SD Public Utilities

Biennial Receiving Waters Monitoring and Assessment Report for the Point Loma and South Bay Ocean Outfalls

2024–2025



City of San Diego Ocean Monitoring Program
Environmental Monitoring and Technical Services Division

SD Public Utilities

Biennial Receiving Waters Monitoring and Assessment Report for the Point Loma and South Bay Ocean Outfalls

2024–2025

Point Loma Wastewater Treatment Plant
(NPDES CA0107409; Order No. R9–2026–0002)

South Bay Water Reclamation Plant
(NPDES CA0109045; Order No. R9-2021-0011 as amended by Order No. R9-2026-0006)

South Bay International Wastewater Treatment Plant
(NPDES CA0108928; Order No. R9-2021-0001 as amended by Order No. R9-2023-0009 and 2026-0005)

Prepared by:
City of San Diego Ocean Monitoring Program
Environmental Monitoring & Technical Services Division, Public Utilities Department

Ryan Kempster, Managing Editor

June 2026

Table of Contents

Executive Summary **1**
R. Kempster

Chapter 1. General Introduction **8**
R. Kempster

Chapter 2. Coastal Oceanographic Conditions **17**
C. Lantz, W. Enright., S. Jaeger

Chapter 3. Water Quality Compliance **60**
S. Smith

Chapter 4. Plume Dispersion **94**
S. Jaeger, C. Lantz, S. Smith, W. Enright

Chapter 5. Sediment Quality **139**
S. Smith, A. Latker

Chapter 6. Macrobenthic Communities **174**
W. Enright, V. Rodriguez-Villanueva, A. Webb

Chapter 7. San Diego Regional Benthic Condition Assessment **199**
W. Enright, S. Smith, A. Latker, L. Nanninga, V. Rodriguez-Villanueva, A. Webb

Chapter 8. Demersal Fishes and Megabenthic Invertebrates **237**
M. Kasuya, G. Rodriguez, Z. Scott

Chapter 9. Contaminants in Marine Fishes **277**
L. Valentino, A. Latker

Appendices - Supplemental Analyses

Appendix A: NPDES Permit Questions
Appendix B: Coastal Oceanographic Conditions
Appendix C: Plume Dispersion
Appendix D: Sediment Quality
Appendix E: Macrobenthic Communities
Appendix F: San Diego Regional Benthic Conditions Assessment
Appendix G: Demersal Fishes and Megabenthic Invertebrates
Appendix H: Contaminants in Marine Fishes

Appendices - Enhanced Monitoring Reports

Appendix I: Evaluation of Anthropogenic Impacts on the San Diego Coastal Kelp Forest Ecosystem, Spring 2023 to Fall 2025
L. Ladah, J. Leichter, K. Riser, B. Bulach, R. Sanders, P. Dayton
Scripps Institution of Oceanography, UC San Diego

Table of Contents

Appendix J: Satellite & Aerial Coastal Water Quality Monitoring in the San Diego/Tijuana Region, Annual Summary Reports: 1 January 2024 to 31 December 2024; and 1 January 2025 to 31 December 2025
M. Hess,
Ocean Imaging, Littleton, CO

Appendix K: Ocean Acidification Monitoring Progress Report for the Point Loma and South Bay Ocean Outfall Regions, San Diego, California, 2019 to 2024
C. Lantz,
City of San Diego

Production Credits and Acknowledgements

Managing Editor:
R. Kempster

GIS Graphics:
M. Kasuya, A. Webb

Production Editors:
L. Valentino, R. Kempster

Production Team:
L. Valentino, W. Enright, S. Smith, C. Lantz, R. Kempster

Acknowledgments:
We are grateful to the personnel of the City's Marine Biology, Marine Microbiology, and Environmental Chemistry Services Laboratories for their assistance in the collection and/or processing of all samples, and for discussions of the results. The completion of this report would not have been possible without their continued efforts and contributions. Complete staff listings for the above labs and additional details concerning relevant QA/QC activities for the receiving waters monitoring data reported herein are available upon request.

How to cite this document:
City of San Diego. (2026). Biennial Receiving Waters Monitoring and Assessment Report for the Point Loma and South Bay Ocean Outfalls, 2024–2025. City of San Diego Ocean Monitoring Program, Public Utilities Department, Environmental Monitoring and Technical Services Division, San Diego, CA.

Executive Summary

Executive Summary

Monitoring results from 2024–2025 indicate that treated wastewater discharges from the Point Loma and South Bay Ocean Outfalls (PLOO and SBOO, respectively) did not measurably impact coastal water quality, benthic habitats, demersal fishes, or offshore biological communities. Observed water quality impairments were primarily associated with stormwater, transboundary flows, and natural oceanographic variability.

Background

The City of San Diego (City) conducts an extensive Ocean Monitoring Program to evaluate potential environmental effects associated with the discharge of treated wastewater to the Pacific Ocean via the PLOO and SBOO. Data collected are used to determine compliance with receiving water quality requirements as specified in National Pollutant Discharge Elimination System (NPDES) permits, and associated orders; these permits and orders are issued by the San Diego Regional Water Quality Control Board (SDRWQCB) and the U.S. Environmental Protection Agency (USEPA) for the City's Point Loma Wastewater Treatment Plant (PLWTP), South Bay Water Reclamation Plant (SBWRP), and the South Bay International Wastewater Treatment Plant (SBIWTP), which is operated by the U.S. Section of the International Boundary and Water Commission (USIBWC). Treated effluent from both the SBWRP and SBIWTP commingle before being discharged to the ocean via the SBOO, thus a single monitoring and reporting program, approved by the SDRWQCB and USEPA, is conducted to comply with these two permits.

The principal objectives of the combined ocean monitoring efforts for both the PLOO and SBOO are to: (1) measure and document compliance with NPDES permit requirements and California Ocean Plan (Ocean Plan) water quality objectives and standards; (2) track movement and dispersion of the wastewater plumes discharged via the outfalls; (3) assess any impact of wastewater discharge on the local marine ecosystem, including effects on coastal water quality, seafloor sediments, and marine life.

Regular (core) monitoring is conducted on a weekly, quarterly, semiannual, and annual basis at a total of 142 discrete sites arranged in grids surrounding the PLOO and SBOO. The PLOO terminates at a discharge depth of around 100 m and is located approximately 7.2 km west of the PLWTP on the Point Loma peninsula. The SBOO terminates at a discharge depth of around 27 m and is located approximately 5.6 km offshore of southern San Diego, just north of the USA/Mexico border. Core monitoring in the PLOO region extends from Mission Beach southward to the tip of Point Loma along the shoreline, and from the nearshore to offshore waters from depths of around 9 to 116 m. Core monitoring of the SBOO region extends from Coronado, San Diego southward to Playa Blanca in northern Baja California, extending offshore from depths of around 9 to 55 m. In addition to monitoring at permanent core stations, an annual survey of benthic conditions (sediment quality and macrobenthic communities) is typically conducted each year at 40 randomly selected "regional" stations, which range from northern San Diego County southward to near the international border, extending offshore to depths of up to 500 m. These broader geographic surveys are useful for evaluating patterns over the entire San Diego coastal region and provide information important for distinguishing reference areas from those impacted by human activities. Additional information on background conditions for San

Diego's coastal marine environment is also available from pre-discharge baseline studies conducted by the City for the PLOO region (1991–1993) and SBOO region (1995–1998).

Results of all receiving waters monitoring activities conducted for the PLOO and SBOO regions, between January 1, 2024 and December 31, 2025, are presented in this report (Chapters 2–9, Appendices A–H), and supplemental studies are included in Appendices I-K. All raw data for the 2024-2025 sampling period have been submitted to either the Regional Water Quality Control Board, the California Environmental Data Exchange Network (CEDEN) or the City's Open Data Portal and may be accessed upon request.

Chapter 1 represents a general introduction and overview of the combined Ocean Monitoring Program for the PLOO and SBOO regions, while chapters 2–9 include results of the primary monitoring components conducted at the core and regional stations. In Chapter 2, data characterizing coastal oceanographic conditions and water mass transport for the region are evaluated. Chapter 3 presents the results of shoreline and offshore water quality compliance, including measurements of fecal indicator bacteria to assess compliance with water contact standards defined in the Ocean Plan. Chapter 4 presents the results of various plume tracking data collection efforts to assess the fate of discharged wastewater via the PLOO and SBOO. Assessments of regional benthic conditions, including benthic sediment quality (physical properties, sediment chemistry, and sediment toxicity), and the status of macrobenthic invertebrate communities are presented in Chapters 5, 6 and 7. Chapter 8 presents the results of trawling activities designed to monitor communities of bottom dwelling demersal fishes and megabenthic invertebrates. Finally, bioaccumulation assessments to measure contaminants in marine fishes are presented in Chapter 9.

In addition to the core monitoring activities described above, the City supports other projects relevant to assessing the status of receiving waters, including: (1) an ongoing long-term assessment of the health and status of San Diego's kelp forest ecosystems conducted by the Scripps Institution of Oceanography (SIO) and funded by the City (see Appendix I); (2) satellite imaging of the San Diego/Tijuana coastal region to assess wastewater plume dispersion and coastal runoff (see Appendix J); (3) an assessment of ongoing efforts to better understand the accuracy of pH measurements used to calculate aragonite saturation state for ocean acidification monitoring (see Appendix K).

Coastal Ocean Conditions

Oceanographic conditions, such as water temperature, salinity, dissolved oxygen (DO) concentrations, pH, natural light levels (transmissivity or water clarity), and concentrations of chlorophyll *a* were generally within historical ranges and followed typical seasonal patterns reported for the PLOO and SBOO monitoring regions. As is characteristic for these waters, ocean conditions indicative of local coastal upwelling, such as relatively cold, dense waters with low DO and high salinity at subsurface depths, were most evident during the spring and winter months of both years. These observations suggest that overall, the temporal and spatial variability observed in oceanographic conditions for coastal San Diego can be explained by a combination of local (e.g., coastal upwelling, rain-related runoff) and large-scale oceanographic-climatic processes, notably the transition from La Niña to ENSO neutral conditions in late 2025, which allowed for the intrusion of warmer water masses from offshore heatwave events once La Niña conditions broke down. As a result, proximity to either outfall is not considered a significant driver of the variations observed in oceanographic parameters discussed in this chapter.

Water Quality Compliance

The 2024–2025 reporting period saw little-to-no improvement in water quality following a decline in compliance, particularly in the SBOO region. All bacterial compliance metrics in the SBOO region, from the shoreline to offshore, indicate a decline in compliance when compared with results from years following the initiation of secondary treatment in 2011. PLOO shore and nearshore stations remained highly compliant overall during the reporting period, with occasional exceedances associated primarily with wet-season conditions. However, despite the very low occurrence of exceedances offshore in the PLOO region, elevated fecal indicator bacteria (FIB) detections at > 60m depths at the stations nearest the outfall and outside of state waters (F29, F30, and F31) have started to emerge in recent years since maximum compliance rates were achieved in 2013.

Precipitation, which is known to drive declines in water quality, especially at shore and kelp stations, remained notably high in 2024 (11.16 in.), following a very wet 2023 (14.43 in.), compared to prior years (9.59 in. on average). Rain events in the wet season are a significant driver of non-compliance region wide, with the largest effect along the shore. However, despite this seasonal pattern, dry-season non-compliance at SBOO region shore and nearshore stations occurred at rates an order of magnitude greater than dry-season noncompliance in the PLOO region. Therefore, although the impact of rain events on shoreline water quality is clear region wide, there remains an additional significant driver of dry-weather noncompliance in the South Bay. This observation is likely explained by the northward transport of contaminated water, particularly from undertreated and untreated wastewater discharging into the Pacific Ocean via San Antonio de Los Buenos Creek, Mexico, by the shallow southern swell. These swells are known to be strongest along the San Diego coast in the summertime. Improvements to nearshore water quality, apparent in 2025, may be driven by repairs to the San Antonio de Los Buenos treatment plant completed in April 2025. This plant treats ~18 MGD of wastewater that had previously been discharged to the coast untreated since 2020. Additionally, periodic excess flows from the South Bay International Wastewater Treatment Plant (SBIWTP) to the SBOO have occurred in response to infrastructure failure, storm-related damage, and resulting ongoing repairs, especially prior to November of 2024. Despite ongoing repairs, flows from the SBIWTP were largely in compliance with the permitted 25 MGD limit from November 2024 – September 2025. An additional ~5 MGD, comprised of effluent treated to advanced primary standards, were added to SBIWTP discharge in September –November of 2025 to relieve pumping constraints in the Tijuana system and enable diversion of sewage away from the Tijuana River. Additional flows have been scaled back since November 2025 due to storm-related interruptions and system maintenance and repair. Increased flows are expected to resume and reach up to 10 MGD in 2026. All combined, these factors were likely driving the observed decrease in water quality at stations in the SBOO region.

Overall, the primary source of contamination in San Diego coastal receiving waters is of known origin and, at shore and nearshore stations, is likely associated with precipitation-driven runoff, contaminated outflows from the Tijuana River, and transboundary flows not related to wastewater discharge. The relatively low number of samples with elevated FIB near the outfalls, compared to the nearshore, highlight the minimal impact of treated wastewater discharge. As a result, we conclude that noncompliance with receiving water limitations for bacterial characteristics is primarily driven by known contaminated outflows from rivers, such as the Tijuana River Estuary, and other non-point source runoff and not a result of treated wastewater discharge.

Plume Dispersion

Observations of potential plume detections throughout the 2024–2025 reporting period demonstrated that the PLOO effluent plume generally remained offshore and below a depth of 30 m, while the SBOO plume was generally trapped below the pycnocline during seasonal periods of water column stratification. However, unlike the PLOO plume, the SBOO plume showed evidence of rising to the surface when waters became more mixed and stratification broke down, typically during the late fall and winter months. Despite differences in observed plume vertical rise heights between the outfalls, both effluent plumes generally remained offshore and were transported along the coast with no evidence of nearshore movement. Although variable over space and time, the general axes of subsurface current velocities in the PLOO and SBOO regions follow a N:NW by S:SE trajectory regardless of season. Thus, as effluent mixed with ambient seawater, it generally travelled along the coast rather than being directed inshore toward the kelp beds, shoreline, or other recreational waters. As a result, there was no evidence that wastewater discharged to the ocean, via either the PLOO or SBOO, reached recreational waters along the shore or nearshore kelp beds. These findings concur with prior plume tracking studies, as well as historical satellite imagery observations that have not shown visual evidence of wastewater ever reaching the shoreline or having any significant impact on recreational waters.

Regional Benthic Conditions

Benthic habitats, and associated biological communities, found on the continental shelf and upper slope off San Diego were found to be in excellent condition during the 2024–2025 reporting period. There was no evidence of fine particle loading related to wastewater discharge via the PLOO or SBOO, and no evidence of degraded benthic habitats, based on the chemical properties of the sediments, or contaminant distribution patterns. Instead, contaminant concentrations near the outfalls were generally within the range of variability observed throughout both outfall regions. While several indicators of organic loading, trace metals, pesticides, PCBs, PAHs, and PBDEs were detected in sediment samples throughout the San Diego region, almost all occurred at concentrations below available ERL (Effects Range Low) and ERM (Effects Range Median) thresholds, consistent with previous years. This is further supported by results from sediment toxicity testing in offshore San Diego waters that revealed minimal or low toxicity at all regional stations tested.

Benthic macrofaunal communities off San Diego also appeared to be healthy, with most assemblages appearing to be similar to those observed in the region from 1991 through to the present, and throughout southern California and northern Baja California. A modest decrease in condition assessment in the SBOO region compared to the previous reporting period is within the range of natural background variability observed historically. Although communities varied across depth and sediment gradients, there was no evidence of disturbance or significant environmental degradation that could be attributed to anthropogenic factors, such as wastewater discharge. Instead, these communities segregated by habitat characteristics, such as depth and sediment particle size, often corresponding with the “patchy” habitats reported to occur naturally in southern California’s offshore coastal waters. Finally, the Benthic Response Index (BRI) further confirmed little evidence of disturbance off San Diego with 90% of all calculated BRI values being indicative of reference conditions, in line with previous reporting periods (2018–2019: 89%; 2020–2021: 94%; 2022-2023: 95%). These results, when integrated with sediment chemistry and sediment toxicity results, demonstrated that the shelf off San Diego remains unimpacted

by the PLOO or SBOO. Consequently, there is presently no evidence to suggest that wastewater discharge via the PLOO or SBOO is affecting the quality of benthic sediments off San Diego to the point that it may degrade resident marine biological communities.

Demersal Fishes and Megabenthic Invertebrates

Demersal fishes and megabenthic invertebrate populations monitored in 2024 and 2025 did not show evidence of negative impacts associated with proximity to wastewater discharge from the PLOO and SBOO. Although highly variable, patterns in the abundance and distribution of individual species were similar regardless of proximity to either outfall and were representative of similar habitats throughout the SCB.

A total of 26,411 fishes were captured from 52 trawls conducted within the PLOO and SBOO monitoring regions during 2024 and 2025, representing at least 52 different species from 26 families in the PLOO region, and 32 species from 17 families in the SBOO region. Pacific Sanddabs dominated assemblages surrounding the PLOO, and Speckled Sanddab dominated assemblages surrounding the SBOO, as they have done since monitoring began in each region. Halfbanded Rockfish were also prevalent in PLOO assemblages, while California Lizardfish were prevalent within the SBOO region. Other commonly captured, but less abundant fishes, collected from the PLOO and SBOO regions included California Tonguefish, Dover Sole, English Sole, Longfin Sanddab, Northern Anchovy, Longspine Combfish, Shortspine Combfish, and White Croaker. External examination of fish collected indicated that fish populations remained healthy off San Diego, with fewer than 0.2% of all fish having external parasites or showing any evidence of disease or other abnormalities. As abnormalities or parasites were present across nearly all stations between regions, there does not appear to be a relationship between these anomalies and proximity to either outfall. Most abnormalities observed in the study period were limited to single occurrences distributed across the different stations and seasons with no apparent relationship with proximity to outfall discharge.

A total of 52,926 invertebrates were captured from the 52 trawls conducted within the PLOO and SBOO monitoring regions in 2024 and 2025, representing 85 taxa from five phyla (Arthropoda, Echinodermata, Mollusca, Cnidaria, Silicea). The sea urchin *Lytechinus pictus* dominated PLOO trawls-caught invertebrates and accounted for 98% of total abundance across trawls in that region. The sea star *Astropecten californicus* and the sea cucumber *Apostichopus californicus* were caught in more than 50% of the trawls but their abundances were very low (≤2 haul). The sea star *Astropecten californicus* dominated the SBOO region and accounted for 74% of total abundance. The brittle star *Ophiothrix spiculata,* the shrimp *Sicyonia penicillata*, and the sea star *Luidia armata* occurred in more than 50% of the trawls and accounted for 2% to 3% of the total catch.

The abundance and distribution of fish and invertebrate species varied similarly at stations located near and far from the outfalls in both regions. The high degree of variability in these assemblages during this reporting period was similar to that observed in previous years, including before wastewater discharge began through either outfall. Furthermore, similar variability has been observed in comparable habitats elsewhere off the coast of southern California. Consequently, changes in local community structure of these fishes and invertebrates are more likely due to natural factors, such as changes in ocean temperatures associated with El Niño or other large-scale oceanographic events.

Contaminants in Marine Fishes

The accumulation of chemical contaminants in San Diego marine fishes varied across species and stations, but most values were within ranges reported previously for southern California fishes. Although several different trace metals, pesticides, PCB congeners, PBDEs and various PAHs were detected in both liver and muscle tissues, these contaminants occurred in fishes distributed throughout both regions, with no patterns that could be attributed to wastewater discharge via the outfalls. Consequently, the occurrence of these contaminants in some local fishes off San Diego is likely influenced by other factors, such as the widespread distribution of many contaminants in southern California sediments, differences in the physiology and life history traits of various species of fish, different exposure pathways, and differences in the migration pathways of various species. For example, an individual fish may be exposed to contaminants at a polluted site but then migrate to an area that is less contaminated. This is of particular concern for fishes collected in the vicinity of the PLOO and SBOO, as there are many other nearby potential point and non-point sources of contamination. These results are consistent with findings of other assessments of bioaccumulation in fishes off San Diego and are further supported by the lack of other indicators of poor fish health in the region, such as the presence of fin rot or other signs of disease. Overall, there was no evidence of contaminant accumulation in PLOO or SBOO fishes that could be associated with wastewater discharge from either outfall, which is consistent with historical findings.

Conclusions

The 2024–2025 Ocean Monitoring Program results indicate that the Point Loma and South Bay Ocean Outfalls generally remained in compliance with regulatory objectives and that treated wastewater discharges did not measurably degrade coastal water quality, benthic habitats, marine communities, or fish health in the San Diego region. Oceanographic conditions and biological communities largely reflected natural, seasonal, and regional variability rather than impacts from wastewater discharge, while plume tracking demonstrated that discharged effluent remained offshore and away from recreational waters. Although bacterial water quality impairments persisted, particularly in the South Bay region, the evidence indicates that these issues were primarily driven by transboundary contamination, stormwater runoff, and Tijuana River-related flows rather than the treated ocean discharges themselves. Overall, long-term monitoring data continues to support the conclusion that the PLOO and SBOO are not causing significant adverse environmental impacts to the receiving marine environment.

Chapter 1
General Introduction

Chapter 1. General Introduction

Program Requirements & Objectives

Ocean monitoring within the Point Loma and South Bay outfall regions is conducted by the City of San Diego (City) in accordance with requirements set forth in National Pollution Discharge Elimination System (NPDES) permits and associated orders for the following: the Point Loma Wastewater Treatment Plant (PLWTP), the South Bay Water Reclamation Plant (SBWRP), and the South Bay International Wastewater Treatment Plant (SBIWTP), which is owned and operated by the U.S. Section of the International Boundary and Water Commission (USIBWC) (see Table 1.1). These documents specify the terms and conditions that allow treated effluent to be discharged to the Pacific Ocean via the Point Loma Ocean Outfall (PLOO) and South Bay Ocean Outfall (SBOO). In addition, the Monitoring and Reporting Program (MRP), included within each of these orders, defines the requirements for monitoring ocean (receiving) waters surrounding the two outfalls. These requirements include sampling design, frequency of sampling, field operations and equipment, regulatory compliance criteria, types of laboratory tests and analyses, data management and analysis, statistical methods and procedures, environmental assessment, and reporting guidelines. Although this report aims to provide a comprehensive discussion, evaluation, and interpretation of the state of receiving waters throughout the Point Loma and South Bay regions, to ensure all regulatory questions are answered clearly and concisely, Appendix A has been included with direct answers to specific permit-related questions.

The combined Ocean Monitoring Program for these regions is designed to assess the impact of wastewater discharged through the PLOO and SBOO on the coastal marine environment off San Diego. The main objectives of the program are to: (1) measure and document compliance with NPDES permit requirements and California Ocean Plan (Ocean Plan) water quality objectives and standards; (2) track movement and dispersion of the wastewater plumes discharged via the outfalls; (3) assess any impact of wastewater discharge on the local marine ecosystem, including effects on coastal water quality, seafloor sediments, and marine life.

Background

Point Loma Ocean Outfall

The City began operation of the PLWTP and original PLOO off Point Loma in 1963, at which time treated effluent was discharged approximately 3.9 km west of the Point Loma peninsula at a depth of around 60 m. The PLWTP operated as a primary treatment facility from 1963 to 1985, after which it was upgraded to advanced primary treatment between mid-1985 and July 1986. This improvement involved the addition of chemical coagulation to the treatment process, which resulted in an increase in removal of total suspended solids (TSS) to about 75%. Since then, the treatment process has continued to be improved with the addition of more sedimentation basins, expanded aerated grit removal, and refinements in chemical treatment, which together further reduced mass emissions from the plant. For example, TSS removals are now consistently greater than the 80%, as required by the NPDES permit.

The structure of the PLOO was significantly modified in the early 1990s when it was extended about 3.3 km farther offshore in order to prevent intrusion of the waste field into nearshore waters and to increase compliance with Ocean Plan standards for water-contact sports areas. Discharge from the original 60-m terminus was discontinued in November 1993 following completion of the outfall extension. Currently, the PLOO extends approximately 7.2 km west of the PLWTP to a depth of around 94 m, where the main outfall pipe splits into a Y-shaped (wye) multiport diffuser system. The two diffuser legs extend an additional 762 m to the north and south, each terminating at a depth of about 98 m. The average discharge of effluent through the PLOO in 2024–2025 was about 139.88 –147.97 mgd (million gallons per day).

South Bay Ocean Outfall

The SBOO is located just north of the international border between the United States and Mexico where it terminates approximately 5.6 km offshore and west of Imperial Beach at a depth of around 27 m. Unlike other southern California ocean outfalls that lie on the surface of the seafloor, the SBOO pipeline begins as a tunnel on land that extends from the SBWRP and SBIWTP facilities to the coastline, after which it continues beneath the seabed 4.3 km offshore. The outfall pipe connects to a vertical riser assembly that conveys effluent to a pipeline buried just beneath the surface of the seafloor. This subsurface pipeline then splits into a Y-shaped (wye) multiport diffuser system with the two diffuser legs each extending an additional 0.6 km to the north or south. The SBOO was originally designed to discharge wastewater through 165 diffuser ports and risers, which included one riser at the center of the wye and 82 risers spaced along each diffuser leg. Since discharge began, however, low flow rates have required closure of all ports along the northern diffuser leg and many along the southern diffuser leg in order for the outfall to operate effectively. Consequently, wastewater discharge is restricted primarily to the distal end of the southern diffuser leg and to a few intermediate points at or near the center of the wye. The average discharge of effluent through the SBOO in 2024–2025 was about 25.91–27.61 mgd, including about 2.61-3.01 mgd of secondary and tertiary treated effluent from the SBWRP, and 23.3-24.6 mgd of secondary treated effluent from the SBIWTP.

Receiving Waters Monitoring

The total area for the PLOO and SBOO monitoring program covers approximately 881 km^2 (~340 mi^2) of coastal marine waters from Northern San Diego County into Northern Baja California. Core monitoring for the Point Loma region is conducted at 82 stations, located from the shore to a depth of around 116 m. Core monitoring for the South Bay region is conducted at a total of 53 stations, ranging from the shore to depths of around 61 m (Figure 2.1 and 5.1). Each of the core monitoring stations is sampled for specific parameters as stated in their respective MRPs. A summary of the results for all quality assurance procedures performed during 2024 and 2025, in support of these requirements, can be found in City of San Diego (2025, 2026a). Data collected during the 2024–2025 reporting period have been submitted to either the Regional Water Quality Control Board, the California Environmental Data Exchange Network (CEDEN) or the City's Open Data Portal (City of San Diego 2026b) and may be accessed upon request.

Prior to 1994, the City conducted an extensive ocean monitoring program off Point Loma surrounding the original 60-m discharge site. This program was subsequently expanded with the construction and operation of the deeper outfall, as discussed previously. Data from the last year of regular monitoring near the original PLOO discharge site are presented in City of San Diego (1995a), while the results of a 3-year "recovery study" are summarized in City of San Diego (1998). Additionally, a more detailed assessment

of spatial and temporal patterns surrounding the original discharge site is available (Zmarzly et al. 1994). From 1991 through 1993, the City also conducted "pre-discharge" monitoring for the new PLOO discharge site in order to collect baseline data prior to wastewater discharge into these deeper waters (City of San Diego 1995a, b). All permit mandated ocean monitoring for the South Bay region has also been performed by the City since wastewater discharge through the SBOO began in 1999; this included pre-discharge monitoring for 3½ years (July 1995–December 1998) in order to provide background information against which post-discharge conditions could be compared (City of San Diego, 2000). Results of NPDES mandated monitoring for the extended PLOO from 1994 to present, and the SBOO from 1999 to present, are available in previous annual receiving waters monitoring reports. Finally, additional detailed assessments of the PLOO region have been completed as part of past modified NPDES permit renewal applications for the PLWTP submitted by the City (e.g., City of San Diego 2022) and subsequent technical decisions issued by the USEPA (e.g., USEPA 2017).

The City has also conducted annual region-wide surveys off the coast of San Diego since 1994, either as part of regular outfall monitoring requirements (e.g., City of San Diego 1999), or as part of larger multi-agency surveys of the entire Southern California Bight (SCB) (e.g., Gillett et al. 2017). The latter include the 1994 Southern California Bight Pilot Project (SCCWRP 1998) and subsequent Bight programs from 1998 through 2023. These large-scale surveys are useful for characterizing the ecological health of diverse coastal areas to distinguish reference sites from those impacted by wastewater or storm water discharges, urban runoff, or other sources of contamination. In addition to the above activities, the City participates as a member of the Region Nine Kelp Survey Consortium to fund aerial surveys of all the major kelp beds in San Diego and Orange Counties (e.g., MBC 2025).

Report Components & Organization

This report presents a comprehensive biennial assessment of the results of all receiving waters monitoring activities conducted during 2024 and 2025 for both the Point Loma and South Bay outfall regions. Included herein are results from all regular core stations that comprise the fixed-site monitoring grids surrounding the two outfalls (see Figure 2.1 and 5.1), as well as results from the 2024 and 2025 summer benthic surveys of randomly selected sites that range from near the USA/Mexico border to northern San Diego County (see Figure 7.1). The main components of the combined monitoring program are covered in the following sections or chapters: Executive Summary; General Introduction (Chapter 1); Coastal Oceanographic Conditions (Chapter 2); Water Quality Compliance (Chapter 3); Plume Dispersion (Chapter 4); Sediment Quality (Chapter 5); Macrobenthic Communities (Chapter 6); San Diego Regional Benthic Condition Assessment (Chapter 7); Demersal Fish and Megabenthic Invertebrate Communities (Chapter 8); Contaminants in Marine Fishes (Chapter 9). Supplemental analyses for Chapters 2–9 are included in Appendices B-H.

Special Studies & Enhanced Monitoring

In addition to the core monitoring highlighted above, the City has actively participated in, or supported, numerous important special projects, or enhanced ocean monitoring studies, over the past 10 years or more. Many of these projects to date were identified as part of a scientific review of the City's Ocean Monitoring Program, conducted by the Scripps Institution of Oceanography (SIO) and other participating institutions (SIO 2004). This review evaluated the environmental monitoring needs

of the region, and recommended special projects based on priorities identified. Examples of special projects currently underway, or being initiated include:

- **San Diego Kelp Forest Ecosystem Monitoring Project:** This project represents continuation of a long-term commitment by the City to support important research conducted on local kelp forests by SIO. This work is essential to assessing the health of San Diego's kelp forests and monitoring the effects of wastewater discharge on the local coastal ecosystem relative to other anthropogenic and natural influences (see Appendix I).

- **Remote Sensing of the San Diego / Tijuana Coastal Region:** This project represents a long-term effort, funded by the City and the USIBWC since 2002, to utilize satellite and aerial imagery to better understand regional water quality conditions off San Diego. The project is conducted by Ocean Imaging (Littleton, CO) and is focused on detecting and tracking the dispersion of wastewater plumes from local ocean outfalls and nearshore sediment plumes caused by stormwater runoff or outflows from local bays and rivers (see Appendix J and City of San Diego, 2026c).

- **Ocean Acidification Monitoring:** In 2021, new requirements were established in the NPDES permits for the South Bay Water Reclamation Plant (SBWRP) and the South Bay International Wastewater Treatment Plant (SBIWTP) to monitor pH by spectrophotometric analysis to calibrate the pH results measured by a conductivity-temperature-depth (CTD) profiler. Further, pH and total alkalinity are required to be used to calculate aragonite saturation state for ocean acidification monitoring. To achieve these objectives, the City's Ocean Monitoring Program has since been collecting discrete bottle samples for pH and total alkalinity (TA) analysis in the South Bay Ocean Outfall (SBOO) monitoring region. Based on the findings of this study, the City requested amendments to be applied upon renewal of the NPDES permits for the PLWTP, SBWRP, and the SBIWTP, including the discontinuation of quarterly pH bottle sampling for the purpose of CTD pH correction given the high quality of the City's pH calibration procedures (see Appendix K).

- **Euphotic Zone Study:** The National Marine Fisheries Service (NMFS) concluded that certain federally listed threatened and endangered marine species could be at risk of exposure to phytoplankton blooms, including harmful algal blooms, as a result of nutrient loads from the Point Loma Wastewater Treatment Plant (PLWTP). Consequently, the City agreed to study the euphotic zone depth of the receiving waters in order to evaluate whether nutrients from the discharge plume reach the euphotic zone and thereby potentially stimulate phytoplankton productivity. Phase two of this Euphotic Zone Study begin in 2024 and involves quarterly sampling throughout the Point Loma region with the final report due by December 1, 2027. Interim Progress reports are provided annually in March (see City of San Diego, 2026c).

Literature Cited

City of San Diego. (1995a). Receiving Waters Monitoring Report for the Point Loma Ocean Outfall, 1994. City of San Diego Ocean Monitoring Program, Metropolitan Wastewater Department, Environmental Monitoring and Technical Services Division, San Diego, CA.

City of San Diego. (1995b). Outfall Extension Pre-Construction Monitoring Report (July 1991–October 1992). City of San Diego Ocean Monitoring Program, Metropolitan Wastewater Department, Environmental Monitoring and Technical Services Division, San Diego, CA.

City of San Diego. (1998). Recovery Stations Monitoring Report for the Original Point Loma Ocean Outfall (1991–1996). City of San Diego Ocean Monitoring Program, Metropolitan Wastewater Department, Environmental Monitoring and Technical Services Division, San Diego, CA.

City of San Diego. (1999). San Diego Regional Monitoring Report for 1994–1997. City of San Diego Ocean Monitoring Program, Metropolitan Wastewater Department, Environmental Monitoring and Technical Services Division, San Diego, CA.

City of San Diego. (2000). Final Baseline Monitoring Report for the South Bay Ocean Outfall (1995–1998). City of San Diego Ocean Monitoring Program, Metropolitan Wastewater Department, Environmental Monitoring and Technical Services Division, San Diego, CA.

City of San Diego. (2022). Application for Renewal of NPDES CA0107409 and 301(h) Modified Secondary Treatment Requirements for Biochemical Oxygen Demand and Total Suspended Solids, Point Loma Ocean Outfall and Point Loma Wastewater Treatment Plant. Volumes I–X, Appendices A–U. The City of San Diego, Public Utilities Department, San Diego, CA.

City of San Diego. (2025). Annual Receiving Waters Monitoring & Toxicity Testing Quality Assurance Report, 2024. City of San Diego Ocean Monitoring Program, Public Utilities Department, Environmental Monitoring and Technical Services Division, San Diego, CA.

City of San Diego. (2026a). Annual Receiving Waters Monitoring & Toxicity Testing Quality Assurance Report, 2025. City of San Diego Ocean Monitoring Program, Public Utilities Department, Environmental Monitoring and Technical Services Division, San Diego, CA.

City of San Diego. (2026b). Ocean Monitoring Program Reports and Data. https://www.sandiego.gov/public-utilities/sustainability/ocean-monitoring/reports

City of San Diego. (2026c). Euphotic Zone Study Progress Report for the Point Loma Ocean Outfall Region, San Diego. City of San Diego Ocean Monitoring Program, Public Utilities Department, Environmental Monitoring and Technical Services Division, San Diego, CA.

Gillett, D.J., L.L. Lovell, and K.C. Schiff. (2017). Southern California Bight 2013 Regional Monitoring Program: Volume VI. Benthic Infauna. Technical Report 971. Southern California Coastal Water Research Project. Costa Mesa, CA.

[MBC] MBC Aquatic Sciences. (2025). Status of the Kelp Beds 2023–2024, Kelp Bed Surveys: Orange, and San Diego Counties. Final Report, August 2025. MBC Aquatic Sciences, Costa Mesa CA.

Rogowski, P., E. Terrill, M. Otero, L. Hazard, S.Y. Kim, P.E. Parnell, and P. Dayton. (2012a). Final Report: Point Loma Ocean Outfall Plume Behavior Study. Prepared for City of San Diego Public Utilities Department by Scripps Institution of Oceanography, University of California, San Diego, CA.

Rogowski, P., E. Terrill, M. Otero, L. Hazard, and W. Middleton. (2012b). Mapping ocean outfall plumes and their mixing using Autonomous Underwater Vehicles. Journal of Geophysical Research, 117: C07016.

Rogowski, P., E. Terrill, M. Otero, L. Hazard, and W. Middleton. (2013). Ocean outfall plume characterization using an Autonomous Underwater Vehicle. Water Science & Technology, 67(4): 925–933.

[SCCWRP] Southern California Coastal Water Research Project. (1998). Southern California Bight 1994 Pilot Project: Volumes I–VI. Southern California Coastal Water Research Project, Westminster, CA .

[SCCWRP] Southern California Coastal Water Research Project. (2018). Southern California Bight 2018 Regional Monitoring Program: Contaminant Impact Assessment Field Operations Manual. Southern California Coastal Water Research Project. Costa Mesa, CA.

[SIO] Scripps Institution of Oceanography. (2004). Point Loma Outfall Project, Final Report, September 2004. Scripps Institution of Oceanography, University of California, La Jolla, CA.

Terrill, E., K. Sung Yong, L. Hazard, and M. Otero. (2009). IBWC/Surfrider – Consent Decree Final Report. Coastal Observations and Monitoring in South Bay San Diego. Scripps Institution of Oceanography, University of California, San Diego, CA.

[USEPA] United States Environmental Protection Agency. (2017). City of San Diego's Point Loma Wastewater Treatment Plant Application for a Modified NPDES Permit under Sections 301(h) and (j)(5) of the Clean Water Act. Technical Decision Document. United States Environmental Protection Agency, Region IX, San Francisco, CA.

Zmarzly, D.L., T.D. Stebbins, D. Pasko, R.M. Duggan, and K.L. Barwick. (1994). Spatial patterns and temporal succession in soft-bottom macroinvertebrate assemblages surrounding an ocean outfall on the southern San Diego shelf: relation to anthropogenic and natural events. Marine Biology, 118: 293–307.

CHAPTER 1

FIGURES & TABLES

Table 1.1

NPDES permits and associated orders issued by the San Diego Water Board for the Point Loma Wastewater Treatment Plant (PLWTP), South Bay Water Reclamation Plant (SBWRP), and South Bay International Wastewater Treatment Plant (SBIWTP) discharges to the Pacific Ocean via the PLOO and SBOO.

Facility	Outfall	NPDES Permit No.	Order No.	Effective Dates
PLWTP	PLOO	CA0107409	R9-2026-0002	May 1, 2026–April 30, 2031
SBWRP	SBOO	CA0109045	R9-2021-0011[a]	July 1, 2021–June 30, 2026
SBIWTP	SBOO	CA0108928	R9-2021-0001[b]	July 1, 2021–June 30, 2026

[a] as amended by Order R9-2026-0006

[b] as amended by Orders R9-2023-0009 and 2026-0005

Chapter 2
Coastal Oceanographic Conditions

Chapter 2. Coastal Oceanographic Conditions

Introduction

The City of San Diego (City) collects a comprehensive suite of oceanographic data from coastal waters surrounding the Point Loma Ocean Outfall (PLOO) and South Bay Ocean Outfall (SBOO) to characterize regional conditions and to identify possible impacts of wastewater discharge and other factors on the marine environment. These data include measurements of ocean temperature, salinity, light transmittance (transmissivity), dissolved oxygen, pH, and chlorophyll *a* throughout the water column, all of which are considered important indicators of physical and biological processes that can impact marine life (Skirrow 1975, Mann 1982, Mann and Lazier 1991). As the fate of wastewater discharged into the ocean is determined by multiple factors (e.g., outfall geometry, rate of effluent discharge, water column mixing, ocean currents, tidal flows), evaluations of physical parameters that influence the mixing potential of the water column are important components of many ocean monitoring programs (Bowden 1975, Pickard and Emery 1990).

In the nearshore coastal waters of the Southern California Bight (SCB), including the PLOO and SBOO monitoring regions, ocean conditions are influenced by multiple factors. These include: (1) large-scale climatic processes, such as El Niño Southern Oscillations (ENSO), Pacific Decadal Oscillations (PDO), and North Pacific Gyre Oscillations (NPGO), which can affect long-term oceanographic trends (Peterson et al. 2006, McClatchie et al. 2008, 2009, Bjorkstedt et al. 2010, 2011, 2012, Wells et al. 2013, NOAA/NWS 2024); (2) the California Current System, coupled with local gyres that transport distinct water masses into and out of the SCB (Lynn and Simpson 1987, Leising et al. 2014); (3) seasonal changes in local weather patterns (Bowden 1975, Skirrow 1975, Pickard and Emery 1990), which are a primary driver of water column stratification typically observed off San Diego and in coastal waters throughout the rest of southern California (Terrill et al. 2009, Rogowski et al. 2012a,b, 2013). These seasonal patterns include typically warmer and more stratified waters in the dry season, from May through September, and cooler, weakly stratified and well-mixed waters, in the wet season, from October through April (e.g., City of San Diego 2022a, Hess 2019, 2020).

Understanding changes in oceanographic conditions due to natural processes, such as the seasonal patterns described above, is of utmost importance since they will likely affect the transport and distribution of wastewater, storm water, and other nearshore plumes. In the PLOO and SBOO monitoring regions, nearshore plumes include sediment or turbidity plumes associated with outflows from local bays, major rivers, lagoons and estuaries, discharges from storm drains or other point sources, surface runoff from local watersheds, seasonal upwelling, and variable ocean currents or eddies. Outflow plumes from the San Diego River, San Diego Bay, and the Tijuana River can contribute significantly to patterns of nearshore turbidity, sediment deposition, and bacterial contamination (see Largier et al. 2004, Terrill et al. 2009, Svejkovsky 2010, 2017, Hess 2018, 2019, 2020).

In order to assess conditions on a comprehensive spatial scale, quarterly water quality surveys have historically been conducted across the two outfall regions (beginning in 1991 at PLOO and 1995 at

SBOO). Subsequent studies of the fate and behavior of wastewater discharged to the ocean via the SBOO (Terrill et al. 2009) and the PLOO (Rogowski et al. 2012a,b, 2013) included recommendations to use real-time oceanographic mooring systems (RTOMS) and advanced sampling technologies to better understand nearshore coastal water quality and the impacts of local ocean currents and tidal fluxes on effluent plume dynamics. This higher temporal resolution data collection began in 2017 at SBOO and in 2018 at PLOO (City of San Diego 2018a, 2020). While quarterly surveys provide a snapshot of conditions across a large regional area, the RTOMS provide near-continuous information on how ocean conditions change over time near the two ocean outfalls. As such, some variations in ranges and seasonal comparisons between quarterly surveys and RTOMS data are expected, and differences between these sampling approaches are discussed in relevant sections.

This chapter presents analysis and interpretation of the oceanographic monitoring data collected during 2024 and 2025 for the coastal waters surrounding the PLOO and SBOO. The primary goals of this chapter are to: (1) summarize coastal oceanographic conditions in these regions to provide information on the state of local receiving waters; (2) determine if water clarity, pH or dissolved oxygen are significantly altered at any point outside of the Zone of Initial Dilution (ZID) as a result of the outfall discharge; (3) evaluate local ocean conditions off the coast of San Diego within the context of regional climatic processes. In addition, results of remote sensing observations (e.g., satellite imagery) are combined with measurements of physical oceanographic parameters to provide further insight on the horizontal transport of surface waters off San Diego. The results reported herein are also referred to in subsequent chapters to explain patterns of fecal indicator bacteria distributions and plume dispersion (see Chapters 3 and 4) as well as other changes in the local marine environment (see Chapters 5-9).

Materials and Methods

Quarterly CTD surveys

Data Collection

A total of 69 offshore water quality monitoring stations were sampled quarterly to assess coastal oceanographic conditions in the two outfall regions (Figure 2.1). These include 36 stations surrounding the PLOO and 33 stations surrounding the SBOO. The PLOO stations are designated F1–F36 and are located along or adjacent to the 18, 60, 80, and 98-m depth contours. The SBOO stations are designated I1–I18, I20–I23, I27–I31, and I33–I38, and are located along the 9, 19, 28, 38 and 55-m depth contours, respectively. All 69 stations were monitored during winter (February), spring (May), summer (August), and fall (November) in 2024 and 2025, and were sampled over a four-day period during each survey (Appendix B.1). Sampling at an additional eight kelp bed stations off Point Loma (i.e., stations A1, A6, A7, C4–C8) and seven kelp/nearshore stations in the South Bay region (i.e., stations I19, I24–I26, I32, I39, I40) was conducted four to five times per month to meet bacterial monitoring requirements (see Chapter 3). However, only data collected at these 15 kelp bed stations that occurred within one week of the quarterly offshore stations are analyzed in this chapter (see Appendix B.1).

Oceanographic data were collected using a SeaBird SBE 25 Plus conductivity, temperature, and depth instrument (CTD). The CTD was lowered through the water column at each station to collect continuous measurements of water temperature, conductivity (used to calculate salinity), pressure (used to calculate depth), dissolved oxygen (DO), pH, transmissivity (a proxy for water clarity), chlorophyll *a* fluorescence (a proxy for phytoplankton), and colored dissolved organic material (CDOM). Vertical profiles of each

parameter were constructed for each station per survey by averaging the data values recorded within each 1-m depth bin. This level of data reduction ensures that physical measurements used in subsequent analyses will correspond to discrete sampling depths required for bacterial monitoring (see Chapter 3). Visual observations of weather and water conditions were recorded just prior to each CTD cast. These observations were previously reported in monthly receiving waters monitoring reports submitted to the San Diego Regional Water Quality Control Board (see City of San Diego 2024–2025a,b).

Data Analysis

Water column parameters were summarized as quarterly means pooled over all stations by the following depth layers: 1–20 m, 21–60 m, 61–80 m, 81–98 m (PLOO); 1–9 m, 10–19 m, 20–28 m, 29–38 m, 39–55 m (SBOO). The top layer is herein referred to as surface water, while the subsurface layers account for mid and bottom waters. Unless otherwise noted, analyses were performed using R (R Core Team, 2026) and various functions within the reshape2, Rmisc, mixOmics, tidyverse, Hmisc, RODBC, and oce packages (Wickham 2007, Hope 2013, Rohart et al. 2017, Wickham et al. 2019, Harrell 2021, Ripley and Lapsley 2021, Kelley and Richards 2022).

Vertical density profiles were constructed from CTD data to depict the pycnocline (i.e., depth layer where the density gradient was greatest) for each survey and to illustrate seasonal changes in water column stratification. Data for these density profiles were limited to stations located along the 98-m depth contour in the PLOO region (i.e., stations F26–F36) and the 28-m depth contour in the SBOO region (i.e., stations I2, I3, I6, I9, I12, I14, I17, I22, I27, I30, I33) to prevent masking trends that occur when data from multiple depth contours are combined. Buoyancy frequency (BF), a measure of the static stability of the water column, was used to quantify the magnitude of stratification for each station per survey and was calculated as follows:

$$BF = \sqrt{(g/\rho * (d\rho/dz))}$$

where g is the acceleration due to gravity, ρ is the seawater density, and dρ/dz is the density gradient (Mann and Lazier 1991). The depth of maximum BF was used as a proxy for the depth at which stratification was the greatest.

Additionally, time series of anomalies for water temperature, salinity, and DO were calculated to evaluate regional oceanographic events within the context of large-scale climatic processes (i.e., ENSO events). These analyses were limited to data from the discharge depth stations for each outfall, with all water column depths combined. Anomalies were then calculated as the difference between the quarterly historical average and quarterly means for each year.

RTOMS

Data Collection

Two real-time oceanographic mooring systems were deployed at the terminal ends of the PLOO and SBOO (Figure 2.1), in partnership with Scripps Institution of Oceanography (SIO). The PLOO RTOMS was anchored at a nominal depth of 98 m, just east of the northern diffuser leg, and the SBOO RTOMS was anchored at a nominal depth of 30 m, just west of the southern diffuser leg terminus (Appendix B.2). Each mooring was deployed for a period of approximately one year. The PLOO RTOMS were deployed on three separate occasions during the 2024-25 reporting period: December 20, 2023 to December 9, 2024, April 14, 2025 to October 29, 2025, and December 11, 2025 to present (retrieval anticipated for

December, 2026). Similarly, the SBOO RTOMS were deployed on three separate occasions during this period: June 29, 2023 to May 21, 2024, July 30, 2024 to June 4, 2025, and July 10, 2025 to present (retrieval anticipated for July, 2026). Data presented here include only data collected in real-time from all deployments. Data are not available for the first half of 2024 at the PLOO due to manufacturer delays in instrument service and calibration and staffing shortages. For a summary of critical data loss issues for 2025, see Appendix B.3 and for 2024, see Appendix A.1 in City of San Diego (2025a). For a more comprehensive list of all RTOMS issues for 2024-25, see annual progress reports (City of San Diego 2025b, 2026a).

Each RTOMS was outfitted with a series of instruments/sensors at fixed depths (Table 2.1). Critical parameters that were measured on a real-time basis, by both systems, included temperature, conductivity (salinity), total pH, DO, dissolved carbon dioxide (xCO_2), nitrogen (nitrate + nitrite), chlorophyll *a*, CDOM, and current direction and velocity. Note that pH is reported in total scale (pH_T) from RTOMS with a more accurate calibration and measurement method for seawater, while pH has been reported in National Bureau of Standards (NBS) scale from CTD casts; it is not recommended to convert between these scales (Marion et al. 2011). In general, pH_T ranges reported by RTOMS may be lower than those recorded by the CTD, and any pH comparisons should be interpreted with caution due to method differences. All parameters were recorded at 10-minute intervals, except for nitrate + nitrite and xCO_2, which were recorded at 1-hour intervals.

Temperature and ocean current data from static moorings were used to supplement data gaps between RTOMS deployments. These non-telemetered (static) upward-facing bottom-mounted acoustic doppler current profilers (ADCPs) (Teledyne RD Instruments 300 KHz Workhorse Monitor) and thermistor (Onset Tidbit temperature loggers) string arrays were moored near the RTOMS at the terminal end of the PLOO and SBOO (Figure 2.1, Appendix B.4), as part of the original Moored Observation System Pilot Study (Storms et al. 2006). These instrument packages are much smaller and less logistically challenging to retrieve and deploy compared to RTOMS. Data from ADCPs were collected every five minutes in 4-m depth bins, ranging from 9 to 93 m at the PLOO and from 6 to 30 m at the SBOO. Temperature data were collected from vertical series of thermistors every 10 minutes from duplicate arrays at the PLOO (100 m) and a single array at the SBOO (36 m). The thermistors were deployed on mooring lines at each site starting at 2 m above the seafloor and extending through the water column every 4 m to within 6 m of the surface.

Data Processing and Analysis

Prior to conducting analyses, RTOMS data were subject to a comprehensive suite of quality assurance/quality control (QA/QC) procedures following Quality Assurance of Real-Time Oceanographic Data (QARTOD) methodologies (US IOOS 2017, 2020). This collaborative effort was developed to address data quality issues of the U.S. Integrated Ocean Observing System (US IOOS) community and provides recommendations for applying automated data qualifier flags specific to each parameter. Methodology for ADCP data differed slightly and is described separately. For all other RTOMS data, QARTOD tests were applied to all data prior to analysis (Appendices B.5–B.7, City of San Diego 2025a). In addition to these automated tests, all data were reviewed manually and flagged to identify questionable data, which may result from biofouling, interference from bubbles, sensor drift, or other malfunctions. Major data and sensor problems are highlighted by parameter and location (Appendix B.3, City of San Diego 2025a), and a detailed log of data flagged manually by parameter, site, depth, and date range is available upon request. When possible, additional QA/QC procedures included analyzing quarterly CTD casts near RTOMS sites to validate data from RTOMS sensors and using seawater bottle samples to validate and drift correct

nitrate + nitrate results from RTOMS sensors. After review, all data that were flagged as suspect or bad were excluded from further analyses and are not presented in this report.

Analyses were performed in R (R Core Team 2026) using functions within various packages (i.e., zoo, reshape2, Rmisc, mixOmics, tidyverse, scales, pracma, data.table, gtools) (Zeileis and Grothendieck 2005, Wickham 2007, Hope 2013, Rohart et al. 2017, Wickham et al. 2019, Wickham and Seidel 2020, Borchers 2021, Dowle and Srinivasan 2021, Warnes et al. 2021). Annual time series of raw and daily averaged data were plotted at each depth and site for all parameters, except for ADCP data (described subsequently). Contour plots were generated in MATLAB (2022) using default settings, which display fixed isolines, and fill areas between isolines with constant colors. Density calculations and temperature-salinity plots were created using the SEAWATER toolbox library for MATLAB, version 3.3.1 (Morgan and Pender 2014). Vertical profiles were constructed for daily averages of temperature, salinity, and density, as these parameters had the most coverage through the water column. Density and thermal gradients were calculated by differences in daily-averaged values between sensors and dividing by the depth. In addition, summary statistics were completed at each depth and site with the following seasonal periods that align with quarterly water quality sampling: winter (January–March); spring (April–June); summer (July–September); fall (October–December). Large data gaps were identified as seasons with <40% data recovery, based on expected number of samples for sensor-specific sampling intervals, and were excluded from summary analyses.

Ocean current data collected by ADCP were checked for quality by eliminating those measurements that did not meet echo intensity criteria (i.e., minimum correlation among the four beams of > 75%). Following this initial screening, tidal frequency data were removed using the PL33 filter (Alessi et al. 1984), compass direction was corrected to true north (-11.0 degrees) [NOAA/NCEI 2026], and data were hourly averaged. For all RTOMS and static ADCP deployments in 2024 and 2025, data were summarized as counts of observed velocities by season and select depth bins. Current direction and magnitude for the entire reporting period from RTOMS-based ADCP measurements were summarized as compass rose frequency distributions for select depth bins. Current data not reported previously were summarized by season and depth bin.

Data collected during 2024 were reported previously (City of San Diego 2025a), and all raw data for the 2024-2025 sampling period have been submitted to either the Regional Water Quality Control Board, the California Environmental Data Exchange Network (CEDEN) or the City's Open Data Portal (City of San Diego 2026b) and may be accessed upon request.

Results and Discussion

Oceanographic Conditions in 2024-2025

Water Temperature

Ocean temperatures recorded during the 2024–2025 quarterly CTD surveys followed expected seasonal patterns throughout the PLOO and SBOO regions, ranging from a minimum of 10.6 to a maximum of 15.3°C in winter, 9.8 to 17.9°C in spring, 10.5 to 23.6°C in summer, and 10.0 to 15.9°C in fall (Figures 2.2–2.5, City of San Diego 2025a). Regardless of the year or season, water temperature decreased throughout the water column with increasing depth. Surface waters during the summer were typically the warmest, and deeper waters during the spring were the coldest. Over the past two years, maximum water

temperatures were recorded in surface waters of both regions during summer 2024 (PLOO: 23.6°C; SBOO: 21.7°C) (City of San Diego 2025a). Conversely, the coldest water temperatures were recorded in the deepest waters of both regions (PLOO: 81–98 m stations; SBOO: 39–55 m stations) during spring 2024 (PLOO: 9.8°C), SBOO: 10.2°C) (City of San Diego 2025a).

Ocean temperatures observed by RTOMS and thermistor arrays showed similar seasonal patterns and comparable ranges to quarterly CTD surveys. Temperatures recorded during 2024–2025 from moorings near the PLOO and SBOO ranged from a minimum of 9.8 to a maximum of 17.6°C in winter, 9.5 to 22.8°C in spring, 9.8 to 24.5°C in summer, and 9.8 to 20.7°C in fall (Figures 2.6–2.7, Appendices B.8–B.12; City of San Diego 2025a). The warmest seasonal mean water temperatures were recorded at the surface in both regions during summer 2025 (PLOO: 24.7°C; SBOO: 21.2°C) (Appendices B.10–B.11). Conversely, the coldest seasonal mean water temperatures were recorded in the deepest locations for PLOO (89 m) during spring 2025 (9.9°C), with minimums occurring in mid April (9.5°C). Overall, cooler temperatures (< 9.8°C) occurred during the winter and spring of both years at deep depths (>45 m), and warmer temperatures (>22°C) occurred near the surface in the summer of both years. As a result of higher frequency sampling, maximum surface summer temperatures from moorings were up to 0.9°C higher than observations from any sites during quarterly surveys.

Salinity

Salinities recorded during the 2024–2025 quarterly surveys also followed expected seasonal patterns throughout the PLOO and SBOO regions, ranging from a minimum of 32.29 to a maximum of 34.12 ppt in winter, 33.27 to 34.10 ppt in spring, 33.07 to 33.83 ppt in summer, and 33.10 to 33.88 ppt in fall (Figures 2.2–2.5, City of San Diego 2025a). Within the PLOO region, the highest salinity values (>34.0 ppt) were typically recorded at bottom depths (80 and 98-m stations) during spring 2024 and winter 2025. Similarly, high salinities in the SBOO region (>33.8 ppt) were recorded at bottom depths (55-m stations) during spring and winter 2025. High salinity values, associated with deep waters during the spring in both the PLOO and SBOO regions, corresponded with the coldest temperatures, as described previously. Taken together, these results support the observation that local coastal upwelling appears to be strongest during the spring months and, to a lesser extent, winter months (Jackson 1986).

Low salinity values in the PLOO (<33.5 ppt) and SBOO (<33.3 ppt) regions were limited to mostly surface waters in winter and fall in the PLOO region (Figures 2.2–2.5). Given the proximity of these SBOO locations to the mouth of the Tijuana River, the occurrence of the low salinity events may be correlated with winter rain events and the resultant influx of freshwater input into local receiving waters (Hess 2019, NOAA/NWS 2024).

Salinities observed from moorings near the PLOO and SBOO ranged from a minimum of 31.92 to a maximum of 34.02 PSU (Practical Salinity Unit) in winter, 32.67 to 34.16 PSU in spring, 32.60 to 33.90 PSU in summer, and 32.83 to 33.80 PSU during fall (Figures 2.8–2.9, Appendices B.10–B.12; City of San Diego 2025a). As described in Materials and Methods, salinity data from PLOO mooring is not available in winter 2025. High seasonal mean salinities (>33.6 PSU) generally occurred at depth at both sites (PLOO: >30 m; SBOO: >18 m) and peaked during spring 2024 and 2025 when upwelling conditions were strongest. The highest maximum salinities during this period occurred across all depths (surface: 33.8; bottom: 34.2 PSU) at both sites in April 2025, likely due to an upwelling event on the San Diego shelf that mixed throughout the water column (Figures 2.8–2.9, Appendices B.10–B.12).

Density and Ocean Stratification

Seasonal changes in thermal stratification over the past two years were mirrored by density stratification of the water column during each survey (Figures 2.2–2.5). These results align with regional studies showing that density in shallow coastal waters of southern California, and elsewhere, is primarily influenced by temperature differences, since salinity is relatively uniform (Bowden 1975, Jackson 1986, Pickard and Emery 1990). Additionally, maximum buoyancy frequency for both regions ranged from a minimum of 6.74 to a maximum of 7.84 cycles/min during the winter, 10.84 to 12.82 cycles/min during the spring, 11.72 to 15.98 cycles/min during the summer, and 8.47 to 9.74 cycles/min during the fall (Figure 2.10, Appendix B.13). As expected, the depth of the pycnocline also varied by season. Shallower pycnocline depths (≤11 m) occurred in spring and summer, which typically corresponded to greater stratification.

Dissolved Oxygen and pH

Levels of DO and pH in the coastal waters off San Diego generally followed expected patterns in 2024 and 2025 that corresponded to seasonal fluctuations in water mass inputs. Additionally, changes in DO and pH tended to be closely linked, since both parameters reflect fluctuations in dissolved carbon dioxide, an indicator of biological activity in coastal waters (Skirrow 1975). Concentrations of DO across the PLOO and SBOO regions ranged from a minimum of 2.0 to a maximum of 10.0 mg/L in winter, 2.1 to 14.3 mg/L in spring, 3.5 to 14.6 mg/L in summer, and 3.6 to 11.2 mg/L in fall. The recorded pH ranged from a minimum of 7.6 to a maximum of 8.3 in winter, 7.6 to 8.5 in spring, 7.7 to 8.4 in summer, and 7.7 to 8.4 in fall (Figures 2.2–2.5, Appendices B.14–B.17, City of San Diego 2025a).

Maximum DO and pH were recorded in surface waters of PLOO and SBOO during spring (PLOO: 14.3 mg/L and pH 8.4) and the surface waters of SBOO during spring (SBOO: 14.6 mg/L and pH 8.5) (Figures 2.2–2.5, Appendices B.14–B.17; City of San Diego 2025a). Conversely, minimum DO and pH were recorded in the bottom depths of nearshore stations (9 and 18-m stations) of both regions during winter and spring 2025 (PLOO: 2.0 mg/L and pH 7.6; SBOO: 3.0 mg/L and pH 7.6) (City of San Diego 2025a), likely due to the upwelling of cold, saline, oxygen-poor water moving inshore like the pattern described previously for temperature and salinity.

Changes in DO and pH at the PLOO and SBOO RTOMS were also generally aligned and showed similar seasonal patterns to quarterly CTD surveys. Concentrations of DO ranged from a minimum of 2.3 to a maximum of 11.8 mg/L in winter, 1.3 to 14.6 mg/L in spring, 1.4 to 17.6 mg/L in summer, and from 2.3 to 16.0 mg/L in fall (Appendices B.10–B.12, City of San Diego 2025a). Similarly, pH_T (total scale) recorded ranged from a minimum of 7.65 to a maximum of 8.23 in winter, 7.52 to 8.43 in spring, 7.56 to 8.28 in summer, and 7.55 to 8.47 pH_T units in fall (Appendices B.10–B.12, City of San Diego 2025a). As described in Materials and Methods, DO and pH_T data from the PLOO mooring are not available in winter 2025, and generally RTOMS sensors report slightly lower pH values compared to quarterly CTD surveys due to difference in pH units (total scale and NBS units, respectively).

High seasonal maximum DO and pH_T levels were observed during phytoplankton blooms at the PLOO RTOMS at the surface in spring 2024 and 2025 and fall 2024, and at SBOO in fall 2024 and spring 2025 (DO >13.5 mg/L and pH_T >8.3) (Appendices B.10–B.12; City of San Diego 2025a). Conversely, the lowest DO and pH_T levels were observed at deep depths in spring 2025 (DO <1.7 mg/L and pH_T <7.53) (Appendices B.10–B.12; City of San Diego 2025a). At the PLOO, the lowest DO values (< 3 mg/L) at mid depths were closely associated with the coldest and highest salinity water masses in the spring

(Figure 2.11). Similarly, low DO values at the bottom depth at the SBOO were generally recorded in coldest, saline waters, in both winter and spring (Figure 2.12). These observations further support the role of upwelling in the spring as a significant driver of local conditions.

Dissolved CO_2

Surface seawater carbon dioxide levels (xCO_2) recorded from the RTOMS generally aligned with surface DO and pH_T levels. Concentrations of xCO_2 at the PLOO region ranged from a minimum of 142 to a maximum of 519 ppm in spring 2024 and spring 2025, respectively (City of San Diego 2025a). Concentrations of xCO_2 at SBOO ranged from a minimum of 168 to a maximum of 795 ppm in the spring of 2025 for both values (Appendices B.10–B.12; City of San Diego 2025a). The largest variability in both regions was generally observed in the spring, along with lowest seasonal mean levels (PLOO: 331 ppm; SBOO: 337 ppm). Generally, biological productivity and surface water temperatures drive large seasonal amplitudes in xCO_2 (Sutton et al. 2019). The relatively large short-term variability (> 100 ppm change between days) observed during the spring and summer at both regions was due to this biological productivity, as concentrations of xCO_2 followed trends in DO due to phytoplankton blooms (and subsequent respiration and remineralization of organic matter). In addition, upwelling brings cold and saline waters enriched in carbon dioxide, and an upwelling event in April 2025 was observed to reach surface waters with peak xCO_2 values (Appendix B.12). In contrast, winter generally shows more stable daily values (Appendix B.12) with similar seasonal variability and ranges to the closest near-coastal SIO carbon mooring (California Current Ecosystem mooring 2, NOAA/PMEL 2024).

Transmissivity

Although water clarity (transmissivity) ranged widely, from a minimum of 1 to a maximum of 100% (Appendices B.14–B.17). During winter and spring, low transmissivity (<75%) was most often observed at shallow monitoring stations in the SBOO region, located close to shore, where the influence of waves, currents, and land-based turbidity plumes was most acute. Low transmissivity during spring/winter surveys in both regions appeared to be associated with high concentrations of chlorophyll *a*, possibly indicative of dense accumulations of phytoplankton cells (see next section), most obvious during spring and winter. Finally, low transmissivity values were also occasionally observed in the midwater (~25 m) at stations located along deeper depth contours (<60 m) in the PLOO region during summer 2024 and spring 2025, indicating a possible resuspension of soft sediments caused by the CTD approaching or hitting the seafloor. These low transmissivity values coincided with relatively high chlorophyll *a* concentration at the same midwater contour.

***Chlorophyll* a**

Concentrations of chlorophyll *a* ranged from a minimum of 0.1 to a maximum of 49.0 µg/L across the PLOO and SBOO regions in 2024 and 2025 (Appendices B.14–B.17; City of San Diego 2025a). Elevated chlorophyll concentrations (>5 µg/L) were recorded at depths from the surface to 40 m along all depth contours in the PLOO region during spring 2025, and to depths associated with (or just below) the mixed layer. Prolonged elevated concentrations (>40 µg/L) were observed in the PLOO and SBOO region during summer 2024 and spring 2025 and the maximum concentrations temporarily observed (49 µg/L) were in the SBOO region in spring 2025 (Figure 2.13; City of San Diego 2025a, Ocean Imaging 2025). Elevated concentrations were also recorded at depths from 25 to 60 m along deeper depth contours (<60 m) in the PLOO region during summer 2024 and spring 2025. Elevated chlorophyll *a* concentrations at these depths reflect the tendency for phytoplankton to accumulate along natural barriers such as isopycnals near the thermocline, where deeper water nutrients are available, and light is not yet limiting (Lalli and Parsons 1993).

Chlorophyll *a* observed at the PLOO and SBOO moorings ranged from a minimum of <0.1 to a maximum of >30 µg/L, with higher values generally occurring from March through September (Appendices B.10–B.12; City of San Diego 2025a). Multiple sensor failures or fouling events occurred at both moorings, resulting in some data gaps during these periods (Appendix B.3; City of San Diego 2025a). Generally, the highest chlorophyll *a* concentration occurred at midwater depth at SBOO (18 m) in March and August 2024 and in April and May 2025 (>15 µg/L) (Appendix B.12). These elevated concentrations coincided with relatively high DO and pH_T levels at the surface, particularly in spring 2025, and were indicative of phytoplankton blooms.

Nitrate (plus Nitrite)

Nitrate + nitrite concentrations observed at the RTOMS from 2024 through 2025 at the PLOO ranged from <0.01 to 29.4 µM, and from <0.01 to 21.8 µM at the SBOO (Appendices C.10–C.12, City of San Diego 2025a). . The lowest seasonal mean levels were observed at SBOO during the summer of 2024 and summer/fall of 2025 near the surface (<1 µM), and at PLOO during the summer/fall of 2025 at mid-depth (<10 µM) likely due to uptake from phytoplankton. Generally, nitrate + nitrite concentrations increased with increasing depth and higher salinities, with the highest seasonal mean occurring in the spring of 2025 at PLOO (26 µM at 89 m) (Appendix B.10). These observations generally showed similar ranges to that of historical data (1969–2023) from nearby regional stations reported by the California Cooperative Oceanic Fisheries Investigations (CalCOFI) surveys, where the lowest nitrate levels occurred near the surface (< 10 m: < 0.1–11.2 µM) and higher levels occurred at depth, associated with higher salinities (70–130 m: < 0.1–33.4 µM) (CalCOFI 2024, Weber et al. 2021).

Direction and Velocity of Subsurface Currents

Ocean currents surrounding the PLOO and SBOO varied by depth and season during the 2024–2025 reporting period. Seasonal mean current velocities (1-m depth bin for RTOMS deployments) at the PLOO ranged from a minimum of 20 to a maximum of 175 mm/s during winter, 23 to 291 mm/s during spring, 36 to 136 mm/s during summer, and 20 to 140 mm/s during fall (Appendix B.18). Seasonal mean current velocities (by 1-m depth bin for RTOMS deployments) at the SBOO ranged from a minimum of 63 to a maximum of 108 mm/s during winter, 46 to 110 mm/s during spring, 44 to 130 mm/s during summer, and 51 to 105 mm/s in the fall (Appendix B.19; City of San Diego 2025a). The highest seasonal mean current velocities typically occurred in near-surface waters during the winter at the PLOO and the spring in the SBOO region. Generally, for all seasons, the highest mean current velocities occurred in the upper 20 m at the PLOO and the upper 10 m at the SBOO. Below these thresholds, velocities decreased with depth around both outfalls, with the lowest mean velocities roughly 15 m from the bottom at the PLOO and 5 m from the bottom at the SBOO.

Historically, currents predominantly flow along a north-northwest/south-southeast axis, regardless of season or outfall location, however during this reporting period currents around the PLOO exhibited a higher variability and a stronger northeastern-southwestern flow at several depths and seasons while currents around the SBOO had stronger than normal north-south oriented flows (Figures 2.14, 2.15). Much of the variability observed from the PLOO RTOMS was due to currents during 2024 directed north-south more frequently than in 2025 (City of San Diego 2025a). Surface currents for the reporting period at both locations were most frequently observed heading strongly south while mid-depth and bottom currents were more evenly distributed along their directional axes (Figure 2.16). These results are generally consistent with observations from the nearby bottom-mounted static ADCPs at both locations (Appendices C.20–C.23).

Historical Assessment of Oceanographic Conditions

A review of temperature, salinity, and DO anomalies from all discharge depth stations sampled from 1991 through 2025 demonstrates how the PLOO and SBOO regions have responded to long-term climate-related changes in the SCB (Figure 2.17). Overall, these results are consistent with largescale temporal patterns in the California Current System (CCS) associated with ENSO, PDO and NPGO events (Peterson et al. 2006, McClatchie et al. 2008, 2009, Bjorkstedt et al. 2010, 2011, 2012, Wells et al. 2013, Leising et al. 2014, 2015, Thompson et al. 2018, 2019, Harvey et al. 2021, Weber et al. 2021, NOAA/ NWS 2024). Several major events in the CCS have affected SCB coastal waters since 1997 (Table 2.2), notably transition periods between La Niña and El Niño conditions.

Temperature and salinity data for the entire San Diego region were overall consistent with the CCS events in Table 2.2, but there have been some notable deviations from these trends, where coastal waters may lag in response to transitions between El Niño/ La Niña conditions and temporarily differ from offshore, open ocean trends. For example, since the onset of marine heatwaves in 2012, the mean SST anomaly across the North Pacific Ocean has been steadily increasing, reaching a record high in 2022 (Thompson et al. 2024). However, surface temperature SBOO and PLOO regions were roughly 0.5 to 1.0°C below average in 2022 and early 2023, likely due to regional effects of a negative PDO and an ongoing La Niña trend, which acted to increase upwelling and decrease coastal California ocean temperatures (Harvey et al. 2023).

The overall heating of eastern Pacific Ocean temperatures has been evident in the SBOO and PLOO region since roughly 2013-14 (Figure 2.17), with a marine heatwave event recorded in the North Pacific Ocean every year since. Ocean temperatures were notably warmer than the long-term average during the majority of 2016 which corresponded to El Niño conditions that lasted until spring 2016 before switching to a La Niña that lasted from late 2016 through winter 2017. Deviations from the long-term average were minor, reflecting the ENSO neutral conditions that endured for most of 2017 (NOAA/NWS 2024). Ocean temperatures observed throughout the water column were warmer than the historical average during most of 2018, as confirmed by both CTD surveys and RTOMS (City of San Diego 2024a), and closer to average conditions during 2019 for the PLOO region.

In contrast, the CCS north of Monterey Bay showed surface water temperatures far above average in summer and fall 2019, consistent with a regionwide marine heat wave, as well as positive PDO and negative NPGO phases. With the switch to negative PDO in 2020, overall ocean temperatures were roughly average, with surface temperatures above average in 2020. Despite the negative PDO, the 2020 heatwave affected the Southern California Bight region similarly to 2014, with surface temperatures above average in 2020 (Weber et al. 2021). Surface temperatures were 0.5 to 3.0°C above normal in 2020, except for fall in the PLOO region. 2021 was more typical, apart from a cooler than normal summer in the SBOO region. Above average salinity observed during 2018 through 2021 was consistent with conditions all along the west coast, shifting from relatively low salinities during the warm period of 2014–2016. These anomalous conditions were remotely observed moving towards the SCB prior to 2018, suggesting a shifting balance of water mass source waters being responsible for these temperature and salinity anomalies, which have remained through 2021 (Thompson et al. 2018, 2019, Harvey et al. 2021, Weber et al. 2021).

From 2019 to 2022, Pacific climate indices were generally negative (PDO, NPGO) indicating three consecutive years of La Niña conditions (Thompson et al. 2024). During La Niña events, upwelling tends

to be prevalent region wide and introduces deeper cold and saline water masses to coastal surface waters (Bond et al. 2008). This was evident by the negative temperature and positive salinity anomalies in both the SBOO and PLOO region from 2019 to 2022. La Niña conditions persisted into early 2023 when the PDO stopped decreasing and the NPGO began to trend positively, indicating the transition to an incoming El Niño phase by the fall of 2023 (Harvey et al. 2023). This transition weakened coastal upwelling along California and allowed the penetration of warmer, less saline offshore waters starting in late summer and fall of 2023 relative to 2022 (Figure 2.18), consistent with the same El Niño trends observed in the SCB region in 2016. Subsurface temperatures were average in 2023 along much of the California coastline, indicating that the 2023 heatwave did not penetrate relatively deep into the water column and effect DO trends along the coastline (e.g., Harmful Algal Bloom [HAB] events; Leising et al. 2024)

In the beginning of 2024, the California Current experienced a strong El Niño which caused widespread warmer than normal coastal ocean temperatures during early spring of 2024 (Leising et al. 2025). This led to a transition back into La Niña or neutral conditions in 2025. These trends are reflected in the positive to negative shift in temperature anomalies for 2024 to 2025, respectively (Figure 2.17). By the end of 2025, temperature began to shift to above average (positive anomaly) reflecting a transition back into El Niño forecasted 2026.

Historical trends in local DO concentrations reflect several periods during which lower than normal DO has corresponded with low water temperatures and high salinity (Figure 2.17). The alignment of these anomalies is generally consistent with cold, saline, less oxygenated ocean waters, which coincided with relatively high salinities (e.g., 2002, 2005–2012, 2019–2021). The overall decrease observed in DO in the PLOO and SBOO regions through 2012 was also observed throughout the entire CCS and deep North Pacific and was thought to be linked to changing ocean climate and increased occurrence of El Niño events (Bjorkstedt et al. 2012). However, no significant long-term trend has been shown over the last 70 years in the North Pacific shelf depths (Schmidtko et al. 2017). These large negative anomalies have been absent since mid-2013 in the PLOO and SBOO regions but were present for some of 2024 and 2025 in both the PLOO and SBOO region.

Summary

Oceanographic conditions in the PLOO and SBOO regions during 2024 and 2025 generally followed typical seasonal patterns for the coastal waters off San Diego. Maximum water column stratification occurred during spring and summer months, whereas waters were well mixed or weakly stratified in the winter. Ocean conditions indicative of local coastal upwelling, such as relatively cold, dense waters with low DO and high salinity at subsurface depths, were most evident during the spring and winter months of both years (Figure 2.13). These upwelling signatures were corroborated by decreased pH and DO at the surface in both the SBOO and PLOO region, particularly in December 2024 and April 2025 (Figure 2.18). This local upwelling was driven by a combination of localized processes (seasonal, wind-driven upwelling) and large-scale oceanographic trends in the Pacific Ocean (La Niña conditions that persisted from throughout 2024).

Results are similar to findings reported previously for the San Diego region (City of San Diego 2015a,b, 2016a,b, 2018b, 2020, 2022a,b, 2023a, 2024a,b, 2025a,b) and are generally consistent with conditions and long-term trends in the SCB (Peterson et al. 2006, McClatchie et al. 2008, 2009, Bjorkstedt et al. 2010, 2011, 2012, Wells et al. 2013, Leising et al. 2014, 2015, NOAA/NWS 2024), and northern Baja

California waters (Peterson et al. 2006). The origins of the more northeasterly-southwesterly current flows during 2025 around the PLOO are difficult to ascertain. Swell direction for both 2024 and 2025 was predominantly from the west (CDIP 2026) while local wind forcing was also similar across years (SCCOOS 2026). It's possible that changes to remote forcing driving this difference are due to the persistence of large-scale marine heatwaves but further data are needed (NOAA/IEA 2026).

In addition to oceanographic processes, policy changes also introduced potential impacts to water quality in the SBOO region. During the reporting period, the International Boundary and Water Commission (IBWC) proposed to increase flows to the SBOO by 10 MGD starting August 24th 2025. Subsequently, approximately 5MGD of additional flows, comprising of effluent treated to advanced primary standards, were added to SBIWTP discharge in September–November of 2025 to relieve pumping constraints in the Tijuana system and enable diversion of sewage away from the Tijuana River. Additional flows have been scaled back since November 2025 due to storm-related interruptions and system maintenance and repair. Increased flows are expected to resume and reach up to 10MGD in 2026. This prompted heightened vigilance during water quality sampling efforts at the SBOO. To date, the impact of these increased flows appears negligible on receiving water conditions. Observations from the SBOO RTOMS of parameters such as DO, chlorophyll *a*, and nitrate across all depths did not show apparent deviations from typical conditions after August 2025, or between 2024 and 2025 for the fall period (Appendix B.12). However, given the treated sewage flows increased only recently, more data are needed over a larger timeframe to ascertain the impact. The IBWC plans to increase flows further over the coming years and continued water quality monitoring around the SBOO will be critical. The impact of these increased flows are further discussed in Chapter 4 – Plume Dispersion.

These observations suggest that overall, the temporal and spatial variability observed in oceanographic conditions for coastal San Diego for this 2024-2025 report period can be explained by a combination of local (e.g., coastal upwelling, rain-related runoff) and large-scale oceanographic-climatic processes, notably the transition from La Niña to El Niño conditions in late 2025 (i.e., shift from negative to positive PDO) which allowed for the intrusion of warm water masses from offshore heatwave events once La Niña conditions broke down (Leising et al. 2025). As a result, proximity to either outfall is not considered a significant driver of the variations observed in oceanographic parameters discussed in this chapter.

Literature Cited

Alessi, C.A., R. Beardsley, R. Limeburner, and L.K. Rosenfeld. (1984). CODE-2: Moored Array and Large-Scale Data Report. Woods Hole Oceanographic Institution Technical Report. 85–35: 21.

Bjorkstedt, E.P., R. Goericke, S. McClatchie, E. Weber, W. Watson, N. Lo, B. Peterson, B. Emmett, J. Peterson, R. Durazo, G. Gaxiola-Castro, F. Chavez, J.T. Pennington, C.A. Collins, J. Field, S. Ralston, K. Sakuma, S.J. Bograd, F.B. Schwing, Y. Xue, W.J. Sydeman, S.A. Thompson, J.A. Santora, J. Largier, C. Halle, S. Morgan, S.Y. Kim, K.B.P. Merkins, J.A. Hildebrand, and L.M. Munger. (2010). State of the California Current 2009–2010: Regional variation persists through transition from La Niña to El Niño (and back?). California Cooperative Oceanic Fisheries Investigations (CalCOFI) Reports, 51: 39–69.

Bjorkstedt, E.P., R. Goericke, S. McClatchie, E. Weber, W. Watson, N. Lo, B. Peterson, B. Emmett, R. Brodeur, J. Peterson, M. Litz, J. Gómez-Valdés, G. Gaxiola-Castro, B. Lavaniegos, F. Chavez, C.A.

Collins, J. Field, K. Sakuma, S.J. Bograd, F.B. Schwing, P. Warzybok, R. Bradley, J. Jahncke, G.S. Campbell, J.A. Hildebrand, W.J. Sydeman, S.A. Thompson, J.L. Largier, C. Halle, S.Y. Kim, and J. Abell. (2011). State of the California Current 2010–2011: Regionally variable responses to a strong (but fleeting?) La Niña. California Cooperative Oceanic Fisheries Investigations (CalCOFI) Reports, 52: 36–68.

Bjorkstedt, E.P., R. Goericke, S. McClatchie, E. Weber, W. Watson, N. Lo, W.T. Peterson, R.D. Brodeur, T. Auth, J. Fisher, C. Morgan, J. Peterson, J. Largier, S.J. Bograd, R. Durazo, G. Gaxiola-Castro, B. Lavaniegos, F.P. Chavez, C.A. Collins, B. Hannah, J. Field, K. Sakuma, W. Satterthwaite, M. O'Farrell, S. Hayes, J. Harding, W.J. Sydeman, S.A. Thompson, P. Warzybok, R. Bradley, J. Jahncke, R.T. Golightly, S.R. Schneider, R.M. Suryan, A.J. Gladics, C.A. Horton, S.Y. Kim, S.R. Melin, R.L. DeLong, and J. Abell. (2012). State of the California Current 2011–2012: Ecosystems respond to local forcing as La Niña wavers and wanes. California Cooperative Oceanic Fisheries Investigations (CalCOFI) Reports, 53: 41–76.

Bond, N. A., Batchelder, H. P., & Bograd, S. J. (2008). Forecasting northeastern Pacific ecosystem responses to La Nina. Eos, Transactions American Geophysical Union, 89(35), 321-322.

Borchers, H.W. (2021). pracma: Practical Numerical Math Functions. R package version 2.3.6. https://CRAN.R-project.org/package=pracma.

Bowden, K.F. (1975). Oceanic and Estuarine Mixing Processes. In: J.P. Riley and G. Skirrow (eds.). Chemical Oceanography, 2nd Ed., Vol.1. Academic Press, San Francisco, CA. p 1–41.

[CalCOFI] California Cooperative Oceanic Fisheries Investigations (2024). Archive of nutrient bottle data, January 1969–January 2023. https://calcofi.org/data/oceanographic-data/bottle-database/.

[CDIP] Coastal Data Information Program (2026). Summary of buoy 191 – Point Loma South, CA. https://cdip.ucsd.edu/m/products/?stn=191p1.

City of San Diego. (2015a). Point Loma Ocean Outfall Annual Receiving Waters Monitoring and Assessment Report, 2014. City of San Diego Ocean Monitoring Program, Public Utilities Department, Environmental Monitoring and Technical Services Division, San Diego, CA.

City of San Diego. (2015b). South Bay Ocean Outfall Annual Receiving Waters Monitoring and Assessment Report, 2014. City of San Diego Ocean Monitoring Program, Public Utilities Department, Environmental Monitoring and Technical Services Division, San Diego, CA.

City of San Diego. (2016a). Point Loma Ocean Outfall Annual Receiving Waters Monitoring and Assessment Report, 2015. City of San Diego Ocean Monitoring Program, Public Utilities Department, Environmental Monitoring and Technical Services Division, San Diego, CA.

City of San Diego. (2016b). South Bay Ocean Outfall Annual Receiving Waters Monitoring and Assessment Report, 2015. City of San Diego Ocean Monitoring Program, Public Utilities Department, Environmental Monitoring and Technical Services Division, San Diego, CA.

City of San Diego. (2018a). Plume Tracking Monitoring Plan for the Point Loma and South Bay Ocean Outfall Regions, San Diego, California. Submitted by the City of San Diego Public Utilities Department to the San Diego Water Board and USEPA, Region IX, March 28, 2018 (approved 4/25/2018).

City of San Diego. (2018b). Biennial Receiving Waters Monitoring and Assessment Report for the Point Loma and South Bay Ocean Outfalls, 2016–2017. City of San Diego Ocean Monitoring Program, Public Utilities Department, Environmental Monitoring and Technical Services Division, San Diego, CA.

City of San Diego. (2020). Biennial Receiving Waters Monitoring and Assessment Report for the Point Loma and South Bay Ocean Outfalls, 2018–2019. City of San Diego Ocean Monitoring Program, Public Utilities Department, Environmental Monitoring and Technical Services Division, San Diego, CA.

City of San Diego. (2022a). Biennial Receiving Waters Monitoring and Assessment Report for the Point Loma and South Bay Ocean Outfalls, 2020–2021. City of San Diego Ocean Monitoring Program, Public Utilities Department, Environmental Monitoring and Technical Services Division, San Diego, CA.

City of San Diego. (2022b). Appendix P. Oceanography. In: Application for Renewal of NPDES CA0107409 and 301(h) Modified Secondary Treatment Requirements, Point Loma Ocean Outfall. Volume X, Appendices O thru U. Public Utilities Department, Environmental Monitoring and Technical Services Division, San Diego, CA.

City of San Diego. (2023a). Interim Receiving Waters Monitoring Report for the Point Loma and South Bay Ocean Outfalls, 2022. City of San Diego Ocean Monitoring Program, Public Utilities Department, Environmental Monitoring and Technical Services Division, San Diego, CA.

City of San Diego. (2024a). Biennial Receiving Waters Monitoring and Assessment Report for the Point Loma and South Bay Ocean Outfalls, 2022–2023. City of San Diego Ocean Monitoring Program, Public Utilities Department, Environmental Monitoring and Technical Services Division, San Diego, CA.

City of San Diego. (2025a). Interim Receiving Waters Monitoring Report for the Point Loma and South Bay Ocean Outfalls, 2024. City of San Diego Ocean Monitoring Program, Public Utilities Department, Environmental Monitoring and Technical Services Division, San Diego, CA.

City of San Diego. (2025b). Plume Tracking Monitoring Plan Progress Report for the Point Loma and South Bay Ocean Outfall Regions, San Diego, California; Report Period: January – December 2024. Submitted by the City of San Diego Public Utilities Department to the San Diego Water Board and USEPA, Region IX, March 1, 2025.

City of San Diego. (2026a). Plume Tracking Monitoring Plan Progress Report for the Point Loma and South Bay Ocean Outfall Regions, San Diego, California; Report Period: January – December 2025. Submitted by the City of San Diego Public Utilities Department to the San Diego Water Board and USEPA, Region IX, March 1, 2026.

City of San Diego. (2026b). Ocean Monitoring Program Reports and Data. https://www.sandiego.gov/public-utilities/sustainability/ocean-monitoring/reports

Dowle, M. and A. Srinivasan. (2021). data.table: Extension of `data.frame`. R package version 1.14.2. https://CRAN.R-project.org/package=data.table.

Harrell, F.E., Jr. (2021). Hmisc: Harrell Miscellaneous. R package version 4.6-0. http://CRAN.R-project.org/package=Hmisc.

Harvey, C.J., N. Garfield, G.D. Williams, and N. Tolimieri, editors. (2021). Ecosystem Status Report of the California Current for 2020–21: A Summary of Ecosystem Indicators Compiled by the California Current Integrated Ecosystem Assessment Team (CCIEA). U.S. Department of Commerce, NOAA Technical Memorandum NMFS-NWFSC-170.

Harvey, C.J., N. Garfield, G.D. Williams, and N. Tolimieri, editors. (2023). Ecosystem status report of the California Current for 2022-23: A summary of ecosystem indicators compiled by the California Current Integrated Ecosystem Assessment Team (CCIEA). U.S. Department of Commerce, National Oceanic and Atmospheric Administration, National Marine Fisheries Service, Northwest Fisheries Science Center.

Hess, M. (2018). Satellite & Aerial Coastal Water Quality Monitoring in the San Diego/Tijuana Region: Annual Summary Report 1 January 2017–31 December 2018. Littleton, CO.

Hess, M. (2019). Satellite & Aerial Coastal Water Quality Monitoring in the San Diego/Tijuana Region: Annual Summary Report 1 January 2018–31 December 2019. Littleton, CO.

Hess, M. (2020). Satellite & Aerial Coastal Water Quality Monitoring in the San Diego/Tijuana Region: Annual Summary Report 1 January 2019–31 June 2019. Littleton, CO.

Hope, R.M. (2013). Rmisc: Ryan Miscellaneous. R package version 1.5. http://CRAN.R-project.org/package=Rmisc.

Jackson, G.A. (1986). Physical Oceanography of the Southern California Bight. In: R. Eppley (ed.). Plankton Dynamics of the Southern California Bight. Springer Verlag, New York. p 13–52.

Kelley, D. and C. Richards. (2022). oce: Analysis of Oceanographic Data. R package version 1.5.0. http://CRAN.R-project.org/package=oce.

Lalli, C.M. and T.R. Parsons. (1993). Biological Oceanography: an introduction. Pergamon, New York.

Largier, J., L. Rasmussen, M. Carter, and C. Scearce. (2004). Consent Decree – Phase One Study Final Report. Evaluation of the South Bay International Wastewater Treatment Plant Receiving Water Quality Monitoring Program to Determine Its Ability to Identify Source(s) of Recorded Bacterial Exceedances. Scripps Institution of Oceanography, University of California, San Diego, CA.

Leising, A.W., I.D. Schroeder, S.J. Bograd, E.P. Bjorkstedt, J. Field, K. Sakuma, J. Abell, R.R. Robertson, J. Tyburczy, W.T. Peterson, R. Brodeur, C. Barcelo, T.D. Auth, E.A. Daly, G.S. Campbell,

J.A. Hildebrand, R.M. Suryan, A.J. Gladics, C.A. Horton, M. Kahru, M. Manzano-Sarabia, S. McClatchie, E.D. Weber, W. Watson, J.A. Santora, W.J. Sydeman, S.R. Melin, R.L. DeLong, J. Largier, S.Y. Kim, F.P. Chavez, R.T. Golightly, S.R. Schneider, P. Warzybok, R. Bradley, J. Jahncke, J. Fisher, and J. Peterson. (2014). State of the California Current 2013-2014: El Niño Looming. California Cooperative Oceanic Fisheries Investigations (CalCOFI) Reports, 55: 51–87.

Leising, A.W., I.D. Schroeder, S.J. Bograd, J. Abell, R. Durazo, G. Gaxiola-Castro, E.P. Bjorkstedt, J. Field, K. Sakuma, R.R. Robertson, R. Goericke, W.T. Peterson, R.D. Brodeur, C. Barceló, T.D. Auth, E.A. Daly, R.M. Suryan, A.J. Gladics, J.M. Porquez, S. McClatchie, E.D. Weber, W. Watson, J.A. Santora, W.J. Sydeman, S.R. Melin, F.P. Chavez, R.T. Golightly, S.R. Schneider, J. Fisher, C. Morgan, R. Bradley, and P. Warybok. (2015). State of the California Current 2014-2015: Impacts of the Warm-Water "Blob". California Cooperative Oceanic Fisheries Investigations (CalCOFI) Reports, 56: 31–69.

Leising, A.W., M. Hunsicker, G.D. Williams, and N. Tolimieri, editors. (2024) State of the California Current 2023-24. A report of the NOAA California Current Integrated Ecosystem Assessment Team (CCIEA) to the Pacific Fishery Management Council.

Leising, A.W., M. Hunsicker, G.D. Williams, and N. Tolimieri, editors. (2025) State of the California Current 2024-25. A report of the NOAA California Current Integrated Ecosystem Assessment Team (CCIEA) to the Pacific Fishery Management Council.

Lynn, R.J. and J.J. Simpson. (1987). The California Current System: The Seasonal Variability of its Physical Characteristics. Journal of Geophysical Research, 92(C12): 12947–12966.

Mann, K.H. (1982). Ecology of Coastal Waters, A Systems Approach. University of California Press, Berkeley.

Mann. K.H. and J.R.N. Lazier. (1991). Dynamics of Marine Ecosystems, Biological–Physical Interactions in the Oceans. Blackwell Scientific Publications, Boston.

Marion, G.M, F.J. Millero, M.F. Camões, P. Spitzer, R. Feistel, and C.-T.A. Chen. (2011). pH of seawater. Marine Chemistry. 126: 89–96.

MATLAB. (2022). Version R2022b. The MathWorks Inc., Natick, Massachusetts. URL https://www.mathworks.com/products/matlab.html.

McClatchie, S., R. Goericke, J.A. Koslow, F.B. Schwing, S.J. Bograd, R. Charter, W. Watson, N. Lo, K. Hill, J. Gottschalck, M. l'Heureux, Y. Xue, W.T. Peterson, R. Emmett, C. Collins, G. Gaxiola-Castro, R. Durazo, M. Kahru, B.G. Mitchell, K.D. Hyrenbach, W.J. Sydeman, R.W. Bradley, P. Warzybok, and E. Bjorkstedt. (2008). The state of the California Current, 2007–2008: La Niña conditions and their effects on the ecosystem. California Cooperative Oceanic Fisheries Investigations (CalCOFI) Reports, 49: 39–76.

McClatchie, S., R. Goericke, J.A. Koslow, F.B. Schwing, S.J. Bograd, R. Charter, W. Watson, N. Lo, K. Hill, J. Gottschalck, M. l'Heureux, Y. Xue, W.T. Peterson, R. Emmett, C. Collins, J. Gomez-Valdes, B.E. Lavaniegos, G. Gaxiola-Castro, B.G. Mitchell, M. Manzano-Sarabia, E. Bjorkstedt. S.

Ralston, J. Field, L. Rogers-Bennet, L. Munger, G. Campbell, K. Merkens, D. Camacho, A. Havron, A. Douglas, and J. Hildebrand. (2009). The state of the California Current, Spring 2008–2009: Cold conditions drive regional differences in coastal production. California Cooperative Oceanic Fisheries Investigations (CalCOFI) Reports, 50: 43–68.

Morgan, P. and L. Pender. (2014). SEAWATER library for calculating EOS-80 properties of seawater in MATLAB. CSIRO Marine Research, version 3.3.1. http://www.cmar.csiro.au/datacentre/ext_docs/seawater.html.

[NOAA/IEA] National Oceanic and Atmospheric Administration/Integrated Ecosystem Assessment. (2026) Blob tracker. https://www.integratedecosystemassessment.noaa.gov/regions/california-current/california-current-marine-heatwave-tracker-blobtracker.

[NOAA/NCEI] National Oceanic and Atmospheric Administration/National Center for Environmental Information. (2026). Magnetic field calculators. https://www.ngdc.noaa.gov/geomag/calculators/magcalc.shtml.

[NOAA/NWS] National Oceanic and Atmospheric Administration/National Weather Service. (2024). Climate Weather Linkage Website. http://www.cpc.ncep.noaa.gov/products/precip/CWlink/MJO/enso.shtml.

[NOAA/PMEL] National Oceanic and Atmospheric Administration/Pacific Marine Environmental Laboratory (2024). Carbon group data from California Current Ecosystem Mooring 2 (CCE2). https://www.ncei.noaa.gov/access/ocean-carbon-acidification-data-system/oceans/Moorings/CCE2.html.

Ocean Imaging. (2026). Ocean Imaging Corporation archive of aerial and satellite-derived images. http://www.oceani.com/SanDiegoWater/index.html.

Peterson, B., R. Emmett, R. Goericke, E. Venrick, A. Mantyla, S.J. Bograd, F.B. Schwing, R. Hewitt, N. Lo, W. Watson, J. Barlow, M. Lowry, S. Ralston, K.A. Forney, B.E. Lavaniegos, W.J. Sydeman, D. Hyrenbach, R.W. Bradley, P. Warzybok, F. Chavez, K. Hunter, S. Benson, M. Weise, J. Harvey, G. Gaxiola-Castro, and R. Durazo. (2006). The state of the California Current, 2005–2006: Warm in the north, cool in the south. California Cooperative Oceanic Fisheries Investigations (CalCOFI) Reports, 47: 30–74.

Pickard, D.L. and W.J. Emery. (1990). Descriptive Physical Oceanography. 5th Ed. Pergamon Press, Oxford.

R Core Team. (2026). R: A language and environment for statistical computing. R Foundation for Statistical Computing, Vienna, Austria. URL https://www.R-project.org/.

Ripley, B. and M. Lapsley. (2021). RODBC: ODBC Database Access. R package version 1.3-19. http://CRAN.R-project.org/package=RODBC.

Rogowski, P., E. Terrill, M. Otero, L. Hazard, S.Y. Kim, P.E. Parnell, and P. Dayton. (2012a). Final Report: Point Loma Ocean Outfall Plume Behavior Study. Prepared for City of San Diego Public Utilities Department by Scripps Institution of Oceanography, University of California, San Diego, CA.

Rogowski, P., E. Terrill, M. Otero, L. Hazard, and W. Middleton. (2012b). Mapping ocean outfall plumes and their mixing using Autonomous Underwater Vehicles. Journal of Geophysical Research, 117: C07016.

Rogowski, P., E. Terrill, M. Otero, L. Hazard, and W. Middleton. (2013). Ocean outfall plume characterization using an Autonomous Underwater Vehicle. Water Science & Technology, 67(4): 925–933.

Rohart F., B. Gautier, A. Singh, and K-A Le Cao. (2017) mixOmics: An R package for 'omics feature selection and multiple data integration. PLoS computational biology, 13(11):e1005752.

[SCCOOS] Southern California Coastal Ocean Observing System. (2026) High-frequency radar surface currents. https://data.caloos.org/#module-metadata/de91c282-01e2-11e2-ad19-00219bfe5670.

Schmidtko, S., L. Stramma, M. Visbeck. (2017). Decline in global oceanic oxygen content during the past five decades. Nature, 542(7641): 335-339.

Skirrow, G. (1975). Chapter 9. The Dissolved Gases–Carbon Dioxide. In: Chemical Oceanography. J.P. Riley and G. Skirrow, eds. Academic Press, London. Vol. 2. p 1–181.

Storms, W.E., T.D Stebbins, and P.E. Parnell. (2006). San Diego Moored Observation System Pilot Study Workplan for Pilot Study of Thermocline and Current Structure off Point Loma, San Diego, California. City of San Diego, Metropolitan Wastewater Department, Environmental Monitoring and Technical Services Division, and Scripps Institution of Oceanography, La Jolla, CA.

Sutton, A. J., R. A. Feely, S. Maenner-Jones, S. Musielwicz, J. Osborne, C. Dietrich, N. Monacci, J. Cross, R. Bott, A. Kozyr, A. J. Andersson, N. R. Bates, W. Cai, M. F. Cronin, E. H. De Carlo, B. Hales, S. D. Howden, C. M. Lee, D. P. Manzello, M. J. McPhaden, M. Meléndez, J. B. Mickett, J. A. Newton, S. E. Noakes, J. H. Noh, S. R. Olafsdottir, J. E. Salisbury, U. Send, T. W. Trull, D. C. Vandemark, R. A. Weller. (2019). Autonomous seawater pCO2 and pH time series from 40 surface buoys and the emergence of anthropogenic trends. Earth System Science Data, 11(1): 421–439.

Svejkovsky, J. (2010). Satellite and Aerial Coastal Water Quality Monitoring in the San Diego/Tijuana Region: Annual Summary Report for: 1 January 2009–31 December 2009. Solana Beach, CA.

Svejkovsky J. (2017). Satellite and Aerial Coastal Water Quality Monitoring in the San Diego/Tijuana Region: Annual Summary Report for: 1 January 2016–31 December 2016. Solana Beach, CA.

Terrill, E., K. Sung Yong, L. Hazard, and M. Otero. (2009). IBWC/Surfrider – Consent Decree Final Report. Coastal Observations and Monitoring in South Bay San Diego. Scripps Institution of Oceanography, University of California, San Diego, CA.

Thompson, A.R., I.D. Schroeder, S.J. Bograd, E.L. Hazen, M.G. Jacox, A. Leising, B.K. Wells, J. Largier, J. Fisher, E. Bjorkstedt, R.R. Robertson, F.P. Chavez, M. Kahru, R. Goericke, S. McClatchie, C.E. Peabody, T. Baumgartner, B.E. Lavaniegos, J. Gomez-Valdes, R.D. Brodeur, E.A. Daly, C.A. Morgan, T.D. Auth, B.J. Burke, J. Field, K. Sakuma, E.D. Weber, W. Watson, J. Coates, R.

Schoenbaum, L. Rogers-Bennett, R.M. Suryan, J. Dolliver, S. Loredo, J. Zamon, S.R. Schneider, R.T. Golightly, P. Warzybok, J. Jahncke, J.A. Santora, S. A. Thompson, W. Sydeman, and S.R. Melin. (2018). State of the California Current 2017-2018: Still Not Quite Normal in the North and Getting Interesting in the South. California Cooperative Oceanic Fisheries Investigations (CalCOFI) Reports, 59: 1-66.

Thompson, A.R., I.D. Schroeder, S.J. Bograd, E.L. Hazen, M.G. Jacox, A. Leising, B.K. Wells, J. Fisher, K. Jacobson, S. Zemen, E. Bjorkstedt, R.R. Robertson, M. Kahru, R. Goericke, C.E. Peabody, T. Baumgartner, B.E. Lavaniegos, L.E. Miranda, E. Gomez-Ocampo, J. Gomez-Valdez, T. Auth, E.A. Daly, C.A. Morgan, B.J. Burke, J.C. Field, K.M. Sakuma, E.D. Weber, W. Watson, J.M. Porquez, J. Dolliver, D. Lyons, R.A. Orben, J. Zamon, P. Warzybok, J. Jahncke, J.A. Santora, S. A. Thompson, B. Hoover, W. Sydeman, and S.R. Melin. (2019). State of the California Current 2018-2019: a Novel Anchovy Regime and a New Marine Heat Wave? California Cooperative Oceanic Fisheries Investigations (CalCOFI) Reports, 60: 1-65.

Thompson, A. R., Swalethorp, R., Alksne, M., Santora, J. A., Hazen, E. L., Leising, A., ... & Wells, B. (2024). State of the California Current Ecosystem report in 2022: a tale of two La Niñas. Frontiers in Marine Science, 11, 1294011.

[US IOOS] U.S. Integrated Ocean Observing System. (2017). Manual for the Use of Real-Time Oceanographic Data Quality Control Flags, Version 1.1. Silver Spring, MD, U.S. Department of Commerce, National Oceanic and Atmospheric Administration, National Ocean Service, Integrated Ocean Observing System, 43 pp.

[US IOOS] U.S. Integrated Ocean Observing System (2020). Quality Assurance/Quality Control of Real Time Oceanographic Data. https://ioos.noaa.gov/project/qartod/.

Warnes, G.R., B. Bolker, T. Lumley. (2021). gtools: Various R Programming Tools. R package version 3.9.2. https://CRAN.R-project.org/package=gtools.

Weber, E.D., T.D. Auth, S. Baumann-Pickering, T.R. Baumgartner, E.P. Bjorkstedt, S.J. Bograd, B.J. Burke, J.L. Cadena-Ramirez, E.A. Daly, M. de la Cruz, H. Dewar, J.C. Field, J.L. Fisher, A. Giddings, R. Goericke, E. Gomez-Ocampo, J. Gomez-Valdes, E.L. Hazen, J. Hildebrand, C.A. Horton, K.C. Jacobson, M.G. Jacox, J. Jahncke, M. Kahru, R.M. Kudela, B.E. Lavaniegos, A. Leising, S.R. Melin, L.E. Miranda-Bojorquez, C.A. Morgan, C.F. Nickels, R.A. Orben, J.M. Porquez, E.J. Portner, R.R. Robertson, D.L. Rudnick, K.M. Sakuma, J.A. Santora, I.D. Schroeder, O.E. Snodgrass, W.J. Sydeman, A.R. Thompson, S.A. Thompson, J.S. Trickey, J. Villegas-Mendoza, P. Warzybok, W. Watson, and S.M. Zeman. (2021). State of the California Current 2019-2020: Back to the Future with Marine Heatwaves? Frontiers in Marine Science, 8: 1-23.

Wells, B.K., I.D. Schroeder, J.A. Santora, E.L. Hazen, S.J. Bograd, E.P. Bjorkstedt, V.J. Loeb, S. McClatchie, E.D. Weber, W. Watson, A.R. Thompson, W.T. Peterson, R.D. Brodeur, J. Harding, J. Field, K. Sakuma, S. Hayes, N. Mantua, W.J. Sydeman, M. Losekoot, S.A. Thompson, J. Largier, S.Y. Kim, F.P. Chavez, C. Barcelo, P. Warzybok, R. Bradley, J. Jahncke, R. Goericke, G.S. Campbell, J.A. Hildebrand, S.R. Melin, R.L. DeLong, J. Gomez-Valdes, B. Lavaniegos, G. Gaxiola-Castro, R.T. Golightly, S.R. Schneider, N. Lo, R.M. Suryan, A.J. Gladics, C.A. Horton, J. Fisher, C. Morgan, J. Peterson, E.A. Daly, T.D. Auth, and J. Abell. (2013). State of the California

Current 2012-2013: no such thing as an “average” year. California Cooperative Oceanic Fisheries Investigations (CalCOFI) Reports, 54: 37–71.

Wickham, H. (2007). Reshaping Data with the reshape Package. Journal of Statistical Software, 21(12): 1–20. URL http://www.jstatsoft.org/v21/i12/.

Wickham, H., M. Averick, J. Bryan, W. Chang, L. D’Agostino McGowan, R. François, G.Grolemund, A. Hayes, L. Henry, J. Hester, M. Kuhn, T. Lin Pedersen, E. Miller, S. Milton Bache, K. Müller, J. Ooms, D. Robinson, D. P. Seidel, V. Spinu, K. Takahashi, D. Vaughan, C. Wilke, K. Woo, H. Yutani. (2019). Welcome to the tidyverse. Journal of Open Source Software, 4(43), 1686, https://doi.org/10.21105/joss.01686.

Wickham, H. and D. Seidel. (2020). scales: Scale Functions for Visualization. R package version 1.1.1. https://CRAN.R-project.org/package=scales.

Zeileis, A. and G Grothendieck. (2005). zoo: S3 Infrastructure for Regular and Irregular Time Series. Journal of Statistical Software,14(6), 1-27. https://doi.org/10.18637/jss.v014.i06.

CHAPTER 2

FIGURES & TABLES

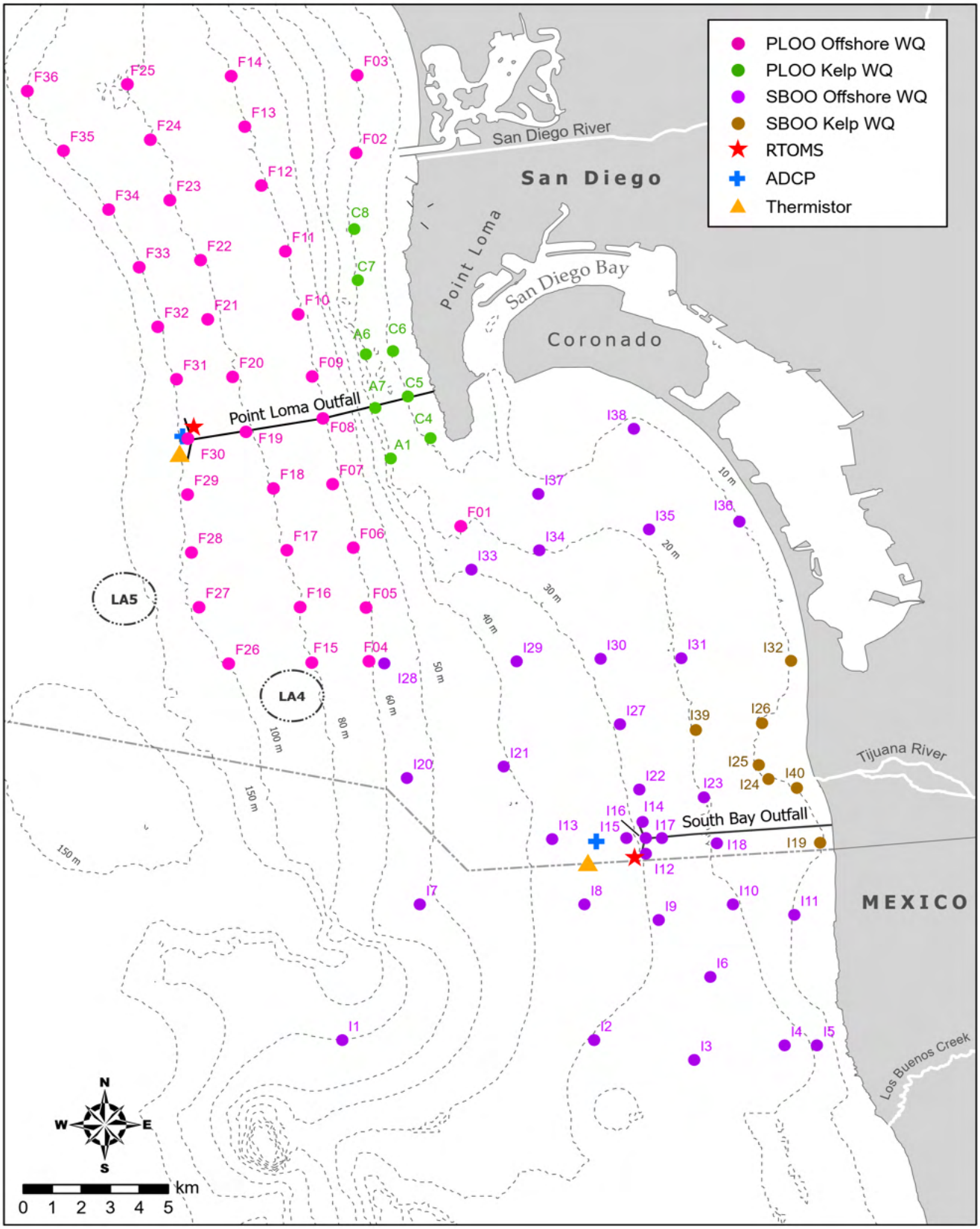


Figure 2.1
Locations of CTD water quality monitoring stations and mooring sites (RTOMS, ADCP, and thermistor arrays) sampled around the PLOO and SBOO as part of the City of San Diego's Ocean Monitoring Program.

Table 2.1

Sensor configuration and model type for RTOMS by site and depth during 2024 and 2025.

Sensor Depth		
PLOO	**SBOO**	**Parameters Measured (Sensor Types)**
1 m (surface)	1 m (surface)	Temperature, conductivity, pH_T (total scale), DO (Sea-Bird SeapHOx)
		Ocean currents (RDI 300kHz ADCP)
		Partial pressure of carbon dioxide (Pro-Oceanus pCO_2 System)
		Chlorophyll *a*, CDOM, turbidity (Sea-Bird ECO triplet)
10 m	10 m	Temperature, conductivity (Sea-Bird MicroCAT)
	18 m	Temperature, conductivity, DO (Sea-Bird MicroCAT ODO)
		Chlorophyll *a*, CDOM, turbidity (Sea-Bird ECO triplet)
20 m		Temperature, conductivity (Sea-Bird MicroCAT)
	26 m (cage)	Temperature, conductivity, pH_T, DO (Sea-Bird SeapHOx)
		Chlorophyll *a*, CDOM, turbidity (Sea-Bird ECO triplet)
		Nitrate + nitrite (Sea-Bird SUNA V2)
30 m (cage-1)		Temperature, conductivity, pH_T, DO (Sea-Bird SeapHOx)
		Chlorophyll *a*, CDOM, turbidity (Sea-Bird ECO triplet)
		Nitrate + nitrite (Sea-Bird SUNA V2)
45 m		Temperature, conductivity (Sea-Bird MicroCAT)
60 m		Temperature, conductivity (Sea-Bird MicroCAT)
75 m		Temperature, conductivity, DO (Sea-Bird MicroCAT ODO)
89 m (cage-2)		Temperature, conductivity, pH_T, DO (Sea-Bird Deep SeapHOx)
		Chlorophyll *a*, CDOM, turbidity (Sea-Bird ECO triplet)
		Nitrate + nitrite (Sea-Bird SUNA V2)

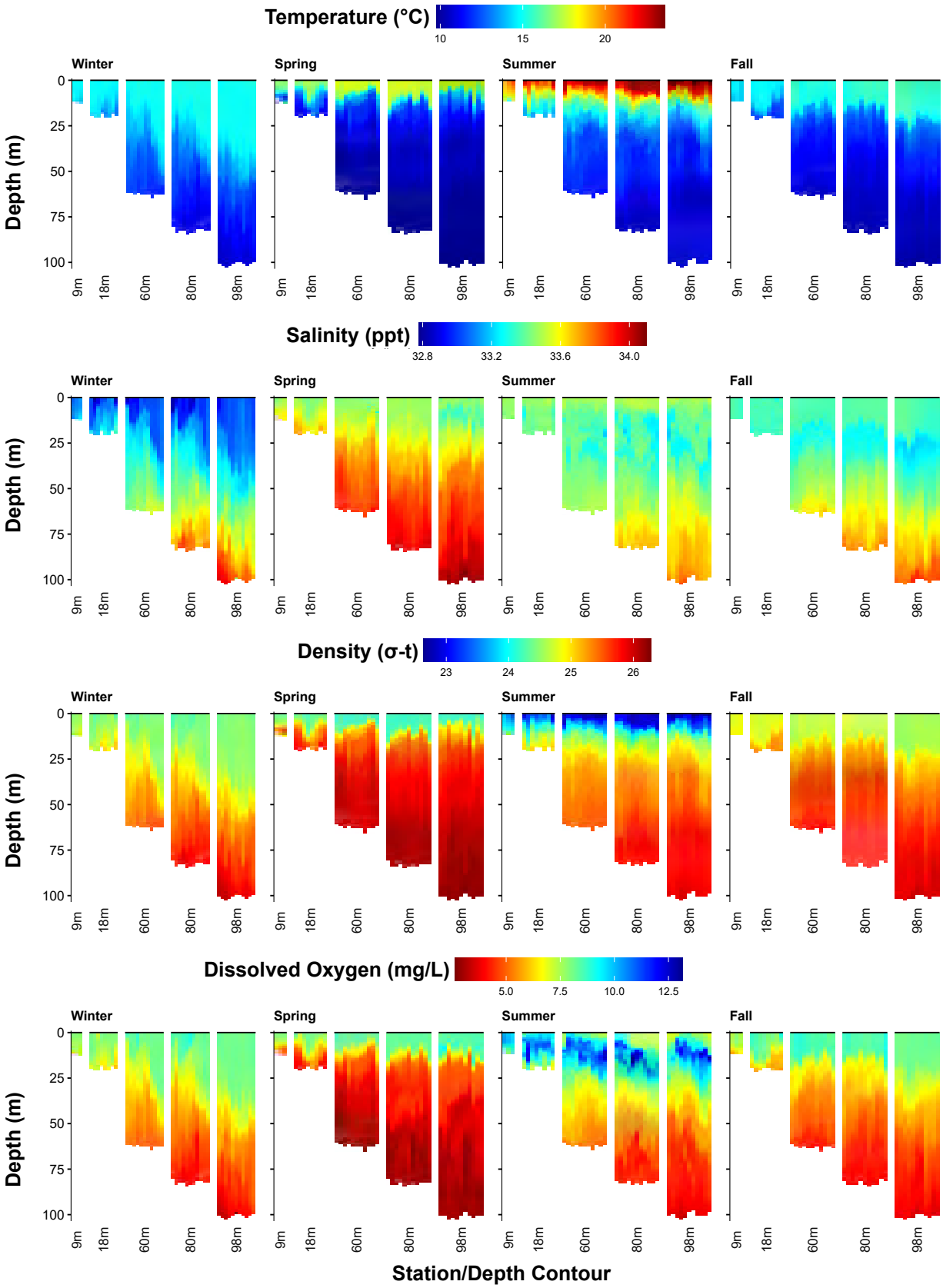


Figure 2.2

Temperature, density, salinity, and dissolved oxygen recorded in the PLOO region during 2024. Data are 1-m binned values per depth for each station and were collected over 4–5 days during each quarterly survey. Stations are depicted from north to south along each depth contour.

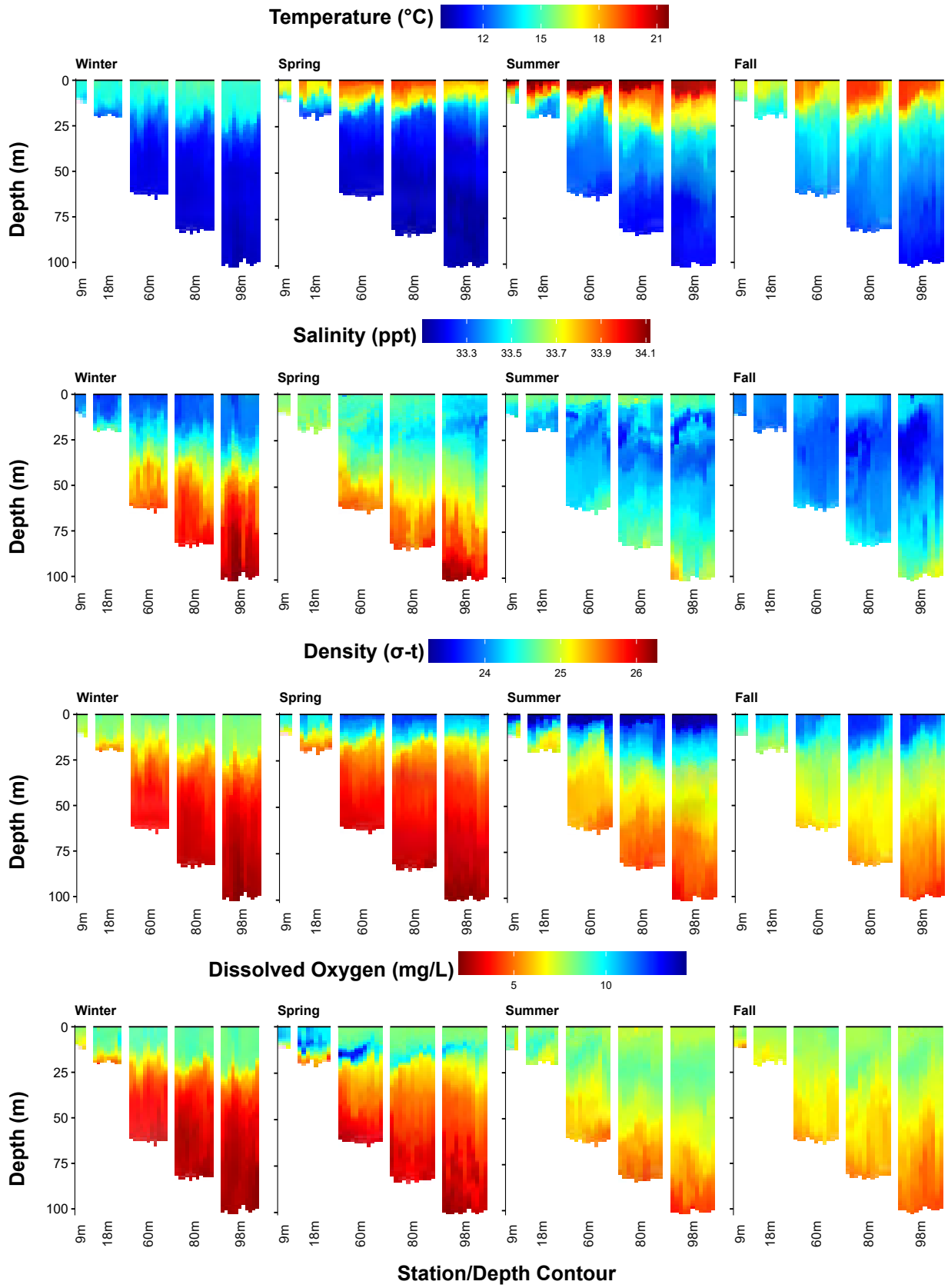


Figure 2.3

Temperature, density, salinity, and dissolved oxygen recorded in the PLOO region during 2025. Data are 1-m binned values per depth for each station and were collected over 4–5 days during each quarterly survey. Stations are depicted from north to south along each depth contour.

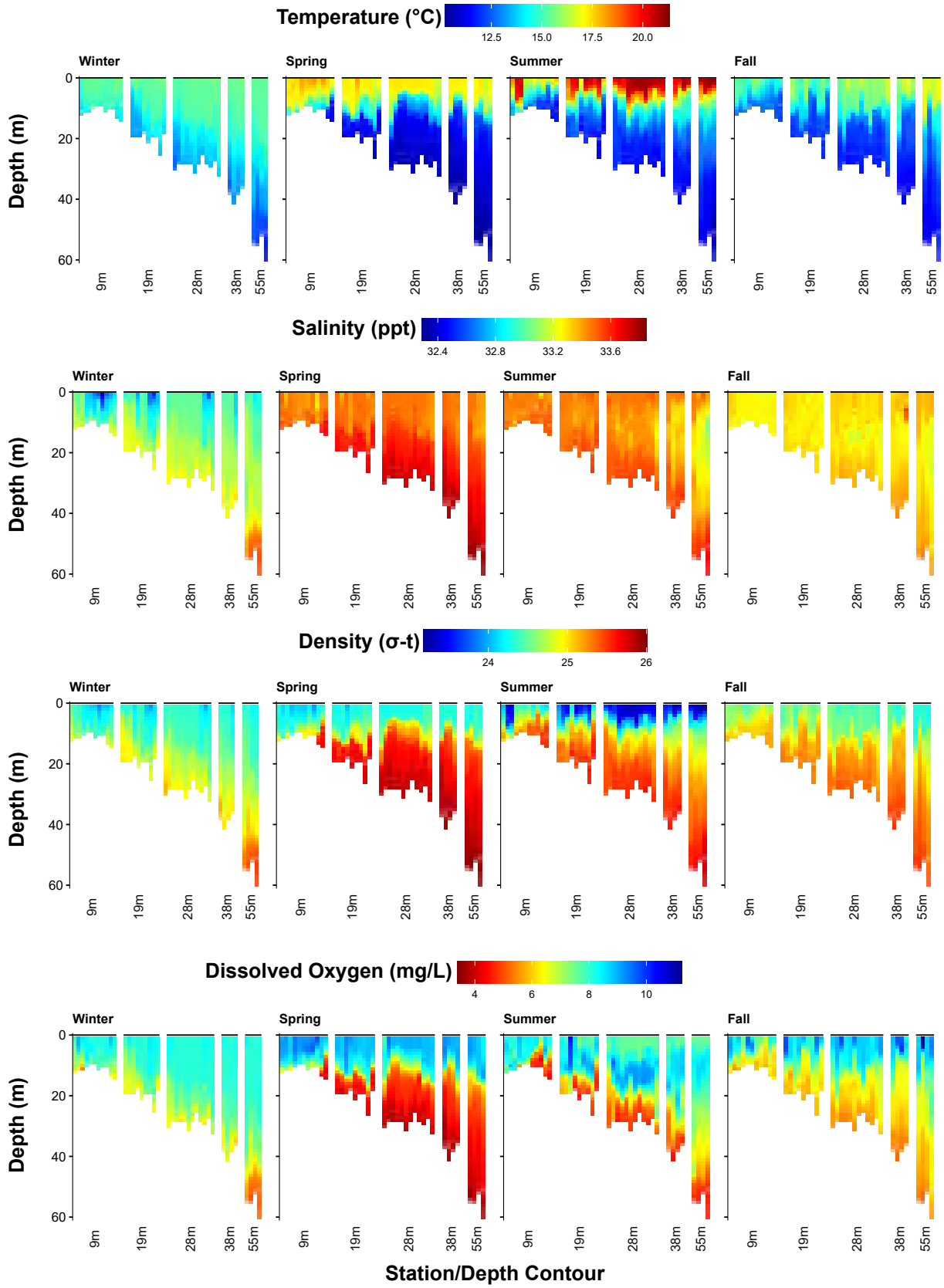


Figure 2.4

Temperature, density, salinity, and dissolved oxygen recorded in the SBOO region during 2024. Data are 1-m binned values per depth for each station and were collected over 4–5 days during each quarterly survey. Stations are depicted from north to south along each depth contour.

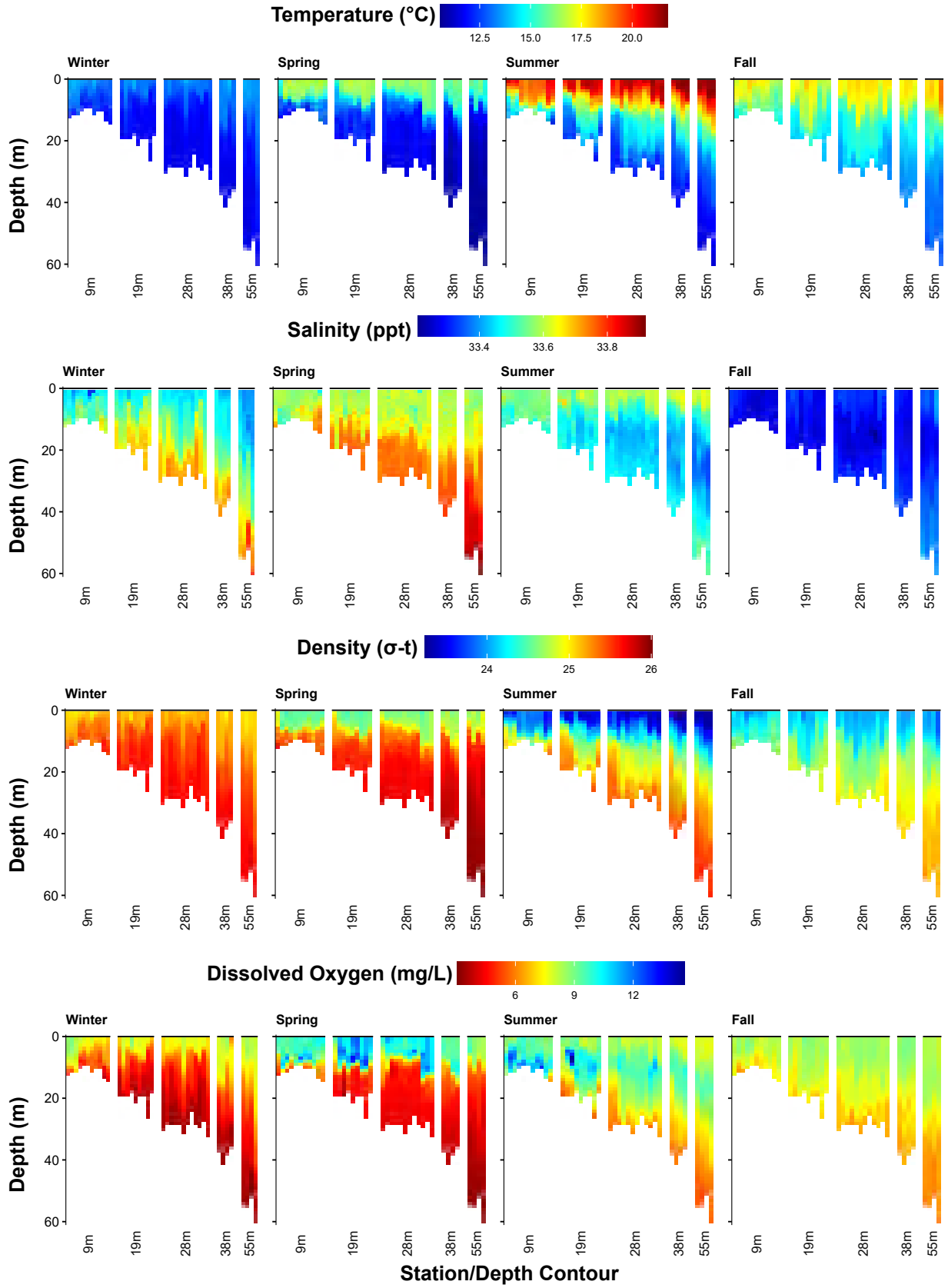


Figure 2.5

Temperature, density, salinity, and dissolved oxygen recorded in the SBOO region during 2025. Data are 1-m binned values per depth for each station and were collected over 4–5 days during each quarterly survey. Stations are depicted from north to south along each depth contour.

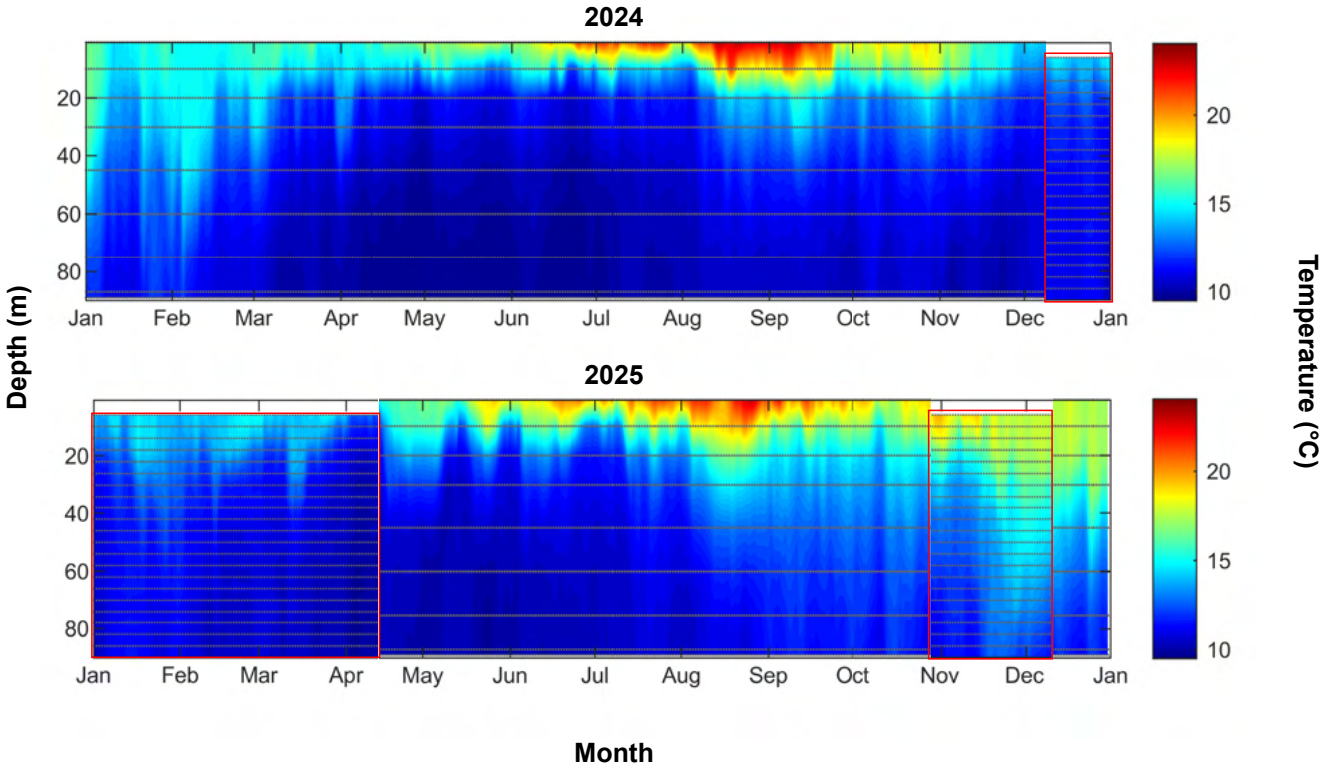


Figure 2.6

Daily averaged temperature recorded near the PLOO by the RTOMS during 2024 and 2025. Horizontal gray lines indicate depths at which sensors were located. Thermistor array data were used to replace missing RTOMS data for all periods within a red border. Additional missing data shown as white spaces.

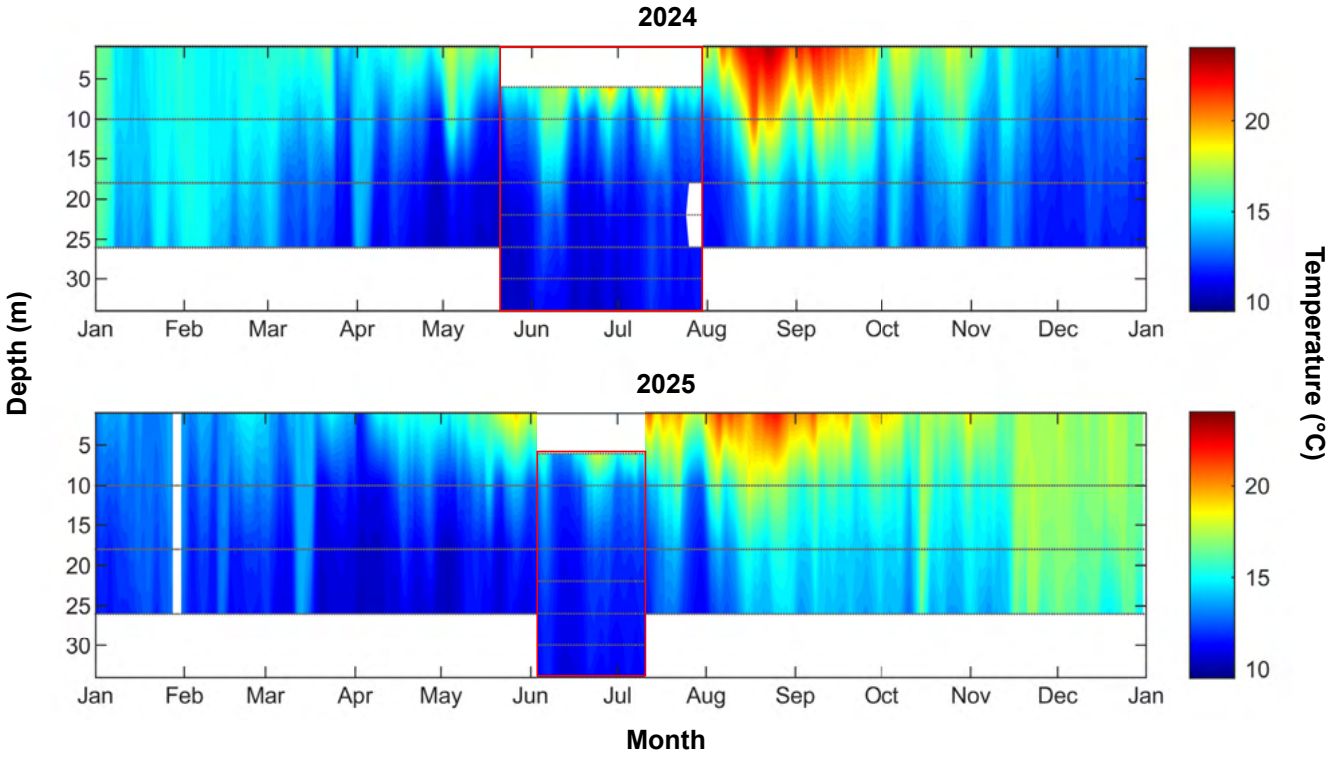


Figure 2.7

Daily averaged temperature recorded near the SBOO by the RTOMS or thermistor array during 2024 and 2025. Horizontal gray lines indicate depths at which sensors were located. Thermistor array data were used to replace missing RTOMS data for all periods within a red border. Additional missing data shown as white spaces.

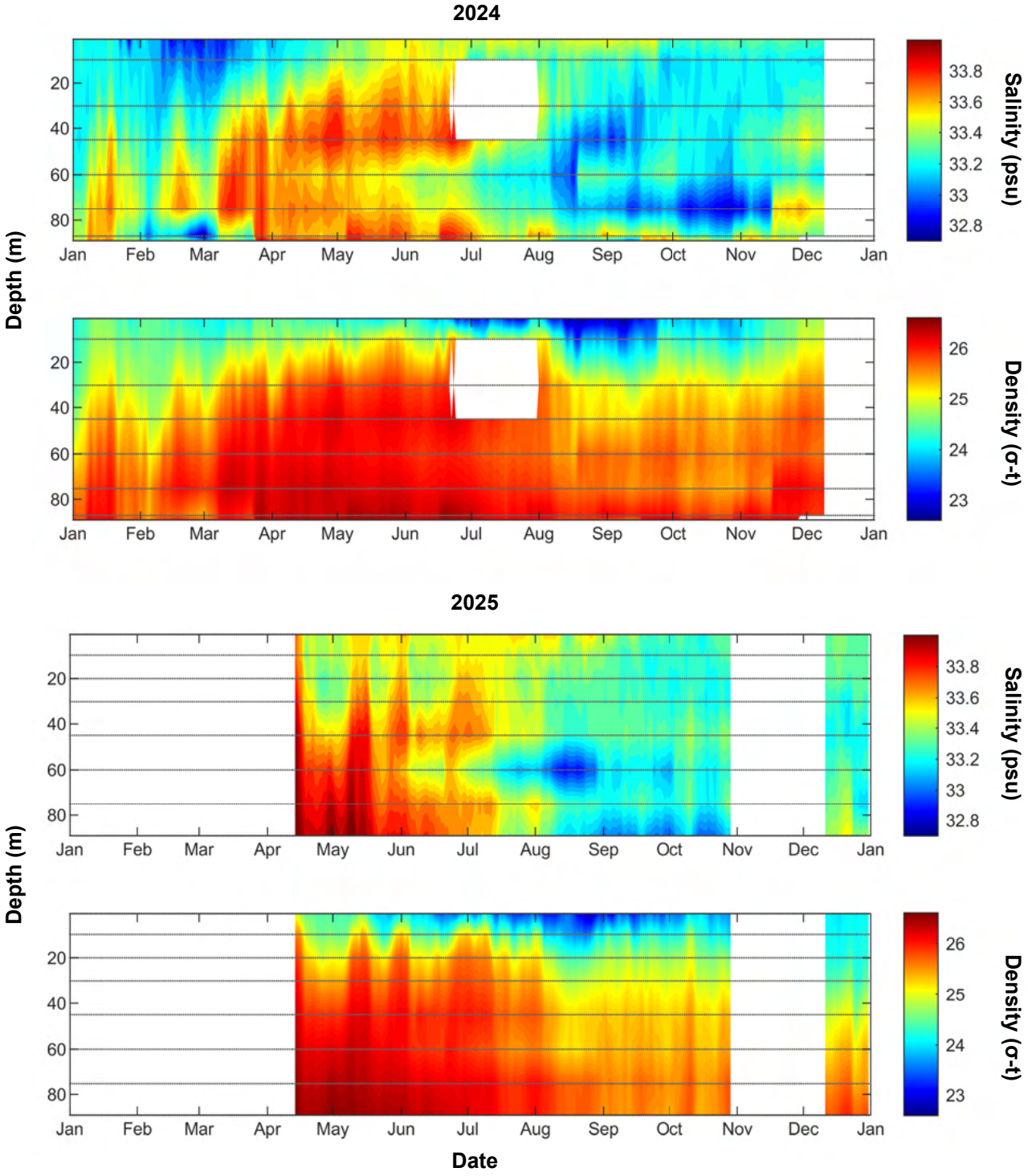


Figure 2.8
Daily averaged salinity and density recorded by the PLOO RTOMS during 2024 and 2025. Horizontal gray lines indicate depths at which sensors were located. Missing data (due to instrument failure or an RTOMs rebuild period) shown as white spaces.

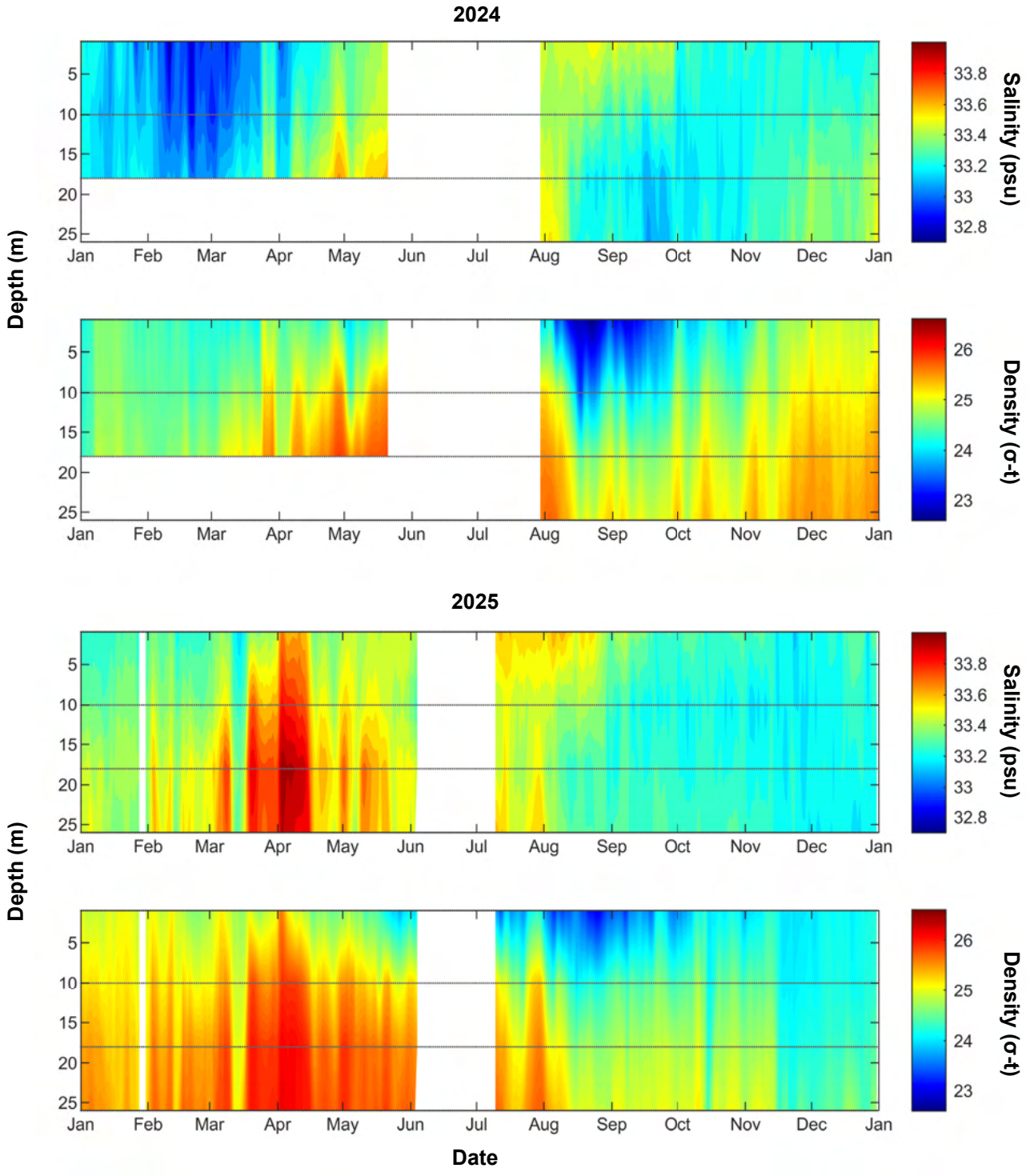


Figure 2.9

Daily averaged salinity and density recorded by the SBOO RTOMS during 2024 and 2025. Horizontal gray lines indicate depths at which sensors were located. Missing data (due to instrument failure or or an RTOMs rebuild period) shown as white spaces.

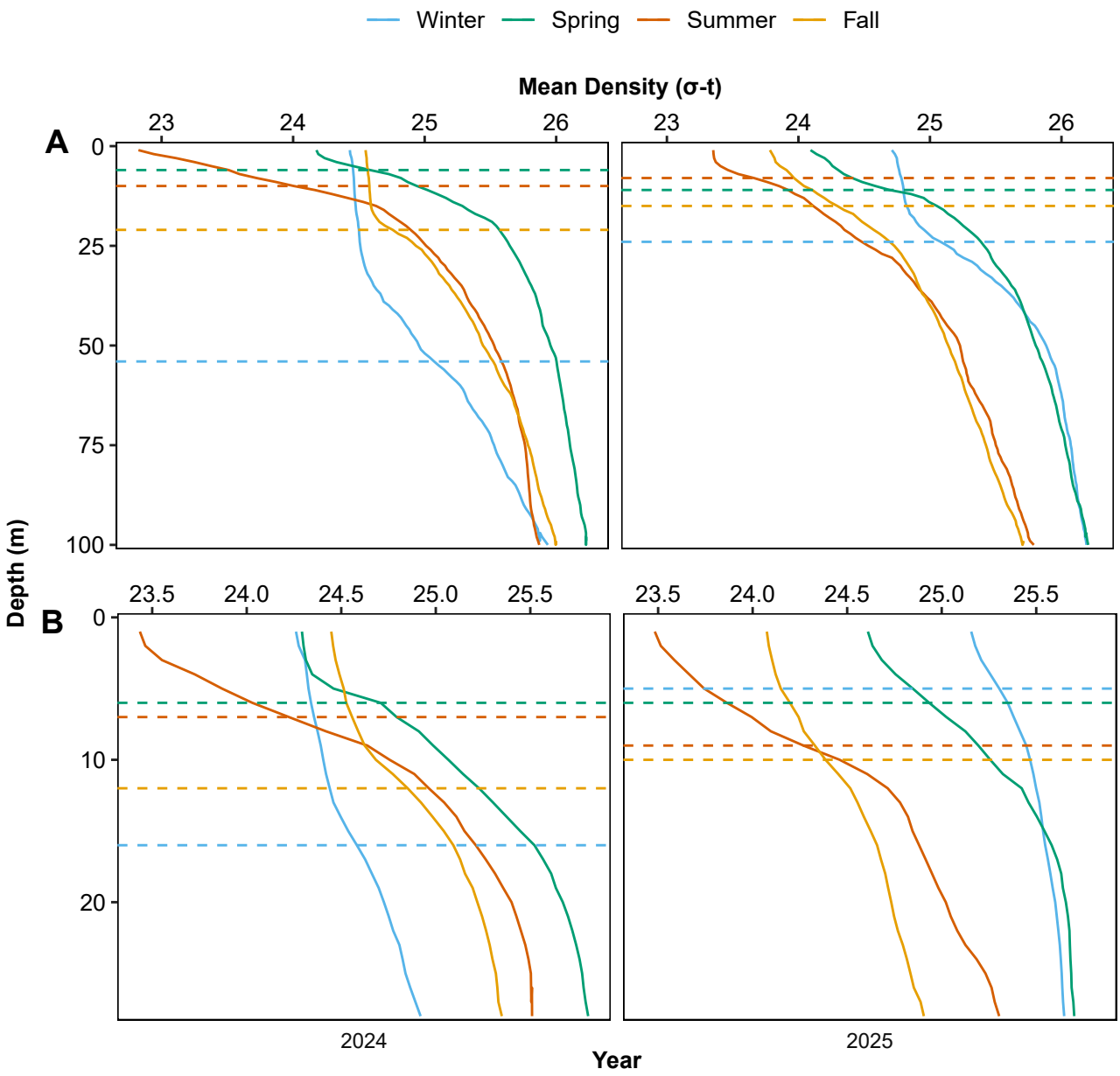


Figure 2.10
Mean density for each survey conducted during 2024 and 2025 at (A) PLOO discharge depth stations (n = 11) and (B) SBOO discharge depth stations (n = 13). Horizontal dashed lines indicate depth of maximum buoyancy frequency per respective season. Dashed line not shown for buoyancy frequencies less than 5.5 cycles/minute indicating a well mixed water column.

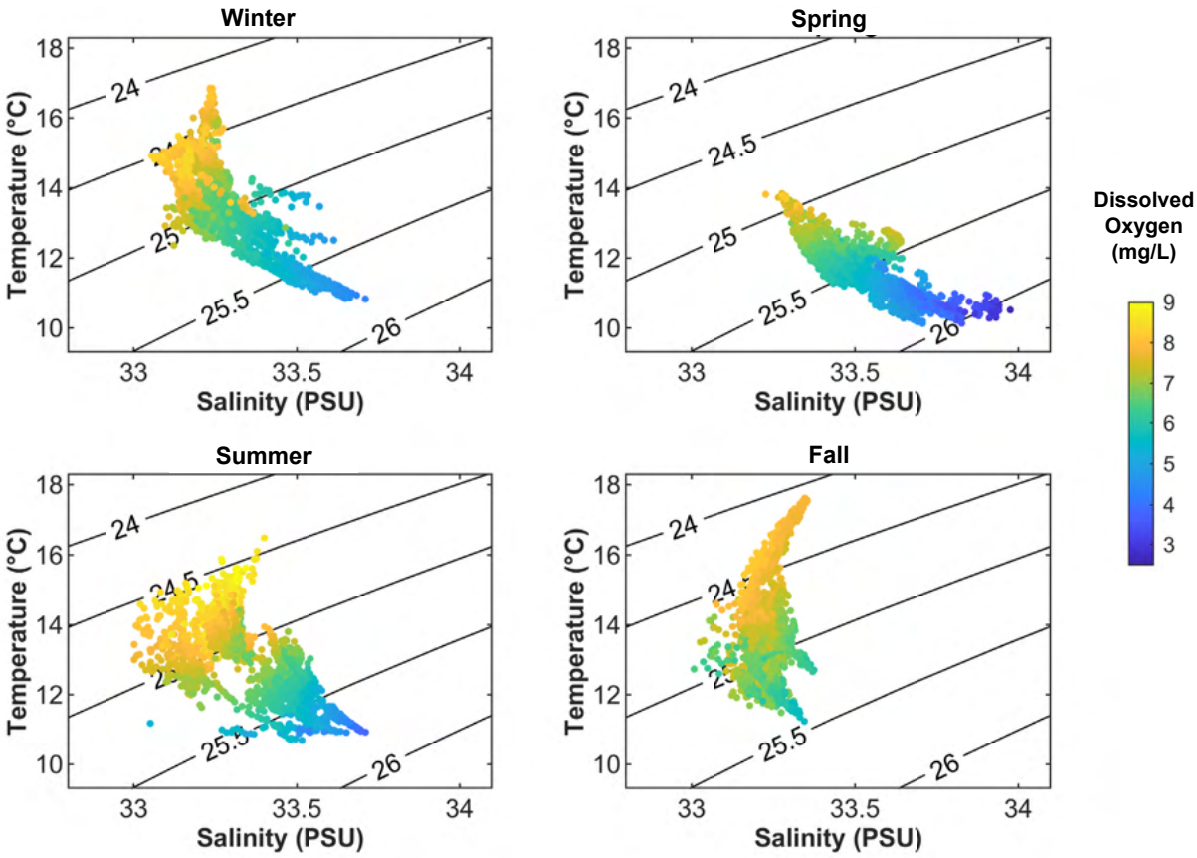


Figure 2.11
Hourly averaged DO by season shown on temperature versus salinity plots at 30 m for all available PLOO mooring data from 2024 to 2025. Isopycnals and corresponding σ-t values shown by black lines.

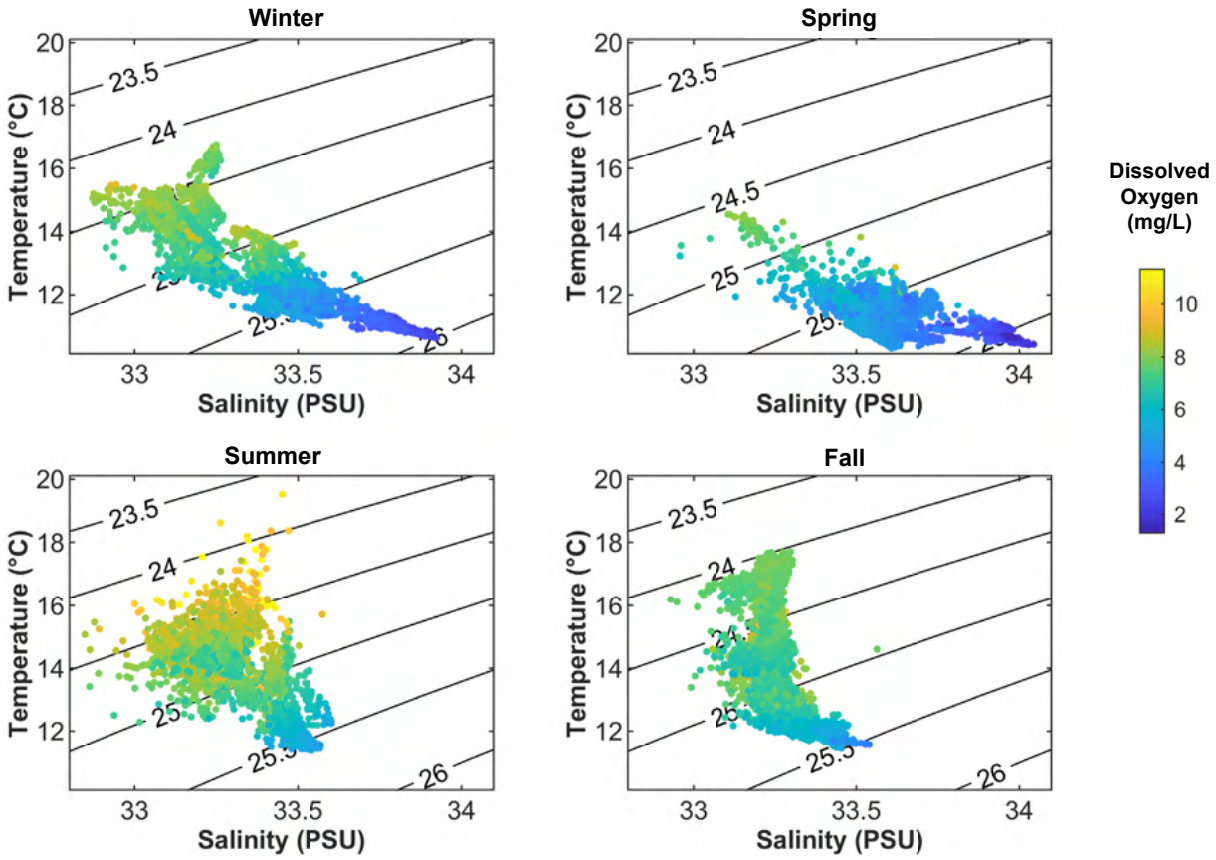


Figure 2.12

Hourly averaged DO by season shown on temperature versus salinity plots at 18 m for all available SBOO mooring data from 2024 to 2025. Isopycnals and corresponding σ-t values shown by black lines.

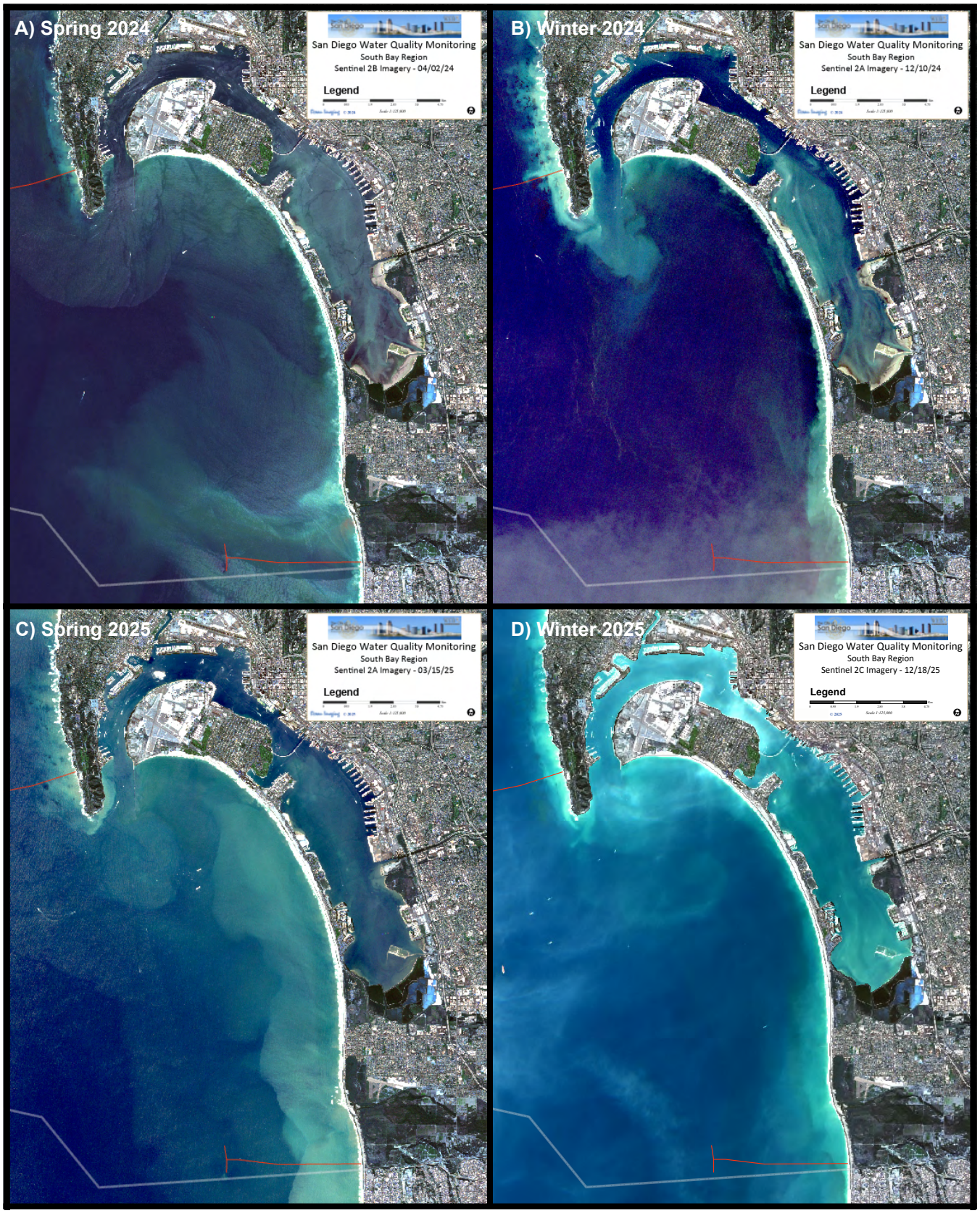


Figure 2.13
Sentinel 2 satellite images of the San Diego region acquired nearest to the date of upwelling events for A) Spring 2024 (April), B) Winter 2024 (December), C) Spring 2025 (March) and, D) Winter 2025 (December) (Ocean Imaging 2025).

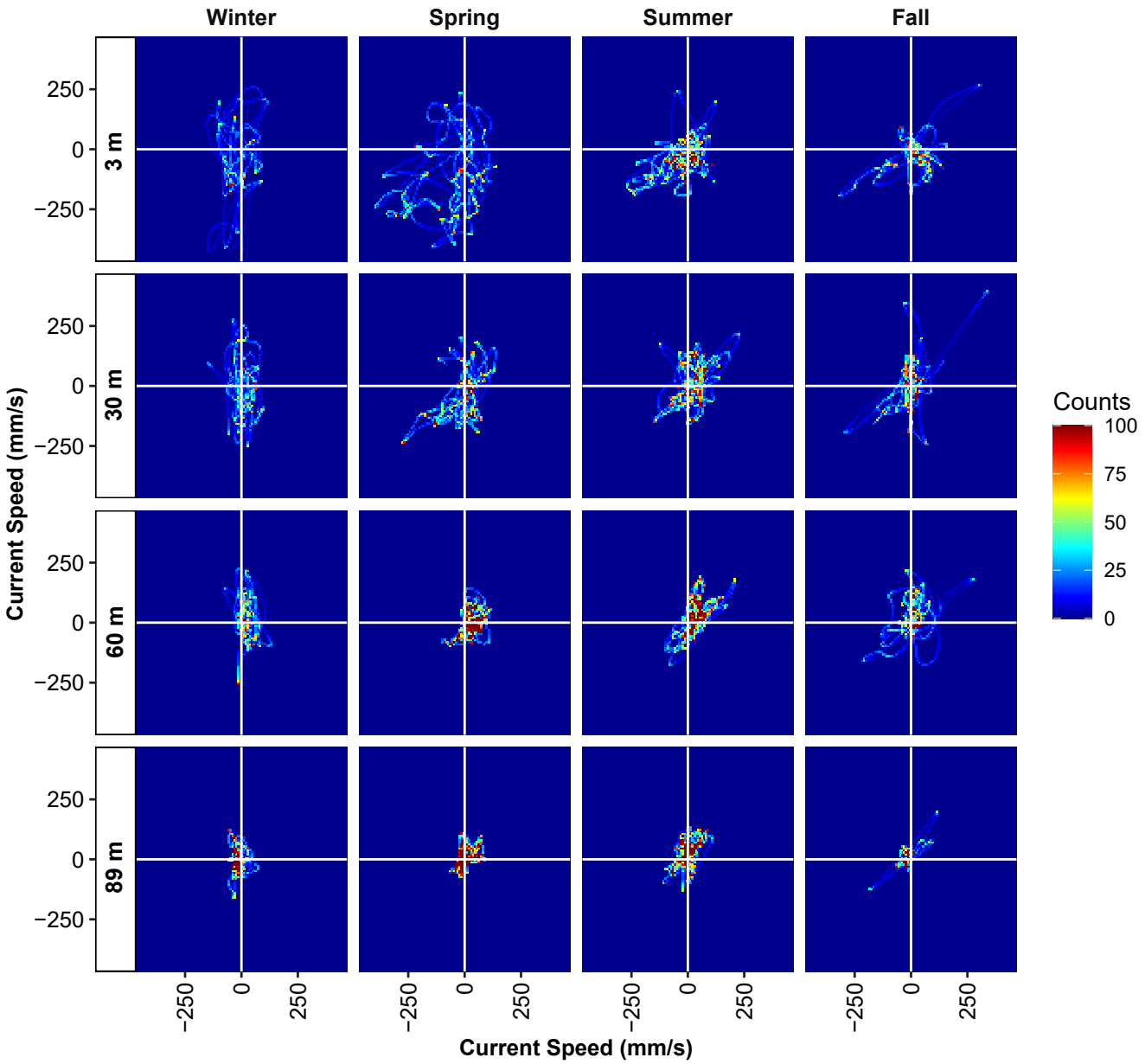


Figure 2.14

Frequency distribution (counts) by season of current speed (mm/s) and direction from 2024-2025 at the PLOO RTOMS ADCP location at representative depth bins. The winter season is for 2024 only. On the x-axis, positive values indicate an eastward direction while negative values indicate a westward direction. On the y-axis, positive values indicate a northward direction while negative values indicate a southward direction.

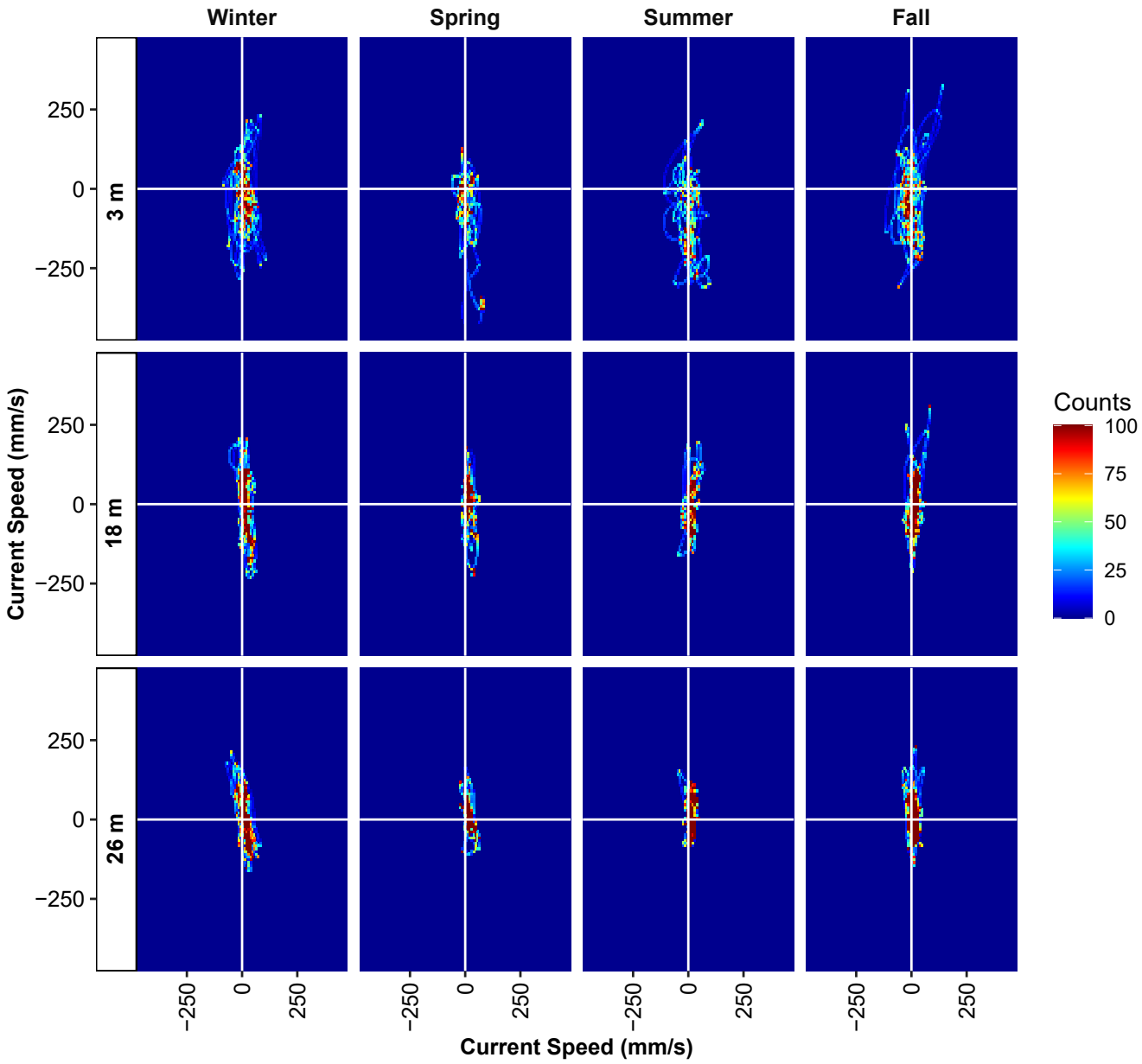


Figure 2.15
Frequency distribution (counts) by season of current speed (mm/s) and direction from 2024-2025 at the SBOO RTOMS ADCP location at representative depth bins. On the x-axis, positive values indicate an eastward direction while negative values indicate a westward direction. On the y-axis, positive values indicate a northward direction while negative values indicate a southward direction.

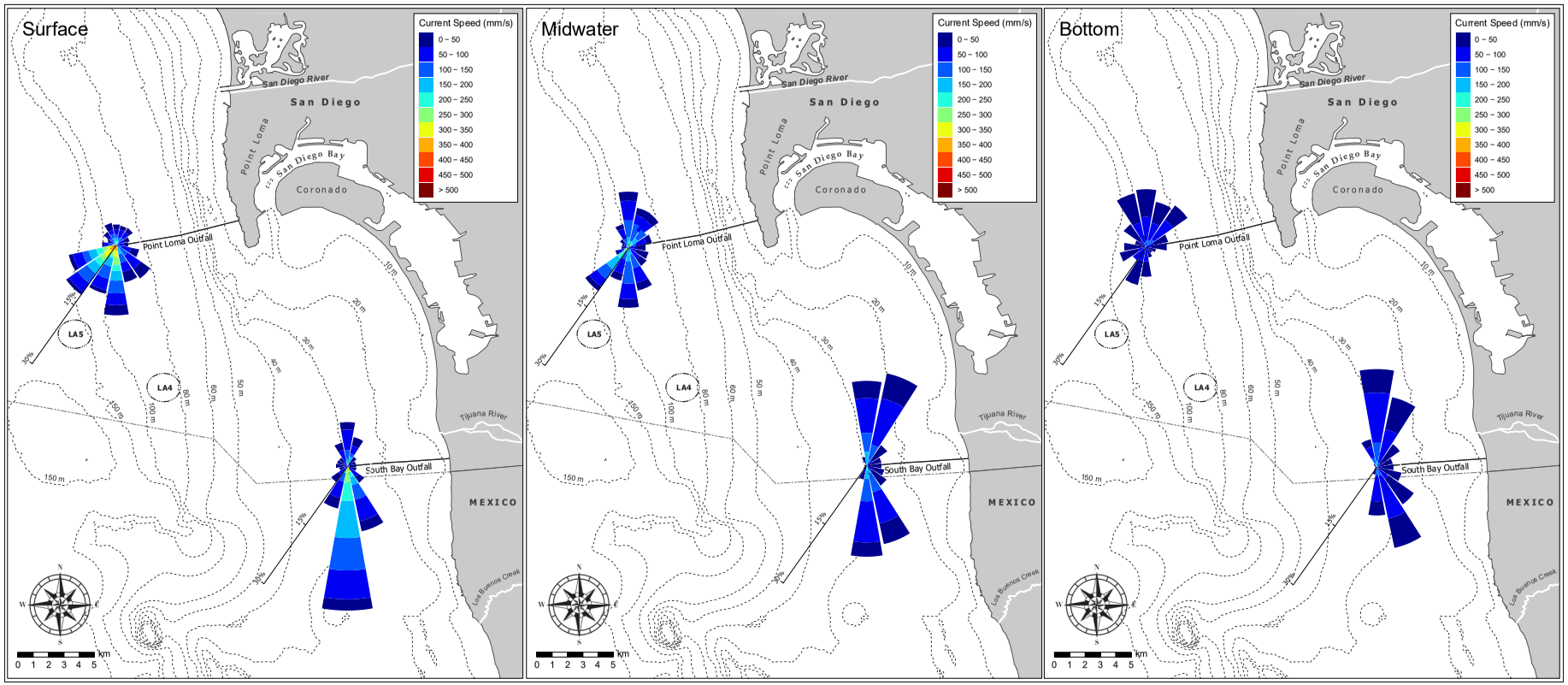


Figure 2.16

Windrose plots of current speed and direction at the surface, midwater, and bottom at PLOO (3m, 30m, and 89m) and SBOO (3m, 18m, and 26m) RTOMS locations.during the 2024-2025 deployment. Length of each slice and colored blocks within reflect the relative frequency of currents in that direction and speed (all slices sum to 100%). Block color corresponds to magnitude of the current speed.(see legend).

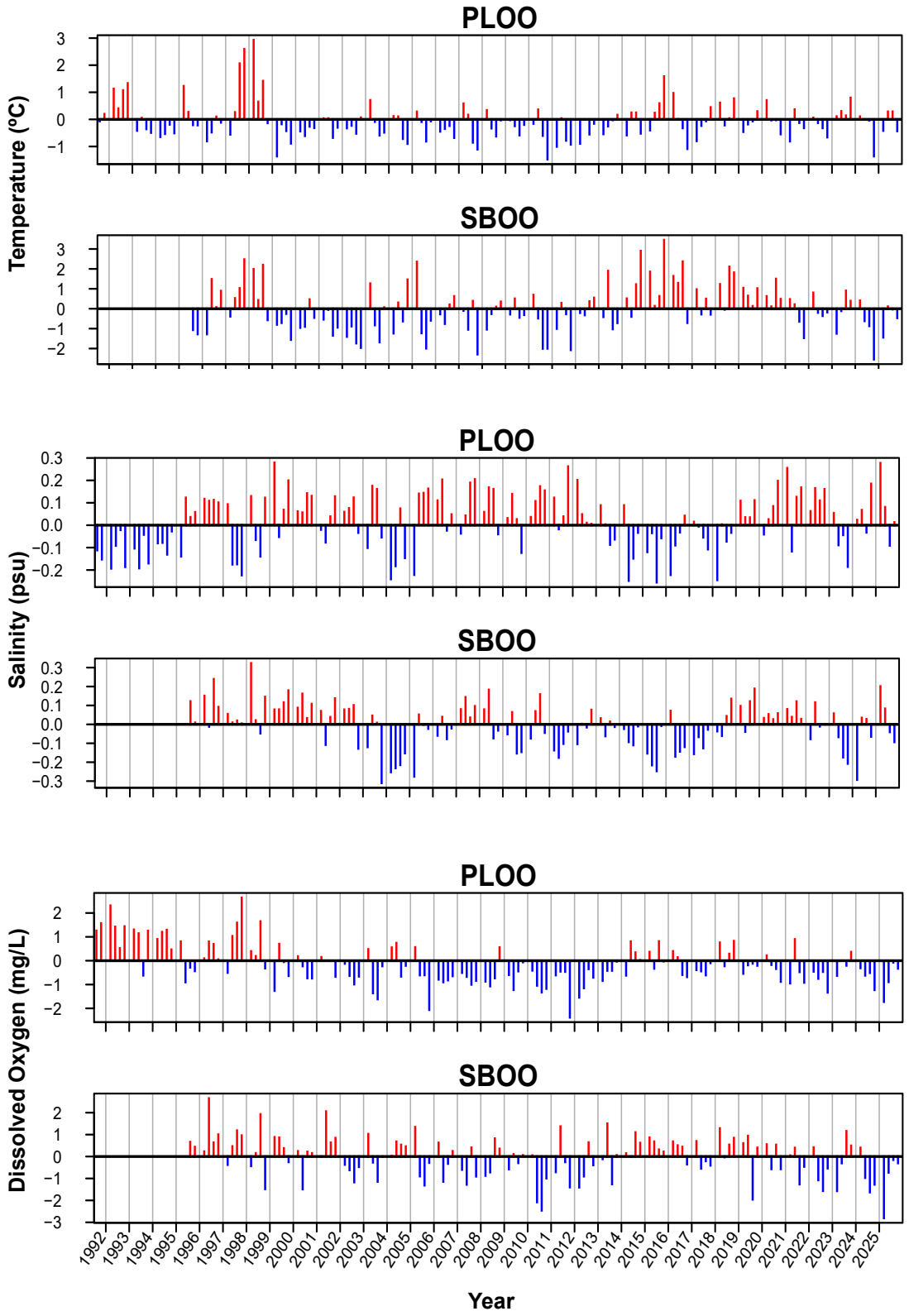


Figure 2.17

Time series of temperature, salinity, and dissolved oxygen (DO) anomalies from 1991 through 2025 at PLOO discharge depth stations (n = 11) and SBOO discharge depth stations (n = 13), all depths combined. Monitoring at the SBOO stations began in 1995.

Table 2.2

Long-term climate-related events in the Southern California Bight. El Niño Southern Oscillation (ENSO); Pacific Decadal Oscillation (PDO); California Current System (CCS); North Pacific Gyre Oscillation (NPGO); Multivariate ENSO Index (MEI)

Approximate Timespan	Large-Scale Climatic Event
1997-1998	Colossal El Niño
1998-2002	Phase change to (-) ENSO and (-) PDO indices to cold conditions
2002-2006	Return to warm ocean conditions in CCS
2002-2004	Intrusion of subarctic waters into CSS with lower than normal salinities
2007	Moderate to strong La Niña, negative PDO cooling event
2010	Moderate to strong La Niña
2013-2014	Phase change to (+) PDO , (-) NPGO, and (+) MEI, resulting in region-wide warming
2014-2015	Largest marine heatwave (BLOB) in NE Pacific
2015	Colossal El Niño
2016-2018	Weak La Niña to Neutral ENSO conditions
2018-2019	Weak El Niño. Marine heatwave in the CCS (2019)
2020-2021	Phase change to (-) PDO and (-) MEI, with weak La Niña. Offshore marine heatwave
2022-2023	Phase change from La Niña (2019-2022) to El Niño in late 2023
2024-2025	Strong El Niño in 2024. Phase change to La Niña in 2025

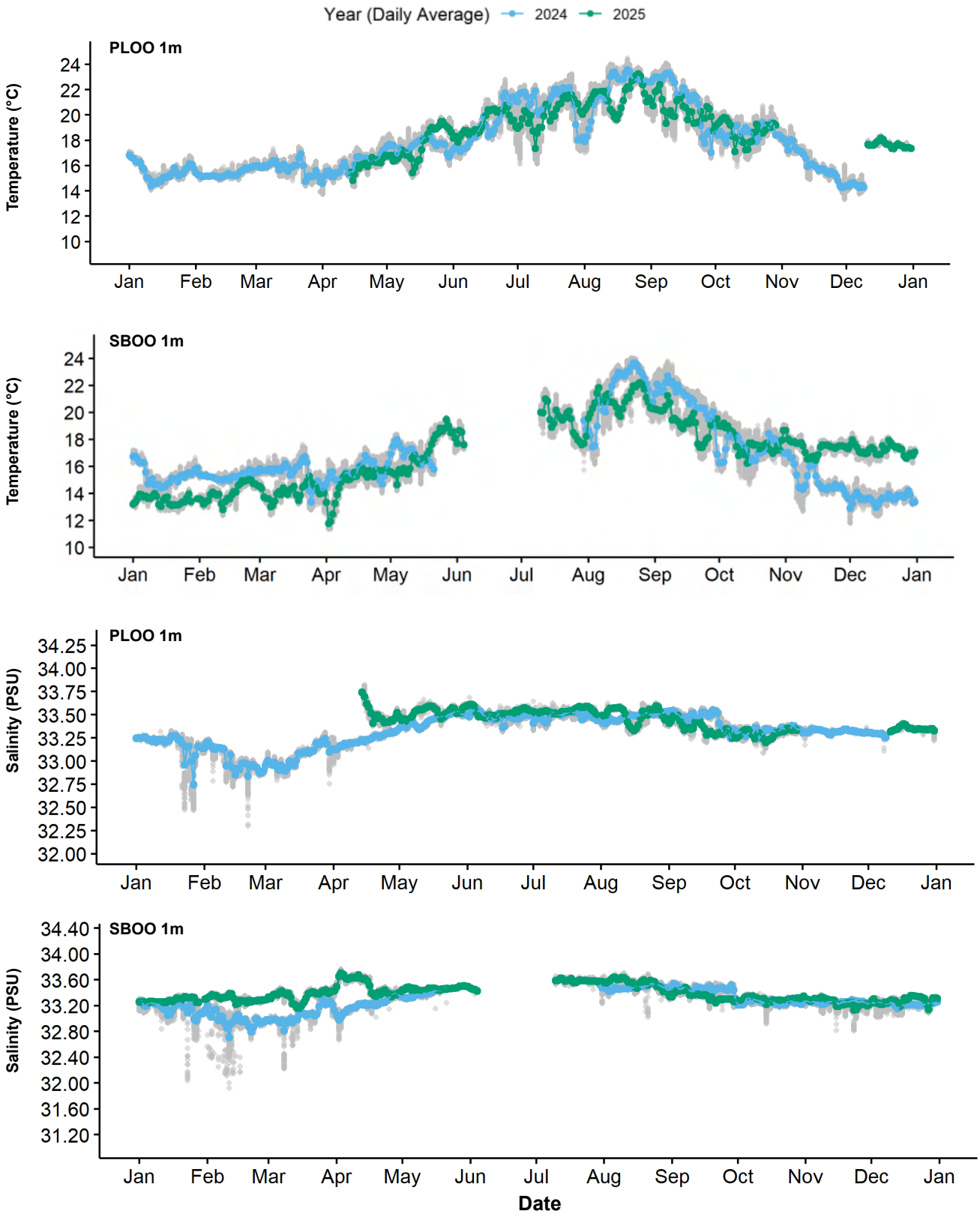


Figure 2.18

Surface (1 m) temperature, salinity, pH, and dissolved oxygen data recorded at the PLOO and SBOO RTOMS during 2024–2025. Data presented as daily averages shown in color and raw values shown in gray.

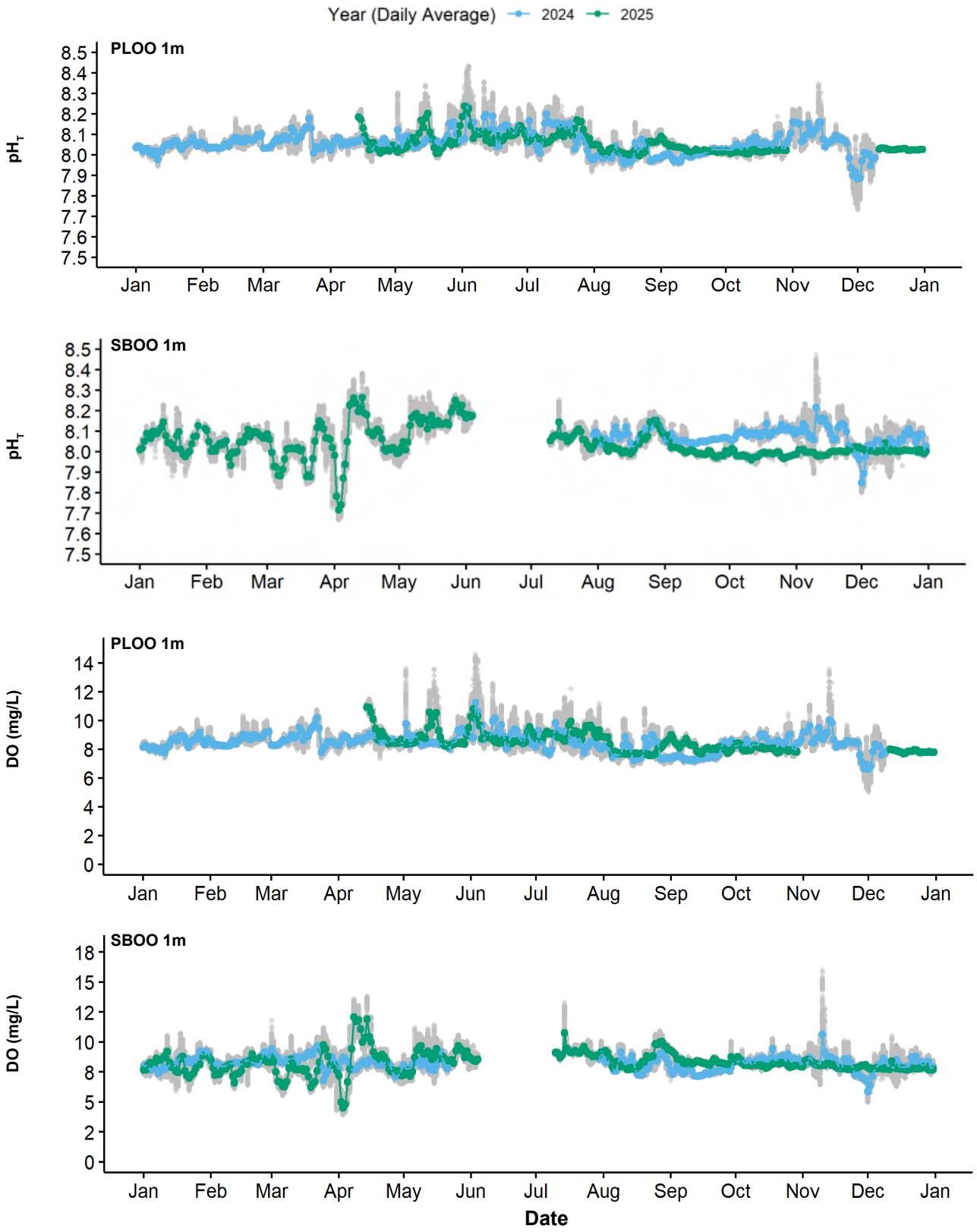


Figure 2.18 *continued*

Chapter 3
Water Quality Compliance

Chapter 3. Water Quality Compliance

Introduction

The City of San Diego (City) conducts extensive monitoring along the shoreline (beaches), nearshore (e.g., kelp forests), and other offshore coastal waters surrounding the Point Loma and South Bay Ocean Outfalls (PLOO and SBOO, respectively) to characterize regional water quality conditions and to identify possible impacts of wastewater discharge, or other contaminant sources, on the marine environment. Densities of fecal indicator bacteria (FIB), including total coliforms, fecal coliforms, and *Enterococcus*, are measured and evaluated to provide information about the dispersion of potentially contaminated water throughout the regions surrounding the two outfalls. Evaluation of these data may also help to identify the source of bacterial contamination throughout the region. In addition, the City's water quality monitoring efforts are designed to assess compliance with the bacterial water contact standards and other physical and chemical water quality objectives specified in the California Ocean Plan (Ocean Plan) that are intended to help protect the beneficial uses of State ocean waters (SWRCB 2019).

Multiple sources of bacterial contamination exist in the Point Loma and South Bay monitoring regions and being able to separate any impact that may be associated with wastewater discharge from other point, or non-point, sources of contamination is often challenging. Examples include outflows from the San Diego River, San Diego Bay, the Tijuana River, and the San Antonio de Los Buenos Creek in northern Baja California (Largier et al. 2004, Nezlin et al. 2007, Gersberg et al. 2008, Terrill et al. 2009). Likewise, storm water discharges and terrestrial runoff from local watersheds during storms, or other wet weather events, can also flush sediments and contaminants into nearshore coastal waters (Noble et al. 2003, Reeves et al. 2004, Sercu et al. 2009, Griffith et al. 2010). Moreover, decaying kelp and seagrass (beach wrack), sediments and sludge accumulating in storm drains, and sandy beach sediments themselves can serve as reservoirs for bacteria until release into coastal waters by returning tides, rain events, or other disturbances (Gruber et al. 2005, Martin and Gruber 2005, Noble et al. 2006, Yamahara et al. 2007, Phillips et al. 2011). Further, the presence of shore birds and their droppings has been associated with high bacterial counts that may impact nearshore water quality (Grant et al. 2001, Griffith et al. 2010).

This chapter presents an analysis and assessment of bacterial distribution patterns collected during 2024 and 2025, at more than 100 permanent water quality monitoring stations surrounding the PLOO and SBOO. The primary goals are to: (1) document bacteriological conditions off San Diego; (2) distinguish elevated bacteriological signals that may result from the PLOO and SBOO wastewater plumes versus other possible sources of contamination; (3) assess compliance with Ocean Plan water contact standards; (4) identify any unknown sources of fecal bacteria contamination and determine if human fecal waste is the cause. Results of remote sensing observations (i.e., satellite imagery) for the San Diego and Tijuana regions are also evaluated to provide insight into the transport and dispersal of wastewater and other types of surface water plumes during the study period. To better understand potential impacts of a wastewater plume on ocean conditions, Chapter 4 discusses natural chemical tracers that can be leveraged to detect and distinguish an outfall's effluent signal from other non-point sources.

Materials and Methods

Field Sampling

Shore stations

Seawater samples were collected weekly at 19 shoreline stations to monitor concentrations of FIB in waters adjacent to public beaches (Figure 3.1). Sixteen of these stations are in California State waters and are therefore subject to Ocean Plan water contact standards (Box 3.1; SWRCB 2019). Eight PLOO stations (D4, D5, D7, D8-B, D9, D10, D11, D12) are located from Mission Beach southward to the tip of Point Loma. Eight SBOO stations (S4, S5, S6, S8, S9, S10, S11, S12) are located between the USA/Mexico border and Coronado, while the other three SBOO shoreline stations (S0, S2, S3) are located south of the border and are not subject to Ocean Plan standards.

Seawater samples were collected from the surf zone at each of the above stations in sterile 250 mL bottles, after which they were transported on blue ice to the City's Marine Microbiology Laboratory and analyzed to determine concentrations of three types of FIB (i.e. total coliform, fecal coliform, *Enterococcus* bacteria). In addition, weather conditions and visual observations of water color and clarity, surf height, and human or animal activity were recorded at the time of sample collection. Wind speed and direction were measured using a hand-held anemometer with a compass. These observations were previously reported in monthly receiving waters monitoring reports submitted to the SDRWQCB (see City of San Diego 2024–2026). These reports are available online (City of San Diego 2026a).

Kelp and offshore stations

Fifteen stations located in relatively shallow waters within or near the Point Loma or Imperial Beach kelp beds (i.e., referred to as "kelp" stations herein) were monitored weekly to assess water quality conditions and Ocean Plan compliance in nearshore areas used for recreational activities such as SCUBA diving, surfing, fishing, and kayaking (Figure 3.1). These included PLOO stations C4, C5 and C6 located along the 9-m depth contour near the inner edge of the Point Loma kelp forest; PLOO stations A1, A6, A7, C7 and C8 located along the 18-m depth contour near the outer edge of the Point Loma kelp forest; SBOO stations I25, I26 and I39 located at depths of 9–18 m contiguous to the Imperial Beach kelp bed; and SBOO stations I19, I24, I32 and I40 located in other nearshore waters along the 9-m depth contour.

An additional 69 offshore stations were sampled quarterly over consecutive days in winter (February), spring (May), summer (August), and fall (November) to monitor water quality conditions and to estimate dispersion of the PLOO and SBOO wastewater plumes (Figure 3.1). These included 36 stations surrounding the PLOO, and 33 stations surrounding the SBOO. The PLOO stations are designated F1–F36 and are located along or adjacent to the 18, 60, 80, and 98-m depth contours. Seawater samples for FIB were collected at all of these stations. The SBOO stations are designated I1–I18, I20–I23, I27–I31, and I33–I38 and are located along the 9, 19, 28, 38 and 55 m depth contours, respectively. Only a subset of SBOO sites (n = 21; I3, I5, I7, I8, I9, I10–I14, I16, I18, I20–I23, I30, I33, I36–I38), are sampled for FIB. Additionally, 15 of the PLOO stations (F01–F03, F06–F14, F18–F20) and 15 of the SBOO stations (I12, I14, I16–I18, I22–I23, I27, I31, I33–I38) are located within State jurisdictional waters (i.e., within 3 nautical miles of shore) and therefore subject to the Ocean Plan compliance standards.

Seawater samples for FIB analyses were collected from three to five discrete depths at the kelp and offshore stations as indicated in Table 3.1. These samples were typically collected using a rosette sampler fitted with Niskin bottles surrounding a central Conductivity, Temperature, and Depth (CTD) instrument,

although replacement samples due to misfires or other causes may have been collected from a separate follow-up cast using stand-alone Van Dorn bottles if necessary. All weekly kelp/nearshore samples and quarterly offshore SBOO samples were analyzed for all three types of FIB, while the quarterly offshore PLOO samples were only analyzed for *Enterococcus* per permit requirements. All samples were refrigerated at sea and then transported on blue ice to the City's Marine Microbiology Laboratory for processing and analysis. Oceanographic data were collected simultaneously with the water samples at each station (see Chapter 2). Visual observations of weather, sea conditions, and human or animal activity were also recorded at the time of sampling. These latter observations were reported previously in monthly receiving waters monitoring reports submitted to the SDRWQCB (see City of San Diego 2024–2026).

Laboratory Analyses

The City Marine Microbiology Laboratory follows guidelines issued by the U.S. Environmental Protection Agency (USEPA) Water Quality Office, State Water Resources Control Board (SWRCB) including the 2019 Ocean Plan and Environmental Laboratory Accreditation Program (ELAP) with respect to sampling and analytical procedures (Bordner et al. 1978, APHA 2012, USEPA 2014). All bacterial analyses were initiated within eight hours of sample collection and conformed to standard membrane filtration techniques, for which the laboratory is certified (ELAP Field of Testing 126).

FIB densities were determined and validated in accordance with USEPA and APHA guidelines (Bordner et al. 1978, APHA 2012, USEPA 2014). Plates with FIB densities above or below the ideal counting range were given greater than (>), greater than or equal to (≥), less than (<), or estimated (e) qualifiers. However, all qualifiers were dropped, and densities were treated as discrete values, when determining compliance with Ocean Plan standards.

Quality assurance tests were performed routinely on bacterial samples to ensure that analyses and sampling variability did not exceed acceptable limits. Laboratory and field duplicate bacteriological samples were processed according to method requirements to measure analyst precision and variability between samples, respectively. Results of these procedures were reported under separate cover (City of San Diego 2025a, 2026b).

Data Analyses

Bacteriology

Compliance with the running geometric mean standards for fecal coliforms and *Enterococcus* was assessed using running 30-day and 42-day windows, respectively. Compliance with the median standard for total coliforms was assessed over a running 30-day window. Compliance with the statistical threshold value (STV) metrics for total coliforms and *Enterococcus* was calculated at monthly intervals. Compliance calculations were limited to shore, kelp and offshore stations located within State waters, excluding resamples. In all instances, compliance was rounded to the nearest whole number (e.g. 99.5% equates to 100%). For the purpose of visualization, to assess temporal and spatial trends, and to assess compliance with the HF183 sampling standards (Box 3.2), elevated FIB was determined by the number of analyses in which FIB concentrations exceeded the threshold established by the 2019 Ocean Plan's water quality bacterial objectives for single sample maximum (SSM) or STV benchmark levels (Box 3.1) (SWRCB 2019). Due to the nature of the STV metric, elevated FIB does not necessarily indicate out-of-compliance for individual analyses of *Enterococcus*

and total coliform densities. Compliance with the HF183 sampling metrics was calculated as the proportion of analyses showing elevated FIB within the rolling window specified in Box 3.2, assessed daily over the report period.

Bacterial densities were compared to rainfall data from San Diego International Airport, San Diego, CA (NOAA 2026). For the purpose of analyses contained within this report, the San Diego dry season was defined as all days between May 1st and September 30th in any given year, while the wet season occurs October 1st through April 30th. Satellite images of the San Diego coastal region were provided by Ocean Imaging of Solana Beach, California and used to aid in the analysis and interpretation of water quality data (see Appendix J). All analyses were performed using R (R Core Team 2019) and various functions within the reshape2, tidyverse, Hmisc, flextable, gtools, psych, RODBC, ggpubr, quantreg, and openxlsx packages (Wickham 2007, 2017, Harrell et al. 2015, Gohel 2024, Warnes et al. 2015, Revelle 2015, Ripley and Lapsley 2017, Kassambara 2019, Koenker 2019, Schauberger and Walker 2019).

Data collected during 2024 were reported previously (City of San Diego 2025b), and all raw data for the 2024-2025 sampling period have been submitted to either the Regional Water Quality Control Board, the California Environmental Data Exchange Network (CEDEN) or the City's Open Data Portal (City of San Diego 2026a) and may be accessed upon request.

Results and Discussion

Bacteriological Compliance and Distribution

Shore stations

Seawater samples collected from the eight PLOO shore stations were 100% compliant with the 30-day fecal coliform geometric mean standard, while the 42-day *Enterococcus* geometric mean standard and the 30-day total coliform median standard were in compliance 99% and 78% of the time over the report period, respectively (Figure 3.2A). Compliance with the fecal coliform SSM standard at these sites was 100% (Figure 3.2B). Compliance with the STV standards for *Enterococcus* and total coliforms ranged from 38–100% of stations each month (Figure 3.2B, Table 3.2). In contrast, compliance rates were more variable during these two years at the eight SBOO shore stations located in State waters. For example, the eight SBOO shore stations were 70% compliant with the 30-day fecal coliform geometric mean standard, while the 42-day *Enterococcus* geometric mean standard and the 30-day total coliform median standard were in compliance 52% and 32% of the time over the report period, respectively (Figure 3.3A). Furthermore, compliance with the SSM for fecal coliforms was 71% (Figure 3.3B). Compliance with the STV standards for *Enterococcus* ranged from 0–88% of stations each month, while compliance with the standard for total coliforms ranged from 0–62% (Figure 3.3B, Table 3.2). However, it is important to note that six of these eight stations (S4, S5, S6, S10, S11, S12) are located near or within areas listed as 'impaired waters' and are not anticipated to comply with State water contact standards (State of California 2010).

Of the 6,016 analyses run on seawater samples collected at the PLOO and SBOO shore stations in 2024–2025 (not including resamples), about 24% (n = 1,466) had elevated FIB, 96% of which occurred at SBOO shore stations (Table 3.3). In state waters, elevated FIB was detected in 19% of analyses (957 of 5,101 total analyses). A majority (66%) of the shore samples with elevated FIB were collected during the wet seasons when rainfall totaled 20.81 inches over both years. This general relationship between rainfall and elevated bacterial levels at shore stations has been evident since water quality monitoring began in both regions (Figure 3.4). Analysis of all data from PLOO and SBOO shore stations over the history of the Ocean

Monitoring Program indicates that the occurrence of a sample with elevated FIB is significantly more likely during the wet season than during the dry season (14% versus 5%, respectively; n = 79,926, $\chi 2 = 1{,}518$, $p < 0.0001$).

Regionally, elevated FIB densities occurred most often at SBOO shore stations S4, S5, S10 and S11 located near the mouth of the Tijuana River, as well as in northern Baja California waters at stations S0, S2 and S3 over the past two years (Table 3.3). Results from historical analyses also indicated that elevated FIB occurred more frequently at stations near the Tijuana River and south of the border near San Antonio de Los Buenos Creek, than at other PLOO or SBOO shore stations, especially during the wet seasons (Figure 3.4). Over the past several years, high FIB densities at these stations have consistently corresponded to outflows from the Tijuana River and San Antonio de Los Buenos Creek, typically following rain events (City of San Diego 2022). In addition, several sanitary sewer overflow events impacted the Tijuana River Valley during 2024 and 2025 (USIBWC 2024–2025).

Kelp bed stations

Seawater samples from the PLOO kelp stations were 100% compliant with the 30-day fecal coliform geometric mean standard, the 42-day *Enterococcus* geometric mean standard, and the 30-day total coliform median standard. Compliance with the fecal coliform SSM standard at these sites was 100% (Figure 3.5B). Compliance with the STV standards for *Enterococcus* was 100% of stations each month, while compliance with the standard for total coliforms was 88–100% (Table 3.2). In the SBOO region, as was noted above for the shore stations, compliance rates were variable at the seven kelp bed, or nearshore, stations. For example, SBOO kelp bed stations were 87% compliant with the 30-day fecal coliform geometric mean standard, while the 42-day *Enterococcus* geometric mean standard and the 30-day total coliform median standard were in compliance 75% and 55% of the time over the report period, respectively (Figure 3.6A). The SSM standard for fecal coliforms was met in 87% of samples (Figure 3.6B). Compliance with the STV standards for *Enterococcus* and total coliforms ranged from 0–100% of stations each month (Table 3.2).

Of the 14,175 analyses run on samples collected at the PLOO and SBOO kelp stations in 2024–2025, approximately 9% (n = 1,286) had elevated FIB, of which 99% occurred in the SBOO region and 80% occurred during the wet season (Table 3.4). However, analysis of water quality monitoring data collected at PLOO kelp stations over the course of the monitoring program (since 1991) shows that the difference in the occurrence of elevated FIB between wet and dry seasons is, though statistically significant, small in magnitude, indicating that rainfall alone has a reduced impact on water quality in the PLOO nearshore region (2.7% in the dry season versus 3.5% in the wet season; n = 179,556, $\chi 2 = 94$, $p < 0.0001$). The likelihood of encountering elevated FIB at these stations was significantly higher before the PLOO was extended to its present discharge site in late 1993 (13.2% before versus 0.4% after extension; n = 179,556, $\chi 2 = 15{,}985$, $p < 0.0001$) (see Figure 3.7). The influence of rainfall on FIB is typically much more pronounced in the SBOO region, with elevated FIB significantly more likely to occur at these stations during the wet season than during the dry season (12.8% versus 2.9%, respectively, since the onset of monitoring; n = 72,398, $\chi 2 = 2{,}160$, $p < 0.0001$) (Figure 3.7). As at the shore stations, high FIB densities at the SBOO kelp stations have historically corresponded to outflows from the Tijuana River and San Antonio de Los Buenos Creek following rain events in the area (City of San Diego 2026a). Such rain-driven turbidity plumes have often been observed in satellite images of the region overlapping SBOO kelp stations with elevated FIB counts (e.g. Figure 3.8). The increasing incidence of elevated FIB at the SBOO kelp bed stations during the wet season since 2017 is likely related to a series of large sewage spills that originated in Tijuana before

spreading through the Tijuana River Valley and eventually reaching ocean waters and moving offshore (see USIBWC 2017–2025).

Offshore stations

Of the 2,640 analyses run on samples collected at offshore stations in the PLOO and SBOO over the past two years, only about 5% (n = 134) had elevated FIB, 67% of which occurred during the wet season (Table 3.5). Unlike shore and nearshore stations, offshore station exceedances were not overrepresented in either region (47% of exceedances occurred in the SBOO region while 53% occurred in the PLOO region). The STV standard for *Enterococcus* at the 15 PLOO offshore stations located within State of California jurisdictional waters, where Ocean Plan water contact standards apply, ranged from 75–100% over the report period (Figure 3.9A, Table 3.2). Additionally, the 10 SBOO stations located within State of California jurisdictional waters were 100% compliant with the SSM standard for fecal coliforms (Figure 3.9B). Compliance with the STV standards for *Enterococcus* ranged from 90–100% of stations each month, while compliance with the standard for total coliforms ranged from 50–100% (Table 3.2).

In the PLOO region, 6.3% of offshore sample analyses had elevated FIB during the two-year reporting period (Table 3.5). Most analyses showing elevated FIB were sampled at stations located along the 80 or 98-m depth contours and from depths of 25 m or deeper (Table 3.5). 30% of these analyses were from stations F29, F30 and F31 located within 1000 m of the PLOO discharge site (i.e., nearfield stations). These results suggest that the PLOO wastewater plume continues to be restricted to relatively deep, offshore waters throughout the year (see also Figure 3.8). Additionally, there were no visual indications of wastewater at any of the 36 offshore PLOO stations based on visual observations of the surface. This conclusion is consistent with historical remote sensing observations that have provided no indication of the PLOO plume reaching surface waters (see Appendix J: Svejkovsky and Hess 2025, 2026).

These findings are also generally consistent with historical ocean monitoring results, which revealed that 0.5% of samples collected at shallow depths (≤ 25 m) from the PLOO 98-m (i.e., discharge depth) stations had elevated levels of Enterococcus during the pre-chlorination years (1993–2008) (Figure 3.10). This percentage dropped to 0.1% at these depths following the initiation of partial chlorination at the Point Loma Wastewater Treatment Plant (PLWTP) in 2008 (City of San Diego 2009). Across all sample depths, detection of elevated Enterococcus has been significantly more likely at the three nearfield stations (F29, F30, F31) than at any other 98-m site (13.7% versus 4.4%, respectively; $n = 7{,}785$, $\chi^2 = 216$, $p < 0.0001$). The addition of chlorination significantly decreased the number of samples with elevated Enterococcus at these three stations (i.e., 15.8% before versus 10.8% after, $n = 2{,}491$, $\chi^2 = 15$, $p = 0.00013$), and the other 98-m stations (5.5% before versus 3.4% after; $n = 5{,}294$, $\chi^2 = 15$, $p < 0.0001$). However, although offshore compliance improved following chlorination, elevated FIB detections at depths of 60 m or greater have increased in recent years, particularly at stations proximal to the outfall (i.e. nearfield and nearfield-adjacent stations) (Figure 3.10).

In the SBOO region, 4.2% of offshore sample analyses had elevated FIB during the two-year reporting period (Table 3.5). Historically, elevated bacterial levels were more likely at the three nearfield stations (i.e., I12, I14, I16) when compared to other SBOO 28-m (i.e., discharge depth) stations (10.2% versus 2.8%; $n = 19{,}506$, $\chi^2 = 473$, $p < 0.0001$) (Figure 3.11). Since the initiation of secondary treatment at the South Bay Wastewater Treatment Plant in January 2011, elevated FIB detections at nearfield stations

have remained low compared to such detections prior to initiation of secondary treatment (56.3% of analyses showing elevated FIB per year prior to secondary versus 3.7% after).

Receiving Water Bacterial Compliance

The 2024–2025 reporting period saw little-to-no improvement following a decline in water quality compliance throughout San Diego coastal waters in both the PLOO and SBOO regions which was first noted in the 2022-2023 Biennial Report (City of San Diego 2024a). All bacterial compliance metrics in the SBOO region, from the shoreline to offshore, indicate a decline in compliance when compared with results from years following the initiation of secondary treatment in 2011. A number of factors may be influencing compliance. Precipitation remained high in 2024 (11.16 in.), following a very wet 2023 (14.43 in.), compared to prior years (9.59 in. on average). Periodic excess flows from the South Bay International Wastewater Treatment Plant (SBIWTP) to the SBOO have occurred in response to infrastructure failure, storm-related damage, and resulting ongoing repairs, especially prior to November of 2024. Despite ongoing repairs, flows from the SBIWTP were largely in compliance with the permitted 25 MGD limit from November 2024 – September 2025. An additional ~5 MGD comprised of effluent treated to advanced primary standards were added to SBIWTP discharge in September –November of 2025 to relieve pumping constraints in the Tijuana system and enable diversion of sewage away from the Tijuana River. Additional flows have been scaled back since November 2025 due to storm-related interruptions and system maintenance and repair. Increased flows are expected to resume and reach up to 10 MGD in 2026. All combined, these factors were likely driving the observed decrease in water quality in the SBOO region. PLOO shore and nearshore stations remained highly compliant overall during the reporting period, with occasional exceedances associated primarily with wet-season conditions. However, despite very low occurrence of exceedances offshore in the PLOO region, elevated FIB detections at deep (60 m or greater) depths at the stations nearest the PLOO (F29, F30, and F31), as well as adjacent stations (F17, F18, F19, F20, F21, F28, F32) has started to emerge in recent years since maximum compliance rates were achieved in 2013 (Figure 3.10). Multiple factors potentially contributing to this trend are currently under evaluation.

During the summer (i.e. dry season), there is typically a significant improvement in shoreline water quality compliance (Tables 3.3 and 3.4), with less of a dramatic effect apparent at offshore stations (Table 3.5). Thus, rain events in the wet season are a significant driver of non-compliance region-wide, with the largest effect along the shore. However, despite this seasonal pattern, dry season non-compliance at SBOO region shore and nearshore stations occurs at rates an order of magnitude greater than dry season non-compliance in the PLOO region (Table 3.3). Therefore, although the impact of rain events on shoreline water quality is clear region wide, there remains an additional significant driver of dry weather non-compliance in the South Bay. This observation is likely explained by the northward transport of contaminated water, particularly from undertreated and untreated wastewater which discharges into the Pacific Ocean via San Antonio de Los Buenos Creek, by the shallow southern swell, which is known to be strongest along the San Diego coast in the summertime (Fedderson et al. 2021, Bray et al. 1999). Improvements to nearshore water quality apparent in 2025 (Figure 3.7) may be driven by repairs to the San Antonio de Los Buenos treatment plant completed in April 2025, which treats ~18 MGD of wastewater that had previously been discharged to the coast untreated since 2020. These results should be interpreted with caution, as the region is characterized by high variability.

Despite the factors highlighted above, compliance with receiving water limitations for bacterial characteristics (Box 3.2) in the PLOO region was above the minimum threshold for all metrics (for each parameter) throughout the report period (Table 3.6). Whereas the nearshore in the SBOO region

continues to show water quality impacts, as has been reported in the past, with overall compliance below the minimum threshold (90%) for fecal coliforms on 585 of the 731 days (80% days out of compliance) in the report period, and on all 731 days (100%) in the report period for *Enterococcus* and total coliforms (Table 3.6). Stations with the highest occurrence of elevated FIB were shore and nearshore stations located close to the mouth of the Tijuana River Estuary. Furthermore, compliance with the kelp station metric was below the minimum threshold for fecal coliforms and Enterococcus at station I19 and I40 on one or more days in the report period, and at I19, I24, I25, I26, and I40 for total coliforms (Table 3.6). Compliance with the offshore station metric in the SBOO region was above the minimum threshold for each of the three indicators throughout the report period (Table 3.6). Observed patterns in SBOO shore and nearshore regulatory exceedances are consistent with documented sources of shore-based contamination (e.g. runoff and northward transport combined with wastewater infrastructure failure). Therefore, additional source tracking in the form of HF183 analysis, as outlined in Box 3.2, is not expected to materially alter management interpretation of the results presented herein.

SUMMARY

Water quality patterns observed during this reporting period were consistent with historical trends. FIB exceedances were most frequent at shore stations in the SBOO region (40%), decreasing somewhat in the nearshore (19%), and were lowest offshore (4%), indicating that the source of reduced water quality is largely shore-based and unrelated to the discharge of treated effluent. Water quality in the PLOO region was generally better, with exceedance rates of 2% at shore stations, 0.2% in the nearshore, and 6% offshore. In both regions, exceedances at shore and kelp bed stations were more common during the wet season, where elevated FIB has historically been associated with storm activity, heavy recreational use, seabirds, and decaying kelp or surfgrass (City of San Diego 2024a). The consistently poorer water quality observed at SBOO stations relative to PLOO is largely attributable to transboundary flows associated with wastewater infrastructure failures in Tijuana, Mexico. Although these general patterns persist, notable deviations have occurred in response to specific events. For example, Hurricane Hilary resulted in reduced compliance during August 2023, reflecting wet-season conditions during a typically dry month. Similarly, elevated bacteria observed at PLOO shore and kelp stations in 1992 followed a catastrophic outfall rupture within the Point Loma kelp forest (Tegner et al. 1995). More recently, a gradual increase in elevated FIB concentrations has been observed in deeper waters surrounding the PLOO. Although the cause remains unclear, these elevated concentrations remain offshore, in the vicinity of the outfall, and below the surface. Evaluation of local currents (see Chapter 2) and plume indicators (see Chapter 4) show no evidence that the PLOO effluent plume reaches the shore or nearshore kelp beds.

The spatial and temporal distribution of elevated FIB observed in recent years corroborate the findings of previous City reports and other studies, which suggest that the Tijuana River and other terrestrial inputs are the largest drivers of contamination in the South Bay region (Svejkovsky and Jones 2001, Noble et al. 2003, Gersberg et al. 2004, 2006, 2008, Largier et al. 2004, Terrill et al. 2009, Svejkovsky and Hess 2022). For example, coastal runoff from rivers and creeks were more likely to impact coastal water quality than wastewater discharge from the outfall, especially during and immediately after significant rain events (Svejkovsky and Jones 2001, Terrill et al. 2009). Further, the general relationship between rainfall levels and elevated FIB densities in the SBOO region existed before wastewater discharge began in 1999 (City of San Diego 2000). Shore stations located near the mouths of the Tijuana River and in Mexican waters near San Antonio de Los Buenos Creek have historically had higher numbers of elevated FIB samples than stations located farther to the north. It is also well established that sewage-laden

discharges from the Tijuana River and San Antonio de Los Buenos Creek are likely sources of bacteria during or after storms or other periods of increased flows (Svejkovsky and Jones 2001, Noble et al. 2003, Gersberg et al. 2004, 2006, 2008, Largier et al. 2004, Terrill et al. 2009, Svejkovsky and Hess 2024). The failure of the San Antonio de Los Buenos Treatment Plant in 2020 is believed to be a major source of poor water quality that has been observed in recent years at SBOO shore and nearshore stations during the dry season, when along-shore currents are known to travel northward (Fedderson et al. 2021, Bray et al. 1999). A modest improvement in shore and nearshore water quality in the dry season in 2025, compared to the dry season of other recent years, coincides temporally with the completion of repairs to that facility. Despite increased flows from the SBIWTP, the occurrence of samples with elevated FIB near the SBOO outfall remains low compared to that of samples taken before the initiation of secondary treatment, which began in January 2011 at the South Bay International Treatment Plant. Repairs that improved compliance with SBIWTP's permitted flow rates beginning in November 2024 did not immediately yield an improvement in water quality in the vicinity of the outfall. However, shore-based contamination can overlap with outfall nearfield stations during rain events, making it difficult to assign a source of contamination in the winter. Following improved water quality in August of 2025, a slight increase in the occurrence of samples with elevated FIB in November of 2025 coincided with planned increased flows to the SBOO as well as moderate rainfall, again rendering sources inconclusive. Continued monitoring through the 2026 dry season is necessary to inform conclusions regarding any potential effects of planned increased flows from the SBIWTP. Most analyses showing elevated FIB continue to be associated with stations near the mouth of the Tijuana River Estuary and they continue to be more prevalent in the wet season. As a result, we conclude that non-compliance with receiving water limitations for bacterial characteristics is primarily driven by known contaminated outflows from the Tijuana River Estuary and other non-point source runoff.

Literature Cited

[APHA] American Public Health Association. (2012). Standard Methods for the Examination of Water and Wastewater, 22nd edition. E.W. Rice, R. Baird, A. Eaton and L. Clesceri (eds.). American Public Health Association, American Water Works Association, and Water Pollution Control Federation.

Bordner, R., J. Winter, and P. Scarpino, eds. (1978). Microbiological Methods for Monitoring the Environment: Water and Wastes, EPA Research and Development, EPA-600/8-78-017.

Bray, N.A., A. Keyes, and W. M. L. Morawitz. (1999). The California Current system in the Southern California Bight and the Santa Barbara Channel. Journal of Geophysical Research, 104: 7695-7714.

City of San Diego. (2000). International Wastewater Treatment Plant Final Baseline Ocean Monitoring Report for the South Bay Ocean Outfall (1995–1998). City of San Diego Ocean Monitoring Program, Metropolitan Wastewater Department, Environmental Monitoring and Technical Services Division, San Diego, CA.

City of San Diego. (2009). Biennial Receiving Waters Monitoring and Assessment Report for the Point Loma and South Bay Ocean Outfalls, 2007–2008. City of San Diego Ocean Monitoring Program, Public Utilities Department, Environmental Monitoring and Technical Services Division, San Diego, CA.

City of San Diego. (2022). Biennial Receiving Waters Monitoring and Assessment Report for the Point Loma and South Bay Ocean Outfalls, 2020–2021. City of San Diego Ocean Monitoring Program, Public Utilities Department, Environmental Monitoring and Technical Services Division, San Diego, CA.

City of San Diego. (2024–2026). Monthly Receiving Waters Monitoring Reports for the South Bay Ocean Outfall (South Bay Water Reclamation Plant), January 2024–December 2025. City of San Diego Ocean Monitoring Program, Public Utilities Department, Environmental Monitoring and Technical Services Division, San Diego, CA.

City of San Diego. (2024a). Biennial Receiving Waters Monitoring Report for the Point Loma Ocean Outfall and South Bay Ocean Outfalls, 2022-2023. City of San Diego Ocean Monitoring Program, Public Utilities Department, Environmental Monitoring and Technical Services Division, San Diego, CA.

City of San Diego. (2025a). Annual Receiving Waters Monitoring and Toxicity Testing Quality Assurance Report, 2024. City of San Diego Ocean Monitoring Program, Public Utilities Department, Environmental Monitoring and Technical Services Division, San Diego, CA.

City of San Diego. (2025b). Interim Receiving Waters Monitoring Report for the Point Loma Ocean Outfall and South Bay Ocean Outfalls, 2024. City of San Diego Ocean Monitoring Program, Public Utilities Department, Environmental Monitoring and Technical Services Division, San Diego, CA.

City of San Diego. (2026a). Ocean Monitoring Program Reports and Data. https://www.sandiego.gov/public-utilities/sustainability/ocean-monitoring/reports

City of San Diego. (2026b). Annual Receiving Waters Monitoring and Toxicity Testing Quality Assurance Report, 2025. City of San Diego Ocean Monitoring Program, Public Utilities Department, Environmental Monitoring and Technical Services Division, San Diego, CA.

Feddersen, F., Boehm, A. B., Giddings, S. N., Wu, X., & Liden, D. (2021). Modeling untreated wastewater evolution and swimmer illness for four wastewater infrastructure scenarios in the San Diego-Tijuana (US/MX) border region. Geo Health, 5, 1-20.

Gersberg, R.M., D. Daft, and D. Yorkey. (2004). Temporal pattern of toxicity in runoff from the Tijuana River Watershed. Water Research, 38: 559–568.

Gersberg, R.M., M.A. Rose, R. Robles-Sikisaka, and A.K. Dhar. (2006). Quantitative detection of hepatitis a virus and enteroviruses near the United States-Mexico Border and correlation with levels of fecal indicator bacteria. Applied and Environmental Microbiology, 72: 7438–7444.

Gersberg, R., J. Tiedge, D. Gottstein, S. Altmann, K. Watanabe, and V. Luderitz. (2008). Effects of the South Bay Ocean Outfall (SBOO) on beach water quality near the USA-Mexico border. International Journal of Environmental Health Research, 18: 149–158.

Gohel D, Skintzos P (2024). flextable: Functions for Tabular Reporting. R package version 0.9.5, https://davidgohel.github.io/flextable/, https://ardata-fr.github.io/flextable-book/.

Grant, S.B., B.F. Sanders, A. Boehm, J. Redman, R. Kim, A. Chu, M. Gouldin, C. McGee, N. Gardiner, B. Jones, J. Svejkovsky, and G. Leipzig. (2001). Generation of enterococci bacteria in a coastal saltwater marsh and its impact on surf zone water quality. Environmental Science Technology, 35: 2407–2416.

Griffith, J., K.C. Schiff, G. Lyon, and J. Fuhrman. (2010). Microbiological water quality at non-human influenced reference beaches in southern California during wet weather. Marine Pollution Bulletin, 60: 500–508.

Gruber, S., L. Aumand, and A. Martin. (2005). Sediments as a reservoir of indicator bacteria in a coastal embayment: Mission Bay, California, Technical paper 0506. Weston Solutions, Inc. Presented at StormCon 2005. Orlando, FL, USA. July 2005.

Harrell, F.E. Jr, C. Dupont et al. (2015). Hmisc: Harrell Miscellaneous. R package version 3.17-0. http://CRAN.R-project.org/package=Hmisc.

Kassambara, A. (2019). ggpubr: 'ggplot2' Based Publication Ready Plots. R package version 0.2.4. https://CRAN.R-project.org/package=ggpubr.

Koenker, R. (2019). quantreg: Quantile Regression. R package version 5.52. https://CRAN.R-project.org/package=quantreg.

Largier, J., L. Rasmussen, M. Carter, and C. Scearce. (2004). Consent Decree – Phase One Study Final Report. Evaluation of the South Bay International Wastewater Treatment Plant Receiving Water Quality Monitoring Program to Determine Its Ability to Identify Source(s) of Recorded Bacterial Exceedances. Scripps Institution of Oceanography, University of California, San Diego, CA.

Martin, A., and S. Gruber. (2005). Amplification of indicator bacteria in organic debris on southern California beaches. Technical Paper 0507. Weston Solutions, Inc. Presented at StormCon 2005. Orlando, FL, USA. July 2005.

Nezlin, N.P., P.M. DiGiacomo, S.B. Weisberg, D.W. Diehl, J.A. Warrick, M.J. Mengel, B.H. Jones, K.M. Reifel, S.C. Johnson, J.C. Ohlmann, L. Washburn, and E.J. Terrill. (2007). Southern California Bight 2003 Regional Monitoring Program: V. Water Quality. Southern California Coastal Water Research Project. Costa Mesa, CA.

[NOAA] National Oceanic and Atmospheric Administration. (2026). National Climatic Data Center. https://www.ncdc.noaa.gov/cdo-web/datatools

Noble, R.T., D.F. Moore, M.K. Leecaster, C.D. McGee, and S.B. Weisberg. (2003). Comparison of total coliform, fecal coliform, and Enterococcus bacterial indicator response for ocean recreational water quality testing. Water Research, 37: 1637–1643.

Noble, M.A., J.P. Xu, G.L. Robertson, and K.L. Rosenfeld. (2006). Distribution and sources of surfzone bacteria at Huntington Beach before and after disinfection of an ocean outfall–A frequency-domain analysis. Marine Environmental Research, 61: 494–510.

Phillips, C.P., H.M. Solo-Gabriele, A.J. Reneiers, J.D. Wang, R.T. Kiger, and N. Abdel-Mottaleb. (2011). Pore water transport of enterococci out of beach sediments. Marine Pollution Bulletin, 62: 2293–2298.

R Core Team. (2019). R: A language and environment for statistical computing. R Foundation for Statistical Computing, Vienna, Austria. URL https://www.R-project.org/.

Reeves, R.L., S.B. Grant, R.D. Mrse, C.M. Copil Oancea, B.F. Sanders, and A.B. Boehm. (2004). Scaling and management of fecal indicator bacteria in runoff from a coastal urban watershed in southern California. Environmental Science and Technology, 38: 2637–2648.

Revelle, W. (2015). psych: Procedures for Personality and Psychological Research, Northwestern University, Evanston, Illinois, USA, http://CRAN.R-project.org/package=psych version 1.5.8.

Ripley, B. and M. Lapsley. (2017). RODBC: ODBC Database Access. R package version 1.3-12. http://CRAN.R-project.org/package=RODBC.

Schauberger, P and A. Walker (2019). openxlsx: Read, Write and Edit xlsx Files. R package version 4.1.4. https://CRAN.R-project.org/package=openxlsx.

Sercu, B., L.C. Van de Werfhorst, J. Murray, and P.A. Holden. (2009). Storm drains are sources of human fecal pollution during dry weather in three urban southern California watersheds. Environmental Science and Technology, 43: 293–298.

State of California. (2010). Integrated Report (Clean Water Act Section 303(d) List/305(b) Report). http://www.waterboards.ca.gov/water_issues/programs/tmdl/integrated2010.shtml.

Svejkovsky, J. and B. Jones. (2001). Detection of coastal urban storm water and sewage runoff with synthetic aperture radar satellite imagery. Eos, Transactions, American Geophysical Union, 82, 621–630.

Svejkovsky, J. and Hess, M. (2025). Satellite & Aerial Coastal Water Quality Monitoring in the San Diego/Tijuana Region: Annual Summary Report: 1 January 2024 – 31 December 2024. Littleton, CO.

Svejkovsky, J. and Hess, M. (2026). Satellite & Aerial Coastal Water Quality Monitoring in the San Diego/Tijuana Region: Annual Summary Report: 1 January 2025 – 31 December 2025. Littleton, CO.

[SWRCB] California State Water Resources Control Board. (2019). California Ocean Plan, Water Quality Control Plan, Ocean Waters of California. California Environmental Protection Agency, Sacramento, CA.

Tegner, M.J., P.K. Dayton, P.B. Edwards, K.L. Riser, D.B. Chadwick, T.A. Dean, and L. Deysher. (1995). Effects of a large sewage spill on a kelp forest community: Catastrophe or disturbance? Marine Environmental Research, 40: 181–224.

Terrill, E., K. Sung Yong, L. Hazard, and M. Otero. (2009). IBWC/Surfrider – Consent Decree Final Report. Coastal Observations and Monitoring in South Bay San Diego. Scripps Institution of Oceanography, University of California, San Diego, CA.

[USEPA] United States Environmental Protection Agency. (2014). Method 1600: Enterococci in Water by Membrane Filtration Using membrane-Enterococcus Indoxyl-β-D-Glucoside Agar (mEI). EPA Document EPA-821-R-14-011. Office of Water (4303T), Washington, DC.

[USIBWC] United States International Boundary Water Commission (2017–2025). Executive Officer's Reports. https://www.waterboards.ca.gov/sandiego/publications_forms/publications/eoreports.html

Warnes, G., B. Bolker, and T. Lumley. (2015). gtools: Various R Programming Tools. R package version 3.5.0. http://CRAN.R-project.org/package=gtools.

Wickham, H. (2007). Reshaping Data with the reshape Package. Journal of Statistical Software, 21(12), 1-20. URL http://www.jstatsoft.org/v21/i12/.

Wickham, H. (2017). tidyverse: Easily Install and Load the 'Tidyverse'. R package version 1.2.1. https://CRAN.R-project.org/package=tidyverse.

Yamahara, K.M., B.A. Layton, A.E. Santoro, and A.B. Boehm. (2007). Beach sands along the California coast are diffuse sources of fecal bacteria to coastal waters. Environmental Science and Technology, 41: 4515–4521.

CHAPTER 3

FIGURES & TABLES

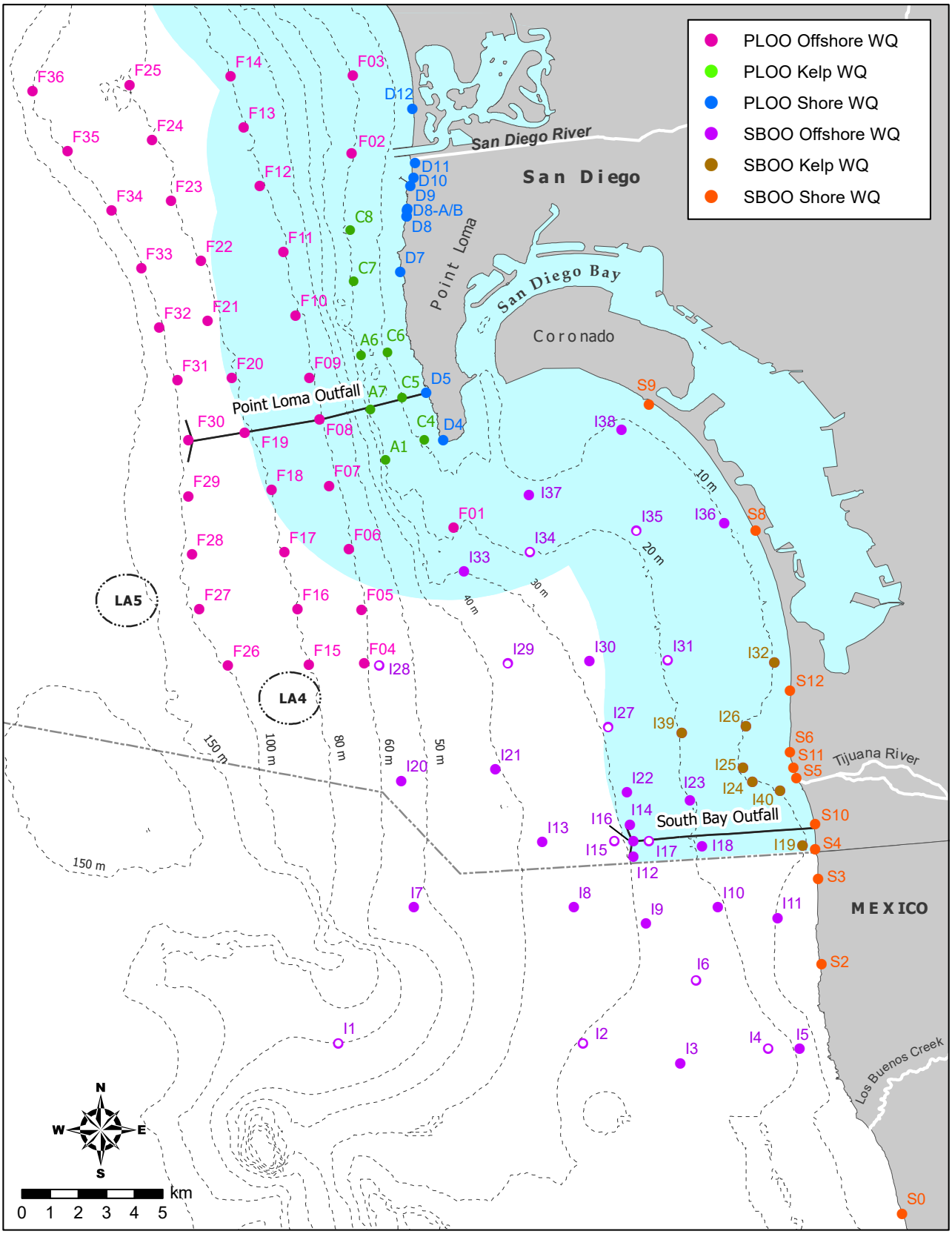


Figure 3.1
Water quality (WQ) monitoring station locations sampled around the PLOO and SBOO as part of the City of San Diego's Ocean Monitoring Program. Open circles are sampled by CTD only. Light blue shading represents State jurisdictional waters.

Box 3.1

Water quality objectives for water contact areas, California Ocean Plan (SWRCB 2019).

A. Bacterial Characteristics – Water Contact Standards; CFU = colony forming units.

(a) *Fecal Coliforms:*
   1) A 30-day geometric mean of fecal coliform density shall not exceed 200 CFU/100 mL, calculated based on the five most recent samples from each site
   2) A single sample maximum of fecal coliform density shall not exceed 400 CFU/100 mL.

(b) *Enterococcus*:
   1) A 42-day geometric mean of *Enterococcus* density shall not exceed 30 CFU/100 mL, calculated weekly
   2) A statistical threshold value of *Enterococcus* density shall not exceed 110 CFU/100 mL in more than 10% of samples per calendar month.

(c) *Total Coliforms:*
   1) The median of total coliform density shall not exceed 70 CFU/100 mL*.
   2) A statistical threshold value of total coliform density shall not exceed 230 CFU/100 mL in more than 10% of samples.

B. Physical Characteristics

(a) Floating particulates and oil and grease shall not be visible.
(b) The discharge of waste shall not cause aesthetically undesirable discoloration of the ocean surface.
(c) Natural light shall not be significantly reduced at any point outside of the initial dilution zone as the result of the discharge of waste.

C. Chemical Characteristics

(a) The dissolved oxygen concentration shall not at any time be depressed more than 10% from what occurs naturally, as a result of the discharge of oxygen demanding waste materials.
(b) The pH shall not be changed at any time more than 0.2 units from that which occurs naturally.

D. A time period is not specified for the total coliforms running median calculation. For the purposes of this report, the median was calculated over a 30-day running window,

Table 3.1

Depths from which seawater samples are collected for bacteriological analysis from kelp and offshore stations.

Station Contour	PLOO Sample Depth (m)								
	1	3	9	12	18	25	60	80	98
Kelp Bed									
9-m	x	x	x						
18-m	x			x	x				
Offshore									
18-m	x			x	x				
60-m	x					x	x		
80-m	x					x	x	x	
98-m	x					x	x	x	x

Station Contour	SBOO Sample Depth (m)							
	2	6	9/11	12	18	27	37	55
Kelp Bed								
9-m	x	x	x[a]					
18-m	x			x	x			
Offshore								
9-m	x	x	x[a]					
18-m	x			x	x			
28-m	x				x	x		
38-m	x				x		x	
55-m	x				x			x

[a] Stations I25, I26, I32, and I40 sampled at 9 m; stations I11, I19, I24, I36, I37, and I38 sampled at 11 m

Box 3.2

Receiving Water Bacterial Compliance (NPDES Permit No. CA0109045, Order No. R9-2021-0011; NPDES Permit No. CA0108928, Order No. R9-2021-0001).

Receiving water monitoring for human marker HF183 and effluent monitoring for fecal indicator bacteria may be required if any of the following conditions are true, and if the source of contamination is unknown.

A. The overall compliance rate with the receiving water limitations for bacterial characteristics is below 90% within a rolling one-year period.
B. A single monitoring location exceeds the bacteria receiving water limitations more than 50% of the time within a rolling one-year period for offshore monitoring locations.
C. A single monitoring location exceeds the bacteria receiving water limitations more than 50% of the time within a rolling quarterly period for kelp/nearshore monitoring locations.

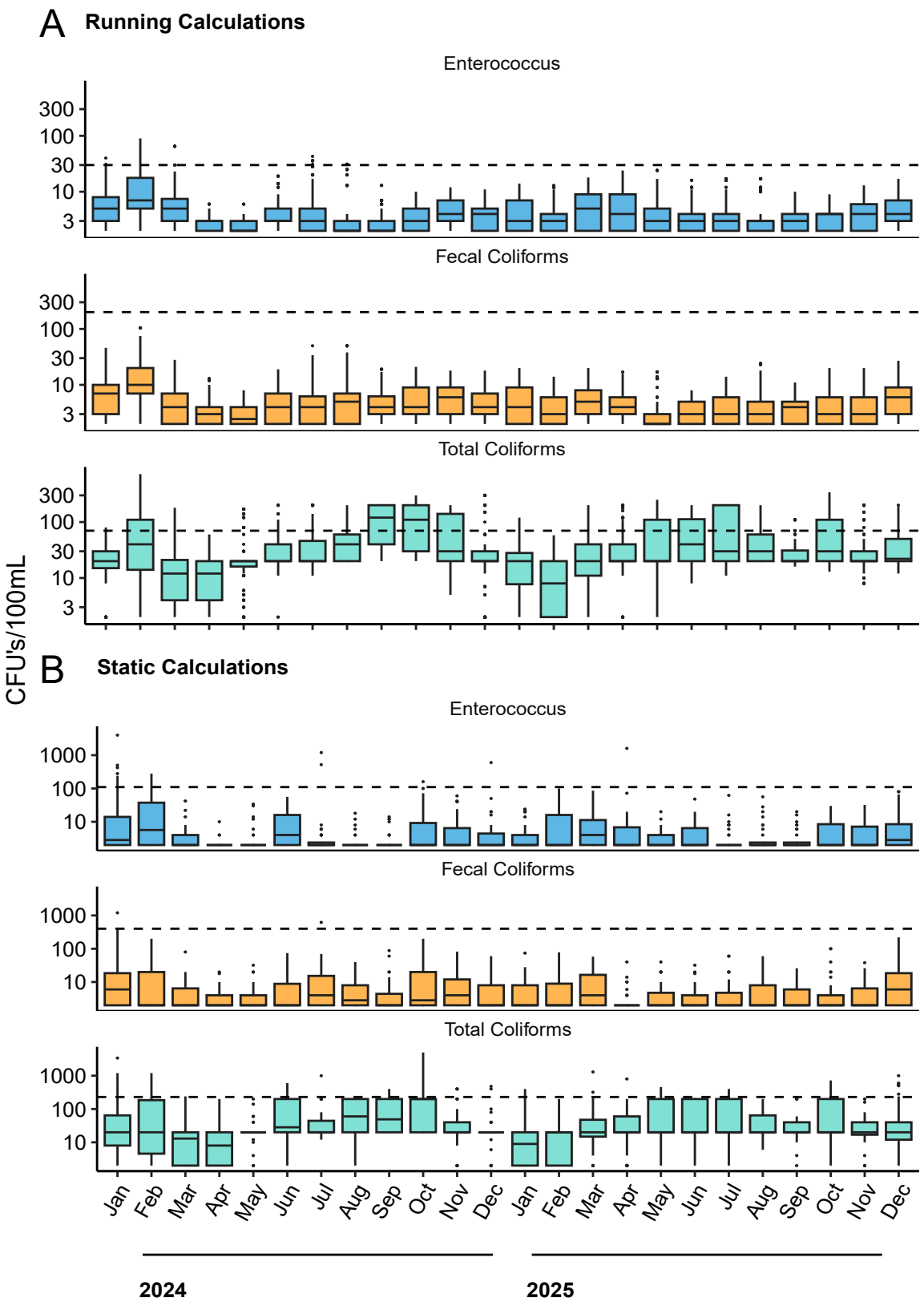


Figure 3.2

Distribution of values at PLOO shore stations across the report period, binned monthly, for (A) running mean and median calculations and (B) single sample values. Dashed line represents the water contact standard compliance threshold*. Boxes = median, upper and lower quantiles; whiskers = 1.5x interquartile range, dots = outliers. *STV compliance is calculated separately and shown in Table 3.2.

Table 3.2

Percent compliance with STV standards across all months in the report period, binned by year and region.

Enterococcus

Year	Project		Jan	Feb	Mar	Apr	May	Jun	Jul	Aug	Sep	Oct	Nov	Dec
2024	**PLOO**	*Shore*	38	88	100	100	100	100	88	100	100	88	100	88
		Kelp	100	100	100	100	100	100	100	100	100	100	100	100
		Offshr	—	75	—	—	75	—	—	92	—	—	75	—
	SBOO	*Shore*	12	0	50	25	25	25	25	25	62	88	50	50
		Kelp	0	14	43	29	57	57	71	86	100	100	71	86
		Offshr	—	100	—	—	100	—	—	100	—	—	90	—
2025	**PLOO**	*Shore*	100	100	100	88	100	100	100	100	100	100	100	100
		Kelp	100	100	100	100	100	100	100	100	100	100	100	100
		Offshr	—	85	—	—	83	—	—	83	—	—	100	—
	SBOO	*Shore*	25	25	62	25	38	50	25	88	62	50	38	25
		Kelp	43	43	71	71	100	100	100	100	29	71	14	43
		Offshr	—	100	—	—	100	—	—	100	—	—	100	—

Total Coliforms

Year	Project		Jan	Feb	Mar	Apr	May	Jun	Jul	Aug	Sep	Oct	Nov	Dec
2024	**PLOO**	*Shore*	38	50	88	100	100	75	88	100	88	88	62	75
		Kelp	100	100	100	100	100	100	100	100	100	100	100	100
	SBOO	*Shore*	0	0	25	25	25	12	12	25	62	62	25	50
		Kelp	0	14	0	0	14	0	57	71	86	86	14	57
		Offshr	—	90	—	—	90	—	—	100	—	—	80	—
2025	**PLOO**	*Shore*	88	100	75	88	75	100	88	100	100	62	100	38
		Kelp	100	88	100	100	100	100	100	100	100	100	100	100
	SBOO	*Shore*	25	25	38	25	38	12	25	50	25	25	12	25
		Kelp	0	0	29	29	57	57	86	100	29	0	0	0
		Offshr	—	50	—	—	100	—	—	100	—	—	90	—

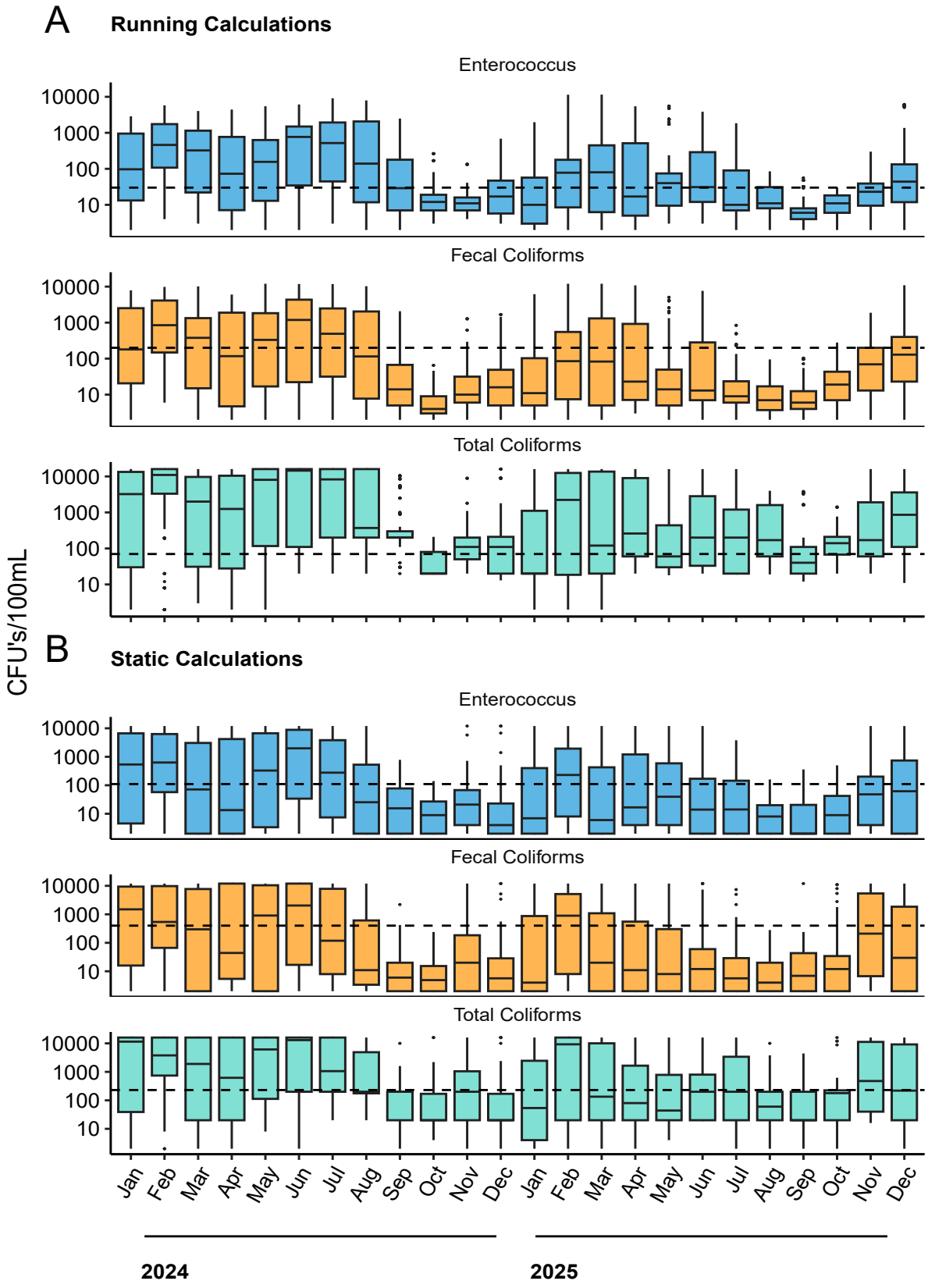


Figure 3.3

Distribution of values at SBOO shore stations across the report period, binned monthly, for (A) running mean and median calculations and (B) single sample values. Dashed line represents the water contact standard compliance threshold*. Boxes = median, upper and lower quantiles; whiskers = 1.5x interquartile range, dots = outliers. *STV compliance is calculated separately and shown in Table 3.2.

Table 3.3

Number of analyses showing elevated FIB (eFIB) collected from shore stations during wet and dry seasons, and percent occuring in the wet season (% wet) during 2024 and 2025. Stations are listed north to south from top to bottom. Stations not listed had no analyses showing elevated FIB during the report period.

		Seasons		
		Wet	Dry	% Wet
PLOO				
	D12	2	0	100
	D11	12	7	63
	D10	6	2	75
	D9	7	0	100
	D8	4	0	100
	D8-B	6	1	86
	D7	2	0	100
	D5	3	0	100
Total eFIB		42	10	81
Total Analyses		1,485	1,032	59
SBOO				
	S9	8	2	80
	S8	12	2	86
	S12	55	37	60
	S6	64	55	54
	S11	82	73	53
	S5	145	84	63
	S10	108	44	71
	S4	93	41	69
	S3	102	33	76
	S2	83	22	79
	S0	167	102	62
Total eFIB		919	495	65
Total Analyses		2,067	1,432	59

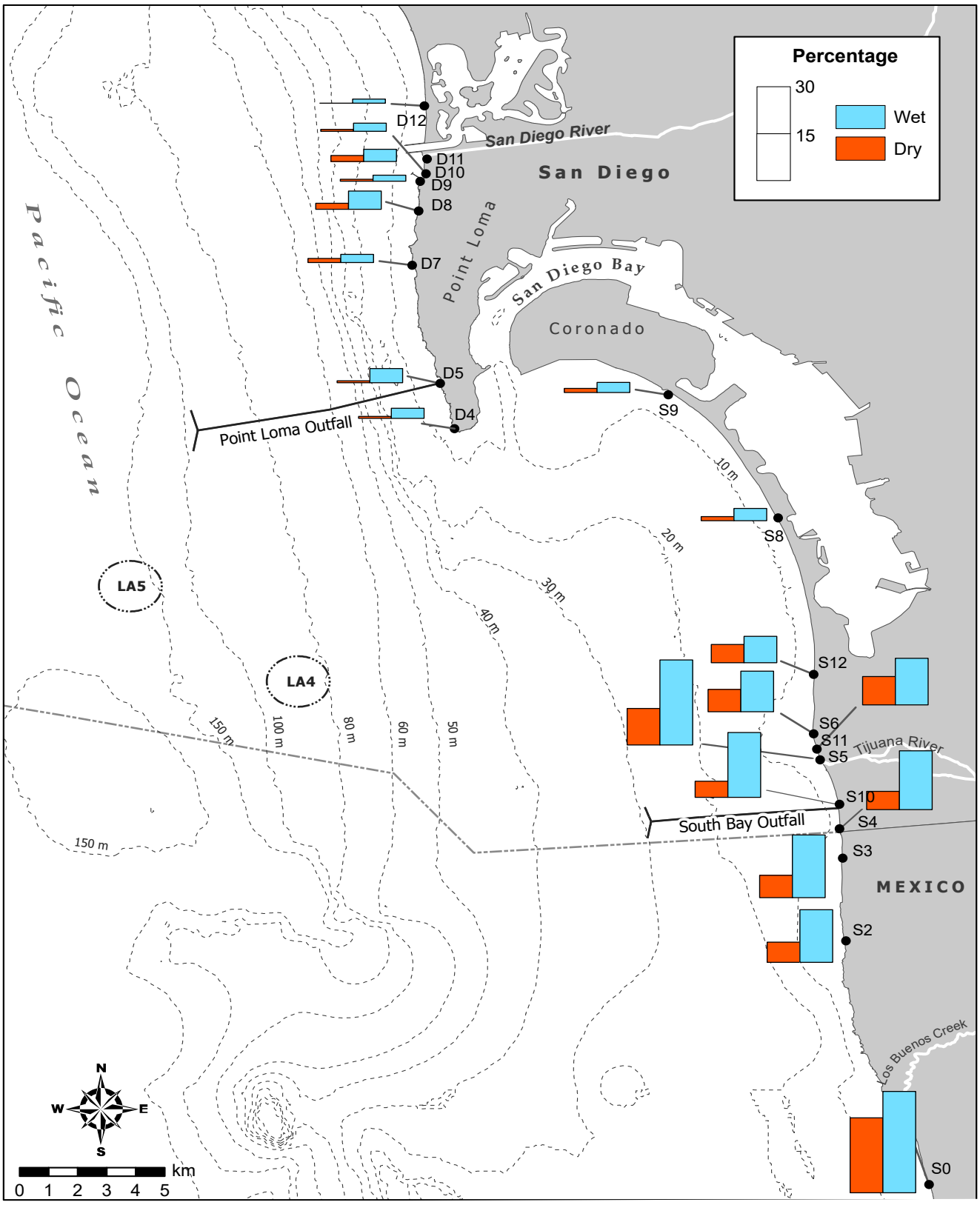


Figure 3.4

Percentage of samples with elevated FIB densities in wet versus dry seasons at shore stations from 1991 through 2025. Shore sampling in the SBOO region began in 1995.

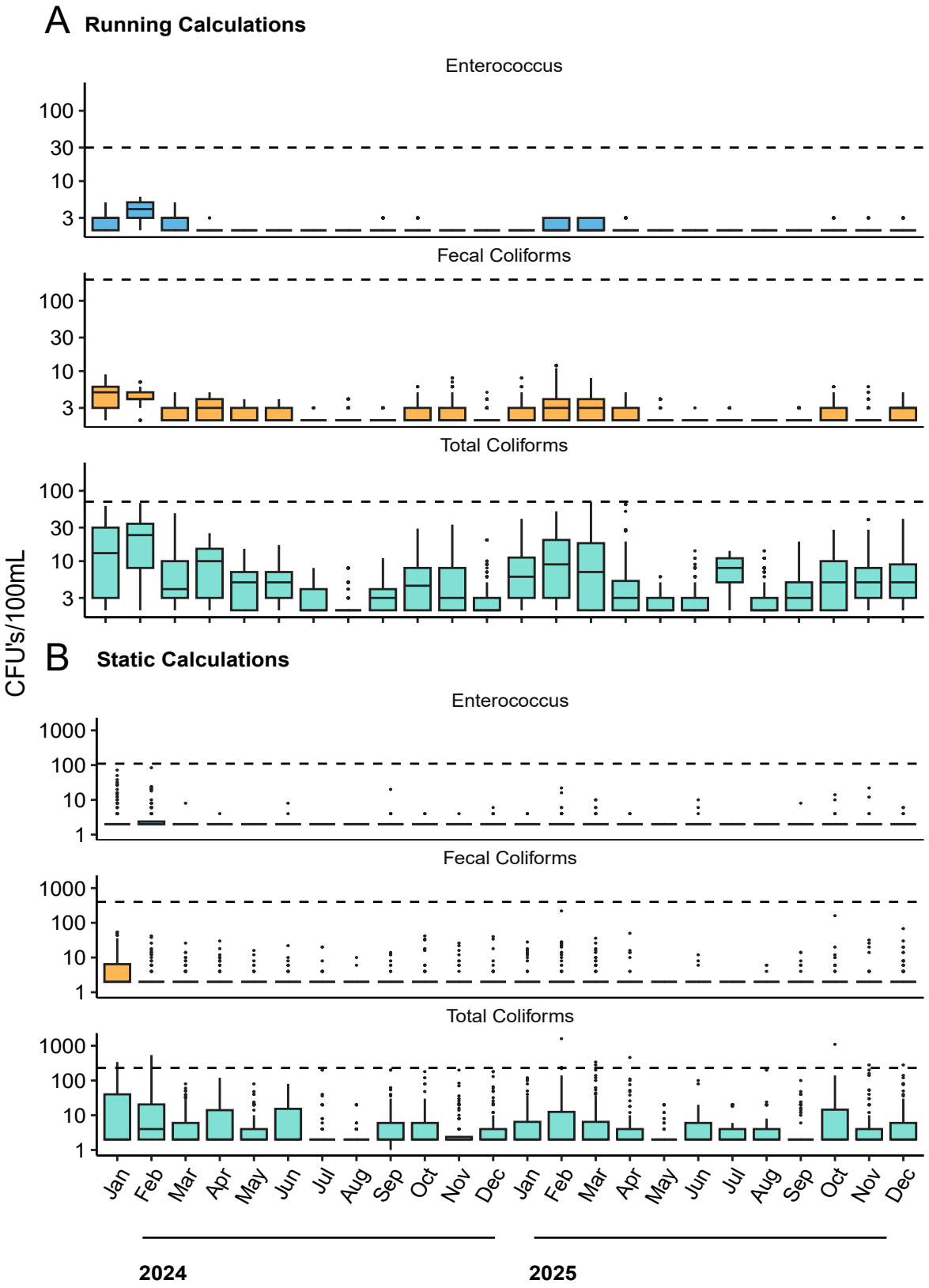


Figure 3.5
Distribution of values at PLOO kelp stations during the report period, binned monthly, for (A) running mean and median calculations and (B) single sample values. Dashed line represents the water contact standard compliance threshold*. Boxes = median, upper and lower quantiles; whiskers = 1.5x interquartile range, dots = outliers. *STV compliance is calculated separately and shown in Table 3.2.

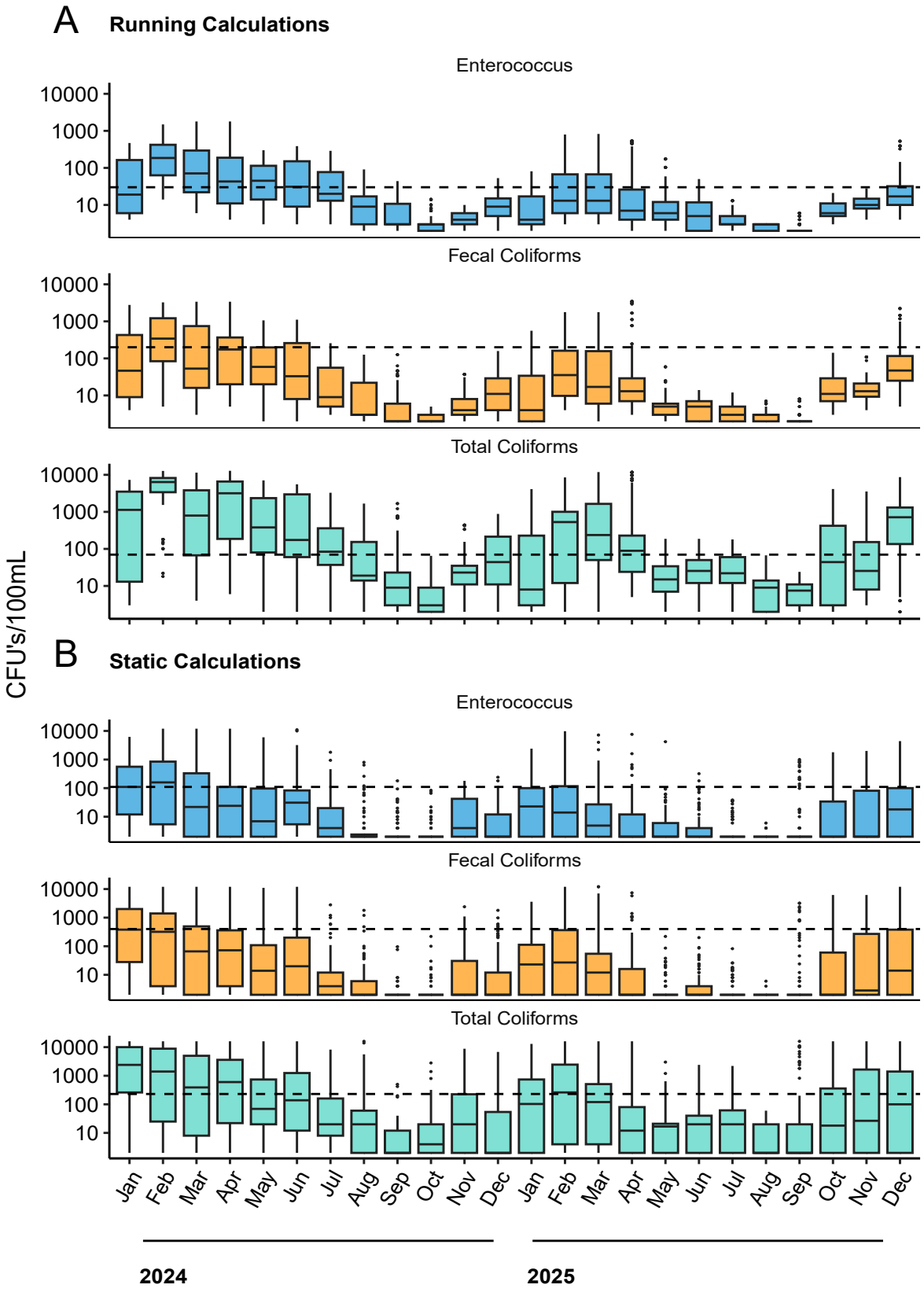


Figure 3.6

Distribution of values at SBOO kelp stations during the report period, binned monthly, for (A) running mean and median calculations and (B) single sample values. Dashed line represents the water contact standard compliance threshold*. Boxes = median, upper and lower quantiles; whiskers = 1.5x interquartile range, dots = outliers. *STV compliance is calculated separately and shown in Table 3.2.

Table 3.4

Number of analyses showing elevated FIB (eFIB) collected from kelp stations during wet and dry seasons, and percent occurring in the wet season (% wet) during 2024 and 2025. Within each contour stations are listed from north to south. Stations not listed had no analyses showing elevated FIB during the report period.

	Seasons		
	Wet	Dry	% Wet
PLOO			
9-m Depth Contour			
C6	1	0	100
18-m Depth Contour			
C8	1	0	100
C7	1	0	100
A6	2	0	100
A7	4	0	100
A1	3	0	100
Total eFIB	12	0	100
Total Analyses	4,392	3,168	58
SBOO			
9-m Depth Contour			
I32	74	44	63
I26	105	19	85
I25	117	17	87
I24	158	27	85
I40	284	74	79
I19	227	73	76
18-m Depth Contour			
I39	52	3	95
Total eFIB	1,017	257	80
Total Analyses	3,843	2,772	58

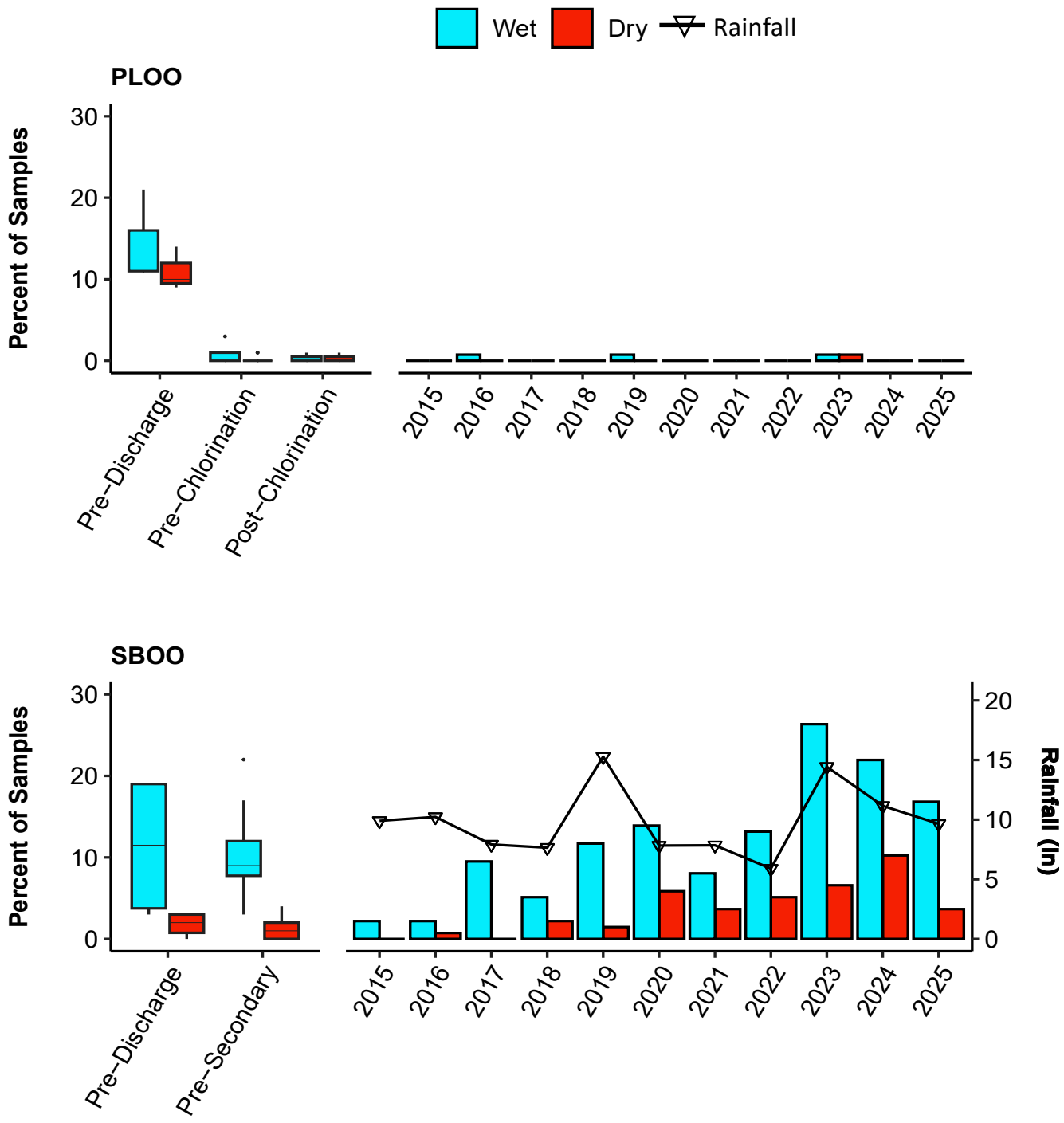


Figure 3.7

Comparison of annual rainfall with occurrence of elevated FIB densities in wet (blue bars) versus dry (red bars) seasons at PLOO and SBOO kelp stations over the last decade. Boxed data show the distriution of % exceedances for each season over monitoring periods pre-dating the last decade. For PLOO, the Pre-Discharge period spanned from 1991 until the extension of the outfall to its current location in 1993. Chlorination of PLOO effluent began in 2008. For SBOO, Pre-Discharge data were collected in 1999, and secondary treatment began in 2011. Rain data are from San Diego International Airport, San Diego, CA.

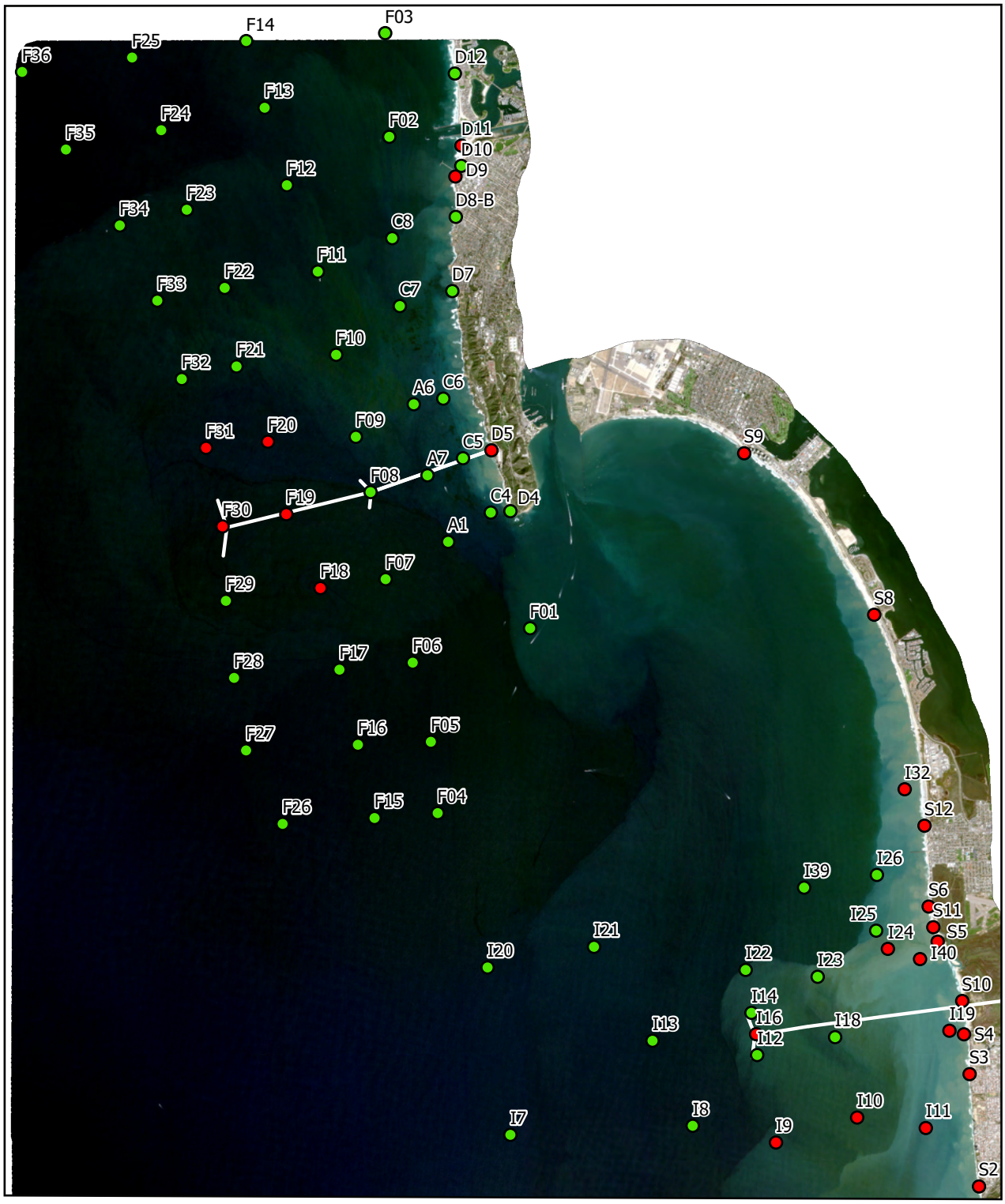


Figure 3.8

Sentinel 2 satellite image captured on February 12th, 2024 (Ocean Imaging 2026) combined with bacteria levels sampled at shore, kelp, and offshore stations sampled between February 6th and 10th. Green circles indicate FIB met and red circles indicate at least one analysis with elevated FIB relative to 2019 OceanPlan thresholds. Station S0 is excluded as it lies outside the southern boundary of the image. Turbid waters followed heavy rains in January and February. In this instance, there is a clear spatial demarcation between FIB exceedances resulting from land-based sources vs oufall-based sources, despite turbidity from the Tijuana River Estuary overlapping visually with the SBOO.

Table 3.5

Number of analyses showing elevated FIB (eFIB) collected from offshore stations during wet and dry seasons, and percent occurring in the wet season (% wet) during 2024 and 2025. Within each contour stations are listed from north to south. Stations not listed had no analyses showing elevated FIB during the report period.

	Seasons		
	Wet	Dry	% Wet
PLOO			
60-m Depth Contour			
F10	1	0	100
80-m Depth Contour			
F25	0	1	0
F23	0	1	0
F22	2	1	67
F21	1	3	25
F20	3	4	43
F19	2	5	29
F18	3	3	50
100-m Depth Contour			
F34	1	0	100
F33	3	3	50
F32	4	3	57
F31	5	3	62
F30	5	5	50
F29	1	2	33
F28	1	2	33
F27	1	1	50
F26	0	1	0
Total eFIB	33	38	46
Total Analyses	564	564	50
SBOO			
9-m Depth Contour			
I36	1	0	100
I11	9	2	82
I5	11	2	85
18-m Depth Contour			
I18	3	0	100
I10	5	1	83
28-m Depth Contour			
I22	1	0	100
I14	1	0	100
I16	4	0	100
I12	3	1	75
I9	7	0	100
I3	3	0	100
38-m Depth Contour			
I21	2	0	100
I13	1	0	100
I8	3	0	100
55-m Depth Contour			
I20	1	0	100
I7	2	0	100
Total eFIB	57	6	90
Total Analyses	756	756	50

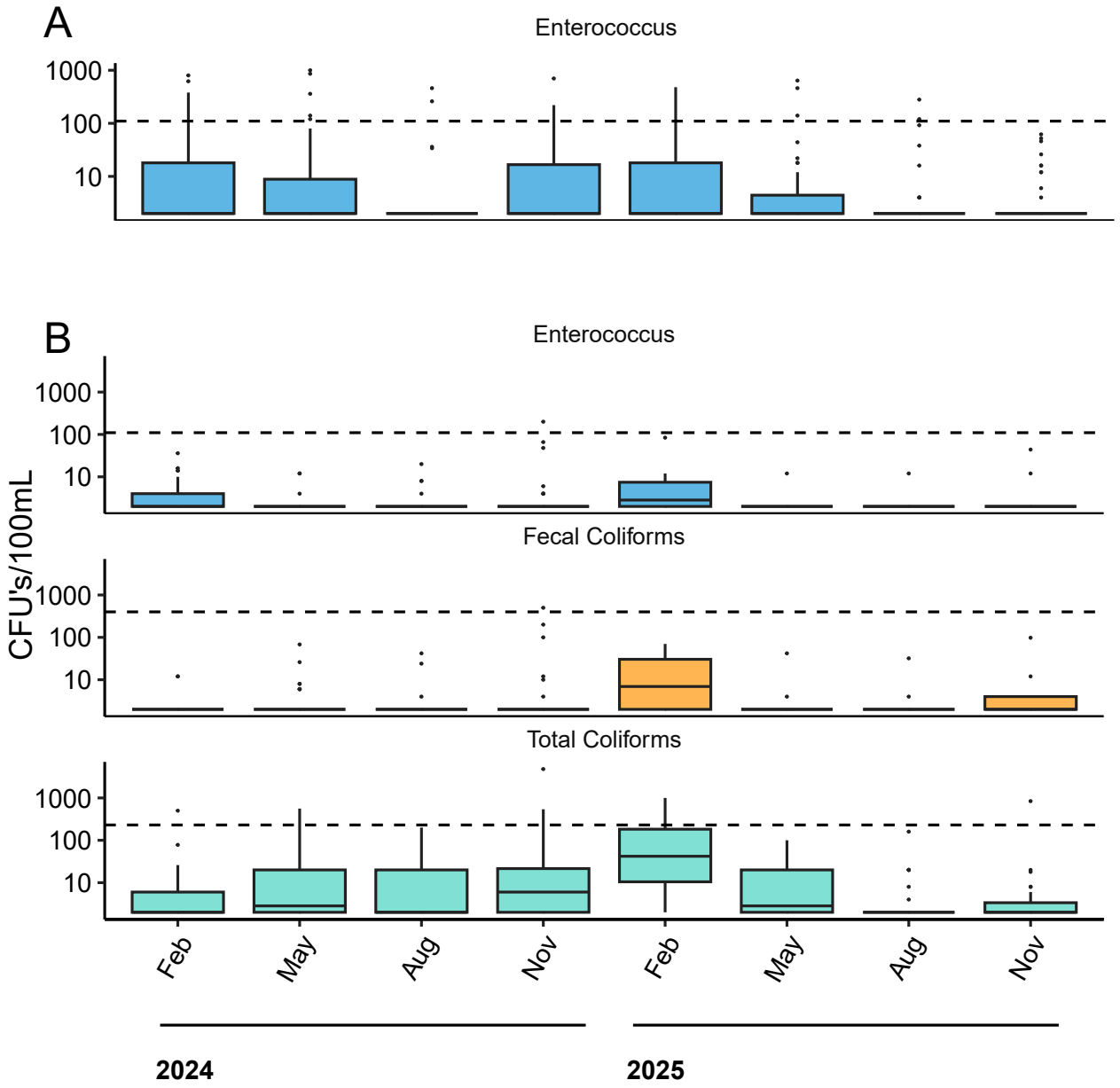


Figure 3.9
Distribution of values for PLOO (A) and SBOO (B) offshore stations during the report period, binned monthly. Dashed line represents the water contact standard compliance threshold*. Boxes = median, upper and lower quantiles; whiskers = 1.5x interquartile range, dots = outliers. *STV compliance is calculated separately and shown in Table 3.2. Only *Enterococcus* is measured at PLOO offshore stations.

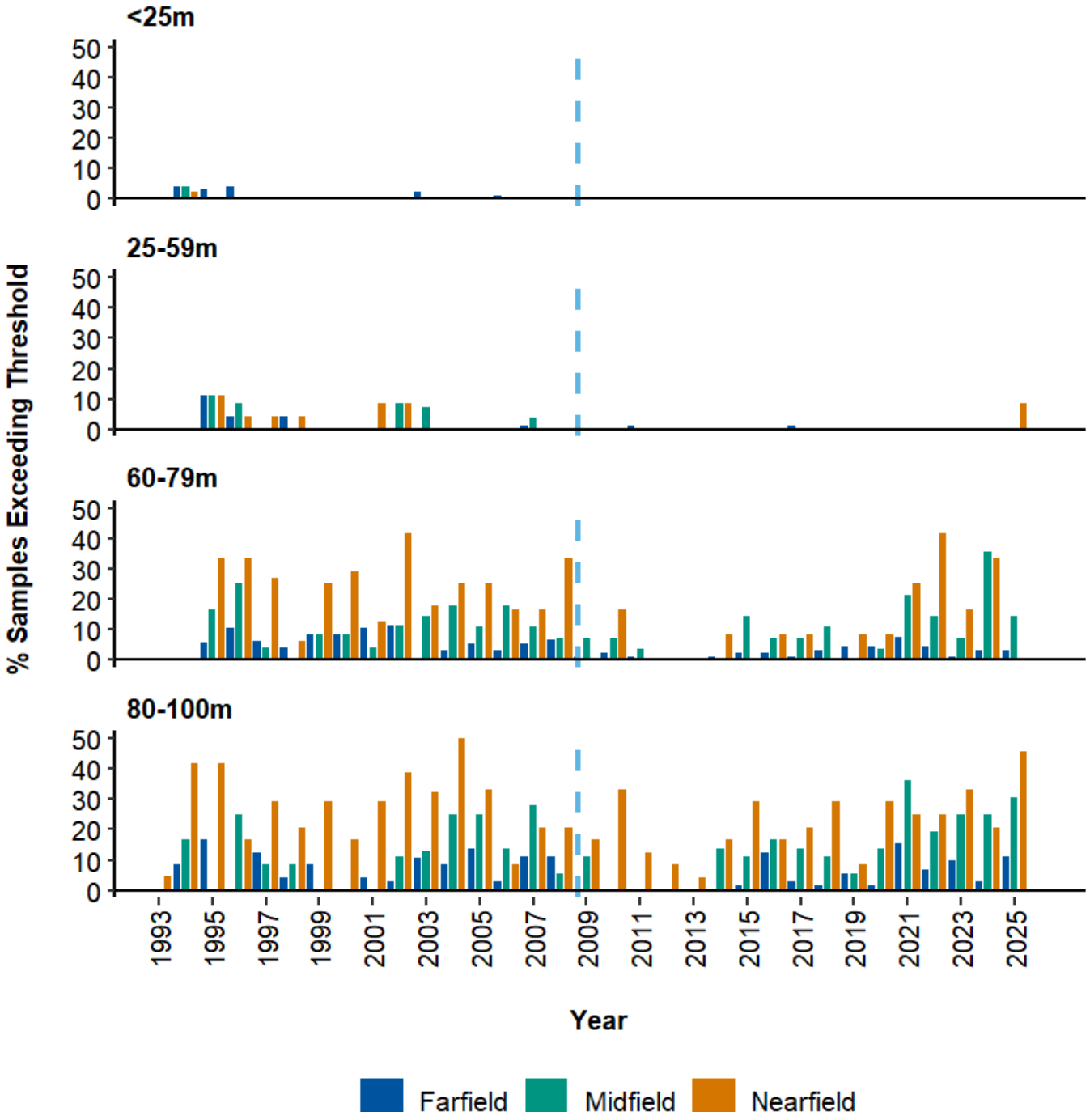


Figure 3.10

Percent of analyses with elevated FIB in samples collected from PLOO offshore stations. Nearfield stations are F29, F30, and F31. Midfield stations, a category not used in other analyses in this report but employed here to provide improved spatial context, include stations F17, F18, F19, F20, F21, F28, and F32. Farfield stations include all other PLOO region offshore "F" stations. The pale blue dotted line marks the onset of chlorination at the PLWTP.

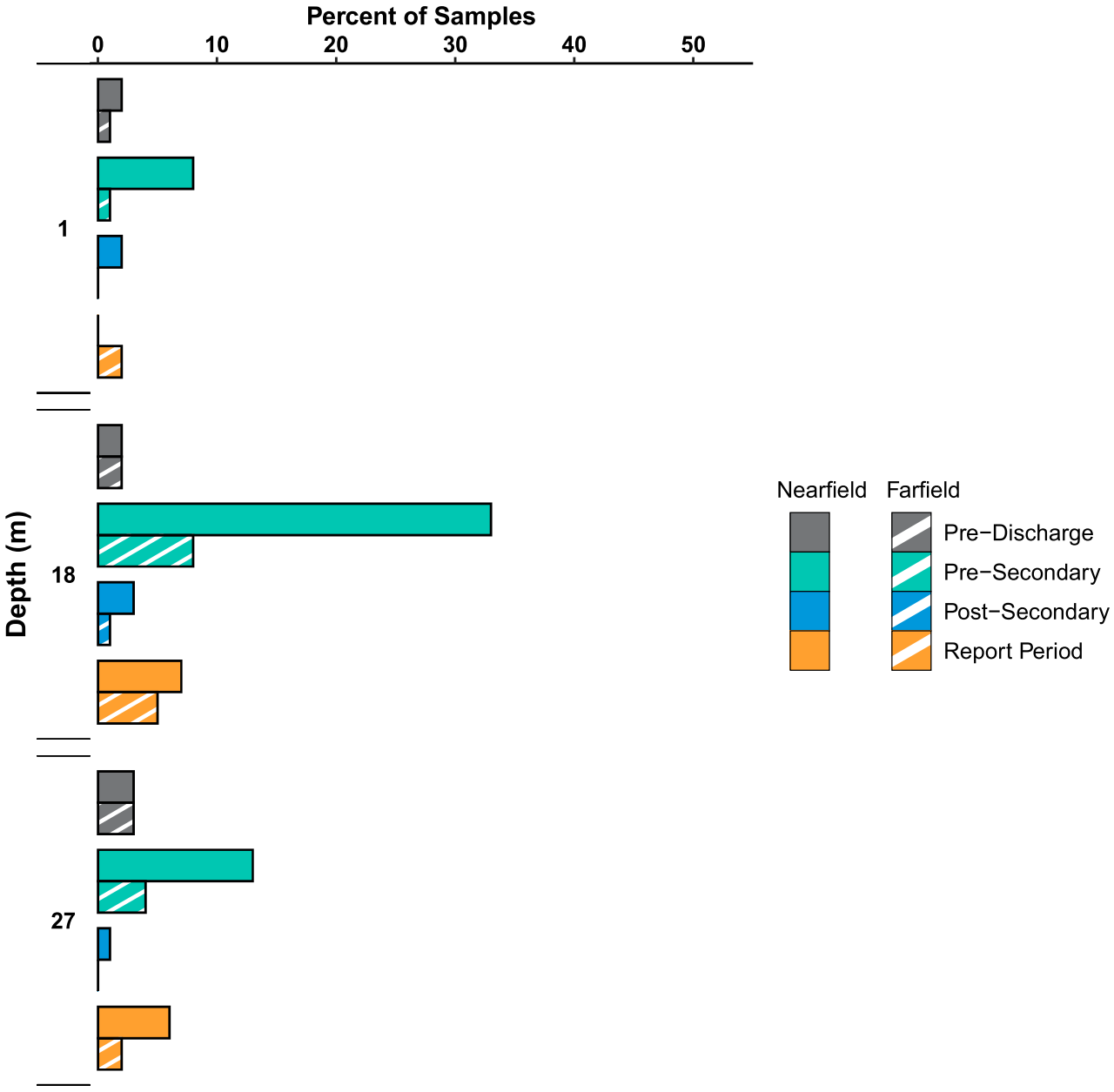


Figure 3.11
Percent of analyses of samples collected from SBOO 28-m offshore stations with elevated FIB. Samples from 2024 and 2025 are compared to those collected since the onset of monitoring in the South Bay in 1995.

Table 3.6

Percent compliance with the HF183 sampling standards, calculated as the proportion of rolling window calculations, taken daily over the report period, showing compliance rates above the threshold established for each metric (90% overall, 50% kelp, 50% offshore). In the case of kelp and offshore compliance metrics, any stations with compliance < 100% are listed individually.

		Fecal Coliforms	Total Coliforms	*Enterococcus*
PLOO				
Overall		100	100	100
Kelp		100	100	100
Offshore		—	—	100
SBOO				
Overall		20	0	0
Kelp	I19	84	56	82
	I24	100	73	100
	I25	100	90	100
	I26	100	93	100
	I40	83	50	74
Offshore		100	100	100

Chapter 4
Plume Dispersion

Chapter 4. Plume Dispersion

Introduction

The City of San Diego (City) collects a comprehensive suite of oceanographic data in nearshore (e.g., kelp forests) and offshore coastal waters surrounding the Point Loma and South Bay Ocean Outfalls (PLOO and SBOO, respectively) to identify the presence of discharged treated wastewater effluent ('plume') and characterize regional water quality conditions. A range of specialized equipment are used to facilitate this data collection both temporally and spatially, including a conductivity, temperature, and depth (CTD) instrument package deployed weekly at nearshore stations, and quarterly at offshore stations; two real-time oceanographic mooring systems (RTOMS) anchored near the terminal ends of the PLOO and SBOO; and a remotely operated towed vehicle (ROTV) deployed quarterly in the PLOO and SBOO regions. The ability to monitor over a large spatial scale using a CTD and continuously in real-time using RTOMS, and to track potential wastewater discharge directly using an ROTV, ensures that the City has the most comprehensive suite of tools available to both assess plume dispersion and predict potential shoreward movement of wastewater plumes.

The specialized equipment utilized for plume tracking comes equipped with auxiliary instruments that help to distinguish an outfall's effluent signal from ambient ocean water. For example, colored dissolved organic material (CDOM) has proven useful in identifying wastewater plumes from the PLOO and SBOO in the San Diego region (Terrill et al. 2009, Rogowski et al. 2012a, b, 2013). The reliability of plume detection can be further improved by combining measurements of CDOM with additional parameters (e.g., low chlorophyll *a* concentrations), thus facilitating evaluation of possible wastewater impacts on coastal waters.

Historically, the City has assessed for the presence of effluent plumes via quarterly CTD surveys alone, which provide discrete measurements over a large spatial scale, but lack the temporal and spatial resolution that may be necessary to fully assess plume behavior and the ocean conditions that impact plume dispersion. Following an independent review of the City's Ocean Monitoring Program (SIO 2004), the Scripps Institution of Oceanography (SIO) was contracted to develop and conduct enhanced monitoring intended to provide an improved understanding of physical circulation and current movement patterns in local coastal waters surrounding the PLOO. Initially, non-telemetered moored temperature loggers (thermistor arrays) and acoustic doppler current profilers (ADCPs) were utilized to characterize the thermocline structure and current regime in the area surrounding the PLOO (Storms et al. 2006). The use of these "static" moorings was later expanded to include both the PLOO and SBOO regions where the resultant data have been a valuable part of the City's annual receiving waters reports (e.g., City of San Diego 2022a).

Subsequent studies of the fate and behavior of wastewater discharged to the ocean via the SBOO (Terrill et al. 2009) and the PLOO (Rogowski et al. 2012a,b, 2013) included recommendations to use RTOMS and advanced mobile sampling technologies (i.e., ROTVs or autonomous underwater vehicles) to better understand nearshore coastal water quality and the impacts of local ocean currents

and tidal fluxes on effluent plume dynamics. The ability to monitor in near real-time is an essential component of wastewater plume tracking, as it provides the City with the opportunity to predict potential shoreward movement of wastewater plumes, which may otherwise present a hazard to people utilizing recreational waters along the shoreline. Furthermore, real-time monitoring allows the City to quickly identify issues with mooring equipment to facilitate long-term maintenance. Used in conjunction with the RTOMS, optimized and adaptive sampling using ROTV surveys can improve evaluation of plume dispersion from outfalls. Based on these recommendations, the City, U.S. Section of the International Boundary and Water Commission (USIBWC), San Diego Regional Water Quality Control Board (SDRWQCB) and U.S. Environmental Protection Agency (USEPA) reached an agreement that real-time monitoring should be developed for the PLOO and SBOO regions. Therefore, between 2017 and 2021, the City developed and carried out the Plume Tracking Monitoring Plan (PTMP) for the Point Loma and South Bay Ocean Outfall Regions (City of San Diego 2018, 2020b). As of July 1, 2021, the PTMP was included as a requirement in the National Pollutant Discharge Elimination System (NPDES) permit for the South Bay International Wastewater Treatment Plant (SBIWTP) and the South Bay Water Reclamation Plant (SBWRP). An updated PTMP was submitted in January 2026 that reflected modifications to improve operational performance and data utility of the ongoing monitoring efforts (City of San Diego 2026a, 2026b).

This chapter presents the preliminary analysis and interpretation of available plume tracking data collected by CTD, RTOMS, and ROTV in 2024 and 2025 in the PLOO and SBOO regions. The primary goals of this chapter are to: (1) provide in-depth evaluations, interpretations, discussions, and conclusions concerning wastewater plume behavior in receiving waters; (2) determine if the wastewater plume is encroaching upon receiving water areas used for swimming, surfing, diving, and shellfish harvesting; (3) assess the fate of the discharged wastewater plume.

Materials and Methods

CTD

Deployment and Configuration

Oceanographic data were collected using a Sea-Bird SBE 25 Plus CTD. The CTD was lowered through the water column at each station to collect continuous measurements of water temperature, conductivity (used to calculate salinity), pressure (used to calculate depth), dissolved oxygen (DO), pH, transmissivity (a proxy for water clarity), chlorophyll *a* fluorescence (a proxy for phytoplankton), and colored dissolved organic material (CDOM). Vertical profiles of each parameter were constructed for each station, per survey, by averaging the data values recorded within each 1-m depth bin (see Chapter 2).

Data Collection

Fifteen stations located in relatively shallow waters within or near the Point Loma or Imperial Beach kelp beds (i.e., referred to as "kelp" stations herein) were monitored weekly to assess water quality conditions and California Ocean Plan (Ocean Plan) (SWRCB 2019) compliance in nearshore areas used for recreational activities such as SCUBA diving, surfing, fishing, and kayaking (Figure 4.1). These included PLOO stations C4, C5, and C6, located along the 9 m depth contour near the inner edge of the Point Loma kelp forest, PLOO stations A1, A6, A7, C7, and C8, located along the 18m depth contour near the outer edge of the Point Loma kelp forest, SBOO stations I25, I26, and I39, located at depths of 9–18 m contiguous to the Imperial Beach kelp bed, and SBOO stations I19, I24, I32, and I40 located in other nearshore waters along the 9 m depth contour.

An additional 69 offshore stations were sampled quarterly over 3 to 4 days in winter (February), spring (May), summer (August), and fall (November) to monitor water quality conditions and to estimate dispersion of the PLOO and SBOO wastewater plumes (Figure 4.1). These included 36 stations surrounding the PLOO, and 33 stations surrounding the SBOO. The PLOO stations are designated F1–F36 and are located along or adjacent to the 18, 60, 80, and 98m depth contours. The SBOO stations are designated I1–I18, I20–I23, I27–I31, and I33–I38, and are located along the 9, 19, 28, 38 and 55m depth contours, respectively. Fifteen of the PLOO stations (F01–F03, F06–F14, F18–F20) and 15 of the SBOO stations (I12, I14, I16–I18, I22–I23, I27, I31, I33–I38) are located within State jurisdictional waters (i.e., within 3 nautical miles of shore) and therefore subject to the Ocean Plan compliance standards (see Chapter 3 for further details).

Data Analyses

Presence or absence of the wastewater plume at the PLOO and SBOO offshore stations was estimated by evaluating a combination of oceanographic parameters (i.e., detection criteria). All stations along the 9 m depth contour were excluded from these analyses, due to the potential for coastal runoff or sediment resuspension in shallow nearshore waters to confound any CDOM signal that could be associated with plume dispersion from the outfalls (see Hess 2026, Appendices C.1, C.2). Previous monitoring results have consistently shown that the PLOO plume remains trapped below the pycnocline with no evidence of surfacing throughout the year (City of San Diego 2020a, Rogowski et al. 2012a, b, 2013, Hess 2019, 2025, 2026). In contrast, the SBOO plume stays trapped below the pycnocline during seasonal periods of water column stratification but may rise to the surface when waters become more mixed and stratification breaks down. Water column stratification and pycnocline depth were quantified using buoyancy frequency (BF, cycles/min) calculations for each quarterly survey. This measure of the water column's static stability was used to quantify the magnitude of stratification for each survey and was calculated as follows:

$$BF = \sqrt{g/\rho} * (d\rho/dz)$$

where g is the acceleration due to gravity, ρ is the seawater density, and dρ/dz is the density gradient (Mann and Lazier 1991). The depth of maximum BF was used as a proxy for the depth at which stratification was the greatest. If the water column was determined to be stratified (i.e., maximum BF > 5.5 cycles/min), subsequent analyses were limited to depths below the pycnocline.

Identification of potential plume signal was determined for each quarterly survey at each monitoring station based on a combination of CDOM, chlorophyll *a*, and salinity levels, as well as a visual review of the overall water column profile. Detection thresholds for the PLOO and SBOO stations were set adaptively for each quarter according to the criteria described in City of San Diego (2016a, b). It should be noted that these thresholds are based on observations of ocean properties specific to the distinct PLOO and SBOO monitoring regions and thus constrained to only those regions. Finally, water column profiles were visually interpreted to remove stations with spurious signals (e.g., CDOM signals near the seafloor that were likely caused by sediment resuspension). All analyses were performed using R (R Core Team 2026) and various functions within the reshape2, Rmisc, RODBC, oce and tidyverse packages (Wickham 2007, Hope 2013, Ripley and Lapsley 2017, Kelley and Richards 2019, Wickham et al. 2019). Further confirmation of these CTD-based parameters as being indicative of the effluent plume was determined by comparison of potential plume detections with fecal indicator bacteria (FIB) data at the same stations and similar depths (see Chapter 3).

The effect of any potential "plume detection" on local water quality, during each quarterly survey, was evaluated by comparing mean values of DO, pH, and transmissivity within the possible plume boundaries to thresholds calculated for the same depths from reference stations. For each quarter, stations with all CDOM values below the 85th percentile of that region's values were considered "reference". Individual non-reference stations were then determined to be out-of-range (OOR) compared to the reference stations if values exceeded narrative water quality standards defined in the Ocean Plan (see Chapter 3, Box 3.1). For example, the Ocean Plan defines OOR thresholds for DO as a 10% reduction from naturally occurring concentrations, for pH as a 0.2 pH unit change, and for transmissivity as below the lower 95% confidence interval from the mean. For purposes of this report, "naturally" is defined for DO as the mean concentration minus one standard deviation (see Nezlin et al. 2016).

RTOMS

Deployment and Configuration

The RTOMS are anchored buoys suspended in the water column configured with a range of instruments, collecting near continuous oceanographic data and providing near real-time information of changing conditions. The RTOMS are outfitted with a series of instruments at various depths throughout the water column (see Chapter 2, Table 2.1). Critical parameters that were measured on a real-time basis included temperature, conductivity (salinity), total pH, DO, dissolved carbon dioxide (xCO_2), nitrate (nitrate + nitrite), chlorophyll *a*, CDOM, backscatter (turbidity), and current direction and velocity. Parameters were recorded at 10-minute intervals, with the exception of nitrate + nitrite and xCO_2, which were recorded at 1-hour intervals.

Data Collection

Two RTOMS were anchored near the terminal ends of the PLOO and SBOO (nearfield), at a distance far enough from the diffuser ports to be outside the area of active plume rise. The PLOO RTOMS was anchored at a depth of approximately 95 m, just east of the northern diffuser leg, and the SBOO RTOMS was anchored at a depth of approximately 30 m, just west of the southern diffuser leg terminus (Figure 4.1). Each mooring was deployed for a period of approximately one year, with a gap in the PLOO deployment from mid-December 2024 to mid-April 2025 due to instrument service delays from manufacturers and staffing shortages (see Chapter 2).

In addition, temperature and ocean current data from static moorings were used to supplement data gaps between RTOMS deployments (see Chapter 2, Appendix B.2). These non-telemetered (static) upward-facing bottom-mounted ADCPs (Teledyne RD Instruments 300 KHz Workhorse Monitor) and thermistor (Onset Tidbit temperature loggers) string arrays were moored near the RTOMS at the terminal ends of the PLOO and SBOO (Figure 4.1; see Chapter 2 for details).

Data Processing and Analysis

Prior to conducting analyses, RTOMS data were subject to a comprehensive suite of quality assurance/quality control (QA/QC) procedures following Quality Assurance of Real-Time Oceanographic Data (QARTOD) methodologies (see Chapter 2). After review, all data that were flagged as suspect or bad were excluded from further analyses and are not presented in this report.

Ocean current data analyses were performed in R (R Core Team 2026) using functions within various packages (i.e., Rmisc, mixOmics, tidyverse, scales, pracma, and gtools) (Hope 2013, Le Cao et al. 2017, Wickham et al. 2019, Wickham and Seidel 2020, Borchers 2021, Warnes et al. 2021). Specifically, after

data QA/QC, tidal frequency data were removed using the PL33 filter (Alessi et al. 1984), compass corrected from magnetic to true north (NOAA/NCEI 2026) and then hourly averaged. Plots and analyses for all other RTOMS data were completed in MATLAB (2022). Contour plots were generated for parameters with sufficient vertical coverage in the water column using default settings, which display fixed isolines and fill areas between isolines with constant colors. Density calculations and temperature-salinity plots were created using the SEAWATER toolbox library for MATLAB, version 3.3.1 (Morgan and Pender 2014).

Temperature gradients were evaluated from RTOMS and thermistor data to illustrate daily and seasonal changes in thermal stratification. Vertical gradients were calculated by the daily average temperature difference between adjacent sensors in the water column (e.g., from 6 to 10 m at thermistor arrays) and then divided by the depth between sensors. Depths of the maximum daily temperature gradients were used to evaluate stratification, with moderate stratification defined as greater than 0.2°C/m gradients. Ocean conditions during ROTV surveys were evaluated by calculating the maximum temperature difference (from surface to bottom sensor) and the maximum thermocline depth was described as the sensor depth with the greatest temperature gradient.

During time periods when the wastewater effluent plumes overlap with the fixed locations of the RTOMS, observations may be assessed for potential plume detections. In order to compare potential freshwater signals from effluent plumes to background ocean salinity levels, time series anomalies of RTOMS salinity were calculated and compared to historical salinity data from CTD surveys. Since there were no equivalent moorings deployed in similar ocean water masses to use as a farfield reference site on the same time scale, this approach provided a baseline comparison to typical salinity ranges by region and depth. The historical CTD salinity data included data from the last two decades (2001–2025) and excluded data from nearfield stations (F29, F30, F31 for PLOO; I12, I14, I15, I16 for SBOO). Historical CTD data averages and percentiles were calculated within a similar depth range for each mooring sensor (1–3 m for the surface bin for both RTOMS; other target depths spanned ±3 m for PLOO and ±1 m for SBOO). Salinity anomalies from RTOMS data were then calculated as the difference between the historical CTD average for each depth range and the daily means for each RTOMS sensor depth. Relatively low subsurface salinities (33.2–33.5 Practical Salinity Unit [PSU]) are frequently observed in the San Diego region (City of San Diego 2024), likely influenced by seasonal evaporation at the surface and the incursion of the low salinity and low temperature Pacific Subarctic water mass within the California Current System (Lynn and Simpson 1987, Jones et al. 2002). Therefore, RTOMS salinity anomalies were compared to minimum CTD salinity observations at each depth range using the 99th percentile, in order to assess for high likelihood of potential influence from freshwater effluent plumes. In addition, average salinities across the region were lower than normal in the winter and early spring in 2024, continuing from summer and fall in 2023 (see Chapter 2; City of San Diego 2024). Therefore, mean CTD salinity from farfield stations for each quarterly CTD survey in 2024 was calculated for comparison to 2024 RTOMS data.

While previous studies in the region used salinity signatures to estimate effluent dilution near outfalls (e.g., Washburn et al. 1992), more recent work has improved upon the impracticality of discerning effluent plumes using salinity signatures alone by examining additional identifying characteristics such as elevated CDOM (Rogowski et al. 2012a, b, 2013, City of San Diego 2016a, 2022a, 2024). Preliminary analyses of other parameters (i.e., CDOM, turbidity, nitrate + nitrite) that may aid in potential plume detections by the PLOO and SBOO RTOMS are presented, where an example is highlighted for each site along with challenges in deciphering plume signals. The primary goals of the RTOMS data are to evaluate

oceanographic conditions in receiving waters and provide information on factors that influence plume dispersion (City of San Diego 2026a). Further work will be completed to evaluate potential wastewater plume evaluations by RTOMS to continue to refine and improve this monitoring approach.

ROTV

Deployment and Configuration

The ScanFish III is a wing-shaped ROTV that is towed behind the sampling vessel using a "live-wire" tow cable with ethernet communication capabilities to surface computing platforms aboard the sampling vessel. The surface computing platforms control the ROTV and process, display, and record data as the data are collected. Using surface communication, the ROTV can be programmed to sample a variable depth range in the water column, moving in an undulating pattern from ocean surface to seabed, or moving in a fixed depth or terrain-following mode. Its large payload enables a variety of modular sensors to be outfitted to the vehicle frame. The City's current package includes a Sea-Bird SBE-25 Plus CTD with a Sea-Bird pump, temperature, conductivity (salinity), and DO sensors, a Sea-Bird SeaOwl sensor with CDOM, chlorophyll, and turbidity channels, a Sea-Bird WetStar fluorometer (CDOM), and three Turner Designs Cyclops-7F fluorometers tuned for CDOM, chlorophyll and optical brightener (OB) measurements, and a Chelsea Uvilux biochemical oxygen demand (BOD) sensor (uses tryptophan proxy for BOD).

During all surveys, vessel speed while towing the ROTV was kept below 11 knots. The tow cable payout varied from 200 to 600 m depending on the depth of the transect and vessel speed. Data from the ROTV were continuously monitored in real-time to ensure instrument function. Fathometer readings from both the ROTV and the shipboard instruments were also closely monitored to ensure capture of the largest possible portion of the water column without damage to the ROTV. To prevent altimeter errors, the ROTV was typically flown no less than 10–15 m below the surface in the deeper PLOO region, and 5m below the surface in the SBOO region, as shallow depths have been determined to be a cause of altimeter failure. To prevent collision with the seafloor, the ROTV was kept 2-5 m from the bottom.

Data Collection

ROTV surveys are conducted on a time- and resource-permitting basis, with effort made to complete 2—4 surveys per year in both the PLOO and SBOO regions (City of San Diego 2026a). In 2024, ROTV surveys were conducted in the PLOO region on March 1, March 4—6, and December 3—5 and in 2025 on March 5 and 10, August 27, December 18 and 23. In the South Bay region, surveys were conducted on March 7 and December 5 in 2024, and on March 10, August 26, September 15, and December 22 in 2025. SBOO region surveys are typically more limited in scope than PLOO region surveys due to the increased risk of damage to the equipment associated with subsurface fishing gear and other obstructions on the bottom. Survey extent varied among dates due to weather conditions, vessel availability, instrument troubleshooting, and operational constraints specific to each outfall region (see City of San Diego 2026b).

Survey strategy prioritized identification and characterization of wastewater plume extent. Initial transects targeted the expected plume location based on prior observations, tidal conditions, and available current information, with staff adjusting the survey extent adaptively based on real-time findings. Each transect aimed to capture the longitudinal (north to south) extent of the plume when observed by monitoring changes in the output of sensors detecting plume-associated signals such as CDOM and OB (Cao et al. 2009). When time permitted and equipment was performing as expected, additional transects were conducted inshore and offshore of the outfall depth contour to characterize cross-shore (east to west) plume extent, with priority generally placed on capturing the inshore plume boundary.

Operational constraints differ between regions. In the SBOO region, the presence of submerged fishing gear requires visual inspection for floats or buoys in each survey area prior to deployment to reduce entanglement risk, increasing the time needed to prepare in advance of each transect. In the PLOO region, surveys were often lengthy due to the large spatial extent of detectable plume signals and the broader area requiring investigation. Depending on field conditions and instrument performance, between one and four transects were typically completed per survey day. At times, equipment failures occurred that could not be resolved within the survey window, resulting in shortened surveys and less coverage of sampling area. Despite operational inefficiencies associated with ROTV deployment and troubleshooting, the approach provided substantially greater vertical and horizontal sampling resolution compared to conventional CTD profiling, with approximately 3–4 times greater vertical resolution and 2–4 times greater horizontal spatial coverage achievable within a comparable survey period.

Data Processing and Analysis

Data from the ROTV were processed and displayed shipboard in real-time while staff monitored for potential plume detection and equipment malfunction. For analyses presented herein, distinct longitudinal transects were extracted from the data via timestamp and named for the average fathometer depth recorded over the duration of the transect, rounded to the nearest 5m. Values outside of climatological ranges established for RTOMS QA/QC were flagged as suspect and removed prior to analysis, as were data that appeared suspect upon initial manual review. For example, CDOM values equal to zero were found to be due to instrument malfunction and were therefore removed. Sensor observations were aligned in time manually to account for differences in sensor response time and pump lag by comparing downcast and upcast values across matched depth bins. A single pump lag value was assigned to each pumped parameter, respectively. Variability in pump lag across surveys may result in some minor misalignment in downcast versus upcast readings. Data from the ROTV surveys were processed and analyzed using the R statistical programming language (R Core Team 2026), employing functions from several packages including tidyverse, fields, and marelac (Wickham et al. 2019; Nychka et al. 2021; Soetaert et al. 2020). To visualize the spatial structure and extent of plume-associated signals observed during individual transects, interpolated contour plots were generated for each surveyed isobath over the water column. Interpolated surfaces were generated from the irregularly spaced observations using thin plate spline interpolation implemented through the R package *fields* (Nychka et al. 2021). Interpolation was constrained to the observed sampling domain to reduce extrapolation into unsampled regions. Interpolated color contour maps were overlaid with the actual ROTV tow path and associated raw data values within the water column to allow visual comparison between interpolated surfaces and the underlying observations. Thermocline depth was calculated for each transect independently using ROTV temperature readings to provide a visual indicator of stratification. Common color scales were applied among transects within individual survey days to facilitate qualitative comparison of plume structure, vertical distribution, and spatial extent among transects. Parameter- and region-specific color scales were standardized across all surveys within a region using global plotting limits defined by the distribution of values (bounded by the 2nd and 98th percentiles) across the report period. This facilitates qualitative comparison of plume structure, signal intensity, vertical distribution, and spatial extent across transects and survey dates within each region.

Data Reporting

CTD and RTOMS data collected during 2024 were reported previously (City of San Diego 2025a), and all raw data (collected by CTD, RTOMS, and ROTV surveys) for the 2024-2025 sampling period have been submitted to either the Regional Water Quality Control Board, the California Environmental Data Exchange Network (CEDEN) or the City's Open Data Portal (City of San Diego 2026c) and may be accessed upon request.

Results and Discussion

Potential Plume Signals Determined via CTD

PLOO Region

The dispersion of the treated wastewater plume from the PLOO and its effects on natural light (percent transmissivity), DO, and pH levels were assessed by evaluating the results of 328 CTD profile casts performed in 2024 and 2025. Based on the criteria described previously (City of San Diego 2016a, b), potential evidence of a plume signal was detected 68 times during the report period from 24 different stations, while between 7 to 16 stations were identified as reference sites during each quarterly survey (Table 4.1, Figure 4.2, Appendix C.1-C.3). In total, about 21% of the total number of casts (n = 328) showed possible plume detections. Overall, the variation in plume dispersion observed near Point Loma in 2024 and 2025 appeared similar to flow-mediated dispersal patterns reported previously for the region (Rogowski et al. 2012a, b, 2013).

The width and rise height of potential PLOO plume detections varied between stations throughout the year (Figure 4.3, Appendix C.3). In general, the plume was detected between a depth of 37 and 98 m (average depth = 70 m) and exhibited a width between 1 and 43 m (average width = 10 m). Despite fluctuations in depth of the pycnocline, plume detections remained below 37 m even during periods of weak water column stratification. Additionally, detection depths were similar between nearfield and farfield stations when excluding chlorophyll blooms. This finding aligns with historical satellite imagery observations that have not shown visual evidence of the plume surfacing (e.g., Svejkovsky 2010, Hess 2019, 2025, 2026).

Of the 68 potential plume signals that occurred during the reporting period, a total of 41 out-of-range (OOR) events were identified at various stations throughout the year, which consisted of 32 OOR events for natural light and 7 OOR events for DO (Table 4.1, Appendix C.3). Representative quarterly profiles from station F30 are shown in Appendices C.4–C.11. There were no OOR events for pH. Nine of the natural light OOR events and two of the OOR events for DO occurred at nearfield stations. None of the DO or natural light OOR events occurred at stations located within State jurisdictional waters where Ocean Plan compliance standards apply.

SBOO Region

The dispersion of the SBOO plume and its effects on natural light, DO and pH levels were assessed by evaluating the results of 232 CTD profile casts performed in 2024 and 2025. Potential evidence of a plume signal was detected 30 times during the reporting period from 14 different stations, while between 6 to 15 stations were identified as reference sites during each quarterly survey (Table 4.1, Figure 4.2). In addition to chlorophyll blooms (surface production), plume signals at SBOO farfield stations can also be associated with terrestrial sources of CDOM. For example, stations I23 and I27 are located within the possible influence of Tijuana River outflows.

The width and rise height of potential SBOO plume detections varied between stations throughout the reporting period (Figure 4.3, Appendix C.12). Unlike the observations at the PLOO, potential SBOO plume signals were detected throughout the water column, ranging from a depth of 2 to 15 m (average depth = 12 m) and a width of 3 to 11 m (average width = 4 m). Potential plume detection depths in the SBOO region were similar between nearfield and farfield stations, except in February of 2024 where no nearfield plumes were detected (Figure 4.3)

The effects of the SBOO wastewater plume on the three physical water quality indicators described above were calculated for each station and depth where a possible plume signal was detected (Table 4.1, Appendix C.12). Representative profiles from station I12 are shown in Appendices C.13–C.20. Of the 30 potential plume signals that occurred during the reporting period, a total of 19 OOR events were identified for transmissivity, while 5 OOR events occurred for DO. There were no OOR events for pH. Five of the natural light OOR events and one of the DO OOR events occurred at nearfield stations. Fifteen of the natural light OOR events and five of the DO OOR events occurred at stations within State jurisdictional waters where Ocean Plan compliance standards apply.

Receiving Waters Conditions and Potential Plume Signals Determined via RTOMS

Receiving Waters Conditions

Ocean conditions surrounding the PLOO and SBOO RTOMS that could potentially affect the dispersion of wastewater plumes, such as ocean currents and density structure of the water column, were generally within historical ranges and align with expected seasonality patterns for the region (see Chapter 2; Terrill et al. 2009, Rogowski et al. 2012a, City of San Diego 2022c).

Changes in ocean stratification are primarily influenced by water column temperature structure in the region, where larger differences in temperature between depths (thermal gradients) result in stronger stratification (see Chapter 2; Bowden 1975, Jackson 1986, Pickard and Emery 1990). The weakest thermal stratification (<0.2°C/m) was observed during late fall and early winter months (December through February) in 2024 and 2025, with daily maximum thermal gradients occurring more frequently at mid to deep depths (PLOO: 10–60m; SBOO: 10–22m) (Appendix C.21). Conversely, moderate (>0.2°C/m) to strong (>0.5°C/m) daily thermal stratification persisted from spring to fall (April through October) in 2024 and 2025 more frequently at shallower depths (PLOO: <10 to 20m; SBOO: <10m), with more variability in stratification occurring during transition months in the spring and fall (March and November) of both years. As described in the CTD results in this chapter, previous monitoring results have consistently shown that the PLOO plume remains at depth even during periods of weak stratification, while the SBOO plume has a greater likelihood of reaching the surface during these periods when the water column is more mixed (Figure 4.3).

Ocean currents predominantly flowed along a north-northwest/south-southeast axis of variation near the PLOO and SBOO (see Figures 2.14, 2.15, 2.16, Appendices C.22, C.23). Generally, along-coast currents tended to dominate, regardless of season although in 2025 there were several northeast-southwestern excursions in the PLOO region (see Chapter 2, Appendix B). These periods were unlikely to impact the dispersion of the plume as these layers were generally above the pycnocline. Variability in currents occurred throughout 2024 to 2025, with distinct periods of predominantly N:NW and S:SE directed currents throughout the water column from days to weeks at a time (Appendices C.22, C.23). Transitions in current direction and speed often indicate a shift in local conditions that may also result in further

mixing of the water column, especially when there is increased vertical shear (i.e., one section of the water column moving in a different direction than the other part of the water column) (see Pickard and Emery 1990). Additionally, ocean currents in the vicinity of the outfalls can influence the initial rise height and horizontal dispersion of the wastewater effluent plumes, as well as the rate of transport of effluent out of the discharge area on longer time scales (days to weeks) (City of San Diego 2022b).

PLOO Region

At the PLOO RTOMS, the lowest salinity values (daily average values <33.1 PSU) were observed from 45 to 89 m in the winter, summer and fall in 2024 and in the summer and fall in 2025, and in the upper water column (< 30 m) in the winter in 2024 (see Chapter 2, Figure 2.8). Anomalously low salinity measurements from the PLOO RTOMS have occurred at deep depths throughout prior deployments regardless of season and are lower than what has historically been reported from CTD data or the more recent ROTV surveys (Figure 4.4). In addition, these depths of lowest salinities overlapped with other observations of potential PLOO plume rise heights (Figure 4.3; Rogowski et al. 2012a). Given the proximity of the mooring to the PLOO, these low salinity values at deep depths (>45 m) may likely be attributable to the effluent plume. Additionally, the observations by the RTOMS of lower-than-normal salinities in deep waters in nearfield sites near the PLOO were likely due to the increased frequency of sampling that captured a larger range of variability, as well as a potential reduction in mixing between the freshwater effluent plume and ocean water masses by the equipment itself. For example, the mooring instruments are suspended passively in the water column at a fixed location, while large towed or profiling packages such as the ROTV or CTD rosette may result in turbulence and additional mixing as moved through the water (e.g., Paver et al. 2020). Given these factors, it is expected that the potential presence of the plume may be better discerned using salinity at the RTOMS as a supplement to other methods. With an exception during the reporting period, during September through October 2023, salinity values at nearly all RTOMS depths approached or exceeded minimum CTD salinity observations (99th percentile) (Figure 4.4). Notably, in late 2023, salinity values across the region were lower than typical seasonal patterns due to a regionwide shift in ocean conditions (see Chapter 2), which was reflected in lower-than-normal mean CTD salinity (open red circles in Figure 4.4). Therefore, the anomalously low salinity observed by RTOMS in late 2023 at shallow and mid-depths aligned with regional ambient salinity at the time and is unlikely to be related to the effluent plume.

Auxiliary measurements from RTOMS, such as CDOM, were also assessed to assist with possible plume detection. Time periods with a strong potential for plume detection (e.g., low salinities at typical plume depths) and fewer confounding factors (such as during dry periods or low phytoplankton concentrations) may be targeted initially to identify other possible plume characteristics. As one example, near the PLOO in early March 2024, possible plume detections were evident from low salinity values at depths from 75 to 89 m (Figure 4.5). Beginning March 7, the plume appeared to be advected away from the sensors, likely influenced by an earlier shift to a more prominent south-easterly current. During the same period, no clear changes in CDOM and turbidity levels were evident at the deepest depth (89 m) (Figure 4.5). Nitrate + nitrite measurements were relatively low for this time period of potential plume detections compared to other periods (Appendix B.12, City of San Diego 2024), and values increased with the shift to higher salinity waters, likely associated with upwelling (Figure 4.5). This pattern aligns with the typical PLOO effluent's relatively low nitrate proportion of nitrogen (see City of San Diego 2024–2026a, CSWRCB 2024). This range falls within a similar range of ambient ocean nitrate levels (see Weber et al. 2021). Generally, higher nitrate levels were observed in cold, high salinity water masses during winter 2024, while very slightly elevated CDOM levels tended to occur at warmer temperatures and lower salinities (Figure 4.6). This supports the role of upwelling in bringing cold, saline, nutrient-rich, oxygen-

poor water masses into the region (see Chapter 2, Weber et al. 2021). Overall, salinity observations, used in conjunction with CDOM, turbidity, and chlorophyll *a* levels may provide potential evidence of effluent plume signals at the PLOO RTOMS and further work will be completed to better evaluate these detections throughout the year.

SBOO Region

At the SBOO RTOMS, the detection of potential SBOO plume signals was not discernable solely by examining salinity values. Low salinity anomalies were observed across depths from January to March in 2024 (Figure 4.4), which coincided with regionwide low salinities as described above. In order to target possible plume characteristics, time periods were examined in the same manner as the PLOO RTOMS data (e.g., during dry periods and low phytoplankton concentrations) where other auxiliary parameters were available. As one example, during early December 2025 near the SBOO, weak stratification and southerly currents occurred on the same days as observations of slightly reduced salinity near the surface (1 m) (Figure 4.7). Additionally, these lower salinity periods coincided with slightly elevated CDOM and nitrate + nitrite levels at the surface, while these characteristics were not observed at the deepest sensor depth (26 m) of the mooring (Figure 4.7). Taken together, these near surface signals may be attributed to effluent plume influence. In addition, high resolution satellite monitoring captured a surfacing event related to the SBOO wastewater plume during this same one-week period (Figure 4.8). Typically, the highest number of SBOO effluent surface plumes detected by satellite occur from November to January during periods of weak stratification. In 2024, there were 22 days in which the SBOO surface plume was evident by satellite while in 2025, there were 19 days (Hess 2025, 2026).

Elevated CDOM levels were generally observed with slightly lower salinities at the surface during winter 2024 and 2025 (Figure 4.9). While the highest nitrate + nitrite levels corresponded to the highest salinities and coldest temperatures at the surface, likely due to upwelling, slightly elevated nitrate + nitrite levels occurred at the lowest salinities (Figure 4.9). In contrast to the PLOO, treated effluent from the SBWRP and SBIWTP discharged through the SBOO generally contained concentrations of nitrate higher than ambient ocean nitrate levels (for effluent levels, see City of San Diego 2024–2026b, CSWRCB 2024; for ocean levels, see Weber et al. 2021). Depending on the conditions and mixing regime, nitrate may be another potential indicator of SBOO plume presence. However, other confounding factors such as coastal runoff and influence from the Tijuana River estuary may also bring water masses into the region that are less saline, CDOM, and nutrient-rich, resulting in a complex environment in the SBOO region (Hess 2019, 2025, 2026). The main goals of the RTOMS data include providing information on oceanographic conditions that influence plume dispersion and supplementing evaluation of potential SBOO plume signals that can be mapped spatially with satellite imagery and ROTV surveys. Further analyses with RTOMS data and other available data will be completed in the future to address these challenges with determining potential SBOO plume signals.

Potential Plume Signals Determined via ROTV

Instrumentation

Multiple sensor technologies were evaluated concurrently for CDOM and chlorophyll to assess agreement among instruments and support future optimization of the monitoring platform. Agreement between Turner CDOM and SeaOwl CDOM measurements was generally strong, with both sensors identifying similar plume structures and spatial patterns. Turner CDOM data plots for all transects conducted during the report period are provided (Appendix C.24, C.25). In contrast, the WetStar CDOM sensor exhibited comparatively poor alignment with other CDOM measurements and experienced sensor

malfunction during portions of the study period. Chlorophyll fluorescence measurements from the Turner and SeaOwl sensors also showed broadly similar spatial structure, although absolute measurement ranges differed between instruments. Turner chlorophyll measurements were used preferentially in subsequent analyses due to closer agreement with values observed in RTOMS and CTD datasets. Tryptophan fluorescence measurements were discontinued in early 2024 due to persistent data quality issues and hardware limitations. BOD measurements were collected during portions of the study period; however, persistent sensor performance issues prevented reliable interpretation, and these data were excluded from subsequent analyses.

PLOO Region

Wastewater plume signals were successfully detected during all completed PLOO ROTV surveys (Table 4.2). Plume-associated signals were consistently observed below 30 m depth and were most typically found at 40-80m depth. On several survey dates, plume signals remained detectable at the longitudinal limit of completed transects, indicating that reported plume widths likely represent minimum observed extents rather than complete characterization of plume boundaries. Observations suggest that stratification and relatively weak ambient currents exert substantial influence on plume transport and spatial extent in the PLOO region. Alongshore plume displacement frequently aligned with the dominant alongshore current direction, even during periods characterized by weak measured current velocities, indicating that persistent low-velocity transport may substantially influence plume position over time.

In the PLOO region on December 4, 2024, the 90 m transect was surveyed twice under differing tidal conditions (Figure 4.10). Plume concentration and overall spatial extent were broadly similar between the morning and afternoon surveys, with some variation in the vertical distribution in the plume. During the morning flood tide survey, plume-associated signals extended upward to approximately 40 m depth, whereas during the afternoon survey, conducted later in the ebb tide cycle, the plume signal was largely confined below approximately 60 m depth. The plume was also detected along the 105 m transect shortly following the transition to ebb tide, but was not observed along the 80 m transect despite sampling occurring near peak flood tide conditions. Alongshore and cross-shore currents were relatively weak throughout the survey period, suggesting that vertical mixing and stratification likely exerted greater influence on plume structure than short-term current variability during this event. Relatively weak thermocline strength observed during this survey may have enhanced dilution to reduce detectability outside of the immediate vicinity of the outfall.

SBOO Region

Potential plume signals were successfully detected during all completed SBOO ROTV surveys (Table 4.3). Compared to the PLOO region, plume expression in the SBOO region was generally shallower and exhibited greater variability in both depth and lateral extent among surveys. During periods of weak stratification, plume-associated signals occasionally approached near-surface waters. Surveys conducted during periods of stronger stratification exhibited broader and more spatially coherent plume signatures. This pattern suggests that reduced vertical mixing during strongly stratified conditions may substantially enhance detectable plume persistence and lateral extent within the SBOO region.

Elevated background CDOM and optical brightener signals observed during the March 10, 2025 survey were corroborated by satellite imagery collected that day, which showed widespread shore-associated discoloration extending offshore beyond the 25 m bathymetric contour (Figure 4.11). These conditions followed substantial precipitation during the preceding week and suggest that land-based runoff and nearshore contamination may have contributed substantially to the elevated background fluorescence signals observed during the survey. Surveys conducted in August and September 2025 coincided temporally with the period immediately preceding and during planned increased flows from the South Bay International Wastewater Treatment

Plant (SBIWTP). Comparison of plume structure and fluorescence signatures between these surveys did not reveal an obvious increase in plume extent or intensity associated with the planned flow increase. However, interpretation is complicated by differences in oceanographic conditions, including substantially stronger stratification during the August survey, as well as potential interference from shore-associated contamination visible in satellite imagery collected during both survey periods (Figure 4.12, Figure 4.13) (Ocean Imaging 2026). Interpretation is further limited by the occurrence of intermittent elevated flows associated with infrastructure failures and maintenance activities prior to November 2024, which reduced the ability to establish a clearly defined baseline condition preceding planned flow increases. Additional surveys spanning a broader range of environmental conditions and operational flow states are needed to determine whether planned increased SBIWTP flows measurably affect plume characteristics in the SBOO region.

In the SBOO region on December 22, 2025, the 30 m transect was surveyed twice under differing tidal conditions (Figure 4.14). During the morning survey, conducted during flood tide conditions, plume-associated fluorescence signals appeared stronger and more coherent than during the afternoon repeat survey, which occurred approximately 2–2.5 hours following the transition to ebb tide. Plume signals were not clearly detected along the 20 m transect despite sampling occurring near peak flood tide conditions, nor were plume signals observed along the 35 m transect following the transition to ebb tide. Thermocline strength during this survey was relatively weak, highlighting the potential for vertical mixing to enhance dilution and dispersion of the plume, reducing detectability across transects.

Summary

Historically, the City has evaluated the fate and dispersal of treated wastewater effluent plumes through quarterly and weekly monitoring of a fixed grid of stations utilizing CTD instrumentation and bacteriological evidence (e.g., City of San Diego 2024). Although this technique covers a large spatial area, the infrequent temporal sampling rate limits observations to just a few "snapshots" in time. This limited timeframe may not capture sporadic events, such as storm-driven transport or other oceanographic phenomena. To address this issue, the City installed non-telemetered ADCP and thermistor instrumentation to document hydrographic conditions in the immediate vicinity of the outfalls over much finer timescales (Storms et al. 2006). Although variable over space and time, the general axes of current velocities were consistently observed to follow N:NW and S:SE trajectories with occasional excursions along the northeast-southwest axes. This has indicated that as effluent mixes with ambient seawater, it generally travels along the coast rather than being directed inshore toward the shoreline, kelp beds, or other recreational waters. These types of ADCP data have improved temporal coverage of conditions in the area; however, the 4-month recovery cycle for the data rendered it useful only to understand events in retrospect and did not include auxiliary measurements for potential plume characterization.

More recently, real-time data have become available via the City's RTOMS, which incorporate a variety of sensors at multiple depths providing near-continuous information from a single platform. These observations have enhanced the assessment of environmental conditions and the potential impacts of oceanographic and anthropogenic events in coastal waters. While it is not possible to understand the dispersion and spatial extent of plumes using RTOMS alone, these near-continuous data may show potential vertical spread of plumes as well as events that would otherwise be missed by fixed grid surveys. For example, they provided the ability to capture SBOO effluent plume surfacing events that aligned with observations from satellite monitoring (Figure 4.8, Hess 2026). In addition, these high

frequency data at a single, fixed location provide context on the state and variability of the receiving waters into which the PLOO and SBOO discharge. For example, the rise height of the effluent plume is highly dependent on density structure and stratification of the water column, as well as ambient currents (Rogowski et al. 2012a, b, 2013, City of San Diego 2022b, c). Stronger currents may result in greater initial mixing while weaker currents may result in shallower rise heights depending on stratification. Other local ocean dynamics, such as internal waves, can result in further mixing and impact observed plume rise heights (Rogowski et al. 2012a). These data can be further used to validate predictive models that seek to characterize changes, which may cause environmental degradation. While initial RTOMS results presented show examples of potential indicators of effluent plume signals, one challenge remains: there is no equivalent farfield reference mooring station in similar water masses to use for comparison at the same time scales. Thus, it is difficult to confirm plume presence as well as any possible plume effects on DO, pH, or natural light water quality indicators (also note that moorings are located outside State jurisdictional waters where Ocean Plan compliance standards do not apply). To strengthen the ability to discern plume signals, further analyses are planned.

In addition to the limitations in the temporal resolution of fixed grad sampling, spatial extent and resolution are also limited in the fixed-grid method. In order to produce a more focused and higher resolution method for tracking plumes over a large spatial scale, and to complement the findings of the RTOMS, the City deploys an ROTV with an array of sensors chosen for their ability to characterize plume distribution. In the 2024-2025 survey period, survey methods were improved to allow greater use of the ROTV in the SBOO region, though challenges associated with shallow survey and risk of entanglement with kelp and underwater fishing gear remain.

ROTV observations during the report period indicate that PLOO plume signals were consistently deep, spatially extensive, and frequently extended beyond the offshore survey grid, whereas SBOO plume expression was generally shallower and appeared more sensitive to small changes in stratification and circulation. Across both regions, plume displacement frequently aligned with dominant alongshore current direction, even during periods of relatively weak measured current velocities, suggesting that persistent low-velocity transport substantially influences plume position over time. Stronger stratification generally coincided with broader and more spatially coherent plume signatures. These observations are consistent with reduced vertical mixing under strongly stratified conditions, allowing plume waters to remain confined within narrower density layers and maintain detectable fluorescence signatures over greater horizontal distances.

Despite the different spatial and temporal coverages of the CTD, RTOMS, and ROTV instrument packages utilized by the City, all observations from 2024–2025 demonstrated that the Point Loma effluent plume generally remained offshore below a depth of 30 m, and was transported along the coast. This finding concurs with prior plume tracking studies (Rogowski et al. 2012a, b, 2013), as well as historical satellite imagery observations that have not shown visual evidence of the plume surfacing (e.g., Svejkovsky 2010, Hess 2019, 2025, 2026). These observations support previous studies showing that there is no evidence that wastewater discharged to the ocean via the current configuration of the PLOO has ever reached the shoreline or had any significant impact on recreational waters (City of San Diego 2022b, c).

Within the shallower SBOO region, past studies have shown that other sources, such as coastal runoff from rivers and creeks, were more likely to impact coastal water quality than wastewater discharge from the outfall, especially during and immediately after significant rain events (Svejkovsky and Jones

2001, Terrill et al. 2009). Bacteriological analyses indicate widespread and persistent reduced water quality in the region for the last several years, with contamination from known sources including runoff following wet-weather events and dry-weather transboundary flows through the Tijuana River Estuary and San Antonio de Los Buenos Creek associated with infrastructure failures in Tijuana, Mexico. These factors confound efforts to decipher SBOO effluent plume signals from other coastal influences. While the SBOO plume generally stays trapped below the pycnocline during seasonal periods of water column stratification, it may rise to the surface when waters become more mixed and stratification breaks down (Terrill et al. 2009, Hess 2019, 2025, 2026, City of San Diego 2020a, 2024). However, given predominant along-shore currents, it does not appear that wastewater discharged via the SBOO reaches the shoreline or impacts recreational waters, particularly compared to other coastal inputs (Largier et al. 2004, Terrill et al. 2009).

In addition to oceanographic and coastal processes, policy changes also introduced potential impacts to water quality in the SBOO region. During the reporting period, the International Boundary and Water Commission (IBWC) proposed to increase flows to the SBOO by 10 MGD starting August 24th, 2025. Subsequently, approximately 5MGD of additional flows, comprising of effluent treated to advanced primary standards, were added to SBIWTP discharge in September–November of 2025 to relieve pumping constraints in the Tijuana system and enable diversion of sewage away from the Tijuana River. Additional flows have been scaled back since November 2025 due to storm-related interruptions and system maintenance and repair. Increased flows are expected to resume and reach up to 10MGD in 2026. This prompted heightened vigilance during plume survey efforts at the SBOO, and additional ROTV surveys were added in August and September 2025, before and after the planned change, respectively. To date, the impact of these increased flows appears negligible on receiving water conditions and did not yield detectable changes in plume characteristics. However, more observations are needed to overcome limitations in interpretation associated with variability in oceanographic conditions and effluent volume over the course of the City's plume tracking monitoring program.

Literature Cited

Alessi, C.A., R. Beardsley, R. Limeburner, and L.K. Rosenfeld. (1984). CODE-2: Moored Array and Large-Scale Data Report. Woods Hole Oceanographic Institution Technical Report. 85–35: 21.

Borchers, H.W. (2021). pracma: Practical Numerical Math Functions. R package version 2.3.3. https://CRAN.R-project.org/package=pracma.

Bowden, K.F. (1975). Oceanic and Estuarine Mixing Processes. In: J.P. Riley and G. Skirrow (eds.). Chemical Oceanography, 2nd Ed., Vol.1. Academic Press, San Francisco, CA. p 1–41.

Cao, Y., J.F. Griffith, and S.B. Weisberg. (2009). Evaluation of optical brightener photodecay characteristics for detection of human fecal contamination. Water Research, 43(8), 2273–2279.

City of San Diego. (2016a). Point Loma Ocean Outfall Annual Receiving Waters Monitoring and Assessment Report, 2015. City of San Diego Ocean Monitoring Program, Public Utilities Department, Environmental Monitoring and Technical Services Division, San Diego, CA.

City of San Diego. (2016b). South Bay Ocean Outfall Annual Receiving Waters Monitoring and Assessment Report, 2015. City of San Diego Ocean Monitoring Program, Public Utilities Department,

Environmental Monitoring and Technical Services Division, San Diego, CA.

City of San Diego. (2018). Plume Tracking Monitoring Plan for the Point Loma and South Bay Ocean Outfall Regions, San Diego, California. Submitted by the City of San Diego Public Utilities Department to the San Diego Water Board and USEPA, Region IX, March 28, 2018 (approved 4/25/2018).

City of San Diego. (2020a). Biennial Receiving Waters Monitoring and Assessment Report for the Point Loma Ocean Outfall and South Bay Ocean Outfall, 2018-2019. City of San Diego Ocean Monitoring Program, Public Utilities Department, Environmental Monitoring and Technical Services Division, San Diego, CA.

City of San Diego. (2020b). Plume Tracking Monitoring Plan Progress Report for the Point Loma and South Bay Ocean Outfall Regions, San Diego, California; Report Period: January – December 2019. Submitted by the City of San Diego Public Utilities Department to the San Diego Water Board and USEPA, Region IX, March 3, 2020.

City of San Diego. (2022a). Biennial Receiving Waters Monitoring and Assessment Report for the Point Loma and South Bay Ocean Outfalls, 2020–2021. City of San Diego Ocean Monitoring Program, Public Utilities Department, Environmental Monitoring and Technical Services Division, San Diego, CA.

City of San Diego. (2022b). Appendix D. Plume Behavior and Tracking Summary. In: Report of Waste Discharge and Application for Renewal of NPDES CA 0107409 and 301(h) Modified Secondary Treatment Requirements. Volume VI, Appendices D–G. Public Utilities Department, San Diego, CA.

City of San Diego. (2022c). Appendix P. Oceanography. Appendix Q. Initial Dilution Simulation Models. In: Report of Waste Discharge and Application for Renewal of NPDES CA 0107409 and 301(h) Modified Secondary Treatment Requirements. Volume X, Appendices O–U. Public Utilities Department, San Diego, CA.

City of San Diego. (2024). Biennial Receiving Waters Monitoring and Assessment Report for the Point Loma and South Bay Ocean Outfalls, 2022–2023. City of San Diego Ocean Monitoring Program, Public Utilities Department, Environmental Monitoring and Technical Services Division, San Diego, CA.

City of San Diego. (2024–2026a). Monthly Monitoring Reports for the Point Loma Wastewater Treatment Plant and Ocean Outfall, January 2024–December 2025. City of San Diego, Public Utilities Department, Environmental Monitoring and Technical Services Division, San Diego, CA.

City of San Diego. (2024–2026b). Monthly Monitoring Reports for the South Bay Water Reclamation Plant and Ocean Outfall, January 2024–December 2025. City of San Diego, Public Utilities Department, Environmental Monitoring and Technical Services Division, San Diego, CA.

City of San Diego. (2025a). Interim Receiving Waters Monitoring Report for the Point Loma and South Bay Ocean Outfalls, 2024. City of San Diego Ocean Monitoring Program, Public Utilities Department, Environmental Monitoring and Technical Services Division, San Diego, CA.

City of San Diego. (2025b). Plume Tracking Monitoring Plan Progress Report for the Point Loma and

South Bay Ocean Outfall Regions, San Diego, California; Report Period: January – December 2024. Submitted by the City of San Diego Public Utilities Department to the San Diego Water Board and USEPA, Region IX, March 1, 2025.

City of San Diego. (2026a). Plume Tracking Monitoring Plan for the Point Loma and South Bay Ocean Outfall Regions, San Diego, California. Submitted by the City of San Diego Public Utilities Department to the San Diego Water Board and USEPA, Region IX, January 31, 2026 (approved 4/25/2018).

City of San Diego. (2026b). Plume Tracking Monitoring Plan Progress Report for the Point Loma and South Bay Ocean Outfall Regions, San Diego, California; Report Period: January – December 2025. Submitted by the City of San Diego Public Utilities Department to the San Diego Water Board and USEPA, Region IX, March 1, 2026.

City of San Diego. (2026c). Ocean Monitoring Program Reports and Data. https://www.sandiego.gov/public-utilities/sustainability/ocean-monitoring/reports

[CSWRCB] California State Water Resources Control Board, Office of Information Management and Analysis (2024). California Integrated Water Quality System Project, Water Quality Effluent Electronic Self-Monitoring Report (eSMR) Data. https://data.ca.gov/dataset/water-quality-effluent-electronic-self-monitoring-report-esmr-data.

Hess, M. (2019). Satellite & Aerial Coastal Water Quality Monitoring in the San Diego/Tijuana Region: Annual Summary Report 1 January 2018 – 31 December 2018. Littleton, CO.

Hess, M. (2025). Satellite & Aerial Coastal Water Quality Monitoring in the San Diego/Tijuana Region: Annual Summary Report 1 January 2024 – 31 December 2024. Littleton, CO.

Hess, M. (2026). Satellite & Aerial Coastal Water Quality Monitoring in the San Diego/Tijuana Region: Annual Summary Report 1 January 2025 – 31 December 2025. Littleton, CO.

Hope, R.M. (2013). Rmisc: Ryan Miscellaneous. R package version 1.5. http://CRAN.R-project.org/package=Rmisc.

Jackson, G.A. (1986). Physical Oceanography of the Southern California Bight. In: R. Eppley (ed.). Plankton Dynamics of the Southern California Bight. Springer Verlag, New York. p 13–52.

Jones, B., M.A. Noble, and T.D. Dickey. (2002). Hydrographic and particle distributions over the Palos Verdes continental shelf: Spatial, seasonal and daily variability. Continental Shelf Research. 22: 945–965.

Kelley, D. and C. Richards. (2019). oce: Analysis of Oceanographic Data. R package version 1.1-1. http://CRAN.R-project.org/package=oce.

Largier, J., L. Rasmussen, M. Carter, and C. Scearce. (2004). Consent Decree – Phase One Study Final Report. Evaluation of the South Bay International Wastewater Treatment Plant Receiving Water Quality Monitoring Program to Determine Its Ability to Identify Source(s) of Recorded Bacterial Exceedances. Scripps Institution of Oceanography, University of California, San Diego, CA.

Le Cao, K-A., F. Rohart, I. Gonzalez, S. Dejean, B. Gautier, F. Bartolo, P. Monget, J. Coquery, F. Yao, and B. Liquet. (2017). mixOmics: Omics. R package version 6.8.0. https://CRAN.R-project.org/package=mixOmics.

Lynn, R.J. and J.J. Simpson. (1987). The California Current System: The Seasonal Variability of its Physical Characteristics. Journal of Geophysical Research. 92(C12): 12947–12966.

Mann. K.H. and J.R.N. Lazier. (1991). Dynamics of Marine Ecosystems, Biological–Physical Interactions in the Oceans. Blackwell Scientific Publications, Boston.

MATLAB. (2022). Version R2022b. The MathWorks Inc., Natick, Massachusetts. URL https://www.mathworks.com/products/matlab.html.

Morgan, P., and L. Pender. (2014). SEAWATER library for calculating EOS-80 properties of seawater in MATLAB. CSIRO Marine Research, version 3.3.1. http://www.cmar.csiro.au/datacentre/ext_docs/seawater.htm.

Nezlin, N.P, J.A.T. Booth, C. Beegan, C.L. Cash, J.R. Gully, A. Latker, M.J. Mengel, G.L. Robertson, A. Steele, and S.B. Weisberg. (2016). Assessment of wastewater impact on dissolved oxygen around southern California's submerged ocean outfalls. Regional Studies in Marine Science. In Press.

[NOAA/NCEI] National Oceanic and Atmospheric Administration/National Center for Environmental Information. (2026). Magnetic field calculators. https://www.ngdc.noaa.gov/geomag/calculators/magcalc.shtml.

Nychka, D., R. Furrer, J. Paige, S. Sain. (2021). "fields: Tools for spatial data." R package version 13.3, https://github.com/dnychka/fieldsRPackage.

Ocean Imaging. (2026). Ocean Imaging Corporation archive of aerial and satellite-derive images. http://www.oceani.com/SanDiegoWater/index.html.

Paver, C.R., L.A. Codispoti, V.J. Coles, and L.W. Cooper. (2020). Sampling errors arising from carousel entrainment and insufficient flushing of oceanographic samples bottles. Limnology & Oceanography: Methods, 18: 311–326.

Pickard, D.L. and W.J. Emery. (1990). Descriptive Physical Oceanography. 5th Ed. Pergamon Press, Oxford.

R Core Team. (2026). R: A language and environment for statistical computing. R Foundation for Statistical Computing, Vienna, Austria. URL https://www.R-project.org/.

Ripley, B. and M. Lapsley. (2017). RODBC: ODBC Database Access. R package version 1.3-12. http://CRAN.R-project.org/package=RODBC.

Rogowski, P., E. Terrill, M. Otero, L. Hazard, S.Y. Kim, P.E. Parnell, and P. Dayton. (2012a). Final Report: Point Loma Ocean Outfall Plume Behavior Study. Prepared for City of San Diego Public Utilities Department by Scripps Institution of Oceanography, University of California, San Diego, CA.

Rogowski, P., E. Terrill, M. Otero, L. Hazard, and W. Middleton. (2012b). Mapping ocean outfall plumes and their mixing using Autonomous Underwater Vehicles. Journal of Geophysical Research, 117: C07016.

Rogowski, P., E. Terrill, M. Otero, L. Hazard, and W. Middleton. (2013). Ocean outfall plume characterization using an Autonomous Underwater Vehicle. Water Science & Technology, 67(4): 925–933.

[SIO] Scripps Institution of Oceanography. (2004). Point Loma Outfall Project, Final Report, September 2004. Scripps Institution of Oceanography, University of California, La Jolla, CA.

Soetaert, K., T. Petzoldt, F. Meysman, and L. Meire. (2020). "marelac: tools for aquatic sciences" R package version 2.1.10. https://CRAN.R-project.org/package=marelac.

Storms, W.E., T.D Stebbins, and P.E. Parnell. (2006). San Diego Moored Observation System Pilot Study Workplan for Pilot Study of Thermocline and Current Structure off Point Loma, San Diego, California. City of San Diego, Metropolitan Wastewater Department, Environmental Monitoring and Technical Services Division, and Scripps Institution of Oceanography, La Jolla, CA.

Svejkovsky, J. (2010). Satellite and Aerial Coastal Water Quality Monitoring in the San Diego/Tijuana Region: Annual Summary Report, 1 January 2009–31 December 2009. Ocean Imaging, Solana Beach, CA.

Svejkovsky, J. and B. Jones. (2001). Detection of coastal urban storm water and sewage runoff with synthetic aperture radar satellite imagery. Eos, Transactions, American Geophysical Union, 82, 621–630.

[SWRCB] California State Water Resources Control Board. (2019). California Ocean Plan, Water Quality Control Plan, Ocean Waters of California. California Environmental Protection Agency, Sacramento, CA.

Terrill, E., K. Sung Yong, L. Hazard, and M. Otero. (2009). IBWC/Surfrider – Consent Decree Final Report. Coastal Observations and Monitoring in South Bay San Diego. Scripps Institution of Oceanography, University of California, San Diego, CA.

Warnes, G., B. Bolker, and T. Lumley. (2021). gtools: Various R Programming Tools. R package version 3.5.0. http://CRAN.R-project.org/package=gtools.

Washburn, L., B.H. Jones, A. Bratkovich, T.D. Dickey, and M.S. Chen. (1992). Mixing, dispersion, and resuspension in vicinity of ocean wastewater plume. Journal of Hydraulic Engineering, 118: 38–58.

Weber, E.D., T.D. Auth, S. Baumann-Pickering, T.R. Baumgartner, E.P. Bjorkstedt, S.J. Bograd, B.J. Burke, J.L. Cadena-Ramirez, E.A. Daly, M. de la Cruz, H. Dewar, J.C. Field, J.L. Fisher, A. Giddings, R. Goericke, E. Gomez-Ocampo, J. Gomez-Valdes, E.L. Hazen, J. Hildebrand, C.A. Horton, K.C. Jacobson, M.G. Jacox, J. Jahncke, M. Kahru, R.M. Kudela, B.E. Lavaniegos, A. Leising, S.R. Melin, L.E. Miranda-Bojorquez, C.A. Morgan, C.F. Nickels, R.A. Orben, J.M. Porquez, E.J. Portner, R.R. Robertson, D.L. Rudnick, K.M. Sakuma, J.A. Santora, I.D. Schroeder, O.E. Snodgrass, W.J. Sydeman, A.R. Thompson, S.A. Thompson, J.S. Trickey, J. Villegas-Mendoza, P. Warzybok, W. Watson, and S.M. Zeman. (2021). State of the California Current 2019-2020: Back to the Future with Marine Heatwaves? Frontiers in Marine Science, 8: 1-23.

Wickham, H. (2007). Reshaping Data with the reshape Package. Journal of Statistical Software, 21(12), 1–20. URL http://www.jstatsoft.org/v21/i12/.

Wickham, H., M. Averick, J. Bryan, W. Chang, L. D'Agostino McGowan, R. François, G. Grolemund, A. Hayes, L. Henry, J. Hester, M. Kuhn, T. Lin Pedersen, E. Miller, S. Milton Bache, K. Müller, J. Ooms, D. Robinson, D. P. Seidel, V. Spinu, K. Takahashi, D. Vaughan, C. Wilke, K. Woo, H. Yutani. (2019). Welcome to the tidyverse. Journal of Open Source Software, 4(43), 1686, https://doi.org/10.21105/joss.01686.

Wickham, H. and D. Seidel. (2020). scales: Scale Functions for Visualization. R package version 1.1.1. https://CRAN.R-project.org/package=scales.

CHAPTER 4

FIGURES & TABLES

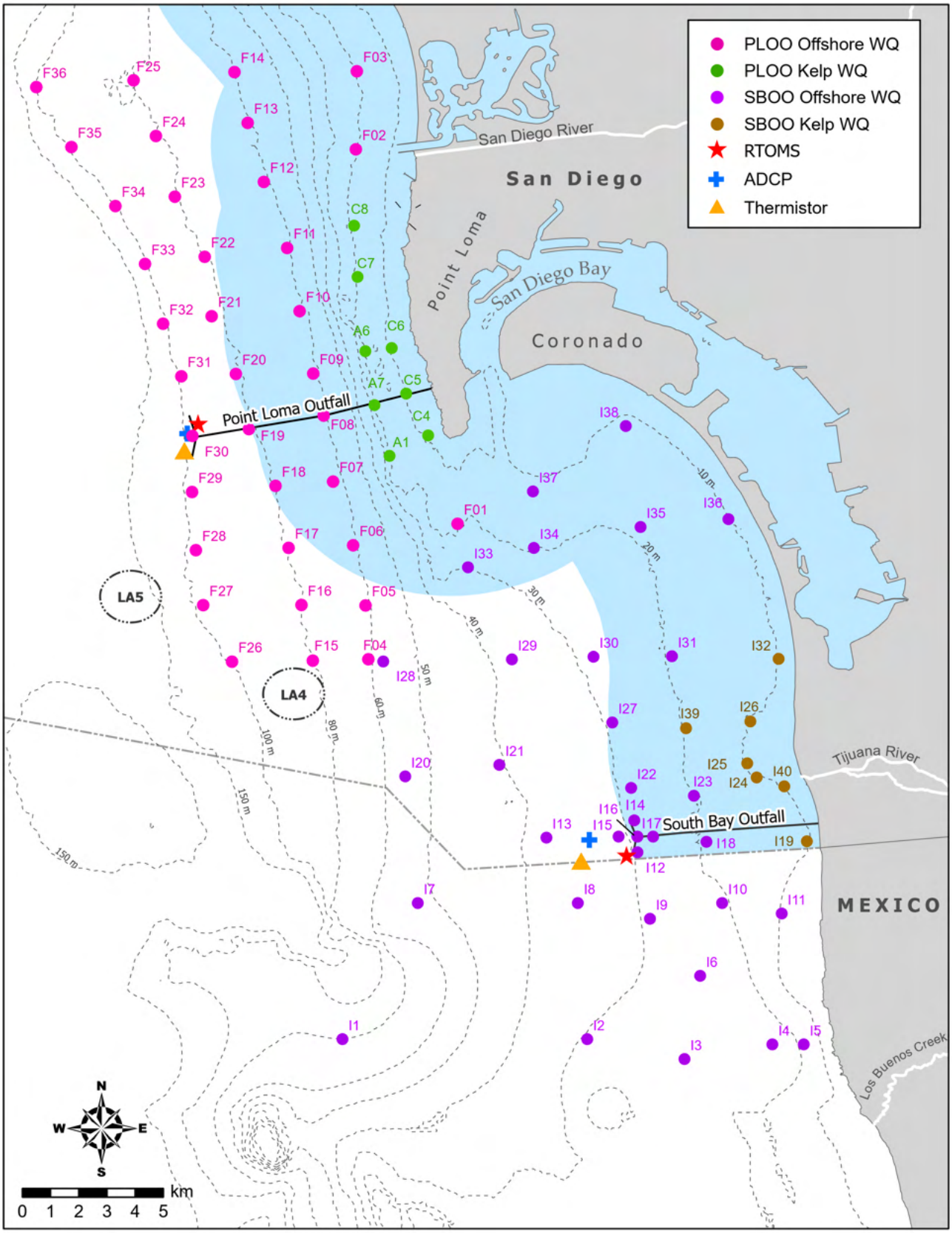


Figure 4.1
Oceanographic mooring and monitoring station locations around the PLOO and SBOO sampled as part of the City of San Diego's Ocean Monitoring Program. Light blue shading represents State jurisdictional waters.

Table 4.1

Summary of the numbers of reference stations, potential wastewater plume detections, and out-of-range values at offshore stations during 2024 and 2025. DO = dissolved oxygen; XMS = transmissivity.

			Reference Stations	Potential Plume Detections	Out of Range		
					DO	pH	XMS
PLOO	*2024*	Feb	16	4	1	0	3
		May	7	8	2	0	5
		Aug	7	3	0	0	3
		Nov	8	10	2	0	7
	2025	Feb	14	12	1	0	8
		May	4	14	0	0	1
		Aug	3	10	0	0	0
		Nov	13	7	1	0	5
			Detection Rate (%)	21	2	0	10
			Total Count	68	7	0	32
			Total Samples	328	328	328	328
SBOO	*2024*	Feb	15	1	0	0	1
		May	7	4	0	0	2
		Aug	14	2	0	0	2
		Nov	6	5	0	0	1
	2025	Feb	8	6	1	0	4
		May	10	6	4	0	2
		Aug	13	0	0	0	0
		Nov	15	6	0	0	7
			Detection Rate (%)	13	2	0	8
			Total Count	30	5	0	19
			Total Samples	232	232	232	232

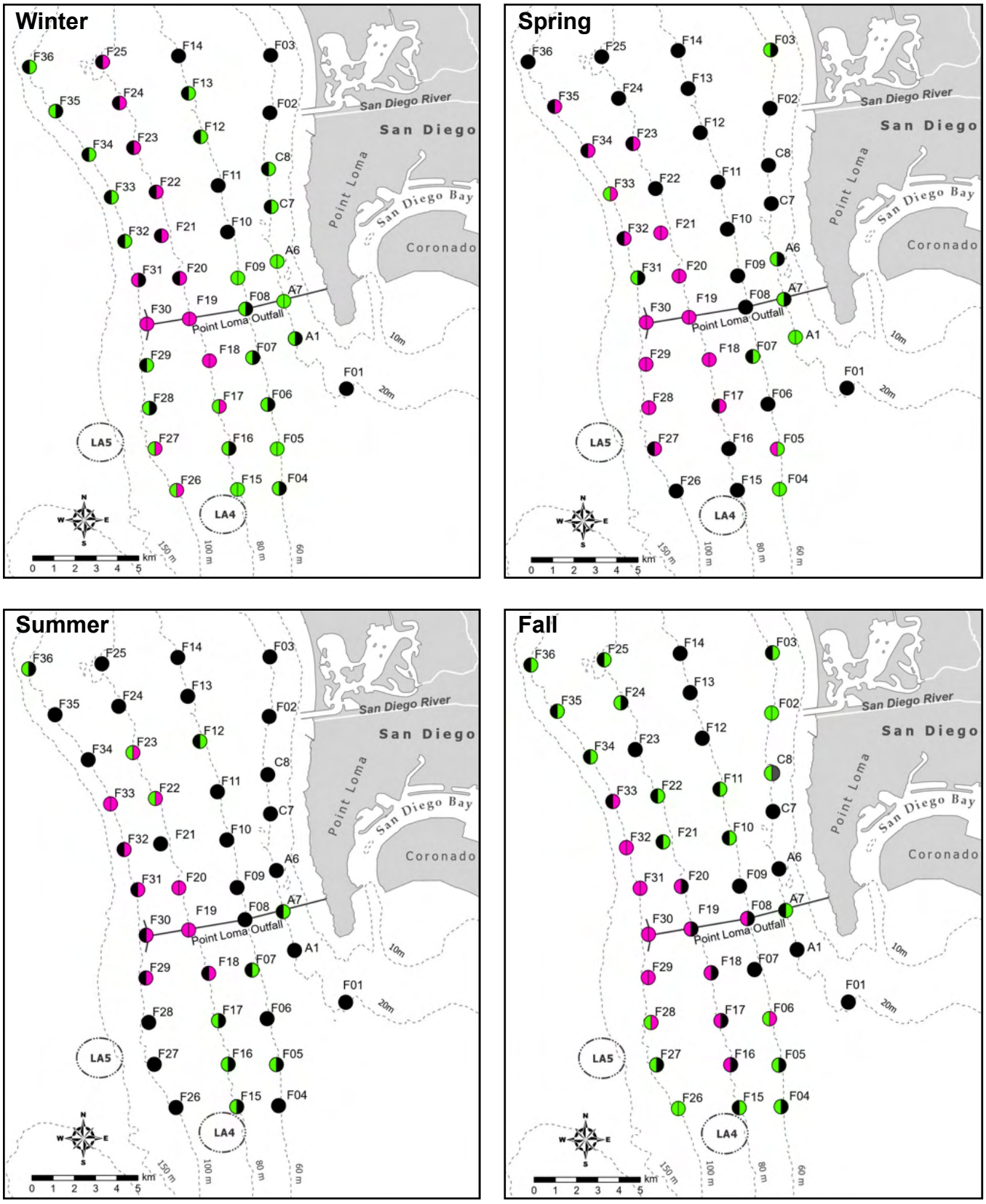


Figure 4.2

Distribution of stations meeting potential plume criteria (pink), those used as reference stations (green), and stations meeting neither criteria (grey) near the PLOO (this page) and SBOO (facing page) during quarterly surveys in 2024 (left half of circle) and 2025 (right half).

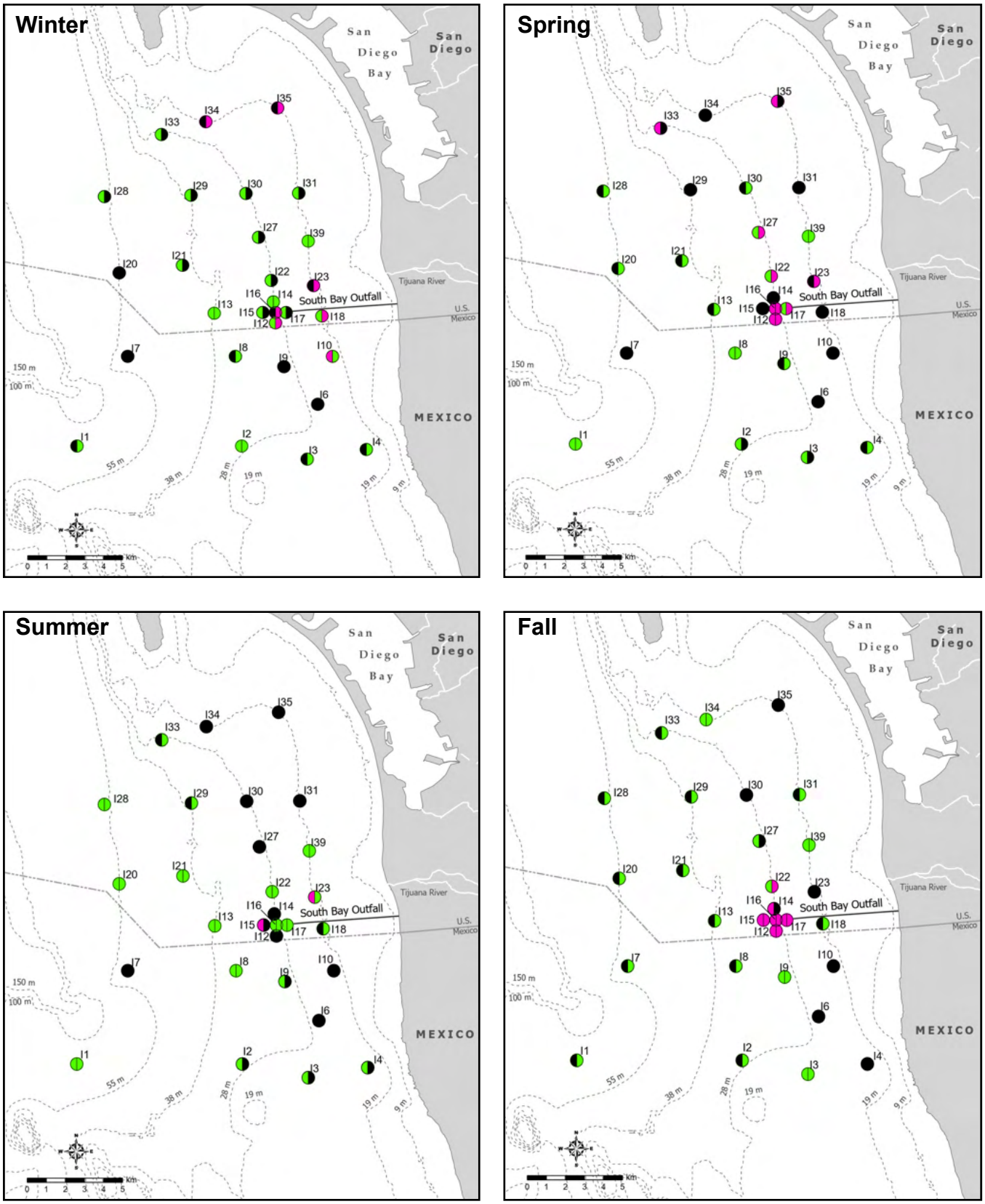


Figure 4.2 *continued*

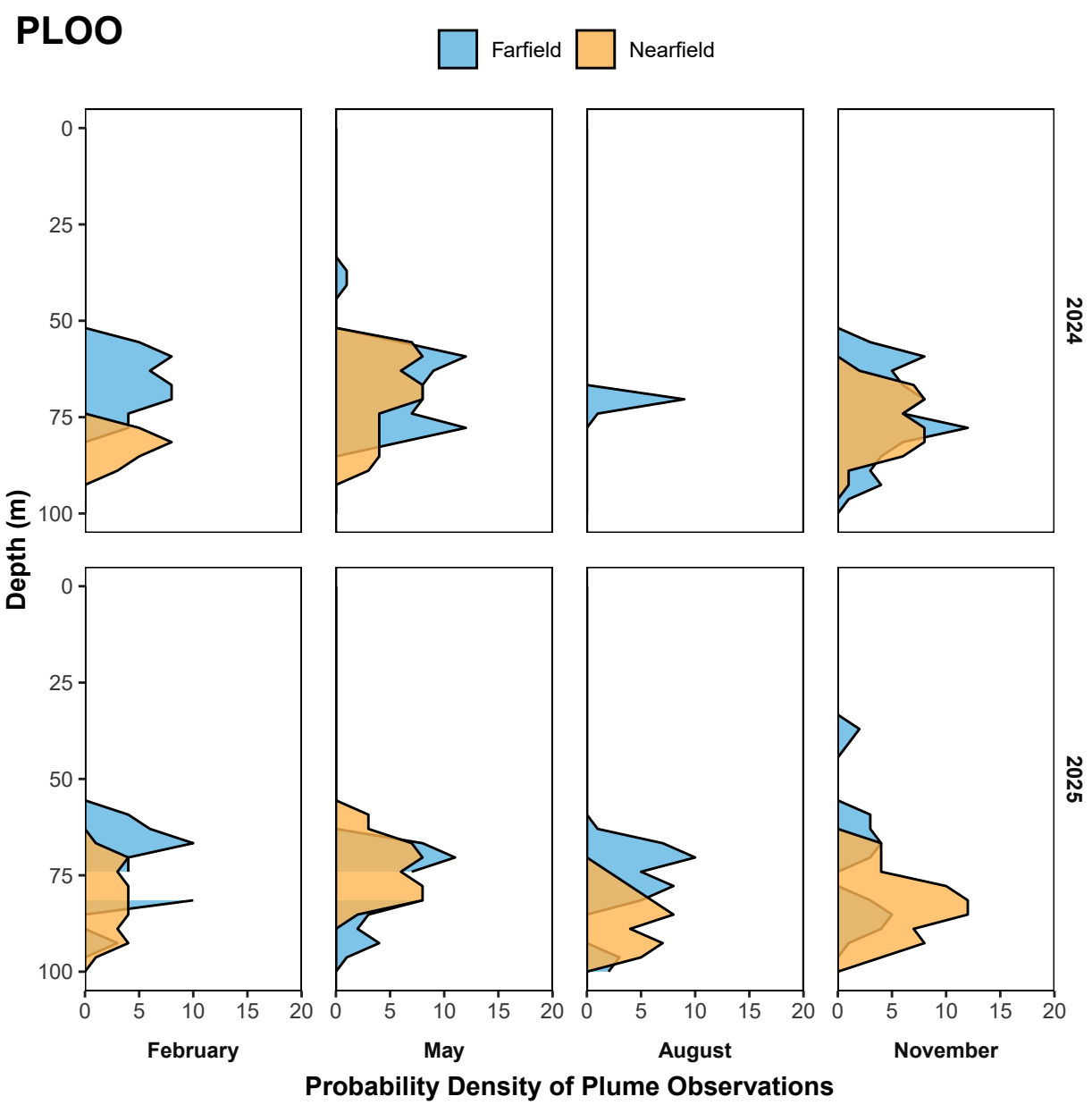


Figure 4.3

Depth profiles by season of the probability density of potential plume detections at PLOO and SBOO offshore stations during 2024 and 2025. Nearfield stations for PLOO are F29, F30, F31; nearfield stations for SBOO are I12, I14, I15, I16.

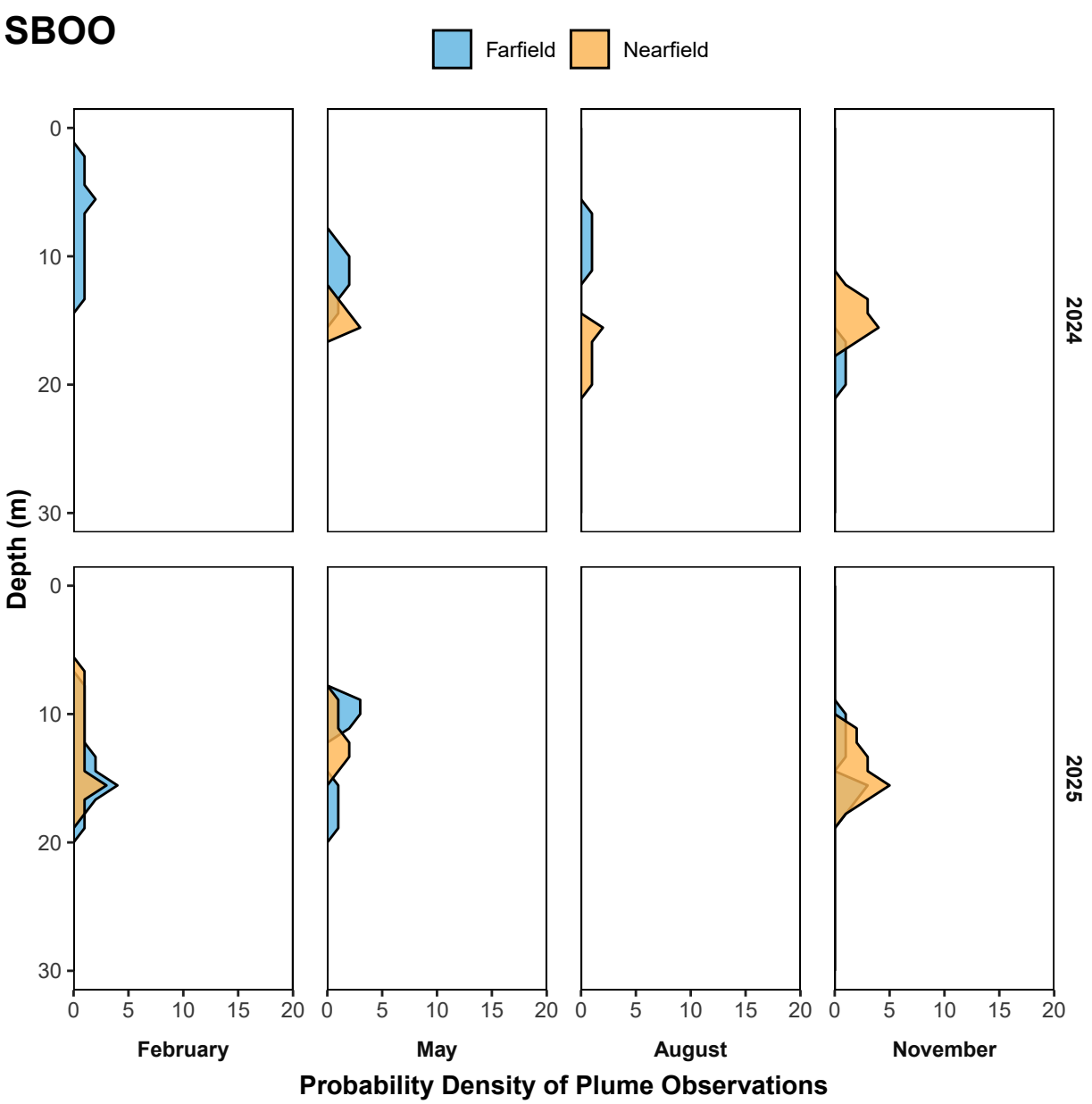


Figure 4.3 *continued*

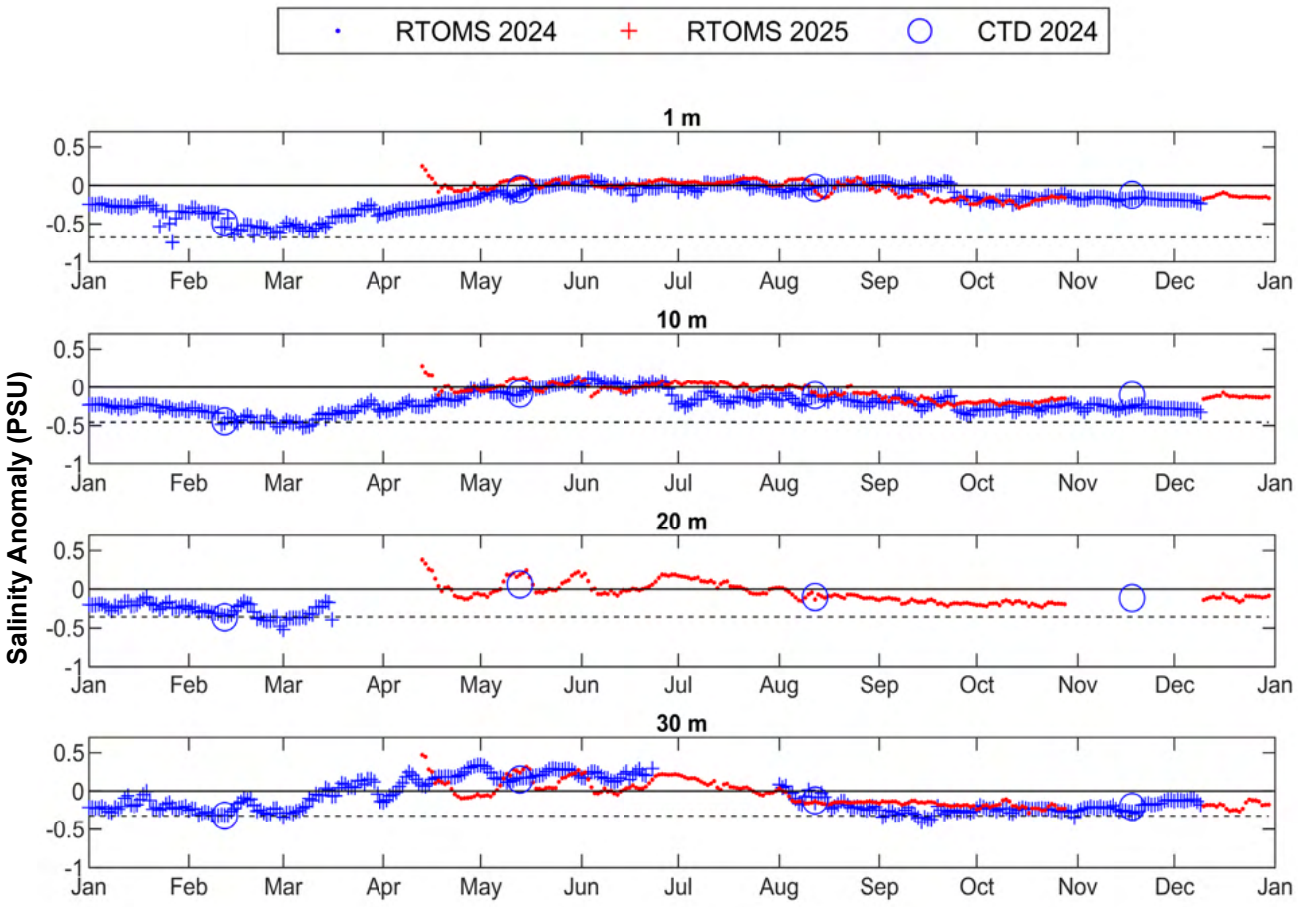


Figure 4.4

Daily averaged salinity anomalies from 2024 (blue) to 2025 (red) for each mooring sensor depth shown using available RTOMS data. Anomalies calculated from historical CTD survey data from 2001–2025 for each monitoring region and depth range, excluding nearfield stations (see text). Dashed line indicates 99th percentile minimum from CTD survey data. Due to low regional salinities in early 2024, mean salinity anomalies from each quarterly CTD survey from farfield stations are also shown for 2024 (open blue circles; see text).

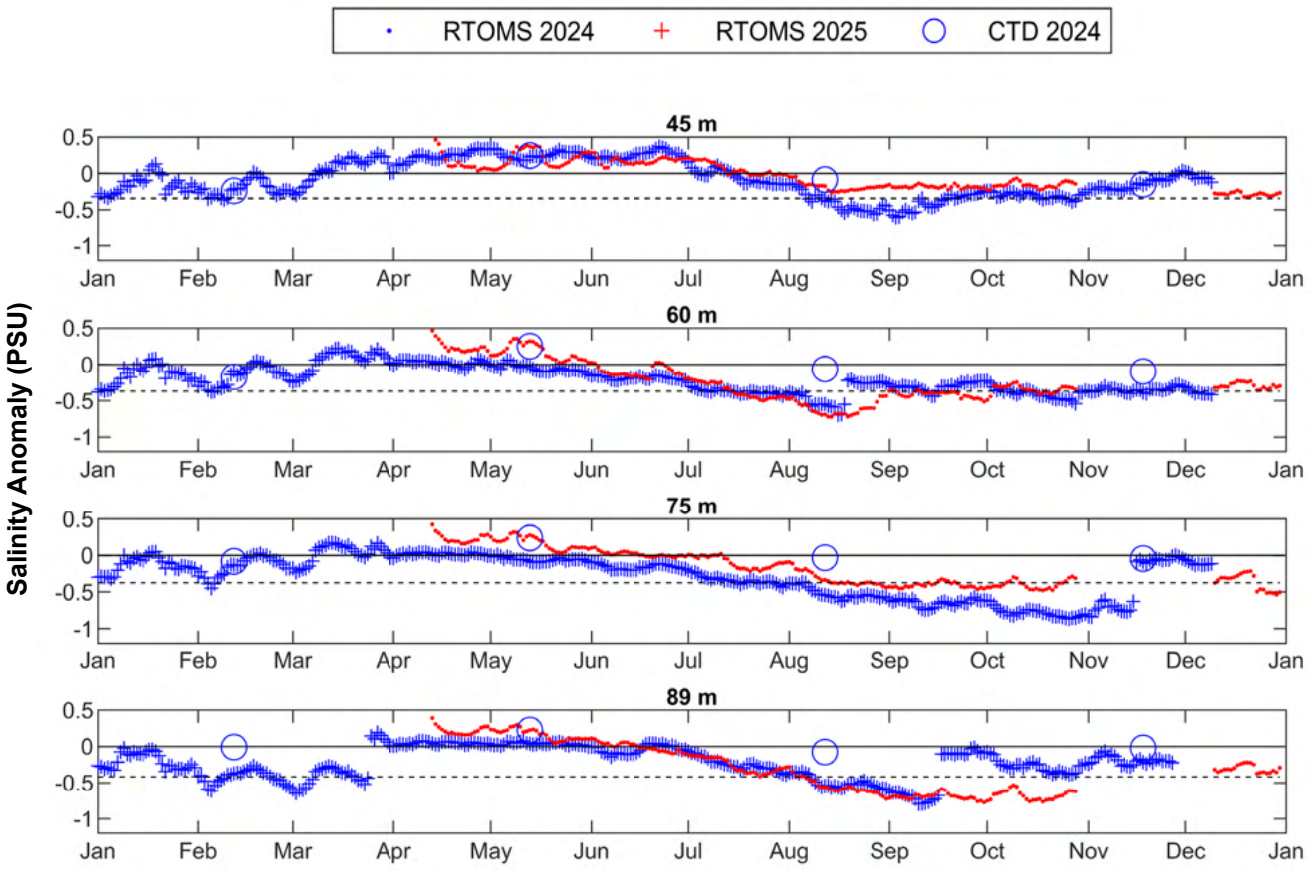


Figure 4.4 *continued*

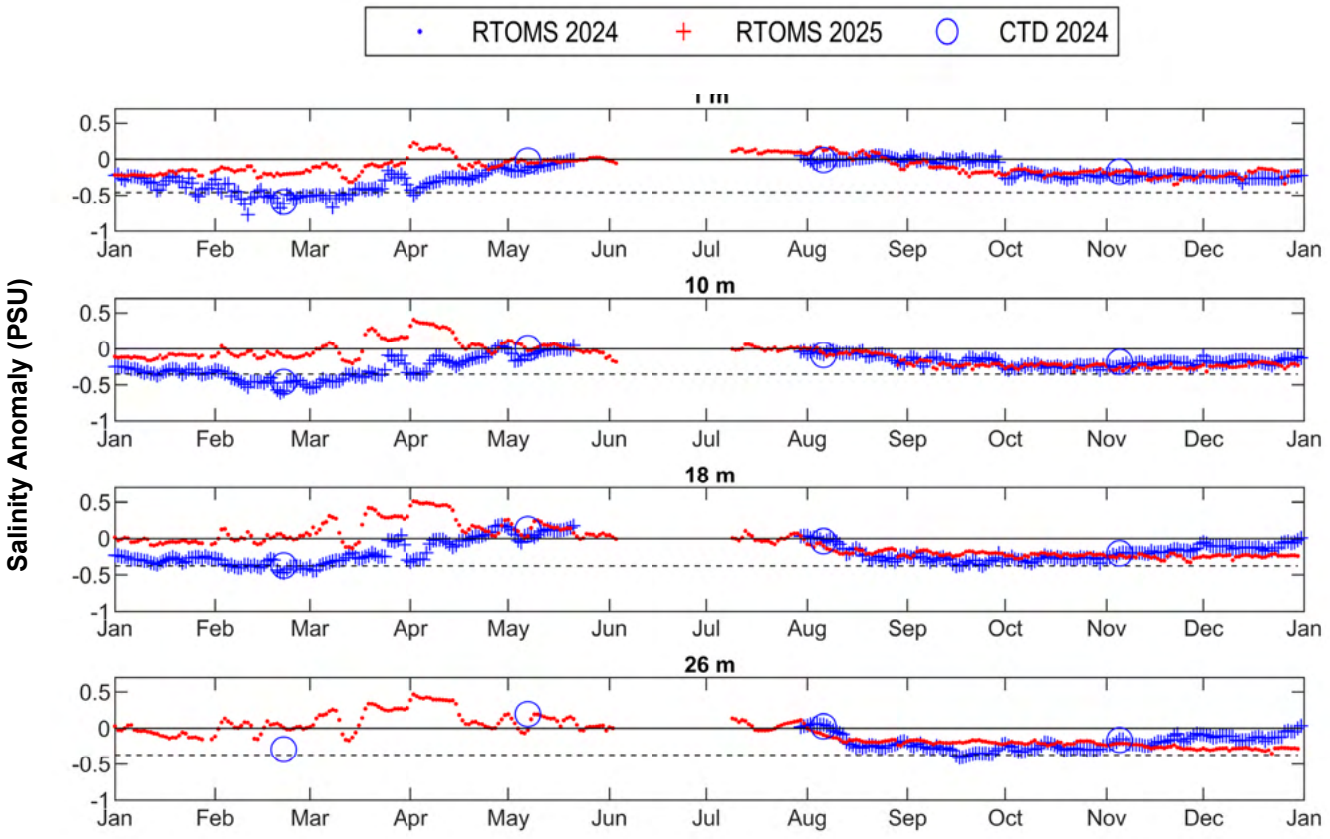


Figure 4.4 *continued*

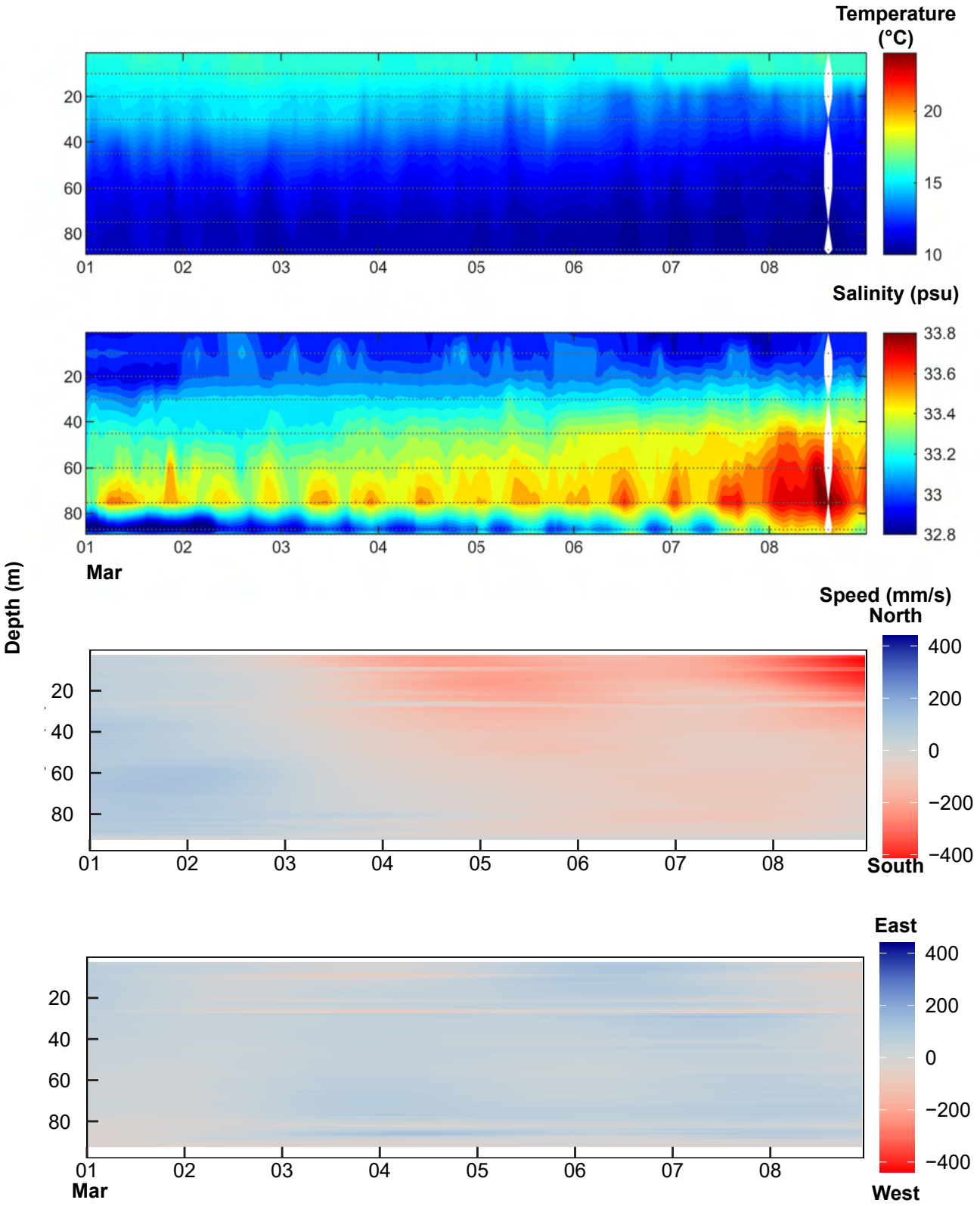


Figure 4.5

PLOO RTOMS hourly averaged ocean temperature, salinity, and current speeds (tides removed) interpolated for entire water column plus chlorophyll *a* (chl), CDOM, turbidity, and nitrate + nitrite for subsurface depths to show a change in conditions during the week of March 1-8, 2024. Gaps and white areas indicate loss of data due to instrumentation issues or failure to meet data quality criteria (see text).

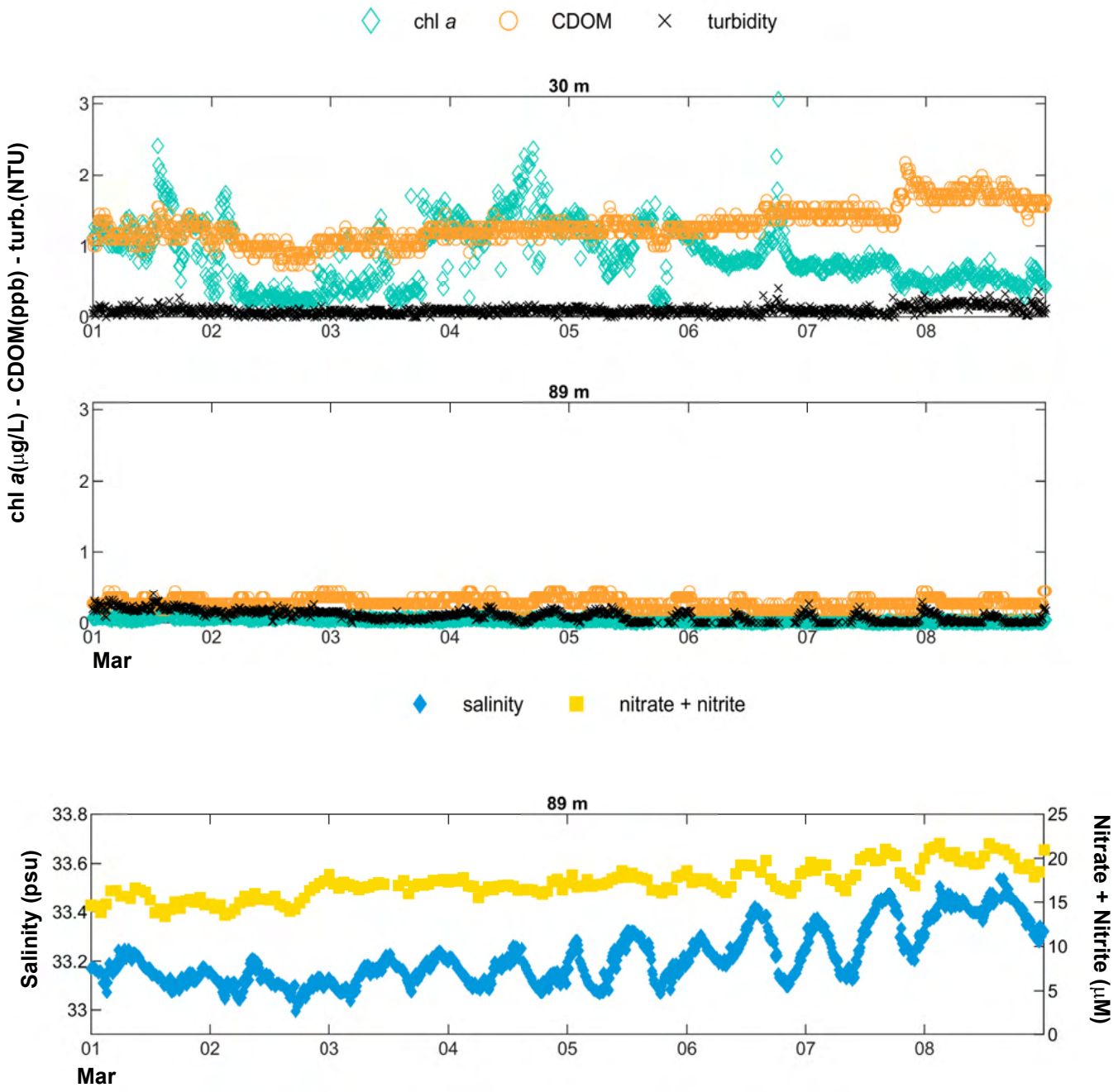


Figure 4.5 *continued*

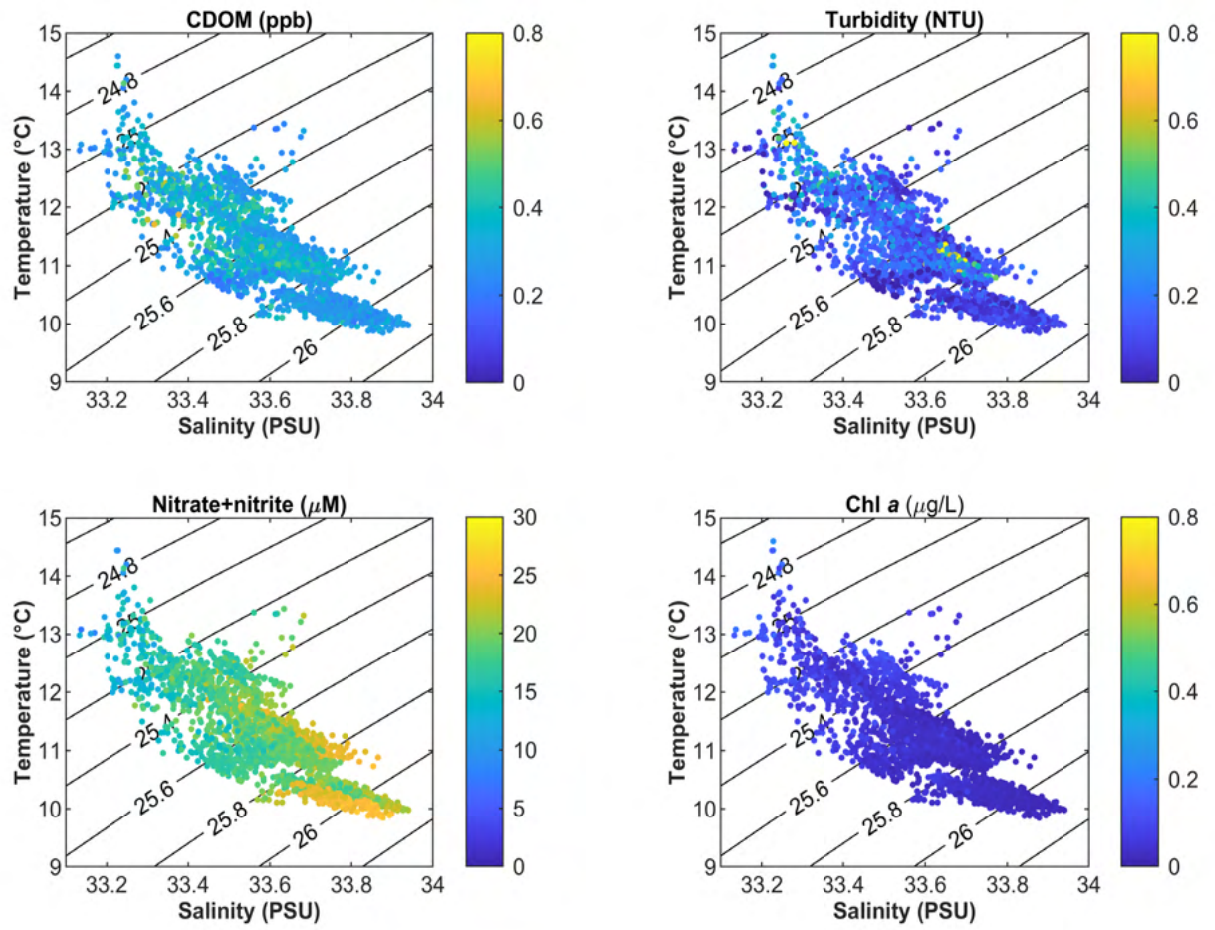


Figure 4.6

PLOO RTOMS hourly averaged CDOM, turbidity, nitrate + nitrite, and chlorophyll *a* shown on temperature versus salinity plots at 89 m for winter 2024 (January–March). No PLOO RTOMS data are available for winter 2025 (see text). Isopycnals and corresponding σ-t values shown by black lines.

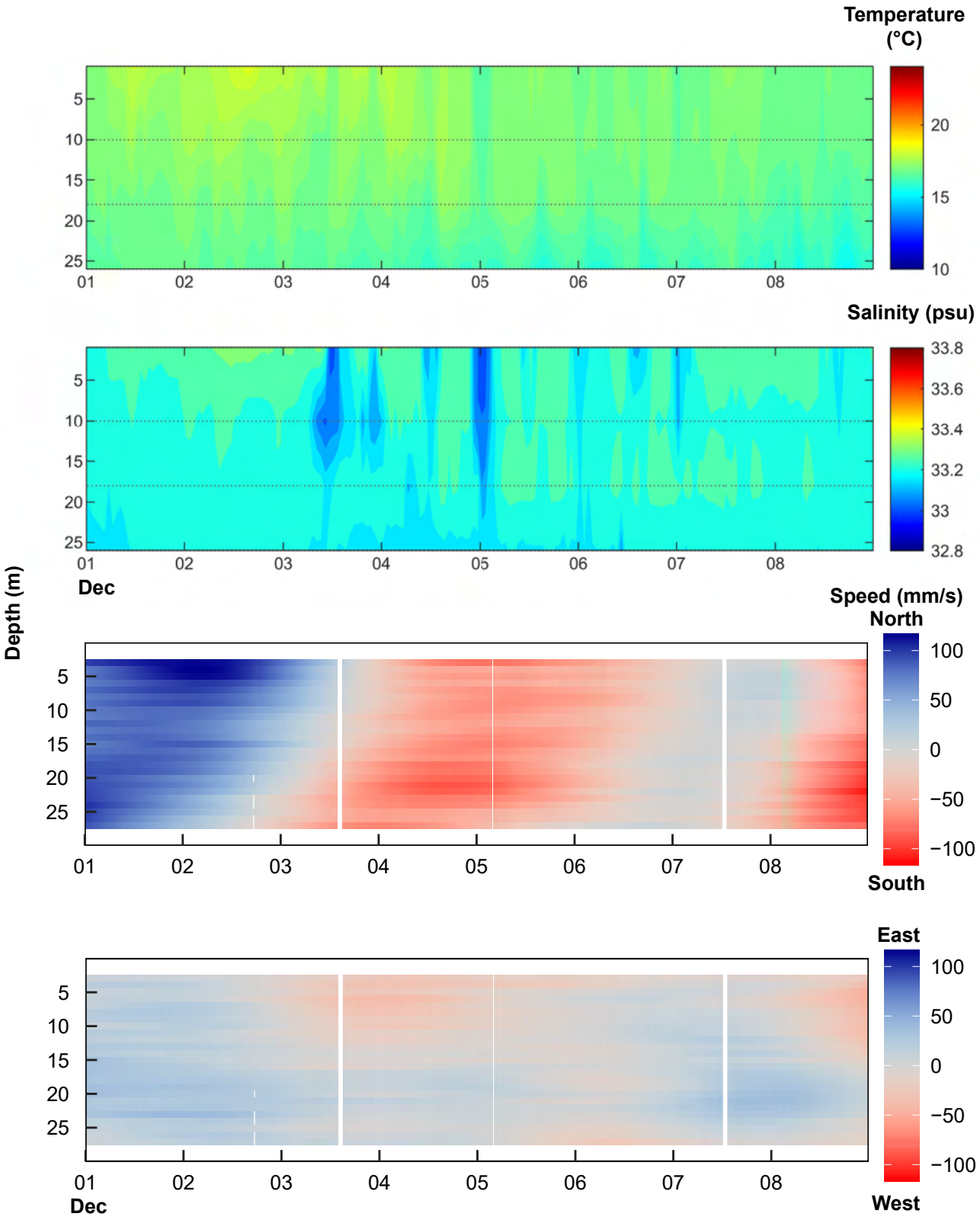


Figure 4.7

SBOO RTOMS hourly averaged ocean temperature, salinity, and current speeds (tides removed) interpolated for entire water column plus chlorophyll *a* (chl), CDOM, turbidity, and nitrate + nitrite for surface and bottom depths to show a change in conditions during the week of December 1-8, 2025. Gaps and white areas indicate loss of data due to instrumentation issues or failure to meet data quality criteria (see text).

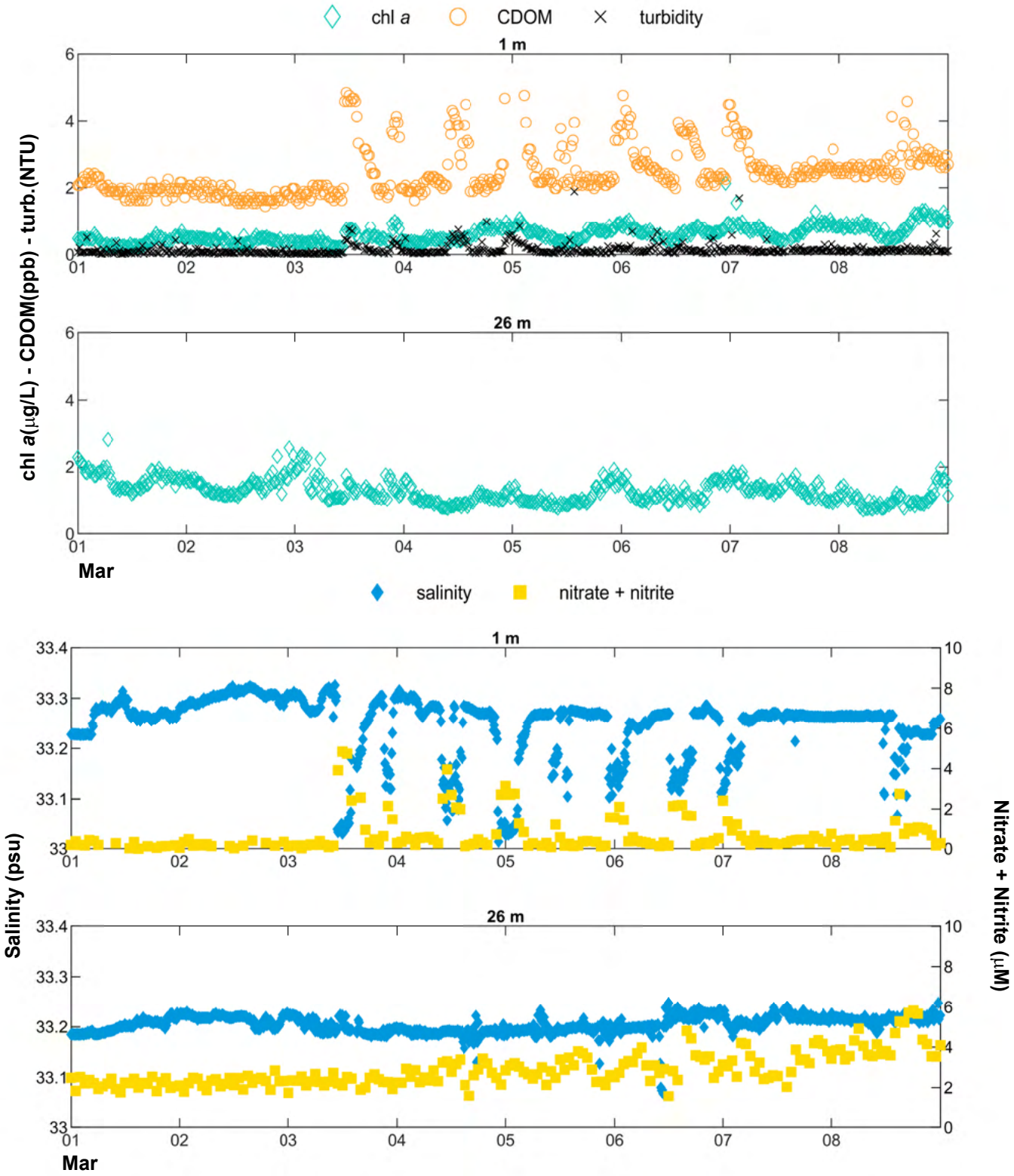


Figure 4.7 *continued*

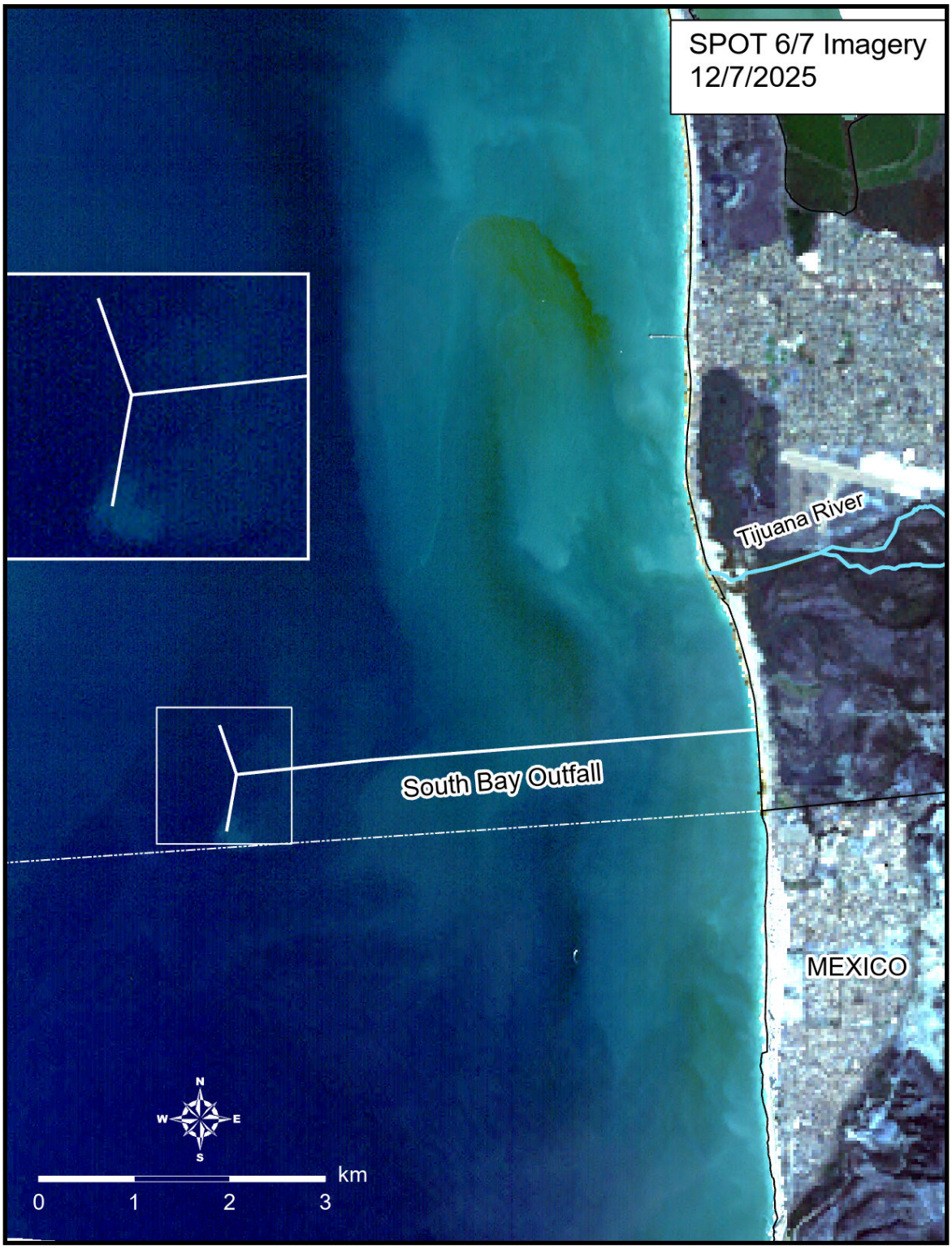


Figure 4.8

SPOT 6/7 high resolution satellite images of the South Bay region acquired that show SBOO-related wastewater plume at the surface on December 7, 2025. (Ocean Imaging 2026).

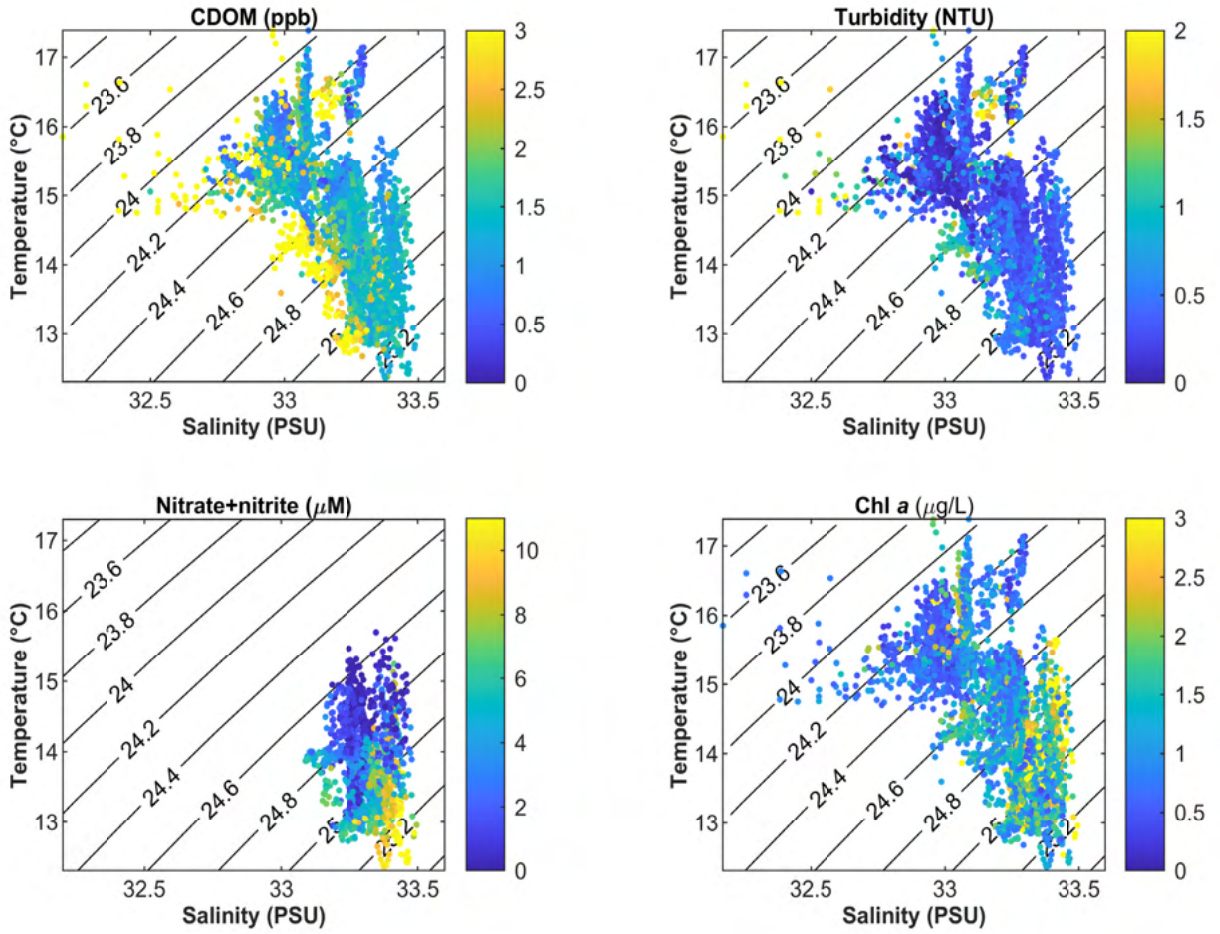


Figure 4.9

SBOO RTOMS hourly averaged CDOM, turbidity, nitrate + nitrite, and chlorophyll *a* shown on temperature versus salinity plots at 1 m for winter 2024 and 2025 (January–March). Isopycnals and corresponding σ-t values shown by black lines.

Table 4.2

Ocean conditions in the PLOO region on dates corresponding to ROTV surveys, and description of plume extent as observed with the ROTV. ΔT = change in temperature between surface and bottom (RTOMS). Plume extent assessed visually using interpolation of CDOM from ROTV Turner sensors (Appendix C.24).

	Thermocline			Currents[b]			Tides	Plume Extent				
Date	Qualitative Strength	Max ΔT (°C)	Max depth (m)	Dominant alongshore	Dominant cross-shore	Mean deep speed (mm/s)	Tidal State	Transects Completed	Plume width (m)	Min. plume depth (m)	Plume max relative to outfall	Max plume transect depth
01 Mar 2024	Weak to Moderate	5	<30	weak north	weak east; week west below 80m	97	Ebb; recent transition from Flood	90m, 90m	2500	60	north (3300m)	90m [d]
04 Mar 2024	Weak to Moderate	5	<30	weak south; moderate south above 30 m	weak east	59	Flood; recent transition from Ebb	100m, 100m, 85m	6000	60	centered	85m
05 Mar 2024	Weak to Moderate	5.3	<20	weak south; moderate south above 30 m	weak east; weak west 30-70m	72	Ebb	60m, 75m, 110m, 90m	6000	60	slightly south (800m)	90m
06 Mar 2024	Weak to Moderate	5.4	<20	weak south	weak east	90	Ebb	80m	7000	60	south (5000m)	80m [d]
03 Dec 2024	Weak	3.9	<20	weak north; weak south below 45m	weak east	43 [c]	Ebb; recent transition from Flood	85m, 100m, 90m	3000	40	centered	100m
04 Dec 2024	Weak	3.9	<20	weak north	weak east	66 [c]	Ebb [e]	90m, 80m, 105m, 90m, 120m	4000	40	north (2000m)	90m
05 Dec 2024	Weak	3.7	<20	weak north; weak south above 20m	weak east; weak west above 30m	24 [c]	Flood	110m, 85m, 105m	5500	40	north (2500m)	85m
05 Mar 2025	Weak	4.2[a]	<18[a]	–	–	–	Flood	100m, 75m, 85m	8500+	30	south (4000m)	100m
10 Mar 2025	Weak	3.9[a]	<10[a]	–	–	–	Ebb	100m, 85m	12000	45	south (5000m)	85m
27 Aug 2025	Strong	11.9	<10	weak north; weak south above 15m	weak east; weak west above 15 m	86	Flood; nearing peak	100 m, 80m	10000+	60	north (10000m)	100m
18 Dec 2025	Moderate	6.6	<20	weak north; weak south above 40m	weak east	30	Ebb	100m, 90m, 90m	6500+	60	north (1800m)	90m
23 Dec 2025	Weak to Moderate	5.8	<20	weak north	weak east; weak west below 85 m	81	Flood; nearing peak	100m, 80m	15000+	65	north (5000m)	100m

a RTOMS data not available from March 2025. Thermocline calculated from static thermistor data (from 4 to 98m depth, spaced 4m apart).

b ADCP data not available from either RTOMS or static mooring in March 2025.

c RTOMS ADCP data not available below 60 m depth due to quality control failure. Current measurements from static ADCP (4 m bins, upward facing).

d Only one transect depth available on this date

e sampled twice, strongest plume signature chosen to match tidal state

Table 4.3

Ocean conditions and plume extend observed in the SBOO region on dates corresponding to ROTV surveys. ΔT = change in temperature between surface and bottom (RTOMS). Plume extent assessed visually using interpolation of CDOM from ROTV Turner sensors (Appendix C.25).

	Thermocline			Currents			Tides	Plume Extent				
Date	Qualitative Strength	Max ΔT (°C)	Max depth (m)	Dominant alongshore	Dominant cross-shore	Mean deep speed (mm/s)	Tidal State	Transects Completed	Plume width (m)	Min. plume depth (m)	Plume max relative to outfall	Max plume transect depth
07 Mar 2024	Weak to Moderate	3	<20	weak south	weak east	17	Ebb	30m	1000	15	south (1000m)	30m[a]
05 Dec 2024	Weak	2.2	<20	weak north; weak south above 12 m	weak east	27	Ebb	30m	3000	7	centered	30m[a]
10 Mar 2025	Weak to Moderate	2.9	<10[a]	very weak south below 10m transitioning to weak north	weak east below 15m transitioning to weak west	58	Ebb	25m	500	10	south (500m)	25m[a]
26 Aug 2025	Strong	7.5	<10	weak north	weak east; weak west above 5 m	79	Flood	30m, 20m	9000+	5	centered	20m
15 Sep 2025	Moderate	5.1	<10	weak south transitioning to weak north; weak south above 12 m	weak east; weak west above 15 m	15	Ebb	30m, 25m, 25m	9000+	8	centered	30m
22 Dec 2025	Weak	2	<18	weak south; moderate south above 8 m	weak east; weak west above 10 m	54	Flood [b]	30m, 20m, 35m, 35m, 30m	500	15	south	30m

a Only one transect depth available on this date

b sampled twice, strongest plume signature chosen to match tidal state

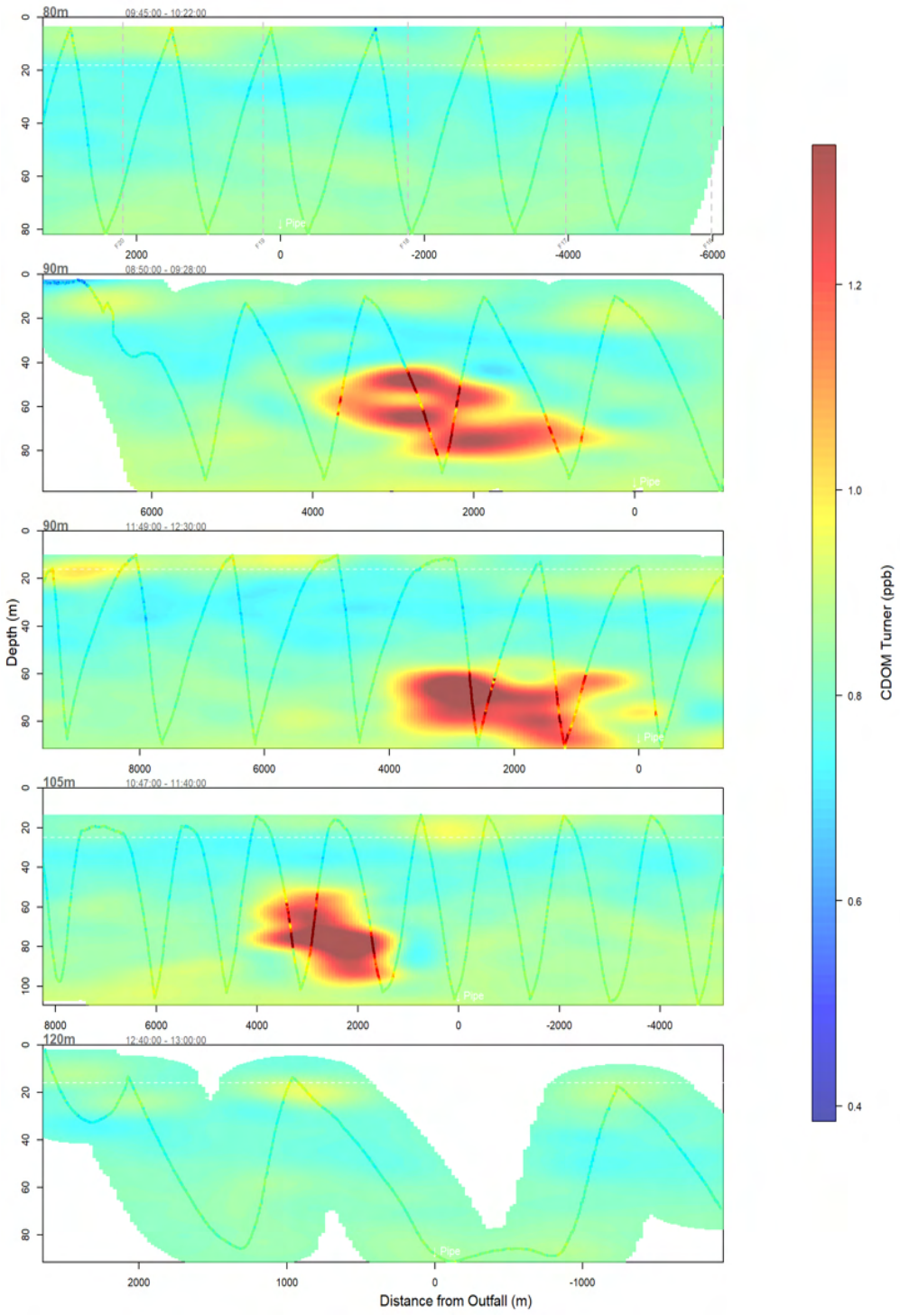


Figure 4.10

Interpolated CDOM data for each transect along an isobath from an example ROTV survey of the PLOO region conducted on December 4th, 2024 (see text for methods). Opaque color lines indicate the position of the ROTV in the water column and associated raw data values. The position of the outfall is designated by text ("Pipe") and arrow in white. Vertical grey dashed lines indicate the position of nearby CTD sampling stations. A horizontal white line indicates the position of the thermocline.

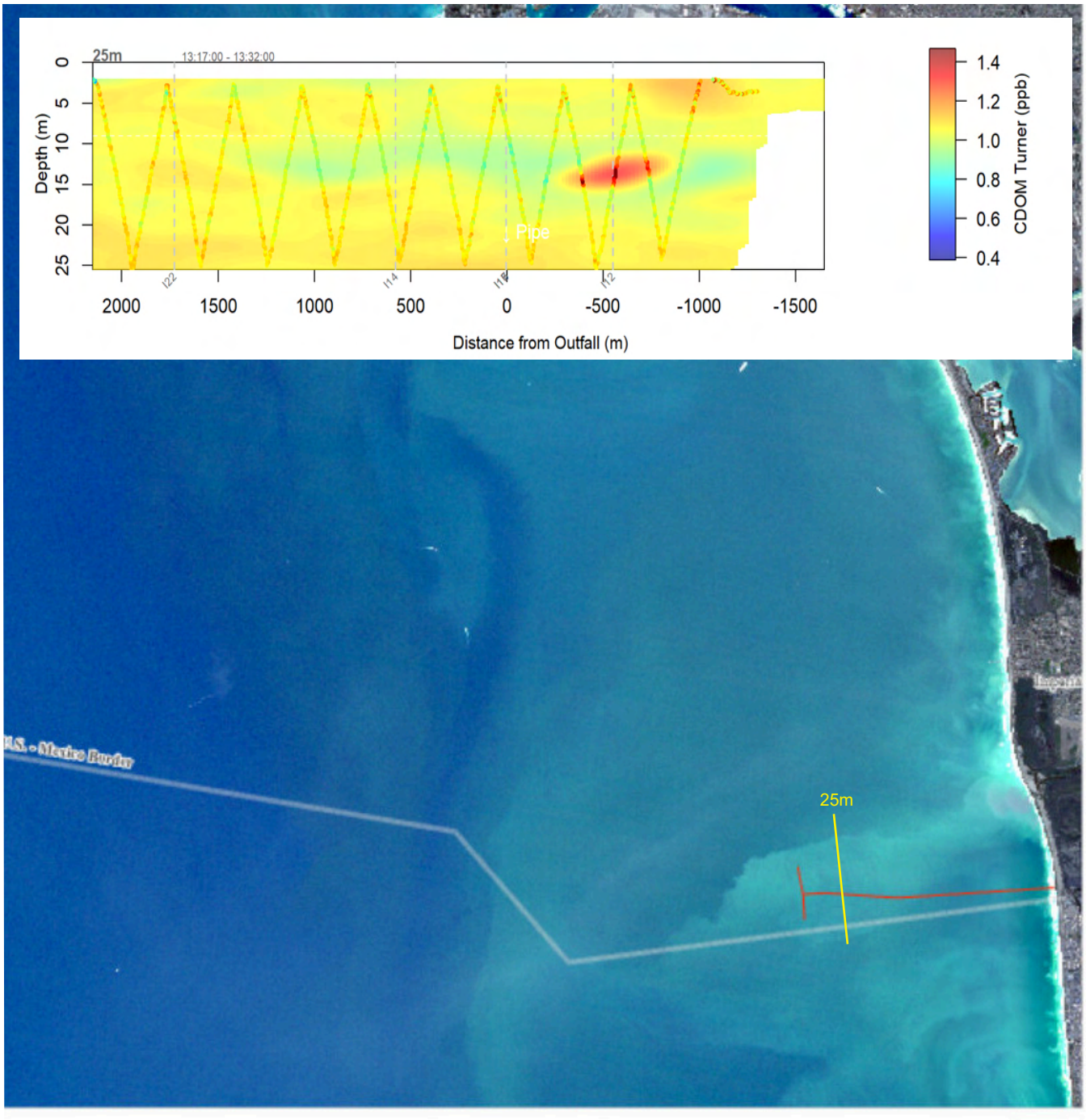


Figure 4.11

Inset: Interpolated CDOM data for a single transect along an isobath from an example ROTV survey of the SBOO region conducted on March 10th, 2025 (see text for methods). Opaque color lines indicate the position of the ROTV in the water column and associated raw data values. The position of the outfall is designated by text ("Pipe") and arrow in white. Vertical grey dashed lines indicate the position of nearby CTD sampling stations. A horizontal white line indicates the position of the thermocline. Background: A corresponding satellite image was also captured on March 10th, 2025 (Ocean Imaging 2026). The approximate location of the ROTV transect is indicated by the yellow bar.

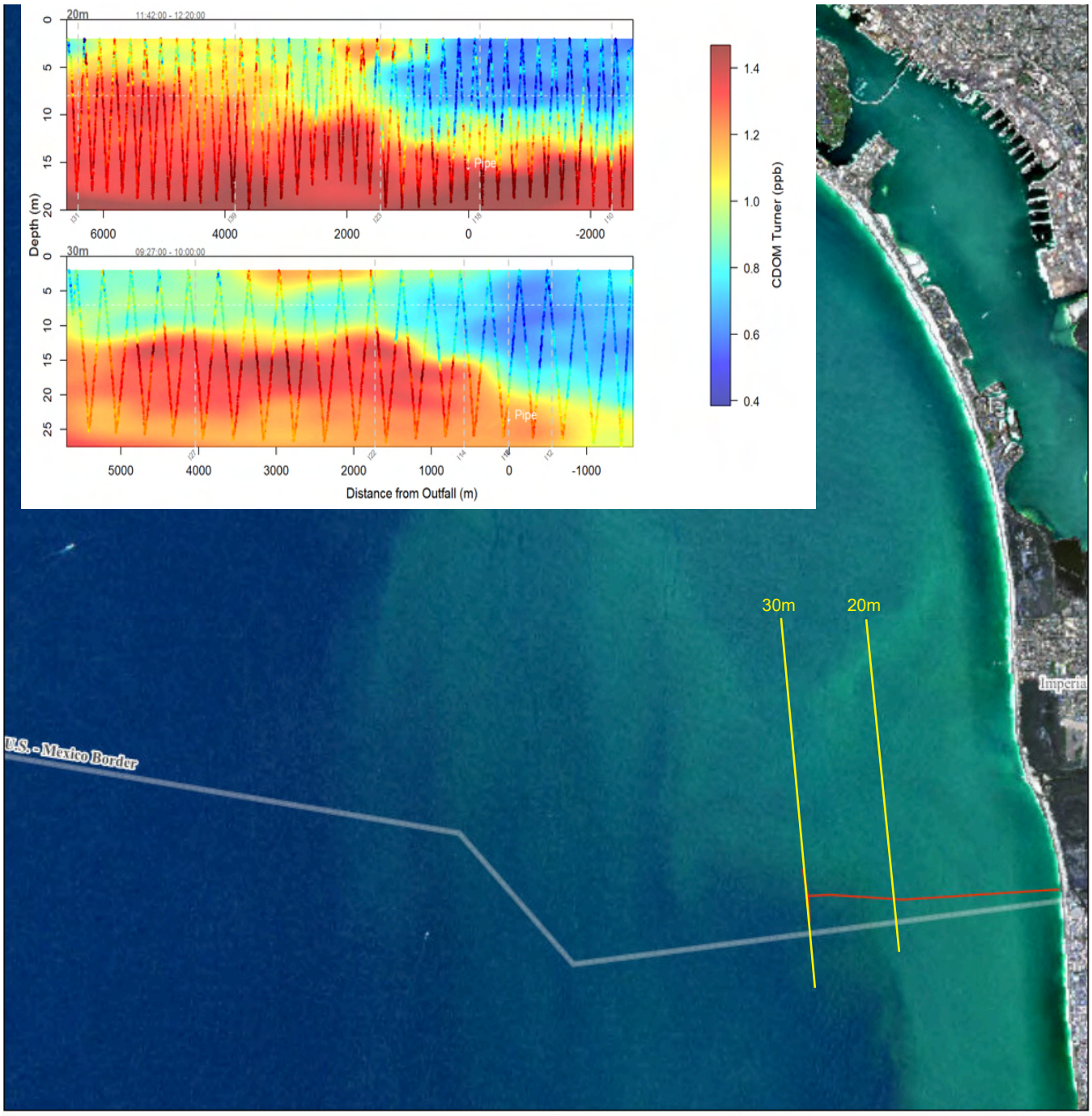


Figure 4.12

Inset: Interpolated CDOM data for each transect along an isobath from an example ROTV survey of the SBOO region conducted on August 26th, 2025 (see text for methods). Opaque color lines indicate the position of the ROTV in the water column and associated raw data values. The position of the outfall is designated by text ("Pipe") and arrow in white. Vertical grey dashed lines indicate the position of nearby CTD sampling stations. A horizontal white line indicates the position of the thermocline. Background: A corresponding satellite image was captured on August 27th, 2025 (Ocean Imaging 2026). An exact date match was not available. The approximate location of each ROTV transect is indicated by the yellow bars.

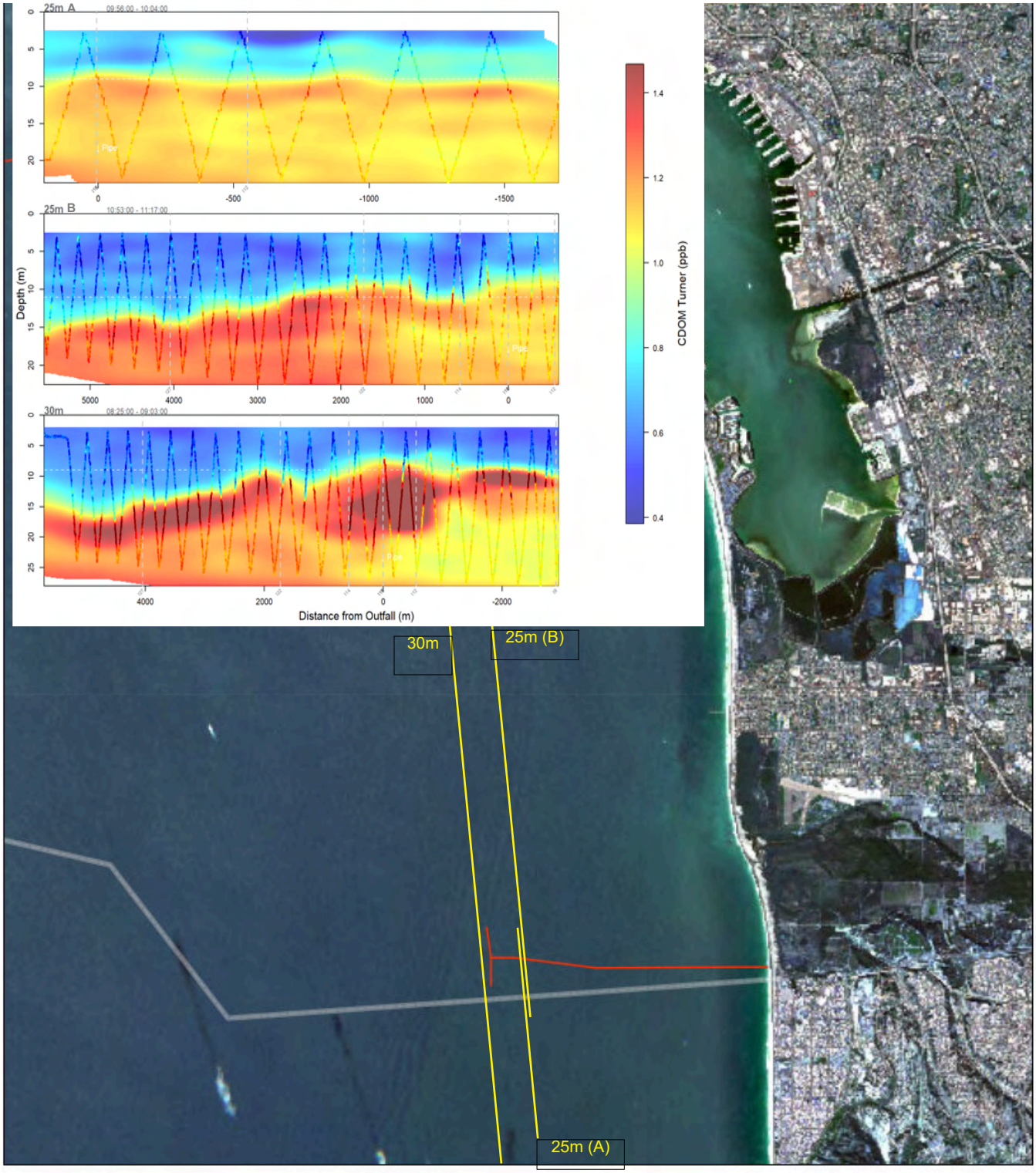


Figure 4.13

Inset: Interpolated CDOM data for each transect along an isobath from an example ROTV survey of the SBOO region conducted on September 15th, 2025 (see text for methods). Opaque color lines indicate the position of the ROTV in the water column and associated raw data values. The position of the outfall is designated by text ("Pipe") and arrow in white. Vertical grey dashed lines indicate the position of nearby CTD sampling stations. A horizontal white line indicates the position of the thermocline. Background: A corresponding satellite image was captured on September 16th, 2025 (Ocean Imaging 2026). An exact date match was not available. The approximate location of each ROTV transect is indicated by the yellow bars.

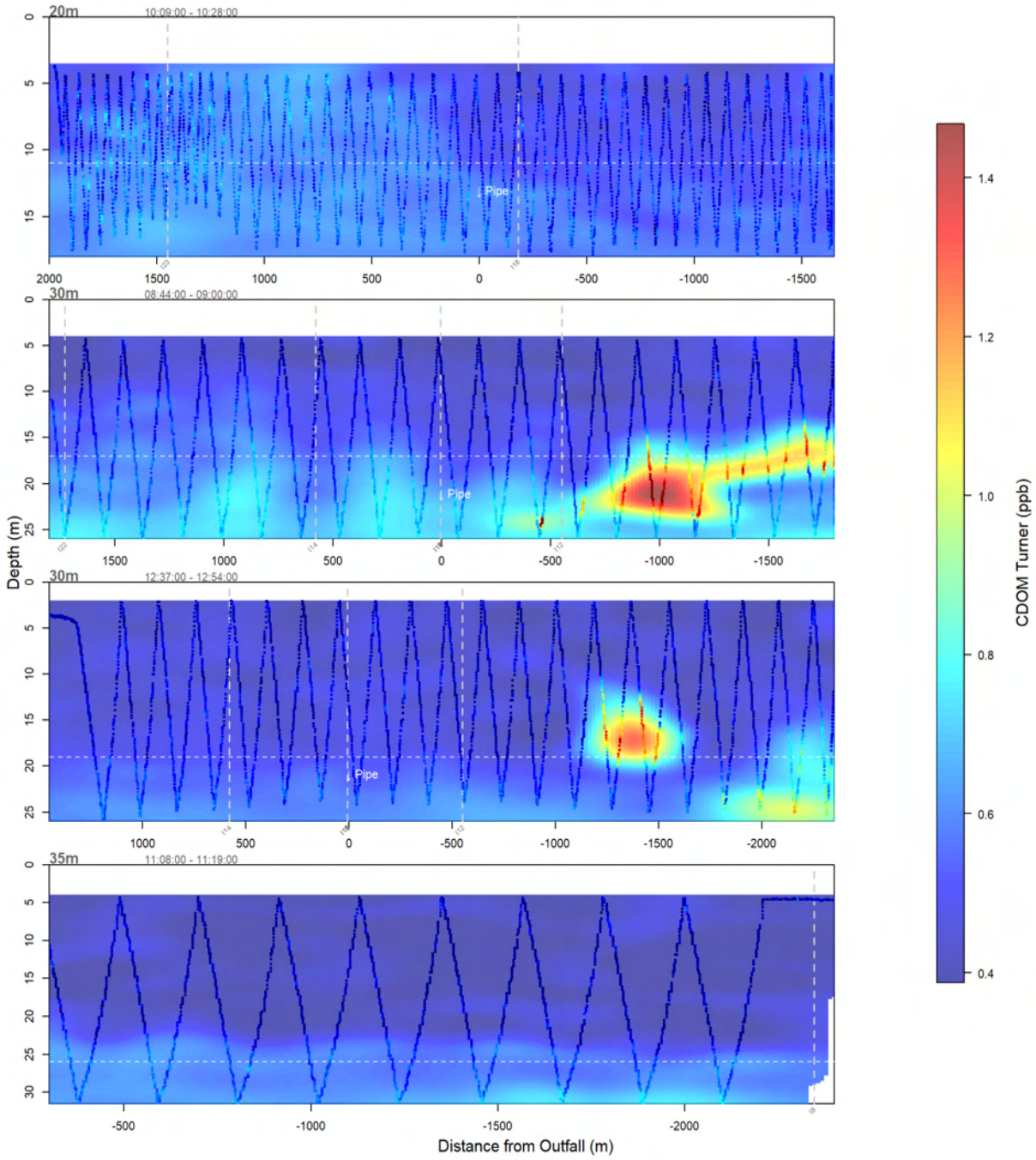


Figure 4.14

Interpolated CDOM data for each transect along an isobath from an example ROTV survey of the SBOO region conducted on December 22nd, 2025 (see text for methods). Opaque color lines indicate the position of the ROTV in the water column and associated raw data values. The position of the outfall is designated by text ("Pipe") and arrow in white. Vertical grey dashed lines indicate the position of nearby CTD sampling stations. A horizontal white line indicates the position of the thermocline.

Chapter 5
Sediment Quality

Chapter 5. Sediment Quality

Introduction

Ocean sediment samples are analyzed by the City of San Diego (City) as part of the Ocean Monitoring Program to examine the effects of wastewater discharge from the Point Loma Ocean Outfall (PLOO) and South Bay Ocean Outfall (SBOO), and other anthropogenic inputs, on the marine benthic environment. Analyses of various sediment contaminants are conducted as anthropogenic inputs to the marine ecosystem, including municipal wastewater, can lead to increased concentrations of pollutants within the local environment. The relative proportions of sand, silt, clay, and other particle size parameters are also examined as concentrations of some compounds are known to be directly linked to sediment composition (Emery 1960, Eganhouse and Venkatesan 1993). Physical and chemical sediment characteristics are also analyzed as they define the primary microhabitats for benthic macroinvertebrates (macrofauna) that live within or on the seafloor, and therefore influence the distribution and presence of various species. For example, differences in sediment composition and organic loading impact the burrowing, tube building, and feeding abilities of infaunal invertebrates, thus affecting benthic community structure (Gray 1981, Snelgrove and Butman 1994). Many demersal fish species are also associated with specific sediment types that reflect the habitats of their preferred invertebrate prey (Cross and Allen 1993). Thus, understanding changes in sediment condition and quality over time and space is crucial to assessing corresponding changes in benthic invertebrate and demersal fish populations (see Chapters 6 and 8, respectively).

Both natural and anthropogenic factors affect the composition, distribution, and stability of seafloor sediments on the continental shelf. Natural factors that affect sediment conditions include geologic history, strength and direction of bottom currents, exposure to wave action, seafloor topography, inputs from rivers and bays, beach erosion, runoff, bioturbation by fish and benthic invertebrates, and decomposition of calcareous organisms (Emery 1960). These processes affect the size and distribution of sediment particles, as well as the chemical composition of sediments. For example, erosion from coastal cliffs and shores, and flushing of terrestrial sediment and debris from bays, rivers, and streams strongly influence the overall organic content and particle size of coastal sediments (Emery 1960). These inputs can also contribute to the deposition and accumulation of trace metals, or other contaminants, on the sea floor. In addition, primary productivity by phytoplankton, and decomposition of marine and terrestrial organisms, are major sources of organic loading in coastal shelf sediments (Mann 1982, Parsons et al. 1990).

Municipal wastewater outfalls, such as the PLOO and SBOO off San Diego, are one of many anthropogenic sources which may influence sediment characteristics through the discharge of treated effluent and the subsequent deposition of a wide variety of organic and inorganic compounds. Some of the most commonly detected contaminants discharged via ocean outfalls are trace metals, pesticides, and various indicators of organic loading such as organic carbon, nitrogen, and sulfides (Anderson et al. 1993). In particular, organic enrichment due to wastewater discharge is of concern as it may impair habitat quality for resident marine organisms and, thus, disrupt ecological processes (Gray 1981). Lastly, the physical presence of a large outfall, and associated ballast materials (e.g., rock, sand) on the seafloor, may alter the hydrodynamic regime in surrounding areas, thus affecting sediment movement and transport, as well as the structure of local fish and invertebrate communities.

This chapter presents analysis and interpretation of sediment particle size and chemistry data collected during 2024 and 2025, from core benthic monitoring stations throughout the PLOO and SBOO regions. The three primary goals of this chapter are to: (1) document sediment conditions at core monitoring stations; (2) identify if concentrations of pollutants in marine sediments are at levels that would degrade the benthic communities; (3) identify possible effects of wastewater discharge on sediment quality; (4) identify other potential natural or anthropogenic sources of sediment contamination. For additional information, a broader regional assessment of benthic conditions throughout the entire San Diego region is presented in Chapter 7.

Materials and Methods

Field Sampling

Benthic samples analyzed in this chapter were collected at a total of 49 core monitoring stations, located at inner shelf (≤ 30 m) to middle shelf (> 30 –120 m) depths, surrounding the PLOO and SBOO, during winter (January) and summer (July) of 2024 and 2025 (Figure 5.1). The PLOO sites include 12 primary core stations located along the 98-m discharge depth contour, and 10 secondary core stations located along or adjacent to the 88-m or 116-m depth contours. The SBOO sites include 12 primary core stations located along the 28-m discharge depth contour, and 15 secondary core stations located along or adjacent to the 19, 38, or 55-m depth contours. Stations located within 1000 m of the boundary of the zone of initial dilution (ZID), for either outfall, are considered to represent near-ZID conditions. These include PLOO stations E11, E14, E15 and E17, and SBOO stations I12, I14, I15 and I16.

Samples for benthic analyses were collected using a double 0.1-m^2 Van Veen grab, with one grab per cast used for sediment quality analyses, one grab per cast used for benthic community analysis, and subsequent grabs used for sediment toxicity testing where required (see Chapters 6 and 7). Visual observations of weather, sea conditions, and human/animal activity were also recorded at the time of sampling. Criteria established by the U.S. Environmental Protection Agency (USEPA) to ensure consistency of these types of samples were followed with regard to sample disturbance and depth of penetration (USEPA 1987). Sub-samples for particle size and sediment chemistry analyses were taken from the top 2 cm of the sediment surface and handled according to standard guidelines (USEPA 1987, SCCWRP 2018).

Laboratory Analyses

All sediment chemistry and particle size analyses were performed at the City's Environmental Chemistry Services Laboratory. Detailed analytical protocols are available upon request. Briefly, sediment sub-samples were analyzed on a dry weight basis to determine concentrations of various indictors of organic loading (biochemical oxygen demand, total organic carbon, total nitrogen, total sulfides, total volatile solids), 17 trace metals, nine chlorinated pesticides, 42 polychlorinated biphenyl compound congeners (PCBs), 24 polycyclic aromatic hydrocarbons (PAHs), and 13 polybrominated ethers (PBDEs). Data were limited to values above the method detection limit (MDL) for each parameter (Appendix D.1). A variety of laboratory technical issues resulted in a number of non-reportable sediment chemistry data for the 2024 and 2025 benthic surveys, see Appendices D.2–D.12.

Particle size analysis was performed using either a Horiba LA-950V2 laser scattering particle analyzer or a set of nested sieves. The Horiba measures particles ranging in size from 0.5 to 2000 µm.

Coarser sediments were removed and quantified prior to laser analysis by screening samples through a 2000 µm mesh sieve. These data were later combined with the Horiba results to obtain a complete distribution of particle sizes totaling 100%, and then classified into 11 sub-fractions and four main size fractions based on the Wentworth scale (Folk 1980) (see Appendix D.13). When a sample contained substantial amounts of coarse sand, gravel, shell hash or other large materials that could damage the Horiba analyzer, or where the general distribution of sediments would be poorly represented by laser analysis, a set of nested sieves was used with mesh sizes of 2000 µm, 1000 µm, 500 µm, 250 µm, 125 µm, 75 µm, and 63 µm to divide the samples into seven sub-fractions. See Appendix D.14 for visual observations for each PLOO and SBOO core station.

Data Analyses

Data collected during 2024 were reported previously (City of San Diego 2025), and all raw data for the 2024-2025 sampling period have been submitted to the Regional Water Quality Control Board, the California Environmental Data Exchange Network (CEDEN) and the City's Open Data Portal (City of San Diego 2026) and will be provided upon request.

Data summaries for the various sediment parameters included detection rate, minimum, maximum, and mean values for all samples combined by outfall region (i.e., PLOO, SBOO). Historical summaries were generated using data from current primary and secondary core stations but limited to samples collected during winter and summer surveys. For chemistry parameters, all means were calculated using detected values only, with no substitutions made for non-detects in the data (i.e., analyte concentrations < method detection limit [MDL]). Limiting analyses to detected values (i.e., excluding non-detects) is considered a conservative way of handling contaminant concentrations as it creates a strong upward bias in the data and respective summary statistics, and therefore may represent a worst-case scenario (e.g., see Helsel 2005a, b, 2006 for discussions of non-detect data). In contrast to previous reports (e.g., City of San Diego 2022c), estimated values that fell below method detection limits but were confirmed by mass-spectrometry were excluded from all data (1991–2025). Instead, estimated values were treated as non-detects for this report. Total chlordane, total DDT (tDDT), total hexachlorocyclohexane (tHCH), total PCB (tPCB), total PAH (tPAH), and total PBDE (tPBDE) were calculated for each sample as the sum of all individual constituents with reported values. When applicable, contaminant concentrations were compared to the Effects Range Low (ERL) and Effects Range Median (ERM) sediment quality guidelines of Long et al. (1995). The ERLs represent chemical concentrations below which adverse biological effects are rarely observed, while values above ERLs, but below ERMs, represent levels at which effects occasionally occur. Concentrations above the ERM indicate likely biological effects, although these may not always be validated by toxicity testing results (Schiff and Gossett 1998). Analyses were performed using R (R Core Team 2022) and various functions within the zoo, reshape2, plyr, stringr, Rmisc, ROBDC, tidyr, ggpubr, vegan, psych, tidyverse, ggplot2, and dplyr (Zeileis and Grothendieck 2005, Wickham 2007, 2011, 2019, Hope 2013, Ripley and Lapsley 2017, Wickham and Henry 2018, Kassambara 2019, Oksanen et al. 2019, Revelle 2019, Wickham et al. 2019a,b, 2020).

RESULTS

Particle Size Distribution

Ocean sediments sampled at the core PLOO stations during 2024 and 2025 were composed primarily of fine silts and clays (fine particles, or percent fines), plus fine sands. Percent fines ranged from 19.7 to 71.0% per sample, while fine sands ranged from 15.5 to 69.5%, medium-coarse sands ranged from 0 to 49.6%, and coarse particles ranged from 0 to 24.4% (Table 5.1). Coarser particles often included shell hash, black sand, and/or gravel (Appendix D.14). Overall, there were no spatial patterns in sediment composition relative to proximity to the PLOO discharge site over the past two years (Figure 5.2). For example, most samples from the near-ZID stations (E11, E14, E15, and E17) had proportions of fine particles that fell within the range of the farfield stations (31.7-54.7% versus 19.7-71.0% per sample, respectively). Occasionally, larger proportions of medium-coarse sands (>10% per sample) and coarse particles (>5% per sample) were found at the near-ZID stations, the B stations to the north of the region (stations B9, B11, B12), and to the south of the region (stations E1, E5, E9).

There was no evidence that fine sediments have been accumulating over time at any of the nearfield or farfield primary core PLOO stations since wastewater discharge began at the current discharge site in late 1993 (Figure 5.3). Instead, temporal variability of sediment composition at these sites has been primarily in the sand and coarse fractions (see City of San Diego 2014a, 2022a). This variability has corresponded to occasional patches of coarse sands (e.g., black sand) or larger particles (e.g., gravel, shell hash). For example, black sands have been observed at stations E9, E15, and E14 over the years (e.g., City of San Diego 2020, 2022c, 2023, 2024) possibly due in part to the presence of ballast or bedding material near the outfall (City of San Diego 2022a). In addition to the sporadic occurrence of coarser sediments at a few stations, a sudden, region-wide increase in fine particles was observed starting in winter 2019. This abrupt change remains unexplained.

In contrast to the PLOO region, seafloor sediments were much more diverse at the SBOO monitoring sites during 2024 and 2025. Percent fines ranged from 0 to 93.6% per sample at these stations, while fine sands ranged from 0.6 to 90.9%, medium-coarse sands ranged from 0 to 93.3%, and coarse particles ranged from 0 to 48.0% (Table 5.2). Coarser particles at the SBOO stations often comprised shell hash, red relict sands, black sand, or organic debris (Appendix D.14). There were no spatial patterns in sediment composition relative to proximity to the SBOO discharge site over the past two years (Figure 5.2). Similar to the rest of the SBOO region, sediments from near-ZID stations (I12, I14, I15, and I16) were highly variable, with proportions of fine particles ranging from 1.9-52.9%, fine sands ranging from 3.9-82.4%, medium-coarse sands ranging from 0.6-89.8%, and coarse particles ranging from 0-9.3%.

It is interesting to note that fine particles also appeared to increase starting in winter 2019 at some SBOO primary core stations (Figure 5.3). Previous analysis of particle size data revealed considerable temporal variability at some sites within the SBOO region and relative stability at others, with no clear patterns evident relative to depth, proximity to the outfall, or other sources of nearshore sediment plumes, such as San Diego Bay and the Tijuana River (City of San Diego 2014b).

Indicators of Organic Loading

Detection rates and concentrations of the various indicators of organic loading in benthic sediments, surrounding the PLOO and SBOO, varied both within and between regions during 2024 and 2025

(Tables 5.1, 5.2). Only the parameter total volatile solids (TVS) was detected in all sediment samples from both regions. In contrast, total nitrogen (TN) and total organic carbon (TOC) were detected in 95-99% of the PLOO sediment samples, but only in 42% and 32% of the SBOO samples, respectively. Detection rates for sulfides were 85% in the PLOO region and 32% in the SBOO region. Although not a required parameter for any of the PLOO or SBOO permits, biochemical oxygen demand (BOD) has long been measured by the City at PLOO benthic stations; this parameter was detected in all PLOO primary core station sediment samples for which it was analyzed during 2024 and 2025. Detection rates for all of these parameters were similar to, or lower than, those recorded historically since monitoring began. Lower detection rates likely reflect changes in MDLs; for example, the MDL for sulfides went from 0.14 ppm in summer 2017 to 2.2 ppm for the current reporting period (Appendix D.1).

Sediments off Point Loma, in 2024 and 2025, had BOD concentrations ≤ 727 ppm per sample, while sulfides were ≤ 51.6 ppm, TN was ≤ 0.172% weight, TOC was ≤ 2.88% weight, and TVS was ≤ 4.1% weight per sample (Table 5.1). The highest concentrations of TN, TOC, and TVS were consistently detected in sediments from the northern 'B' stations located at least 10 km north of the PLOO (Figure 5.4). In contrast, BOD and sulfide distributions were more variable over this period. The highest concentration of BOD occurred in one sample from station B12 north of the PLOO. The highest concentrations of sulfides occurred in one sample each from near-ZID stations E14 and E17, as well as in one sample each from farfield stations B8 and E7 during the report period. In general, only sulfide and BOD have shown any changes in concentrations near the PLOO that appear consistent with possible organic enrichment (Figure 5.3) (see also City of San Diego 2022a,b, 2023, 2024).

Sediments surrounding the SBOO, in 2024 and 2025, had sulfide concentrations ≤ 15.6 ppm per sample, while TN concentrations were ≤ 0.067% weight, TOC concentrations were ≤ 2.13% weight, and TVS concentrations were ≤ 1.8% weight per sample (Table 5.2). There was little evidence of any organic enrichment near the SBOO discharge site during these two years; the highest concentrations of the various organic loading indicators were widely distributed throughout the region (Figure 5.4). For TOC, TN and TVS, variable concentrations may be linked to regional differences in sediment particle composition since these parameters can co-vary with the amount of percent fines (see City of San Diego 2014b and Chapter 7). In contrast to the overall survey area, concentrations of these organic indicators have been less variable at the SBOO primary core stations, with no patterns indicative of organic enrichment being evident since wastewater discharge began in early 1999 (Figure 5.3). For both regions, all reported concentrations of TN and TOC over the past 29-33 years generally fell within ranges reported regionally off San Diego (e.g., Chapter 7; see also City of San Diego 2022b), and elsewhere in the SCB (e.g., Dodder et al. 2016, Du et al. 2020, Wong et al. in review).

Trace Metals

Eleven of the 17 trace metals analyzed were detected in all sediment samples collected at the PLOO and SBOO core benthic stations, in 2024 and 2025, including: aluminum, arsenic, barium, beryllium, chromium, copper, iron, lead, manganese, nickel, and zinc (Tables 5.1, 5.2). Antimony, cadmium, and tin also had high detection rates in both regions (≥ 70%). Mercury and selenium were found more often in the PLOO region (100% and 85%, respectively) than in the SBOO region (51% and 38%, respectively). Silver was not detected in any samples collected during the 2-year reporting period.

Of the nine metals with published ERLs and ERMs (Long et al. 1995), only arsenic was reported at levels above its threshold during 2024 or 2025 (Table 5.3). Arsenic exceeded its ERL in three of the four sediment samples collected from SBOO farfield station I21 collected during 2024 and 2025. None

of these exceeded the ERM for arsenic. In addition to low overall values, metal concentrations tended to vary in sediments throughout the two regions, with no discernible patterns relative to proximity to either outfall (Figure 5.5, Appendix D.15). Several of the highest concentrations of aluminum, antimony, barium, beryllium, chromium, copper, lead, manganese, mercury, nickel, and zinc, were found in sediments from one or more of the northern 'B' stations or southern 'E' stations within the PLOO region. As with TOC, TN and TVS, this pattern may be linked to regional differences in sediment particle composition since several of these metals can co-vary with the amount of percent fines (see City of San Diego 2014b and Chapter 7). Cadmium tended to be highest near the PLOO, with the five highest values (≥ 0.101) recorded in sediments from near-ZID stations E11, E14 and E17, and at SBOO station I35. Note, though, that the maximum value recorded at these sites (0.119 ppm) was an order of magnitude below the ERL of 1.2 ppm.

Historically, detection rates have been relatively high for several different metals at PLOO and SBOO stations. For example, aluminum, arsenic, barium, chromium, copper, iron, lead, manganese, nickel, and zinc have been detected in ≥ 69% of the sediment samples collected in these areas since monitoring began (Tables 5.1, 5.2). Mercury and tin were also detected frequently (≥ 69%) at PLOO stations, but less frequently at SBOO stations (31% and 54%, respectively). Concentrations of mercury have remained below the ERL, while exceedances for arsenic, cadmium, chromium, copper, lead, nickel, silver, and zinc have also been rare (historical rates ≤ 6.7% within each region; Table 5.3). Concentrations of the remaining metals have been extremely variable with most being detected within ranges reported regionally off San Diego (e.g., Chapter 7; see also City of San Diego 2022b), and elsewhere in the Southern California Bight (SCB) (e.g., Dodder et al. 2016, Du et al. 2020, Wong et al. in review). While high metal concentrations have been occasionally recorded in sediments collected from both PLOO and SBOO near-ZID stations, no discernible long-term patterns have been identified that could be associated with proximity to either outfall or to the onset of wastewater discharge (Figure 5.6, Appendix D.16). It should be noted, however, that cadmium has been slightly higher at near-ZID station E14 versus other sites in several of the surveys over the past two decades. These values rarely exceeded the ERL of 1.2 ppm, never exceeded the ERM of 9.6 ppm, and there is no indication that cadmium is accumulating in the sediments around the outfall or within the region.

Pesticides, PCBs, PAHs, PBDEs

A total of four chlorinated pesticides were detected in benthic sediments off San Diego during 2024 and 2025, including chlordanes, DDT, hexachlorobenzene (HCB), and endosulfan (Tables 5.1, 5.2). The most common of these pesticides, DDT, was detected in 97% of the PLOO samples and 18% of the SBOO samples, with total DDT concentrations ≤ 18,000 ppt and ≤ 1112 ppt per region, respectively. Chlordanes had a detection rate of 1% for each of the PLOO and SBOO regions, concentrations did not exceed 94 ppt in the PLOO and 341 ppt in the SBOO. HCB had a detection rate of 6% for the PLOO region, at concentrations ≤389 ppt, but was not detected in the SBOO region this reporting period. Endosulfan was detected in one SBOO sample, at a concentration 92 ppt for beta-endosulfan and 66 ppt for alpha-ensosulfan. Aldrin, dieldrin, other endosulfans (endosulfan sulfate), endrin, endrin aldehyde, and mirex were not detected in any PLOO or SBOO sediment samples during this reporting period. The spatial distribution of these pesticides varied in sediments from throughout the two regions over the past two years, with no discernible patterns relative to either outfall (e.g., Figure 5.7). Only one sample, taken from station E5 in the PLOO region, exceeded the ERL threshold of 1580 ppt. This sample did not exceed the ERM threshold of 461,000 ppt.

During the 2024–2025 reporting period, PCBs were detected in 20% of sediment samples from the PLOO region at concentrations up to 24,938 ppt, and in 3% of samples from the SBOO region, at concentrations up to 720 ppt (Tables 5.1, 5.2, Figure 5.7). The highest values were found in sediments collected adjacent to the LA-5 dredge materials dumpsite at stations E1, E2 and E3, an area known for elevated PCBs (see City of San Diego 2022a and Parnell et al 2008). All other total PCB concentrations from the PLOO region were below 2,039 ppt. PAHs were also detected more frequently in the PLOO region than the SBOO region (23% and 3%, respectively). Total PAH occurred at concentrations ≤ 192.3 ppb at all stations, well below the ERL threshold of 4022 ppb, with no discernable patterns relative to either outfall. Total PBDEs were only quantified for the SBOO region. Total PBDEs in the SBOO region were detected in 6% of samples at concentrations ≤ 338 ppt at all stations, including two near-ZID stations (I14, I15) and four farfield stations (I4, I22, I27, I30).

Historically, pesticide, PCB and PAH concentrations have been consistently low, with total DDT exceeding its ERL in just 8.3% of the samples collected in the PLOO region, and 2.2% of the samples in the SBOO region between 1991 or 1995 – 2023 (Table 5.3). Over this time period, total DDT exceeded its ERM in only 0.1% of PLOO sediment samples. Total PAH exceeded its ERL in 0.1% of the samples from PLOO stations, and never exceeded its ERM. These thresholds do not exist for PCBs measured as congeners, and historical comparisons cannot be made for PBDEs, since reporting of these only began in 2022. For both regions, all reported concentrations of total DDT, chlordanes, total PCB, and total PAHs were generally within values reported regionally off San Diego (e.g., Chapter 7; see also City of San Diego 2022b, 2023, 2024), and well below maximum values reported elsewhere in the SCB (e.g., Dodder et al. 2016, Du et al. 2020, Wong et al. in review). Finally, changes in DDT, PCB and PAH demonstrated no discernible long-term patterns that can be associated with wastewater discharge via either outfall (Figure 5.8).

Discussion

Particle size composition during the current reporting period (2024–2025) at PLOO and SBOO stations varied as expected by outfall region and depth stratum (e.g., Emery 1960, MBC 1988), and was generally consistent with results of previous surveys off San Diego (e.g., City of San Diego 2020, 2022a,b,c, 2024, Wong et al. in review). Within the PLOO region, percent fines (silt and clay) and fine sands continued to comprise the largest proportion of sediments. Within the SBOO region, sands continued to comprise the largest proportion of sediments, with the relative amounts of coarser and finer particles varying among sites. No spatial relationship was evident between sediment particle size composition and proximity to either the PLOO or SBOO discharge site. Further, there has not been any substantial accumulation of fine particles at any of the near-ZID stations or elsewhere since wastewater discharge began at the current PLOO discharge site in late 1993 or the SBOO discharge site in early 1999. Instead, a sudden increase in fine particles was observed across the entire PLOO region and part of the SBOO region starting in winter 2019 that has persisted through summer 2025. Further investigation is required to determine the origins of this dramatic change.

The diversity of sediment types in these areas reflect multiple geologic origins and complex patterns of transport and deposition. Variability in the composition of Point Loma sediments is likely affected by both anthropogenic and natural influences, including outfall construction or ballast materials, offshore disposal of dredged materials, and recent deposition of sediment and detrital materials (Emery 1960, Parnell et al. 2008, City of San Diego 2022a). For example, the PLOO lies within the Mission Bay littoral cell (Patsch and Griggs 2007), which has natural sources of sediments, such as outflows from Mission Bay, the San Diego River, and San Diego Bay. However, fine particles may also travel in suspension across littoral cell

borders up and down the coast (e.g., Farnsworth and Warrick 2007, Svejkovsky 2013), thus widening the range of potential sediment sources to the region. Additionally, the presence of relict red sands at some stations in the SBOO region is indicative of minimal sediment deposition in recent years (Emery 1960). Several SBOO stations are also located within or near an accretion zone for sediments moving within the Silver Strand littoral cell (MBC-ES 1988, Patsch and Griggs 2007). Therefore, higher proportions of fine sands, silts, and clays at these sites are also likely associated with the transport of fine materials originating from the Tijuana River, the Silver Strand beach, and to a lesser extent from San Diego Bay (MBC-ES 1988).

Various organic loading indicators, trace metals, pesticides, PCBs, PAHs, and PBDEs were detected in sediment samples collected throughout the PLOO and SBOO regions in 2024 and 2025. However, concentrations of these parameters were below ERM thresholds, mostly below ERL thresholds, and typically within historical ranges at regional sites (e.g., City of San Diego 2020, 2022b,c, 2024). Additionally, values for most sediment parameters remained within ranges typical for other areas of the southern California continental shelf (see Schiff and Gossett 1998, City of San Diego 2022b, Noblet et al. 2002, Schiff et al. 2006, 2011, Maruya and Schiff 2009, Dodder et al. 2016, Du et al. 2020, Wong et al. in review).

There have been few, if any, clear spatial patterns consistent with outfall discharge effects on sediment chemistry values over the past several years, with concentrations of most contaminants at near-ZID sites falling within the range of values observed at farfield stations. The only exceptions off San Diego have been slightly higher BOD, sulfide, and cadmium levels measured in sediments near the PLOO discharge site (see also City of San Diego 2022a). Instead, the highest concentrations of several organic indicators, trace metals, pesticides, PCBs, and PAHs have historically occurred in sediments from southern and/or northern farfield stations. The driver of elevated contaminants at the northern PLOO stations is unknown, while sediments from the southern PLOO stations are known to be impacted by the dumping of dredged materials destined originally for the LA-5 dredged disposal dumpsite (Anderson et al. 1993, Steinberger et al. 2003, Parnell et al. 2008). In the SBOO region, relatively high values of most parameters could be found distributed throughout the region, and several organic indicators and metals co-occurred in samples characterized by finer sediments. This association is expected due to the known correlation between particle size and concentrations of these chemical parameters (Eganhouse and Venkatesan 1993). For the four parameters found at slightly higher concentrations at PLOO near-ZID stations, there has been no indication of contaminant accumulation in the sediments.

The broad distribution of various contaminants in sediments throughout the PLOO and SBOO regions is likely derived from several sources. Mearns et al. (1991) described the distribution of contaminants, such as arsenic, mercury, DDT, and PCBs as being ubiquitous in the SCB. Additionally, Brown et al. (1986) concluded that there may be no coastal areas in southern California that are sufficiently free of chemical contaminants to be considered reference sites. This has been supported by more recent surveys of SCB continental shelf habitats (Schiff and Gossett 1998, Noblet et al. 2002, Schiff et al. 2006, 2011, Dodder et al. 2016, Du et al. 2020). The lack of contaminant-free reference areas clearly pertains to the PLOO and SBOO regions as demonstrated by the presence of many contaminants in sediments prior to wastewater discharge (see City of San Diego 2000, 2022a). In addition, historical assessments of benthic sediments off the coast of Los Angeles have shown that as wastewater treatment improved, sediment conditions were more likely affected by other factors (Stein and Cadien 2009). Such factors may include bioturbative re-exposure of buried legacy sediments (Niedoroda et al. 1996, Stull et al. 1996), large storms that assist redistribution of legacy contaminants (Sherwood et al. 2002), and stormwater discharges (Schiff et al. 2006, Nezlin et al. 2007). Possible non-outfall sources and pathways of contaminant dispersal off San Diego include transport of contaminated sediments from San Diego Bay via tidal exchange, offshore

disposal of dredged sediments, nearshore turbidity plumes emanating from the Tijuana River, and surface runoff from local watersheds (Parnell et al. 2008).

In conclusion, there was no evidence of fine particle loading related to wastewater discharge via the PLOO or SBOO, during the current reporting period, or since the discharge originally began through either outfall in the 1990s. Likewise, contaminant concentrations at near-ZID stations were generally within the range of variability observed throughout both outfall regions and do not appear to reflect any significant organic enrichment. The only sustained effects have been restricted to a few sites located within 200 m of the PLOO (near-ZID stations E11, E14 and E17). These minor effects include sporadic occurrences of slightly higher values of BOD, sulfide, and cadmium. Finally, the quality of PLOO and SBOO sediments in 2024 and 2025 was similar to previous years with overall contaminant concentrations remaining relatively low compared to available thresholds, or values found in other southern California coastal areas (Schiff and Gossett 1998, Noblet et al. 2002, Schiff et al. 2006, 2011, Maruya and Schiff 2009, Dodder et al. 2016, Du et al. 2020, Wong et al. in review). Consequently, there is presently no evidence to suggest that wastewater discharge via the PLOO or SBOO is affecting the quality of benthic sediments off San Diego to the point that it may degrade resident marine biological communities (i.e., Chapters 6–8).

Literature Cited

Anderson, J.W., D.J. Reish, R.B. Spies, M.E. Brady, and E.W. Segelhorst. (1993). Human Impacts. In: M.D. Dailey, D.J. Reish, and J.W. Anderson (eds.). Ecology of the Southern California Bight: A Synthesis and Interpretation. University of California Press, Berkeley, CA. p 682–766.

Brown, D.A., R.W. Gossett, G.P. Hershelman, C.G. Word, A.M. Westcott, and J.N. Cross. (1986). Municipal wastewater contamination in the Southern California Bight: Part I–metal and organic contaminants in sediments and organisms. Marine Environmental Research, 18: 291–310.

City of San Diego. (2000). International Wastewater Treatment Plant Final Baseline Ocean Monitoring Report for the South Bay Ocean Outfall (1995–1998). City of San Diego Ocean Monitoring Program, Metropolitan Wastewater Department, Environmental Monitoring and Technical Services Division, San Diego, CA.

City of San Diego. (2014a). Point Loma Ocean Outfall Annual Receiving Waters Monitoring and Assessment Report, 2013. City of San Diego Ocean Monitoring Program, Public Utilities Department, Environmental Monitoring and Technical Services Division, San Diego, CA.

City of San Diego. (2014b). South Bay Ocean Outfall Annual Receiving Waters Monitoring and Assessment Report, 2013. City of San Diego Ocean Monitoring Program, Public Utilities Department, Environmental Monitoring and Technical Services Division, San Diego, CA.

City of San Diego. (2020). Biennial Receiving Waters Monitoring and Assessment Report for the Point Loma and South Bay Ocean Outfalls, 2018–2019. City of San Diego, Public Utilities Department, Environmental Monitoring and Technical Services Division, San Diego, CA.

City of San Diego. (2022a). Appendix C.1 Benthic Sediments, Invertebrates and Fishes. In: Application for Renewal of NPDES CA0107409 and 301(h) Modified Secondary Treatment Requirements Point Loma Ocean Outfall. Volume V, Appendices C thru D. Public Utilities Department, Environmental Monitoring and Technical Services Division, San Diego, CA.

City of San Diego. (2022b). Appendix C.2 San Diego Benthic Tolerance Intervals; 24-Year San Diego Regional Benthic Assessment and Reference Tolerance Intervals. In: Application for Renewal of NPDES CA0107409 and 301(h) Modified Secondary Treatment Requirements Point Loma Ocean Outfall. Volume V, Appendices C thru D. Public Utilities Department, Environmental Monitoring and Technical Services Division, San Diego, CA.

City of San Diego. (2022c). Biennial Receiving Waters Monitoring and Assessment Report for the Point Loma and South Bay Ocean Outfalls, 2020–2021. City of San Diego, Public Utilities Department, Environmental Monitoring and Technical Services Division, San Diego, CA.

City of San Diego. (2023). Interim Receiving Waters Monitoring Report for the Point Loma and South Bay Ocean Outfalls, 2022. City of San Diego, Public Utilities Department, Environmental Monitoring and Technical Services Division, San Diego, CA.

City of San Diego. (2024). Biennial Receiving Waters Monitoring and Assessment Report for the Point Loma and South Bay Ocean Outfalls, 2022–2023. City of San Diego, Public Utilities Department, Environmental Monitoring and Technical Services Division, San Diego, CA.

City of San Diego. (2026). Ocean Monitoring Program Reports and Data. https://www.sandiego.gov/public-utilities/sustainability/ocean-monitoring/reports

Cross, J.N. and L.G. Allen. (1993). Fishes. In: M.D. Dailey, D.J. Reish, and J.W. Anderson (eds.). Ecology of the Southern California Bight: A Synthesis and Interpretation. University of California Press, Berkeley, CA. p 459–540.

Dodder, N., K. Schiff, A. Latker, C-L Tang. (2016). Southern California Bight 2013 Regional Monitoring Program: IV. Sediment Chemistry. Southern California Coastal Water Research Project, Westminster, CA.

Du, B., C.S. Wong, K. Mclaughlin, and K. Schiff. (2020). Southern California Bight 2018 Regional Monitoring Program: II. Sediment Chemistry. Southern California Coastal Water Research Project, Westminster, CA.

Eganhouse, R.P. and M.I. Venkatesan. (1993). Chemical Oceanography and Geochemistry. In: M.D. Dailey, D.J. Reish, and J.W. Anderson (eds.). Ecology of the Southern California Bight: A Synthesis and Interpretation. University of California Press, Berkeley, CA. p 71–189.

Emery, K.O. (1960). The Sea off Southern California. John Wiley, New York, NY.

Farnsworth, K.L. and J.A. Warrick. (2007). Sources, dispersal, and fate of fine sediment supplied to coastal California. U.S. Geological Survey Scientific Investigations Report 2007–5254. Reston, VA.

Folk, R.L. (1980). Petrology of Sedimentary Rocks. Hemphill, Austin, TX.

Gray, J.S. (1981). The Ecology of Marine Sediments: An Introduction to the Structure and Function of Benthic Communities. Cambridge University Press, Cambridge, England.

Helsel, D.R. (2005a). More than obvious: better methods for interpreting nondetect data. Environmental Science & Technology (October 15, 2005), 419A-423A.

Helsel, D.R. (2005b). Nondetects and Data Analysis: Statistics for Censored Environmental Data. John Wiley, New York.

Helsel, D.R. (2006). Fabrication data: how substituting values for nondetects can ruin results, and what can be done about it. Chemosphere 65: 2434–2439.

Hope, R.M. (2013). Rmisc: Ryan Miscellaneous. R package version 1.5. http://CRAN.R-project.org/package=Rmisc.

Kassambara, A. (2019). ggpubr: 'ggplot2' Based Publication Ready Plots. R package version 0.2.5. https://CRAN.R-project.org/package=ggpubr.

Long, E.R., D.L. MacDonald, S.L. Smith, and F.D. Calder. (1995). Incidence of adverse biological effects within ranges of chemical concentration in marine and estuarine sediments. Environmental Management, 19: 81–97.

[MBC] MBC Applied Environmental Sciences and Engineering-Science. (1988). Part F: Biological studies. In: Tijuana Oceanographic Engineering Study, Volume 1. Ocean Measurement Program. Prepared for the City of San Diego, CA.

Mann, K.H. (1982). The Ecology of Coastal Marine Waters: A Systems Approach. University of California Press, Berkeley, CA.

Maruya, K.A. and K. Schiff. (2009). The extent and magnitude of sediment contamination in the Southern California Bight. Geological Society of America Special Paper, 454: 399–412.

Mearns, A.J., M. Matta, G. Shigenaka, D. MacDonald, M. Buchman, H. Harris, J. olas, and G. Lauenstein. (1991). Contaminant Trends in the Southern California Bight: Inventory and Assessment. NOAA Technical Memorandum NOS ORCA 62. Seattle, WA.

Nezlin, N.P., P.M. DiGiacomo, S.B. Weisberg, D.W. Diehl, J.A. Warrick, M.J. Mengel, B.H. Jones, K.M. Reifel, S.C. Johnson, J.C. Ohlmann, L. Washburn, and E.J. Terrill. (2007). Southern California Bight 2003 Regional Monitoring Program: V. Water Quality. Southern California Coastal Water Research Project. Costa Mesa, CA.

Niedoroda, A.W., D.J.P. Swift, C.W. Reed, and J.K. Stull. (1996). Contaminant dispersal on the Palos Verdes continental margin. Science of the Total Environment, 179: 109–133.

Noblet, J.A., E.Y. Zeng, R. Baird, R.W. Gossett, R.J. Ozretich, and C.R. Phillips. (2002). Southern California Bight 1998 Regional Monitoring Program: VI. Sediment Chemistry. Southern California Coastal Water Research Project, Westminster, CA.

Oksanen, J., F.G. Blanchet, R. Kindt, P. Legendre, P.R. Minchin, R.B. O'Hara, G.L. Simpson, P. Solymos, M.H.H. Stevens, and H. Wagner. (2019). vegan: Community Ecology Package. R package version 2.5-6. http://CRAN.R-project.org/package=vegan.

Parnell, P.E., A.K. Groce, T.D. Stebbins, and P.K. Dayton. (2008). Discriminating sources of PCB contamination in fish on the coastal shelf off San Diego, California (USA). Marine Pollution Bulletin, 56: 1992–2002.

Parsons, T.R., M. Takahashi, and B. Hargrave. (1990). Biological Oceanographic Processes 3rd Edition. Pergamon Press, Oxford.

Patsch, K. and G. Griggs. (2007). Development of Sand Budgets for California's Major Littoral Cells. Institute of Marine Sciences, University of California, Santa Cruz, CA.

R Core Team. (2022). R: A language and environment for statistical computing. R Foundation for Statistical Computing, Vienna, Austria. URL https://www.R-project.org/.

Revelle, W. (2019) psych: Procedures for Personality and Psychological Research, Northwestern University, Evanston, Illinois, USA, https://CRAN.R-project.org/package=psych Version = 1.9.12.31.

Ripley, B. and M. Lapsley. (2017). RODBC: ODBC Database Access. R package version 1.3-12. http://CRAN.R-project.org/package=RODBC.

[SCCWRP] Southern California Coastal Water Research Project. (2018). Southern California Bight 2018 Regional Monitoring Program: Contaminant Impact Assessment Field Operations Manual. Southern California Coastal Water Research Project. Costa Mesa, CA.

Schiff, K.C. and R.W. Gossett. (1998). Southern California Bight 1994 Pilot Project: III. Sediment Chemistry. Southern California Coastal Water Research Project. Westminster, CA.

Schiff, K., R. Gossett, K. Ritter, L. Tiefenthaler, N. Dodder, W. Lao, and K. Maruya. (2011). Southern California Bight 2008 Regional Monitoring Program: III. Sediment Chemistry. Southern California Coastal Water Research Project, Costa Mesa, CA.

Schiff, K., K. Maruya, and K. Christenson. (2006). Southern California Bight 2003 Regional Monitoring Program: II. Sediment Chemistry. Southern California Coastal Water Research Project, Westminster, CA.

Sherwood, C.R., D.E. Drake, P.L. Wiberg, and R.A. Wheatcroft. (2002). Prediction of the fate of p,p-DDE in sediment on the Palos Verdes shelf, California, USA. Continental Shelf Research, 32: 1025–1058.

Snelgrove, P.V.R. and C.A. Butman. (1994). Animal-sediment relationships revisited: cause versus effect. Oceanography and Marine Biology Annual Review, 32: 111–177.

Stein, E.D. and D.B. Cadien. (2009). Ecosystem response to regulatory and management actions: The Southern California experience in long-term monitoring. In: K. Schiff (ed.). Southern California Coastal Water Research Project Annual Report 2009. Southern California Coastal Water Research Project, Costa Mesa, CA.

Steinberger, A., E. Stein, and K. Schiff. (2003). Characteristics of dredged material disposal to the Southern California Bight between 1991 and 1997. In: Southern California Coastal Water Research Project Biennial Report 2001–2002. Long Beach, CA. p 50–60.

Stull, J.K., D.J.P. Swift, and A.W. Niedoroda. (1996). Contaminant dispersal on the Palos Verdes Continental margin. Science of the Total Environment, 179: 73–90.

Svejkovsky, J. (2013). Satellite and Aerial Coastal Water Quality Monitoring in the San Diego/Tijuana Region: Annual Summary Report, 1 January, 2012–31 December, 2012. Ocean Imaging, Solana Beach, CA.

[USEPA] United States Environmental Protection Agency. (1987). Quality Assurance and Quality Control for 301(h) Monitoring Programs: Guidance on Field and Laboratory Methods. EPA Document 430/9-86-004. Office of Marine and Estuary Protection, Washington, DC.

Wickham, H. (2007). Reshaping Data with the reshape Package. Journal of Statistical Software, 21(12), 1–20. URL http://www.jstatsoft.org/v21/i12/.

Wickham, H. (2011). The Split-Apply-Combine Strategy for Data Analysis. Journal of Statistical Software, 40(1), 1–29. URL http://www.jstatsoft.org/v40/i01/.

Wickham, H. (2019). stringr: Simple, Consistent Wrappers for Common String Operations. R package version 1.4.0. https://CRAN.R-project.org/package=stringr.

Wickham, H., R. Francois, L. Henry and K. Müller. (2020). dplyr: A Grammar of Data Manipulation. R package version 1.2.0. https://CRAN.R-project.org/package=dplyr.

Wickham, H., M. Averick, J. Bryan, W. Chang, L. D'Agostino McGowan, R. François, G.Grolemund, A. Hayes, L. Henry, J. Hester, M. Kuhn, T. Lin Pedersen, E. Miller, S. Milton Bache, K. Müller, J. Ooms, D. Robinson, D. P. Seidel, V. Spinu, K. Takahashi, D. Vaughan, C. Wilke, K. Woo, H. Yutani. (2019a). Welcome to the tidyverse. Journal of Open Source Software, 4(43), 1686, https://doi.org/10.21105/joss.01686.

Wickham, H., W. Chang, L. Henry, T.L. Pedersen, K. Takahashi, C. Wilke, K. Woo, (2019b). Ggplot2: Create Elegant Data Visualizations Using the Grammar of Graphics. Version 3.2.0. Rstudio. URL https://ggplot2.tidyverse.org/.

Wickham H. and L. Henry. (2018). tidyr: Easily Tidy Data with 'spread()' and 'gather()' Functions. R package version 0.7.2. https://CRAN.R-project.org/package=tidyr.

Wickham, H., Francois, L. Henry and K. Müller (2020). dplyr: A Grammar of Data Manipulation. R package version 0.8.5. https://CRAN.R-project.org/package=dplyr.

Wong, C., Schiff, K., and R. Butler. (in review). Southern California Bight 2023 Regional Monitoring Program: Volume II. Sediment Chemistry. Technical Report No. 1469, Southern California Coastal Water Research Project, Long Beach, CA.

Zeileis, A and G. Grothendieck. (2005). zoo: S3 Infrastructure for Regular and Irregular Time Series. Journal of Statistical Software, 14(6), 1-27. URL http://www.jstatsoft.org/v14/i06/

CHAPTER 5

FIGURES & TABLES

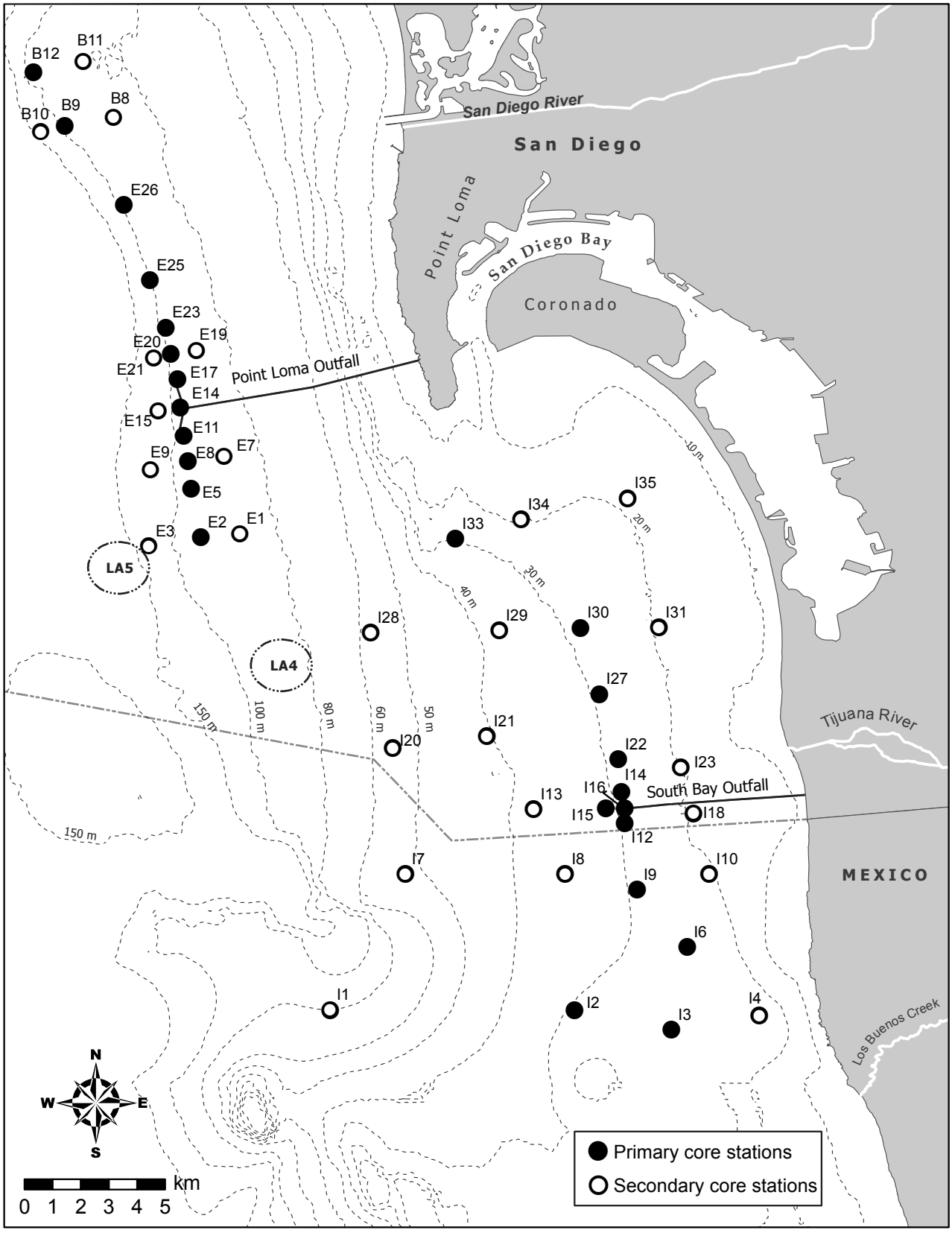


Figure 5.1
Benthic station locations sampled around the PLOO and SBOO as part of the City of San Diego's Ocean Monitoring Program.

Table 5.1

Summary of particle sizes and chemistry concentrations in sediments from PLOO benthic stations sampled historically (1991–2023) and during the current reporting period (2024–2025). Data include the total number of samples analyzed (n), detection rate (DR, %), minimum, maximum, and mean values for the entire survey area during each time period. For chemistry parameters, minimum and maximum values were calculated based on all samples, whereas means were calculated on detected values only; nd = not detected.

	Historical (1991–2023)					Current (2024–2025)				
Parameter	**n**	**DR**	**Min**	**Max**	**Mean**	**n**	**DR**	**Min**	**Max**	**Mean**
Particle Size (%)										
Coarse Particles	1320	27	0	64.2	1.4	88	30	0	24.4	1.5
Med-Coarse Sands	1320	96	0	66.5	3.6	88	97	0	49.6	5.3
Fine Sands	1320	100	0	85.6	51.5	88	100	15.5	69.5	43.2
Fine Particles	1320	100	0	80.9	43.5	88	100	19.7	71.0	50.0
Organic Indicators										
BOD (ppm)	1098	>99	nd	980	303	48	100	198	727	292
Sulfides (ppm)	1339	93	nd	108.0	5.4	88	85	nd	51.6	12.0
TN (% weight)	1274	99	nd	0.192	0.052	88	95	nd	0.172	0.056
TOC (% weight)	1275	100	0.13	4.85	0.69	88	99	nd	2.88	0.70
TVS (% weight)	1314	100	0.2	5.4	2.4	88	100	1.5	4.1	2.2
Metals (ppm)										
Aluminum	1232	100	3130	31800	9134	88	100	2720	11400	6926
Antimony	1324	52	nd	13.90	1.61	88	94	nd	1.23	0.54
Arsenic	1342	100	0.75	8.82	3.01	88	100	1.11	5.94	2.79
Barium	836	100	10.3	155.0	35.4	88	100	9.7	55.2	27.9
Beryllium	1342	50	nd	6.760	0.396	88	100	0.061	0.313	0.165
Cadmium	1342	46	nd	6.270	0.566	88	100	0.021	0.119	0.073
Chromium	1342	>99	nd	40.6	17.1	88	100	6.0	24.6	14.4
Copper	1342	>99	nd	82.4	8.0	88	100	2.3	14.2	6.2
Iron	1276	100	4840	31900	12749	88	100	3850	21200	10147
Lead	1342	71	nd	326.0	5.5	88	100	1.3	6.5	2.9
Manganese	1143	100	32	319	99	88	100	31	115	76
Mercury	1325	70	nd	0.142	0.029	88	100	0.011	0.100	0.031
Nickel	1342	97	nd	29.0	7.0	88	100	2.4	8.8	5.5
Selenium	1342	45	nd	0.90	0.28	88	85	nd	0.74	0.38
Silver	1342	12	nd	67.4	1.6	88	0	—	—	—
Tin	1143	69	nd	42.00	1.24	88	100	0.22	1.10	0.70
Zinc	1342	>99	nd	176.0	29.7	88	100	10.6	40.4	24.1
Pesticides (ppt)										
Total DDT	1304	56	nd	63580	1153	88	97	nd	18000	440
Total Chlordane	1304	2	nd	2000	305	88	1	nd	94	94
Total HCH	1304	1	nd	980	213	88	0	—	—	—
HCB	1097	5	nd	3300	704	88	6	nd	389	277
Endrin aldehyde	1304	<1	nd	970	970	88	0	—	—	—
Mirex	1304	<1	nd	66	66	88	0	—	—	—
Total PCB (ppt)	994	24	nd	60730	2382	88	20	nd	24938	2860
Total PAH (ppb)	1322	25	nd	9751.3	111.7	88	23	nd	192.3	48.7

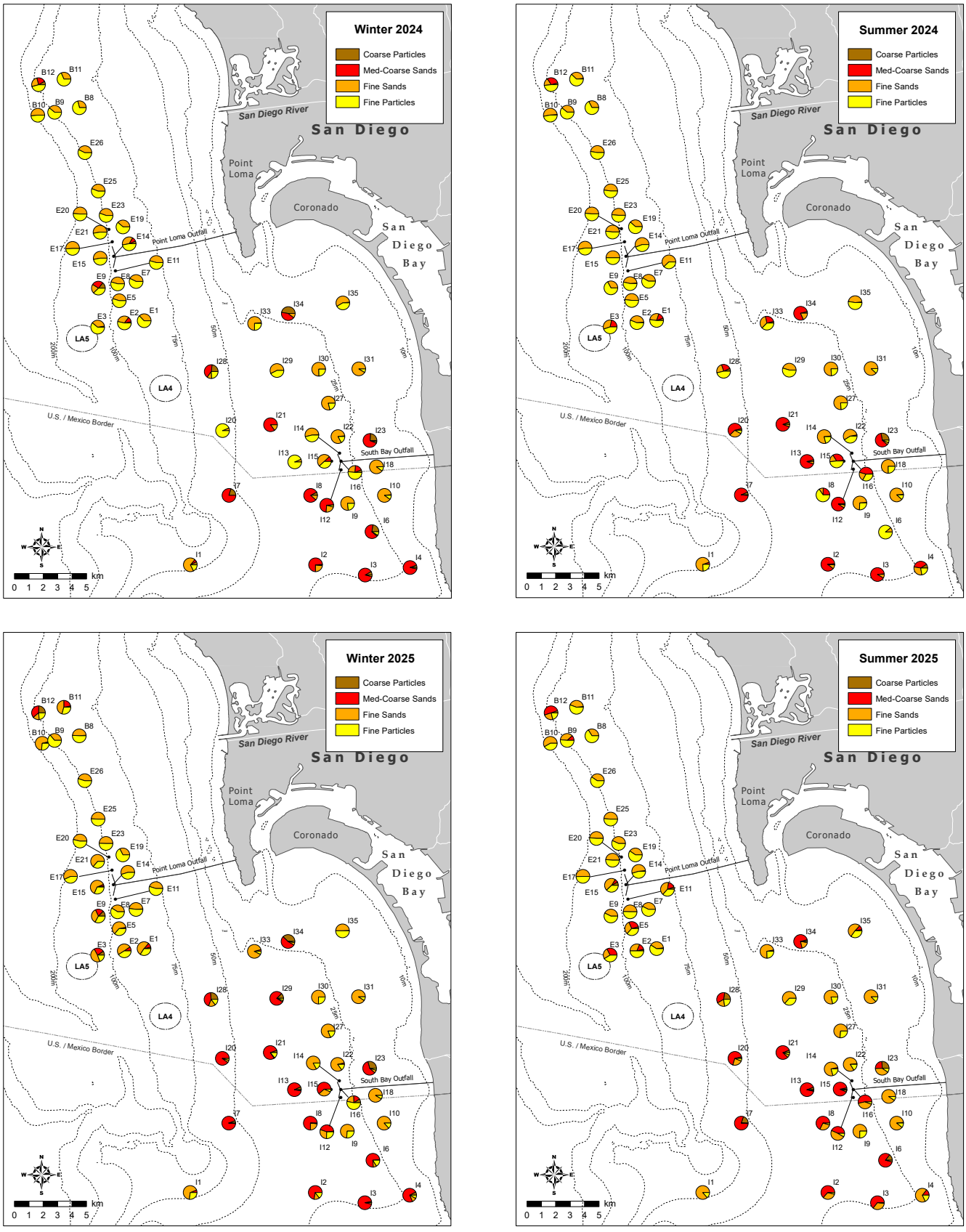


Figure 5.2
Sediment composition at PLOO and SBOO benthic stations during winter and summer surveys of 2024 and 2025.

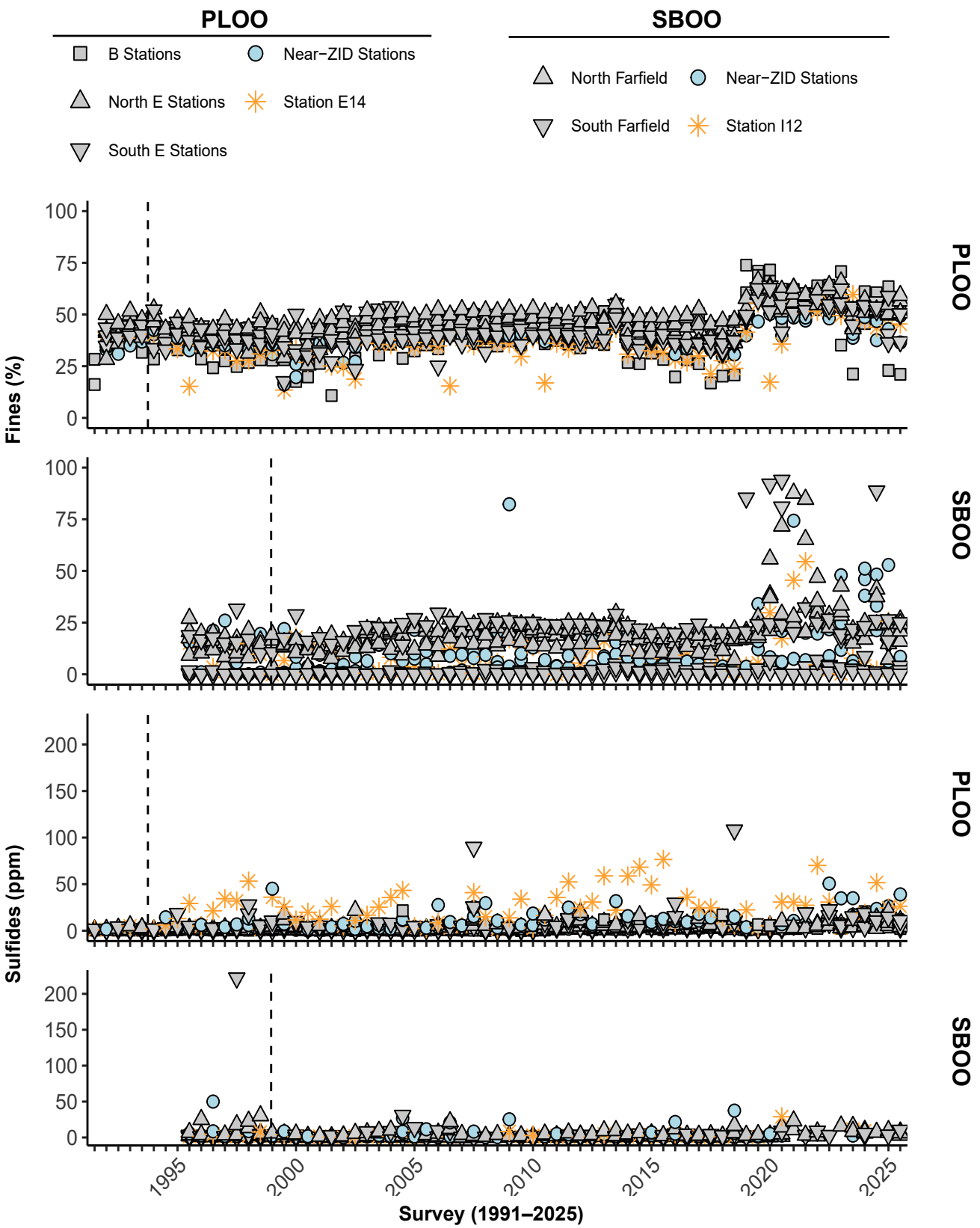


Figure 5.3

Percent fines and concentrations of organic indicators in sediments sampled during winter and summer surveys at PLOO primary core stations from 1991 through 2025 and at SBOO primary core stations from 1995 through 2025. Data represent detected values from each station, n ≤ 12 samples per survey. Dashed lines indicate onset of discharge from the PLOO or SBOO. Biochemical Oxygen Demand (BOD) only measured at PLOO stations.

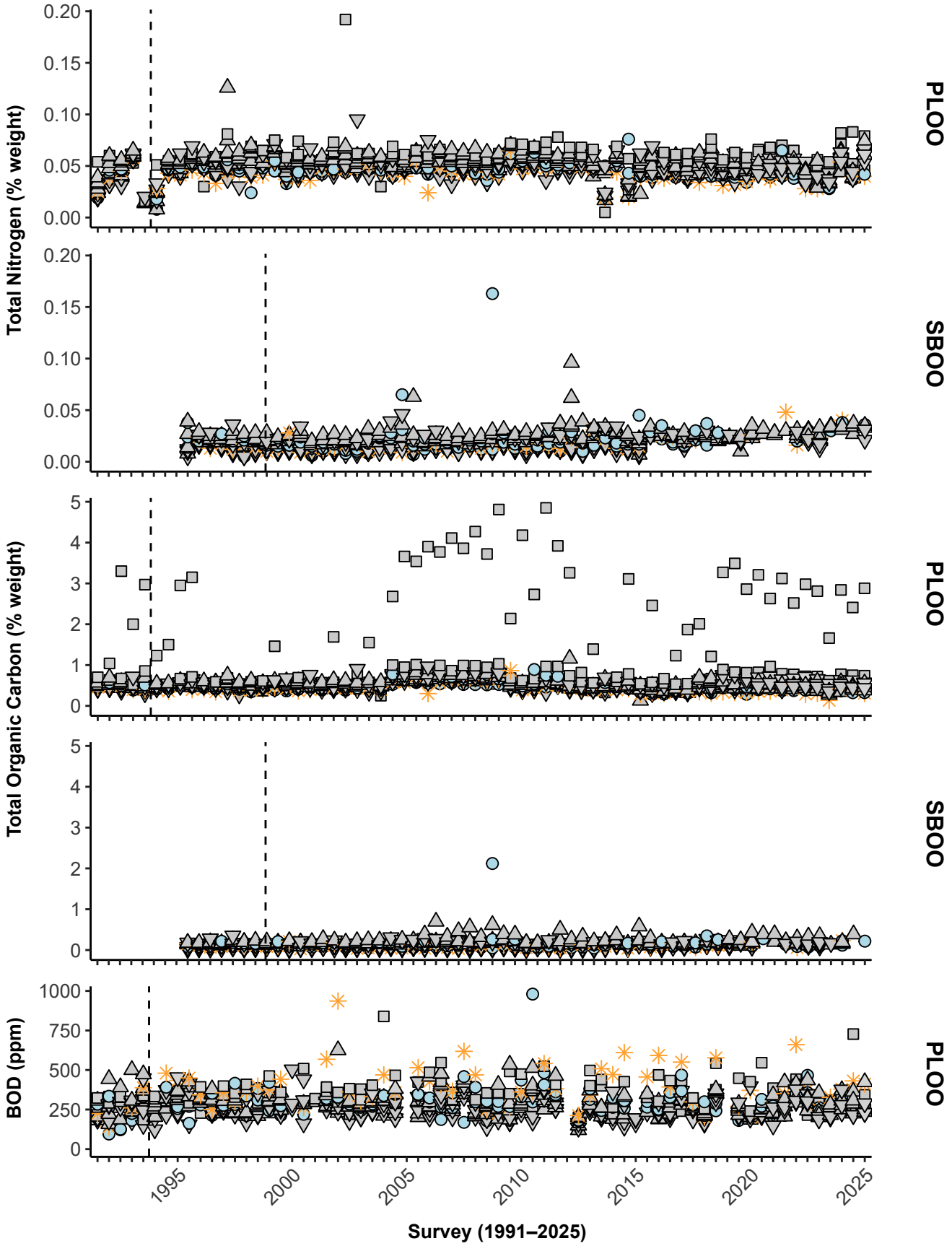


Figure 5.3 *continued*

Table 5.2

Summary of particle sizes and chemistry concentrations in sediments from SBOO benthic stations sampled historically (1995–2023) and during the current reporting period (2024–2025). Data include the total number of samples analyzed (n), detection rate (DR, %), minimum, maximum, and mean values for the entire survey area during each time period. For chemistry parameters, minimum and maxium values were calculated based on all samples, whereas means were calculated on detected values only; nd = not detected.

	Historical (1995–2023)					Current (2024–2025)				
Parameter	**n**	**DR**	**Min**	**Max**	**Mean**	**n**	**DR**	**Min**	**Max**	**Mean**
Particle Size (%)										
Coarse Particles	1503	45	0	56.8	2.8	108	54	0	48.0	4.8
Med-Coarse Sands	1503	99	0	99.8	34.9	108	99	0	93.3	35.6
Fine Sands	1503	100	0	97.4	49.0	108	100	0.6	90.9	41.0
Fine Particles	1503	89	0	100.1	13.2	108	93	0	93.6	18.6
Organic Indicators										
Sulfides (ppm)	1490	76	nd	222.0	3.2	98	32	nd	15.6	7.2
TN (% weight)	1508	82	nd	0.163	0.022	108	42	nd	0.067	0.035
TOC (% weight)	1508	92	nd	6.85	0.20	108	32	nd	2.13	0.38
TVS (% weight)	1436	100	0.2	39.8	0.9	108	100	0.3	1.8	0.8
Metals (ppm)										
Aluminum	1508	100	495	30100	4445	108	100	658	7760	3334
Antimony	1508	38	nd	6.40	0.68	108	70	nd	0.93	0.35
Arsenic	1508	99	nd	11.90	2.42	108	100	0.74	10.30	2.41
Barium	1104	100	nd	177.0	19.1	108	100	1.3	42.0	15.0
Beryllium	1508	43	nd	3.090	0.175	108	100	0.022	0.141	0.069
Cadmium	1508	27	nd	2.000	0.132	108	82	nd	0.102	0.034
Chromium	1508	>99	nd	39.0	9.6	108	100	2.4	13.6	8.2
Copper	1508	74	nd	99.2	3.4	108	100	0.3	5.8	1.9
Iron	1508	100	559	29300	6087	108	100	1170	8130	4858
Lead	1508	69	nd	20.0	2.2	108	100	0.7	5.5	1.5
Manganese	1481	100	5	621	61	108	100	7	86	42
Mercury	1454	31	nd	0.135	0.010	108	51	nd	0.022	0.009
Nickel	1508	78	nd	22.8	2.8	108	100	0.5	5.4	2.0
Selenium	1508	13	nd	0.62	0.22	108	38	nd	0.48	0.30
Silver	1508	11	nd	11.2	1.0	108	0	—	—	—
Tin	1481	54	nd	4.50	0.75	108	98	nd	3.02	0.32
Zinc	1508	96	nd	136.0	13.2	108	100	1.7	22.2	9.8

Table 5.2 *continued*

Parameter	Historical (1995–2023)					Current (2024–2025)				
	n	DR	Min	Max	Mean	n	DR	Min	Max	Mean
Pesticides (ppt)										
Total DDT	1453	17	nd	23380	901	108	18	nd	1112	289
Total Chlordane	1453	<1	nd	600	221	108	1	nd	341	341
Total HCH	1453	1	nd	3550	549	108	0	—	—	—
HCB	1085	7	nd	6200	695	108	0	—	—	—
Dieldrin	1453	<1	nd	59.6	59.6	108	0	—	—	—
Endrin	1453	<1	nd	133	133	108	0	—	—	—
Alpha-Endosulfan	1433	0	—	—	—	108	<1	nd	66	66
Beta-Endosulfan	1453	<1	nd	820	820	108	1	nd	91.7	91.7
Mirex	1453	<1	nd	50	41	108	0	—	—	—
Total PCB (ppt)	1298	4	nd	106390	2615	108	3	nd	720	380
Total PAH (ppb)	1484	13	nd	1819.5	74.5	108	3	nd	22.2	10.7
Total PBDE (ppt)	93	11	nd	142	73	108	6	nd	338	174

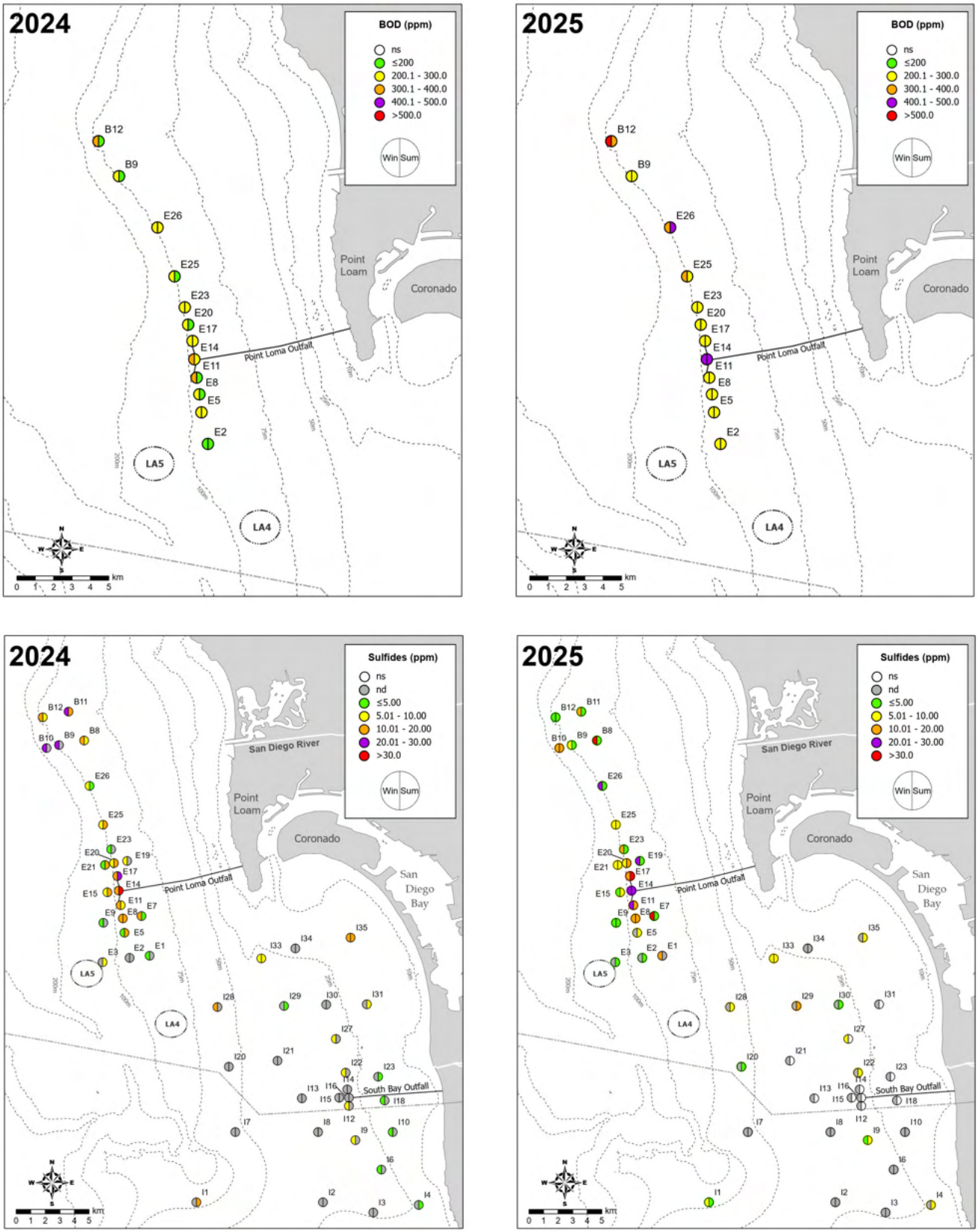
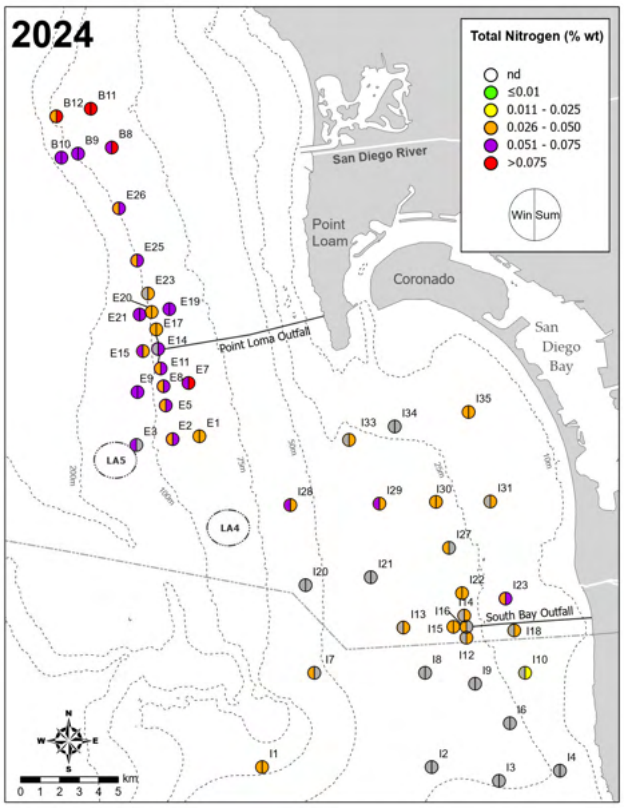
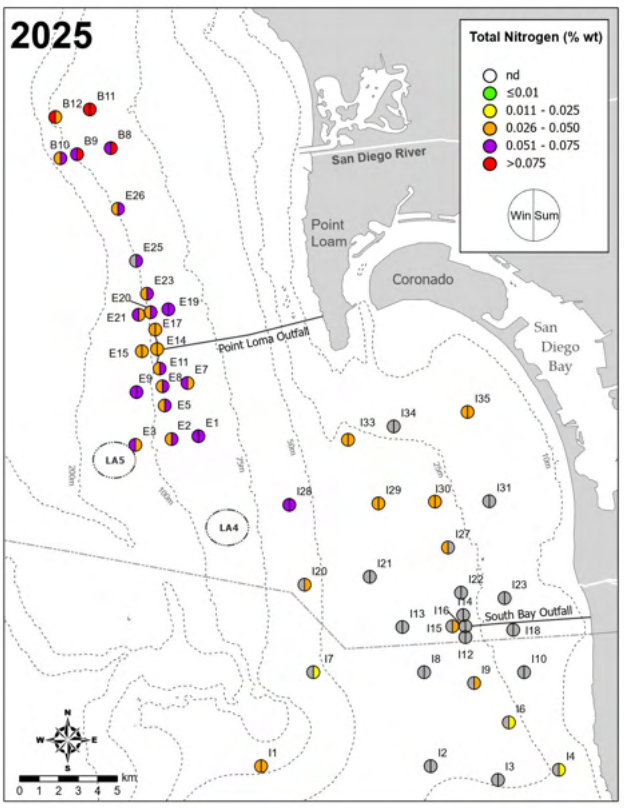
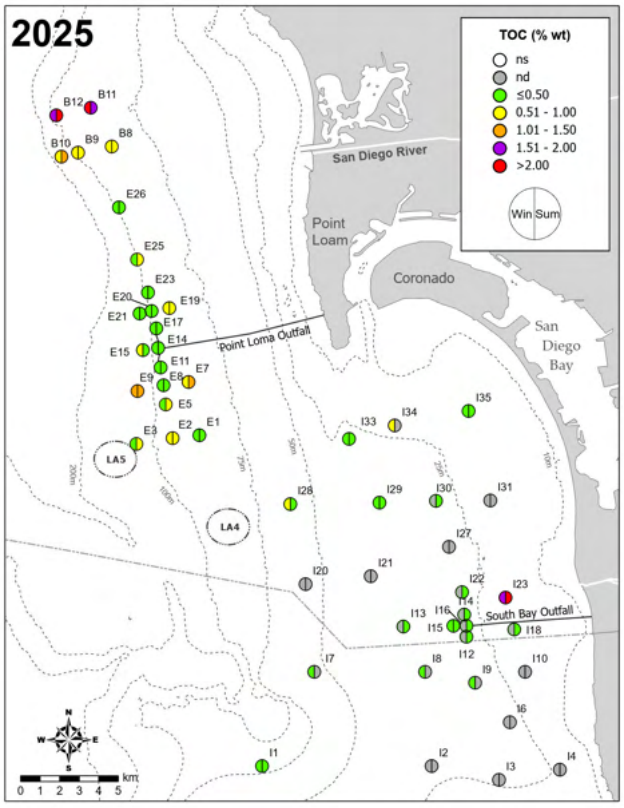


Figure 5.4

Distribution of select organic loading indicators in sediments from the PLOO and SBOO regions during winter and summer surveys of 2024 and 2025. BOD is only measured at PLOO primary core stations; ns = not sampled (or not reportable, see text); nd = not detected.







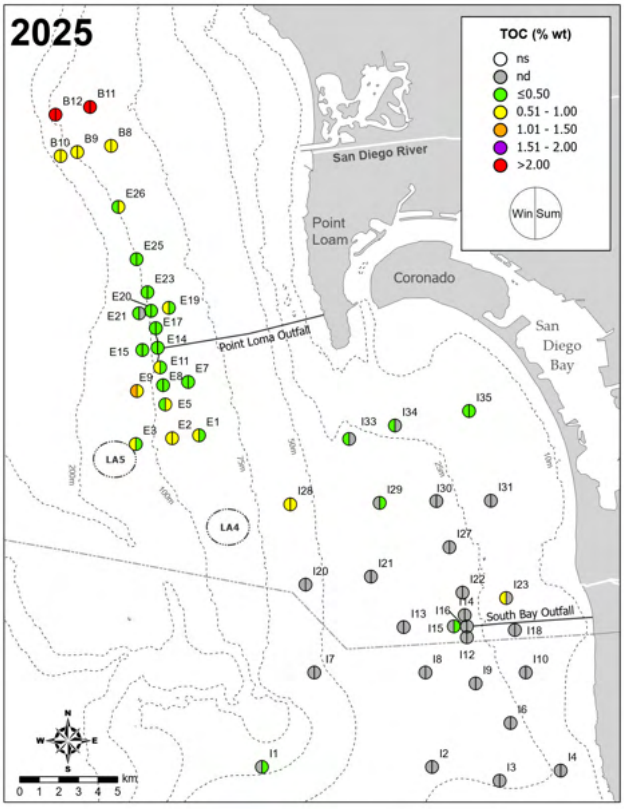


Figure 5.4 *continued*

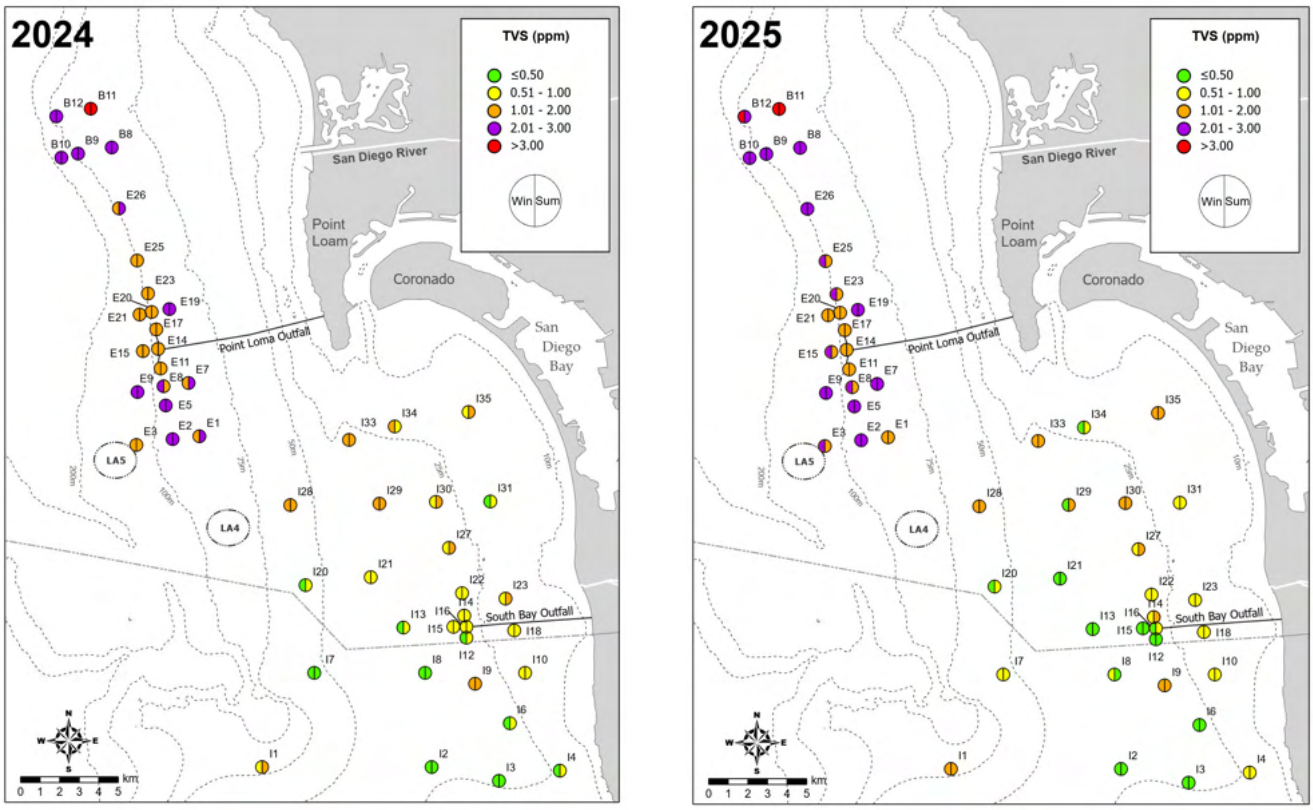


Figure 5.4 *continued*

Table 5.3

Summary of samples with chemistry concentrations that exceeded Effects Range Low (ERL) and Effects Range Median (ERM) thresholds (see Long et al 1995) in sediments from PLOO and SBOO benthic stations sampled historically (1991–2023) and during the current reporting period (2024–2025). Data include the percent of samples that exceeded the ERL (%ERL) and ERM (%ERM) thresholds during each time period. See Tables 5.1 and 5.2 for total number of samples analyzed.

			PLOO				SBOO			
	Thresholds		1991–2023		2024–2025		1995–2023		2024–2025	
Parameter	ERL	ERM	%ERL	%ERM	%ERL	%ERM	%ERL	%ERM	%ERL	%ERM
Metals (ppm)										
Arsenic	8.2	70.0	0.1	0.0	0	0	2.6	0	2.8	0
Cadmium	1.2	9.6	6.7	0.0	0	0	0.2	0	0	0
Chromium	81	370	0.3	0.0	0	0	0	0	0	0
Copper	34	270	0.1	0.1	0	0	0.1	0.0	0	0
Lead	46.7	218.0	0.2	0.1	0	0	0	0	0	0
Mercury	0.15	0.71	0	0	0	0	0	0	0	0
Nickel	20.9	51.6	0.1	0.0	0	0	0.1	0	0	0
Silver	1.0	3.7	5.1	0.5	0	0	3.5	1.0	0	0
Zinc	150	410	0.1	0	0	0	0	0	0	0
tDDT (ppt)	1580	461,000	8.3	0.1	1.1	0	2.2	0	0	0
tPAH (ppb)	4022	44,792	0.1	0.0	0	0	0	0	0	0

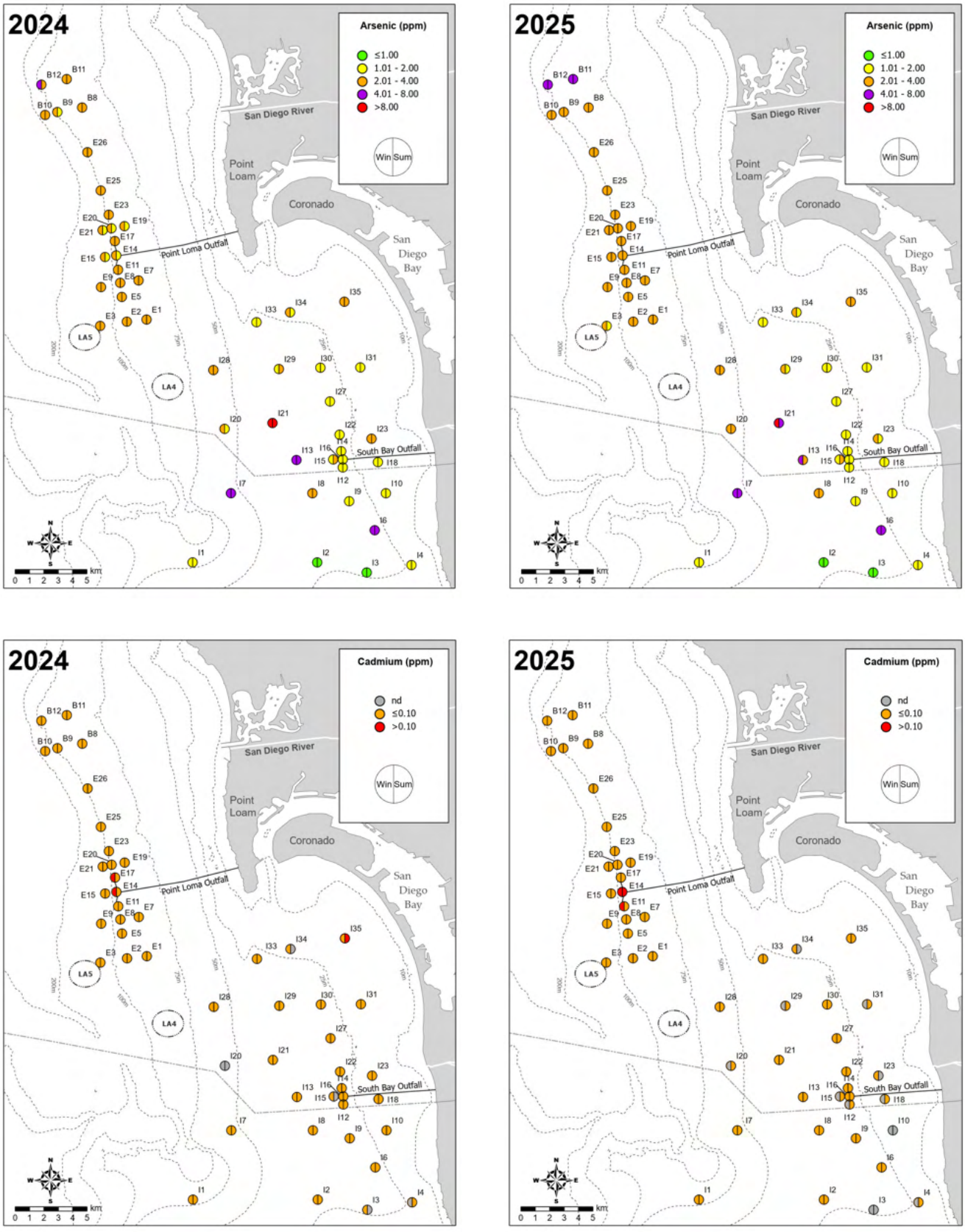
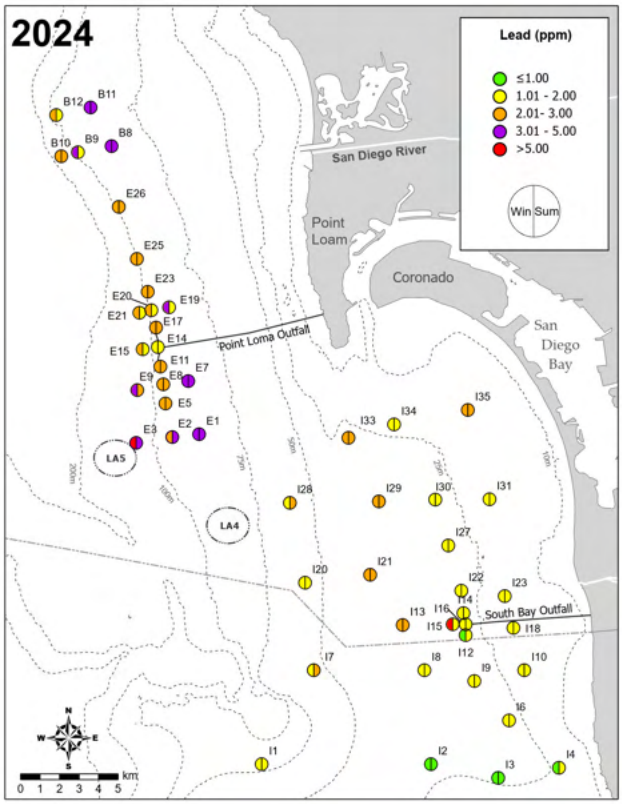
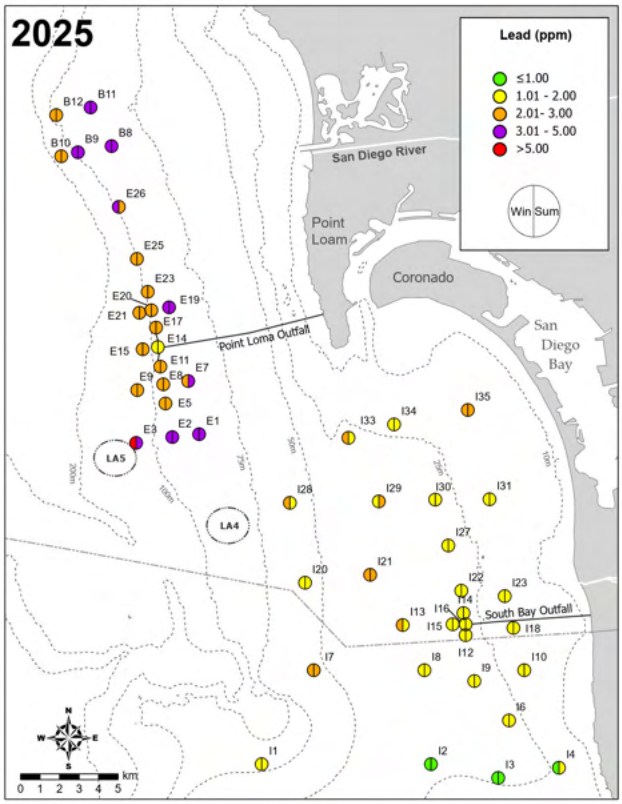
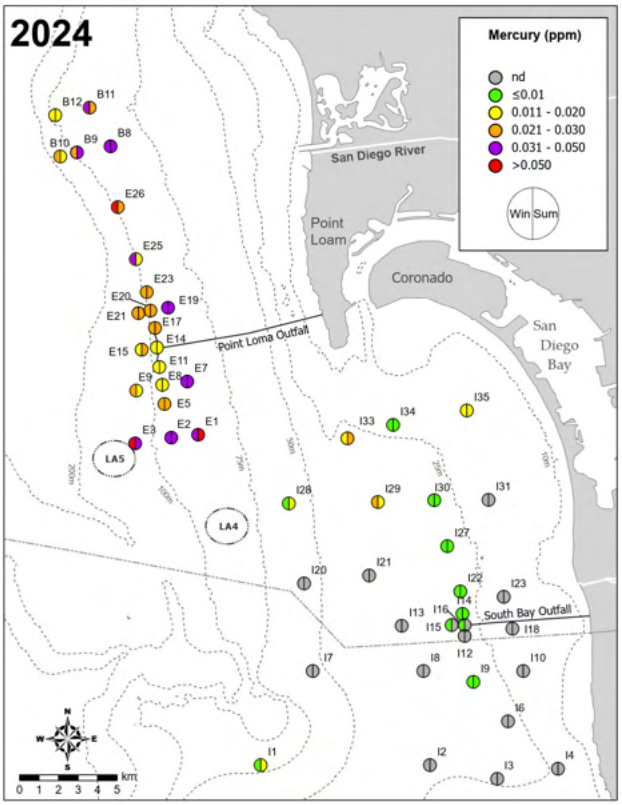


Figure 5.5

Distribution of select metals (ppm) in sediments from the PLOO and SBOO regions during winter and summer surveys of 2024 and 2025; ns = not sampled (or not reportable, see text); nd = not detected.







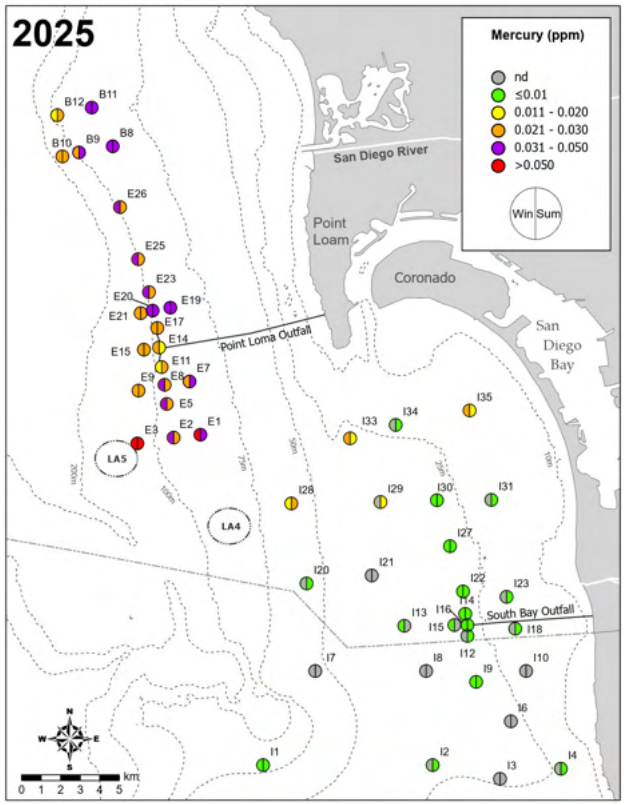


Figure 5.5 *continued*

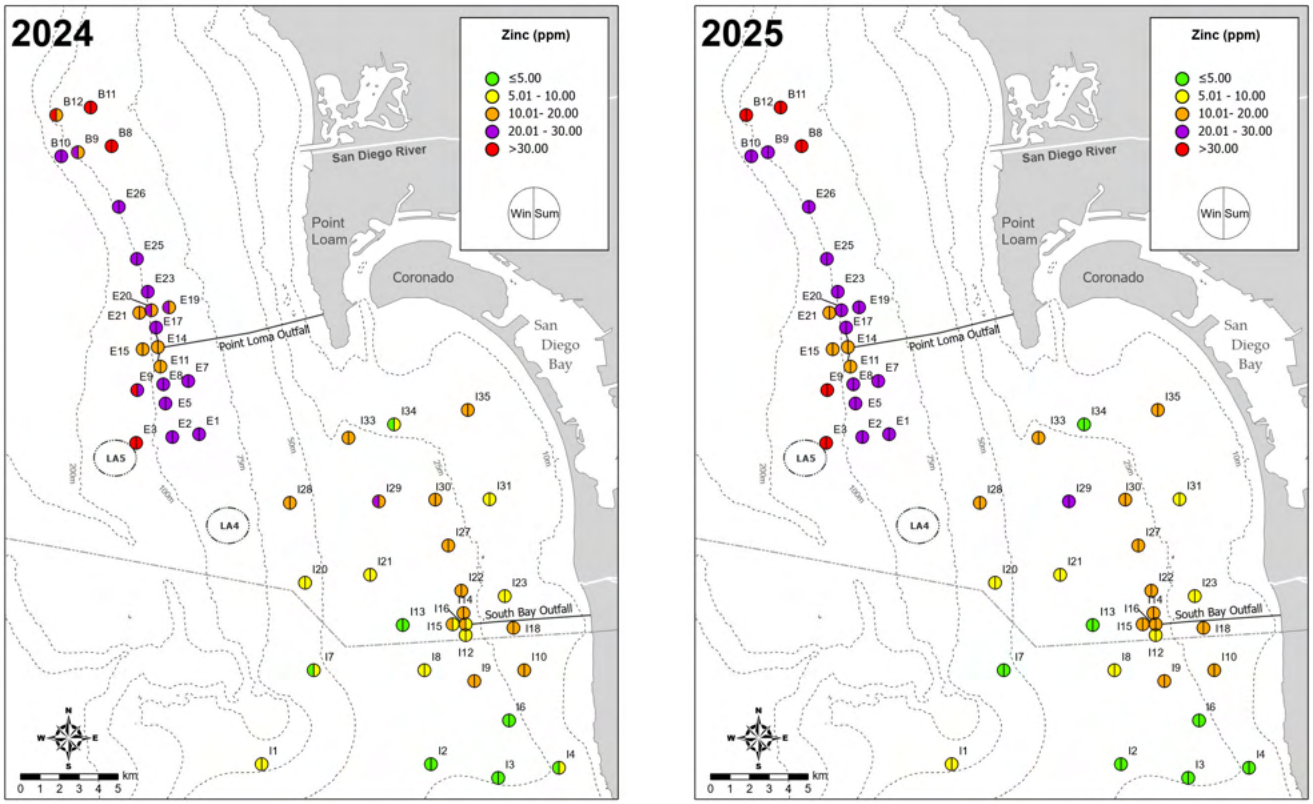


Figure 5.5 *continued*

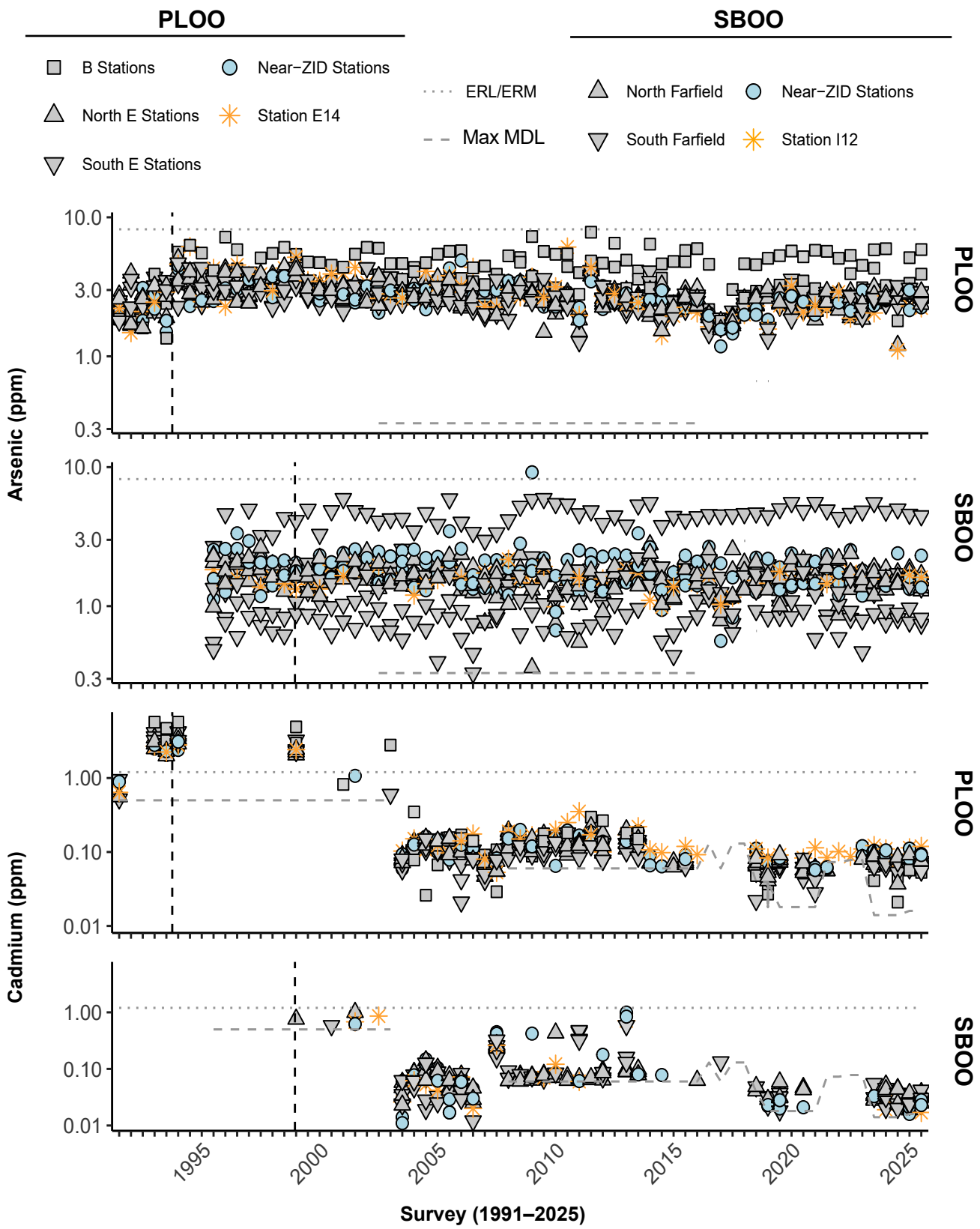


Figure 5.6

Concentrations of select metals in sediments sampled during winter and summer surveys at PLOO primary core stations from 1991 through 2025 and at SBOO primary core stations from 1995 through 2025. Data represent detected values from each station, n≤12 samples per survey. Dashed lines indicate onset of discharge from the PLOO or SBOO. Thresholds included (ERLs, ERMs) when relevant (see Table 5.3), along with the maximum MDL per survey.

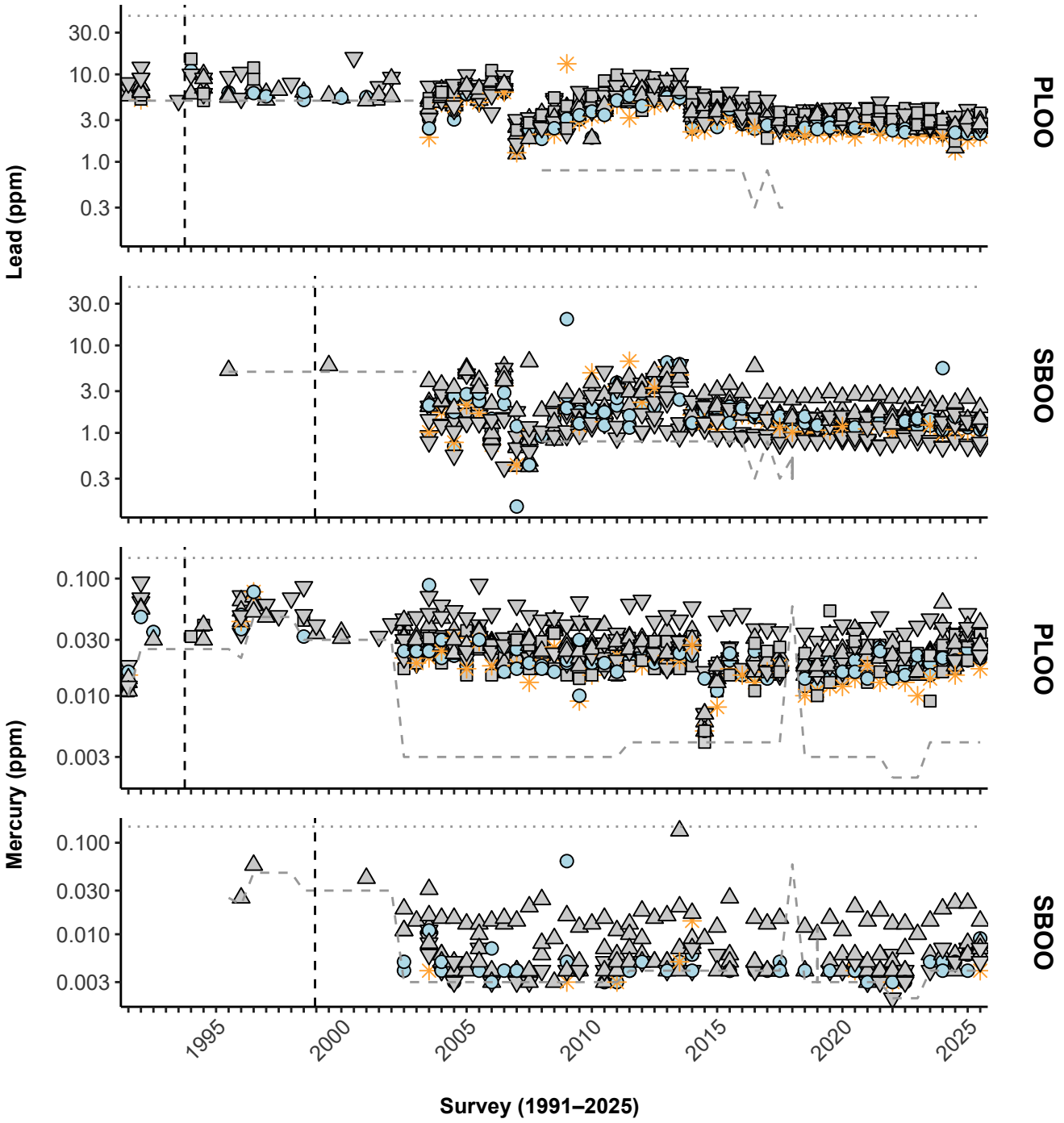


Figure 5.6 *continued*

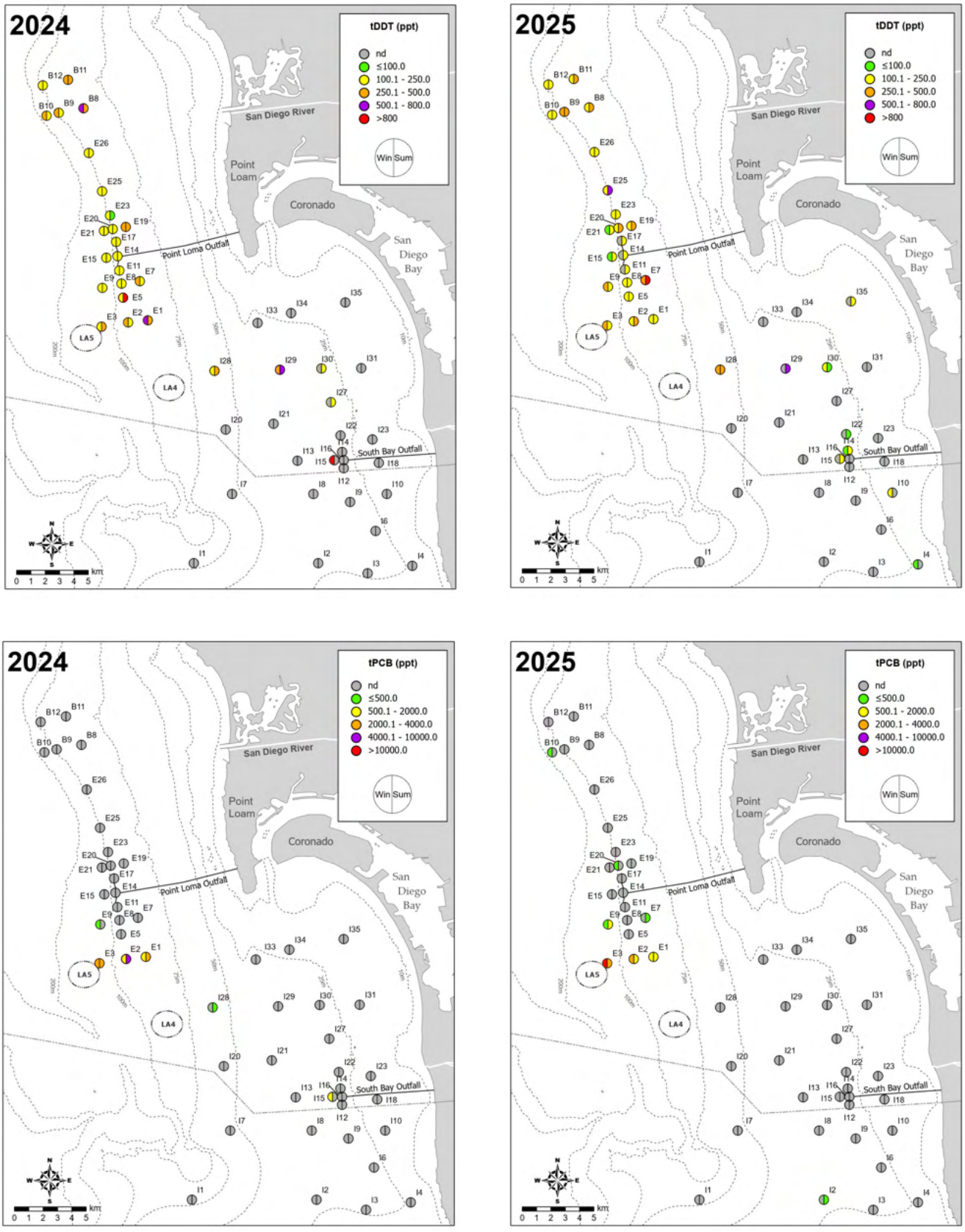
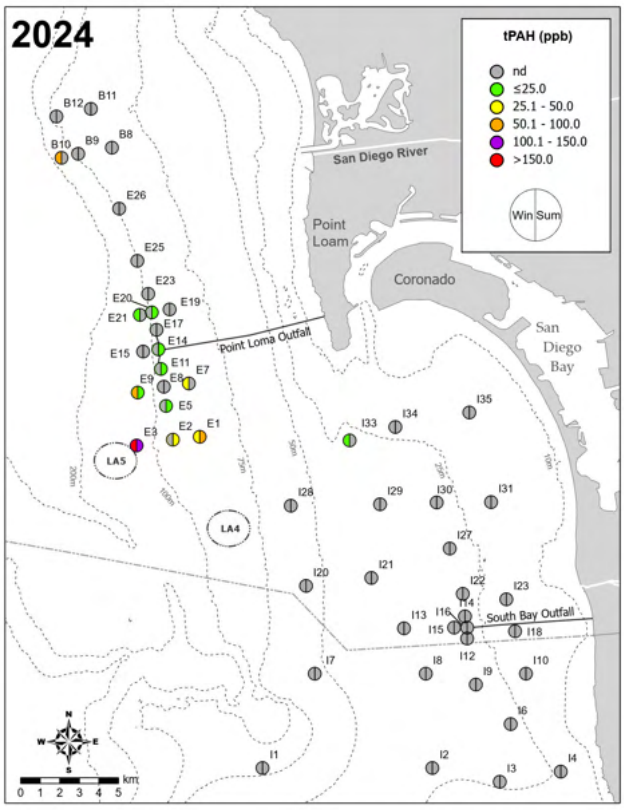
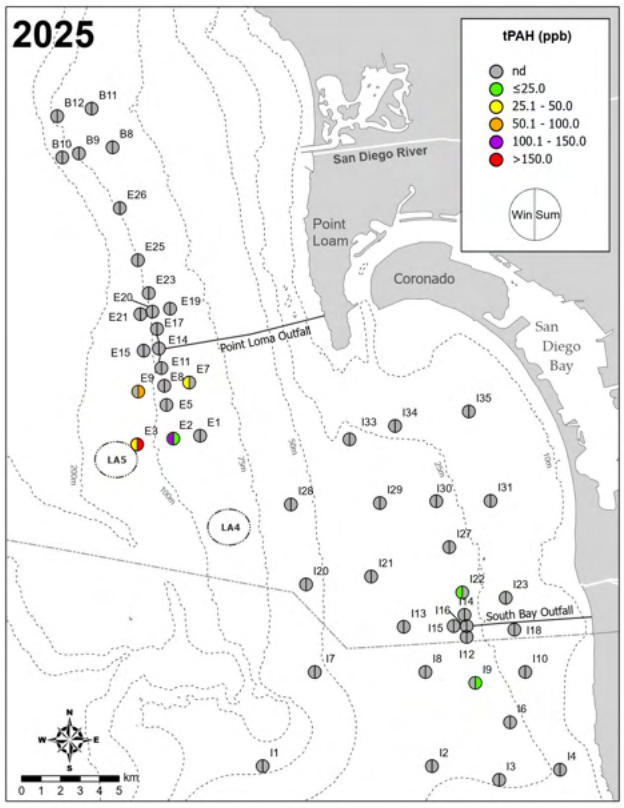
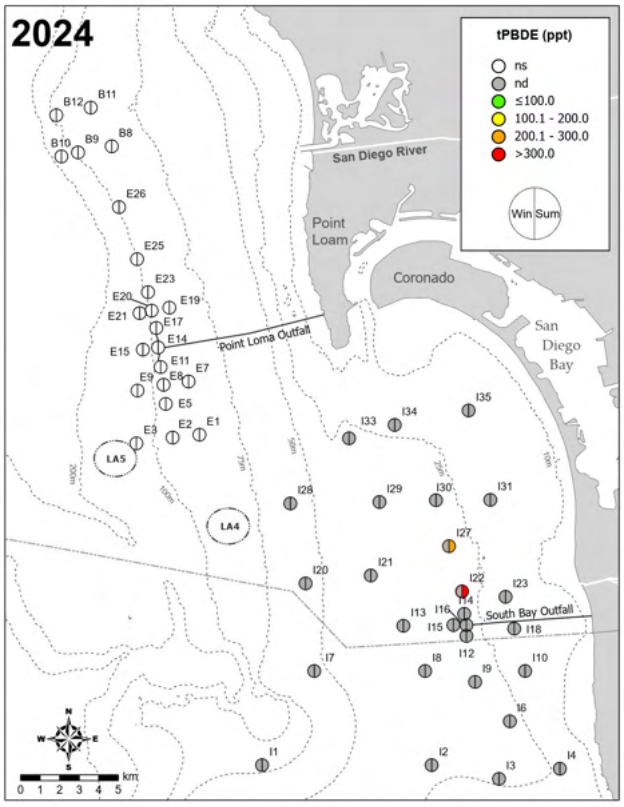


Figure 5.7
Distribution of total DDT, total PCB and total PAH in sediments from the PLOO and SBOO regions during winter and summer surveys of 2024 and 2025; ns = not sampled (or not reportable, see text); nd = not detected.







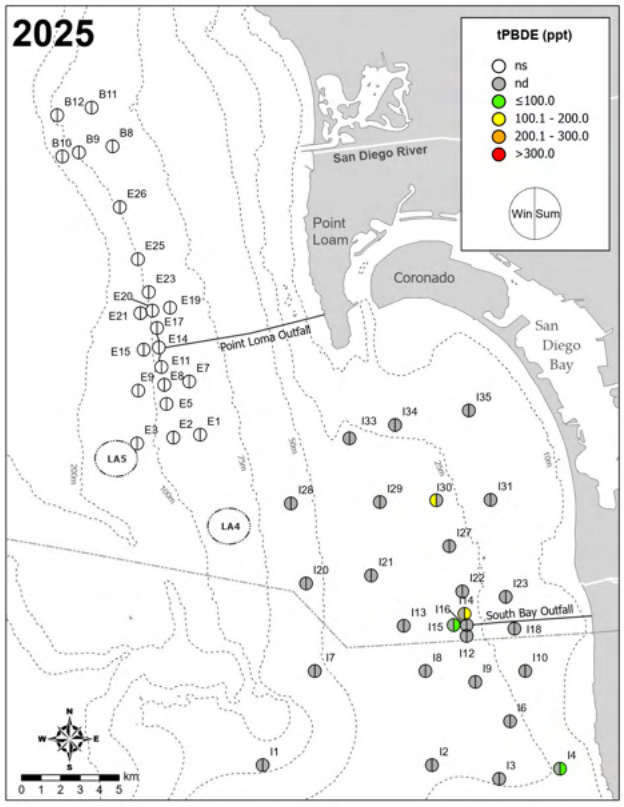


Figure 5.7 *continued*

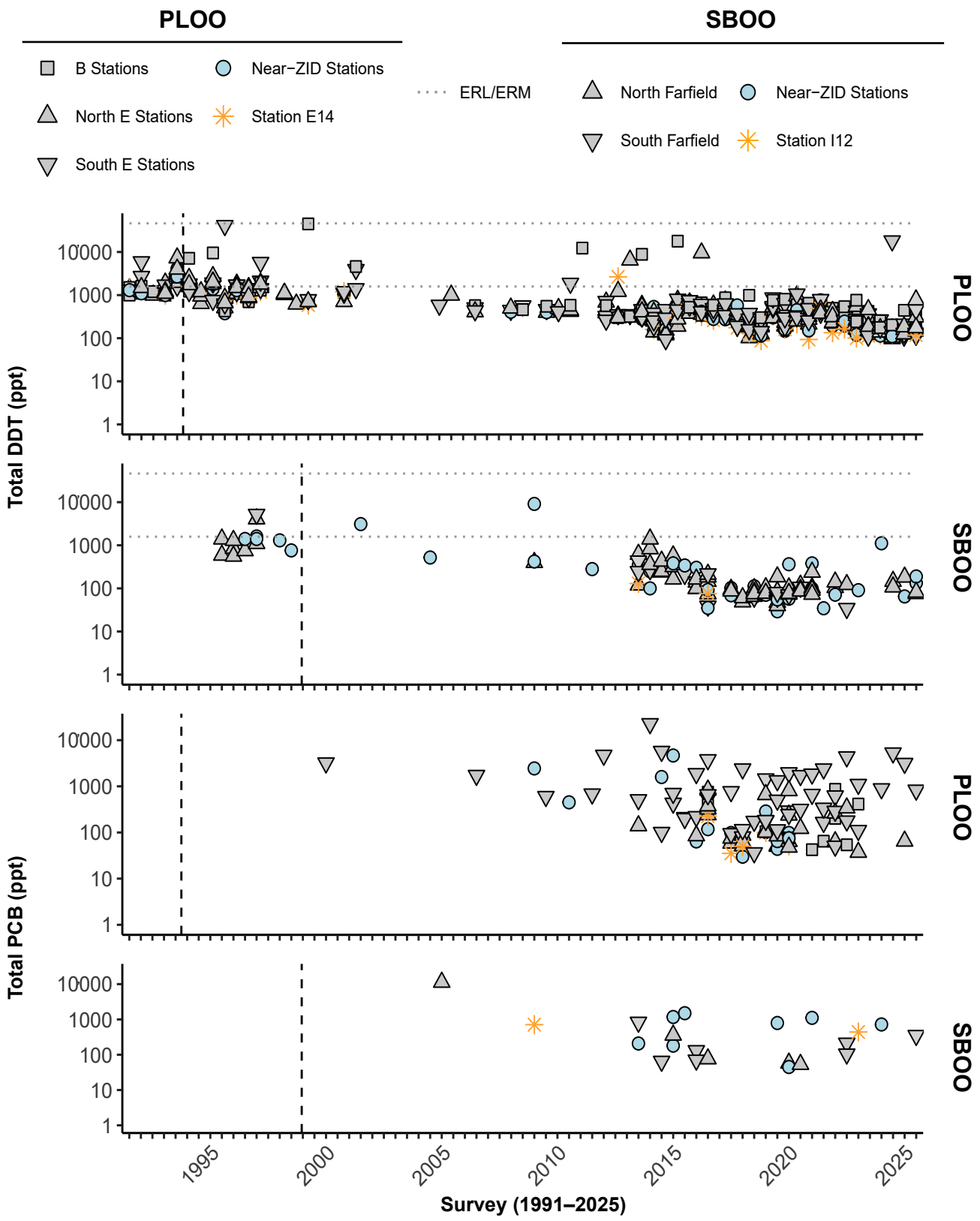


Figure 5.8

Concentrations of total DDT, total PCB, and total PAH in sediments sampled during winter and summer surveys at PLOO primary core stations from 1991 through 2025 and at SBOO primary core stations from 1995 through 2025. Data represent detected values from each station, n ≤ 12 samples per survey. Dashed lines indicate onset of discharge from the PLOO or SBOO. Thresholds included (ERLs, ERMs) when relevant (see Table 5.3).

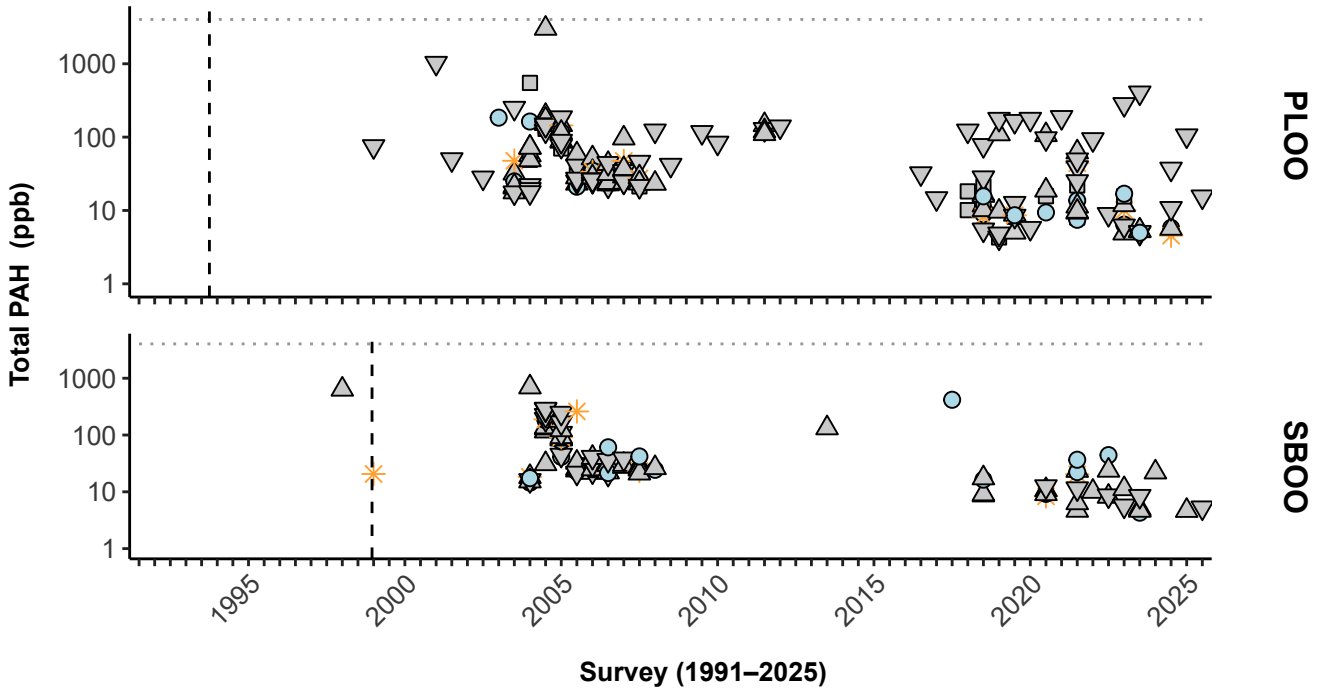


Figure 5.8 *Continued*

Chapter 6
Macrobenthic Communities

Chapter 6. Macrobenthic Communities

INTRODUCTION

The City of San Diego (City) conducts extensive monitoring of soft-bottom marine macrobenthic communities at permanent (core) monitoring sites surrounding the Point Loma Ocean Outfall (PLOO) and South Bay Ocean Outfall (SBOO). Additionally, a number of randomly selected (regional) stations, distributed throughout the broader San Diego coastal region are sampled in order to characterize the status of the local marine ecosystem and to identify any possible effects of wastewater discharge or other anthropogenic or natural influences. Benthic macrofauna (e.g., worms, crabs, clams, brittle stars, other small invertebrates) are targeted when monitoring seafloor habitats, because such organisms play important ecological roles in coastal marine ecosystems off southern California, and throughout the world (e.g., Fauchald and Jones 1979, Thompson et al. 1993a, Snelgrove et al. 1997). As many macrobenthic species live relatively long and stationary lives, changes in their populations may exhibit effects of pollution, or other disturbances over time (Hartley 1982, Bilyard 1987). The response of many of these species to environmental stressors is also well documented, and thus monitoring changes in discrete populations, or more complex communities, can help identify areas impacted by anthropogenic inputs (Pearson and Rosenberg 1978, Bilyard 1987, Warwick 1993, Smith et al. 2001). For example, pollution-tolerant species are often opportunistic, successfully colonizing impacted areas, and can therefore displace more sensitive species. In contrast, populations of pollution-sensitive species will typically decrease in response to contamination, oxygen depletion, nutrient loading, or other forms of environmental degradation (Gray 1979). For these reasons, the assessment of benthic community structure has become a major component of many ocean monitoring programs (e.g., Gillett et al. 2022).

The City relies on a suite of ecological indices to evaluate potential changes in local marine macrobenthic communities. Biological indices, such as the Benthic Response Index (BRI), Shannon Diversity Index (H'), and Swartz Dominance Index (Dom) are used as important metrics of community structure (e.g., Smith et al. 2001). The use of multiple measures of community health also provides better resolution than the evaluation of single parameters, some of which include established benchmarks for determining environmental impacts caused by anthropogenic influences. Collectively, these data are used to evaluate whether macrobenthic assemblages from habitats with comparable depth and sediment particle size are similar, or whether impacts from local ocean outfalls, or other sources, may be occurring. For example, minor organic enrichment due to wastewater discharge should be evident through increases in species richness and abundance in macrofaunal assemblages. Additionally, more severe impacts should result in decreases in the overall number of species, coupled with increases in dominance by a few pollution-tolerant species (Pearson and Rosenberg 1978).

This chapter presents analysis and interpretation of macrofaunal data collected at core benthic monitoring stations throughout the PLOO and SBOO regions during 2024 and 2025. Included are descriptions of the different macrobenthic communities present in these two regions, along with comparisons of spatial patterns and long-term changes over time. The three primary goals of the chapter are to: (1) characterize and document the benthic assemblages present during the reporting period; (2) assess whether benthic communities are degraded as a result of wastewater discharge; (3) identify other potential natural or

anthropogenic sources of variability in the San Diego coastal marine ecosystem. A broader regional assessment of benthic conditions throughout the entire San Diego region, based on a subset of data reported in this chapter combined with a suite of randomly selected stations sampled during the summers of 2024 and 2025 is presented in Chapter 7.

Materials and Methods

Field Sampling

Benthic samples analyzed in this chapter were collected at a total of 49 core monitoring stations located from inner shelf (≤ 30 m) to middle shelf (> 30–120 m) depths, surrounding the PLOO and SBOO, during winter (January) and summer (July) of 2024 and 2025 (Figure 6.1). The PLOO sites include 12 primary core stations located along the 98 m discharge depth contour, and 10 secondary core stations located along or adjacent to the 88 m or 116 m depth contours. The SBOO sites include 12 primary core stations located along the 28 m discharge depth contour, and 15 secondary core stations located along or adjacent to the 19, 38, or 55 m depth contours. Stations located within 1000 m of the boundary of the Zone of Initial Dilution (ZID) for either outfall are considered to represent near-ZID conditions. These include PLOO stations E11, E14, E15, and E17, and SBOO stations I12, I14, I15, and I16. All other stations are considered farfield.

Samples for benthic analyses were collected using a double 0.1 m^2 Van Veen grab, with one grab per cast used for sediment quality analysis (see Chapters 5 and 7) and one grab per cast used for benthic community analysis. Criteria established by the U.S. Environmental Protection Agency (USEPA) to ensure consistency of these types of samples were followed with regard to sample disturbance and depth of penetration (USEPA 1987). Samples for infauna analysis were transferred to a wash table aboard ship, rinsed with seawater, and then sieved through a 1.0 mm mesh screen in order to remove as much sediment as possible. The macroinvertebrates (macrofauna or infauna) retained on the screen were transferred to sample jars, relaxed for 30 minutes in a magnesium sulfate solution, and then fixed with buffered formalin. The preserved samples were then transferred back to the City's Marine Biology Laboratory. After a minimum of 72 hours, but no more than 10 days in formalin, each sample was thoroughly rinsed with fresh water and transferred to 70% ethanol for final preservation. All organisms were separated from the raw material (e.g., sediment grunge, shell hash, debris) and sorted into the following six taxonomic groups by an external contract lab: Annelids (e.g., polychaete and oligochaete worms), Arthropods (e.g., crustaceans, pycnogonids), Molluscs (e.g., bivalves, gastropods, scaphopods), non-ophiuroid Echinoderms (e.g., sea urchins, sea stars, sea cucumbers), Ophiuroids (i.e., brittle stars), and other phyla (e.g., Platyhelminthes, Nemertea, Cnidaria). The sorted macrofaunal samples were then returned to the City's Marine Biology Laboratory where all animals were identified to species or to the lowest taxon possible by staff marine biologists. All identifications during this reporting period followed nomenclatural standards established by the Southern California Association of Marine Invertebrate Taxonomists (SCAMIT 2023).

Data Analyses

Macrofaunal community parameter data for each PLOO and SBOO core station sampled in 2025 are listed in Appendices E.1 and E.2 while taxonomic listings of all specimens identified are listed in Appendices E.3 and E.4. The following community metrics were determined for each station and

expressed per 0.1 m^2 grab: species richness (number of species or distinct taxa), abundance (number of individuals), Shannon Diversity Index (H'), Pielou's Evenness Index (J'), Swartz Dominance Index (Dom) (see Swartz et al. 1986, Ferraro et al. 1994), and Benthic Response Index (BRI) (see Smith et al. 2001). Outfall contour stations are analyzed by three station groups: (1) north farfield stations (i.e., PLOO stations B9, B12, E20, E23, E25, E26 and SBOO stations I22, I27, I30, I33); (2) near-ZID stations (i.e., PLOO stations E11, E14, E17 and SBOO stations I12, I14, I15, I16); (3) south farfield stations (i.e., PLOO stations E2, E5, E8 and SBOO stations I2, I3, I6, I9). Unless otherwise noted, the above analyses were performed using the computational software package R (R Core Team 2021) and various functions within the ggpubr, reshape2, Rmisc, RODBC, scales, tidyverse, and vegan packages (Kassambara 2019, Wickham 2007, 2017, 2018, Hope 2013, Oksanen et al. 2017, Ripley and Lapsley 2017).

Data collected during 2024 were reported previously (City of San Diego 2025), and all raw data for the 2024-2025 sampling period have been submitted to either the Regional Water Quality Control Board, the California Environmental Data Exchange Network (CEDEN) or the City's Open Data Portal (City of San Diego 2026) and may be accessed upon request.

Results and Discussion

Community Parameters

Species richness

A total of 975 different taxa were identified from 196 grabs collected at 22 core PLOO stations and 27 core SBOO stations during 2024 and 2025 (Appendices E.1, E.2, City of San Diego 2025). Approximately 80% (n = 777) of these taxa were identified to species, while the remainder could only be identified to genus or higher taxonomic levels. From the relatively deeper (88–116 m) mid-shelf waters off Point Loma, 603 taxa were identified during this period, of which 486 (81%) were identified at the species level. In contrast, 832 taxa were identified from the shallower (19–55 m) inner to mid-shelf stations in the SBOO region. Of these, 665 (80%) were distinguished at the species level. Most taxa occurred at multiple stations, although 24% (n = 145) of the PLOO taxa and 25% (n = 211) of the SBOO taxa were recorded only once. Thirteen new taxa were reported that had not previously been recorded by the City's Ocean Monitoring Program, including six polychaetes, three arthropods, one brachiopod, two mollusks, and one flatworm.

During 2024 and 2025, species richness ranged from a mean of 82 to 123 taxa per grab at the PLOO stations, and 37 to 150 taxa per grab at the SBOO stations (Tables 6.1 and 6.2, respectively). The greatest number of taxa (n = 145) collected from a single grab in the PLOO region was identified at station E9 during summer of 2025, while the fewest taxa (n = 71) were identified during summer of 2024 at near-ZID station E11 (Appendix E.1, City of San Diego 2025). In the SBOO region, the summer sample from 2025 at northern station I29 had the greatest number of taxa (n = 183), while southern farfield station I4 from winter of 2024 had the fewest taxa identified (n = 22) (Appendix E.2, City of San Diego 2025). These values were similar to the historical range of 19–198 taxa per grab for mid-shelf stations reported from 1994 through 2020 at regional stations (City of San Diego 2022). Comparisons of these parameters among near-ZID stations, versus northern and southern farfield stations, sampled during pre-discharge, historical post-discharge, and current discharge periods did not reveal any clear spatial patterns that could be attributed to wastewater discharge (Figure 6.2).

Macrofaunal abundance

A total of 68,803 macrofaunal animals were recorded for all core PLOO and SBOO stations sampled during 2024 and 2025. Mean abundance per station ranged from 282 to 600 animals in the PLOO region (Table 6.1) and from 109 to 918 animals in the SBOO region (Table 6.2). As shown for species richness, there were no clear patterns in abundance relative to their proximity to either outfall (see Figure 6.2). The highest abundance, per grab, in the PLOO region occurred during summer of 2025 at near-ZID station E14 (n = 879), while the lowest abundance occurred at northern station B12 in winter of 2024 (n = 201) (Appendix E.1, City of San Diego 2025). In the SBOO region, the highest abundance occurred in winter 2025 at northern station I34 (n = 2373), while the lowest abundance was observed at southern station I3 (n = 62) in winter of 2025 (Appendix E.2). The maximum number of individuals in the SBOO area exceeded the range of 47–1467 organisms per grab reported at mid-shelf stations from 1994 to 2020 (City of San Diego 2022). Many of the specimens at I34 in winter 2025 were small, interstitial polychaetes.

Species diversity, evenness, and dominance

Shannon Diversity Index (H') values ranged from a mean of 3.6 to 4.3 at the PLOO stations (Table 6.1), and 2.6 to 4.3 at the SBOO stations (Table 6.2), during 2024 and 2025. In the PLOO region, the highest diversity per grab sample occurred at station E9 in summer 2025 (H' = 4.5), and the lowest diversity was observed at near-ZID station E14 in the winter of 2024 and summer of 2025, as well as E11 and E21 in summer of 2025 (H' = 3.5) (Appendix E.1, City of San Diego 2025). In the SBOO region, the highest diversity per grab sample occurred at northern farfield station I33 in summer 2025 (H' = 4.4), and the lowest diversity was observed at southern farfield station I4 in winter of 2024 (H' = 1.9) (Appendix E.2, City of San Diego 2025).

Pielou's Evenness Index (J') values ranged from a mean of 0.78 to 0.91 in the PLOO region (Table 6.1), and 0.65 to 0.92 in the SBOO region (Table 6.2). In the PLOO region, the highest evenness values per grab sample occurred at northern farfield station B11 in winter and southern farfield station E3 in summer 2025 (J' = 0.92), and the lowest evenness values occurred at near-ZID station E14 in summer of 2025 (J' = 0.75) (Appendix E.1). In the SBOO region, the highest evenness occurred at station I31 in winter of 2025 (J' = 0.95), and the lowest value occurred at northern station I34 in summer of 2024 (J' = 0.43) (Appendix E.2, City of San Diego 2025).

Swartz Dominance Index values ranged from a mean of 20 to 46 taxa at PLOO stations (Table 6.1), and 8 to 46 taxa at SBOO stations (Table 6.2). In the PLOO region, the highest dominance (i.e., lowest index value) per grab sample occurred at near-ZID station E14 in summer 2024 (19 taxa), and the lowest dominance (i.e., highest index value) occurred at station E9 in summer of 2025 (60 taxa) (Appendix E.1, City of San Diego 2025). In the SBOO region, the highest dominance occurred at southern farfield station I4 in winter of 2024 (4 taxa) (Appendix E.2), and the lowest dominance occurred at northern station I28 in both winter and summer of 2025 (51 taxa) (Appendix E.2, City of San Diego 2025).

Overall, these results indicate that the PLOO and SBOO benthic communities remain characterized by relatively diverse assemblages of evenly distributed species. Values for all three of the above parameters in 2024 and 2025 (Appendices E.1, E.2, City of San Diego 2025), were within historical ranges (see City of San Diego 2022), and there remain no patterns that appear related to wastewater discharge in either region (see Figure 6.2).

Benthic response index

The BRI is an important tool for evaluating anthropogenic impacts on coastal seafloor habitats off southern California: BRI values less than 25 are considered indicative of reference conditions (i.e., not impacted by natural and/or anthropogenic disturbance), values between 25 and 34 represent possible minor deviation from reference conditions, and values greater than 34 represent increasing levels of degradation (Smith et al. 2001). Overall, 90% (n = 177) of all individual benthic samples collected in the combined PLOO and SBOO regions during 2024 and 2025 were characteristic of reference conditions (Appendices E.1, E.2, City of San Diego 2025). No stations had BRI values considered indicative of degradation (i.e., all stations had a BRI ≤ 34).

Almost all the individual samples (99%) in the PLOO region had BRI values indicative of reference conditions. Only the sample from near-ZID station E14 in summer 2025, with a BRI score of 26, appeared to show evidence of slight deviation from reference conditions (Appendix E.1). Station E14 is often distinguished from the other primary core "E" stations, located along the 98-m PLOO discharge depth contour, by the presence of higher proportions of coarse sediment particles and lower proportion of very fine particles (see Chapter 5). This difference in habitat may contribute to the slightly elevated BRI score at station E14, as it may decrease the presence of certain pollution-sensitive species (e.g., the brittle star *Amphiodia urtica*) that are known to prefer finer sediments (Bergen 1995). No other spatial patterns relative to depth or sediments were observed (see Figures 5.2, 6.3, Tables 6.1, 6.2).

In the SBOO region, BRI values ranged from -9 at southern farfield station I4 in winter of 2024 to 34 at northern station I35 during winter 2025, with about 83% of samples indicative of reference conditions (Appendix E.2, City of San Diego 2025). No SBOO samples had BRI values > 34 that would indicate environmental degradation. Individual sample BRI values corresponding to possible minor deviation from reference conditions (> 25) occurred at 11 stations throughout the SBOO region (Appendix E.2, City of San Diego 2025). The slightly higher BRI values at these stations may be due to naturally higher levels of organic matter that often occur at depths < 30 m due to proximity to terrestrial inputs (Smith et al. 2001) or more coarse sediment particles that inhibit pollution sensitive species (Bergen 1995). Historically, BRI values at the near-ZID SBOO stations have been similar to values observed for northern farfield SBOO stations, while BRI has been consistently lower at the southern farfield SBOO stations (Figure 6.3). These apparent deviations from reference condition have been present in these stations even before the onset of the operation of the SBOO in 1999. In 1995, when monitoring began, over 28% of stations in the SBOO area had BRI values greater than 25 and from 2011 to 2013, up to 26% of samples exceeded the threshold for possible moderate disturbance (Appendix E.5). Other stations in the SBOO with lower BRI values have sediments favoring the presence of aggregations of the sand dollar, *Dendraster terminalis*, a pollution sensitive species that yields low BRI values.

Species of Interest

Dominant taxa

Annelid polychaete worms were the dominant taxonomic group found in both the PLOO and SBOO regions during 2024–2025, accounting for 48% and 47% of all taxa collected, respectively (Table 6.3). Crustaceans accounted for 20% and 21%, molluscs for 15% and 16%, and echinoderms 5% and 4% in PLOO and SBOO, respectively. All other taxa combined equated to 11 and 12% respectively. Polychaetes were also the most abundant organisms encountered, accounting for 65% and 67% of all macrofauna in both the PLOO and SBOO regions, respectively. Crustaceans, molluscs, echinoderms, and "other phyla" each contributed to ≤ 18% of the total abundance in each region. Overall, the percentage of taxa that occurred within each of the above major taxa groups, and their relative abundances, have shown

little change since monitoring began (City of San Diego 2022) and are similar to the rest of the Southern California Bight (SCB) (see Ranasinghe et al. 2010, Gillett et al. 2022.

The 10 most abundant taxa in the PLOO region during 2024–2025 included seven species of polychaetes, one species of echinoderm, and two species of arthropod (Table 6.4). Together, these species accounted for about 33% of all invertebrates identified during this period. The numerically dominant polychaetes included the spionids *Spiophanes duplex, S. kimballi, Prionospio jubata* and *P. dubia,* capitellids in the genus *Mediomastus*, the amphinomid *Chloeia pinnata,* and the onuphid *Paradiopatra parva.* The two dominant ostracods were *Euphilomedes carcharodonta* and *E. producta,* while the brittle star *Amphiodia urtica* was the dominant ophiuroid. *Amphiodia urtica* populations have been declining across the region since monitoring at the current stations began in 1991, and especially since the warm water period of 2014–2016 (see Chapter 2, Figure 2.17, Table 2.2). However, they are still a dominant taxon, accounting for approximately 3% of all invertebrates collected in the region and occurring in 88% of grabs with a mean abundance of approximately 11 individuals per grab. Historically, *Amphiodia urtica* and *Spiophanes duplex* (Figure 6.4), as well as *Proclea* sp A (Figure 6.5) have also been numerically dominant. However, other historically dominant polychaete taxa, the oweniid *Myriochele striolata*, and the terebellid, *Phisidia sanctaemariae* were not as abundant during the most recent reporting period (Appendix E.6). *Proclea* sp A and *M. striolata* have not been abundant in the region since 2005, while *P. sanctaemariae* has been largely absent since 2000.

The 10 most abundant taxa in the SBOO region during 2024–2025, included seven polychaetes, one tanaid, one Cnidarian, and members of the phylum Nematoda (Table 6.5). The dominant polychaetes included the spionids *Spiophanes norrisi* and *S. duplex*, the undescribed maldanid Euclymeninae sp A, the cirratullid *Kirkegaardia siblina,* the sigalionid *Pisione* sp, the phyllodocid *Hesionura coineaui difficilis*, and the undescribed terebellid *Polycirrus* sp SD3. The dominant tanaid was represented by *Chondrochelia dubia* Cmplx*,* while the other most abundant taxa were Nematoda and the anemone *Edwardsia juliae.* The polychaete worm *Spiophanes norrisi* was the most abundant of all these species during the past two years, accounting for 7% of invertebrates collected in the SBOO area and occurring in 94% of all grabs. Although not as numerous as in previous surveys, *S. norrisi* has remained the most abundant species recorded in the SBOO region since 2007 (Figure 6.6), with up to 3009 individuals found in a single grab from station I6 during the summer of 2010 (City of San Diego 2011). Aside from *S. duplex*, all other taxa collected during the current reporting period averaged 12 individuals or fewer per grab (Table 6.5). Three other numerically dominant species occurred in ≥ 65% of the samples, including Euclymeninae sp A*, Chondrochelia dubia* Cmplx*,* and large nematodes (Table 6.5). The remaining five of the top 10 taxa occurred in 5–60% of the samples with average abundances per grab of 5–7 animals. Historically*, S. norrisi*, *S. duplex*, *Kirkegaardia siblina* and *Chondrochelia dubi*a Cmplx (Figure 6.6), along with the capitellid polychaete *Mediomastus* sp have been the most numerically dominant taxa (Appendix E.7).

Indicator species

Several species known to be useful indicators of environmental change that occur in the PLOO and SBOO regions include members of the capitellid polychaete species complex *Capitella capitata*, amphipods in the genera *Ampelisca* and *Rhepoxynius*, the terebellid polychaete *Proclea* sp A, the bivalve *Petrasma pervernicosa*, and the brittle star *Amphiodia urtica*. For example, increased abundances of pollution-tolerant species such as *C. capitata* Cmplx and *P. pervernicosa* and decreased abundances of pollution-sensitive taxa such as *A. urtica*, are often indicative of organic enrichment and may indicate habitats impacted by human activity (Barnard and Ziesenhenne 1961, Anderson et al. 1998, Linton and

Taghon 2000, Smith et al. 2001, Kennedy et al. 2009, McLeod and Wing 2009). During 2024 and 2025, a total of 287 individuals of *C. capitata* Cmplx were found in samples collected across the entire region distributed among 26 different sites, while a total of 250 individuals of *P. pervernicosa* were identified in samples from 13 different sites. Despite occasionally exceeding regional tolerance intervals of 0 to 1 animal per grab (see City of San Diego 2022), abundances of *C. capitata* Cmplx and *P. pervernicosa* remained characteristic of relatively undisturbed habitats (Figures 6.5, 6.7). For example, *C. capitata* Cmplx commonly reaches densities as high as 600 individuals per $0.1m^2$ grab in polluted sediments (Reish 1957, Swartz et al. 1986). Changes in abundance of *Ampelisca* and *Rhepoxynius* amphipod species varied at all PLOO primary core stations regardless of proximity to the outfall, which may have been influenced by the presence of large populations of pelagic red crabs from 2016 to 2019 (see City of San Diego 2020).

Summary

Analyses of macrofaunal data for the 2024–2025 reporting period demonstrate that wastewater discharged through the Point Loma and South Bay outfalls has not negatively impacted macrobenthic communities in the coastal waters off San Diego. Values for most community parameters are similar at stations located both near to and far from the discharge areas. Major community metrics, such as species richness, abundance, diversity, evenness, and dominance were within historical ranges reported for the San Diego region (City of San Diego 2022), and were representative of those characteristic of similar SCB benthic habitats (Barnard and Ziesenhenne 1961, Jones 1969, Fauchald and Jones 1979, Thompson et al. 1987, 1993b, Zmarzly et al. 1994, Diener and Fuller 1995, Bergen et al. 2000, 2001, Ranasinghe et al. 2010, Mikel et al. 2007, Gillett et al. 2022). BRI values for 99% of the PLOO sites and 83% of the SBOO sites were considered characteristic of undisturbed habitats, while the remaining stations had values suggesting only a possible minor deviation from reference conditions. Additionally, BRI values at the shallower (i.e., less than 28 m) stations in the SBOO region have typically been higher than BRI values for deeper water stations since monitoring began. However, this pattern is not unexpected, since naturally higher levels of organic matter often occur closer to shore and particle sizes tend to be coarser (see Chapter 5). A similar phenomenon has been reported across the SCB where Smith et al. (2001) found a pattern of lower BRI values at mid-depth stations (25–130 m) versus shallower (10–35 m) or deeper (110–324 m) sites.

Changes in populations of pollution-sensitive and pollution-tolerant species, or other indicators of benthic condition, provide little or no evidence of habitat degradation in either outfall region. For example, the brittle star *Amphiodia urtica* is a well-known dominant species of the mid-shelf in fine sediment habitats in the SCB, which is known to be sensitive to environmental changes near wastewater outfalls (Swartz et al. 1986). However, abundances of *A. urtica* off Point Loma remained within the range of natural variation in SCB populations (Gillett et al. 2022). Additionally, populations of opportunistic species, such as the polychaete *Capitella capitata* Cmplx and the bivalve *Petrasma pervernicosa,* remained low during 2024 and 2025, while populations of pollution-sensitive amphipods in the genera *Ampelisca* and *Rhepoxynius* have generally varied similarly between near-ZID and farfield stations. Furthermore, although spionid polychaetes are often abundant in other coastal areas of the world that possess high levels of organic matter (e.g., Díaz-Jaramillo et al. 2008), in the SCB these worms are known to be a stable, dominant component of many healthy environments with normal levels of organic inputs (Rodríguez-Villanueva et al. 2003). Thus, the presence of large populations of *Spiophanes norrisi*, observed at many SBOO stations since 2007, is not considered to

be indicative of habitat degradation related to wastewater discharge. Instead, population fluctuations of this spionid, in recent years, may correspond to natural changes in large-scale oceanographic conditions. Further support for this hypothesis is shown by the continued relatively low abundances of *S. norrisi* at all station groups during 2024 and 2025, compared to what would be expected at negatively impacted areas.

In conclusion, benthic macrofaunal communities appear to be in good condition overall throughout the PLOO and SBOO regions. A modest decrease in condition assessment in the SBOO region compared to the previous reporting period is within the range of natural background variability observed historically. Communities remain largely similar to those observed prior to outfall operations and are representative of natural communities from similar habitats on the southern California continental shelf. Overall, 90% of all benthic sites surveyed for the combined region in 2024 and 2025 were classified as being in reference condition, based on assessments using the BRI. The few moderate indicators of potential disturbance remain below the threshold of community degradation. Thus, no significant effects of wastewater discharge on the local macrobenthic communities off San Diego could be identified during this past 2-year reporting period.

Literature Cited

Anderson, B.S., J.W. Hunt, B.M. Philips, S. Tudor, R. Fairey, J. Newman, H.M. Puckett, M. Stephenson, E.R. Long, and R.S. Tjeerdema. (1998). Comparison of marine sediment toxicity test protocols for the amphipod *Rhepoxynius abronius* and the polychaete worm *Nereis* (*Neanthes*) *arenaceodentata*. Environmental Toxicology and Chemistry. 17(5): 859–866.

Barnard, J.L. and F.C. Ziesenhenne. (1961). Ophiuroidea communities of southern Californian coastal bottoms. Pacific Naturalist, 2: 131–152.

Bergen, M. (1995). Distribution of Brittlestar Amphiodia (Amphispina) spp. in the Southern California Bight in 1956 to 1959. Bulletin of the Southern California Academy of Sciences. 94(3): 190–203.

Bergen, M., D.B. Cadien, A. Dalkey, D.E. Montagne, R.W. Smith, J.K. Stull, R.G. Velarde, and S.B. Weisberg. (2000). Assessment of benthic infaunal condition on the mainland shelf of southern California. Environmental Monitoring Assessment, 64: 421–434.

Bergen, M., S.B. Weisberg, R.W. Smith, D.B. Cadien, A. Dalkey, D.E. Montagne, J.K. Stull, R.G. Velarde, and J.A. Ranasinghe. (2001). Relationship between depth, sediment, latitude, and the structure of benthic infaunal assemblages on the mainland shelf of southern California. Marine Biology, 138: 637–647.

Bilyard, G.R. (1987). The value of benthic infauna in marine pollution monitoring studies. Marine Pollution Bulletin, 18(11): 581–585.

City of San Diego. (2011). Annual Receiving Waters Monitoring Report for the South Bay Ocean Outfall (South Bay Water Reclamation Plant), 2010. City of San Diego Ocean Monitoring Program, Public Utilities Department, Environmental Monitoring and Technical Services Division, San Diego, CA.

City of San Diego. (2020). Biennial Receiving Waters Monitoring and Assessment Report for the Point Loma and South Bay Ocean Outfalls, 2018-2019. City of San Diego Ocean Monitoring Program, Public Utilities Department, Environmental Monitoring and Technical Services Division, San Diego, CA.

City of San Diego. (2022). Appendix C2: San Diego Benthic Tolerance Intervals. In: Report of Waste Discharge and Application for Renewal of NPDES CA 0107409 and 301(h) Modified Secondary Treatment Requirements. Volume V: Appendix C. City of San Diego Public Utilities Department, San Diego, CA.

City of San Diego. (2025). Interim Receiving Waters Monitoring Report for the Point Loma and South Bay Ocean Outfalls, 2022. City of San Diego Ocean Monitoring Program, Public Utilities Department, Environmental Monitoring and Technical Services Division, San Diego, CA.

City of San Diego. (2026). Ocean Monitoring Program Reports and Data. https://www.sandiego.gov/public-utilities/sustainability/ocean-monitoring/reports

Díaz-Jaramillo, M., P. Muñoz, V. Delgado-Blas, and C. Bertrán. (2008). Spatio-temporal distribution of spionids (Polychaeta-Spionidae) in an estuarine system in south-central Chile. Revista Chilena de Historia Natural, 81: 501–514.

Diener, D.R. and S.C. Fuller. (1995). Infaunal patterns in the vicinity of a small coastal wastewater outfall and the lack of infaunal community response to secondary treatment. Bulletin of the Southern California Academy of Science, 94: 5–20.

Fauchald, K. and G.F. Jones. (1979). Variation in community structures on shelf, slope, and basin macrofaunal communities of the Southern California Bight. Report 19, Series 2. In: Southern California Outer Continental Shelf Environmental Baseline Study, 1976/1977 (Second Year) Benthic Program. Principal Investigators Reports, Vol. II. Science Applications, Inc. La Jolla, CA.

Ferraro, S.P., R.C. Swartz, F.A. Cole, and W.A. Deben. (1994). Optimum macrobenthic sampling protocol for detecting pollution impacts in the Southern California Bight. Environmental Monitoring and Assessment, 29: 127–153.

Gillett, D.J., W. Enright, J.B. Walker. 2022. Southern California Bight 2018 Regional Monitoring Program: Volume III. Benthic Infauna. Technical Report 1289. Southern California Coastal Water Research Project. Costa Mesa, CA.

Gray, J.S. (1979). Pollution-induced changes in populations. Philosophical Transactions of the Royal Society of London (Series B), 286: 545–561.

Hartley, J.P. (1982). Methods for monitoring offshore macrobenthos. Marine Pollution Bulletin, 12: 150–154.

Hope, R.M. (2013). Rmisc: Ryan Miscellaneous. R package version 1.5. http://CRAN.R-project.org/package=Rmisc.

Jones, G.F. (1969). The benthic macrofauna of the mainland shelf of southern California. Allan Hancock Monographs of Marine Biology, 4: 1–219.

Kassambara, A. (2019). ggpubr: 'ggplot2' Based Publication Ready Plots. R package version 0.2.2. https://CRAN.R-project.org/package=ggpubr.

Kennedy, A.J., J.A. Stevens, G.R. Lotufo, J.D. Farrar, M.R. Reiss, R.K. Kropp, J. Doi, and T.S. Bridges. (2009). A comparison of acute and chronic toxicity methods for marine sediments. Marine Environmental Research, 68: 118–127.

Linton, D.L. and G.L. Taghon. (2000). Feeding, growth, and fecundity of *Capitella* sp. I in relation to sediment organic concentration. Marine Ecology Progress Series, 205: 229–240.

McLeod, R.J. and S.R. Wing. (2009). Strong pathways for incorporation of terrestrially derived organic matter into benthic communities. Estuarine, Coastal and Shelf Science, 82: 645–653.

Mikel T.K., J.A Ranasinghe, and D.E. Montagne. (2007). Characteristics of benthic macrofauna of the Southern California Bight. Appendix F. Southern California Bight 2003 Regional Monitoring Program, SCCWRP, Costa Mesa, CA.

Oksanen, J., F. G. Blanchet, R. Kindt, P. Legendre, P. R. Minchin, R. B. O'Hara, G. L. Simpson, P. Solymos, M. H. H. Stevens and H. Wagner (2017). vegan: Community Ecology Package. R package version 2.3-1. http://CRAN.R-project.org/package=vegan.

Pearson, T.H. and R. Rosenberg. (1978). Macrobenthic succession in relation to organic enrichment and pollution of the marine environment. Oceanography and Marine Biology Annual Review, 16: 229–311.

R Core Team (2021). R: A language and environment for statistical computing. R Foundation for Statistical Computing, Vienna, Austria. URL https://www.R-project.org/.

Ranasinghe, J.A., K.C. Schiff, D.E. Montagne, T.K. Mikel, D.B. Cadien, R.G. Velarde, and C.A. Brantley. (2010). Benthic macrofaunal community condition in the Southern California Bight, 1994–2003. Marine Pollution Bulletin, 60: 827–833.

Reish, D. J. (1957). The relationship of the polychaetous annelid *Capitella capitata* (Fabricius) to waste discharges of biological origin. In: C.M. Tarzwell (ed.). Biological Problems in Water Pollution. U.S. Public Health Service, Washington, DC. p 195–200.

Ripley, B. and M. Lapsley. (2017). RODBC: ODBC Database Access. R package version 1.3-15. http://CRAN.R-project.org/package=RODBC.

Rodríguez-Villanueva, V., R. Martínez-Lara, and V. Macías Zamora. (2003). Polychaete community structure of the northwestern coast of Mexico: patterns of abundance and distribution. Hydrobiologia, 496: 385–399.

[SCAMIT] Southern California Association of Marine Invertebrate Taxonomists. (2023). A taxonomic listing of benthic macro- and megainvertebrates from infaunal and epibenthic monitoring programs in the Southern California Bight, Edition 14. Southern California Association of Marine Invertebrate Taxonomists, Natural History Museum of Los Angeles County Research and Collections, Los Angeles, CA.

Smith, R.W., M. Bergen, S.B. Weisberg, D. Cadien, A. Dalkey, D. Montagne, J.K. Stull, and R.G. Velarde. (2001). Benthic response index for assessing infaunal communities on the southern California mainland shelf. Ecological Applications, 11(4): 1073–1087.

Snelgrove, P.V.R., T.H. Blackburn, P.A. Hutchings, D.M. Alongi, J.F. Grassle, H. Hummel, G. King, I. Koike, P.J.D. Lambshead, N.B. Ramsing, and V. Solis-Weiss. (1997). The importance of marine sediment biodiversity in ecosystem processes. Ambio, 26: 578–583.

Swartz, R.C., F.A. Cole, and W.A. Deben. (1986). Ecological changes in the Southern California Bight near a large sewage outfall: benthic conditions in 1980 and 1983. Marine Ecology Progress Series, 31: 1–13.

Thompson, B.E., J.D. Laughlin, and D.T. Tsukada. (1987). 1985 reference site survey. Technical Report No. 221, Southern California Coastal Water Research Project, Long Beach, CA.

Thompson, B., J. Dixon, S. Schroeter, and D.J. Reish. (1993a). Chapter 8. Benthic invertebrates. In: M.D. Dailey, D.J. Reish, and J.W. Anderson (eds.). Ecology of the Southern California Bight: A Synthesis and Interpretation. University of California Press, Berkeley, CA.

Thompson, B.E., D. Tsukada, and D. O'Donohue. (1993b). 1990 reference site survey. Technical Report No. 269, Southern California Coastal Water Research Project, Long Beach, CA.

[USEPA] United States Environmental Protection Agency. (1987). Quality Assurance and Quality Control (QA/QC) for 301(h) Monitoring Programs: Guidance on Field and Laboratory Methods. EPA Document 430/9-86-004. Office of Marine and Estuarine Protection.

Warwick, R.M. (1993). Environmental impact studies on marine communities: pragmatical considerations. Australian Journal of Ecology, 18: 63–80.

Wickham, H. (2007). Reshaping Data with the reshape Package. Journal of Statistical Software, 21(12), 1-20. URL http://www.jstatsoft.org/v21/i12/.

Wickham, H. (2017). tidyverse: Easily Install and Load the 'Tidyverse'. R package version 1.2.1. https://CRAN.R-project.org/package=tidyverse.

Wickham, H. (2018). scales: Scale Functions for Visualization. R package version 1.0.0. https://CRAN.R-project.org/package=scales

Zmarzly, D.L., T.D. Stebbins, D. Pasko, R.M. Duggan, and K.L. Barwick. (1994). Spatial patterns and temporal succession in soft-bottom macroinvertebrate assemblages surrounding an ocean outfall on the southern San Diego shelf: Relation to anthropogenic and natural events. Marine Biology, 118: 293–307.

CHAPTER 6

FIGURES & TABLES

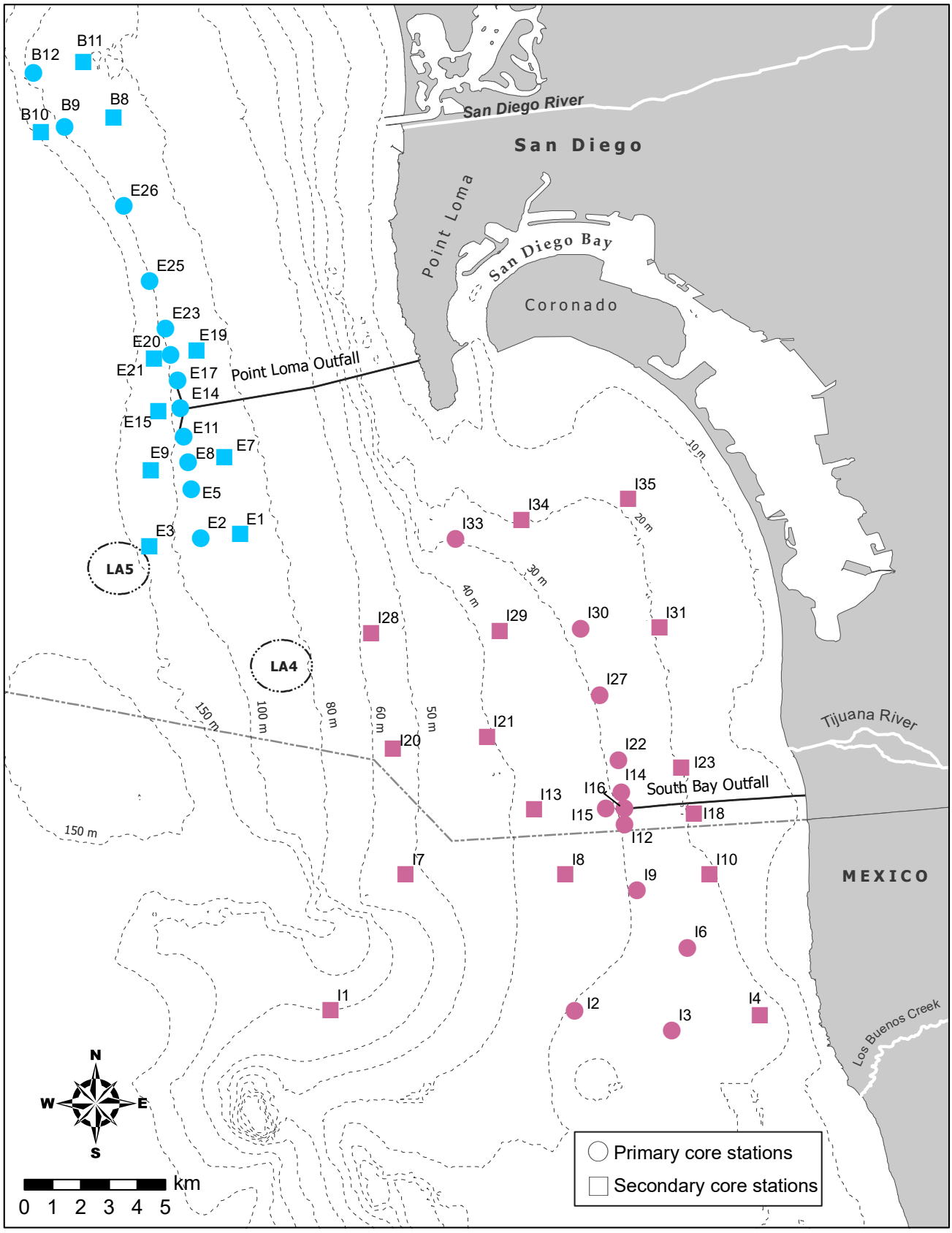


Figure 6.1
Benthic station locations sampled around the PLOO (blue) and SBOO (magenta) as part of the City of San Diego's Ocean Monitoring Program.

Table 6.1

Summary of macrofaunal community parameters for PLOO benthic stations sampled during 2024 and 2025. Data for each station are expressed as biennial means (n ≤ 4). SR = species richness; Abun = abundance; H' = Shannon diversity index; J' = Pielou's evenness; Dom = Swartz dominance; BRI = Benthic Response Index; CI = confidence interval. Stations are listed north to south from top to bottom for each depth contour.

	Station	SR	Abun	H'	J'	Dom	BRI
88-m Depth Contour	B11	104	324	4.2	0.89	40	12
	B8	105	428	4.1	0.87	35	11
	E19	101	452	4.0	0.86	30	12
	E7	96	370	4.0	0.87	30	12
	E1	96	350	3.9	0.87	32	10
98-m Depth Contour	B12	104	316	4.2	0.91	42	12
	B9	102	348	4.1	0.89	37	11
	E26	100	407	4.1	0.88	33	10
	E25	98	390	4.0	0.87	32	12
	E23	95	438	3.9	0.85	28	11
	E20	82	344	3.7	0.85	25	11
	E17[a]	90	419	3.8	0.84	27	17
	E14[a]	94	600	3.6	0.78	20	24
	E11[a]	84	322	3.8	0.86	28	15
	E8	88	318	3.9	0.87	31	12
	E5	94	373	3.9	0.86	32	12
	E2	104	460	3.9	0.85	32	12
116-m Depth Contour	B10	93	282	4.1	0.90	37	14
	E21	88	391	3.7	0.82	24	12
	E15[a]	96	398	3.9	0.85	31	12
	E9	122	412	4.3	0.89	46	12
	E3	123	378	4.3	0.90	46	12
All Grabs	Mean	98	387	4.0	0.86	33	13
	95% CI	3	22	0.0	0.01	2	1
	Minimum	71	201	3.5	0.75	19	5
	Maximum	145	879	4.5	0.92	60	26

[a] Near-ZID station

Table 6.2

Summary of macrofaunal community parameters for SBOO benthic stations sampled during 2024 and 2025. Data for each station are expressed as biennial means (n ≤ 4). SR = species richness; Abun = abundance; H' = Shannon diversity index; J' = Pielou's evenness; Dom = Swartz dominance; BRI = Benthic Response Index; CI = confidence interval. Stations are listed north to south from top to bottom for each depth contour.

	Station	SR	Abun	H'	J'	Dom	BRI
19-m Depth Contour	I35	62	215	3.5	0.86	23	28
	I34	54	892	2.6	0.65	9	19
	I31	63	166	3.8	0.92	26	19
	I23	56	350	3.2	0.79	13	17
	I18	54	144	3.5	0.88	21	19
	I10	47	109	3.6	0.91	24	18
	I4	41	140	3.0	0.81	16	12
28-m Depth Contour	I33	123	446	4.3	0.88	44	24
	I30	79	280	3.7	0.85	28	24
	I27	87	336	3.8	0.85	29	25
	I22	89	265	4.1	0.92	38	23
	I14[a]	67	198	3.8	0.90	28	24
	I16[a]	68	273	3.4	0.82	20	24
	I15[a]	59	273	3.2	0.78	16	25
	I12[a]	76	353	3.4	0.81	20	20
	I9	96	383	4.0	0.87	32	26
	I6	43	164	3.0	0.79	13	12
	I2	44	181	3.1	0.81	14	20
	I3	37	181	2.6	0.74	8	13
38-m Depth Contour	I29	134	918	3.9	0.79	32	19
	I21	67	302	3.3	0.79	18	14
	I13	54	230	3.2	0.80	16	13
	I8	47	180	3.2	0.83	16	20
55-m Depth Contour	I28	150	612	4.2	0.84	46	16
	I20	74	384	3.3	0.76	18	15
	I7	64	204	3.6	0.86	24	11
	I1	113	503	4.0	0.83	34	16
All Grabs	Mean	72	322	3.5	0.83	23	19
	95% CI	6	55	0.1	0.02	2	1
	Minimum	22	62	1.9	0.61	4	-9
	Maximum	183	2373	4.4	0.95	51	34

[a] Near-ZID station

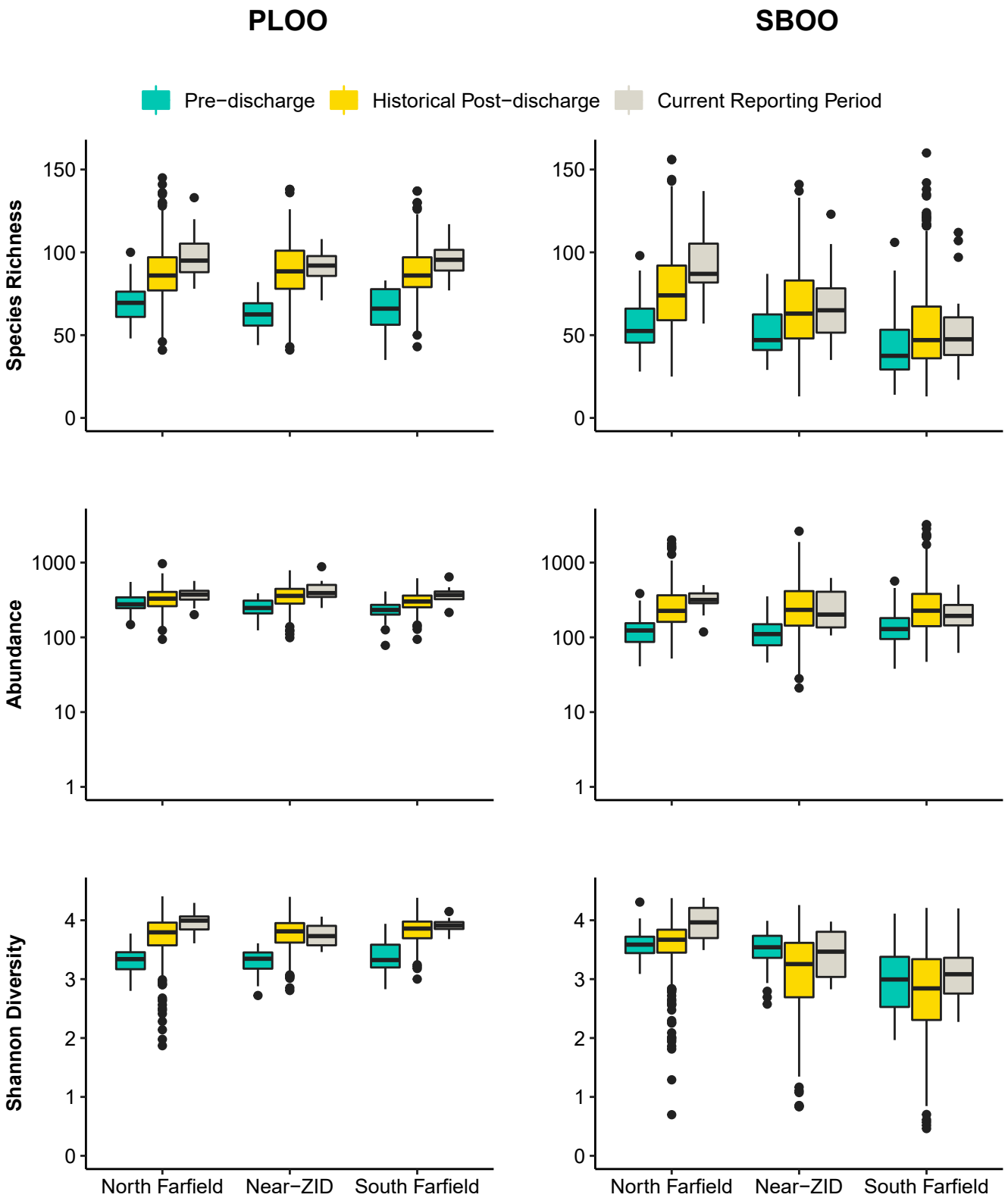


Figure 6.2

Species richness, abundance, and diversity (H') of benthic infauna collected from PLOO and SBOO north farfield, near-ZID, and south farfield primary core stations during pre-discharge, historical post-discharge, and current reporting period; Boxes = median, upper, and lower quantiles; whiskers = 1.5x interquantile range; circles = outliers; see Chapter 1 for description of pre- versus post-discharge time periods for the two outfalls.

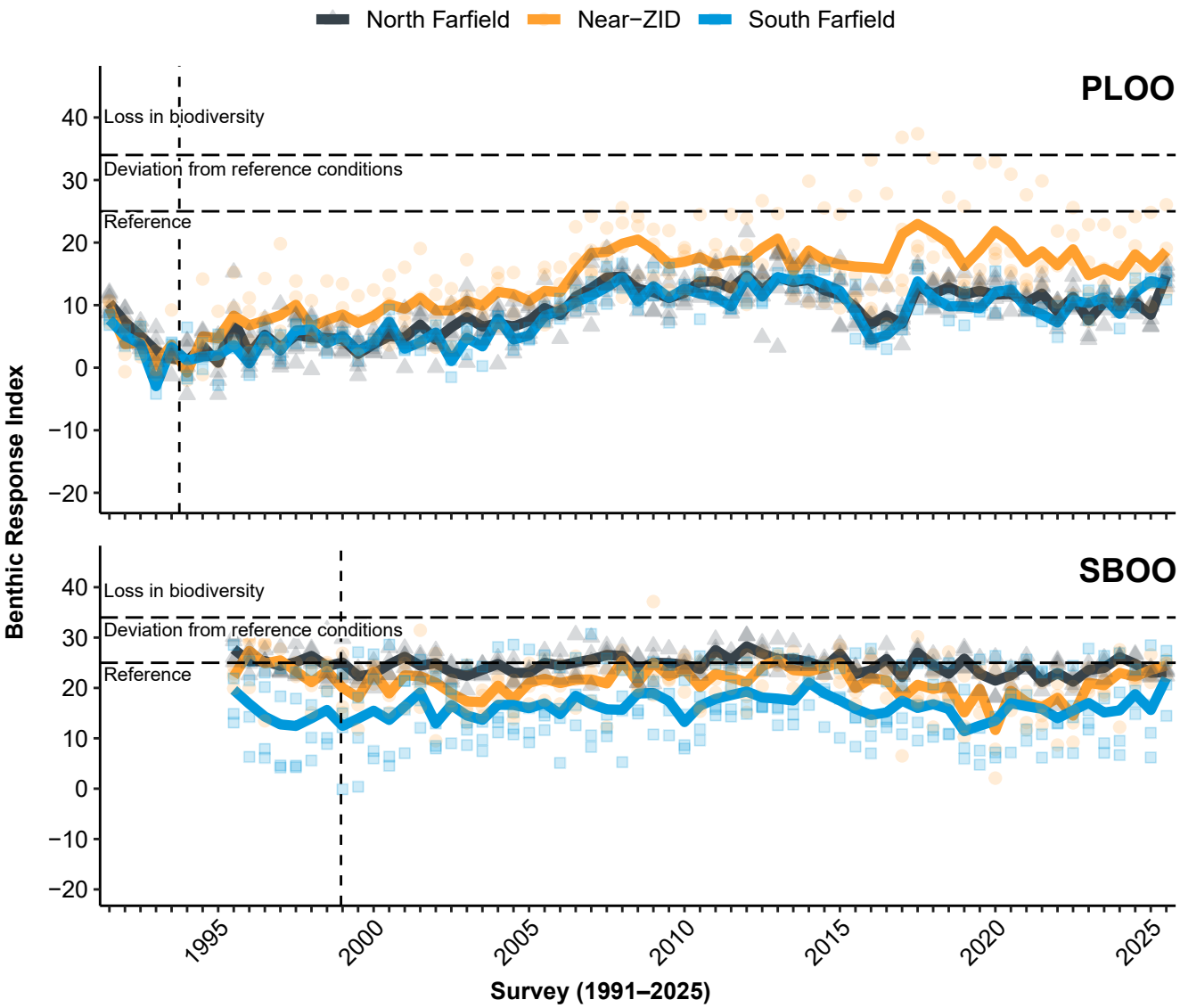


Figure 6.3

Benthic Response Index at PLOO and SBOO north farfield, near-ZID, and south farfield primary core stations sampled in the PLOO region from 1991 through 2025 and in the SBOO region from 1995 through 2025. For each station group, mean BRI per survey is shown by the solid line ($n \leq 8$) while BRI per station is shown by the symbols. Vertical dashed lines indicate onset of wastewater discharge at each outfall's current location.

Table 6.3

Percent composition and abundance of major taxonomic groups in PLOO and SBOO benthic grabs sampled during 2024 and 2025. Percentages may not add up to 100 due to rounding artifacts.

	PLOO		SBOO	
Phyla	**Species (%)**	**Abundance (%)**	**Species (%)**	**Abundance (%)**
Annelida (Polychaeta)	48	65	47	67
Arthropoda (Crustacea)	20	18	21	13
Echinodermata	5	8	4	3
Mollusca	15	5	16	6
Other Phyla	11	3	12	11

Table 6.4

The 10 most abundant macroinvertebrate taxa collected from PLOO benthic stations during 2024 and 2025. Data are expressed as percent abundance (number of individuals per species/total abundance of all species), frequency of occurrence (percentage of grabs in which a species occurred), and abundance per grab (mean number of individuals per grab, n = 88).

Taxon	Taxonomic Classification	Percent Abundance	Frequency of Occurrence	Abundance per Grab
Euphilomedes carcharodonta	Arthropoda: Ostracoda	7	90	28
Spiophanes duplex	Polychaeta: Spionidae	5	99	19
Mediomastus sp	Polychaeta: Capitellidae	4	99	17
Prionospio jubata	Polychaeta: Spionidae	3	99	11
Amphiodia urtica	Echinodermata: Ophiuroidea	3	88	11
Euphilomedes producta	Arthropoda: Ostracoda	3	91	11
Paradiopatra parva	Polychaeta: Onuphidae	2	99	10
Prionospio dubia	Polychaeta: Spionidae	2	97	9
Chloeia pinnata	Polychaeta: Amphinomidae	2	68	9
Spiophanes kimballi	Polychaeta: Spionidae	2	89	9

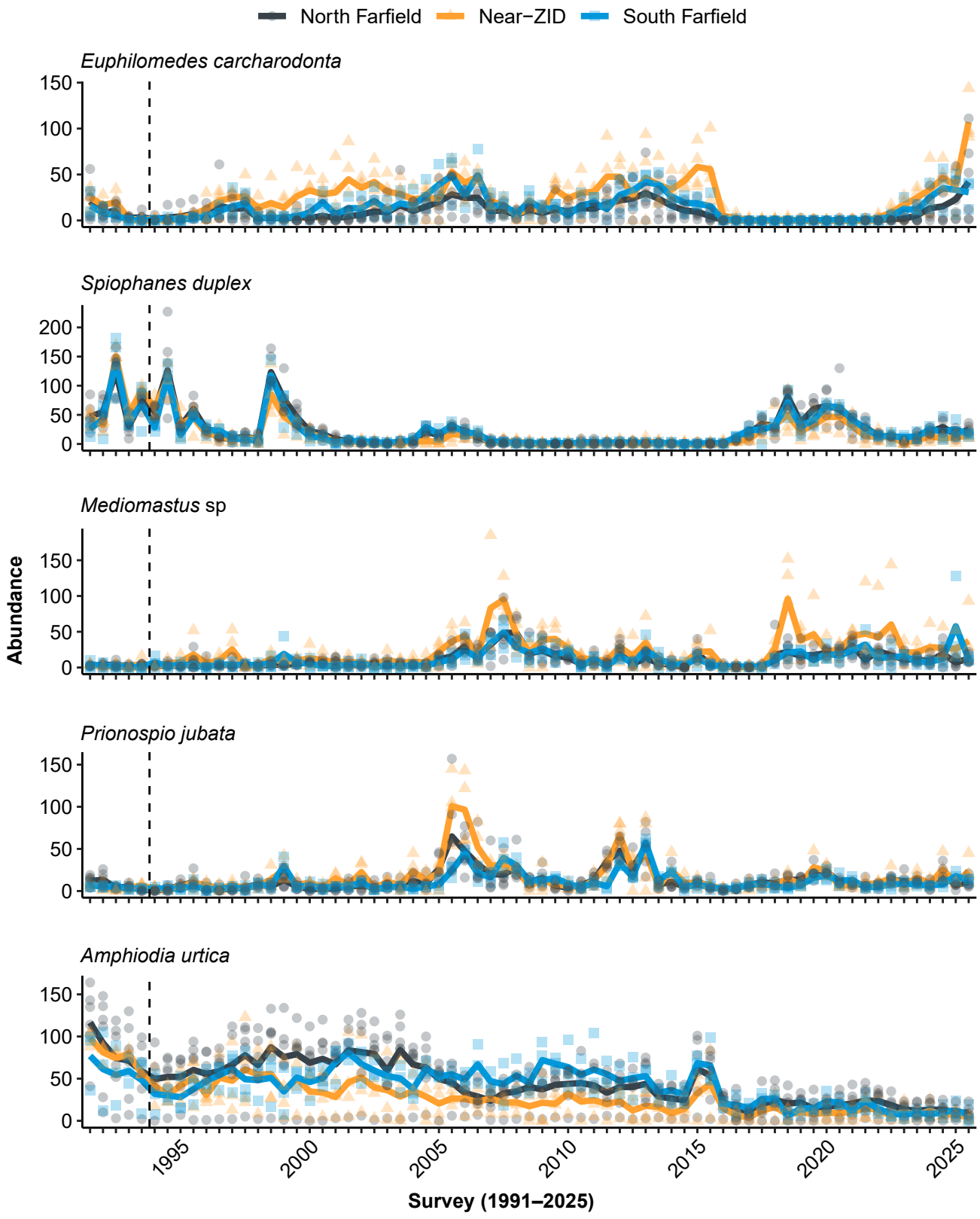


Figure 6.4

Abundances of the five most numerically dominant species recorded during 2024 and 2025 (presented in order) at PLOO north farfield, near-ZID, and south farfield primary core stations from 1991 through 2025. For each station group, mean abundance per survey is shown by the solid line ($n \leq 8$) while abundance per station is shown by the symbols. Dashed lines indicate onset of wastewater discharge at its current location.

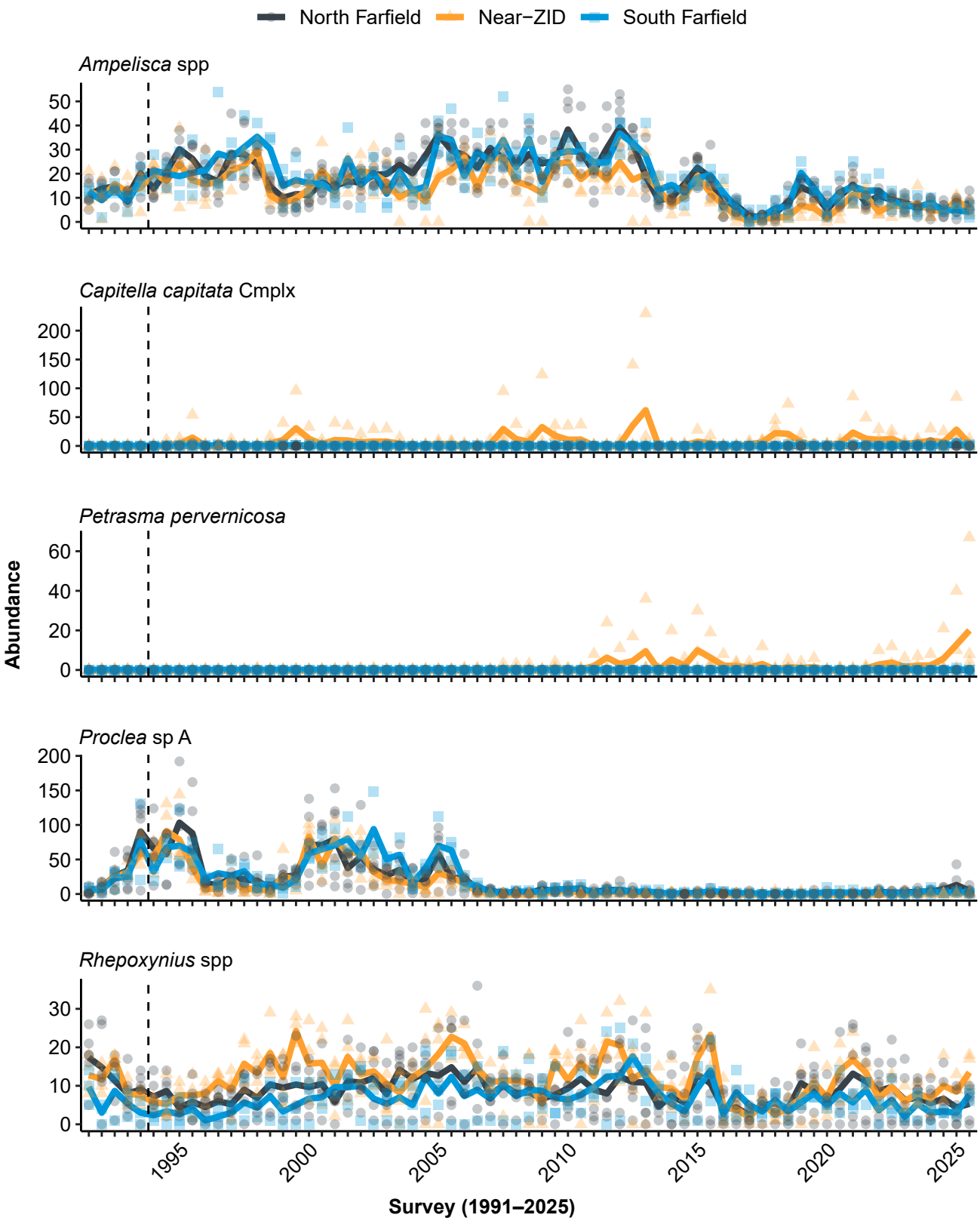


Figure 6.5

Abundances of representative ecologically important indicator taxa collected at PLOO north farfield, near-ZID, and south farfield primary core stations from 1991 through 2025. For each station group, mean abundance per survey is shown by the solid line ($n \leq 8$) while abundance per station is shown by the symbols. Dashed lines indicate onset of wastewater discharge at its current location.

Table 6.5

The 10 most abundant macroinvertebrate taxa collected from SBOO benthic stations during 2024 and 2025. Data are expressed as percent abundance (number of individuals per species/total abundance of all species), frequency of occurrence (percentage of grabs in which a species occurred), and abundance per grab (mean number of individuals per grab, n = 108).

Taxon	Taxonomic Classification	Percent Abundance	Frequency of Occurrence	Abundance per Grab
Spiophanes norrisi	Polychaeta: Spionidae	7	94	24
Spiophanes duplex	Polychaeta: Spionidae	4	71	12
Euclymeninae sp A	Polychaeta: Maldanidae	2	65	8
Kirkegaardia siblina	Polychaeta: Cirratulidae	2	59	7
Edwardsia juliae	Cnidaria: Actiniaria	2	60	7
Pisione sp	Polychaeta: Sigalionidae	2	6	6
Nematoda		2	65	6
Chondrochelia dubia Cmplx	Arthropoda: Tanaidacea	2	68	5
Hesionura coineaui difficilis	Polychaeta: Phyllodocidae	2	7	5
Polycirrus sp SD3	Polychaeta: Terebellidae	2	5	5

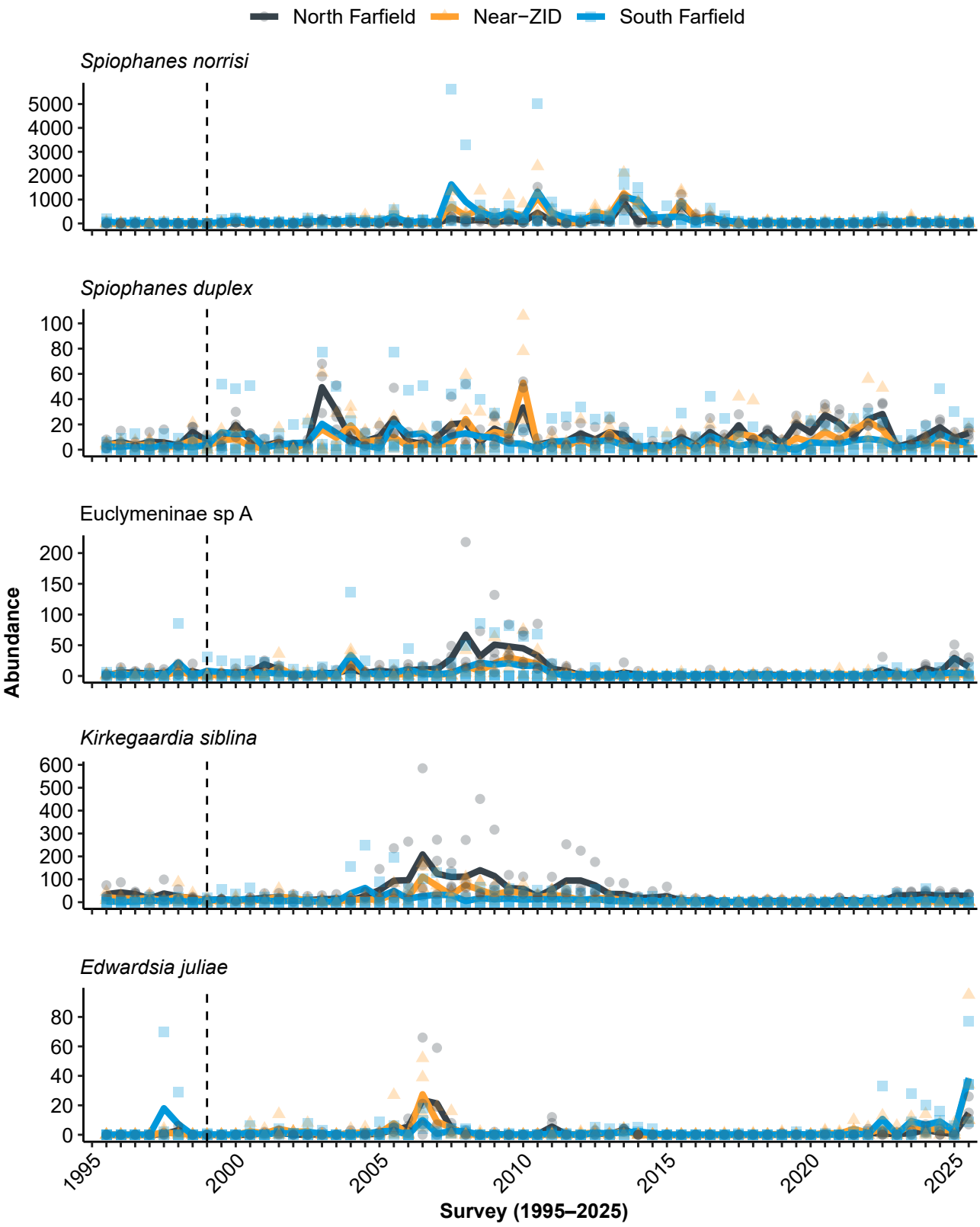


Figure 6.6

Abundances of the five most numerically dominant species (presented in order) recorded during 2024 and 2025 at SBOO north farfield, near-ZID, and south farfield primary core stations from 1995 through 2025. For each station group, mean abundance per survey is shown by the solid line ($n \leq 8$) while abundance per station is shown by the symbols. Dashed lines indicate onset of wastewater discharge.

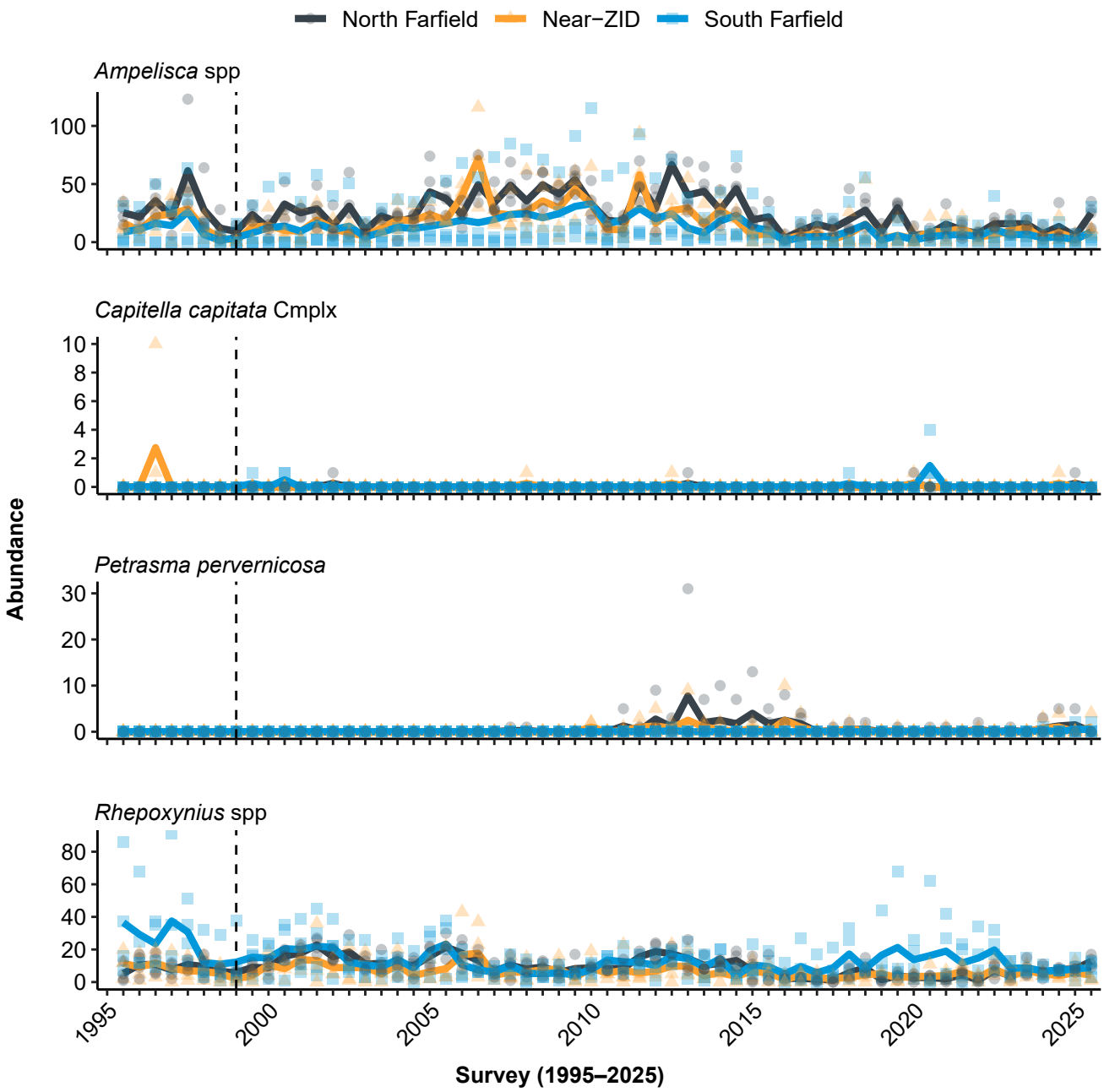


Figure 6.7

Abundances of representative ecologically important indicator taxa collected at SBOO north farfield, near-ZID, and south farfield primary core stations from 1995 through 2025. For each station group, mean abundance per survey is shown by the solid line ($n \leq 8$) while abundance per station is shown by the symbols. Dashed lines indicate onset of wastewater discharge.

Chapter 7
San Diego Regional
Benthic Condition Assesssment

Chapter 7. San Diego Regional Benthic Condition Assessment

Introduction

The City of San Diego (City) has conducted annual surveys of randomly selected (regional) benthic stations off the coast of San Diego since 1994 (see Chapter 1). The location of these regional surveys typically range from offshore of Del Mar in northern San Diego County southward to the USA/Mexico border. An array of 40 stations are selected each year using a probability-based, random stratified sampling design as described in Bergen (1996), Stevens (1997), and Stevens and Olsen (2004). During 1995–1997, 1999–2002, and 2005–2007, the surveys off San Diego were restricted to continental shelf depths < 200 m. However, beginning in 2009, the survey area was expanded to include deeper habitats along the upper continental slope (200–500 m). No separate San Diego regional survey was conducted in 2004 due to sampling for a special sediment mapping project (Stebbins et al. 2004), while the 1994, 1998, 2003, 2008, 2013, 2018, and 2023 regional surveys were conducted as part of the larger Southern California Bight (SCB) Regional Monitoring Program (Bergen et al. 1998, 2001, Schiff and Gossett 1998, Noblet et al. 2002, Schiff et al. 2006, 2011, Maruya and Schiff 2009, Ranasinghe et al. 2003, 2007, 2010, 2012, Dodder et al. 2016, Gillett et al. 2022, SCCWRP 2018, Du et al. 2020, Wong et al. in review). In total more than 1146 samples have been collected off San Diego over the past 31 years (1994–2025).

This chapter presents an overall assessment of regional benthic conditions on the continental shelf and upper slope off San Diego during 2024–2025. Included are analyses of sediment particle size, sediment chemistry, sediment toxicity, and macrofaunal community data collected from a total of 80 regional benthic stations and 49 core benthic stations sampled during summer 2024 and 2025. These data provide a snapshot of the region's sediment quality and benthic community structure across the major depth strata defined by the SCB regional monitoring programs (e.g., SCCWRP 2018). Additional analyses of spatial patterns, winter vs. summer differences, and long-term changes over time at the core Point Loma Ocean Outfall (PLOO) and South Bay Ocean Outfall (SBOO) stations are presented in Chapters 5 and 6.

In an effort to provide a more comprehensive assessment of sediment quality in this region, sediment toxicity results have been integrated with other lines of evidence (LOEs), including sediment chemistry and benthic community structure. These LOEs were integrated using a framework adopted by the State of California to assess sediment quality within enclosed bays and estuaries (SWRCB 2009; Bay et al. 2013), but with the same modifications used for the coastal shelf as part of Southern California Bight (SCB) Regional Monitoring Program surveys (i.e., Bight regional surveys; see B13CIA 2017). These modifications included applying the results from the 10-day amphipod sediment toxicity test prescribed by the Sediment Toxicity Monitoring Plan (versus the two sediment toxicity tests available for embayments) (City of San Diego 2015a) and the benthic response index (BRI) that was developed specifically for evaluation of benthic macrofaunal (e.g., worms, crabs, clams, brittle stars, other small invertebrates) communities in offshore waters (Bergen et al. 2000, Smith et al. 2001). The same two sediment chemistry assessment indices developed for embayments were used, even though these indices have not been calibrated or validated for continental shelf sediments, as these are the best tools currently available (B13CIA 2017). The integration of each line of evidence using the State of

California's sediment quality assessment framework resulted in the classification of each site into one of five potential categories: (1) unimpacted; (2) likely unimpacted; (3) possibly impacted; (4) likely impacted; (5) clearly impacted. The State Water Board considers the first two categories as healthy, or representative of conditions undisturbed by pollutants in sediment (SWRCB 2009, B13CIA 2017). The primary objectives of this chapter are to: (1) describe the overall condition and quality of the diverse benthic habitats that occur in the offshore coastal waters off San Diego; (2) characterize sediment quality, sediment toxicity, and the health of the soft-bottom marine benthos in the region; (3) gain a better understanding of regional variation in order to distinguish between the effects of anthropogenic and natural factors; (4) put into context the results of more frequent sampling at permanent (core) monitoring sites surrounding the PLOO and SBOO.

Materials and Methods

Collection and Processing of Samples

Benthic samples analyzed in this chapter were collected during the summer of 2024 and 2025 at 129 stations that ranged from Del Mar southward to below the USA/Mexico border (Figure 7.1). A total of 80 of these stations were selected using a probability-based random stratified sampling design as described in Bergen (1996), Stevens (1997), and Stevens and Olsen (2004). These "regional" stations were sampled at depths ranging from 8 to 453 m spanning four distinct depth strata off southern California. These included 16 regional stations along the inner shelf (4–30 m), 34 regional stations along the midshelf (30–120 m), 17 regional stations along the outer shelf (120–200 m), and 13 regional stations on the upper slope (200–485 m). In addition to the above, the results of 2024 and 2025 summer sampling at the 49 primary and secondary core PLOO and SBOO monitoring stations located at inner to mid-shelf depths as described in Chapters 5 and 6 are also analyzed in this chapter. Stations located within 1000 m of the boundary of the zone of initial dilution (ZID) for either outfall are considered to represent near-ZID conditions. These include PLOO stations E11, E14, E15, E17, and SBOO stations I12, I14, I15, I16.

Samples for benthic analyses were collected using a double 0.1-m^2 Van Veen grab, with one grab per cast used for sediment quality analysis (see Chapter 5), one grab per cast used for benthic community analysis (see Chapter 6), and subsequent grabs used for sediment toxicity testing where required. Visual observations of weather, sea conditions, and human/animal activity were also recorded at the time of sampling. Criteria established by the U.S. Environmental Protection Agency (USEPA) to ensure consistency of these types of samples were followed with regard to sample disturbance and depth of penetration (USEPA 1987).

Sub-samples for particle size and sediment chemistry analyses were taken from the top 2 cm of the sediment surface and handled according to standard guidelines (USEPA 1987, SCCWRP 2018). For infauna analysis, sediment from an entire grab was transferred to a wash table aboard ship, rinsed with seawater, and then sieved through a 1.0-mm mesh screen in order to remove as much sediment as possible. The macroinvertebrates retained on the screen were transferred to sample jars, relaxed for 30 minutes in a magnesium sulfate solution, and then fixed with buffered formalin. The preserved samples were then transferred back to the City's Marine Biology Laboratory. After a minimum of 72 hours, but no more than 10 days, in formalin, each sample was thoroughly rinsed with fresh water and transferred to 70% ethanol for final preservation.

For sediment toxicity samples, a plastic (high-density polyethylene [HDPE], polycarbonate, or Teflon) or stainless-steel scoop was used to collect sediment from the top 2 cm of the undisturbed surface material in the grab. Contact with sediment within 1 cm of the sides of the grab was avoided in order to minimize cross-contamination. In most cases, multiple grabs were required to obtain enough sediment for toxicity testing (i.e., up to 6 L of sediment). If more than one grab was required, sediment from each grab was added to a Teflon bag and homogenized thoroughly using either a clean Teflon or plastic spoon, or by kneading the sample within the bag. Once collected, the toxicity samples were stored in the dark at 4°C in the laboratory for no longer than four weeks prior to testing.

Laboratory Analyses

Sediment Particle Size

All sediment chemistry and particle size analyses were performed at the City's Environmental Chemistry Services Laboratory. Particle size analysis was performed using either a Horiba LA-950V2 laser scattering particle analyzer or a set of nested sieves. The Horiba measures particles ranging in size from 0.5 to 2000 µm. Coarser sediments were removed and quantified prior to laser analysis by screening samples through a 2000 µm mesh sieve. These data were later combined with the Horiba results to obtain a complete distribution of particle sizes totaling 100%, and then classified into 11 sub-fractions and four main size fractions based on the Wentworth scale (Folk 1980) (see Appendix D.13). When a sample contained substantial amounts of coarse sand, gravel, shell hash or other large materials that could damage the Horiba analyzer or where the general distribution of sediments would be poorly represented by laser analysis, a set of nested sieves with mesh sizes of 2000 µm, 1000 µm, 500 µm, 250 µm, 125 µm, 75 µm and 63 µm was used to divide the samples into seven sub-fractions. See Appendix F.1 for visual observations for each regional station; see Appendix D.14 for visual observations for each PLOO and SBOO core station.

Sediment Chemistry

A detailed description of the analytical protocols is available upon request. Briefly, sediment sub-samples were analyzed on a dry weight basis to determine concentrations of various indictors of organic loading (i.e., biochemical oxygen demand, total organic carbon, total nitrogen, total sulfides, total volatile solids), 18 trace metals, 9 chlorinated pesticides, 42 polychlorinated biphenyl compound congeners (PCBs), and 24 polycyclic aromatic hydrocarbons (PAHs), and 13 polybrominated ethers (PBDEs) (see Appendix F.1). A variety of laboratory technical issues resulted in a number of non-reportable sediment chemistry data for the 2024 and 2025 benthic surveys, see Appendices D.2–D.12 and Appendices F.2–F.7.

Sediment Toxicity Testing

A detailed description of the sediment toxicity testing protocols can be found in City of San Diego (2024). Briefly, all sediment toxicity testing was conducted by the City of San Diego Toxicology Laboratory (CSDTL) using the marine amphipod *Eohaustorius estuarius*. The 10-day amphipod tests were conducted in accordance with EPA 600/R-94/0925 (USEPA 1994) and the procedures approved for Southern California Bight 2018 Regional Monitoring Program (Bight'23 Toxicology Committee 2023). Juvenile *E. estuarius* were exposed for 10 days to both test and control sediments. Response criteria included amphipod mortality, emergence from sediment during exposure, and, if considered a measurement of interest, the ability of amphipods to rebury in clean sediment at the end of the bioassay. In addition, a reference toxicant test (using seawater only) was

conducted concurrently and under identical environmental conditions as the sediment toxicity tests to determine test-organism sensitivity.

Macrobenthic Assemblages

All organisms were separated from the raw material (e.g., sediment grunge, shell hash, debris) and sorted into the following six taxonomic groups by an external contract lab: Annelids (e.g., polychaete and oligochaete worms), Arthropods (e.g., crustaceans and pycnogonids), Molluscs (e.g., clams, snails, and scaphopods), non-ophiuroid Echinoderms (e.g., sea urchins, sea stars, and sea cucumbers), Ophiuroids (i.e., brittle stars), and other phyla (e.g., flatworms, nemerteans, and cnidarians). The sorted macrofaunal samples were then returned to the City's Marine Biology Laboratory where all animals were identified to species, or to the lowest taxon possible, by City Marine Biologists. All identifications followed nomenclatural standards established by the Southern California Association of Marine Invertebrate Taxonomists (SCAMIT 2023). See Appendix F.8 for a complete listing of encountered taxa from 2025 Regional stations, Appendices E.3 and E.4 for taxa from 2025 PLOO and SBOO core stations, and City of San Diego (2025) for taxa collected during 2024.

Data Analyses

Data collected during 2024 were reported previously (City of San Diego 2025), and all raw data for the 2024-2025 sampling period have been submitted to either the Regional Water Quality Control Board, the California Environmental Data Exchange Network (CEDEN) or the City's Open Data Portal (City of San Diego 2026a) and will be provided upon request.

Sediment Chemistry

Data summaries for the various sediment parameters included detection rate, minimum, maximum, and mean values. For chemistry parameters, all means were calculated using detected values only, with no substitutions made for non-detects in the data (analyte concentrations < method detection limit [MDL]). Limiting analyses to detected values (i.e., excluding non-detects) is considered a conservative way of handling contaminant concentrations as it creates a strong upward bias in the data and respective summary statistics, and therefore may represent a worst-case scenario (e.g., see Helsel 2005a,b, 2006 for discussions of non-detect data). For continuity, and in contrast to previous reports (e.g., City of San Diego 2020), estimated values that fell below method detection limits but were confirmed by mass-spectrometry were excluded from all data (1991–2025). Estimated values were treated as non-detects for this report. Total chlordane, total DDT (tDDT), total hexachlorocyclohexane (tHCH), total PCB (tPCB), total PAH (tPAH), and total PBDE (tPBDE) were calculated for each sample as the sum of all individual constituents with reported values. When applicable, contaminant concentrations were compared to the Effects Range Low (ERL) and Effects Range Median (ERM) sediment quality guidelines (Long et al. 1995). The ERLs represent chemical concentrations below which adverse biological effects are rarely observed, while values above the ERL but below the ERM represent levels at which effects occasionally occur. Concentrations above the ERM indicate likely biological effects, although these are not always validated by toxicity testing (Schiff and Gossett 1998). Unless stated otherwise, analyses were performed using R (R Core Team 2023) and various functions within the zoo, reshape2, plyr, ggplot2, tidyverse, Rmisc, vegan, RODBC, stringr, ggpubr, psych, tidyr, and dplyr packages (Zeileis and Grothendieck 2005, Wickham 2007, 2011, 2016, Wickham et al. 2019, Hope 2022, Oksanen et al. 2022, Ripley and Lapsley 2022, Wickham 2022, Kassambara 2023, Revelle 2023, Wickham et al. 2023a, 2023b).

Spearman rank correlations were calculated to assess if values for the various parameters co-varied in the sediments. This non-parametric analysis accounts for non-detects in the data without the use of value substitutions (Helsel 2005b). However, depending on the data distribution, the instability in rank-based analyses may intensify with increased censoring (Conover 1980). Therefore, a criterion of <50% non-detects was used to screen eligible constituents for this analysis.

Sediment Toxicity Testing

All data were analyzed in accordance with procedures outlined in Sections 12 and 13 of EPA 600/R-94/0925 using the acceptability criterion of ≥90% mean control survival at test termination. Additional information and the standard operation procedures for sediment toxicity testing are provided in Appendix B of the CSDTL's Quality Assurance Manual (City of San Diego 2026b).

Macrobenthic Assemblages

The following community metrics were determined for each station and expressed per 0.1-m^2 grab: species richness (number of species or distinct taxa), abundance (number of individuals), Shannon Diversity Index (H'), Pielou's Evenness Index (J'), Swartz dominance index (see Swartz et al. 1986, Ferraro et al. 1994), and Benthic Response Index (BRI) (see Smith et al. 2001). Due to limitations in the validation dataset, BRI values were not calculated for samples collected at depths <10 m or >200 m (Smith et al. 2001). Unless otherwise noted, analyses were performed using the computational software package R (R Core Team 2023) and various functions within the zoo, reshape2, tidyverse, Rmisc, vegan, RODBC, scales, ggpubr, tidyr, and dplyr packages (Zeileis and Grothendieck 2005, Wickham 2007, Wickham et al. 2019, Hope 2022, Oksanen et al. 2022, Ripley and Lapsley 2022, Wickham and Seidel 2022, Kassambara 2023, Wickham et al. 2023a, 2023b).

Sediment Quality Triad Assessment

Following instructions provided in Bay et al. (2013), benthic macrofauna and sediment chemistry results were combined with sediment toxicity results from the 16 stations where sediment toxicity was conducted during 2024-2025 to determine relevant condition categories. The benthic community LOE was determined by assigning condition categories to each sample collected at acceptable depths as follows: BRI values <25 = reference conditions, 25–33 = minor deviation from reference conditions, 34–43 = moderate disturbance, 44–71 = high disturbance (defined as loss in community function in Smith et al. 2001), and >72 = defaunation. The sediment toxicity LOE was determined by assigning scores to samples using the following thresholds: percent control ≥90% = nontoxic, ≥82% = low toxicity, ≥59% = moderate toxicity, and <59% = high toxicity. The sediment chemistry LOE was determined by using the California Logistic Regression Model Index (LRM) and the Chemical Score Index (CSI) to calculate scores for each sample with sufficient parameters analyzed, calculating the mean score as (LRM + CSI)/2, and assigning the overall integrated chemistry category LOE as follows: mean score ≤1.0 = minimal exposure, 1.1–2.0 = low exposure, 2.1–3.0 = moderate exposure, and 3.1–4.0 = high exposure.

After the scores were converted to LOE categories, they were combined using the integration framework defined in Bay et al (2013). This framework is based on a conceptual approach that addresses two key elements: (1) is there biological degradation at the site, and (2) is chemical exposure at the site high enough to potentially result in a biological response? (see SWRCB 2009, Bay and Weisberg 2012). Station assessment (site condition) categories were assigned using benthic community condition as determined by the BRI (reference, or low, moderate, high disturbance), sediment toxicity (nontoxic, or low, moderate, high toxicity), and sediment chemistry exposure (minimal, low, moderate, high) according to Table 6.1 in Bay et al (2013). For example, if a sample had a benthic community in

reference condition, the sediments were found to be nontoxic, and the sediment chemistry exposure was minimal, then the station assessment (site condition) was deemed unimpacted. There is a total of 64 combinations resulting in the five categories: (1) unimpacted; (2) likely unimpacted; (3) possibly impacted; (4) likely impacted; (5) clearly impacted. The station assessment could also be inconclusive (e.g., reference benthic conditions plus moderate sediment toxicity exposure plus high sediment chemistry exposure).

Multivariate Analyses

Multivariate analyses were performed using PRIMER v7 software to examine spatial and temporal patterns in macrofaunal data collected at the 80 regional stations and 49 core stations sampled during summer 2024 and 2025 (total samples = 178) (Clarke et al. 2008, Clarke et al. 2014). These included ordination and hierarchical agglomerative clustering (cluster analysis) with group-average linking and similarity profile analysis (SIMPROF) to confirm the non-random structure of the resultant cluster dendrograms. Prior to these analyses, macrofaunal abundance data were square-root transformed to lessen the influence of overly abundant species and increase the importance (or presence) of rare species. Measures of similarity used as the basis for clustering included the Bray-Curtis measure of similarity for macrofaunal data. Major ecologically-relevant clusters receiving SIMPROF support were retained, and similarity percentages analysis (SIMPER) was used to determine which species were responsible for the greatest contributions to within-group similarity (characteristic species) and between-group dissimilarity for retained clusters. BEST tests, using the BVSTEP procedure, were conducted to determine which subset of species best described patterns within the dendrogram resulting from the cluster analyses. Additional BEST tests, using the BIO-ENV procedure, were conducted to determine which subsets of sediment sub-fractions were the best explanatory variables for similarity between the particle size and macrofaunal resemblance matrices.

RESULTS

Regional Sediment Quality

Particle Size Composition

Ocean sediment composition was diverse across the 129 benthic stations sampled during the 2024 and 2025 summer surveys. The proportion of fine silt and clay particles (combined as ‘fine particles’ or ‘percent fines’) ranged from a minimum of 0 to a maximum of 88.6% per sample, while fine sands ranged from 0.8 to 90.1%, medium-coarse sands ranged from 0 to 91.8%, and coarse particles ranged from 0 to 28.1% (Table 7.1). Overall, and as expected, sediment composition varied by depth and region (Table 7.1, Figure 7.2, Figure 7.3). For example, the amount of percent fines at regional stations increased with depth, with a mean of 23.1% per sample along the inner shelf, 45.4% along the midshelf, 52.9% along the outer shelf, and 73.3% along the upper slope (Table 7.1). Percent fines were also higher at PLOO core stations located at mid-shelf depths of 88–116 m (mean = 50.0%) versus SBOO core stations located at inner shelf depths of 19–28 m (mean = 18.4%) and at mid-shelf depths of 38–55 m (mean = 19.6%). Furthermore, correlation analysis confirmed that percent fines tended to increase with depth throughout the San Diego area (r_s = 0.63; Figure 7.2, Appendix F.9). Several exceptions to this overall pattern were observed during the current reporting period, where percent fines were higher or lower than expected by depth. For example, several regional stations (9417, 9425, 9426, 9523, 9525, 9530) located between the 50 and 75 m depth contours off Point Loma had finer sediments (>60% fines) than deeper stations in that same area. Sediments were also finer than expected by depth at regional stations 9441 off Coronado Island and 9414 off the southern tip of Point Loma (Figure 7.3).

Sediment Chemistry

As with sediment particle size composition, regional patterns of sediment contamination during summer 2024 and 2025 were similar to patterns seen in previous years (e.g., City of San Diego 2018, 2020, 2022a, 2024). There was no evidence of degraded sediment quality in the general San Diego region. While various indictors of organic loading (Figure 7.4), trace metals (Figure 7.5), chlorinated pesticides (e.g. DDT, see Figure 7.6), PCBs (Appendix F.10), PAHs (Figure 7.7 and PBDEs (Figure 7.8) were detected at variable concentrations in sediment samples collected throughout the region, no gradients were observed with proximity to either outfall and almost all contaminants occurred at levels below both ERL and ERM thresholds, within tolerance intervals calculated for the PLOO region, and within historical ranges (Table 7.1; see also Chapter 5 and City of San Diego 2022a). Of the 129 samples collected during these summer surveys, only 8.5% (n = 11) had elevated concentrations of a parameter with available thresholds. Arsenic exceeded its ERL in one summer sample from SBOO farfield station I21, and one sample from regional station 9503, which is located on the midshelf near I21(Figure 7.5). Nickel exceeded its ERL at regional station 9433, located on the upper slope off Point La Jolla. Total DDT exceeded its ERL in a total of 6 sediment samples from one regional station and one PLOO core station located along the midshelf (station 9426, E5), station 9411 located on the outer shelf, and three samples from regional stations located along the upper slope (stations 9419, 9433, 9440) (Figure 7.6). Regional station 9426 also exceeded the ERM threshold for total DDT. The ERL and ERM thresholds for total PAH were exceeded at one regional station (9510), located on the midshelf.

As in previous surveys (e.g., City of San Diego 2018, 2020, 2022a, 2024), concentrations of most metals increased with increasing proportions of fine particles ($r_s \geq 0.70$), including aluminum, barium, beryllium, cadmium, chromium, copper, iron, mercury, nickel, selenium, and zinc (Appendix F.9). Because of the relationship between fines and depth, several of these also increased across depth strata (aluminum, barium, beryllium, cadmium, chromium, copper, iron, mercury, nickel, selenium, zinc) (Table 7.1, Figure 7.4, Figure 7.5, Appendix F.9, Appendix F.10). The organic loading indicators sulfides, total nitrogen, total organic carbon, and total volatile solids also increased across depth strata (Table 7.1). However, only total volatile solids co-varied with proportions of fine particles (Appendix F.9).

Sediment Toxicity

During summer 2024, sediments were collected and tested for toxicity at eight near-ZID stations in both the PLOO and SBOO regions, and in summer 2025, from eight regional stations that ranged in depth from 13 to 178 m (Figure 7.1, Appendix F.11). Mean survival rates for near-ZID stations in 2024 ranged from 88 to 99%, while survival rates from regional stations ranged from 85 to 99%. One near ZID-station (E15) and one regional station (9525) were categorized as having low toxicity, while all other stations were categorized as nontoxic. Regional station 9525 was located in the midshelf in the PLOO region at 75m depth.

Regional Macrobenthic Communities

A total of 62,904 macrobenthic invertebrates were identified from the 178 grabs collected during summer 2024 and 2025 surveys at depths ranging from 8 to 453 m off San Diego. Of the 980 taxa recorded, 80% (n = 786) were identified to the level of species, while the rest could only be identified to higher taxonomic levels. Macrofaunal community structure varied across both the continental shelf and slope, with species richness ranging from 8 to 183 taxa per grab; macrofaunal abundance ranging from 28 to 1561 individuals per grab; Shannon Diversity Index (H') ranging from 1.2 to 4.5 per grab; Pielou's Evenness Index (J') ranging from 0.44 to 0.95 per grab; and Swartz Dominance Index ranging from 2 to

61 per grab (Table 7.2). Reported values for each parameter, and the variation observed between strata, generally correspond to findings reported previously for the San Diego region (e.g., City of San Diego 2020, 2022b). For example, species richness and abundance values were lowest at upper-slope stations. However, abundance values at SBOO mid-shelf station I34 exceeded expected ranges, possibly due to greater than normal amounts of small interstitial polychaetes (see Chapter 6). As has also been reported previously, BRI values off San Diego have generally been indicative of reference, or non-impacted conditions (BRI ≤ 25) (Smith et al. 2001). This remained true for the 2024 and 2025 summer surveys with 92% of samples collected from BRI-validated depths (n = 164) having BRI values indicative of reference condition (Appendix F.12). A total of 13 samples had slightly elevated BRI values > 25, which may indicate a minor deviation from reference condition. These samples were collected at one near-ZID PLOO station (E14), seven SBOO stations, and five regional stations located south of San Diego Bay. None of the stations sampled in summer 2024 or 2025 had BRI values > 34, which would indicate increasing levels of disturbance or environmental degradation.

Cluster and ordination analyses of the macrofaunal data, described above, resulted in eight ecologically-relevant SIMPROF-supported cluster groups (groups A–H) (Figures 7.9, 7.10). These macrofauna cluster groups comprised 1 to 95 grabs. The composition of each cluster group varied in terms of the specific taxa present and their relative abundance, as well as depth and sediment composition. For example, the macrofaunal assemblages represented by cluster groups A and G occurred along the outer shelf to upper slope at depths of 193–485 m, but differed from each other due to the presence or absence of key polychaete and bivalve taxa as well as differences in their ratio of fine particles to very fine sands (Figure 7.10, Appendices F.13, F.14). Macrofaunal assemblages associated with cluster group H, the largest group (n = 95), spanned a significant portion of the middle shelf, as well as a smaller portion of the outer shelf, off San Diego. Assemblages associated with cluster groups B, C, D, and E represented a total of four samples that occurred along the inner to midshelf at depths of 4–43 m.

Fine particles and four subfractions of sand (excluding very coarse sand) were most highly correlated with the macrofaunal communities (BEST/BIOENV $\rho = 0.374$, $p < 0.01$, number of permutations = 999). Of these subfractions, coarse sand accounted for most of the variation (corr. = 0.271). This marks a departure from previous results that tended to show fine particles as having the most influence over the distribution of infaunal communities. According to BEST/BVSTEP ($\rho = 0.95$, $p < 0.01$, number of permutations = 999), a total of 20 species best described the overall pattern (gradient) of the cluster dendrogram, including 13 polychaetes, 3 arthropod taxa, and one each from the molluscan, nemertean, cnidarian, and echinoderm phyla. The main characteristics and distribution of each cluster group are described below.

Macrofauna cluster group A represented a small group (4 grabs) of samples from the upper slope of the continental shelf, all at depths > 400m, during the summers of 2024 and 2025, with sediments comprising mostly fine particles and very fine sands (Figures 7.9, 7.10, Appendix F.13). According to SIMPER, group A assemblages were characterized by the polychaetes *Prionospio lobulata, Paraprionospio alata, Maldane sarsi,* and *Chone* sp SD3, along with the bivalve *Yoldiella nana* (Appendix F.14).

Macrofauna cluster groups B–E (n = 4) each represented a single sample along the inner and midshelf regions located south of the mouth of San Diego Bay (Figures 7.9, 7.10). These samples were distinguished from the other communities in the sampling region by the abundances of polychaetes or ostracods that were not found at similar levels in the other communities. For instance, cluster group B

was the only community to have high numbers of the polychaete *Prionospio pygmaeus* in conjunction with the ostracod *Euphilomedes carcharodonta*. (Appendix F.14). Sediments at these four groups also varied widely with groups B, C, and D having high proportions of medium and coarse sand (26.5-45.9% and 17.7-45.9%, respectively) while group E had the highest proportion of very fine sand (59.4%) of all groups (Appendix F.13).

Macrofauna cluster group F was the second largest group (n = 63), representing assemblages from most of the samples collected south of Point Loma at depths from 12 to 52m (Figures 7.9, 7.10). Two regional stations offshore of Mission Bay were also part of this group. Sediments associated with this cluster group were largely a mix of fine particles (mean = 19.4% per grab), very fine sand (mean = 30.3% per grab) and fine sand (mean = 17.0% per grab) (Appendix F.13). Group F averaged 72 taxa and 282 individuals per grab. The five most characteristic taxa for cluster group F were *Spiophanes norrisi* (mean = 5 per grab), *Edwardsia juliae* (mean = 3 per grab), *S. duplex* (mean = 2 per grab), *Ampharete labrops* (mean = 2 per grab), and *Spiochaetopterus costarum* Cmplx (mean = 1 per grab) (Appendix F.14).

Macrofauna cluster group G communities were encountered at the edge of the outer shelf and down the upper slope in depths from 193 to 357m (Figures 7.9, 7.10). Sediments at these stations contained the second highest proportion of fine particles and averaged less than 1% each of medium, coarse, and very coarse sand as well as almost zero larger granules (Appendix F.13). The most characteristic species of this cluster group were all polychaetes including *Phyllochaetopterus limicolus, Paraprionospio alata, Spiophanes kimballi, Maldane sarsi,* and *Mediomastus* sp. Group G was distinguished from Group H by lower numbers of *Spiophanes duplex* as well as having very few ophiuroids in the Amphiuridae family.

Macrofauna cluster group H comprised the largest number of samples (n = 95) in the area spanning mid-shelf depths of 35-198m (Figures 7.9, 7.10). These stations represented all of the core monitoring stations in the PLOO region, three of the deeper stations from the SBOO monitoring region, as well as 43 regional stations. The communities in this cluster group were most characterized by spionid, maldanid, and capitellid polychaetes, although amphiurid ophiuroids were also distinctive (Appendix F.14). Sediments in this group mostly comprised fine particles and very fine sand (mean = 48.8% and 30.6%, respectively), although larger grain sizes, such as coarse sand, were encountered in concentrations as high as 43.3% (Appendix F.13). This cluster group had the highest average number of taxa (mean = 104) and number of animals (mean = 442 individuals) per sample of all cluster groups.

Integrated Benthic Conditions Assessment

Overall, benthic community conditions were excellent off San Diego during the summers of 2024 and 2025. Sediment toxicity was absent (percent control ≥ 97%, condition ≥ 90% = nontoxic) at 14 of the 16 samples tested, while one sample in each year exhibited low toxicity (station E15, in the PLOO near ZID, and regional station 9525, located on the midshelf north of the PLOO) (Table 7.3). All of these samples had combined sediment chemistry concentrations indicative of minimal exposure, which is the lowest level of exposure measured by the California Logistic Regression Model Index (LRM) and the Chemical Score Index (CSI). BRI scores at each of the near-ZID stations, and at seven of the eight sample locations ranged from 13 to 24, indicative of reference stations (i.e., <25). One station, 9519, an inner-shelf station located off the coast of Coronado Island, had a BRI score of 27, which is considered low disturbance (Table 7.3). Thus, all BRI scores, when integrated with SQOs and sediment toxicity scores, resulted in 100% of the stations assessed in summer 2024 and 2025 deemed unimpacted.

Discussion

Benthic habitats and associated macrofaunal communities found on the continental shelf and upper slope off San Diego remained in good condition during the 2024–2025 reporting period. Overall, this regional assessment is consistent with the findings from the more extensive sampling of the core PLOO and SBOO stations reported in Chapter 5 for sediment quality and Chapter 6 for macrofaunal communities.

The physical composition of the sediments at the regional and core benthic stations, sampled during the summer 2024 and 2025, was typical for this portion of the southern California coast (Emery 1960), and is consistent with results of previous surveys off San Diego (e.g., City of San Diego 2018, 2020, 2022a,b). Overall, particle size composition varied as expected by outfall region and depth stratum. For example, stations sampled along the inner and midshelf within the SBOO monitoring area tended to be composed of medium and coarse sands, whereas stations sampled along the middle and outer shelf within the PLOO region were typically characterized by much finer sediments (see also Chapter 5). Much of the variability in particle size distributions off San Diego is likely related to the complexities of local seafloor geology, topography, and current patterns all of which can significantly affect sediment transport and deposition (Emery 1960, Patsch and Griggs 2007).

Sediment quality was excellent throughout the entire San Diego region in summer 2024–2025. There was no evidence of degraded benthic habitats, in terms of the chemical properties of the sediments, or spatial patterns in the distribution of the different types of contaminants, which may accumulate over time (e.g., organic indicators, trace metals). In addition, results of sediment toxicity testing in offshore San Diego waters revealed minimal toxicity at nearly all regional stations tested, with two stations incurring a result indicative of low toxicity. These results, when integrated with benthic infauna and sediment chemistry results, demonstrated that the shelf off San Diego remains unimpacted by the PLOO or SBOO.

Sediment contamination patterns during the current reporting period were also similar to those seen in previous years. Although, a number of indicators of organic loading, trace metals, pesticides, PCBs, PAHs, and PBDEs were detected in sediment samples throughout the San Diego region, almost all occurred at concentrations below critical ERL and ERM thresholds, similar to that observed in previous years (e.g., City of San Diego 2018, 2020, 2022a,b). Furthermore, examination of spatial patterns revealed no evidence of sediment contamination that could be attributed to local wastewater discharges via the PLOO or SBOO. Instead, concentrations of several trace metals were found to increase with increasing percent fines, and to a lesser degree, with increasing depth. Total nitrogen and total volatile solids also increased with increasing depth. This association is expected, due to the known correlation between sediment size and concentrations of organics and trace metals (Eganhouse and Venkatesan 1993). A cluster of PAH detections at regional and core monitoring stations sampled during this report period appear proximal to the LA-5 dredged materials disposal site (Figure 7.7). Finally, concentrations of these contaminants in San Diego waters remained relatively low compared to other coastal areas located off southern California (Schiff and Gossett 1998, Noblet et al. 2002, Schiff et al. 2006, 2011, Maruya and Schiff 2009, Dodder et al. 2016, Du et al 2020).

Macrofaunal communities in the San Diego region also appeared healthy in summer 2024–2025, with assemblages consistent with those observed during previous regional surveys conducted from 1994 to 2022 (City of San Diego 2010–2013, 2015b, 2016, 2018, 2020, 2022a,b). BRI results revealed little

evidence of disturbance off San Diego, with 92% of all calculated BRI values being indicative of reference condition. No samples showed evidence of moderate disturbance. Bight-wide, reference and low disturbance condition categories are indicative of "good condition" (e.g., Gillett et al. 2022). These results reflect assemblages characterized by expected abundances of pollution sensitive species, such as amphipods in the genera *Ampelisca* and *Rhepoxynius*, and low abundances of pollution tolerant species, such as the polychaete *Capitella capitata* Cmplx and the sulfur-oxidizing bivalve *Petrasma pervernicosa* (see also Chapter 6). Comparison of the results for other major benthic community metrics (e.g., species richness, macrofaunal abundance, diversity, evenness, and dominance) also showed no evidence of wastewater impact or significant habitat degradation during the 2024 and 2025 surveys. Furthermore, values for each of these community structure metrics remain within, or near, the range of tolerance intervals calculated for their specific habitats (see City of San Diego 2022a).

Most of the macrofaunal assemblages identified in summer 2024–2025 segregated by habitat characteristics such as depth and sediment particle size, often corresponding with the "patchy" habitats reported to occur naturally across the SCB (Fauchald and Jones 1979, Jones 1969, Bergen et al. 2000, Mikel et al. 2007). Several of the inner to mid-shelf assemblages described in this chapter were similar to those previously described in other shallow habitats across southern California (Barnard 1963, Jones 1969, Thompson et al. 1987, 1993a,b, MBC 1988, Mikel et al. 2007). These assemblages occurred in sandy sediments and were characterized by several species of polychaetes, including the spionids *Spiophanes norrisi* and *Spiophanes duplex*, and the capitellid *Mediomastus* sp. However, differences between these groups were probably driven by minor variations in sediment type (e.g., shell hash, relict red sand) or depth that differentially affected populations of the resident species. The middle to outer shelf strata off San Diego were described mainly by macrofauna cluster group H, which represented assemblages from 53% of all samples analyzed during the current reporting period. These assemblages occurred in sediments with close to 50% fines and large proportions of very fine and fine sand. Benthic communities dominated by polychaete worms such as *S. duplex* have long been common off Point Loma, and in similar seafloor habitats in other areas of southern California (Jones 1969, Fauchald and Jones 1979, Thompson et al. 1987, 1993a,b, Zmarzly et al. 1994, Diener and Fuller 1995, Bergen et al. 1998, 2000, 2001, Mikel et al. 2007, City of San Diego 2022a). The even finer sediments of upper slope stations sampled off San Diego in summer 2024–2025 were characterized by macrofaunal assemblages with much lower total abundances and fewer species than at most shelf stations. This pattern is similar to results reported previously for the region since regular monitoring of these deeper slope habitats began (e.g., City of San Diego 2010–2013, 2015b, 2016, 2018, 2020, 2022a,b).

Although benthic habitats and their associated macrofaunal communities continue to vary across depth and sediment gradients throughout the San Diego region, there was no evidence of disturbance or environmental degradation in 2024–2025 which may be attributed to anthropogenic factors, such as wastewater discharge via the PLOO or SBOO or other point sources. Macrobenthic communities appeared to be in good condition overall, with none of the sites surveyed showing evidence consistent with environmental disturbance. This result is similar to findings in Gillett et al. (2022) who reported that at least 98% of the entire SCB mainland shelf is in good condition, based on BRI data from bight-wide regional monitoring programs.

Literature Cited

Barnard, J.L. (1963). Relationship of benthic Amphipoda to invertebrate communities of inshore sublittoral sands of southern California. Pacific Naturalist, 3: 439–467.

Bay, S.M., D.J. Greenstein, J.A. Ranasinghe, D.W. Diehl, and A.E. Fetscher. (2013). Sediment Quality Assessment Technical Support Manual. Technical Report 777. Southern California Coastal Water Research Project. Costa Mesa, CA.

Bay S.M. and S.B. Weisberg. (2012). Framework for interpreting sediment quality triad data. Integrated Environ Assess Manag 8:589-596.

Bergen, M. (1996). The Southern California Bight Pilot Project: Sampling Design. In: M.J. Allen, C. Francisco, D. Hallock (Eds.). Southern California Coastal Water Research Project: Annual Report 1994–1995. Southern California Coastal Water Research Project, Westminster, CA.

Bergen, M., D.B. Cadien, A. Dalkey, D.E. Montagne, R.W. Smith, J.K. Stull, R.G. Velarde, and S.B. Weisberg. (2000). Assessment of benthic infaunal condition on the mainland shelf of southern California. Environmental Monitoring Assessment, 64: 421–434.

Bergen, M., S.B. Weisberg, D. Cadien, A. Dalkey, D. Montagne, R.W. Smith, J.K. Stull, and R.G. Velarde. (1998). Southern California Bight 1994 Pilot Project: IV. Benthic Infauna. Southern California Coastal Water Research Project, Westminster, CA.

Bergen, M., S.B. Weisberg, R.W. Smith, D.B. Cadien, A. Dalkey, D.E. Montagne, J.K. Stull, R.G. Velarde, and J.A. Ranasinghe. (2001). Relationship between depth, sediment, latitude, and the structure of benthic infaunal assemblages on the mainland shelf of southern California. Marine Biology, 138: 637–647.

[B13CIA] Bight '13 Contaminant Impact Assessment Planning Committee. (2017). Southern California Bight 2013 Regional Monitoring Program: Volume VIII. Contaminant Impact Assessment Synthesis Report. Technical Report 973. Southern California Coastal Water Research Project. Costa Mesa, CA.

Bight’23 Toxicology Committee. (2023). Bight’23 Toxicology Laboratory Manual. Southern California Bight 2023 Regional Monitoring Program. Southern California Coastal Water Research Project. Costa Mesa, CA.

City of San Diego. (2010–2013). Annual Receiving Waters Monitoring Report for the South Bay Ocean Outfall (South Bay Water Reclamation Plant), 2009-2012. City of San Diego Ocean Monitoring Program, Public Utilities Department, Environmental Monitoring and Technical Services Division, San Diego, CA.

City of San Diego. (2015a). Sediment Toxicity Monitoring Plan for the South Bay Ocean Outfall and Point Loma Ocean Outfall Monitoring Regions, San Diego, California. Submitted by the City of San Diego Public Utilities Department to the San Diego Water Board and USEPA, Region IX, August 28, 2015 [approved 9/29/2015].

City of San Diego. (2015b). South Bay Ocean Outfall Annual Receiving Waters Monitoring and Assessment Report, 2014. City of San Diego Ocean Monitoring Program, Public Utilities Department, Environmental Monitoring and Technical Services Division, San Diego, CA.

City of San Diego. (2016). South Bay Ocean Outfall Annual Receiving Waters Monitoring and Assessment Report, 2015. City of San Diego Ocean Monitoring Program, Public Utilities Department, Environmental Monitoring and Technical Services Division, San Diego, CA.

City of San Diego. (2018). Biennial Receiving Waters Monitoring and Assessment Report for the Point Loma and South Bay Ocean Outfalls, 2016–2017. City of San Diego, Public Utilities Department, Environmental Monitoring and Technical Services Division, San Diego, CA.

City of San Diego. (2020). Biennial Receiving Waters Monitoring and Assessment Report for the Point Loma and South Bay Ocean Outfalls, 2018–2019. City of San Diego, Public Utilities Department, Environmental Monitoring and Technical Services Division, San Diego, CA.

City of San Diego. (2022a). Appendix C. Ocean Benthic Conditions. In: Application for Renewal of NPDES CA0107409 and 301(h) Modified Secondary Treatment Requirements, Point Loma Ocean Outfall. Volume V, Appendix C. Public Utilities Department, Environmental Monitoring and Technical Services Division, San Diego, CA.

City of San Diego. (2022b). Biennial Receiving Waters Monitoring and Assessment Report for the Point Loma and South Bay Ocean Outfalls, 2020–2021. City of San Diego, Public Utilities Department, Environmental Monitoring and Technical Services Division, San Diego, CA.

City of San Diego. (2024). Biennial Receiving Waters Monitoring and Assessment Report for the Point Loma and South Bay Ocean Outfalls, 2022–2023. City of San Diego, Public Utilities Department, Environmental Monitoring and Technical Services Division, San Diego, CA.

City of San Diego. (2025). Interim Receiving Waters Monitoring Report for the Point Loma and South Bay Ocean Outfalls, 2024. City of San Diego, Public Utilities Department, Environmental Monitoring and Technical Services Division, San Diego, CA.

City of San Diego. (2026a). Ocean Monitoring Program Reports and Data. https://www.sandiego.gov/public-utilities/sustainability/ocean-monitoring/reports

City of San Diego. (2026b). Quality Assurance Manual for Toxicity Testing. City of San Diego Toxicology Laboratory, Environmental Monitoring and Technical Services Division, Public Utilities Department, San Diego, CA.

Clarke, K.R., R.N. Gorley, P.J. Somerfield, and R.M. Warwick. (2014). Change in marine communities: an approach to statistical analysis and interpretation, 3rd edition. PRIMER-E, Plymouth, England.

Clarke, K.R., P.J. Somerfield, and R.N. Gorley. (2008). Testing of null hypotheses in exploratory community analyses: similarity profiles and biota-environment linkage. Journal of Experimental Marine Biology and Ecology, 366: 56–69.

Conover, W.J. (1980). Practical Nonparametric Statistics, 2nd ed. John Wiley & Sons, Inc., New York, NY.

Diener, D.R. and S.C. Fuller. (1995). Infaunal patterns in the vicinity of a small coastal wastewater outfall and the lack of infaunal community response to secondary treatment. Bulletin of the Southern California Academy of Science, 94: 5–20.

Dodder, N., K. Schiff, A. Latker, and C-L Tang. (2016). Southern California Bight 2013 Regional Monitoring Program: IV. Sediment Chemistry. Southern California Coastal Water Research Project, Westminster, CA.

Du, B., C.S. Wong, K. Mclaughlin, and K. Schiff. (2020). Southern California Bight 2018 Regional Monitoring Program: II. Sediment Chemistry. Southern California Coastal Water Research Project, Westminster, CA.

Eganhouse, R.P. and M.I. Venkatesan. (1993). Chemical Oceanography and Geochemistry. In: M.D. Dailey, D.J. Reish, and J.W. Anderson (eds.). Ecology of the Southern California Bight: A Synthesis and Interpretation. University of California Press, Berkeley, CA. p 71–189.

Emery, K. O. (1960). The Sea Off Southern California. John Wiley, New York, NY.

Fauchald, K. and G.F. Jones. (1979). Variation in community structures on shelf, slope, and basin macrofaunal communities of the Southern California Bight. Report 19, Series 2. In: Southern California Outer Continental Shelf Environmental Baseline Study, 1976/1977 (Second Year) Benthic Program. Principal Investigators Reports, Vol. II. Science Applications, Inc. La Jolla, CA.

Ferraro, S.P., R.C. Swartz, F.A. Cole, and W.A. Deben. (1994). Optimum macrobenthic sampling protocol for detecting pollution impacts in the Southern California Bight. Environmental Monitoring and Assessment, 29: 127–153.

Folk, R.L. (1980). Petrology of Sedimentary Rocks. Hemphill, Austin, TX.

Gillett, D.J., W. Enright, J.B. Walker. 2022. Southern California Bight 2018 Regional Monitoring Program: Volume III. Benthic Infauna. Technical Report 1289. Southern California Coastal Water Research Project. Costa Mesa, CA.

Helsel, D.R. (2005a). More than obvious: better methods for interpreting nondetect data. Environmental Science & Technology (October 15, 2005), 419A-423A.

Helsel, D.R. (2005b). Nondetects and Data Analysis: Statistics for Censored Environmental Data. John Wiley, New York.

Helsel, D.R. (2006). Fabrication data: how substituting values for nondetects can ruin results, and what can be done about it. Chemosphere 65: 2434-2439.

Hope, R.M. (2022). Rmisc: Ryan Miscellaneous. R package version 1.5.1. http://CRAN.R-project.org/package=Rmisc.

Jones, G.F. (1969). The benthic macrofauna of the mainland shelf of southern California. Allan Hancock Monographs of Marine Biology, 4: 1–219.

Kassambara, A. (2023). ggpubr: Based Publication Ready Plots R package version 0.6.0. http://www.sthda.com/english/rpkgs/ggpubr.

Long, E.R., D.L. MacDonald, S.L. Smith, and F.D. Calder. (1995). Incidence of adverse biological effects within ranges of chemical concentration in marine and estuarine sediments. Environmental Management, 19(1): 81–97.

Maruya, K.A. and K. Schiff. (2009). The extent and magnitude of sediment contamination in the Southern California Bight. Geological Society of America Special Paper, 454: 399–412.

[MBC] MBC Applied Environmental Sciences and Engineering-Science. (1988). Part F: Biological studies. In: Tijuana Oceanographic Engineering Study, Volume 1. Ocean Measurement Program. Prepared for the City of San Diego, CA.

Mikel T.K., J.A Ranasinghe, and D.E. Montagne. (2007). Characteristics of benthic macrofauna of the Southern California Bight. Appendix F. Southern California Bight 2003 Regional Monitoring Program, SCCWRP, Costa Mesa, CA.

Noblet, J.A., E.Y. Zeng, R. Baird, R.W. Gossett, R.J. Ozretich, and C.R. Phillips. (2002). Southern California Bight 1998 Regional Monitoring Program: VI. Sediment Chemistry. Southern California Coastal Water Research Project, Westminster, CA.

Oksanen, J., F.G. Blanchet, R. Kindt, P. Legendre, P.R. Minchin, R.B. O'Hara, G.L. Simpson, P. Solymos, M.H.H. Stevens, and H. Wagner. (2022). vegan: Community Ecology Package. R package version 2.6-4. http://CRAN.R-project.org/package=vegan.

Patsch, K. and G. Griggs. (2007). Development of Sand Budgets for California's Major Littoral Cells. Institute of Marine Sciences, University of California, Santa Cruz, CA.

R Core Team. (2023). R: A language and environment for statistical computing. R Foundation for Statistical Computing, Vienna, Austria. URL https://www.R-project.org/.

Ranasinghe, J.A., A.M. Barnett, K. Schiff, D.E. Montagne, C. Brantley, C. Beegan, D.B. Cadien, C. Cash, G.B. Deets, D.R. Diener, T.K. Mikel, R.W. Smith, R.G. Velarde, S.D. Watts, and S.B. Weisberg. (2007). Southern California Bight 2003 Regional Monitoring Program: III. Benthic Macrofauna. Southern California Coastal Water Research Project. Costa Mesa, CA.

Ranasinghe, J.A., D. Montagne, R.W. Smith, T.K. Mikel, S.B. Weisberg, D. Cadien, R. Velarde, and A. Dalkey. (2003). Southern California Bight 1998 Regional Monitoring Program: VII. Benthic Macrofauna. Southern California Coastal Water Research Project. Westminster, CA.

Ranasinghe, J.A., K.C. Schiff, C.A. Brantley, L.L. Lovell, D.B. Cadien, T.K. Mikel, R.G. Velarde, S. Holt, and S.C. Johnson. (2012). Southern California Bight 2008 Regional Monitoring Program:

VI. Benthic Macrofauna. Technical Report No. 665, Southern California Coastal Water Research Project, Costa Mesa, CA.

Ranasinghe, J.A., K.C. Schiff, D.E. Montagne, T.K. Mikel, D.B. Cadien, R.G. Velarde, and C.A. Brantley. (2010). Benthic macrofaunal community condition in the Southern California Bight, 1994–2003. Marine Pollution Bulletin, 60: 827–833.

Revelle, W. (2023) psych: Procedures for Personality and Psychological Research, Northwestern University, Evanston, Illinois, USA, https://CRAN.R-project.org/package=psych Version = 2.3.6.

Ripley, B. and M. Lapsley. (2022). RODBC: ODBC Database Access. R package version 1.3-20. http://CRAN.R-project.org/package=RODBC.

[SCAMIT] Southern California Association of Marine Invertebrate Taxonomists. (2023). A taxonomic listing of benthic macro- and megainvertebrates from infaunal and epibenthic monitoring programs in the Southern California Bight, Edition 14. Southern California Association of Marine Invertebrate Taxonomists, Natural History Museum of Los Angeles County Research and Collections, Los Angeles, CA.

[SCCWRP] Southern California Coastal Water Research Project. (2018). Southern California Bight 2018 Regional Monitoring Program: Contaminant Impact Assessment Field Operations Manual. Southern California Coastal Water Research Project. Costa Mesa, CA.

Schiff, K.C. and R.W. Gossett. (1998). Southern California Bight 1994 Pilot Project: III. Sediment Chemistry. Southern California Coastal Water Research Project. Westminster, CA.

Schiff, K., R. Gossett, K. Ritter, L. Tiefenthaler, N. Dodder, W. Lao, and K. Maruya. (2011). Southern California Bight 2008 Regional Monitoring Program: III. Sediment Chemistry. Southern California Coastal Water Research Project, Costa Mesa, CA.

Schiff, K., K. Maruya, and K. Christenson. (2006). Southern California Bight 2003 Regional Monitoring Program: II. Sediment Chemistry. Southern California Coastal Water Research Project, Westminster, CA.

Smith, R.W., M. Bergen, S.B. Weisberg, D. Cadien, A. Dalkey, D. Montagne, J.K. Stull, and R.G. Velarde. (2001). Benthic response index for assessing infaunal communities on the southern California mainland shelf. Ecological Applications, 11(4): 1073–1087.

[SWRCB] State Water Resource Control Board. (2009). Water Quality Control Plan for Enclosed Bays and Estuaries – Part 1 Sediment Quality. Resolution Number 2008-0070, State Water Resources Control Board, Sacramento, CA.

Stebbins, T.D., K.C. Schiff, and K. Ritter. (2004). San Diego Sediment Mapping Study: Workplan for Generating Scientifically Defensible Maps of Sediment Conditions in the San Diego Region. City of San Diego, Metropolitan Wastewater Department, Environmental Monitoring and Technical Services Division, and Southern California Coastal Water Research Project, Westminster, CA.

Stevens Jr., D.L. (1997). Variable density grid-based sampling designs for continuous spatial populations. Environmetrics, 8: 167–195.

Stevens Jr., D.L. and A.R. Olsen. (2004). Spatially-balanced sampling of natural resources in the presence of frame imperfections. Journal of the American Statistical Association, 99: 262–278.

Swartz, R.C., F.A. Cole, and W.A. Deben. (1986). Ecological changes in the Southern California Bight near a large sewage outfall: benthic conditions in 1980 and 1983. Marine Ecology Progress Series, 31: 1–13.

Thompson, B.E., J.D. Laughlin, and D.T. Tsukada. (1987). 1985 reference site survey. Technical Report No. 221, Southern California Coastal Water Research Project, Long Beach, CA.

Thompson, B., J. Dixon, S. Schroeter, and D.J. Reish. (1993a). Chapter 8. Benthic invertebrates. In: M.D. Dailey, D.J. Reish, and J.W. Anderson (eds.). Ecology of the Southern California Bight: A Synthesis and Interpretation. University of California Press, Berkeley, CA.

Thompson, B.E., D. Tsukada, and D. O'Donohue. (1993b). 1990 reference site survey. Technical Report No. 269, Southern California Coastal Water Research Project, Long Beach, CA.

[USEPA] United States Environmental Protection Agency. (1987). Quality Assurance and Quality Control (QA/QC) for 301(h) Monitoring Programs: Guidance on Field and Laboratory Methods. EPA Document 430/9-86-004. Office of Marine and Estuarine Protection.

[USEPA] United States Environmental Protection Agency. (1994). Methods for assessing the toxicity of sediment-associated contaminants with estuarine and marine amphipods. EPA/600/R-94/025. Office of Research and Development, UEPA. Narragansett, RI.

Wickham, H. (2007). Reshaping Data with the reshape Package. Journal of Statistical Software, 21(12), 1-20. URL http://www.jstatsoft.org/v21/i12/.

Wickham, H. (2011). The Split-Apply-Combine Strategy for Data Analysis. Journal of Statistical Software, 40(1), 1-29. URL http://www.jstatsoft.org/v40/i01/.

Wickham, H. (2016). Ggplot2: Elegant Graphics for Data Analysis. Springer-Verlag, New York.

Wickham, H., M. Averick, J. Bryan, W. Chang, L. D'Agostino McGowan, R. François, G.Grolemund, A. Hayes, L. Henry, J. Hester, M. Kuhn, T. Lin Pedersen, E. Miller, S. Milton Bache, K. Müller, J. Ooms, D. Robinson, D. P. Seidel, V. Spinu, K. Takahashi, D. Vaughan, C. Wilke, K. Woo, H. Yutani. (2019). Welcome to the tidyverse. Journal of Open Source Software, 4(43), 1686, https://doi.org/10.21105/joss.01686.

Wickham, H. (2022). stringr: Simple, Consistent Wrappers for Common String Operations. R package version 1.5.0. https://CRAN.R-project.org/package=stringr.

Wickham, H. and D. Seidel. (2022). Scales: Scale Functions for Visualization Rstudio. R package version 1.2.1. https://scales.r-lib.org/.

Wickham, H. D. Vaughan, and M. Girlich. (2023a). tidyr: Easily Tidy Data with 'spread()' and 'gather()' Functions. R package version 1.3.0. https://CRAN.R-project.org/package=tidyr.

Wickham, H., R. Francois, L. Henry, K. Müller, and D. Vaughan. (2023b). dplyr: A Grammar of Data Manipulation. R package version 1.1.2. https://CRAN.R-project.org/package=dplyr.

Wong, C., Schiff, K., and R. Butler. (in review). Southern California Bight 2023 Regional Monitoring Program: Volume II. Sediment Chemistry. Technical Report No. 1469, Southern California Coastal Water Research Project, Long Beach, CA.

Zeileis, A and G. Grothendieck. (2005). zoo: S3 Infrastructure for Regular and Irregular Time Series. Journal of Statistical Software, 14(6), 1-27. URL http://www.jstatsoft.org/v14/i06/.

Zmarzly, D.L., T.D. Stebbins, D. Pasko, R.M. Duggan, and K.L. Barwick. (1994). Spatial patterns and temporal succession in soft-bottom macroinvertebrate assemblages surrounding an ocean outfall on the southern San Diego shelf: Relation to anthropogenic and natural events. Marine Biology, 118: 293–307.

CHAPTER 7

FIGURES & TABLES

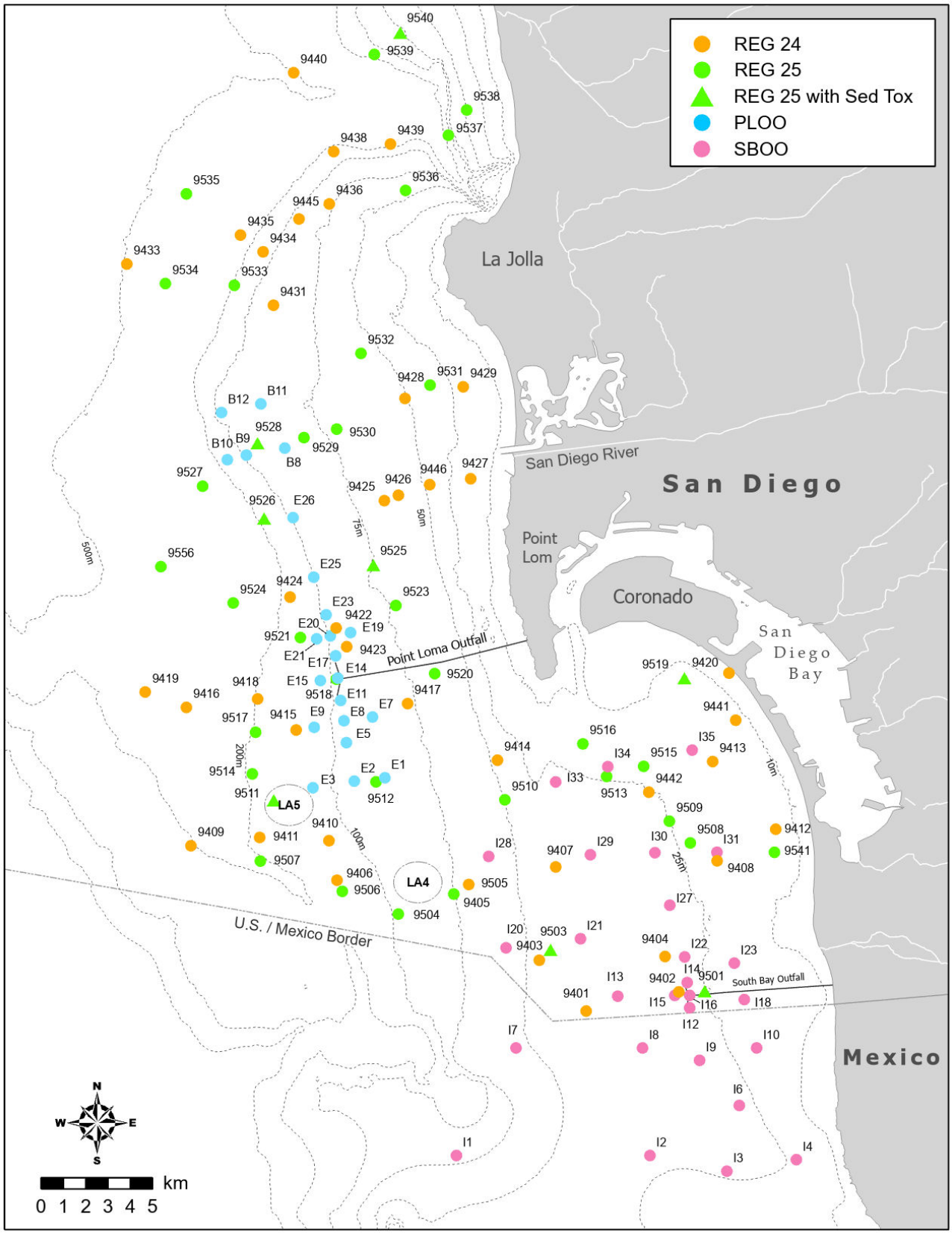


Figure 7.1
Distribution of 80 regional and 49 core (PLOO/SBOO) benthic stations sampled off San Diego and northern Baja California during summer 2024 and 2025.

Table 7.1

Summary of particle sizes and chemistry concentrations in sediments from San Diego regional (Reg) and core benthic stations sampled during summer 2024 and 2025. Data include detection rate (DR; %), minimum, maximum, and mean values for the entire survey area, as well as mean value by depth stratum. For chemistry parameters, minimum and maximum values were calculated using all samples, whereas means were calculated with detected values only; n = number of samples; nd = not detected.

					Depth Strata						
					Inner Shelf		Middle Shelf			Outer Shelf	Upper Slope
	2024–2025 Survey Area				SBOO	Reg	PLOO	SBOO	Reg	Reg	Reg
Parameter	DR	Min	Max	Mean	n=17	n=16	n=22	n=10	n=34	n=17	n=13
Particle Size (%)											
Coarse particles	30	0.0	28.1	1.9	4.1	0.2	1.5	6.4	2.1	2.5	0.0
Med-coarse sands	96	0.0	91.8	16.4	28.9	7.0	5.3	51.6	15.9	7.6	0.2
Fine sands	100	0.8	90.1	42.1	48.8	69.7	43.2	22.4	36.7	37.0	26.5
Fine particles	97	0.0	88.6	39.6	18.4	23.1	50.0	19.6	45.4	52.9	73.3
Organic Indicators											
Sulfides (ppm)	67	nd	121.0	15.8	7.0	13.8	12.0	7.7	16.2	15.5	43.3
TN (% weight)	78	nd	0.28	0.07	0.03	0.03	0.06	0.04	0.06	0.08	0.17
TOC (% weight)	72	nd	3.35	0.78	0.43	0.23	0.70	0.33	0.51	1.05	2.13
TVS (% weight)	100	0.4	9.5	2.1	0.9	0.9	2.2	0.8	2.1	3.4	6.6
Trace Metals (ppm)											
Aluminum	100	874	20600	6340	3884	4154	6926	2401	7016	9323	14469
Antimony	90	nd	1.75	0.55	0.33	0.32	0.54	0.38	0.57	0.72	1.05
Arsenic	100	0.74	10.30	2.65	1.80	1.66	2.79	3.45	3.16	2.78	3.68
Barium	100	1.4	123.0	28.8	19.1	20.7	27.9	8.2	32.7	41.6	71.6
Beryllium	100	0.022	0.459	0.140	0.071	0.072	0.165	0.065	0.152	0.220	0.325
Cadmium	92	nd	0.531	0.088	0.033	0.037	0.073	0.036	0.088	0.157	0.300
Chromium	100	3.7	39.7	13.4	8.1	7.9	14.4	8.3	14.4	18.6	29.9
Copper	100	0.3	22.3	5.5	2.2	2.3	6.2	1.4	5.7	10.5	16.0
Iron	100	1170	22800	8513	4756	4994	10147	5030	9499	12312	16331
Lead	100	0.7	62.0	2.9	1.4	1.6	2.9	1.8	4.8	4.0	4.8
Manganese	100	7	364	72	50	60	76	28	83	105	132
Mercury	82	nd	0.143	0.030	0.008	0.012	0.031	0.011	0.031	0.053	0.066
Nickel	100	0.6	21.5	5.0	2.1	2.1	5.5	1.8	5.4	7.9	14.9
Selenium	57	nd	1.65	0.46	0.29	0.25	0.38	0.31	0.40	0.52	0.98
Silver	0	—	—	—	—	—	—	—	—	—	—
Tin	100	0.05	3.02	0.63	0.37	0.40	0.70	0.24	0.76	0.90	1.23
Zinc	100	1.8	63.9	20.9	11.0	12.6	24.1	7.9	23.7	31.3	47.5

Table 7.1 *Continued*

					Depth Strata						
					Inner Shelf		Middle Shelf			Outer Shelf	Upper Slope
	2024–2025 Survey Area				SBOO	Reg	PLOO	SBOO	Reg	Reg	Reg
Parameter	**DR**	**Min**	**Max**	**Mean**	**n=17**	**n=16**	**n=22**	**n=10**	**n=34**	**n=17**	**n=13**
Pesticides (ppt)											
Total DDT	65	nd	70973	1229	123	230	440	474	2738	446	1752
Total HCH	0	—	—	—	—	—	—	—	—	—	—
Total Chlordane	0	—	—	—	341	—	94	—	—	—	—
Hexachlorobenzene	3	nd	389	251	—	—	277	—	—	122	—
Mirex	0	—	—	—	—	—	—	—	—	—	—
Total PCB (ppt)	20	nd	91340	3798	—	—	2860	380	650	13078	704
Total PAH (ppb)	16	nd	54741.1	2012.6	10.7	39.2	48.7	—	13693.3	417.4	49.0
Total PBDE (ppt)	13	nd	558.7	182.6	194.1	458.7	—	75.6	142.9	85.1	291.9

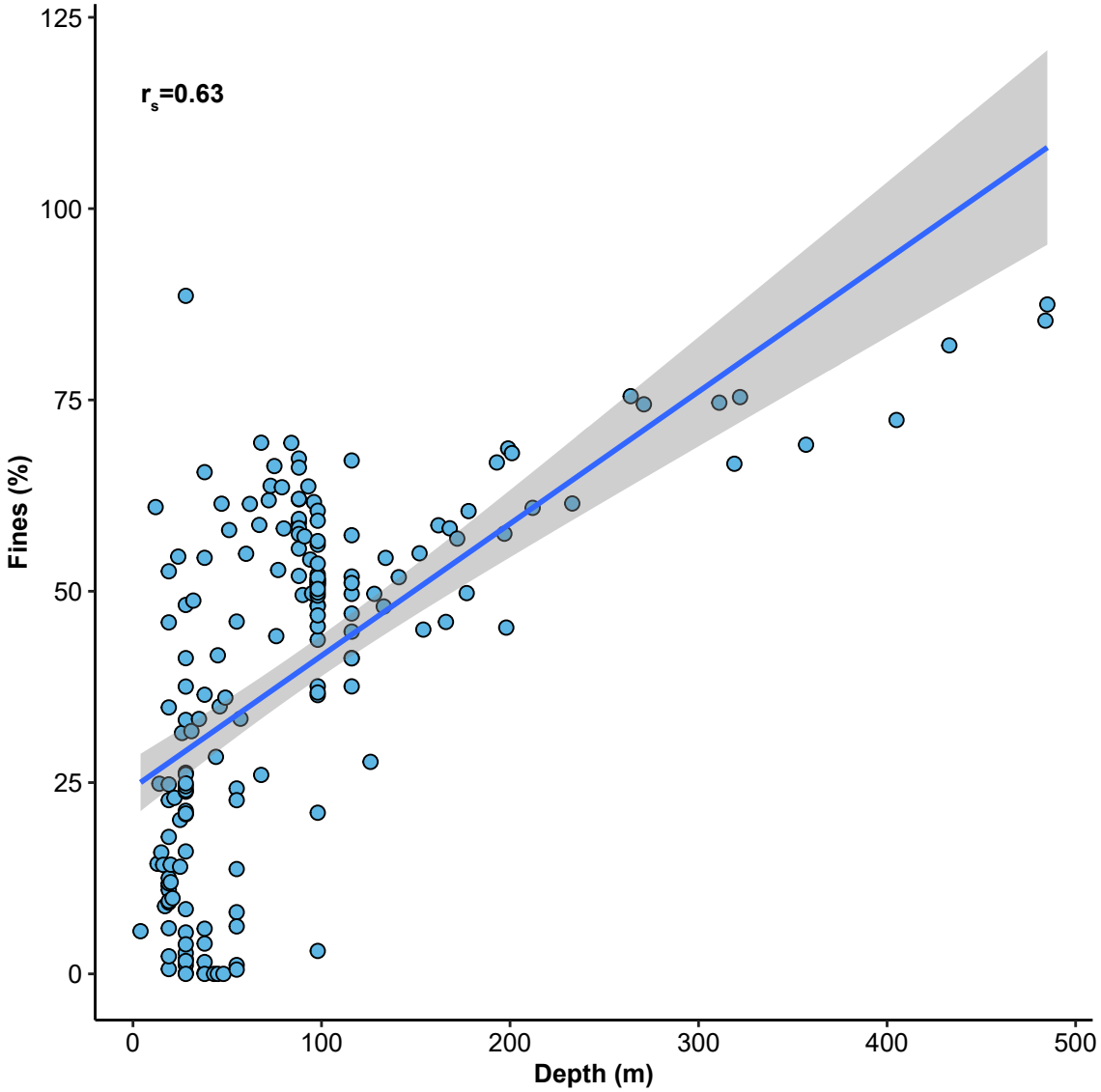


Figure 7.2

Scatterplot of concentrations of fine particles (Fines) versus depth for sediments collected from San Diego regional and core benthic stations during summer 2024 and 2025. Shaded area indicates 95% confidence interval.

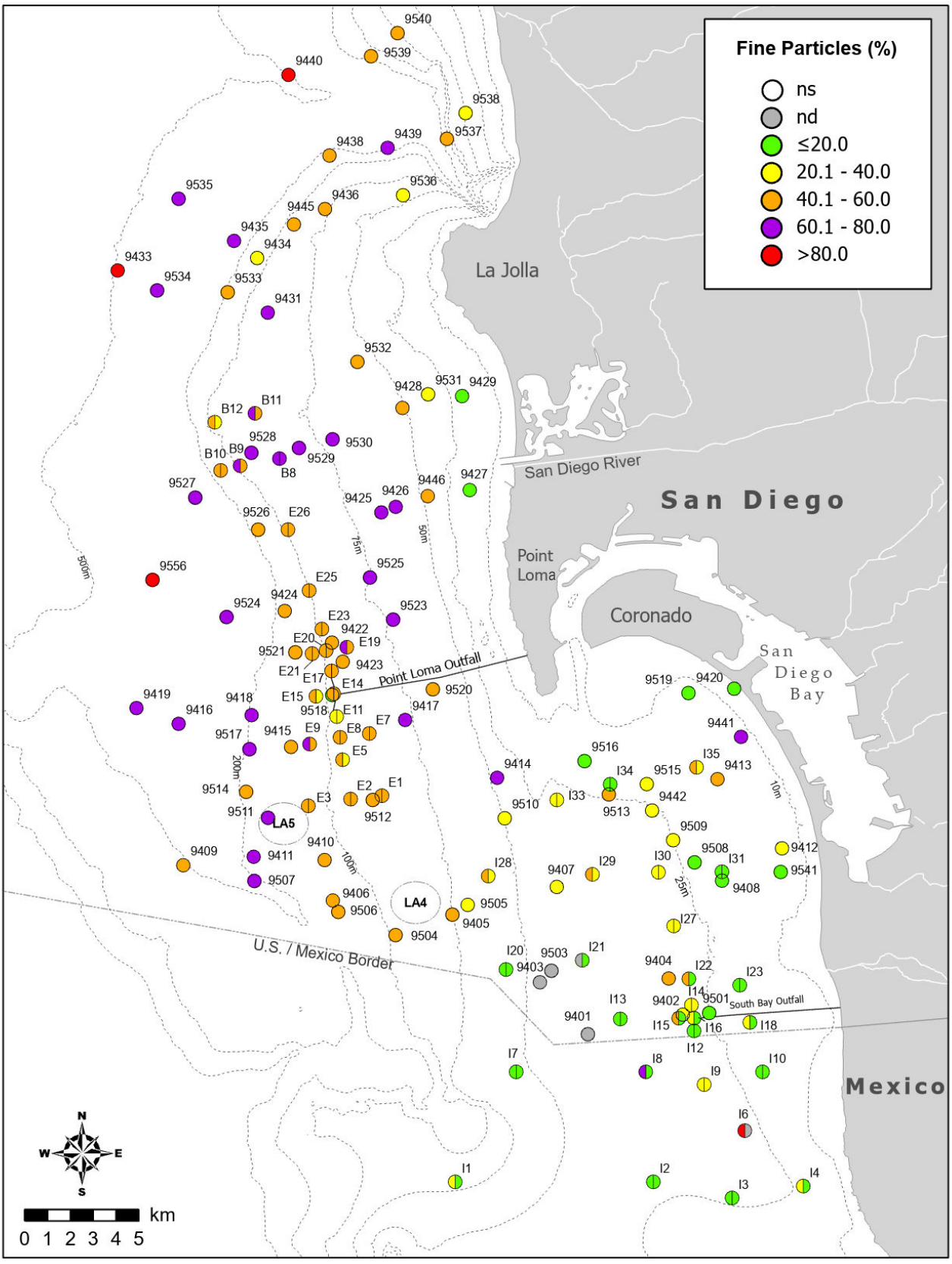


Figure 7.3
Distribution of fine particles in sediments from San Diego regional and core benthic stations sampled during summer 2024 and 2025; ns = not sampled.

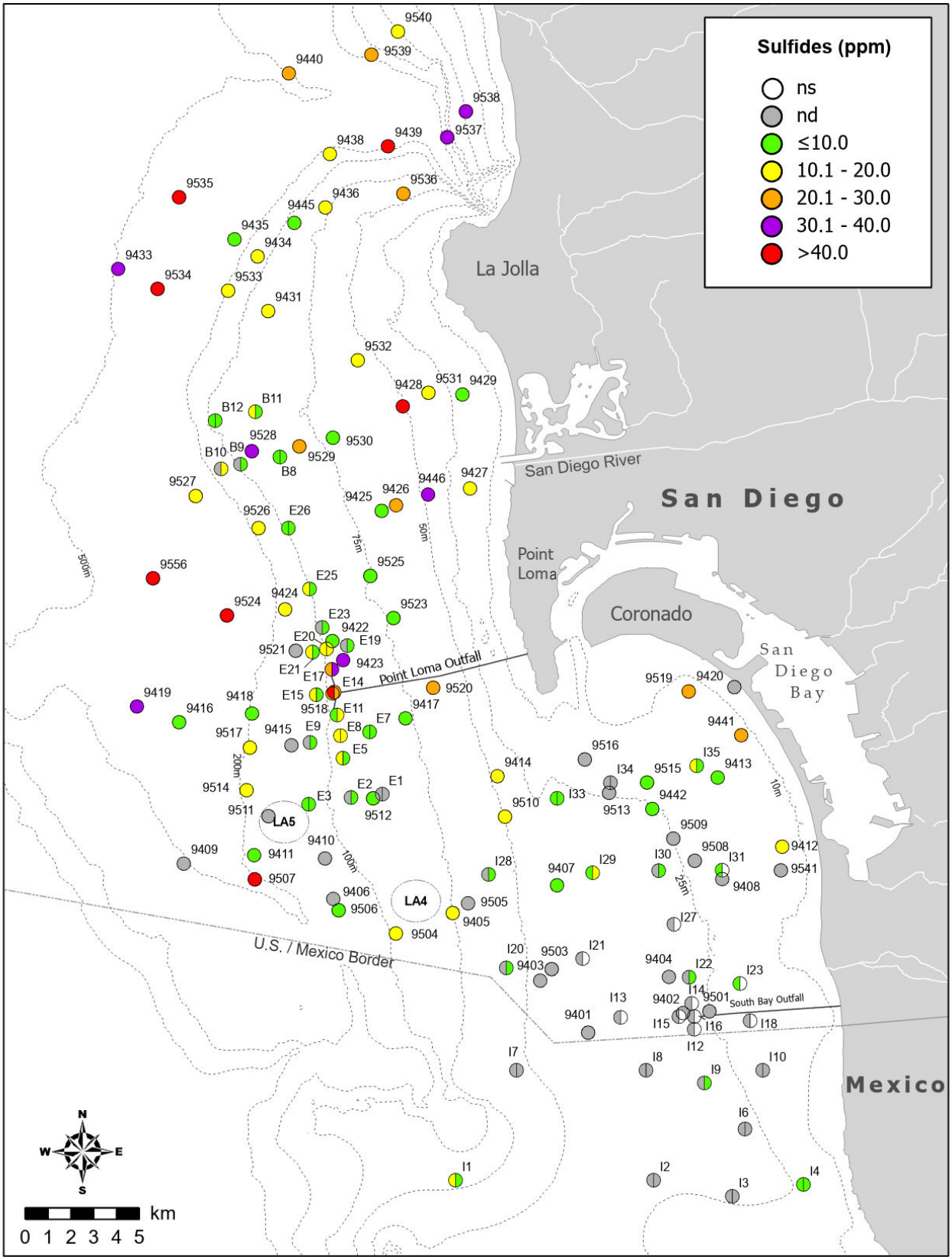


Figure 7.4
Distribution of organic loading indicators in sediments from San Diego regional and core benthic stations sampled during summer 2024 and 2025; ns = not sampled (or not reportable, see text); nd = not detected.

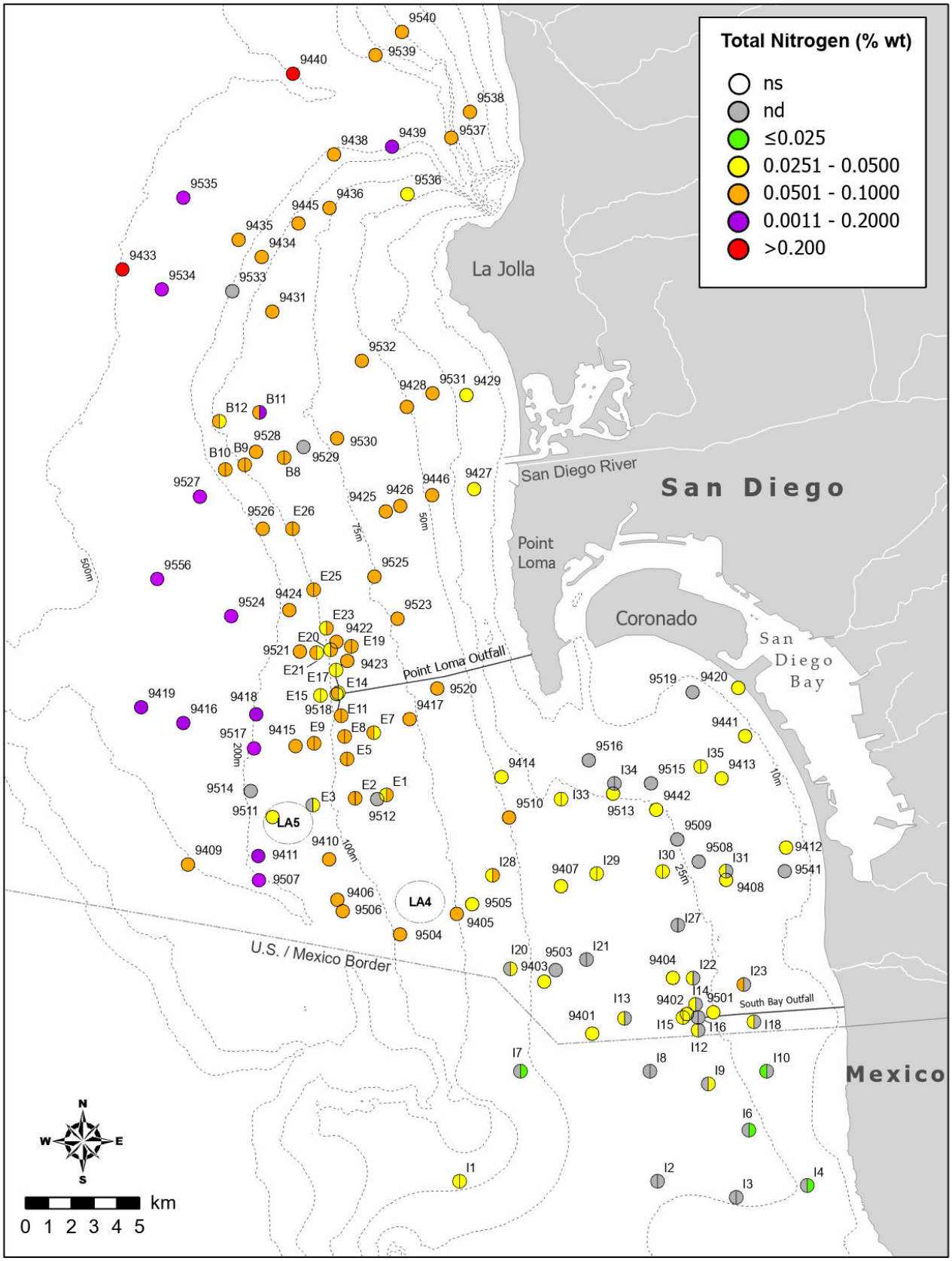


Figure 7.4 *continued*

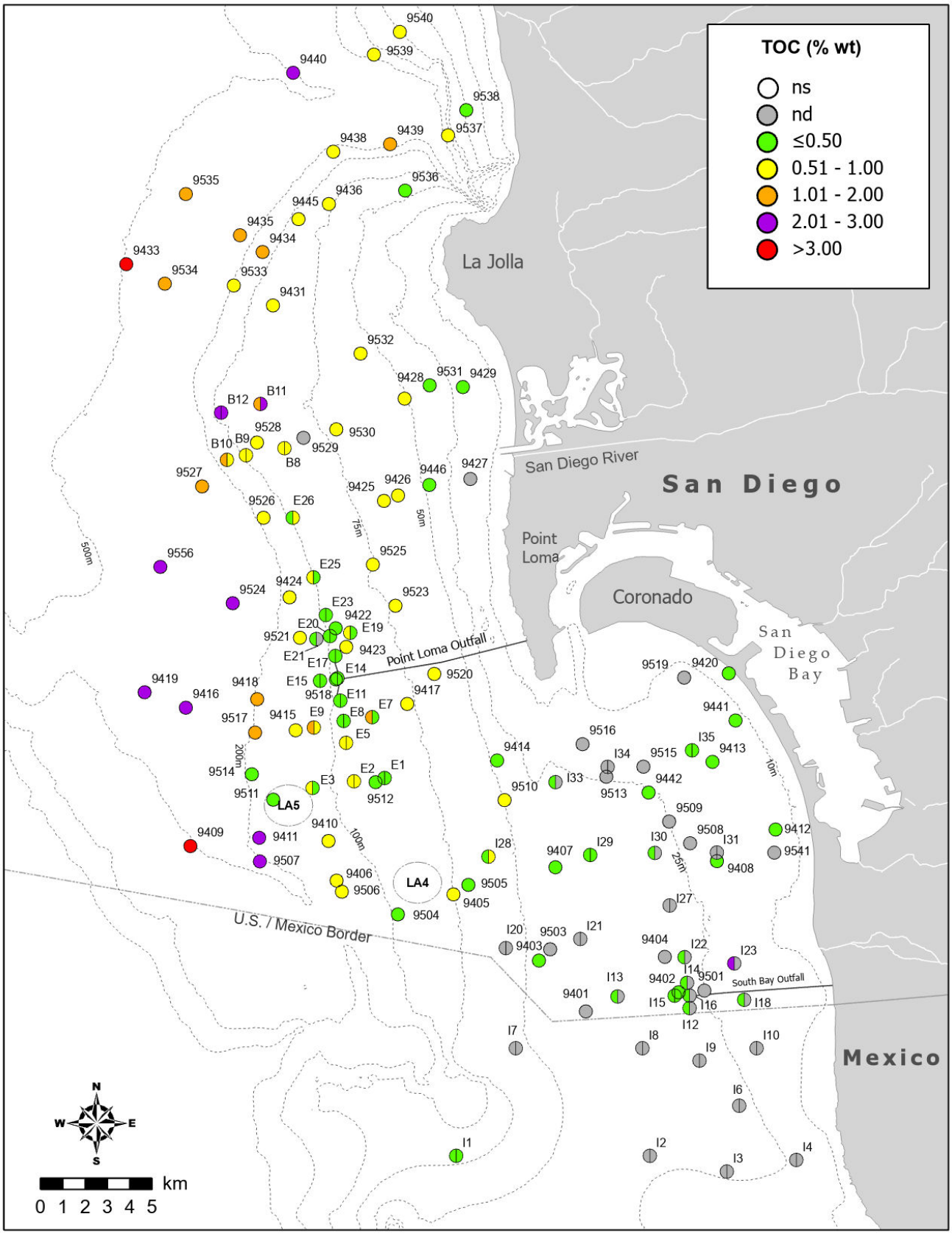


Figure 7.4 *continued*

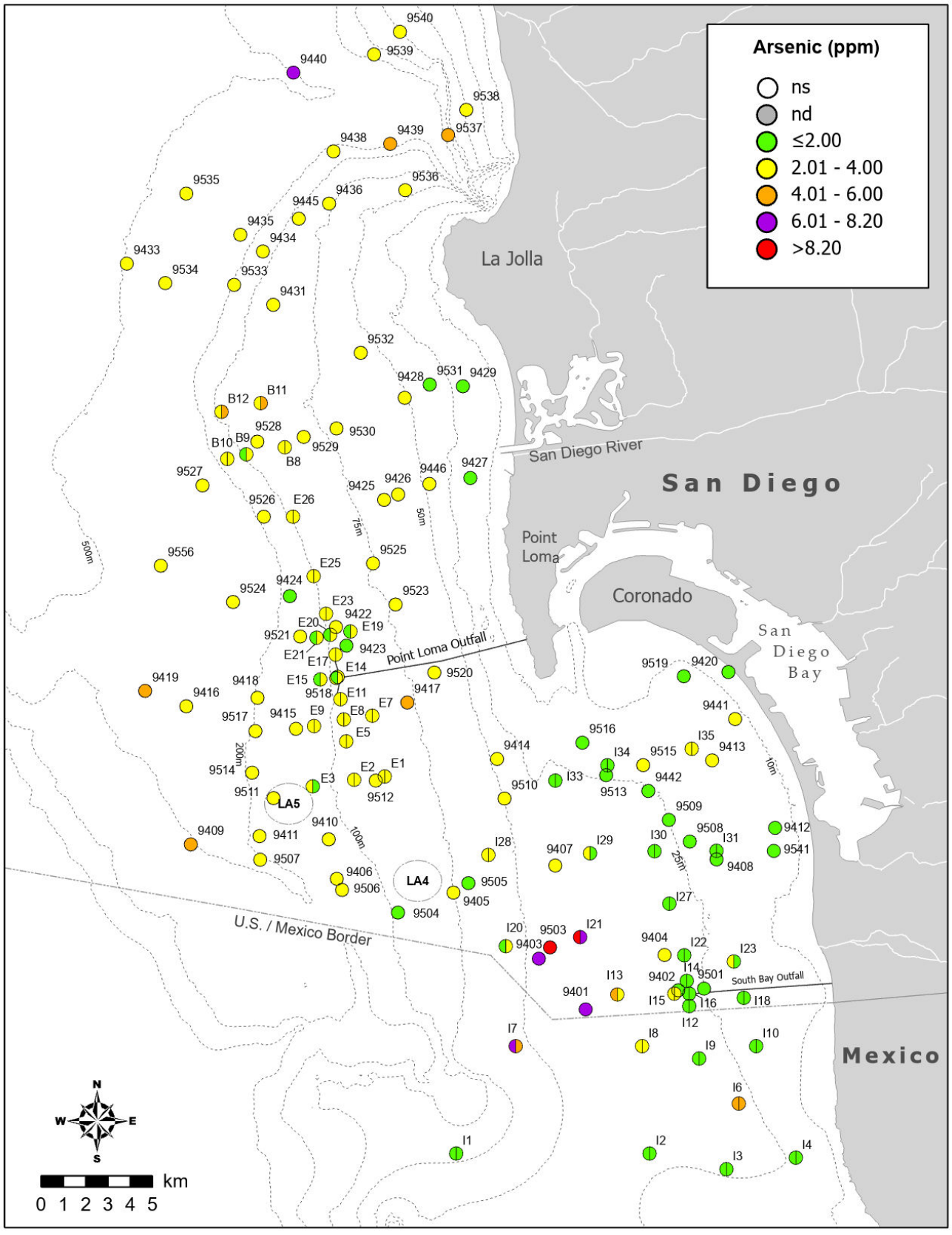


Figure 7.5
Distribution of select metals in sediments from San Diego regional and core benthic stations sampled during summer 2024 and 2025; ns = not sampled (or not reportable, see text); nd = not detected.

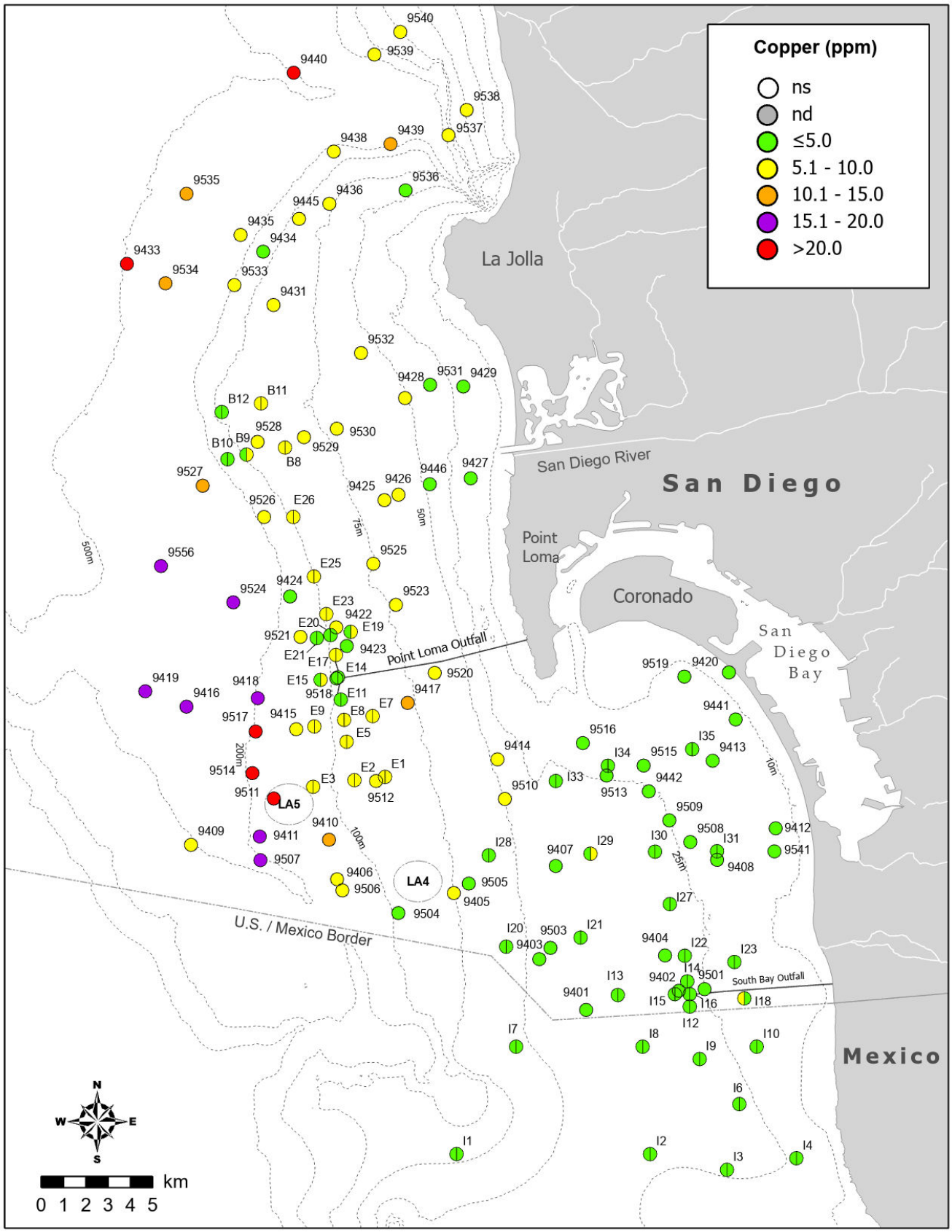


Figure 7.5 *continued*

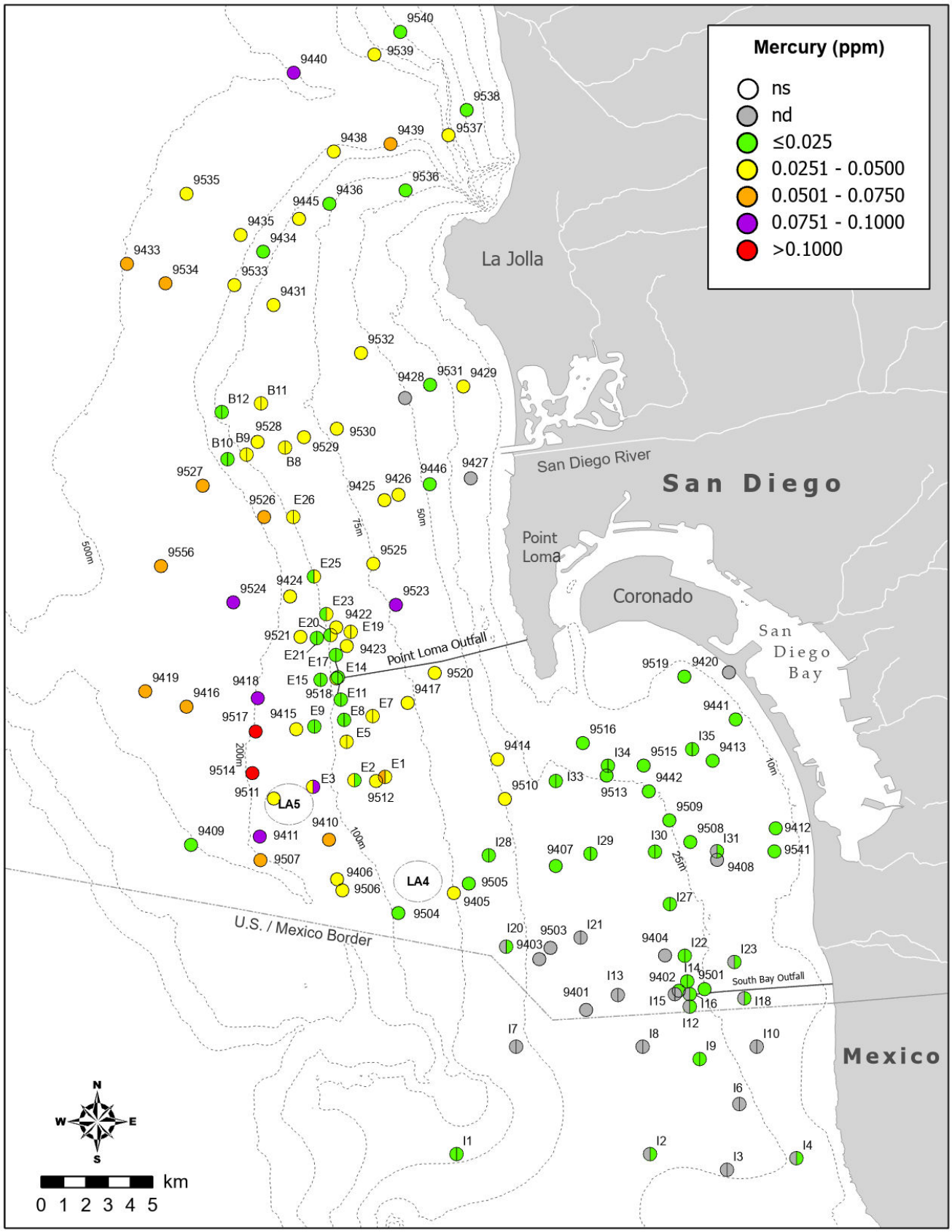


Figure 7.5 *continued*

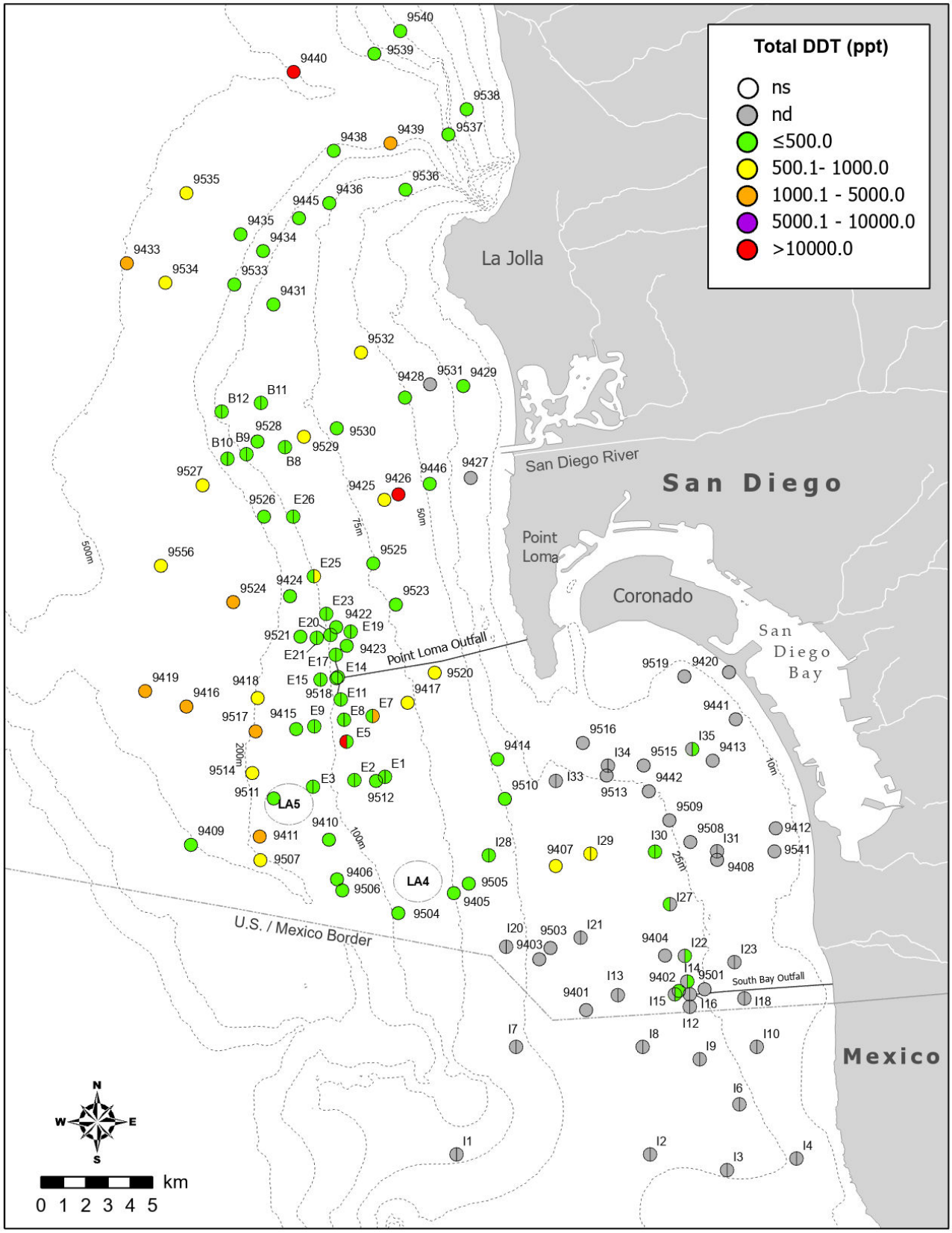


Figure 7.6
Distribution of total DDT in sediments from San Diego regional and core benthic stations sampled during summer 2024 and 2025; ns = not sampled (or not reportable, see text); nd = not detected.

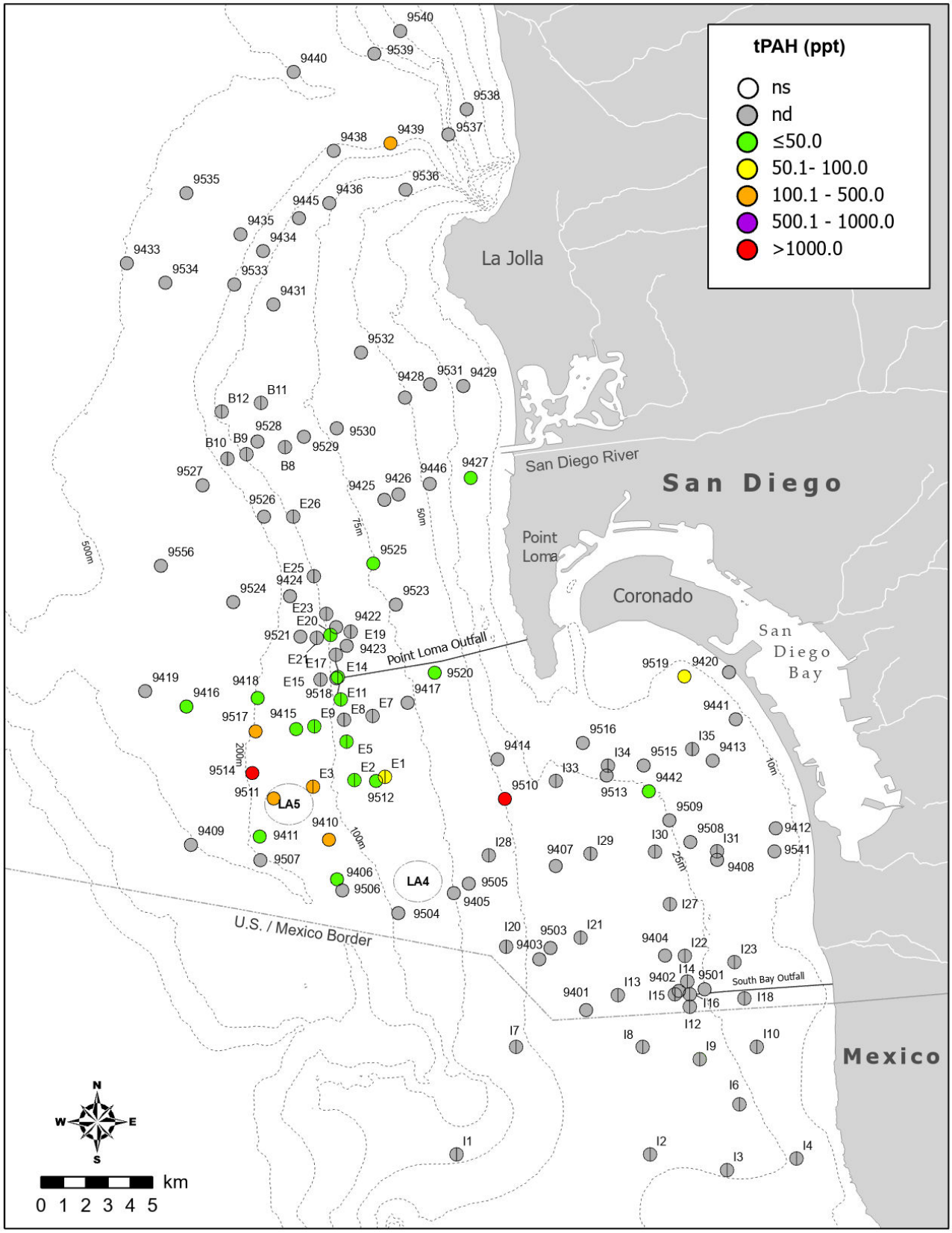


Figure 7.7
Distribution of total PAHs in sediments from San Diego regional and core benthic stations sampled during summer 2024 and 2025; ns = not sampled (or not reportable, see text); nd = not detected.

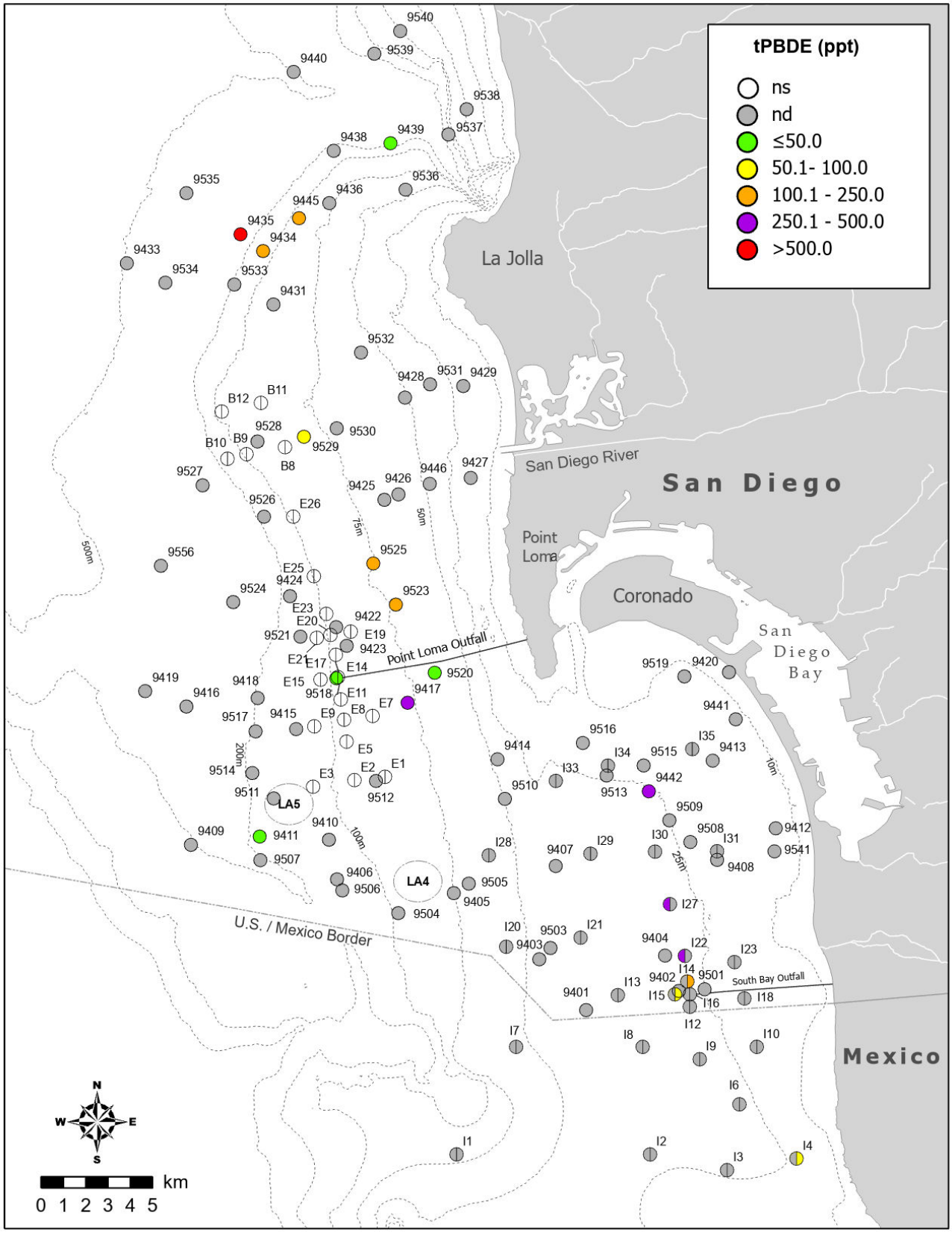


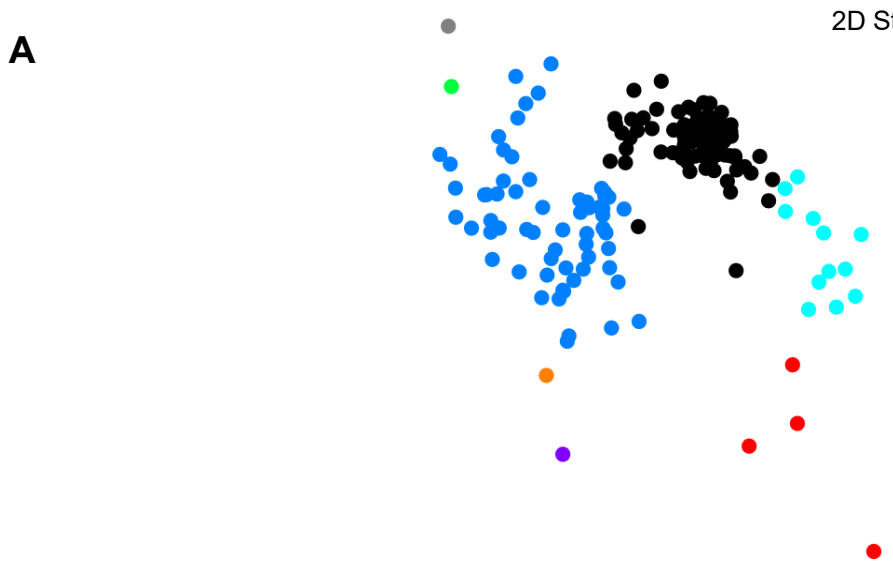
Figure 7.8
Distribution of total PBDEs in sediments from San Diego regional and core benthic stations sampled during summer 2024 and 2025; ns = not sampled (or not reportable, see text); nd = not detected.

Table 7.2

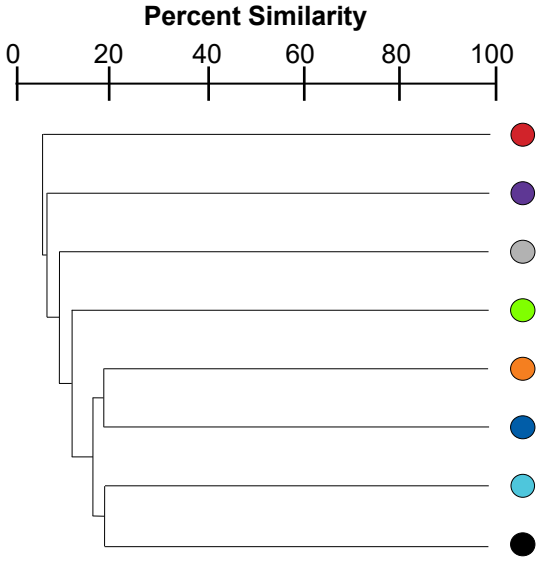
Macrofaunal community summary statistics calculated for San Diego regional and core benthic stations sampled during summer 2024 and 2025. Data are presented as means (ranges) by stratum; n = number of grabs; SR = species richness; Abun = abundance; H' = Shannon diversity index; J' = Pielou's evenness; Dom = Swartz dominance; BRI = benthic response index. See Appendices G.1, G.2, and H.15 for individual sample values.

Stratum		n	SR	Abun	H'	J'	Dom	BRI[a]
Inner Shelf	SBOO	34	74 (37-137)	290 (81-623)	3.5 (2.3-4.4)	0.83 (0.61-0.93)	25 (7-50)	22 (14-30)
	Regional	16	63 (14-109)	235 (84-616)	3.4 (1.2-4.3)	0.83 (0.44-0.93)	22 (2-46)	23 (16-33)
	All Inner Shelf	50	70 (14-137)	272 (81-623)	3.5 (1.2-4.4)	0.83 (0.44-0.93)	24 (2-50)	22 (14-33)
Middle Shelf	PLOO	44	101 (71-145)	407 (215-879)	3.9 (3.5-4.5)	0.85 (0.75-0.92)	33 (19-60)	13 (5-26)
	SBOO	20	90 (38-183)	441 (158-1561)	3.5 (2.8-4.3)	0.8 (0.67-0.90)	25 (11-51)	19 (12-27)
	Regional	34	108 (36-170)	453 (69-1086)	4 (3.1-4.4)	0.85 (0.74-0.94)	34 (13-61)	16 (9-27)
	All Middle Shelf	98	101 (36-183)	430 (69-1561)	3.9 (2.8-4.5)	0.84 (0.67-0.94)	32 (11-61)	15 (5-27)
Outer Shelf	Regional	17	76 (36-128)	326 (137-588)	3.4 (1.7-4.4)	0.79 (0.47-0.90)	22 (3-46)	15 (8-22)
Upper Slope	Regional	13	31 (8-58)	126 (28-274)	2.5 (1.4-3.1)	0.76 (0.45-0.95)	10 (2-18)	—
	All Stations	178	85 (8-183)	353 (28-1561)	3.6 (1.2-4.5)	0.83 (0.44-0.95)	27 (2-61)	17 (5-33)

[a]BRI statistic not calculated for stations located at depths < 10 m or > 200 m



B



Cluster Group	n	Depth Range (m)	Community Metric SR	Community Metric Abun
A	4	405-485	21	52
B	1	4	14	134
C	1	21	68	335
D	1	43	36	69
E	1	14	47	91
F	63	12-52	72	282
G	12	193-357	40	196
H	95	35-198	104	442

Figure 7.9

Results of ordination and cluster analysis of macrofauna data from San Diego regional and core benthic stations sampled during summer 2024 and 2025. Results are presented as (A) nMDS ordination and (B) a dendrogram of main cluster groups. Data are mean values over all stations in each group (n); SR = species richness; Abun = abundance.

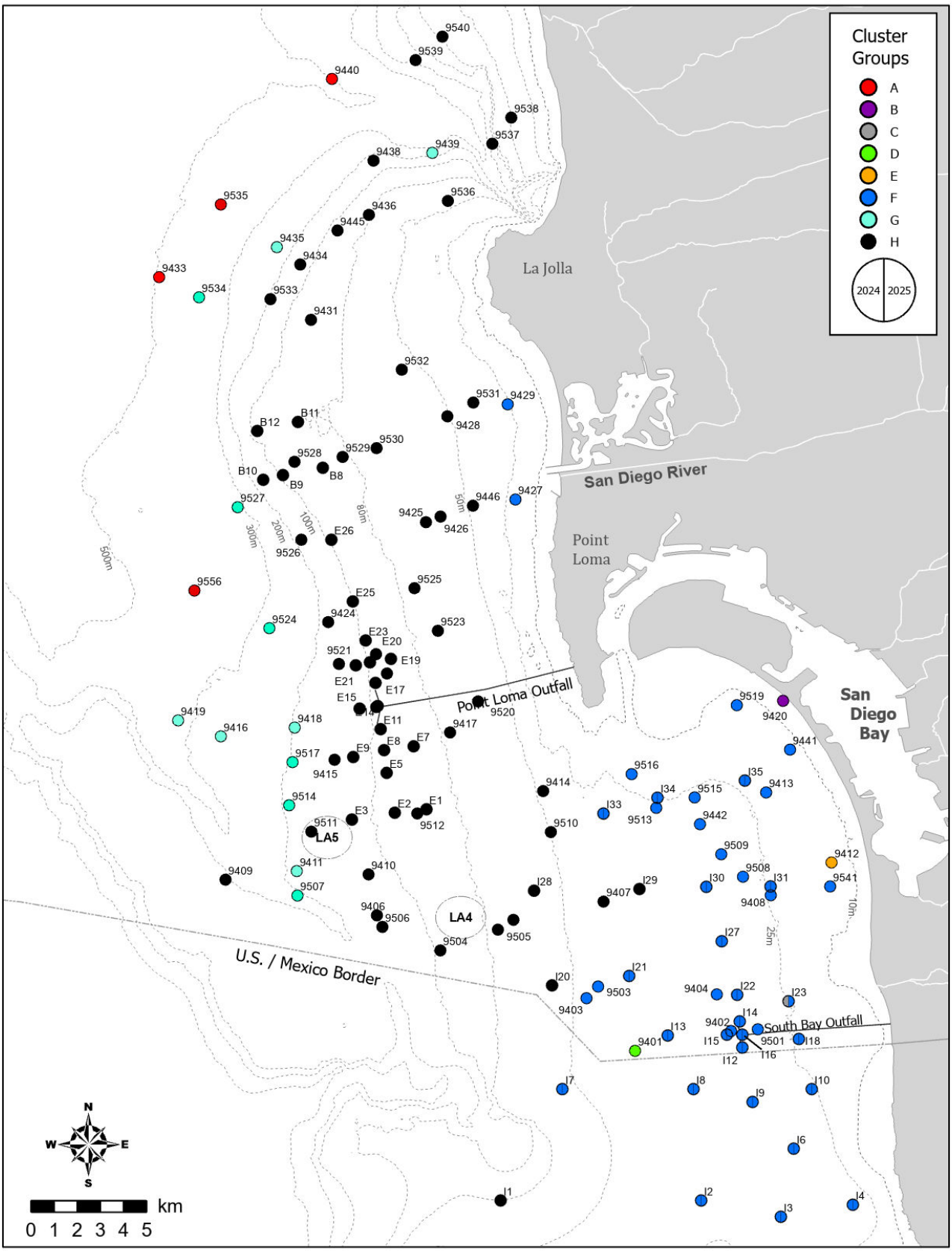


Figure 7.10
Spatial distribution of macrofaunal cluster groups A–H defined in Figure 7.7.

Table 7.3

Results for the benthic response index (BRI), sediment toxicity, and sediment quality objective (SQO) lines of evidence for San Diego regional benthic stations sampled during summer 2024 and 2025 at which sediment toxicity testing was conducted. Cond = condition; TR = test result; TC = test control; %C = percent control; LRM = logistic regression model; CSI = chemical score index; Ref = reference; LD = low disturbance; NT = non-toxic; LT=low toxicity; ME = minimal exposure; LE = low exposure; NA = not available (see text).

		Depth	Fines	BRI		Sediment Toxicity				SQOs			Site
Survey	Station	(m)	(%)	Value	Cond	TR	TC	%C	Cond	LRM	CSI	Cond	Condition
2024	I12	28	21	19	Ref	97	99	98	NT	0.12	1.00	ME	Unimpacted
	I14	28	2	24	Ref	99	99	100	NT	0.07	1.00	ME	Unimpacted
	I15	28	48	13	Ref	99	99	100	NT	0.07	1.00	ME	Unimpacted
	I16	28	33	16	Ref	98	99	99	NT	0.12	1.00	ME	Unimpacted
	E11	98	38	21	Ref	97	99	98	NT	0.06	1.00	ME	Unimpacted
	E14	98	41	24	Ref	95	99	96	NT	0.10	1.00	ME	Unimpacted
	E15	98	50	22	Ref	88	99	89	LT	0.05	1.00	ME	Unimpacted
	E17	98	47	22	Ref	97	99	98	NT	0.06	1.00	ME	Unimpacted
2025	9501	25	14	23	Ref	98	99	99	NT	0.08	1.00	ME	Unimpacted
	9503	45	0	15	Ref	93	99	94	NT	0.03	1.00	ME	Unimpacted
	9511	178	60	14	Ref	91	99	92	NT	0.23	1.00	ME	Unimpacted
	9519	13	14	27	LD	99	99	100	NT	0.08	1.00	ME	Unimpacted
	9525	75	66	13	Ref	85	99	86	LT	0.20	1.00	ME	Unimpacted
	9526	166	46	16	Ref	98	99	99	NT	0.16	1.00	ME	Unimpacted
	9528	96	62	13	Ref	98	99	99	NT	0.18	1.00	ME	Unimpacted
	9540	77	53	13	Ref	90	99	91	NT	0.17	1.00	ME	Unimpacted

Chapter 8
Demersal Fishes and Megabenthic Invertebrates

Chapter 8. Demersal Fishes and Megabenthic Invertebrates

Introduction

The City of San Diego (City) collects bottom dwelling (demersal) fishes, and relatively large (megabenthic) surface dwelling invertebrates, by otter trawl to examine the potential effects of wastewater discharge or other natural and/or anthropogenic disturbances, on the marine environment around the Point Loma and South Bay Ocean Outfalls (PLOO and SBOO, respectively). These fish and invertebrate communities are targeted for monitoring as they are known to play critical ecological roles on the southern California coastal shelf (e.g., Allen et al. 2006, Thompson et al. 1993a,b). Trawled species typically live on or near the seafloor, and are therefore exposed to sediment conditions, which may be affected by both point and non-point disturbances, such as discharges from ocean outfalls, runoff from watersheds, outflows from rivers and bays, or the disposal of dredged sediments (see Chapter 5: Sediment Quality). For these reasons, assessment of bottom dwelling fish and invertebrate communities has become an important focus of ocean monitoring programs throughout the world, but especially in the Southern California Bight (SCB) where they have been sampled extensively on the mainland shelf for the past four decades (e.g., Stein and Cadien 2009).

In healthy coastal marine ecosystems, demersal fish and megabenthic invertebrate communities vary widely and are influenced by many natural factors. For example, prey availability, seafloor topography, sediment composition, and changes in water temperatures associated with large scale oceanographic events, such as El Niño, may affect migration patterns or the recruitment of certain fish species (Cross et al. 1985, Helvey and Smith 1985, Karinen et al. 1985, Murawski 1993, Stein and Cadien 2009). Therefore, an understanding of natural background conditions is essential to determine whether changes in community structure may be related to anthropogenic activity. Pre-discharge and regional monitoring efforts by the City and others since 1991 provide baseline information on the variability of demersal fish and megabenthic invertebrate communities in the San Diego region critical for such comparative analyses (e.g., Allen et al. 1998, 2002, 2007, 2011, City of San Diego 1995, 1998, 2000, Walther et al. 2017).

The City relies on a suite of scientifically accepted indices and statistical analyses to evaluate changes in local fish and invertebrate communities. These include univariate measures of community structure, such as species richness, abundance, and diversity, while multivariate analyses are used to detect spatiotemporal differences among communities (e.g., Warwick 1993). The use of multiple types of analyses allows for more robust inference than relying on single parameters for determining anthropogenic environmental impacts. In addition, physical abnormalities or diseases on trawl-caught fishes can be indicators of degraded habitats (e.g., Cross and Allen 1993, Stein and Cadien 2009). Collectively, these data are used to determine whether demersal fish and megabenthic invertebrate assemblages from habitats with comparable depth and sediment characteristics are similar, or if observable impacts from wastewater discharge or other sources have occurred.

This chapter presents analysis and interpretation of demersal fish and megabenthic invertebrate data collected at designated monitoring stations throughout the PLOO and SBOO regions during 2024 and 2025. Included are descriptions of the different fish and invertebrate communities present in these two

regions during the reporting period, along with comparisons of spatial patterns and long-term changes over time. The four primary goals of this chapter are to: (1) characterize and document the demersal fish and megabenthic invertebrate assemblages present during the current reporting period; (2) determine the presence or absence of impacts on these assemblages that may be associated with wastewater discharge from the PLOO and SBOO; (3) identify other potential natural or anthropogenic sources of variability in the San Diego coastal marine ecosystem; (4) determine if the populations of selected species of fish and invertebrates are changing over time.

Materials and Methods

Field Sampling

Trawls were conducted at 13 stations throughout the PLOO and SBOO regions to monitor demersal fishes and megabenthic invertebrates during the winters and summers of 2024 and 2025 (Figure 8.1). These included six PLOO stations located along the 100-m depth contour (PLOO discharge depth), ranging from 9 km south to 8 km north of the outfall, and seven SBOO stations located along the 28-m depth contour (SBOO discharge depth), ranging from 7 km south to 8.5 km north of the outfall. Stations located within 1000 m of the boundary of the Zone of Initial Dilution (ZID) for either outfall are considered to represent near-ZID conditions (i.e. nearfield stations). These include two PLOO stations (SD10, SD12) and two SBOO stations (SD17, SD18). All other stations are categorized as farfield, either north or south of the outfall discharge.

A single trawl was performed at each station during each survey using a 7.6-m Marinovich otter trawl fitted with a 1.3-cm cod-end mesh net. Standard sampling procedure requires towing the net for a total of at least 10 minutes of bottom time per trawl, at a speed of around 2 knots, along a predetermined heading that follows the isobath at each station. A pressure-temperature sensor was attached to one of the trawl doors to measure water temperature, depth, and time of the individual trawls; these data were used to confirm time at depth of the trawl. The catch from each successful trawl was sorted, recorded, and immediately returned to the water to minimize mortality. All captured fish and invertebrates were individually identified to species, or to the lowest taxon possible, based on accepted taxonomic protocols for the region (Eschmeyer and Herald 1998, Page et al. 2013, SCAMIT 2023, Miller 2020). If an animal could not be accurately identified to species in the field, it was returned to the laboratory for further identification where possible. The total number of individuals and total biomass (kg, wet weight) were recorded for each species of fish. Additionally, each fish was inspected for the presence of physical abnormalities (e.g., tumors, lesions, fin erosion, discoloration) or external parasites (e.g., copepods, cymothoid isopods, leeches). The length of each fish was measured to the nearest centimeter to determine size class; total length (TL) was measured for cartilaginous fishes while standard length (SL) was measured for bony fishes (SCCWRP 2018, 2023). For invertebrates, the total number of individuals was recorded for each species. As of 2022, parasitic invertebrates that are no longer attached to their hosts, including the cymothoid isopod *Elthusa vulgaris* and leeches in the subclass Hirudinea, were recorded as present/absent rather than being counted individually, and are therefore no longer included in the analyses presented herein. This change aligns with Southern California Bight Regional Marine Monitoring Program methods (SCCWRP 2018, 2023). Visual observations of weather, sea conditions, and human and animal activity were also recorded at the time of sampling.

Data Analyses

Population characteristics of fish and invertebrate species among sites and between regions were summarized as percent abundance (PA; number of individuals per species/total abundance of all species), frequency of occurrence (FO; percentage of stations at which a species was collected), mean abundance per haul (MAH; number of individuals per species/total number of trawls sampled), and mean abundance per occurrence (MAO; number of individuals per species/number of stations at which the species was collected). Additionally, the following community structure parameters were calculated per station for fishes and invertebrates separately: species richness (number of species), total abundance (number of individuals per species), and the Shannon Diversity Index (H'). For fishes, total biomass was also calculated per station. These analyses were performed using R (R Core Team 2021) and various functions within the reshape2, lubridate, tidyverse, glue, Rmisc, magrittr, vegan, RODBC, devtools, webshot, officer, flextable, ggpubr, and patchwork packages (Wickham 2007, Grolemund and Wickham 2011, Bolker et al. 2022, Hester and Bryan 2022, Hope 2022, Milton Bache and Wickham 2022, Oksanen et al. 2022, Ripley and Lapsley 2022, Wickham et al. 2022, Chang 2023, Gohel 2023, Gohel and Skintzos 2023, Kassambara 2023, Lin Pedersen 2023).

To determine if the populations of fish and invertebrates are changing over time, multivariate analyses were performed in PRIMER v7 software using fish and invertebrate abundance data collected from 10-minute trawls conducted in the PLOO and SBOO regions from 1991 through 2025 (see Clarke 1993, Warwick 1993, Clarke et al. 2014). Prior to these analyses, all data were limited to summer surveys to reduce variability from natural seasonal variations. Additionally, data were transformed as appropriate to characterize the natural variability in species abundance more accurately. Additional multivariate analyses included Bray-Curtis measure of dissimilarity to serve as the basis for ordination (non-metric multidimensional scaling; nMDS) and hierarchical agglomerative clustering (cluster analysis) with group-average linking. Similarity profile analysis (SIMPROF) was used to confirm the non-random structure of the resultant cluster dendrogram (Clarke et al. 2008), with major ecologically-relevant clusters receiving SIMPROF support retained as cluster groups. A BEST test using the BVSTEP procedure was conducted to determine which subset of species best described patterns within the resulting cluster dendrograms. Similarity percentages analysis (SIMPER) was used to determine which species were responsible for > 70% of the contributions to within-group similarity (characteristic species) by cluster group to support cluster group selection.

Data collected during 2024 were reported previously (City of San Diego 2025), and all raw data for the 2024–2025 sampling period have been submitted to either the Regional Water Quality Control Board, the California Environmental Data Exchange Network (CEDEN) or the City's Open Data Portal (City of San Diego 2026) and may be accessed upon request.

Results and Discussion

Demersal Fish Populations in 2024 and 2025

A total of 26,411 fishes were captured from the 52 trawls conducted within the PLOO and SBOO monitoring regions during 2024 and 2025, representing at least 52 different species from 26 families in the PLOO, and 32 species from 17 families in SBOO (Appendices G.1, G.2). For the purposes of this discussion, individual samples are referred to as "trawls" and "hauls" interchangeably. Pacific Sanddabs

continued to dominate PLOO demersal fish assemblages over the past two years, occurring in every trawl and accounting for 46% of the fishes collected across trawls in that region (Table 8.1). Other species that were present in all PLOO assemblages during this period included Halfbanded Rockfish, Dover Sole and Shortspine Combfish, which accounted for 10%, 5%, and 4% of fishes collected, respectively (Table 8.1). Other species of fish that were collected in at least 85% of the trawls included Longspine Combfish and Longfin Sanddab (Table 8.1). Fish assemblages in the SBOO region were dominated by Speckled Sanddabs, which occurred in all trawls and accounted for 44% of the fishes collected, and by California Lizardfish, which occurred in 86% of the trawls and accounted for 20% of the fishes collected (Table 8.2). Though California Tonguefish occurred in 93% of trawls, they only accounted for 3% of the fishes collected (Table 8.2). Other species that were collected in at least 80% of the trawls included Longfin Sanddab and Hornyhead Turbot (Table 8.2). Rare species in both regions that are not included in Tables 8.1 and 8.2 can be found in Appendices G.1 and G.2.

The vast majority of individuals (>99%) collected in the PLOO and SBOO monitoring regions were < 30 cm in length. Species collected from PLOO stations with individuals measuring ≥ 30 cm were Pacific Angel Shark, California Skate, Spotted Ratfish, California Grenadier, and Pacific Electric Ray, with a total of 15 individuals being caught in 2024 and 2025. In contrast, 51 individuals measuring ≥ 30 cm were caught at SBOO stations, including California Halibut, California Skate, Specklefin Midshipman, English Sole, Fantail Sole, California Lizardfish, and Round Stingray (Appendices G.1 and G.2).

The three most abundant fish species in 2024 and 2025 trawls (Pacific Sanddab, Longspine Combfish and Halfbanded Rockfish) dominated the PLOO surveys, occurring in nearly every trawl and together comprising nearly half of all the biomass collected. Together, these 3 fish species accounted for 70% of all individuals and 163 kg of the total 353kg of the biomass collected. Despite the relatively small size of these fish (9 cm, 9 cm, and 10 cm mean sizes, respectively), their sheer numbers overwhelmed the effect of the few large fish collected, for example, the largest fish (Pacific Angel Shark), which measured 11.3 kg mass (3% total biomass collected) and 99 cm length, but was relatively uncommon, occurring only once in the survey period (Appendix G.1).

Similarly, the three most abundant species of fish collected in SBOO also dominated the trawls, with Speckled Sanddab occurring in every trawl and California Lizardfish and Longfin Sanddab occurring in over 80% of trawls. These fish accounted for 79% of individuals sampled (6,849 of 8,667 individuals) and 46% of the biomass collected (128 of 275 kg) in the 2024–2025 survey period. Like the top 3 fish in PLOO surveys, these fish were relatively small, at 8, 12, and 13 cm mean length, respectively. California Halibut, which did not occur in any PLOO trawls, accounted for 15% of the total biomass collected in the South Bay, despite comprising less than 1% of abundance (57 of 8,667 fish caught). These large (34 cm mean length, 19–57 cm range) fish provided an exception to the pattern of dominance by small, numerically abundant fish in both PLOO and SBOO trawls (Appendix G.2).

Demersal Fish Community Structure

No prominent spatial patterns in the community parameters of demersal fishes were observed relative to the proximity of the PLOO or SBOO discharge sites during 2024 and 2025 (Table 8.3, Figure 8.2). Results were generally consistent with previous findings for the two regions, and elsewhere in the SCB (e.g., Allen et al. 1998, 2002, 2007, 2011, City of San Diego 1995, 1998, Walther et al. 2017, Wisenbaker et al. 2021); mean species richness and diversity were consistently low (SR ≤ 22 species,

H' ≤ 1.8, respectively); and fish abundance and biomass remained variable among both nearfield and farfield stations and between surveys over the past two years, with values ranging from 21–1,581 fishes/haul and 1–28.1 kg/haul (Table 8.3).

Abundance was highly variable among stations and seasons in the PLOO region, with total abundance per trawl ranging from 270 to 1,581 fish (mean 739 ± 333 sd). Despite variability in abundance, species richness and diversity were relatively consistent by comparison (mean SR 18.1 ± 3.0 sd, mean H' 1.6 ± 0.22 sd) indicating that the individual trawls were representative, even if the number of fish caught was highly variable. Community parameters (H' and SR) were also relatively consistent among stations groups, indicating that proximity to the outfall had no effect on fish community structure (Table 8.3).

Similarly, within the SBOO region, abundance was also highly variable among stations and seasons, with total abundance per trawl ranging from 21 to 790 fish (mean 309 ± 245 sd). Additionally, mean abundance in the SBOO region was about half of PLOO abundance, indicative of some spatial effect on abundance beyond any that could be attributed to outfall discharge. Furthermore, species richness in the SBOO region showed slightly lower mean richness (mean SR 11.4 ± 3.3 sd) when compared to PLOO stations. Despite lower richness values, diversity was similar among stations regardless of region (mean H' 1.5 ± 0.26 sd) further supporting the hypothesis that outfall activities are not adversely affecting fish populations in the PLOO and SBOO region (Table 8.3).

Historical comparisons indicate no noteworthy spatial patterns in demersal fish community parameters relative to their proximity to the discharge sites, but varying degrees of stability relative to the onset of wastewater discharge that began in the PLOO and SBOO regions in 1994 and 1999, respectively (Figure 8.2). Since the initiation of discharge, mean species richness and diversity values for demersal fishes collected from PLOO and SBOO stations have remained low (SR ≤ 17 species; H' ≤ 1.6, respectively). However, there has been considerably greater variability in abundance, with post-discharge trawls generally having greater abundances of fishes. The latter was largely due to population fluctuations of a few numerically dominant species in each region (Figures 8.3, 8.4). For example, differences in overall trawl catch abundances tended to track changes in Pacific Sanddab populations at the PLOO stations, and Speckled Sanddab populations at the SBOO stations, since these two species have been numerically dominant in these regions since monitoring began. In addition, occasional spikes in abundances within the PLOO region have been due to population fluctuations of other common species, such as Yellowchin Sculpin, Halfbanded Rockfish, Longspine Combfish, Dover Sole, Plainfin Midshipman, Stripetail Rockfish, California Lizardfish, Longfin Sanddab, and Pink Seaperch (Figure 8.3). In contrast, periodic spikes within the SBOO region have been due to population dynamics of California Lizardfish, Longfin Sanddab, White Croaker, Yellowchin Sculpin, Roughback Sculpin, Hornyhead Turbot, California Tonguefish, English Sole, and Northern Anchovy (Figure 8.4). Population dynamics of these species and communities over time do not appear to be associated with proximity to wastewater discharge from either outfall.

Physical Abnormalities and Parasitism in Demersal Fishes

Demersal fish populations appeared healthy in the PLOO and SBOO regions in 2024 and 2025, with parasites and abnormalities reported for just 0.17% of fishes collected. Generally, eye parasites appear to occur more frequently in the PLOO region, whereas gill and external parasites appear to occur more frequently in the SBOO region (Appendix G.5). As abnormalities or parasites were present across nearly all stations between regions, there does not appear to be a relationship between these anomalies and

proximity to either outfall. Most abnormalities observed in the study period (fin rot, tumors, lesions, ambicoloration, etc.) were limited to single occurrences distributed across the different stations and seasons with no apparent relationship with proximity to outfall discharge. Several *E. vulgaris* specimens were noted as being present during each trawl, but since they often become detached from their hosts during retrieval and sorting of the trawl catch, it is unknown which fishes were parasitized by these isopods. However, *E. vulgaris* is known to be especially common on Pacific and Speckled Sanddab, and California Lizardfish in southern California waters where it may reach infestation rates of up to 80% (see Brusca 1978, 1981).

Classification of Demersal Fishes Assemblages

PLOO Region

Cluster and ordination analyses of a total of 178 trawls resulted in six ecologically-relevant SIMPROF-supported groups, or types of assemblages, in the PLOO region since the initiation of monitoring in 1991 (cluster groups A–G; Figure 8.5, Appendix G.6). These assemblages represented from 1 to 126 hauls each and varied in both species richness and abundance per haul. A BEST/BVSTEP test implicated California Lizardfish, Dover Sole, English Sole, Halfbanded Rockfish, Longfin Sanddab, Longspine Combfish, Pacific Argentine, Pacific Sanddab, Pink Seaperch, Plainfin Midshipman, Shortspine Combfish, Slender Sole, Spotfin Sculpin, Stripetail Rockfish, and Yellowchin Sculpin as being influential to the overall pattern (gradient) of the cluster dendrogram ($\rho = 0.952$, $p \leq 0.001$, number of permutations = 999). Overall, the data show that when stations are compared over time, the outfall stations are not different from the farfield stations (Figure 8.5). Instead, assemblages appeared to be influenced by the distribution of the more abundant species or unique characteristics of specific station locations (e.g., habitat differences). For example, assemblages from stations SD7 and SD8 located south of the outfall often grouped apart from the remaining stations between 1991 and 2006 (see group E). The species composition and main descriptive characteristics of each of the cluster groups are included below.

Cluster group A represented a unique assemblage sampled at nearfield trawl station SD12 in 1998 (Figure 8.5). The assemblage represented by cluster group B was characterized by 261 individuals comprising 16 species, and 75 Pacific Sanddabs per haul. Plainfin Midshipman (116/haul), Dover Sole (36/haul), Longspine Combfish (7/haul), and Gulf Sanddab (5/haul) also contributed to the dissimilarity between this and other cluster groups (Appendix G.6).

Cluster group B represented a unique assemblage sampled at nearfield trawl station SD12 in 1997 (Figure 8.5). The assemblage represented by cluster group C was characterized by 231 individuals comprising 19 species, and 110 Pacific Sanddabs per haul. Halfbanded Rockfish (60/haul), Squarespot Rockfish (23/haul), Greenblotched Rockfish (8/haul), and Vermillion Rockfish (6/haul) also contributed to the dissimilarity between this and other cluster groups (Appendix G.6).

Cluster group C represented nine assemblages sampled across stations in 2009 and 2014 (Figure 8.5). These assemblages included moderately sized hauls, averaging 13 species and 280 individuals per haul, and was characterized by a high abundance of California Lizardfish ($\bar{x} = 140$/haul) (Appendix G.6).

Cluster group D was the largest group, representing assemblages from a total of 126 hauls that were conducted across the entire monitoring period (Figure 8.5). Most of the trawls conducted from 1993 through 2008 were in this cluster group, including mostly nearfield and north farfield station

assemblages, and all the samples from 2010 to 2013. Assemblages in cluster group D averaged 15 species of fish, 414 individuals per haul, and was characterized by the highest average abundance of Pacific Sanddab among cluster groups (Figure 8.5, Appendix G.6).

Cluster group E was the second largest cluster group, representing assemblages from a total of 44 hauls that consisted almost exclusively of south farfield trawls from 1991 through 2006 (Figure 8.5). Trawls at station SD7 in 2009, 2016, 2019, and 2020 were also included in this cluster group. These assemblages averaged 14 species and 180 individuals per haul. The most characteristic species of cluster group G were Pacific Sanddab ($\bar{x}$ = 112/haul), Dover Sole ($\bar{x}$ = 13/haul), and Plainfin Midshipman ($\bar{x}$ = 12/haul) (Appendix G.6).

Cluster group F represented 4 trawls from all station groupings between 1994 and 2001 (Figure 8.5). These assemblages included the smallest hauls, averaging just 10 species and 60 individuals per haul, and had the lowest average Pacific Sanddab abundance ($\bar{x}$ = 39/haul) (Appendix G.6).

SBOO Region

Cluster and ordination analyses of a total of 201 trawls resulted in six ecologically-relevant SIMPROF-supported groups, or types of assemblages in the South Bay outfall region since the initiation monitoring in 1995 (cluster groups A–F; Figure 8.6, Appendix G.7). These assemblages represented from 1 to 105 hauls each and represented a wide range of mean species richness (7–16 species/haul) and mean abundances (59–489/haul). A BEST/BVSTEP test implicated Speckled Sanddab, California Lizard fish, Pacific Sanddab, Longspine Combfish, Longfin Sanddab, Yellowchin Sculpin, Hornyhead Turbot and White Croaker as being influential to the overall pattern (gradient) of the cluster dendrogram ($\rho = 0.951$, $p \leq 0.001$, number of permutations = 999). Overall, there were no discernable patterns associated with proximity to the SBOO discharge site. Instead, as observed in the PLOO region, SBOO fishes assemblages appear to be influenced by the distribution of the more abundant species or the unique characteristics of a specific station location. For example, cluster group F was distinguished by comparatively low abundances of Speckled Sanddab that generally coincided with or followed warm water El Niño events in 1994–1995, 1997–1998 and 2014–2016 (NOAA/NWS 2022). Additionally, station SD15, located farthest south of the SBOO in northern Baja California waters, often grouped apart from the remaining stations (see cluster group A), possibly due to habitat differences such as sandier sediments (see Chapter 5: Sediment Quality). The species composition and main descriptive characteristics of each of the six cluster groups are included below.

Cluster group A comprised 53 hauls, including 66% (n = 20) of the trawls from south farfield station SD15 and 33% (n = 10) of the trawls from south farfield station SD16 over the past 30 years (Figure 8.6). This cluster group also included 55% (n = 31) of the trawls conducted at most stations from 1995 through 2002, with the exception of SD21, which never grouped as “A”. The assemblages represented by cluster group A averaged 7 species and 82 fishes per haul. These assemblages averaged 98 Speckled Sanddab per haul and were also characterized by Hornyhead Turbot ($\bar{x}$ = 4/haul) (Appendix G.7).

Cluster group B represented a unique assemblage sampled at north farfield trawl station SD21 in 2011 (Figure 8.6). The assemblage represented by cluster group A was characterized by 59 individuals from 16 species, and relatively few (26 individuals) Speckled Sanddabs. California Lizardfish (75 individuals), Longspine Combfish (79 individuals), Longfin Sanddab (8 individuals), and White Croaker (22 individuals) also contributed to the dissimilarity between this and other cluster groups (Appendix G.7).

Cluster group C represented assemblages from 34 trawls that included trawls, mostly from north farfield stations from 1995 to 2002, especially SD21 (Figure 8.6). This cluster group averaged 7 species and the smallest mean abundance per haul (27 individuals per haul). The most characteristic species for this group were relatively low abundance of Speckled Sanddab ($\bar{x}$ = 53/haul) and the highest mean abundance of Longfin Sanddab ($\bar{x}$ = 33/haul) (Appendix G.7).

Cluster group D represented a unique assemblage sampled at south farfield trawl station SD15 in 2013 (Figure 8.6). Cluster group D had the highest total abundance (489 individuals), and the highest abundance of California Lizardfish (118 individuals) and Longspine Combfish (153 individuals) recorded (Appendix G.7).

Cluster group E was the largest cluster group comprising 105 hauls and was the dominant assemblage from all station groupings from 2002 to 2025 (Figure 8.6). Assemblages represented by cluster group E averaged 9 species and 59 individuals per haul. This cluster group had the highest mean abundance of Speckled Sanddab ($\bar{x}$ = 180/haul) and relatively high abundance of Longfin Sanddab ($\bar{x}$ = 30/haul) (Appendix G.7).

Cluster group F comprised 7 hauls, mostly from sample year 2001 (Figure 8.6). Assemblages in this cluster group averaged 7 species and 121 individuals per haul and had the lowest mean abundance of Speckled Sanddab ($\bar{x}$ = 13/haul). Low numbers of California Lizardfish ($\bar{x}$ = 1/haul), Longfin Sanddab ($\bar{x}$ = 1/haul), and Hornyhead Turbot ($\bar{x}$ = 2/haul) were also characteristic of these trawls (Appendix G.7).

Megabenthic Invertebrate Populations in 2024 and 2025

A total of 52,926 invertebrates were captured from the 52 trawls conducted within the PLOO and SBOO monitoring regions in 2024 and 2025, representing 85 taxa from five phyla (Arthropoda, Echinodermata, Mollusca, Cnidaria, Silicea) (Appendices G.8, G.9). The sea urchin *Lytechinus pictus* dominated PLOO trawls-caught invertebrates and accounted for 98% of total abundance across trawls in that region (Table 8.4). The sea star *Astropecten californicus* and the sea cucumber *Apostichopus californicus* were caught in more than 50% of the trawls but their abundances were very low (2 haul) (Table 8.4). The sea star *Astropecten californicus* dominated the SBOO region and accounted for 74% of total abundance (Table 8.5). The brittle star *Ophiothrix spiculate*, the shrimp *Sicyonia penicillata,* and the sea star *Luidia armata* occurred in more than 50% of the trawls and accounted for 2% to 3% of the total catch (Table 8.5). Rare species in both regions that are not included in Tables 8.4 and 8.5 can be found in Appendices G.8 and G.9.

Megabenthic Invertebrate Community Structure Parameters

No notable spatial patterns in megabenthic invertebrate community parameters were observed relative to the proximity of the PLOO or SBOO discharge sites during 2024 and 2025. Results were generally consistent with previous findings for the two regions and elsewhere in the SCB (e.g., Allen et al. 1998, 2002, 2007, 2011, City of San Diego 1995, 1998, Walther et al. 2017, Wisenbaker et al. 2021). For example, species richness and diversity were consistently low (SR $\leq$ 21, H' $\leq$ 2.3, respectively), whereas abundance remained highly variable among both nearfield and farfield stations and between surveys over the past two years, with values ranging from 15 to 8,523 individuals per haul (Table 8.6).

Within the PLOO region, species richness and diversity varied both over time and across nearfield and farfield stations. Much of this variation may be correlated with the population dynamics of the urchins *Lytechinus pictus* and *Strongylocentrotus fragilis*. When abundance of one or a combination of these species significantly increases, diversity tends to decline. For instance, some of the lowest diversity in the region (H' ≤ 0.02–0.1) was observed at station SD8 between 2024 and 2025 (Table 8.6). *L. pictus* was collected in large abundances at station SD8 in 2025, including 5,425 individuals in the winter and 8,466 individuals in the summer. The highest diversity was recorded at station SD13 in the winter of 2024 (H' = 2.3) and no dominant species were observed in this trawl. Species richness does not seem to follow the same trend as diversity since the second highest species richness value was recorded at south farfield station SD8 (SR = 21) in the summer of 2025 when a high number of *L. pictus* (8,466/haul) was recorded (Table 8.6).

Within the SBOO region, the abundance of the dominant species, *A. californicus*, appears to be correlated with both species richness and diversity. For example, the highest diversity (H' = 1.9) was recorded at SD17 in the winter of 2024 and 2025 and at SD21 in the winter of 2024 when relatively low numbers of *A. californicus* were observed (1–35/haul). Conversely, the lowest diversity (H' = 0.1) was recorded at SD19 in the summer of 2025 when the highest abundance of *A. californicus* was observed (354/haul). Similarly, SD17 exhibited two of the highest species richness values (SR = 14 and 17, respectively) during the summer and winter of 2025 when *A. californicus* abundance remained relatively low (16 and 54/haul) (Table 8.6).

Historical comparisons indicate no notable spatial patterns in megabenthic invertebrate community parameters relative to the proximity of the PLOO or SBOO discharge sites, or to the onset of wastewater discharge that began in 1994 or 1999, respectively (Figure 8.7). Since the initiation of discharge, mean species richness and diversity for megabenthic invertebrates collected from the PLOO and SBOO regions have remained low (SR ≤ 12 species; H' ≤ 1.3, respectively). However, total abundance has shown substantially greater variability (1−46,255/haul). This variability seems to be driven by population fluctuations of a few numerically dominant species in each region, rather than station proximity to either outfall (Figures 8.8, 8.9). For example, differences in overall megabenthic invertebrate abundances at the PLOO stations tended to track population changes of the pelagic red crab *Grimothea planipes*, the sea urchins *L. pictus* and *S. fragilis*, the brittle star *Ophiura luetkenii*, the sea stars *Luidia foliolata* and *Astropecten californicus*, the sea pen *Acanthoptilum* sp, the sea cucumber *Apostichopus californicus*, the shrimp *Sicyonia ingentis,* and the crab *Platymera gaudichaudii* (Figure 8.8). Large hauls of *G. planipes* from PLOO trawl stations SD12 and SD13 in 2018 and 2020 were followed by decreased species richness and diversity (SR = 4–7, H' = 0.03–0.8). Following a *G. planipes* population decline in 2021, species richness has slowly recovered to pre-2018 levels (City of San Diego 2019, 2020, 2021). Since then, the sea urchin *L. pictus* has become the dominant species. Although species richness at stations SD12 and SD13 has improved (SR = 8–13), diversity has only shown substantial improvement at station SD12 (H' = 0.9–2.3) (Table 8.6). Similarly, *S. fragilis* were previously abundant at north farfield stations SD13 and SD14 before *G. planipes* became the dominant species at these stations between 2016 and 2020. As *G. planipes* expanded in the north, *S. fragilis* appears to have migrated to the south farfield region where its population increased rapidly before declining as *L. pictus* became dominant across the PLOO region (Figure 8.8).

Differences in overall abundances at SBOO stations generally tracked population changes of several influential species including the sea stars *L. pictus* and *A. californicus*, the shrimps *C. nigromaculata* and *S. penicillata*, the crab *Latulambrus occidentalis*, the snail *Philine auriformis*, the sand dollar

Dendraster terminalis, the brittle star *Ophiothrix spiculata*, the swimming crab *Achelous xantusii*, and the rock crab *Metacarcinus gracilis* (Figure 8.9). *A. californicus* population declined significantly following the large 2014–2016 El Niño events; however, they started to recover quickly and their abundances have since returned to pre-2014 levels. An ecologically interesting note is the consistent recent presence of *S. penicillata* in the SBOO region. This species is typically documented from Puntarenas, Costa Rica in the south to Punta Canoas, Mexico in the north, with noted incursions into the SCB only during El Niño events (Jensen 2014). However, since the 2014–2016 El Niño, *S. penicillata* appears to have established a resident population and has been seen with increasing frequency and abundance in SBOO trawls (Figure 8.9). None of the observed trends in either region appears to be associated with proximity to wastewater discharge from either outfall.

Classification Analysis of Invertebrate Assemblages

PLOO Region

Cluster and ordination analyses of a total of 184 trawls resulted in seven ecologically-relevant SIMPROF-supported groups or types of megabenthic invertebrate assemblages in the PLOO region since the initiation monitoring in 1991 (cluster groups A–F). These assemblages represented from 2 to 164 hauls each and varied in terms of species present, as well as the relative abundances per haul (Figure 8.10). A BEST/BVSTEP test implicated 21 invertebrate species including the pelagic red crab *Grimothea planipes*, the sea urchins *Lytechinus pictus* and *Strongylocentrotus fragilis*, the shrimp *Sicyonia ingentis*, and the sea pen *Acanthoptilum sp* as influences on the overall pattern (gradient) of the cluster dendrogram ($\rho = 0.952$, $p \leq 0.001$, number of permutations = 999) (Appendix G.10). Overall, there were no discernible patterns associated with proximity to the PLOO discharge site. Instead, assemblages appear to be influenced by the distribution of more abundant species or the unique characteristics of specific station locations. The species composition and main descriptive characteristics of each of the five cluster groups are included below.

Cluster group A occurred in 2021 and consisted of assemblages from two trawls (Figure 8.10). These assemblages had the lowest average species richness (SR = 4) and the second lowest average abundance ($\bar{x}$ = 94/haul). This cluster group was primarily characterized by the shrimp *Sicyonia ingentis* ($\bar{x}$ = 89/haul) and the octopus *Octopus veligero* ($\bar{x}$ = 3/haul) (Appendix G.10).

Cluster group B consisted of assemblages from ten trawls and was primarily dominated by the pelagic red crab *G. planipes* ($\bar{x}$ = 5,261/haul) (Figure 8.10, Appendix G.10). Assemblages in this cluster group were sampled between 2016 and 2020 during the period when *G. planipes* migrated to the PLOO region and its abundance peaked. These assemblages had a low average species richness of 6 species per haul and the highest average abundance of 5,492 individuals per haul (Figure 8.10).

Cluster group C included two trawls from stations SD7 in 2020 and SD13 in 2021. This cluster group was characterized by a single species, the sea urchin *L. pictus* ($\bar{x}$ = 12/haul) (Figure 8.10, Appendix G.10). This cluster group had the lowest average abundance ($\bar{x}$ = 21/haul) and second lowest species richness (SR = 6) (Figure 8.10).

Cluster group D comprised two trawl assemblages and had an average abundance of 708 individuals per haul and the second highest mean species richness (SR = 22) (Figure 8.10). This cluster group was primarily characterized by the high abundance of the two sea urchin species, *L. pictus* ($\bar{x}$ = 619/haul) and *S. fragilis* ($\bar{x}$ = 27/haul) (Appendix G.10). Other characteristic species

included the sea star *Astropecten californicus* ($\bar{x}$ = 12/haul), the snail *Megasurcula carpenteriana* ($\bar{x}$ = 6/haul), the brittle star *Amphichondrius granulatus* ($\bar{x}$ = 5/haul), and the shrimp *Neocrangon zacae* ($\bar{x}$ = 4/haul) (Appendix, G.10).

Cluster group E was the largest group, representing assemblages from a total of 164 trawls. The hauls occurred across all spatial and temporal ranges (Figure 8.10). These assemblages had the moderate average species richness (SR = 12) and the second highest mean abundance ($\bar{x}$ = 1685/haul). This cluster group was characterized by the highest average number of the sea urchin *L. pictus* ($\bar{x}$ = 1516/haul) and other echinoderms including *Astropecten californicus* ($\bar{x}$ = 5/haul), *Luidia foliolate* ($\bar{x}$ = 4/haul), and *Apostichopus californicus* ($\bar{x}$ = 4/haul) (Appendix G.10).

Cluster group F was comprised of four hauls with average of 133 individuals per haul (Figure 8.10). These hauls occurred at the three most nothern stations SD12, SD13 and SD14. The two most characteristic species were the sea pen *Acanthoptilum* sp ($\bar{x}$ = 73/haul) and the sea urchin *S. fragilis* ($\bar{x}$ = 24/haul) (Appendix G.10). This cluster group and cluster group A are the only groups that are not influenced by *L. pictus.*

SBOO Region

Cluster and ordination analyses of a total of 201 trawls resulted in six ecologically-relevant SIMPROF-supported groups or types of megabenthic invertebrate assemblages in the SBOO region since the initiation of monitoring in 1995 (cluster groups A–F; Figure 8.11, Appendix G.11). These assemblages represented from 1 to 172hauls each, and varied in terms of species present, as well as the relative abundances of individual species. A BEST/BVSTEP test implicated 19 invertebrate species including the urchin *Lytechinus pictu*s, the brittle star *Ophiura luetkenii*, the sea star *Astropecten californicu*s, the sand dollar *Dendraster terminalis*, and the shrimp *Sicyonia penicillata* as influences on the overall pattern (gradient) of the cluster dendrogram ($\rho = 0.952$, $p \leq 0.001$, number of permutations = 999) (Appendix G.11). There were no discernible patterns associated with proximity to the SBOO discharge site (Figure 8.11). Instead, assemblages appear influenced by the distribution of the more abundant species during specific time periods (groups E and F) versus background conditions (group D). The species composition and main descriptive characteristics of each of the four cluster groups are included below.

Cluster group A was one of the smallest clusters, containing a single haul from station SD15 in 2009 (Figure 8.11). The brittle star *Ophiura luetkenii* was the dominant species ($\bar{x}$ = 72/haul) and other species characteristic of this assemblage include the brittle star *O. spiculata* ($\bar{x}$ = 3/haul), the sand dollar *D. terminalis* ($\bar{x}$ = 3/haul), the octopus *O. rubescens* ($\bar{x}$ = 1/haul), and the crab *Pyromaia tuberculata* ($\bar{x}$ = 1/haul) (Appendix G.11).

Cluster group B represented one haul from station SD19 in 1998 and had the lowest species richness of 4 and abundance of 4 individuals/haul (Figure 8.11). The sea stars *A. californicus* (1/haul) and *Pisaster brevispinus* (1/haul), and the snail *Crossata ventricosa* (1/haul) were representative species of this group (Appendix G.11).

Cluster group C comprised two unique assemblages collected at stations SD17 in 1995 and SD15 in 1997 (Figure 8.11). This cluster was represented by heavily dominant the sea urchin *L. pictus* with the

highest recorded abundance in the SBOO region ($\bar{x}$ = 647/haul). Due to the large abundance of *L. pictus,* the average abundance of all individuals was also the highest *(*$\bar{x}$ = 694/haul) (Figure 8.11)

Cluster group D was the largest cluster group, comprising 172 hauls found across all stations between 1995 and 2025, likely reflecting background conditions within the region (Figure 8.11). Assemblages represented by cluster group D averaged 8 species per haul and 63 individuals per haul. This cluster group was primarily characterized by two sea star species, *A. californicus* ($\bar{x}$ = 39/haul) and *P. brevispinus* ($\bar{x}$ = <1/haul) (Appendix G.11).

Cluster group E represented assemblages from a total of 18 hauls collected between 2009 and 2019 across all stations (Figure 8.11). Average species richness of hauls in this cluster was 7 species per haul and average abundance was 28 individuals per haul (Figure 8.11). The most characteristic species for cluster group E assemblages were the sea star *A. californicus* ($\bar{x}$ = 2/haul), the shrimp *S. penicillata* ($\bar{x}$ = 7/haul), the octopus *O. rubescens (*$\bar{x}$ = 2/haul), and the snail *Kelletia kelletii* ($\bar{x}$ = 2/haul) (Appendix G.11).

Cluster group F comprised four hauls collected over three years, 2000, 2017, and 2019 across several stations and had a moderate species richness of 13 and an average abundance of 133 individuals per haul. (Figure 8.11) The characteristic species included the sea urchin *L. pictus*, ($\bar{x}$ = 2/haul), the snail *C. ventricosa* ($\bar{x}$ = 1/haul), and the shrimp *Crangon nigromaculata* ($\bar{x}$ = <1/haul) (Appendix G.11)

Summary

Demersal fishes and megabenthic invertebrate populations monitored in 2024 and 2025 do not show evidence of negative impacts associated with proximity to wastewater discharge from the PLOO and SBOO. Community parameters are similar at stations located both near and far from the outfall discharge sites in both regions. Major community metrics, such as species richness, abundance, and diversity were generally within historical ranges reported for the San Diego region (City of San Diego 1995, 1998, 2000, 2022) and were representative of those characteristic of similar habitats throughout the SCB (e.g., Allen et al. 1998, 2002, 2007, 2011, Walther et al. 2017).

Over the past two years, Pacific Sanddab dominated assemblages surrounding the PLOO, and Speckled Sanddab dominated assemblages surrounding the SBOO, as they have done so since monitoring began in each region. Halfbanded Rockfish were also prevalent in PLOO assemblages during 2024 and 2025, while California Lizardfish were also prevalent within the SBOO region during this period, as they have in eleven of the past thirteen years. Other commonly captured, but less abundant fishes, collected from the PLOO and SBOO regions included California Tonguefish, Dover Sole, English Sole, Longfin Sanddab, Northern Anchovy, Longspine Combfish, Shortspine Combfish, and White Croaker.

Of the 52,926 megabenthic invertebrates encountered during 2024 and 2025, 93% were the sea urchin *Lytechinus pictus*, collected mostly at PLOO trawl stations. *L. pictus* started to become the dominant species at PLOO stations following the collapse of pelagic red crab *Grimothea planipes* populations in 2021 and its abundance continued to increase through 2024–2025. Community metrics, including species richness, diversity, and cluster analysis, indicate that the PLOO region is returning to baseline conditions typically observed prior to the most recent *G. planipes* migration. A comparable pattern was observed in the SBOO region where the sea star *Astropecten californicus* re-emerged as a dominant

species following population declines associated with the 2014–2016 El Nino event and subsequent *G. planipes* incursions in 2018 and 2020. This shift indicates a return to pre-disturbance community structure when *A. californicus* was a principal species of the SBOO trawl assemblage. Additionally, the consistent presence of a historically more southerly located species, the shrimp *Sicyonia penicillata*, is a potential indicator of large-scale climate driven effects of species distribution and occurrence, which will likely only increase in the future (Lilly 2004).

The abundance and distribution of species varied similarly at stations located near and far from the outfalls in both regions. The high degree of variability in these assemblages during this reporting period was similar to that observed in previous years, including before wastewater discharge began through either outfall (City of San Diego 1995, 1998, 2000, 2022). Furthermore, this sort of variability has been observed in similar habitats elsewhere off the coast of southern California (Allen et al. 1998, 2002, 2007, 2011, Walther et al. 2017). Consequently, changes in local community structure of these fishes and invertebrates are more likely due to natural factors, such as changes in ocean temperatures associated with El Niño or other large-scale oceanographic events. Finally, the rarity of disease indicators, or other physical abnormalities, in local fishes suggests that populations in the Point Loma and South Bay outfall regions continue to be unimpacted by wastewater discharge.

Literature Cited

Allen, L.G., D.J. Pondella II, and M.H. Horn. (2006). The Ecology of Marine Fishes: California and Adjacent Waters. University of California Press, Berkeley, CA.

Allen, M.J., S.L. Moore, K.C. Schiff, D. Diener, S.B. Weisburg, J.K. Stull, A. Groce, E. Zeng, J. Mubarak, C.L. Tang, R. Gartman, and C.G. Haydock. (1998). Assessment of demersal fish and megabenthic invertebrate assemblages on the mainland shelf of Southern California in 1994. Southern California Coastal Water Research Project, Westminster, CA.

Allen, M.J., A.K. Groce, D. Diener, J. Brown, S.A. Steinert, G. Deets, J.A. Noblet, S.L. Moore, D. Diehl, E.T. Jarvis, V. Raco-Rands, C. Thomas, Y. Ralph, R. Gartman, D. Cadien, S.B. Weisberg, and T. Mikel. (2002). Southern California Bight 1998 Regional Monitoring Program: V. Demersal Fishes and Megabenthic Invertebrates. Southern California Coastal Water Research Project, Westminster, CA.

Allen, M.J., T. Mikel, D.B. Cadien, J.E. Kalman, E.T. Jarvis, K.C. Schiff, D.W. Diehl, S.L. Moore, S. Walther, G. Deets, C. Cash, S. Watts, D.J. Pondella II, V. Raco-Rands, C. Thomas, R. Gartman, L. Sabin, W. Power, A.K. Groce, and J.L. Armstrong. (2007). Southern California Bight 2003 Regional Monitoring Program: IV. Demersal Fishes and Megabenthic Invertebrates. Southern California Coastal Water Research Project. Costa Mesa, CA.

Allen, M.J., D.B. Cadien, E. Miller, D.W. Diehl, K. Ritter, S.L. Moore, C. Cash, D.J. Pondella, V. Raco-Rands, C. Thomas, R. Gartman, W. Power, A.K. Latker, J. Williams, J.L. Armstrong, and K. Schiff. (2011). Southern California Bight 2008 Regional Monitoring Program: Volume IV. Demersal Fishes and Megabenthic Invertebrates. Southern California Coastal Water Research Project, Costa Mesa, CA.

Bolker, B., G.R. Warnes and T. Lumley (2022). gtools: Various R Programming Tools. R package version 3.9.4. https://CRAN.R-project.org/package=gtools

Brusca, R.C. (1978). Studies on the cymothoid fish symbionts of the eastern Pacific (Crustacea: Cymothoidae). II. Systematics and biology of Livoneca vulgaris Stimpson 1857. Occasional Papers of the Allan Hancock Foundation. (New Series), 2: 1–19.

Brusca, R.C. (1981). A monograph on the Isopoda Cymothoidae (Crustacea) of the eastern Pacific. Zoological Journal of the Linnean Society, 73: 117–199.

Chang, W. (2023). webshot: Take Screenshots of Web Pages. R package version 0.5.5. https://CRAN.R-project.org/package=webshot

City of San Diego. (1995). Outfall Extension Pre-Construction Monitoring Report (July 1991–October 1992). City of San Diego Ocean Monitoring Program, Metropolitan Wastewater Department, Environmental Monitoring and Technical Services Division, San Diego, CA.

City of San Diego. (1998). San Diego Regional Monitoring Report for 1994–1997. City of San Diego Ocean Monitoring Program, Metropolitan Wastewater Department, Environmental Monitoring and Technical Services Division, San Diego, CA.

City of San Diego. (2000). International Wastewater Treatment Plant Final Baseline Ocean Monitoring Report for the South Bay Ocean Outfall (1995–1998). City of San Diego Ocean Monitoring Program, Metropolitan Wastewater Department, Environmental Monitoring and Technical Services Division, San Diego, CA.

City of San Diego. (2019). Interim Receiving Waters Monitoring Report for the Point Loma Ocean Outfall and South Bay Ocean Outfalls, 2018. City of San Diego Ocean Monitoring Program, Public Utilities Department, Environmental Monitoring and Technical Services Division, San Diego, CA.

City of San Diego. (2020). Biennial Receiving Waters Monitoring and Assessment Report for the Point Loma and South Bay Ocean Outfalls, 2018–2019. City of San Diego Ocean Monitoring Program, Public Utilities Department, Environmental Monitoring and Technical Services Division, San Diego, CA.

City of San Diego. (2021). Interim Receiving Waters Monitoring Report for the Point Loma Ocean Outfall and South Bay Ocean Outfalls, 2020. City of San Diego Ocean Monitoring Program, Public Utilities Department, Environmental Monitoring and Technical Services Division, San Diego, CA.

City of San Diego. (2022). Appendix C.1 Benthic Sediments, Invertebrates, and Fishes. In: Application for Renewal of NPDES CA0107409 and 301(h) Modified Secondary Treatment Requirements Point Loma Ocean Outfall. Volume V, Appendix C. Public Utilities Department, Environmental Monitoring and Technical Services Division, San Diego, CA.

City of San Diego. (2025). Interim Receiving Waters Monitoring Report for the Point Loma Ocean Outfall and South Bay Ocean Outfalls, 2024. City of San Diego Ocean Monitoring Program, Public Utilities Department, Environmental Monitoring and Technical Services Division, San Diego, CA.

City of San Diego. (2026). Ocean Monitoring Program Reports and Data. https://www.sandiego.gov/public-utilities/sustainability/ocean-monitoring/reports

Clarke, K.R. (1993). Non-parametric multivariate analyses of changes in community structure. Australian Journal of Ecology, 18: 117–143.

Clarke, K.R., R.N. Gorley, P.J. Somerfield, and R.M. Warwick. (2014). Change in marine communities: an approach to statistical analysis and interpretation, 3rd edition. PRIMER-E, Plymouth, England.

Clarke, K.R., P.J. Somerfield, and R.N. Gorley. (2008). Testing of null hypotheses in exploratory community analyses: similarity profiles and biota-environment linkage. Journal of Experimental Marine Biology and Ecology, 366: 56–69.

Cross, J.N. and L.G. Allen. (1993). Chapter 9. Fishes. In: M.D. Dailey, D.J. Reish, and J.W. Anderson (eds.). Ecology of the Southern California Bight: A Synthesis and Interpretation. University of California Press, Berkeley, CA. 459–540.

Cross, J.N., J.N. Roney, and G.S. Kleppel. (1985). Fish food habits along a pollution gradient. California Fish and Game, 71: 28–39.

Eschmeyer, W.N. and E.S. Herald. (1998). A Field Guide to Pacific Coast Fishes of North America. Houghton and Mifflin Company, New York.

Gohel, D. (2023). officer: Manipulation of Microsoft Word and PowerPoint Documents. R package version 0.6.2. https://CRAN.R-project.org/package=officer

Gohel, D. and P. Skintzos (2023). flextable: Functions for Tabular Reporting. R package version 0.9.3. https://CRAN.R-project.org/package=flextable

Grolemund, G. and H. Wickham (2011). Dates and Times Made Easy with lubridate. Journal of Statistical Software, 40(3), 1-25. URL https://www.jstatsoft.org/v40/i03/

Helvey, M. and R.W. Smith. (1985). Influence of habitat structure on the fish assemblages associated with two cooling-water intake structures in southern California. Bulletin of Marine Science, 37: 189–199.

Hester, J. and J. Bryan (2022). glue: Interpreted String Literals. R package version 1.6.2. https://CRAN.R-project.org/package=glue

Hope, R. M. (2022). Rmisc: Ryan Miscellaneous. R package version 1.5. http://CRAN.R-project.org/package=Rmisc

Jensen, G.C. (2014). Crabs and Shrimps of the Pacific Coast. A Guide to Shallow Water Decapods from Southeastern Alaska to the Mexican Border. MolaMarine Publication. WA. 240 pp.

Karinen, J.B., B.L. Wing, and R.R. Straty. (1985). Records and sightings of fish and invertebrates in the eastern Gulf of Alaska and oceanic phenomena related to the 1983 El Niño event. In: W.S. Wooster and D.L. Fluharty (eds.). El Niño North: El Niño Effects in the Eastern Subarctic Pacific Ocean. Washington Sea Grant Program, Seattle, WA. 253–267.

Kassambara, A. (2023). ggpubr: Based Publication Ready Plots R package version 0.2. http://www.sthda.com/english/rpkgs/ggpubr

Lilly, M. (2004). *Octopus veligero*: Permanent Resident or Fair-Weather Friend? The Festivus. Vol XXXVI(1): pp 3-8.

Lin Pedersen, T. (2023). patchwork: The Composer of Plots. R package version 1.1.3. https://CRAN.R-project.org/package=patchwork

Miller, D. J. (2020). Miller and Lea's Guide to the Coastal Marine Fishes of California. United States: University of California Agriculture and Natural Resources.

Milton Bache, S. and H. Wickham (2022). magrittr: A Forward-Pipe Operator for R. R package version 2.0.3. https://CRAN.R-project.org/package=magrittr

Murawski, S.A. (1993). Climate change and marine fish distribution: forecasting from historical analogy. Transactions of the American Fisheries Society, 122: 647–658.

[NOAA/NWS] National Oceanic and Atmospheric Administration/National Weather Service. (2022). Climate Prediction Center Website. https://origin.cpc.ncep.noaa.gov/products/analysis_monitoring/ensostuff/ONI_v5.php

Oksanen, J., F.G. Blanchet, R. Kindt, P. Legendre, P.R. Minchin, R.B. O'Hara, G.L. Simpson, P. Solymos, M. Henry, H. Stevens and H. Wagner. (2022). vegan: Community Ecology Package. R package version 2.3-0. http://CRAN.R-project.org/package=vegan

Page, L., M., H. Espinosa-Pérez, L. T. Findley, C. R. Gilbert, R. N. Lea, N. E. Mandrak, R. L. Mayden, and J. S. Nelson. (2013). Common and Scientific names of fishes from the United States, Canada and Mexico. Special Publication 34. The American Fisheries Society, Bethesda, Maryland.

R Core Team. (2021). R: A language and environment for statistical computing. R Foundation for Statistical Computing, Vienna, Austria. URL https://www.R-project.org/

Ripley, B. and M. Lapsley. (2022). RODBC: ODBC Database Access. R package version 1.3-12. http://CRAN.R-project.org/package=RODBC

[SCAMIT] Southern California Association of Marine Invertebrate Taxonomists. (2023). A taxonomic listing of benthic macro- and megainvertebrates from infaunal and epibenthic monitoring programs in the Southern California Bight, edition 14. Southern California Associations of Marine Invertebrate Taxonomists, Natural History Museum of Los Angeles County, Research and Collections, Los Angeles, CA.

[SCCWRP] Southern California Coastal Water Research Project. (2018). Southern California Bight 2018 Regional Monitoring Program: Contaminant Impact Assessment Field Operations Manual. Southern California Coastal Water Research Project. Costa Mesa, CA.

[SCCWRP] Southern California Coastal Water Research Project. (2023). Southern California Bight 2023 Regional Monitoring Program: Sediment Quality Assessment Workplan. Southern California Coastal Water Research Project. Costa Mesa, CA.

Stein, E.D. and D.B. Cadien. (2009). Ecosystem response to regulatory and management actions: The southern California experience in long-term monitoring. Marine Pollution Bulletin, 59: 91–100.

Thompson, B., J. Dixon, S. Schroeter, and D.J. Reish. (1993a). Chapter 8. Benthic invertebrates. In: M.D. Dailey, D.J. Reish, and J.W. Anderson (eds.). Ecology of the Southern California Bight: A Synthesis and Interpretation. University of California Press, Berkeley, CA. 369–458.

Thompson, B., D. Tsukada, and J. Laughlin. (1993b). Megabenthic assemblages of coastal shelves, slopes, and basins off Southern California. Bulletin of the Southern California Academy of Sciences, 92: 25–42.

Walther, S.M., J.P. Williams, A. Latker, D.B. Cadien, D.W. Diehl, K. Wisenbaker, E. Miller, R. Gartman, C. Stransky and K. Schiff. (2017). Southern California Bight 2013 Regional Monitoring Program: Volume VII. Demersal Fishes and Megabenthic Invertebrates. Southern California Coastal Water Research Project. Costa Mesa, CA.

Warwick, R.M. (1993). Environmental impact studies on marine communities: pragmatical considerations. Australian Journal of Ecology, 18: 63–80.

Wickham, H. (2007). Reshaping Data with the reshape Package. Journal of Statistical Software, 21(12), 1-20. URL http://www.jstatsoft.org/v21/i12/

Wickham, H., J. Hester, W. Chang and J. Bryan (2022). devtools: Tools to Make Developing R Packages Easier. R package version 2.4.5. https://CRAN.R-project.org/package=devtools

Wisenbaker, K., K. McLaughlin, D. Diehl, A. Latker, K. Stolzenbach, R. Gartman, K. Schiff. (2021). Southern California Bight 2018 Regional Monitoring Program: Volume IV. Demersal Fishes and Megabenthic Invertebrates. Technical Report #1183. Southern California Coastal Water Research Project. Costa Mesa, CA.

CHAPTER 8

FIGURES & TABLES

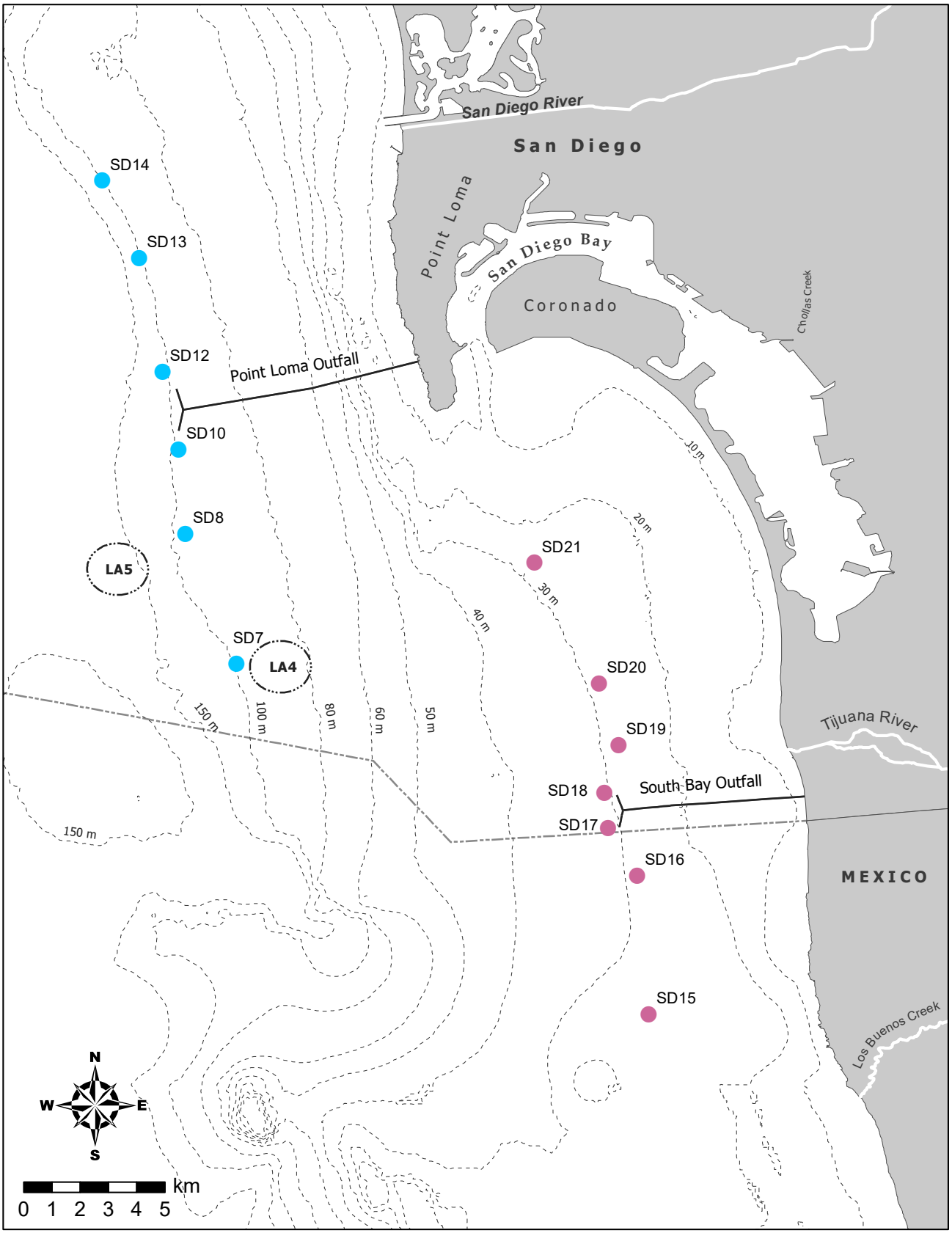


Figure 8.1
Trawl station locations sampled around the Point Loma and South Bay Ocean Outfalls as part of the City of San Diego's Ocean Monitoring Program.

Table 8.1

Top 10 most abundant demersal fish species collected from 24 trawls conducted in the PLOO region during 2024 and 2025. PA = percent abundance; FO = frequency of occurrence; MAH = mean abundance per haul; MAO = mean abundance per occurrence.

Species	PA	FO	MAH	MAO
Pacific Sanddab	46	100	338	338
Longspine Combfish	14	96	106	111
Halfbanded Rockfish	10	100	74	74
Longfin Sanddab	6	96	42	44
Dover Sole	5	100	34	34
Shortspine Combfish	4	100	31	31
Stripetail Rockfish	4	75	29	39
Yellowchin Sculpin	3	54	24	44
California Lizardfish	1	54	8	15
California Tonguefish	1	100	11	11

Table 8.2

Top 10 most abundant demersal fish species collected from 28 trawls conducted in the SBOO region during 2024 and 2025. PA = percent abundance; FO = frequency of occurrence; MAH = mean abundance per haul; MAO = mean abundance per occurrence.

Species	PA	FO	MAH	MAO
Speckled Sanddab	44	100	135	135
California Lizardfish	20	86	62	72
Longfin Sanddab	16	82	48	59
Kelp Pipefish	4	18	11	63
California Tonguefish	3	93	8	8
English Sole	3	71	9	13
Hornyhead Turbot	2	86	6	6
Longspine Combfish	2	39	7	17
Roughback Sculpin	2	79	6	7
Yellowchin Sculpin	2	39	5	13

Table 8.3

Summary of demersal fish community parameters for PLOO and SBOO trawl stations sampled during 2024 and 2025. Data are included for species richness, abundance, diversity (H'), and biomass (kg, wet weight).

			Richness		*Abundance*		*Diversity*		*Biomass*	
Region	**Year**	**Station**	**Winter**	**Summer**	**Winter**	**Summer**	**Winter**	**Summer**	**Winter**	**Summer**
PLOO	2024	SD7	19	13	344	322	2.0	1.2	7.5	7.7
		SD8	18	16	648	369	1.9	1.4	18.9	10.6
		SD10	21	15	1,260	357	1.4	1.4	28.1	7.6
		SD12	18	17	1,134	490	1.8	1.6	16.8	13.1
		SD13	19	14	451	270	1.9	1.4	9.2	5.9
		SD14	16	13	506	282	2.0	1.5	7.4	22.6
	2025	SD7	18	14	681	596	2.0	1.4	14.3	9.3
		SD8	20	21	743	708	1.6	1.6	27.4	14.2
		SD10	22	17	1,581	783	1.7	1.5	16.0	11.1
		SD12	20	22	1,327	942	1.4	1.5	24.4	15.4
		SD13	22	21	914	1,150	1.6	1.5	17.6	22.3
		SD14	22	16	984	902	1.7	1.6	14.7	11.0
SBOO	2024	SD15	9	10	21	114	1.9	1.0	1.9	4.8
		SD16	11	9	63	140	1.7	1.5	3.0	9.6
		SD17	13	11	81	116	2.0	1.5	5.7	7.4
		SD18	13	16	83	506	1.7	1.2	9.0	15.6
		SD19	5	12	37	379	1.2	1.8	1.0	22.2
		SD20	6	13	86	364	1.2	1.5	1.0	14.9
		SD21	8	16	29	412	1.6	1.6	4.7	12.9
	2025	SD15	6	9	111	404	1.1	1.0	1.2	9.0
		SD16	14	12	306	625	1.7	1.5	7.5	20.7
		SD17	18	12	313	644	1.9	1.4	8.7	13.4
		SD18	9	11	96	611	1.8	1.3	7.6	16.7
		SD19	7	13	61	571	1.5	1.4	1.4	24.9
		SD20	14	13	736	567	1.2	1.4	11.5	17.4
		SD21	15	15	401	790	1.5	1.6	8.7	13.1

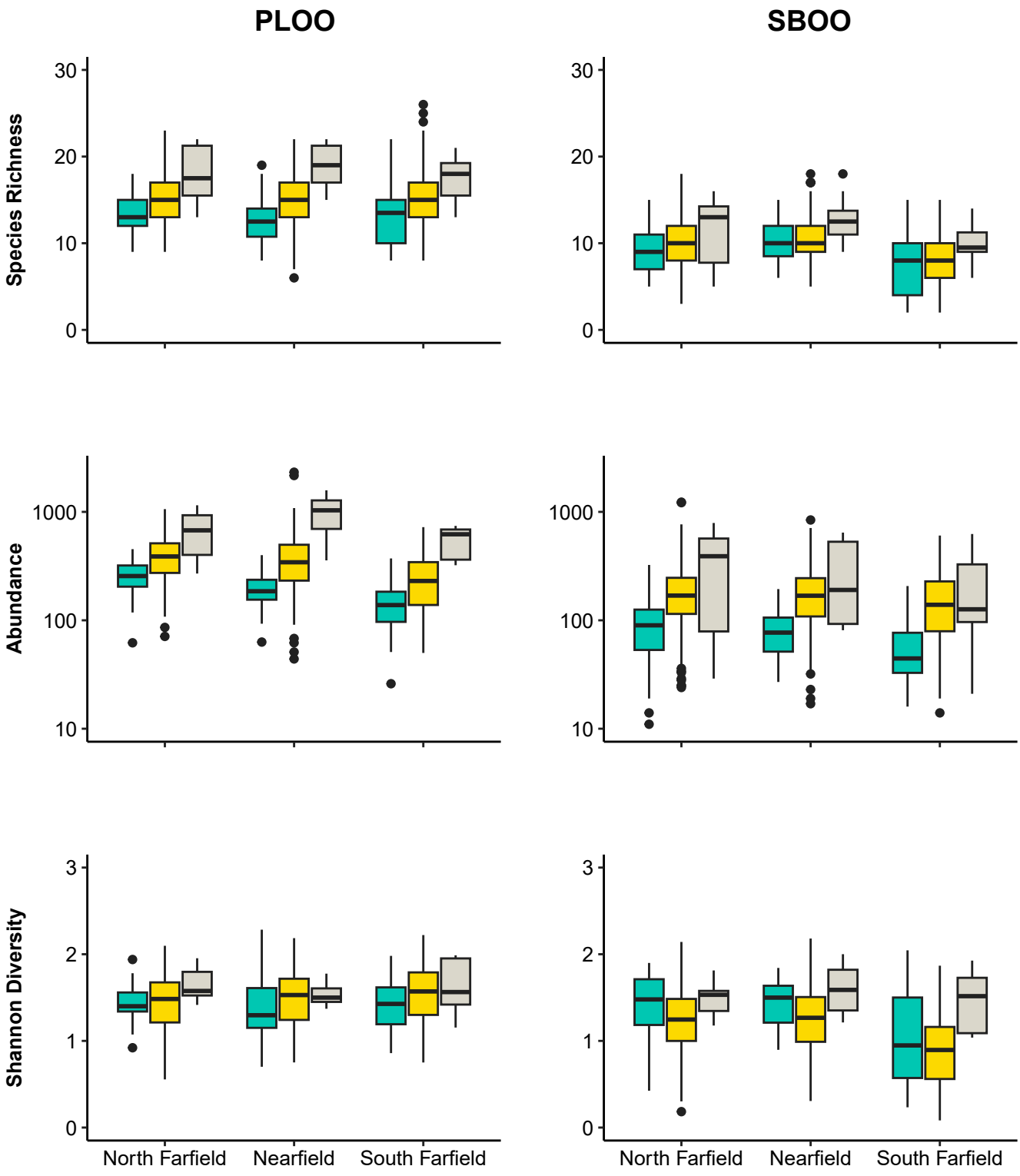


Figure 8.2
Species richness, abundance, and diversity (H') of demersal fishes collected from PLOO and SBOO north farfield, near-ZID, and south farfield stations during pre-discharge (green), historical post-discharge (yellow), and during 2024–2025 (grey). Data limited to 10-minute trawls. Boxes = median, upper, and lower quantiles; whiskers = 1.5x interquantile range; circles = outliers; see text for description of pre- versus post-discharge periods for the two outfalls.

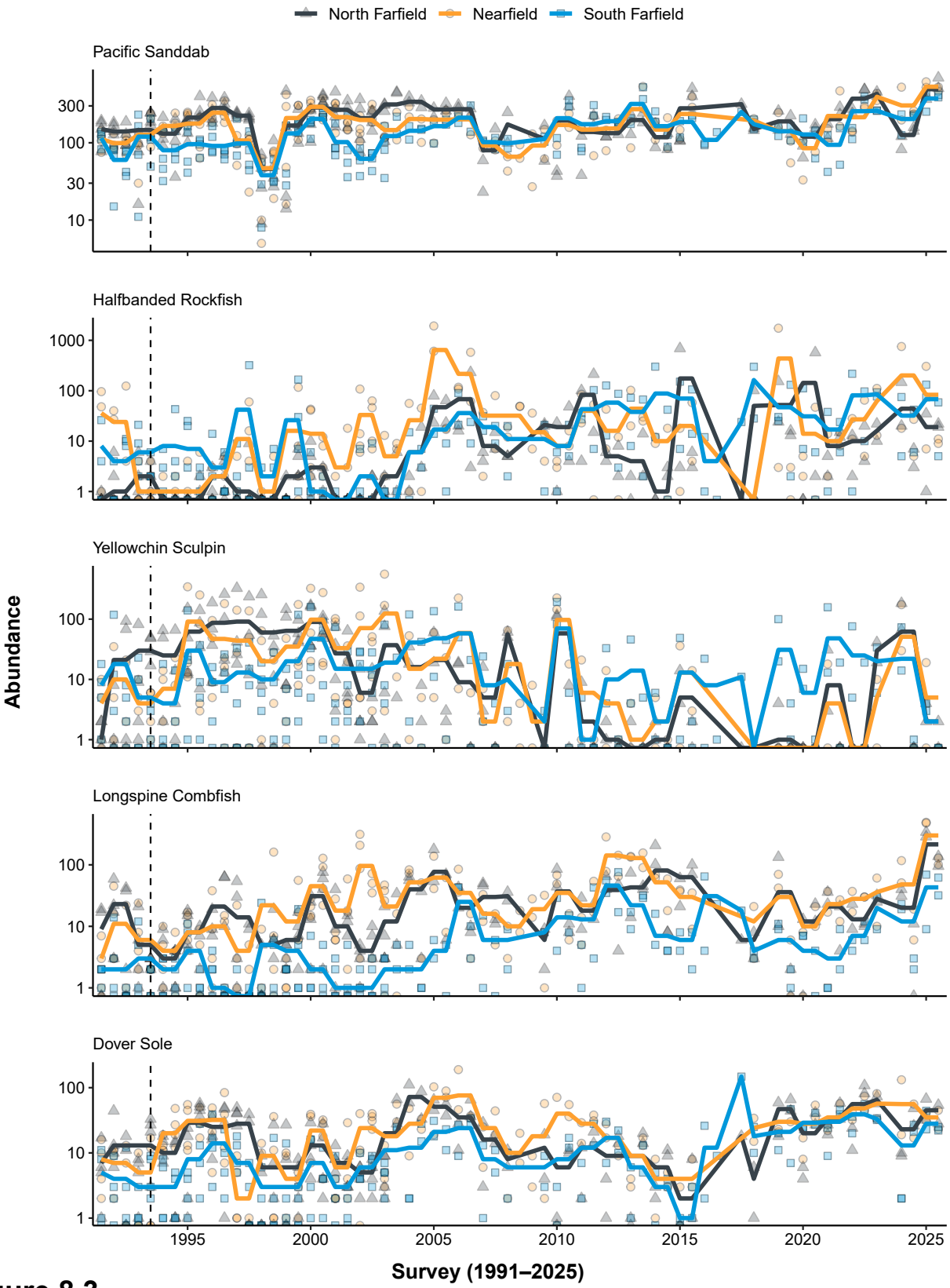


Figure 8.3

The ten most abundant demersal fish species (presented in order) collected from PLOO trawl stations sampled from 1991 through 2025. Data are limited to 10-minute trawls and are presented as quarterly means (lines) and total values per haul for north farfield (triangles), near-ZID (circles), and south farfield (squares) stations. Dashed lines indicate onset of wastewater discharge.

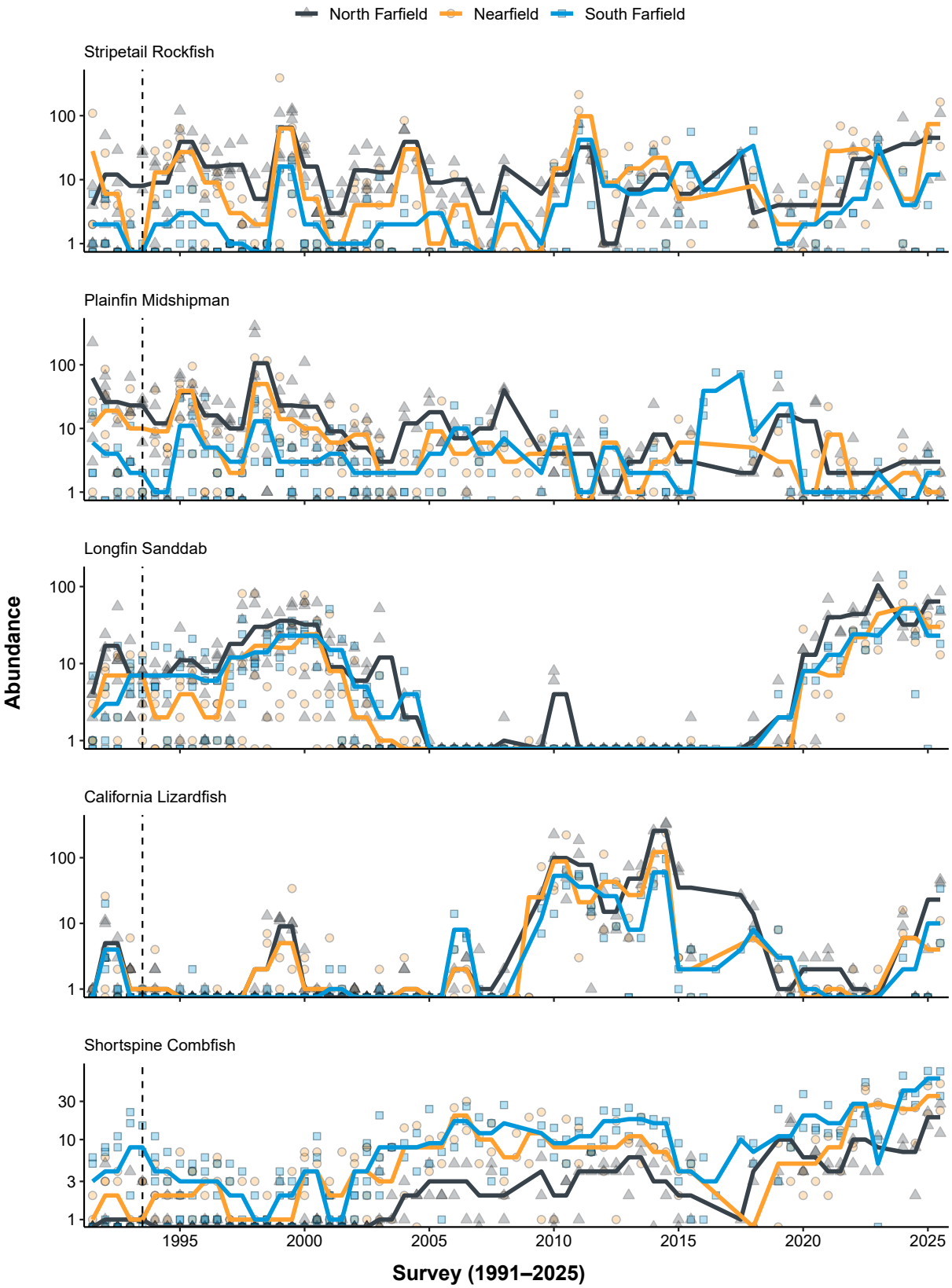


Figure 8.3 *continued*

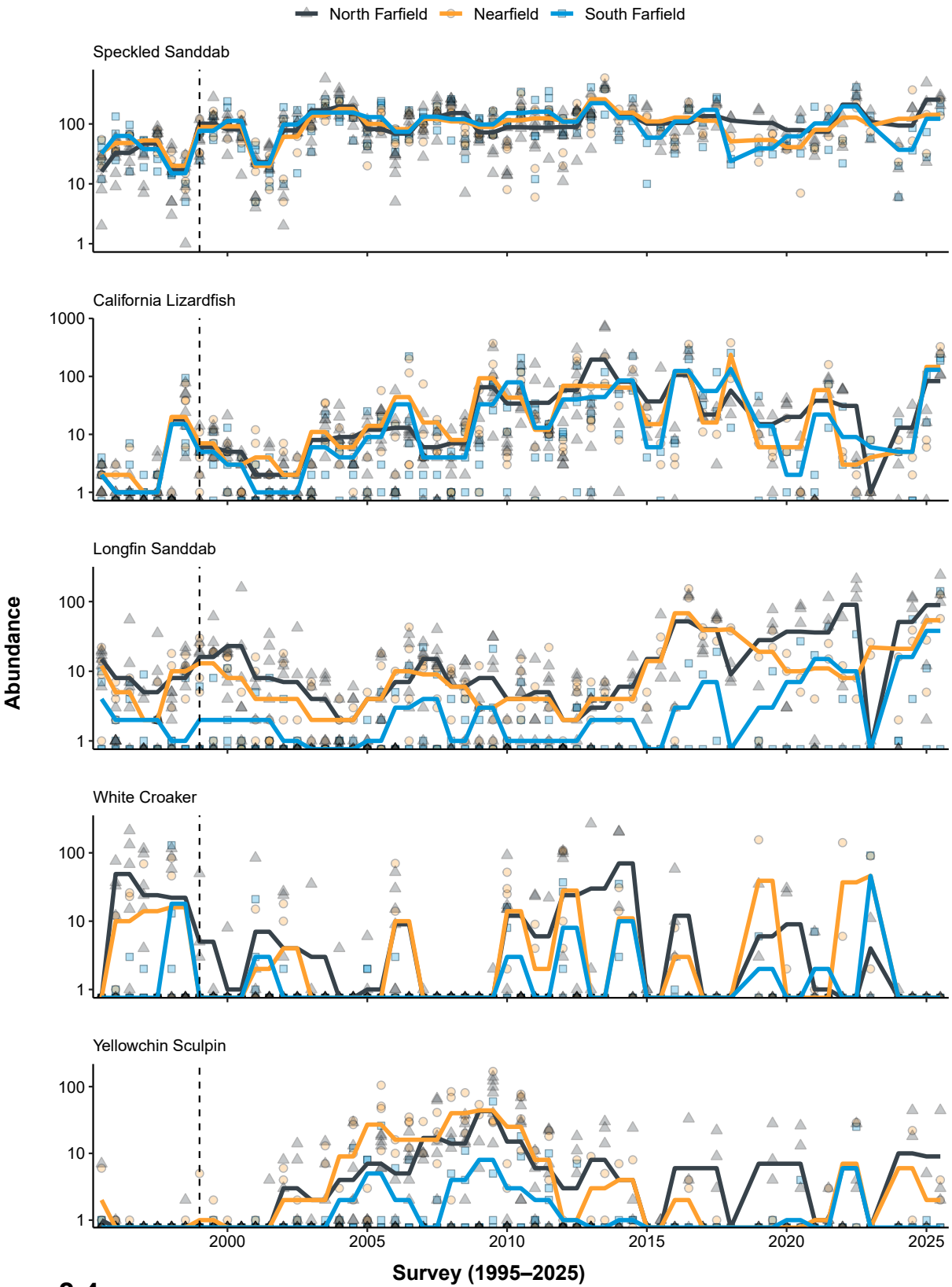


Figure 8.4

The ten most abundant demersal fish species (presented in order) collected from SBOO trawl stations sampled from 1995 through 2025. Data are limited to 10-minute trawls and are presented as quarterly means (lines) and total values per haul for north farfield (triangles), near-ZID (circles), and south farfield (squares) stations. Dashed lines indicate onset of wastewater discharge.

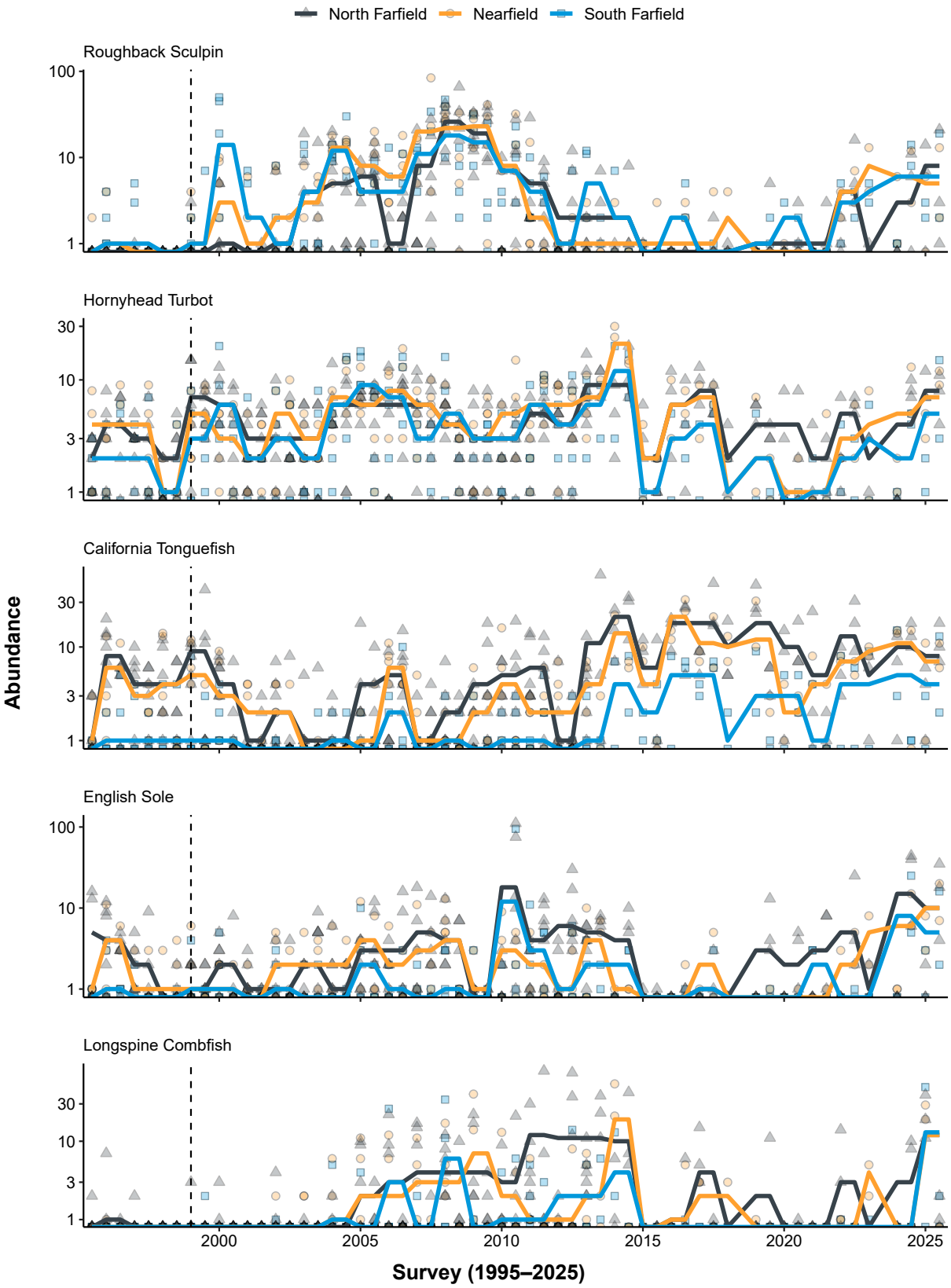


Figure 8.4 *continued*

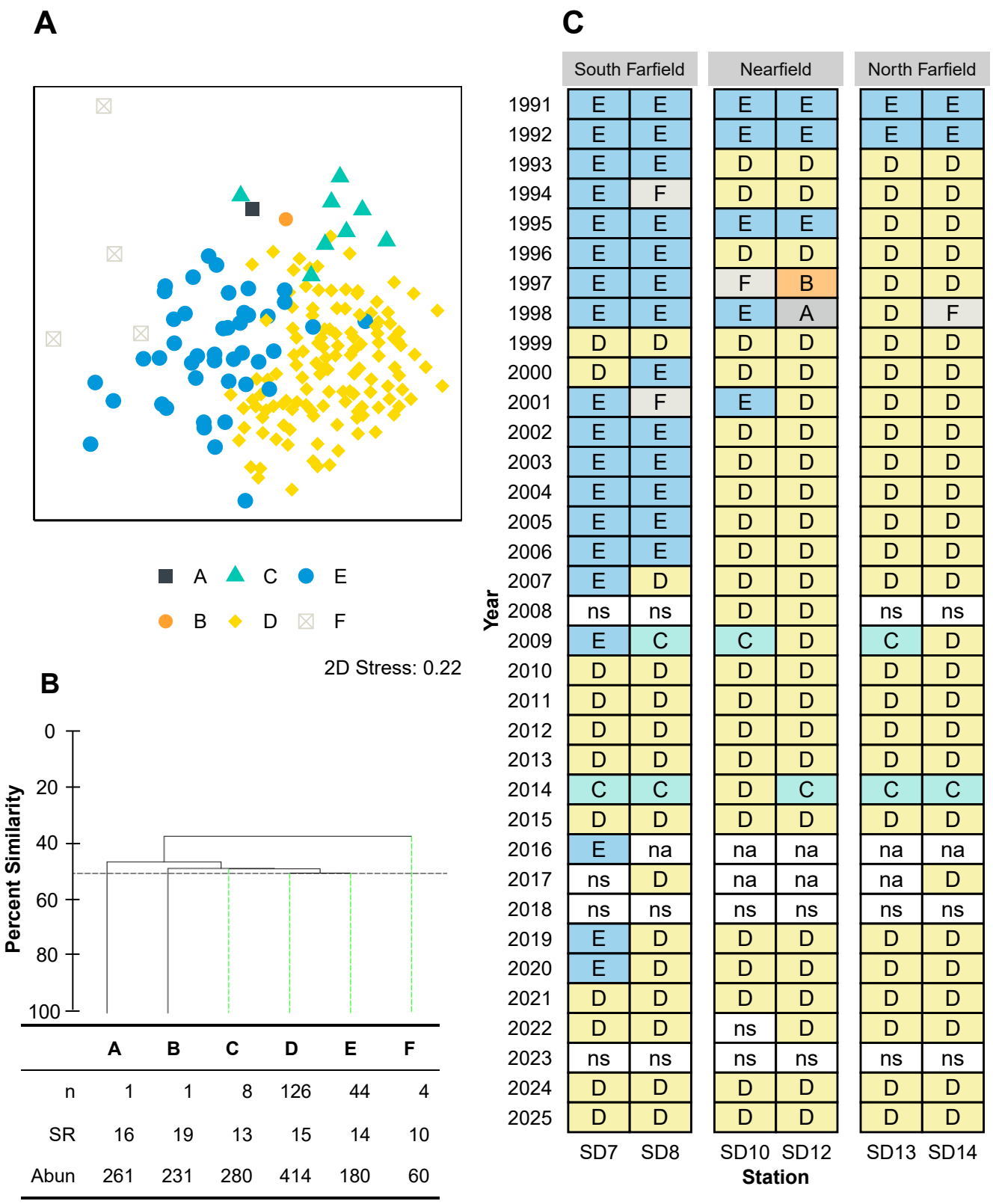


Figure 8.5

Results of ordination and cluster analysis of demersal fish assemblages from PLOO trawl stations sampled from 1991 through 2025. Data are limited to 10-minute trawls from summer surveys and presented as (A) nMDS ordination; (B) a dendrogram of main cluster groups; (C) a matrix showing distribution of cluster groups over time; n = number of hauls; SR = mean species richness; Abun = mean abundance; na = not analyzed; ns=not sampled.

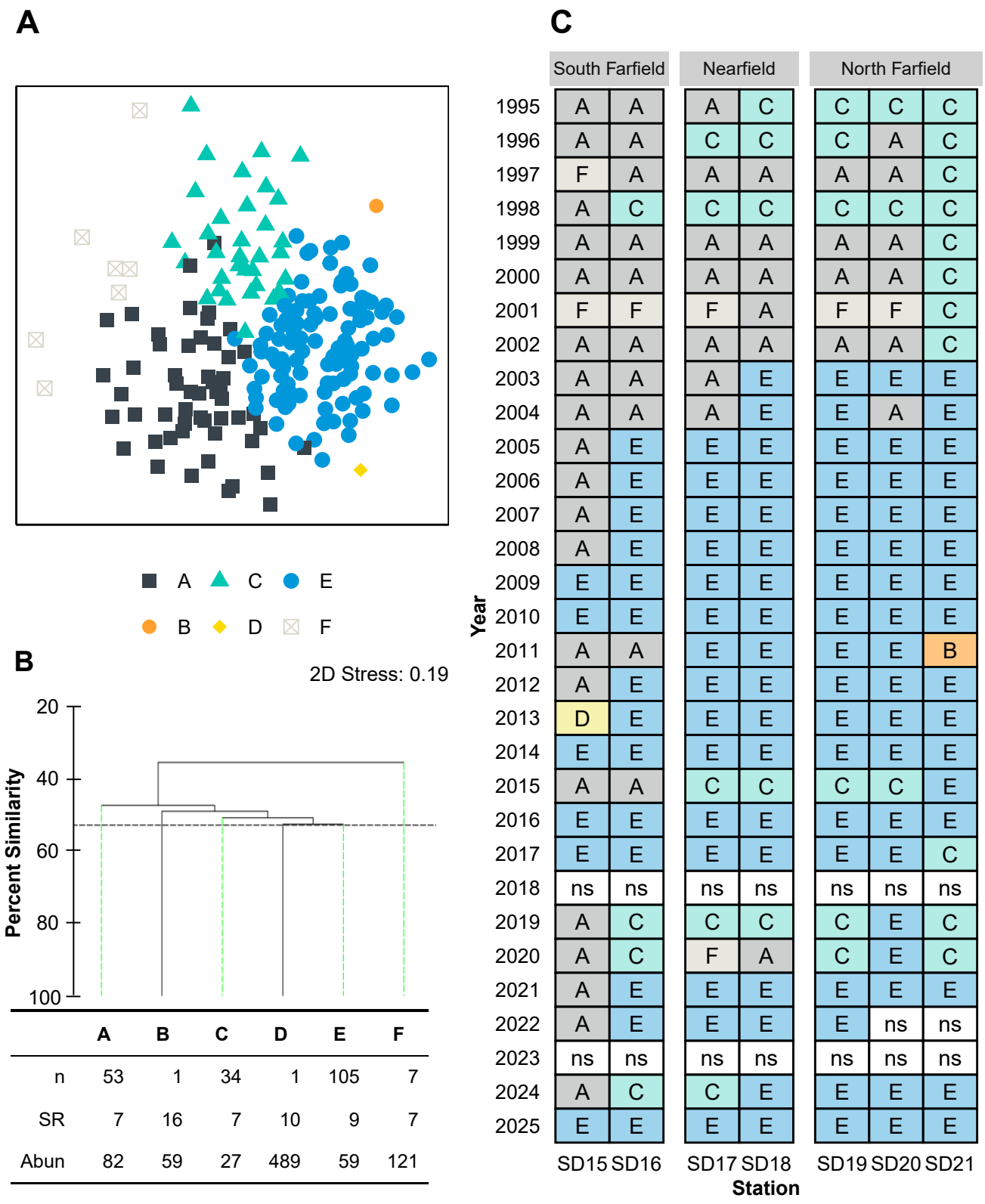


Figure 8.6

Results of ordination and cluster analysis of demersal fish assemblages from SBOO trawl stations sampled from 1995 through 2025. Data are limited to 10-minute trawls from summer surveys and presented as (A) nMDS ordination; (B) a dendrogram of main cluster groups; (C) a matrix showing distribution of cluster groups over time; n = number of hauls; SR = mean species richness; Abun = mean abundance; ns = not sampled.

Table 8.4

Top 10 most abundant megabenthic invertebrate species collected from 24 trawls conducted in the PLOO region during 2024 and 2025. PA = percent abundance; FO = frequency of occurrence; MAH = mean abundance per haul; MAO = mean abundance per occurrence.

Species	PA	FO	MAH	MAO
Lytechinus pictus	98	100	2053	2053
Astropecten californicus	1	96	20	21
Acanthoptilum sp	<1	46	1	2
Adelogorgia phyllosclera	<1	12	<1	1
Antiplanes catalinae	<1	21	<1	1
Aphrodita refulgida	<1	8	<1	1
Apostichopus californicus	<1	62	2	3
Astropecten ornatissimus	<1	8	<1	1
Baptodoris mimetica	<1	4	<1	1
Calliostoma turbinum	<1	4	<1	1

Table 8.5

Top 10 most abundant megabenthic invertebrate species collected from 28 trawls conducted in the SBOO region during 2024 and 2025. PA = percent abundance; FO = frequency of occurrence; MAH = mean abundance per haul; MAO = mean abundance per occurrence.

Species	PA	FO	MAH	MAO
Astropecten californicus	74	100	67	67
Crangon nigromaculata	3	46	3	6
Lytechinus pictus	3	39	2	6
Ophiothrix spiculata	3	50	2	5
Sicyonia penicillata	3	64	3	5
Luidia armata	2	68	2	3
Philine auriformis	2	18	2	11
Hemisquilla californiensis	1	29	<1	2
Lovenia cordiformis	1	11	1	7
Pagurus spilocarpus	1	32	1	3

Table 8.6

Summary of megabenthic invertebrate community parameters for PLOO and SBOO trawl stations sampled during 2024 and 2025. Data are included for species richness, abundance, diversity (H').

			Richness		*Abundance*		*Diversity*	
Region	**Year**	**Station**	**Winter**	**Summer**	**Winter**	**Summer**	**Winter**	**Summer**
PLOO	2024	SD7	9	11	1,328	2,095	0.2	0.2
		SD8	8	13	2,604	4,167	0.0	0.1
		SD10	16	9	81	1,250	2.0	0.2
		SD12	8	12	27	289	1.5	0.7
		SD13	13	8	36	686	2.3	0.2
		SD14	7	8	25	156	1.7	0.5
	2025	SD7	11	11	5,435	2,891	0.1	0.2
		SD8	15	21	5,469	8,523	0.1	0.1
		SD10	19	9	307	2,408	1.3	0.1
		SD12	9	9	3,859	3,116	0.1	0.1
		SD13	11	13	859	2,701	0.2	0.1
		SD14	12	10	1,464	658	0.3	0.3
SBOO	2024	SD15	11	7	56	57	1.4	0.9
		SD16	8	5	21	15	1.8	0.9
		SD17	10	5	22	16	1.9	1.0
		SD18	12	9	55	76	1.8	1.5
		SD19	6	5	45	116	1.3	0.3
		SD20	6	3	36	59	1.2	0.3
		SD21	8	7	17	52	1.9	1.1
	2025	SD15	8	9	56	244	1.4	0.7
		SD16	8	8	50	174	1.6	0.7
		SD17	14	17	45	91	1.9	1.7
		SD18	8	14	55	111	1.3	1.2
		SD19	8	6	127	361	1.1	0.1
		SD20	7	7	268	99	0.3	0.5
		SD21	13	7	169	29	1.5	1.0

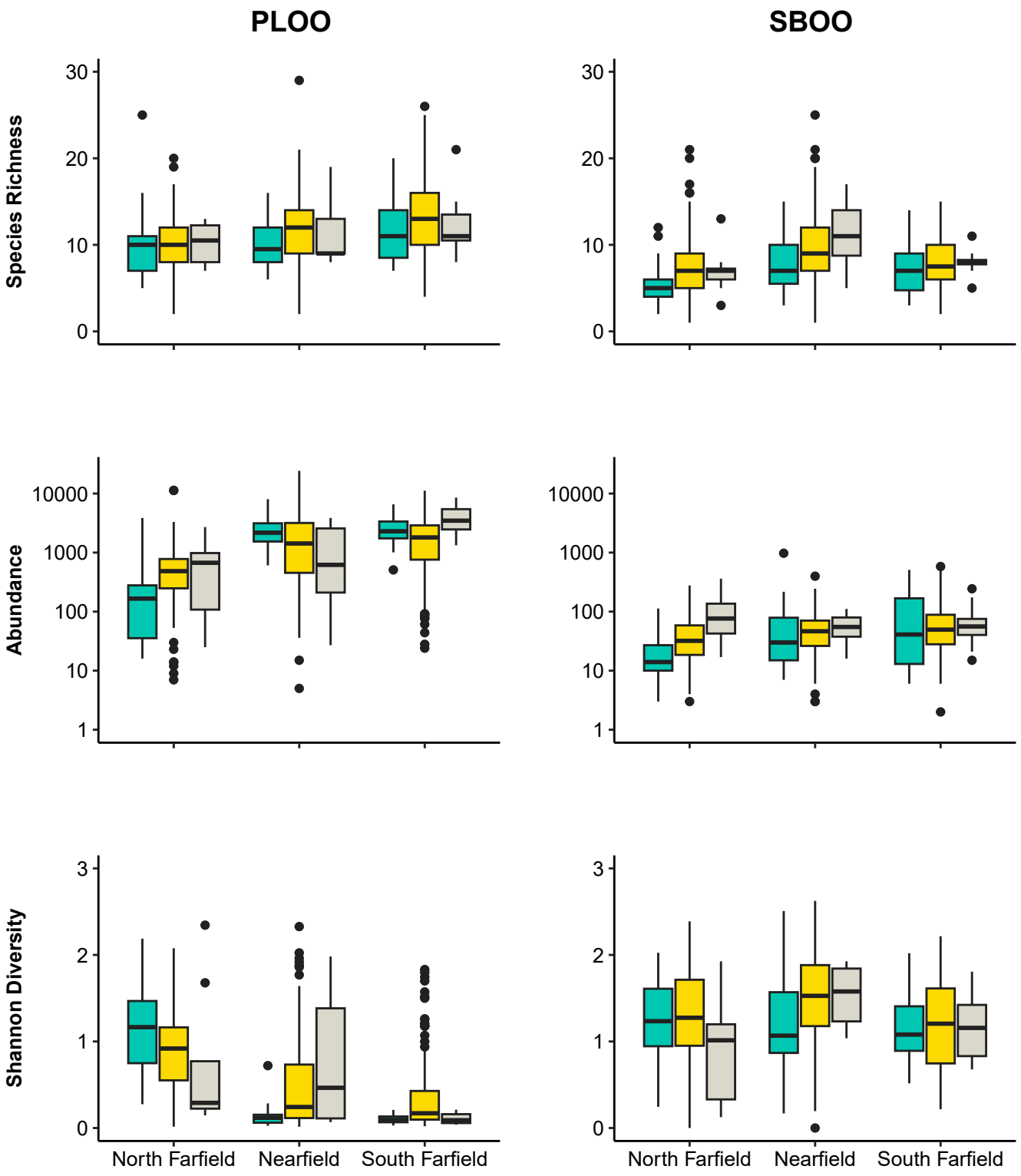


Figure 8.7

Species richness, abundance, and diversity (H') of megabenthic invertebrates collected from PLOO and SBOO north farfield, near-ZID, and south farfield stations during pre-discharge (green), historical post-discharge (yellow), and 2024–2025 (grey). Data limited to 10-minute trawls. Boxes = median, upper, and lower quantiles; whiskers = 1.5x interquantile range; circles = outliers; see text for description of pre- versus post-discharge periods for the two outfalls.

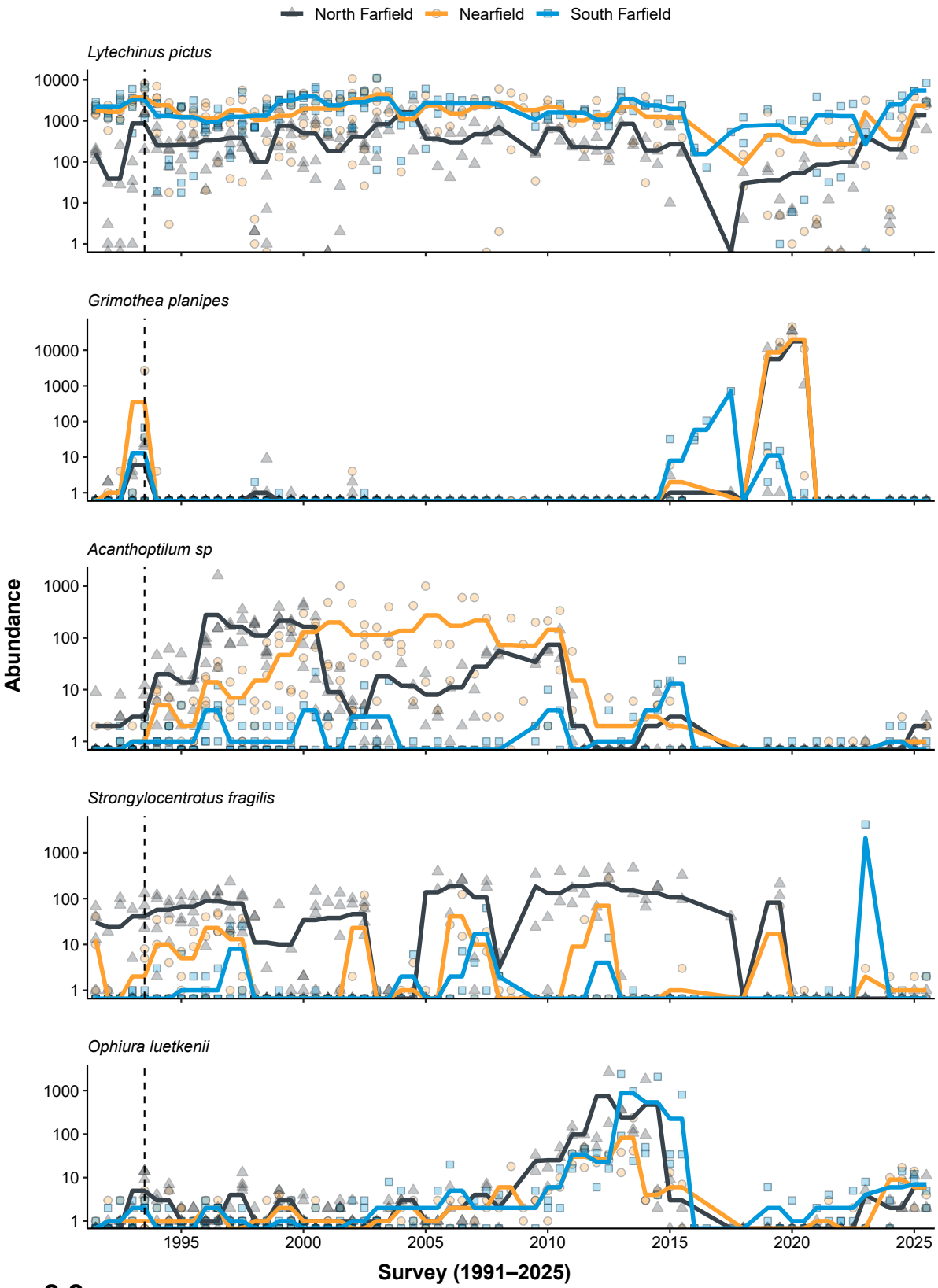


Figure 8.8

The ten most abundant megabenthic invertebrate species (presented in order) collected from PLOO trawl stations sampled from 1991 through 2025. Data are limited to 10-minute trawls and are presented as quarterly means (lines) and total values per haul for north farfield (triangles), near-ZID (circles), and south farfield (squares) stations. Dashed lines indicate onset of wastewater discharge.

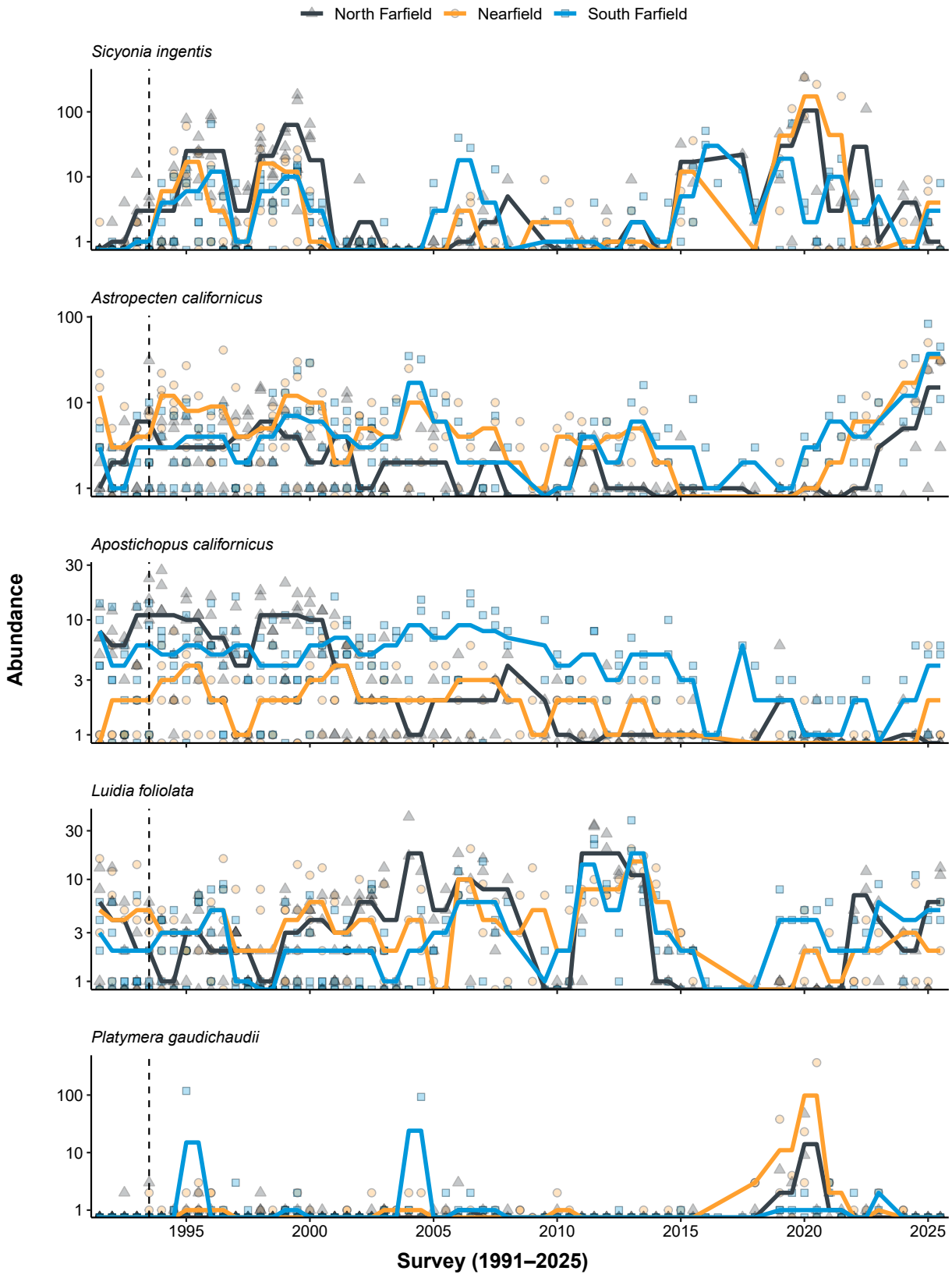


Figure 8.8 *continued*

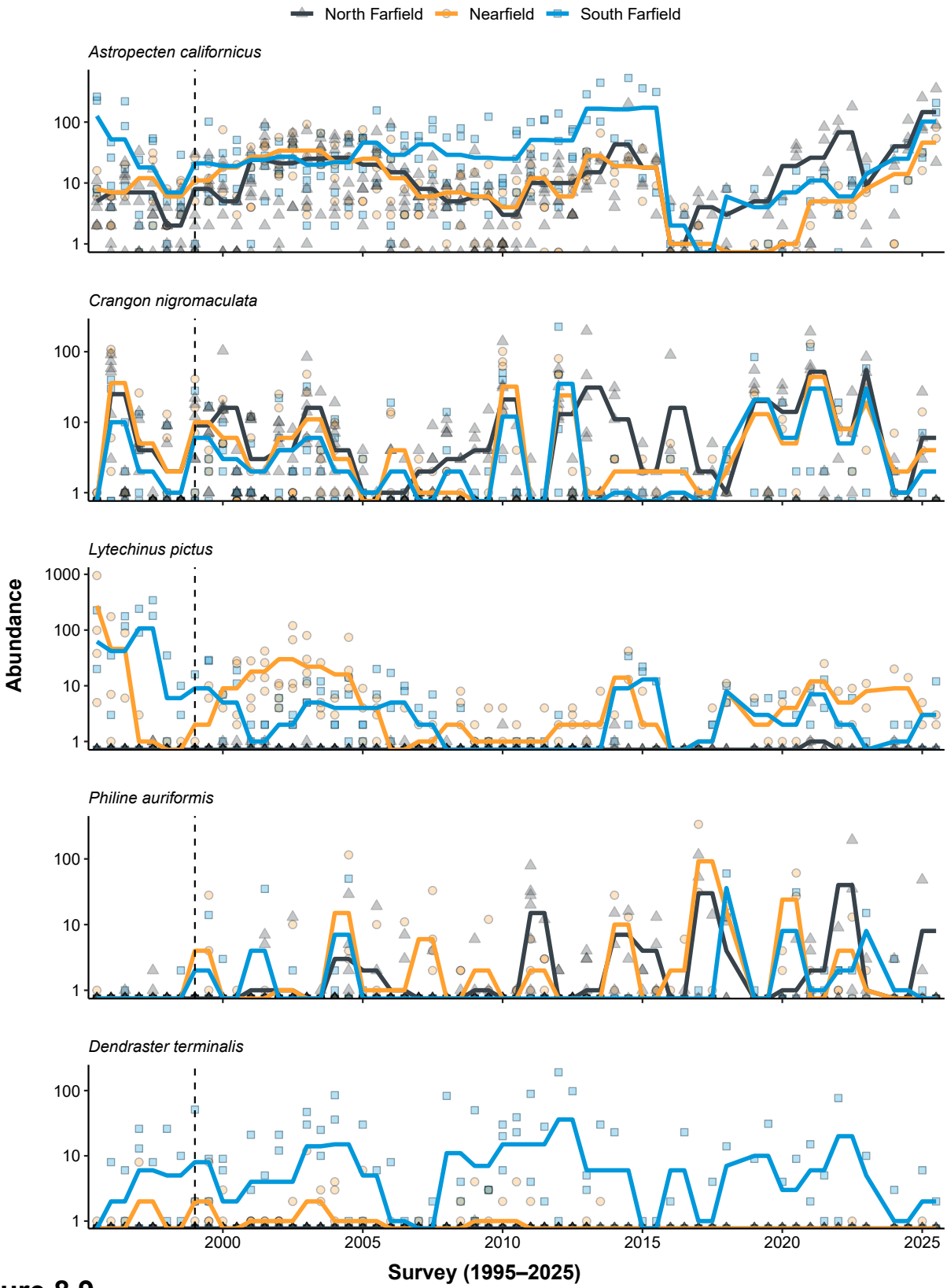


Figure 8.9
The ten most abundant megabenthic invertebrate species (presented in order) collected from SBOO trawl stations sampled from 1995 through 2025. Data are limited to 10-minute trawls and are presented as quarterly means (lines) and total values per haul for north farfield (triangles), near-ZID (circles), and south farfield (squares) stations. Dashed lines indicate onset of wastewater discharge.

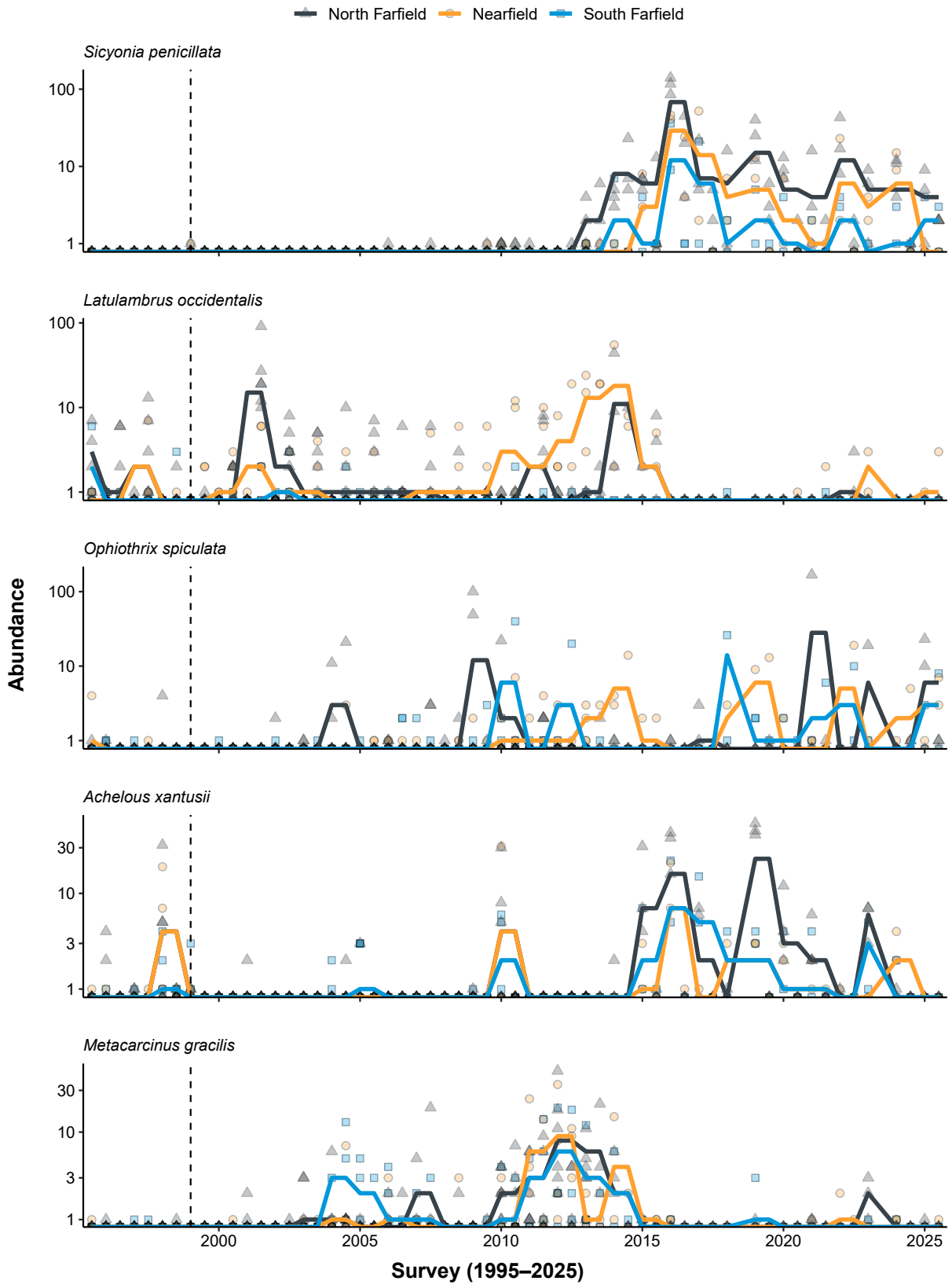


Figure 8.9 *continued*

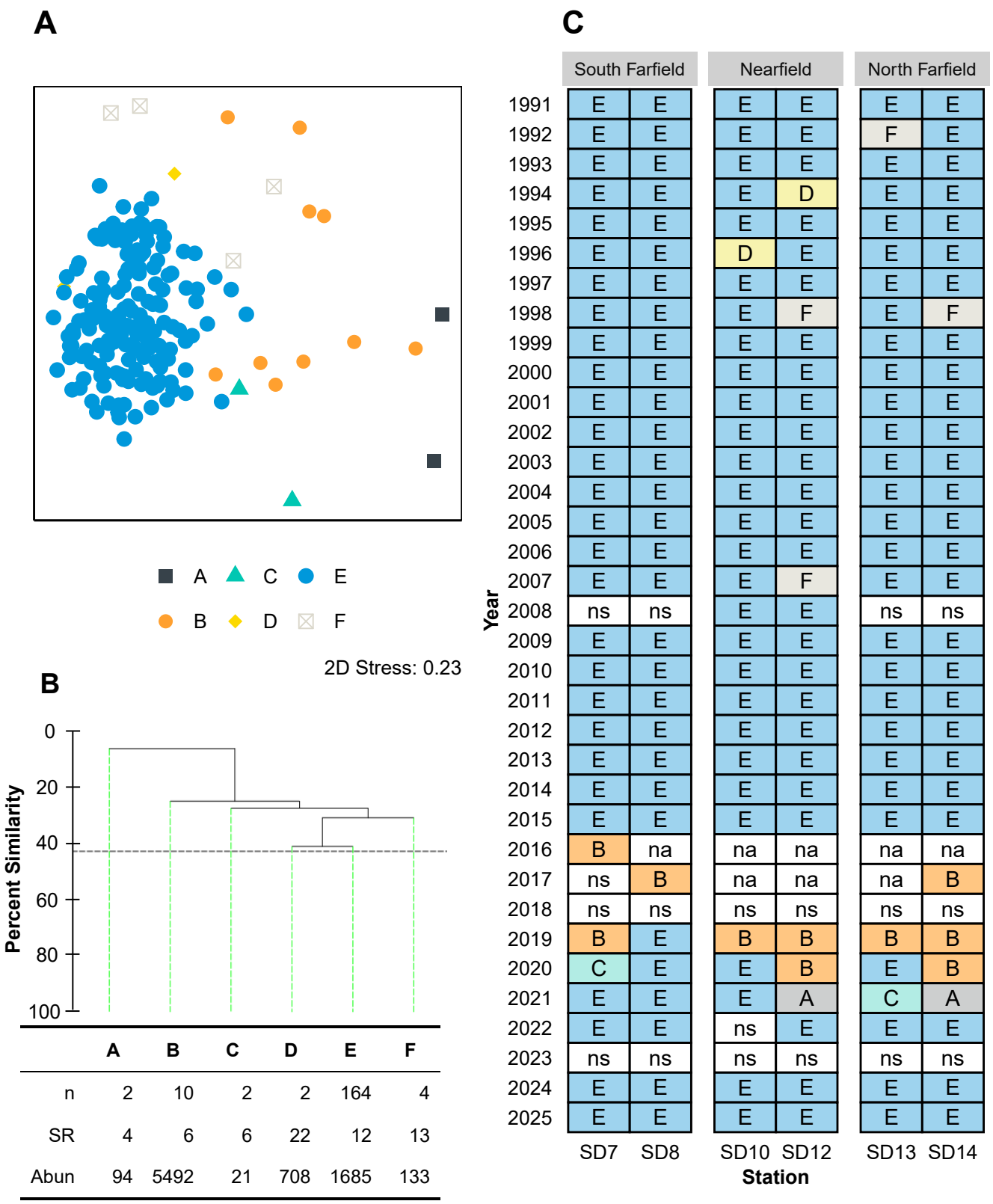


Figure 8.10

Results of ordination and cluster analysis of megabenthic invertebrate assemblages from PLOO trawl stations sampled from 1991 through 2025. Data are limited to 10-minute trawls from summer surveys and presented as (A) nMDS ordination; (B) a dendrogram of main cluster groups; (C) a matrix showing distribution of cluster groups over time; n = number of hauls; SR = mean species richness; Abun = mean abundance; na = not analyzed; ns=not sampled.

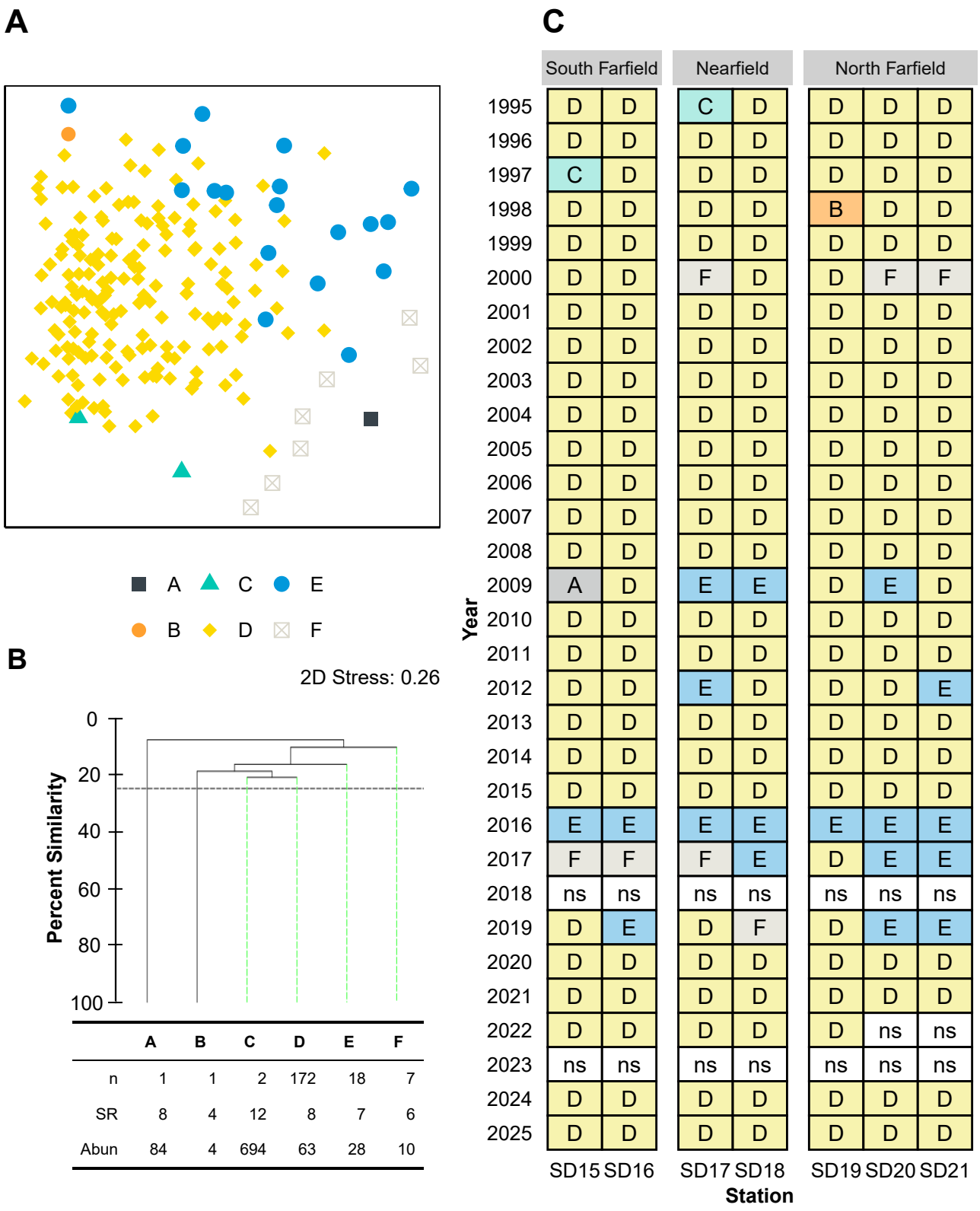


Figure 8.11

Results of ordination and cluster analysis of megabenthic invertebrate assemblages from SBOO trawl stations sampled from 1995 through 2025. Data are limited to 10-minute trawls from summer surveys and presented as (A) nMDS ordination; (B) a dendrogram of main cluster groups; (C) a matrix showing distribution of cluster groups over time; n = number of hauls; SR = mean species richness; Abun = mean abundance; ns=not sampled.

Chapter 9
Contaminants in Marine Fishes

Chapter 9. Contaminants in Marine Fishes

Introduction

Bottom dwelling (demersal) fishes are collected by the City of San Diego (City) as part of the Ocean Monitoring Program to evaluate the presence of contaminants in their tissues, which may result from the discharge of wastewater through the Point Loma Ocean Outfall (PLOO) and South Bay Ocean Outfall (SBOO). Anthropogenic inputs to coastal waters can result in increased concentrations of pollutants within the local marine environment, which may subsequently accumulate in the tissues of fishes and their prey. Such accumulation occurs through the biological uptake and retention of chemicals derived via various exposure pathways, including the absorption of dissolved chemicals directly from seawater, and the ingestion/assimilation of pollutants contained in different food sources (Connell 1988, Cardwell 1991, Rand 1995, USEPA 2000). In addition, demersal fishes may accumulate contaminants through the ingestion of suspended particulates or sediments because of their proximity to the seafloor. For this reason, contaminant levels in the tissues of these bottom dwelling fishes throughout the Southern California Bight (SCB) are often linked to those found in the surrounding environment (Schiff and Allen 1997), thus making these types of assessments useful in biomonitoring programs.

This portion of the City's Ocean Monitoring Program consists of two components: (1) analyzing liver tissues from mostly trawl-caught fishes; (2) analyzing muscle tissues from fishes collected by hook and line (rig fishing). Species targeted by trawling activities (see Chapter 8) are considered representative of the general demersal fish community off San Diego. The chemical analysis of liver tissues in target species of these fishes is important for assessing population effects because this is the organ where contaminants typically bioaccumulate. In contrast, species targeted for capture by rig fishing represent fish that are more characteristic of a typical sport fisher's catch and are therefore considered to be of recreational and commercial importance, and thus directly relevant to human health concerns. Consequently, muscle samples are analyzed from these fishes as this is the tissue most often consumed by humans. All liver and muscle tissue samples collected were analyzed for contaminants specified in the National Pollutant Discharge Elimination System (NPDES) discharge permits that govern monitoring requirements for the PLOO and SBOO regions (see Chapter 1).

This chapter presents analysis and interpretation of all chemical analyses performed on the tissues of fishes collected in the PLOO and SBOO regions during 2024 and 2025. The primary goals of this chapter are to: (1) document levels of contaminant loading in local demersal fishes to establish if concentrations accumulate to levels that may degrade marine communities and/or be harmful to human health; (2) identify whether any contaminant bioaccumulation detected in local fishes is changing over time and if the health of fish is changing as a result; (3) identify potential natural and anthropogenic sources of pollutants to the San Diego coastal marine environment that may play a role in contaminant bioaccumulation.

Materials and Methods

Fishes were collected in fall (October) 2024 and 2025 from a total of nine trawl zones (TZ1–TZ9) and four rig fishing zones (RF1–RF4) that span the PLOO and SBOO monitoring regions (Figure 9.1). Each trawl zone represents an area centered on (within a 1-km radius of) one or two trawl stations as specified in Chapter 8. Trawl Zone 1 includes the "nearfield" area of PLOO stations SD10 and SD12, which are located just south and north of the outfall discharge site, respectively. Trawl Zone 2 includes the area surrounding northern "farfield" PLOO stations SD13 and SD14. Trawl Zone 3 represents the area surrounding "farfield" PLOO station SD8, which is located south of the outfall near the LA-5 dredged material disposal site. Trawl Zone 4 is the area surrounding "farfield" PLOO station SD7 located several kilometers south of the outfall. Trawl Zone 5 includes the area surrounding SBOO stations SD17 and SD18, which are located just south and north of the outfall discharge site, respectively. Trawl Zone 6 includes the area surrounding northern SBOO stations SD19 and SD20, while Trawl Zone 7 includes the area surrounding northern SBOO station SD21. Trawl Zone 8 represents the area surrounding southern SBOO station SD16, while Trawl Zone 9 represents the area surrounding southern SBOO station SD15. Rig Fishing Zones 1–4 represent the areas within a 1-km radius of the nominal coordinates for stations RF1, RF2, RF3, and RF4. Stations RF1 and RF3 are located within 1 km of the PLOO and SBOO discharge sites, respectively, and are considered the "nearfield" rig fishing sites. In contrast, station RF2 is located about 11 km northwest of the PLOO, while station RF4 is located about 13.2 km southeast of the SBOO. These two sites are considered "farfield" or reference stations for the analyses herein. Efforts to collect target species by trawl were limited to five 10-minute (bottom time) trawls per site, while rig fishing effort was limited to 5 hours at each station.

A total of 20 species of fish were collected for analysis of liver and muscle tissues during the 2024 and 2025 surveys (Table 9.1). Seven different species of flatfish were collected from the nine trawl zones for analysis of liver tissues, including Pacific Sanddab (*Citharichthys sordidus*), Longfin Sanddab (*Citharichthys xanthostigma*), Hornyhead Turbot (*Pleuronichthys verticalis*), Fantail Sole (*Xystreurys liolepis*), English Sole (*Parophrys vetulus*), Bigmouth Sole (*Hippoglossina stomata*), and Spotted Turbot (*Pleuronichthys ritteri*). These flatfish were collected from regular trawls at the SBOO stations, and by alternative hook and line methods at the PLOO stations. An additional 13 species of fish were collected for analysis of muscle tissues at the rig fishing stations using standard hook and line fishing techniques. These species included Vermilion Rockfish (*Sebastes miniatus*), Squarespot Rockfish (*Sebastes hopkinsi*), Starry Rockfish (*Sebastes constellatus*), Brown Rockfish (*Sebastes auriculatus*), California Scorpionfish (*Scorpaena guttata*), Gopher Rockfish (*Sebastes carnatus*), Copper Rockfish (*Sebastes caurinus*), Flag Rockfish (*Sebastes rubrivinctus*), Speckled Rockfish (*Sebastes ovalis*), Honeycomb Rockfish (*Sebastes umbrosus*), Greenblotched Rockfish (*Sebastes rosenblatti*), Black and Yellow Rockfish (*Sebastes chrysomelas*), and Treefish (*Sebastes serriceps*).

Only fishes with standard lengths ≥12 cm were retained to ensure the collection of sufficient tissue for analysis while minimizing total catch necessary. These fishes were sorted into three composite samples per station, with a minimum of three individuals in each composite. All fishes were wrapped in aluminum foil, labeled, sealed in re-sealable plastic bags, placed on dry ice, and then transported to the City's Marine Biology Laboratory where they were stored at -20°C prior to dissection and tissue processing.

Tissue Processing and Chemical Analyses

All dissections were performed according to standard techniques for tissue analysis. A summary follows, but detailed methods are available in City of San Diego (2023). Prior to dissection, each fish was partially defrosted, cleaned with a paper towel to remove loose scales and excess mucus, and the standard length (cm) and weight (g) were recorded (Appendices H.1, H.2). Dissections were carried out on Teflon® pads that were cleaned between samples. The liver or muscle tissues from each fish were removed and placed in separate glass jars for each composite sample, sealed, labeled, and stored in a freezer at -20°C prior to chemical analyses.

All tissue analyses were performed at the City's Environmental Chemistry Laboratory. Detailed analytical protocols are available upon request. Briefly, all fish tissue samples were analyzed on a wet weight basis to determine the concentrations of 17 different trace metals, nine chlorinated pesticides and their constituents, 42 polychlorinated biphenyl compound congeners (PCBs), 13 polybrominated diphenyl ethers (PBDEs) and 24 polycyclic aromatic hydrocarbons (PAHs). Data were limited to values above the method detection limit (MDL) for each parameter (Appendix H.3). A variety of laboratory technical issues resulted in several non-reportable tissue chemistry data for the 2024 and 2025 surveys, see Appendices H.4–H.13 and City of San Diego 2025.

Data Analyses

Data summaries for each parameter include detection rate, minimum, maximum, and mean values for all samples combined by species for each outfall region. All means were calculated using detected values only, with no substitutions made for non-detects (analyte concentrations < method detection limit (MDL)). Limiting analyses to detected values (i.e., excluding non-detects) is considered a conservative way of handling contaminant concentrations as it creates a strong upward bias in the data and respective summary statistics, and therefore may represent a worst-case scenario (e.g., see Helsel 2005a, b, 2006 for discussions of non-detect data). Results recorded with a qualifier of Detected, but Not Quantified (DNQ) were treated as detected values. Total chlordane, total DDT (tDDT), total hexachlorocyclohexane (tHCH), total PCB (tPCB), total polybrominated diphynel ethers (tPBDE) and total PAH (tPAH) were calculated for each sample as the sum of all constituents with reported values for individual constituents.

For comparative historical analyses, data were limited as follows: (1) fall (October) surveys only; (2) data collected after 1994; (3) specific species feeding guilds (e.g., mixed sanddabs, mixed rockfish) (see Allen et al. 2002) or the most frequently collected species (City of San Diego 2020). Data collected from the PLOO region prior to 1995 were excluded due to incompatible methods used by the external contract lab at the time (see City of San Diego 2015). Barred Sand Bass were also included in the historical analyses because it was the only species collected at SBOO station RF3 in 1995. Missing data from 2018 and 2023 are due to resource exchange agreements with the San Diego Regional Water Quality Control Board for participation in the region-wide Bight'18 and Bight'23 sampling projects. Data analyses were performed using R (R Core Team 2025) using various functions within the zoo, reshape2, plyr, scales, tidyverse, vegan, psych, and ggpubr packages (Zeileis and Grothendieck 2005, Wickham 2007, 2011, 2019, Oksanen et al. 2019, Revelle 2019, Wickham et al. 2019, Kassambara 2020).

Contaminant levels in muscle tissue samples were compared to state, national, and international limits and standards to address seafood safety and public health issues. These included: (1) fish contaminant goals for chlordane, DDT, methylmercury, selenium, and PCBs developed by the California Office of

Environmental Health Hazard Assessment (OEHHA) (Klasing and Brodberg 2008); (2) action limits on the amount of mercury, DDT, and chlordane in seafood that can be sold for human consumption, which are set by the U.S. Food and Drug Administration (USFDA) (Mearns et al. 1991); (3) international standards for acceptable concentrations of various metals and DDT (Mearns et al. 1991).

Data collected during 2024 were reported previously (City of San Diego 2025), and all raw data for the 2024-2025 sampling period have been submitted to the Regional Water Quality Control Board, the California Environmental Data Exchange Network (CEDEN) and the City's Open Data Portal (City of San Diego 2026) and will be provided upon request.

RESULTS

Contaminants in Fish Liver Tissues

Trace Metals

During 2024 and 2025, 8 of 17 trace metals were detected in all fish liver samples, including: arsenic, cadmium, copper, iron, manganese, mercury, selenium, and zinc at concentrations ≤180 ppm (Table 9.2). Detection rates for aluminum, barium, chromium, silver and tin were slightly less at 4–97% per region at concentrations ≤1.12 ppm. Lead and nickel were detected in 24% and 7%, respectively, of liver samples from the SBOO region at concentrations ≤2.56 ppm but were not detected in samples from the PLOO region. Antimony, and beryllium, were not detected in any fish liver tissue samples from either region during 2024 and 2025.

Detection rates have been relatively high for several different metals in liver tissues of fishes collected at trawl zones since 1995 (Table 9.3). Cadmium, copper, iron, manganese, mercury, selenium, and zinc were detected in ≥88% of all Sanddab, Scorpionfish, and Hornyhead Turbot liver samples analyzed from the PLOO and SBOO trawl zones over the past 30 years. Detection rates for other metals varied by species. For example, arsenic was detected in ≥88% of all Sanddab and Hornyhead Turbot liver samples, but only 45% of Scorpionfish samples. Aluminum and barium were detected in 87% and 93% of all California Scorpionfish, respectively, and 46–63% of Sanddab and Hornyhead Turbot samples. Chromium, silver, and tin were detected in 76%, 76%, and 60% of Hornyhead Turbot samples, respectively, and 23–60% of California Scorpionfish and Sanddab samples. Antimony, beryllium, lead, and nickel were detected in ≤25% of all samples from both regions.

Metal concentrations have also been highly variable over these past 30 years, with most being detected within ranges reported elsewhere in the SCB (e.g., Mearns et al. 1991, CLA 2023, OCSD 2024, McLaughlin et al 2020). While relatively high values of various metals have been occasionally recorded in liver tissues from fishes collected from nearfield zones, when compared to farfield zones, there were no discernable intra-species patterns that could be associated with proximity to either outfall (Figure 9.2, Appendix H.14).

Pesticides

Ten chlorinated pesticides were detected in fish liver tissue samples from PLOO or SBOO trawl zones in 2024 and 2025 (Table 9.4). Total DDT was detected in all samples in both regions, at concentrations ≤397.4 ppb. Total chlordane, dieldrin, endrin, endrin aldehyde, alpha-endosulfan, beta-endosulfan, endosulfan sulfate and total HCH, were analyzed but not detected in any of the PLOO samples and ≤7% of the SBOO samples, at concentrations ≤101.26 ppb. Hexachlorobenzene (HCB) was only detected

in 8% of the Sanddab tissues from the PLOO region, at concentrations ≤7.82 ppb. The pesticides (or pesticide constituents) mirex and aldrin were analyzed but not detected in any liver samples from fish collected from either region.

DDT was the most frequently detected pesticide in liver tissues from trawl-zone fishes since 1995 with rates between 98–99% per species (or species group) (Table 9.5). In contrast, long-term detection rates were 6–36% for HCB, 1–32% for total chlordane, 0–8% for total HCH, ≤1% for mirex, alpha-endosulfan, and beta-endosulfan and ≤2% for aldrin, dieldrin, and endrin. Endrin aldehyde, endosulfan sulfate, and toxaphene have been analyzed but never detected in any liver tissue samples from PLOO or SBOO trawl zones. As with metals, pesticide concentrations have been highly variable over time, with most being detected at levels within ranges reported elsewhere in the SCB (e.g., Allen et al. 1998, 2002, Mearns et al. 1991, LACSD 2022, McLaughlin et al 2020). While relatively high values of various pesticides have been occasionally recorded in liver tissues from nearfield zones, when compared to farfield zones, there were no discernable intra-species patterns that could be associated with proximity to either outfall (Figure 9.3, Appendix H.15).

PCBs

PCBs were detected in 83% fish liver tissue samples from PLOO trawl zones and 53% of SBOO trawl zones in 2024 and 2025, at concentrations ≤231.6 ppb (Table 9.4). Since 1995, PCBs have been detected in 93–99% of the liver samples from Sanddabs and Scorpionfish, and in 45% of the liver samples from Hornyhead Turbot (Table 9.5), with total PCB concentrations generally within ranges reported elsewhere in the SCB (e.g., Allen et al. 1998, Mearns et al. 1991, LACSD 2022, McLaughlin et al 2020). There were no discernable intra-species patterns that could be associated with proximity to either outfall over the past 30 years (Figure 9.3).

PBDEs

PBDEs were detected in all fish liver tissue samples from PLOO and 80% of fish liver tissue samples from SBOO trawl zones in 2022, at concentrations ≤85.8 ppb (Table 9.4). Since monitoring PBDEs started recently, no temporal evaluation could be completed. Recorded values for individual PBDE congeners were generally within ranges reported elsewhere in the SCB (Maruya et al 2012). For example, mean concentrations of BDE-47 were 20.9 ppb in Hornyhead Turbot livers from SBOO trawl stations in 2025, versus 156.0 ppm in Hornyhead Turbot livers collected from across the SCB in 2012.

PAHs

PAHs were analyzed but not detected in any liver samples from fish collected in either region during 2024 and 2025 (Table 9.4). Historically, PAHs have been detected in ≤11% of the liver tissue samples from Sanddabs, Scorpionfish, and Hornyhead Turbot analyzed since 1995 (Table 9.5), with total PAH concentrations generally within ranges reported elsewhere in the SCB (e.g., Allen et al. 1998, Mearns et al. 1991, LACSD 2022). There were no discernable intra-species patterns that could be associated with proximity to either outfall during the years that PAH was analyzed (Appendix H.15).

Contaminants in Fish Muscle Tissues

Trace Metals

Eleven of the 17 trace metals analyzed were detected in fish muscle tissue samples from PLOO and SBOO rig fishing zones in 2024 and 2025, including: aluminum, arsenic, barium, chromium, copper, iron, manganese, mercury, selenium, tin, and zinc (Table 9.6). Arsenic, chromium, copper, iron,

manganese, mercury, selenium, tin, and zinc were detected in all muscle samples. Detection rates for barium were 92–100% per region. Aluminum and nickel were found in 8% and 25% of the muscle tissue samples, respectively, from the SBOO region but were not detected in muscle tissue samples from the PLOO region. Silver was detected in 33% of the muscle tissue samples from the PLOO region but not detected in SBOO. Antimony, beryllium, cadmium, and lead were analyzed but not detected in any muscle tissue samples from either region during 2024 and 2025.

Detection rates have been relatively high for several different metals in muscle tissues of fishes captured at rig fishing zones since 1995 (Table 9.7). For example, arsenic, copper, iron, mercury, selenium, and zinc were detected in ≥66% of all California Scorpionfish and rockfish muscle samples analyzed from the PLOO and SBOO rig fishing over the past 30 years. Aluminum, barium, cadmium, chromium, manganese, and tin were detected in 23–80% of all California Scorpionfish and rockfish muscle samples from both regions, while antimony, beryllium, lead, nickel, and silver were detected in ≤17% of muscle samples from these species. In contrast to California Scorpionfish and mixed rockfish, iron, mercury, selenium, and zinc were the only metals detected in Barred Sand Bass muscle samples during the limited period this species was targeted. Metal concentrations in muscle tissues of San Diego fishes have been highly variable, but consistently lower than in liver tissues and within ranges reported elsewhere in the SCB (Mearns et al. 1991, CLA 2023, LACSD 2022, OCSD 2024, McLaughlin et al 2020). While relatively high values of various metals have been occasionally recorded in muscle tissues of fishes collected off San Diego, there were no discernable patterns at the rig fishing zones that could be associated with proximity to either the PLOO or the SBOO (Figure 9.4, Appendix H.16).

Of the 24 rockfish muscle tissue samples collected from PLOO and SBOO rig fishing zones in 2024 and 2025, median international standards were exceeded for arsenic (17–83% per zone) and 100% exceeded this standard for selenium (Table 9.8). The OEHHA limit for mercury was exceeded in 17% of samples from PLOO farfield zone (RF2), but all samples were below the USFDA mercury action limit. All samples were below the OEHHA limit for total chlordane and selenium. Since 1995, median international standards were exceeded for arsenic (49–75% per zone), chromium (≤4% per zone), mercury (1–6% per zone), and selenium (32–77% per zone). Cadmium, copper, lead, tin, and zinc were never found at concentrations above their median international standards. Over this period, the OEHHA fish contaminant goals were exceeded for mercury (9–22% per zone), but not for selenium. The USFDA action limit for mercury exceeded just 4% of the samples from SBOO farfield zone RF4.

Pesticides

Three chlorinated pesticides were detected in fish muscle tissue samples from PLOO or SBOO rig fishing zones in 2024 and 2025 (Table 9.9). Total DDT was detected in all PLOO muscle tissue samples, at concentrations ≤21.48 ppb and 83% of SBOO samples at concentrations ≤5.16 ppb. For PLOO samples HCB was detected at a rate of 8% at concentrations ≤0.72 ppb, and total chlordane was not detected. Total HCB was not detected in any muscle tissue samples from SBOO rig fishing zones. Additionally, the pesticides (or pesticide constituents) aldrin, alpha-endosulfan, beta-endosulfan, dieldrin, endosulfan sulfate, endrin aldehyde, total HCH and mirex were not detected in any muscle samples from fishes collected from either region. None of the detected pesticide values from the past two years exceeded median international standards or the USFDA action limits, however 17% of samples exceeded the OEHHA fish contaminant goals for total DDT (Table 9.8).

Historically, only six pesticides have been found in muscle tissues from Barred Sand Bass, California Scorpionfish, and mixed rockfish samples from the PLOO or SBOO rig fishing zones (Table 9.10).

Longterm detection rates were 50–93% per species (or species group) for DDT, ≤12% for HCB, ≤3% for total chlordane, and ≤2% for total HCH, dieldrin and endrin. Other pesticides such as aldrin, alpha-endosulfan, beta-endosulfan, endrin aldehyde, endosulfan sulfate, mirex, and toxaphene have never been detected in muscle tissue samples from these species collected from the PLOO or SBOO regions over the past 30 years. As with metals, pesticides also typically occurred in lower concentrations in muscle tissues compared to liver tissue, and most were detected at levels within ranges reported elsewhere in the SCB (e.g., Allen et al. 1998, 2002, Mearns et al. 1991, CLA 2023, McLaughlin et al 2020). While relatively high values of various pesticides have been occasionally recorded in muscle tissues of fishes collected off San Diego, there were no discernable patterns at the rig fishing zones that could be associated with proximity to either the PLOO or the SBOO (Figure 9.5, Appendix H.17).

Among the various detected pesticides, the rate of threshold exceedances for the current reporting period were similar to those observed previously (1995–2025) (Table 9.8). Since 1995, median international standards for total chlordane, total DDT, and hexachlorobenzene, the OEHHA fish contaminant goal for total chlordane, and the USFDA action limits for total DDT and hexachlorobenzene were never exceeded, while the OEHHA fish contaminant goal for total DDT was exceeded in ≤17% of samples per zone.

PCBs

During 2024 and 2025, PCBs were detected in 42% and 8% of muscle tissue samples from PLOO and SBOO rig fishing zones, at concentrations ≤12.959 ppb (Table 9.9). Only 17% of samples from PLOO zone RF2 had total PCB levels in exceedance of the OEHHA threshold (Table 9.8). Historically, PCB detection rates were 20–43% per species (or species group) in muscle tissue samples, with highly variable concentrations falling within ranges reported elsewhere in the SCB (e.g., Allen et al. 2002, Mearns et al. 1991, LACSD 2022, OCSD 2024, McLaughlin et al 2020) and with no discernable patterns that could be associated with proximity to either outfall (Table 9.10, Figure 9.5). From 1995 through 2025, the OEHHA fish contaminant goal was exceeded in 4–30% of samples collected per zone (Table 9.8).

PBDEs

PBDEs were detected in 50% of fish muscle tissue samples from PLOO and 17% of fish muscle tissue samples from SBOO trawl zones in 2024 and 2025, at concentrations ≤2.55 ppb (Table 9.9). Since monitoring PBDEs started recently, no temporal evaluation could be completed. Recorded values for individual PBDE congeners were generally within ranges reported elsewhere on the California coast (Brown et al. 2006).

PAHs

During 2024 and 2025 sampling, PAHs were not detected in any of the muscle tissue samples from PLOO or SBOO rig fishing zones. Historically, PAH detection rates were 0–7% per species (or species group) in muscle tissue samples, with highly variable concentrations falling within ranges reported elsewhere in the SCB (e.g., Allen et al. 2002, Mearns et al. 1991, LACSD 2022, OCSD 2024) and with no discernable patterns that could be associated with proximity to either outfall (Table 9.10, Appendix H.17).

Discussion

Several trace metals, pesticides, PCBs, PBDEs and PAHs were detected in liver tissues from various fish species collected in Point Loma and South Bay monitoring regions in 2024 and 20255. Many of the same metals, pesticides, PCBs, and PAHs were detected during this reporting period, as have been documented historically in California Scorpionfish and rockfish muscle tissues, albeit generally less frequently and/or in lower concentrations. Although tissue contaminant concentrations varied among different species of fish and across stations, most values were within ranges reported previously for southern California fishes (e.g., Mearns et al. 1991, Allen et al. 1998, 2002, CLA 2023, LACSD 2022, OCSD 2024, McLaughlin et al 2020). During 2024 and 2025, selenium was found to exceed the median international standards for human consumption in all of the muscle tissue samples from sport fish collected from PLOO and SBOO rig fishing zones. Arsenic was more variable with 17%–83% of samples in exceedance of the median international standards for human consumption. In contrast, all muscle tissue samples had concentrations of mercury, total DDT, and hexachlorobenzene below USFDA action limits. Historically, elevated levels of such contaminants have remained uncommon in sport fish collected from both survey areas.

The frequent occurrence of different trace metals and chlorinated hydrocarbons in the tissues of fish collected from the PLOO and SBOO regions is likely influenced by multiple factors. For example, many metals occur naturally in the environment, although little information is available on background levels in fish tissues. Brown et al. (1986) determined that there may be no area in the SCB sufficiently free of chemical contaminants to be considered a reference site, while Mearns et al. (1991) described the distribution of several contaminants, such as arsenic, mercury, DDT, and PCBs as being ubiquitous. The wide-spread distribution of contaminants in SCB fishes has been supported by more recent work regarding PCBs and DDT (e.g., Allen et al. 1998, 2002).

Other factors that affect contaminant loading in fish tissues include the physiology and life history of different species (see Groce 2002). Exposure to contaminants can also vary greatly between different species and among individuals of the same species depending on migration pathways (Otway 1991). Fishes may be exposed to contaminants in a highly polluted area and then move into areas free of contamination. For example, California Scorpionfish tagged in Santa Monica Bay have been recaptured as far south as the Coronado Islands (Hartmann 1987, Love et al. 1987). This is of particular concern for fishes collected in the vicinity of the PLOO and the SBOO, as there are many point and non-point sources that may contribute to local contamination in the region, including the San Diego River, San Diego Bay, Tijuana River, and offshore dredged material disposal sites (see Chapters 2–7 and Parnell et al. 2008). However, assessments of contaminant loading in San Diego offshore sediments have revealed no evidence to indicate that the PLOO or SBOO are major sources of pollutants in the region (see Chapters 5, 7, and Parnell et al. 2008).

Overall, there was no evidence of contaminant accumulation in PLOO or SBOO fishes during 2024 and 2025 that could be associated with wastewater discharge from either outfall, which is consistent with historical findings. Concentrations of most contaminants were generally similar across trawl or rig fishing zones, and no relationships with the PLOO or SBOO were evident. These results are consistent with findings of other assessments of bioaccumulation in fishes off San Diego (Parnell et al. 2008, City of San Diego 2022). Finally, there were no other indications of poor fish health in the region, such as the presence of fin rot or other indicators of disease (see Chapter 8).

Literature Cited

Allen, M.J., S.L. Moore, K.C. Schiff, D. Diener, S.B. Weisberg, J.K. Stull, A. Groce, E. Zeng, J. Mubarak, C.L. Tang, R. Gartman, and C.I. Haydock. (1998). Assessment of demersal fish and megabenthic invertebrate assemblages on the mainland shelf of Southern California in 1994. Southern California Coastal Water Research Project, Westminster, CA.

Allen, M.J., A.K. Groce, D. Diener, J. Brown, S.A. Steinert, G. Deets, J.A. Noblet, S.L. Moore, D. Diehl, E.T. Jarvis, V. Raco-Rands, C. Thomas, Y. Ralph, R. Gartman, D. Cadien, S.B. Weisberg, and T. Mikel. (2002). Southern California Bight 1998 Regional Monitoring Program: V. Demersal Fishes and Megabenthic Invertebrates. Southern California Coastal Water Research Project, Westminster, CA.

Brown, D.A., R.W. Gossett, G.P. Hershelman, C.G. Word, A.M. Westott, and J.N. Cross. (1986). Municipal wastewater contamination in the Southern California Bight: Part I — Metal and Organic Contaminations in Sediments and Organisms. Marine Environmental Research, 18:291–310

Brown, F.R, J. Winkler, P. Visita, J. Dhaliwal, and M. Petreas. (2006). Levels of PBDEs, PCDDs, PCDFs, and coplanar PCBs in edible fish from California coastal waters. Chemosphere Vol 4, 2:276–286.

Cardwell, R. D. (1991). Methods for evaluating risks to aquatic life and human health from exposure to marine discharges of municipal wastewaters. Pages 253–252 in A. G. Miskiewicz (ed.). Proceedings of a Bioaccumulation Workshop: Assessment of the Distribution, Impacts, and Bioaccumulation of Contaminants in Aquatic Environments. Australian Marine Science Association, Inc./WaterBoard.

[CLA] City of Los Angeles, Environmental Monitoring Division. (2023). Marine Monitoring in Santa Monica Bay: Biennial Assessment Report for the Period January 2021 through December 2022. Report submitted to USEPA and RWQCB (Los Angeles). Department of Public Works, LA Sanitation, Hyperion Treatment Plant, Playa del Rey, California, pp. 1–220 + appendices.

City of San Diego. (2015). Point Loma Ocean Outfall Annual Receiving Waters Monitoring and Assessment Report, 2014. City of San Diego Ocean Monitoring Program, Public Utilities Department, Environmental Monitoring and Technical Services Division, San Diego, CA.

City of San Diego. (2022). Appendix C5. Bioaccumulation Assessment. In: Application for Renewal of NPDES CA0107409 and 301(h) Modified Secondary Treatment Requirements Point Loma Ocean Outfall. Volume V, Appendix C. Public Utilities Department, Environmental Monitoring and Technical Services Division, San Diego, CA.

City of San Diego. (2023). Quality Assurance Plan for Coastal Receiving Waters Monitoring. City of San Diego Ocean Monitoring Program, Public Utilities Department, Environmental Monitoring and Technical Services Division, San Diego, CA.

City of San Diego. (2024). Biennial Receiving Waters Monitoring and Assessment Report for the Point Loma and South Bay Ocean Outfalls, 2022–2023. City of San Diego, Public Utilities Department, Environmental Monitoring and Technical Services Division, San Diego, CA.

City of San Diego, (2025). Interim Receiving Waters Monitoring Report for the Point Loma and South Bay Ocean Outfalls, 2024. City of San Diego, Public Utilities Department, Environmental Monitoring and Technical Services Division, San Diego, CA.

City of San Diego. (2026). Ocean Monitoring Program Reports and Data. https://www.sandiego.gov/public-utilities/sustainability/ocean-monitoring/reports

Connell, D. W. (1988). Bioaccumulation behavior of persistent organic chemicals with aquatic organisms. Review of Environmental Contamination and Toxicology, 101:117–154.

Groce, A.K. (2002). Influence of life history and lipids on the bioaccumulation of organo-chlorines in demersal fishes. Master's thesis. San Diego State University. San Diego, CA.

Hartmann, A.R. (1987). Movement of scorpionfishes (Scorpaenidae: Sebastes and Scorpaena) in the Southern California Bight. California Fish and Game, 73: 68–79.

Helsel, D.R. (2005a). More than obvious: better methods for interpreting nondetect data. Environmental Science & Technology (October 15, 2005), 419A–423A.

Helsel, D.R. (2005b). Nondetects and Data Analysis: Statistics for Censored Environmental Data. John Wiley, New York.

Helsel, D.R. (2006). Fabrication data: how substituting values for nondetects can ruin results, and what can be done about it. Chemosphere 65: 2434–2439.

Kassambara, A. (2020). ggpubr: 'ggplot2' Based Publication Ready Plots. R package version 0.2.5 https://CRAN.R-project.org/package = ggpubr.

Klasing, S. and R. Brodberg. (2008). Development of Fish Contaminant Goals and Advisory Tissue Levels for Common Contaminants in California Sport Fish: Chlordane, DDTs, Dieldrin, Methylmercury, PCBs, Selenium, and Toxaphene. California Environmental Protection Agency, Office of Environmental Health Hazard Assessment, Sacramento, CA.

[LACSD] Los Angeles County Sanitation District. (2022). Joint Water Pollution Control Plant Biennial Receiving Water Monitoring Report 2020–2021. Los Angeles, CA.

Love, M.S., B. Axell, P. Morris, R. Collins, and A. Brooks. (1987). Life history and fishery of the California scorpionfish, Scorpaena guttata, within the Southern California Bight. Fisheries Bulletin, 85: 99–116.

Maruya, K.A, D.E Vidal-Dorsch, S.M. Bay, J.W. Kwon, K. Xia, and K.L. Armbrust. (2012). Organic contaminants of emerging concern in Southern California coastal waters. Environ, Toxicol. Chem 2012; 31:2683–2688.

McLaughlin, K., K. Schiff, B. Du, J. Davis, A. Bonnema, G. Ichikawa, B. Jakl, and W. Heim. (2020). Southern California Bight 2018 Regional Monitoring Program: Volume V. Contaminant Bioaccumulation in Edible Sport Fish Tissue. Technical Report 1155. Southern California Coastal Water Research Project. Costa Mesa, CA.

Mearns, A.J., M. Matta, G. Shigenaka, D. MacDonald, M. Buchman, H. Harris, J. Golas, and G. Lauenstein. (1991). Contaminant Trends in the Southern California Bight: Inventory and Assessment. NOAA Technical Memorandum NOS ORCA 62. Seattle, WA.

Oksanen, J., F.G. Blanchet, R. Kindt, P. Legendre, P.R. Minchin, R.B. O'Hara, G.L. Simpson, P. Solymos, M.H.H. Stevens, and H. Wagner. (2019). vegan: Community Ecology Package. R package version 2.5–6. http://CRAN.R-project.org/package=vegan.

[OCSD] Orange County Sanitation District. (2024). Marine Monitoring Annual Report, Program Year 2022 – 2023. Fountain Valley, CA.

Otway, N. (1991). Bioaccumulation studies on fish: choice of species, sampling designs, problems and implications for environmental management. In: A.G. Miskiewicz (ed.). Proceedings of a Bioaccumulation Workshop: Assessment of the Distribution, Impacts, and Bioaccumulation of Contaminants in Aquatic Environments. Australian Marine Science Association, Inc./Water Board.

Parnell, P.E., A.K. Groce, T.D. Stebbins, and P.K. Dayton. (2008). Discriminating sources of PCB contamination in fish on the coastal shelf off San Diego, California (USA). Marine Pollution Bulletin, 56: 1992–2002.

R Core Team. (2025). R: A language and environment for statistical computing. R Foundation for Statistical Computing, Vienna, Austria. URL https://www.R-project.org/

Rand, G.M., ed. (1995). Fundamentals of Aquatic Toxicology: Effects, Environmental Fate, and Risk Assessment. 2nd ed. Taylor and Francis, Washington, D.C.

Revelle, W. (2019). psych: Procedures for Personality and Psychological Research, Northwestern University, Evanston, Illinois, USA, https://CRAN.R-project.org/package=psych Version = 1.9.12.31.

Schiff, K. and M.J. Allen. (1997). Bioaccumulation of chlorinated hydrocarbons in livers of flatfishes from the Southern California Bight. In: S.B. Weisberg, C. Francisco, and D. Hallock (eds.). Southern California Coastal Water Research Project Annual Report 1995–1996. Southern California Coastal Water Research Project, Westminster, CA.

[USEPA] United States Environmental Protection Agency. (2000). Bioaccumulation Testing and Interpretation for the Purpose of Sediment Quality Assessment. Status and Needs. EPA-823-R-00-001. U.S. Environmental Protection Agency. February 2000.

Wickham, H. (2007). Reshaping Data with the reshape Package. Journal of Statistical Software, 21(12), 1–20. URL http://www.jstatsoft.org/v21/i12/.

Wickham, H. (2011). The Split-Apply-Combine Strategy for Data Analysis. Journal of Statistical Software, 40(1), 1–29. URL http://www.jstatsoft.org/v40/i01/.

Wickham, H. (2019). Scales: Scale Functions for Visualization Rstudio. R package version 1.1.0. https://scales.r-lib.org/.

Wickham, H., M. Averick, J. Bryan, W. Chang, L. D'Agostino McGowan, R. François, G.Grolemund, A. Hayes, L. Henry, J. Hester, M. Kuhn, T. Lin Pedersen, E. Miller, S. Milton Bache, K. Müller, J. Ooms, D. Robinson, D. P. Seidel, V. Spinu, K. Takahashi, D. Vaughan, C. Wilke, K. Woo, H. Yutani. (2019). Welcome to the tidyverse. Journal of Open Source Software, 4(43), 1686, https://doi.org/10.21105/joss.01686.

Zeileis, A and G. Grothendieck. (2005). zoo: S3 Infrastructure for Regular and Irregular Time Series. Journal of Statistical Software, 14(6), 1–27. URL http://www.jstatsoft.org/v14/i06/.

CHAPTER 9

FIGURES & TABLES

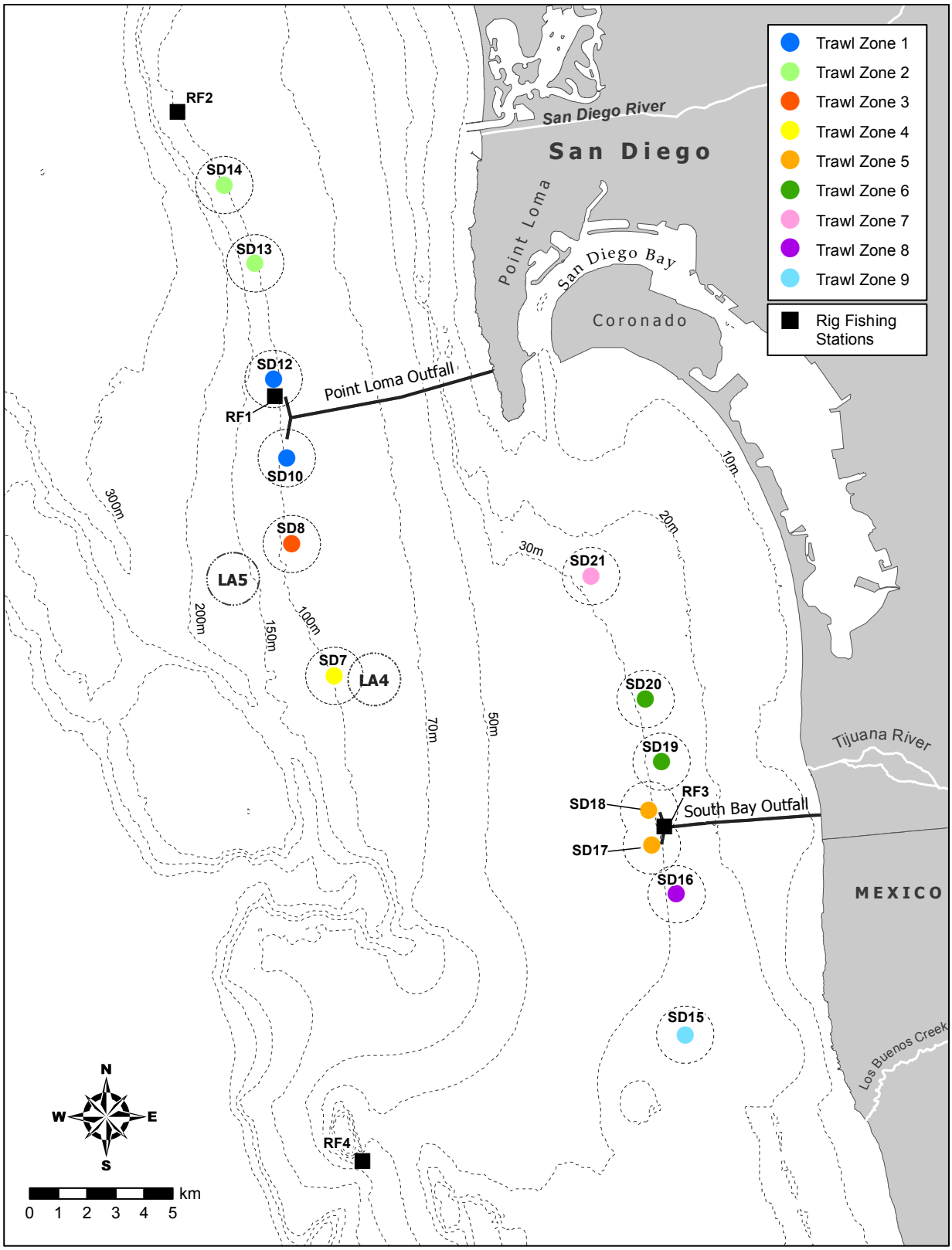


Figure 9.1
Trawl and rig fishing zone locations sampled around the PLOO and SBOO as part of the City of San Diego's Ocean Monitoring Program.

Table 9.1

Species of fish collected from each PLOO and SBOO trawl and rig fishing zone during 2024–2025.

	Zone	Composite 1	Composite 2	Composite 3
PLOO				
2024	Rig Fishing Zone 1 (RF1)	Vermilion Rockfish	Vermilion Rockfish	Vermilion Rockfish
	Rig Fishing Zone 2 (RF2)	Starry Rockfish	Starry Rockfish	Mixed Rockfish[a]
	Trawl Zone 1 (TZ1)	Pacific Sanddab	Pacific Sanddab	Pacific Sanddab
	Trawl Zone 2 (TZ2)	Pacific Sanddab	Pacific Sanddab	Pacific Sanddab
	Trawl Zone 3 (TZ3)	Pacific Sanddab	Pacific Sanddab	Pacific Sanddab
	Trawl Zone 4 (TZ4)	Pacific Sanddab	Pacific Sanddab	Pacific Sanddab
2025	Rig Fishing Zone 1 (RF1)	Vermilion Rockfish	Vermilion Rockfish	Copper Rockfish
	Rig Fishing Zone 2 (RF2)	Speckled Rockfish	Mixed Rockfish[b]	Mixed Rockfish[c]
	Trawl Zone 1 (TZ1)	Pacific Sanddab	Pacific Sanddab	Pacific Sanddab
	Trawl Zone 2 (TZ2)	Pacific Sanddab	Pacific Sanddab	Pacific Sanddab
	Trawl Zone 3 (TZ3)	Pacific Sanddab	Pacific Sanddab	Pacific Sanddab
	Trawl Zone 4 (TZ4)	Pacific Sanddab	Pacific Sanddab	Pacific Sanddab
SBOO				
2024	Rig Fishing Zone 3 (RF3)	Vermilion Rockfish	Vermilion Rockfish	Mixed Rockfish[d]
	Rig Fishing Zone 4 (RF4)	California Scorpionfish	Mixed Rockfish[e]	Mixed Rockfish[f]
	Trawl Zone 5 (TZ5)	Longfin Sanddab	Longfin Sanddab	Hornyhead Turbot
	Trawl Zone 6 (TZ6)	Longfin Sanddab	Longfin Sanddab	Longfin Sanddab
	Trawl Zone 7 (TZ7)	Longfin Sanddab	Longfin Sanddab	Longfin Sanddab
	Trawl Zone 8 (TZ8)	Longfin Sanddab	Longfin Sanddab	Longfin Sanddab
	Trawl Zone 9 (TZ9)	Fantail Sole	English Sole	Hornyhead Turbot
2025	Rig Fishing Zone 3 (RF3)	Vermilion Rockfish	Brown Rockfish	Brown Rockfish
	Rig Fishing Zone 4 (RF4)	Honeycomb Rockfish	California Scorpionfish	Treefish
	Trawl Zone 5 (TZ5)	Hornyhead Turbot	Hornyhead Turbot	Hornyhead Turbot
	Trawl Zone 6 (TZ6)	Longfin Sanddab	Hornyhead Turbot	Longfin Sanddab
	Trawl Zone 7 (TZ7)	Hornyhead Turbot	Hornyhead Turbot	Hornyhead Turbot
	Trawl Zone 8 (TZ8)	Hornyhead Turbot	Hornyhead Turbot	Longfin Sanddab
	Trawl Zone 9 (TZ9)	Hornyhead Turbot	Spotted Turbot	Bigmouth Sole[g]

[a]Includes Greenblotched, Flag, and Speckled Rockfish; [b]includes Starry and Flag Rockfish; [c]includes Squarespot and Vermilion Rockfish; [d]includes Vermilion and Brown Rockfish; [e]includes Treefish, Starry, and Honeycomb Rockfish; [f]includes Black and Yellow and Gopher Rockfish; [g]PAH not analyzed due to insufficient tissue

Table 9.2

Summary of metals (ppm) in liver tissues of fishes collected from PLOO and SBOO trawl zones during 2024–2025. Data include the number of detected values (n), minimum, maximum, and mean[a] detected concentrations for each species, and the total number of samples, detection rate, and maximum value for all species within each region. nd = not detected.

		Al	Sb	As	Ba	Be	Cd	Cr	Cu	Fe	Pb	Mn	Hg	Ni	Se	Ag	Sn	Zn
PLOO	Pacific Sanddab																	
	n	1	0	24	23	0	24	23	24	24	0	24	24	0	24	3	23	24
	min	nd	—	2.54	nd	—	2.23	nd	2.11	55.9	—	0.78	0.048	—	1.59	nd	nd	18.9
	max	0.50	—	5.21	0.038	—	7.08	0.575	4.80	180.0	—	1.34	0.129	—	3.08	0.092	0.69	36.6
	mean	0.50	—	3.84	0.019	—	4.33	0.085	3.50	97.4	—	1.02	0.095	—	2.40	0.078	0.39	26.1
	Total Samples	24	24	24	24	24	24	24	24	24	24	24	24	24	24	24	24	24
	Detection Rate (%)	4	0	100	96	0	100	96	100	100	0	100	100	0	100	13	96	100
	Max	0.50	nd	5.21	0.038	nd	7.08	0.575	4.80	180.0	nd	1.34	0.129	nd	3.08	0.092	0.69	36.6
SBOO	Bigmouth Sole																	
	n	0	0	1	1	0	1	1	1	1	0	1	1	0	1	0	1	1
	value	—	—	9.24	0.042	—	0.86	0.099	1.88	64.1	—	1	0.054	—	1.77	—	0.20	31.4
	English Sole																	
	n	0	0	1	1	0	1	0	1	1	0	1	1	0	1	0	0	1
	value	—	—	3.79	0.096	—	0.42	—	9.51	143.0	—	1.00	0.025	—	3.62	—	—	56.1
	Fantail Sole																	
	n	0	0	0	0	0	0	0	0	0	0	0	1	0	0	0	0	0
	value	—	—	—	—	—	—	—	—	—	—	—	0.150	—	—	—	—	—
	Hornyhead Turbot																	
	n	11	0	12	12	0	12	12	12	12	2	12	12	1	12	12	12	12
	min	nd	—	2.92	0.005	—	3.26	0.055	5.11	26.8	nd	0.82	0.097	nd	1.59	0.054	0.10	45.2
	max	1.12	—	6.31	0.029	—	10.60	0.164	10.60	87.2	0.11	1.66	0.239	0.07	2.08	0.153	0.28	67.8
	mean	0.52	—	4.20	0.011	—	5.70	0.074	7.94	46.5	0.10	1.10	0.135	0.07	1.83	0.092	0.19	59.4
	Longfin Sanddab																	
	n	1	0	14	11	0	14	10	14	14	4	14	14	1	14	11	14	14
	min	nd	—	4.84	nd	—	0.91	nd	3.69	54.0	nd	0.61	0.034	nd	2.14	nd	0.35	16.6
	max	0.56	—	7.49	0.043	—	2.24	0.110	7.16	118.0	0.30	0.91	0.097	2.56	3.40	0.140	0.79	24.4
	mean	0.56	—	5.82	0.015	—	1.68	0.061	5.16	85.0	0.26	0.70	0.062	2.56	3.07	0.094	0.50	21.9
	Spotted Turbot																	
	n	1	0	1	1	0	1	1	1	1	1	1	1	0	1	1	1	1
	value	0.33	—	10.20	0.009	—	0.68	0.085	17.40	128.0	0.15	1.42	0.088	—	1.95	0.103	0.24	57.5
	Total Samples	29	29	29	29	29	29	29	29	29	29	29	30	29	29	29	29	29
	Detection Rate (%)	45	0	100	90	0	100	83	100	100	24	100	100	7	100	83	97	100
	Max	1.12	nd	10.20	0.096	nd	10.60	0.164	17.40	143.0	0.30	1.66	0.239	2.56	3.62	0.153	0.79	67.8

[a] Minimum and maximum values were calculated based on all samples, whereas means were calculated from detected values only

Table 9.3

Summary of metals (ppm) in liver tissues of fishes collected from PLOO and SBOO trawl zones from 1995 through 2025. Data include the total number of samples (n), detection rate (DR%), minimum, maximum, and mean[a] detected concentrations for each guild or species; nd = not detected.

		Al	Sb	As	Ba	Be	Cd	Cr	Cu	Fe	Pb	Mn	Hg	Ni	Se	Ag	Sn	Zn
PLOO	Mixed Sanddabs																	
	n	367	367	367	246	367	367	367	359	367	367	367	369	367	368	367	367	367
	DR%	53	14	92	59	11	94	60	100	100	16	98	91	16	98	23	53	100
	min	nd	nd	nd	nd	nd	nd	nd	0.9	27	nd	nd	nd	nd	nd	nd	nd	8.6
	max	44.6	9.73	123	15.2	0.184	19.2	22.8	28.7	233	8.8	5.47	0.579	18.9	4.37	2.2	277	74.2
	mean	11.96	1.43	5.02	0.221	0.018	4.12	0.58	5.17	96.9	0.87	0.85	0.099	0.68	1.27	0.223	3.55	24.3
	California Scorpionfish																	
	n	105	105	105	43	105	105	105	105	105	105	105	107	105	107	105	105	105
	DR%	87	11	45	93	10	94	54	100	100	14	88	94	25	99	41	26	100
	min	nd	nd	nd	nd	nd	nd	nd	4.06	29.6	nd	nd	nd	nd	nd	nd	nd	20.5
	max	59.8	1.68	8.06	0.584	0.057	6.92	5.34	81.1	481	8.1	2.52	0.695	2.67	2.82	1.16	3.44	207
	mean	13.55	0.85	2.25	0.093	0.01	2.66	0.92	22.85	177.8	1.41	0.58	0.175	0.42	0.89	0.309	1.29	97.2
SBOO	Hornyhead Turbot																	
	n	153	153	153	133	153	153	153	153	153	153	153	153	153	154	153	153	153
	DR%	63	7	92	56	4	99	76	100	100	15	99	98	15	98	76	60	100
	min	nd	nd	nd	nd	nd	nd	nd	2.3	19.4	nd	nd	nd	nd	nd	nd	nd	23
	max	27.8	1.77	25	0.291	0.018	12	7.67	41.7	263	3.3	3.21	0.407	4.61	3.38	1.32	88.2	233
	mean	6.24	1.07	4.3	0.053	0.005	4.1	0.37	8	55.3	0.59	1.11	0.109	0.48	0.95	0.196	1.86	61.9
	Longfin Sanddab																	
	n	196	196	196	149	196	196	196	196	196	196	196	196	196	197	196	196	196
	DR%	51	13	88	46	6	93	58	100	100	13	97	89	17	96	41	57	100
	min	nd	nd	nd	nd	nd	nd	nd	1.38	33	nd	nd	nd	nd	nd	nd	nd	10.3
	max	49	2.38	12.1	0.603	0.043	9.31	3.56	23.2	449	14.3	2.01	0.438	2.56	3.4	1.63	4.61	109
	mean	12.43	0.88	5.49	0.132	0.017	1.83	0.4	6.19	78.4	0.98	0.95	0.079	0.5	1.11	0.195	1.34	23.2

[a] Minimum and maximum values were calculated based on all samples, whereas means were calculated from detected values only

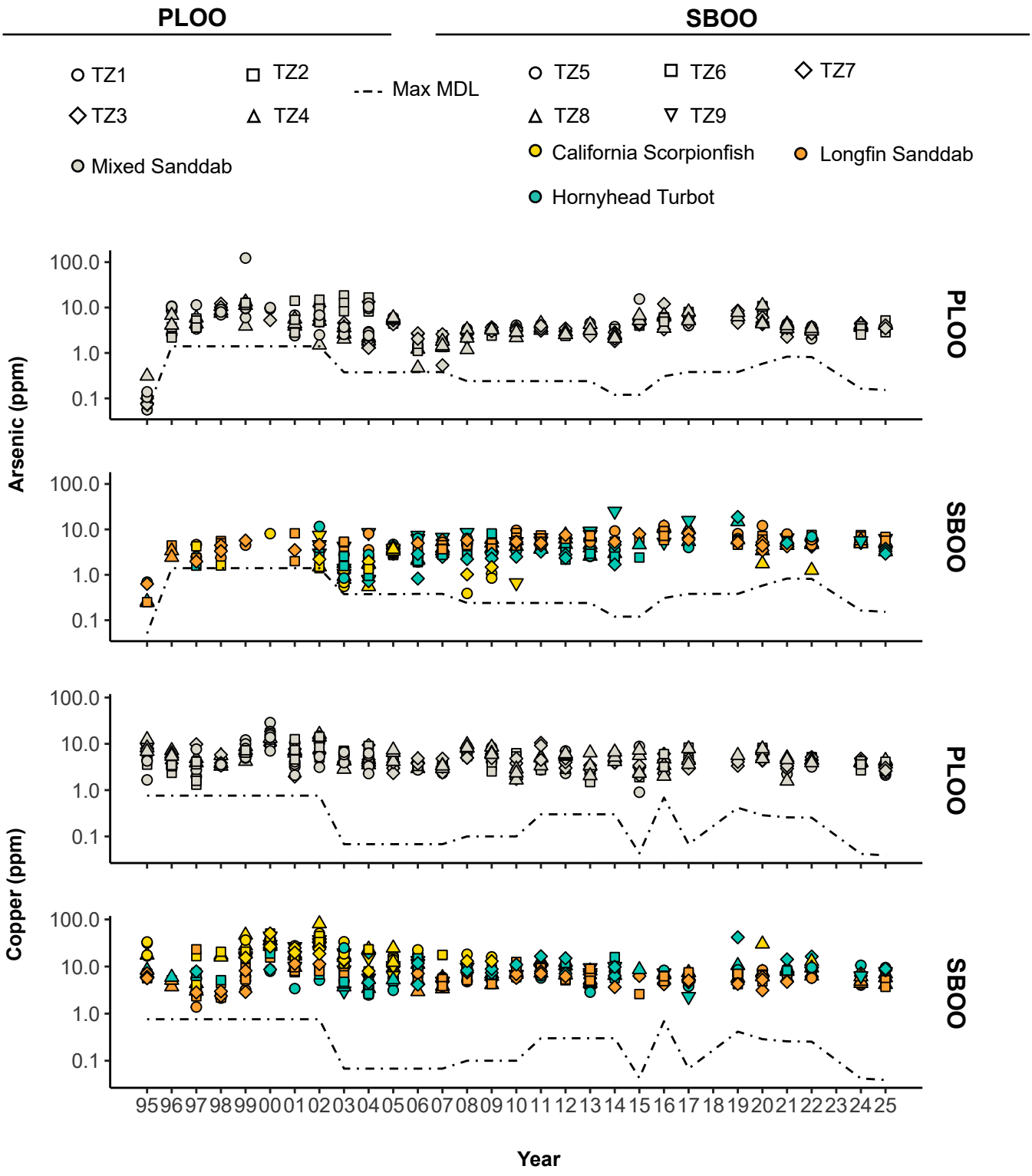


Figure 9.2

Concentrations of select metals in liver tissues of fishes collected from PLOO and SBOO trawl zones from 1995 through 2025. Zones TZ1 and TZ5 are considered nearfield. No samples were collected in 2018 or 2023 as described in text.

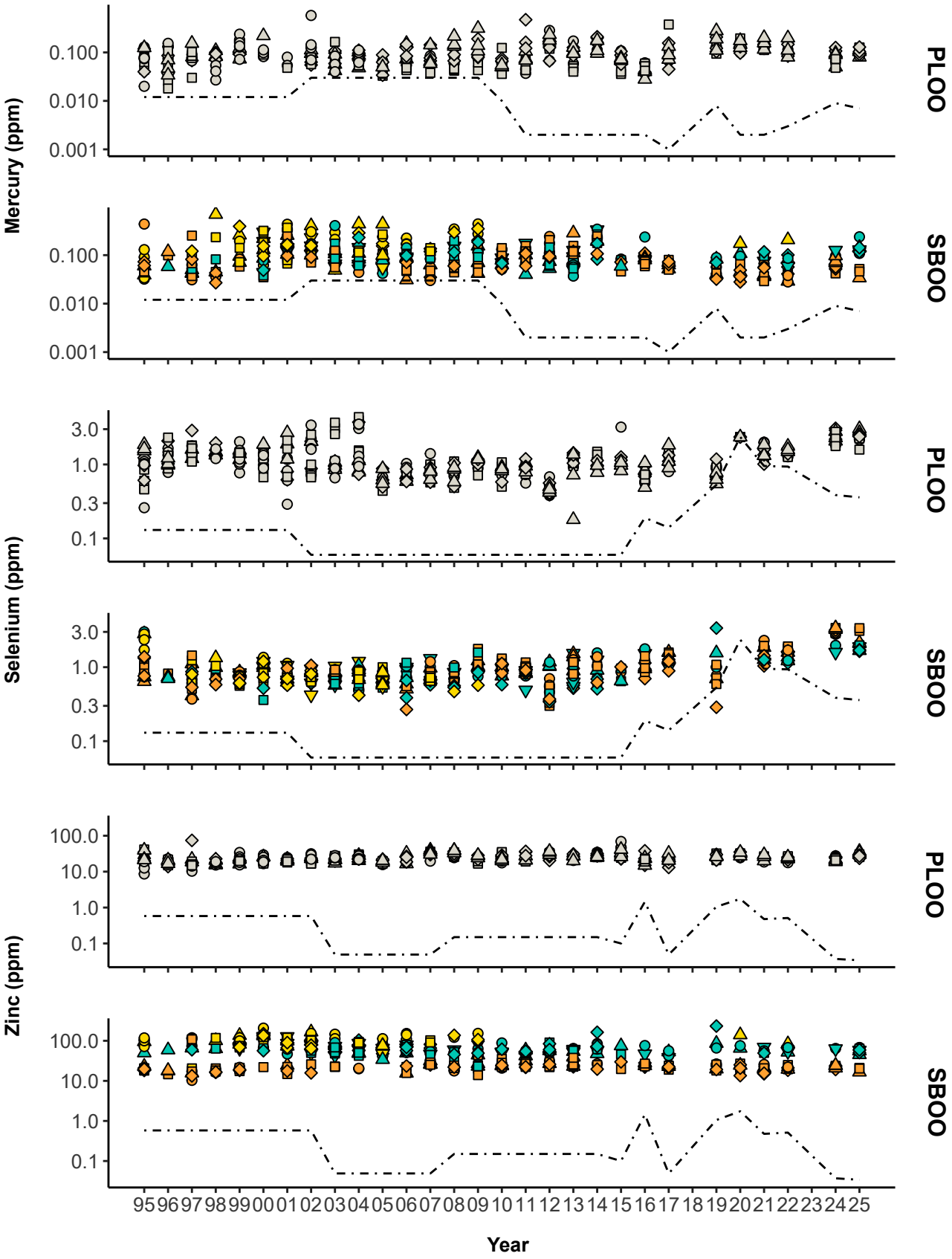


Figure 9.2 *continued*

Table 9.4

Summary of pesticides (ppb), total PCB (ppb), total PAH (ppb), total PBDE (ppb), and lipids (% weight) in liver tissues of fishes collected from PLOO and SBOO trawl zones during 2024-2025. Data include the number of detected values (n), minimum, maximum, and mean[a] detected concentrations for each species, and the total number of samples, detection rate and maximum value for all species within each region. nd = not detected.

		Pesticides												
		tChlor	tDDT	Dieldrin	αEndosulfan	βEndosulfan	Endosulfan sulfate	Endrin	Endrin aldehyde	HCB	tHCH	tPCB	tPBDE	Lipids
PLOO	Pacific Sanddab													
	n	0	24	0	0	0	0	0	0	2	0	20	24	24
	min	—	22.7	—	—	—	—	—	—	nd	—	nd	2.56	15
	max	—	157.5	—	—	—	—	—	—	7.82	—	231.6	24	38.1
	mean	—	97.2	—	—	—	—	—	—	6.905	—	89.5	15.40	26.8
	Total Samples	24	24	24	24	24	24	24	24	24	24	24	24	24
	Detection Rate (%)	0	100	0	0	0	0	0	0	8	0	83	100	100
	Max	nd	157.5	nd	nd	nd	nd	nd	nd	7.82	nd	231.6	24	38.1
SBOO	Bigmouth Sole													
	n	1	1	1	0	1	1	0	1	0	1	0	0	1
	value	25	16.3	6.7	—	3.04	14.9	—	6.93	—	7.28	—	—	2.8
	English Sole													
	n	0	1	0	0	0	0	0	0	0	0	0	1	1
	value	—	15.8	—	—	—	—	—	—	—	—	—	9.37	12.5
	Fantail Sole													
	n	0	1	0	0	0	0	0	0	0	0	1	1	1
	value	—	397.4	—	—	—	—	—	—	—	—	173.2	1.21	4.1
	Hornyhead Turbot													
	n	0	12	0	0	0	0	0	0	0	0	2	8	12
	min	—	7.0	—	—	—	—	—	—	—	—	nd	nd	3.6
	max	—	38.2	—	—	—	—	—	—	—	—	5.9	85.8	7.5
	mean	—	19.7	—	—	—	—	—	—	—	—	5.5	47.20	5.0
	Longfin Sanddab													
	n	1	14	1	1	1	0	1	0	0	1	13	14	14
	min	nd	74.9	nd	nd	nd	—	nd	—	—	nd	nd	11.72	19.2
	max	74.07	185.9	33.5	25.4	3.83	—	6.79	—	—	101.26	164.4	72.66	45.5
	mean	74.07	118.2	33.5	25.4	3.83	—	6.79	—	—	101.26	59.8	29.35	34.5
	Spotted Turbot													
	n	0	1	0	0	0	0	0	0	0	0	0	0	1
	value	—	4.4	—	—	—	—	—	—	—	—	—	—	3.3
	Total Samples	30	30	30	30	30	30	30	30	30	30	30	30	30
	Detection Rate (%)	7	100	7	3	7	3	3	3	0	7	53	80	100
	Max	74.07	397.4	33.5	25.4	3.83	14.9	6.79	6.93	nd	101.26	173.2	85.8	45.5

[a] Minimum and maximum values were based on all samples, whereas means were calculated from detected values only

Table 9.5

Summary of pesticides (ppb), total PCB (ppb), total PAH (ppb), and lipids (% weight) in liver tissues of fishes collected from PLOO and SBOO trawl zones from 1995 through 2025. Data include total number of samples (n), detection rate (DR%), minimum, maximum, and mean[a] detected concentrations per guild or species; nd = not detected.

		Pesticides												
		Aldrin	**tChlor**	**tDDT**	**Dieldrin**	**αEndosulfan**	**βEndosulfan**	**Endrin**	**HCB**	**tHCH**	**Mirex**	**tPCB**	**tPAH**	**Lipids**
PLOO	Mixed Sanddab													
	n	365	376	376	353	365	197	353	356	376	376	377	190	373
	DR%	0	32	98	2	0	0	0	28	8	0	98	11	100
	min	—	nd	nd	nd	—	—	—	nd	nd	nd	nd	nd	6.9
	max	—	94.00	3800.0	15.8	—	—	—	120.0	22.00	48	3179.5	1353	69.6
	mean	—	15.34	638.1	6.3	—	—	—	7.4	3.63	48	404.1	206.7	36.7
SBOO	CA Scorpionfish													
	n	95	95	95	95	95	41	95	94	95	95	109	72	107
	DR%	2	14	98	2	0	0	2	6	4	0	93	0	100
	min	nd	nd	nd	nd	—	—	nd	nd	nd	—	nd	—	6.4
	max	19.00	122	15503.0	63.0	—	—	66	37.3	278.00	—	2187.9	—	45.4
	mean	12.05	32.54	1231.6	38.5	—	—	55	10.3	102.92	—	296.5	—	19.6
	Hornyhead Turbot													
	n	156	159	159	154	156	69	154	153	159	159	161	140	158
	DR%	0	1	99	0	0	0	0	9	0	0	45	4	100
	min	—	nd	nd	—	—	—	—	nd	—	—	nd	nd	0.1
	max	—	32.04	2802.0	—	—	—	—	41.0	—	—	828.4	330.5	32.2
	mean	—	26.17	114.7	—	—	—	—	9.7	—	—	47.2	133.7	9.4
	Longfin Sanddab													
	n	190	193	193	181	190	109	181	174	193	193	197	159	196
	DR%	0	22	99	1	1	1	1	36	6	1	98	3	100
	min	—	nd	nd	nd	nd	nd	nd	nd	nd	nd	nd	nd	6.15
	max	—	120	3600.0	33.5	25.4	3.83	6.79	51.3	101.26	2	6781.9	43167	62.4
	mean	—	10.65	563.7	33.5	25.4	3.83	6.79	4.1	10.10	1.75	478.5	8678.3	35.8

[a] Minimum and maximum values were based on all samples, whereas means were calculated from detected values only

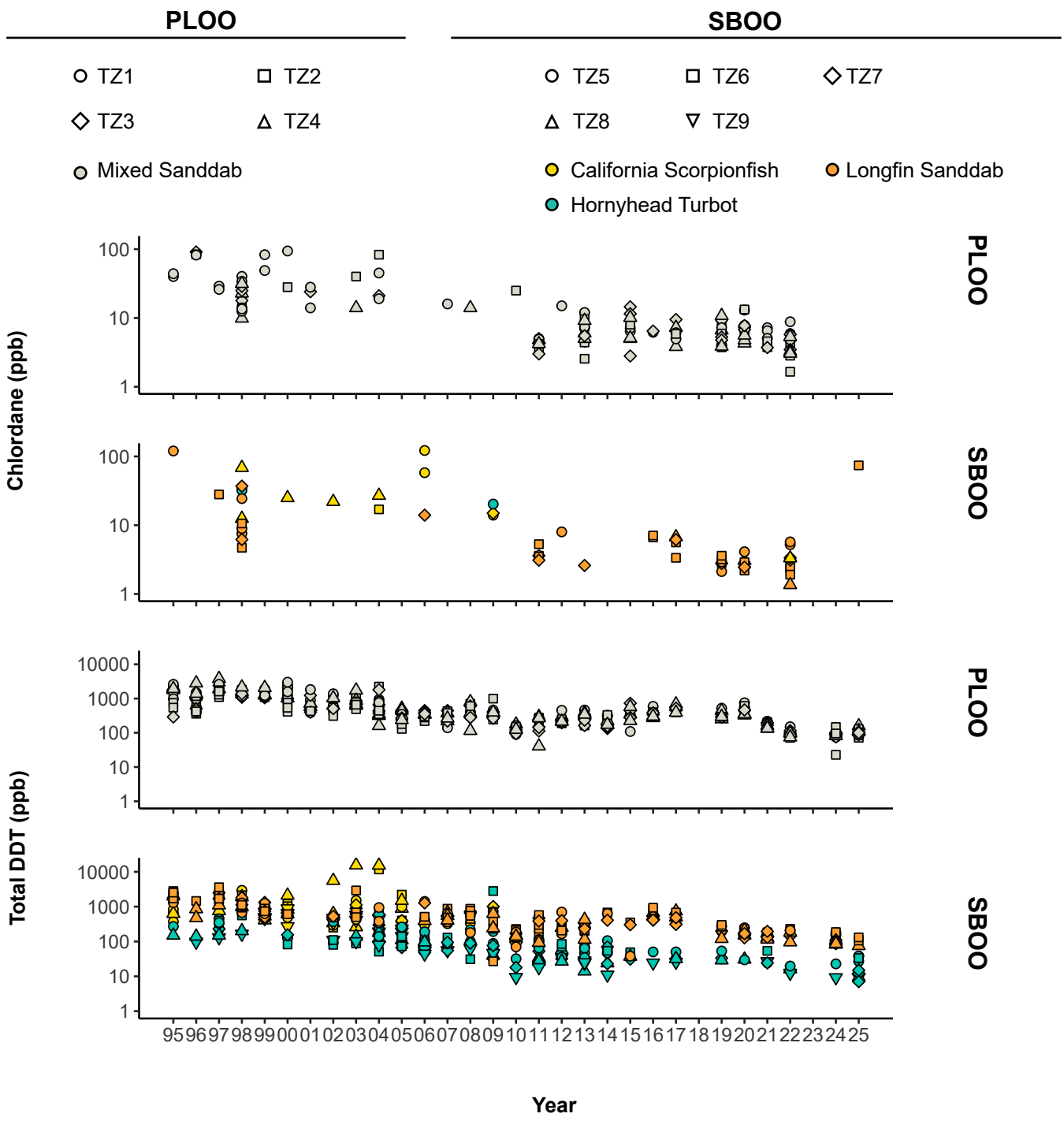


Figure 9.3

Concentrations of pesticides and total PCB in liver tissues of fishes collected from PLOO and SBOO trawl zones from 1995 through 2025. Zones TZ1 and TZ5 are considered nearfield. No samples were collected in 2018 and 2023 as described in text.

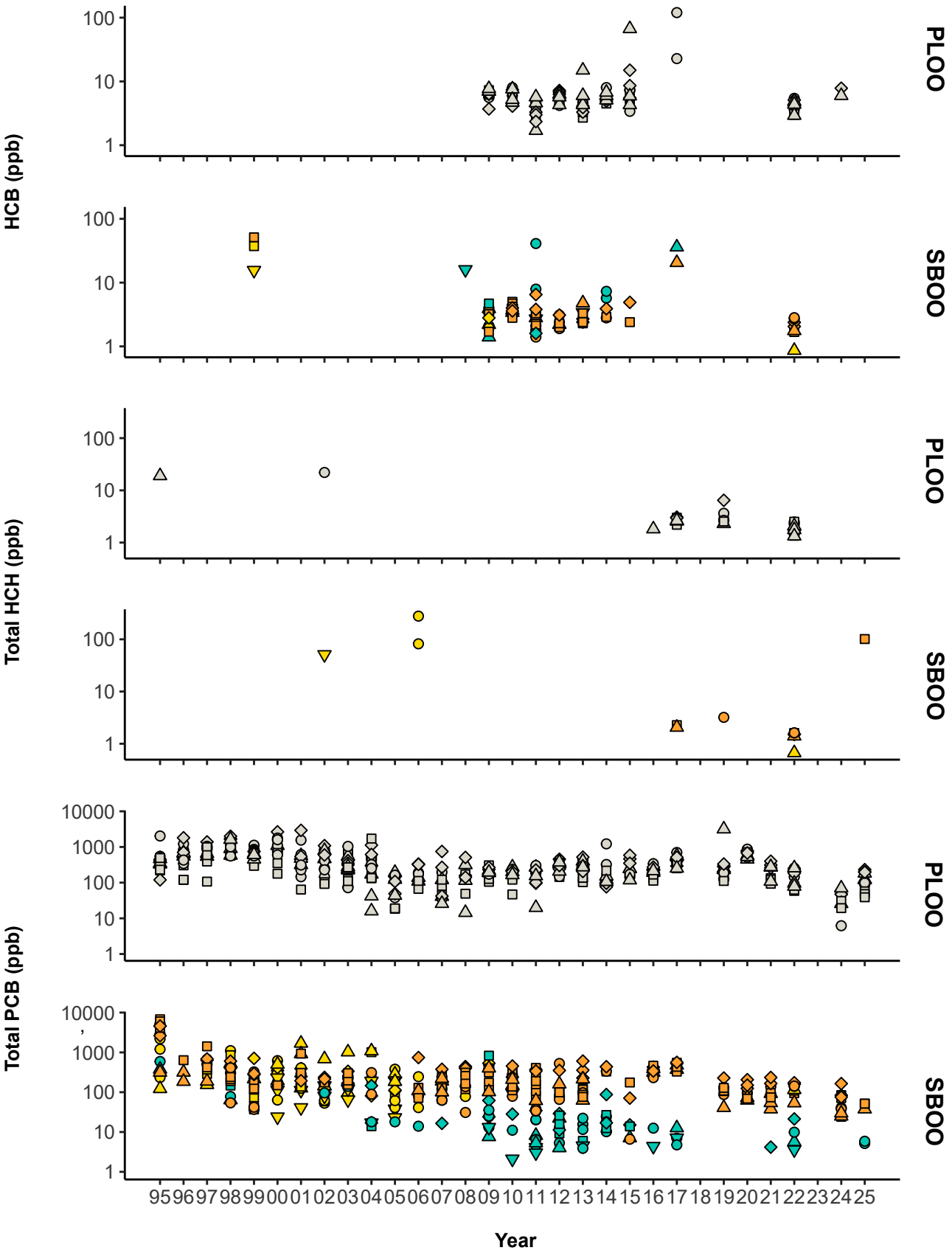


Figure 9.3 *continued*

Table 9.6

Summary of metals (ppm) in muscle tissues of fishes collected from PLOO and SBOO rig fishing zones during 2024-2025. Data include the number of detected values (n), minimum, maximum, and mean[a] detected concentrations per species and the total number of samples, detection rate, and maximum value for all species within each region. nd = not detected.

		Al	Sb	As	Ba	Be	Cd	Cr	Cu	Fe	Pb	Mn	Hg	Ni	Se	Ag	Sn	Zn
PLOO	Copper Rockfish																	
	n	0	0	1	1	0	0	1	1	1	0	1	1	0	1	1	1	1
	value	—	—	2.32	0.019	—	—	0.07	0.38	1.20	—	0.05	0.141	—	1.43	0.037	0.12	3.9
	Mixed Rockfish																	
	n	0	0	3	2	0	0	3	3	3	0	3	3	0	3	1	3	3
	min	—	—	1.24	0	—	—	0.04	0.28	1.45	—	0.03	0.082	—	1.07	nd	0.15	3.3
	max	—	—	1.67	0.024	—	—	0.07	0.43	2.95	—	0.07	0.445	—	1.26	0.032	0.16	6.9
	mean	—	—	1.43	0.021	—	—	0.05	0.35	2.37	—	0.05	0.240	—	1.19	0.032	0.16	4.6
	Speckled Rockfish																	
	n	0	0	1	1	0	0	1	1	1	0	1	1	0	1	0	1	1
	value	—	—	0.89	0.022	—	—	0.06	0.37	2.51	—	0.05	0.088	—	1.09	—	0.13	4.1
	Starry Rockfish																	
	n	0	0	2	2	0	0	2	2	2	0	2	2	0	2	0	2	2
	min	—	—	1.27	0.010	—	—	0.03	0.15	1.30	—	0.07	0.168	—	1.03	—	0.15	2.6
	max	—	—	1.31	0.040	—	—	0.04	0.21	1.34	—	0.08	0.178	—	1.04	—	0.15	2.7
	mean	—	—	1.29	0.025	—	—	0.04	0.18	1.32	—	0.08	0.173	—	1.04	—	0.15	2.7
	Vermilion Rockfish																	
	n	0	0	5	5	0	0	5	5	5	0	5	5	0	5	2	5	5
	min	—	—	1.28	0.006	—	—	0.05	0.30	1.32	—	0.08	0.036	—	0.62	0	0.10	3.1
	max	—	—	2.45	0.010	—	—	0.07	0.96	2.51	—	0.12	0.081	—	1.12	0.026	0.18	3.5
	mean	—	—	1.75	0.009	—	—	0.06	0.54	1.67	—	0.09	0.054	—	0.88	0.026	0.13	3.3
	Total Samples	12	12	12	12	12	12	12	12	12	12	12	12	12	12	12	12	12
	Detection Rate (%)	0	0	100	92	0	0	100	100	100	0	100	100	0	100	33	100	100
	Max	nd	nd	2.45	0.040	nd	nd	0.07	0.96	2.95	nd	0.12	0.445	nd	1.43	0.037	0.18	6.9

Table 9.6 *continued*

	Al	Sb	As	Ba	Be	Cd	Cr	Cu	Fe	Pb	Mn	Hg	Ni	Se	Ag	Sn	Zn
Brown Rockfish																	
n	0	0	2	2	0	0	2	2	2	0	2	2	0	2	0	2	2
min	—	—	0.91	0.010	—	—	0.06	0.11	0.90	—	0.04	0.070	—	0.66	—	0.1	2.8
max	—	—	1.01	0.010	—	—	0.07	0.21	1.23	—	0.04	0.084	—	0.75	—	0.11	3.1
mean	—	—	0.96	0.010	—	—	0.07	0.16	1.07	—	0.04	0.077	—	0.71	—	0.11	3.0
CA Scorpionfish																	
n	0	0	2	2	0	0	2	2	2	0	2	2	1	2	0	2	2
min	—	—	1.49	0.010	—	—	0.04	0.18	0.96	—	0.05	0.126	nd	0.72	—	0.13	2.8
max	—	—	4.05	0.010	—	—	0.05	1.35	1.16	—	0.05	0.212	0.07	0.80	—	0.14	3.0
mean	—	—	2.77	0.010	—	—	0.05	0.77	1.06	—	0.05	0.169	0.07	0.76	—	0.14	2.9
Honeycomb Rockfish																	
n	0	0	1	1	0	0	1	1	1	0	1	1	0	1	0	1	1
value	—	—	1.27	0.010	—	—	0.04	0.18	1.46	—	0.06	0.188	—	0.89	—	0.12	3.3
Mixed Rockfish																	
n	1	0	3	3	0	0	3	3	3	0	3	3	2	3	0	3	3
min	nd	—	1.73	0.004	—	—	0.05	0.17	1.27	—	0.04	0.059	0	0.95	—	0.15	3.2
max	0.48	—	3.04	0.040	—	—	0.05	0.21	1.34	—	0.09	0.160	0.48	1.11	—	0.16	3.8
mean	0.48	—	2.22	0.016	—	—	0.05	0.19	1.31	—	0.06	0.121	0.31	1.01	—	0.15	3.5
Treefish																	
n	0	0	1	1	0	0	1	1	1	0	1	1	0	1	0	1	1
value	—	—	1.50	0.005	—	—	0.04	0.17	1.08	—	0.02	0.189	—	0.80	—	0.08	3.3
Vermilion Rockfish																	
n	0	0	3	3	0	0	3	3	3	0	3	3	0	3	0	3	3
min	—	—	2.58	0.004	—	—	0.05	0.21	1.35	—	0.07	0.030	—	0.65	—	0.08	3.0
max	—	—	2.70	0.010	—	—	0.05	0.28	1.53	—	0.08	0.037	—	1.05	—	0.13	3.4
mean	—	—	2.65	0.008	—	—	0.05	0.24	1.47	—	0.07	0.034	—	0.89	—	0.11	3.2
Total Samples	12	12	12	12	12	12	12	12	12	12	12	12	12	12	12	12	12
Detection Rate (%)	8	0	100	100	0	0	100	100	100	0	100	100	25	100	0	100	100
Max	0.48	nd	4.05	0.040	nd	nd	0.07	1.35	1.53	nd	0.09	0.212	0.48	1.11	nd	0.16	3.8

[a] Minimum and maximum values were based on all samples, whereas means were calculated from detected values only

Table 9.7

Summary of metals (ppm) in muscle tissues of fishes collected from PLOO and SBOO rig fishing zones from 1995 through 2025. Data include the total number of samples (n), detection rate (DR%), minimum, maximum, and mean[a] detected concentrations for each guild or species; nd = not detected.

		Al	Sb	As	Ba	Be	Cd	Cr	Cu	Fe	Pb	Mn	Hg	Ni	Se	Ag	Sn	Zn
PLOO	Mixed Rockfish																	
	n	160	160	160	116	160	160	160	160	160	160	160	157	160	160	160	160	160
	DR%	31	8	87	47	3	27	61	66	79	3	41	97	11	97	7	41	99
	min	nd	nd	nd	nd	nd	nd	nd	nd	nd	nd	nd	nd	nd	nd	nd	nd	nd
	max	22.10	1.11	13.50	0.185	0.042	0.178	1.78	8.96	257.00	0.42	5.30	0.79	0.38	1.43	0.50	2.12	6.88
	mean	6.40	0.62	2.55	0.053	0.010	0.060	0.21	0.83	6.42	0.29	0.46	0.16	0.14	0.47	0.09	0.81	3.67
SBOO	Barred Sand Bass																	
	n	4	4	4	—	4	4	4	4	4	4	4	4	4	4	4	4	4
	DR%	0	0	0	0	0	0	0	0	100	0	0	100	0	75	0	0	75
	min	—	—	—	—	—	—	—	—	3.20	—	—	0.23	—	0	—	—	0
	max	—	—	—	—	—	—	—	—	6.65	—	—	0.36	—	0.71	—	—	5.01
	mean	—	—	—	—	—	—	—	—	4.64	—	—	0.29	—	0.66	—	—	4.41
	California Scorpionfish																	
	n	86	86	86	53	86	86	86	86	86	86	86	86	86	86	86	86	86
	DR%	36	1	74	36	5	23	49	71	81	5	27	97	9	87	3	30	100
	min	nd	nd	nd	nd	nd	nd	nd	nd	nd	nd	nd	nd	nd	nd	nd	nd	1.92
	max	19.40	0.23	5.35	0.151	0.025	0.083	2.21	5.11	21.20	0.38	1.85	1.54	0.22	0.80	0.11	1.96	6.77
	mean	6.50	0.23	2.40	0.055	0.013	0.043	0.26	1.00	5.06	0.28	0.17	0.19	0.10	0.28	0.09	0.78	3.90
	Mixed Rockfish																	
	n	76	76	76	67	76	76	76	76	76	76	76	76	76	76	76	76	76
	DR%	29	12	93	52	0	26	80	79	78	3	55	96	17	96	3	54	100
	min	nd	nd	nd	nd	—	nd	nd	nd	nd	nd	nd	nd	nd	nd	nd	nd	1.42
	max	16.10	1.57	11.20	0.202	—	0.197	0.81	3.80	20.80	0.44	2.60	0.33	0.73	1.22	0.07	2.43	6.16
	mean	5.24	0.77	2.25	0.044	—	0.079	0.22	0.54	3.46	0.38	0.16	0.10	0.21	0.41	0.07	0.78	3.76

[a] Minimum and maximum values were based on all samples, whereas means were calculated from detected values only

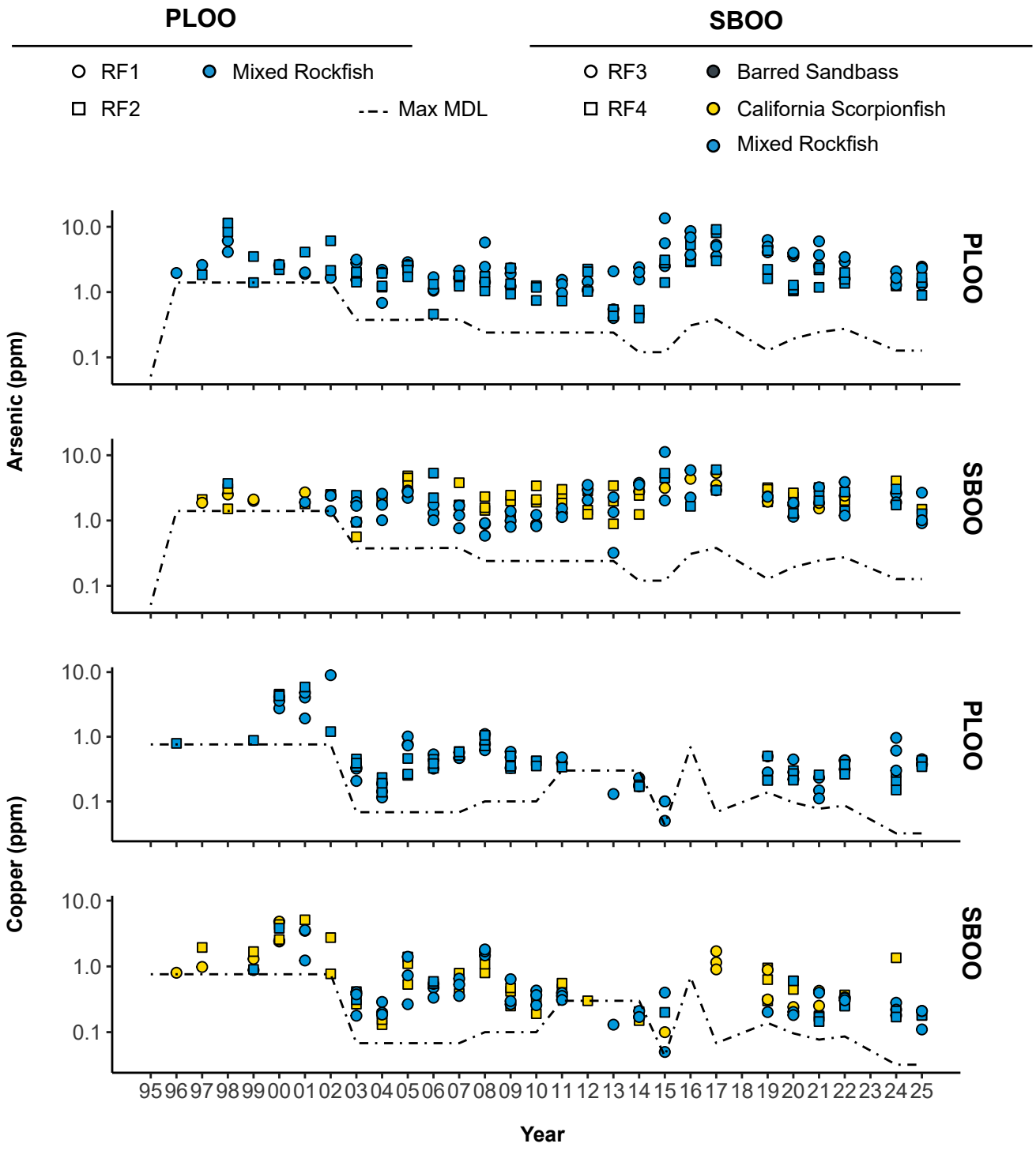


Figure 9.4

Concentrations of select metals detected in muscle tissues of fishes collected from PLOO and SBOO rig fishing zones from 1995 through 2025. Zones RF1 and RF3 are considered nearfield. No samples were collected in 2018 and 2023 as described in text.

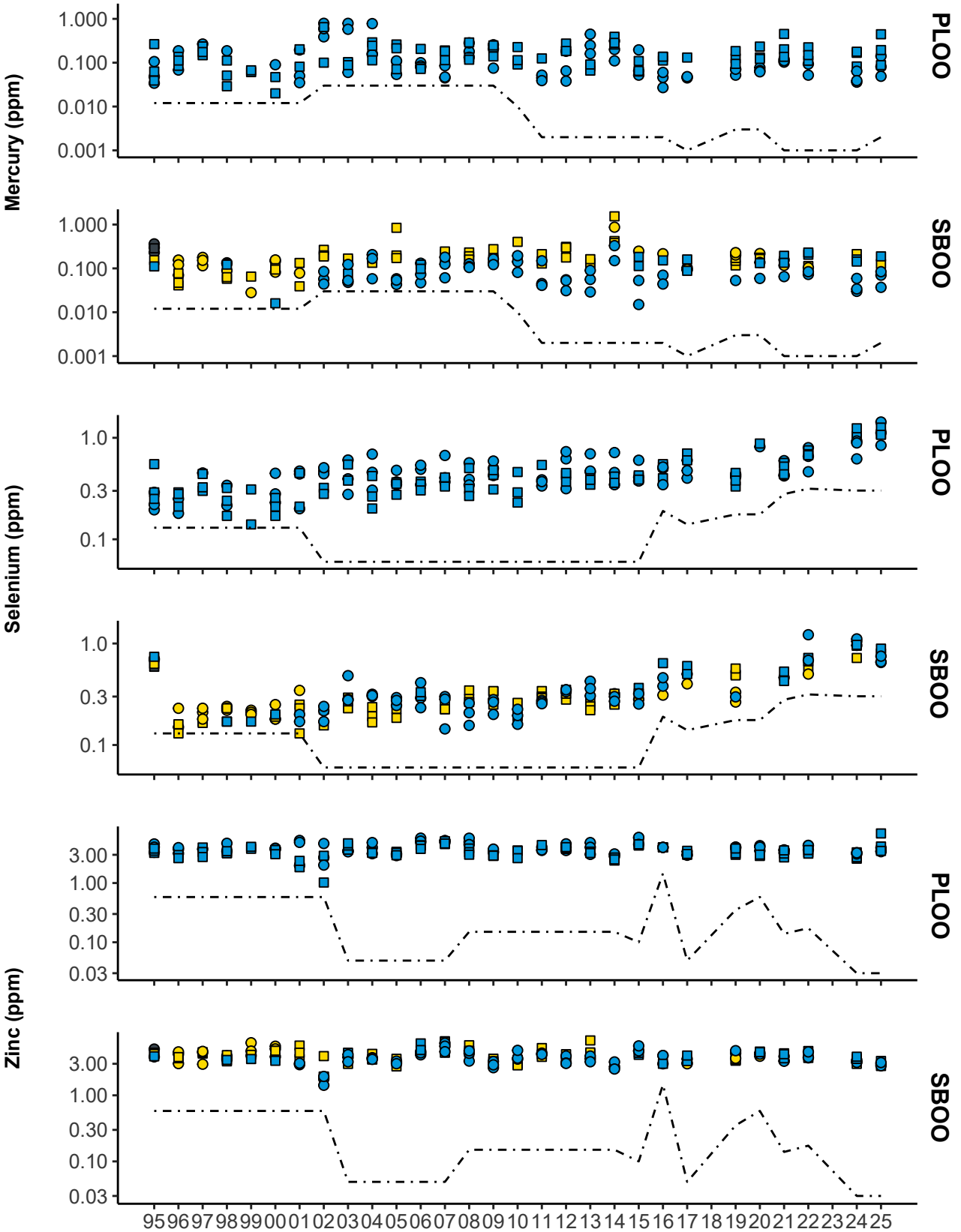


Figure 9.4 *continued*

Table 9.8

Summary of metals (ppm), pesticides (ppb), and total PCB (ppb) in fish muscle samples with chemistry concentrations that exceeded available thresholds (see Mearns et al 1991) from PLOO and SBOO rig fishing zones sampled historically (1995–2023) and during the current reporting period (2024-2025). Data include the percent of samples that exceeded thresholds during each time period. See Tables 9.2–9.7, 9.9–9.10 for total number of samples analyzed.

		PLOO				SBOO			
		1995–2023		2024-2025		1995–2023		2024-2025	
Threshold		**RF1**	**RF2**	**RF1**	**RF2**	**RF3**	**RF4**	**RF3**	**RF4**
Median International Standard [a]									
Arsenic	1	75	49	67	17	53	68	67	83
Cadmium	1	0	0	0	0	0	0	0	0
Chromium	1	1	1	0	0	4	0	0	0
Copper	20	0	0	0	0	0	0	0	0
Lead	2	0	0	0	0	0	0	0	0
Mercury	1	6	1	0	0	1	2	0	0
Selenium	0.30	77	71	100	100	32	37	100	100
Tin	175	0	0	0	0	0	0	0	0
Zinc	70	0	0	0	0	0	0	0	0
Total Chlordane	100	0	0	0	0	0	0	0	0
Total DDT	5000	0	0	0	0	0	0	0	0
Hexachlorobenzene	100	0	0	0	0	0	0	0	0
OEHHA [b]									
Mercury	0.22	18	22	0	17	9	17	0	0
Selenium	7.40	0	0	0	0	0	0	0	0
Total DDT	21	17	9	0	17	12	6	0	0
Total Chlordane	6	0	0	0	0	0	0	0	0
Total PCB	4	30	14	0	17	15	4	0	0
USFDA [a]									
Mercury	1	0	0	0	0	0	4	0	0
Total DDT	5000	0	0	0	0	0	0	0	0
Hexachlorobenzene	300	0	0	0	0	0	0	0	0

[a] From Mearns et al. 1991. USFDA action limits for mercury and all international standards are for shellfish, but are often applied to fish

[b] From the California OEHHA (Klasing and Brodberg 2008)

Table 9.9

Summary of pesticides (ppb), total PCB (ppb), total PBDE (ppb), and lipids (% weight) in muscle tissues of fishes collected from PLOO and SBOO rig fishing stations during 2024-2025. Data include the number of detected values (n), minimum, maximum, and mean[a] detected concentrations for each species, and the total number of samples, detection rate and maximum value for all species within region. nd = not detected.

		Pesticides					
		tChlor	**tDDT**	**HCB**	**tPCB**	**tPBDE**	**Lipids**
PLOO	Copper Rockfish						
	n	0	1	0	1	0	1
	value	—	4.10	—	1.965	—	1.72
	Mixed Rockfish						
	n	0	3	0	2	2	3
	min	—	2.27	—	nd	nd	1.30
	max	—	21.48	—	12.959	2.550	2.67
	mean	—	9.80	—	6.956	1.345	2.19
	Speckled Rockfish						
	n	0	1	0	1	0	1
	value	—	3.19	—	1.416	—	3.06
	Starry Rockfish						
	n	0	2	0	0	2	2
	min	—	2.73	—	—	0.145	0.82
	max	—	4.02	—	—	0.222	0.98
	mean	—	3.38	—	—	0.184	0.90
	Vermilion Rockfish						
	n	0	5	1	1	2	5
	min	—	1.31	0	0	0	0.45
	max	—	2.62	0.72	1.176	0.244	1.02
	mean	—	1.71	0.72	1.176	0.218	0.82
	Total Samples	12	12	12	12	12	12
	Detection Rate (%)	0	100	8	42	50	100
	Max	0	21.48	0.72	12.959	2.55	3.06

Table 9.9 *continued*

		Pesticides					
		tChlor	tDDT	HCB	tPCB	tPBDE	Lipids
SBOO	Brown Rockfish						
	n	0	2	0	0	0	2
	min	—	1.41	—	—	—	1.15
	max	—	3.38	—	—	—	1.79
	mean	—	2.40	—	—	—	1.47
	CA Scorpionfish						
	n	0	2	0	0	1	2
	min	—	0.81	—	—	nd	0.35
	max	—	5.16	—	—	0.259	0.76
	mean	—	2.98	—	—	0.259	0.55
	Honeycomb Rockfish						
	n	1	1	0	1	0	1
	value	2.277	4.9	—	1.572	—	1.06
	Mixed Rockfish						
	n	0	2	0	0	0	2
	min	—	nd	—	—	—	0
	max	—	1.67	—	—	—	0.44
	mean	—	1.45	—	—	—	0.42
	Treefish						
	n	0	1	0	0	0	1
	value	—	2.54	—	—	—	0.58
	Vermilion Rockfish						
	n	0	2	0	0	1	3
	min	—	nd	—	—	nd	1.19
	max	—	1.05	—	—	0.165	1.85
	mean	—	1.02	—	—	0.165	1.41
	Total Samples	12	12	12	12	12	12
	Detection Rate (%)	8	83	0	8	17	92
	Max	2.277	5.16	nd	1.572	0.259	1.85

[a] Minimum and maximum values were based on all samples, whereas means were calculated from detected values only

Table 9.10

Summary of pesticides (ppb), total PCB (ppb), total PAH (ppb), and lipids (% weight) in muscle tissues of fishes collected from PLOO and SBOO rig fishing zones from 1995 through 2025. Data include total number of samples (n), detection rate (DR%), minimum, maximum, and mean[a] detected concentrations per species; nd = not detected.

		Pesticides								
		tChlor	tDDT	Dieldrin	Endrin	HCB	tHCH	tPCB	tPAH	Lipids
PLOO	Mixed Rockfish									
	n	160	160	148	148	147	160	160	87	160
	DR (%)	3	93	0	0	12	2	43	7	98
	min	nd	nd	—	—	nd	nd	nd	nd	nd
	max	2.4	217.3	—	—	15.0	13.4	69.0	360.1	4.4
	mean	1.1	12.2	—	—	1.3	4.5	8.2	166.6	0.9
SBOO	Barred Sand Bass									
	n	4	4	4	4	4	4	4	4	4
	DR (%)	0	50	0	0	0	0	75	0	100
	min	—	nd	—	—	—	—	nd	—	0.7
	max	—	13.0	—	—	—	—	32.0	—	1.4
	mean	—	9.6	—	—	—	—	20.0	—	1
	CA Scorpionfish									
	n	82	82	80	80	76	82	86	64	86
	DR (%)	0	93	0	0	0	0	40	3	100
	min	—	nd	—	—	—	—	nd	nd	0.1
	max	—	195.7	—	—	—	—	49.3	22.7	2.6
	mean	—	16.5	—	—	—	—	5.2	18.4	0.6
	Mixed Rockfish									
	n	74	74	67	67	69	74	76	70	76
	DR (%)	1	76	1	1	6	0	20	4	97
	min	nd	nd	nd	nd	nd	—	nd	nd	nd
	max	2.3	15.1	0.3	0.7	7.2	—	5.6	227	3.0
	mean	2.3	3.1	0.3	0.7	2.0	—	1.4	92.4	0.7

[a] Minimum and maximum values were based on all samples, whereas means were calculated from detected values only

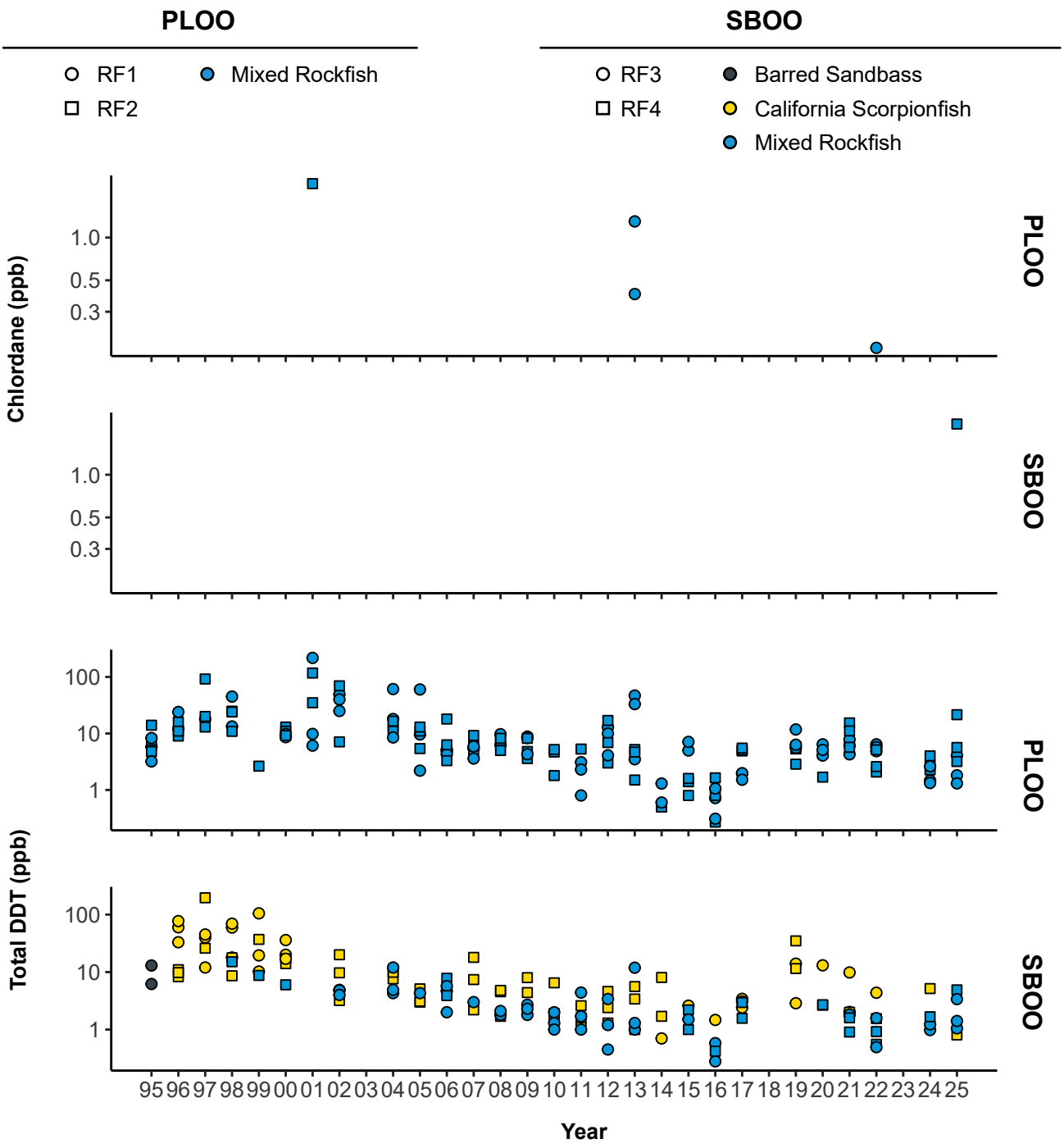


Figure 9.5

Concentrations of pesticides and total PCB in muscle tissues of fishes collected from PLOO and SBOO rig fishing zones from 1995 through 2025. Zones RF1 and RF3 are considered nearfield. No samples were collected in 2018 and 2023 as described in text.

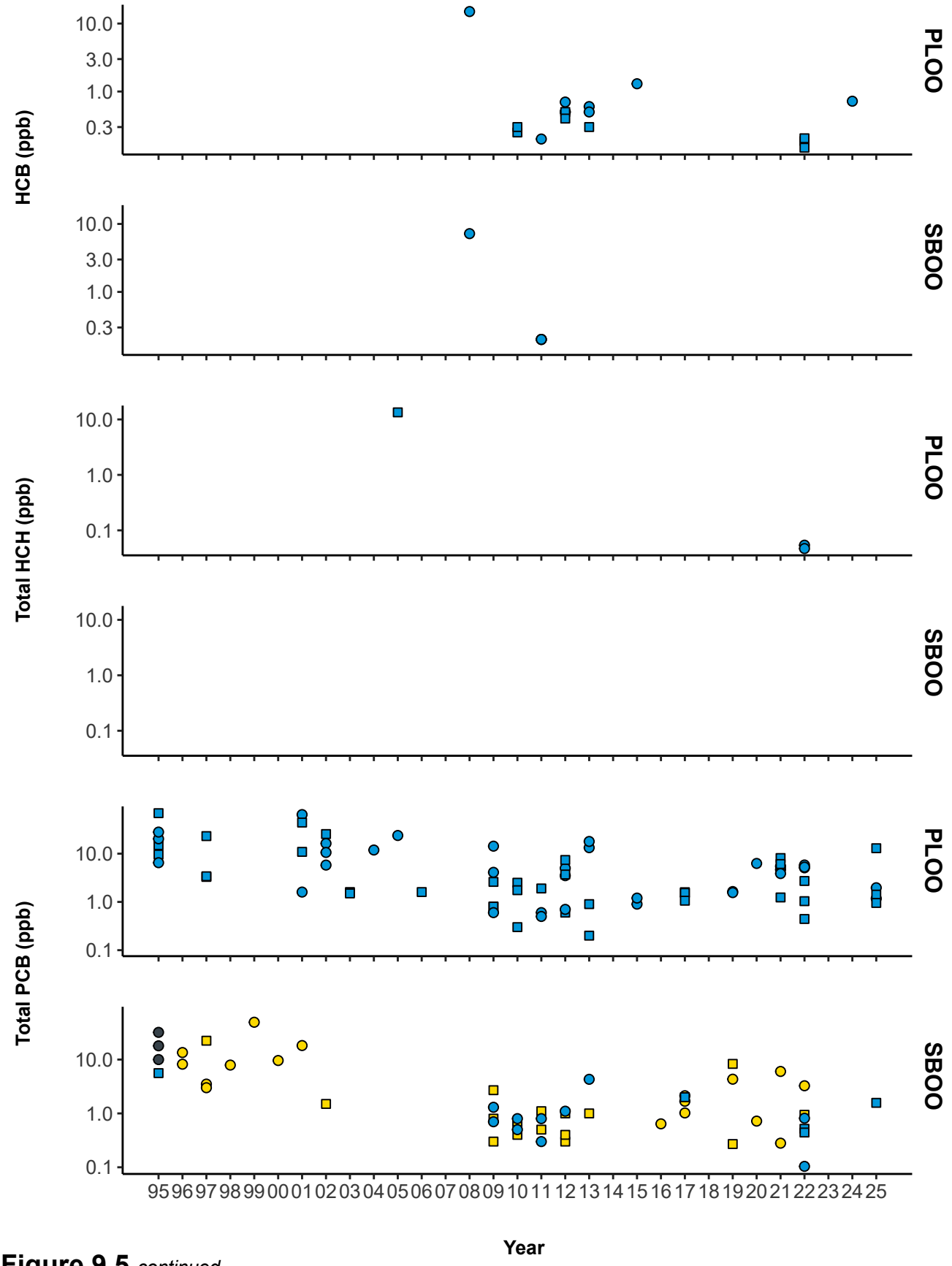


Figure 9.5 *continued*

Appendices

Appendix A

NPDES Permit Questions

Appendix A. NPDES Permit Questions

The following questions are taken directly from *Attachment E - Monitoring and Reporting Program* sections of the National Pollution Discharge Elimination System (NPDES) permits and associated orders for the following facilities: the Point Loma Wastewater Treatment Plant (PLWTP), the South Bay Water Reclamation Plant (SBWRP), and the South Bay International Wastewater Treatment Plant (SBIWTP), which is owned and operated by the U.S. Section of the International Boundary and Water Commission (USIBWC) (see Chapter 1, Table 1.1). Brief responses are provided here but you are encouraged to refer to the appropriate chapters of this Biennial Report for more detailed analyses and discussions.

Receiving Water Monitoring Requirements (SBWRP, SBIWTP, PLWTP)

- **Does the receiving water meet water quality standards?** Compliance with receiving water limitations for bacterial characteristics in the Point Loma Ocean Outfall (PLOO) region were above the minimum threshold for all metrics throughout the 2024-2025 report period. As has been reported in the past, the nearshore South Bay Ocean Outfall (SBOO) region continues to show water quality impacts, with overall compliance below the minimum threshold for fecal coliforms on 585 of the 731 days (80% days out of compliance) in the report period, and all of the 731 days (100%) in the report period for Enterococcus and total coliforms. Stations with the highest occurrence of elevated Fecal Indicator Bacteria (FIB) were shore and nearshore stations located close to the mouth of the Tijuana River Estuary. Consequently, non-compliance was driven primarily by Tijuana River outflows and runoff, not treated wastewater discharge from the SBOO or PLOO.

- **Are the receiving water conditions getting better or worse over time?** Overall conditions, when considering the sediments, fish, invertebrates, and water quality remain good. Historical review of temperature, salinity, and dissolved oxygen changes, sampled from 1991 through 2025, show that ocean conditions in the PLOO and SBOO regions respond most strongly to long-term climate-related changes in the Southern CA Bight, such as transition periods between La Nina and El Nino conditions. Nevertheless, there continues to be a general decline in water quality compliance in the SBOO region. PLOO shore and nearshore stations remained highly compliant overall during the reporting period, with occasional exceedances associated primarily with wet-season conditions. However, all bacterial compliance metrics in the SBOO region, from the shoreline to offshore, indicate a decline in compliance when compared with results from years following the initiation of secondary treatment in 2011. Several factors may influence compliance. Precipitation remained high in 2024 (11.16 in.), following a very wet 2023 (14.43 in.), compared to prior years (9.59 in. on average). Periodic excess flows from the SBIWTP to the SBOO have occurred in response to infrastructure failure, storm-related damage, and resulting ongoing repairs, especially prior to November of 2024. Combined with outflows from the Tijuana River, these factors were likely to drive the observed decrease in water quality throughout the SBOO region.

- **What is the relative contribution of the Facility's discharge to pollution in the receiving water?** Plumes remained offshore with no shoreward transport. Elevated FIB near outfalls remained low relative to pre-secondary treatment levels albeit recent declines in nearshore SBOO water quality are noteworthy. However, the primary source of contamination remains the Tijuana River Estuary outflows and transboundary/non-point source runoff, not treated wastewater discharge.

- **What are the effects of the discharge on the receiving waters?** No significant effects are attributable to discharge beyond occasional non-compliant water quality samples outside of state waters, which are transient. Oceanographic conditions followed natural patterns (upwelling, La Niña/El Niño transition). Benthic habitats, sediments, fish, and invertebrate communities showed no degradation or outfall-related patterns.

Shoreline Water Quality Monitoring Requirements (SBWRP, SBIWTP, PLWTP)

- **Does the effluent cause or contribute to an exceedance of the water quality standards in the receiving water?** Outfall specific exceedances are generally minimal and transient. Non-compliance with bacterial standards is primarily driven by Tijuana River Estuary outflows and non-point source runoff, not treated wastewater discharge from the outfalls.

- **Does the effluent reach water contact zones or commercial shellfish beds?** There was no evidence that wastewater plumes from either outfall reached recreational waters, nearshore kelp beds, or commercial shellfish beds.

- **Are densities of bacteria in water contact areas below levels protective of public health?** Compliance with receiving water limitations for bacterial characteristics in the PLOO region were above the minimum threshold for all metrics throughout the 2024-2025 report period. Whereas the nearshore in the SBOO region continues to show water quality impacts, as has been reported in the past, with overall compliance below the minimum threshold for fecal coliforms on 585 of the 731 days (80% days out of compliance) in the report period, and all of the 731 days (100%) in the report period for Enterococcus and total coliforms. Stations with the highest occurrence of elevated FIB were shore and nearshore stations located close to the mouth of the Tijuana River Estuary. Consequently, non-compliance was driven primarily by Tijuana River outflows and runoff, not treated wastewater discharge from the SBOO or PLOO.

Offshore Water Quality and Kelp Monitoring Requirements (SBWRP, SBIWTP, PLWTP)

- **Is natural light significantly reduced at any point outside the ZID as a result of the discharge?** Natural light levels (transmissivity/water clarity) were within historical ranges; proximity to either outfall was not a significant driver of variations.

- **Does the discharge cause a discoloration of the ocean surface?** Based on visual observations collected throughout the reporting period, the discharges do not appear to cause a discoloration of the ocean surface. In the PLOO region the discharge is trapped below the thermocline and so does not impact surface waters. In the SBOO region, while the discharge does occasionally reach

the surface during the winter when stratification is lacking, no discoloration has been linked to the discharge itself, rather discoloration of the water in the SBOO region is often linked to discharges form the TJ River, as identified in water quality data and satellite imagery.

- **Does the discharge of oxygen demanding waste cause the dissolved oxygen concentration to be depressed at any time more than 10 percent from that which occurs naturally outside the ZID?** Dissolved Oxygen (DO) concentrations were generally within historical ranges; changes in DO are largely driven by natural upwelling, not discharge. Proximity to outfall was not a significant driver.

- **Does the discharge of waste cause the pH to change at any time more than 0.2 units from that which occurs naturally outside the ZID?** pH was within historical ranges; changes in pH are largely driven by natural upwelling or surface production associated with chlorophyll, not discharge. Proximity to outfall was not a significant driver.

- **Is the wastewater plume encroaching upon receiving water areas used for swimming, surfing, diving, and shellfish harvesting?** Plumes remained offshore with no evidence of nearshore movement or encroachment.

- **What is the fate of the discharge plume?** The PLOO plume generally remained offshore and below 30 m depth. The SBOO plume can reach surface waters in the vicinity of the offshore outfall during periods of weak water column stratification, particularly from November through January. Both PLOO and SBOO plumes were transported along the coast (generally N:NW by S:SE trajectory) rather than inshore.

- **Are fecal indicator bacteria present outside the ZID? If so, do the bacteria come from a human source(s)?** No notable sources in the PLOO region, but in the SBOO region yes, especially nearshore. The primary source is Tijuana River Estuary outflows and transboundary flows (not facility discharge).

(PLWTP Only)

- **Does the discharge of waste cause the salinity to become elevated in the receiving water?** Salinity was within historical ranges; changes in salinity are largely driven by natural upwelling, not discharge. Proximity to outfall was not a significant driver.

(SBWRP and SBIWTP Only)

- **What is the potential error associated with the pH samples collected by the conductivity-temperature-depth (CTD) profiler?** On average, CTD pH was 0.036 ± 0.072 pH units higher than the spectrophotometric bottle measurements, highlighting that the City's CTD pH electrode calibration procedure conducted the morning of every deployment (± 0.05 pH units) is adequately ensuring that the CTD pH data are not subject to drift within the accuracy range of these sensors as stated by the manufacturer (± 0.1 pH units).

- **Is the aragonite saturation state at a level which is harmful to aquatic life?** On average, the in-situ aragonite saturation state (Ωarg) was 1.7 ± 0.5. Ωarg was highest at the surface (1 - 10 m) in the summer (3.0 ± 0.3) and lowest at the bottom (51 – 150 m) in the spring (1.0 ± 0.1). Across the PLOO and SBOO regions, Ωarg ranged from a minimum of 0.9 to a maximum of 2.8 in winter, 0.8 to 3.6 in spring, 0.9 to 3.4 in summer, and 0.9 to 2.9 in fall. In general, the ranges of Ωarg observed agree with expectations for nearshore variability in the California current system (maxima > 3 and minima < 1; Feely et al. 2008; Alin et al. 2012).

- **Do nutrients cause objectionable aquatic growth or degrade indigenous biota?** Chlorophyll *a* concentrations were within historical ranges and followed natural seasonal patterns; proximity to outfall was not a significant driver of variations or degradation.

Benthic Monitoring Requirements (SBWRP, SBIWTP, PLWTP)

- **Is the dissolved sulfide concentration of waters in sediments significantly increased above that present under natural conditions?** During 2024 and 2025, sulfide values (measured as total sulfides) remained within range of those reported regionally in San Diego and in other southern California coastal areas. While relatively high concentrations of sulfides were occasionally detected at near-ZID stations, there was no evidence of degraded benthic habitat based on the sediment quality triad.

- **Is the concentration of substances set forth in Table 3 of the Ocean Plan for protection of marine aquatic life in marine sediments at levels which would degrade the benthic community?** Contaminant concentrations were within regional variability and below available ERL/ERM thresholds and sediment quality triad results indicate that all PLOO, SBOO and regional sites evaluated were unimpacted. There was no evidence of degradation from discharge.

- **Is the concentration of organic pollutants in marine sediments at levels that would degrade the benthic community?** During 2024 and 2025, organic loading indicators (i.e. sulfides, TOC, TN, BOD, TVS) remained within range of those reported regionally in San Diego and in other southern California coastal areas, and there was no evidence of degraded benthic habitat based on the sediment quality triad.

- **Are benthic communities degraded as a result of the discharge?** Communities were healthy, similar to 1991–2025 regional/reference conditions, and segregated by natural habitat factors (depth, sediment type). 90% of BRI values indicated reference conditions.

- **Is the sediment quality changing over time?** No significant change attributable to discharge; quality remained similar to previous years and within natural variability across the San Diego region.

Fish and Macroinvertebrates Monitoring Requirements (SBWRP, SBIWTP, PLWTP)

- **Does the concentration of pollutants in fish, shellfish, or other marine organisms used for human consumption bioaccumulate to levels that are harmful to human health?** No evidence of contaminant accumulation associated with discharge; values were within previously reported ranges for southern California fishes.

- **Does the concentration of pollutants in marine life bioaccumulate to levels that degrade marine communities?** No evidence of accumulation associated with discharge that would degrade communities.

- **Are the concentrations of pollutants in fish and other marine organisms changing over time?** Most values were within previously reported ranges for southern California fishes; no outfall-related patterns.

- **Is the health of fish changing over time?** Fish remained healthy (<0.2% with parasites/abnormalities); no relationship to outfall proximity.

- **Are the populations of selected species of fish and invertebrates changing over time?** Populations are highly variable but consistent with previous years; no changes attributable to discharge.

Regional Monitoring Requirements (SBWRP, SBIWTP, PLWTP)

- **What are the status and trends of conditions in ocean waters in the San Diego Region with regard to beneficial uses?** For example: Are fish and shellfish safe to eat? Is water quality safe for swimming? Are ecosystems healthy? Fish and shellfish are healthy and representative of region-wide populations throughout southern California. Ecosystems are healthy (benthic, fish, and invertebrate communities in excellent/reference condition). Water quality showed a continued decline in compliance in the South Bay region, which was largely driven by increased rainfall/runoff and outflows from the Tijuana River.

- **What are the primary stressors causing or contributing to conditions of concern?** Heavier-than-normal rainfall, terrestrial runoff, nearshore contamination, and (in SBOO) increased SBIWTP flows with reduced primary treatment.

- **What are the major sources of the stressors causing or contributing to conditions of concern?** Contaminated outflows from the Tijuana River Estuary, transboundary flows, and other non-point source runoff.

- **Are the actions taken to address such stressors and sources effective (i.e., environmental outcomes)?** Treated wastewater discharge via the outfalls has minimal impact on receiving waters with no outfall-related degradation observed in sediments or biota. However, uncontrolled transboundary outflows continue to heavily impact water quality, particularly in the South Bay region, with no actions to date showing effective solutions to mitigate this stressor.

Kelp Bed Canopy Monitoring Requirements (SBWRP, SBIWTP, PLWTP)

- **What is the maximum areal extent of the coastal kelp bed canopies each year?** The most recent aerial kelp survey report covers the period of 2023 and 2024. The total amount of kelp coverage between Orange County and San Diego County in 2024 was 0.6 km^2, decreasing by 25% from 2023. Of the 25 designated kelp beds in the region (including Corona del Mar), 13 displayed surface canopy in 2024, including one that reappeared, three that increased in size, and seven that decreased in size. The Point Loma and La Jolla kelp beds accounted for 34% of the total kelp coverage in the region.

- **What is the variability of the coastal kelp bed canopy over time?** Kelp canopy and abundance are highly variable across seasons, years, and locations. Since 2007, giant kelp has experienced episodic recruitment pulses, declines in persistence at several historically stable beds, and partial recovery during 2023–2025. Some sites (such as La Jolla South and Point Loma Central) showed densities and plant sizes in the top 10–20% of the long-term record, while other sites remained historically low. Variability is strongly linked to temperature, nutrient availability, light, wave disturbance, sea urchin grazing, and competition from understory algae.

- **Are coastal kelp beds disappearing? If yes, what are factors that could contribute to the disappearance?** Some historically stable kelp beds have shown reduced persistence and lower abundance over the past decade, indicating partial decline. While recovery occurred at some sites during 2023–2025, many areas remain below historical conditions. Contributing factors include warmer water and marine heatwaves that reduce nutrient availability, strong storm waves that remove adult kelp, and competition from understory kelps such as Laminaria, Pterygophora, and Eisenia. As in past sampling and monitoring periods, the relative persistence of the kelp forest at Point Loma when compared with other sites along the coast, continues to suggest that point source impacts of the Point Loma outfall are not controlling kelp population fluctuations. Other factors most likely influencing kelp abundance in the San Diego area are seawater temperature fluctuations, oceanic nutrient availability, light (especially for early life stage kelps), and benthic competition for space.

- **Are new coastal kelp beds forming?** Recruitment of juvenile giant kelp (Macrocystis pyrifera) was documented during 2023–2025, particularly at La Jolla South and Point Loma sites, indicating active formation and recovery of kelp populations following earlier recruitment failures. However, this recruitment occurred in known, existing or previously defined/named kelp beds. No new coastal kelp beds have formed.

Appendix B

Coastal Oceanographic Conditions

2024 – 2025 Supplemental Analyses

Appendix B.1

Sample dates for quarterly oceanographic surveys conducted during 2024 and 2025. All stations in each station group were sampled on a single day (see Figure 2.1 for stations and locations).

	2024				2025			
	Winter	**Spring**	**Summer**	**Fall**	**Winter**	**Spring**	**Summer**	**Fall**
PLOO Station Group								
Kelp WQ	Feb-12	May-13	Aug-12	Nov-18	Feb-19	May-19	Aug-11	Nov-10
18 & 60-m WQ	Feb-14	May-15	Aug-14	Nov-20	Feb-21	May-21	Aug-14	Nov-13
80-m WQ	Feb-15	May-16	Aug-15	Nov-21	Feb-22	May-22	Aug-13	Nov-14
98-m WQ	Feb-13	May-14	Aug-13	Nov-19	Feb-20	May-20	Aug-12	Nov-12
SBOO Station Group								
Kelp WQ	Feb-21	May-6	Aug-5	Nov-4	Feb-3	May-12	Aug-4	Nov-3
North WQ	Feb-24	May-10	Aug-8	Nov-7	Feb-5	May-14	Aug-6	Nov-5
Mid WQ	Feb-23	May-8	Aug-9	Nov-6	Feb-4	May-15	Aug-6	Nov-6
South WQ	Feb-22	May-7	Aug-7	Nov-5	Feb-6	May-13	Aug-5	Nov-4

SBOO North (I28–I31, I33–I38); SBOO Mid (I12–I18, I20–I23, I27); SBOO South (I1–I11)

Appendix B.2

Location, depth, and dates for each year-long deployment of the PLOO and SBOO RTOMS. Dates are displayed by deployment, recovery, and period of real-time (RT) data availability. All times are Pacific Standard Time; DD = decimal degrees.

Site	Deployment #	Lat (DD)	Long (DD)	Total Depth (m)	Deployment	RTdata Start	RTdata End	Recovery
SBOO	5	32.53185	-117.18651	31	29 Jun 2023 11:15	29 Jun 2023 11:30	21 May 2024 8:00	21 May 2024
	6	32.53187	-117.18630	31	30 Jul 2024 12:23	30 Jul 2024 13:00	4 Jun 2025 8:10	4 Jun 2025
	7	32.53195	-117.18613	30.2	10 Jul 2025 11:22	10 Jul 2025 13:30	Present	
PLOO	5	32.67012	-117.32463	96	20 Dec 2023 9:32	20 Dec 2023 9:40	9 Dec 2024 9:50	9 Dec 2024
	6	32.6702	-117.32458	96	14 Apr 2025 12:36	14 Apr 2025 12:40	29 Oct 2025 8:10	29 Oct 2025
	7	32.66926	-117.32382	95	11 Dec 2025 10:30	11 Dec 2025 15:00	Present	

Appendix B.3

Summary of manual QA/QC review findings, including major sensor problems and data quality issues for the PLOO and SBOO RTOMS. Gaps in data resulted during time periods data were not collected or flagged as bad or suspect.

Parameter	Site	Depths	Time Period	Problem	Action Taken
All Parameters	PLOO	All	Jun-2025	Fishing vessel fouled mooring with nets and dragged anchor on 6/17 about 660 m SSE against outfall pipe and mooring relocated on 7/1.	Data evaluated carefully during this period due to fouled fishing nets; if no issues found, data passed and was reported
Chlorophyll a, CDOM, and turbidity	PLOO	30 m	Jun-Oct 2025	ECO triplet sensor face was severely fouled with fishing nets, resulting in noisy and spiky data.	Data qualified as bad and not reported
Salinity	PLOO	87 m	May-Oct 2025	Backup SBE37IM sensor drifted excessively low compared to nearby depths	Data qualified as suspect and not reported
DO	PLOO	75 m	Apr-Oct 2025	SBE37-ODO sensor consistently low compared to all CTD validation casts at same depth and nearby stations in similar depth.	Data drift corrected using minimum correction and applied to duration of deployment
Nitrate + nitrite	PLOO	30 m	Dec-2025	SUNA nitrate sensor reported slightly negative values upon deployment.	Data drift corrected by minimum readings, validated with water samples, and reported
CDOM and turbidity	SBOO	18 m	Jan-Jun 2025	ECO triplet sensor spiked to high values far outside typical ranges not observed at other depths.	Data qualified as suspect and not reported
CDOM and turbidity	SBOO	26 m	Aug-Dec 2025	SeaOwl sensor fouled early in deployment and drifted low and negative	Data qualified as suspect and not reported
xCO2	SBOO	1 m	May-Jun 2025	Unexplained upward spikes that did not correspond with any DO or pH events.	Data qualified as suspect and not reported
Nitrate + nitrite	SBOO	26 m	Jan-Jun 2025	SUNA nitrate sensor showed extreme noise and flatlining through much of deployment.	Data qualified as suspect and not reported
Nitrate + nitrite	SBOO	1 m	Jan-Dec 2025	SUNA nitrate sensors drifted low and showed negative data throughout deployments.	Data drift corrected with water samples and reported
Nitrate + nitrite	SBOO	26 m	Jul-Dec 2025	SUNA nitrate sensor drifted low in slope over time of deployment.	Data drift corrected with water samples and reported

Appendix B.4

Location, depth, and dates for each deployment of static moorings located at the PLOO and SBOO. DD = decimal degrees.

Site	Deployment #	Lat (DD)	Long (DD)	Total Depth (m)	Deployment
PLOO	ADCP (#2)	32.66711	117.32686	100	22 Apr 2024
SBOO	ADCP (#3)	32.53642	117.19796	36	2 May 2024
PLOO	Thermistor (#1) south	32.65941	117.32559	100	25 Apr 2024
PLOO	Thermistor (#2) north	32.66392	117.32718	100	23 Apr 2024
SBOO	Thermistor(#6)	32.53052	117.20138	36	1 May 2024

Appendix B.5

Data qualifier definitions for QC data flags. Follows national data standards for summary real-time data flagging (US IOOS 2017), and post-processing data flagging (ARGO 2020).

QC_Flag	Designation	Use
1	Pass/good	For data reviewed both automatically and manually
2	Provisional/unreviewed	For data that is not reviewed or unable to validate; or passed automated test only
3	Suspect/questionable	Failed automated test but not unreasonable (such as climatology test) or manually flagged as possible instrument drift (such as due to biofouling)
4	Bad	Failed automated test (such as out of range test) or manually flagged as clearly bad (such as due to instrument malfunction)
5	Value changed/drift-corrected	Used only in post-processing. Values have been corrected based on new information, such as water sample results to correct for drift or new calibration factors. For data use purposes, this flag can be treated as a “pass.” Original data are also retained separately.
9	Missing	Placeholder to show missing real-time data; may be able to be filled in later by downloaded data after mooring recovery

Appendix B.6

Ranges used for automated QC data flagging for each parameter for the gross range test. Values outside of these ranges were assigned a qualifier flag value of 4. Ranges were defined by manufacturers for each sensor configuration.

Parameter	Units	Min	Max
CDOM - Eco triplet	ppb	0	375
Chl - Eco triplet	µg/L	0	75
xCO_2	ppm	0	2000
NO_3 (Nitrate + Nitrite)	µM	0	3000
NTU (Turbidity)	NTU	0	100
O_2 (DO)	mg/L	0.1	24
pH (total scale; both internal and external)	pH_T	6.5	9
Sal (Salinity)	PSU	2	42
Temp (Temperature)	°C	-2.5	35

Appendix B.7

Annual ranges used for automated QC data flagging for each parameter, site, and depth for the climatological range test. Temperature, salinity, DO, and pH_T ranges were based on the minimum and maximum values recorded at each site and depth range where the sensors were found to be functional and in reasonable agreement with historical CTD ranges from the City's quarterly surveys. CDOM ranges were based on maximum of multiple readings recorded at the PLOO mooring due to proximity to plume. Chlorophyll *a* and turbidity ranges were based on the maximum sensor range for the ECO triplet. Nitrate ranges were based on values observed at both moorings where the sensors were found to be functional, and verified in a reasonable range compared to nearshore data collected by the California Cooperative Oceanic Fisheries Investigations (see: https://calcofi.org). Ranges for xCO_2 were based on values observed at both moorings, where the phytoplankton bloom in spring 2020 resulted in lower xCO_2 values than prior years, and comparable to ranges recorded by the closest NOAA/SIO carbon program mooring (CCE2, see: https://www.pmel.noaa.gov/c02/story/CCE2).

		PLOO RTOMS						SBOO RTOMS						
		1 m		Mid depths		Bottom depth (>70 m)		1 m		Mid depths		Bottom depth (>25 m)		Qualifer to assign if outside of site/ depth range
Parameter	**Units**	**Min**	**Max**	**Min**	**Max**	**Min**	**Max**	**Min**	**Max**	**Min**	**Max**	**Min**	**Max**	
CDOM-ECO triplet	ppb	0	50	0	50	0	50	0	50	0	50	0	50	3
Chl-ECO triplet	µg/L	0	30	0	30	0	30	0	30	0	30	0	30	3
xCO_2	ppm	50	1000	NA	NA	NA	NA	50	1000	NA	NA	NA	NA	3
NO_3 (Nitrate + Nitrite)	µM	0	39	0	39	0	39	0	39	NA	NA	0	39	3
NTU (Turbidity)	NTU	0	10	0	10	0	10	0	10	0	10	0	10	3
O_2 (DO)	mg/L	5.5	24.0	2.0	9.5	1.5	7.5	5.5	24.0	3.0	11.0	1.5	11.0	3
pH (total scale; both internal and external)	pH_T	7.6	8.9	7.5	8.1	7.4	8.1	7.6	8.7	NA	NA	7.4	8.1	3
Sal (Salinity)	PSU	32.0	34.0	32.3	34.0	32.5	34.0	31.0	34.0	32.0	34.0	33.0	34.0	3
Temp (Temperature)	°C	11.0	26.5	9.0	24.5	9.0	15.0	12.0	26.5	10.0	26.0	9.0	19.0	3

Appendix B.8

Summary of temperature recorded by the PLOO thermistor array (100 m) at nearest depths to the PLOO RTOMS sensors. These data represent all recovered thermistor strings during the seasons between 2024 to 2025. Data include mean, minimum, and maximum values, sample size (n), and proportion recovered (n_prop) for each depth by season.

Season		6 m	10 m	14 m	18 m	22 m	26 m	30 m	34 m	38 m	42 m	46 m	50 m	54 m	58 m	62 m	66 m	70 m	74 m	78 m	82 m	86 m	90 m	94 m	98 m
Winter 2025	mean	14.45	14.15	13.82	13.30	12.71	12.35	11.89	11.83	11.59	11.39	11.27	11.19	11.09	11.00	10.97	10.98	10.91	10.84	10.90	10.75	10.81	10.81	10.67	10.60
	min	12.00	11.04	10.98	10.81	10.62	10.47	10.20	10.42	10.35	10.27	10.40	10.27	10.34	10.20	10.13	10.03	10.13	10.13	10.04	10.00	10.05	10.08	9.98	9.90
	max	15.84	15.60	15.43	14.94	14.75	14.80	14.68	14.64	14.30	14.00	13.47	12.85	12.73	12.71	12.48	12.24	12.00	11.93	12.05	11.78	11.81	11.78	11.64	11.59
	n	12956	12956	12965	12965	12965	12965	12965	12965	12965	12965	12965	12965	12965	12965	12965	12965	12965	12965	12965	12965	12965	12965	12965	12965
	n_prop	1	1	1	1	1	1	1	1	1	1	1	1	1	1	1	1	1	1	1	1	1	1	1	1

Appendix B.9

Summary of temperature recorded by the SBOO thermistor array (36 m) at nearest depths to the SBOO RTOMS sensors, during seasons between 2024 to 2025 where RTOMS data were unavailable. These data represent all recovered thermistor strings during the seasons between 2024 to 2025. Data include mean, minimum, and maximum values, sample size (n), and proportion recovered (n_prop) for each depth by season.

Season	6 m	10 m	14 m	18 m	22 m	26 m	30 m	34 m
NA	NA	NA	NA	NA	NA	NA	NA	NA

SBOO RTOMS Provided full coverage of temperature for both 2024 and 2025

Appendix B.10

Summary of temperature, salinity, DO, pH (total scale), chlorophyll *a*, CDOM, turbidity, nitrate + nitrite, BOD, and xCO2 recorded at various depths by the PLOO RTOMS in 2025. Seasonal summaries from 2024 are available in the interim report by City of San Diego (2025a). Data include mean, minimum, and maximum values, sample size (n), and proportion recovered (n_prop) for each depth by season. Sample sizes differed due to variations in sampling interval, deployment date, and data quality (Appendix C.2—C.7); id = insufficient data (see text).

Parameter	Season		1 m	10 m	20 m	30 m	45 m	60 m	75 m	89 m
Temperature (°C)	*Winter*	mean	—	—	—	—	—	—	—	—
		min	—	—	—	—	—	—	—	—
		max	—	—	—	—	—	—	—	—
		n	id	id	id	id	id	id	id	id
		n_prop	0	0	0	0	0	0	0	0
	Spring	mean	17.96	15.19	12.57	11.5	10.67	10.38	10.28	10.22
		min	14.34	10.91	10.26	10.11	9.83	9.81	9.70	9.65
		max	21.41	20.51	16.31	14.56	11.94	11.07	10.73	10.70
		n	10340	10487	10495	10419	10474	10491	10499	9454
		n_prop	0.79	0.80	0.80	0.80	0.80	0.80	0.80	0.72
	Summer	mean	20.68	17.03	14.39	13.27	12.2	11.58	11.23	11.07
		min	16.11	11.56	11.05	10.75	10.46	10.30	10.30	10.2
		max	23.74	21.63	18.74	17.3	14.28	13.31	12.64	12.36
		n	11864	12002	11991	11920	12011	11983	11914	10805
		n_prop	0.90	0.91	0.91	0.90	0.91	0.90	0.90	0.82
	Fall	mean	18.23	17.16	15.87	14.90	13.53	12.69	12.03	11.66
		min	15.90	13.46	12.96	12.60	11.93	11.22	10.79	10.48
		max	20.28	19.44	18.20	17.64	17.37	15.28	14.70	13.76
		n	6560	6690	6685	6624	6679	6672	6672	6258
		n_prop	0.50	0.50	0.50	0.50	0.50	0.50	0.50	0.47
Salinity (psu)	*Winter*	mean	—	—	—	—	—	—	—	—
		min	—	—	—	—	—	—	—	—
		max	—	—	—	—	—	—	—	—
		n	id	id	id	id	id	id	id	id
		n_prop	0	0	0	0	0	0	0	0
	Spring	mean	33.52	33.49	33.49	33.55	33.70	33.68	33.80	33.87
		min	33.35	33.27	33.14	33.24	33.37	33.16	33.54	33.58
		max	33.82	33.84	33.92	34.05	34.09	34.11	34.16	34.16
		n	10339	10487	10494	10419	10474	10491	10499	9454
		n_prop	0.79	0.80	0.80	0.80	0.80	0.80	0.80	0.72

Appendix B.10 *continued*

Parameter	Season		1 m	10 m	20 m	30 m	45 m	60 m	75 m	89 m
Salinity *(cont.*)	*Summer*	mean	33.46	33.4	33.38	33.38	33.41	33.13	33.4	33.26
		min	33.20	33.14	32.94	33.08	33.17	32.67	32.92	32.94
		max	33.65	33.69	33.79	33.74	33.76	33.48	33.74	33.74
		n	11861	12002	11957	11920	12011	11982	11914	10805
		n_prop	0.90	0.91	0.90	0.90	0.91	0.90	0.90	0.82
	Fall	mean	33.32	33.31	33.29	33.25	33.3	33.27	33.28	33.25
		min	33.08	33.06	32.97	33.01	33.06	32.83	32.97	32.88
		max	33.42	33.43	33.43	33.38	33.49	33.51	33.58	33.71
		n	6556	6688	6684	6623	6679	6672	6672	6258
		n_prop	0.49	0.50	0.50	0.50	0.50	0.50	0.50	0.47
DO (mg/L)	*Winter*	mean	—	—	—	—	—	—	—	—
		min	—	—	—	—	—	—	—	—
		max	—	—	—	—	—	—	—	—
		n	id	—	—	id	—	—	id	id
		n_prop	0	—	—	0	—	—	0	0
	Spring	mean	8.96	—	—	5.45	—	—	2.95	2.71
		min	8.04	—	—	2.38	—	—	1.89	1.70
		max	13.55	—	—	8.32	—	—	4.99	3.87
		n	10349	—	—	10427	—	—	10510	9462
		n_prop	0.79	—	—	0.80	—	—	0.80	0.72
	Summer	mean	8.39	—	—	7.10	—	—	4.33	3.97
		min	7.47	—	—	3.46	—	—	2.24	2.35
		max	12.19	—	—	9.27	—	—	6.84	5.84
		n	11889	—	—	11945	—	—	11938	10826
		n_prop	0.90	—	—	0.90	—	—	0.90	0.82
	Fall	mean	7.94	—	—	7.50	—	—	5.05	4.73
		min	7.59	—	—	5.91	—	—	2.26	2.78
		max	8.70	—	—	8.56	—	—	7.30	6.58
		n	6561	—	—	6627	—	—	6676	6261
		n_prop	0.50	—	—	0.50	—	—	0.50	0.47
Chlorophyll *a*	*Winter*	mean	—	—	—	—	—	—	—	—
(µg/L)		min	—	—	—	—	—	—	—	—
		max	—	—	—	—	—	—	—	—
		n	id	—	—	id	—	—	—	id
		n_prop	0	—	—	0	—	—	—	0

Appendix B.10 *continued*

Parameter	Season		1 m	10 m	20 m	30 m	45 m	60 m	75 m	89 m
Chlorphyll a *(cont.)*	*Spring*	mean	0.49	—	—	0.57	—	—	—	0.11
		min	0	—	—	0.01	—	—	—	0.01
		max	15.28	—	—	9.13	—	—	—	2.82
		n	4874	—	—	8924	—	—	—	10084
		n_prop	0.74	—	—	0.68	—	—	—	0.77
	Summer	mean	0.37	—	—	—	—	—	—	0.1
		min	0	—	—	—	—	—	—	0.02
		max	2.8	—	—	—	—	—	—	4.55
		n	5575	—	—	id	—	—	—	11557
		n_prop	0.84	—	—	0	—	—	—	0.87
	Fall	mean	0.30	—	—	—	—	—	—	0.09
		min	0	—	—	—	—	—	—	0.01
		max	2.45	—	—	—	—	—	—	0.41
		n	3126	—	—	id	—	—	—	6501
		n_prop	0.47	—	—	0.22	—	—	—	0.49
pH_T	*Winter*	mean	—	—	—	—	—	—	—	—
(pH Total scale)		min	—	—	—	—	—	—	—	—
		max	—	—	—	—	—	—	—	—
		n	id	—	—	—	—	—	—	—
		n_prop	0	—	—	—	—	—	—	—
	Spring	mean	8.08	—	—	7.78	—	—	—	7.59
		min	7.99	—	—	7.59	—	—	—	7.52
		max	8.34	—	—	7.99	—	—	—	7.66
		n	10412	—	—	10488	—	—	—	9513
		n_prop	0.79	—	—	0.80	—	—	—	0.73
	Summer	mean	8.05	—	—	7.90	—	—	—	7.66
		min	7.97	—	—	7.64	—	—	—	7.56
		max	8.24	—	—	8.04	—	—	—	7.79
		n	11937	—	—	11999	—	—	—	10869
		n_prop	0.90	—	—	0.91	—	—	—	0.82
	Fall	mean	8.02	—	—	7.96	—	—	—	7.73
		min	7.98	—	—	7.83	—	—	—	7.55
		max	8.04	—	—	8.05	—	—	—	7.89
		n	6384	—	—	6523	—	—	—	6147
		n_prop	0.48	—	—	0.49	—	—	—	0.46

Appendix B.10 *continued*

Parameter	Season		1 m	10 m	20 m	30 m	45 m	60 m	75 m	89 m
CDOM (ppb)	*Winter*	mean	—	—	—	—	—	—	—	—
		min	—	—	—	—	—	—	—	—
		max	—	—	—	—	—	—	—	—
		n	id	—	—	id	—	—	—	id
		n_prop	0	—	—	0	—	—	—	0
	Spring	mean	1.55	—	—	3.35	—	—	—	4.61
		min	0.46	—	—	2.54	—	—	—	3.53
		max	3.01	—	—	5.00	—	—	—	8.15
		n	4874	—	—	8694	—	—	—	10084
		n_prop	0.74	—	—	0.66	—	—	—	0.77
	Summer	mean	0.65	—	—	—	—	—	—	4.64
		min	0	—	—	—	—	—	—	3.53
		max	3.83	—	—	—	—	—	—	8.06
		n	5466	—	—	id	—	—	—	11557
		n_prop	0.83	—	—	0	—	—	—	0.87
	Fall	mean	0.59	—	—	—	—	—	—	4.17
		min	0	—	—	—	—	—	—	2.27
		max	12.06	—	—	—	—	—	—	9.33
		n	3118	—	—	id	—	—	—	6501
		n_prop	0.47	—	—	0.22	—	—	—	0.49
Turbidity (NTU)	*Winter*	mean	—	—	—	—	—	—	—	—
		min	—	—	—	—	—	—	—	—
		max	—	—	—	—	—	—	—	—
		n	id	—	—	id	—	—	—	id
		n_prop	0	—	—	0	—	—	—	0
	Spring	mean	0.25	—	—	0.1	—	—	—	0.23
		min	0.06	—	—	0	—	—	—	0.04
		max	1	—	—	1	—	—	—	0.94
		n	4867	—	—	8725	—	—	—	10079
		n_prop	0.74	—	—	0.67	—	—	—	0.77
	Summer	mean	0.24	—	—	—	—	—	—	0.20
		min	0.08	—	—	—	—	—	—	0.04
		max	0.99	—	—	—	—	—	—	0.88
		n	5574	—	—	id	—	—	—	11556

Appendix B.10 *continued*

Parameter	Season		1 m	10 m	20 m	30 m	45 m	60 m	75 m	89 m
		n_prop	0.47	—	—	0.22	—	—	—	0.49
Nitrate + nitrite (µM)	*Winter*	mean	—	—	—	—	—	—	—	—
		min	—	—	—	—	—	—	—	—
		max	—	—	—	—	—	—	—	—
		n	—	—	—	id	—	—	—	id
		n_prop	—	—	—	0	—	—	—	0
	Spring	mean	—	—	—	18.37	—	—	—	26.03
		min	—	—	—	1.64	—	—	—	21.35
		max	—	—	—	28.31	—	—	—	28.57
		n	—	—	—	1746	—	—	—	1263
		n_prop	—	—	—	0.80	—	—	—	0.58
	Summer	mean	—	—	—	8.78	—	—	—	18.20
		min	—	—	—	0.42	—	—	—	5.27
		max	—	—	—	25.11	—	—	—	28.95
		n	—	—	—	1974	—	—	—	1379
		n_prop	—	—	—	0.89	—	—	—	0.62
	Fall	mean	—	—	—	4.50	—	—	—	14.51
		min	—	—	—	0	—	—	—	2.51
		max	—	—	—	11.49	—	—	—	21.24
		n	—	—	—	1095	—	—	—	902
xCO2 (ppm)	*Winter*	mean	—	—	—	—	—	—	—	—
		min	—	—	—	—	—	—	—	—
		max	—	—	—	—	—	—	—	—
		n	id	—	—	—	—	—	—	—
		n_prop	0	—	—	—	—	—	—	—
	Spring	mean	359.82	—	—	—	—	—	—	—
		min	187.72	—	—	—	—	—	—	—
		max	518.83	—	—	—	—	—	—	—
		n	1827	—	—	—	—	—	—	—
		n_prop	0.84	—	—	—	—	—	—	—
	Summer	mean	375.34	—	—	—	—	—	—	—
		min	221.68	—	—	—	—	—	—	—
		max	463.56	—	—	—	—	—	—	—
		n	2144	—	—	—	—	—	—	—

Appendix B.10 *continued*

Parameter	Season		1 m	10 m	20 m	30 m	45 m	60 m	75 m	89 m
xCO2 *(cont.*)		n_prop	0.97	—	—	—	—	—	—	—
	Fall	mean	—	—	—	—	—	—	—	—
		min	—	—	—	—	—	—	—	—
		max	—	—	—	—	—	—	—	—
		n	id	—	—	—	—	—	—	—
		n_prop	0.29	—	—	—	—	—	—	—

Appendix B.11

Summary of temperature, salinity, DO, pH (total scale), chlorophyll *a*, CDOM, turbidity, nitrate + nitrite, BOD, and xCO2 recorded at various depths by the SBOO RTOMS in 2025. Seasonal summaries from 2024 are available in the interim report by City of San Diego (2025a). Data include mean, minimum, and maximum values, sample size (n), and proportion recovered (n_prop) for each depth by season. Sample sizes differed due to variations in sampling interval, deployment date, and data quality (Appendix C.2 to C.7); id = insufficient data (see text).

Parameter	Season		1 m	10 m	18 m	26 m
Temperature (°C)	*Winter*	mean	13.89	12.83	12.11	11.82
		min	12.34	10.82	10.61	10.61
		max	15.84	14.96	14.22	14.02
		n	12347	12461	11509	12203
		n_prop	0.95	0.96	0.89	0.94
	Spring	mean	16.08	12.57	11.26	10.96
		min	11.35	10.47	10.29	10.36
		max	19.64	19.14	15.23	12.22
		n	8974	9215	7123	8764
		n_prop	0.68	0.70	0.54	0.67
	Summer	mean	19.89	15.8	14.06	13.4
		min	15.71	11.61	11.39	11.25
		max	23.04	22.32	19.97	15.47
		n	11720	11792	11728	11724
		n_prop	0.88	0.89	0.89	0.88
	Fall	mean	17.46	16.41	15.72	15.08
		min	15.11	13.32	13.09	12.61
		max	19.97	18.66	17.76	17.65
		n	13122	13207	13119	13116
		n_prop	0.99	1	0.99	0.99
Salinity (psu)	*Winter*	mean	33.31	33.42	33.53	33.53
		min	32.72	33.13	33.14	33.22
		max	33.50	33.92	33.95	33.84
		n	12325	12443	11509	12203
		n_prop	0.95	0.96	0.89	0.94
	Spring	mean	33.48	33.55	33.68	33.65
		min	33.16	33.07	33.20	33.33
		max	33.76	33.94	34.05	33.97
		n	8972	9174	7123	8462
		n_prop	0.68	0.70	0.54	0.65
	Summer	mean	33.48	33.37	33.34	33.38
		min	33.03	33.00	32.72	33.13
		max	33.70	33.78	33.69	33.67
		n	11719	11792	11728	11724
		n_prop	0.88	0.89	0.89	0.88
	Fall	mean	33.27	33.22	33.24	33.25
		min	32.81	32.89	32.91	32.95
		max	33.39	33.44	33.41	33.4
		n	12990	13207	13118	13116
		n_prop	0.98	1	0.99	0.99

Appendix B.11 *continued*

Parameter	Season		1 m	10 m	18 m	26 m
DO (mg/L)	*Winter*	mean	7.92	—	5.36	4.26
		min	4.27	—	2.24	2.13
		max	11.17	—	9.89	8.55
		n	12434	—	11583	12284
		n_prop	0.96	—	0.89	0.95
	Spring	mean	8.66	—	4.22	3.5
		min	3.91	—	1.28	0.8
		max	13.8	—	9.12	5.27
		n	9162	—	7266	8946
		n_prop	0.70	—	0.55	0.68
	Summer	mean	8.68	—	7.49	6.8
		min	7.59	—	4.67	3.78
		max	13.27	—	10.75	8.92
		n	11810	—	11818	11814
		n_prop	0.89	—	0.89	0.89
	Fall	mean	7.99	—	7.53	7.06
		min	7.02	—	5.91	5.42
		max	10.52	—	8.58	8.2
		n	13210	—	13207	13204
		n_prop	1	—	1	1
Chlorophyll *a*	*Winter*	mean	1.62	—	0.97	0.77
(µg/L)		min	0.27	—	0.08	0.09
		max	7.81	—	6.6	5.04
		n	6026	—	11207	12226
		n_prop	0.93	—	0.86	0.94
	Spring	mean	1.16	—	1.31	1.06
		min	0.13	—	0.11	0.11
		max	9.99	—	29.39	8.65
		n	4379	—	6648	8869
		n_prop	0.67	—	0.51	0.68
	Summer	mean	0.71	—	1.47	—
		min	0.04	—	0.25	—
		max	14.38	—	7.3	—
		n	5863	—	5862	id
		n_prop	0.89	—	0.44	0.25
	Fall	mean	0.70	—	1.12	—
		min	0.01	—	0.27	—
		max	4.55	—	8.51	—
		n	6550	—	6548	id
		n_prop	0.99	—	0.49	0.35

Appendix B.11 *continued*

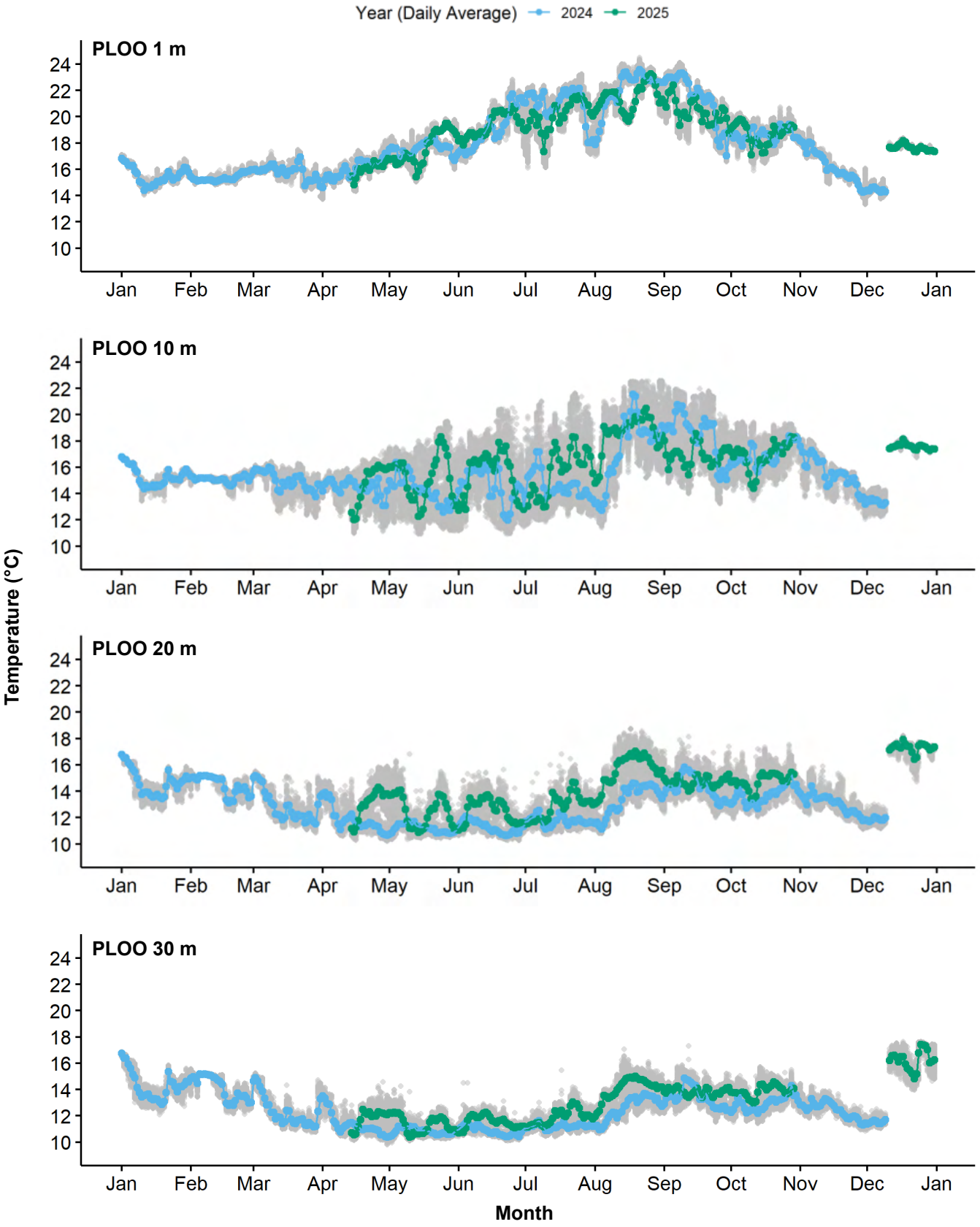
Parameter	Season		1 m	10 m	18 m	26 m
pH_T	*Winter*	mean	8.03	—	—	7.80
(pH Total scale)		min	7.73	—	—	7.65
		max	8.23	—	—	8.12
		n	12433	—	—	12283
		n_prop	0.96	—	—	0.95
	Spring	mean	8.10	—	—	7.74
		min	7.67	—	—	7.53
		max	8.38	—	—	7.86
		n	9164	—	—	8948
		n_prop	0.70	—	—	0.68
	Summer	mean	8.04	—	—	7.89
		min	7.96	—	—	7.66
		max	8.25	—	—	8.03
		n	11809	—	—	11814
		n_prop	0.89	—	—	0.89
	Fall	mean	8.00	—	—	7.93
		min	7.93	—	—	7.81
		max	8.17	—	—	8.03
		n	12933	—	—	13059
		n_prop	0.98	—	—	0.99
CDOM (ppb)	*Winter*	mean	1.48	—	—	4.56
		min	0.09	—	—	2.99
		max	4.99	—	—	9.97
		n	6007	—	id	12177
		n_prop	0.93	—	0	0.94
	Spring	mean	0.90	—	—	3.79
		min	0	—	—	2.63
		max	4.99	—	—	9.88
		n	4167	—	id	8857
		n_prop	0.64	—	0	0.68
	Summer	mean	1.97	—	5.03	—
		min	0.45	—	3.72	—
		max	4.94	—	9.80	—
		n	5827	—	5859	id
		n_prop	0.88	—	0.44	0.11
	Fall	mean	2.48	—	—	—
		min	0.09	—	—	—
		max	4.94	—	—	—
		n	6460	—	id	id
		n_prop	0.98	—	0.23	0

Appendix B.11 *continued*

Parameter	Season		1 m	10 m	18 m	26 m
Turbidity (NTU)	*Winter*	mean	0.41	—	—	0.67
		min	0.10	—	—	0.06
		max	3.00	—	—	3.00
		n	5980	—	id	12159
		n_prop	0.92	—	0	0.94
	Spring	mean	0.36	—	—	0.31
		min	0.07	—	—	0.06
		max	2.95	—	—	2.92
		n	4100	—	id	8868
		n_prop	0.63	—	0	0.68
	Summer	mean	0.23	—	0.30	—
		min	0.01	—	0.05	—
		max	2.98	—	2.35	—
		n	5851	—	5858	id
		n_prop	0.88	—	0.44	0
	Fall	mean	0.18	—	—	—
		min	0.01	—	—	—
		max	2.96	—	—	—
		n	6487	—	id	id
		n_prop	0.98	—	0.23	0
Nitrate + nitrite (µM)	*Winter*	mean	3.15	—	—	—
		min	0	—	—	—
		max	13.55	—	—	—
		n	1867	—	—	id
		n_prop	0.86	—	—	0
	Spring	mean	2.70	—	—	—
		min	0	—	—	—
		max	21.82	—	—	—
		n	1399	—	—	id
		n_prop	0.64	—	—	0
	Summer	mean	0.97	—	—	7.12
		min	0	—	—	0.63
		max	2.38	—	—	21.28
		n	1733	—	—	1949
		n_prop	0.78	—	—	0.88
	Fall	mean	0.70	—	—	4.70
		min	0	—	—	0.32
		max	4.84	—	—	12.11
		n	2008	—	—	2178
		n_prop	0.91	—	—	0.99

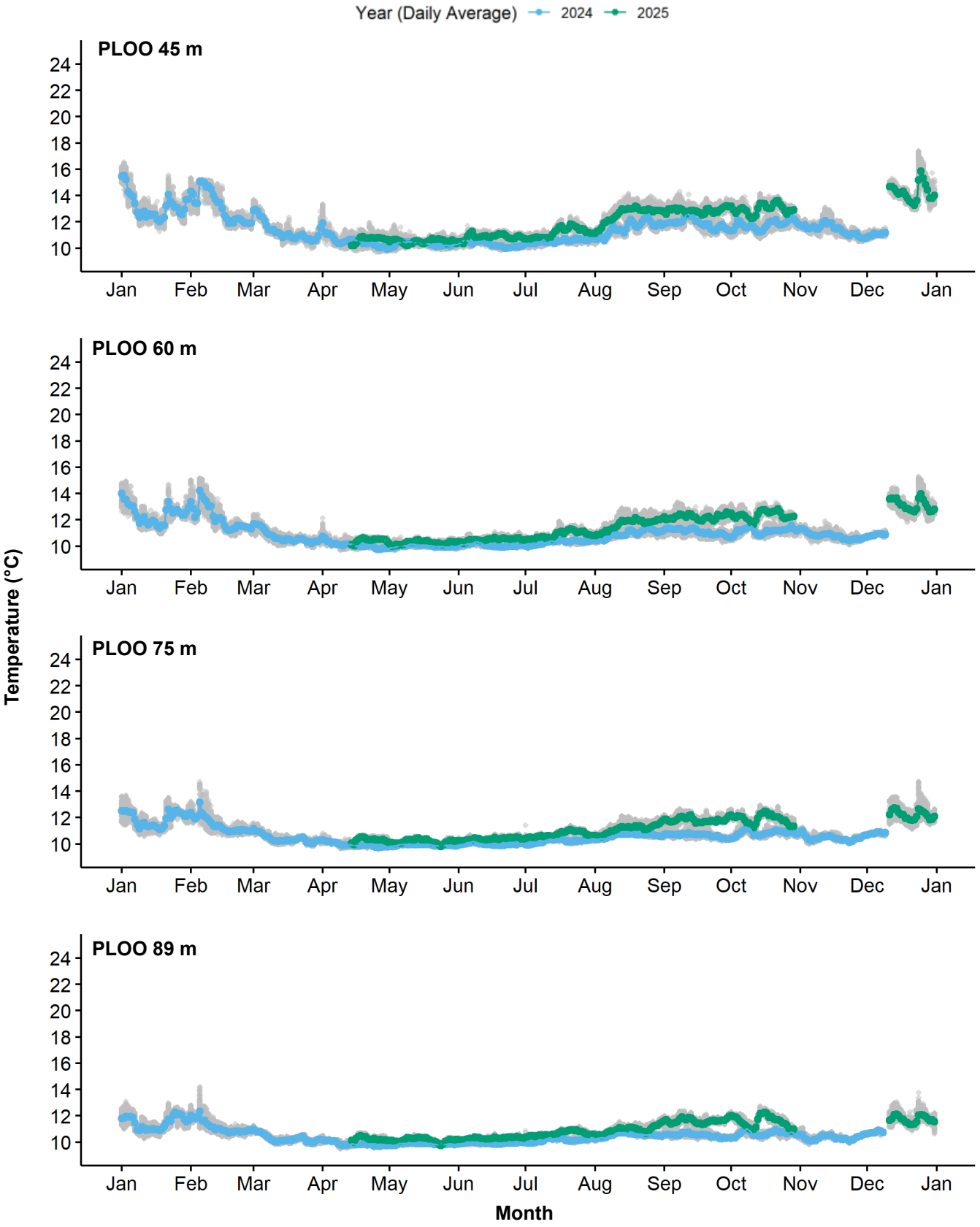
Appendix B.11 *continued*

Parameter	Season		1 m	10 m	18 m	26 m
xCO2 (ppm)	*Winter*	mean	397.58	—	—	—
		min	276.91	—	—	—
		max	593.93	—	—	—
		n	4207	—	—	—
		n_prop	0.97	—	—	—
	Spring	mean	337.29	—	—	—
		min	168	—	—	—
		max	795.38	—	—	—
		n	2402	—	—	—
		n_prop	0.55	—	—	—
	Summer	mean	—	—	—	—
		min	—	—	—	—
		max	—	—	—	—
		n	id	—	—	—
		n_prop	0	—	—	—
	Fall	mean	—	—	—	—
		min	—	—	—	—
		max	—	—	—	—
		n	id	—	—	—
		n_prop	0	—	—	—

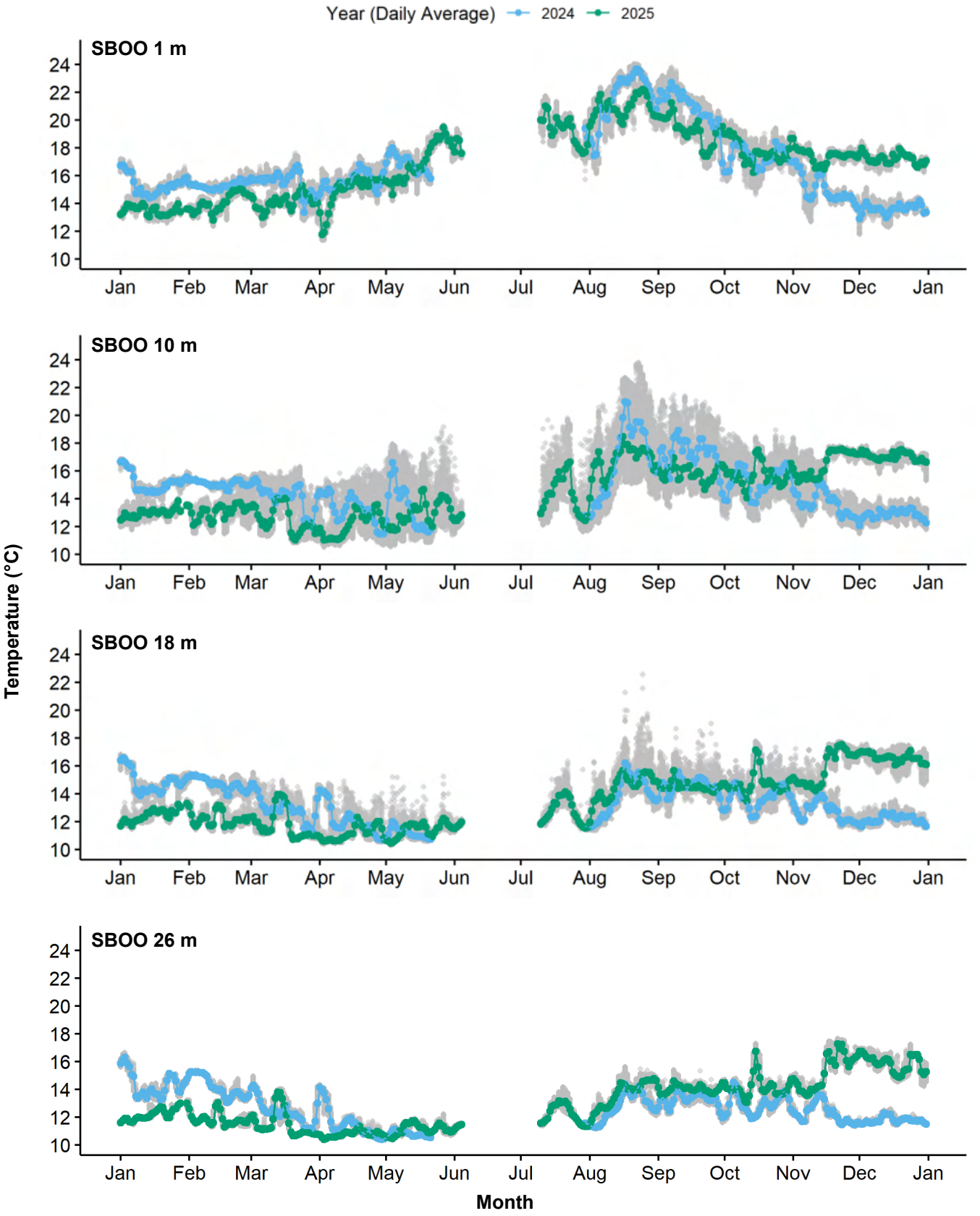


Appendix B.12

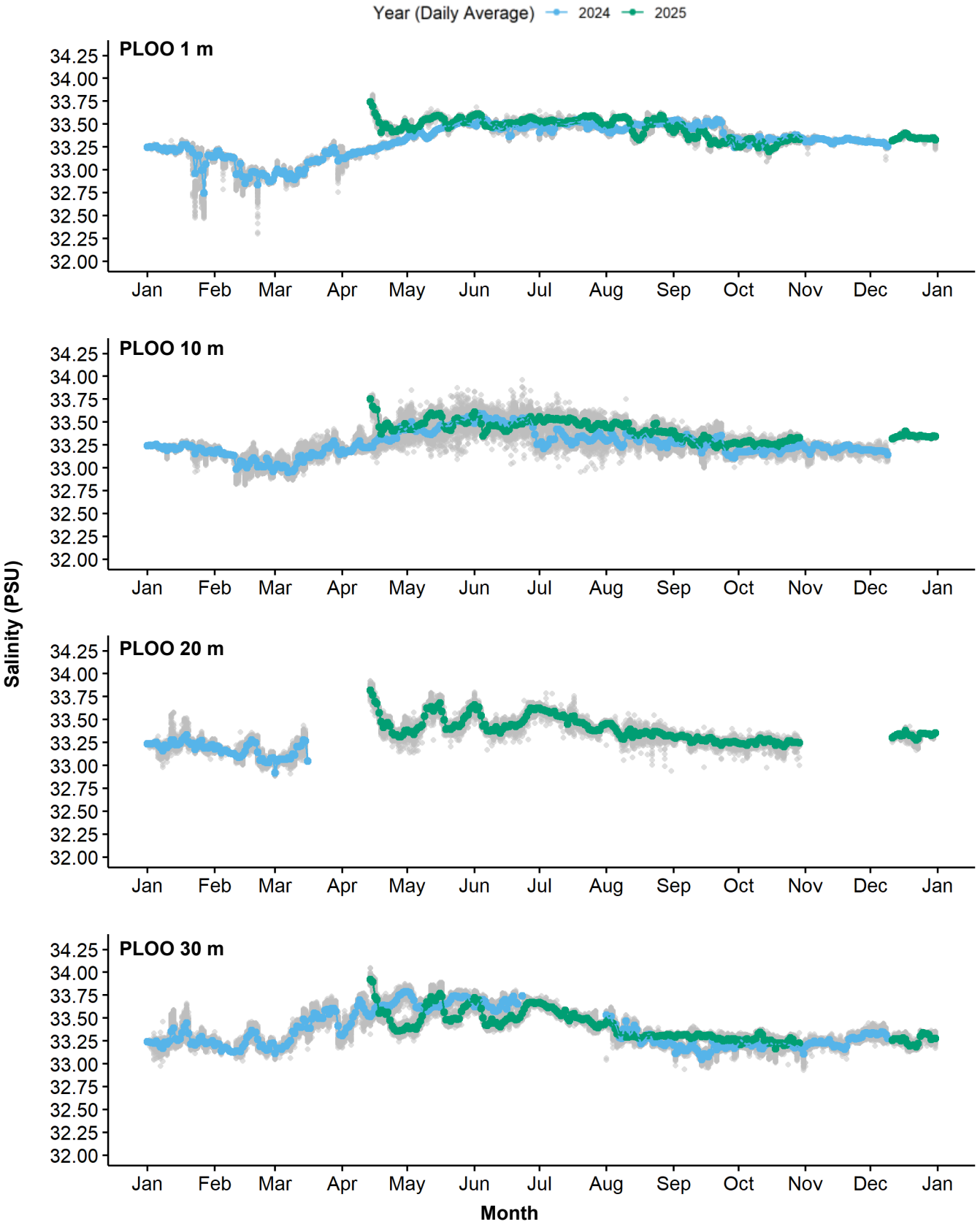
Temperature, salinity, DO, pH (total scale), chlorophyll *a*, CDOM, turbidity, nitrate + nitrite, BOD, and xCO2 recorded at various depths by the PLOO and SBOO RTOMS during 2024 and 2025. Grey points represent raw data while green and blue points represent daily averaged data.



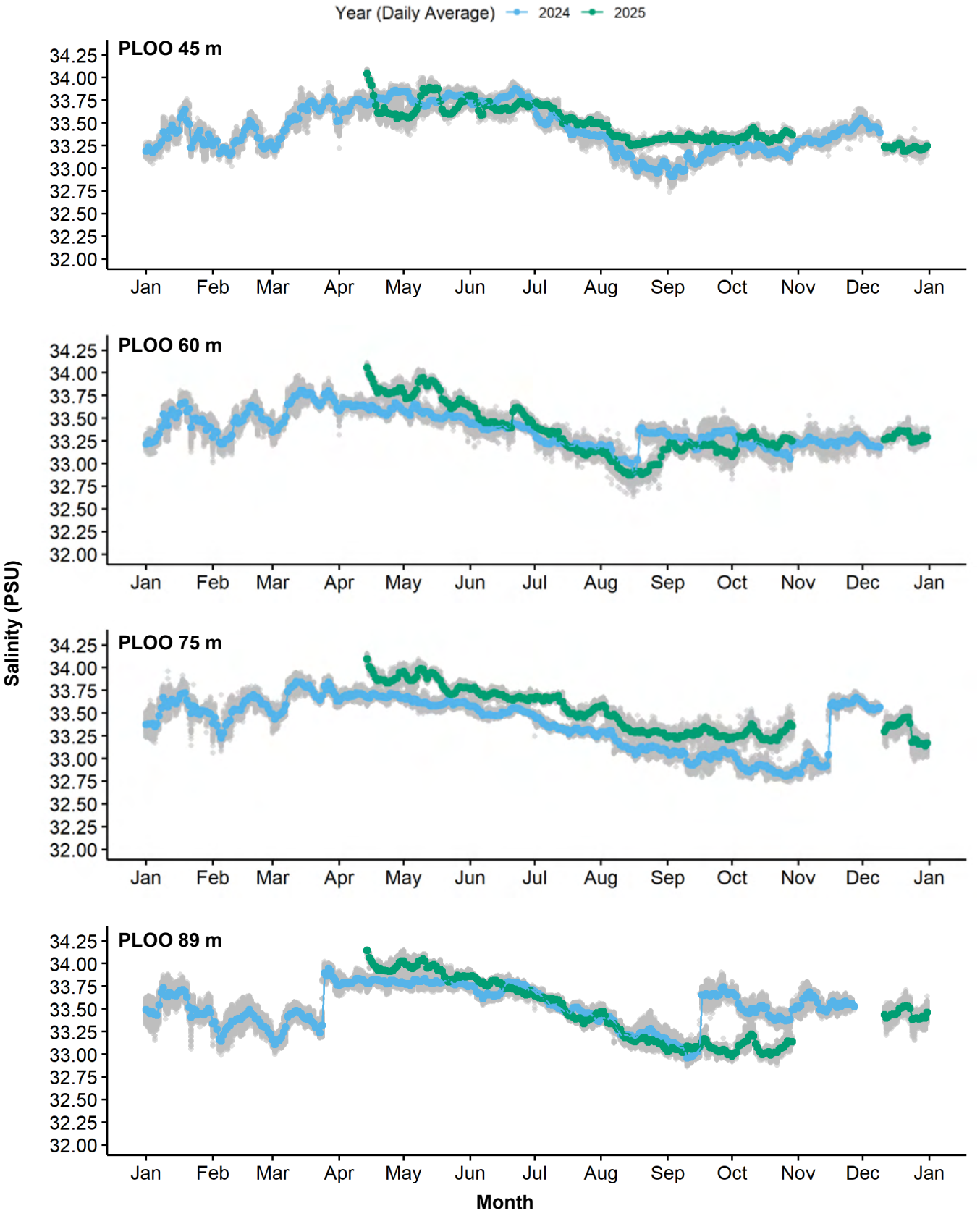
Appendix B.12 *continued*



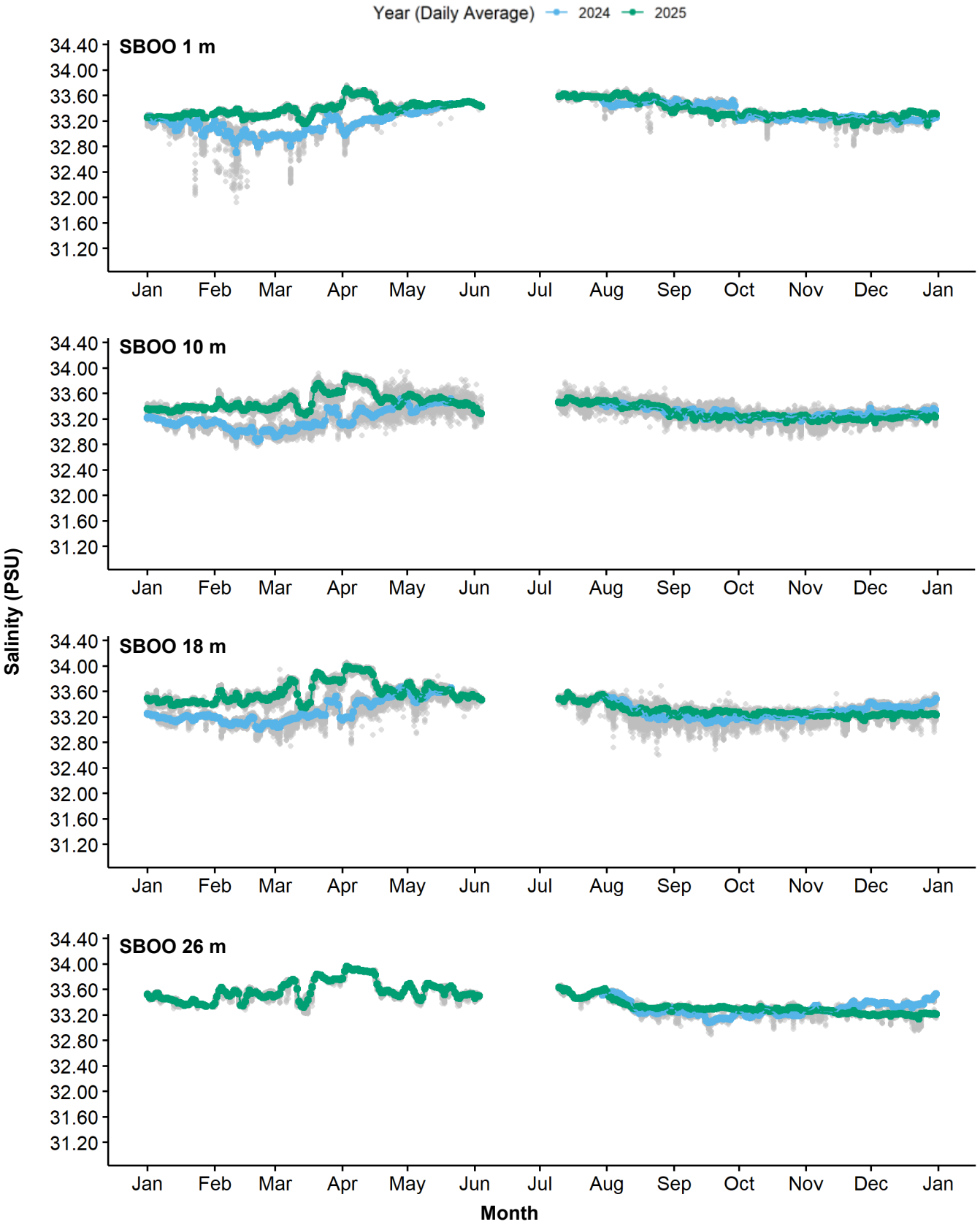
Appendix B.12 *continued*



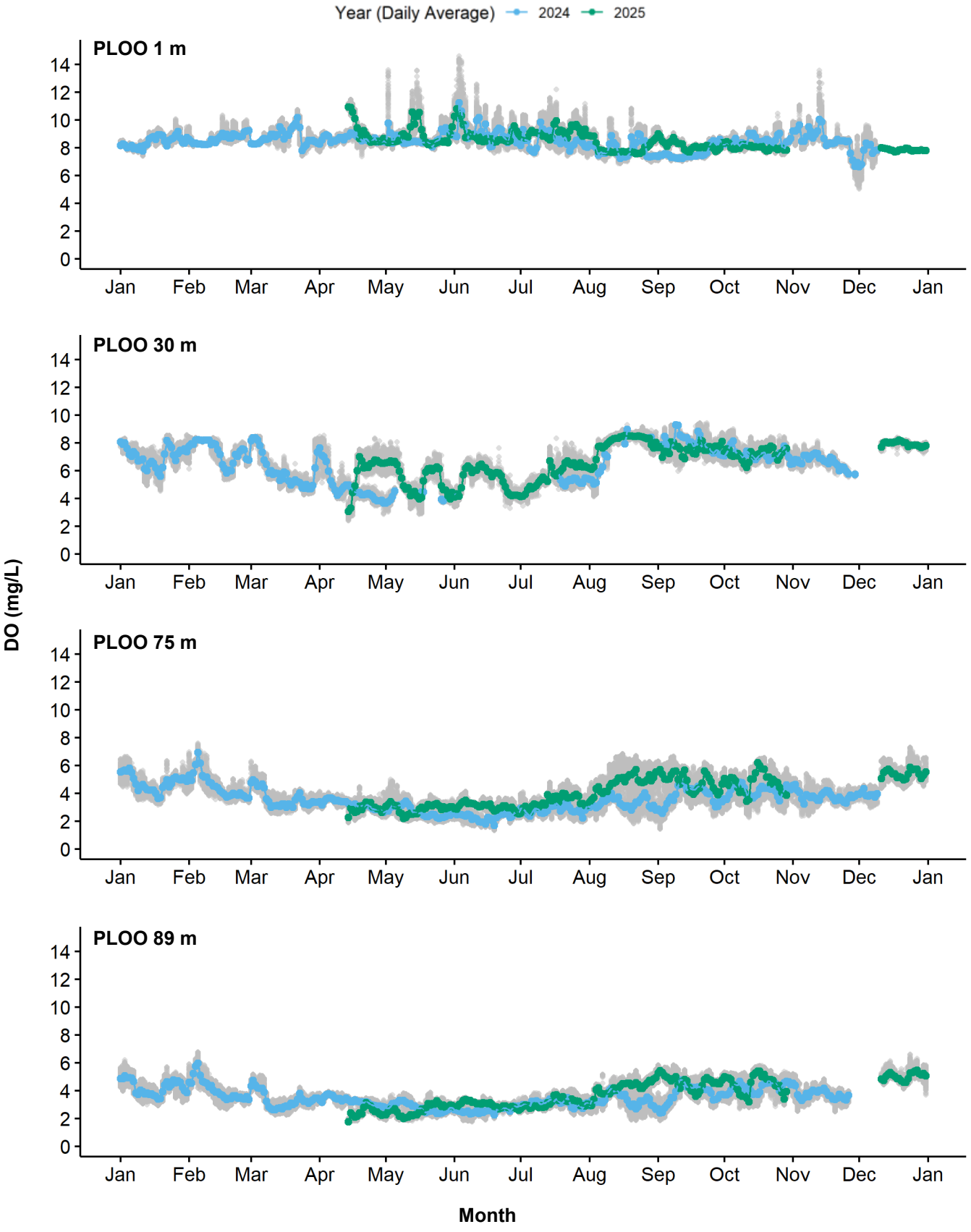
Appendix B.12 *continued*



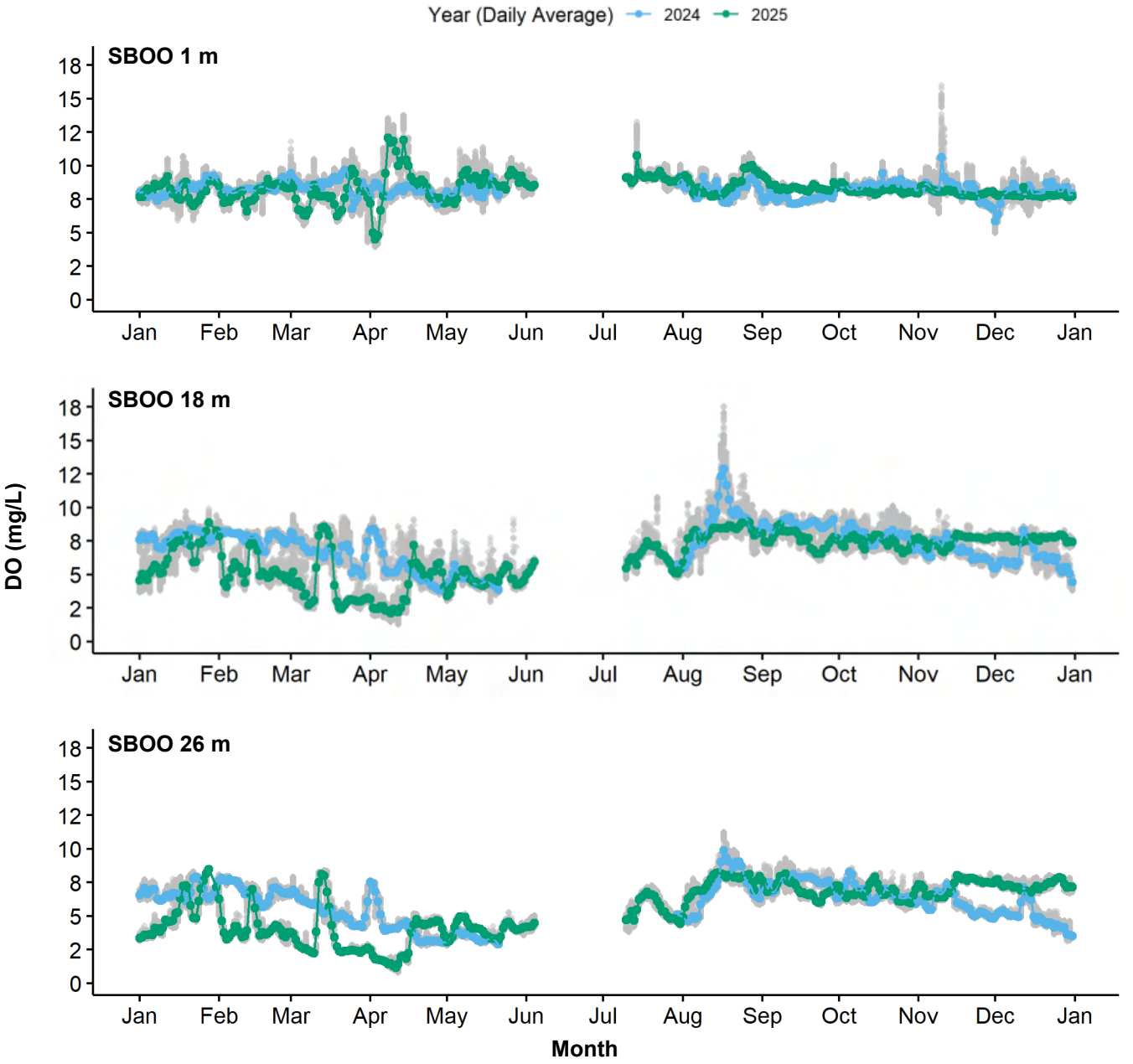
Appendix B.12 *continued*



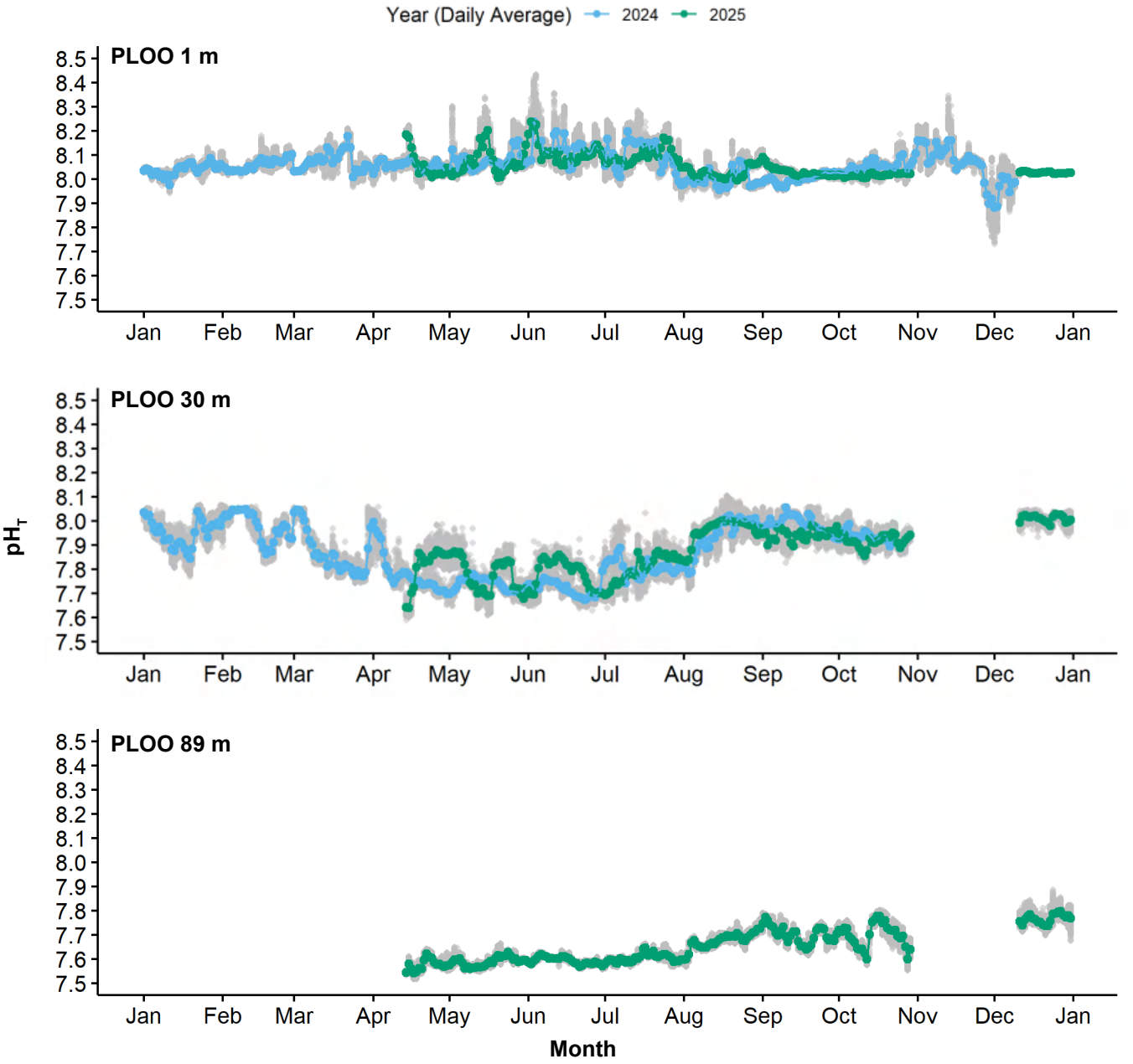
Appendix B.12 *continued*



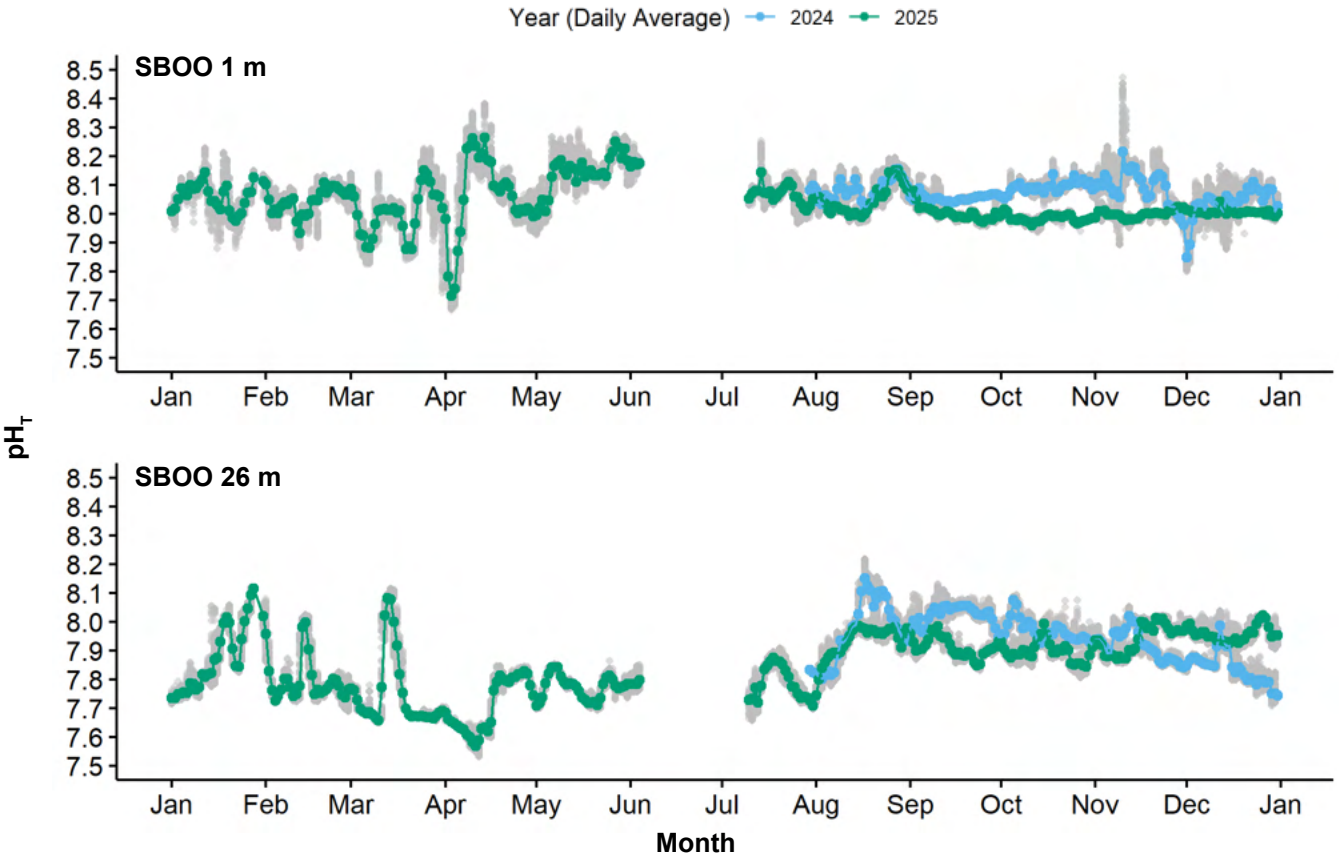
Appendix B.12 *continued*



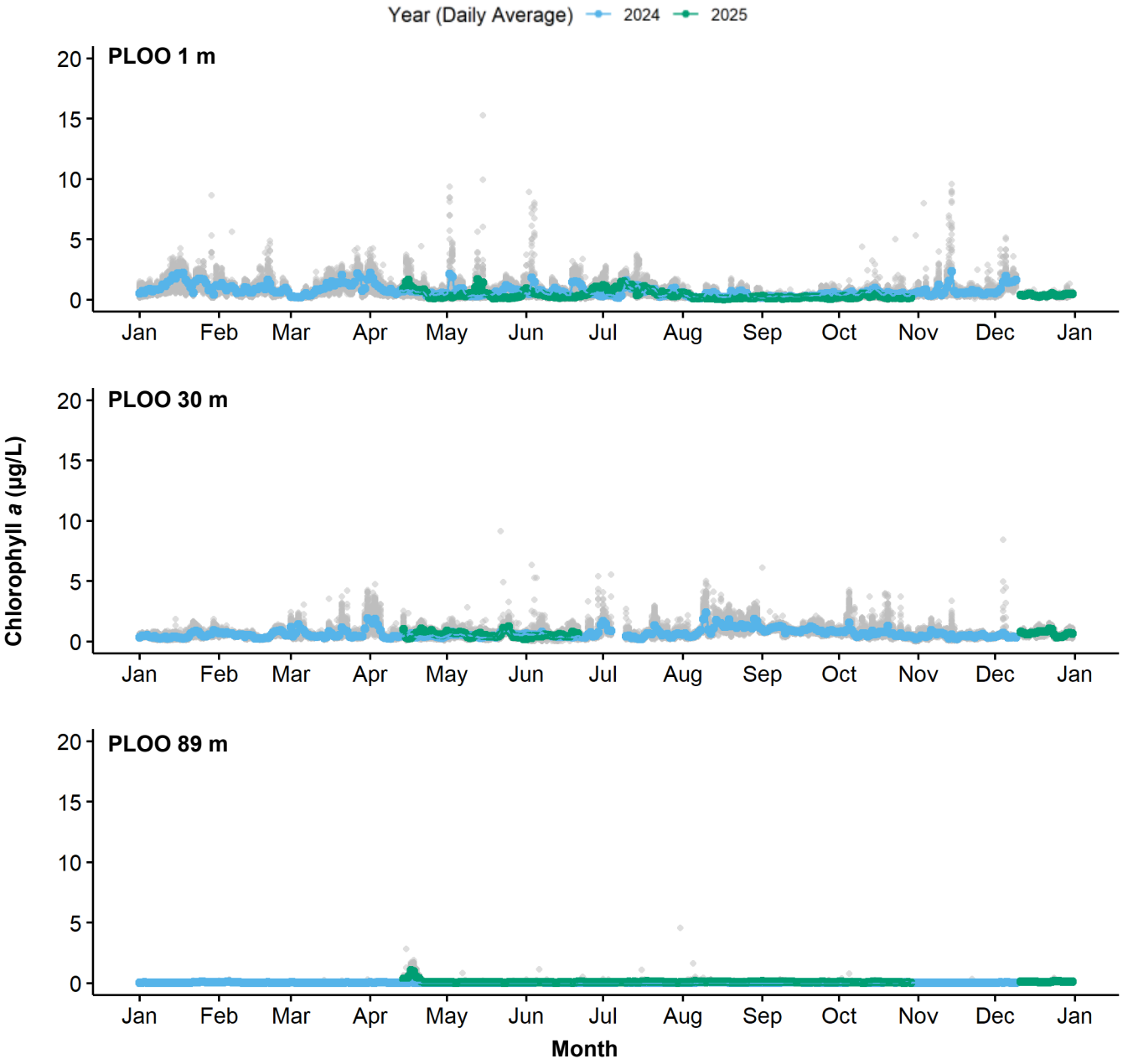
Appendix B.12 *continued*



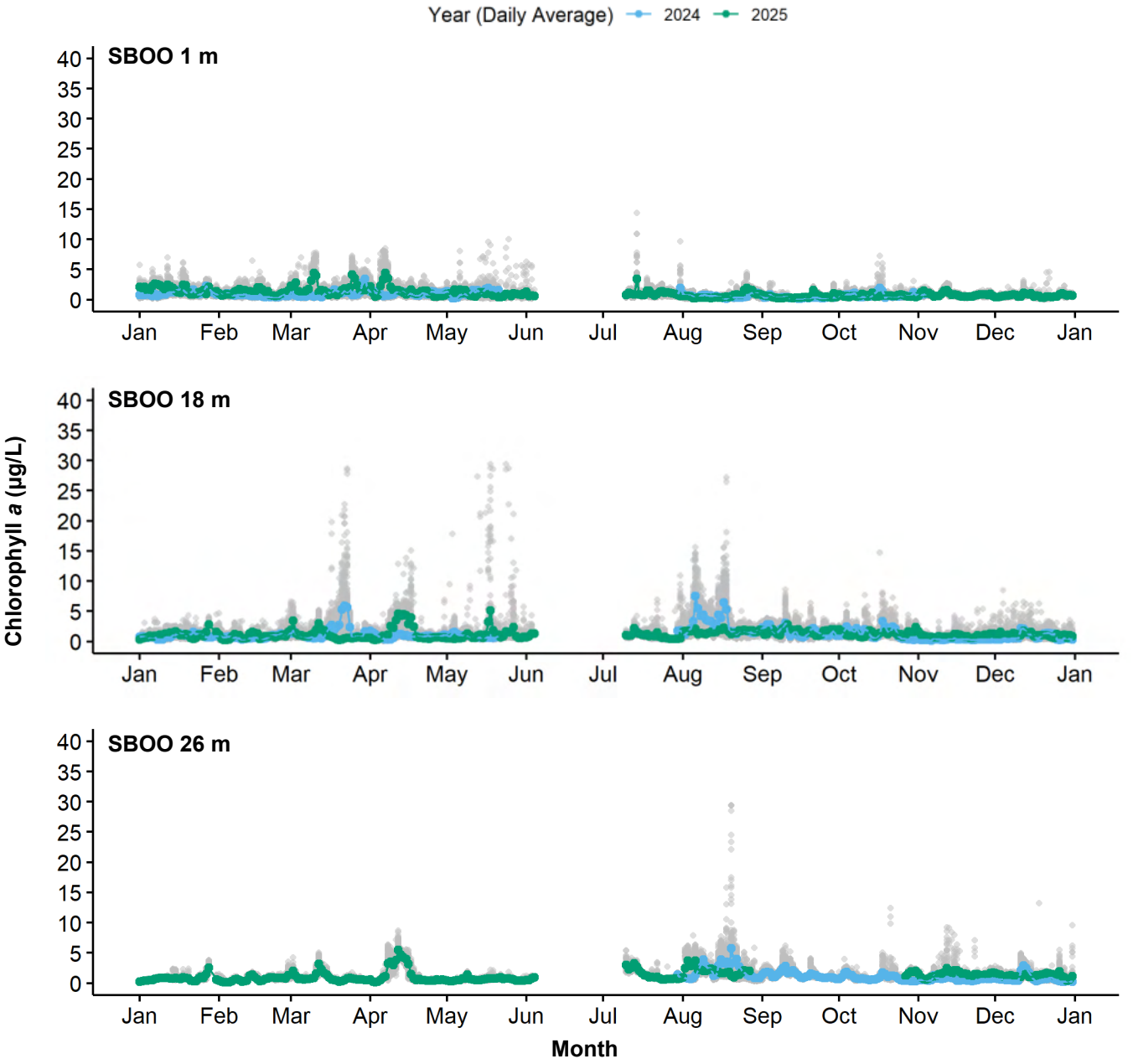
Appendix B.12 *continued*



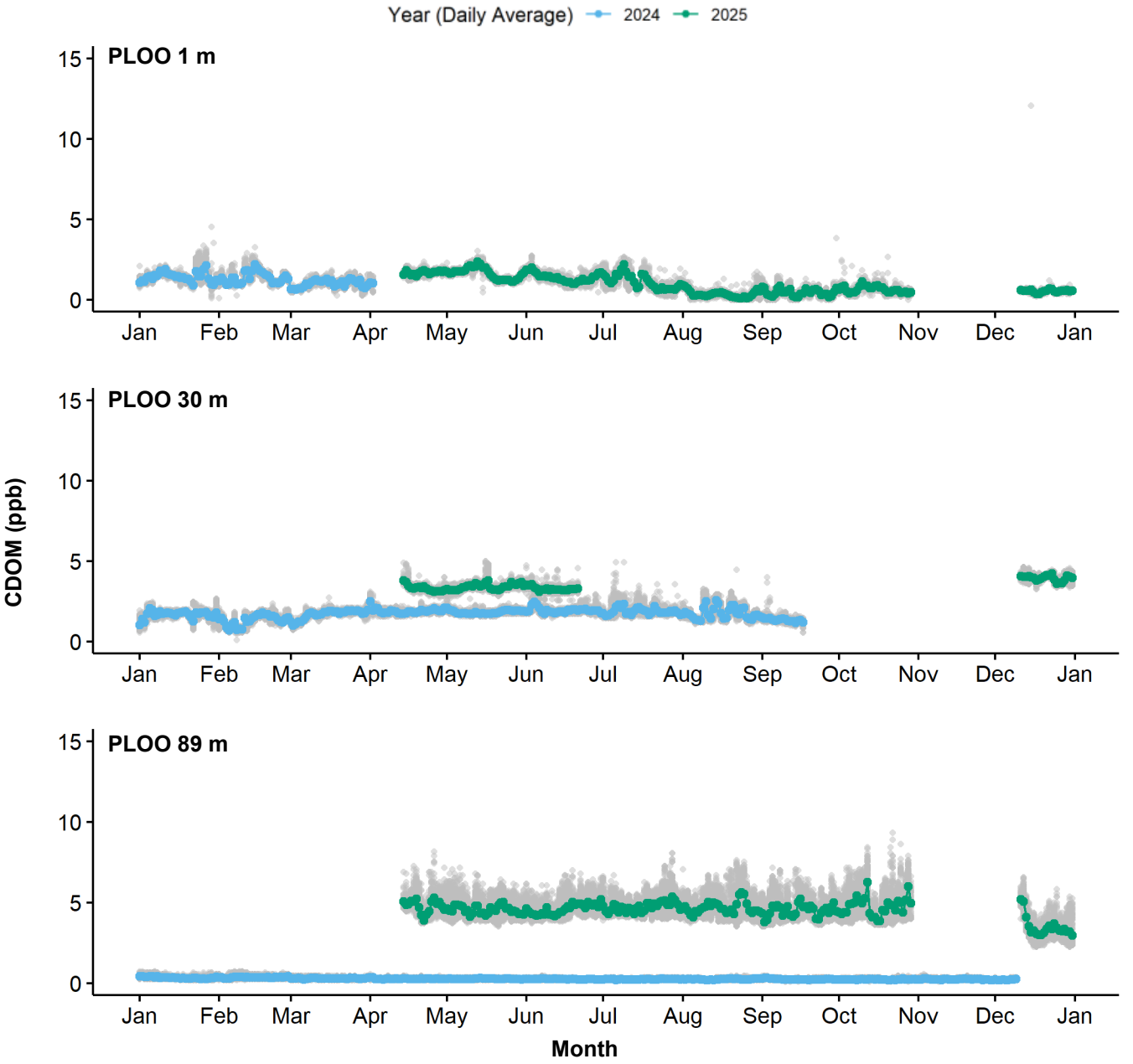
Appendix B.12 *continued*



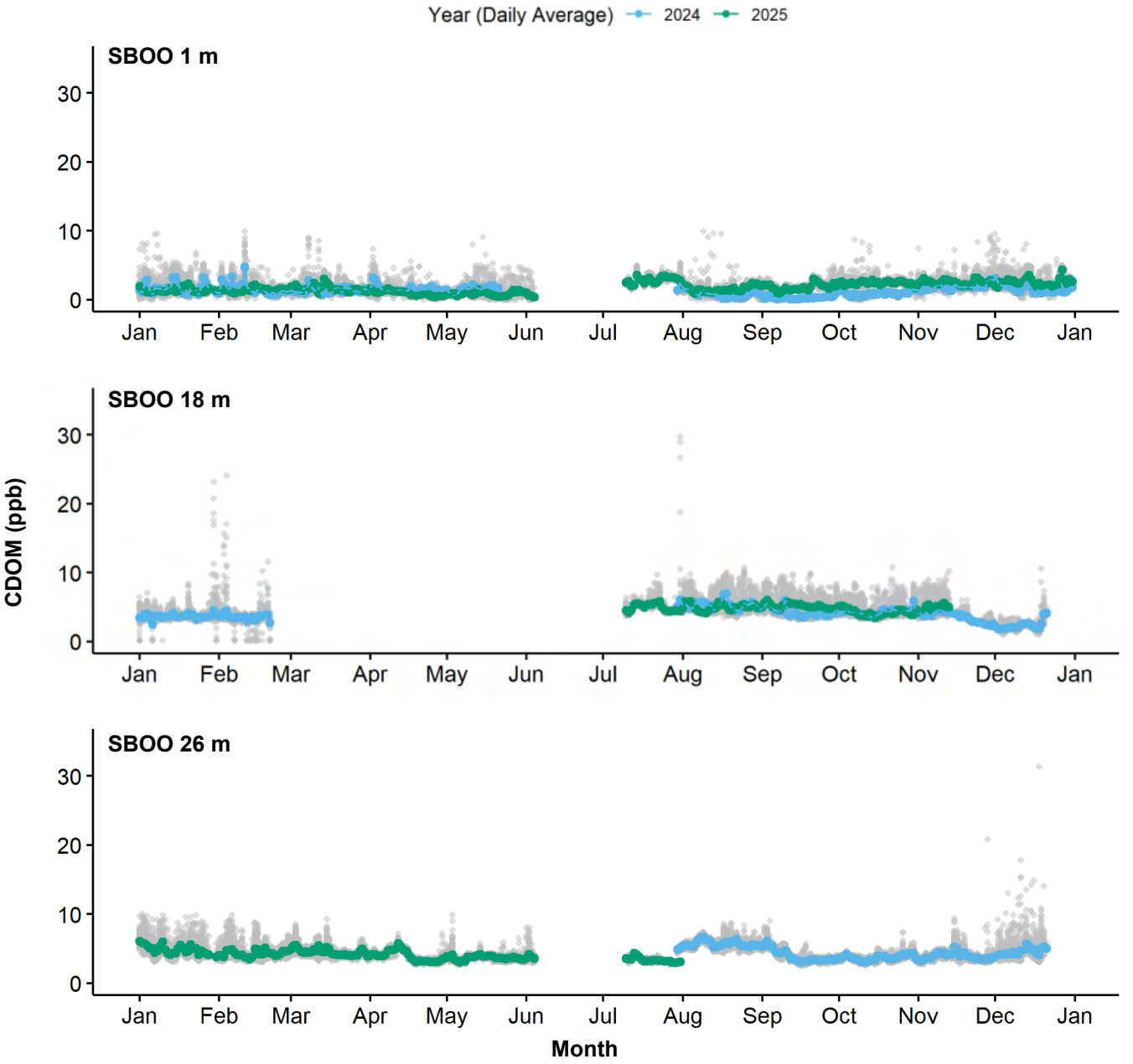
Appendix B.12 *continued*



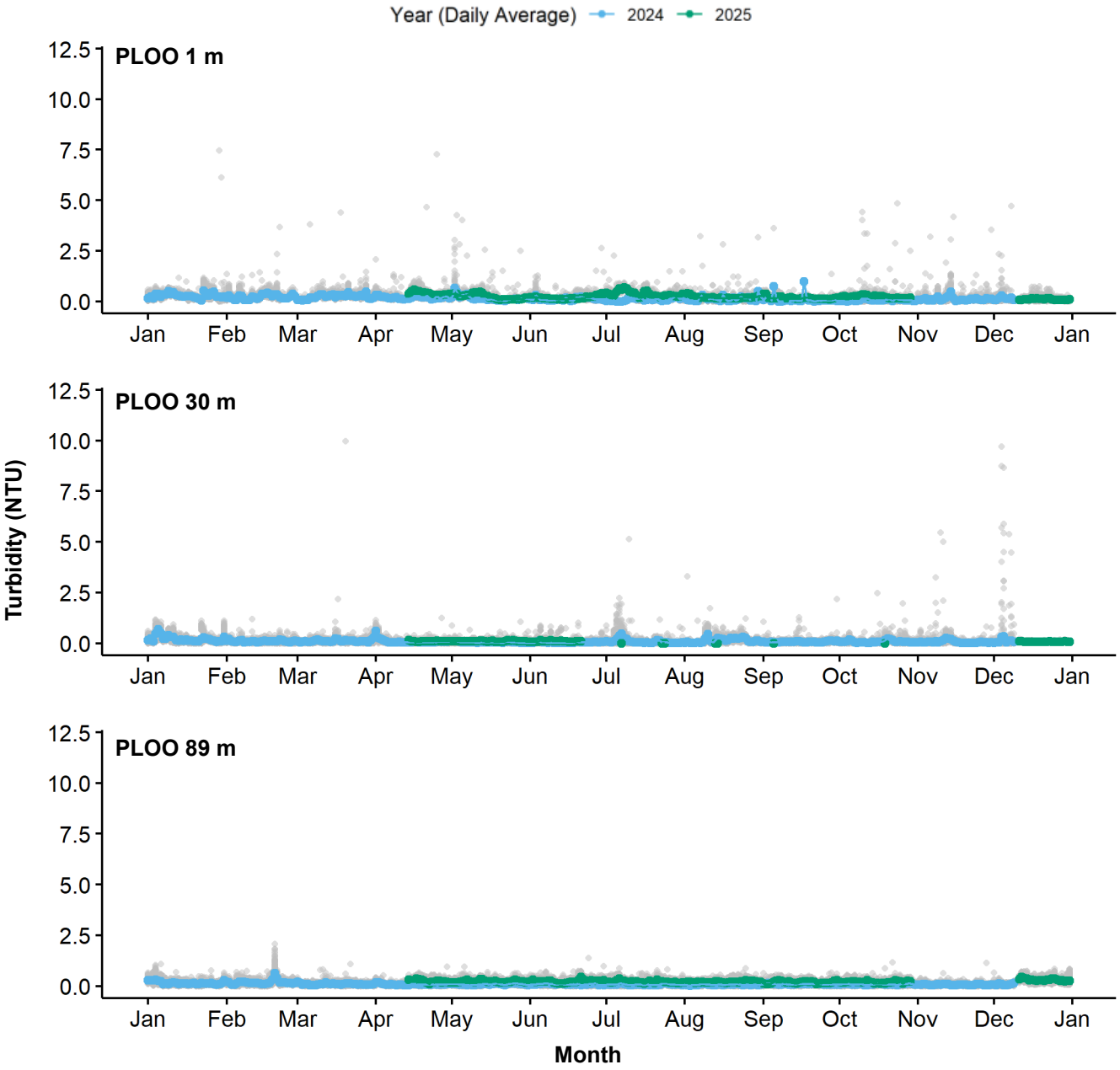
Appendix B.12 *continued*



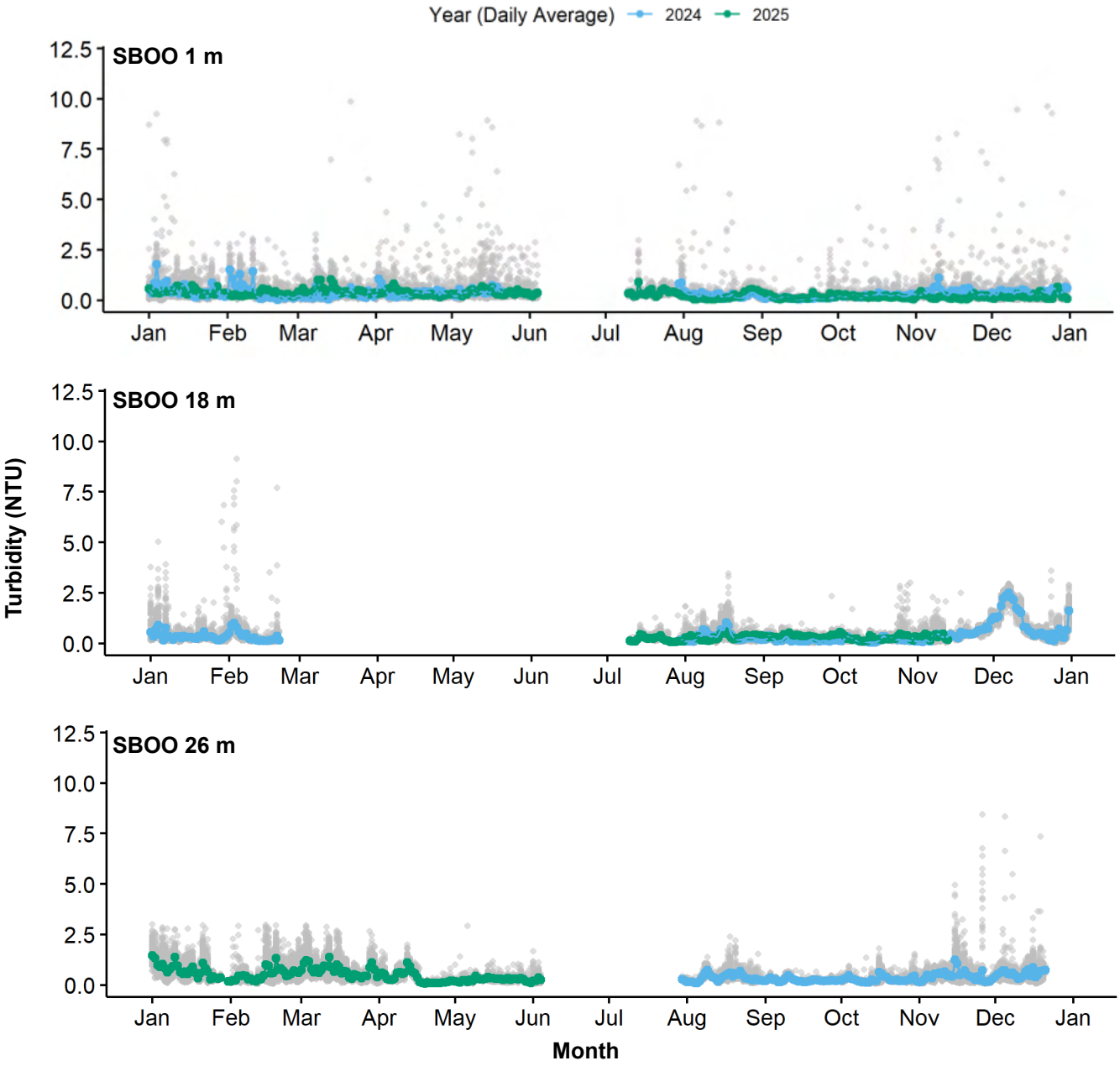
Appendix B.12 *continued*



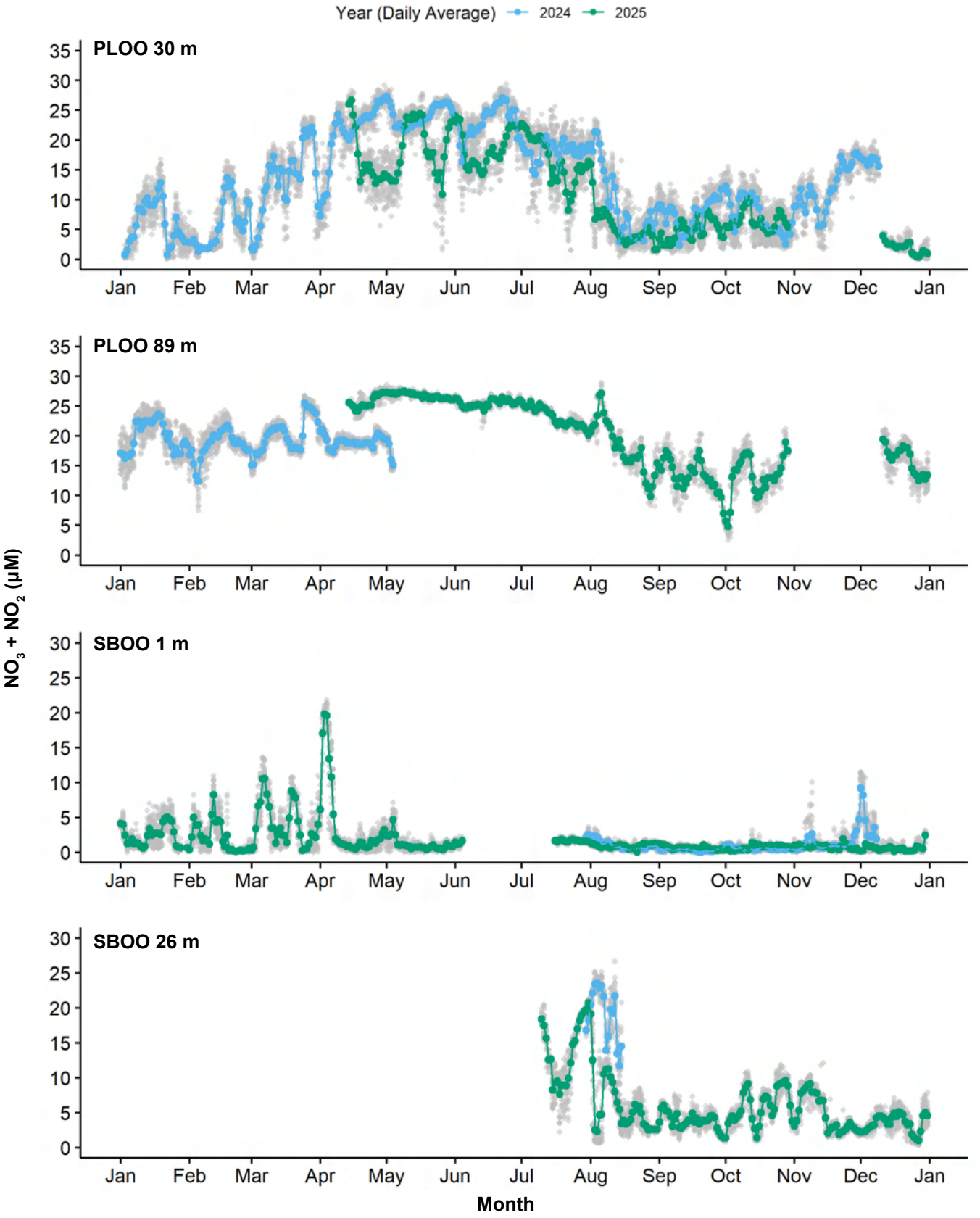
Appendix B.12 *continued*



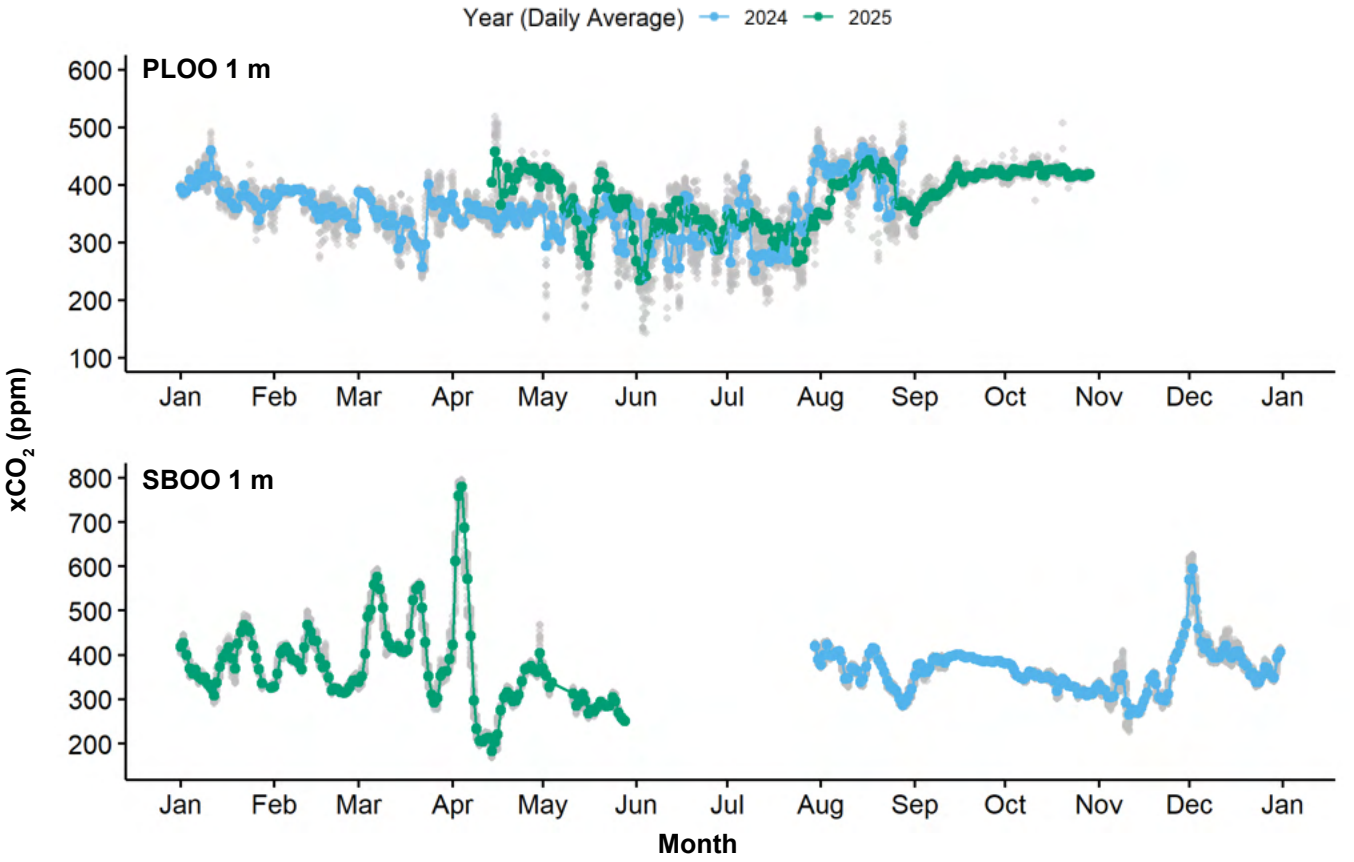
Appendix B.12 *continued*



Appendix B.12 *continued*



Appendix B.12 *continued*

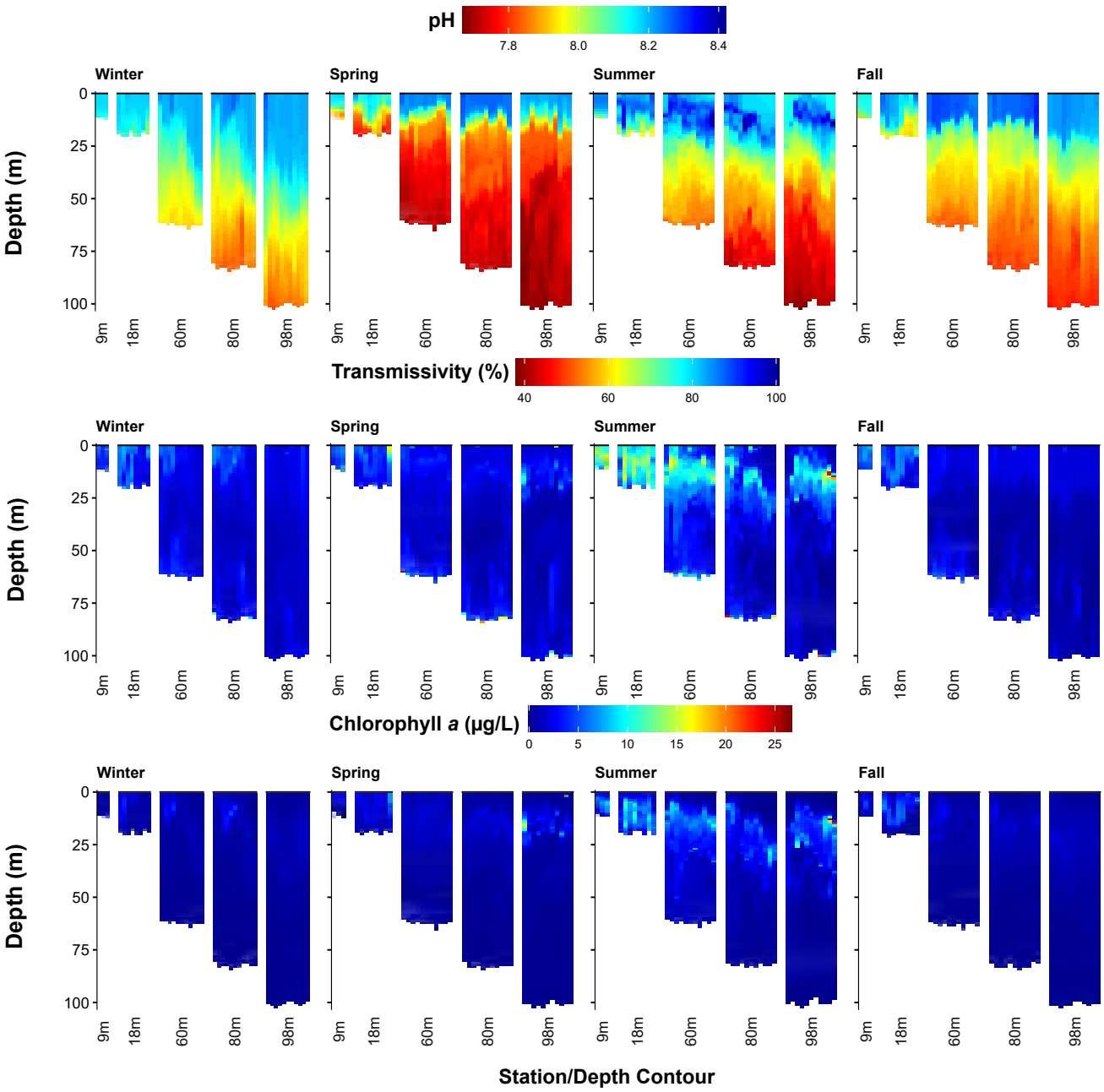


Appendix B.12 *continued*

Appendix B.13

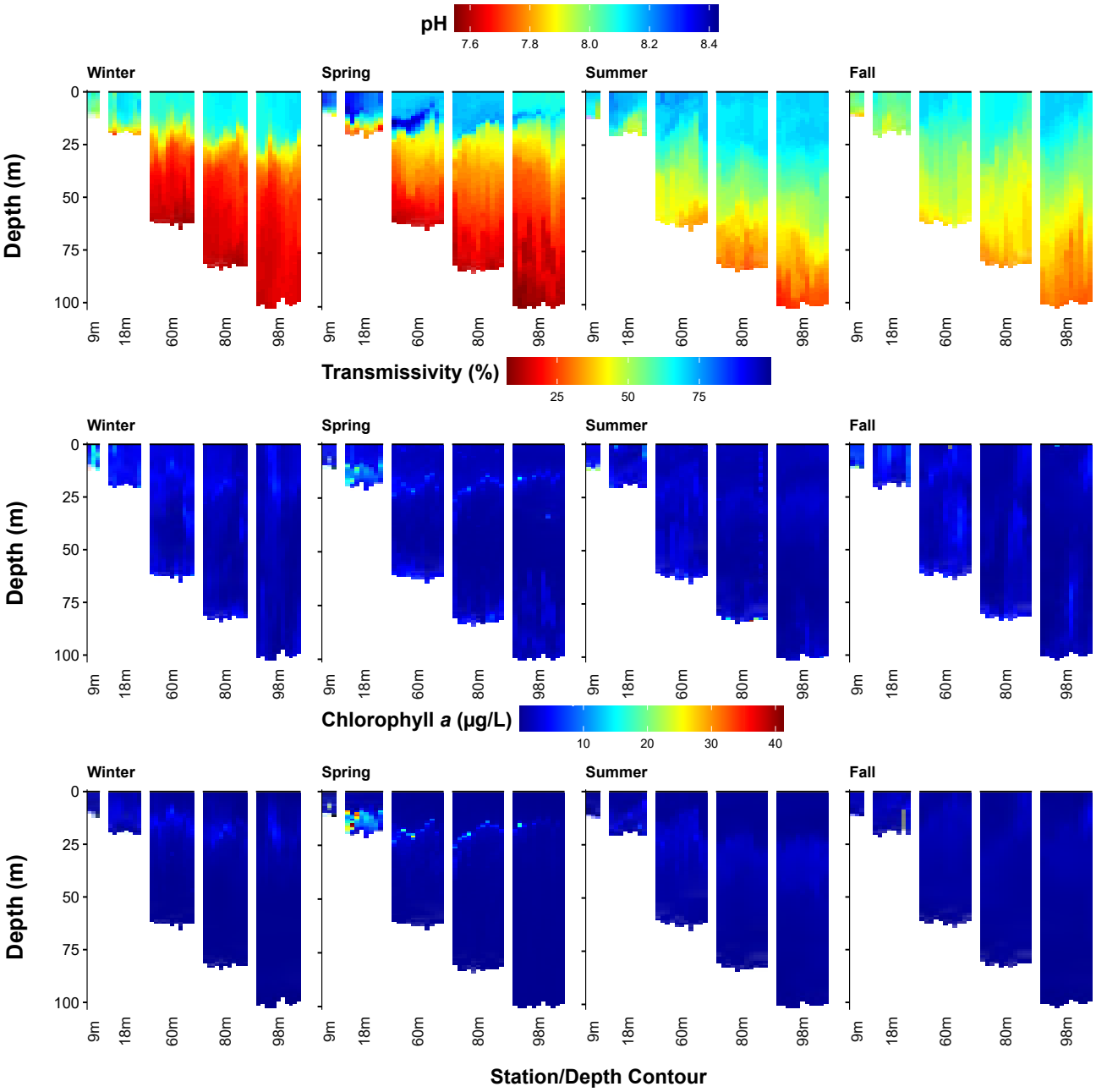
Summary of seasonal buoyancy frequency in the PLOO and SBOO regions during 2024 and 2025. Depth refers to the depth of maximum buoyancy frequency. Max BF refers to the maximum buoyancy frequency, measured in cycles per second. For each quarter: n = 11 (PLOO), n = 13 (SBOO).

	2024		2025	
	Depth (m)	**Max BF (s^{-1})**	**Depth (m)**	**Max BF (s^{-1})**
PLOO Region				
Winter	37	5.33	24	7.85
Spring	6	12.59	11	12.76
Summer	10	13.83	8	11.72
Fall	21	8.63	15	8.48
SBOO Region				
Winter	16	7.51	5	7.50
Spring	6	12.88	67	10.83
Summer	7	15.98	9	14.50
Fall	12	9.73	10	8.00



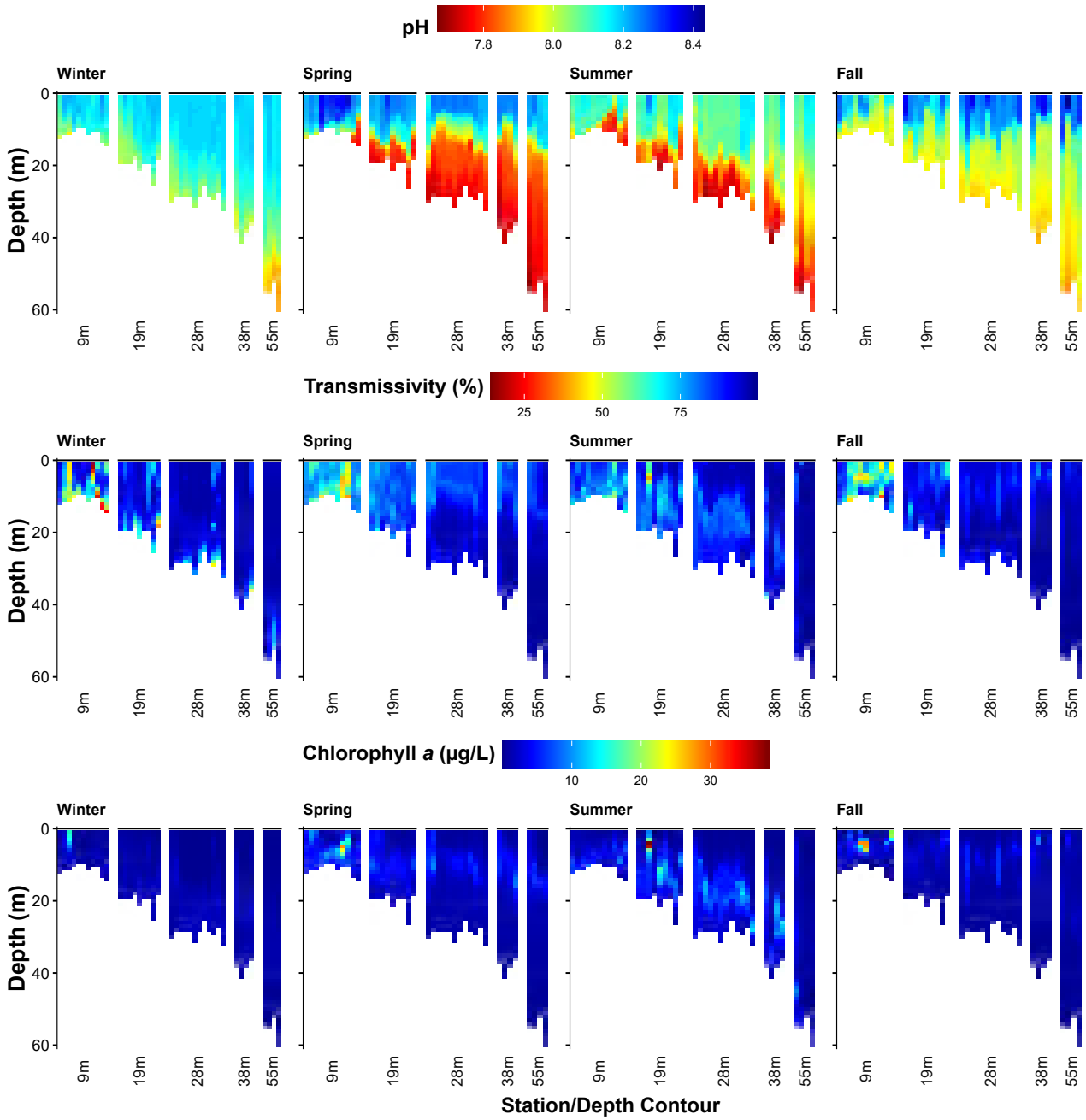
Appendix B.14

Values of pH, transmissivity, and chlorophyll *a* recorded in the PLOO region during 2024. Data are 1-m binned values per depth for each station and were collected over 4–5 days during each quarterly survey. Stations are depicted from north to south along each depth contour.



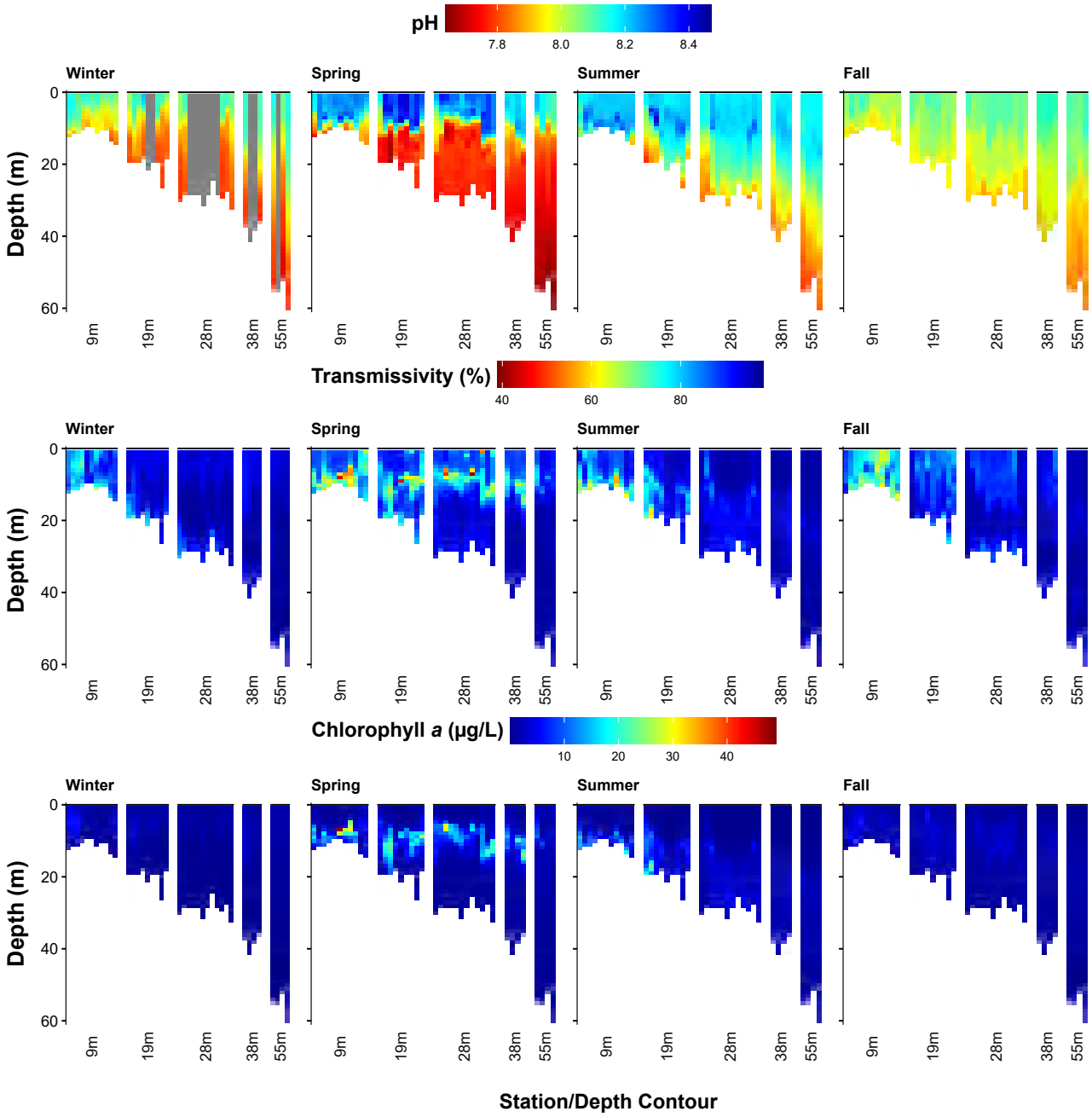
Appendix B.15

Values of pH, transmissivity, and chlorophyll *a* recorded in the PLOO region during 2025. Data are 1-m binned values per depth for each station and were collected over 4–5 days during each quarterly survey. Stations are depicted from north to south along each depth contour.



Appendix B.16

Values of pH, transmissivity, and chlorophyll *a* recorded in the SBOO region during 2024. Data are 1-m binned values per depth for each station and were collected over 4–5 days during each quarterly survey. Stations are depicted from north to south along each depth contour.



Appendix B.17

Values of pH, transmissivity, and chlorophyll *a* recorded in the SBOO region during 2025. Data are 1-m binned values per depth for each station and were collected over 4–5 days during each quarterly survey. Stations are depicted from north to south along each depth contour. Grey areas indicate missing data (sensor failure).

Appendix B.18

Summary of current velocity magnitude and direction from the PLOO RTOMS ADCP during 2024 and 2025. Data are presented by depth bin as seasonal recovered observations (n), minimum (min), maximum (max), and means with 95% confidence intervals (CI). Proportion of recovered observations (n_prop) differed due to variations in data quality (see text). Minimum and maximum angles of velocity are not shown due to the circular nature of the measurement.

				Magnitude (mm/s)				Angle	
Season	**Depth (m)**	**n**	**n_prop**	**Min**	**Max**	**Mean**	**95% CI**	**Mean**	**95% CI**
Winter	3	13104	1	2	495	150	4	199	70
	4	13104	1	15	590	172	5	192	72
	5	13104	1	11	608	175	5	190	71
	6	13104	1	11	593	173	5	190	71
	7	13104	1	3	581	172	5	189	70
	8	13104	1	5	568	169	5	189	70
	9	13104	1	7	494	156	4	199	68
	10	13104	1	4	476	153	4	195	68
	11	13104	1	5	510	163	5	188	70
	12	13104	1	8	496	160	4	186	69
	13	13104	1	10	489	157	4	186	70
	14	13104	1	11	479	153	4	185	69
	15	13104	1	12	468	151	4	184	69
	16	13104	1	12	453	148	4	181	70
	17	13104	1	3	440	145	4	181	70
	18	13104	1	4	428	141	4	180	70
	19	13104	1	4	413	138	4	178	70
	20	13104	1	3	394	133	3	182	70
	21	13104	1	0	363	125	3	195	69
	22	13104	1	3	338	121	3	182	70
	23	13104	1	2	357	128	3	164	71
	24	13104	1	6	336	124	3	169	71
	25	13104	1	3	308	117	3	188	69
	26	13104	1	3	271	112	2	255	62
	27	13104	1	0	206	84	2	271	64
	28	13104	1	3	259	101	2	119	69
	29	13104	1	1	285	112	3	130	69
	30	13104	1	3	276	107	3	143	70
	31	13104	1	2	277	105	2	134	70
	32	13104	1	1	273	102	2	132	70
	33	13104	1	3	274	101	2	120	70
	34	13104	1	5	279	99	2	107	69
	35	13104	1	1	276	96	2	102	69
	36	13104	1	1	273	95	2	91	70

Appendix B.18 *continued*

				Magnitude (mm/s)				Angle	
Season	Depth (m)	n	n_prop	Min	Max	Mean	95% CI	Mean	95% CI
	37	13104	1	2	280	94	2	83	70
	38	13104	1	1	280	93	2	78	70
	39	13104	1	3	271	91	2	70	70
	40	13104	1	1	271	89	2	55	69
	41	13104	1	1	273	87	2	37	69
	42	13104	1	3	267	84	2	42	69
	43	13104	1	1	277	85	2	54	69
	44	13104	1	0	274	86	2	58	69
	45	13104	1	2	277	85	3	54	68
	46	13104	1	1	273	85	2	49	68
	47	13104	1	4	274	85	2	58	69
	48	13104	1	1	282	84	2	57	69
	49	13104	1	1	282	85	2	57	68
	50	13104	1	1	276	83	2	58	69
	51	13104	1	1	271	83	2	55	70
	52	13104	1	3	267	80	2	57	70
	53	13104	1	1	268	81	2	53	70
	54	13104	1	1	267	80	2	50	70
	55	13104	1	3	261	78	2	48	70
	56	13104	1	2	248	78	2	50	71
	57	13104	1	1	246	80	2	58	70
	58	13104	1	3	248	82	2	64	70
	59	13104	1	1	252	82	2	65	70
	60	13104	1	1	252	83	2	62	71
	61	13104	1	1	261	83	2	63	71
	62	13104	1	2	254	83	2	62	71
	63	13104	1	1	248	83	2	65	71
	64	13104	1	2	247	84	2	67	70
	65	13104	1	2	246	84	2	67	71
	66	13104	1	1	254	84	2	69	70
	67	13104	1	6	249	85	2	70	71
	68	13104	1	5	242	85	2	71	71
	69	13104	1	7	248	84	2	72	71
	70	13104	1	4	247	84	2	73	71
	71	13104	1	9	236	84	2	76	71
	72	13104	1	2	236	83	2	76	70
	73	13104	1	3	235	83	2	79	70

Appendix B.18 *continued*

				Magnitude (mm/s)				Angle	
Season	**Depth (m)**	**n**	**n_prop**	**Min**	**Max**	**Mean**	**95% CI**	**Mean**	**95% CI**
	74	13104	1	1	233	82	2	83	70
	75	13104	1	3	234	80	2	83	69
	76	13104	1	1	236	79	2	87	69
	77	13104	1	2	232	76	2	90	69
	78	13104	1	2	232	73	2	91	70
	79	13104	1	1	219	71	2	99	69
	80	13104	1	2	220	69	2	119	69
	81	13104	1	2	223	67	2	210	69
	82	13104	1	1	218	65	2	236	71
	83	13104	1	1	200	63	2	181	70
	84	13104	1	0	201	62	2	105	68
	85	13104	1	1	200	64	2	109	64
	86	13104	1	1	204	66	2	124	62
	87	13104	1	1	207	62	2	144	62
	88	13104	1	2	200	57	2	213	65
	89	13104	1	1	170	51	1	241	67
	90	13104	1	2	135	44	1	258	65
	91	13104	1	1	77	29	1	275	61
	92	13104	1	0	66	20	1	292	51
Spring	3	24060	1	1	462	204	3	210	50
	4	24060	1	2	509	228	4	208	49
	5	24060	1	3	529	233	4	208	49
	6	24060	1	5	530	230	4	208	50
	7	24060	1	3	510	223	4	208	51
	8	24060	1	1	510	217	4	208	51
	9	24060	1	3	489	206	3	208	51
	10	24060	1	3	472	199	3	208	51
	11	24060	1	2	471	197	3	207	51
	12	24060	1	1	468	192	3	207	52
	13	24060	1	2	455	186	3	206	52
	14	24060	1	2	456	181	3	207	52
	15	24060	1	2	445	175	3	206	52
	16	24060	1	1	432	170	3	206	51
	17	24060	1	1	419	165	3	207	51
	18	24060	1	4	418	160	3	207	51
	19	24054	1	1	416	153	3	206	51
	20	24060	1	3	414	149	3	207	51

Appendix B.18 *continued*

				Magnitude (mm/s)				Angle	
Season	Depth (m)	n	n_prop	Min	Max	Mean	95% CI	Mean	95% CI
	21	24054	1	3	421	144	3	208	51
	22	24060	1	2	414	138	3	209	50
	23	24060	1	4	411	137	3	205	51
	24	24060	1	3	405	132	3	207	51
	25	24060	1	4	404	127	3	209	51
	26	24060	1	2	385	118	2	226	51
	27	24060	1	2	369	101	2	235	50
	28	24060	1	2	378	106	2	205	50
	29	24060	1	5	377	114	2	192	51
	30	24060	1	0	366	110	2	200	51
	31	24060	1	2	362	105	2	204	51
	32	24060	1	2	360	101	2	205	52
	33	24060	1	3	343	99	2	203	52
	34	24060	1	2	332	96	2	201	52
	35	24060	1	1	327	94	2	200	52
	36	24060	1	1	322	91	2	198	52
	37	24060	1	0	311	88	2	198	52
	38	24060	1	0	301	87	2	192	52
	39	24054	1	1	291	85	2	192	52
	40	24060	1	1	278	83	2	187	52
	41	24060	1	3	271	82	2	186	52
	42	24060	1	1	265	79	2	187	52
	43	24060	1	3	248	78	1	173	51
	44	24060	1	2	251	77	1	154	51
	45	24060	1	2	233	75	1	147	51
	46	24060	1	1	228	74	1	141	51
	47	24060	1	1	219	73	1	126	51
	48	24060	1	1	210	71	1	113	51
	49	24060	1	3	196	70	1	103	50
	50	24060	1	0	188	69	1	99	51
	51	24060	1	3	176	68	1	94	51
	52	24060	1	1	174	67	1	91	51
	53	24060	1	1	172	66	1	92	51
	54	24060	1	1	167	65	1	90	51
	55	24060	1	0	146	63	1	87	52
	56	24060	1	0	146	62	1	82	52
	57	24060	1	0	147	61	1	84	52

Appendix B.18 *continued*

				Magnitude (mm/s)				Angle	
Season	Depth (m)	n	n_prop	Min	Max	Mean	95% CI	Mean	95% CI
	58	24060	1	0	146	65	1	90	52
	59	24060	1	2	145	65	1	91	52
	60	24060	1	0	144	63	1	90	53
	61	24060	1	1	141	63	1	90	54
	62	24060	1	1	146	63	1	90	53
	63	24060	1	2	142	62	1	90	55
	64	24060	1	1	142	62	1	91	56
	65	24060	1	2	136	62	1	92	55
	66	24060	1	8	138	62	1	92	56
	67	24060	1	8	137	61	1	94	56
	68	24060	1	5	137	62	1	94	56
	69	24060	1	5	136	60	1	95	56
	70	24060	1	9	132	60	1	94	56
	71	24054	1	6	135	59	1	95	56
	72	24054	1	6	132	59	1	96	57
	73	24060	1	0	134	59	1	97	57
	74	24060	1	3	138	58	1	96	58
	75	24060	1	8	131	57	1	98	58
	76	24054	1	6	131	55	1	97	60
	77	24060	1	2	129	54	1	96	57
	78	24060	1	2	136	52	1	94	58
	79	24060	1	3	130	51	1	93	58
	80	24054	1	0	138	48	1	86	57
	81	24054	1	2	137	46	1	72	56
	82	24054	1	1	139	45	1	58	54
	83	24048	1	1	134	44	1	55	52
	84	24048	1	1	134	42	1	60	53
	85	24048	1	1	163	48	1	73	54
	86	24042	1	2	136	50	1	79	54
	87	24018	1	0	145	47	1	73	54
	88	24012	1	1	122	43	1	65	52
	89	23994	1	1	119	40	1	42	51
	90	23994	1	1	144	37	1	26	47
	91	23964	1	1	105	34	1	26	45
	92	23970	1	0	77	29	1	31	43
Summer	3	26022	1	4	310	103	2	220	42
	4	26022	1	2	348	121	2	211	44

Appendix B.18 *continued*

				Magnitude (mm/s)				Angle	
Season	Depth (m)	n	n_prop	Min	Max	Mean	95% CI	Mean	95% CI
	5	26022	1	8	390	131	2	205	44
	6	26022	1	1	400	133	2	203	45
	7	26022	1	6	410	136	2	201	46
	8	26022	1	3	422	136	2	200	45
	9	26022	1	6	400	132	2	201	47
	10	26022	1	6	377	129	2	199	48
	11	26022	1	1	366	131	2	196	48
	12	26022	1	3	346	129	2	193	49
	13	26022	1	4	345	127	2	191	50
	14	26022	1	2	327	125	2	189	51
	15	26022	1	1	324	122	2	185	51
	16	26016	1	4	330	120	2	182	52
	17	26016	1	2	328	116	2	179	52
	18	26022	1	1	319	113	2	172	52
	19	26022	1	0	324	109	2	157	52
	20	26016	1	1	318	108	2	142	54
	21	26022	1	2	325	106	2	129	53
	22	26022	1	2	321	101	2	96	54
	23	26016	1	0	323	102	2	89	53
	24	26022	1	2	322	101	2	74	53
	25	26022	1	2	327	99	2	61	54
	26	26016	1	5	304	94	2	23	53
	27	26016	1	2	280	85	1	8	51
	28	26022	1	0	298	82	1	45	52
	29	26022	1	1	319	92	1	62	53
	30	26022	1	3	316	92	1	53	54
	31	26022	1	2	315	92	1	50	54
	32	26022	1	3	317	91	2	49	54
	33	26022	1	2	312	90	2	47	54
	34	26016	1	2	305	89	2	45	54
	35	26022	1	1	309	88	2	44	54
	36	26022	1	1	300	86	2	44	54
	37	26022	1	0	307	86	2	44	53
	38	26022	1	2	302	85	2	43	53
	39	26016	1	2	302	84	2	42	53
	40	26016	1	6	301	84	2	43	54
	41	26022	1	2	311	83	2	42	53

Appendix B.18 *continued*

				Magnitude (mm/s)				Angle	
Season	Depth (m)	n	n_prop	Min	Max	Mean	95% CI	Mean	95% CI
	42	26016	1	8	298	82	2	40	53
	43	26022	1	1	298	82	2	41	53
	44	26016	1	1	297	83	2	44	53
	45	26016	1	1	301	82	2	43	53
	46	26022	1	1	300	82	2	43	53
	47	26016	1	2	303	82	2	42	53
	48	26022	1	1	305	81	2	43	53
	49	26022	1	3	301	82	2	43	53
	50	26022	1	0	291	81	2	43	53
	51	26022	1	1	298	81	2	44	53
	52	26022	1	3	292	80	2	45	53
	53	26022	1	3	289	81	2	44	54
	54	26016	1	4	286	82	2	46	54
	55	26016	1	1	291	81	2	46	54
	56	26022	1	2	283	81	2	45	54
	57	26022	1	1	275	81	2	47	54
	58	26022	1	2	275	81	1	49	54
	59	26022	1	1	273	81	1	51	54
	60	26022	1	3	277	81	1	52	54
	61	26022	1	2	265	81	1	53	55
	62	26022	1	2	263	80	1	54	55
	63	26022	1	2	274	80	1	55	54
	64	26022	1	6	261	80	1	57	55
	65	26022	1	6	254	79	1	57	54
	66	26022	1	1	259	79	1	59	55
	67	26022	1	3	249	79	1	61	55
	68	26022	1	3	250	77	1	61	55
	69	26022	1	2	237	76	1	63	55
	70	26022	1	7	232	76	1	62	56
	71	26022	1	6	227	75	1	63	56
	72	26022	1	2	222	74	1	64	56
	73	26022	1	2	225	74	1	65	56
	74	26022	1	1	224	73	1	66	55
	75	26022	1	1	211	72	1	66	56
	76	26022	1	2	204	70	1	66	56
	77	26022	1	5	201	70	1	63	56
	78	26022	1	0	190	69	1	61	56

Appendix B.18 *continued*

				Magnitude (mm/s)				Angle	
Season	**Depth (m)**	**n**	**n_prop**	**Min**	**Max**	**Mean**	**95% CI**	**Mean**	**95% CI**
	79	26022	1	1	188	68	1	59	56
	80	26022	1	1	184	67	1	54	55
	81	26022	1	1	167	62	1	45	55
	82	26016	1	1	169	61	1	33	55
	83	26022	1	1	167	60	1	28	55
	84	26016	1	2	194	62	1	19	56
	85	26022	1	0	181	60	1	25	56
	86	26022	1	0	166	58	1	22	54
	87	26022	1	2	157	59	1	18	56
	88	26016	1	1	156	57	1	13	55
	89	26022	1	0	151	57	1	359	55
	90	26022	1	2	145	54	1	358	56
	91	26016	1	2	129	47	1	358	55
	92	26016	1	1	96	36	1	356	56
Fall	3	16860	1	1	407	89	3	168	39
	4	16860	1	1	462	126	4	203	48
	5	16860	1	6	497	144	4	205	51
	6	16860	1	4	493	147	4	205	52
	7	16860	1	4	477	146	4	206	51
	8	16860	1	3	468	143	4	207	51
	9	16860	1	1	462	138	4	208	51
	10	16860	1	2	443	132	4	208	52
	11	16860	1	4	480	134	4	207	52
	12	16860	1	2	478	131	4	207	53
	13	16860	1	2	469	127	4	205	53
	14	16860	1	4	463	124	4	207	54
	15	16860	1	1	462	121	3	207	55
	16	16860	1	0	472	119	3	208	55
	17	16860	1	4	469	117	3	209	55
	18	16860	1	2	459	114	3	213	55
	19	16860	1	4	470	111	3	213	56
	20	16860	1	0	473	111	3	216	56
	21	16860	1	1	484	109	3	226	56
	22	16860	1	1	489	106	3	226	55
	23	16860	1	1	491	106	3	224	56
	24	16860	1	2	496	108	3	230	57
	25	16860	1	2	490	106	3	241	56

Appendix B.18 *continued*

				Magnitude (mm/s)				Angle	
Season	Depth (m)	n	n_prop	Min	Max	Mean	95% CI	Mean	95% CI
	26	16860	1	3	441	102	3	271	55
	27	16860	1	5	465	88	3	285	55
	28	16860	1	3	503	90	3	253	55
	29	16860	1	4	515	98	3	206	56
	30	16854	1	0	518	102	3	296	57
	31	16860	1	6	512	102	3	316	56
	32	16860	1	1	514	100	3	322	57
	33	16860	1	2	511	101	3	336	57
	34	16860	1	2	514	100	3	341	56
	35	16860	1	2	502	98	3	345	56
	36	16860	1	3	504	98	3	349	56
	37	16860	1	1	495	97	3	353	56
	38	16860	1	2	494	97	3	354	56
	39	16860	1	1	482	96	3	356	56
	40	16860	1	3	471	95	3	356	55
	41	16860	1	3	457	93	3	357	55
	42	16860	1	2	444	92	3	360	55
	43	16860	1	2	438	90	3	2	55
	44	16860	1	1	436	93	3	3	55
	45	16860	1	3	423	91	3	2	54
	46	16860	1	1	406	90	2	4	54
	47	16860	1	1	404	89	2	4	54
	48	16860	1	1	402	89	2	6	54
	49	16860	1	2	385	87	2	7	55
	50	16860	1	2	380	87	2	8	54
	51	16860	1	2	371	87	2	8	53
	52	16860	1	2	363	85	2	10	54
	53	16860	1	0	355	85	2	6	53
	54	16860	1	1	339	83	2	12	52
	55	16860	1	2	341	83	2	12	53
	56	16860	1	2	345	81	2	7	53
	57	16860	1	0	342	81	2	14	52
	58	16860	1	2	343	80	2	19	53
	59	16860	1	1	343	82	2	22	52
	60	16860	1	0	331	84	2	15	51
	61	16860	1	2	329	80	2	16	53
	62	6900	0.41	1	327	86	4	85	43

Appendix B.18 *continued*

				Magnitude (mm/s)				Angle	
Season	Depth (m)	n	n_prop	Min	Max	Mean	95% CI	Mean	95% CI
	63	6900	0.41	4	328	87	4	90	43
	64	6900	0.41	3	318	86	4	77	44
	65	6900	0.41	4	322	88	4	82	43
	66	6900	0.41	9	311	87	4	81	43
	67	6900	0.41	9	304	87	4	86	43
	68	6900	0.41	8	296	86	4	83	44
	69	6900	0.41	9	293	86	4	82	44
	70	6900	0.41	9	299	86	4	84	44
	71	6900	0.41	3	303	86	4	86	45
	72	6900	0.41	12	293	87	3	90	45
	73	6900	0.41	8	294	87	3	93	45
	74	6894	0.41	15	294	85	3	97	45
	75	6900	0.41	7	292	86	3	98	46
	76	6894	0.41	15	291	83	3	100	46
	77	6900	0.41	5	296	83	3	102	47
	78	6900	0.41	5	292	79	3	109	47
	79	6900	0.41	10	281	79	3	109	48
	80	6900	0.41	4	282	75	3	103	48
	81	6900	0.41	7	278	71	3	92	48
	82	6900	0.41	4	272	68	3	83	48
	83	6900	0.41	2	274	69	3	55	48
	84	6900	0.41	0	275	68	3	66	47
	85	6900	0.41	1	269	68	3	54	48
	86	6900	0.41	1	261	66	3	22	48
	87	6900	0.41	0	260	63	3	335	49
	88	6900	0.41	2	248	59	3	321	49
	89	6900	0.41	0	232	56	3	325	47
	90	6900	0.41	1	197	44	2	340	47
	91	6900	0.41	1	165	27	2	19	49
	92	6900	0.41	1	96	20	1	43	59

Appendix B.19

Summary of current velocity magnitude and direction from the SBOO RTOMS ADCP during 2024 and 2025. Data are presented by depth bin as seasonal recovered observations (n), minimum (min), maximum (max), and means with 95% confidence intervals (CI). Proportion of recovered observations (n_prop) differed due to variations in data quality (see text). Minimum and maximum angles of velocity are not shown due to the circular nature of the measurement.

				Magnitude (mm/s)				Angle	
Season	**Depth (m)**	**n**	**n_prop**	**Min**	**Max**	**Mean**	**95% CI**	**Mean**	**95% CI**
Winter	3	25487	1	1	282	88	2	155	72
	4	25486	1	2	287	103	2	154	73
	5	25485	1	1	319	108	2	150	74
	6	25486	1	1	308	107	2	147	75
	7	25487	1	1	306	106	2	146	76
	8	25486	1	1	322	106	2	142	76
	9	25485	1	0	271	99	2	142	77
	10	25484	1	2	273	98	2	139	77
	11	25483	1	2	314	102	2	134	77
	12	25482	1	2	314	101	2	132	78
	13	25484	1	1	306	100	2	129	78
	14	25484	1	3	310	99	2	127	78
	15	25483	1	2	297	97	2	121	79
	16	25483	1	1	252	93	2	115	79
	17	25482	1	2	237	87	2	108	78
	18	25479	1	2	234	87	2	102	78
	19	25484	1	1	259	94	2	99	78
	20	25480	1	3	267	93	2	94	77
	21	25484	1	3	220	90	1	88	77
	22	25482	1	0	198	81	1	76	76
	23	25484	1	1	192	73	1	39	75
	24	25485	1	1	197	70	1	360	73
	25	25480	1	0	219	71	1	37	74
	26	25479	1	3	218	70	1	52	72
	27	25483	1	1	207	63	1	38	70
Spring	3	16384	1	1	483	102	4	171	76
	4	16383	1	1	482	112	4	168	78
	5	16383	1	1	493	116	4	164	77
	6	16385	1	2	508	118	4	159	77
	7	16383	1	2	471	113	4	155	77
	8	16383	1	2	437	109	4	152	77
	9	16382	1	0	391	101	4	152	76
	10	16383	1	2	396	96	3	150	75
	11	16382	1	1	383	93	3	146	76
	12	16384	1	1	359	89	3	143	76
	13	16381	1	1	338	84	3	137	76

Appendix B.19 *continued*

				Magnitude (mm/s)				Angle	
Season	**Depth (m)**	**n**	**n_prop**	**Min**	**Max**	**Mean**	**95% CI**	**Mean**	**95% CI**
	14	16383	1	2	319	80	3	131	76
	15	16381	1	4	296	76	2	124	77
	16	16381	1	2	249	72	2	111	77
	17	16383	1	1	223	67	2	91	79
	18	16381	1	1	223	67	2	88	78
	19	16382	1	2	218	69	2	88	78
	20	16380	1	0	214	69	2	85	77
	21	16382	1	4	195	66	1	75	76
	22	16381	1	2	164	59	1	61	77
	23	16379	1	3	152	52	1	42	76
	24	16384	1	1	149	49	1	27	72
	25	16382	1	2	153	50	1	44	71
	26	16383	1	4	162	51	1	57	72
	27	16381	1	7	146	46	1	56	70
Summer	3	20792	1	2	318	130	3	177	72
	4	20792	1	1	344	123	3	175	74
	5	20790	1	2	367	129	3	172	75
	6	20792	1	8	354	126	3	169	76
	7	20792	1	5	361	120	3	166	76
	8	20791	1	2	363	116	3	163	76
	9	20791	1	0	302	99	2	161	75
	10	20792	1	1	290	95	2	158	75
	11	20791	1	1	312	99	2	155	76
	12	20791	1	1	296	94	2	153	77
	13	20791	1	1	268	88	2	150	76
	14	20790	1	1	247	84	2	149	77
	15	20789	1	0	237	80	2	146	77
	16	20790	1	1	224	74	2	137	78
	17	20791	1	1	211	67	1	110	77
	18	20791	1	0	203	67	1	99	76
	19	20791	1	1	187	71	1	109	78
	20	20790	1	1	176	71	1	107	79
	21	20791	1	1	171	69	1	98	79
	22	20790	1	2	172	60	1	70	76
	23	20791	1	1	165	54	1	42	75
	24	20790	1	1	155	50	1	24	74
	25	20791	1	1	152	50	1	58	76
	26	20790	1	0	157	49	1	52	76
	27	20790	1	0	134	44	1	38	74

Appendix B.19 *continued*

				Magnitude (mm/s)				Angle	
Season	**Depth (m)**	**n**	**n_prop**	**Min**	**Max**	**Mean**	**95% CI**	**Mean**	**95% CI**
Fall	3	26234	1	4	353	105	2	182	71
	4	26233	1	1	399	99	2	180	73
	5	26234	1	1	398	100	2	175	73
	6	26234	1	0	376	98	2	169	73
	7	26232	1	0	371	96	2	165	73
	8	26233	1	1	360	93	2	159	74
	9	26233	1	2	323	88	2	158	74
	10	26233	1	2	354	85	2	150	75
	11	26230	1	1	359	85	2	142	75
	12	26234	1	1	366	84	2	134	75
	13	26233	1	1	366	83	2	129	76
	14	26233	1	0	367	81	2	117	76
	15	26231	1	0	340	80	2	108	76
	16	26231	1	0	310	78	2	103	77
	17	26227	1	1	298	75	2	84	78
	18	26228	1	1	322	75	2	78	78
	19	26228	1	2	334	77	2	78	77
	20	26227	1	2	316	77	2	75	78
	21	26228	1	1	274	74	1	70	78
	22	26228	1	3	255	69	1	55	78
	23	26228	1	2	245	64	1	30	77
	24	26228	1	1	250	61	1	13	77
	25	26228	1	1	243	59	1	34	76
	26	26227	1	0	232	56	1	38	75
	27	26226	1	0	205	51	1	32	74

Appendix B.20

Summary of current velocity magnitude and direction from the PLOO static ADCP during 2024 and 2025. Data are presented by depth bin as seasonal recovered observations (n), minimum (min), maximum (max), and means with 95% confidence intervals (CI). Proportion of recovered observations (n_prop) differed due to variations in data quality (see text). Minimum and maximum angles of velocity are not shown due to the circular nature of the measurement.

				Magnitude (mm/s)				Angle	
Season	**Depth (m)**	**n**	**n_prop**	**Min**	**Max**	**Mean**	**95% CI**	**Mean**	**95% CI**
Winter	9	246	0.23	8	201	69	6	129	65
	13	1088	1	9	450	160	6	157	64
	17	1088	1	4	462	164	6	160	67
	21	1088	1	2	418	153	6	157	68
	25	1088	1	7	376	145	6	151	69
	29	1088	1	11	356	139	5	141	70
	33	1088	1	0	332	133	5	123	70
	37	1088	1	2	319	129	4	105	70
	41	1088	1	1	307	125	4	89	70
	45	1088	1	0	287	120	4	74	69
	49	1088	1	3	245	113	3	63	69
	53	1088	1	3	230	106	3	52	69
	57	1088	1	12	222	99	3	39	68
	61	1088	1	4	225	93	3	28	68
	65	1088	1	2	218	87	3	18	68
	69	1088	1	0	204	81	3	12	69
	73	1088	1	6	202	76	3	10	70
	77	1088	1	3	200	73	3	15	71
	81	1088	1	2	192	72	2	26	72
	85	1088	1	3	185	72	2	42	72
	89	1088	1	3	176	71	2	58	71
	93	1085	1	3	183	62	2	69	69
Spring	9	1666	1	1	360	156	4	161	71
	13	1666	1	3	336	134	4	160	72
	17	1666	1	1	305	117	3	159	72
	21	1666	1	2	279	104	3	156	71
	25	1666	1	1	253	92	3	156	71
	29	1666	1	2	221	82	2	153	70
	33	1666	1	1	190	74	2	124	69
	37	1666	1	1	174	68	2	36	68
	41	1666	1	0	158	65	2	5	66
	45	1666	1	1	162	62	1	354	64
	49	1666	1	1	168	60	2	349	63
	53	1666	1	3	173	59	2	345	61
	57	1666	1	2	176	58	2	342	59
	61	1666	1	5	176	57	2	340	58
	65	1666	1	3	172	55	2	342	57

Appendix B.20*continued*

				Magnitude (mm/s)				Angle	
Season	**Depth (m)**	**n**	**n_prop**	**Min**	**Max**	**Mean**	**95% CI**	**Mean**	**95% CI**
	69	1666	1	1	166	52	2	349	59
	73	1666	1	1	163	48	2	359	63
	77	1666	1	1	165	44	2	14	68
	81	1666	1	3	166	45	1	34	72
	85	1666	1	12	153	47	1	52	74
	89	1666	1	1	128	46	1	66	74
	93	1666	1	4	93	39	1	79	75
Summer	9	2128	0.84	13	275	123	2	128	58
	13	2281	0.9	5	279	115	2	111	57
	17	2384	0.94	1	306	105	2	66	58
	21	2490	0.98	2	314	99	2	37	60
	25	2529	1	1	299	94	2	21	61
	29	2533	1	2	275	91	2	15	62
	33	2534	1	9	252	86	2	10	63
	37	2534	1	6	233	83	2	7	64
	41	2534	1	4	217	82	2	4	65
	45	2534	1	2	216	81	2	2	65
	49	2534	1	2	215	80	2	1	64
	53	2534	1	2	206	80	2	358	65
	57	2534	1	1	195	81	2	353	66
	61	2534	1	2	197	80	2	349	67
	65	2534	1	1	199	78	2	347	68
	69	2534	1	1	201	76	2	347	69
	73	2534	1	1	202	73	2	351	71
	77	2534	1	2	196	70	2	358	72
	81	2534	1	2	183	66	1	6	72
	85	2532	1	5	168	62	1	18	72
	89	2522	1	0	155	57	1	32	70
	93	2525	1	3	129	48	1	50	68
Fall	9	4021	0.92	0	306	104	2	134	67
	13	4141	0.95	4	474	123	3	163	72
	17	4332	0.99	2	514	114	3	161	72
	21	4366	1	1	470	107	2	157	71
	25	4376	1	1	420	102	2	146	71
	29	4378	1	1	372	97	2	97	71
	33	4378	1	4	349	92	2	40	72
	37	4378	1	1	338	89	2	22	72
	41	4378	1	1	316	86	2	17	72
	45	4378	1	1	286	84	2	16	71
	49	4378	1	2	268	82	2	15	71
	53	4378	1	0	264	79	2	9	71

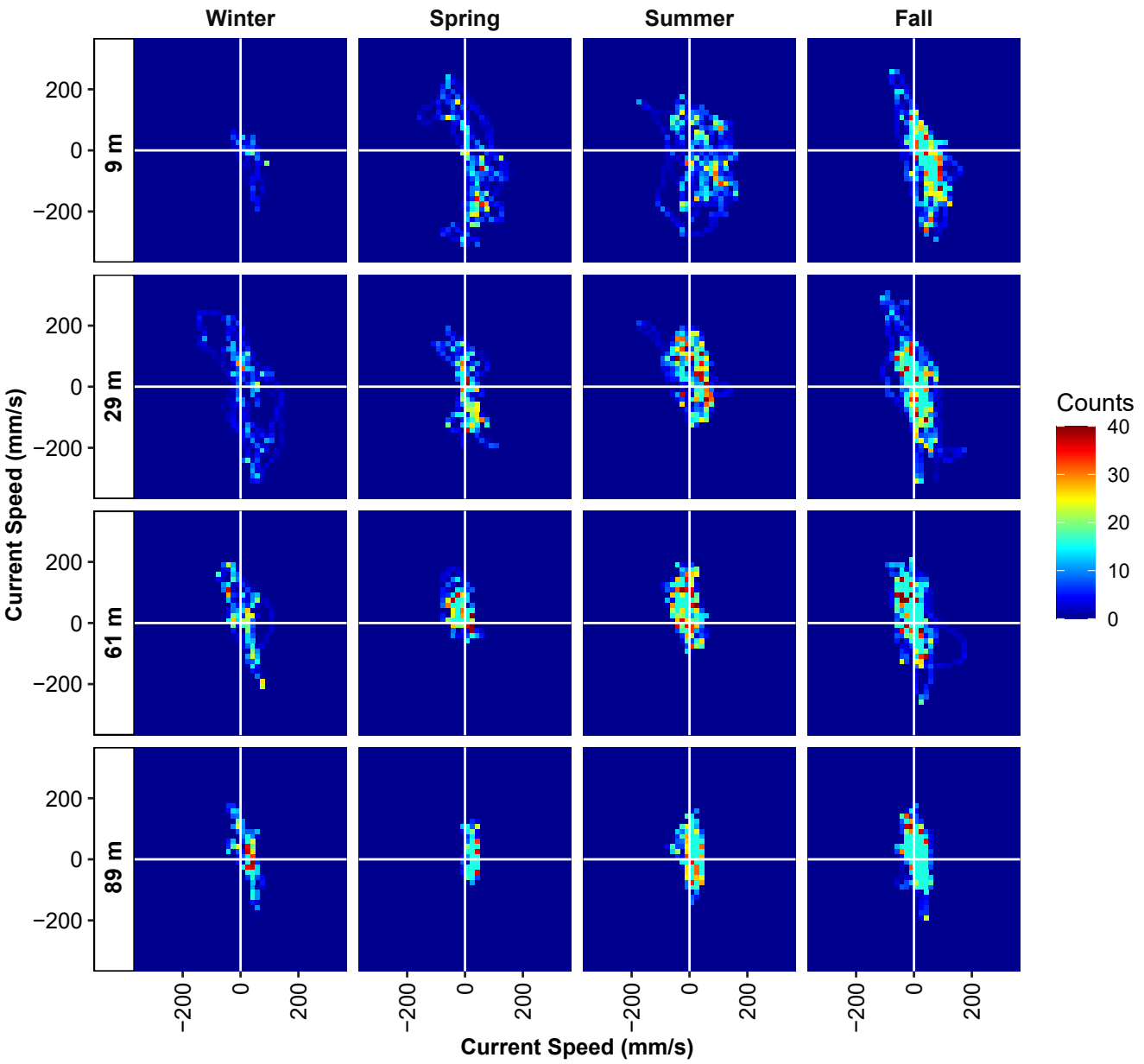
Appendix B.20 *continued*

				Magnitude (mm/s)				Angle	
Season	**Depth (m)**	**n**	**n_prop**	**Min**	**Max**	**Mean**	**95% CI**	**Mean**	**95% CI**
	57	4378	1	1	259	77	2	1	70
	61	4378	1	1	258	76	1	354	69
	65	4378	1	1	254	74	1	348	68
	69	4378	1	0	249	73	1	345	68
	73	4378	1	1	243	71	1	346	70
	77	4378	1	1	236	68	1	353	71
	81	4378	1	1	231	65	1	6	72
	85	4375	1	0	224	63	1	26	72
	89	4355	0.99	0	203	59	1	54	70
	93	4282	0.98	2	169	52	1	92	65

Appendix B.21

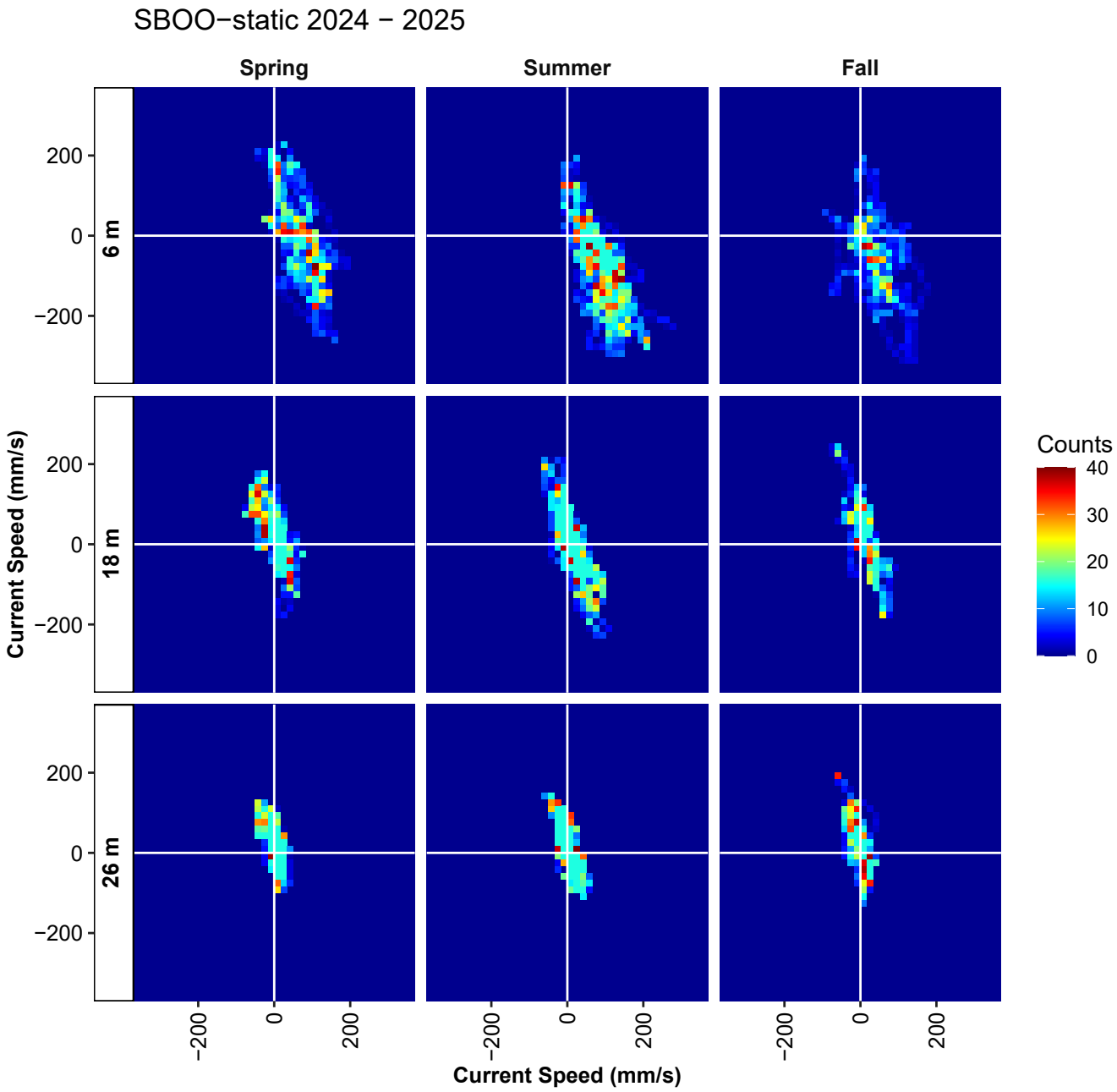
Summary of current velocity magnitude and direction from the SBOO static ADCP during 2024 and 2025. The static mooring was not deployed in winter of either year. Data are presented by depth bin as seasonal recovered observations (n), minimum (min), maximum (max), and means with 95% confidence intervals (CI). Proportion of recovered observations (n_prop) differed due to variations in data quality (see text). Minimum and maximum angles of velocity are not shown due to the circular nature of the measurement.

				Magnitude (mm/s)				Angle	
Season	**Depth (m)**	**n**	**n_prop**	**Min**	**Max**	**Mean**	**95% CI**	**Mean**	**95% CI**
Winter	6								
	10								
	14								
	18								
	22								
	26								
	30								
Spring	6	2183	1	29	380	133	2	120	67
	10	2184	1	5	339	75	2	125	65
	14	2184	1	0	283	67	2	85	66
	18	2184	1	0	233	58	2	46	69
	22	2184	1	1	195	54	2	22	70
	26	2184	1	0	167	50	1	8	69
	30	2184	1	2	137	43	1	356	67
Summer	6	2202	1	3	420	135	3	128	70
	10	2207	1	3	383	123	4	123	71
	14	2207	1	1	406	113	3	77	70
	18	2208	1	2	388	101	3	26	69
	22	2208	1	3	350	92	3	6	69
	26	2208	1	2	305	83	2	359	70
	30	2208	1	1	250	68	2	355	69
Fall	6	944	0.99	2	209	90	3	131	56
	10	949	1	1	178	65	3	42	65
	14	949	1	9	194	67	3	20	68
	18	950	1	5	207	73	3	5	68
	22	950	1	3	204	74	3	355	69
	26	950	1	2	184	67	3	348	70
	30	950	1	2	155	53	2	344	69



Appendix B.22

Frequency distribution (counts) by season of current speed (mm/s) and direction from 2024 and 2025 at the PLOO static ADCP location at representative depth bins. On the x-axis, positive values indicate an eastward direction while negative values indicate a westward direction. On the y-axis, positive values indicate a northward direction while negative values indicate a southward direction.



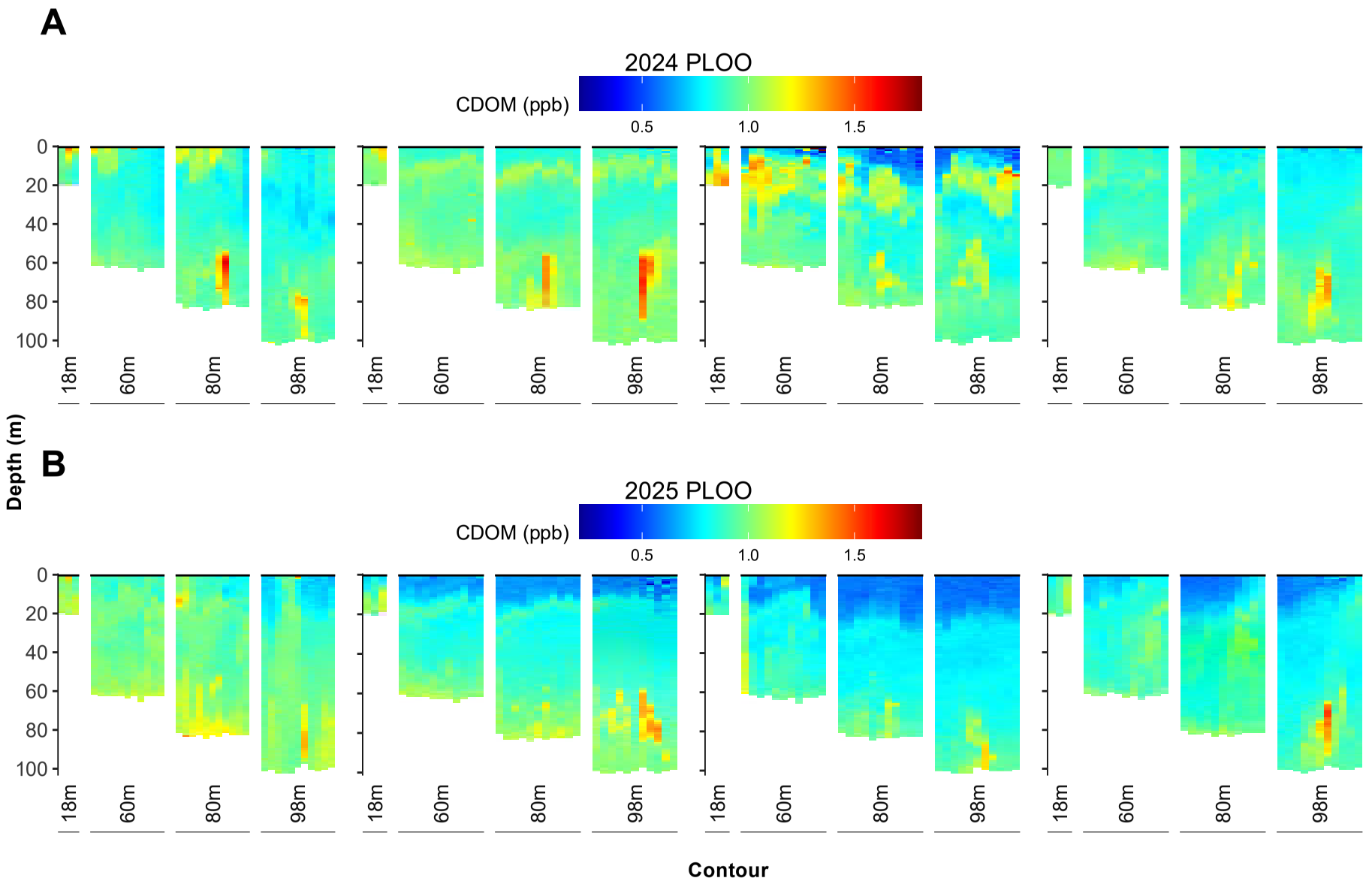
Appendix B.23

Frequency distribution (counts) by season of current speed (mm/s) and direction from 2024 and 2025 at the SBOO static ADCP location at representative depth bins. This instrument was not deployed during winter months of either year. On the x-axis, positive values indicate an eastward direction while negative values indicate a westward direction. On the y-axis, positive values indicate a northward direction while negative values indicate a southward direction.

Appendix C

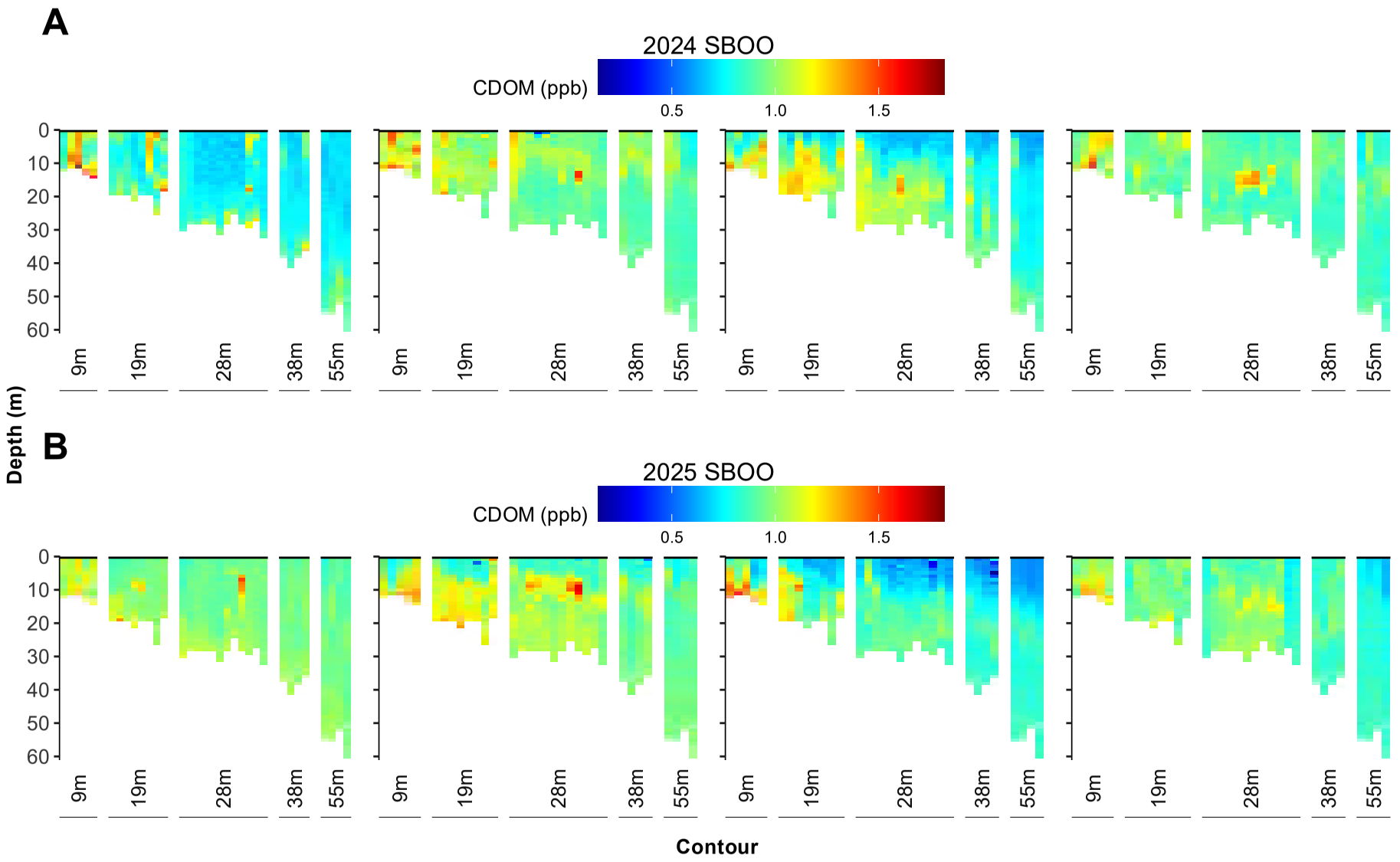
Plume Dispersion

2024 – 2025 Supplemental Analyses



Appendix C.1

Concentrations of CDOM recorded in the PLOO region during (A) 2024 and (B) 2025. Data are 1-m binned values per depth for each station during each quarterly survey. Stations depicted from north to south along each depth contour. See Chapter 2 for additional sampling details.



Appendix C.2

Concentrations of CDOM recorded in the SBOO region during (A) 2024 and (B) 2025. Data are 1-m binned values per depth for each station during each quarterly survey. Stations depicted from north to south along each depth contour. See Chapter 2 for additional sampling details.

Appendix C.3

Summary of oceanographic data within potential detected plume at PLOO offshore stations and corresponding reference values during 2024 and 2025. Plume depth is the minimum depth at which CDOM exceeds the 95th percentile while plume width is the number of meters across which that exceedance occurs. Out-of-range values are in **bold**. DO = dissolved oxygen (mg/L); XMS = transmissivity (%); SD = standard deviation; CI = confidence interval.

		Potential Plume					Reference		
Station	Date	Width (m)	Depth (m)	Mean DO	Mean pH	Mean XMS	DO (Mean - SD)	pH (Mean)	XMS (Mean - 95% CI)
F31	2/13/2024	7	77	4.6	7.9	94.9	4.4	7.9	95
F30	2/13/2024	12	78	4.3	7.9	**94.3**	4.2	7.9	96
F18[a]	2/15/2024	25	54	**4.0**	7.8	**92.8**	4.8	7.9	96
F19[a]	2/15/2024	16	57	4.5	7.9	**94.9**	4.8	7.9	96
F28	5/14/2024	10	54	3.3	7.7	97.3	3.5	7.7	97
F29	5/14/2024	19	54	3.1	7.7	**95.4**	3.4	7.7	97
F30	5/14/2024	35	55	**2.9**	7.7	**93.4**	3.3	7.7	96
F05	5/15/2024	1	38	3.5	7.8	97.2	3.6	7.8	95
F19[a]	5/16/2024	25	56	**2.9**	7.7	**94.6**	3.4	7.7	96
F18[a]	5/16/2024	16	58	3.1	7.7	**94.4**	3.4	7.7	96
F21	5/16/2024	7	74	3.0	7.7	**94.7**	3.3	7.7	96
F20[a]	5/16/2024	5	76	3.1	7.7	96.3	3.3	7.7	96
F33	8/13/2024	2	70	4.2	7.7	**96.3**	4.3	7.8	97
F19[a]	8/15/2024	2	70	4.1	7.8	**96.2**	4.3	7.8	97
F20[a]	8/15/2024	3	70	4.1	7.8	**95.9**	4.3	7.8	97
F31	11/19/2024	23	63	4.1	7.8	**97.3**	4.3	7.8	98
F30	11/19/2024	20	66	4.0	7.8	**95.8**	4.3	7.8	98
F32	11/19/2024	19	76	4.1	7.8	98.7	4.0	7.8	97
F29	11/19/2024	1	90	4.3	7.8	99.3	3.8	7.8	96
F08[a]	11/20/2024	1	59	**4.2**	7.8	**92.3**	4.7	7.9	99
F17	11/21/2024	3	55	**4.4**	7.8	**97.9**	4.9	7.9	99
F18[a]	11/21/2024	20	59	4.3	7.8	**98.2**	4.5	7.9	99
F16	11/21/2024	3	60	4.3	7.8	**97.1**	4.7	7.9	100
F20[a]	11/21/2024	2	67	4.2	7.8	**98.8**	4.6	7.9	100
F19[a]	11/21/2024	11	70	4.1	7.8	97.6	4.3	7.8	97
F30	2/20/2025	27	68	2.7	7.7	96.8	2.5	7.6	97
F26	2/20/2025	2	76	2.5	7.6	**96.0**	2.5	7.6	97
F27	2/20/2025	2	91	2.3	7.6	**95.1**	2.5	7.6	96
F22	2/22/2025	22	58	2.6	7.6	96.2	2.6	7.6	96

[a]Station located within State jurisdictional waters

Appendix C.3 *continued*

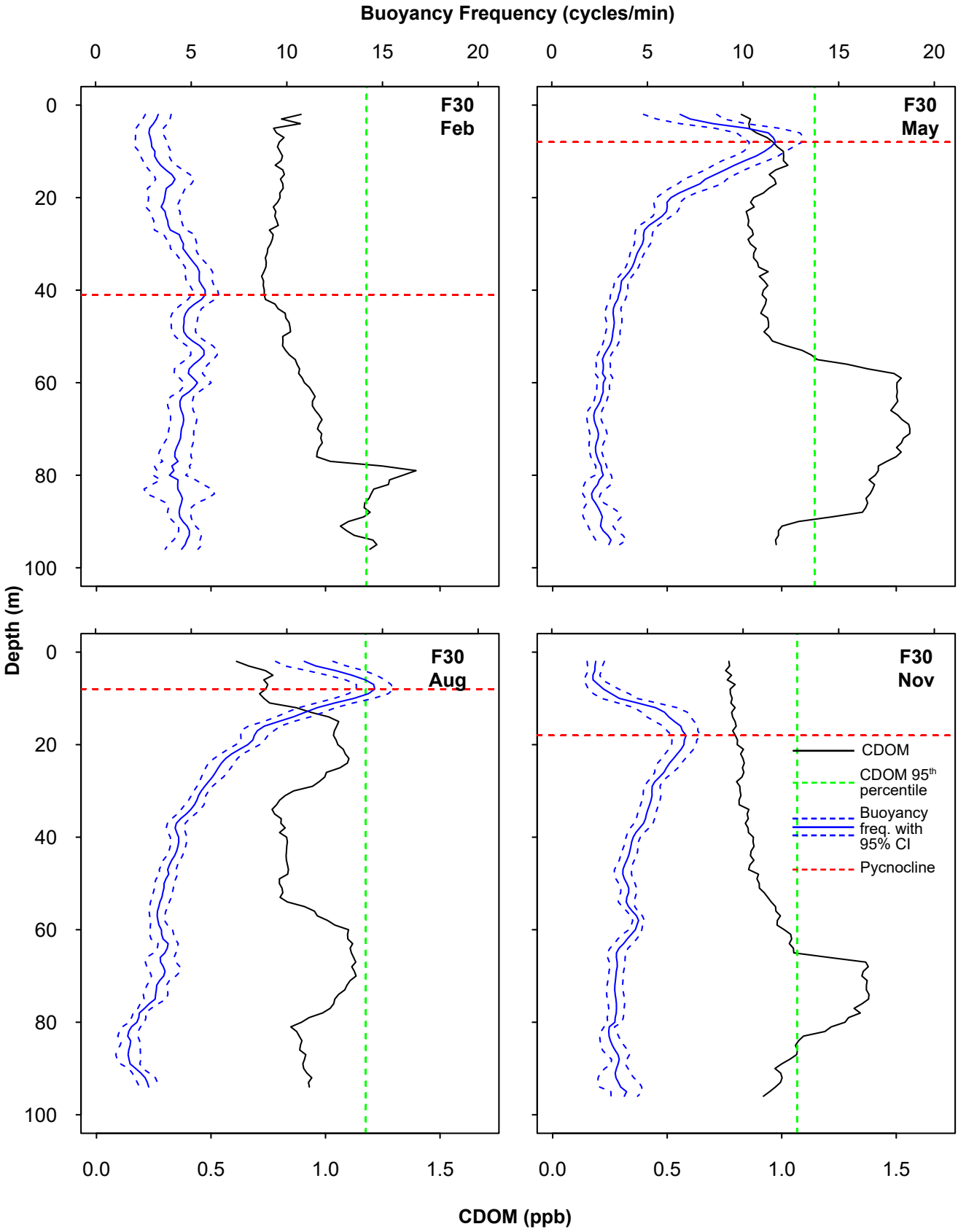
		Potential Plume					Reference		
Station	Date	Width (m)	Depth (m)	Mean DO	Mean pH	Mean XMS	DO (Mean - SD)	pH (Mean)	XMS (Mean - 95% CI)
F24	2/22/2025	5	62	2.6	7.6	**95.4**	2.6	7.6	97
F25	2/22/2025	2	66	2.8	7.6	97.3	2.7	7.7	97
F19[a]	2/22/2025	6	75	2.4	7.6	**95.6**	2.5	7.6	97
F21	2/22/2025	6	76	2.6	7.6	96.6	2.5	7.6	97
F23	2/22/2025	5	76	2.4	7.6	**95.0**	2.5	7.6	97
F20[a]	2/22/2025	3	77	2.4	7.6	**95.5**	2.4	7.6	97
F18[a]	2/22/2025	1	78	2.3	7.6	**92.1**	2.4	7.6	97
F17	2/22/2025	1	79	**2.2**	7.6	**90.9**	2.5	7.6	97
F30	5/20/2025	26	59	3.3	7.6	**94.2**	3.3	7.6	96
F29	5/20/2025	17	66	3.2	7.6	94.6	NaN	NaN	NaN
F32	5/20/2025	3	68	3.3	7.6	96.7	NaN	NaN	NaN
F34	5/20/2025	12	68	2.9	7.6	96.3	NaN	NaN	NaN
F35	5/20/2025	2	71	3.3	7.6	97.6	NaN	NaN	NaN
F28	5/20/2025	12	74	3.0	7.6	93.9	NaN	NaN	NaN
F33	5/20/2025	3	76	2.9	7.6	96.0	NaN	NaN	NaN
F27	5/20/2025	6	89	2.9	7.6	95.7	NaN	NaN	NaN
F19[a]	5/22/2025	4	65	3.4	7.7	97.8	NaN	NaN	NaN
F23	5/22/2025	2	67	3.0	7.6	97.5	NaN	NaN	NaN
F20	5/22/2025	5	75	3.4	7.7	97.6	NaN	NaN	NaN
F17	5/22/2025	2	78	2.7	7.6	87.5	NaN	NaN	NaN
F21	5/22/2025	1	78	3.3	7.6	97.0	NaN	NaN	NaN
F18[a]	5/22/2025	1	79	2.9	7.6	89.9	NaN	NaN	NaN
F31	8/12/2025	14	74	5.1	7.8	97.2	NaN	NaN	NaN
F30	8/12/2025	15	82	4.7	7.7	94.1	NaN	NaN	NaN
F29	8/12/2025	4	92	4.6	7.8	96.2	NaN	NaN	NaN
F32	8/12/2025	2	97	4.6	7.7	97.8	NaN	NaN	NaN
F33	8/12/2025	1	98	4.6	7.7	97.7	NaN	NaN	NaN
F19[a]	8/14/2025	17	64	4.8	7.8	95.8	NaN	NaN	NaN
F18[a]	8/14/2025	6	66	4.8	7.8	95.2	NaN	NaN	NaN
F22	8/14/2025	2	71	5.2	7.8	97.3	NaN	NaN	NaN

[a]**Station located within State jurisdictional waters**

Appendix C.3 *continued*

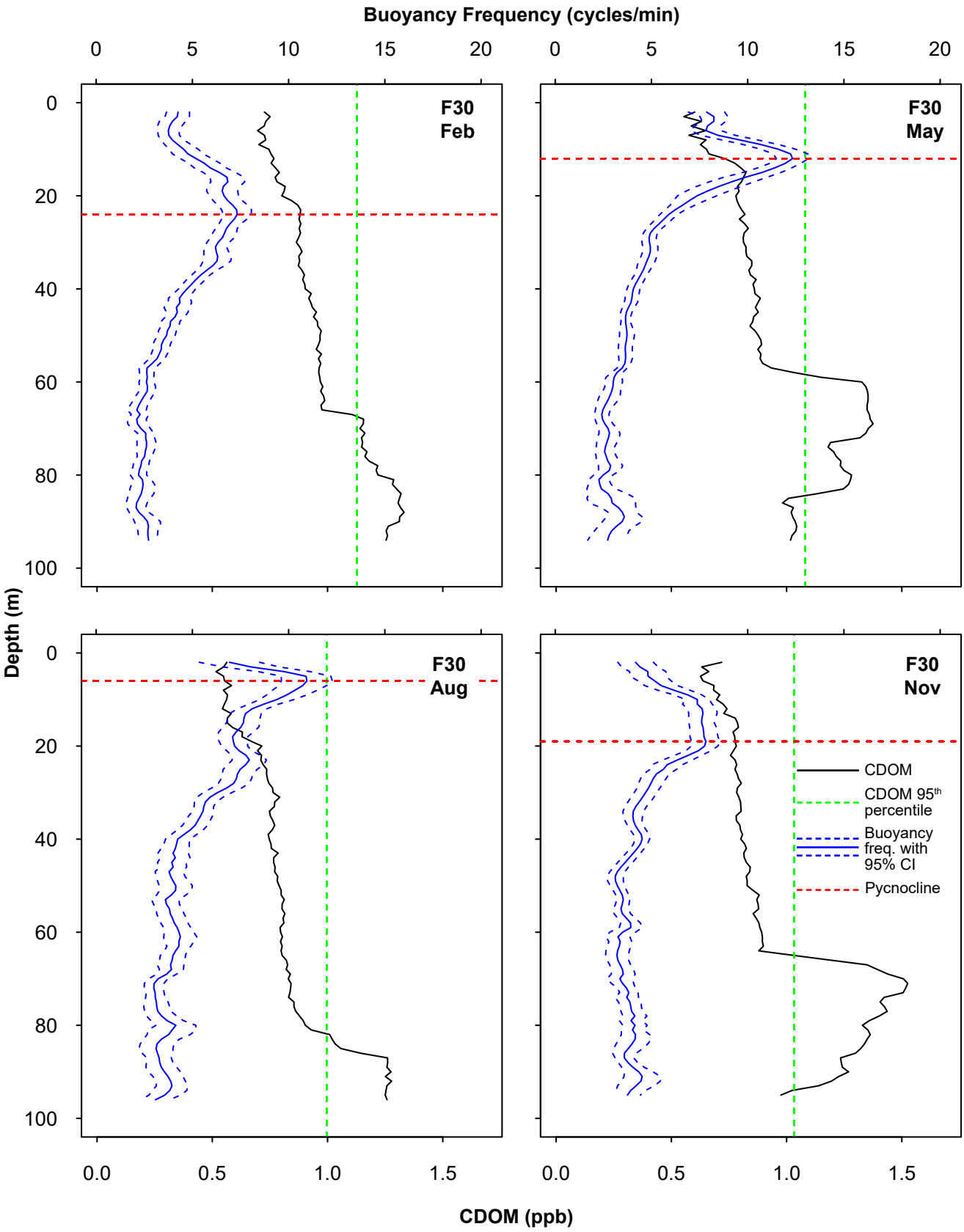
		Potential Plume					Reference		
Station	Date	Width (m)	Depth (m)	Mean DO	Mean pH	Mean XMS	DO (Mean - SD)	pH (Mean)	XMS (Mean - 95% CI)
F23	8/14/2025	5	75	4.7	7.8	95.4	NaN	NaN	NaN
F20[a]	8/14/2025	1	80	4.9	7.8	95.9	NaN	NaN	NaN
F28	11/12/2025	12	59	**5.2**	7.8	**97.3**	6.0	7.9	98
F30	11/12/2025	29	65	**4.8**	7.8	**90.2**	5.4	7.8	97
F31	11/12/2025	23	75	4.9	7.8	**96.4**	5.1	7.8	97
F29	11/12/2025	10	78	4.9	7.8	**96.5**	5.2	7.8	97
F32	11/12/2025	7	81	5.1	7.8	97.4	5.0	7.8	97
F33	11/12/2025	4	87	5.1	7.8	98.1	4.9	7.8	96
F06[a]	11/13/2025	2	37	6.3	7.9	**87.1**	6.9	8.0	97

[a] **Station located within State jurisdictional waters**



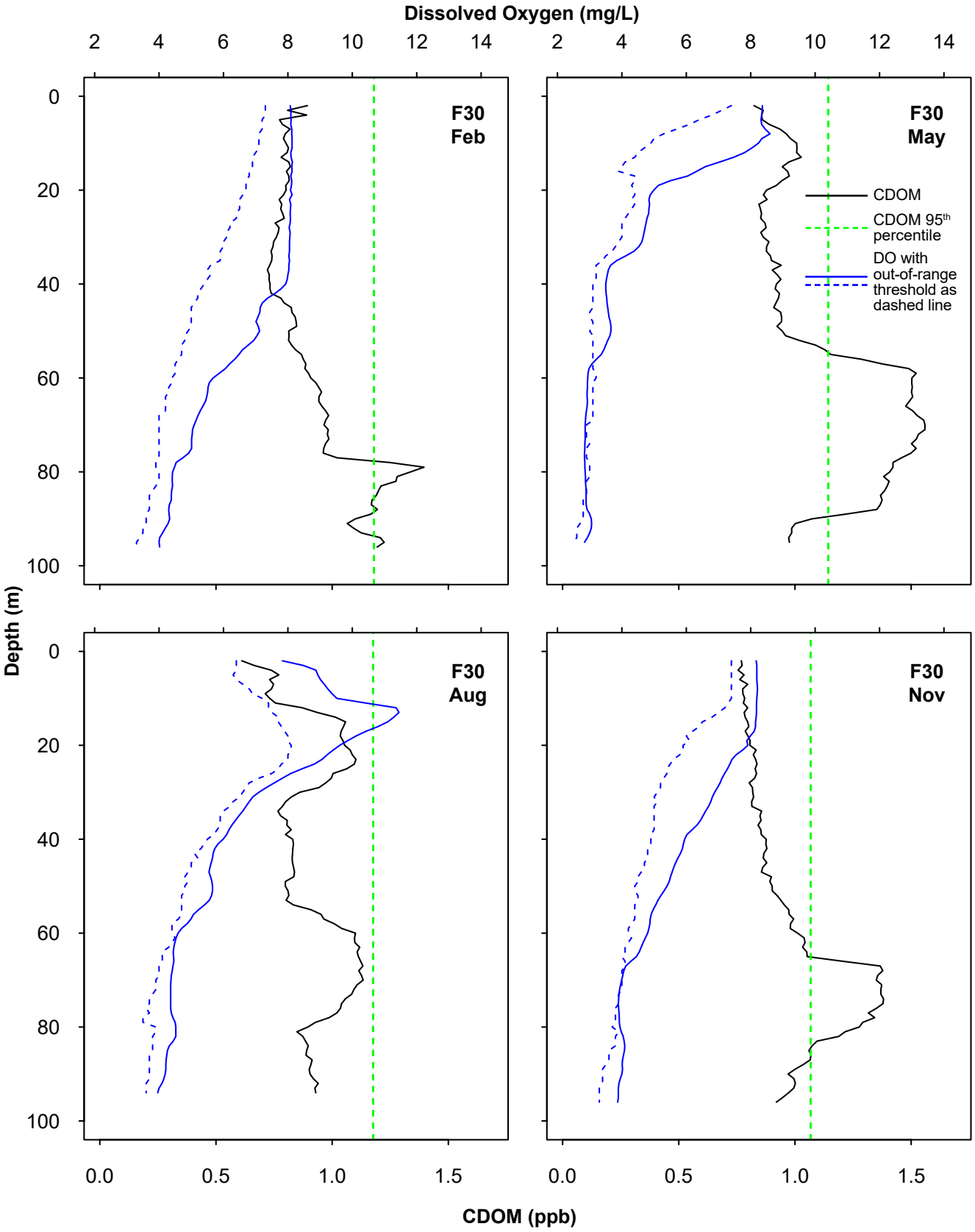
Appendix C.4

Representative vertical profiles of CDOM and buoyancy frequency from PLOO nearfield station F30 during 2024.



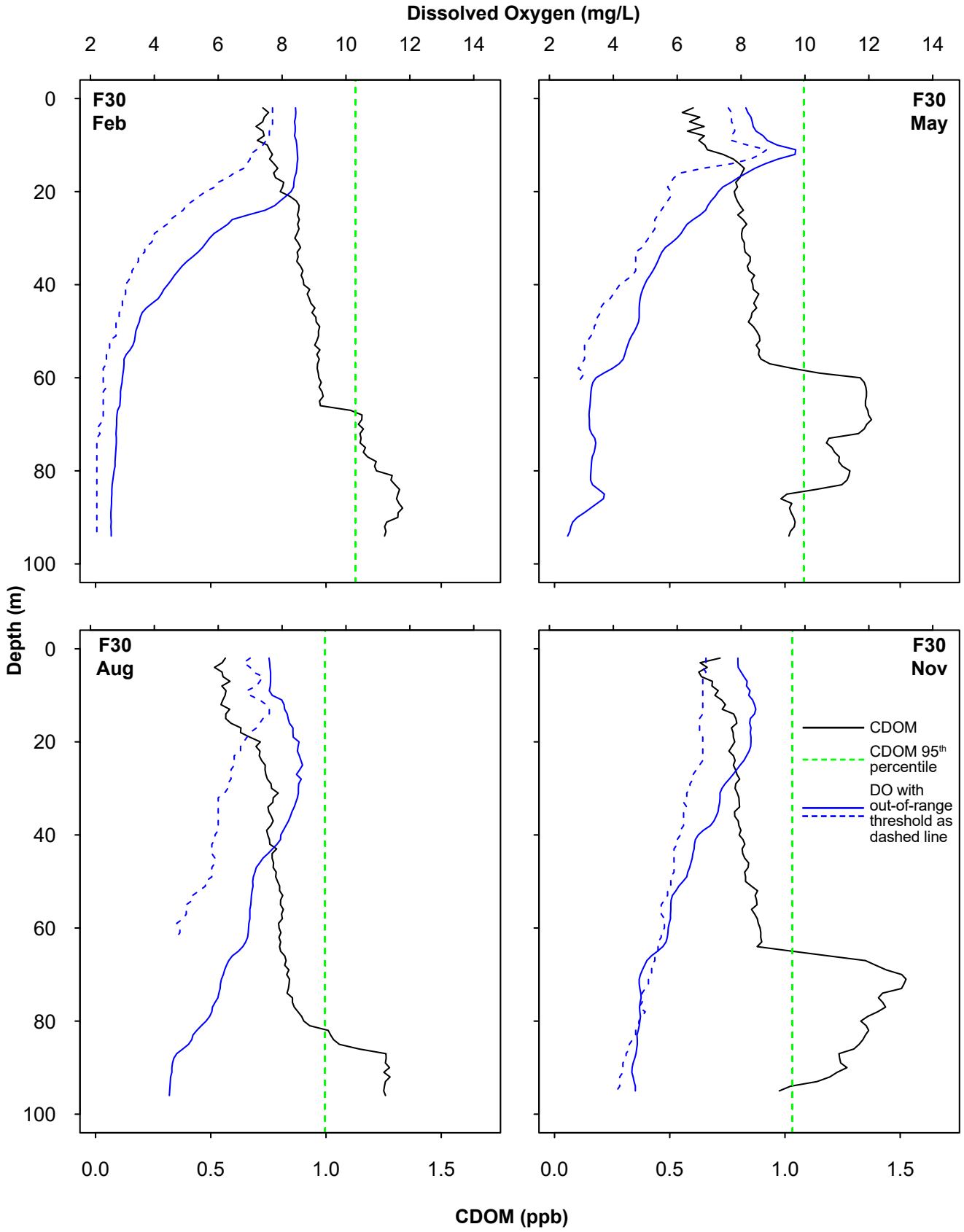
Appendix C.5

Representative vertical profiles of CDOM and buoyancy frequency from PLOO nearfield station F30 during 2025.



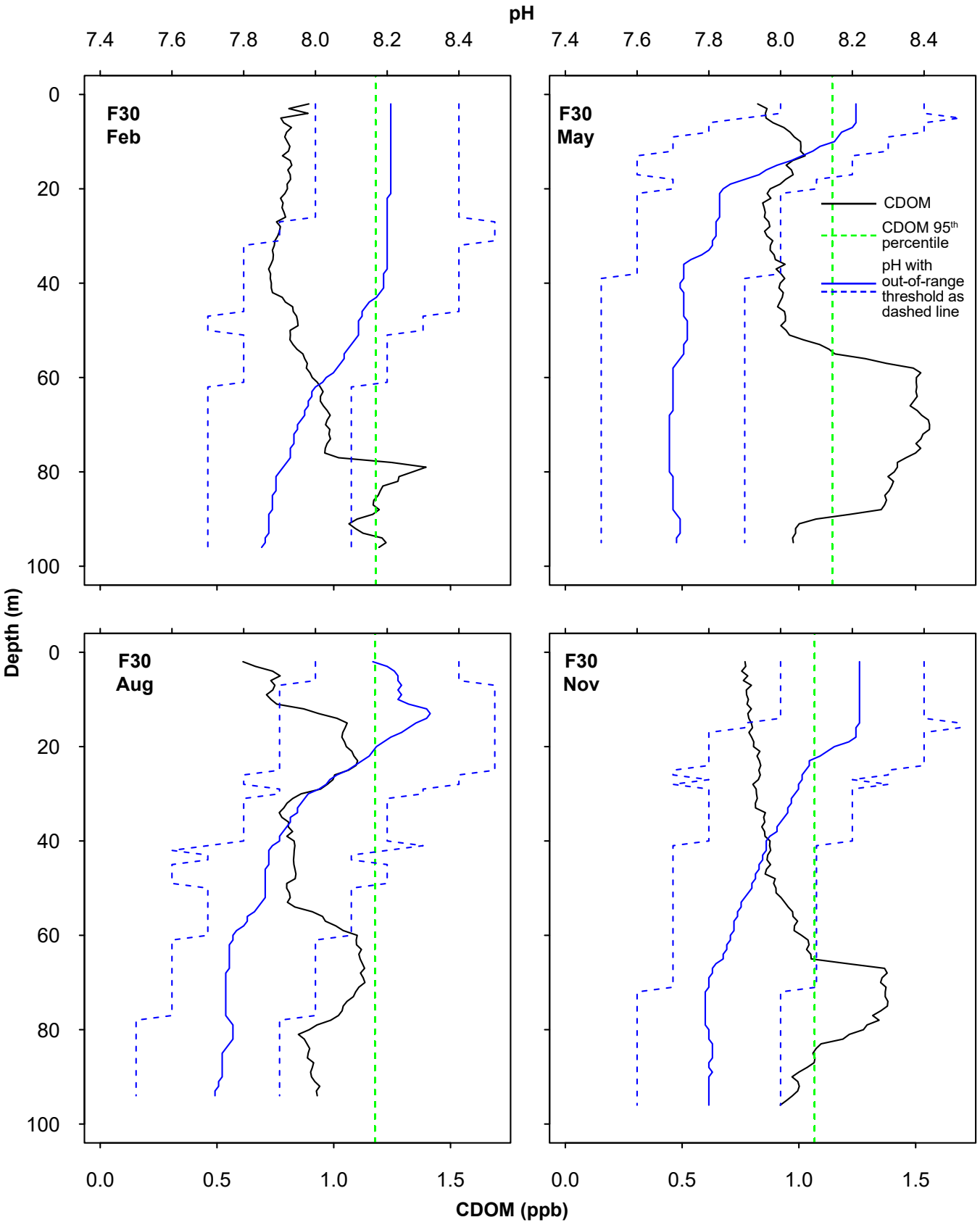
Appendix C.6

Representative vertical profiles of CDOM and DO from PLOO nearfield station F30 during 2024.



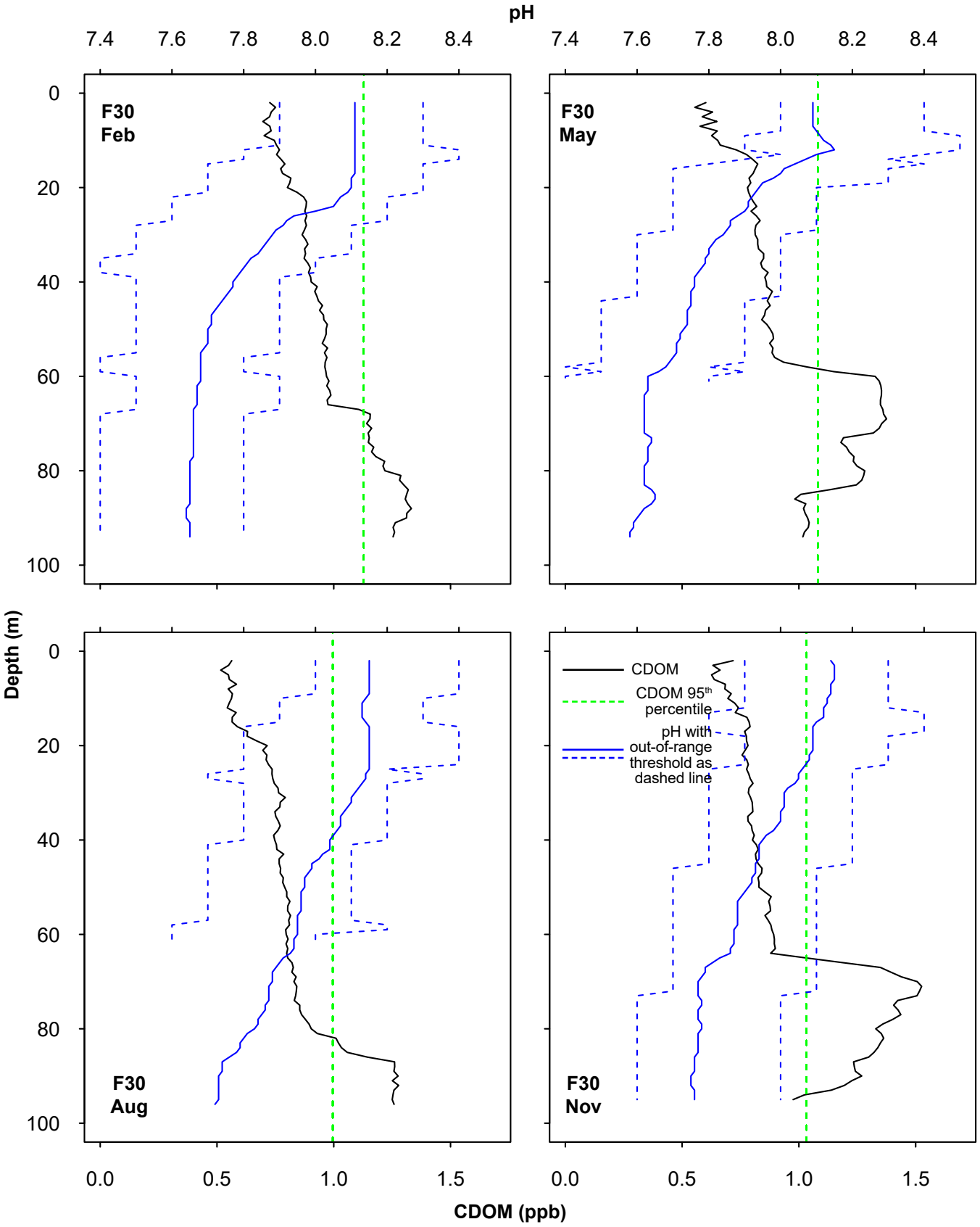
Appendix C.7

Representative vertical profiles of CDOM and DO from PLOO nearfield station F30 during 2025.



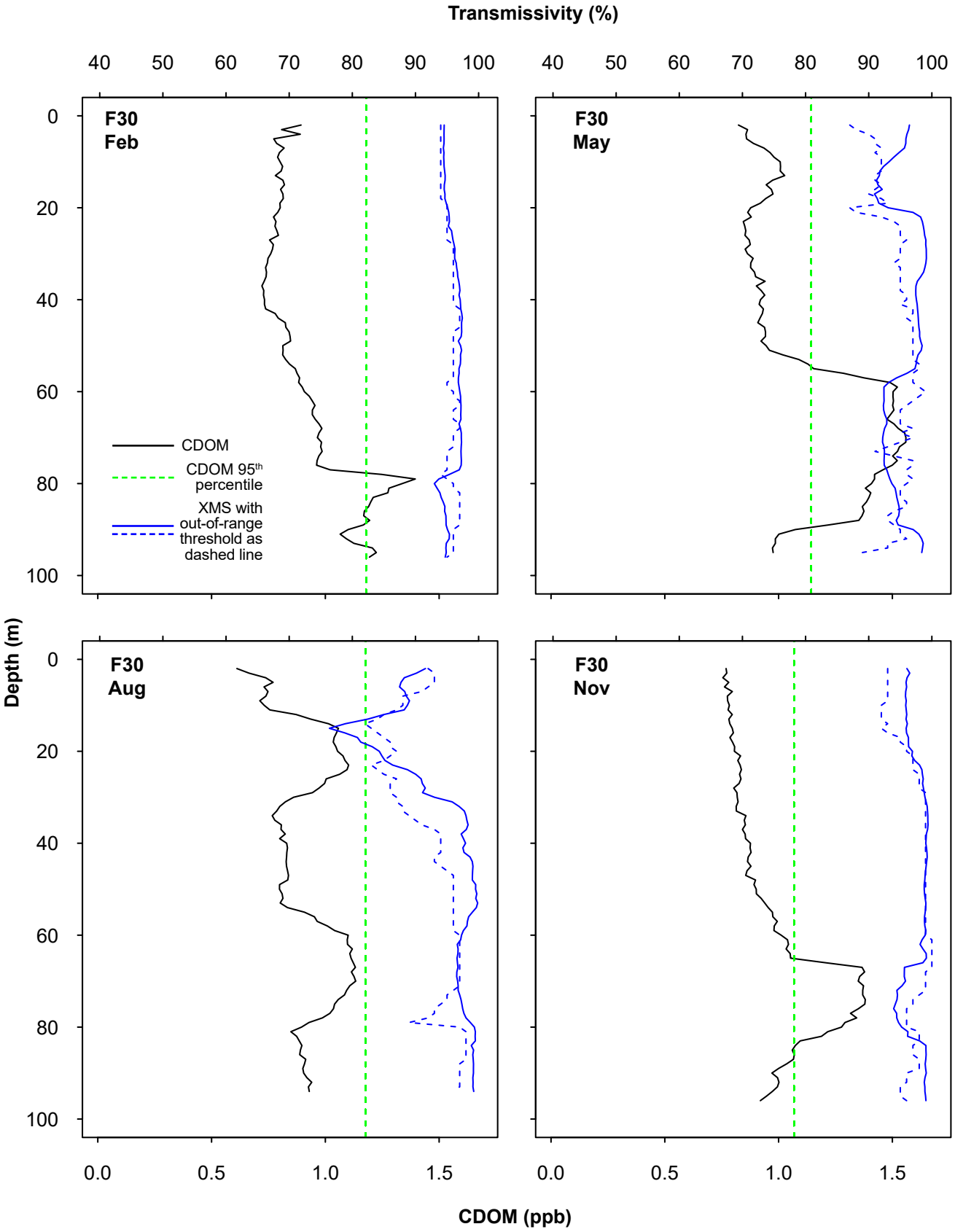
Appendix C.8

Representative vertical profiles of CDOM and pH from PLOO nearfield station F30 during 2024.



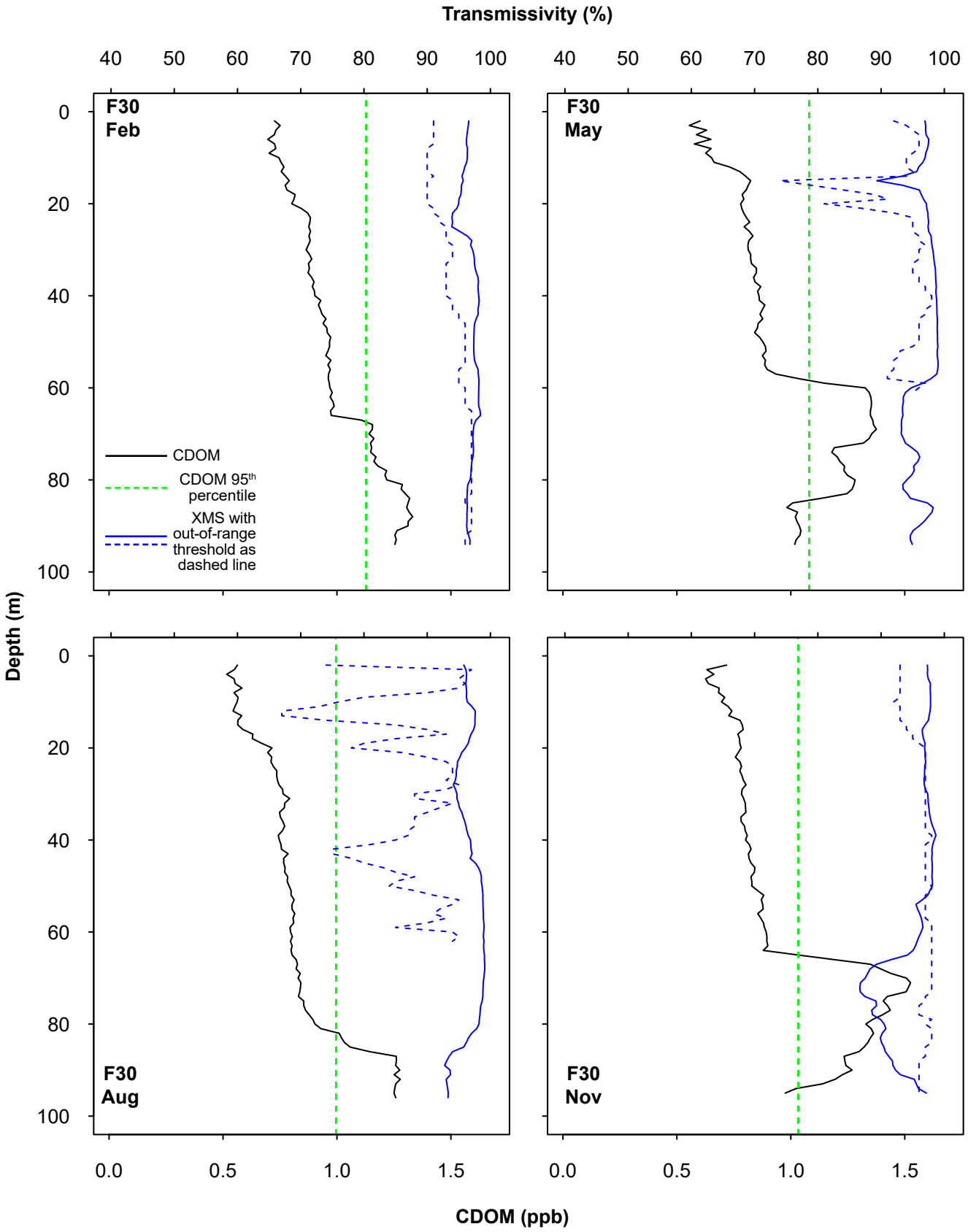
Appendix C.9

Representative vertical profiles of CDOM and pH from PLOO nearfield station F30 during 2025.



Appendix C.10

Representative vertical profiles of CDOM and transmissivity (XMS) from PLOO nearfield station F30 during 2024.



Appendix C.11

Representative vertical profiles of CDOM and transmissivity (XMS) from PLOO nearfield station F30 during 2025.

Appendix C.12

Summary of oceanographic data within potential detected plume at SBOO offshore stations and corresponding reference values during 2024 and 2025. Plume depth is the minimum depth at which CDOM exceeds the 95th percentile while plume width is the number of meters across which that exceedance occurs. Out-of-range values are in **bold**. DO = dissolved oxygen (mg/L); XMS = transmissivity (%); SD = standard deviation; CI = confidence interval.

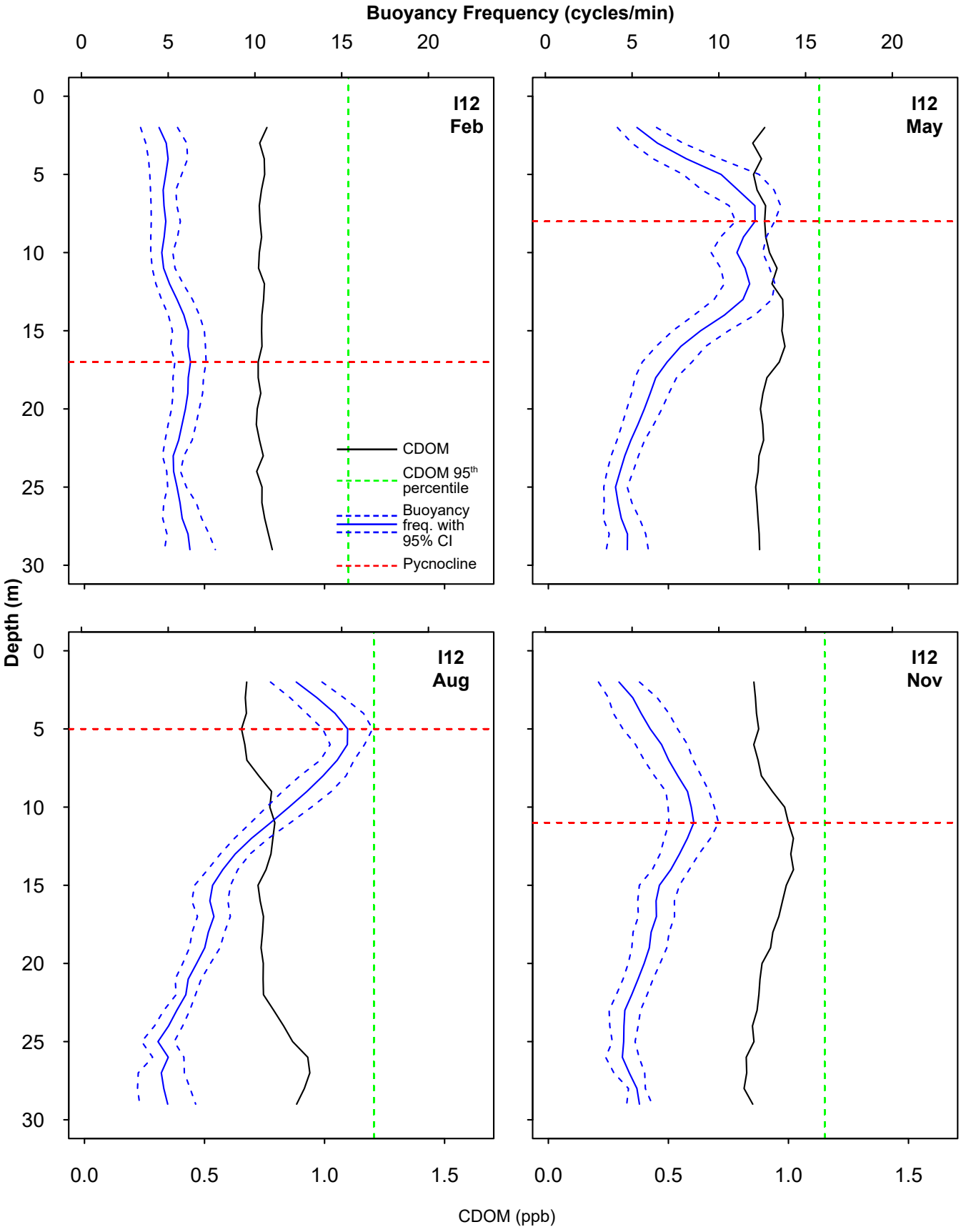
		Potential Plume					Reference		
Station	**Date**	**Width (m)**	**Depth (m)**	**Mean DO**	**Mean pH**	**Mean XMS**	**DO (Mean - SD)**	**pH (Mean)**	**XMS (Mean - 95% CI)**
I10	2/22/2024	11	2	8.4	8.2	**78.0**	7.9	8.2	95
I12[a]	5/8/2024	3	13	4.7	7.8	92.6	4.9	8.0	88
I16[a]	5/8/2024	1	14	5.0	7.8	93.0	4.9	8.0	88
I33[a]	5/10/2024	5	9	7.8	8.1	**79.0**	5.7	8.1	88
I35[a]	5/10/2024	2	10	6.4	8.0	**79.2**	5.4	8.0	88
I15	8/7/2024	5	15	7.1	7.9	**85.1**	7.5	8.0	87
I23[a]	8/7/2024	4	7	8.1	8.0	**74.9**	8.2	8.1	92
I12[a]	11/6/2024	2	12	6.5	8.0	95.0	6.5	8.1	94
I15	11/6/2024	4	13	6.3	8.0	93.7	6.2	8.0	94
I17[a]	11/6/2024	3	17	6.8	8.0	**94.1**	6.0	8.0	97
I16[a]	11/6/2024	4	13	6.5	8.0	94.3	6.2	8.0	94
I12[a]	2/5/2025	9	7	4.6	NaN	94.6	4.7	8.0	95
I16[a]	2/5/2025	2	16	4.3	NaN	96.7	4.0	7.9	96
I23[a]	2/5/2025	2	17	**3.6**	NaN	**84.6**	4.2	7.9	96
I18[a]	2/5/2025	3	8	5.5	NaN	**94.1**	5.0	8.0	95
I34[a]	2/6/2025	4	13	3.8	7.8	**84.1**	4.1	7.9	95
I35[a]	2/6/2025	4	12	5.1	7.9	**86.8**	4.1	7.9	95
I16[a]	5/14/2025	1	12	4.8	7.8	89.0	5.0	8.0	80
I12[a]	5/14/2025	5	9	4.8	**7.8**	90.6	5.6	8.0	78
I17[a]	5/14/2025	2	9	5.2	**7.8**	85.3	6.4	8.1	76
I22[a]	5/14/2025	1	9	5.0	**7.8**	**72.7**	6.7	8.1	78
I23[a]	5/14/2025	3	16	4.5	7.8	**86.9**	4.7	7.8	91
I27[a]	5/14/2025	2	9	4.4	**7.7**	82.2	6.4	8.1	76
I9	11/4/2025	3	15	7.7	8	**91**	7.6	8	94
I12[a]	11/5/2025	6	11	7.9	8	**90.5**	7.7	8	93
I14[a]	11/5/2025	1	17	8	8	**90.4**	7.4	8	94

[a] Station located within State jurisdictional waters

Appendix C.12 *continued*

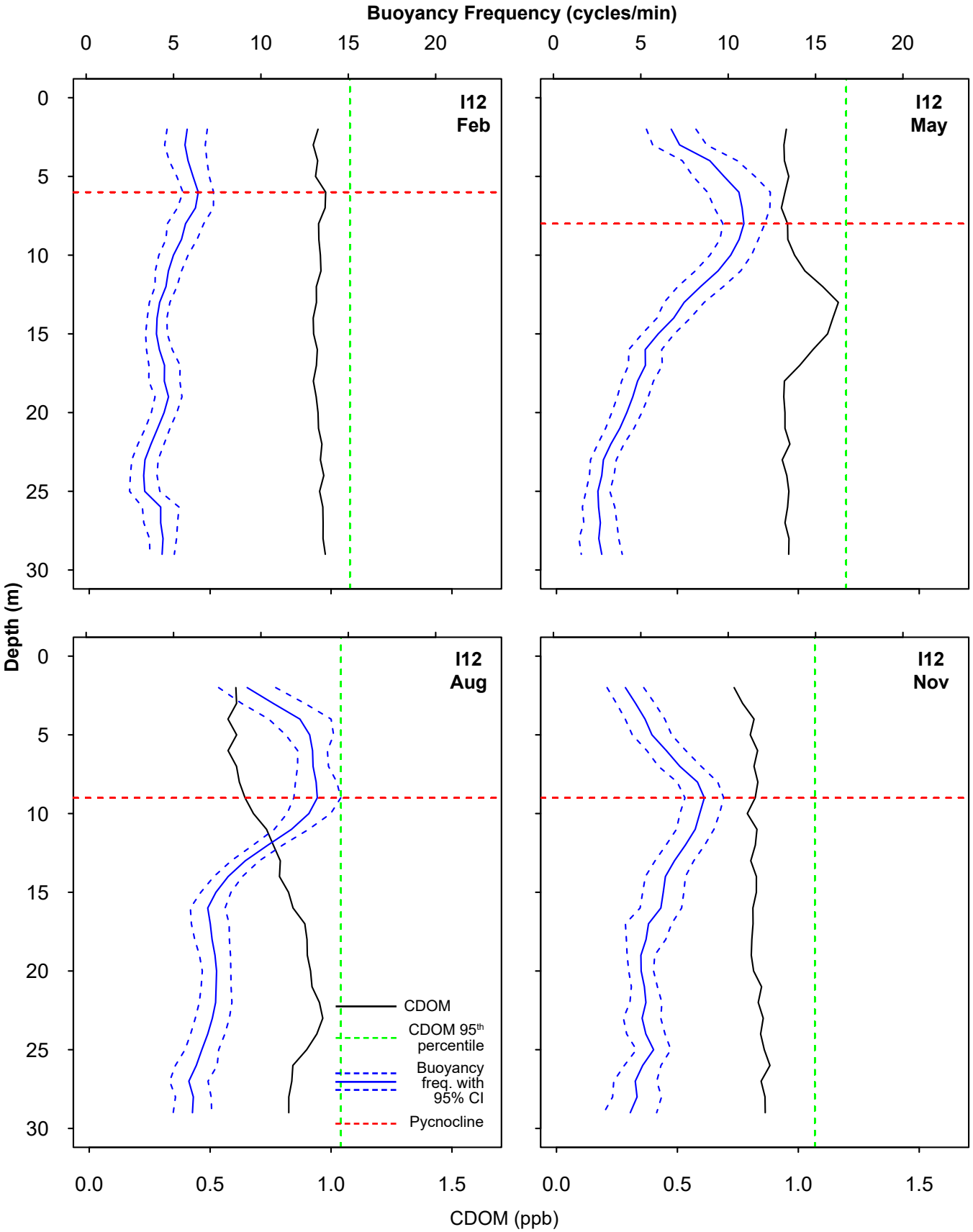
		Potential Plume					Reference		
Station	Date	Width (m)	Depth (m)	Mean DO	Mean pH	Mean XMS	DO (Mean - SD)	pH (Mean)	XMS (Mean - 95% CI)
I15	11/5/2025	4	13	7.9	8	**91**	7.7	8	94
I16[a]	11/5/2025	4	11	7.9	8	**89.9**	7.8	8	92
I17[a]	11/5/2025	1	16	7.9	8	**90.6**	7.6	8	94
I22[a]	11/5/2025	3	10	7.8	8	**91.1**	7.9	8.1	92

[a]**Station located within State jurisdictional waters**



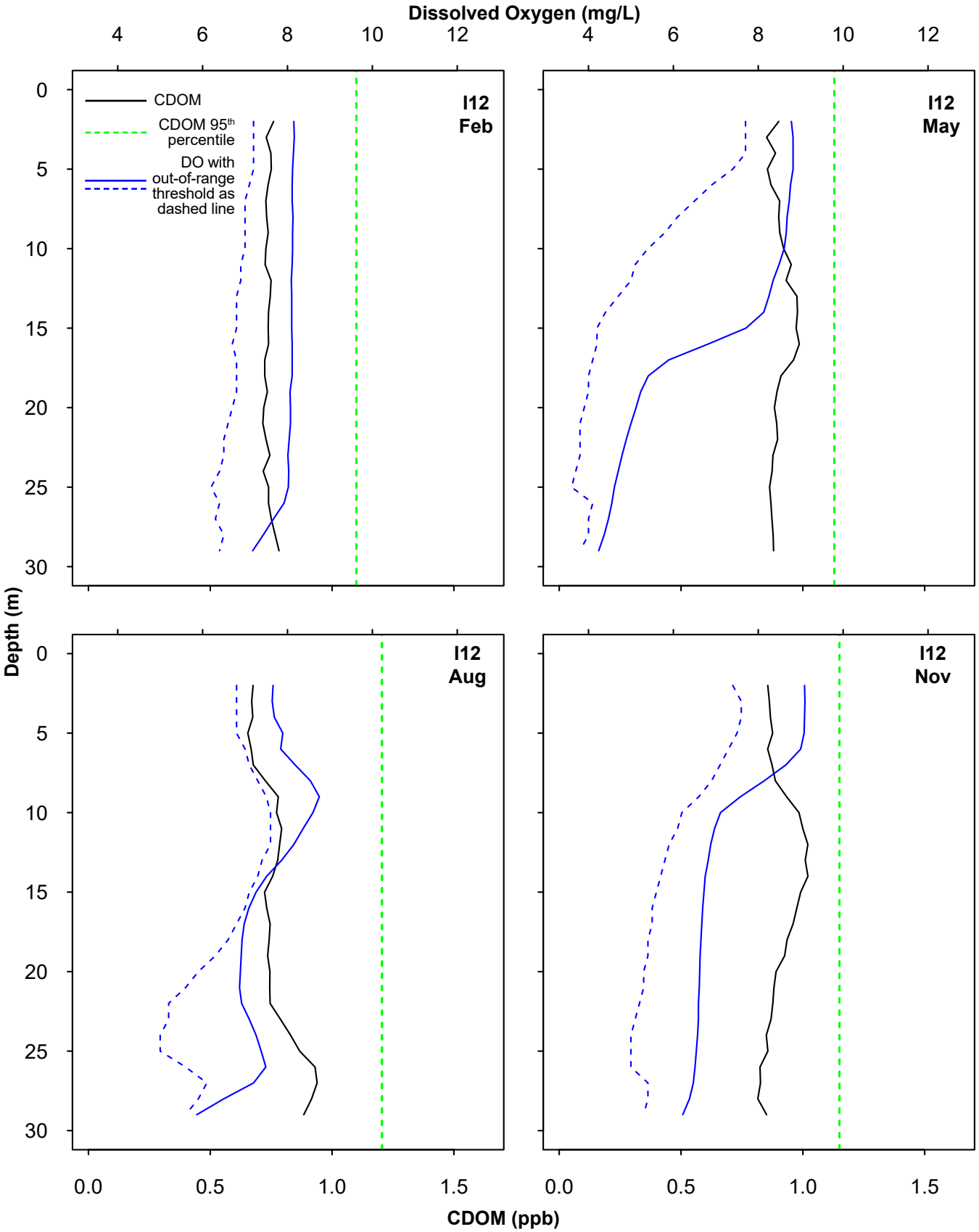
Appendix C.13

Representative vertical profiles of CDOM and buoyancy frequency from SBOO nearfield station I12 during 2024.



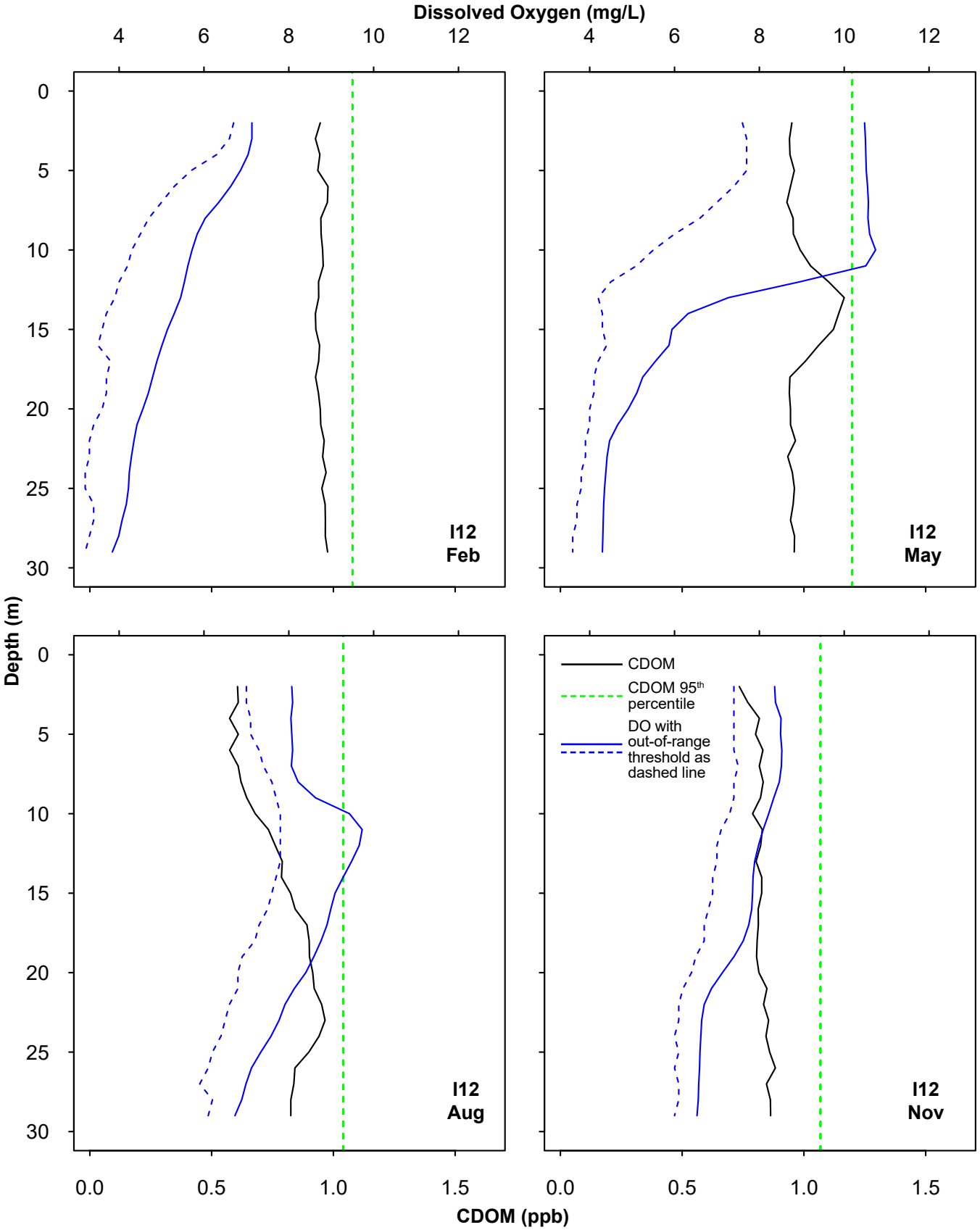
Appendix C.14

Representative vertical profiles of CDOM and buoyancy frequency from SBOO nearfield station I12 during 2025.



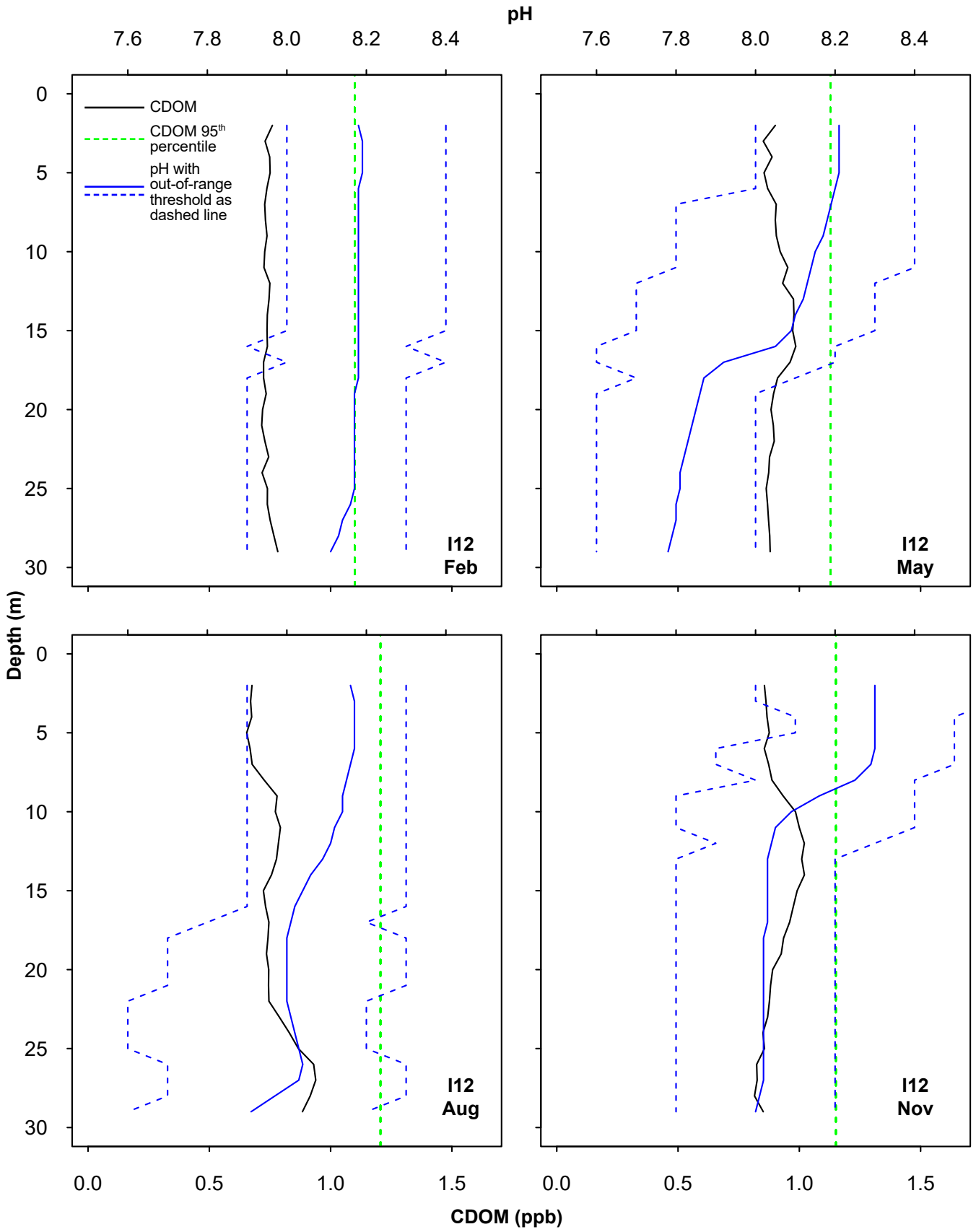
Appendix C.15

Representative vertical profiles of CDOM and DO from SBOO nearfield station I12 during 2024



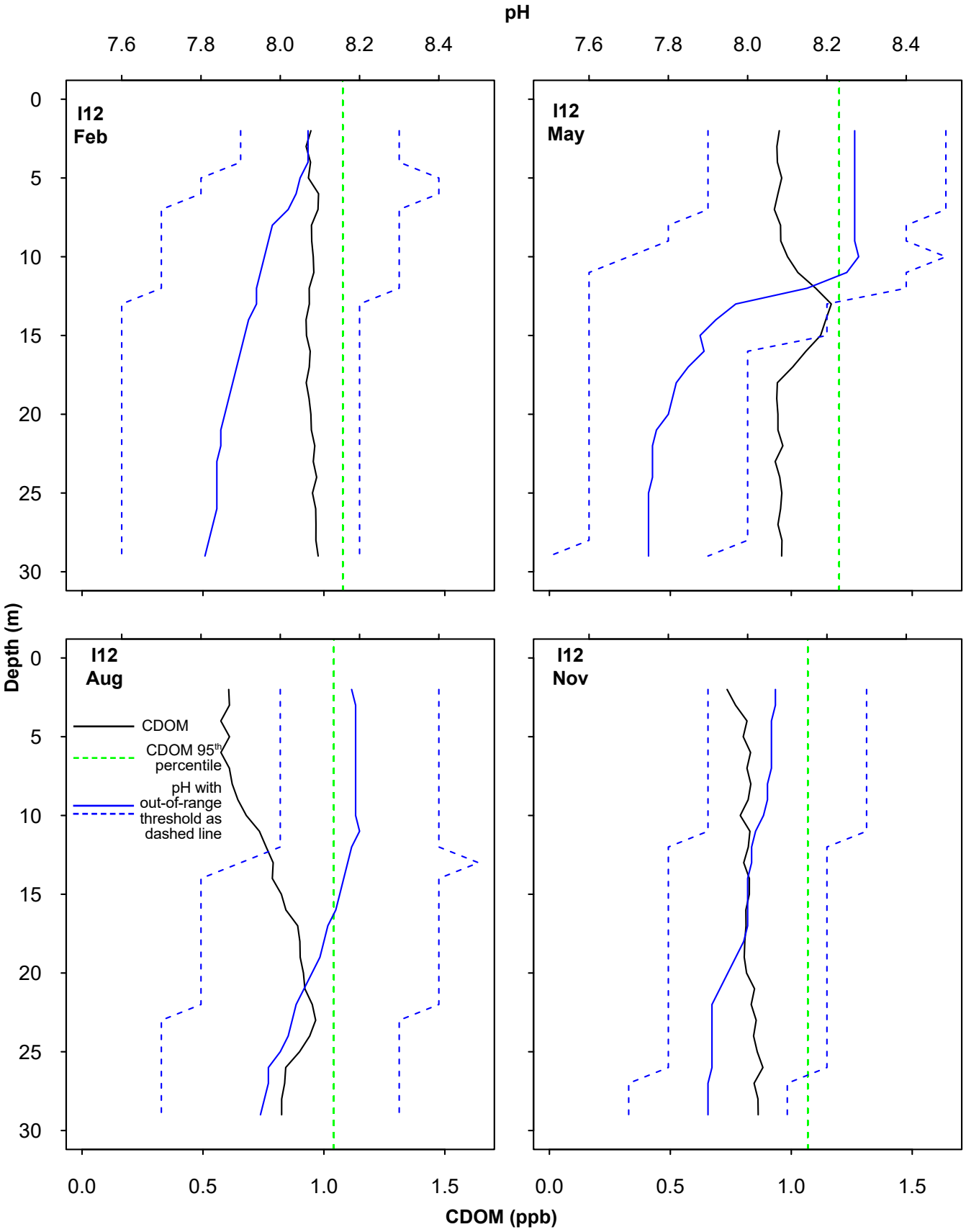
Appendix C.16

Representative vertical profiles of CDOM and DO from SBOO nearfield station I12 during 2025.



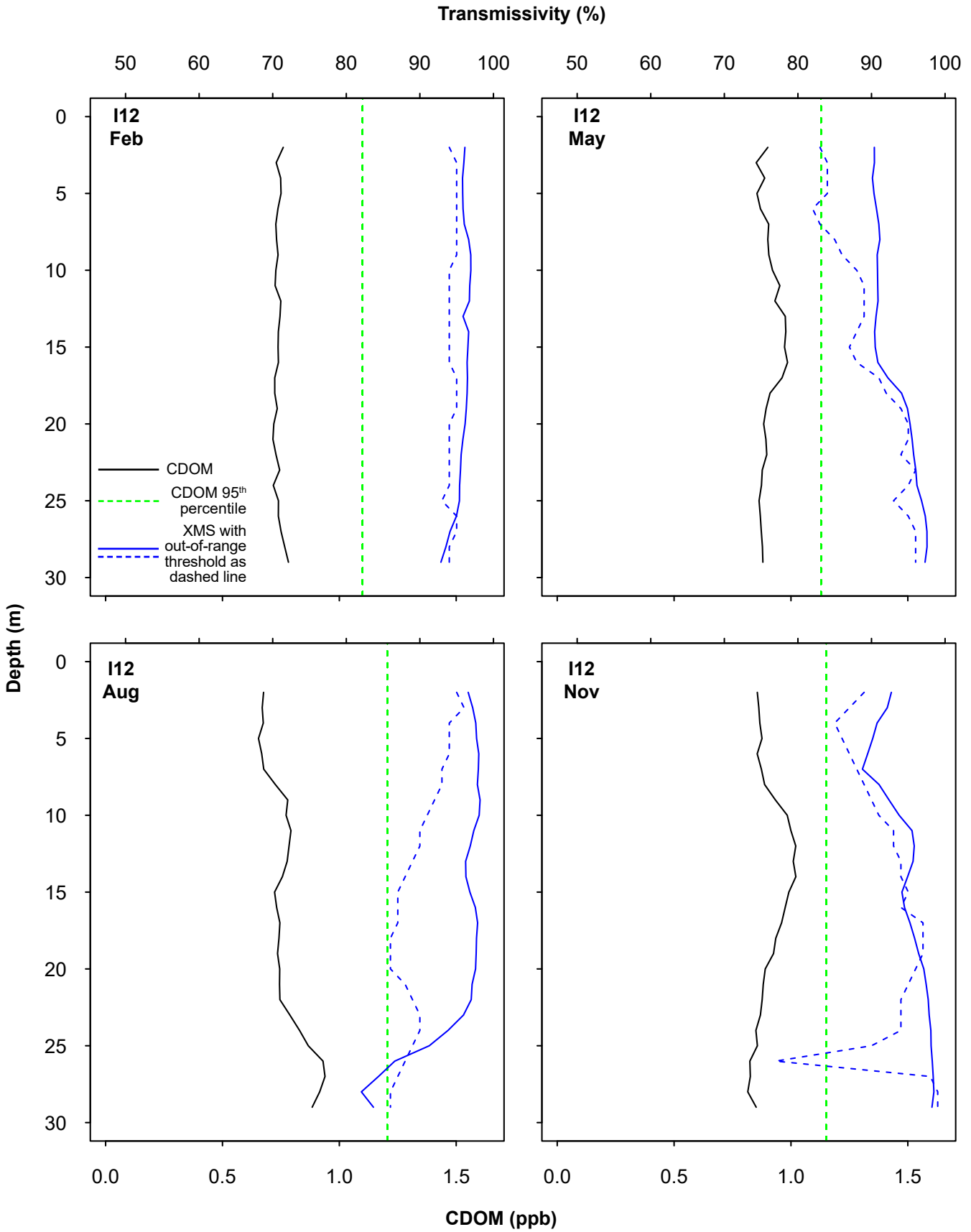
Appendix C.17

Representative vertical profiles of CDOM and pH from SBOO nearfield station I12 during 2024.



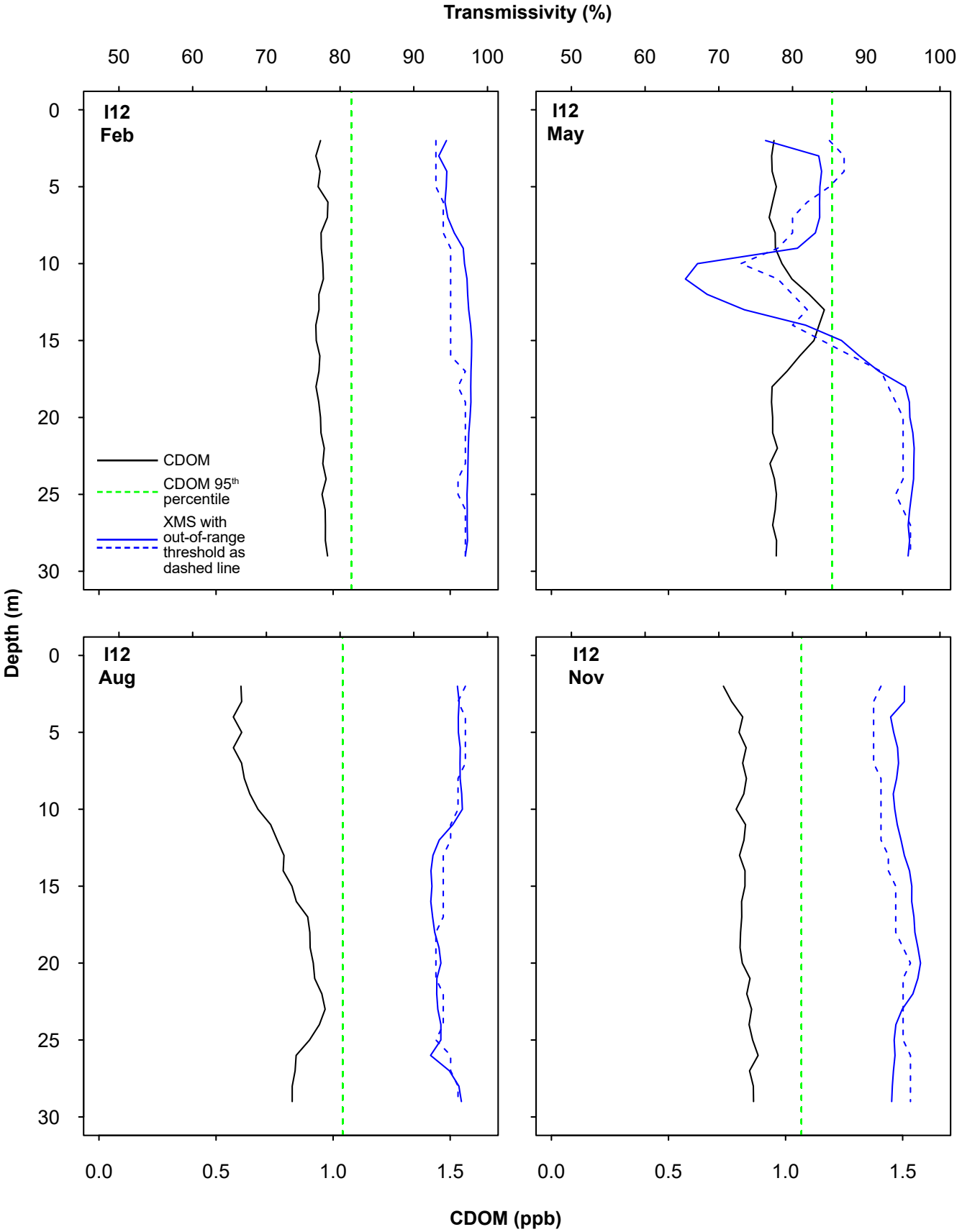
Appendix C.18

Representative vertical profiles of CDOM and pH from SBOO nearfield station I12 during 2025.



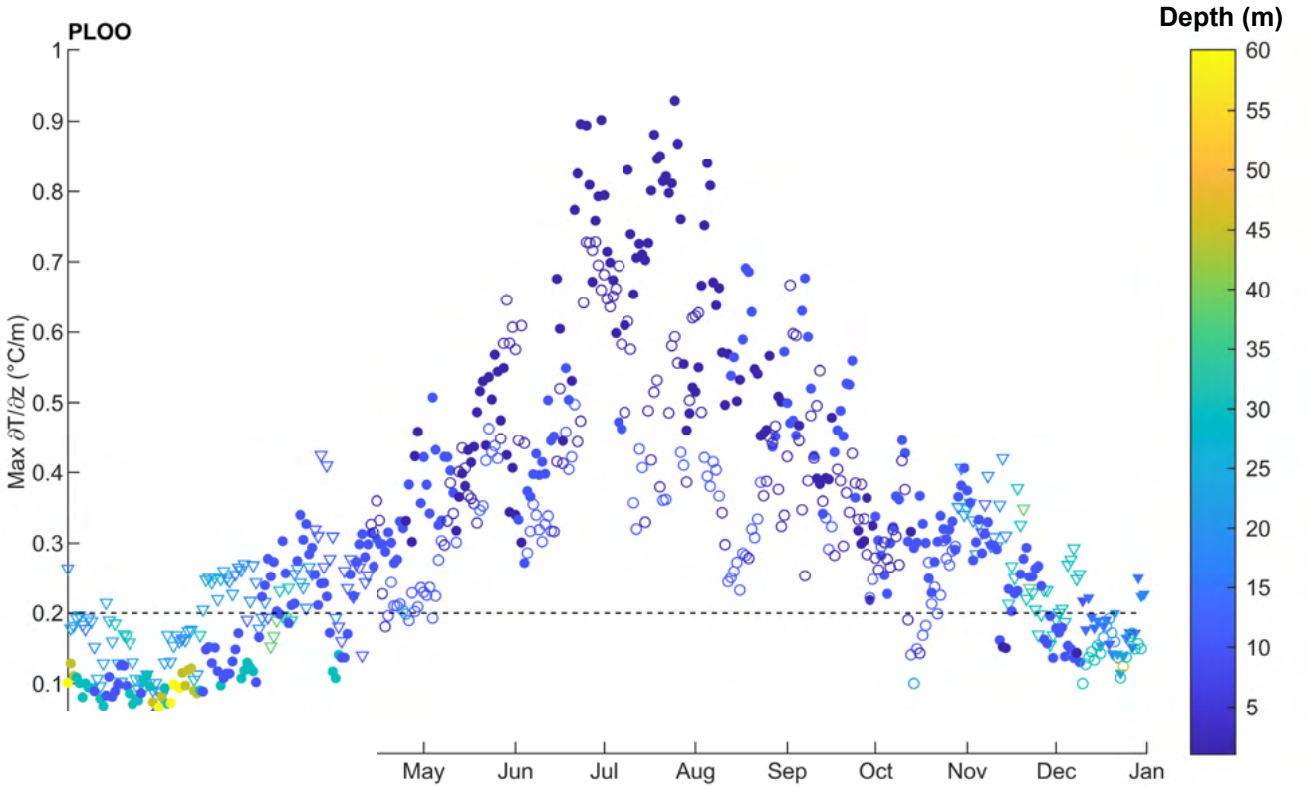
Appendix C.19

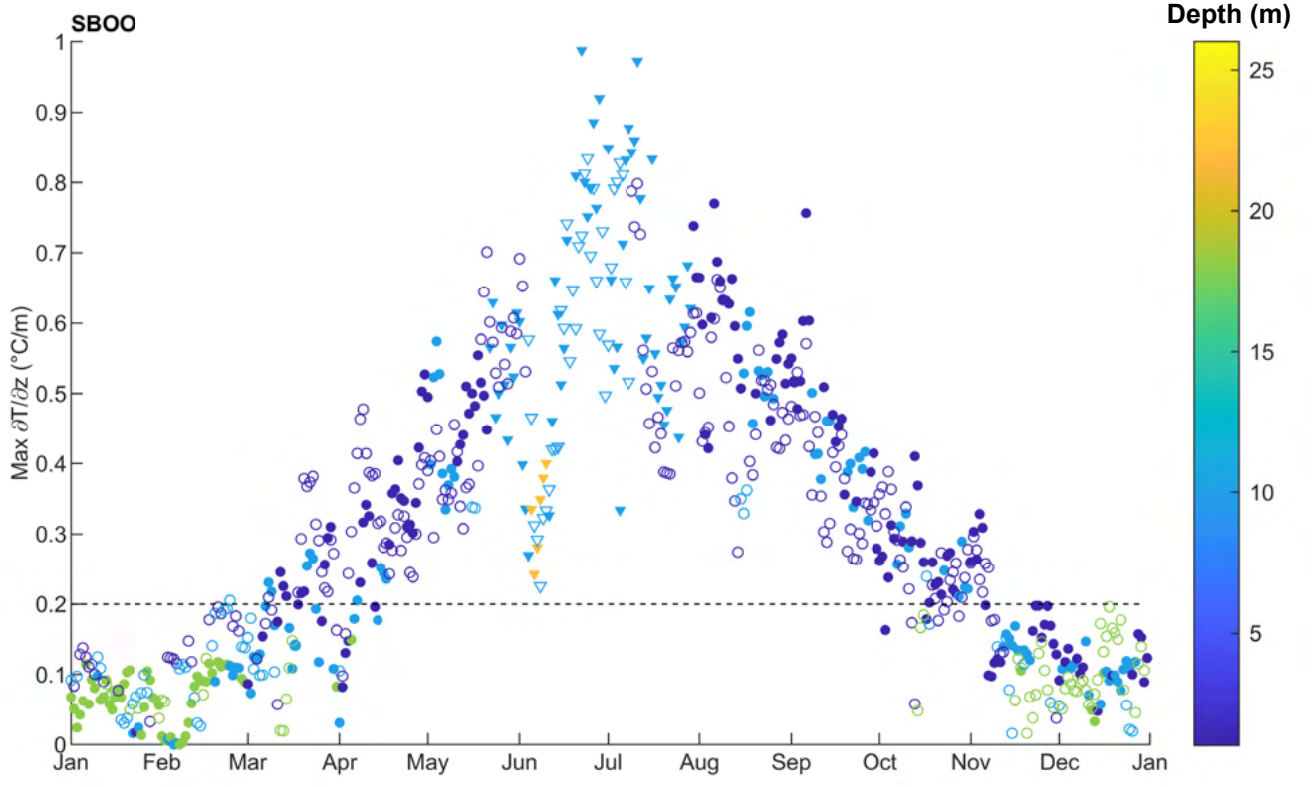
Representative vertical profiles of CDOM and transmissivity (XMS) from SBOO nearfield station I12 during 2024.



Appendix C.20

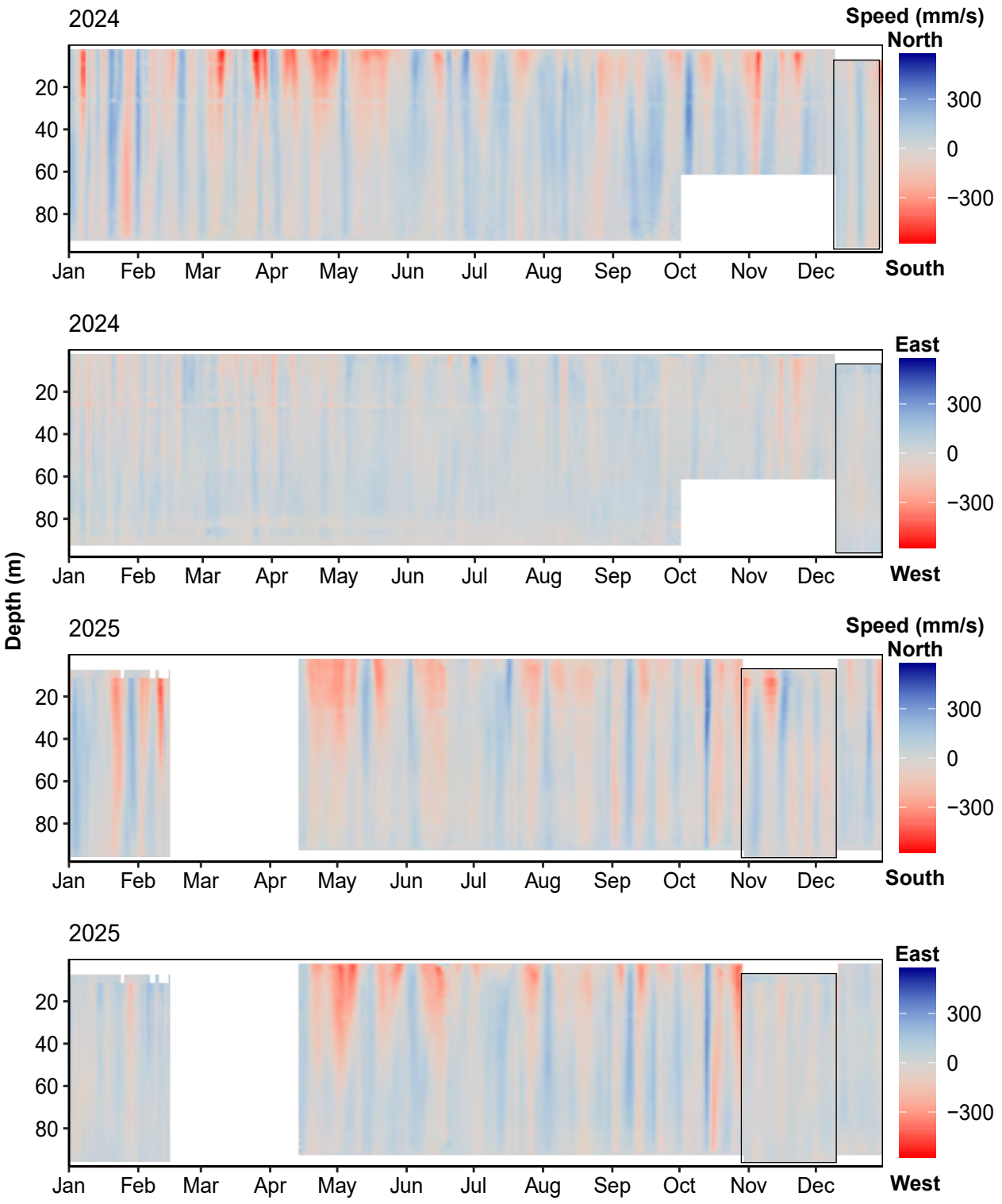
Representative vertical profiles of CDOM and transmissivity (XMS) from SBOO nearfield station I12 during 2025.





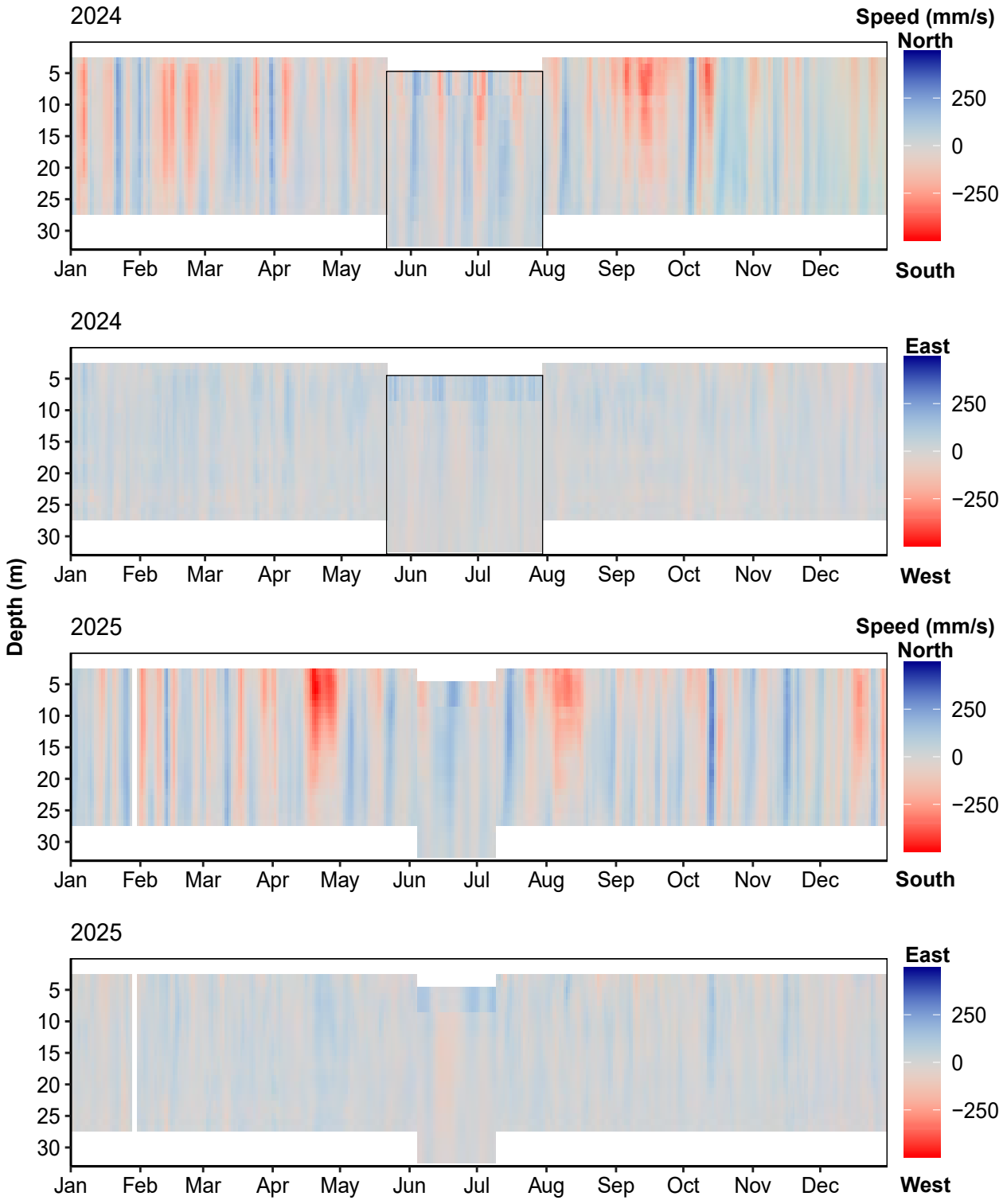
Appendix C.21

Maximum daily averaged thermal gradients (δT/δz) by depth of occurrence collected by RTOMS near PLOO (95 m) and SBOO (31 m) in 2024 (filled circles) and 2025 (open circles), and collected by thermistor arrays during RTOMS deployment gaps in 2024 (filled triangles) and 2025 (open triangles). Dashed line indicates moderate relative stratification (0.2°C/m), with values below line showing more weakly stratified conditions. Thermistor arrays used instead of RTOMS near SBOO due to data availability (see text).



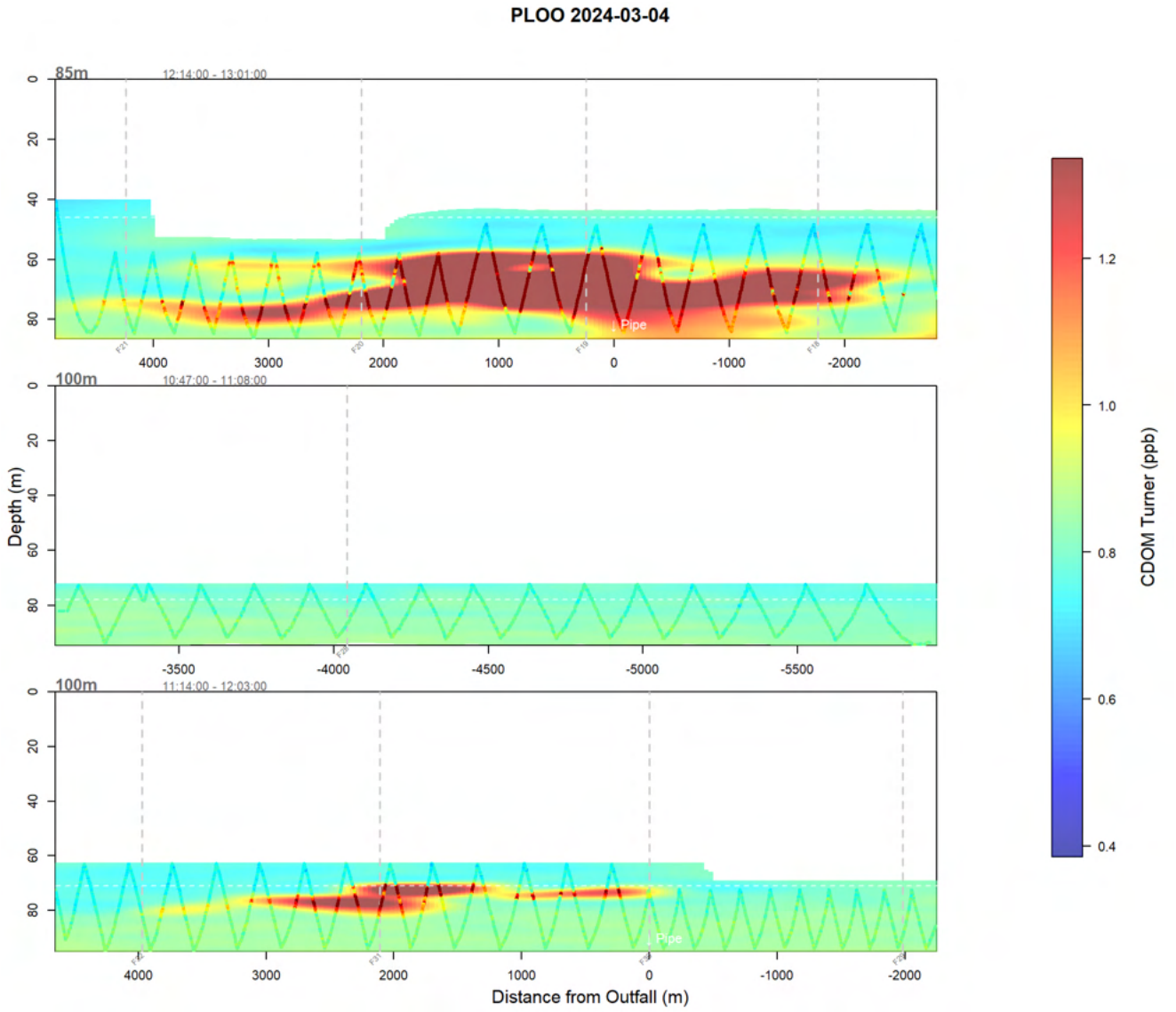
Appendix C.22

North-south and east-west daily averaged current speeds (tides removed) from the PLOO RTOMS in 2024 and 2025. Static ADCP data used to supplement RTOMS data are indicated by a black box. White areas indicate loss of data due to instrumentation issues or failure to meet data quality criteria (see text).



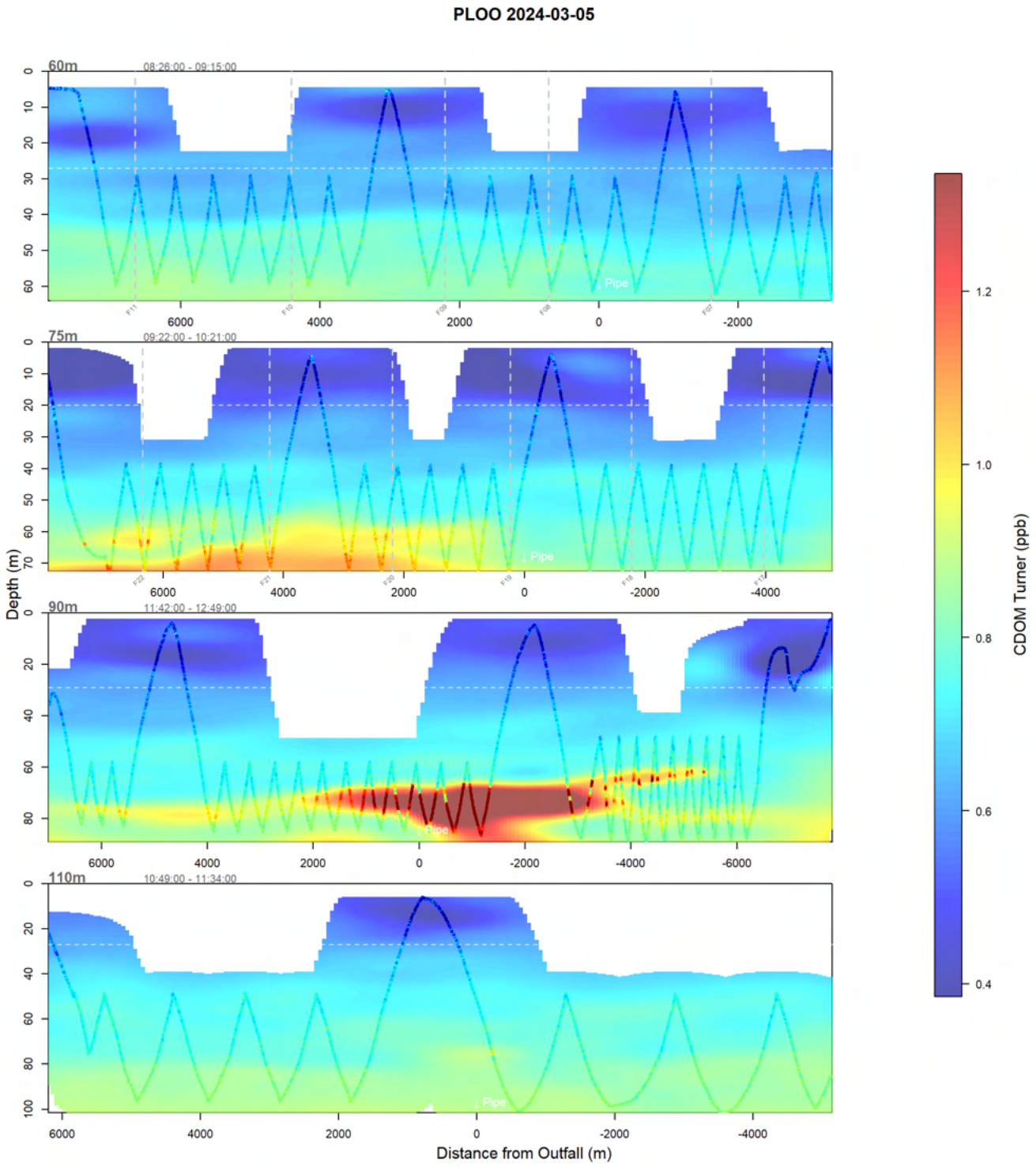
Appendix C.23

North-south and east-west daily averaged current speeds (tides removed) from the SBOO RTOMS in 2024 and 2025. Static ADCP data used to supplement RTOMS data are indicated by a black box. White areas indicate loss of data due to instrumentation issues or failure to meet data quality criteria (see text).

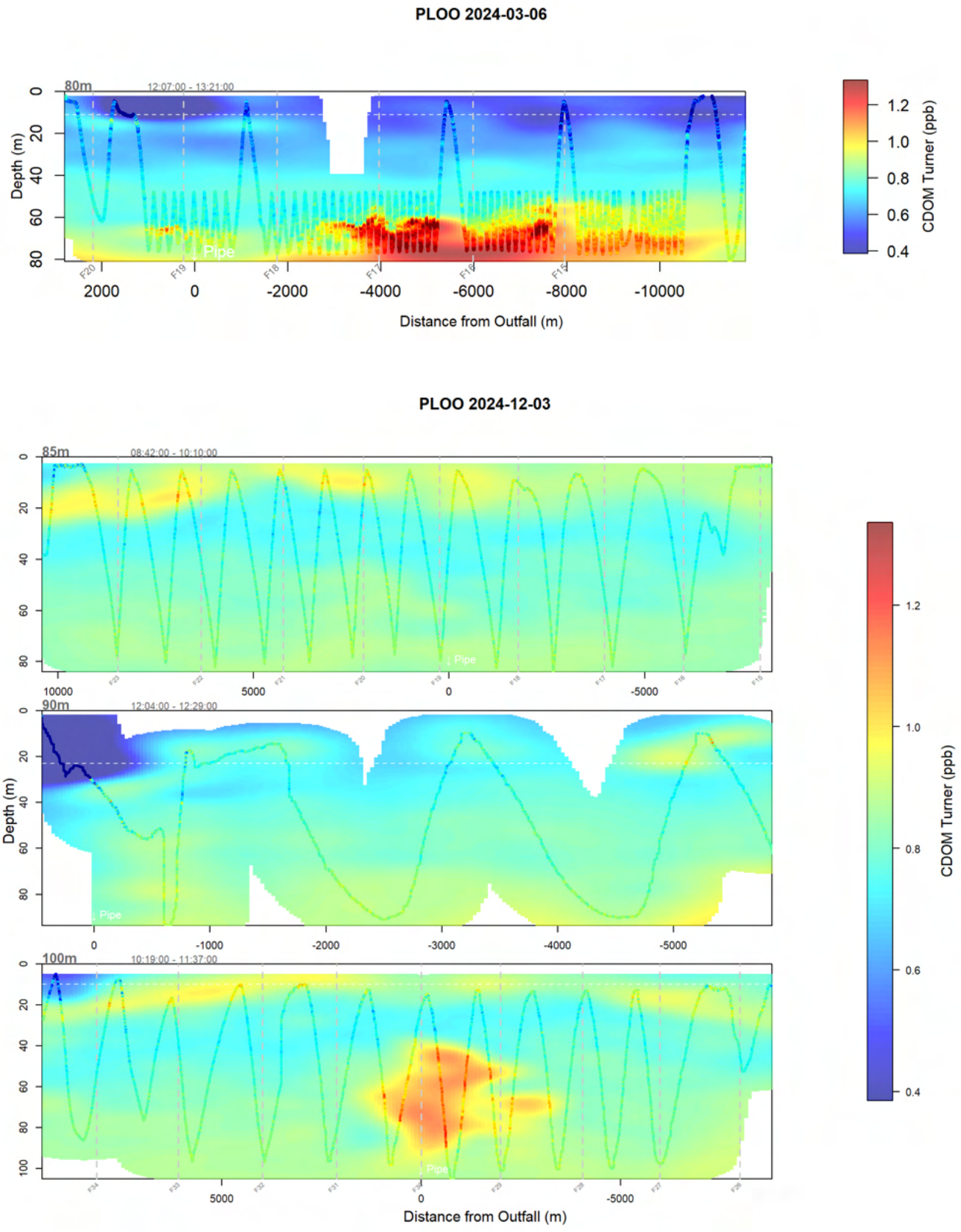


Appendix C.24

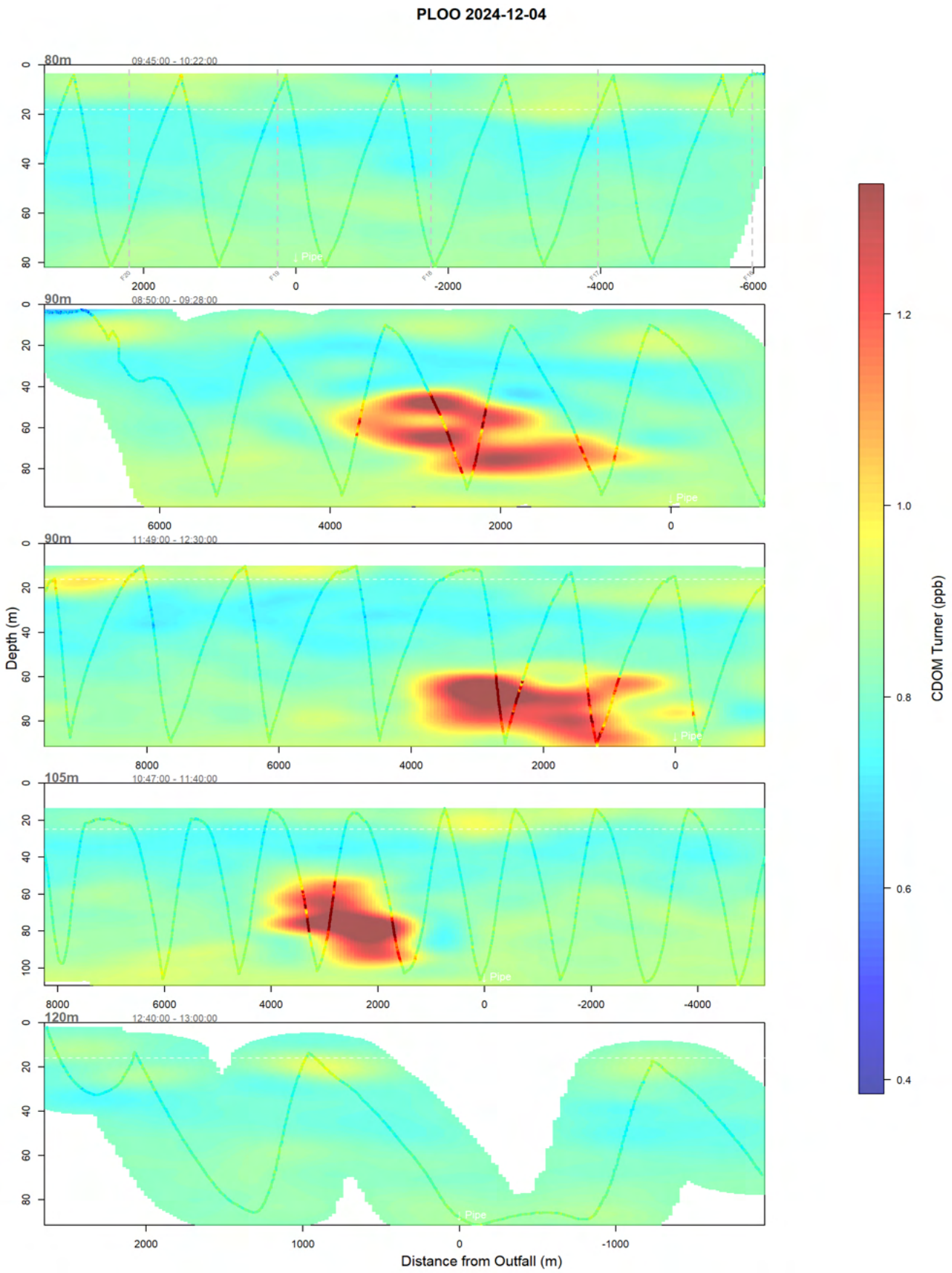
Interpolated CDOM data from ROTV surveys for each transect along an isobath conducted in the PLOO region during the report period (see text for methods). Opaque color lines indicate the position of the ROTV in the water column and associated raw data values. The position of the outfall is designated by text (“Pipe”) and arrow in white. Scales for each parameter are bound by the 2nd and 98th percentile of observed data for the region, using report-period ROTV data from the PLOO region. Vertical grey dashed lines indicate the position of nearby CTD sampling stations. A horizontal white line indicates the position of the thermocline for each transect.



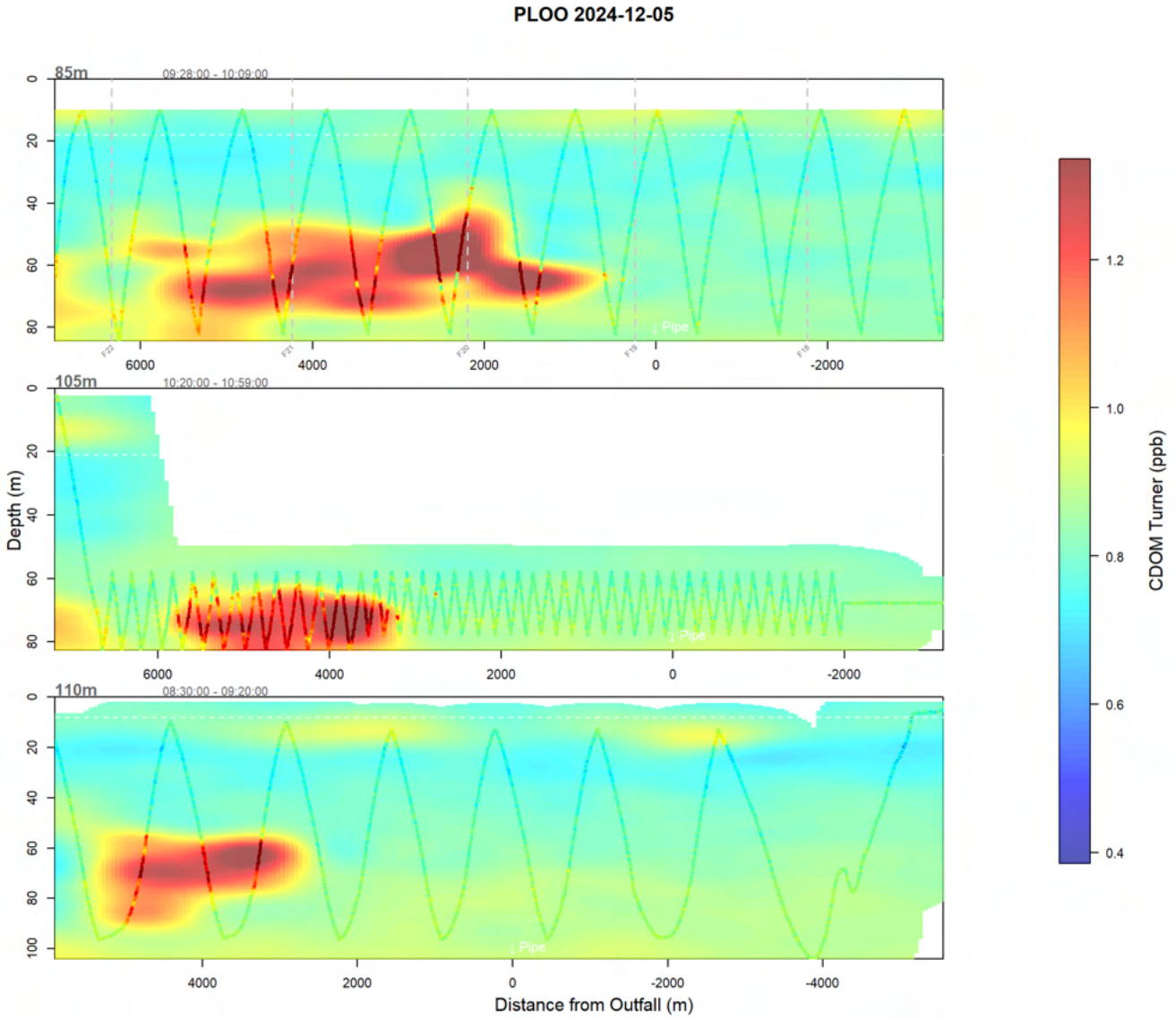
Appendix C.24 *continued*



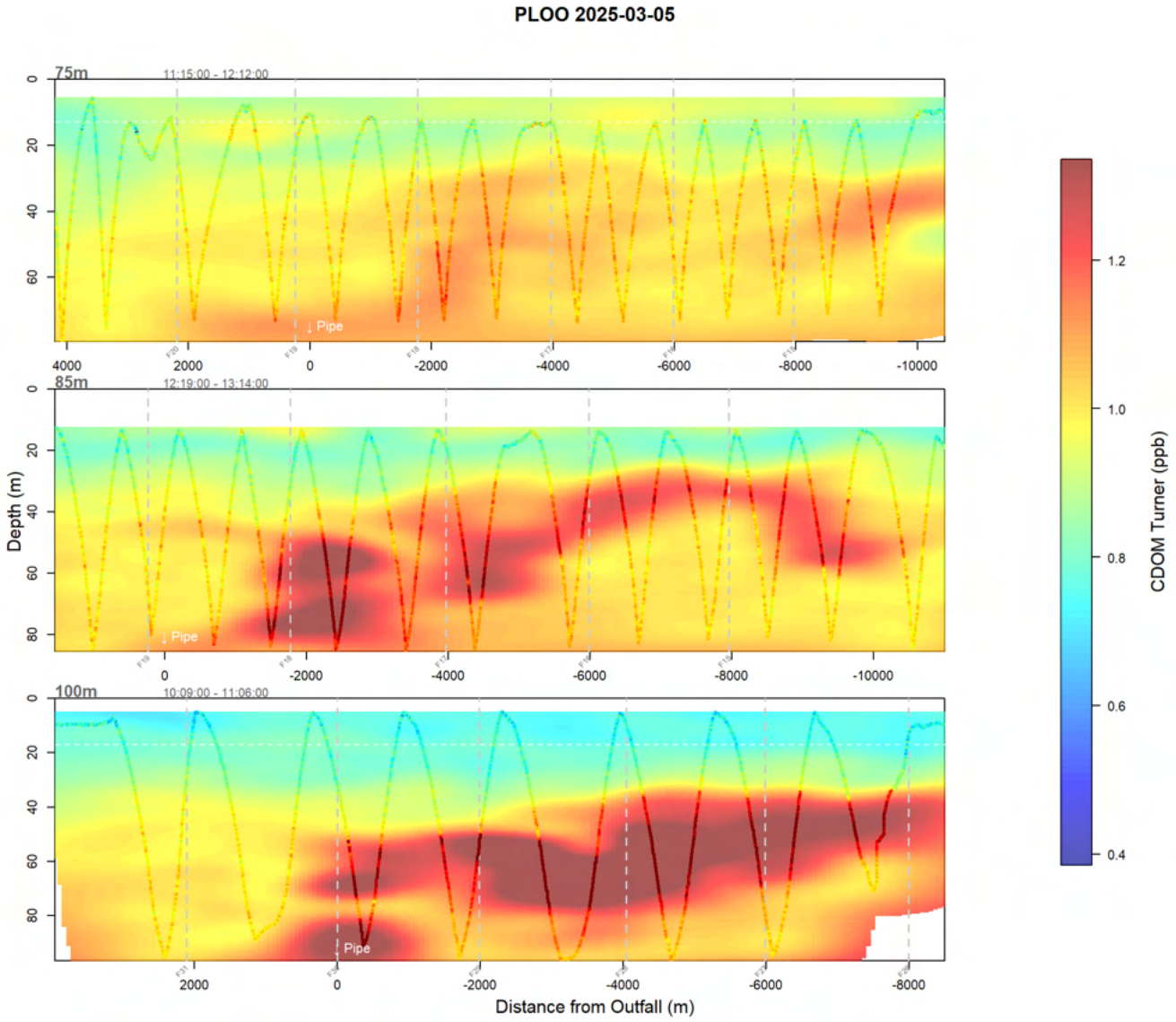
Appendix C.24 *continued*



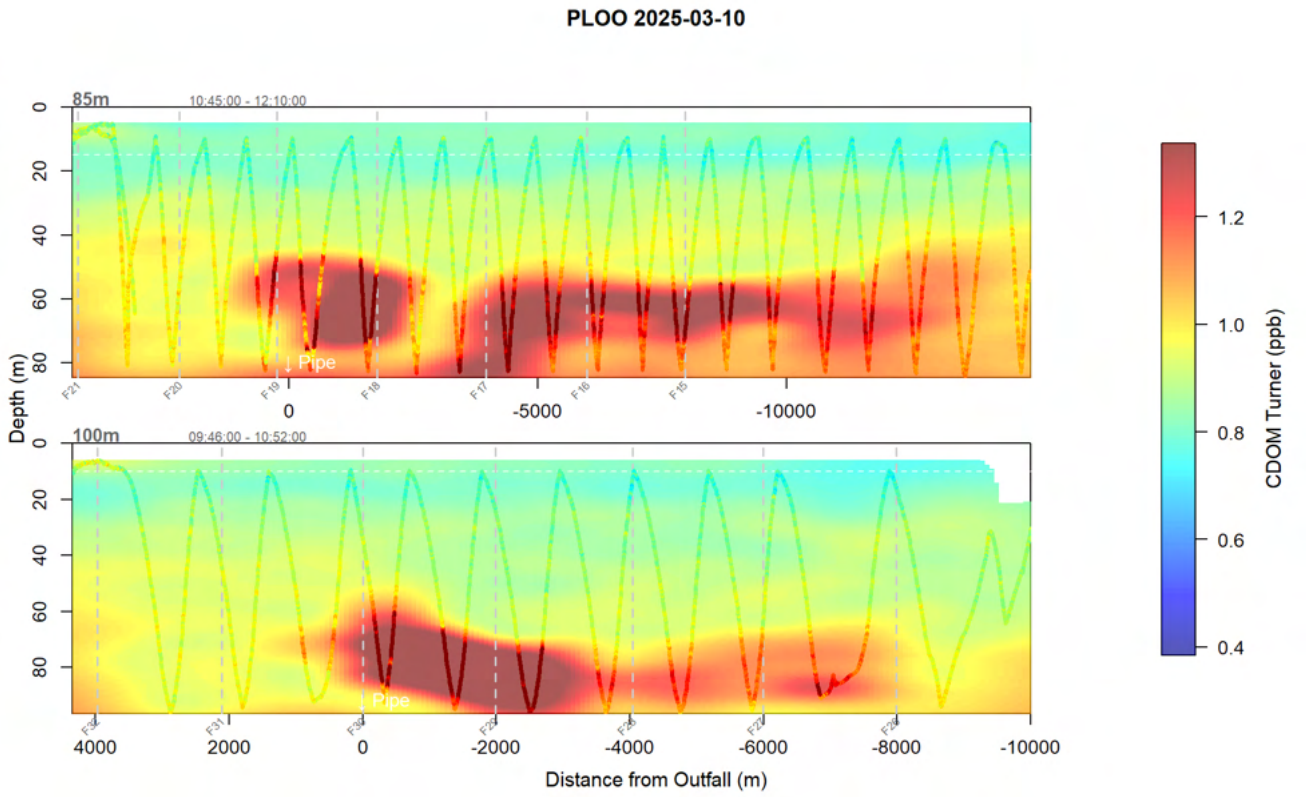
Appendix C.24 *continued*

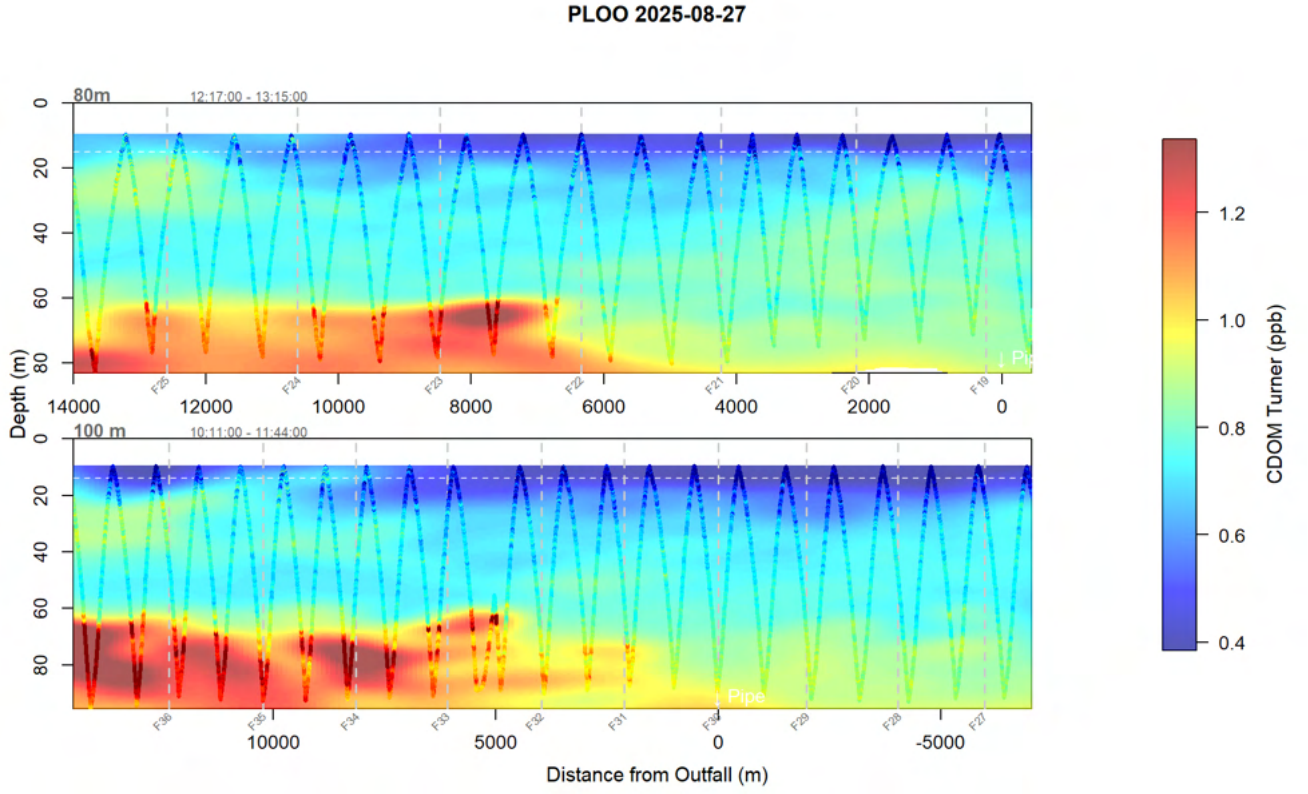


Appendix C.24 *continued*

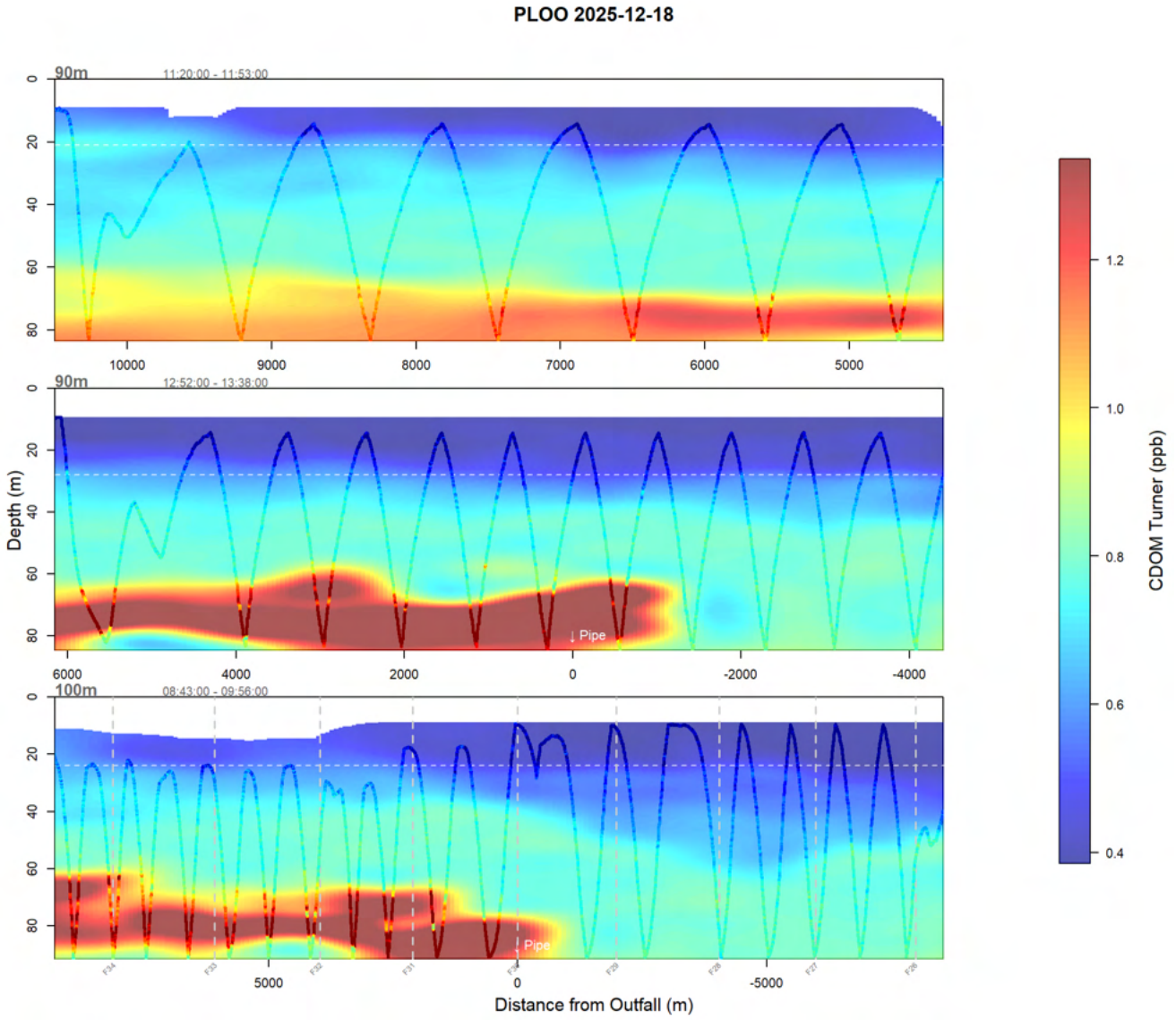


Appendix C.24 *continued*

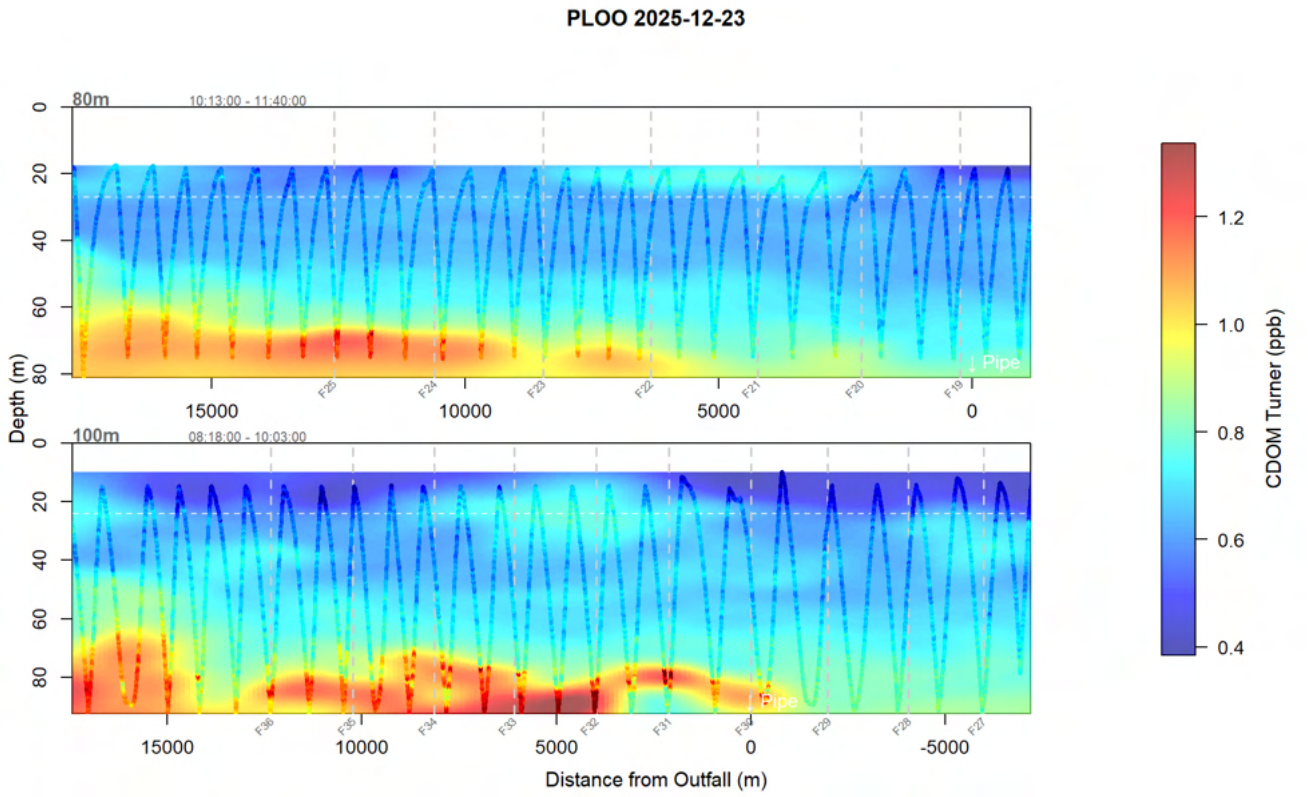




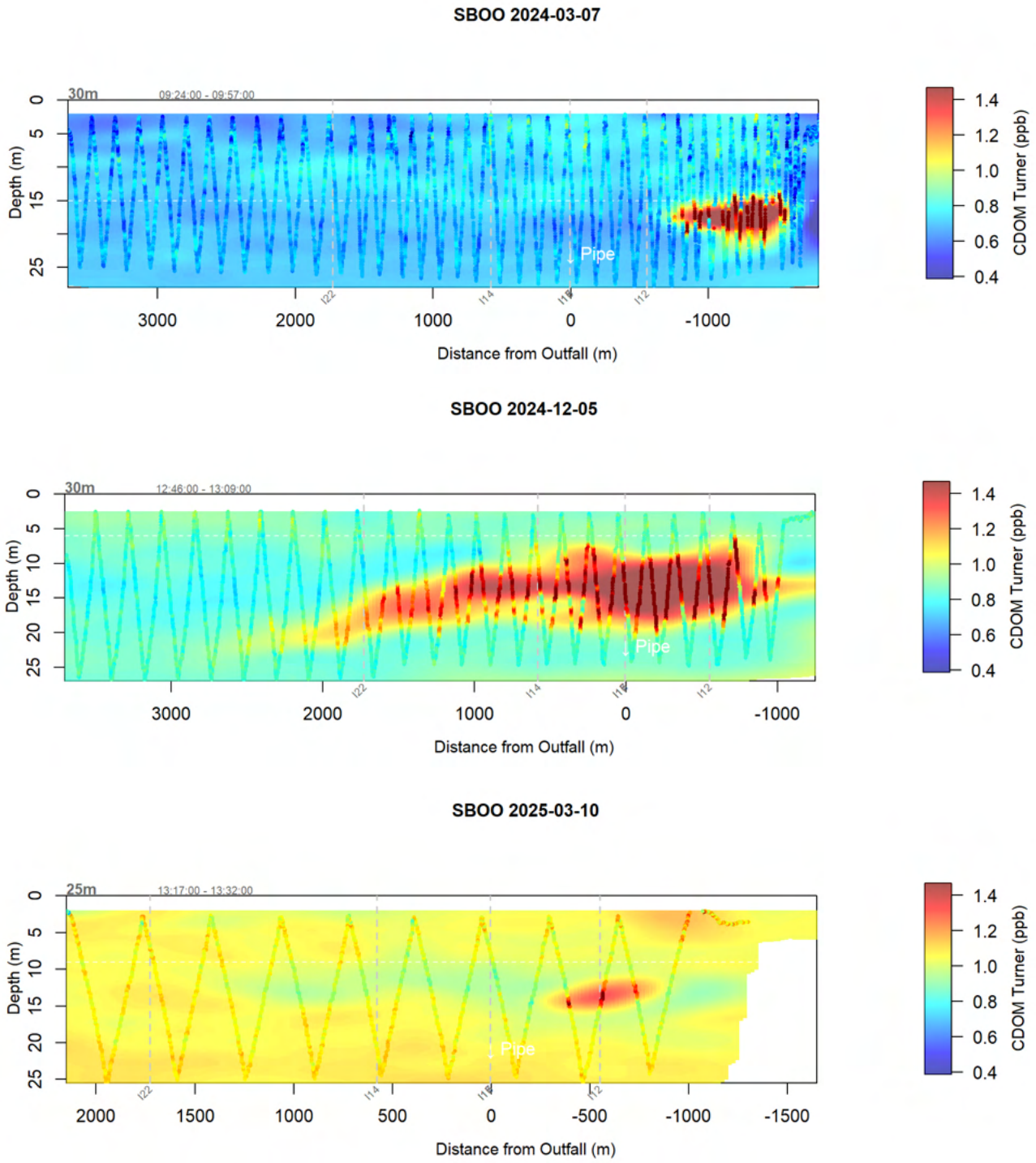
Appendix C.24 *continued*



Appendix C.24 *continued*

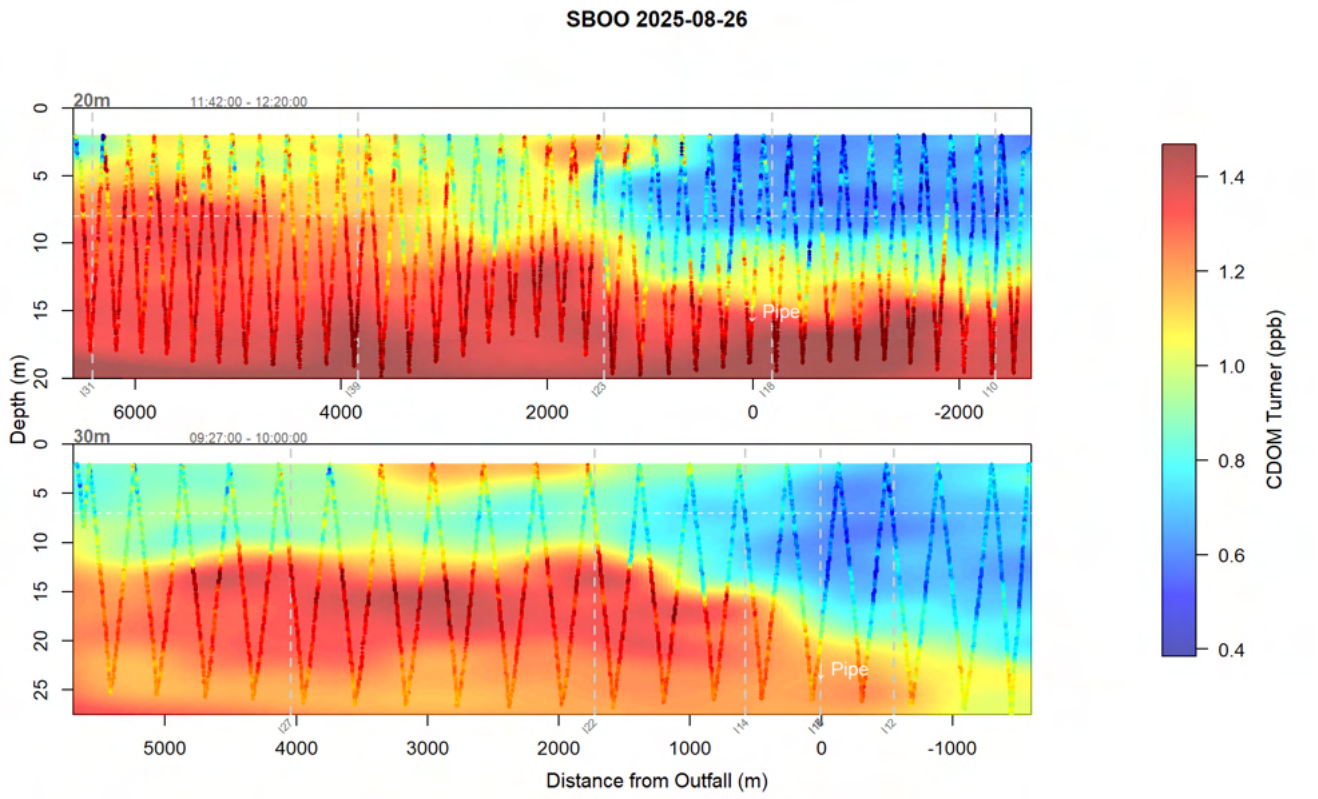


Appendix C.24 *continued*

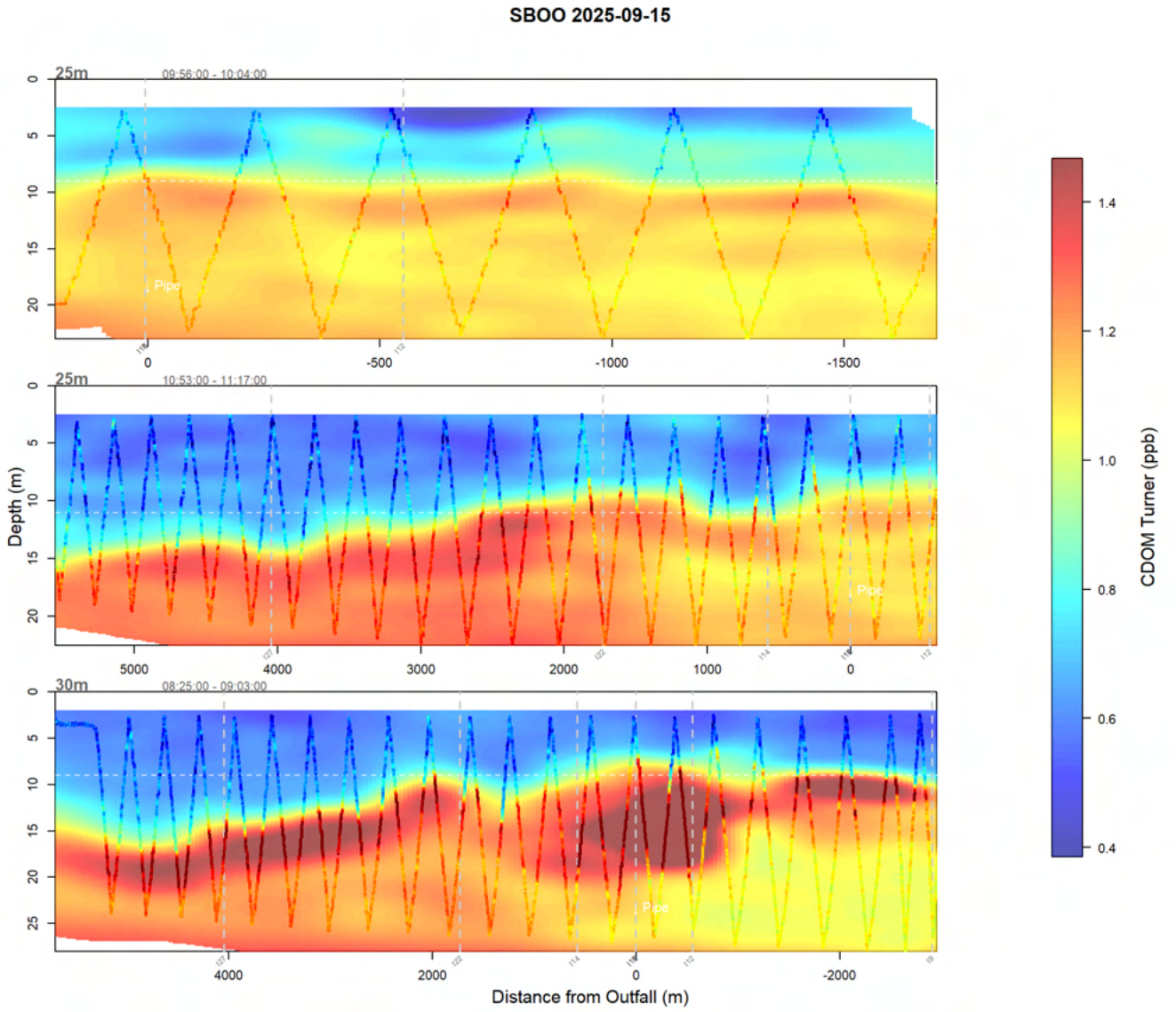


Appendix C.25

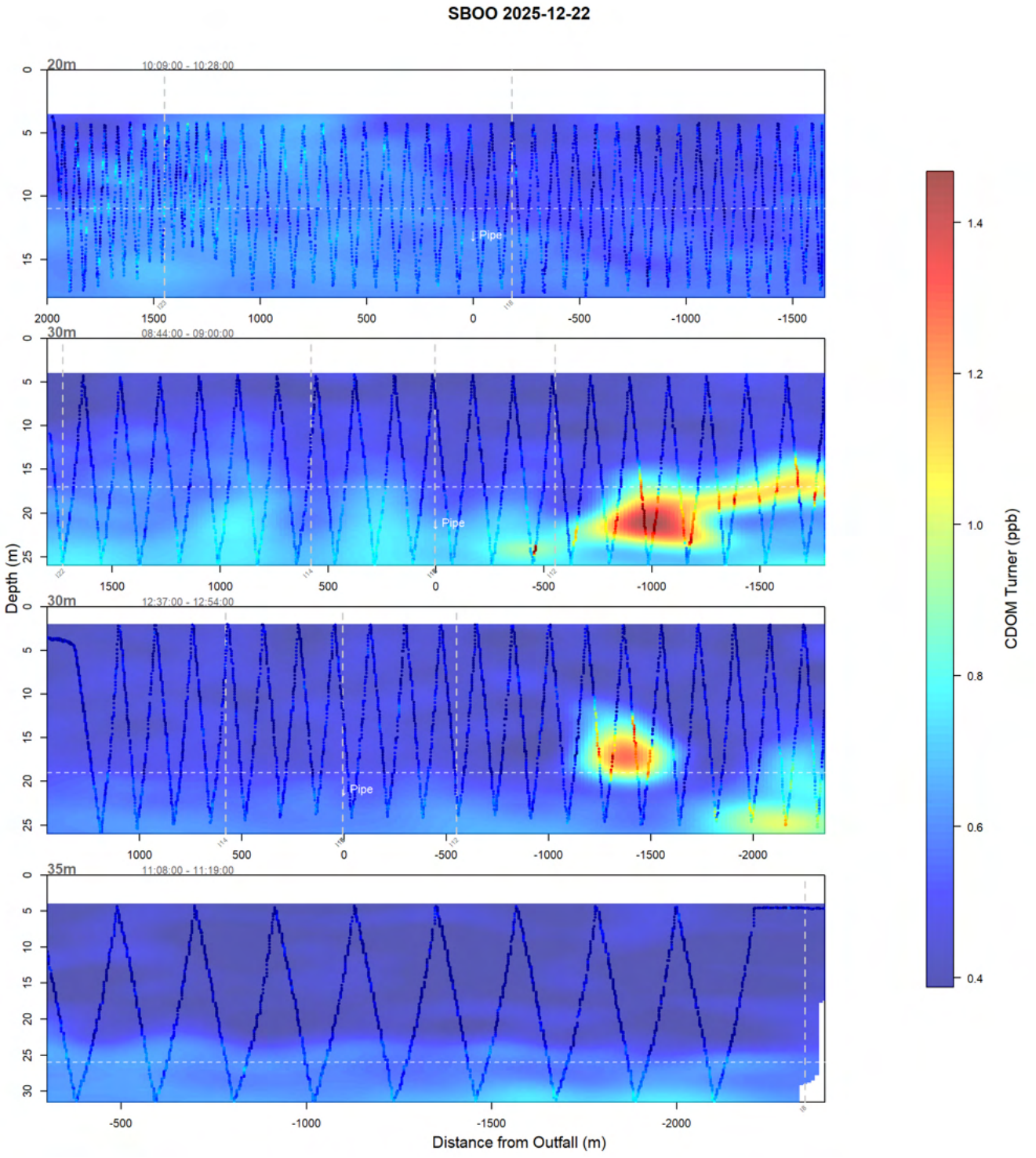
Interpolated CDOM data from ROTV surveys for each transect along an isobath conducted in the SBOO region during the report period (see text for methods). Opaque color lines indicate the position of the ROTV in the water column and associated raw data value. The position of the outfall is designated by text (“Pipe”) and arrow in white. Scales for each parameter are bound by the 2nd and 98th percentile of observed data for the region, using report-period ROTV data from the SBOO region. Vertical grey dashed lines indicate the position of nearby CTD sampling stations. A horizontal white line indicates the position of the thermocline for each transect.



Appendix C.25 *continued*



Appendix C.25 *continued*



Appendix C.25 *continued*

Appendix D

Sediment Quality

2024 – 2025
Raw Data Tables & Supplemental Analyses

Appendix D.1

Constituents and method detection limits (MDL) used for the analysis of sediments during 2024 and 2025. MDLs are summarized as minimum, and maximum values over the two years, abbreviations are in parentheses.

	MDL			MDL	
Parameter	**Min**	**Max**	**Parameter**	**Min**	**Max**
Organic Indicators					
BOD (ppm)	2	2	Sulfides (ppm)	2.2	2.2
TN (% wt.)	0.001	0.15	TVS (% wt.)	0.1	0.1
TOC (% wt.)	0.119	0.226			
Metals (ppm)					
Aluminum (Al)	0.551	1.09	Lead (Pb)	0.101	0.101
Antimony (Sb)	0.167	0.195	Manganese (Mn)	0.021	0.021
Arsenic (As)	0.151	0.151	Mercury (Hg)	0.004	0.005
Barium (Ba)	0.077	0.077	Nickel (Ni)	0.094	0.203
Beryllium (Be)	0.002	0.002	Selenium (Se)	0.213	0.213
Cadmium (Cd)	0.014	0.016	Silver (Ag)	0.032	0.033
Chromium (Cr)	0.029	0.029	Tin (Sn)	0.054	0.058
Copper (Cu)	0.047	0.047	Zinc (Zn)	0.19	0.19
Iron (Fe)	1.97	1.97			
Chlorinated Pesticides (ppt)					
Chlordanes					
Alpha (cis) Chlordane [A(c)C]	73.4	180	Heptachlor epoxide (HeptEpox)	65.4	154
Cis Nonachlor (cNon)	60.7	118	Methoxychlor (Methoxy)	498	988
Gamma (trans) Chlordane [G(t)C]	70.3	141	Oxychlordane (Oxychlor)	52.8	103
Heptachlor (Hept)	68.5	172	Trans Nonachlor (tNon)	801	988
Dichlorodiphenyltrichloroethane (DDT)					
o,p–DDD	49	95.7	p,p–DDE	60	117
o,p–DDE	65	127	p,p–DDMU	61.2	120
o,p–DDT	50.9	99.3	p,p–DDT	65.1	255
p,p–DDD	64	125			
Endrin					
Endrin	92.7	195	Endrin aldehyde (EndAld)	281	821
Endosulfan					
Alpha-Endosulfan	53.9	105	Endosulfan sulfate	100	195
Beta-Endosulfan	71.2	139			
Hexachlorocyclohexane (HCH)					
HCH, Alpha isomer	52.2	102	HCH, Delta isomer	63	123
HCH, Beta isomer	62.4	122	HCH, Gamma isomer	60.5	118
Miscellaneous Pesticides					
Aldrin	72.8	152	Hexachlorobenzene (HCB)	98.9	304
Dieldrin	76.1	208	Mirex	61.3	120

Appendix D.1 *continued*

Parameter	MDL Min	MDL Max	Parameter	MDL Min	MDL Max
Polychlorinated Biphenyl Congeners (PCBs) (ppt)					
PCB 8	63.1	138	PCB 126	65.4	190
PCB 18	60.3	118	PCB 128	66.4	151
PCB 28	56.5	110	PCB 138	58.0	113
PCB 37	64.6	130	PCB 149	62.3	128
PCB 44	61.1	119	PCB 151	56.2	110
PCB 49	61.1	119	PCB 153/168	124	318
PCB 52	64.6	126	PCB 156	72.0	160
PCB 66	51.0	99.6	PCB 157	66.9	131
PCB 70	55.3	108	PCB 158	64.1	131
PCB 74	55.5	108	PCB 167	64.6	137
PCB 77	62.9	123	PCB 169	59.1	115
PCB 81	46.9	91.5	PCB 170	56.1	110
PCB 87	58.5	114	PCB 177	56.5	110
PCB 99	55.9	109	PCB 180	56.3	110
PCB 101	48.0	93.8	PCB 183	58.8	115
PCB 105	63.7	162	PCB 187	58.4	114
PCB 110	59.6	116	PCB 189	63.7	212
PCB 114	59.5	116	PCB 194	62.8	123
PCB 118	51.0	99.6	PCB 195	60.4	118
PCB 119	61.3	120	PCB 201	57.3	112
PCB 123	52.6	103	PCB 206	82.2	160
Polycyclic Aromatic Hydrocarbons (PAHs) (ppb)					
1-methylnaphthalene	5.09	9.13	Benzo[G,H,I]perylene	4.40	21.3
1-methylphenanthrene	4.57	8.20	Benzo[K]fluoranthene	6.14	24.3
2-methylnaphthalene	4.13	7.41	Biphenyl	7.18	15.7
2,3,5-trimethylnaphthalene	10.2	18.3	Chrysene	3.67	6.58
2,6-dimethylnaphthalene	3.75	6.73	Dibenzo(A,H)anthracene	3.43	23.3
3,4-benzo(B)fluoranthene	3.23	21.3	Fluoranthene	5.99	10.8
Acenaphthene	3.97	7.12	Fluorene	3.57	6.40
Acenaphthylene	4.57	8.20	Indeno(1,2,3-CD)pyrene	3.67	22.2
Anthracene	3.99	17.2	Naphthalene	3.87	6.94
Benzo[A]anthracene	2.06	9.64	Perylene	10.2	17.8
Benzo[A]pyrene	4.17	17.0	Phenanthrene	3.31	5.93
Benzo[e]pyrene	3.08	18.5	Pyrene	3.45	10.8

Appendix D.1 *continued*

Parameter	MDL Min	MDL Max	Parameter	MDL Min	MDL Max
Polybrominated Diphenyl Ethers (PBDEs) (ppt)					
BDE-17	18.9	36.9	BDE-100	21.0	46.7
BDE-28	22.9	51.8	BDE-138	28.9	75.4
BDE-47	60.1	150	BDE-153	24.1	47.1
BDE-49	13.5	26.3	BDE-154	22.2	43.7
BDE-66	15.1	29.5	BDE-183	32.7	63.9
BDE-85	40.5	116.0	BDE-190	49.9	101
BDE-99	115	225			

Appendix D.2

Concentrations of organic loading indicators detected in sediments from PLOO stations sampled during winter and summer 2025. See Appendix D.1 for MDLs; ND = not detected; NR = not reportable..

2025	Winter					Summer				
	BOD[b] (ppm)	Sulfides (ppm)	TN (% wt)	TOC (% wt)	TVS (% wt)	BOD (ppm)	Sulfides (ppm)	TN (% wt)	TOC (% wt)	TVS (% wt)
88-m Depth Contour										
B11	—	12.20	0.078	2.290	4.0	—	3.18	0.172	2.330	3.7
B8	—	32.20	0.073	0.763	2.9	—	4.99	0.083	0.629	2.8
E19	—	29.00	0.057	0.569	2.5	—	3.45	0.072	0.486	2.3
E7	—	41.50	0.055	0.486	2.1	—	2.34	0.045	0.441	2.2
E1	—	13.20	0.057	0.595	2.0	—	ND	0.051	0.409	1.8
98-m Depth Contour										
B12	727	3.93	0.083	2.410	3.1	343	3.31	0.046	2.880	3.0
B9	273	8.18	0.052	0.749	2.6	276	2.29	0.079	0.739	2.7
E26	308	20.70	0.045	0.434	2.4	424	4.51	0.074	0.555	2.1
E25	364	8.88	ND	0.481	2.2	253	7.68	0.069	0.470	1.9
E23	288	14.40	0.039	0.399	2.2	237	4.66	0.070	0.489	2.0
E20	226	5.55	0.038	0.448	1.9	236	10.80	0.061	0.384	1.6
E17[a]	260	12.80	0.037	0.323	1.8	267	39.00	0.042	0.325	1.6
E14[a]	431	24.40	0.039	0.385	1.6	411	26.30	0.040	0.310	1.5
E11[a]	283	26.30	0.046	0.534	1.9	278	11.90	0.063	0.481	1.8
E8	214	14.50	0.044	0.454	2.4	288	10.90	0.061	0.431	1.7
E5	214	ND	0.038	0.462	2.2	227	5.17	0.066	0.548	2.1
E2	246	ND	0.040	0.618	2.4	227	2.80	0.054	0.568	2.4
116-m Depth Contour										
B10	—	12.00	0.049	0.934	2.4	—	10.30	0.073	0.974	2.3
E21	—	7.40	0.057	0.411	1.9	—	6.03	0.034	ND	1.9
E15[a]	—	4.43	0.044	0.494	2.1	—	8.53	0.042	0.386	2.0
E9	—	3.27	0.054	1.290	2.2	—	3.15	0.051	0.629	2.1
E3	—	ND	0.052	0.994	2.2	—	4.25	0.043	0.449	1.8
Detection Rate (%)	100	86.36	95	100	100	100	95.45	100	95	100

[a] Near-ZID station

[b] BOD only sampled at PLOO primary core stations

Appendix D.3

Concentrations of organic indicators detected in sediments from SBOO stations sampled during winter and summer 2025. See Appendix D.1 for MDLs; ND = not detected; NR = not reportable.

2025	Winter				Summer			
	Sulfides (ppm)	TN (% wt)	TOC (% wt)	TVS (% wt)	Sulfides (ppm)	TN (% wt)	TOC (% wt)	TVS (% wt)
19-m Stations								
I35	ND	0.041	0.228	1.4	7.4	0.036	0.219	1.6
I34	ND	ND	0.471	0.4	ND	ND	ND	0.6
I31	ND	ND	ND	0.6	NR	ND	ND	0.8
I23	ND	ND	0.520	1.0	NR	ND	ND	1.0
I18	ND	ND	ND	0.7	NR	ND	ND	0.8
I10	ND	ND	ND	0.9	ND	ND	ND	0.8
I4	ND	ND	ND	0.6	7.7	0.025	ND	1.0
28-m Stations								
I33	9.7	0.037	0.389	1.6	6.6	0.035	ND	1.3
I30	ND	0.034	ND	1.2	3.3	0.033	ND	1.3
I27	7.1	0.027	ND	1.0	NR	ND	ND	1.1
I22	ND	ND	ND	1.0	7.7	ND	ND	1.0
I14[a]	ND	ND	ND	1.0	NR	ND	ND	1.5
I16[a]	ND	ND	ND	0.4	NR	ND	ND	0.8
I15	ND	ND	ND	0.5	NR	0.036	0.218	0.5
I12[a]	ND	ND	ND	0.5	NR	ND	ND	0.5
I9	3.3	ND	ND	1.2	10.0	0.031	ND	1.2
I6	ND	ND	ND	0.5	ND	0.021	ND	0.5
I2	ND	ND	ND	0.5	ND	ND	ND	0.5
I3	ND	ND	ND	0.4	ND	ND	ND	0.4
38-m Stations								
I29	ND	0.030	ND	0.4	12.3	0.040	0.342	1.8
I21	ND	ND	ND	0.5	NR	ND	ND	0.5
I13	ND	ND	ND	0.5	NR	ND	ND	0.5
I8	ND	ND	ND	0.6	ND	ND	ND	0.5
55-m Stations								
I28	ND	0.067	0.790	1.5	7.2	0.062	0.750	1.5
I20	ND	ND	ND	0.5	2.2	0.027	ND	0.7
I7	ND	ND	ND	0.6	ND	0.018	ND	0.6
I1	5.3	0.034	ND	1.2	3.9	0.030	0.232	1.2
Detection Rate (%)	15	26	19	100	59	44	19	100

[a] Near-ZID station

Appendix D.4

Concentrations of trace metals (ppm) detected in sediments from PLOO stations sampled during winter and summer 2025. See Appendix D.1 for MDLs and translation of periodic table symbols; DR = detection rate; DNQ= detected not quantified; ND = not detected; NR = not reportable; NA = not analyzed.

Winter 2025	Al	Sb	As	Ba	Be	Cd	Cr	Cu	Fe	Pb	Mn	Hg	Ni	Se	Ag	Sn	Zn
88-m Depth Contour																	
B11	9570	0.78 DNQ	4.08	33.7	0.276	0.083 DNQ	21.3	7.8	17200	3.7	113	0.038	7.4	0.74 DNQ	ND	0.77	36.7
B8	11400	0.30 DNQ	3.12	45.0	0.231	0.076 DNQ	20.5	9.2	13500	4.1	115	0.045	8.8	0.65 DNQ	ND	1.10	33.0
E19	8820	0.45 DNQ	2.94	37.9	0.176	0.099	16.3	7.4	10800	3.6	96	0.038	6.9	0.44 DNQ	ND	0.96	27.1
E7	8040	0.24 DNQ	2.96	31.6	0.159	0.086 DNQ	14.7	6.6	9890	2.8	88	0.029	6.4	0.37 DNQ	ND	0.85	24.0
E1	8430	0.30 DNQ	2.76	35.3	0.170	0.050 DNQ	15.1	8.0	10500	4.5	86	0.057	6.0	0.48 DNQ	ND	0.88	25.5
98-m Depth Contour																	
B12	6630	0.88 DNQ	5.12	18.4	0.279	0.057 DNQ	22.6	4.3	18300	2.7	57	0.020	5.0	0.39 DNQ	ND	0.59	31.7
B9	8110	0.59 DNQ	3.35	36.2	0.222	0.064 DNQ	19.1	5.9	13900	3.3	89	0.029	6.4	0.40 DNQ	ND	0.81	30.8
E26	7810	0.85 DNQ	2.86	30.9	0.172	0.084 DNQ	15.3	6.5	10300	3.1	88	0.039	6.6	0.40 DNQ	ND	0.76	24.8
E25	7260	0.76 DNQ	2.80	29.2	0.158	0.092	14.2	6.2	9670	2.9	82	0.033	6.1	0.45 DNQ	ND	0.73	23.2
E23	7300	0.76 DNQ	2.78	28.1	0.155	0.078 DNQ	14.4	5.9	9640	2.9	83	0.036	6.0	0.41 DNQ	ND	0.69	23.2
E20	6880	0.65 DNQ	2.71	26.2	0.146	0.079 DNQ	13.5	5.7	8990	2.8	78	0.032	5.7	0.36 DNQ	ND	0.69	21.8
E17[a]	5560	0.56 DNQ	2.99	21.6	0.126	0.081 DNQ	11.8	4.9	8110	2.4	65	0.025	4.8	0.42 DNQ	ND	0.59	19.0
E14[a]	4670	0.52 DNQ	2.30	16.0	0.114	0.114	10.4	4.8	6720	1.8	56	0.023	4.3	0.42 DNQ	ND	0.51	17.2
E11[a]	5790	0.60 DNQ	2.15	21.8	0.135	0.111	12.0	5.3	7860	2.1	66	0.020	4.9	0.34 DNQ	ND	0.59	20.0
E8	6720	0.79 DNQ	2.84	25.4	0.155	0.080 DNQ	13.5	6.2	9160	2.6	74	0.038	5.4	0.30 DNQ	ND	0.67	21.9
E5	6550	0.66 DNQ	3.08	26.3	0.148	0.065 DNQ	12.8	5.6	9170	2.5	73	0.035	5.2	0.39 DNQ	ND	0.64	21.3
E2	8540	0.86 DNQ	2.83	43.7	0.171	0.059 DNQ	15.3	9.1	11600	3.9	92	0.050	6.0	0.42 DNQ	ND	0.88	27.8
116-m Depth Contour																	
B10	6600	0.47 DNQ	2.61	22.6	0.193	0.066 DNQ	16.3	4.9	11400	2.6	67	0.023	4.8	0.40 DNQ	ND	0.61	25.2
E21	5990	0.41 DNQ	2.09	22.4	0.131	0.091	12.3	6.2	7910	2.7	67	0.027	5.1	0.30 DNQ	ND	0.64	19.4
E15[a]	6310	0.29 DNQ	2.25	20.1	0.141	0.072 DNQ	12.7	5.5	8010	2.5	65	0.026	4.9	0.37 DNQ	ND	0.62	19.6
E9	6140	0.40 DNQ	3.15	20.8	0.156	0.076 DNQ	14.9	7.6	9990	2.8	62	0.025	5.0	0.33 DNQ	ND	0.64	29.2
E3	8610	0.57 DNQ	3.39	55.2	0.190	0.057 DNQ	15.0	11.5	12900	6.5	92	0.100	5.0	0.30 DNQ	ND	1.03	40.4
DR (%)	100	100	100	100	100	100	100	100	100	100	100	100	100	100	0	100	100

[a] Near-ZID station

Appendix D.4 *continued*

Summer 2025	Al	Sb	As	Ba	Be	Cd	Cr	Cu	Fe	Pb	Mn	Hg	Ni	Se	Ag	Sn	Zn
88-m Depth Contour																	
B11	9280	1.20	4.85	38.4	0.312	0.055 DNQ	24.6	7.4	20000	4.6	107	0.036	7.3	0.74 DNQ	ND	0.97	39.6
B8	10200	0.58 DNQ	2.52	41.8	0.217	0.071 DNQ	19.0	8.3	12500	3.5	113	0.038	8.2	0.54 DNQ	ND	1.00	31.7
E19	8490	0.47 DNQ	2.77	37.0	0.178	0.080 DNQ	16.4	7.2	10700	3.2	97	0.034	7.0	0.44 DNQ	ND	0.93	27.4
E7	7870	0.55 DNQ	3.07	35.3	0.167	0.080 DNQ	15.6	7.3	10000	3.3	89	0.045	6.7	0.47 DNQ	ND	0.86	25.7
E1	6670	0.43 DNQ	2.56	29.8	0.139	0.054 DNQ	12.8	6.5	8690	3.4	75	0.039	5.3	0.34 DNQ	ND	0.78	22.1
98-m Depth Contour																	
B12	6050	1.07	5.86	18.3	0.276	0.074 DNQ	24.4	4.6	18500	2.9	57	0.023	5.2	0.24 DNQ	ND	0.51	33.3
B9	7490	0.92 DNQ	3.90	47.4	0.270	0.053 DNQ	22.2	6.0	16500	3.6	87	0.033	6.6	0.42 DNQ	ND	0.76	32.8
E26	7080	0.54 DNQ	2.91	30.9	0.160	0.077 DNQ	14.5	6.2	9770	3.0	82	0.027	6.4	0.22 DNQ	ND	0.73	24.4
E25	6570	0.47 DNQ	2.62	27.5	0.149	0.076 DNQ	13.4	5.5	8990	2.7	75	0.026	5.7	0.26 DNQ	ND	0.68	22.6
E23	6660	0.51 DNQ	2.63	30.4	0.151	0.083 DNQ	13.9	5.8	9260	2.7	78	0.028	6.0	0.26 DNQ	ND	0.66	23.2
E20	5700	0.41 DNQ	2.37	23.5	0.134	0.078 DNQ	12.2	4.8	7900	2.4	68	0.042	5.1	0.27 DNQ	ND	0.61	19.8
E17[a]	5750	0.60 DNQ	2.25	23.5	0.135	0.094	12.6	5.4	7840	2.5	69	0.022	5.2	0.36 DNQ	ND	0.68	20.5
E14[a]	4490	0.46 DNQ	2.23	17.4	0.114	0.119	10.8	5.0	6480	1.9	58	0.017	4.6	ND	ND	0.58	17.8
E11[a]	5370	0.46 DNQ	2.44	20.5	0.132	0.091	11.6	5.0	7730	2.1	62	0.021	4.6	ND	ND	0.59	19.6
E8	5760	0.51 DNQ	2.47	22.4	0.147	0.065 DNQ	12.3	5.0	8080	2.4	68	0.022	4.9	ND	ND	0.65	20.2
E5	6380	0.51 DNQ	2.43	27.5	0.154	0.074 DNQ	13.5	6.0	9270	2.8	73	0.028	5.5	ND	ND	0.72	23.5
E2	8070	0.76 DNQ	2.91	45.1	0.179	0.055 DNQ	15.5	8.8	11600	3.5	88	0.025	6.1	0.38 DNQ	ND	0.90	28.6
116-m Depth Contour																	
B10	5930	0.52 DNQ	2.43	20.2	0.177	0.077 DNQ	15.3	4.7	10100	2.5	67	0.023	4.9	0.49 DNQ	ND	0.62	23.7
E21	5920	0.54 DNQ	2.43	21.7	0.135	0.076 DNQ	12.2	5.0	7670	2.4	67	0.023	5.1	0.25 DNQ	ND	0.61	19.3
E15[a]	5710	0.52 DNQ	2.71	19.9	0.134	0.070 DNQ	12.2	5.0	7820	2.5	63	0.024	4.7	0.30 DNQ	ND	0.63	19.2
E9	6210	0.52 DNQ	3.38	22.1	0.154	0.057 DNQ	14.9	5.8	9820	2.5	66	0.025	5.0	0.40 DNQ	ND	0.58	23.1
E3	7490	0.52 DNQ	1.84	40.6	0.136	0.051 DNQ	12.3	9.6	10000	4.1	84	0.078	4.6	0.30 DNQ	ND	0.73	26.6
DR (%)	100	100	100	100	100	100	100	100	100	100	100	100	100	82	0	100	100

[a] Near-ZID station

Appendix D.5

Concentrations of trace metals (ppm) detected in sediments from SBOO stations sampled during winter and summer 2025. See Appendix D.1 for MDLs and translation of periodic table symbols; DR = detection rate; DNQ = detected not quantified; ND = not detected; NR = not reportable; NA = not analyzed.

Winter 2025	Al	Sb	As	Ba	Be	Cd	Cr	Cu	Fe	Pb	Mn	Hg	Ni	Se	Ag	Sn	Zn
19-m Stations																	
I35	6660	ND	2.16	30.6	0.111		11.4	4.5	7730	2.7	84	0.022	3.7	ND	ND	0.66	20.9
I34	1030	ND	2.92	4.2	0.024 DNQ		2.7	0.9	2670	1.3	18	ND	0.6	ND	ND	0.15 DNQ	3.9
I31	3480	ND	1.19	18.3	0.056	ND	7.0	1.5	3710	1.0	57	ND	1.4	ND	ND	0.32 DNQ	8.0
I23	1280	ND	2.91	4.8	0.052		4.0	0.7	2830	1.4	16	ND	0.7	ND	ND	0.10 DNQ	4.9
I18	4310	ND	1.44	35.0	0.073	ND	11.7	2.2	6240	1.2	76	ND	2.1	0.27 DNQ	ND	0.40 DNQ	11.2
I10	4830	ND	1.42	23.9	0.078	ND	9.3	2.4	5770	1.3	63	ND	2.4	0.36 DNQ	ND	0.41 DNQ	12.6
I4	1120	ND	1.20	3.7	0.027 DNQ	ND	4.3	0.7	2000	1.0	17	ND	0.8	ND	ND	0.15 DNQ	3.4
28-m Stations																	
I33	4420	ND	1.86	18.8	0.084		8.3	4.0	5750	2.5	68	0.022	2.4	ND	ND	0.56	14.6
I30	5640	0.30 DNQ	1.75	24.1	0.094		9.9	2.9	5570	1.4	58	0.008 DNQ	2.9	0.29 DNQ	ND	0.42 DNQ	14.4
I27	6280	ND	1.53	28.8	0.096		10.0	3.1	5980	1.3	64	0.006 DNQ	3.1	ND	ND	0.44 DNQ	15.6
I22	4310	ND	1.46	22.0	0.078		8.5	2.3	4630	1.2	57	0.006 DNQ	2.5	ND	ND	0.34 DNQ	10.8
I14[a]	5810	0.21 DNQ	1.33	29.3	0.096		10.0	3.1	5950	1.3	67	0.006 DNQ	3.2	0.30 DNQ	ND	0.38 DNQ	15.6
I16[a]	2250	ND	1.62	7.8	0.057		5.9	1.2	3550	1.2	36	0.006 DNQ	1.2	ND	ND	0.21 DNQ	7.8
I15	2530	ND	1.64	7.2	0.063	ND	7.9	1.0	3910	1.4	32	0.004 DNQ	1.4	0.28 DNQ	ND	0.26 DNQ	8.1
I12[a]	2890	ND	1.67	12.5	0.062	ND	6.8	1.5	4030	1.0	40	ND	1.4	ND	ND	0.26 DNQ	9.1
I9	7350	0.28 DNQ	1.41	38.3	0.116		12.0	4.0	7640	1.4	79	0.007 DNQ	4.2	0.26 DNQ	ND	0.51	19.9
I6	1370	0.26 DNQ	4.57	3.4	0.039 DNQ		7.6	0.6	4040	1.5	19	ND	0.9	0.24 DNQ	ND	0.22 DNQ	4.4
I2	1120	ND	0.77 DNQ	1.9	0.026 DNQ		5.4	0.4 DNQ	1260	0.7	11	ND	0.8	ND	ND	0.15 DNQ	2.4
I3	658	0.20 DNQ	0.97 DNQ	6.1	0.022 DNQ	ND	4.9	0.3 DNQ	1390	0.7	9	ND	0.5	0.23 DNQ	ND	0.13 DNQ	1.9
38-m Stations																	
I29	1320	0.24 DNQ	3.71	2.9	0.056	ND	5.0	0.6	5200	1.6	15	ND	0.9	ND	ND	0.12 DNQ	5.0
I21	1130	0.52 DNQ	9.97	2.1	0.065		10.5	0.6	7840	3.0	14	ND	0.9	0.30 DNQ	ND	0.15 DNQ	6.1
I13	1070	0.35 DNQ	6.55	2.3	0.044 DNQ		9.7	0.5	6120	2.1	23	0.005 DNQ	0.7	0.26 DNQ	ND	0.17 DNQ	5.6
I8	1870	0.24 DNQ	2.27	5.1	0.056		8.8	0.8	4230	1.1	22	ND	1.2	0.32 DNQ	ND	0.20 DNQ	7.8
55-m Stations																	
I28	5150	0.25 DNQ	2.54	21.3	0.110		9.1	4.2	6500	2.2	56	0.012	4.7	0.37 DNQ	ND	0.55	14.7
I20	1240	0.23 DNQ	2.97	2.2	0.054	ND	5.1	0.5 DNQ	4660	1.3	18	ND	0.8	0.26 DNQ	ND	0.12 DNQ	5.8
I7	1210	0.48 DNQ	6.75	2.9	0.051		8.9	0.5	7340	2.3	19	ND	0.8	0.27 DNQ	ND	0.21 DNQ	5.7
I1	2820	0.34 DNQ	1.44	9.2	0.064		7.0	1.6	3890	1.4	40	0.009 DNQ	2.6	0.28 DNQ	ND	0.27 DNQ	7.9
DR (%)	100	48	100	100	100	67	100	100	100	100	100	44	100	56	0	100	100

[a] Near-ZID station

Appendix D.5 *continued*

Summer 2025	Al	Sb	As	Ba	Be	Cd	Cr	Cu	Fe	Pb	Mn	Hg	Ni	Se	Ag	Sn	Zn
19-m Stations																	
I35	6550	0.49 DNQ	2.21	34.1	0.118	0.070 DNQ	11.9	4.4	7910	2.6	86	0.018	3.8	0.48 DNQ	ND	0.77	22.0
I34	1940	0.29 DNQ	1.90	7.3	0.038 DNQ	ND	3.9	0.9	3060	1.4	28	0.006 DNQ	0.9	ND	ND	0.22 DNQ	6.4
I31	3060	ND	1.17	12.7	0.054	0.022 DNQ	6.9	1.5	3360	1.0	45	0.004 DNQ	1.5	ND	ND	0.25 DNQ	7.9
I23	4000	0.34 DNQ	1.65	24.3	0.073	ND	8.1	1.8	4470	1.1	56	0.006 DNQ	2.0	0.29 DNQ	ND	0.37 DNQ	10.1
I18	4070	ND	1.51	27.3	0.070	0.020 DNQ	9.8	2.2	5500	1.1	64	0.005 DNQ	2.1	ND	ND	0.36 DNQ	11.1
I10	5090	0.26 DNQ	1.37	28.1	0.085	ND	9.2	2.5	5560	1.2	65	ND	2.6	ND	ND	0.43 DNQ	13.3
I4	4860	0.31 DNQ	1.41	24.0	0.079	0.027 DNQ	8.6	2.5	5210	1.0	59	0.005 DNQ	3.1	0.26 DNQ	ND	0.47 DNQ	12.8
28-m Stations																	
I33	4110	0.37 DNQ	1.69	17.0	0.080	0.025 DNQ	7.6	2.4	5240	2.0	64	0.014	2.2	0.24 DNQ	ND	0.52	13.3
I30	5830	0.48 DNQ	1.53	28.1	0.100	0.033 DNQ	10.5	3.1	5800	1.4	61	0.008 DNQ	3.2	0.29 DNQ	ND	0.47 DNQ	15.8
I27	5500	0.22 DNQ	1.29	28.3	0.095	0.038 DNQ	10.2	3.6	5700	1.5	62	0.007 DNQ	3.3	ND	ND	0.43 DNQ	15.7
I22	3960	ND	1.36	20.4	0.076	0.038 DNQ	8.8	2.3	4530	1.3	50	0.006 DNQ	2.5	0.23 DNQ	ND	0.32 DNQ	11.5
I14 [a]	6090	0.42 DNQ	1.58	33.1	0.107	0.028 DNQ	10.3	3.2	6300	1.3	71	0.009 DNQ	3.3	ND	ND	0.48 DNQ	17.4
I16 [a]	2920	0.21 DNQ	1.36	14.1	0.061	0.023 DNQ	6.9	1.4	3900	1.1	44	0.007 DNQ	1.6	ND	ND	0.26 DNQ	9.0
I15	1610	ND	2.31	5.4	0.052	0.025 DNQ	6.9	0.7	3470	1.3	20	ND	1.0	ND	ND	0.14 DNQ	6.5
I12 [a]	2450	ND	1.61	10.8	0.056	0.017 DNQ	6.8	1.1	3790	1.1	37	0.004 DNQ	1.4	0.23 DNQ	ND	0.25 DNQ	8.2
I9	7760	0.27 DNQ	1.35	42.0	0.126	0.042 DNQ	12.6	4.3	7560	1.3	83	0.007 DNQ	4.5	0.27 DNQ	ND	0.54	21.0
I6	897	0.41 DNQ	4.46	2.5	0.033 DNQ	0.030 DNQ	7.3	0.4 DNQ	3470	1.2	11	ND	0.7	ND	ND	0.13 DNQ	3.3
I2	1170	0.23 DNQ	0.74 DNQ	2.2	0.025 DNQ	0.023 DNQ	5.3	0.3 DNQ	1250	0.7	10	0.005 DNQ	0.7	ND	ND	0.12 DNQ	2.4
I3	990	ND	0.82 DNQ	1.9	0.024 DNQ	ND	6.2	0.3 DNQ	1290	0.8	8	ND	0.7	ND	ND	0.11 DNQ	2.0
38-m Stations																	
I29	7570	0.60 DNQ	1.92	36.9	0.141	0.049 DNQ	13.6	5.6	8050	2.6	82	0.020	5.4	0.41 DNQ	ND	0.72	22.2
I21	1040	0.44 DNQ	7.13	2.2	0.055	0.042 DNQ	10.8	0.5 DNQ	6720	2.6	12	ND	1.0	ND	ND	0.15 DNQ	6.1
I13	929	0.30 DNQ	3.73	2.1	0.039 DNQ	0.024 DNQ	9.3	0.4 DNQ	3870	1.6	12	ND	0.6	ND	ND	0.10 DNQ	4.2
I8	1720	0.29 DNQ	2.37	4.3	0.054	0.021 DNQ	8.7	0.5	3750	1.2	18	ND	1.0	ND	ND	0.13 DNQ	6.7
55-m Stations																	
I28	4180	0.45 DNQ	2.04	17.7	0.097	0.040 DNQ	7.7	3.4	5410	1.9	45	0.022	3.9	0.41 DNQ	ND	0.43 DNQ	12.7
I20	2180	0.32 DNQ	2.28	5.6	0.066	0.029 DNQ	6.4	1.1	4310	1.6	22	0.009 DNQ	1.6	ND	ND	0.23 DNQ	7.8
I7	1360	0.52 DNQ	5.49	3.2	0.057	0.020 DNQ	8.4	0.4 DNQ	6150	2.0	19	ND	0.8	0.23 DNQ	ND	0.17 DNQ	6.0
I1	2920	0.29 DNQ	1.24	9.0	0.067	0.061 DNQ	7.0	1.7	3740	1.3	43	0.008 DNQ	2.9	ND	ND	0.28 DNQ	8.1
DR (%)	100	78	100	100	100	85	100	100	100	100	100	70	100	41	0	100	100

[a] Near-ZID station

Appendix D.6

Concentrations of pesticides (ppt) detected in sediments from PLOO stations sampled during winter and summer 2025. See Appendix D.1 for MDLs and abbreviations; DR = detection rate; DNQ = detected not quantified; ND = not detected; NR = not reportable.

Winter	Chlordane								DDT						
2025	A(c)C	cNon	G(t)C	Hept	HeptEpox	Methoxy	Oxychlor	tNon	o,p-DDD	o,p-DDE	o,p-DDT	p,-p-DDMU	p,p-DDD	p,p-DDE	p,p-DDT
88-m Depth Contour															
B11	ND	ND	ND	ND	ND	ND	ND	ND	ND	ND	ND	ND	ND	144	ND
B8	ND	ND	ND	ND	ND	ND	ND	ND	ND	ND	ND	ND	ND	153	ND
E19	ND	ND	ND	ND	ND	ND	ND	ND	ND	ND	ND	ND	ND	132	ND
E7	ND	ND	ND	ND	ND	ND	ND	ND	ND	ND	ND	ND	ND	285	ND
E1	ND	ND	ND	ND	ND	ND	ND	ND	ND	ND	ND	ND	ND	202	ND
98-m Depth Contour															
B12	ND	ND	ND	ND	ND	ND	ND	ND	ND	ND	ND	ND	ND	191	ND
B9	ND	ND	ND	ND	ND	ND	ND	ND	ND	ND	ND	ND	ND	304	139
E26	ND	ND	ND	ND	ND	ND	ND	ND	ND	ND	ND	ND	ND	184	ND
E25	ND	ND	ND	ND	ND	ND	ND	ND	ND	ND	ND	ND	ND	126	ND
E23	ND	ND	ND	ND	ND	ND	ND	ND	ND	ND	ND	ND	ND	126	ND
E20	ND	ND	ND	ND	ND	ND	ND	ND	ND	ND	ND	ND	ND	159	ND
E17[a]	ND	ND	ND	ND	ND	ND	ND	ND	ND	ND	ND	ND	ND	ND	ND
E14[a]	ND	ND	ND	ND	ND	ND	ND	ND	ND	ND	ND	ND	ND	ND	ND
E11[a]	ND	ND	ND	ND	ND	ND	ND	ND	ND	ND	ND	ND	ND	ND	ND
E8	ND	ND	ND	ND	ND	ND	ND	ND	ND	ND	ND	ND	ND	130	ND
E5	ND	ND	ND	ND	ND	ND	ND	ND	ND	ND	ND	ND	ND	111	ND
E2	ND	ND	ND	ND	ND	ND	ND	ND	ND	ND	ND	ND	ND	211	ND
116-m Depth Contour															
B10	ND	ND	ND	ND	ND	ND	ND	ND	ND	ND	ND	ND	ND	130	ND
E21	ND	ND	ND	ND	ND	ND	ND	ND	ND	ND	ND	ND	ND	96.9	ND
E15[a]	ND	ND	ND	ND	ND	ND	ND	ND	ND	ND	ND	ND	ND	90.1 DNQ	ND
E9	ND	ND	ND	ND	ND	ND	ND	ND	ND	ND	ND	ND	ND	304	190
E3	ND	ND	ND	ND	ND	ND	ND	ND	ND	ND	ND	ND	101	270	ND
DR (%)	0	0	0	0	0	0	0	0	0	0	0	0	5	86	9

[a] Near-ZID station

Appendix D.6 *continued*

Winter 2025	HCH						Endosulfan						
	Alpha	Beta	Delta	Gamma	Aldrin	Dieldrin	Alpha	Beta	Sulfate	Endrin	EndAld	HCB	Mirex
88-m Depth Contour													
B11	ND	ND	ND	ND	ND	ND	ND	ND	ND	ND	ND	ND	ND
B8	ND	ND	ND	ND	ND	ND	ND	ND	ND	ND	ND	ND	ND
E19	ND	ND	ND	ND	ND	ND	ND	ND	ND	ND	ND	ND	ND
E7	ND	ND	ND	ND	ND	ND	ND	ND	ND	ND	ND	ND	ND
E1	ND	ND	ND	ND	ND	ND	ND	ND	ND	ND	ND	ND	ND
98-m Depth Contour													
B12	ND	ND	ND	ND	ND	ND	ND	ND	ND	ND	ND	ND	ND
B9	ND	ND	ND	ND	ND	ND	ND	ND	ND	ND	ND	ND	ND
E26	ND	ND	ND	ND	ND	ND	ND	ND	ND	ND	ND	ND	ND
E25	ND	ND	ND	ND	ND	ND	ND	ND	ND	ND	ND	ND	ND
E23	ND	ND	ND	ND	ND	ND	ND	ND	ND	ND	ND	ND	ND
E20	ND	ND	ND	ND	ND	ND	ND	ND	ND	ND	ND	ND	ND
E17[a]	ND	ND	ND	ND	ND	ND	ND	ND	ND	ND	ND	ND	ND
E14[a]	ND	ND	ND	ND	ND	ND	ND	ND	ND	ND	ND	ND	ND
E11[a]	ND	ND	ND	ND	ND	ND	ND	ND	ND	ND	ND	ND	ND
E8	ND	ND	ND	ND	ND	ND	ND	ND	ND	ND	ND	ND	ND
E5	ND	ND	ND	ND	ND	ND	ND	ND	ND	ND	ND	ND	ND
E2	ND	ND	ND	ND	ND	ND	ND	ND	ND	ND	ND	ND	ND
116-m Depth Contour													
B10	ND	ND	ND	ND	ND	ND	ND	ND	ND	ND	ND	ND	ND
E21	ND	ND	ND	ND	ND	ND	ND	ND	ND	ND	ND	ND	ND
E15[a]	ND	ND	ND	ND	ND	ND	ND	ND	ND	ND	ND	ND	ND
E9	ND	ND	ND	ND	ND	ND	ND	ND	ND	ND	ND	ND	ND
E3	ND	ND	ND	ND	ND	ND	ND	ND	ND	ND	ND	ND	ND
DR (%)	0	0	0	0	0	0	0	0	0	0	0	0	0

[a] Near-ZID station

Appendix D.6 *continued*

Summer	Chlordane								DDT						
2025	**A(c)C**	**cNon**	**G(t)C**	**Hept**	**HeptEpox**	**Methoxy**	**Oxychlor**	**tNon**	**o,p-DDD**	**o,p-DDE**	**o,p-DDT**	**p,-p-DDMU**	**p,p-DDD**	**p,p-DDE**	**p,p-DDT**
88-m Depth Contour															
B11	ND	ND	ND	ND	ND	ND	ND	ND	ND	ND	ND	ND	ND	302	ND
B8	ND	ND	ND	ND	ND	ND	ND	ND	ND	ND	ND	ND	ND	340	135
E19	ND	ND	ND	ND	ND	ND	ND	ND	ND	ND	ND	ND	ND	229	83.5 DNQ
E7	ND	ND	ND	ND	ND	ND	ND	ND	120	ND	83.6	ND	119	802	254
E1	ND	ND	ND	ND	ND	ND	ND	ND	ND	ND	ND	ND	ND	199	ND
98-m Depth Contour															
B12	ND	ND	ND	ND	ND	ND	ND	ND	ND	ND	ND	ND	ND	182	ND
B9	ND	ND	ND	ND	ND	ND	ND	ND	ND	ND	ND	ND	ND	323	ND
E26	ND	ND	ND	ND	ND	ND	ND	ND	ND	ND	ND	ND	ND	176	ND
E25	ND	ND	ND	ND	ND	ND	ND	ND	ND	ND	89.6	ND	ND	274	412
E23	ND	ND	ND	ND	ND	ND	ND	ND	ND	ND	ND	ND	ND	147	ND
E20	ND	ND	ND	ND	ND	ND	ND	ND	ND	ND	ND	ND	ND	163	149
E17[a]	ND	ND	ND	ND	ND	ND	ND	ND	ND	ND	ND	ND	ND	126	ND
E14[a]	ND	ND	ND	ND	ND	ND	ND	ND	ND	ND	ND	ND	ND	118	ND
E11[a]	ND	ND	ND	ND	ND	ND	ND	ND	ND	ND	ND	ND	ND	171	ND
E8	ND	ND	ND	ND	ND	ND	ND	ND	ND	ND	ND	ND	ND	116	ND
E5	ND	ND	ND	ND	ND	ND	ND	ND	ND	ND	ND	ND	ND	130	ND
E2	ND	ND	ND	ND	ND	ND	ND	ND	ND	ND	ND	ND	ND	290	166
116-m Depth Contour															
B10	ND	ND	ND	ND	ND	ND	ND	ND	ND	ND	ND	ND	ND	141	ND
E21	ND	ND	ND	ND	ND	ND	ND	ND	ND	ND	ND	ND	ND	153	ND
E15[a]	ND	ND	ND	ND	ND	ND	ND	ND	ND	ND	ND	ND	ND	211	ND
E9	ND	ND	ND	ND	ND	ND	ND	ND	ND	ND	ND	ND	ND	195	ND
E3	ND	ND	ND	ND	ND	ND	ND	ND	ND	ND	ND	ND	ND	176	ND
DR (%)	0	0	0	0	0	0	0	0	5	0	9	0	5	100	27

[a] Near-ZID station

Appendix D.6 *continued*

Summer	HCH						Endosulfan						
2025	**Alpha**	**Beta**	**Delta**	**Gamma**	**Aldrin**	**Dieldrin**	**Alpha**	**Beta**	**Sulfate**	**Endrin**	**EndAld**	**HCB**	**Mirex**
88-m Depth Contour													
B11	ND	ND	ND	ND	ND	ND	ND	ND	ND	ND	ND	362	ND
B8	ND	ND	ND	ND	ND	ND	ND	ND	ND	ND	ND	389	ND
E19	ND	ND	ND	ND	ND	ND	ND	ND	ND	ND	ND	ND	ND
E7	ND	ND	ND	ND	ND	ND	ND	ND	ND	ND	ND	ND	ND
E1	ND	ND	ND	ND	ND	ND	ND	ND	ND	ND	ND	ND	ND
98-m Depth Contour													
B12	ND	ND	ND	ND	ND	ND	ND	ND	ND	ND	ND	ND	ND
B9	ND	ND	ND	ND	ND	ND	ND	ND	ND	ND	ND	ND	ND
E26	ND	ND	ND	ND	ND	ND	ND	ND	ND	ND	ND	ND	ND
E25	ND	ND	ND	ND	ND	ND	ND	ND	ND	ND	ND	ND	ND
E23	ND	ND	ND	ND	ND	ND	ND	ND	ND	ND	ND	ND	ND
E20	ND	ND	ND	ND	ND	ND	ND	ND	ND	ND	ND	ND	ND
E17[a]	ND	ND	ND	ND	ND	ND	ND	ND	ND	ND	ND	ND	ND
E14[a]	ND	ND	ND	ND	ND	ND	ND	ND	ND	ND	ND	ND	ND
E11[a]	ND	ND	ND	ND	ND	ND	ND	ND	ND	ND	ND	ND	ND
E8	ND	ND	ND	ND	ND	ND	ND	ND	ND	ND	ND	196	ND
E5	ND	ND	ND	ND	ND	ND	ND	ND	ND	ND	ND	189	ND
E2	ND	ND	ND	ND	ND	ND	ND	ND	ND	ND	ND	ND	ND
116-m Depth Contour													
B10	ND	ND	ND	ND	ND	ND	ND	ND	ND	ND	ND	249	ND
E21	ND	ND	ND	ND	ND	ND	ND	ND	ND	ND	ND	ND	ND
E15[a]	ND	ND	ND	ND	ND	ND	ND	ND	ND	ND	ND	ND	ND
E9	ND	ND	ND	ND	ND	ND	ND	ND	ND	ND	ND	ND	ND
E3	ND	ND	ND	ND	ND	ND	ND	ND	ND	ND	ND	ND	ND
DR (%)	0	0	0	0	0	0	0	0	0	0	0	23	0

[a] Near-ZID station

Appendix D.7

Concentrations of pesticides (ppt) detected in sediments from SBOO stations sampled during 2025. See Appendix D.1 for MDLs and abbreviations; DR = detection rate; DNQ = detected not quantified; ND = not detected; NR = not reportable.

Winter 2025	Chlordane								DDT						
	A(c)C	cNon	G(t)C	Hept	HeptEpox	Methoxy	Oxychlor	tNon	o,p-DDD	o,p-DDE	o,p-DDT	p,-p-DDMU	p,p-DDD	p,p-DDE	p,p-DDT
19-m Stations															
I35	ND	ND	ND	ND	ND	ND	ND	ND	ND	ND	ND	ND	ND	ND	ND
I34	ND	ND	ND	ND	ND	ND	ND	ND	ND	ND	ND	ND	ND	ND	ND
I31	ND	ND	ND	ND	ND	ND	ND	ND	ND	ND	ND	ND	ND	ND	ND
I23	ND	ND	ND	ND	ND	ND	ND	ND	ND	ND	ND	ND	ND	ND	ND
I18	ND	ND	ND	ND	ND	ND	ND	ND	ND	ND	ND	ND	ND	ND	ND
I10	ND	182	ND	ND	ND	ND	ND	159	66.1 DNQ	ND	ND	ND	ND	92.8	ND
I4	ND	ND	ND	ND	ND	ND	ND	ND	ND	ND	ND	ND	ND	91.1	ND
28-m Stations															
I33	ND	ND	ND	ND	ND	ND	ND	ND	ND	ND	ND	ND	ND	ND	ND
I30	ND	ND	ND	ND	ND	ND	ND	ND	ND	ND	ND	ND	ND	183	ND
I27	ND	ND	ND	ND	ND	ND	ND	ND	ND	ND	ND	ND	ND	ND	ND
I22	ND	ND	ND	ND	ND	ND	ND	ND	ND	ND	ND	ND	ND	ND	ND
I14[a]	ND	ND	ND	ND	ND	ND	ND	ND	ND	ND	ND	ND	ND	65 DNQ	ND
I16[a]	ND	ND	ND	ND	ND	ND	ND	ND	ND	ND	ND	ND	ND	ND	ND
I15	ND	ND	ND	ND	ND	ND	ND	ND	ND	ND	ND	ND	ND	ND	ND
I12[a]	ND	ND	ND	ND	ND	ND	ND	ND	ND	ND	ND	ND	ND	ND	ND
I9	ND	ND	ND	ND	ND	ND	ND	ND	ND	ND	ND	ND	ND	ND	ND
I6	ND	ND	ND	ND	ND	ND	ND	ND	ND	ND	ND	ND	ND	ND	ND
I2	ND	ND	ND	ND	ND	ND	ND	ND	ND	ND	ND	ND	ND	ND	ND
I3	ND	ND	ND	ND	ND	ND	ND	ND	ND	ND	ND	ND	ND	ND	ND
38-m Stations															
I29	ND	ND	ND	ND	ND	ND	ND	ND	ND	ND	ND	ND	ND	ND	ND
I21	ND	ND	ND	ND	ND	ND	ND	ND	ND	ND	ND	ND	ND	ND	ND
I13	ND	ND	ND	ND	ND	ND	ND	ND	ND	ND	ND	ND	ND	ND	ND
I8	ND	ND	ND	ND	ND	ND	ND	ND	ND	ND	ND	ND	ND	ND	ND
55-m Stations															
I28	ND	ND	ND	ND	ND	ND	ND	ND	ND	ND	ND	ND	ND	259	ND
I20	ND	ND	ND	ND	ND	ND	ND	ND	ND	ND	ND	ND	ND	ND	ND
I7	ND	ND	ND	ND	ND	ND	ND	ND	ND	ND	ND	ND	ND	ND	ND
I1	ND	ND	ND	ND	ND	ND	ND	ND	ND	ND	ND	ND	ND	ND	ND
DR (%)	0	4	0	0	0	0	0	4	4	0	0	0	0	19	0

[a] Near-ZID station

Appendix D.7 *continued*

Winter 2025	HCH						Endosulfan						
	Alpha	Beta	Delta	Gamma	Aldrin	Dieldrin	Alpha	Beta	Sulfate	Endrin	EndAld	HCB	Mirex
19-m Stations													
I35	ND	ND	ND	ND	ND	ND	ND	ND	ND	ND	ND	ND	ND
I34	ND	ND	ND	ND	ND	ND	ND	ND	ND	ND	ND	ND	ND
I31	ND	ND	ND	ND	ND	ND	ND	ND	ND	ND	ND	ND	ND
I23	ND	ND	ND	ND	ND	ND	ND	ND	ND	ND	ND	ND	ND
I18	ND	ND	ND	ND	ND	ND	ND	ND	ND	ND	ND	ND	ND
I10	ND	ND	ND	ND	ND	66 DNQ	91.7	ND	ND	ND	ND	ND	ND
I4	ND	ND	ND	ND	ND	ND	ND	ND	ND	ND	ND	ND	ND
28-m Stations													
I33	ND	ND	ND	ND	ND	ND	ND	ND	ND	ND	ND	ND	ND
I30	ND	ND	ND	ND	ND	ND	ND	ND	ND	ND	ND	ND	ND
I27	ND	ND	ND	ND	ND	ND	ND	ND	ND	ND	ND	ND	ND
I22	ND	ND	ND	ND	ND	ND	ND	ND	ND	ND	ND	ND	ND
I14[a]	ND	ND	ND	ND	ND	ND	ND	ND	ND	ND	ND	ND	ND
I16[a]	ND	ND	ND	ND	ND	ND	ND	ND	ND	ND	ND	ND	ND
I15	ND	ND	ND	ND	ND	ND	ND	ND	ND	ND	ND	ND	ND
I12[a]	ND	ND	ND	ND	ND	ND	ND	ND	ND	ND	ND	ND	ND
I9	ND	ND	ND	ND	ND	ND	ND	ND	ND	ND	ND	ND	ND
I6	ND	ND	ND	ND	ND	ND	ND	ND	ND	ND	ND	ND	ND
I2	ND	ND	ND	ND	ND	ND	ND	ND	ND	ND	ND	ND	ND
I3	ND	ND	ND	ND	ND	ND	ND	ND	ND	ND	ND	ND	ND
38-m Stations													
I29	ND	ND	ND	ND	ND	ND	ND	ND	ND	ND	ND	ND	ND
I21	ND	ND	ND	ND	ND	ND	ND	ND	ND	ND	ND	ND	ND
I13	ND	ND	ND	ND	ND	ND	ND	ND	ND	ND	ND	ND	ND
I8	ND	ND	ND	ND	ND	ND	ND	ND	ND	ND	ND	ND	ND
55-m Stations													
I28	ND	ND	ND	ND	ND	ND	ND	ND	ND	ND	ND	ND	ND
I20	ND	ND	ND	ND	ND	ND	ND	ND	ND	ND	ND	ND	ND
I7	ND	ND	ND	ND	ND	ND	ND	ND	ND	ND	ND	ND	ND
I1	ND	ND	ND	ND	ND	ND	ND	ND	ND	ND	ND	ND	ND
DR (%)	0	0	0	0	0	4	4	0	0	0	0	0	0

[a] Near-ZID station

Appendix D.7 *continued*

Summer 2025	Chlordane								DDT						
	A(c)C	cNon	G(t)C	Hept	HeptEpox	Methoxy	Oxychlor	tNon	o,p-DDD	o,p-DDE	o,p-DDT	p,-p-DDMU	p,p-DDD	p,p-DDE	p,p-DDT
19-m Stations															
I35	ND	ND	ND	ND	ND	ND	ND	ND	ND	ND	ND	ND	ND	189	ND
I34	ND	ND	ND	ND	ND	ND	ND	ND	ND	ND	ND	ND	ND	ND	ND
I31	ND	ND	ND	ND	ND	ND	ND	ND	ND	ND	ND	ND	ND	ND	ND
I23	ND	ND	ND	ND	ND	ND	ND	ND	ND	ND	ND	ND	ND	ND	ND
I18	ND	ND	ND	ND	ND	ND	ND	ND	ND	ND	ND	ND	ND	ND	ND
I10	ND	ND	ND	ND	ND	ND	ND	ND	ND	ND	ND	ND	ND	ND	ND
I4	ND	ND	ND	ND	ND	ND	ND	ND	ND	ND	ND	ND	ND	ND	ND
28-m Stations															
I33	ND	ND	ND	ND	ND	ND	ND	ND	ND	ND	ND	ND	ND	ND	ND
I30	ND	ND	ND	ND	ND	ND	ND	ND	ND	ND	ND	ND	ND	81.9 DNQ	ND
I27	ND	ND	ND	ND	ND	ND	ND	ND	ND	ND	ND	ND	ND	ND	ND
I22	ND	ND	ND	ND	ND	ND	ND	ND	ND	ND	ND	ND	ND	75.9 DNQ	ND
I14[a]	ND	ND	ND	ND	ND	ND	ND	ND	ND	ND	ND	ND	ND	133	ND
I16[a]	ND	ND	ND	ND	ND	ND	ND	ND	ND	ND	ND	ND	ND	ND	ND
I15	ND	ND	ND	ND	ND	ND	ND	ND	ND	ND	ND	ND	ND	80.2 DNQ	109
I12[a]	ND	ND	ND	ND	ND	ND	ND	ND	ND	ND	ND	ND	ND	ND	ND
I9	ND	ND	ND	ND	ND	ND	ND	ND	ND	ND	ND	ND	ND	ND	ND
I6	ND	ND	ND	ND	ND	ND	ND	ND	ND	ND	ND	ND	ND	ND	ND
I2	ND	ND	ND	ND	ND	ND	ND	ND	ND	ND	ND	ND	ND	ND	ND
I3	ND	ND	ND	ND	ND	ND	ND	ND	ND	ND	ND	ND	ND	ND	ND
38-m Stations															
I29	ND	ND	ND	ND	ND	ND	ND	ND	ND	ND	ND	ND	105	490	86.6 DNQ
I21	ND	ND	ND	ND	ND	ND	ND	ND	ND	ND	ND	ND	ND	ND	ND
I13	ND	ND	ND	ND	ND	ND	ND	ND	ND	ND	ND	ND	ND	ND	ND
I8	ND	ND	ND	ND	ND	ND	ND	ND	ND	ND	ND	ND	ND	ND	ND
55-m Stations															
I28	ND	ND	ND	ND	ND	ND	ND	ND	ND	ND	ND	ND	ND	271	ND
I20	ND	ND	ND	ND	ND	ND	ND	ND	ND	ND	ND	ND	ND	ND	ND
I7	ND	ND	ND	ND	ND	ND	ND	ND	ND	ND	ND	ND	ND	ND	ND
I1	ND	ND	ND	ND	ND	ND	ND	ND	ND	ND	ND	ND	ND	ND	ND
DR (%)	0	0	0	0	0	0	0	0	0	0	0	0	4	26	7

[a] Near-ZID station

Appendix D.7 *continued*

Summer 2025	HCH						Endosulfan						
	Alpha	Beta	Delta	Gamma	Aldrin	Dieldrin	Alpha	Beta	Sulfate	Endrin	EndAld	HCB	Mirex
19-m Stations													
I35	ND	ND	ND	ND	ND	ND	ND	ND	ND	ND	ND	ND	ND
I34	ND	ND	ND	ND	ND	ND	ND	ND	ND	ND	ND	ND	ND
I31	ND	ND	ND	ND	ND	ND	ND	ND	ND	ND	ND	ND	ND
I23	ND	ND	ND	ND	ND	ND	ND	ND	ND	ND	ND	ND	ND
I18	ND	ND	ND	ND	ND	ND	ND	ND	ND	ND	ND	ND	ND
I10	ND	ND	ND	ND	ND	ND	ND	ND	ND	ND	ND	ND	ND
I4	ND	ND	ND	ND	ND	ND	ND	ND	ND	ND	ND	ND	ND
28-m Stations													
I33	ND	ND	ND	ND	ND	ND	ND	ND	ND	ND	ND	ND	ND
I30	ND	ND	ND	ND	ND	ND	ND	ND	ND	ND	ND	ND	ND
I27	ND	ND	ND	ND	ND	ND	ND	ND	ND	ND	ND	ND	ND
I22	ND	ND	ND	ND	ND	ND	ND	ND	ND	ND	ND	ND	ND
I14[a]	ND	ND	ND	ND	ND	ND	ND	ND	ND	ND	ND	ND	ND
I16[a]	ND	ND	ND	ND	ND	ND	ND	ND	ND	ND	ND	ND	ND
I15	ND	ND	ND	ND	ND	ND	ND	ND	ND	ND	ND	ND	ND
I12[a]	ND	ND	ND	ND	ND	ND	ND	ND	ND	ND	ND	ND	ND
I9	ND	ND	ND	ND	ND	ND	ND	ND	ND	ND	ND	ND	ND
I6	ND	ND	ND	ND	ND	ND	ND	ND	ND	ND	ND	ND	ND
I2	ND	ND	ND	ND	ND	ND	ND	ND	ND	ND	ND	ND	ND
I3	ND	ND	ND	ND	ND	ND	ND	ND	ND	ND	ND	ND	ND
38-m Stations													
I29	ND	ND	ND	ND	ND	ND	ND	ND	ND	ND	ND	ND	ND
I21	ND	ND	ND	ND	ND	ND	ND	ND	ND	ND	ND	ND	ND
I13	ND	ND	ND	ND	ND	ND	ND	ND	ND	ND	ND	ND	ND
I8	ND	ND	ND	ND	ND	ND	ND	ND	ND	ND	ND	ND	ND
55-m Stations													
I28	ND	ND	ND	ND	ND	ND	ND	ND	ND	ND	ND	ND	ND
I20	ND	ND	ND	ND	ND	ND	ND	ND	ND	ND	ND	ND	ND
I7	ND	ND	ND	ND	ND	ND	ND	ND	ND	ND	ND	ND	ND
I1	ND	ND	ND	ND	ND	ND	ND	ND	ND	ND	ND	ND	ND
DR (%)	0	0	0	0	0	0	0	0	0	0	0	0	0

[a] Near-ZID station

Appendix D.8

Concentrations of PCBs (ppt) detected in sediments from PLOO stations sampled during 2025. See Appendix D.1 for MDLs; DR = detection rate; DNQ = detected not quantified; ND = not detected; NR = not reportable.

Winter 2025	PCB Congener																			
	8	18	28	37	44	49	52	66	70	74	77	81	87	99	101	105	110	114	118	119
88-m Depth Contour																				
B11	ND	ND	ND	ND	ND	ND	ND	ND	ND	ND	ND	ND	ND	ND	ND	ND	ND	ND	ND	ND
B8	ND	ND	ND	ND	ND	ND	ND	ND	ND	ND	ND	ND	ND	ND	ND	ND	ND	ND	ND	ND
E19	ND	ND	ND	ND	ND	ND	ND	ND	ND	ND	ND	ND	ND	ND	ND	ND	ND	ND	ND	ND
E7	ND	ND	ND	ND	ND	ND	ND	ND	ND	ND	ND	ND	ND	ND	ND	ND	ND	ND	ND	ND
E1	ND	ND	ND	ND	ND	ND	ND	ND	ND	ND	ND	ND	78.6 DNQ	80.2 DNQ	170	ND	180	ND	170	ND
98-m Depth Contour																				
B12	ND	ND	ND	ND	ND	ND	ND	ND	ND	ND	ND	ND	ND	ND	ND	ND	ND	ND	ND	ND
B9	ND	ND	ND	ND	ND	ND	ND	ND	ND	ND	ND	ND	ND	ND	ND	ND	ND	ND	ND	ND
E26	ND	ND	ND	ND	ND	ND	ND	ND	ND	ND	ND	ND	ND	ND	ND	ND	ND	ND	ND	ND
E25	ND	ND	ND	ND	ND	ND	ND	ND	ND	ND	ND	ND	ND	ND	ND	ND	ND	ND	ND	ND
E23	ND	ND	ND	ND	ND	ND	ND	ND	ND	ND	ND	ND	ND	ND	ND	ND	ND	ND	ND	ND
E20	ND	ND	ND	ND	ND	ND	ND	ND	ND	ND	ND	ND	ND	ND	ND	ND	ND	ND	65.1 DNQ	ND
E17[a]	ND	ND	ND	ND	ND	ND	ND	ND	ND	ND	ND	ND	ND	ND	ND	ND	ND	ND	ND	ND
E14[a]	ND	ND	ND	ND	ND	ND	ND	ND	ND	ND	ND	ND	ND	ND	ND	ND	ND	ND	ND	ND
E11[a]	ND	ND	ND	ND	ND	ND	ND	ND	ND	ND	ND	ND	ND	ND	ND	ND	ND	ND	ND	ND
E8	ND	ND	ND	ND	ND	ND	ND	ND	ND	ND	ND	ND	ND	ND	ND	ND	ND	ND	ND	ND
E5	ND	ND	ND	ND	ND	ND	ND	ND	ND	ND	ND	ND	ND	ND	ND	ND	ND	ND	ND	ND
E2	ND	ND	ND	ND	86.3 DNQ	ND	190	ND	110	ND	ND	ND	170	150	480	120	380	ND	320	ND
116-m Depth Contour																				
B10	ND	ND	ND	ND	ND	ND	ND	ND	ND	ND	ND	ND	ND	ND	62.3 DNQ	ND	ND	ND	66.1 DNQ	ND
E21	ND	ND	ND	ND	ND	ND	ND	ND	ND	ND	ND	ND	ND	ND	ND	ND	ND	ND	ND	ND
E15[a]	ND	ND	ND	ND	ND	ND	ND	ND	ND	ND	ND	ND	ND	ND	ND	ND	ND	ND	ND	ND
E9	ND	ND	ND	ND	ND	ND	ND	ND	ND	ND	ND	ND	ND	ND	60.2 DNQ	ND	ND	ND	67.3 DNQ	ND
E3	ND	130	130	ND	190	270	400	210	240	103.7 DNQ	ND	ND	230	330	750	230	560	ND	640	ND
DR (%)	0	5	5	0	9	5	9	5	9	5	0	0	14	14	23	9	14	0	27	0

[a] Near-ZID station

Appendix D.8 *continued*

Winter 2025	PCB Congener																					
	123	126	128	138	149	151	153/168	156	157	158	167	169	170	177	180	183	187	189	194	195	201	206
88-m Depth Contour																						
B11	ND	ND	ND	ND	ND	ND	ND	ND	ND	ND	ND	ND	ND	ND	ND	ND	ND	ND	ND	ND	ND	ND
B8	ND	ND	ND	ND	ND	ND	ND	ND	ND	ND	ND	ND	ND	ND	ND	ND	ND	ND	ND	ND	ND	ND
E19	ND	ND	ND	ND	ND	ND	ND	ND	ND	ND	ND	ND	ND	ND	ND	ND	ND	ND	ND	ND	ND	ND
E7	ND	ND	ND	ND	ND	ND	ND	ND	ND	ND	ND	ND	ND	ND	ND	ND	ND	ND	ND	ND	ND	ND
E1	ND	ND	ND	160	150	ND	230	ND	ND	ND	ND	ND	ND	ND	77.6 DNQ	ND	ND	ND	ND	ND	ND	ND
98-m Depth Contour																						
B12	ND	ND	ND	ND	ND	ND	ND	ND	ND	ND	ND	ND	ND	ND	ND	ND	ND	ND	ND	ND	ND	ND
B9	ND	ND	ND	ND	ND	ND	ND	ND	ND	ND	ND	ND	ND	ND	ND	ND	ND	ND	ND	ND	ND	ND
E26	ND	ND	ND	ND	ND	ND	ND	ND	ND	ND	ND	ND	ND	ND	ND	ND	ND	ND	ND	ND	ND	ND
E25	ND	ND	ND	ND	ND	ND	ND	ND	ND	ND	ND	ND	ND	ND	ND	ND	ND	ND	ND	ND	ND	ND
E23	ND	ND	ND	ND	ND	ND	ND	ND	ND	ND	ND	ND	ND	ND	ND	ND	ND	ND	ND	ND	ND	ND
E20	ND	ND	ND	ND	ND	ND	ND	ND	ND	ND	ND	ND	ND	ND	ND	ND	ND	ND	ND	ND	ND	ND
E17[a]	ND	ND	ND	ND	ND	ND	ND	ND	ND	ND	ND	ND	ND	ND	ND	ND	ND	ND	ND	ND	ND	ND
E14[a]	ND	ND	ND	ND	ND	ND	ND	ND	ND	ND	ND	ND	ND	ND	ND	ND	ND	ND	ND	ND	ND	ND
E11[a]	ND	ND	ND	ND	ND	ND	ND	ND	ND	ND	ND	ND	ND	ND	ND	ND	ND	ND	ND	ND	ND	ND
E8	ND	ND	ND	ND	ND	ND	ND	ND	ND	ND	ND	ND	ND	ND	ND	ND	ND	ND	ND	ND	ND	ND
E5	ND	ND	ND	ND	ND	ND	ND	ND	ND	ND	ND	ND	ND	ND	ND	ND	ND	ND	ND	ND	ND	ND
E2	ND	ND	ND	370	240	ND	410	ND	ND	ND	ND	ND	ND	ND	110	ND	ND	ND	ND	ND	ND	ND
116-m Depth Contour																						
B10	ND	ND	ND	75.3 DNQ	ND	ND	ND	ND	ND	ND	ND	ND	ND	ND	ND	ND	ND	ND	ND	ND	ND	ND
E21	ND	ND	ND	ND	ND	ND	ND	ND	ND	ND	ND	ND	ND	ND	ND	ND	ND	ND	ND	ND	ND	ND
E15[a]	ND	ND	ND	ND	ND	ND	ND	ND	ND	ND	ND	ND	ND	ND	ND	ND	ND	ND	ND	ND	ND	ND
E9	ND	ND	ND	ND	ND	ND	ND	ND	ND	ND	ND	ND	ND	ND	ND	ND	ND	ND	ND	ND	ND	ND
E3	63 DNQ	ND	170	630	780	286.85 DNQ	1500	ND	ND	ND	ND	ND	614.75 DNQ	630	4700	1000	3100	ND	3200	820	530	2500
DR (%)	5	0	5	18	14	5	14	0	0	0	0	0	5	5	14	5	5	0	5	5	5	5

[a] Near-ZID station

Appendix D.8 *continued*

Summer 2025	PCB Congener																			
	8	18	28	37	44	49	52	66	70	74	77	81	87	99	101	105	110	114	118	119
88-m Depth Contour																				
B11	ND	ND	ND	ND	ND	ND	ND	ND	ND	ND	ND	ND	ND	ND	ND	ND	ND	ND	ND	ND
B8	ND	ND	ND	ND	ND	ND	ND	ND	ND	ND	ND	ND	ND	ND	ND	ND	ND	ND	ND	ND
E19	ND	ND	ND	ND	ND	ND	ND	ND	ND	ND	ND	ND	ND	ND	ND	ND	ND	ND	ND	ND
E7	ND	ND	ND	ND	ND	ND	ND	ND	ND	ND	ND	ND	ND	ND	ND	ND	ND	ND	90.2 DNQ	ND
E1	ND	ND	ND	ND	ND	ND	ND	ND	ND	ND	ND	ND	74.6 DNQ	89.25 DNQ	140	ND	160	ND	160	ND
98-m Depth Contour																				
B12	ND	ND	ND	ND	ND	ND	ND	ND	ND	ND	ND	ND	ND	ND	ND	ND	ND	ND	ND	ND
B9	ND	ND	ND	ND	ND	ND	ND	ND	ND	ND	ND	ND	ND	ND	ND	ND	ND	ND	ND	ND
E26	ND	ND	ND	ND	ND	ND	ND	ND	ND	ND	ND	ND	ND	ND	ND	ND	ND	ND	ND	ND
E25	ND	ND	ND	ND	ND	ND	ND	ND	ND	ND	ND	ND	ND	ND	ND	ND	ND	ND	ND	ND
E23	ND	ND	ND	ND	ND	ND	ND	ND	ND	ND	ND	ND	ND	ND	ND	ND	ND	ND	ND	ND
E20	ND	ND	ND	ND	ND	ND	ND	ND	ND	ND	ND	ND	ND	ND	ND	ND	ND	ND	ND	ND
E17[a]	ND	ND	ND	ND	ND	ND	ND	ND	ND	ND	ND	ND	ND	ND	ND	ND	ND	ND	ND	ND
E14[a]	ND	ND	ND	ND	ND	ND	ND	ND	ND	ND	ND	ND	ND	ND	ND	ND	ND	ND	ND	ND
E11[a]	ND	ND	ND	ND	ND	ND	ND	ND	ND	ND	ND	ND	ND	ND	ND	ND	ND	ND	ND	ND
E8	ND	ND	ND	ND	ND	ND	ND	ND	ND	ND	ND	ND	ND	ND	ND	ND	ND	ND	ND	ND
E5	ND	ND	ND	ND	ND	ND	ND	ND	ND	ND	ND	ND	ND	ND	ND	ND	ND	ND	ND	ND
E2	ND	ND	ND	ND	ND	ND	ND	ND	ND	ND	ND	ND	ND	74.1 DNQ	120	ND	90	ND	110	ND
116-m Depth Contour																				
B10	ND	ND	ND	ND	ND	ND	ND	ND	ND	ND	ND	ND	ND	ND	ND	ND	ND	ND	ND	ND
E21	ND	ND	ND	ND	ND	ND	ND	ND	ND	ND	ND	ND	ND	ND	ND	ND	ND	ND	ND	ND
E15[a]	ND	ND	ND	ND	ND	ND	ND	ND	ND	ND	ND	ND	ND	ND	ND	ND	ND	ND	ND	ND
E9	ND	ND	ND	ND	ND	ND	81.5 DNQ	ND	ND	ND	ND	ND	ND	ND	140	ND	150	ND	140	ND
E3	ND	ND	ND	ND	ND	79.2 DNQ	130	80.6 DNQ	95	ND	ND	ND	110	150	280	100	280	ND	300	ND
DR (%)	0	0	0	0	0	5	9	5	5	0	0	0	9	14	18	5	18	0	23	0

[a] Near-ZID station

Appendix D.8 *continued*

Summer 2025	PCB Congener																					
	123	126	128	138	149	151	153/168	156	157	158	167	169	170	177	180	183	187	189	194	195	201	206
88-m Depth Contour																						
B11	ND	ND	ND	ND	ND	ND	ND	ND	ND	ND	ND	ND	ND	ND	ND	ND	ND	ND	ND	ND	ND	ND
B8	ND	ND	ND	ND	ND	ND	ND	ND	ND	ND	ND	ND	ND	ND	ND	ND	ND	ND	ND	ND	ND	ND
E19	ND	ND	ND	ND	ND	ND	ND	ND	ND	ND	ND	ND	ND	ND	ND	ND	ND	ND	ND	ND	ND	ND
E7	ND	ND	ND	86 DNQ	ND	ND	ND	ND	ND	ND	ND	ND	ND	ND	ND	ND	ND	ND	ND	ND	ND	ND
E1	ND	ND	ND	160	130	ND	220	ND	ND	ND	ND	ND	ND	ND	110	ND	ND	ND	ND	ND	ND	ND
98-m Depth Contour																						
B12	ND	ND	ND	ND	ND	ND	ND	ND	ND	ND	ND	ND	ND	ND	ND	ND	ND	ND	ND	ND	ND	ND
B9	ND	ND	ND	ND	ND	ND	ND	ND	ND	ND	ND	ND	ND	ND	ND	ND	ND	ND	ND	ND	ND	ND
E26	ND	ND	ND	ND	ND	ND	ND	ND	ND	ND	ND	ND	ND	ND	ND	ND	ND	ND	ND	ND	ND	ND
E25	ND	ND	ND	ND	ND	ND	ND	ND	ND	ND	ND	ND	ND	ND	ND	ND	ND	ND	ND	ND	ND	ND
E23	ND	ND	ND	ND	ND	ND	ND	ND	ND	ND	ND	ND	ND	ND	ND	ND	ND	ND	ND	ND	ND	ND
E20	ND	ND	ND	ND	ND	ND	ND	ND	ND	ND	ND	ND	ND	ND	ND	ND	ND	ND	ND	ND	ND	ND
E17[a]	ND	ND	ND	ND	ND	ND	ND	ND	ND	ND	ND	ND	ND	ND	ND	ND	ND	ND	ND	ND	ND	ND
E14[a]	ND	ND	ND	ND	ND	ND	ND	ND	ND	ND	ND	ND	ND	ND	ND	ND	ND	ND	ND	ND	ND	ND
E11[a]	ND	ND	ND	ND	ND	ND	ND	ND	ND	ND	ND	ND	ND	ND	ND	ND	ND	ND	ND	ND	ND	ND
E8	ND	ND	ND	ND	ND	ND	ND	ND	ND	ND	ND	ND	ND	ND	ND	ND	ND	ND	ND	ND	ND	ND
E5	ND	ND	ND	ND	ND	ND	ND	ND	ND	ND	ND	ND	ND	ND	ND	ND	ND	ND	ND	ND	ND	ND
E2	ND	ND	ND	130	110	ND	190	ND	ND	ND	ND	ND	ND	ND	ND	ND	ND	ND	ND	ND	ND	ND
116-m Depth Contour																						
B10	ND	ND	ND	ND	ND	ND	ND	ND	ND	ND	ND	ND	ND	ND	ND	ND	ND	ND	ND	ND	ND	ND
E21	ND	ND	ND	ND	ND	ND	ND	ND	ND	ND	ND	ND	ND	ND	ND	ND	ND	ND	ND	ND	ND	ND
E15[a]	ND	ND	ND	ND	ND	ND	ND	ND	ND	ND	ND	ND	ND	ND	ND	ND	ND	ND	ND	ND	ND	ND
E9	ND	ND	ND	110	94	ND	144 DNQ	ND	ND	ND	ND	ND	ND	ND	ND	ND	ND	ND	ND	ND	ND	ND
E3	ND	ND	79.1 DNQ	250	230	ND	350	ND	ND	ND	ND	ND	ND	ND	110	ND	130	ND	ND	ND	ND	ND
DR (%)	0	0	5	23	18	0	18	0	0	0	0	0	0	0	9	0	5	0	0	0	0	0

[a] Near-ZID station

Appendix D.9

Concentrations of PCBs (ppt) detected in sediments from SBOO stations sampled during 2025 See Appendix D.1 for MDLs; DR = detection rate; DNQ = detected not quantified; ND = not detected; NR = not reportable.

Winter 2025	PCB Congener																			
	8	18	28	37	44	49	52	66	70	74	77	81	87	99	101	105	110	114	118	119
19-m Stations																				
I35	ND	ND	ND	ND	ND	ND	ND	ND	ND	ND	ND	ND	ND	ND	ND	ND	ND	ND	ND	ND
I34	ND	ND	ND	ND	ND	ND	ND	ND	ND	ND	ND	ND	ND	ND	ND	ND	ND	ND	ND	ND
I31	ND	ND	ND	ND	ND	ND	ND	ND	ND	ND	ND	ND	ND	ND	ND	ND	ND	ND	ND	ND
I23	ND	ND	ND	ND	ND	ND	ND	ND	ND	ND	ND	ND	ND	ND	ND	ND	ND	ND	ND	ND
I18	ND	ND	ND	ND	ND	ND	ND	ND	ND	ND	ND	ND	ND	ND	ND	ND	ND	ND	ND	ND
I10	ND	ND	ND	ND	ND	ND	ND	ND	ND	ND	ND	ND	ND	ND	ND	ND	ND	ND	ND	ND
I4	ND	ND	ND	ND	ND	ND	ND	ND	ND	ND	ND	ND	ND	ND	ND	ND	ND	ND	ND	ND
28-m Stations																				
I33	ND	ND	ND	ND	ND	ND	ND	ND	ND	ND	ND	ND	ND	ND	ND	ND	ND	ND	ND	ND
I30	ND	ND	ND	ND	ND	ND	ND	ND	ND	ND	ND	ND	ND	ND	ND	ND	ND	ND	ND	ND
I27	ND	ND	ND	ND	ND	ND	ND	ND	ND	ND	ND	ND	ND	ND	ND	ND	ND	ND	ND	ND
I22	ND	ND	ND	ND	ND	ND	ND	ND	ND	ND	ND	ND	ND	ND	ND	ND	ND	ND	ND	ND
I14[a]	ND	ND	ND	ND	ND	ND	ND	ND	ND	ND	ND	ND	ND	ND	ND	ND	ND	ND	ND	ND
I16[a]	ND	ND	ND	ND	ND	ND	ND	ND	ND	ND	ND	ND	ND	ND	ND	ND	ND	ND	ND	ND
I15	ND	ND	ND	ND	ND	ND	ND	ND	ND	ND	ND	ND	ND	ND	ND	ND	ND	ND	ND	ND
I12[a]	ND	ND	ND	ND	ND	ND	ND	ND	ND	ND	ND	ND	ND	ND	ND	ND	ND	ND	ND	ND
I9	ND	ND	ND	ND	ND	ND	ND	ND	ND	ND	ND	ND	ND	ND	ND	ND	ND	ND	ND	ND
I6	ND	ND	ND	ND	ND	ND	ND	ND	ND	ND	ND	ND	ND	ND	ND	ND	ND	ND	ND	ND
I2	ND	ND	ND	ND	ND	ND	ND	ND	ND	ND	ND	ND	ND	ND	ND	ND	ND	ND	ND	ND
I3	ND	ND	ND	ND	ND	ND	ND	ND	ND	ND	ND	ND	ND	ND	ND	ND	ND	ND	ND	ND
38-m Stations																				
I29	ND	ND	ND	ND	ND	ND	ND	ND	ND	ND	ND	ND	ND	ND	ND	ND	ND	ND	ND	ND
I21	ND	ND	ND	ND	ND	ND	ND	ND	ND	ND	ND	ND	ND	ND	ND	ND	ND	ND	ND	ND
I13	ND	ND	ND	ND	ND	ND	ND	ND	ND	ND	ND	ND	ND	ND	ND	ND	ND	ND	ND	ND
I8	ND	ND	ND	ND	ND	ND	ND	ND	ND	ND	ND	ND	ND	ND	ND	ND	ND	ND	ND	ND
55-m Stations																				
I28	ND	ND	ND	ND	ND	ND	ND	ND	ND	ND	ND	ND	ND	ND	ND	ND	ND	ND	ND	ND
I20	ND	ND	ND	ND	ND	ND	ND	ND	ND	ND	ND	ND	ND	ND	ND	ND	ND	ND	ND	ND
I7	ND	ND	ND	ND	ND	ND	ND	ND	ND	ND	ND	ND	ND	ND	ND	ND	ND	ND	ND	ND
I1	ND	ND	ND	ND	ND	ND	ND	ND	ND	ND	ND	ND	ND	ND	ND	ND	ND	ND	ND	ND
DR (%)	0	0	0	0	0	0	0	0	0	0	0	0	0	0	0	0	0	0	0	0

[a] Near-ZID station

Appendix D.9 *continued*

Winter 2025	PCB Congener																					
	123	126	128	138	149	151	153/168	156	157	158	167	169	170	177	180	183	187	189	194	195	201	206
19-m Stations																						
I35	ND	ND	ND	ND	ND	ND	ND	ND	ND	ND	ND	ND	ND	ND	ND	ND	ND	ND	ND	ND	ND	ND
I34	ND	ND	ND	ND	ND	ND	ND	ND	ND	ND	ND	ND	ND	ND	ND	ND	ND	ND	ND	ND	ND	ND
I31	ND	ND	ND	ND	ND	ND	ND	ND	ND	ND	ND	ND	ND	ND	ND	ND	ND	ND	ND	ND	ND	ND
I23	ND	ND	ND	ND	ND	ND	ND	ND	ND	ND	ND	ND	ND	ND	ND	ND	ND	ND	ND	ND	ND	ND
I18	ND	ND	ND	ND	ND	ND	ND	ND	ND	ND	ND	ND	ND	ND	ND	ND	ND	ND	ND	ND	ND	ND
I10	ND	ND	ND	ND	ND	ND	ND	ND	ND	ND	ND	ND	ND	ND	ND	ND	ND	ND	ND	ND	ND	ND
I4	ND	ND	ND	ND	ND	ND	ND	ND	ND	ND	ND	ND	ND	ND	ND	ND	ND	ND	ND	ND	ND	ND
28-m Stations																						
I33	ND	ND	ND	ND	ND	ND	ND	ND	ND	ND	ND	ND	ND	ND	ND	ND	ND	ND	ND	ND	ND	ND
I30	ND	ND	ND	ND	ND	ND	ND	ND	ND	ND	ND	ND	ND	ND	ND	ND	ND	ND	ND	ND	ND	ND
I27	ND	ND	ND	ND	ND	ND	ND	ND	ND	ND	ND	ND	ND	ND	ND	ND	ND	ND	ND	ND	ND	ND
I22	ND	ND	ND	ND	ND	ND	ND	ND	ND	ND	ND	ND	ND	ND	ND	ND	ND	ND	ND	ND	ND	ND
I14[a]	ND	ND	ND	ND	ND	ND	ND	ND	ND	ND	ND	ND	ND	ND	ND	ND	ND	ND	ND	ND	ND	ND
I16[a]	ND	ND	ND	ND	ND	ND	ND	ND	ND	ND	ND	ND	ND	ND	ND	ND	ND	ND	ND	ND	ND	ND
I15	ND	ND	ND	ND	ND	ND	ND	ND	ND	ND	ND	ND	ND	ND	ND	ND	ND	ND	ND	ND	ND	ND
I12[a]	ND	ND	ND	ND	ND	ND	ND	ND	ND	ND	ND	ND	ND	ND	ND	ND	ND	ND	ND	ND	ND	ND
I9	ND	ND	ND	ND	ND	ND	ND	ND	ND	ND	ND	ND	ND	ND	ND	ND	ND	ND	ND	ND	ND	ND
I6	ND	ND	ND	ND	ND	ND	ND	ND	ND	ND	ND	ND	ND	ND	ND	ND	ND	ND	ND	ND	ND	ND
I2	ND	ND	ND	ND	ND	ND	ND	ND	ND	ND	ND	ND	ND	ND	ND	ND	ND	ND	ND	ND	ND	ND
I3	ND	ND	ND	ND	ND	ND	ND	ND	ND	ND	ND	ND	ND	ND	ND	ND	ND	ND	ND	ND	ND	ND
38-m Stations																						
I29	ND	ND	ND	ND	ND	ND	ND	ND	ND	ND	ND	ND	ND	ND	ND	ND	ND	ND	ND	ND	ND	ND
I21	ND	ND	ND	ND	ND	ND	ND	ND	ND	ND	ND	ND	ND	ND	ND	ND	ND	ND	ND	ND	ND	ND
I13	ND	ND	ND	ND	ND	ND	ND	ND	ND	ND	ND	ND	ND	ND	ND	ND	ND	ND	ND	ND	ND	ND
I8	ND	ND	ND	ND	ND	ND	ND	ND	ND	ND	ND	ND	ND	ND	ND	ND	ND	ND	ND	ND	ND	ND
55-m Stations																						
I28	ND	ND	ND	ND	ND	ND	ND	ND	ND	ND	ND	ND	ND	ND	ND	ND	ND	ND	ND	ND	ND	ND
I20	ND	ND	ND	ND	ND	ND	ND	ND	ND	ND	ND	ND	ND	ND	ND	ND	ND	ND	ND	ND	ND	ND
I7	ND	ND	ND	ND	ND	ND	ND	ND	ND	ND	ND	ND	ND	ND	ND	ND	ND	ND	ND	ND	ND	ND
I1	ND	ND	ND	ND	ND	ND	ND	ND	ND	ND	ND	ND	ND	ND	ND	ND	ND	ND	ND	ND	ND	ND
DR (%)	0	0	0	0	0	0	0	0	0	0	0	0	0	0	0	0	0	0	0	0	0	0

[a] Near-ZID station

Appendix D.9 *continued*

Summer 2025	PCB Congener																			
	8	18	28	37	44	49	52	66	70	74	77	81	87	99	101	105	110	114	118	119
19-m Stations																				
I35	ND	ND	ND	ND	ND	ND	ND	ND	ND	ND	ND	ND	ND	ND	ND	ND	ND	ND	ND	ND
I34	ND	ND	ND	ND	ND	ND	ND	ND	ND	ND	ND	ND	ND	ND	ND	ND	ND	ND	ND	ND
I31	ND	ND	ND	ND	ND	ND	ND	ND	ND	ND	ND	ND	ND	ND	ND	ND	ND	ND	ND	ND
I23	ND	ND	ND	ND	ND	ND	ND	ND	ND	ND	ND	ND	ND	ND	ND	ND	ND	ND	ND	ND
I18	ND	ND	ND	ND	ND	ND	ND	ND	ND	ND	ND	ND	ND	ND	ND	ND	ND	ND	ND	ND
I10	ND	ND	ND	ND	ND	ND	ND	ND	ND	ND	ND	ND	ND	ND	ND	ND	ND	ND	ND	ND
I4	ND	ND	ND	ND	ND	ND	ND	ND	ND	ND	ND	ND	ND	ND	ND	ND	ND	ND	ND	ND
28-m Stations																				
I33	ND	ND	ND	ND	ND	ND	ND	ND	ND	ND	ND	ND	ND	ND	ND	ND	ND	ND	ND	ND
I30	ND	ND	ND	ND	ND	ND	ND	ND	ND	ND	ND	ND	ND	ND	ND	ND	ND	ND	ND	ND
I27	ND	ND	ND	ND	ND	ND	ND	ND	ND	ND	ND	ND	ND	ND	ND	ND	ND	ND	ND	ND
I22	ND	ND	ND	ND	ND	ND	ND	ND	ND	ND	ND	ND	ND	ND	ND	ND	ND	ND	ND	ND
I14[a]	ND	ND	ND	ND	ND	ND	ND	ND	ND	ND	ND	ND	ND	ND	ND	ND	ND	ND	ND	ND
I16[a]	ND	ND	ND	ND	ND	ND	ND	ND	ND	ND	ND	ND	ND	ND	ND	ND	ND	ND	ND	ND
I15	ND	ND	ND	ND	ND	ND	ND	ND	ND	ND	ND	ND	ND	ND	ND	ND	ND	ND	ND	ND
I12[a]	ND	ND	ND	ND	ND	ND	ND	ND	ND	ND	ND	ND	ND	ND	ND	ND	ND	ND	ND	ND
I9	ND	ND	ND	ND	ND	ND	ND	ND	ND	ND	ND	ND	ND	ND	ND	ND	ND	ND	ND	ND
I6	ND	ND	ND	ND	ND	ND	ND	ND	ND	ND	ND	ND	ND	ND	ND	ND	ND	ND	ND	ND
I2	350	ND	ND	ND	ND	ND	ND	ND	ND	ND	ND	ND	ND	ND	ND	ND	ND	ND	ND	ND
I3	ND	ND	ND	ND	ND	ND	ND	ND	ND	ND	ND	ND	ND	ND	ND	ND	ND	ND	ND	ND
38-m Stations																				
I29	ND	ND	ND	ND	ND	ND	ND	ND	ND	ND	ND	ND	ND	ND	ND	ND	ND	ND	ND	ND
I21	ND	ND	ND	ND	ND	ND	ND	ND	ND	ND	ND	ND	ND	ND	ND	ND	ND	ND	ND	ND
I13	ND	ND	ND	ND	ND	ND	ND	ND	ND	ND	ND	ND	ND	ND	ND	ND	ND	ND	ND	ND
I8	ND	ND	ND	ND	ND	ND	ND	ND	ND	ND	ND	ND	ND	ND	ND	ND	ND	ND	ND	ND
55-m Stations																				
I28	ND	ND	ND	ND	ND	ND	ND	ND	ND	ND	ND	ND	ND	ND	ND	ND	ND	ND	ND	ND
I20	ND	ND	ND	ND	ND	ND	ND	ND	ND	ND	ND	ND	ND	ND	ND	ND	ND	ND	ND	ND
I7	ND	ND	ND	ND	ND	ND	ND	ND	ND	ND	ND	ND	ND	ND	ND	ND	ND	ND	ND	ND
I1	ND	ND	ND	ND	ND	ND	ND	ND	ND	ND	ND	ND	ND	ND	ND	ND	ND	ND	ND	ND
DR (%)	4	0	0	0	0	0	0	0	0	0	0	0	0	0	0	0	0	0	0	0

[a] Near-ZID station

Appendix D.9 *continued*

Summer 2025	PCB Congener																					
	123	126	128	138	149	151	153/168	156	157	158	167	169	170	177	180	183	187	189	194	195	201	206
19-m Stations																						
I35	ND	ND	ND	ND	ND	ND	ND	ND	ND	ND	ND	ND	ND	ND	ND	ND	ND	ND	ND	ND	ND	ND
I34	ND	ND	ND	ND	ND	ND	ND	ND	ND	ND	ND	ND	ND	ND	ND	ND	ND	ND	ND	ND	ND	ND
I31	ND	ND	ND	ND	ND	ND	ND	ND	ND	ND	ND	ND	ND	ND	ND	ND	ND	ND	ND	ND	ND	ND
I23	ND	ND	ND	ND	ND	ND	ND	ND	ND	ND	ND	ND	ND	ND	ND	ND	ND	ND	ND	ND	ND	ND
I18	ND	ND	ND	ND	ND	ND	ND	ND	ND	ND	ND	ND	ND	ND	ND	ND	ND	ND	ND	ND	ND	ND
I10	ND	ND	ND	ND	ND	ND	ND	ND	ND	ND	ND	ND	ND	ND	ND	ND	ND	ND	ND	ND	ND	ND
I4	ND	ND	ND	ND	ND	ND	ND	ND	ND	ND	ND	ND	ND	ND	ND	ND	ND	ND	ND	ND	ND	ND
28-m Stations																						
I33	ND	ND	ND	ND	ND	ND	ND	ND	ND	ND	ND	ND	ND	ND	ND	ND	ND	ND	ND	ND	ND	ND
I30	ND	ND	ND	ND	ND	ND	ND	ND	ND	ND	ND	ND	ND	ND	ND	ND	ND	ND	ND	ND	ND	ND
I27	ND	ND	ND	ND	ND	ND	ND	ND	ND	ND	ND	ND	ND	ND	ND	ND	ND	ND	ND	ND	ND	ND
I22	ND	ND	ND	ND	ND	ND	ND	ND	ND	ND	ND	ND	ND	ND	ND	ND	ND	ND	ND	ND	ND	ND
I14[a]	ND	ND	ND	ND	ND	ND	ND	ND	ND	ND	ND	ND	ND	ND	ND	ND	ND	ND	ND	ND	ND	ND
I16[a]	ND	ND	ND	ND	ND	ND	ND	ND	ND	ND	ND	ND	ND	ND	ND	ND	ND	ND	ND	ND	ND	ND
I15	ND	ND	ND	ND	ND	ND	ND	ND	ND	ND	ND	ND	ND	ND	ND	ND	ND	ND	ND	ND	ND	ND
I12[a]	ND	ND	ND	ND	ND	ND	ND	ND	ND	ND	ND	ND	ND	ND	ND	ND	ND	ND	ND	ND	ND	ND
I9	ND	ND	ND	ND	ND	ND	ND	ND	ND	ND	ND	ND	ND	ND	ND	ND	ND	ND	ND	ND	ND	ND
I6	ND	ND	ND	ND	ND	ND	ND	ND	ND	ND	ND	ND	ND	ND	ND	ND	ND	ND	ND	ND	ND	ND
I2	ND	ND	ND	ND	ND	ND	ND	ND	ND	ND	ND	ND	ND	ND	ND	ND	ND	ND	ND	ND	ND	ND
I3	ND	ND	ND	ND	ND	ND	ND	ND	ND	ND	ND	ND	ND	ND	ND	ND	ND	ND	ND	ND	ND	ND
38-m Stations																						
I29	ND	ND	ND	ND	ND	ND	ND	ND	ND	ND	ND	ND	ND	ND	ND	ND	ND	ND	ND	ND	ND	ND
I21	ND	ND	ND	ND	ND	ND	ND	ND	ND	ND	ND	ND	ND	ND	ND	ND	ND	ND	ND	ND	ND	ND
I13	ND	ND	ND	ND	ND	ND	ND	ND	ND	ND	ND	ND	ND	ND	ND	ND	ND	ND	ND	ND	ND	ND
I8	ND	ND	ND	ND	ND	ND	ND	ND	ND	ND	ND	ND	ND	ND	ND	ND	ND	ND	ND	ND	ND	ND
55-m Stations																						
I28	ND	ND	ND	ND	ND	ND	ND	ND	ND	ND	ND	ND	ND	ND	ND	ND	ND	ND	ND	ND	ND	ND
I20	ND	ND	ND	ND	ND	ND	ND	ND	ND	ND	ND	ND	ND	ND	ND	ND	ND	ND	ND	ND	ND	ND
I7	ND	ND	ND	ND	ND	ND	ND	ND	ND	ND	ND	ND	ND	ND	ND	ND	ND	ND	ND	ND	ND	ND
I1	ND	ND	ND	ND	ND	ND	ND	ND	ND	ND	ND	ND	ND	ND	ND	ND	ND	ND	ND	ND	ND	ND
DR (%)	0	0	0	0	0	0	0	0	0	0	0	0	0	0	0	0	0	0	0	0	0	0

[a] Near-ZID station

Appendix D.10

Concentrations of PAHs (ppb) detected in sediments from PLOO stations sampled during 2025. See Appendix D.1 for MDLs; DR = detection rate; DNQ = detected not quantified; ND = not detected; NR = not reportable.

Winter 2025	1-methyl naphthalene	1-methyl phenanthrene	2-methyl naphthalene	2,3,5-trimethyl naphthalene	2,6-dimethyl naphthalene	3,4-benzo(B) fluoranthene	Acenaphthene	Acenaphthylene	Anthracene	Benzo[A] anthracene	Benzo[A] pyrene
88-m Depth Contour											
B11	ND	ND	ND	ND	ND	ND	ND	ND	ND	ND	ND
B8	ND	ND	ND	ND	ND	ND	ND	ND	ND	ND	ND
E19	ND	ND	ND	ND	ND	ND	ND	ND	ND	ND	ND
E7	ND	ND	ND	ND	ND	19.7	ND	ND	NR	ND	ND
E1	ND	ND	ND	ND	ND	ND	ND	ND	ND	ND	ND
98-m Depth Contour											
B12	ND	ND	ND	ND	ND	ND	ND	ND	NR	ND	ND
B9	ND	ND	ND	ND	ND	ND	ND	ND	ND	ND	ND
E26	ND	ND	ND	ND	ND	ND	ND	ND	NR	ND	ND
E25	ND	ND	ND	ND	ND	ND	ND	ND	NR	ND	ND
E23	ND	ND	ND	ND	ND	ND	ND	ND	NR	ND	ND
E20	ND	ND	ND	ND	ND	ND	ND	ND	NR	ND	ND
E17[a]	ND	ND	ND	ND	ND	ND	ND	ND	NR	ND	ND
E14[a]	ND	ND	ND	ND	ND	ND	ND	ND	ND	ND	ND
E11[a]	ND	ND	ND	ND	ND	ND	ND	ND	ND	ND	ND
E8	ND	ND	ND	ND	ND	ND	ND	ND	NR	ND	ND
E5	ND	ND	ND	ND	ND	ND	ND	ND	ND	ND	ND
E2	ND	ND	ND	ND	ND	32.1	ND	ND	NR	ND	ND
116-m Depth Contour											
B10	ND	ND	ND	ND	ND	ND	ND	ND	ND	ND	ND
E21	ND	ND	ND	ND	ND	ND	ND	ND	ND	ND	ND
E15[a]	ND	ND	ND	ND	ND	ND	ND	ND	ND	ND	ND
E9	ND	ND	ND	ND	ND	ND	ND	ND	NR	ND	ND
E3	ND	ND	ND	ND	ND	19.2	ND	ND	NR	ND	ND
DR (%)	0	0	0	0	0	14	0	0	0	0	0

[a] Near-ZID station

Appendix D.10 *continued*

Winter 2025	Benzo[e] pyrene	Benzo[G,H,I] perylene	Benzo[K] fluoranthene	Biphenyl	Chrysene	Dibenzo(A,H) anthracene	Fluoranthene	Fluorene	Indeno(1,2,3-CD) pyrene	Naphthalene	Perylene	Phenanthrene	Pyrene
88-m Depth Contour													
B11	ND	ND	ND	ND	ND	ND	ND	ND	ND	ND	ND	ND	ND
B8	ND	ND	ND	ND	ND	ND	ND	ND	ND	ND	ND	ND	ND
E19	ND	ND	ND	ND	ND	ND	ND	ND	ND	ND	ND	ND	ND
E7	ND	ND	ND	ND	6.06 DNQ	ND	ND	ND	ND	ND	ND	ND	8.68
E1	ND	ND	ND	ND	ND	ND	ND	ND	ND	ND	NR	ND	ND
98-m Depth Contour													
B12	ND	ND	ND	ND	ND	ND	ND	ND	ND	ND	ND	ND	ND
B9	ND	ND	ND	ND	ND	ND	ND	ND	ND	ND	ND	ND	ND
E26	ND	ND	ND	ND	ND	ND	ND	ND	ND	ND	ND	ND	ND
E25	ND	ND	ND	ND	ND	ND	ND	ND	ND	ND	ND	ND	ND
E23	ND	ND	ND	ND	ND	ND	ND	ND	ND	ND	ND	ND	ND
E20	ND	ND	ND	ND	ND	ND	ND	ND	ND	ND	ND	ND	ND
E17[a]	ND	ND	ND	ND	ND	ND	ND	ND	ND	ND	ND	ND	ND
E14[a]	ND	ND	ND	ND	ND	ND	ND	ND	ND	ND	NR	ND	ND
E11[a]	ND	ND	ND	ND	ND	ND	ND	ND	ND	ND	ND	ND	ND
E8	ND	ND	ND	ND	ND	ND	ND	ND	ND	ND	ND	ND	ND
E5	ND	ND	ND	ND	ND	ND	ND	ND	ND	ND	NR	ND	ND
E2	15.9	16.6	ND	ND	ND	ND	19.4	ND	ND	ND	ND	ND	20.8
116-m Depth Contour													
B10	ND	ND	ND	ND	ND	ND	ND	ND	ND	ND	ND	ND	ND
E21	ND	ND	ND	ND	ND	ND	ND	ND	ND	ND	ND	ND	ND
E15[a]	ND	ND	ND	ND	ND	ND	ND	ND	ND	ND	NR	ND	ND
E9	ND	ND	ND	ND	ND	ND	ND	ND	ND	ND	ND	ND	ND
E3	ND	ND	ND	ND	5.82	ND	ND	ND	ND	ND	ND	ND	8.56
DR (%)	5	5	0	0	9	0	5	0	0	0	0	0	14

[a] Near-ZID station

Appendix D.10 *continued*

Summer 2025	1-methyl NRphthalene	1-methyl pheNRnthrene	2-methyl NRphthalene	2,3,5-trimethyl NRphthalene	2,6-dimethyl NRphthalene	3,4-benzo(B) fluoranthene	AceNRphthene	AceNRphthylene	Anthracene	Benzo[A] anthracene	Benzo[A] pyrene
88-m Depth Contour											
B11	ND	ND	ND	ND	ND	ND	ND	ND	NR	ND	ND
B8	ND	ND	ND	ND	ND	ND	ND	ND	NR	ND	ND
E19	ND	ND	ND	ND	ND	ND	ND	ND	NR	ND	ND
E7	ND	ND	ND	ND	ND	ND	ND	ND	NR	ND	ND
E1	ND	ND	ND	ND	ND	ND	ND	ND	NR	ND	ND
98-m Depth Contour											
B12	ND	ND	ND	ND	ND	ND	ND	ND	NR	ND	ND
B9	ND	ND	ND	ND	ND	ND	ND	ND	ND	ND	ND
E26	ND	ND	ND	ND	ND	ND	ND	ND	ND	ND	ND
E25	ND	ND	ND	ND	ND	ND	ND	ND	ND	ND	ND
E23	ND	ND	ND	ND	ND	ND	ND	ND	ND	ND	ND
E20	ND	ND	ND	ND	ND	ND	ND	ND	NR	ND	ND
E17[a]	ND	ND	ND	ND	ND	ND	ND	ND	ND	ND	ND
E14[a]	ND	ND	ND	ND	ND	ND	ND	ND	ND	ND	ND
E11[a]	ND	ND	ND	ND	ND	ND	ND	ND	NR	ND	ND
E8	ND	ND	ND	ND	ND	ND	ND	ND	NR	ND	ND
E5	ND	ND	ND	ND	ND	ND	ND	ND	ND	ND	ND
E2	ND	ND	ND	ND	ND	15.4	ND	ND	NR	ND	ND
116-m Depth Contour											
B10	ND	ND	ND	ND	ND	ND	ND	ND	NR	ND	ND
E21	ND	ND	ND	ND	ND	ND	ND	ND	NR	ND	ND
E15[a]	ND	ND	ND	ND	ND	ND	ND	ND	NR	ND	ND
E9	ND	ND	ND	ND	ND	16.7	ND	ND	NR	ND	ND
E3	ND	ND	ND	ND	ND	25.5	ND	ND	NR	ND	23.5
DR (%)	0	0	0	0	0	14	0	0	0	0	5

[a] Near-ZID station

Appendix D.10 *continued*

Summer 2025	Benzo[e] pyrene	Benzo[G,H,I] perylene	Benzo[K] fluoranthene	Biphenyl	Chrysene	Dibenzo(A,H) anthracene	Fluoranthene	Fluorene	Indeno(1,2,3-CD) pyrene	Naphthalene	Perylene	Phenanthrene	Pyrene
88-m Depth Contour													
B11	ND	ND	ND	ND	ND	ND	ND	ND	ND	ND	ND	ND	ND
B8	ND	ND	ND	ND	ND	ND	ND	ND	ND	ND	ND	ND	ND
E19	ND	ND	ND	ND	ND	ND	ND	ND	ND	ND	ND	ND	ND
E7	ND	ND	ND	ND	NR	ND	ND	ND	ND	ND	ND	ND	ND
E1	ND	ND	ND	ND	NR	ND	ND	ND	ND	ND	ND	ND	ND
98-m Depth Contour													
B12	ND	ND	ND	ND	ND	ND	ND	ND	ND	ND	ND	ND	ND
B9	ND	ND	ND	ND	ND	ND	ND	ND	ND	ND	ND	ND	ND
E26	ND	ND	ND	ND	ND	ND	ND	ND	ND	ND	ND	ND	ND
E25	ND	ND	ND	ND	ND	ND	ND	ND	ND	ND	ND	ND	ND
E23	ND	ND	ND	ND	ND	ND	ND	ND	ND	ND	ND	ND	ND
E20	ND	ND	ND	ND	NR	ND	ND	ND	ND	ND	ND	ND	ND
E17[a]	ND	ND	ND	ND	ND	ND	ND	ND	ND	ND	ND	ND	ND
E14[a]	ND	ND	ND	ND	ND	ND	ND	ND	ND	ND	ND	ND	ND
E11[a]	ND	ND	ND	ND	NR	ND	ND	ND	ND	ND	ND	ND	ND
E8	ND	ND	ND	ND	NR	ND	ND	ND	ND	ND	ND	ND	ND
E5	ND	ND	ND	ND	ND	ND	ND	ND	ND	ND	ND	ND	ND
E2	ND	ND	ND	ND	NR	ND	ND	ND	ND	ND	ND	ND	ND
116-m Depth Contour													
B10	ND	ND	ND	ND	ND	ND	ND	ND	ND	ND	ND	ND	ND
E21	ND	ND	ND	ND	NR	ND	ND	ND	ND	ND	ND	ND	ND
E15[a]	ND	ND	ND	ND	NR	ND	ND	ND	ND	ND	ND	ND	ND
E9	ND	ND	ND	ND	NR	ND	ND	ND	ND	ND	ND	ND	10.7
E3	ND	15.5	ND	ND	NR	ND	13.1	ND	ND	ND	ND	8.72	20.2
DR (%)	0	5	0	0	0	0	5	0	0	0	0	5	9

[a] Near-ZID station

Appendix D.11

Concentrations of PAHs (ppb) detected in sediments from SBOO stations sampled during 2025. See Appendix D.1 for MDLs; DR = detection rate; DNQ = detected not quantified; ND = not detected; NR = not reportable.

Winter 2025	1-methyl naphthalene	1-methyl phenanthrene	2-methyl naphthalene	2,3,5-trimethyl naphthalene	2,6-dimethyl naphthalene	3,4-benzo(B) fluoranthene	Acenaphthene	Acenaphthylene	Anthracene	Benzo[A] anthracene	Benzo[A] pyrene
19-m Stations											
I35	ND	ND	ND	ND	ND	ND	ND	ND	NR	ND	ND
I34	ND	ND	ND	ND	ND	ND	ND	ND	ND	ND	ND
I31	ND	ND	ND	ND	ND	ND	ND	ND	NR	ND	ND
I23	ND	ND	ND	ND	ND	ND	ND	ND	ND	ND	ND
I18	ND	ND	ND	ND	ND	ND	ND	ND	NR	ND	ND
I10	ND	ND	ND	ND	ND	ND	ND	ND	ND	ND	ND
I4	ND	ND	ND	ND	ND	ND	ND	ND	ND	ND	ND
28-m Stations											
I33	ND	ND	ND	ND	ND	ND	ND	ND	ND	ND	ND
I30	ND	ND	ND	ND	ND	ND	ND	ND	ND	ND	ND
I27	ND	ND	ND	ND	ND	ND	ND	ND	ND	ND	ND
I22	ND	ND	ND	ND	ND	ND	ND	ND	ND	ND	ND
I14[a]	ND	ND	ND	ND	ND	ND	ND	ND	NR	ND	ND
I16[a]	ND	ND	ND	ND	ND	ND	ND	ND	ND	ND	ND
I15	ND	ND	ND	ND	ND	ND	ND	ND	NR	ND	ND
I12[a]	ND	ND	ND	ND	ND	ND	ND	ND	NR	ND	ND
I9	ND	ND	ND	ND	ND	ND	ND	ND	ND	ND	ND
I6	ND	ND	ND	ND	ND	ND	ND	ND	ND	ND	ND
I2	ND	ND	ND	ND	ND	ND	ND	ND	ND	ND	ND
I3	ND	ND	ND	ND	ND	ND	ND	ND	ND	ND	ND
38-m Stations											
I29	ND	ND	ND	ND	ND	ND	ND	ND	NR	ND	ND
I21	ND	ND	ND	ND	ND	ND	ND	ND	NR	ND	ND
I13	ND	ND	ND	ND	ND	ND	ND	ND	ND	ND	ND
I8	ND	ND	ND	ND	ND	ND	ND	ND	ND	ND	ND
55-m Stations											
I28	ND	ND	ND	ND	ND	ND	ND	ND	ND	ND	ND
I20	ND	ND	ND	ND	ND	ND	ND	ND	ND	ND	ND
I7	ND	ND	ND	ND	ND	ND	ND	ND	ND	ND	ND
I1	ND	ND	ND	ND	ND	ND	ND	ND	ND	ND	ND
DR (%)	0	0	0	0	0	0	0	0	0	0	0

[a] Near-ZID station

Appendix D.11 *continued*

Winter 2025	Benzo[e] pyrene	Benzo[G,H,I] perylene	Benzo[K] fluoranthene	Biphenyl	Chrysene	Dibenzo(A,H) anthracene	Fluoranthene	Fluorene	Indeno(1,2,3-CD) pyrene	Naphthalene	Perylene	Phenanthrene	Pyrene
19-m Stations													
I35	ND	ND	ND	ND	ND	ND	ND	ND	ND	ND	ND	ND	ND
I34	ND	ND	ND	ND	ND	ND	ND	ND	ND	ND	NR	ND	ND
I31	ND	ND	ND	ND	ND	ND	ND	ND	ND	ND	ND	ND	ND
I23	ND	ND	ND	ND	ND	ND	ND	ND	ND	ND	NR	ND	ND
I18	ND	ND	ND	ND	ND	ND	ND	ND	ND	ND	ND	ND	ND
I10	ND	ND	ND	ND	ND	ND	ND	ND	ND	ND	ND	ND	ND
I4	ND	ND	ND	ND	ND	ND	ND	ND	ND	ND	ND	ND	ND
28-m Stations													
I33	ND	ND	ND	ND	ND	ND	ND	ND	ND	ND	ND	ND	ND
I30	ND	ND	ND	ND	ND	ND	ND	ND	ND	ND	ND	ND	ND
I27	ND	ND	ND	ND	ND	ND	ND	ND	ND	ND	NR	ND	ND
I22	ND	ND	ND	ND	ND	ND	ND	4.66 DNQ	ND	ND	NR	ND	ND
I14[a]	ND	ND	ND	ND	ND	ND	ND	ND	ND	ND	ND	ND	ND
I16[a]	ND	ND	ND	ND	ND	ND	ND	ND	ND	ND	ND	ND	ND
I15	ND	ND	ND	ND	ND	ND	ND	ND	ND	ND	ND	ND	ND
I12[a]	ND	ND	ND	ND	ND	ND	ND	ND	ND	ND	ND	ND	ND
I9	ND	ND	ND	ND	ND	ND	ND	ND	ND	ND	ND	ND	ND
I6	ND	ND	ND	ND	ND	ND	ND	ND	ND	ND	ND	ND	ND
I2	ND	ND	ND	ND	ND	ND	ND	ND	ND	ND	ND	ND	ND
I3	ND	ND	ND	ND	ND	ND	ND	ND	ND	ND	ND	ND	ND
38-m Stations													
I29	ND	ND	ND	ND	ND	ND	ND	ND	ND	ND	ND	ND	ND
I21	ND	ND	ND	ND	ND	ND	ND	ND	ND	ND	ND	ND	ND
I13	ND	ND	ND	ND	ND	ND	ND	ND	ND	ND	ND	ND	ND
I8	ND	ND	ND	ND	ND	ND	ND	ND	ND	ND	ND	ND	ND
55-m Stations													
I28	ND	ND	ND	ND	ND	ND	ND	ND	ND	ND	NR	ND	ND
I20	ND	ND	ND	ND	ND	ND	ND	ND	ND	ND	NR	ND	ND
I7	ND	ND	ND	ND	ND	ND	ND	ND	ND	ND	ND	ND	ND
I1	ND	ND	ND	ND	ND	ND	ND	ND	ND	ND	ND	ND	ND
DR (%)	0	0	0	0	0	0	0	4	0	0	0	0	0

[a] Near-ZID station

Appendix D.11 *continued*

Summer 2025	1-methyl naphthalene	1-methyl phenanthrene	2-methyl naphthalene	2,3,5-trimethyl naphthalene	2,6-dimethyl naphthalene	3,4-benzo(B) fluoranthene	Acenaphthene	Acenaphthylene	Anthracene	Benzo[A] anthracene	Benzo[A] pyrene
19-m Stations											
I35	ND	ND	ND	ND	ND	ND	ND	ND	ND	ND	ND
I34	ND	ND	ND	ND	ND	ND	ND	ND	ND	ND	ND
I31	ND	ND	ND	ND	ND	ND	ND	ND	ND	ND	ND
I23	ND	ND	ND	ND	ND	ND	ND	ND	ND	ND	ND
I18	ND	ND	ND	ND	ND	ND	ND	ND	ND	ND	ND
I10	ND	ND	ND	ND	ND	ND	ND	ND	ND	ND	ND
I4	ND	ND	ND	ND	ND	ND	ND	ND	ND	ND	ND
28-m Stations											
I33	ND	ND	ND	ND	ND	ND	ND	ND	ND	ND	ND
I30	ND	ND	ND	ND	ND	ND	ND	ND	ND	ND	ND
I27	ND	ND	ND	ND	ND	ND	ND	ND	ND	ND	ND
I22	ND	ND	ND	ND	ND	ND	ND	ND	ND	ND	ND
I14[a]	ND	ND	ND	ND	ND	ND	ND	ND	ND	ND	ND
I16[a]	ND	ND	ND	ND	ND	ND	ND	ND	ND	ND	ND
I15	ND	ND	ND	ND	ND	ND	ND	ND	ND	ND	ND
I12[a]	ND	ND	ND	ND	ND	ND	ND	ND	ND	ND	ND
I9	ND	ND	ND	ND	5.25 DNQ	ND	ND	ND	ND	ND	ND
I6	ND	ND	ND	ND	ND	ND	ND	ND	ND	ND	ND
I2	ND	ND	ND	ND	ND	ND	ND	ND	ND	ND	ND
I3	ND	ND	ND	ND	ND	ND	ND	ND	ND	ND	ND
38-m Stations											
I29	ND	ND	ND	ND	ND	ND	ND	ND	ND	ND	ND
I21	ND	ND	ND	ND	ND	ND	ND	ND	ND	ND	ND
I13	ND	ND	ND	ND	ND	ND	ND	ND	ND	ND	ND
I8	ND	ND	ND	ND	ND	ND	ND	ND	ND	ND	ND
55-m Stations											
I28	ND	ND	ND	ND	ND	ND	ND	ND	ND	ND	ND
I20	ND	ND	ND	ND	ND	ND	ND	ND	ND	ND	ND
I7	ND	ND	ND	ND	ND	ND	ND	ND	ND	ND	ND
I1	ND	ND	ND	ND	ND	ND	ND	ND	NA	ND	
DR (%)	0	0	0	0	4	0	0	0	0	0	0

[a] Near-ZID station

Appendix D.11 *continued*

Summer 2025	Benzo[e] pyrene	Benzo[G,H,I] perylene	Benzo[K] fluoranthene	Biphenyl	Chrysene	Dibenzo(A,H) anthracene	Fluoranthene	Fluorene	Indeno(1,2,3-CD) pyrene	Naphthalene	Perylene	Phenanthrene	Pyrene
19-m Stations													
I35	ND	ND	ND	ND	ND	ND	ND	ND	ND	ND	ND	ND	ND
I34	ND	ND	ND	ND	ND	ND	ND	ND	ND	ND	ND	ND	ND
I31	ND	ND	ND	ND	ND	ND	ND	ND	ND	ND	ND	ND	ND
I23	ND	ND	ND	ND	ND	ND	ND	ND	ND	ND	ND	ND	ND
I18	ND	ND	ND	ND	ND	ND	ND	ND	ND	ND	ND	ND	ND
I10	ND	ND	ND	ND	ND	ND	ND	ND	ND	ND	ND	ND	ND
I4	ND	ND	ND	ND	ND	ND	ND	ND	ND	ND	ND	ND	ND
28-m Stations													
I33	ND	ND	ND	ND	ND	ND	ND	ND	ND	ND	ND	ND	ND
I30	ND	ND	ND	ND	ND	ND	ND	ND	ND	ND	ND	ND	ND
I27	ND	ND	ND	ND	ND	ND	ND	ND	ND	ND	ND	ND	ND
I22	ND	ND	ND	ND	ND	ND	ND	ND	ND	ND	ND	ND	ND
I14[a]	ND	ND	ND	ND	ND	ND	ND	ND	ND	ND	ND	ND	ND
I16[a]	ND	ND	ND	ND	ND	ND	ND	ND	ND	ND	ND	ND	ND
I15	ND	ND	ND	ND	ND	ND	ND	ND	ND	ND	ND	ND	ND
I12[a]	ND	ND	ND	ND	ND	ND	ND	ND	ND	ND	ND	ND	ND
I9	ND	ND	ND	ND	ND	ND	ND	ND	ND	ND	ND	ND	ND
I6	ND	ND	ND	ND	ND	ND	ND	ND	ND	ND	ND	ND	ND
I2	ND	ND	ND	ND	ND	ND	ND	ND	ND	ND	ND	ND	ND
I3	ND	ND	ND	ND	ND	ND	ND	ND	ND	ND	ND	ND	ND
38-m Stations													
I29	ND	ND	ND	ND	ND	ND	ND	ND	ND	ND	ND	ND	ND
I21	ND	ND	ND	ND	ND	ND	ND	ND	ND	ND	ND	ND	ND
I13	ND	ND	ND	ND	ND	ND	ND	ND	ND	ND	ND	ND	ND
I8	ND	ND	ND	ND	ND	ND	ND	ND	ND	ND	ND	ND	ND
55-m Stations													
I28	ND	ND	ND	ND	ND	ND	ND	ND	ND	ND	ND	ND	ND
I20	ND	ND	ND	ND	ND	ND	ND	ND	ND	ND	ND	ND	ND
I7	ND	ND	ND	ND	ND	ND	ND	ND	ND	ND	ND	ND	ND
I1	ND	ND	ND	ND	NA	NA	ND	ND	ND	ND	ND	ND	ND
DR (%)	0	0	0	0	0	0	0	0	0	0	0	0	0

[a] Near-ZID station

Appendix D.12

Concentrations of PBDEs (ppt) detected in sediments from SBOO stations sampled during 2025. See Appendix D.1 for MDLs; DR = detection rate; DNQ = detected not quantified; ND = not detected; NR = not reportable.

Winter 2025	BDE-17	BDE-28	BDE-47	BDE-49	BDE-66	BDE-85	BDE-99	BDE-100	BDE-138	BDE-153	BDE-154	BDE-183	BDE-190
19-m Stations													
I35	ND	ND	ND	ND	ND	ND	ND	ND	ND	ND	ND	ND	ND
I34	ND	ND	ND	ND	ND	ND	ND	ND	ND	ND	ND	ND	ND
I31	ND	ND	ND	ND	ND	ND	ND	ND	ND	ND	ND	ND	ND
I23	ND	ND	ND	ND	ND	ND	ND	ND	ND	ND	ND	ND	ND
I18	ND	ND	ND	ND	ND	ND	ND	ND	ND	ND	ND	ND	ND
I10	ND	ND	ND	ND	ND	ND	ND	ND	ND	ND	ND	ND	ND
I4	ND	ND	ND	ND	ND	ND	ND	ND	ND	ND	ND	ND	ND
28-m Stations													
I33	ND	ND	ND	ND	ND	ND	ND	ND	ND	ND	ND	ND	ND
I30	ND	ND	122	ND	ND	ND	ND	31.8 DNQ	ND	ND	ND	ND	ND
I27	ND	ND	ND	ND	ND	ND	ND	ND	ND	ND	ND	ND	ND
I22	ND	ND	ND	ND	ND	ND	ND	ND	ND	ND	ND	ND	ND
I14[a]	ND	ND	ND	ND	ND	ND	ND	ND	ND	ND	ND	ND	ND
I16[a]	ND	ND	ND	ND	ND	ND	ND	ND	ND	ND	ND	ND	ND
I15	ND	ND	ND	ND	ND	ND	ND	ND	ND	ND	ND	ND	ND
I12[a]	ND	ND	ND	ND	ND	ND	ND	ND	ND	ND	ND	ND	ND
I9	ND	ND	ND	ND	ND	ND	ND	ND	ND	ND	ND	ND	ND
I6	ND	ND	ND	ND	ND	ND	ND	ND	ND	ND	ND	ND	ND
I2	ND	ND	ND	ND	ND	ND	ND	ND	ND	ND	ND	ND	ND
I3	ND	ND	ND	ND	ND	ND	ND	ND	ND	ND	ND	ND	ND
38-m Stations													
I29	ND	ND	ND	ND	ND	ND	ND	ND	ND	ND	ND	ND	ND
I21	ND	ND	ND	ND	ND	ND	ND	ND	ND	ND	ND	ND	ND
I13	ND	ND	ND	ND	ND	ND	ND	ND	ND	ND	ND	ND	ND
I8	ND	ND	ND	ND	ND	ND	ND	ND	ND	ND	ND	ND	ND
55-m Stations													
I28	ND	ND	ND	ND	ND	ND	ND	ND	ND	ND	ND	ND	ND
I20	ND	ND	ND	ND	ND	ND	ND	ND	ND	ND	ND	ND	ND
I7	ND	ND	ND	ND	ND	ND	ND	ND	ND	ND	ND	ND	ND
I1	ND	ND	ND	ND	ND	ND	ND	ND	ND	ND	ND	ND	ND
DR (%)	0	0	4	0	0	0	0	4	0	0	0	0	0

[a] Near-ZID station

Appendix D.12 *continued*

Summer 2025	BDE-17	BDE-28	BDE-47	BDE-49	BDE-66	BDE-85	BDE-99	BDE-100	BDE-138	BDE-153	BDE-154	BDE-183	BDE-190
19-m Stations													
I35	ND	ND	ND	ND	ND	ND	ND	ND	ND	ND	ND	ND	ND
I34	ND	ND	ND	ND	ND	ND	ND	ND	ND	ND	ND	ND	ND
I31	ND	ND	ND	ND	ND	ND	ND	ND	ND	ND	ND	ND	ND
I23	ND	ND	ND	ND	ND	ND	ND	ND	ND	ND	ND	ND	ND
I18	ND	ND	ND	ND	ND	ND	ND	ND	ND	ND	ND	ND	ND
I10	ND	ND	ND	ND	ND	ND	ND	ND	ND	ND	ND	ND	ND
I4	ND	ND	93.5	ND	ND	ND	ND	ND	ND	ND	ND	ND	ND
28-m Stations													
I33	ND	ND	ND	ND	ND	ND	ND	ND	ND	ND	ND	ND	ND
I30	ND	ND	ND	ND	ND	ND	ND	ND	ND	ND	ND	ND	ND
I27	ND	ND	ND	ND	ND	ND	ND	ND	ND	ND	ND	ND	ND
I22	ND	ND	ND	ND	ND	ND	ND	ND	ND	ND	ND	ND	ND
I14[a]	ND	ND	102	ND	ND	ND	ND	29.2 DNQ	ND	ND	ND	ND	ND
I16[a]	ND	ND	ND	ND	ND	ND	ND	ND	ND	ND	ND	ND	ND
I15	ND	ND	75.6 DNQ	ND	ND	ND	ND	ND	ND	ND	ND	ND	ND
I12[a]	ND	ND	ND	ND	ND	ND	ND	ND	ND	ND	ND	ND	ND
I9	ND	ND	ND	ND	ND	ND	ND	ND	ND	ND	ND	ND	ND
I6	ND	ND	ND	ND	ND	ND	ND	ND	ND	ND	ND	ND	ND
I2	ND	ND	ND	ND	ND	ND	ND	ND	ND	ND	ND	ND	ND
I3	ND	ND	ND	ND	ND	ND	ND	ND	ND	ND	ND	ND	ND
38-m Stations													
I29	ND	ND	ND	ND	ND	ND	ND	ND	ND	ND	ND	ND	ND
I21	ND	ND	ND	ND	ND	ND	ND	ND	ND	ND	ND	ND	ND
I13	ND	ND	ND	ND	ND	ND	ND	ND	ND	ND	ND	ND	ND
I8	ND	ND	ND	ND	ND	ND	ND	ND	ND	ND	ND	ND	ND
55-m Stations													
I28	ND	ND	ND	ND	ND	ND	ND	ND	ND	ND	ND	ND	ND
I20	ND	ND	ND	ND	ND	ND	ND	ND	ND	ND	ND	ND	ND
I7	ND	ND	ND	ND	ND	ND	ND	ND	ND	ND	ND	ND	ND
I1	ND	ND	ND	ND	ND	ND	ND	ND	ND	ND	ND	ND	ND
DR (%)	0	0	11	0	0	0	0	4	0	0	0	0	0

[a] Near-ZID station

Appendix D.13

Particle size classifiction schemes (based on Folk 1980) used in the analysis of sediments during 2024 and 2025. Included is a subset of the Wentworth scale presented as “phi” categories with corresponding Horiba channels, sieve sizes, and size fractions.

Wentworth Scale

	Horiba[a]				
Phi size	**Min µm**	**Max µm**	**Sieve Size**	**Sub-Fraction**	**Fraction**
-1	—	—	SIEVE_2000	Granules	Coarse Particles
0	1100	2000	SIEVE_1000	Very coarse sand	Coarse Particles
1	590	1000	SIEVE_500	Coarse sand	Med-Coarse Sands
2	300	500	SIEVE_250	Medium sand	Med-Coarse Sands
3	149	250	SIEVE_125	Fine sand	Fine Sands
4	64	125	SIEVE_75	Very fine sand	Fine Sands
4	64	125	SIEVE_63	Very fine sand	Fine Sands
5	32	62.5	SIEVE_0[b]	Coarse silt	Fine Particles[c]
6	16	31	—	Medium silt	Fine Particles[c]
7	8	15.6	—	Fine silt	Fine Particles[c]
8	4	7.8	—	Very fine silt	Fine Particles[c]
9	≤	3.9	—	Clay	Fine Particles[c]

[a] Values correspond to Horiba channels; particles > 2000 µm measured by sieve

[b] SIEVE_0 = sum of all silt and clay, which cannot be distinguished for samples processed by nested sieves

[c] Fine particles also referred to as percent fines

Appendix D.14

Summary of visual observations for each PLOO and SBOO station sampled during 2024–2025. Visual observations are from sieved "grunge" (i.e., particles retained on 1-mm mesh screen and preserved with infauna for benthic community analysis).

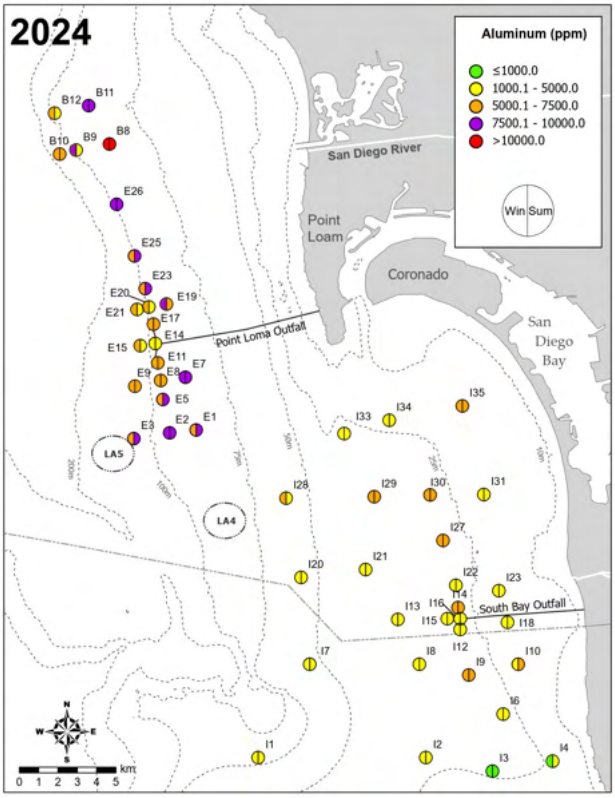
		Winter 2024	Summer 2024	Winter 2025	Summer 2025
PLOO					
88-m Stations	B11	shell hash, coarse sand, gravel	pea gravel, shell hash	pea gravel; shell hash	cobble; gravel
	B8	organic debris, coarse sand		organic debris	-
	E19	shell hash, coarse sand		-	shell hash; organic debris
	E7	-		-	coarse sand; organic debris
	E1	shell hash	cobble, shell has	shell hash	shell hash; cobble
98-m Stations	B12	shell hash, coarse sand	pea gravel, shell hash	coarse sand; shell hash	coarse sand
	B9	-		cobble	cobble; gravel
	E26	-		-	coarse sand; shell hash
	E25	organic debris, shell hash	shell hash	coarse sand; organic debris	coarse sand; shell hash
	E23	shell hash	coarse sand, shell hash	-	shell hash; organic debris
	E20	shell hash		-	-
	E17[a]	-		-	organic debris
	E14[a]	coarse black sand, shell hash	organic debris, coarse black sand	organic debris; shell hash	pea gravel; shell hash
	E11[a]	-		-	-
	E8	-		-	-
	E5	shell hash, coarse sand	cobble, shell has	-	-
	E2			pea gravel; shell hash	pea gravel; shell hash
116-m Stations	B10	-	shell hash	-	shell hash
	E21	coarse sand		-	shell hash; organic debris
	E15[a]	coarse black sand	coarse black sand	coarse sand	coarse sand; shell hash
	E9	-		coarse black sand; pea gravel; shell hash	coarse black sand; pea gravel; shell hash
	E3	shell hash, coarse sand	shell hash	cobble; coarse sand; shell hash	gravel; coarse sand

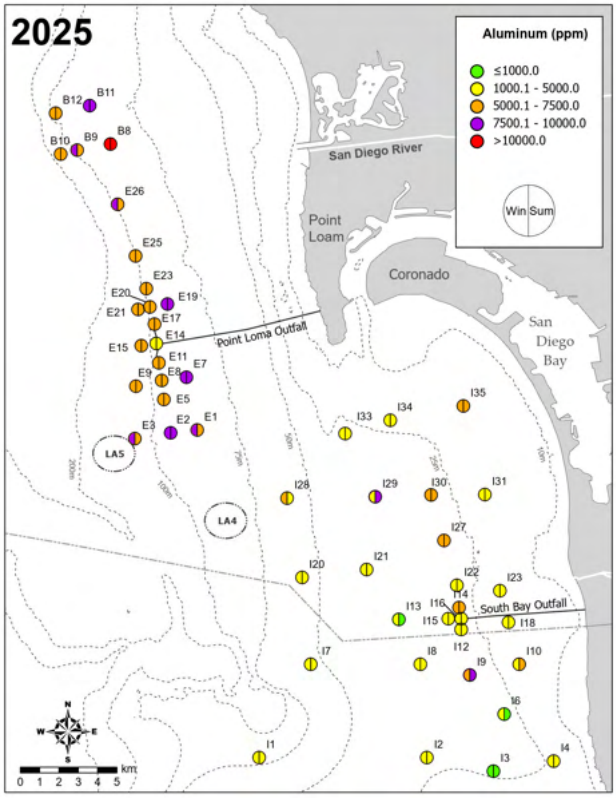
[a] Near-ZID station

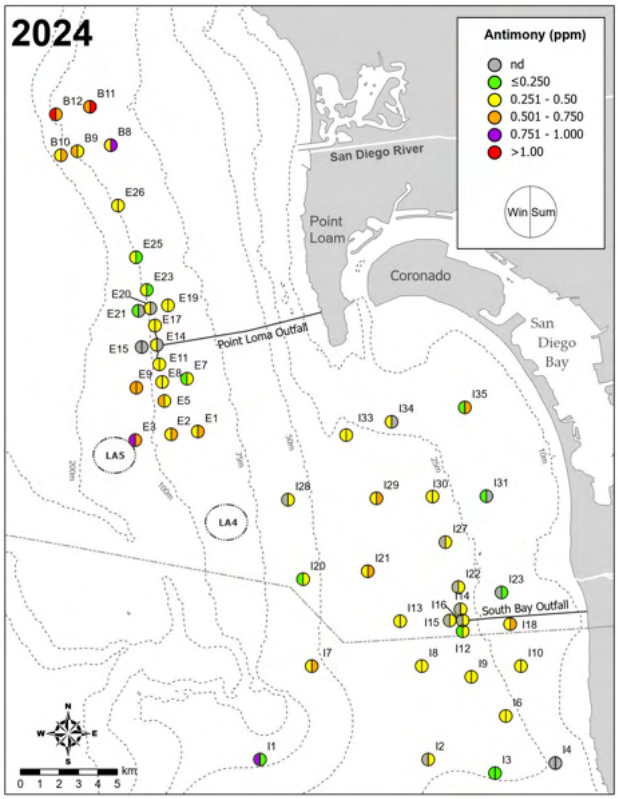
Appendix D.14 *continued*

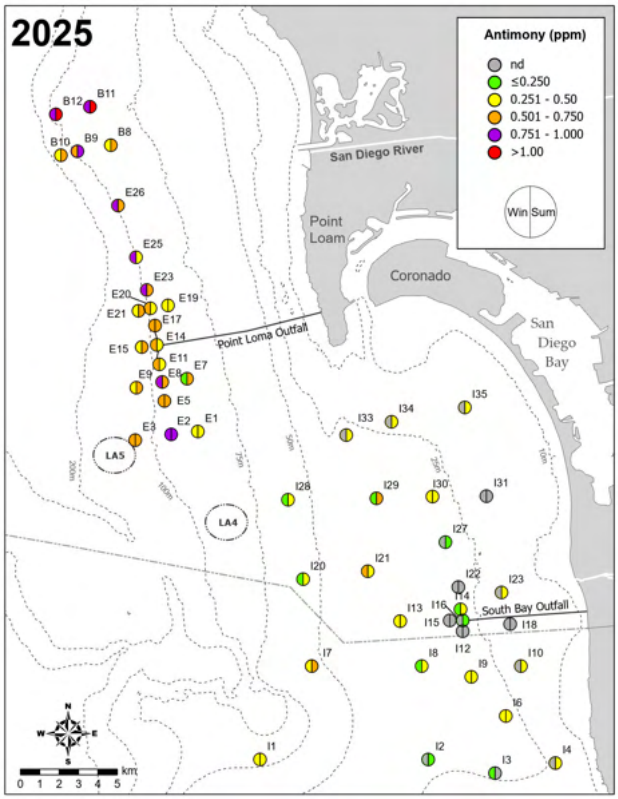
		Winter 2024	Summer 2024	Winter 2025	Summer 2025
SBOO					
19-m Stations	I35	—	—	—	shell hash; organic debris
	I34	shell hash, coarse sand	—	coarse sand; large shell hash	shell hash
	I31	-	coarse black sand, organic debris	—	—
	I23	coarse sand, large shell hash	coarse sand, shell hash	very coarse sand	shell hash; coarse black sand
	I18	coarse sand	—	—	—
	I10	—	—	—	—
	I4	shell hash, gravel	—	shell hash	—
28-m Stations	I33	organic debris, coarse sand	—	shell hash; organic debris	organic debris
	I30	—	—	—	—
	I27	—	—	—	—
	I22	—	—	—	organic debris
	I14[a]	—	—	—	—
	I16[a]	—	—	shell hash	organic debris
	I15[a]	organic debris, shell hash	—	—	—
	I12[a]	—	shell hash	—	shell hash; organic debris
	I9	organic debris, shell hash	—	—	coarse sand; organic debris
	I6	shell hash	—	—	red relict sand; shell hash
	I2	—	—	—	—
	I3	shell hash, coarse sand	—	—	—
38-m Stations	I29	—	—	coarse sand	organic debris
	I21	—	relict red sand, shell hash	—	—
	I13	—	—	shell hash	shell hash
	I8	—	—	—	—
55-m Stations	I28	coarse black sand, shell hash	coarse black sand, organic debris	coarse sand; pea gravel; shell hash	coarse black sand
	I20	red relict sand	—	red relict sand; organic debris	—
	I7	fine red relict sand, shell hash	relict red sand	red relict sand	red relict sand
	I1	—	—	—	—

[a] Near-ZID station



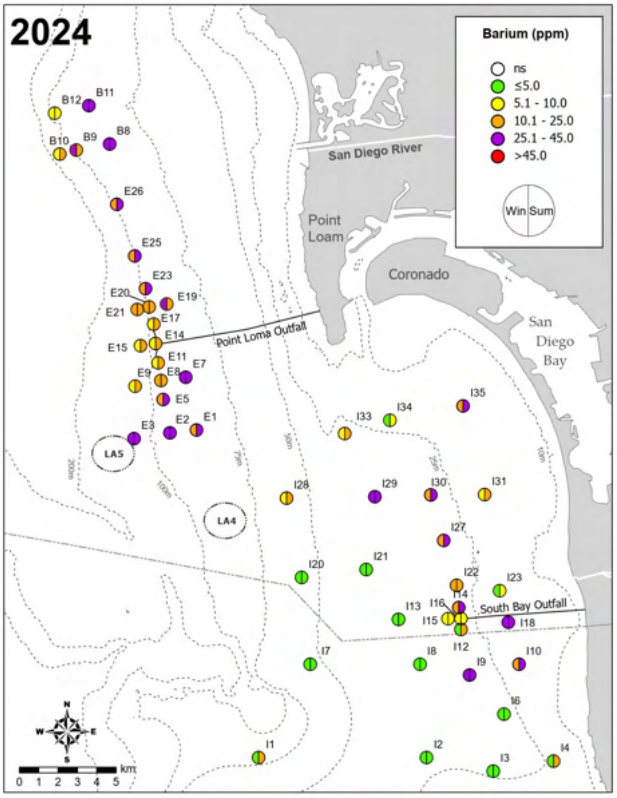


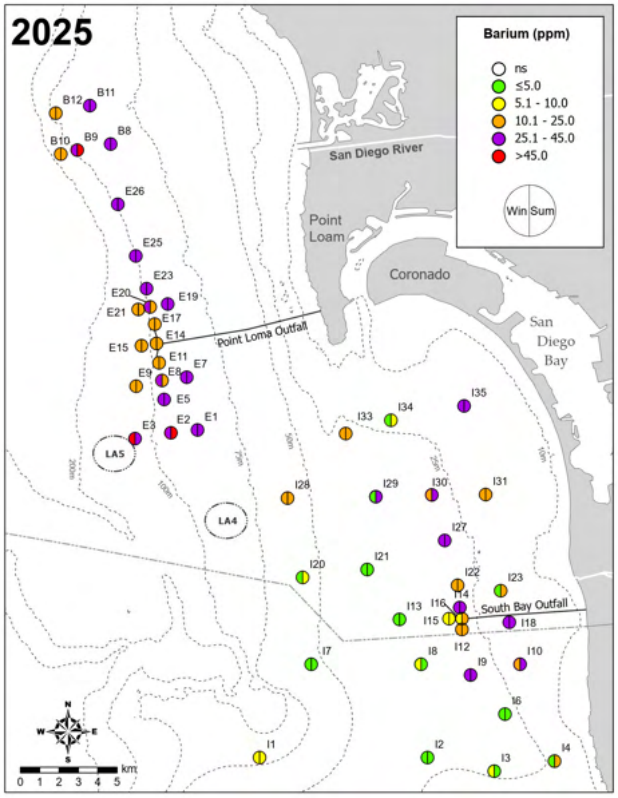


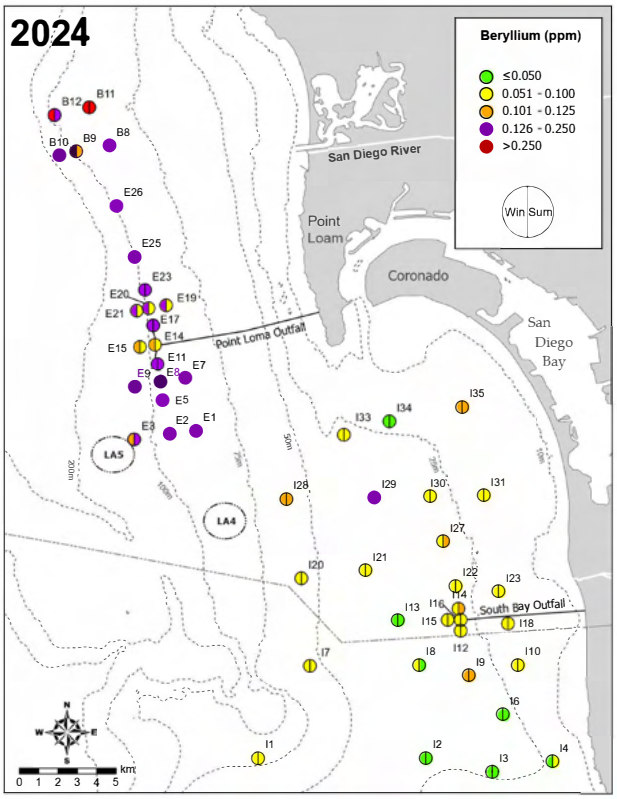


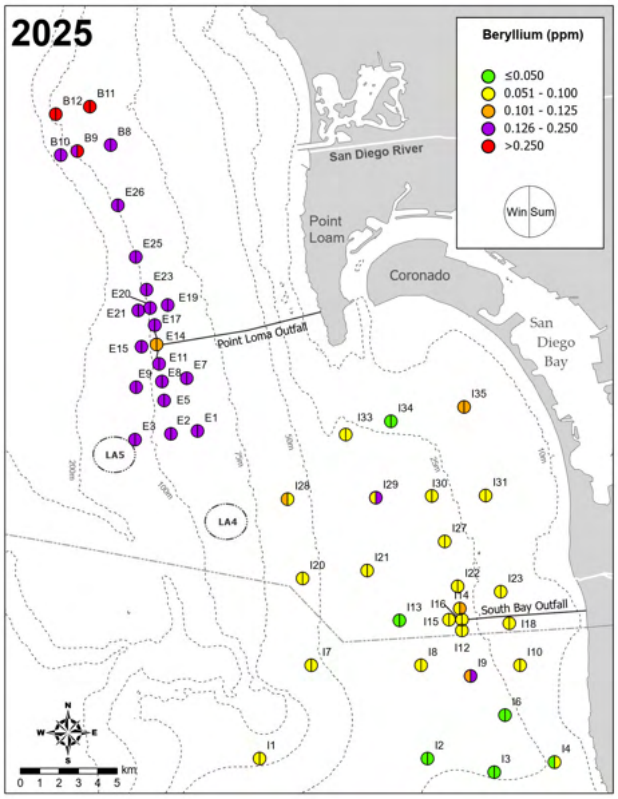
Appendix D.15

Distribution of select metals (ppm) in sediments from the PLOO and SBOO regions during winter and summer surveys of 2024 and 2025; ns = not sampled (or not reportable, see text); nd = not detected.

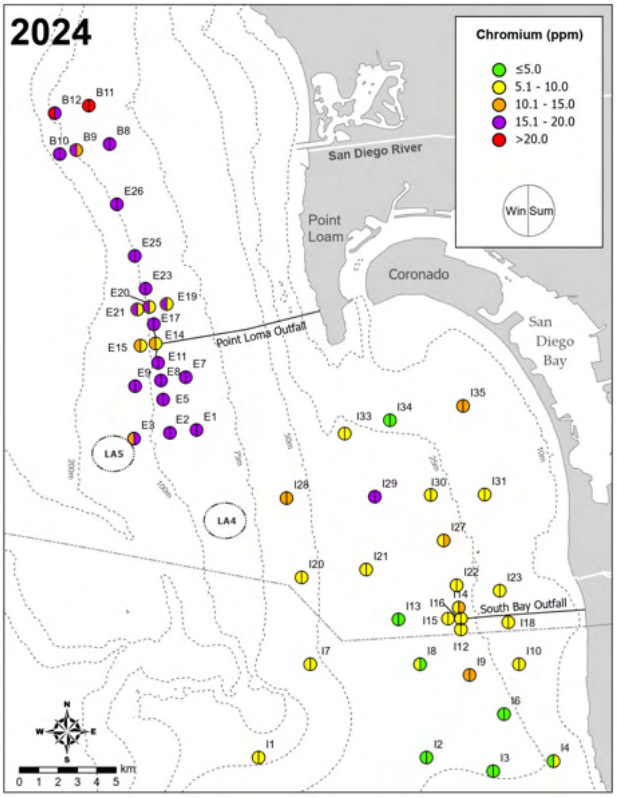


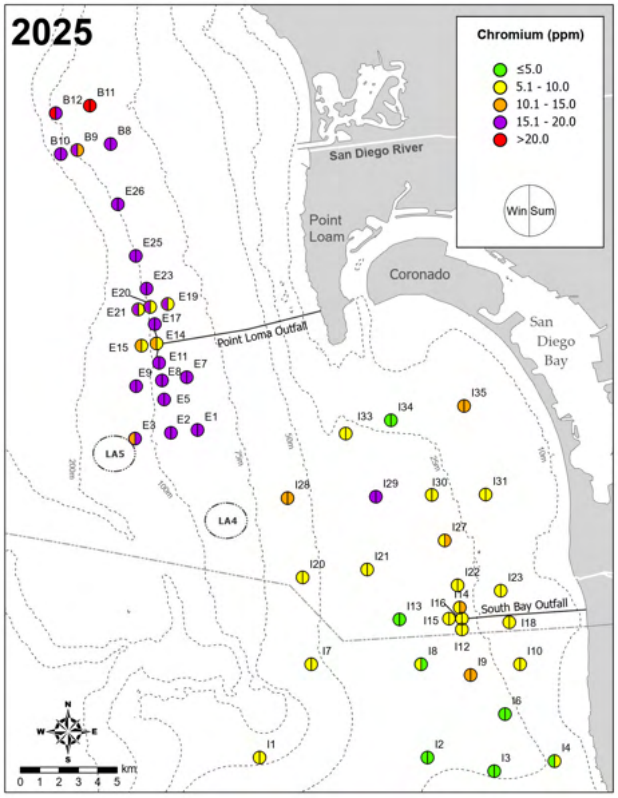


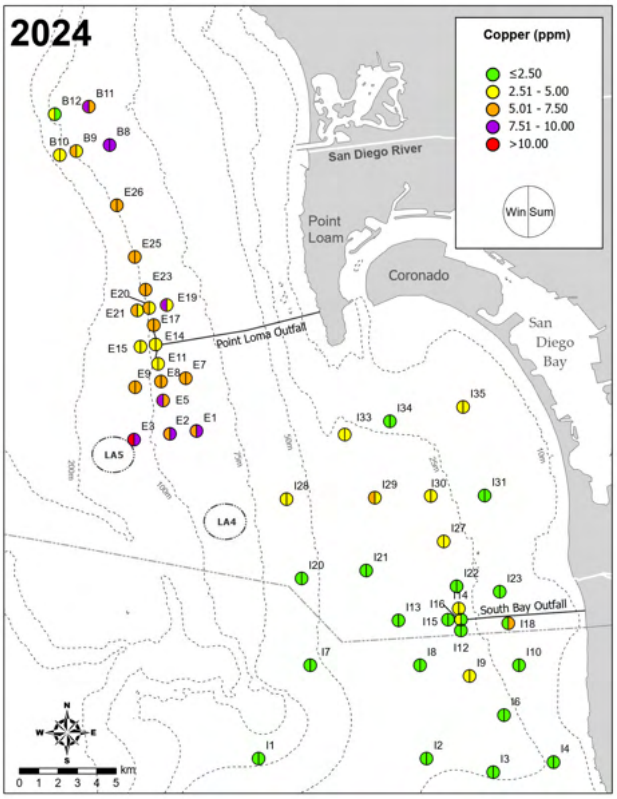


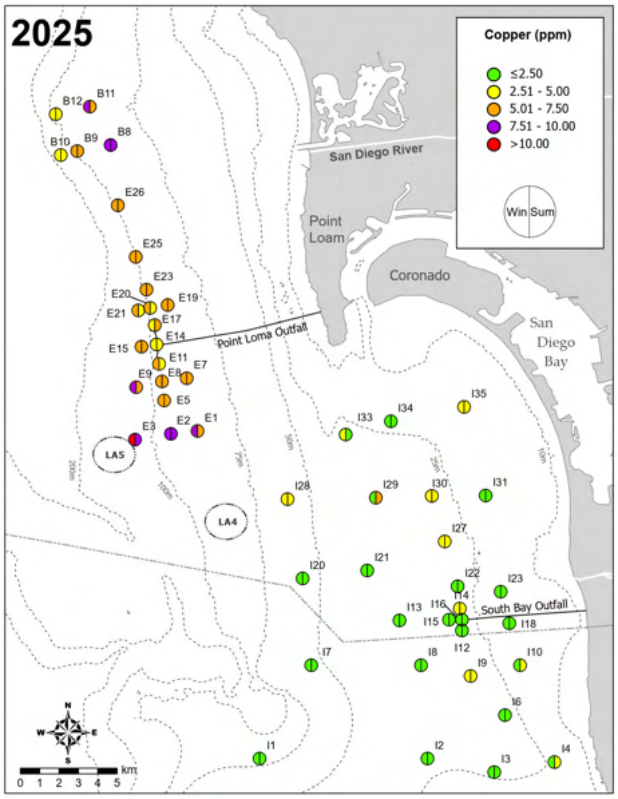


Appendix D.15 *continued*

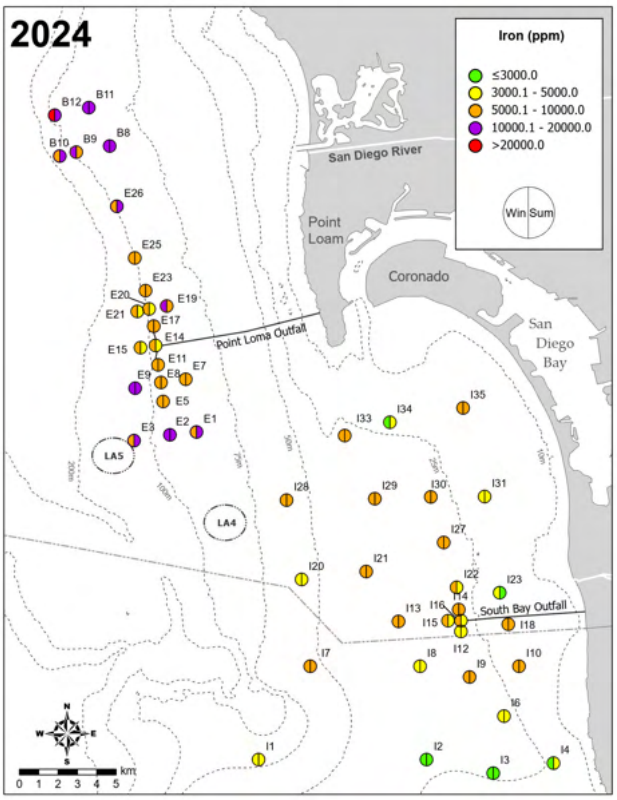


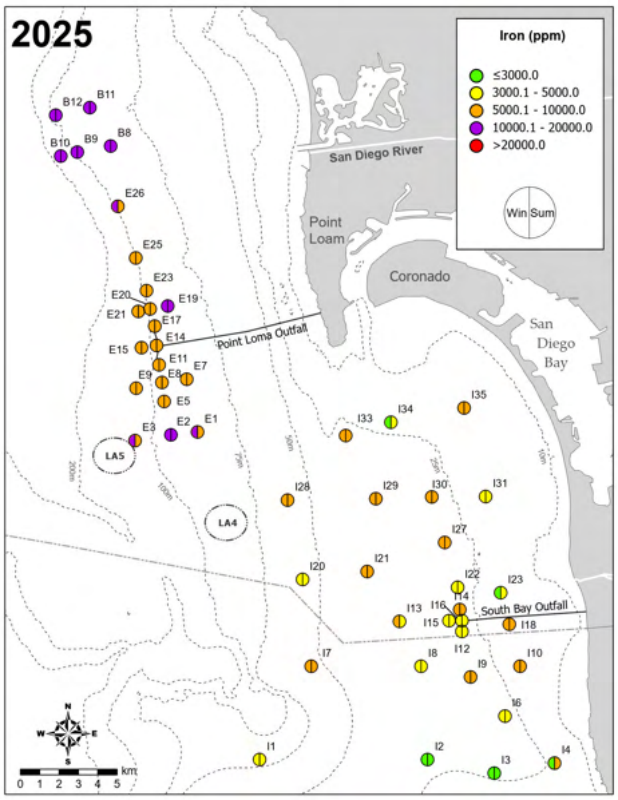


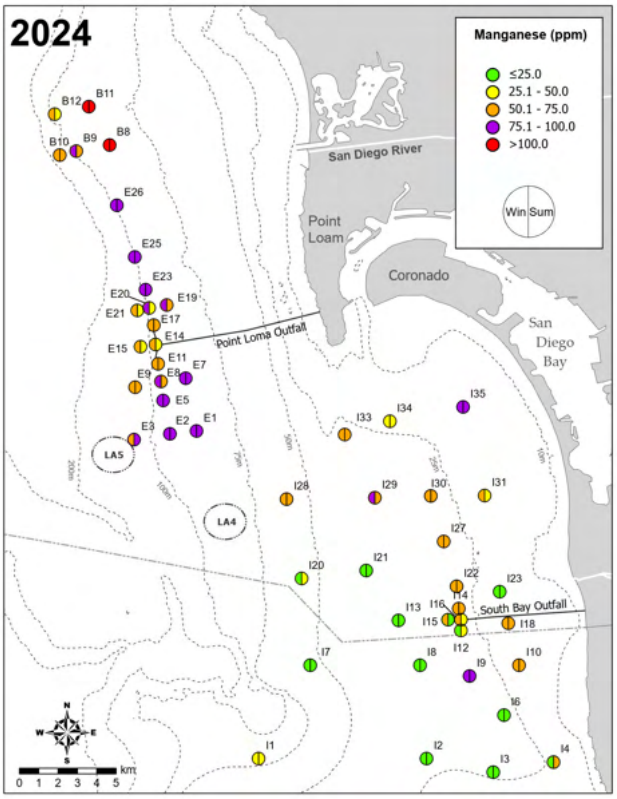


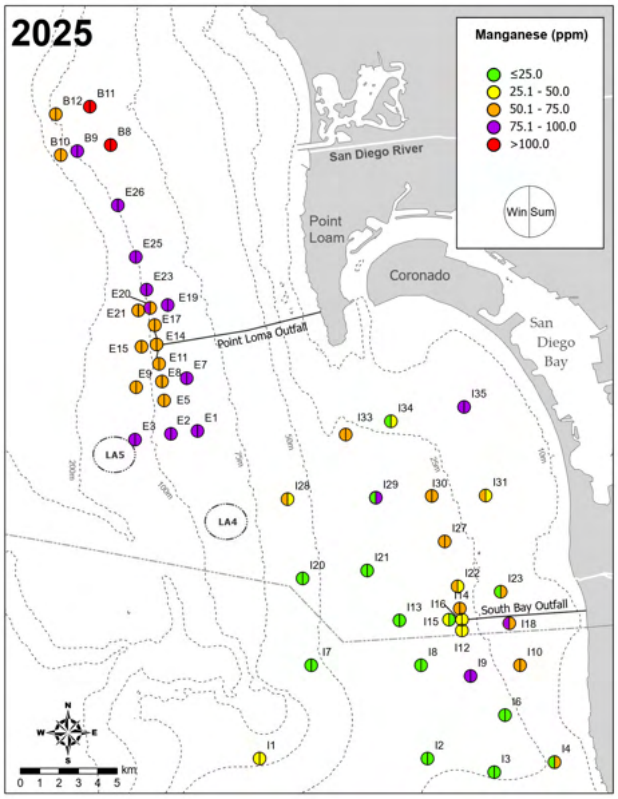


Appendix D.15 *continued*

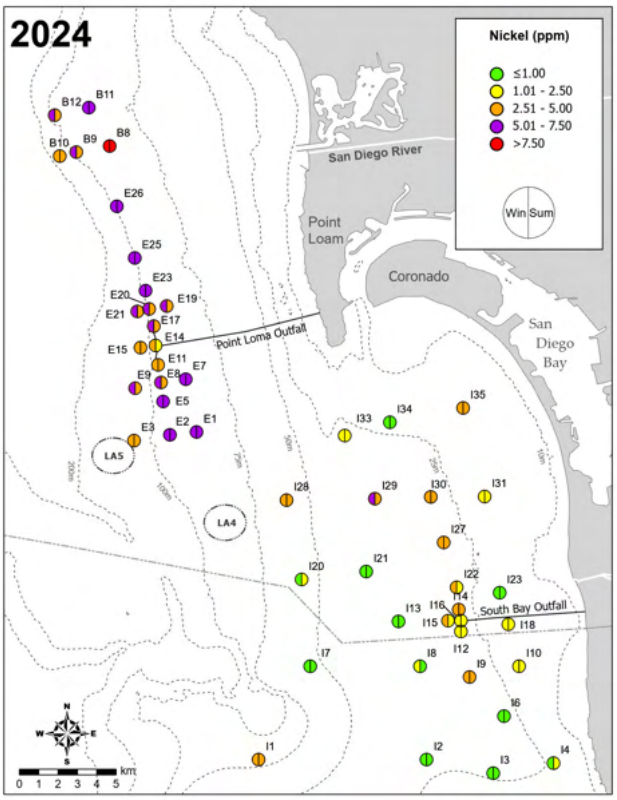


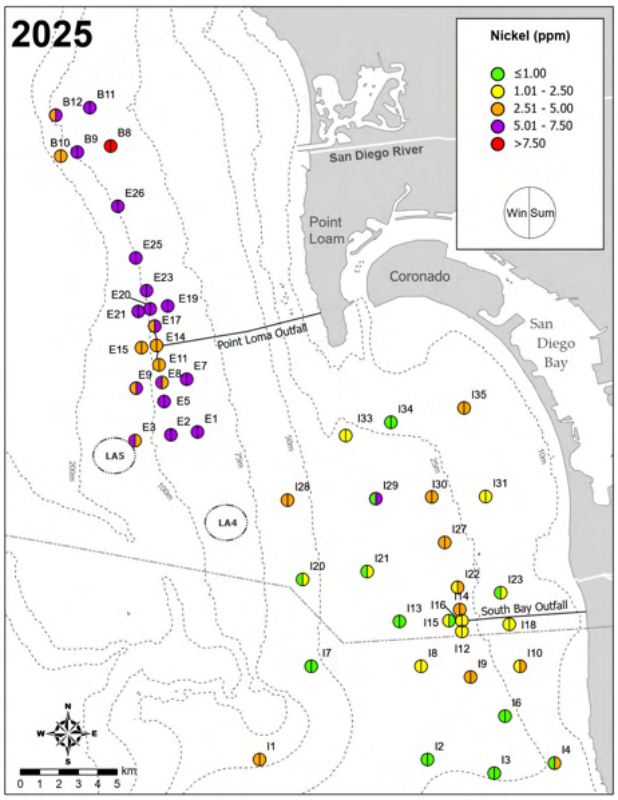


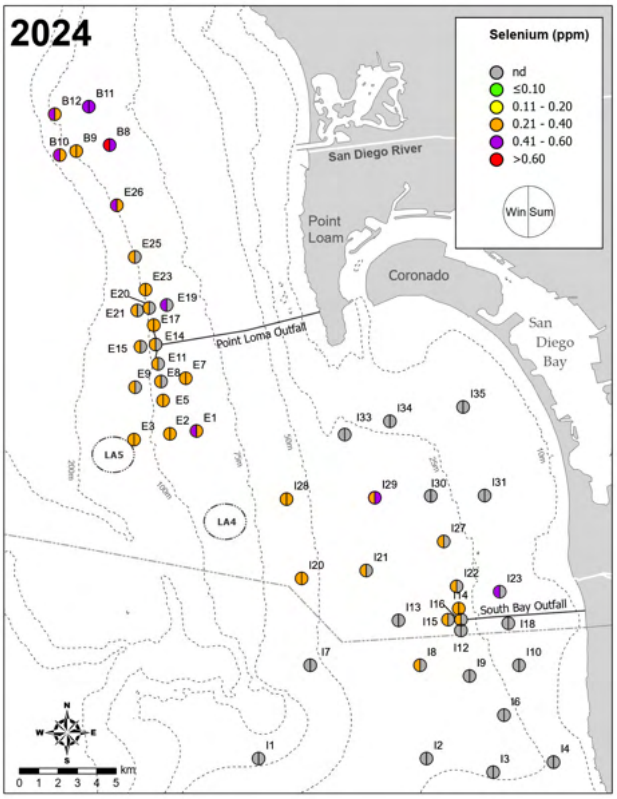


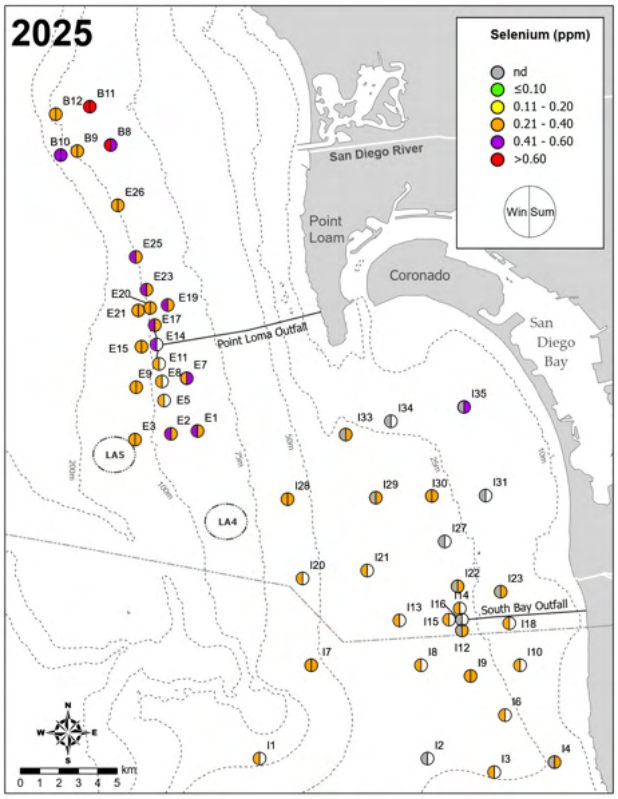


Appendix D.15 *continued*

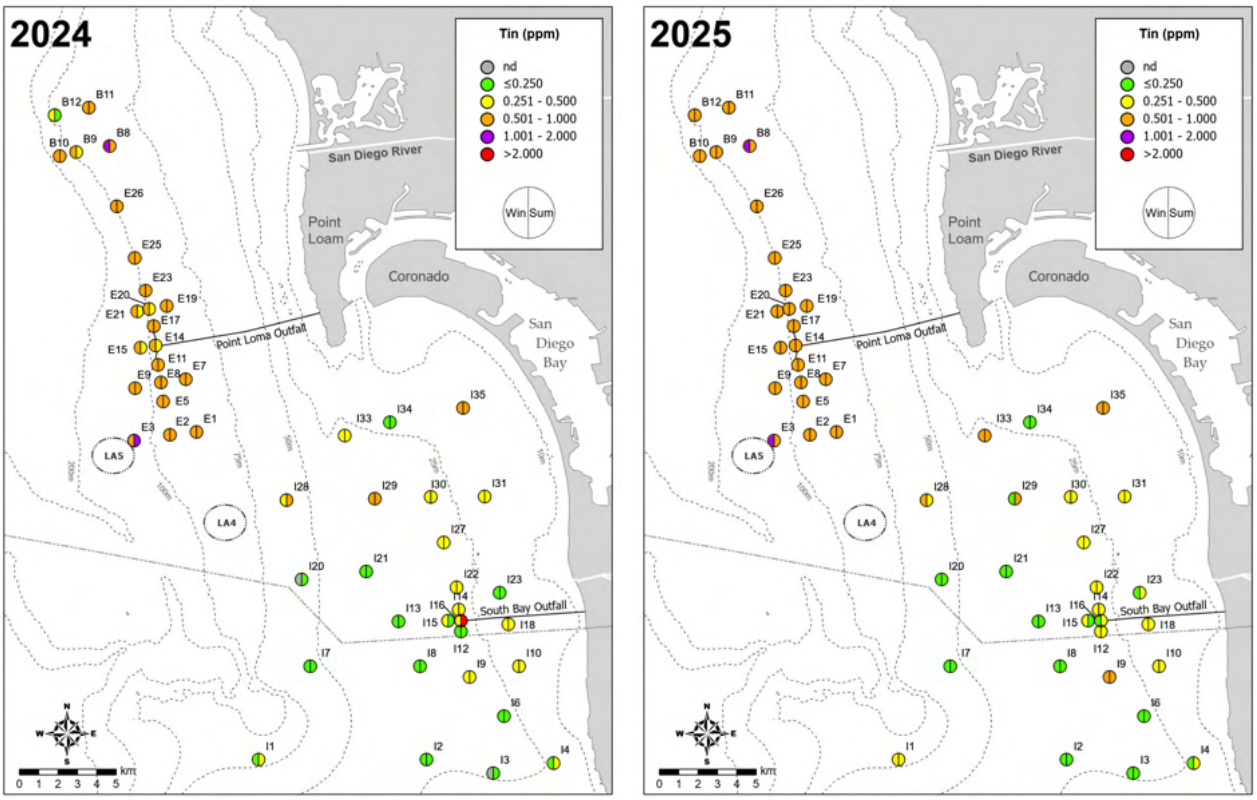




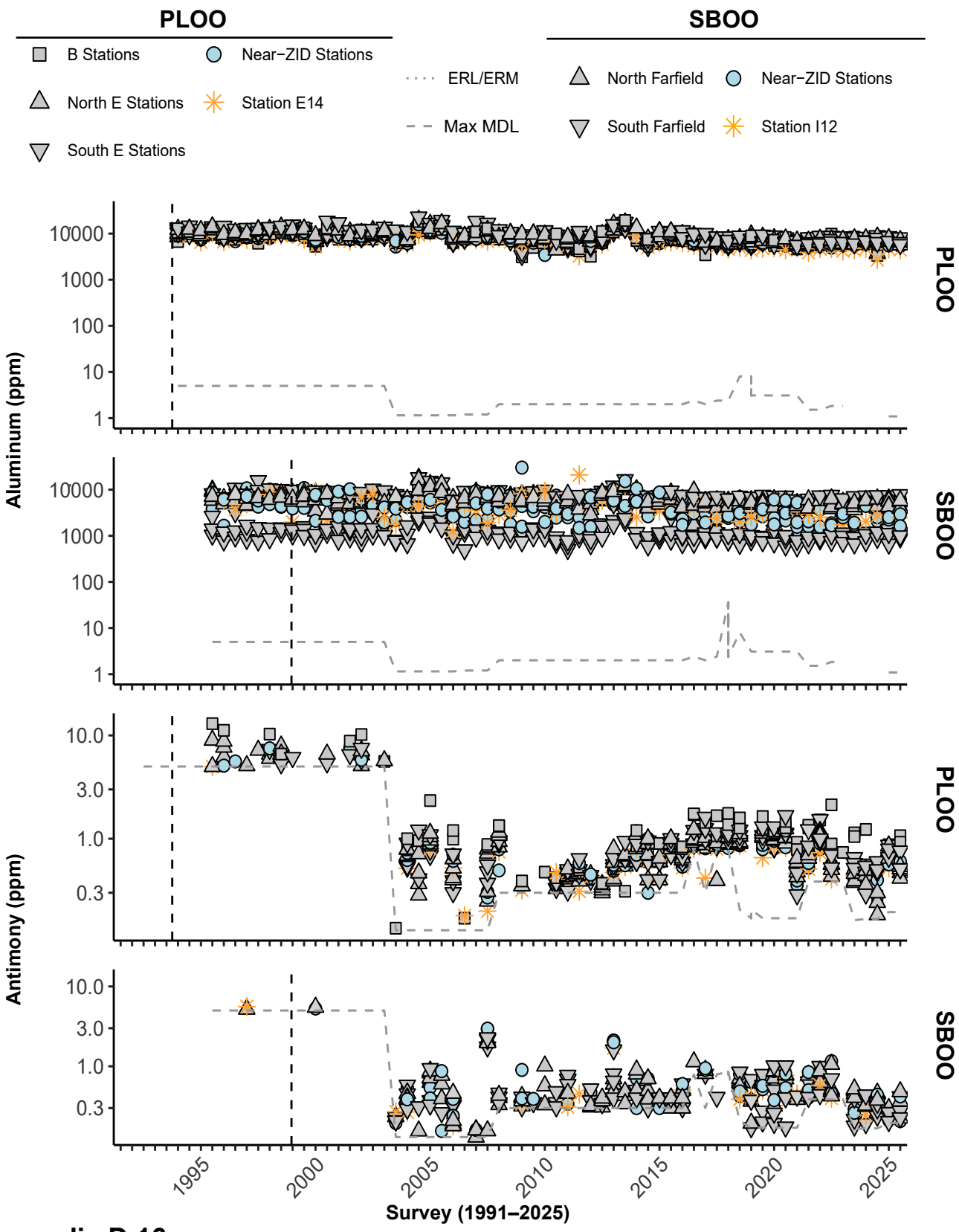




Appendix D.15 *continued*

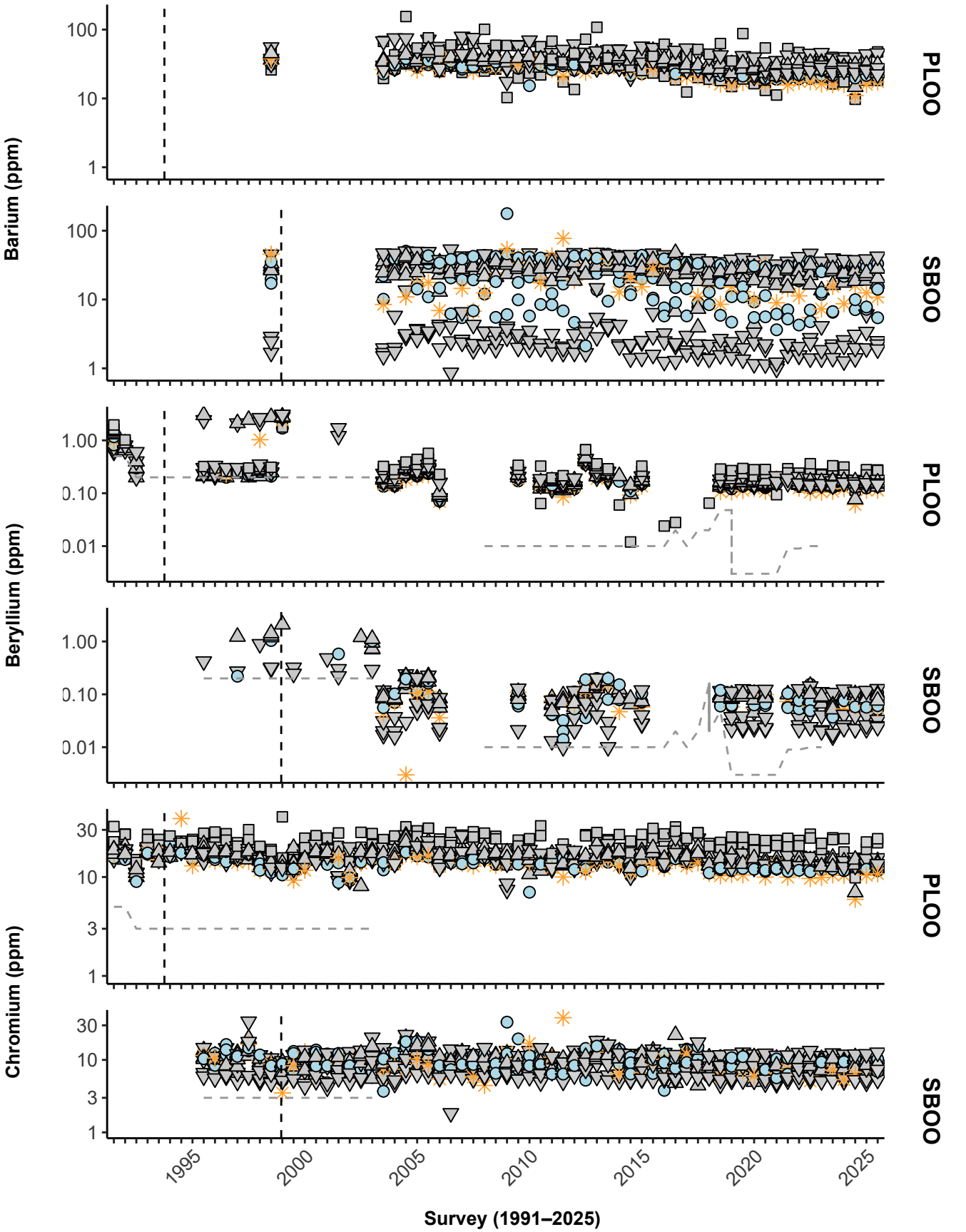


Appendix D.15 *continued*

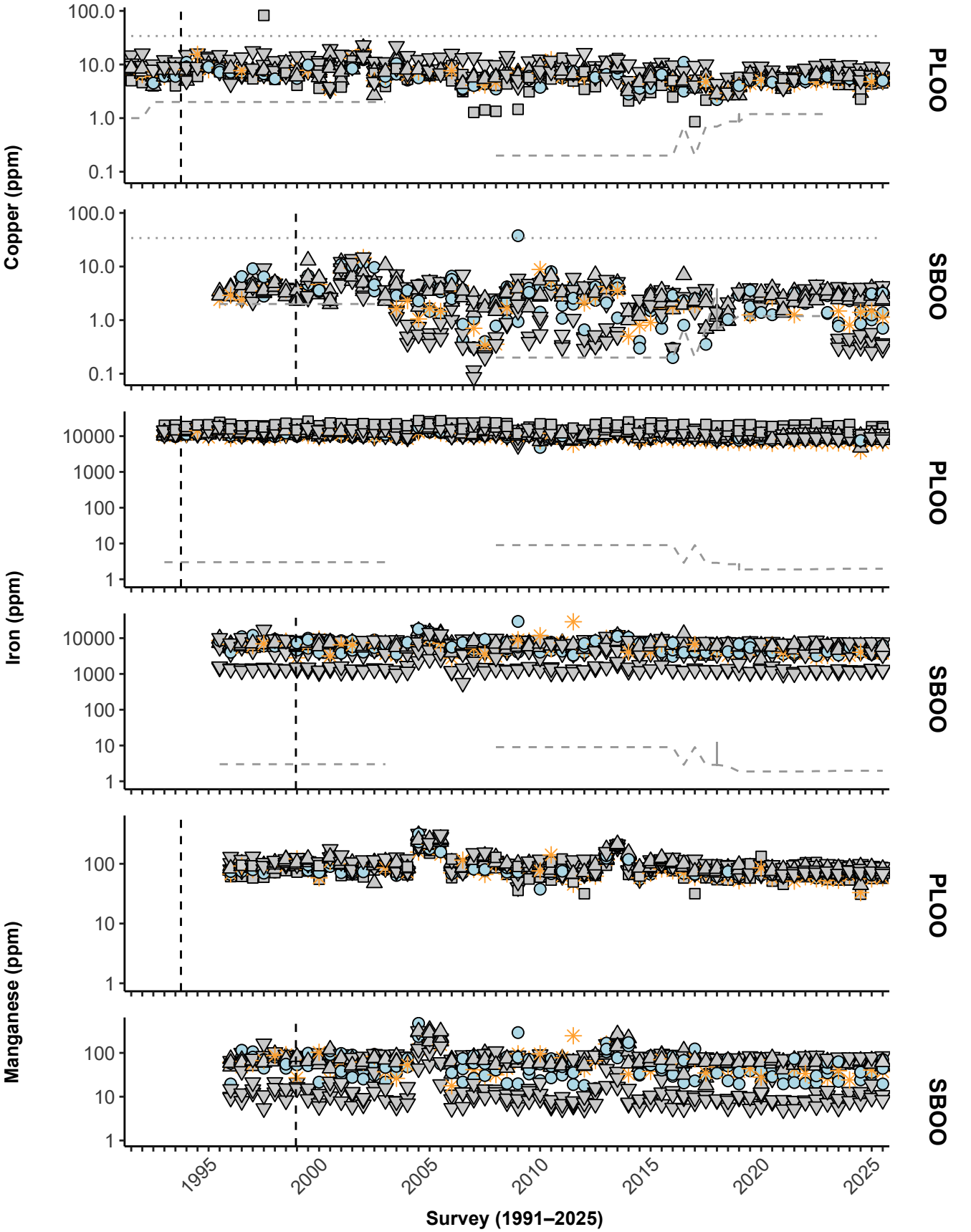


Appendix D.16

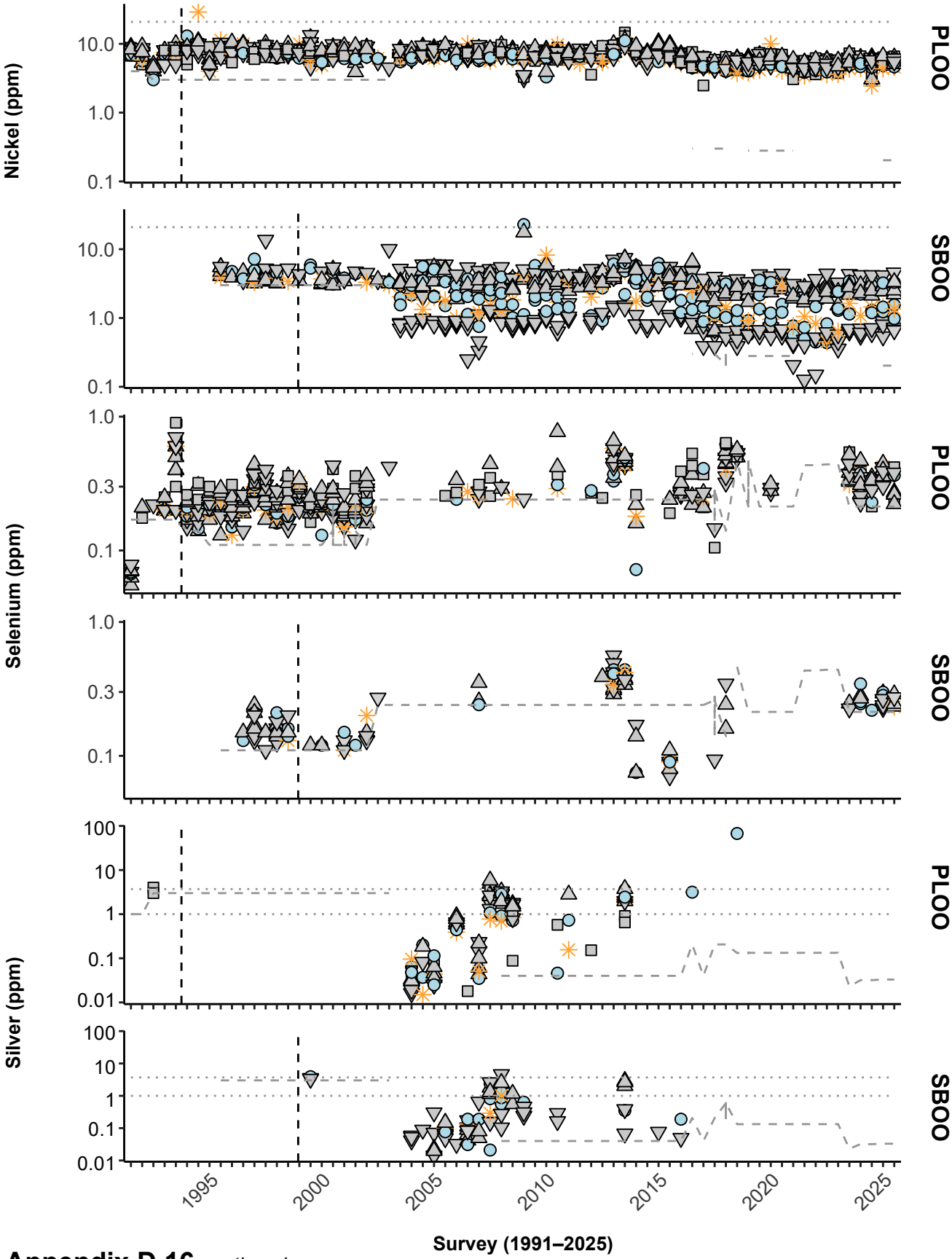
Concentrations of select metals in sediments sampled during winter and summer surveys at PLOO primary core stations from 1991 through 2025 and at SBOO primary core stations from 1995 through 2025. Data represent detected values from each station, n ≤ 12 samples per survey. Vertical dashed lines indicate onset of discharge from the PLOO or SBOO. Thresholds included (ERLs, ERMs) when relevant (see Table 5.3), along with the maximum MDL per survey.



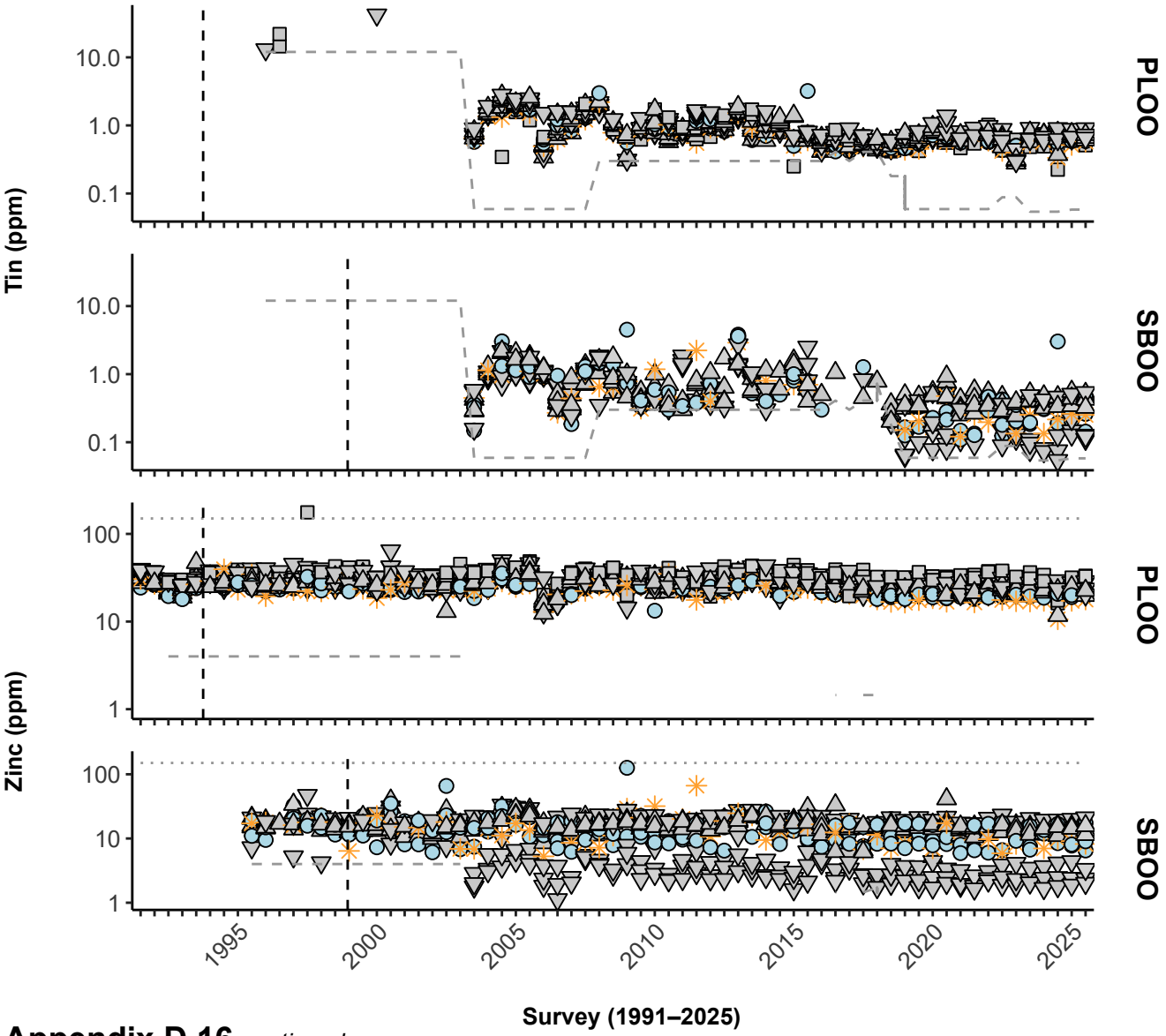
Appendix D.16 *continued*



Appendix D.16 *continued*



Appendix D.16 *continued*



Appendix D.16 *continued*

Appendix E

Macrobenthic Communities

2024 – 2025 Supplemental Analyses

Appendix E.1

Macrofaunal community parameters by grab for PLOO benthic stations sampled during 2025. SR = species richness; Abun = abundance; H' = Shannon diversity index; J' = Pielou's evenness; Dom = Swartz dominance; BRI = Benthic Response Index.

Depth Contour	Station	Survey	SR	Abun	H'	J'	Dom	BRI
88-m	B11	winter	118	309	4.4	0.92	50	11
		summer	93	256	4.0	0.88	33	12
	B8	winter	105	350	4.2	0.90	40	11
		summer	110	451	4.1	0.88	37	14
	E19	winter	86	371	4.0	0.89	31	12
		summer	106	398	3.9	0.84	34	15
	E7	winter	82	280	3.8	0.87	26	14
		summer	113	500	3.9	0.83	32	13
	E1	winter	95	346	3.9	0.87	29	9
		summer	121	520	4.1	0.86	39	12
98-m	B12	winter	108	288	4.2	0.90	45	10
		summer	120	411	4.3	0.90	43	16
	B9	winter	79	254	3.9	0.89	29	8
		summer	101	331	4.1	0.88	36	15
	E26	winter	110	568	4.0	0.85	28	7
		summer	119	457	4.2	0.89	41	13
	E25	winter	98	378	4.0	0.88	32	10
		summer	106	461	3.9	0.83	30	14
	E23	winter	91	387	3.8	0.85	28	7
		summer	94	512	3.6	0.79	24	15
	E20	winter	78	374	3.7	0.84	23	10
		summer	90	341	3.7	0.82	26	16
	E17[a]	winter	91	443	3.8	0.85	28	16
		summer	91	499	3.6	0.79	23	19
	E14[a]	winter	93	569	3.6	0.79	22	25
		summer	108	879	3.5	0.75	20	26
	E11[a]	winter	97	370	4.1	0.89	36	13
		summer	87	390	3.5	0.79	24	17
	E8	winter	94	364	4.0	0.87	35	14
		summer	82	322	3.7	0.84	24	15
	E5	winter	97	396	3.9	0.85	29	14
		summer	100	408	3.9	0.84	33	14
	E2	winter	117	642	3.8	0.80	29	14
		summer	109	467	4.0	0.86	34	11

[a] Near-ZID station

Appendix E.1 *continued*

Depth Contour	Station	Survey	SR	Abun	H'	J'	Dom	BRI
116-m	B10	winter	95	302	4.1	0.91	38	12
		summer	100	266	4.1	0.89	42	17
	E21	winter	92	439	3.8	0.84	26	13
		summer	101	531	3.5	0.76	22	13
	E15[a]	winter	88	386	3.9	0.86	28	10
		summer	102	514	3.7	0.80	25	12
	E9	winter	110	399	4.1	0.88	40	12
		summer	145	443	4.5	0.90	60	11
	E3	winter	131	481	4.2	0.86	39	11
		summer	113	274	4.4	0.92	49	14

[a] Near-ZID station

Appendix E.2

Macrofaunal community parameters by grab for SBOO benthic stations sampled during 2025. SR = species richness; Abun = abundance; H' = Shannon diversity index; J' = Pielou's evenness; Dom = Swartz dominance; BRI = Benthic Response Index.

Depth Contour	Station	Survey	SR	Abun	H'	J'	Dom	BRI
19-m	I35	winter	60	139	3.6	0.88	26	34
		summer	70	303	3.2	0.76	16	25
	I34	winter	63	2373	2.6	0.63	6	21
		summer	48	160	2.5	0.66	13	16
	I31	winter	59	119	3.9	0.95	30	22
		summer	70	215	3.8	0.89	27	19
	I23	winter	58	574	2.9	0.71	8	10
		summer	60	312	3.3	0.81	16	22
	I18	winter	59	153	3.5	0.85	22	15
		summer	51	135	3.6	0.91	24	24
	I10	winter	53	131	3.7	0.93	26	21
		summer	53	144	3.7	0.92	24	17
	I4	winter	37	70	3.3	0.91	20	5
		summer	44	189	3.0	0.79	12	30
28-m	I33	winter	129	451	4.3	0.89	48	23
		summer	129	500	4.4	0.90	48	24
	I30	winter	84	296	3.8	0.85	30	22
		summer	89	379	3.9	0.87	30	23
	I27	winter	85	375	3.6	0.81	24	24
		summer	102	396	4.1	0.88	37	23
	I22	winter	101	310	4.2	0.91	41	22
		summer	84	313	4.0	0.91	34	22
	I14[a]	winter	74	201	4.0	0.92	33	23
		summer	77	255	3.9	0.91	32	26
	I16[a]	winter	82	407	3.4	0.76	17	24
		summer	55	135	3.6	0.89	23	25
	I15[a]	winter	50	180	3.1	0.80	15	27
		summer	63	407	2.9	0.70	11	22
	I12[a]	winter	43	113	3.0	0.80	15	21
		summer	105	623	3.8	0.82	24	25
	I9	winter	97	307	4.0	0.88	34	28
		summer	112	507	4.2	0.89	38	27
	I6	winter	40	146	3.2	0.87	14	11
		summer	52	231	3.3	0.84	16	14
	I2	winter	45	140	3.3	0.86	18	17
		summer	53	228	3.2	0.80	14	25
	I3	winter	23	62	2.8	0.88	9	6
		summer	58	350	2.9	0.71	9	21

[a] Near-ZID station

Appendix E.2 *continued*

Depth Contour	Station	Survey	SR	Abun	H'	J'	Dom	BRI
38-m	I29	winter	75	855	2.9	0.68	12	16
		summer	183	1561	4.1	0.79	38	24
	I21	winter	46	326	2.6	0.67	8	9
		summer	84	406	3.4	0.76	18	19
	I13	winter	45	147	3.2	0.85	16	4
		summer	68	299	3.4	0.81	17	16
	I8	winter	56	214	3.5	0.86	21	18
		summer	40	158	3.1	0.84	13	20
55-m	I28	winter	165	611	4.2	0.83	51	16
		summer	151	599	4.3	0.86	51	17
	I20	winter	85	503	3.4	0.77	18	12
		summer	102	465	3.9	0.84	30	18
	I7	winter	39	74	3.3	0.90	21	11
		summer	84	310	3.9	0.87	28	15
	I1	winter	138	626	4.2	0.85	41	15
		summer	119	650	4.0	0.83	34	16

Appendix E.3

Summary taxonomic listing of benthic infauna taxa identified from PLOO stations during 2025. Data are total number of individuals (n). Taxonomic arrangement follows SCAMIT (2023).

Phylum	Class	Family	Taxon	n
Cnidaria	Hydrozoa	Corymorphidae	Euphysa sp A	2
	Octocorallia		Pennatuloidea	1
		Virgulariidae	Acanthoptilum sp	2
	Ceriantharia			1
		Arachnactidae	Arachnanthus sp A	1
	Hexacorallia		Actiniaria	1
		Edwardsiidae		3
			Edwardsia juliae	1
			Edwardsia olguini	9
			Edwardsia sp SD1	1
			Scolanthus triangulus	9
		Halcampidae	Halcampa decemtentaculata	5
			Halianthella sp A	1
Platyhelminthes	Rhabditophora	Cryptocelidae	Cryptocelis occidentalis	1
		Plehniidae	Diplehnia caeca	3
		Faubelidae	Diplandros singularis	2
Nemertea				12
	Palaeonemertea			1
		Cephalotrichidae	Cephalothrix sp	2
		Carinomidae	Carinoma mutabilis	6
		Carinomellidae	Carinomella lactea	2
		Tubulanidae		6
			Tubulanus cingulatus	9
			Tubulanus polymorphus	27
			Tubulanus sp A	2
			Tubulanidae sp E	8
	Pilidiophora		Heteronemertea	2
		Lineidae		44
			Cerebratulus californiensis	4
			Micrura wilsoni	1
			Siphonenteron bilineatum	79
			Zygeupolia rubens	3
			Lineidae sp SD1	3
		--	Heteronemertea sp SD2	170
	Hoplonemertea			13
		Neesidae	Paranemertes californica	10
		Oerstediidae	Oerstedia dorsalis Cmplx	3
		Amphiporidae	Amphiporus californicus	4
		Zygonemertidae	Zygonemertes virescens	1
		--	Quasitetrastemma nigrifrons	1
			Hoplonemertea sp SD3	1
Mollusca	Caudofoveata		Chaetodermatida	2
		Chaetodermatidae	Chaetoderma marinellii	2
			Chaetoderma pacificum	1
			Chaetoderma sp	2
			Falcidens longus	7
	Polyplacophora	Leptochitonidae	Leptochiton rugatus	1

Appendix E.3 *continued*

Phylum	Class	Family	Taxon	n
	Gastropoda	Solariellidae	Minolia peramabilis	9
		Cerithiidae	Lirobittium rugatum Cmplx	2
		Rissoidae	Alvania rosana	1
		Caecidae	Caecum crebricinctum	4
		Eulimidae	Eulima raymondi	2
			Hypermastus rosa	1
			Polygireulima rutila	5
			Vitreolina columbiana	1
		Mangeliidae	Kurtzia arteaga	18
			Kurtzina beta	38
		Acteonidae	Acteon traskii	2
		Goniodoridídae	Okenia sp A	1
		Pyramidellidae	Odostomia sp	10
			Turbonilla chocolata	2
			Turbonilla santarosana	1
			Turbonilla sp A	4
			Turbonilla sp SD5	5
			Turbonilla sp	3
		Rhizoridae	Volvulella californica	17
			Volvulella cylindrica	7
			Volvulella panamica	6
		Tornatinidae	Acteocina cerealis	2
		Cylichnidae	Cylichna diegensis	27
		Aglajidae	Aglaja ocelligera	12
		Gastropteridae	Gastropteron pacificum	1
		Philinidae	Philine auriformis	10
		--	Bullomorpha sp A	1
		Parvaplustridae	Parvaplustrum cadieni	1
	Bivalvia			1
		Nuculidae	Ennucula tenuis	13
		Solemyidae	Petrasma pervernicosa	132
		Nucinellidae	Huxleyia munita	2
		Nuculanidae	Nuculana hamata	4
			Saccella sp A	85
		Mytilidae	Crenella decussata	2
			Solamen columbianum	1
			Amygdalum pallidulum	18
		Pectinidae		1
		Lucinidae	Lucinoma annulatum	5
			Parvilucina tenuisculpta	49
		Thyasiridae	Adontorhina cyclia	5
			Axinopsida serricata	51
		Thyasiridae	Thyasira flexuosa	6
		Basterotiidae	Saxicavella nybakkeni	3
			Saxicavella pacifica	6
		Lasaeidae	Kurtiella grippi	1
			Kurtiella mortoni	3
			Kurtiella tumida	24
			Kurtiella sp D	17

Appendix E.3 *continued*

Phylum	Class	Family	Taxon	n
			Kurtiella sp	1
			Neaeromya compressa	2
		Carditidae	Coanicardita ventricosa	1
		Cardiidae	Keenaea centifilosa	28
		Tellinidae		2
			Tellina cadieni	237
			Tellina carpenteri	82
			Macoma yoldiformis	2
		Veneridae	Nutricola cymata	1
			Nutricola ovalis	1
		Petricolidae	Cooperella subdiaphana	11
		Cuspidariidae	Cuspidaria parapodema	12
		Pandoridae	Pandora bilirata	4
		Lyonsiidae		1
			Lyonsia californica	1
		--	Thracioidea	2
		Thraciidae	Thracia trapezoides	5
	Scaphopoda	Dentaliidae	Dentalium vallicolens	1
		--	Gadilida	2
		Gadilidae	Polyschides quadrifissatus	71
		--	Compressidens stearnsii	2
Annelida			Sipuncula	2
		Golfingiidae	Phascolion sp A	35
			Thysanocardia nigra	1
		Phascolosomatidae	Apionsoma misakianum	2
	Polychaeta	Thalassematidae	Listriolobus pelodes	1
		Amphinomidae	Chloeia pinnata	631
		Dorvilleidae	Ophryotrocha sp	1
			Parougia caeca	3
		Eunicidae	Leodice americana	4
		Lumbrineridae	Eranno bicirrata	5
			Eranno lagunae	8
			Lumbrineris cruzensis	428
			Lumbrineris latreilli	77
			Lumbrineris ligulata	45
			Lumbrineris limicola	20
			Lumbrineris sp Group I	398
			Ninoe tridentata	3
			Scoletoma tetraura Cmplx	15
			Scoletoma sp	4
		Oenonidae	Drilonereis falcata	14
			Drilonereis mexicana	2
			Drilonereis sp A	1
			Drilonereis sp	9
			Notocirrus californiensis	5
		Onuphidae		2
			Nothria occidentalis	4
			Diopatra splendidissima	1
			Diopatra tridentata	1

Appendix E.3 *continued*

Phylum	Class	Family	Taxon	n
			Mooreonuphis exigua	3
			Mooreonuphis nebulosa	2
			Mooreonuphis segmentispadix	1
			Mooreonuphis sp SD1	3
			Mooreonuphis sp	1
			Onuphis geophiliformis	2
			Onuphis iridescens	2
			Onuphis sp A	11
			Onuphis sp	3
			Paradiopatra parva	309
		Polynoidae		4
			Lepidasthenia berkeleyae	1
			Hesperonoe laevis	1
			Malmgreniella baschi	23
			Malmgreniella macginitiei	2
			Malmgreniella sanpedroensis	14
			Malmgreniella scriptoria	4
			Malmgreniella sp A	65
			Malmgreniella sp SD2	1
			Subadyte mexicana	2
			Tenonia priops	7
		Sigalionidae	Pholoides asperus	8
			Sigalion spinosus	25
			Sthenelais tertiaglabra	20
			Sthenelais verruculosa	1
			Pholoe glabra	94
			Sthenelanella uniformis	101
		Glyceridae	Glycera americana	3
			Glycera macrobranchia	1
			Glycera nana	138
			Glycera oxycephala	3
			Glycera robusta	1
		Goniadidae	Glycinde armigera	62
			Goniada brunnea	2
			Goniada maculata	34
		Hesionidae	Podarkeopsis glabrus	18
			Micropodarke dubia	1
		Nereididae	Gymnonereis crosslandi	3
			Alitta succinea	2
			Nereis sp A	26
		Syllidae		2
			Epigamia-Myrianida Cmplx	1
			Eusyllis blomstrandi Cmplx	1
			Eusyllis habei	2
			Paraehlersia articulata	2
			Exogone dwisula	3
			Exogone lourei	29
			Parexogone molesta	1
			Syllis gracilis Cmplx	3

Appendix E.3 *continued*

Phylum	Class	Family	Taxon	n
			Syllis heterochaeta	10
			Syllis sp SD2	2
		Nephtyidae	Aglaophamus verrilli	10
			Bipalponephtys cornuta	5
			Nephtys caecoides	6
			Nephtys ferruginea	23
			Nephtys simoni	6
			Nephtys sp SD2	1
		Phyllodocidae	Eteone leptotes	1
			Eteone pigmentata	11
			Eulalia levicornuta Cmplx	1
			Eumida longicornuta	5
			Sige sp A	17
			Nereiphylla sp 2	2
			Paranaitis polynoides	2
			Phyllodoce groenlandica	6
			Phyllodoce hartmanae	70
			Phyllodoce longipes	44
			Phyllodoce pettiboneae	2
			Phyllodoce sp	1
		Oweniidae	Galathowenia pygidialis	1
			Myriochele gracilis	51
			Myriochele olgae	4
			Myriochele striolata	19
			Myriowenia californiensis	2
			Owenia collaris	1
		Sabellidae	Acromegalomma splendidum	3
			Dialychone albocincta	13
			Dialychone trilineata	111
			Dialychone veleronis	2
			Euchone arenae	6
			Euchone hancocki	15
			Euchone incolor	34
			Euchone sp A	9
			Jasmineira sp B	16
			Paradialychone bimaculata	1
			Paradialychone paramollis	1
			Potamethus sp A	7
		Serpulidae		1
		Longosomatidae	Heterospio catalinensis	1
		Magelonidae	Magelona berkeleyi	2
			Magelona hartmanae	2
			Magelona longicornis	1
			Magelona sp B	2
			Magelona sp	1
		Poecilochaetidae	Poecilochaetus johnsoni	3
		Spionidae	Dipolydora socialis	1
			Laonice cirrata	9
			Laonice nuchala	21

Appendix E.3 *continued*

Phylum	Class	Family	Taxon	n
			Malacoceros indicus	1
			Microspio pigmentata	13
			Paraprionospio alata	115
			Prionospio dubia	429
			Prionospio jubata	466
			Prionospio lighti	7
			Prionospio lobulata	1
			Prionospio pygmaeus	2
			Scolelepis (Scolelepis) occidentalis	2
			Spio filicornis	15
			Spio maciolekae	4
			Spio maculata	7
			Spiophanes berkeleyorum	100
			Spiophanes duplex	767
			Spiophanes kimballi	523
			Spiophanes wigleyi	12
			Spiophanes sp	1
		Cirratulidae		1
			Aphelochaeta glandaria Cmplx	119
			Aphelochaeta monilaris	40
			Aphelochaeta petersenae	1
			Aphelochaeta phillipsi	16
			Aphelochaeta tigrina	8
			Aphelochaeta williamsae	6
			Aphelochaeta sp D	116
			Aphelochaeta sp E	5
			Aphelochaeta sp	3
			Chaetozone armata	2
			Chaetozone corona	1
			Chaetozone hartmanae	91
			Chaetozone lunula	2
			Chaetozone sp A	1
			Chaetozone sp SD5	2
			Chaetozone sp SD7	1
			Chaetozone sp	2
			Kirkegaardia cryptica	53
			Kirkegaardia serratiseta	20
			Kirkegaardia siblina	82
			Kirkegaardia tesselata	19
			Kirkegaardia sp SD9	12
		Fauveliopsidae	Fauveliopsis sp SD1	9
		Flabelligeridae	Bradabyssa pilosa	5
			Bradabyssa pluribranchiata	5
			Lamispina schmidtii	2
			Pherusa neopapillata	8
			Trophoniella harrisae	1
		Sternaspidae	Sternaspis affinis	93
		Ampharetidae		10
			Amage anops	3

Appendix E.3 *continued*

Phylum	Class	Family	Taxon	n
			Amage scutata	11
			Ampharete finmarchica	23
			Ampharete labrops	25
			Ampharete lineata	6
			Ampharete manriquei	3
			Ampharete sp	4
			Amphicteis mucronata	4
			Amphicteis scaphobranchiata	17
			Anobothrus bimaculatus	49
			Eclysippe trilobata	230
			Lysippe sp A	52
			Lysippe sp B	86
			Samytha californiensis	2
			Sosane occidentalis	25
			Sosanopsis sp A	3
			Ampharetidae sp SD1	6
			Melinna oculata	16
		Pectinariidae	Pectinaria californiensis	130
		Terebellidae	Amaeana occidentalis	18
			Polycirrus californicus	95
			Polycirrus sp A	195
			Polycirrus sp OC1	205
			Polycirrus sp SD3	3
			Polycirrus sp	84
			Terebellinae	5
			Artacama coniferi	5
			Lanassa venusta venusta	165
			Phisidia sanctaemariae	206
			Pista brevibranchiata	9
			Pista estevanica	109
			Pista moorei	8
			Pista pacifica	2
			Pista wui	6
			Proclea sp A	211
			Scionella japonica	1
			Streblosoma sp B	5
		Trichobranchidae	Terebellides californica	163
			Terebellides sp Type C	1
			Terebellides sp Type D	1
			Trichobranchus hancocki	7
		Chaetopteridae		2
			Phyllochaetopterus limicolus	11
			Phyllochaetopterus prolifica	2
			Spiochaetopterus costarum Cmplx	42
		Capitellidae	Capitella capitata Cmplx	170
			Decamastus gracilis	15
			Mediomastus sp	767
			Notomastus hemipodus	59
		Cossuridae	Cossura candida	10

Appendix E.3 *continued*

Phylum	Class	Family	Taxon	n
			Cossura sp A	2
		Maldanidae		85
			Euclymeninae	14
			Axiothella sp	2
			Petaloclymene pacifica	61
			Praxillella gracilis	2
			Praxillella pacifica	191
			Euclymeninae sp A	406
			Clymenura gracilis	140
			Maldane sarsi	94
			Metasychis disparidentatus	1
			Notoproctus pacificus	4
			Rhodine bitorquata	103
		Opheliidae		1
			Ophelina acuminata	3
		Orbiniidae	Leitoscoloplos sp A	5
			Scoloplos armiger Cmplx	341
		Paraonidae		2
			Aricidea (Acmira) catherinae	80
			Aricidea (Acmira) lopezi	45
			Aricidea (Acmira) rubra	5
			Aricidea (Acmira) simplex	143
			Aricidea (Acmira) sp	1
			Aricidea (Aricidea) wassi	5
			Aricidea (Aricidea) sp SD1	1
			Aricidea (Strelzovia) antennata	39
			Aricidea (Strelzovia) hartleyi	1
			Aricidea (Strelzovia) sp A	13
			Levinsenia gracilis	19
			Levinsenia kirbyorum	19
			Paradoneis sp SD1	1
		Scalibregmatidae	Scalibregma californicum	43
		Travisiidae	Travisia brevis	46
Arthropoda	Ostracoda	Cypridinidae	Vargula tsujii	2
		Cylindroleberididae	Xenoleberis californica	47
		Philomedidae	Euphilomedes carcharodonta	1569
			Euphilomedes producta	448
			Scleroconcha trituberculata	4
		Sarsiellidae	Eusarsiella sp A	1
		Rutidermatidae	Rutiderma lomae	4
			Rutiderma sp	1
	Malacostraca	Nebaliidae	Nebalia pugettensis Cmplx	6
		Mysidae	Heteromysis odontops	2
			Mysidella americana	1
		--	Amphipoda	1
		Caprellidae	Caprella mendax	34
			Mayerella banksia	1
		Kamakidae	Amphideutopus oculatus	1
		Photidae	Gammaropsis thompsoni	2

Appendix E.3 *continued*

Phylum	Class	Family	Taxon	n
			Photis bifurcata	1
			Photis californica	37
			Photis lacia	34
			Photis macrotica	1
			Photis sp SD10	11
			Photis sp	30
		Aoridae		2
			Aoroides inermis	1
			Aoroides sp	4
		Corophiidae	Protomedeia articulata Cmplx	41
		Oedicerotidae	Americhelidium shoemakeri	11
			Americhelidium sp	11
			Bathymedon pumilus	34
			Deflexilodes enigmaticus	1
			Deflexilodes similis	37
			Monoculodes emarginatus	74
			Westwoodilla tone	10
		Eusiridae	Rhachotropis sp A	4
		Liljeborgiidae	Listriella eriopisa	1
			Listriella goleta	7
		Amphilochidae	Gitana calitemplado	1
		Stenothoidae	Stenothoe frecanda	4
		Melphidippidae	Melphisana bola	2
		Pardaliscidae	Halicoides synopiae	16
			Nicippe tumida	9
		Ampeliscidae	Ampelisca agassizi	1
			Ampelisca brevisimulata	28
			Ampelisca cf brevisimulata	6
			Ampelisca careyi	80
			Ampelisca cristata	2
			Ampelisca hancocki	30
			Ampelisca indentata	2
			Ampelisca microdentata	1
			Ampelisca pacifica	45
			Ampelisca pugetica	39
			Ampelisca sp	21
			Byblis millsi	14
			Byblis sp	1
		Lysianassidae	Aruga holmesi	2
			Aruga oculata	3
		Opisidae	Opisa tridentata	4
		Uristidae	Anonyx lilljeborgi	12
		Tryphosidae	Hippomedon sp A	5
			Hippomedon sp	1
			Lepidepecreum serraculum	1
		Pakynidae	Pachynus barnardi	1
			Prachynella lodo	4
		Cirolanidae	Eurydice caudata	2

Appendix E.3 *continued*

Phylum	Class	Family	Taxon	n
		Gnathiidae	Caecognathia crenulatifrons	175
		Anthuridae	Haliophasma geminatum	18
		Serolidae	Heteroserolis carinata	1
		Paramunnidae	Pleurogonium californiense	1
		--	Tanaidacea	10
		Akanthophoreidae	Chauliopleona dentata	5
		Anarthruridae	Siphonolabrum californiensis	1
		Leptocheliidae	Chondrochelia dubia Cmplx	99
		Tanaellidae	Araphura breviaria	52
			Araphura cuspirostris	3
			Araphura sp SD1	2
			Tanaella propinquus	25
		Pseudotanaidae	Pseudotanais californiensis	1
		Tanaopsidae	Tanaopsis cadieni	28
		--	Cumacea	2
		Leuconidae	Eudorella pacifica	4
			Leucon subnasica	2
		Nannastacidae	Campylaspis canaliculata	3
			Campylaspis rubromaculata	1
			Procampylaspis caenosa	19
		Lampropidae	Mesolamprops bispinosus	6
		Diastylidae		1
			Diastylis crenellata	32
			Leptostylis calva	2
		Crangonidae	Neocrangon zacae	1
		Cyclodorippidae	Deilocerus planus	4
			Deilocerus sp	1
		Pinnotheridae	Rathbunixa occidentalis Cmplx	12
Nematoda				9
Echinodermata	Asteroidea			27
		Astropectinidae	Astropecten californicus	3
		Astropectinidae	Astropecten sp	1
	Ophiuroidea			65
		Ophiuridae	Ophiura luetkenii	43
		Amphiuridae		357
			Amphichondrius granulatus	57
			Amphiodia digitata	30
			Amphiodia urtica	434
			Amphiodia sp	205
			Amphioplus strongyloplax	1
			Amphipholis squamata	2
			Amphiura arcystata	12
			Dougaloplus amphacanthus	5
			Dougaloplus sp A	8
			Dougaloplus sp	1
	Echinoidea			8
		Toxopneustidae	Lytechinus pictus	18
		Strongylocentrotidae	Strongylocentrotus fragilis	4
		--	Spatangoida	1

Appendix E.3 *continued*

Phylum	Class	Family	Taxon	n
		Spatangidae	Spatangus californicus	2
	Holothuroidea		Dendrochirotida	3
		Phyllophoridae	Pentamera rigida	3
		Synaptidae	Leptosynapta sp	62
		Chiridotidae	Chiridota sp	27
Phoronida		Phoronidae		5
			Phoronis sp	19
Brachiopoda	Lingulata	Lingulidae	Glottidia albida	2
Chordata	Enteropneusta			7
		Ptychoderidae	Balanoglossus sp	2
		Spengelidae	Schizocardium sp	1
		Harrimaniidae	Stereobalanus sp	11

Appendix E.4

Summary taxonomic listing of benthic infauna taxa identified from SBOO stations during 2025. Data are total number of individuals (n). Taxonomic arrangement follows SCAMIT (2023).

Phylum	Class	Family	Taxon	n
Cnidaria				1
	Hydrozoa	Corymorphidae	Corymorpha bigelowi	1
			Euphysa sp A	6
	Octocorallia		Pennatuloidea	1
		Virgulariidae		1
			Stylatula sp	1
	Ceriantharia			13
		Arachnactidae	Arachnanthus sp A	6
	Hexacorallia		Actiniaria	18
		Edwardsiidae		133
			Edwardsia californica	3
			Edwardsia juliae	606
			Edwardsia olguini	1
			Scolanthus triangulus	22
		Halcampidae	Halcampa decemtentaculata	80
			Halianthella sp A	4
		Isanthidae	Zaolutus actius	3
		Haloclavidae	Anemonactis sp A	3
		Limnactiniidae	Limnactiniidae sp A	1
		Halcampoididae	Pentactinia californica	2
Platyhelminthes	Rhabditophora	Hoploplanidae	Hoploplana californica	1
		Stylochidae	Stylochus exiguus	16
		Cryptocelidae	Cryptocelis occidentalis	2
		Leptoplanidae	Leptoplanidae sp A	1
		Stylochoplanidae	Armatoplana reishi	1
		--	Rhabdocoela sp A	2
			Rhabditophora sp A	2
			Rhabditophora sp C	3
Nemertea				26
	Palaeonemertea			6
		Cephalotrichidae	Cephalothrix sp	3
		Carinomidae	Carinoma mutabilis	76
		Carinomellidae	Carinomella lactea	1
		Tubulanidae	Tubulanidae	9
			Tubulanus cingulatus	17
			Tubulanus polymorphus	81
			Tubulanus sp A	2
			Tubulanidae sp B	2
			Tubulanidae sp D	1
			Tubulanidae sp E	3
	Pilidiophora		Heteronemertea	2
		Lineidae		75
			Cerebratulus californiensis	3
			Cerebratulus marginatus	1
			Maculaura alaskensis Cmplx	1
			Micrura wilsoni	3
			Siphonenteron bilineatum	51

Appendix E.4 *continued*

Phylum	Class	Family	Taxon	n
			Zygeupolia rubens	4
			Lineidae sp SD1	17
		--	Heteronemertea sp SD2	90
	Hoplonemertea			55
		Emplectonematidae	Cryptonemertes actinophila	4
		Neesidae	Paranemertes californica	9
		Ototyphlonemertidae	Ototyphlonemertes (Macintoshi) spiralis	36
		Prosorhochmidae	Prosorhochmus albidus	7
		Oerstediidae	Oerstedia dorsalis Cmplx	38
		Amphiporidae	Amphiporus californicus	3
		Amphiporidae	Amphiporus flavescens	1
		Tetrastemmatidae	Tetrastemma candidum	19
		Tetrastemmatidae	Tetrastemma sp HYP1	1
		Zygonemertidae	Zygonemertes virescens	1
		--	Quasitetrastemma nigrifrons	11
			Enopla sp A	1
Mollusca	Caudofoveata		Chaetodermatida	2
		Chaetodermatidae	Chaetoderma marinellii	3
			Chaetoderma pacificum	2
			Falcidens longus	9
	Gastropoda			1
		Trochidae	Halistylus pupoideus	8
		Cerithiidae	Lirobittium rugatum Cmplx	1
		Calyptraeidae	Calyptraea fastigiata	9
			Crepidula sp	2
			Crepipatella lingulata	1
		Naticidae	Glossaulax reclusiana	2
		Barleeiidae	Lirobarleeia kelseyi	1
		Caecidae	Caecum crebricinctum	5
		Eulimidae	Eulima raymondi	3
			Melanella oldroydi	3
			Polygireulima rutila	27
		Epitoniidae	Epitonium bellastriatum	9
			Epitonium berryi	1
			Opalia spongiosa	1
		Columbellidae	Amphissa undata	10
		Nassariidae	Caesia perpinguis	1
		Olividae	Callianax alectona	66
		Borsoniidae	Ophiodermella inermis	1
		Mangeliidae	Kurtziella plumbea	9
			Kurtzina beta	11
		Pseudomelatomidae	Megasurcula carpenteriana	1
		Terebridae	Neoterebra hemphilli	1
			Neoterebra pedroana	1
		Acteonidae	Acteon traskii	1
			Rictaxis punctocaelatus	16
		Goniodoridae		1
			Okenia sp A	3

Appendix E.4 *continued*

Phylum	Class	Family	Taxon	n
		Pleurobranchaeidae	Pleurobranchaea californica	1
		Pyramidellidae	Odostomia sp	16
			Turbonilla chocolata	5
			Turbonilla santarosana	20
			Turbonilla sp A	1
			Turbonilla sp SD5	1
			Turbonilla sp SD7	1
		Rhizoridae	Volvulella californica	1
			Volvulella cylindrica	7
			Volvulella panamica	4
			Volvulella sp	1
		Tornatinidae	Acteocina culcitella	1
		Cylichnidae	Cylichna diegensis	16
		Diaphanidae	Diaphana californica	1
		Aglajidae	Aglaja ocelligera	1
		Philinidae	Philine auriformis	3
		Philinoglossidae	Philinoglossa sp A	5
	Bivalvia			6
		Nuculidae	Ennucula tenuis	5
		Solemyidae	Petrasma pervernicosa	44
		Nuculanidae	Nuculana hamata	4
			Saccella penderi	1
			Saccella taphria	68
		Mytilidae		2
			Crenella decussata	23
			Solamen columbianum	18
			Gregariella coarctata	3
			Mytilus sp	1
			Modiolinae	11
			Amygdalum pallidulum	1
		Glycymerididae	Glycymeris septentrionalis	2
		Pectinidae		2
			Leptopecten latiauratus	34
		Lucinidae	Lucinoma annulatum	5
			Lucinisca nuttalli	1
			Parvilucina tenuisculpta	46
		Thyasiridae	Axinopsida serricata	9
			Thyasira flexuosa	12
		Lasaeidae	Kurtiella coani	1
			Kurtiella grippi	1
			Kurtiella tumida	64
			Kurtiella sp	2
		Carditidae	Scalaricarditinae	3
			Coanicardita ventricosa	2
			Keenaea centifilosa	12
		Tellinidae		1
			Tellina bodegensis	3
			Tellina cadieni	52

Appendix E.4 *continued*

Phylum	Class	Family	Taxon	n
			Tellina carpenteri	26
			Tellina idae	3
			Tellina modesta	111
			Macoma yoldiformis	80
			Macoma sp	3
		Semelidae	Semele venusta	1
		Mactridae	Simomactra falcata	14
		Veneridae	Compsomyax subdiaphana	14
			Venerinae	1
		Neoleptonidae	Neolepton subtrigonum	1
		Petricolidae	Cooperella subdiaphana	46
		Hiatellidae	Hiatella arctica	1
		Solenidae	Solen sicarius	12
		Pharidae	Ensis myrae	8
			Siliqua lucida	4
		Cuspidariidae	Cardiomya pectinata	3
			Cardiomya planetica	4
			Cuspidaria parapodema	2
		Lyonsiidae		4
			Entodesma navicula	12
			Lyonsia californica	16
		--	Thracioidea	2
		Thraciidae	Cyathodonta pedroana	4
			Thracia trapezoides	3
		Periplomatidae	Periploma discus	10
			Periploma sp	9
	Scaphopoda			2
		Dentaliidae	Antalis pretiosa	1
		--	Gadilida	2
		Gadilidae	Polyschides quadrifissatus	30
			Gadila aberrans	49
Annelida			Sipuncula	9
		Golfingiidae	Phascolion sp A	8
			Thysanocardia nigra	20
		Phascolosomatidae	Apionsoma misakianum	64
	Polychaeta		Echiura	1
		Amphinomidae	Paramphinome sp	201
			Pareurythoe californica	51
			Chloeia pinnata	158
		Dorvilleidae	Dorvillea (Schistomeringos) longicornis	2
			Meiodorvillea sp SD1	1
			Parougia caeca	5
			Pettiboneia sanmatiensis	4
			Protodorvillea gracilis	279
			Protodorvillea sp SD1	3
		Eunicidae	Leodice americana	6
			Marphysa sp	2
		Lumbrineridae	Eranno sp	1

Appendix E.4 *continued*

Phylum	Class	Family	Taxon	n
			Lumbrinerides platypygos	223
			Lumbrineris cruzensis	57
			Lumbrineris latreilli	253
			Lumbrineris ligulata	25
			Lumbrineris limicola	10
			Lumbrineris sp Group I	58
			Lumbrineris sp Group II	1
			Lumbrineris sp	2
			Scoletoma tetraura Cmplx	8
			Scoletoma sp	4
		Oenonidae	Drilonereis falcata	2
			Drilonereis mexicana	1
			Drilonereis sp	3
			Notocirrus californiensis	1
		Onuphidae		34
			Hyalinoecia juvenalis	2
			Nothria occidentalis	4
			Diopatra ornata	32
			Diopatra splendidissima	12
			Diopatra tridentata	18
			Diopatra sp	1
			Mooreonuphis exigua	66
			Mooreonuphis nebulosa	54
			Mooreonuphis sp SD1	107
			Mooreonuphis sp SD2	2
			Mooreonuphis sp	79
			Onuphis eremita parva	1
			Onuphis iridescens	12
			Onuphis sp A	76
			Onuphis sp	55
			Paradiopatra parva	91
			Rhamphobrachium longisetosum	3
		Aphroditidae		2
			Aphrodita sp	1
		Polynoidae		2
			Halosydna brevisetosa	1
			Lepidonotus spiculus	1
			Malmgreniella macginitiei	3
			Malmgreniella sanpedroensis	1
			Malmgreniella scriptoria	6
			Malmgreniella sp A	8
			Subadyte mexicana	1
			Tenonia priops	18
		Sigalionidae	Pholoides asperus	2
			Sigalion spinosus	126
			Sthenelais berkeleyi	3
			Sthenelais tertiaglabra	10
			Sthenelais verruculosa	4

Appendix E.4 *continued*

Phylum	Class	Family	Taxon	n
			Pholoe glabra	7
			Pisione sp	554
			Sthenelanella uniformis	286
		Glyceridae	Glycera americana	4
			Glycera macrobranchia	1
			Glycera nana	10
			Glycera oxycephala	161
			Hemipodia borealis	13
		Goniadidae	Glycinde armigera	131
			Goniada littorea	40
			Goniada maculata	36
		Chrysopetalidae	Paleanotus bellis	3
		Hesionidae	Oxydromus pugettensis	8
			Podarkeopsis glabrus	5
			Micropodarke dubia	287
		Microphthalmidae	Microphthalmus sp	7
		Nereididae		9
			Ceratonereis mirabilis	1
			Nereis sp A	70
			Nereis sp	10
			Platynereis bicanaliculata	107
		Pilargidae	Ancistrosyllis groenlandica	1
			Hermundura fauveli	1
			Hermundura ocularis	2
		Syllidae		1
			Streptosyllis sp SD1	4
			Syllides minutus	1
			Syllides reishi	1
			Syllides sp SD1	3
			Epigamia-Myrianida Cmplx	4
			Eusyllis blomstrandi Cmplx	4
			Eusyllis habei	130
			Eusyllis longicirrata	49
			Eusyllis transecta	11
			Eusyllis sp SD2	19
			Odontosyllis phosphorea	12
			Opisthodonta sp SD2	7
			Paraehlersia articulata	6
			Exogone dwisula	296
			Exogone lourei	136
			Parexogone acutipalpa	6
			Parexogone breviseta	8
			Parexogone molesta	56
			Salvatoria mediodentata	4
			Sphaerosyllis californiensis	9
			Sphaerosyllis ranunculus	12
			Syllis elongata	4
			Syllis farallonensis	2

Appendix E.4 *continued*

Phylum	Class	Family	Taxon	n
			Syllis gracilis Cmplx	6
			Syllis heterochaeta	45
			Syllis sp SD1	264
			Syllis sp SD2	143
			Syllis sp	2
			Trypanosyllis (Trypanedentata) sp SD1	2
		Nephtyidae	Aglaophamus verrilli	2
			Bipalponephtys cornuta	7
			Nephtys caecoides	25
			Nephtys ferruginea	2
			Nephtys simoni	11
			Nephtys sp SD2	6
		Sphaerodoridae	Sphaerephesia biserialis	3
		Phyllodocidae	Eteone brigitteae	2
			Eteone fauchaldi	1
			Eteone pigmentata	8
			Eulalia californiensis	5
			Eulalia levicornuta Cmplx	9
			Eulalia quadrioculata	1
			Eulalia sp SD1	10
			Eulalia sp	1
			Eumida longicornuta	99
			Hesionura coineaui difficilis	478
			Mystides sp	2
			Protomystides sp SD1	7
			Protomystides sp SD2	1
			Sige sp A	4
			Nereiphylla sp 2	2
			Nereiphylla sp SD1	1
			Paranaitis polynoides	2
			Phyllodoce cuspidata	1
			Phyllodoce hartmanae	174
			Phyllodoce longipes	103
			Phyllodoce medipapillata	7
			Phyllodoce pettiboneae	35
			Phyllodoce sp	7
		Fabriciidae	Pseudofabriciola californica	7
		Oweniidae	Galathowenia pygidialis	13
			Myriochele gracilis	6
			Myriochele striolata	15
			Owenia collaris	12
		Sabellariidae	Sabellaria gracilis	2
		Sabellidae		3
			Acromegalomma pigmentum	5
			Bispira sp	1
			Dialychone albocincta	12
			Dialychone trilineata	8
			Dialychone veleronis	82

Appendix E.4 *continued*

Phylum	Class	Family	Taxon	n
			Euchone arenae	43
			Euchone hancocki	11
			Euchone incolor	16
			Euchone sp A	9
			Euchone sp	1
			Jasmineira sp B	57
			Myxicola sp	2
			Paradialychone bimaculata	27
			Paradialychone eiffelturris	1
			Paradialychone harrisae	4
			Paradialychone paramollis	11
			Potamethus sp A	5
		Apistobranchidae	Apistobranchus ornatus	1
		Magelonidae	Magelona hartmanae	1
			Magelona pitelkai	3
			Magelona sacculata	8
			Magelona sp B	2
		Poecilochaetidae	Poecilochaetus johnsoni	11
		Spionidae		1
			Aonides sp SD1	1
			Dipolydora socialis	23
			Dipolydora sp	1
			Dispio sp SD1	12
			Dispio sp SD2	12
			Laonice cirrata	11
			Laonice nuchala	1
			Malacoceros indicus	2
			Microspio pigmentata	5
			Paraprionospio alata	82
			Polydora cirrosa	6
			Polydora cornuta	3
			Polydora heterochaeta	1
			Polydora narica	6
			Polydora nuchalis	1
			Prionospio dubia	31
			Prionospio jubata	132
			Prionospio lighti	25
			Prionospio pygmaeus	138
			Spio filicornis	4
			Spio maculata	52
			Spiophanes berkeleyorum	249
			Spiophanes duplex	605
			Spiophanes kimballi	13
			Spiophanes norrisi	1018
		Acrocirridae	Macrochaeta sp A	13
		Cirratulidae	Aphelochaeta glandaria Cmplx	45
			Aphelochaeta monilaris	13
			Aphelochaeta petersenae	2

Appendix E.4 *continued*

Phylum	Class	Family	Taxon	n
			Aphelochaeta sp D	76
			Aphelochaeta sp	2
			Caulleriella alata	1
			Caulleriella pacifica	5
			Caulleriella sp SD2	3
			Caulleriella sp	1
			Chaetozone armata	1
			Chaetozone corona	43
			Chaetozone hartmanae	10
			Chaetozone lunula	6
			Chaetozone sp A	11
			Chaetozone sp SD1	7
			Chaetozone sp SD2	7
			Chaetozone sp SD5	61
			Chaetozone sp SD7	5
			Chaetozone sp	3
			Cirratulus sp	3
			Cirriformia sp SD2	45
			Cirriformia sp SD3	6
			Kirkegaardia cryptica	13
			Kirkegaardia siblina	339
			Kirkegaardia tesselata	29
			Kirkegaardia sp SD9	5
			Kirkegaardia sp	2
			Protocirrineris sp B	1
		Flabelligeridae	Bradabyssa pilosa	6
			Bradabyssa pluribranchiata	1
			Pherusa neopapillata	23
			Trophoniella harrisae	1
		Sternaspidae	Sternaspis affinis	12
		Ampharetidae		48
			Amage anops	3
			Amage scutata	8
			Ampharete finmarchica	4
			Ampharete labrops	194
			Ampharete lineata	3
			Ampharete manriquei	29
			Amphicteis scaphobranchiata	57
			Amphisamytha bioculata	1
			Anobothrus bimaculatus	22
			Eclysippe trilobata	6
			Lysippe sp A	38
			Lysippe sp B	6
			Lysippe sp	2
			Phyllocomus hiltoni	3
			Phyllocomus sp A	2
			Melinna oculata	92
		Pectinariidae	Pectinaria californiensis	24

Appendix E.4 *continued*

Phylum	Class	Family	Taxon	n
		Terebellidae	Amaeana occidentalis	6
			Polycirrus californicus	40
			Polycirrus sp I	2
			Polycirrus sp A	115
			Polycirrus sp OC1	2
			Polycirrus sp SD3	482
			Polycirrus sp	46
			Artacama coniferi	8
			Lanassa venusta venusta	96
			Phisidia sanctaemariae	23
			Pista brevibranchiata	2
			Pista estevanica	55
			Pista pacifica	6
			Pista wui	63
			Pista sp	5
			Proclea sp A	3
			Scionella japonica	1
			Streblosoma crassibranchia	2
			Streblosoma sp B	53
			Streblosoma sp C	23
			Streblosoma sp SF1	5
			Streblosoma sp	4
		Trichobranchidae	Terebellides californica	5
			Terebellides sp Type C	6
			Trichobranchus hancocki	18
		Chaetopteridae	Phyllochaetopterus prolifica	5
			Spiochaetopterus costarum Cmplx	130
		Capitellidae	Capitella capitata Cmplx	12
			Mediomastus acutus	2
			Mediomastus sp	335
			Notomastus hemipodus	27
			Notomastus latericeus	249
			Notomastus magnus	1
			Notomastus sp	1
		Cossuridae	Cossura candida	4
		Maldanidae		51
			Euclymeninae	10
			Axiothella sp	6
			Clymenella complanata	4
			Clymenella sp SD1	5
			Clymenella sp	1
			Petaloclymene pacifica	93
			Praxillella pacifica	42
			Praxillella sp	4
			Euclymeninae sp A	523
			Clymenura gracilis	14
			Maldane sarsi	12
			Metasychis disparidentatus	24

Appendix E.4 *continued*

Phylum	Class	Family	Taxon	n
			Petaloproctus neoborealis	7
			Rhodine bitorquata	9
		Opheliidae	Ophelia pulchella	26
			Armandia brevis	4
			Ophelina sp SD1	3
		Orbiniidae		1
			Leitoscoloplos pugettensis	8
			Naineris uncinata	8
			Scoloplos acmeceps	21
			Scoloplos armiger Cmplx	132
		Paraonidae	Aricidea (Acmira) catherinae	12
			Aricidea (Acmira) cerrutii	7
			Aricidea (Acmira) horikoshii	2
			Aricidea (Acmira) lopezi	3
			Aricidea (Acmira) rubra	1
			Aricidea (Acmira) simplex	20
			Aricidea (Aricidea) wassi	5
			Aricidea (Strelzovia) antennata	5
			Aricidea (Strelzovia) hartleyi	2
			Aricidea (Strelzovia) sp A	1
			Cirrophorus branchiatus	11
			Cirrophorus furcatus	1
			Levinsenia barwicki	1
			Levinsenia gracilis	5
			Levinsenia kirbyorum	2
			Paradoneis sp SD1	33
		Scalibregmatidae	Scalibregma californicum	19
		Travisiidae	Travisia brevis	2
			Travisia gigas	1
		Polygordiidae	Polygordius sp SD1	8
		Saccocirridae	Pharyngocirrus eroticus	208
			Saccocirrus sp	133
	Clitellata		Oligochaeta	35
Arthropoda	Pycnogonida	Ammotheidae	Prototrygaeus jordanae	1
	Ostracoda	Cylindroleberididae	Cylindroleberididae	1
			Leuroleberis sharpei	8
			Xenoleberis californica	4
		Philomedidae	Euphilomedes carcharodonta	171
		Sarsiellidae	Eusarsiella thominx	3
		Rutidermatidae	Rutiderma rotundum	5
		--	Podocopida	3
	Malacostraca		Leptostraca	8
		Nebaliidae	Nebalia daytoni	11
			Nebalia pugettensis Cmplx	2
		Mysidae	Heteromysis odontops	1
			Alienacanthomysis macropsis	3
			Neomysis kadiakensis	7
			Pacifacanthomysis nephrophthalma	1

Appendix E.4 *continued*

Phylum	Class	Family	Taxon	n
			Mysidopsis californica	1
		--	Amphipoda	2
			Corophiida	1
		Caprellidae		1
			Caprella californica Cmplx	4
			Caprella mendax	2
			Mayerella banksia	1
		Ischyroceridae	Ericthonius brasiliensis	12
			Notopoma sp A	9
		Kamakidae	Amphideutopus oculatus	31
		Photidae	Ampelisciphotis podophthalma	26
			Gammaropsis thompsoni	33
			Photis bifurcata	8
			Photis brevipes	30
			Photis californica	89
			Photis lacia	1
			Photis sp C	17
			Photis sp OC1	109
			Photis sp SD10	1
			Photis sp	32
		Aoridae		1
			Aoroides exilis	1
			Aoroides inermis	4
			Aoroides intermedia	3
			Aoroides sp A	3
			Aoroides sp	9
		Unciolidae	Rudilemboides stenopropodus	5
			Rudilemboides sp A	17
		Ampithoidae		4
		Corophiidae	Laticorophium baconi	29
			Protomedeia articulata Cmplx	3
		Megaluropidae	Gibberosus myersi	15
			Megaluropidae sp A	1
		Oedicerotidae		1
			Americhelidium shoemakeri	21
			Americhelidium sp SD1	26
			Americhelidium sp SD4	12
			Americhelidium sp	3
			Bathymedon pumilus	1
			Deflexilodes similis	4
			Hartmanodes hartmanae	11
			Hartmanodes sp SD1	1
			Monoculodes emarginatus	1
			Westwoodilla tone	17
		Eusiridae	Rhachotropis sp A	2
		Liljeborgiidae	Listriella diffusa	1
			Listriella eriopisa	2
			Listriella goleta	3

Appendix E.4 *continued*

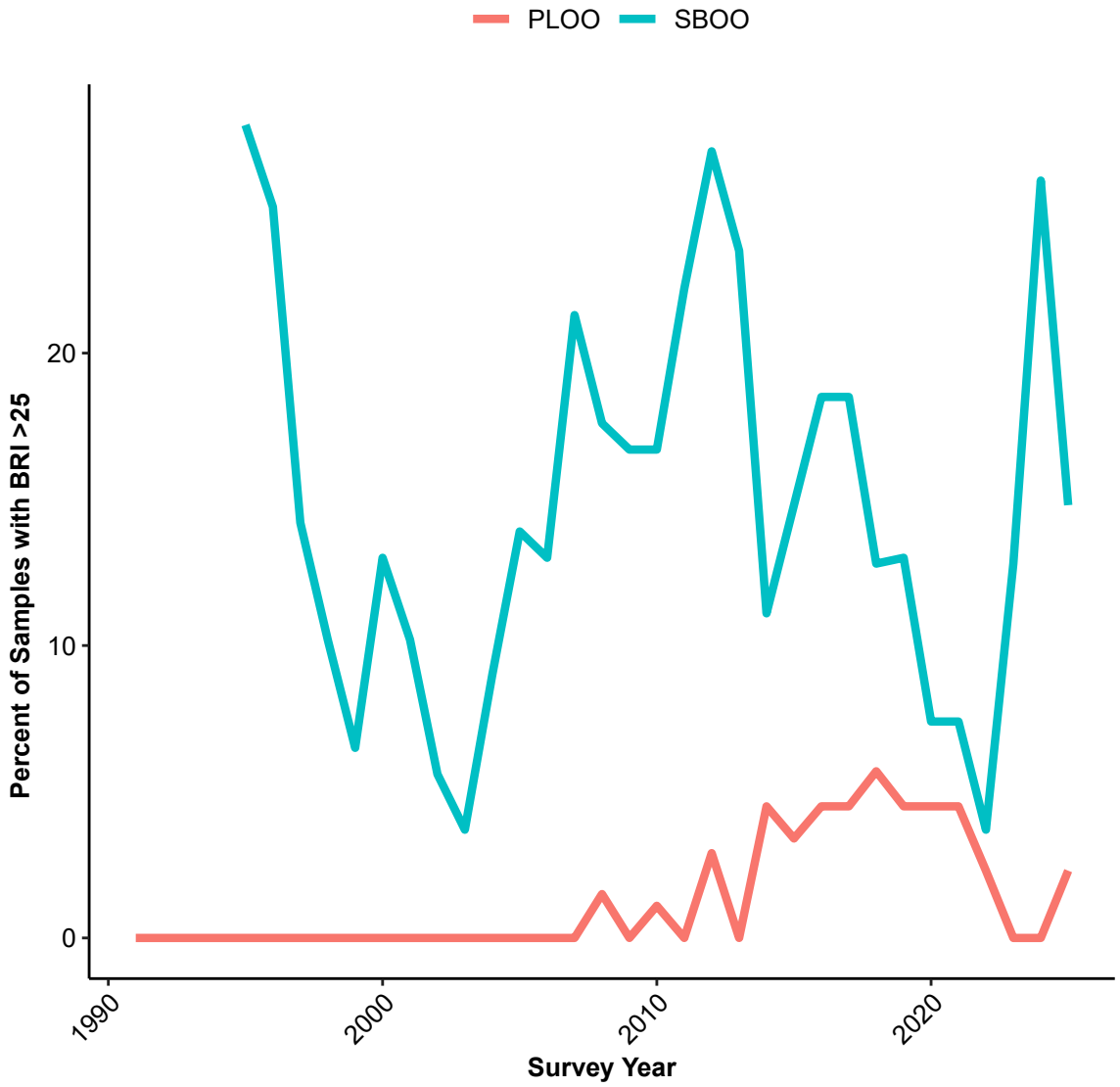
Phylum	Class	Family	Taxon	n
			Listriella melanica	4
		Pleustidae		2
			Pleusymtes subglaber	2
		Stenothoidae	Stenothoides bicoma	2
		Melphidippidae	Melphisana bola	2
		Pardaliscidae	Halicoides synopiae	10
		Ampeliscidae	Ampelisca agassizi	68
			Ampelisca brachycladus	18
			Ampelisca brevisimulata	121
			Ampelisca cf brevisimulata	9
			Ampelisca careyi	34
			Ampelisca cristata	71
			Ampelisca hancocki	2
			Ampelisca indentata	2
			Ampelisca lobata	2
			Ampelisca microdentata	70
			Ampelisca pacifica	1
			Ampelisca pugetica	35
			Ampelisca romigi	3
			Ampelisca sp	13
			Byblis millsi	22
		Synopiidae	Metatiron tropakis	4
			Tiron biocellata	6
		Argissidae	Argissa hamatipes	26
		Haustoriidae	Eohaustorius barnardi	5
		Platyischnopidae	Tiburonella viscana	4
		Phoxocephalidae		11
			Foxiphalus golfensis	2
			Foxiphalus obtusidens	103
			Rhepoxynius abronius	1
			Rhepoxynius daboius	9
			Rhepoxynius fatigans	3
			Rhepoxynius heterocuspidatus	102
			Rhepoxynius lucubrans	20
			Rhepoxynius menziesi	104
			Rhepoxynius stenodes	84
			Rhepoxynius variatus	2
			Rhepoxynius sp	2
		Lysianassidae	Aruga oculata	1
		Tryphosidae	Hippomedon zetesimus	6
			Lepidepecreum serraculum	3
			Orchomene anaquelus	1
			Orchomenella decipiens	1
			Orchomenella pacifica	1
			Tryphosinae incertae sedis ental-ladurus	13
		Acidostomatidae	Acidostoma hancocki	4
		Pakynidae	Pachynus barnardi	3

Appendix E.4 *continued*

Phylum	Class	Family	Taxon	n
		Cirolanidae	Eurydice caudata	13
		Gnathiidae	Caecognathia crenulatifrons	41
		Anthuridae	Haliophasma geminatum	43
		Arcturidae	Neastacilla californica	1
		Idoteidae	Edotia sublittoralis	27
			Synidotea magnifica	16
		Serolidae	Heteroserolis carinata	5
		Microparasellidae	Microcharon sp A	11
		--	Tanaidacea	3
		Akanthophoreidae	Chauliopleona dentata	5
		Anarthruridae	Siphonolabrum californiensis	1
		Leptocheliidae	Chondrochelia dubia Cmplx	373
		Tanaellidae	Araphura breviaria	6
			Araphura sp SD1	11
		Pseudotanaidae	Pseudotanais californiensis	4
		Tanaopsidae	Tanaopsis cadieni	5
		Bodotriidae	Cyclaspis nubila	5
		Nannastacidae	Campylaspis canaliculata	11
			Campylaspis rubromaculata	5
			Procampylaspis caenosa	6
		Lampropidae	Hemilamprops californicus	48
			Mesolamprops bispinosus	17
		Diastylidae	Anchicolurus occidentalis	1
			Diastylis californica	4
			Diastylis crenellata	1
			Diastylopsis tenuis	1
			Leptostylis abditis	1
			Oxyurostylis pacifica	3
		Crangonidae		1
			Crangon alba	1
		Callianassidae	Neotrypaea sp	3
		Diogenidae	Paguristes turgidus	1
		Blepharipodidae	Blepharipoda occidentalis	36
		--	Majoidea	1
		Inachidae	Erileptus spinosus	2
		Inachoididae	Pyromaia tuberculata	1
		Cancridae		1
			Metacarcinus gracilis	1
		Pinnotheridae		16
			Scleroplax franciscana	6
			Scleroplax tubicola	2
			Pinnixa longipes	2
			Rathbunixa occidentalis Cmplx	13
	Hexanauplia	Scalpellidae	Hamatoscalpellum californicum	1
		Balanidae	Balanus sp	3
Nematoda				179
Echinodermata	Asteroidea			80
		Astropectinidae	Astropecten californicus	17

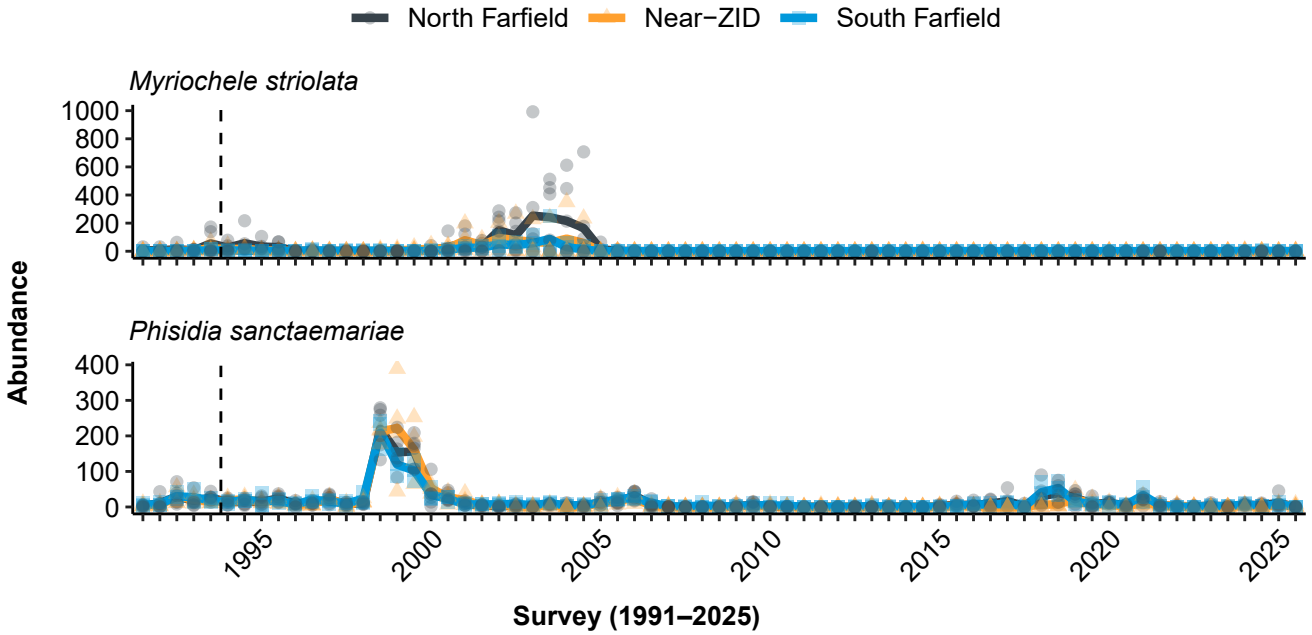
Appendix E.4 *continued*

Phylum	Class	Family	Taxon	n
			Astropecten sp	3
	Ophiuroidea			11
		Ophiuridae	Ophiura luetkenii	16
		Ophioscolecidae	Ophiuroconis bispinosa	17
		Amphiuridae		65
			Amphiodia digitata	4
			Amphiodia psara	1
			Amphiodia urtica	16
			Amphiodia sp	28
			Amphioplus strongyloplax	1
			Amphioplus sp A	1
			Amphioplus sp	12
			Amphipholis squamata	11
			Amphipholis sp	6
			Dougaloplus sp A	4
		Ophiotrichidae	Ophiothrix spiculata	17
	Echinoidea			7
		Toxopneustidae	Lytechinus pictus	14
		Dendrasteridae	Dendraster terminalis	50
			Dendraster sp	23
		Loveniidae	Lovenia cordiformis	3
	Holothuroidea		Dendrochirotida	8
		Phyllophoridae		4
			Pentamera sp	2
			Phyllophoridae sp A	1
		Synaptidae	Leptosynapta sp	14
		Chiridotidae	Chiridota sp	4
Phoronida			Phoronidae	7
			Phoronis sp	58
			Phoronopsis sp	11
Brachiopoda	Lingulata	Lingulidae	Glottidia albida	83
Chordata	Enteropneusta	Ptychoderidae	Balanoglossus sp	2
		Spengelidae	Schizocardium sp	9
		Harrimaniidae	Saccoglossus sp	3
	Ascidiacea			1
		Agneziidae	Agnezia septentrionalis	6
		Styelidae	Cnemidocarpa rhizopus	10
		Molgulidae		22
			Eugyra arenosa californica	1
			Eugyra sp	3
			Molgula pugetiensis	6
			Molgula regularis	4
	Leptocardii	Branchiostomatidae	Branchiostoma californiense	30



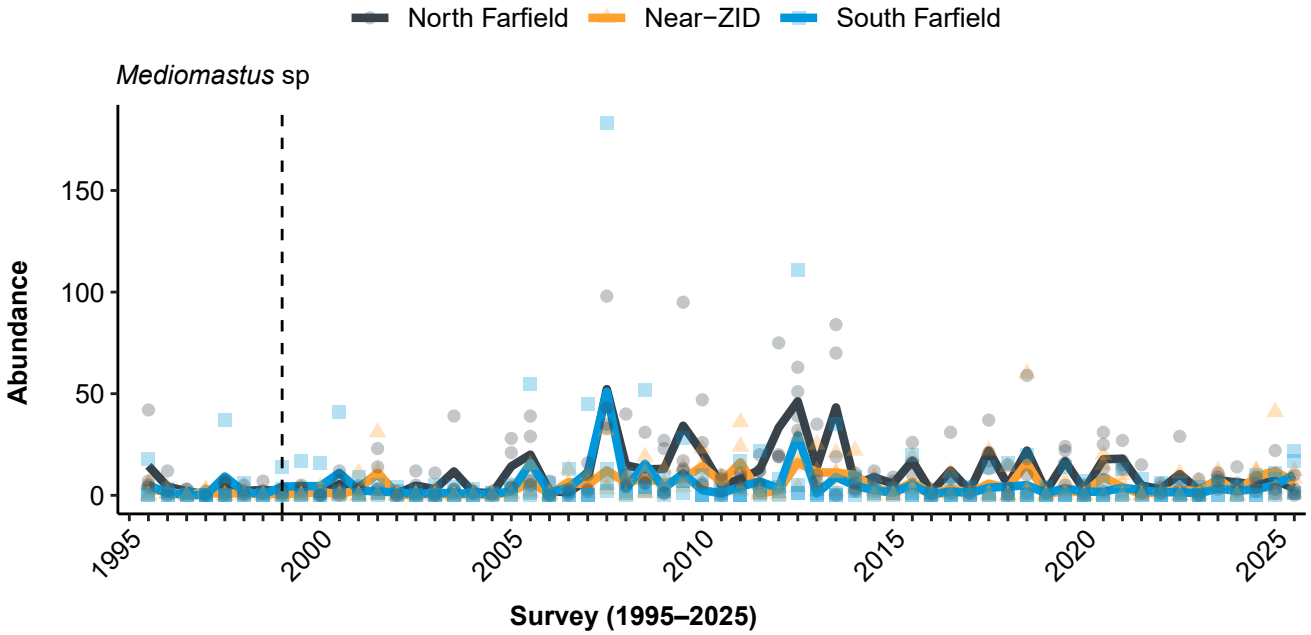
Appendix E.5

Percent of stations with BRI values greater than 25 over time. Monitoring in the PLOO region's current station configuration began in 1991. Monitoring in the SBOO region began in 1995.



Appendix E.6

Two of the five historically most abundant species recorded from 1991 through 2025 at PLOO north farfield, near-ZID, and south farfield primary core stations. The other historically dominant taxa, *Amphiodia urtica, Spiophanes duplex,* and *Proclea* sp A, are shown in Figures 6.4 and 6.5. For each station group, mean abundance per survey is shown by the solid line ($n \leq 8$) while abundance per station is shown by the symbols. Dashed lines indicate onset of wastewater discharge.



Appendix E.7

One of the five historically most abundant species recorded from 1995 through 2025 at SBOO north farfield, near-ZID, and south farfield primary core stations. The other historically dominant taxa, *Spiophanes norrisi, Spiophanes duplex,* Euclymeninae sp A, and *Kirkegaardia siblina*, are shown in Figure 6.6. For each station group, mean abundance per survey is shown by the solid line ($n \leq 8$) while abundance per station is shown by the symbols. Dashed lines indicate onset of wastewater discharge.

Appendix F

San Diego Regional Benthic Condition Assessment

2024 – 2025
Raw Data Tables & Supplemental Analyses

Appendix F.1

Summary of visual observations for each regional station sampled during summer 2025. Visual observations are from sieved "grunge" (i.e., particles retained on 1-mm mesh screen and preserved with infauna for benthic community analysis).

	Station	Depth (m)	Vis Obs
Inner Shelf	9519	13	-
	9541	15	shell hash; organic debris
	9516	17	shell hash
	9508	21	-
	9515	22	-
	9513	24	organic debris
	9501	25	-
	9509	25	-
Mid Shelf	9531	35	organic debris
	9503	45	fine red relict sand
	9538	46	organic debris
	9510	49	shell hash; coarse sand
	9536	57	-
	9532	60	gravel
	9520	67	-
	9530	72	shell hash
	9523	73	-
	9525	75	organic debris
	9505	76	-
	9540	77	-
	9529	84	-
	9512	90	shell hash
	9528	96	organic debris
	9504	98	-
	9518	98	coarse sand; organic debris
Outer Shelf	9506	128	-
	9539	152	organic debris
	9521	154	organic debris
	9537	162	pea gravel; organic debris; shell hash
	9526	166	organic debris
	9533	177	organic debris
	9511	178	pea gravel; coarse sand
	9514	197	pea gravel; organic debris; coarse sand
	9517	199	organic debris
Upper Slope	9507	212	organic debris
	9524	271	organic debris
	9527	319	organic debris
	9534	357	organic debris
	9535	405	-
	9556	433	shell hash; organic debris

Appendix F.2

Concentrations of organic indicators detected in sediments from the San Diego regional benthic stations sampled during summer 2025. See Appendix F.1 for MDLs; DR = detection rate; DNQ = do not quantify; ND = not detected; NR = not reportable.

	Station	Depth (m)	Sulfides (ppm)	TN (% wt)	TOC (% wt)	TVS (% wt)
Inner Shelf	9519	13	25.9	ND	ND	0.8
	9541	15	ND	ND	ND	0.6
	9516	17	ND	ND	ND	0.7
	9508	21	ND	ND	ND	0.8
	9515	22	5.32	ND	ND	0.9
	9513	24	ND	0.029	ND	0.6
	9501	25	ND	0.039	ND	0.9
	9509	25	ND	ND	ND	1.0
Mid Shelf	9531	35	11	0.054	0.28	1.4
	9503	45	ND	ND	ND	0.5
	9538	46	31.7	0.051	0.40	2.1
	9510	49	10.9	0.059	0.54	1.9
	9536	57	25.5	0.046	0.42	1.8
	9532	60	18.8	0.098	0.75	3.0
	9520	67	26.5	0.072	0.66	2.9
	9530	72	6.22	0.082	0.59	2.4
	9523	73	5.26	0.076	0.73	2.8
	9525	75	2.26	0.084	0.74	2.8
	9505	76	14	0.080	0.54	1.8
	9540	77	11.9	0.060	0.51	2.3
	9529	84	22.1	ND	ND	3.4
	9512	90	7.53	ND	0.29	2.1
	9528	96	31.1	0.078	0.74	2.9
	9504	98	15.6	0.072	0.49	1.9
	9518	98	10.8	0.034	0.30	1.7
Outer Shelf	9506	128	6.94	0.079	0.94	2.8
	9539	152	29.8	0.068	0.64	3.1
	9521	154	ND	0.068	0.70	2.9
	9537	162	34.9	0.069	0.81	4.0
	9526	166	13.3	0.074	0.72	2.6
	9533	177	13.8	ND	0.81	2.8
	9511	178	ND	0.046	0.23	3.0
	9514	197	13.1	ND	0.25	4.6
	9517	199	11.9	0.156	1.87	6.0
Upper Slope	9507	212	44.6	0.157	2.35	5.9
	9524	271	86	0.173	2.18	6.5
	9527	319	19.2	0.124	1.68	5.9
	9534	357	42.1	0.133	1.76	5.9
	9535	405	43.7	0.156	1.87	5.2
	9556	433	93.4	0.165	2.11	6.1
	DR (%)		77	72	75	100

Appendix F.3

Concentrations of metals (ppm) detected in sediments from the San Diego regional benthic stations sampled during summer 2025. See Appendix F.1 for MDLs and translation of periodic table symbols; DR = detection rate; DNQ = do not quantify; ND = not detected; NR = not reportable.

	Station	Depth (m)	Al	Sb	As	Ba	Be	Cd	Cr	Cu	Fe
Inner Shelf	9519	13	3660	0.24 DNQ	1.78	18.5	0.06	ND	7.0	2.3	4860
	9541	15	3190	ND	1.62	19.6	0.06	0.04 DNQ	8.9	1.8	4900
	9516	17	2760	0.38 DNQ	1.65	15.9	0.06	ND	6.7	1.9	5080
	9508	21	3500	ND	1.03	15.3	0.06	0.02 DNQ	7.2	1.5	3390
	9515	22	4910	0.25 DNQ	2.30	25.7	0.09	0.03 DNQ	8.6	3.1	6300
	9513	24	2530	ND	1.62	13.9	0.05 DNQ	ND	4.9	1.5	3650
	9501	25	4850	0.29 DNQ	1.40	26.8	0.09	0.02 DNQ	8.9	2.4	5230
	9509	25	4700	0.30 DNQ	1.44	19.3	0.08	0.04 DNQ	8.9	2.4	4560
Mid Shelf	9531	35	3800	0.32 DNQ	1.89	22.5	0.08	0.12	8.3	2.3	5100
	9503	45	975	0.55 DNQ	9.47	1.8	0.05	0.04 DNQ	8.7	0.4 DNQ	7220
	9538	46	9380	0.64 DNQ	3.23	60.5	0.20	0.08 DNQ	17.7	7.1	11900
	9510	49	6510	0.47 DNQ	2.83	29.0	0.13	0.10	12.4	5.7	8040
	9536	57	5900	0.41 DNQ	2.45	34.2	0.13	0.14	11.9	4.2	7470
	9532	60	9400	0.70 DNQ	3.22	46.3	0.21	0.12	19.3	7.3	13000
	9520	67	10600	0.78 DNQ	3.13	54.1	0.21	0.16	19.2	9.5	12400
	9530	72	8190	0.65 DNQ	3.01	37.5	0.18	0.07 DNQ	16.9	7.2	11300
	9523	73	10700	0.75 DNQ	3.55	53.3	0.22	0.12	20.3	9.8	13400
	9525	75	10500	0.76 DNQ	3.49	50.5	0.22	0.11	20.2	9.4	13400
	9505	76	5440	0.47 DNQ	2.22	22.8	0.13	0.07 DNQ	12.0	5.2	7500
	9540	77	8620	0.60 DNQ	3.01	46.3	0.24	0.07 DNQ	17.8	6.3	12500
	9529	84	10700	0.87 DNQ	3.59	49.1	0.24	0.09 DNQ	21.5	9.9	14300
	9512	90	6750	0.56 DNQ	2.38	28.0	0.14	0.06 DNQ	13.4	6.9	8690
	9528	96	8050	0.60 DNQ	2.78	42.3	0.21	0.06 DNQ	18.6	7.2	12700
	9504	98	4420	0.40 DNQ	1.92	16.1	0.11	0.06 DNQ	10.2	3.9	6470
	9518	98	4340	0.43 DNQ	2.19	18.8	0.11	0.13	10.3	4.9	6260
Outer Shelf	9506	128	7690	0.47 DNQ	2.32	29.4	0.18	0.08 DNQ	15.4	7.2	9880
	9539	152	8360	0.74 DNQ	3.18	44.3	0.21	0.35	17.5	9.4	11300
	9521	154	8300	0.65 DNQ	2.45	33.1	0.19	0.10	17.6	8.0	10600
	9537	162	11100	0.81 DNQ	4.45	55.6	0.26	0.31	19.7	9.7	13700
	9526	166	7600	0.58 DNQ	2.30	31.9	0.18	0.15	16.2	7.3	9980
	9533	177	7490	0.61 DNQ	2.75	30.8	0.18	0.25	15.6	6.1	9800
	9511	178	16200	0.81 DNQ	2.44	89.2	0.33	ND	19.5	20.1	20900
	9514	197	12300	0.83 DNQ	2.50	62.7	0.26	0.11	24.6	22.2	14900
	9517	199	14600	1.12	2.82	66.0	0.32	0.14	29.7	20.9	16600
Upper Slope	9507	212	12600	0.90 DNQ	3.39	57.1	0.30	0.16	27.0	16.1	15200
	9524	271	14000	0.88 DNQ	3.00	67.6	0.32	0.21	29.6	16.5	16000
	9527	319	12100	1.02	3.21	61.2	0.30	0.29	28.1	14.6	15300
	9534	357	13100	1.18	3.38	59.9	0.34	0.25	31.6	13.7	16000
	9535	405	12900	0.91 DNQ	2.65	67.4	0.30	0.31	28.6	13.8	14800
	9556	433	12500	1.02	2.77	75.4	0.29	0.31	27.1	15.2	14500
	DR (%)		100	92	100	100	100	90	100	100	100

Appendix F.3 *continued*

	Station	Depth (m)	Pb	Mn	Hg	Ni	Se	Ag	Sn	Zn
Inner Shelf	9519	13	1.8	55	0.011	2.0	0.28 DNQ	ND	0.38 DNQ	13.3
	9541	15	1.3	58	0.004 DNQ	1.7	ND	ND	0.35 DNQ	9.6
	9516	17	2.3	65	0.015	1.4	ND	ND	0.41 DNQ	9.9
	9508	21	1.0	47	0.008 DNQ	1.6	ND	ND	0.28 DNQ	8.4
	9515	22	2.5	69	0.016	2.5	0.24 DNQ	ND	0.49 DNQ	16.5
	9513	24	1.6	38	0.010	1.2	ND	ND	0.43 DNQ	8.8
	9501	25	1.1	64	0.005 DNQ	2.5	ND	ND	0.39 DNQ	13.0
	9509	25	1.4	53	0.009 DNQ	2.4	ND	ND	0.38 DNQ	12.3
Mid Shelf	9531	35	1.7	66	0.014	2.4	0.23 DNQ	ND	0.49 DNQ	13.0
	9503	45	2.7	12	ND	0.7	0.28 DNQ	ND	0.14 DNQ	5.3
	9538	46	2.7	133	0.013	6.2	ND	ND	0.76	36.5
	9510	49	3.0	77	0.031	5.0	0.35 DNQ	ND	1.01	21.2
	9536	57	2.7	80	0.019	4.5	ND	ND	0.58	20.2
	9532	60	4.1	116	0.039	6.7	0.55 DNQ	ND	1.02	35.7
	9520	67	4.1	126	0.049	8.0	0.73 DNQ	ND	1.14	36.3
	9530	72	4.0	95	0.035	6.7	ND	ND	0.93	28.7
	9523	73	4.5	126	0.076	8.6	0.62 DNQ	ND	1.25	36.1
	9525	75	4.1	122	0.044	8.7	0.55 DNQ	ND	1.11	34.9
	9505	76	3.2	63	0.034	5.5	ND	ND	0.67	19.8
	9540	77	3.6	104	0.020	6.0	ND	ND	0.79	29.7
	9529	84	4.3	120	0.045	9.4	0.50 DNQ	ND	1.12	36.7
	9512	90	62.0	75	0.041	5.4	0.34 DNQ	ND	0.82	22.5
	9528	96	3.7	97	0.042	7.3	0.28 DNQ	ND	0.84	31.1
	9504	98	2.3	54	0.020	4.4	0.23 DNQ	ND	0.51	15.6
	9518	98	1.9	54	0.027	4.2	0.30 DNQ	ND	0.55	17.4
Outer Shelf	9506	128	2.9	82	0.037	7.4	0.37 DNQ	ND	0.92	25.7
	9539	152	3.8	98	0.030	6.8	0.25 DNQ	ND	0.77	29.4
	9521	154	3.5	90	0.045	8.0	0.51 DNQ	ND	0.88	28.0
	9537	162	4.4	132	0.034	8.0	0.34 DNQ	ND	0.97	39.2
	9526	166	3.5	87	0.068	7.3	0.41 DNQ	ND	0.80	26.6
	9533	177	3.2	78	0.032	6.6	ND	ND	0.64	24.9
	9511	178	2.8	364	0.029	7.8	0.77 DNQ	ND	0.91	41.5
	9514	197	7.1	122	0.126	10.9	0.68 DNQ	ND	1.51	44.9
	9517	199	6.5	137	0.143	14.9	0.99 DNQ	ND	1.56	50.0
Upper Slope	9507	212	4.5	109	0.069	13.5	0.88 DNQ	ND	1.71	41.6
	9524	271	5.2	137	0.079	15.9	0.91 DNQ	ND	1.33	48.4
	9527	319	4.9	119	0.062	13.9	0.81 DNQ	ND	1.10	44.4
	9534	357	4.4	115	0.059	13.0	0.70 DNQ	ND	1.07	42.8
	9535	405	3.9	120	0.050	12.9	0.85 DNQ	ND	1.04	43.4
	9556	433	4.4	126	0.062	14.4	1.15	ND	1.11	45.6
	DR (%)		100	100	97	100	70	0	100	100

Appendix F.4

Concentrations of pesticides (ppt) detected in sediments from the San Diego regional benthic stations sampled during summer 2025. See Appendix F.1 for MDLs and abbreviations; DR = detection rate; DNQ = do not quantify; ND = not detected; NR = not reportable.

			Chlordane							
	Station	Depth (m)	A(c)C	cNon	G(t)C	Hept	HeptEpox	Methoxy	Oxychlor	tNon
Inner Shelf	9519	13	ND	ND	ND	ND	ND	ND	ND	ND
	9541	15	ND	ND	ND	ND	ND	ND	ND	ND
	9516	17	ND	ND	ND	ND	ND	ND	ND	ND
	9508	21	ND	ND	ND	ND	ND	ND	ND	ND
	9515	22	ND	ND	ND	ND	ND	ND	ND	ND
	9513	24	ND	ND	ND	ND	ND	ND	ND	ND
	9501	25	ND	ND	ND	ND	ND	ND	ND	ND
	9509	25	ND	ND	ND	ND	ND	ND	ND	ND
Mid Shelf	9531	35	ND	ND	ND	ND	ND	ND	ND	ND
	9503	45	ND	ND	ND	ND	ND	ND	ND	ND
	9538	46	ND	ND	ND	ND	ND	ND	ND	ND
	9510	49	ND	ND	ND	ND	ND	ND	ND	ND
	9536	57	ND	ND	ND	ND	ND	ND	ND	ND
	9532	60	ND	ND	ND	ND	ND	ND	ND	ND
	9520	67	ND	ND	ND	ND	ND	ND	ND	ND
	9530	72	ND	ND	ND	ND	ND	ND	ND	ND
	9523	73	ND	ND	ND	ND	ND	ND	ND	ND
	9525	75	ND	ND	ND	ND	ND	ND	ND	ND
	9505	76	ND	ND	ND	ND	ND	ND	ND	ND
	9540	77	ND	ND	ND	ND	ND	ND	ND	ND
	9529	84	ND	ND	ND	ND	ND	ND	ND	ND
	9512	90	ND	ND	ND	ND	ND	ND	ND	ND
	9528	96	ND	ND	ND	ND	ND	ND	ND	ND
	9504	98	ND	ND	ND	ND	ND	ND	ND	ND
	9518	98	ND	ND	ND	ND	ND	ND	ND	ND
Outer Shelf	9506	128	ND	ND	ND	ND	ND	ND	ND	ND
	9539	152	ND	ND	ND	ND	ND	ND	ND	ND
	9521	154	ND	ND	ND	ND	ND	ND	ND	ND
	9537	162	ND	ND	ND	ND	ND	ND	ND	ND
	9526	166	ND	ND	ND	ND	ND	ND	ND	ND
	9533	177	ND	ND	ND	ND	ND	ND	ND	ND
	9511	178	ND	ND	ND	ND	ND	ND	ND	ND
	9514	197	ND	ND	ND	ND	ND	ND	ND	ND
	9517	199	ND	ND	ND	ND	ND	ND	ND	ND
Upper Slope	9507	212	ND	ND	ND	ND	ND	ND	ND	ND
	9524	271	ND	ND	ND	ND	ND	ND	ND	ND
	9527	319	ND	ND	ND	ND	ND	ND	ND	ND
	9534	357	ND	ND	ND	ND	ND	ND	ND	ND
	9535	405	ND	ND	ND	ND	ND	ND	ND	ND
	9556	433	ND	ND	ND	ND	ND	ND	ND	ND
DR (%)			0	0	0	0	0	0	0	0

Appendix F.4 *continued*

	Station	Depth (m)	DDT						
			o,p-DDD	o,p-DDE	o,p-DDT	p,-p-DDMU	p,p-DDD	p,p-DDE	p,p-DDT
Inner Shelf	9519	13	ND	ND	ND	ND	ND	ND	ND
	9541	15	ND	ND	ND	ND	ND	ND	ND
	9516	17	ND	ND	ND	ND	ND	ND	ND
	9508	21	ND	ND	ND	ND	ND	ND	ND
	9515	22	ND	ND	ND	ND	ND	ND	ND
	9513	24	ND	ND	ND	ND	ND	ND	ND
	9501	25	ND	ND	ND	ND	ND	ND	ND
	9509	25	ND	ND	ND	ND	ND	ND	ND
Mid Shelf	9531	35	ND	ND	ND	ND	ND	ND	ND
	9503	45	ND	ND	ND	ND	ND	ND	ND
	9538	46	ND	ND	ND	ND	ND	137	ND
	9510	49	ND	ND	ND	ND	ND	286	ND
	9536	57	ND	ND	ND	ND	ND	923 DNQ	ND
	9532	60	ND	ND	ND	ND	ND	246	344
	9520	67	ND	ND	ND	ND	ND	463	133
	9530	72	ND	ND	ND	ND	ND	230	ND
	9523	73	ND	ND	ND	ND	ND	245	ND
	9525	75	ND	ND	ND	ND	ND	280	ND
	9505	76	ND	ND	ND	ND	ND	495	ND
	9540	77	ND	ND	ND	ND	ND	201	ND
	9529	84	ND	ND	ND	ND	ND	504	ND
	9512	90	ND	ND	ND	ND	ND	272	ND
	9528	96	ND	ND	ND	ND	ND	260	ND
	9504	98	ND	ND	ND	ND	ND	244	ND
	9518	98	ND	ND	ND	ND	ND	109	ND
Outer Shelf	9506	128	ND	ND	ND	ND	ND	287	ND
	9539	152	ND	ND	ND	ND	ND	312	ND
	9521	154	ND	ND	ND	ND	ND	393	ND
	9537	162	ND	ND	ND	ND	ND	423	ND
	9526	166	ND	ND	ND	ND	ND	205	ND
	9533	177	ND	ND	ND	ND	ND	208	ND
	9511	178	ND	ND	ND	ND	ND	108	ND
	9514	197	ND	ND	ND	ND	167	813	ND
	9517	199	ND	ND	ND	ND	118	930	ND
Upper Slope	9507	212	ND	ND	ND	ND	ND	753	ND
	9524	271	ND	ND	ND	ND	ND	962	105 DNQ
	9527	319	ND	ND	ND	ND	ND	654	ND
	9534	357	ND	ND	ND	ND	ND	710	ND
	9535	405	ND	ND	ND	ND	ND	745	ND
	9556	433	ND	ND	ND	ND	ND	675	ND
DR (%)			0	0	0	0	5	75	8

Appendix F.4 *continued*

	Station	Depth (m)	HCH				Endosulfan		
			Alpha	Beta	Delta	Gamma	Alpha	Beta	Sulfate
Inner Shelf	9519	13	ND	ND	ND	ND	ND	ND	ND
	9541	15	ND	ND	ND	ND	ND	ND	ND
	9516	17	ND	ND	ND	ND	ND	ND	ND
	9508	21	ND	ND	ND	ND	ND	ND	ND
	9515	22	ND	ND	ND	ND	ND	ND	ND
	9513	24	ND	ND	ND	ND	ND	ND	ND
	9501	25	ND	ND	ND	ND	ND	ND	ND
	9509	25	ND	ND	ND	ND	ND	ND	ND
Mid Shelf	9531	35	ND	ND	ND	ND	ND	ND	ND
	9503	45	ND	ND	ND	ND	ND	ND	ND
	9538	46	ND	ND	ND	ND	ND	ND	ND
	9510	49	ND	ND	ND	ND	ND	ND	ND
	9536	57	ND	ND	ND	ND	ND	ND	ND
	9532	60	ND	ND	ND	ND	ND	ND	ND
	9520	67	ND	ND	ND	ND	ND	ND	ND
	9530	72	ND	ND	ND	ND	ND	ND	ND
	9523	73	ND	ND	ND	ND	ND	ND	ND
	9525	75	ND	ND	ND	ND	ND	ND	ND
	9505	76	ND	ND	ND	ND	ND	ND	ND
	9540	77	ND	ND	ND	ND	ND	ND	ND
	9529	84	ND	ND	ND	ND	ND	ND	ND
	9512	90	ND	ND	ND	ND	ND	111	ND
	9528	96	ND	ND	ND	ND	ND	ND	ND
	9504	98	ND	ND	ND	ND	ND	ND	ND
	9518	98	ND	ND	ND	ND	ND	ND	ND
Outer Shelf	9506	128	ND	ND	ND	ND	ND	ND	ND
	9539	152	ND	ND	ND	ND	ND	ND	ND
	9521	154	ND	ND	ND	ND	ND	ND	ND
	9537	162	ND	ND	ND	ND	ND	ND	ND
	9526	166	ND	ND	ND	ND	ND	ND	ND
	9533	177	ND	ND	ND	ND	ND	ND	ND
	9511	178	ND	ND	ND	ND	ND	ND	ND
	9514	197	ND	ND	ND	ND	ND	ND	ND
	9517	199	ND	ND	ND	ND	ND	213	ND
Upper Slope	9507	212	ND	ND	ND	ND	ND	ND	ND
	9524	271	ND	ND	ND	ND	ND	ND	ND
	9527	319	ND	ND	ND	ND	ND	ND	ND
	9534	357	ND	ND	ND	ND	ND	ND	ND
	9535	405	ND	ND	ND	ND	ND	ND	ND
	9556	433	ND	ND	ND	ND	ND	ND	ND
DR (%)			0	0	0	0	0	5	0

Appendix F.4 *continued*

	Station	Depth (m)	Aldrin	Dieldrin	Endrin	EndAld	HCB	Mirex
Inner Shelf	9519	13	ND	ND	ND	ND	ND	ND
	9541	15	ND	ND	ND	ND	ND	ND
	9516	17	ND	ND	ND	ND	ND	ND
	9508	21	ND	ND	ND	ND	ND	ND
	9515	22	ND	ND	ND	ND	ND	ND
	9513	24	ND	ND	ND	ND	ND	ND
	9501	25	ND	ND	ND	ND	ND	ND
	9509	25	ND	ND	ND	ND	ND	ND
Mid Shelf	9531	35	ND	ND	ND	ND	ND	ND
	9503	45	ND	ND	ND	ND	ND	ND
	9538	46	ND	ND	ND	ND	ND	ND
	9510	49	ND	ND	ND	ND	ND	ND
	9536	57	ND	ND	ND	ND	ND	ND
	9532	60	ND	ND	ND	ND	ND	ND
	9520	67	ND	ND	ND	ND	ND	ND
	9530	72	ND	ND	ND	ND	ND	ND
	9523	73	ND	ND	ND	ND	ND	ND
	9525	75	ND	ND	ND	ND	ND	ND
	9505	76	ND	ND	ND	ND	ND	ND
	9540	77	ND	ND	ND	ND	ND	ND
	9529	84	ND	ND	ND	ND	ND	ND
	9512	90	ND	ND	ND	ND	ND	ND
	9528	96	ND	ND	ND	ND	ND	ND
	9504	98	ND	ND	ND	ND	ND	ND
	9518	98	ND	ND	ND	ND	ND	ND
Outer Shelf	9506	128	ND	ND	ND	ND	ND	ND
	9539	152	ND	ND	ND	ND	ND	ND
	9521	154	ND	ND	ND	ND	ND	ND
	9537	162	ND	ND	ND	ND	ND	ND
	9526	166	ND	ND	ND	ND	ND	ND
	9533	177	ND	ND	ND	ND	ND	ND
	9511	178	ND	ND	ND	ND	ND	ND
	9514	197	ND	ND	ND	ND	ND	ND
	9517	199	ND	ND	ND	ND	ND	ND
Upper Slope	9507	212	ND	ND	ND	ND	ND	ND
	9524	271	ND	ND	ND	ND	ND	ND
	9527	319	ND	ND	ND	ND	ND	ND
	9534	357	ND	ND	ND	ND	ND	ND
	9535	405	ND	ND	ND	ND	ND	ND
	9556	433	ND	ND	ND	ND	ND	ND
	DR (%)		0	0	0	0	0	0

Appendix F.5

Concentrations of PCBs (ppt) detected in sediments from the San Diego regional benthic stations sampled during summer 2025. See Appendix F.1 for MDLs; DR = detection rate; DNQ = do not quantify; ND = not detected; NR = not reportable.

			PCB									
	Station	Depth (m)	8	18	28	37	44	49	52	66	70	74
Inner Shelf	9519	13	ND	ND	ND	ND	ND	ND	ND	ND	ND	ND
	9541	15	ND	ND	ND	ND	ND	ND	ND	ND	ND	ND
	9516	17	ND	ND	ND	ND	ND	ND	ND	ND	ND	ND
	9508	21	ND	ND	ND	ND	ND	ND	ND	ND	ND	ND
	9515	22	ND	ND	ND	ND	ND	ND	ND	ND	ND	ND
	9513	24	ND	ND	ND	ND	ND	ND	ND	ND	ND	ND
	9501	25	ND	ND	ND	ND	ND	ND	ND	ND	ND	ND
	9509	25	ND	ND	ND	ND	ND	ND	ND	ND	ND	ND
Mid Shelf	9531	35	ND	ND	ND	ND	ND	ND	ND	ND	ND	ND
	9503	45	ND	ND	ND	ND	ND	ND	ND	ND	ND	ND
	9538	46	ND	ND	ND	ND	ND	ND	ND	ND	ND	ND
	9510	49	ND	ND	ND	ND	ND	ND	ND	ND	ND	ND
	9536	57	ND	ND	ND	ND	ND	ND	ND	ND	ND	ND
	9532	60	ND	ND	ND	ND	ND	ND	ND	ND	ND	ND
	9520	67	ND	ND	ND	ND	ND	ND	ND	ND	ND	ND
	9530	72	ND	ND	ND	ND	ND	ND	ND	ND	ND	ND
	9523	73	ND	ND	ND	ND	ND	ND	ND	ND	ND	ND
	9525	75	ND	ND	ND	ND	ND	ND	ND	ND	ND	ND
	9505	76	ND	ND	ND	ND	ND	ND	ND	ND	ND	ND
	9540	77	ND	ND	ND	ND	ND	ND	ND	ND	ND	ND
	9529	84	ND	ND	ND	ND	ND	ND	ND	ND	ND	ND
	9512	90	ND	ND	ND	ND	ND	140	100	68 DNQ	ND	ND
	9528	96	ND	ND	ND	ND	ND	ND	ND	ND	ND	ND
	9504	98	ND	ND	ND	ND	ND	ND	ND	ND	ND	ND
	9518	98	ND	ND	ND	ND	ND	ND	ND	ND	ND	ND
Outer Shelf	9506	128	ND	ND	ND	ND	ND	ND	ND	ND	ND	ND
	9539	152	ND	ND	ND	ND	ND	ND	ND	ND	ND	ND
	9521	154	ND	ND	ND	ND	ND	ND	ND	ND	ND	ND
	9537	162	ND	ND	ND	ND	ND	ND	ND	ND	ND	ND
	9526	166	ND	ND	ND	ND	ND	ND	ND	ND	ND	ND
	9533	177	ND	ND	ND	ND	ND	ND	ND	ND	ND	ND
	9511	178	ND	ND	ND	ND	ND	ND	ND	76 DNQ	ND	ND
	9514	197	ND	ND	ND	ND	630	590	950	1100	2700	900
	9517	199	ND	ND	ND	ND	ND	ND	ND	78 DNQ	ND	ND
Upper Slope	9507	212	ND	ND	ND	ND	ND	ND	ND	ND	ND	ND
	9524	271	ND	ND	ND	ND	ND	ND	ND	ND	ND	ND
	9527	319	ND	ND	ND	ND	ND	ND	ND	ND	ND	ND
	9534	357	ND	ND	ND	ND	ND	ND	ND	ND	ND	ND
	9535	405	ND	ND	ND	ND	ND	ND	ND	ND	ND	ND
	9556	433	ND	ND	ND	ND	ND	ND	ND	ND	ND	ND
	DR (%)		0	0	0	0	3	5	5	10	3	3

Appendix F.5 *continued*

	Station	Depth (m)	PCB 77	81	87	99	101	105	110	114	118	119
Inner Shelf	9519	13	ND	ND	ND	ND	ND	ND	ND	ND	ND	ND
	9541	15	ND	ND	ND	ND	ND	ND	ND	ND	ND	ND
	9516	17	ND	ND	ND	ND	ND	ND	ND	ND	ND	ND
	9508	21	ND	ND	ND	ND	ND	ND	ND	ND	ND	ND
	9515	22	ND	ND	ND	ND	ND	ND	ND	ND	ND	ND
	9513	24	ND	ND	ND	ND	ND	ND	ND	ND	ND	ND
	9501	25	ND	ND	ND	ND	ND	ND	ND	ND	ND	ND
	9509	25	ND	ND	ND	ND	ND	ND	ND	ND	ND	ND
Mid Shelf	9531	35	ND	ND	ND	ND	ND	ND	ND	ND	ND	ND
	9503	45	ND	ND	ND	ND	ND	ND	ND	ND	ND	ND
	9538	46	ND	ND	ND	ND	ND	ND	ND	ND	ND	ND
	9510	49	ND	ND	ND	ND	68 DNQ	ND	ND	ND	ND	ND
	9536	57	ND	ND	ND	ND	ND	ND	ND	ND	ND	ND
	9532	60	ND	ND	ND	ND	ND	ND	ND	ND	ND	ND
	9520	67	ND	ND	ND	ND	96 DNQ	ND	80 DNQ	ND	88 DNQ	ND
	9530	72	ND	ND	ND	ND	ND	ND	ND	ND	ND	ND
	9523	73	ND	ND	ND	ND	ND	ND	ND	ND	ND	ND
	9525	75	ND	ND	ND	ND	97	ND	ND	ND	69 DNQ	ND
	9505	76	ND	ND	ND	ND	88 DNQ	ND	79 DNQ	ND	ND	ND
	9540	77	ND	ND	ND	ND	ND	ND	ND	ND	ND	ND
	9529	84	ND	ND	ND	ND	ND	ND	ND	ND	ND	ND
	9512	90	ND	ND	79 DNQ	200	280	ND	250	ND	260	ND
	9528	96	ND	ND	ND	ND	ND	ND	ND	ND	ND	ND
	9504	98	ND	ND	ND	ND	ND	ND	ND	ND	ND	ND
	9518	98	ND	ND	ND	ND	ND	ND	ND	ND	ND	ND
Outer Shelf	9506	128	ND	ND	ND	ND	ND	ND	ND	ND	ND	ND
	9539	152	ND	ND	ND	ND	ND	ND	ND	ND	ND	ND
	9521	154	ND	ND	ND	ND	ND	ND	ND	ND	ND	ND
	9537	162	ND	ND	ND	ND	ND	ND	ND	ND	ND	ND
	9526	166	ND	ND	ND	ND	ND	ND	ND	ND	ND	ND
	9533	177	ND	ND	ND	ND	ND	ND	ND	ND	ND	ND
	9511	178	ND	ND	ND	160	260	ND	190	ND	180	ND
	9514	197	ND	ND	5400	5400	11000	3000	9700	330	12000	420
	9517	199	ND	ND	90 DNQ	190	280	94 DNQ	250	ND	290	ND
Upper Slope	9507	212	ND	ND	ND	ND	130	ND	130	ND	150	ND
	9524	271	ND	ND	ND	ND	ND	ND	ND	ND	82 DNQ	ND
	9527	319	ND	ND	ND	ND	ND	ND	ND	ND	ND	ND
	9534	357	ND	ND	ND	ND	ND	ND	ND	ND	ND	ND
	9535	405	ND	ND	ND	ND	ND	ND	ND	ND	ND	ND
	9556	433	ND	ND	ND	ND	ND	ND	ND	ND	ND	ND
	DR (%)		0	0	8	10	23	5	18	3	20	3

Appendix F.5 *continued*

	Station	Depth (m)	PCB 123	126	128	138	149	151	153/168	156	157	158	167
Inner Shelf	9519	13	ND	ND	ND	ND	ND	ND	ND	ND	ND	ND	ND
	9541	15	ND	ND	ND	ND	ND	ND	ND	ND	ND	ND	ND
	9516	17	ND	ND	ND	ND	ND	ND	ND	ND	ND	ND	ND
	9508	21	ND	ND	ND	ND	ND	ND	ND	ND	ND	ND	ND
	9515	22	ND	ND	ND	ND	ND	ND	ND	ND	ND	ND	ND
	9513	24	ND	ND	ND	ND	ND	ND	ND	ND	ND	ND	ND
	9501	25	ND	ND	ND	ND	ND	ND	ND	ND	ND	ND	ND
	9509	25	ND	ND	ND	ND	ND	ND	ND	ND	ND	ND	ND
Mid Shelf	9531	35	ND	ND	ND	ND	ND	ND	ND	ND	ND	ND	ND
	9503	45	ND	ND	ND	ND	ND	ND	ND	ND	ND	ND	ND
	9538	46	ND	ND	ND	ND	ND	ND	ND	ND	ND	ND	ND
	9510	49	ND	ND	ND	ND	ND	ND	ND	ND	ND	ND	ND
	9536	57	ND	ND	ND	ND	ND	ND	ND	ND	ND	ND	ND
	9532	60	ND	ND	ND	ND	ND	ND	ND	ND	ND	ND	ND
	9520	67	ND	ND	ND	86 DNQ	98	ND	ND	ND	ND	ND	ND
	9530	72	ND	ND	ND	ND	ND	ND	ND	ND	ND	ND	ND
	9523	73	ND	ND	ND	ND	ND	ND	ND	ND	ND	ND	ND
	9525	75	ND	ND	ND	86 DNQ	140	ND	179 DNQ	ND	ND	ND	ND
	9505	76	ND	ND	ND	96	110	ND	168 DNQ	ND	ND	ND	ND
	9540	77	ND	ND	ND	ND	ND	ND	ND	ND	ND	ND	ND
	9529	84	ND	ND	ND	ND	90	ND	ND	ND	ND	ND	ND
	9512	90	ND	ND	ND	320	360	72 DNQ	550	ND	ND	ND	ND
	9528	96	ND	ND	ND	ND	ND	ND	ND	ND	ND	ND	ND
	9504	98	ND	ND	ND	ND	ND	ND	ND	ND	ND	ND	ND
	9518	98	ND	ND	ND	ND	ND	ND	ND	ND	ND	ND	ND
Outer Shelf	9506	128	ND	ND	ND	ND	83	ND	ND	ND	ND	ND	ND
	9539	152	ND	ND	ND	ND	ND	ND	ND	ND	ND	ND	ND
	9521	154	ND	ND	ND	ND	ND	ND	ND	ND	ND	ND	ND
	9537	162	ND	ND	ND	ND	ND	ND	ND	ND	ND	ND	ND
	9526	166	ND	ND	ND	ND	ND	ND	ND	ND	ND	ND	ND
	9533	177	ND	ND	ND	ND	ND	ND	ND	ND	ND	ND	ND
	9511	178	ND	ND	ND	240	320	ND	440	ND	ND	ND	ND
	9514	197	910	ND	1700	9400	7200	1000	11000	1100	340	880	340
	9517	199	ND	ND	96 DNQ	410	420	89 DNQ	670	ND	ND	ND	ND
Upper Slope	9507	212	ND	ND	ND	190	170	ND	300	ND	ND	ND	ND
	9524	271	ND	ND	ND	ND	ND	ND	ND	ND	ND	ND	ND
	9527	319	ND	ND	ND	ND	ND	ND	ND	ND	ND	ND	ND
	9534	357	ND	ND	ND	ND	ND	ND	ND	ND	ND	ND	ND
	9535	405	ND	ND	ND	ND	ND	ND	ND	ND	ND	ND	ND
	9556	433	ND	ND	ND	ND	ND	ND	ND	ND	ND	ND	ND
	DR (%)		3	0	5	20	25	8	18	3	3	3	3

Appendix F.5 *continued*

	Station	Depth (m)	PCB 169	170	177	180	183	187	189	194	195	201	206
Inner Shelf	9519	13	ND	ND	ND	ND	ND	ND	ND	ND	ND	ND	ND
	9541	15	ND	ND	ND	ND	ND	ND	ND	ND	ND	ND	ND
	9516	17	ND	ND	ND	ND	ND	ND	ND	ND	ND	ND	ND
	9508	21	ND	ND	ND	ND	ND	ND	ND	ND	ND	ND	ND
	9515	22	ND	ND	ND	ND	ND	ND	ND	ND	ND	ND	ND
	9513	24	ND	ND	ND	ND	ND	ND	ND	ND	ND	ND	ND
	9501	25	ND	ND	ND	ND	ND	ND	ND	ND	ND	ND	ND
	9509	25	ND	ND	ND	ND	ND	ND	ND	ND	ND	ND	ND
Mid Shelf	9531	35	ND	ND	ND	ND	ND	ND	ND	ND	ND	ND	ND
	9503	45	ND	ND	ND	ND	ND	ND	ND	ND	ND	ND	ND
	9538	46	ND	ND	ND	ND	ND	ND	ND	ND	ND	ND	ND
	9510	49	ND	ND	ND	ND	ND	ND	ND	ND	ND	ND	ND
	9536	57	ND	ND	ND	ND	ND	ND	ND	ND	ND	ND	ND
	9532	60	ND	ND	ND	ND	ND	ND	ND	ND	ND	ND	ND
	9520	67	ND	ND	ND	ND	ND	ND	ND	ND	ND	ND	ND
	9530	72	ND	ND	ND	ND	ND	ND	ND	ND	ND	ND	ND
	9523	73	ND	ND	ND	ND	ND	ND	ND	ND	ND	ND	ND
	9525	75	ND	ND	ND	100	ND	ND	ND	ND	ND	ND	ND
	9505	76	ND	ND	ND	ND	ND	ND	ND	ND	ND	ND	ND
	9540	77	ND	ND	ND	ND	ND	ND	ND	ND	ND	ND	ND
	9529	84	ND	ND	ND	ND	ND	ND	ND	ND	ND	ND	ND
	9512	90	ND	68 DNQ	ND	140	ND	94	ND	ND	ND	ND	ND
	9528	96	ND	ND	ND	ND	ND	ND	ND	ND	ND	ND	ND
	9504	98	ND	ND	ND	ND	ND	ND	ND	ND	ND	ND	ND
	9518	98	ND	ND	ND	ND	ND	ND	ND	ND	ND	ND	ND
Outer Shelf	9506	128	ND	ND	ND	ND	ND	ND	ND	ND	ND	ND	ND
	9539	152	ND	ND	ND	ND	ND	ND	ND	ND	ND	ND	ND
	9521	154	ND	ND	ND	ND	ND	ND	ND	ND	ND	ND	ND
	9537	162	ND	ND	ND	ND	ND	ND	ND	ND	ND	ND	ND
	9526	166	ND	ND	ND	ND	ND	ND	ND	ND	ND	ND	ND
	9533	177	ND	ND	ND	ND	ND	ND	ND	ND	ND	ND	ND
	9511	178	ND	83 DNQ	ND	160	ND	140	ND	ND	ND	ND	ND
	9514	197	ND	750	300	1100	280	510	ND	170	ND	ND	240
	9517	199	ND	110	88 DNQ	200	ND	230	ND	ND	ND	ND	120
Upper Slope	9507	212	ND	ND	ND	ND	ND	96 DNQ	ND	ND	ND	ND	ND
	9524	271	ND	ND	ND	ND	ND	ND	ND	ND	ND	ND	ND
	9527	319	ND	ND	ND	ND	ND	ND	ND	ND	ND	ND	ND
	9534	357	ND	ND	ND	ND	ND	ND	ND	ND	ND	ND	ND
	9535	405	ND	ND	ND	ND	ND	ND	ND	ND	ND	ND	ND
	9556	433	ND	ND	ND	ND	ND	ND	ND	ND	ND	ND	ND
	DR (%)		0	10	5	13	3	13	0	3	0	0	5

Appendix F.6

Concentrations of PAHs (ppb) detected in sediments from the San Diego regional benthic stations sampled during summer 2025. See Appendix F.1 for MDLs; DR = detection rate; DNQ = do not quantify; ND = not detected; NR = not reportable.

	Station	Depth (m)	1-methyl naphthalene	1-methyl phenanthrene	2-methyl naphthalene	2,3,5-trimethyl naphthalene	2,6-dimethyl naphthalene	3,4-benzo(B) fluoranthene	Acenaphthene	Acenaphthylene
Inner Shelf	9519	13	ND	ND	ND	ND	ND	14.8	ND	12.7
	9541	15	ND	ND	ND	ND	ND	ND	ND	ND
	9516	17	ND	ND	ND	ND	ND	ND	ND	ND
	9508	21	ND	ND	ND	ND	ND	ND	ND	ND
	9515	22	ND	ND	ND	ND	ND	ND	ND	ND
	9513	24	ND	ND	ND	ND	ND	ND	ND	ND
	9501	25	ND	ND	ND	ND	ND	ND	ND	ND
	9509	25	ND	ND	ND	ND	ND	ND	ND	ND
Mid Shelf	9531	35	ND	ND	ND	ND	ND	ND	ND	ND
	9503	45	ND	ND	ND	ND	ND	ND	ND	ND
	9538	46	ND	ND	ND	ND	ND	ND	ND	ND
	9510	49	669.0	339.0	528.0	29.1	185.0	4730.0	598.0	246.0
	9536	57	ND	ND	ND	ND	ND	ND	ND	ND
	9532	60	ND	ND	ND	ND	ND	ND	ND	ND
	9520	67	ND	ND	ND	ND	ND	ND	ND	ND
	9530	72	ND	ND	ND	ND	ND	ND	ND	ND
	9523	73	ND	ND	ND	ND	ND	ND	ND	ND
	9525	75	ND	ND	ND	ND	ND	ND	ND	ND
	9505	76	ND	ND	ND	ND	ND	ND	ND	ND
	9540	77	ND	ND	ND	ND	ND	ND	ND	ND
	9529	84	ND	ND	ND	ND	ND	ND	ND	ND
	9512	90	ND	ND	ND	ND	ND	ND	ND	ND
	9528	96	ND	ND	ND	ND	ND	ND	ND	ND
	9504	98	ND	ND	ND	ND	ND	ND	ND	ND
	9518	98	ND	ND	ND	ND	ND	ND	ND	ND
Outer Shelf	9506	128	ND	ND	ND	ND	ND	ND	ND	ND
	9539	152	ND	ND	ND	ND	ND	ND	ND	ND
	9521	154	ND	ND	ND	ND	ND	ND	ND	ND
	9537	162	ND	ND	ND	ND	ND	ND	ND	ND
	9526	166	ND	ND	ND	ND	ND	ND	ND	ND
	9533	177	ND	ND	ND	ND	ND	ND	ND	ND
	9511	178	ND	ND	ND	ND	ND	118.0	ND	10.4
	9514	197	16.1	ND	ND	ND	ND	223.0	12.3	ND
	9517	199	ND	ND	ND	ND	ND	31.6	ND	ND
Upper Slope	9507	212	ND	ND	ND	ND	ND	ND	ND	ND
	9524	271	ND	ND	ND	ND	ND	ND	ND	ND
	9527	319	ND	ND	ND	ND	ND	ND	ND	ND
	9534	357	ND	ND	ND	ND	ND	ND	ND	ND
	9535	405	ND	ND	ND	ND	ND	ND	ND	ND
	9556	433	ND	ND	ND	ND	ND	ND	ND	ND
DR (%)			5	3	3	3	3	13	5	8

Appendix F.6 *continued*

	Station	Depth (m)	Anthracene	Benzo[A] anthracene	Benzo[A] pyrene	Benzo[e] pyrene	Benzo[G,H,I] perylene	Benzo[K] fluoranthene	Biphenyl	Chrysene
Inner Shelf	9519	13	ND	ND	23.5	ND	ND	ND	ND	10.4
	9541	15	ND	ND	ND	ND	ND	ND	ND	ND
	9516	17	ND	ND	ND	ND	ND	ND	ND	ND
	9508	21	ND	ND	ND	ND	ND	ND	ND	ND
	9515	22	ND	ND	ND	ND	ND	ND	ND	ND
	9513	24	NR	ND	ND	ND	ND	ND	ND	ND
	9501	25	ND	ND	ND	ND	ND	ND	ND	ND
	9509	25	ND	ND	ND	ND	ND	ND	ND	ND
Mid Shelf	9531	35	NR	ND	ND	ND	ND	ND	ND	ND
	9503	45	NR	ND	ND	ND	ND	ND	ND	ND
	9538	46	ND	ND	ND	ND	ND	ND	ND	ND
	9510	49	2520.0	4420.0	3970.0	2010.0	1820.0	1290.0	123.0	3780.0
	9536	57	ND	ND	ND	ND	ND	ND	ND	ND
	9532	60	NR	ND	ND	ND	ND	ND	ND	ND
	9520	67	ND	ND	ND	ND	ND	ND	ND	ND
	9530	72	ND	ND	ND	ND	ND	ND	ND	ND
	9523	73	ND	ND	ND	ND	ND	ND	ND	ND
	9525	75	ND	ND	ND	ND	ND	ND	ND	5.7
	9505	76	ND	ND	ND	ND	ND	ND	ND	ND
	9540	77	ND	ND	ND	ND	ND	ND	ND	ND
	9529	84	NR	ND	ND	ND	ND	ND	ND	ND
	9512	90	ND	ND	ND	ND	ND	ND	ND	7.0
	9528	96	ND	ND	ND	ND	ND	ND	ND	ND
	9504	98	ND	ND	ND	ND	ND	ND	ND	ND
	9518	98	ND	ND	ND	ND	ND	ND	ND	ND
Outer Shelf	9506	128	ND	ND	ND	ND	ND	ND	ND	ND
	9539	152	ND	ND	ND	ND	ND	ND	ND	ND
	9521	154	ND	ND	ND	ND	ND	ND	ND	ND
	9537	162	ND	ND	ND	ND	ND	ND	ND	ND
	9526	166	ND	ND	ND	ND	ND	ND	ND	ND
	9533	177	ND	ND	ND	ND	ND	ND	ND	ND
	9511	178	ND	ND	77.7	40.5	30.3	52.5	ND	ND
	9514	197	58.6	163.0	221.0	106.0	115.0	102.0	ND	200.0
	9517	199	ND	ND	27.2	18.1	26.0	ND	ND	15.8
Upper Slope	9507	212	ND	ND	ND	ND	ND	ND	ND	ND
	9524	271	ND	ND	ND	ND	ND	ND	ND	ND
	9527	319	ND	ND	ND	ND	ND	ND	ND	ND
	9534	357	ND	ND	ND	ND	ND	ND	ND	ND
	9535	405	ND	ND	ND	ND	ND	ND	ND	ND
	9556	433	ND	ND	ND	ND	ND	ND	ND	ND
	DR (%)		6	5	13	10	10	8	3	15

Appendix F.6 *continued*

	Station	Depth (m)	Dibenzo(A,H) anthracene	Fluoranthene	Fluorene	Indeno(1,2,3-CD) pyrene	Naphthalene	Perylene	Phenanthrene	Pyrene
Inner Shelf	9519	13	ND	14.1	ND	ND	ND	ND	ND	ND
	9541	15	ND	ND	ND	ND	ND	ND	ND	ND
	9516	17	ND	ND	ND	ND	ND	ND	ND	ND
	9508	21	ND	ND	ND	ND	ND	ND	ND	ND
	9515	22	ND	ND	ND	ND	ND	ND	ND	ND
	9513	24	ND	ND	ND	ND	ND	ND	ND	ND
	9501	25	ND	ND	ND	ND	ND	ND	ND	ND
	9509	25	ND	ND	ND	ND	ND	ND	ND	ND
Mid Shelf	9531	35	ND	ND	ND	ND	ND	ND	ND	ND
	9503	45	ND	ND	ND	ND	ND	ND	ND	ND
	9538	46	ND	ND	ND	ND	ND	ND	ND	ND
	9510	49	726.0	7830.0	1150.0	1720.0	750.0	808.0	7520.0	6980.0
	9536	57	ND	ND	ND	ND	ND	ND	ND	ND
	9532	60	ND	ND	ND	ND	ND	ND	ND	ND
	9520	67	ND	ND	ND	ND	ND	ND	ND	9.5
	9530	72	ND	ND	ND	ND	ND	ND	ND	ND
	9523	73	ND	ND	ND	ND	ND	ND	ND	ND
	9525	75	ND	ND	ND	ND	ND	ND	ND	ND
	9505	76	ND	ND	ND	ND	ND	ND	ND	ND
	9540	77	ND	ND	ND	ND	ND	ND	ND	ND
	9529	84	ND	ND	ND	ND	ND	ND	ND	ND
	9512	90	ND	ND	ND	ND	ND	ND	ND	9.9
	9528	96	ND	ND	ND	ND	ND	ND	ND	ND
	9504	98	ND	ND	ND	ND	ND	ND	ND	ND
	9518	98	ND	ND	ND	ND	ND	ND	ND	ND
Outer Shelf	9506	128	ND	ND	ND	ND	ND	ND	ND	ND
	9539	152	ND	ND	ND	ND	ND	ND	ND	ND
	9521	154	ND	ND	ND	ND	ND	ND	ND	ND
	9537	162	ND	ND	ND	ND	ND	ND	ND	ND
	9526	166	ND	ND	ND	ND	ND	ND	ND	ND
	9533	177	ND	ND	ND	ND	ND	ND	ND	ND
	9511	178	ND	8.7	ND	34.3	ND	ND	ND	23.0
	9514	197	ND	292.0	12.6	97.1 DNQ	ND	48.5	165.0	302.0
	9517	199	ND	ND	ND	ND	ND	ND	ND	20.3
Upper Slope	9507	212	ND	ND	ND	ND	ND	ND	ND	ND
	9524	271	ND	ND	ND	ND	ND	ND	ND	ND
	9527	319	ND	ND	ND	ND	ND	ND	ND	ND
	9534	357	ND	ND	ND	ND	ND	ND	ND	ND
	9535	405	ND	ND	ND	ND	ND	ND	ND	ND
	9556	433	ND	ND	ND	ND	ND	ND	ND	ND
	DR (%)		3	10	5	8	3	5	5	15

Appendix F.7

Concentrations of PBDEs (ppt) detected in sediments from the San Diego regional benthic stations sampled during summer 2025. See Appendix F.1 for MDLs; DR = detection rate; DNQ = do not quantify; ND = not detected; NR = not reportable.

	Station	Depth (m)	BDE-17	BDE-28	BDE-47	BDE-49	BDE-66	BDE-85	BDE-99
Inner Shelf	9519	13	ND	ND	ND	ND	ND	ND	ND
	9541	15	ND	ND	ND	ND	ND	ND	ND
	9516	17	ND	ND	ND	ND	ND	ND	ND
	9508	21	ND	ND	NR	ND	ND	ND	ND
	9515	22	ND	ND	ND	ND	ND	ND	ND
	9513	24	ND	ND	ND	ND	ND	ND	ND
	9501	25	ND	ND	ND	ND	ND	ND	ND
	9509	25	ND	ND	ND	ND	ND	ND	ND
Mid Shelf	9531	35	ND	ND	NR	ND	ND	ND	NR
	9503	45	ND	ND	ND	ND	ND	ND	ND
	9538	46	ND	ND	ND	ND	ND	ND	ND
	9510	49	ND	ND	NR	ND	ND	ND	ND
	9536	57	ND	ND	ND	ND	ND	ND	ND
	9532	60	ND	ND	NR	ND	ND	ND	NR
	9520	67	ND	ND	NR	NR	ND	ND	NR
	9530	72	ND	ND	NR	ND	ND	ND	NR
	9523	73	ND	ND	100	ND	ND	ND	ND
	9525	75	ND	ND	83 DNQ	ND	ND	ND	ND
	9505	76	ND	ND	NR	ND	ND	ND	ND
	9540	77	ND	ND	ND	ND	ND	ND	ND
	9529	84	ND	ND	NR	NR	ND	ND	NR
	9512	90	ND	ND	NR	ND	ND	ND	ND
	9528	96	ND	ND	ND	ND	ND	ND	ND
	9504	98	ND	ND	ND	ND	ND	ND	ND
	9518	98	ND	ND	NR	35 DNQ	ND	ND	NR
Outer Shelf	9506	128	ND	ND	ND	ND	ND	ND	ND
	9539	152	ND	ND	ND	ND	ND	ND	ND
	9521	154	ND	ND	ND	ND	ND	ND	ND
	9537	162	ND	ND	ND	ND	ND	ND	ND
	9526	166	ND	ND	ND	ND	ND	ND	ND
	9533	177	ND	ND	ND	ND	ND	ND	ND
	9511	178	ND	ND	ND	ND	ND	ND	ND
	9514	197	ND	ND	ND	NR	ND	ND	ND
	9517	199	ND	ND	ND	ND	ND	ND	ND
Upper Slope	9507	212	ND	ND	ND	ND	ND	ND	ND
	9524	271	ND	ND	ND	ND	ND	ND	ND
	9527	319	ND	ND	ND	ND	ND	ND	ND
	9534	357	ND	ND	ND	ND	ND	ND	ND
	9535	405	ND	ND	ND	ND	ND	ND	ND
	9556	433	ND	ND	ND	ND	ND	ND	ND
DR (%)			0	0	7	3	0	0	0

Appendix F.7 *continued*

	Station	Depth (m)	BDE-100	BDE-138	BDE-153	BDE-154	BDE-183	BDE-190
Inner Shelf	9519	13	ND	ND	ND	ND	ND	ND
	9541	15	ND	ND	ND	ND	ND	ND
	9516	17	ND	ND	ND	ND	ND	ND
	9508	21	ND	ND	ND	ND	ND	ND
	9515	22	ND	ND	ND	ND	ND	ND
	9513	24	ND	ND	ND	ND	ND	ND
	9501	25	ND	ND	ND	ND	ND	ND
	9509	25	ND	ND	ND	ND	ND	ND
Mid Shelf	9531	35	NR	ND	ND	ND	ND	ND
	9503	45	ND	ND	ND	ND	ND	ND
	9538	46	ND	ND	ND	ND	ND	ND
	9510	49	NR	ND	ND	ND	ND	ND
	9536	57	ND	ND	ND	ND	ND	ND
	9532	60	NR	ND	ND	ND	ND	ND
	9520	67	NR	ND	ND	32 DNQ	ND	ND
	9530	72	NR	ND	ND	ND	ND	ND
	9523	73	40 DNQ	ND	ND	ND	ND	ND
	9525	75	28 DNQ	ND	ND	ND	ND	ND
	9505	76	NR	ND	ND	ND	ND	ND
	9540	77	ND	ND	ND	ND	ND	ND
	9529	84	66 DNQ	ND	ND	34 DNQ	ND	ND
	9512	90	NR	ND	ND	ND	ND	ND
	9528	96	ND	ND	ND	ND	ND	ND
	9504	98	ND	ND	ND	ND	ND	ND
	9518	98	NR	ND	ND	ND	ND	ND
Outer Shelf	9506	128	ND	ND	ND	ND	ND	ND
	9539	152	ND	ND	ND	ND	ND	ND
	9521	154	ND	ND	ND	ND	ND	ND
	9537	162	ND	ND	ND	ND	ND	ND
	9526	166	ND	ND	ND	ND	ND	ND
	9533	177	ND	ND	ND	ND	ND	ND
	9511	178	ND	ND	ND	ND	ND	ND
	9514	197	ND	ND	ND	ND	ND	ND
	9517	199	ND	ND	ND	ND	ND	ND
Upper Slope	9507	212	ND	ND	ND	ND	ND	ND
	9524	271	ND	ND	ND	ND	ND	ND
	9527	319	ND	ND	ND	ND	ND	ND
	9534	357	ND	ND	ND	ND	ND	ND
	9535	405	ND	ND	ND	ND	ND	ND
	9556	433	ND	ND	ND	ND	ND	ND
	DR (%)		9	0	0	5	0	0

Appendix F.8

Summary taxonomic listing of benthic infauna taxa identified from regional stations during 2025. Data are total number of individuals (n). Taxonomic arrangement follows SCAMIT (2023).-- indicates taxon is not within previous family.

Phylum	Class	Family	Taxon	n
Cnidaria	Hydrozoa	Corymorphidae	Corymorpha bigelowi	1
			Euphysa sp A	2
	Octocorallia		Pennatuloidea	3
		Virgulariidae	Stylatula sp A	3
			Stylatula sp	1
			Virgularia agassizii	7
	Ceriantharia			9
		Arachnactidae	Arachnanthus sp A	8
	Hexacorallia		Actiniaria	3
		Edwardsiidae		53
			Edwardsia juliae	414
			Scolanthus triangulus	14
		Halcampidae	Halcampa decemtentaculata	7
			Halianthella sp A	3
		Isanthidae	Zaolutus actius	3
		Limnactiniidae	Limnactiniidae sp A	2
Platyhelminthes	Rhabditophora	Stylochidae	Stylochus exiguus	3
		Plehniidae	Diplehnia caeca	5
		--	Rhabditophora sp A	2
Nemertea				21
	Palaeonemertea			5
		Cephalotrichidae	Cephalothrix sp	3
		Carinomidae		1
			Carinoma mutabilis	40
		Carinomellidae	Carinomella lactea	1
		Tubulanidae		13
			Tubulanus cingulatus	2
			Tubulanus polymorphus	30
			Tubulanus sp A	3
			Tubulanidae sp B	2
			Tubulanidae sp E	25
	Pilidiophora		Heteronemertea	7
		Lineidae		54
			Cerebratulus californiensis	2
			Siphonenteron bilineatum	78
			Zygeupolia rubens	3
			Lineidae sp SD1	10
		--	Heteronemertea sp SD2	121
	Hoplonemertea			7
		Emplectonematidae	Cryptonemertes actinophila	4
		Neesidae	Paranemertes californica	6
		Oerstediidae	Oerstedia dorsalis Cmplx	9
		Tetrastemmatidae	Tetrastemma candidum	1
		--	Quasitetrastemma nigrifrons	8
		--	Hoplonemertea sp D	1
			Enopla sp A	1
			Enopla sp B	1

Appendix F.8 *continued*

Phylum	Class	Family	Taxon	n
Mollusca	Caudofoveata		Chaetodermatida	9
		Chaetodermatidae	Chaetoderma marinellii	1
			Chaetoderma pacificum	19
			Chaetoderma sp	2
			Falcidens longus	28
		Limifossoridae	Limifossor fratula	2
	Gastropoda	Naticidae	Glossaulax reclusiana	1
		Caecidae	Caecum crebricinctum	1
		Eulimidae	Hypermastus rosa	6
			Polygireulima rutila	3
		Epitoniidae	Epitonium bellastriatum	4
		Columbellidae	Amphissa bicolor	2
			Amphissa undata	3
		Olividae	Callianax alectona	10
		Mangeliidae	Kurtzia arteaga	6
			Kurtziella plumbea	4
			Kurtzina beta	31
		Terebridae	Neoterebra hemphilli	1
		--	Euthyneura	1
		Acteonidae	Acteon traskii	2
			Rictaxis punctocaelatus	10
		Dendronotidae	Dendronotus sp	1
		Apataidae	Apata pricei	1
		Ringiculidae	Microglyphis brevicula	1
		Pyramidellidae	Odostomia sp	8
			Turbonilla santarosana	5
			Turbonilla sp A	5
			Turbonilla sp SD5	2
			Turbonilla sp SD6	2
			Turbonilla sp	2
		Rhizoridae	Volvulella californica	5
			Volvulella cylindrica	4
			Volvulella panamica	26
		Tornatinidae	Acteocina cerealis	1
			Acteocina harpa	1
		Cylichnidae	Cylichna diegensis	15
		Aglajidae	Aglaja ocelligera	7
		Philinidae	Philine auriformis	9
	Bivalvia			5
		Nuculidae	Ennucula tenuis	29
		Solemyidae	Petrasma pervernicosa	60
		Nuculanidae	Propeleda conceptionis	1
			Saccella penderi	2
			Saccella taphria	19
			Saccella sp A	34
		Mytilidae	Crenella decussata	1
			Solamen columbianum	10
			Gregariella coarctata	1
			Modiolinae	12

Appendix F.8 *continued*

Phylum	Class	Family	Taxon	n
			Amygdalum pallidulum	15
		Pectinidae	Leptopecten latiauratus	10
		Lucinidae	Lucinoma annulatum	10
			Lucinisca nuttalli	1
			Parvilucina tenuisculpta	50
		Thyasiridae	Axinopsida serricata	70
			Thyasira flexuosa	18
		Basterotiidae	Saxicavella pacifica	9
		Lasaeidae	Kurtiella tumida	15
			Kurtiella sp D	1
			Neaeromya compressa	2
		Carditidae	Scalaricarditinae	1
		Cardiidae	Keenaea centifilosa	11
		Tellinidae		1
			Tellina cadieni	163
			Tellina carpenteri	13
			Tellina modesta	17
			Macoma carlottensis	5
			Macoma yoldiformis	23
			Macoma sp	1
		Mactridae	Simomactra falcata	1
		Veneridae	Compsomyax subdiaphana	18
		Petricolidae	Cooperella subdiaphana	19
		Hiatellidae	Hiatella arctica	2
		Solenidae	Solen sicarius	3
		Pharidae	Ensis myrae	2
			Siliqua lucida	3
		Cuspidariidae	Cuspidaria parapodema	29
		Pandoridae	Pandora bilirata	2
		Lyonsiidae		4
			Lyonsia californica	8
		--	Thracioidea	1
		Periplomatidae	Periploma discus	1
			Periploma sp	1
	Scaphopoda			9
		Rhabdidae	Rhabdus rectius	2
		Gadilidae	Polyschides quadrifissatus	32
			Cadulus californicus	6
			Gadila aberrans	10
		--	Compressidens stearnsii	18
Annelida			Sipuncula	4
		Golfingiidae	Nephasoma sp	1
			Phascolion sp A	46
			Thysanocardia nigra	9
		Phascolosomatidae	Apionsoma misakianum	4
	Polychaeta	Bonelliidae	Nellobia eusoma	1
		Amphinomidae	Chloeia pinnata	290
		Dorvilleidae		1
			Meiodorvillea sp SD1	3

Appendix F.8 *continued*

Phylum	Class	Family	Taxon	n
			Parougia caeca	3
			Pettiboneia sanmatiensis	3
			Protodorvillea gracilis	2
			Protodorvillea sp SD1	7
		Eunicidae		2
			Eunice sp	1
			Leodice americana	11
			Marphysa sp B	1
			Paucibranchia disjuncta	3
		Lumbrineridae		12
			Eranno bicirrata	3
			Eranno lagunae	20
			Lumbrinerides platypygos	3
			Lumbrineris cruzensis	287
			Lumbrineris index	2
			Lumbrineris japonica	4
			Lumbrineris latreilli	18
			Lumbrineris ligulata	6
			Lumbrineris limicola	8
			Lumbrineris sp Group I	158
			Scoletoma tetraura Cmplx	53
			Scoletoma sp	6
		Oenonidae	Arabella iricolor Cmplx	1
			Drilonereis falcata	16
			Drilonereis sp A	3
			Drilonereis sp	10
			Notocirrus californiensis	1
		Onuphidae		34
			Diopatra ornata	9
			Diopatra tridentata	4
			Mooreonuphis exigua	12
			Mooreonuphis nebulosa	19
			Mooreonuphis sp SD2	2
			Mooreonuphis sp	4
			Onuphis geophiliformis	1
			Onuphis iridescens	7
			Onuphis sp A	40
			Onuphis sp	2
			Paradiopatra parva	229
		Acoetidae	Acoetes pacifica	2
		Aphroditidae	Aphrodita sp	1
		Polynoidae		3
			Lepidonotus spiculus	4
			Harmothoe hirsuta	2
			Malmgreniella baschi	13
			Malmgreniella liei	1
			Malmgreniella macginitiei	4
			Malmgreniella sanpedroensis	3
			Malmgreniella scriptoria	3

Appendix F.8 *continued*

Phylum	Class	Family	Taxon	n
			Malmgreniella sp A	28
			Malmgreniella sp	1
			Subadyte mexicana	1
			Tenonia priops	5
		Sigalionidae	Pholoides asperus	1
			Sigalion spinosus	42
			Sthenelais tertiaglabra	7
			Sthenelais verruculosa	4
			Pholoe glabra	30
			Pisione sp	5
			Sthenelanella uniformis	186
		Glyceridae		1
			Glycera americana	2
			Glycera macrobranchia	5
			Glycera nana	74
			Glycera oxycephala	33
			Glycera tesselata	2
			Hemipodia borealis	2
		Goniadidae	Glycinde armigera	73
			Goniada brunnea	4
			Goniada littorea	26
			Goniada maculata	61
		Chrysopetalidae	Paleanotus bellis	1
			Dysponetus caecus	1
		Hesionidae	Gyptis sp	2
			Oxydromus pugettensis	2
			Podarkeopsis glabrus	16
			Micropodarke dubia	7
		Nereididae	Ceratocephale hartmanae	1
			Nereis sp A	57
			Nereis sp	1
			Platynereis bicanaliculata	67
		Pilargidae	Ancistrosyllis groenlandica	3
		Syllidae	Epigamia-Myrianida Cmplx	4
			Eusyllis blomstrandi Cmplx	1
			Eusyllis habei	13
			Eusyllis transecta	5
			Eusyllis sp	5
			Odontosyllis phosphorea	4
			Exogone dwisula	18
			Exogone lourei	60
			Exogone sp	1
			Parexogone breviseta	5
			Sphaerosyllis californiensis	2
			Syllis elongata	5
			Syllis farallonensis	6
			Syllis heterochaeta	72
			Syllis sp SD1	16
			Syllis sp SD2	3

Appendix F.8 *continued*

Phylum	Class	Family	Taxon	n
			Syllis sp	1
		Nephtyidae	Aglaophamus erectans	1
			Aglaophamus verrilli	14
			Bipalponephtys cornuta	13
			Nephtys caecoides	10
			Nephtys ferruginea	22
			Nephtys simoni	2
		Sphaerodoridae	Sphaerephesia biserialis	1
		Phyllodocidae	Eteone pigmentata	6
			Eulalia levicornuta Cmplx	4
			Eumida longicornuta	14
			Hesionura coineaui difficilis	30
			Protomystides sp SD2	1
			Sige sp A	13
			Nereiphylla ferruginea Cmplx	1
			Nereiphylla sp 2	1
			Nereiphylla sp SD1	3
			Paranaitis polynoides	1
			Phyllodoce groenlandica	3
			Phyllodoce hartmanae	140
			Phyllodoce longipes	37
			Phyllodoce pettiboneae	5
			Phyllodoce sp	1
		Oweniidae	Galathowenia pygidialis	1
			Myriochele gracilis	25
			Myriochele olgae	1
			Myriochele striolata	35
			Myriowenia californiensis	2
			Owenia collaris	20
		Sabellariidae	Sabellaria gracilis	1
		Sabellidae	Acromegalomma pigmentum	8
			Acromegalomma splendidum	1
			Chone sp SD3	7
			Dialychone albocincta	6
			Dialychone trilineata	17
			Dialychone veleronis	10
			Euchone arenae	12
			Euchone hancocki	7
			Euchone incolor	17
			Euchone sp A	5
			Jasmineira sp B	12
			Paradialychone bimaculata	1
			Paradialychone ecaudata	1
			Paradialychone eiffelturris	2
			Paradialychone harrisae	3
			Potamethus sp A	4
			Pseudopotamilla sp 1	5
			Pseudopotamilla sp	14
		Magelonidae	Magelona hartmanae	6

Appendix F.8 *continued*

Phylum	Class	Family	Taxon	n
			Magelona pitelkai	1
			Magelona sacculata	6
			Magelona sp B	9
			Magelona sp	1
		Poecilochaetidae	Poecilochaetus johnsoni	1
			Poecilochaetus martini	1
			Poecilochaetus sp	3
		Spionidae		1
			Dipolydora socialis	12
			Dipolydora sp	5
			Dispio sp SD2	2
			Laonice cirrata	12
			Laonice nuchala	18
			Microspio pigmentata	5
			Paraprionospio alata	148
			Polydora cirrosa	3
			Polydora limicola	2
			Prionospio dubia	193
			Prionospio jubata	233
			Prionospio lighti	24
			Prionospio lobulata	10
			Prionospio pygmaeus	48
			Prionospio sp	1
			Scolelepis sp	1
			Spio filicornis	6
			Spio maciolekae	6
			Spio maculata	2
			Spiophanes berkeleyorum	259
			Spiophanes duplex	632
			Spiophanes kimballi	627
			Spiophanes norrisi	257
			Spiophanes wigleyi	4
			Spiophanes sp	1
		Cirratulidae	Aphelochaeta glandaria Cmplx	44
			Aphelochaeta monilaris	32
			Aphelochaeta petersenae	4
			Aphelochaeta phillipsi	74
			Aphelochaeta tigrina	13
			Aphelochaeta williamsae	10
			Aphelochaeta sp D	67
			Aphelochaeta sp E	1
			Chaetozone columbiana	2
			Chaetozone commonalis	1
			Chaetozone corona	10
			Chaetozone hartmanae	17
			Chaetozone spinosa	3
			Chaetozone sp SD2	1
			Chaetozone sp SD5	17
			Chaetozone sp SD7	1

Appendix F.8 *continued*

Phylum	Class	Family	Taxon	n
			Chaetozone sp	3
			Cirriformia sp SD2	2
			Kirkegaardia cryptica	58
			Kirkegaardia serratiseta	1
			Kirkegaardia siblina	166
			Kirkegaardia tesselata	30
			Kirkegaardia sp SD9	32
			Protocirrineris sp B	1
		Fauveliopsidae	Fauveliopsis glabra	3
		Flabelligeridae	Bradabyssa pilosa	5
			Pherusa neopapillata	9
			Pherusa sp	9
			Piromis capulata	2
			Trophoniella harrisae	1
		Sternaspidae	Sternaspis affinis	73
		Ampharetidae		24
			Amage anops	2
			Amage scutata	3
			Ampharete finmarchica	9
			Ampharete labrops	65
			Ampharete lineata	1
			Ampharete manriquei	17
			Amphicteis scaphobranchiata	23
			Amphisamytha bioculata	1
			Anobothrus bimaculatus	31
			Eclysippe trilobata	57
			Lysippe sp A	15
			Lysippe sp B	27
			Phyllocomus sp A	8
			Phyllocomus sp	1
			Samytha californiensis	5
			Sosane occidentalis	19
			Melinna heterodonta	11
			Melinna oculata	19
		Pectinariidae	Pectinaria californiensis	41
		Terebellidae		2
			Amaeana occidentalis	7
			Polycirrus californicus	36
			Polycirrus sp A	48
			Polycirrus sp OC1	34
			Polycirrus sp	6
			Terebellinae	1
			Eupolymnia heterobranchia	1
			Lanassa venusta venusta	12
			Lanice conchilega	1
			Phisidia sanctaemariae	28
			Pista brevibranchiata	8
			Pista estevanica	44
			Pista moorei	1

Appendix F.8 *continued*

Phylum	Class	Family	Taxon	n
			Pista pacifica	6
			Pista wui	45
			Pista sp	2
			Proclea sp A	89
			Scionella japonica	2
			Streblosoma crassibranchia	1
			Streblosoma sp B	9
			Streblosoma sp C	2
			Streblosoma sp SF1	1
			Streblosoma sp	5
			Thelepus hamatus	1
		Trichobranchidae	Terebellides californica	46
			Trichobranchus hancocki	7
		Chaetopteridae		2
			Phyllochaetopterus limicolus	718
			Phyllochaetopterus prolifica	6
			Phyllochaetopterus sp	1
			Spiochaetopterus costarum Cmplx	48
		Capitellidae	Capitella capitata Cmplx	35
			Decamastus gracilis	11
			Mediomastus sp	471
			Notomastus hemipodus	64
			Notomastus latericeus	5
			Notomastus magnus	1
			Notomastus sp	1
		Cossuridae	Cossura candida	31
			Cossura sp A	8
		Maldanidae		72
			Euclymeninae	39
			Clymenella complanata	1
			Petaloclymene pacifica	125
			Praxillella gracilis	5
			Praxillella pacifica	92
			Euclymeninae sp A	265
			Clymenura gracilis	29
			Maldane sarsi	170
			Metasychis disparidentatus	22
			Rhodine bitorquata	31
		Opheliidae	Armandia brevis	7
			Ophelina sp	1
		Orbiniidae	Leitoscoloplos pugettensis	7
			Leitoscoloplos sp A	2
			Naineris uncinata	1
			Protoariciella sp A	1
			Scoloplos acmeceps	2
			Scoloplos armiger Cmplx	102
		Paraonidae		4
			Aricidea (Acmira) catherinae	22
			Aricidea (Acmira) horikoshii	1

Appendix F.8 *continued*

Phylum	Class	Family	Taxon	n
			Aricidea (Acmira) lopezi	1
			Aricidea (Acmira) rubra	1
			Aricidea (Acmira) simplex	27
			Aricidea (Aricidea) pseudoarticulata	1
			Aricidea (Aricidea) wassi	6
			Aricidea (Strelzovia) antennata	7
			Aricidea (Strelzovia) hartleyi	6
			Aricidea (Strelzovia) sp A	26
			Cirrophorus branchiatus	5
			Cirrophorus furcatus	1
			Levinsenia gracilis	16
			Levinsenia kirbyorum	8
			Levinsenia oculata	1
			Paradoneis lyra	2
			Paradoneis spinifera	1
			Paradoneis sp SD1	169
		Scalibregmatidae	Scalibregma californicum	41
		Travisiidae	Travisia brevis	53
			Travisia pupa	1
	Clitellata		Hirudinea	1
Arthropoda	Ostracoda	Cylindroleberididae		1
			Leuroleberis sharpei	3
			Xenoleberis californica	11
		Philomedidae	Euphilomedes carcharodonta	197
			Euphilomedes producta	58
		Rutidermatidae	Rutiderma lomae	1
	Malacostraca	Nebaliidae	Nebalia daytoni	1
			Nebalia pugettensis Cmplx	3
		Mysidae	Alienacanthomysis macropsis	1
			Inusitatomysis insolita	1
		Caprellidae	Mayerella banksia	1
		Ischyroceridae	Ericthonius brasiliensis	4
			Notopoma sp A	3
		Kamakidae	Amphideutopus oculatus	5
		Photidae	Ampelisciphotis podophthalma	12
			Gammaropsis thompsoni	1
			Photis bifurcata	5
			Photis californica	42
			Photis lacia	3
			Photis sp C	1
			Photis sp OC1	82
			Photis sp	11
		Aoridae	Aoroides spinosa	5
			Aoroides sp A	16
			Aoroides sp	7
			Bemlos audbettius	3
		Unciolidae	Rudilemboides stenopropodus	3
		Corophiidae	Laticorophium baconi	2
			Protomedeia articulata Cmplx	7

Appendix F.8 *continued*

Phylum	Class	Family	Taxon	n
		Megaluropidae	Gibberosus myersi	1
		Oedicerotidae		1
			Americhelidium shoemakeri	11
			Americhelidium sp SD1	1
			Americhelidium sp SD4	2
			Americhelidium sp	1
			Bathymedon pumilus	16
			Bathymedon vulpeculus	2
			Deflexilodes similis	9
			Hartmanodes hartmanae	7
			Hartmanodes sp SD1	1
			Monoculodes emarginatus	46
			Westwoodilla tone	20
		Bateidae	Batea transversa	1
		Eusiridae	Rhachotropis sp SD1	1
		Liljeborgiidae	Listriella diffusa	1
			Listriella goleta	13
		Stenothoidae	Stenothoides bicoma	1
		Melphidippidae	Melphisana bola	5
		Pardaliscidae	Nicippe tumida	5
		Ampeliscidae	Ampelisca agassizi	12
			Ampelisca brevisimulata	49
			Ampelisca cf brevisimulata	2
			Ampelisca careyi	32
			Ampelisca cristata	13
			Ampelisca hancocki	16
			Ampelisca indentata	2
			Ampelisca microdentata	29
			Ampelisca pacifica	17
			Ampelisca pugetica	37
			Ampelisca unsocalae	10
			Ampelisca sp	9
			Byblis millsi	7
			Byblis veleronis	1
		Synopiidae	Tiron biocellata	5
		Argissidae	Argissa hamatipes	9
		Phoxocephalidae		1
			Foxiphalus golfensis	1
			Foxiphalus obtusidens	19
			Rhepoxynius abronius	1
			Rhepoxynius bicuspidatus	49
			Rhepoxynius fatigans	3
			Rhepoxynius heterocuspidatus	4
			Rhepoxynius lucubrans	2
			Rhepoxynius menziesi	52
			Rhepoxynius stenodes	21
			Rhepoxynius variatus	3
			Rhepoxynius sp	1
			Eyakia robusta	4

Appendix F.8 *continued*

Phylum	Class	Family	Taxon	n
			Heterophoxus conlanae	2
			Heterophoxus ellisi	5
			Heterophoxus oculatus	5
			Heterophoxus sp	3
		Lysianassidae	Aruga holmesi	1
			Aruga oculata	4
		Tryphosidae	Hippomedon zetesimus	2
			Hippomedon sp A	1
			Lepidepecreum serraculum	1
		Pakynidae	Pachynus barnardi	1
			Prachynella lodo	2
		Cirolanidae	Eurydice caudata	4
		Gnathiidae	Caecognathia crenulatifrons	41
			Caecognathia sp SD1	3
		Anthuridae	Haliophasma geminatum	14
		Idoteidae	Edotia sublittoralis	2
			Synidotea magnifica	6
		Munnopsidae	Eurycope californiensis	1
		Paramunnidae	Pleurogonium californiense	2
		--	Tanaidacea	4
		Akanthophoreidae	Chauliopleona dentata	2
		Anarthruridae		2
		Leptocheliidae	Chondrochelia dubia Cmplx	67
		Tanaellidae	Araphura breviaria	14
			Araphura sp SD1	12
			Tanaella propinquus	25
		Pseudotanaidae	Pseudotanais californiensis	5
		Tanaopsidae	Tanaopsis cadieni	13
		Bodotriidae	Cyclaspis nubila	1
		Leuconidae	Eudorella pacifica	3
		Nannastacidae	Campylaspis canaliculata	3
			Campylaspis rubromaculata	1
			Procampylaspis caenosa	6
		Lampropidae	Hemilamprops californicus	23
			Mesolamprops bispinosus	17
		Diastylidae	Diastylis californica	2
			Diastylis crenellata	14
			Diastylis pellucida	2
			Leptostylis calva	1
			Oxyurostylis pacifica	1
		Crangonidae	Neocrangon zacae	2
		Albuneidae	Lepidopa californica	2
		Calappidae	Platymera gaudichaudii	1
		Cancridae	Metacarcinus gracilis	1
		Pinnotheridae		3
			Pinnixa hiatus	1
			Pinnixa longipes	1
			Rathbunixa occidentalis Cmplx	32
	Hexanauplia	Scalpellidae	Hamatoscalpellum californicum	1

Appendix F.8 *continued*

Phylum	Class	Family	Taxon	n
		Balanidae	Balanus sp	2
Nematoda				43
Echinodermata	Asteroidea			73
		Astropectinidae	Astropecten californicus	3
			Astropecten sp	2
	Ophiuroidea			57
		Ophiuridae	Ophiura luetkenii	14
		Ophioscolecidae	Ophiuroconis bispinosa	5
		Amphiuridae		422
			Amphichondrius granulatus	12
			Amphiodia digitata	4
			Amphiodia psara	1
			Amphiodia urtica	329
			Amphiodia sp	119
			Amphioplus strongyloplax	2
			Amphioplus sp A	1
			Amphioplus sp	16
			Amphipholis squamata	1
			Amphipholis sp	16
			Amphiura arcystata	3
			Dougaloplus amphacanthus	17
			Dougaloplus sp	1
	Echinoidea			5
		Toxopneustidae	Lytechinus pictus	2
		Strongylocentrotidae	Strongylocentrotus fragilis	1
		Dendrasteridae	Dendraster sp	1
		--	Spatangoida	5
		Schizasteridae	Brisaster latifrons	1
			Brisaster sp	1
		Brissidae	Brissopsis pacifica	4
			Brissopsis sp LA1	4
	Holothuroidea		Dendrochirotida	4
		Phyllophoridae	Phyllophoridae	6
			Pentamera pseudopopulifera	1
		Synaptidae	Leptosynapta sp	16
		Chiridotidae	Chiridota sp	23
Phoronida		Phoronidae		9
			Phoronis sp	84
			Phoronopsis sp	1
Brachiopoda	Lingulata	Lingulidae	Glottidia albida	28
	Rhynchonellata	Cancellothyrididae	Terebratulina unguicula	1
Chordata	Enteropneusta			3
		Spengelidae	Schizocardium sp	1
		Harrimaniidae	Stereobalanus sp	37
		--	Enteropneusta sp SD1	2
	Ascidiacea	Agneziidae	Agnezia septentrionalis	3
		Styelidae	Cnemidocarpa rhizopus	1
		Molgulidae		4
			Molgula pugetiensis	1

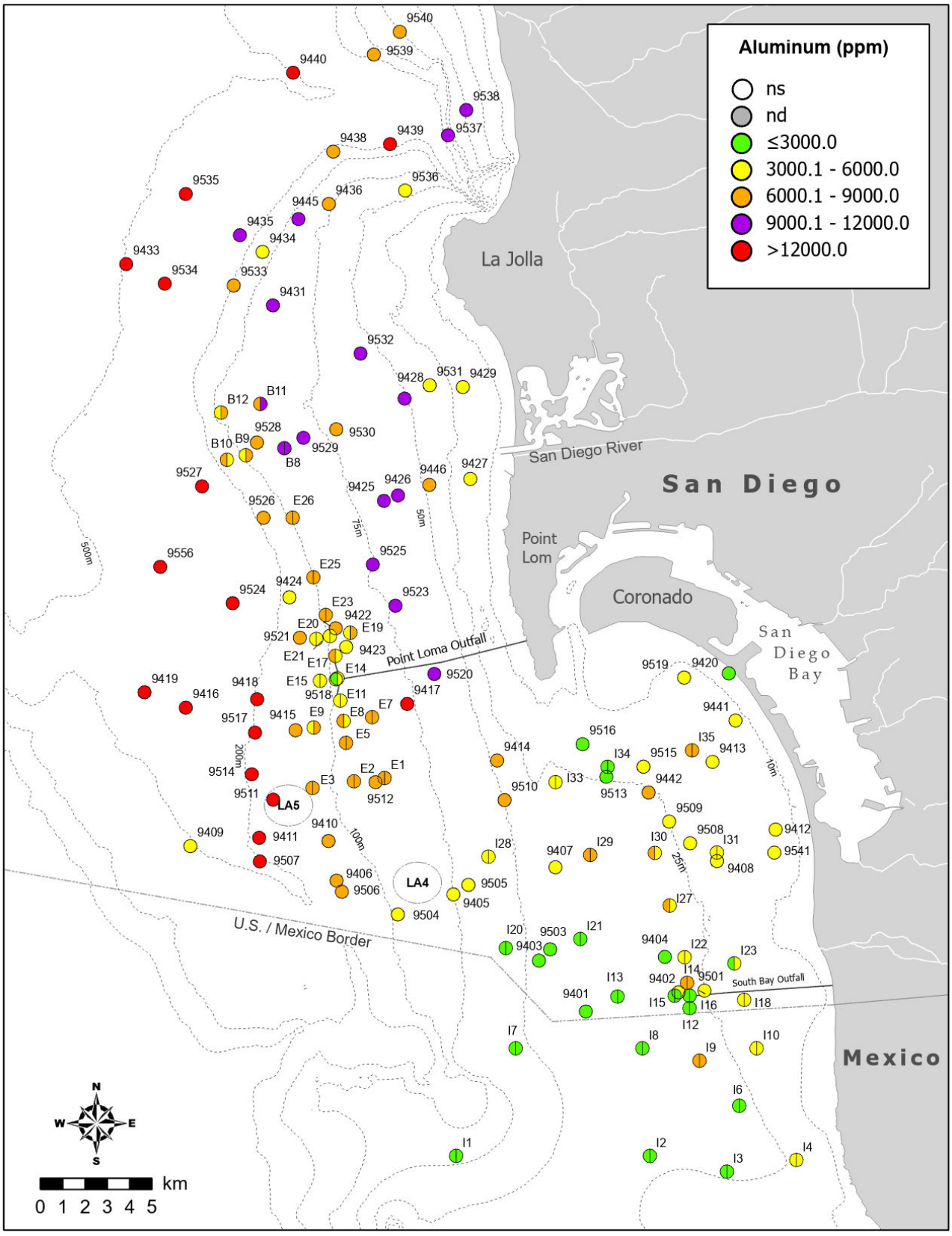
Appendix F.8 *continued*

Phylum	Class	Family	Taxon	n
			Molgula regularis	1
			Molgula sp	2
	Leptocardii	Branchiostomatidae	Branchiostoma californiense	1
	--	--	Craniata	1

Appendix F.9

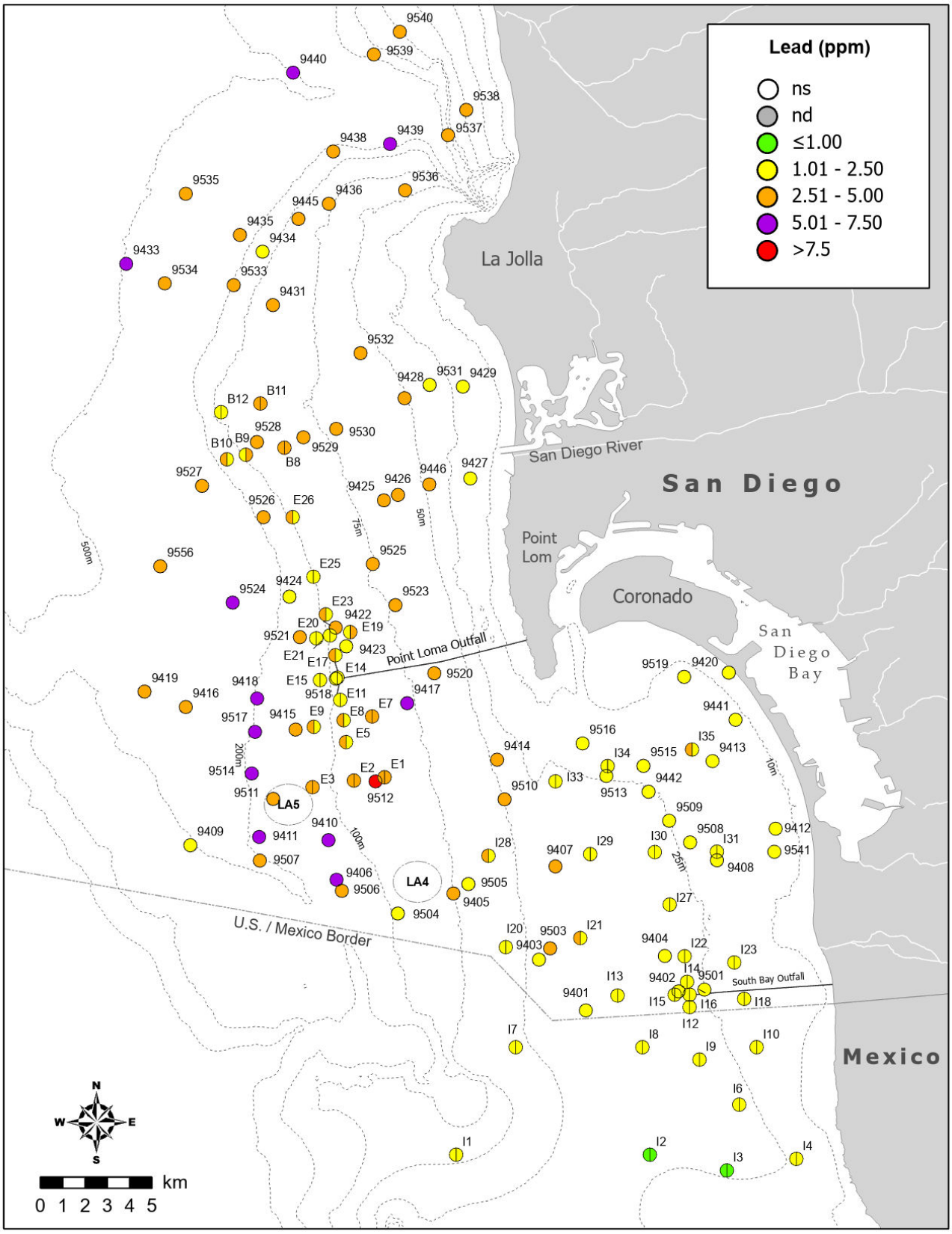
Results of Spearman Rank correlation analyses of various sediment parameters from San Diego regional and core benthic stations sampled during summer 2024 and 2025. Data include the correlation coefficient (r_s) for all parameters with detection rates ≥ 50% (see Table 7.1). Correlation coefficients $r_s \geq 0.70$ are highlighted.

	Depth	Fines	Sul	TN	TOC	TVS	Al	Sb	As	Ba	Be	Cd	Cr	Cu	Fe	Pb	Mn	Hg	Ni	Se	Sn	Zn
Fines	0.63																					
Sul	0.55	0.41																				
TN	0.82	0.69	0.51																			
TOC	0.76	0.55	0.39	0.85																		
TVS	0.89	0.73	0.54	0.89	0.83																	
Al	0.75	0.76	0.46	0.78	0.64	0.90																
Sb	0.69	0.58	0.38	0.71	0.70	0.79	0.76															
As	0.28	0.12	0.08	0.26	0.32	0.27	0.19	0.55														
Ba	0.73	0.69	0.50	0.75	0.59	0.85	0.96	0.73	0.15													
Be	0.81	0.75	0.45	0.83	0.79	0.92	0.94	0.85	0.34	0.89												
Cd	0.83	0.58	0.60	0.74	0.63	0.80	0.73	0.67	0.29	0.73	0.74											
Cr	0.83	0.72	0.47	0.84	0.78	0.94	0.92	0.87	0.40	0.88	0.97	0.77										
Cu	0.81	0.73	0.45	0.77	0.67	0.92	0.95	0.77	0.21	0.92	0.92	0.71	0.91									
Fe	0.73	0.72	0.38	0.77	0.74	0.85	0.90	0.86	0.45	0.84	0.97	0.66	0.95	0.87								
Pb	0.20	0.23	0.10	0.12	0.15	0.23	0.25	0.24	0.11	0.22	0.25	0.17	0.25	0.27	0.25							
Mn	0.56	0.65	0.39	0.59	0.42	0.70	0.90	0.61	0.09	0.90	0.81	0.55	0.75	0.83	0.81	0.20						
Hg	0.71	0.68	0.37	0.69	0.60	0.82	0.81	0.65	0.16	0.74	0.79	0.58	0.79	0.89	0.75	0.30	0.64					
Ni	0.86	0.76	0.51	0.87	0.75	0.97	0.95	0.78	0.24	0.91	0.94	0.78	0.95	0.95	0.87	0.25	0.76	0.84				
Se	0.79	0.61	0.43	0.80	0.72	0.87	0.83	0.78	0.31	0.81	0.85	0.69	0.86	0.85	0.81	0.24	0.68	0.76	0.88			
Sn	0.56	0.67	0.37	0.60	0.49	0.70	0.79	0.63	0.14	0.74	0.75	0.54	0.73	0.78	0.73	0.26	0.69	0.74	0.76	0.67		
Zn	0.78	0.77	0.50	0.81	0.72	0.92	0.97	0.82	0.26	0.94	0.97	0.75	0.96	0.94	0.95	0.26	0.85	0.83	0.95	0.84	0.80	
tDDT	0.07	0.14	0.12	0.12	0.07	0.13	0.16	0.14	0.09	0.14	0.14	0.12	0.14	0.13	0.13	0.04	0.13	0.12	0.13	0.11	0.17	0.14

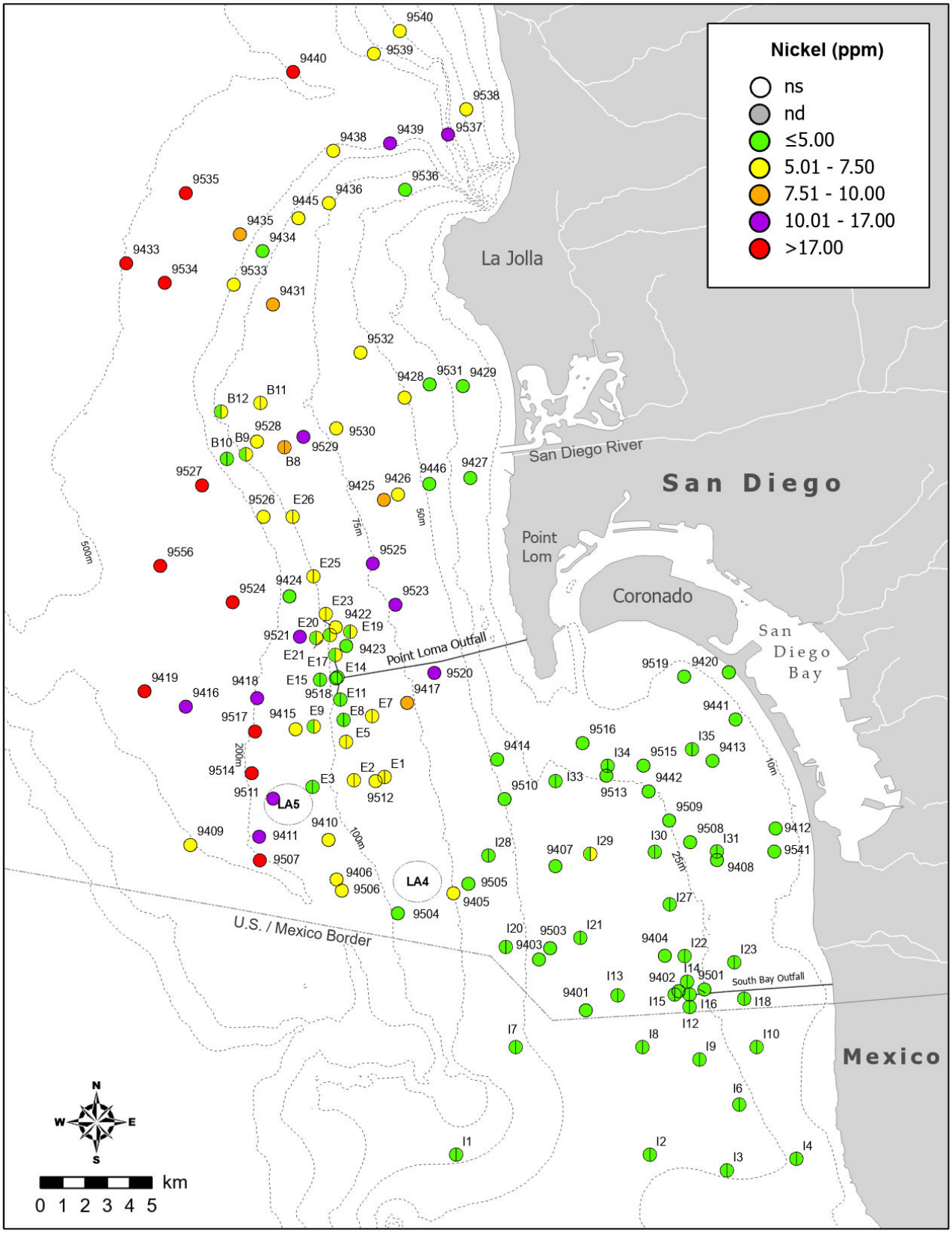


Appendix F.10

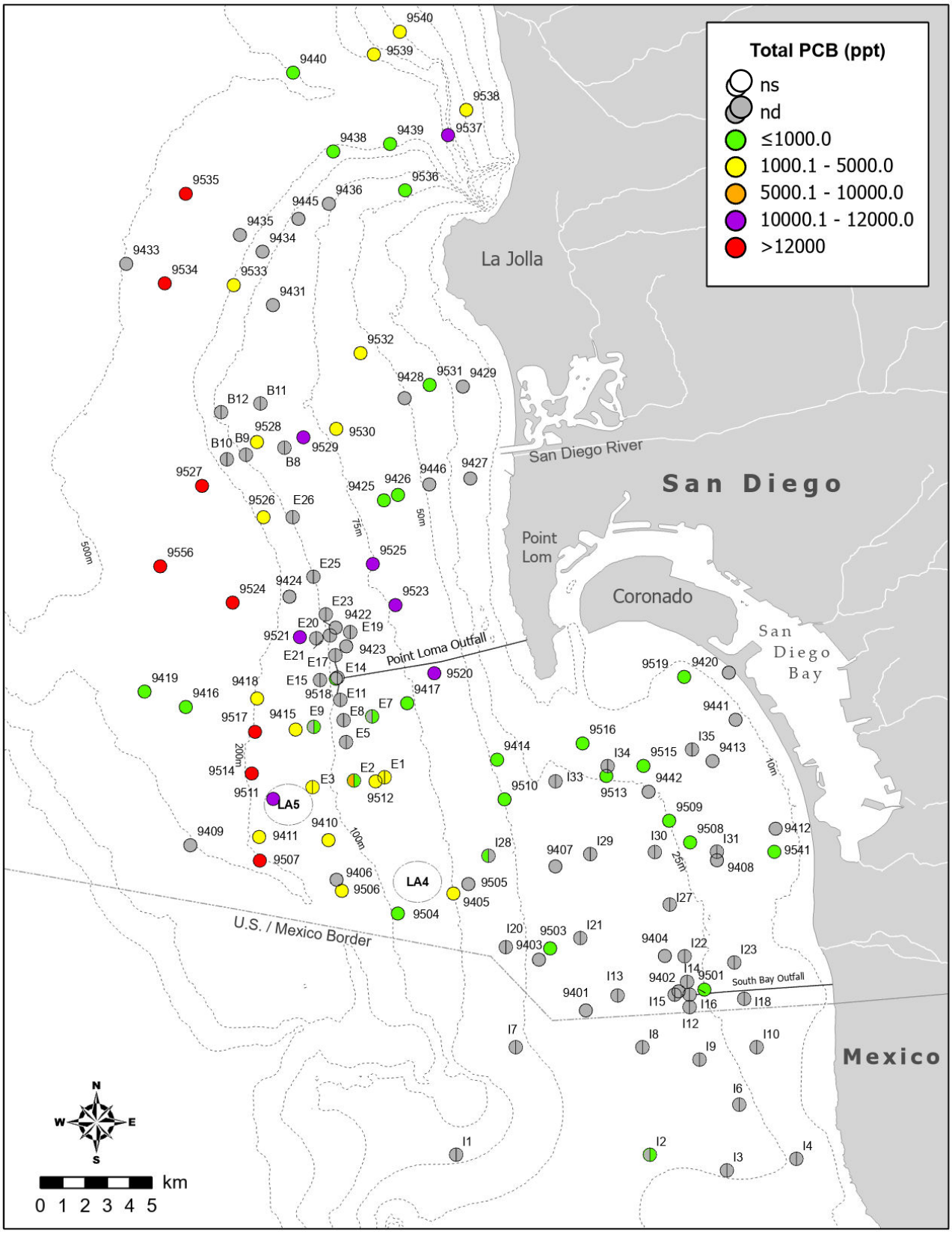
Distribution of select metals (ppm) and Total PCBs (ppt) in sediments from San Diego regional and core benthic stations sampled during summer 2024 and 2025; ns = not sampled (or not reportable, see text); nd = not detected.



Appendix F.10 *continued*



Appendix F.10 *continued*

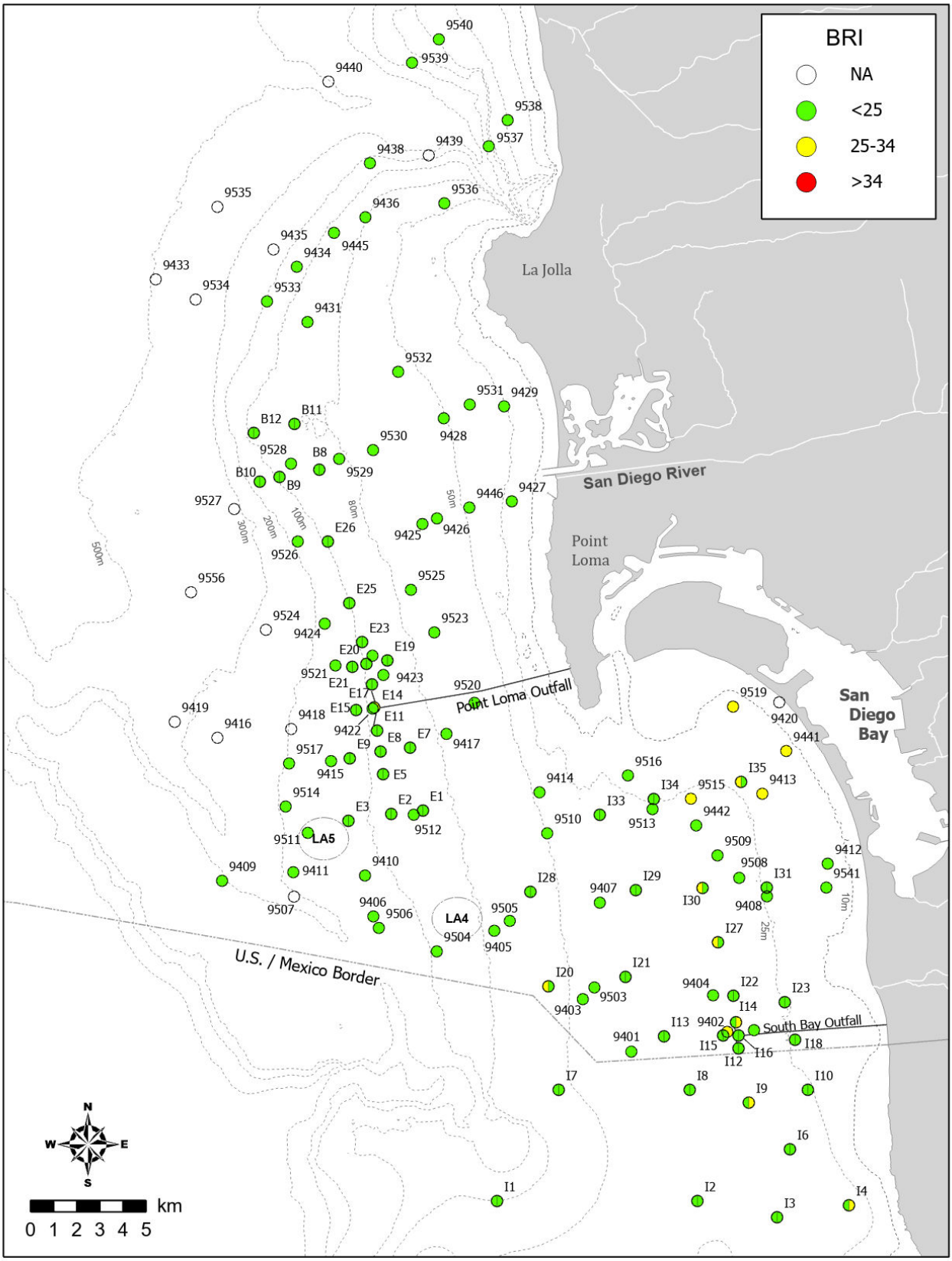


Appendix F.10 *continued*

Appendix F.11

Bioassay results (10-day amphipod survival tests) for sediment toxicity testing conducted for San Diego regional benthic stations sampled during summer 2024 and 2025. Percent fines = percentage of silt + clay combined. Test results (% Survival) are expressed as mean percent survival ± 1 standard deviation.

	Site/Sample	Depth Stratum	Station Depth (m)	Percent Fines	Sample Date	Test Initiation	% Survival (Mean ± SD)
Summer 2024	Lab Control	—	—	—	—	2 Aug 2024	99 ± 2.2
	I12	Inner Shelf	28	21.3	16 Jul 2024	2 Aug 2024	97 ± 4.5
	I14	Inner Shelf	28	1.9	16 Jul 2024	2 Aug 2024	99 ± 2.2
	I15	Inner Shelf	28	48.2	16 Jul 2024	2 Aug 2024	99 ± 2.2
	I16	Inner Shelf	28	33.2	16 Jul 2024	2 Aug 2024	98 ± 2.7
	E11	Mid Shelf	98	37.6	17 Jul 2024	2 Aug 2024	97 ± 2.7
	E14	Mid Shelf	98	43.7	17 Jul 2024	2 Aug 2024	95 ± 6.1
	E15	Mid Shelf	98	49.7	17 Jul 2024	2 Aug 2024	88 ± 14.0*
	E17	Mid Shelf	98	46.9	17 Jul 2024	2 Aug 2024	97 ± 6.7
Summer 2025	Lab Control	—	—	—	—	22 Jul 2025	99±2.2
	9501	Inner Shelf	25	14.0	14 Jul 2025	22 Jul 2025	98±2.7
	9503	Mid Shelf	45	0.0	14 Jul 2025	22 Jul 2025	93±6.7
	9511	Outer Shelf	178	60.5	14 Jul 2025	22 Jul 2025	91±7.4
	9519	Inner Shelf	13	14.4	14 Jul 2025	22 Jul 2025	99±2.2
	9525	Mid Shelf	75	66.4	15 Jul 2025	22 Jul 2025	85±11.2
	9526	Outer Shelf	166	46.0	15 Jul 2025	22 Jul 2025	98±2.7
	9528	Mid Shelf	96	61.7	15 Jul 2025	22 Jul 2025	98±2.7
	9540	Mid Shelf	77	52.8	16 Jul 2025	22 Jul 2025	90±11.7



Appendix F.12

Distribution of BRI values from San Diego regional and core benthic stations sampled during summer 2024 (left side of circle, where applicable) and 2025 (right side of circle, where applicable); NA = not applicable.

Appendix F.13

Particle size summary for each macrofauna cluster group A–H (defined in Figure 7.5). Data are presented as means (ranges) calculated over all grabs within a cluster group. VF = very fine; F = fine; M = medium; C = coarse; VC = very coarse.

Cluster		Particle Size (%)						
Group	n	Fines	VFSand	FSand	MSand	CSand	VCSand	Granules
A	4	81.8 (72.4-87.5)	14.1 (9.8-21.6)	4.0 (2.8-5.9)	0.1 (0.1-0.1)	0 —	0 —	0 —
B	1	5.6 —	9.6 —	34.2 —	30.1 —	17.7 —	2.9 —	0 —
C	1	6.0 —	2.9 —	2.5 —	26.5 —	34.1 —	16.3 —	11.8 —
D	1	0 —	3.8 —	4.7 —	45.9 —	45.9 —	3.1 —	0 —
E	1	24.9 —	59.4 —	15.3 —	0.5 —	0 —	0 —	0 —
F	63	19.4 (0-88.6)	30.3 (0-76.3)	17.0 (0.8-59.9)	16.3 (0.1-58.7)	14.7 (0-73.5)	2.1 (0-21.3)	0.2 (0-9.2)
G	12	68.3 (57.5-75.5)	24.4 (18.9-32.5)	5.8 (3.3-10.2)	0.5 (0-4.7)	0.6 (0-6.8)	0.4 (0-5.0)	<0.1 (0-0.3)
H	95	48.8 (3-69.4)	30.6 (4-50.7)	11.0 (2.3-45.4)	3.7 (0-42.9)	4.3 (0-43.3)	1.4 (0-15.5)	0.3 (0-9.5)

Appendix F.14

Mean abundance of the characteristic species found in each macrofauna cluster group A–H (defined in Figure 7.6). Highlighted values indicate the top most characteristic species according to SIMPER analysis.

	Cluster Group							
Taxon	**A**	**B[a]**	**C[a]**	**D[a]**	**E[a]**	**F**	**G**	**H**
Prionospio lobulata	2	0	0	0	0	0	0	0
Paraprionospio alata	1	0	0	0	0	0	4	2
Yoldiella nana	1	0	0	0	0	0	0	0
Maldane sarsi	2	0	0	0	0	0	2	0
Chone sp SD3	1	0	0	0	0	0	0	0
Prionospio pygmaeus	0	97	0	0	0	2	0	0
Euphilomedes carcharodonta	0	14	0	0	0	0	0	3
Rhepoxynius menziesi	0	7	0	0	0	0	0	0
Macoma carlottensis	0	2	0	0	0	0	0	0
Nephtys caecoides	0	2	0	0	0	0	0	0
Alienacanthomysis macropsis	0	2	0	0	0	0	0	0
Carinoma mutabilis	0	2	0	0	0	0	0	0
Edotia sublittoralis	0	2	0	0	0	0	0	0
Pisione sp	0	0	35	0	0	0	0	0
Nematoda	0	0	33	0	4	1	0	0
Artacama coniferi	0	0	27	0	0	0	0	0
Eulalia levicornuta Cmplx	0	0	26	0	0	0	0	0
Spiophanes norrisi	0	0	0	5	0	5	0	0
Mooreonuphis sp SD1	0	0	0	5	0	0	0	0
Spio maculata	0	0	0	5	0	0	0	0
Americhelidium sp SD1	0	0	0	5	0	0	0	0
Spiophanes berkeleyorum	0	0	0	4	0	1	0	2
Phyllochaetopterus prolifica	0	0	0	4	0	0	0	0
Laticorophium baconi	0	0	0	4	0	0	0	0
Ampharete labrops	0	0	0	0	14	2	0	0
Goniada littorea	0	0	0	0	13	0	0	0
Polydora cirrosa	0	0	0	0	6	0	0	0
Lucinisca nuttalli	0	0	0	0	2	0	0	0
Gadila aberrans	0	0	0	0	2	0	0	0
Phyllodoce hartmanae	0	0	0	0	2	2	0	0
Phyllodoce longipes	0	0	0	0	2	0	0	0
Leitoscoloplos pugettensis	0	0	0	0	2	0	0	0
Callianax alectona	0	0	0	0	2	0	0	0
Spiophanes duplex	0	0	0	0	2	2	0	5
Mooreonuphis sp	0	0	0	0	2	0	0	0
Diastylopsis tenuis	0	0	0	0	2	0	0	0
Aoroides sp	0	0	0	0	2	0	0	0
Sthenelais verruculosa	0	0	0	0	2	0	0	0
Edwardsia juliae	0	0	0	0	0	3	0	0
Spiochaetopterus costarum Cmplx	0	0	0	0	0	1	0	0

[a] SIMPER analyses not conducted on cluster groups that contain only one grab. For these groups, highlight indicates taxa with the five highest abundances.

Appendix F.14 *continued*

Taxon	Cluster Group							
	A	B[a]	C[a]	D[a]	E[a]	F	G	H
Mediomastus sp	0	0	0	0	0	2	2	3
Sigalion spinosus	0	0	0	0	0	2	0	0
Glycinde armigera	0	0	0	0	0	1	0	0
Euclymeninae sp A	0	0	0	0	0	2	0	3
Kirkegaardia siblina	0	0	0	0	0	2	0	0
Tellina modesta	0	0	0	0	0	1	0	0
Phyllochaetopterus limicolus	0	0	0	0	0	0	7	0
Spiophanes kimballi	0	0	0	0	0	0	3	2
Prionospio jubata	0	0	0	0	0	0	0	3
Prionospio dubia	0	0	0	0	0	0	0	3
Paradiopatra parva	0	0	0	0	0	0	0	3
Amphiuridae	0	0	0	0	0	0	0	3
Chloeia pinnata	0	0	0	0	0	0	0	3
Amphiodia urtica	0	0	0	0	0	0	0	3
Scoloplos armiger Cmplx	0	0	0	0	0	0	0	2
Lumbrineris cruzensis	0	0	0	0	0	0	0	2
Eclysippe trilobata	0	0	0	0	0	0	0	2
Heteronemertea sp SD2	0	0	0	0	0	0	0	2
Tellina cadieni	0	0	0	0	0	0	0	2
Amphiodia sp	0	0	0	0	0	0	0	2
Terebellides californica	0	0	0	0	0	0	0	2
Glycera nana	0	0	0	0	0	0	0	1
Lumbrineris sp Group I	0	0	0	0	0	0	0	2
Siphonenteron bilineatum	0	0	0	0	0	0	0	1

Appendix F.15

Macrofaunal community parameters by grab for regional benthic stations sampled during 2025. SR = species richness; Abun = abundance; H' = Shannon diversity index; J' = Pielou's evenness; Dom = Swartz dominance; BRI = Benthic Response Index. BRI not calculated at depths < 10m or > 200m.

Stratum	Station	Depth (m)	SR	Abun	H'	J'	Dom	BRI
Inner Shelf	9519	13	44	141	3.2	0.85	15	27
	9541	15	39	84	3.4	0.93	19	25
	9516	17	50	141	3.5	0.89	18	19
	9508	21	50	141	3.3	0.83	19	19
	9515	22	97	371	3.6	0.78	26	29
	9513	24	93	616	3.3	0.72	18	22
	9501	25	75	195	3.9	0.90	31	23
	9509	25	79	324	3.6	0.83	22	21
Mid Shelf	9531	35	122	680	4.0	0.84	35	25
	9503	45	107	387	4.1	0.87	35	15
	9538	46	145	1086	3.9	0.79	29	22
	9510	49	169	544	4.4	0.86	61	21
	9536	57	133	527	4.2	0.86	41	19
	9532	60	133	511	4.2	0.86	45	19
	9520	67	100	474	3.8	0.82	28	16
	9530	72	115	541	4.0	0.84	33	16
	9523	73	97	426	3.8	0.83	27	14
	9525	75	90	338	3.8	0.85	29	13
	9505	76	120	404	4.2	0.88	42	13
	9540	77	93	362	4.0	0.87	31	13
	9529	84	83	266	3.9	0.88	30	13
	9512	90	114	479	4.1	0.87	37	15
	9528	96	105	429	4.0	0.86	33	13
	9504	98	98	295	4.0	0.88	38	14
	9518	98	103	649	3.7	0.79	23	24
Outer Shelf	9506	128	105	470	3.8	0.81	30	13
	9539	152	74	396	3.6	0.83	21	19
	9521	154	94	420	3.7	0.81	28	16
	9537	162	100	588	3.4	0.73	20	21
	9526	166	84	323	3.7	0.83	26	16
	9533	177	72	450	3.1	0.73	11	19
	9511	178	60	191	3.2	0.77	18	14
	9514	197	72	371	3.0	0.71	15	18
	9517	199	36	265	1.7	0.47	3	22
Upper Slope	9507	212	58	274	2.8	0.69	11	—
	9524	271	27	69	2.9	0.88	11	—
	9527	319	45	111	3.0	0.80	18	—
	9534	357	34	105	3.0	0.85	15	—
	9535	405	36	104	3.0	0.85	16	—
	9556	433	17	28	2.7	0.95	11	—

Appendix G

Demersal Fishes and Megabenthic Invertebrates

2024 – 2025 Supplemental Analyses

Appendix G.1

Taxonomic listing of demersal fish species collected at PLOO trawl stations during 2024 and 2025. Data are reported as total number of fish (n), biomass (BM, wet weight, kg), minimum, maximum, and mean length (standard length, cm unless otherwise noted). Taxonomic arrangement follows Eschmeyer and Herald (1998) and Page et al. (2013).

					Length (cm)		
Taxonomic Classification		**Common Name**	**n**	**Bm**	**Min**	**Max**	**Mean**
CHIMAERIFORMES							
Chimaeridae	*Hydrolagus colliei*	Spotted Ratfish	2	1.2	44	45	44
SQUATINIFORMES							
Squatinidae	*Squatina californica*	Pacific Angel Shark	1	11.5	—	—	99
TORPEDINIFORMES							
Torpedinidae	*Torpedo californica*	Pacific Electric Ray	1	1.2	—	—	36
RAJIFORMES							
Rajidae	*Bathyraja interrupta*	Sandpaper Skate[a]	1	0.1	—	—	25
	Raja inornata	California Skate[a]	21	7.3	15	56	31
ARGENTINIFORMES							
Argentinidae	*Argentina sialis*	Pacific Argentine	56	1.0	3	10	7
STOMIIFORMES							
Sternoptychidae	*Argyropelecus lychnus*	Tropical Hatchetfish	4	0.2	11	15	13
AULOPIFORMES							
Synodontidae	*Synodus lucioceps*	California Lizardfish	200	2.6	9	26	12
GADIFORMIS							
Macrouridae	*Nezumia stelgidolepis*	California Grenadier	1	0.3	—	—	38
OPHIDIIFORMES							
Ophidiidae	*Chilara taylori*	Spotted Cusk-eel	3	0.3	15	20	17
BATRACHOIDIFORMES							
Batrachoididae	*Porichthys notatus*	Plainfin Midshipman	46	2.5	10	19	14
GASTEROSTEIFORMES							
Syngnathidae	*Syngnathus californiensis*	Kelp Pipefish	4	0.3	21	24	23
SCORPAENIFORMES							
Scorpaenidae	*Scorpaena guttata*	California Scorpionfish	24	5.8	13	25	19
Sebastidae	*Sebastes dallii*	Calico Rockfish	8	0.1	4	5	5
	Sebastes elongatus	Greenstriped Rockfish	15	1.0	5	12	8
	Sebastes eos	Pink Rockfish	5	0.2	9	14	10
	Sebastes goodei	Chilipepper	4	0.3	10	13	11
	Sebastes hopkinsi	Squarespot Rockfish	9	0.4	9	15	12
	Sebastes jordani	Shortbelly Rockfish	1	0.1	—	—	14
	Sebastes levis	Cowcod	14	0.9	7	15	10
	Sebastes miniatus	Vermilion Rockfish	2	0.3	16	20	18
	Sebastes rosenblatti	Greenblotched Rockfish	25	1.3	5	19	10
	Sebastes rubrivinctus	Flag Rockfish	19	0.4	4	15	6

Appendix G.1 *continued*

Taxonomic Classification		Common Name	n	Bm	Length (cm)		
					Min	Max	Mean
Sebastidae	*Sebastes saxicola*	Stripetail Rockfish	697	8.2	4	12	8
	Sebastes semicinctus	Halfbanded Rockfish	1788	36.9	5	15	10
	Sebastes sp	Rockfish Unidentified	13	0.7	4	6	5
Hexagrammidae	*Zaniolepis frenata*	Shortspine Combfish	736	13.4	7	26	12
	Zaniolepis latipinnis	Longspine Combfish	2551	18.3	6	18	9
Cottidae	*Chitonotus pugetensis*	Roughback Sculpin	27	0.7	7	11	9
	Icelinus quadriseriatus	Yellowchin Sculpin	575	3.2	4	17	6
	Icelinus tenuis	Spotfin Sculpin	9	0.2	7	10	8
	Scorpaenichthys marmoratus	Cabezon	1	0.3	—	—	17
Agonidae	*Xeneretmus latifrons*	Blacktip Poacher	4	0.4	12	14	13
PERCIFORMES							
Malacanthidae	*Caulolatilus princeps*	Ocean Whitefish	1	0.1	—	—	4
Sciaenidae	*Genyonemus lineatus*	White Croaker	5	0.9	17	22	19
Embiotocidae	*Cymatogaster aggregata*	Shiner Perch	1	0.1	—	—	12
	Zalembius rosaceus	Pink Seaperch	262	5.2	4	18	9
Bathymasteridae	*Rathbunella alleni*	Stripefin Ronquil	1	0.1	—	—	17
Zoarcidae	*Lycodes diapterus*	Black Eelpout	1	0.1	—	—	22
	Lycodes pacificus	Blackbelly Eelpout	6	0.3	13	22	17
Uranoscopidae	*Kathetostoma averruncus*	Smooth Stargazer	1	0.1	—	—	10
Stromateidae	*Peprilus simillimus*	Pacific Pompano	1	0.1	—	—	6
PLEURONECTIFORMES							
Paralichthyidae	*Citharichthys sordidus*	Pacific Sanddab	8123	108.1	3	29	9
	Citharichthys xanthostigma	Longfin Sanddab	1018	42.3	5	20	13
	Hippoglossina stomata	Bigmouth Sole	71	8.8	14	27	19
Pleuronectidae	*Glyptocephalus zachirus*	Rex Sole	24	2.4	11	25	20
	Lyopsetta exilis	Slender Sole	96	2.0	8	15	12
	Microstomus pacificus	Dover Sole	804	30.1	5	25	13
	Parophrys vetulus	English Sole	154	16.5	11	28	18
	Pleuronichthys decurrens	Curlfin Sole	2	0.5	18	19	18
	Pleuronichthys verticalis	Hornyhead Turbot	47	6.3	12	20	16
Cynoglossidae	*Symphurus atricaudus*	California Tonguefish	259	7.5	6	16	14

Appendix G.2

Taxonomic listing of demersal fish species collected at SBOO trawl stations during 2024 and 2025. Data are reported as total number of fish (n), biomass (BM, wet weight, kg), minimum, maximum, and mean length (standard length, cm unless otherwise noted). Taxonomic arrangement follows Eschmeyer and Herald (1998) and Page et al. (2013).

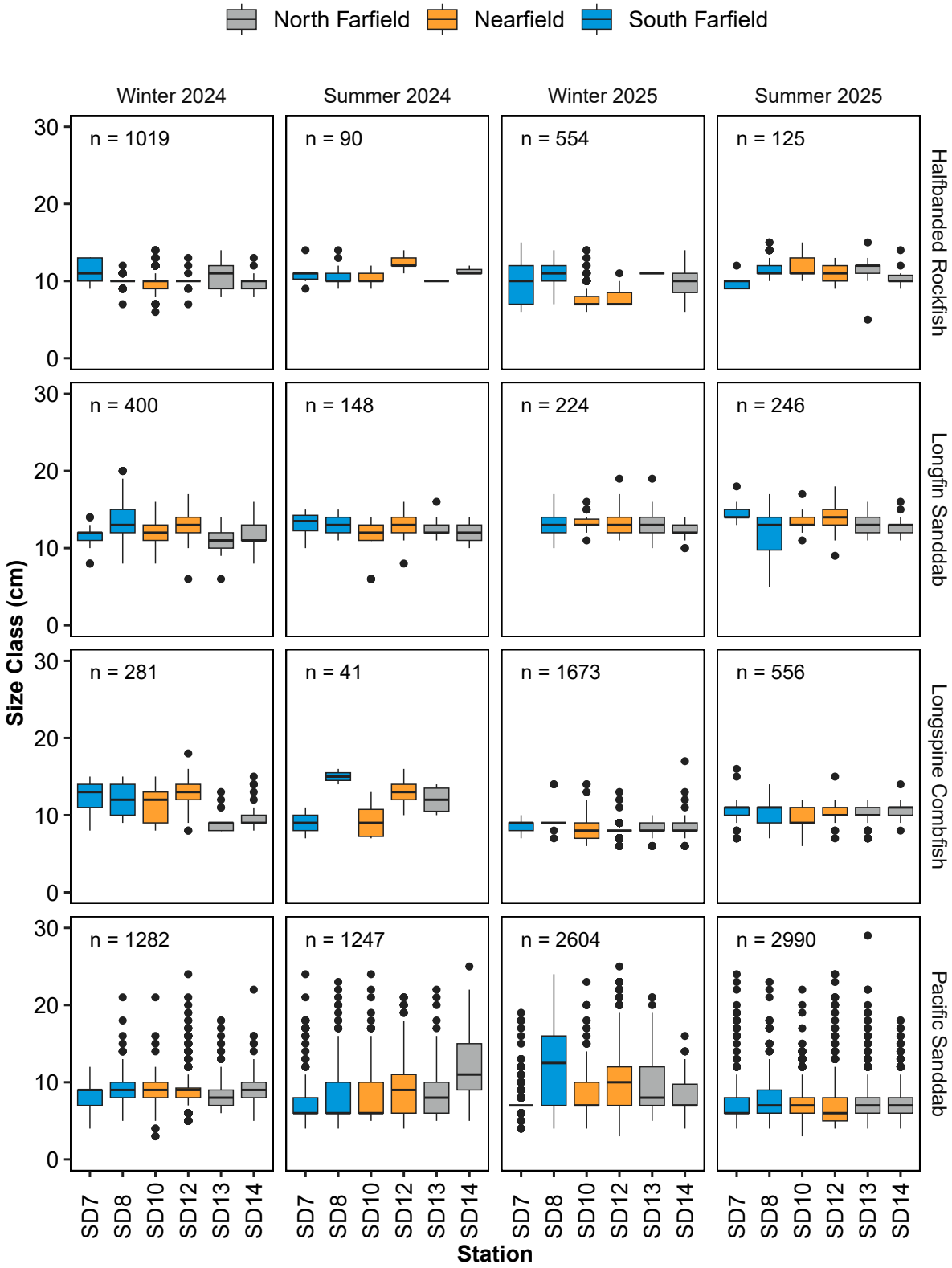
					Length (cm)		
Taxonomic Classification		**Common Name**	**n**	**Bm**	**Min**	**Max**	**Mean**
RAJIFORMES							
Rajidae	*Raja inornata*	California Skate[a]	13	7.8	23	53	40
MYLIOBATIFORMES							
Urolophidae	*Urobatis halleri*	Round Stingray	3	1.3	24	31	27
CLUPEIFORMES							
Engraulidae	*Engraulis mordax*	Northern Anchovy	1	0.1	—	—	12
AULOPIFORMES							
Synodontidae	*Synodus lucioceps*	California Lizardfish	1722	25.6	7	31	12
BATRACHOIDIFORMES							
Batrachoididae	*Porichthys myriaster*	Specklefin Midshipman	32	2.6	6	37	13
	Porichthys notatus	Plainfin Midshipman	21	0.6	6	14	9
ATHERINIFORMES							
Atherinopsidae	*Leuresthes tenuis*	California Grunion	15	0.4	15	17	16
GASTEROSTEIFORMES							
Syngnathidae	*Syngnathus californiensis*	Kelp Pipefish	315	1.3	12	29	22
	Syngnathus exilis	Barcheek Pipefish	43	0.7	16	26	21
SCORPAENIFORMES							
Scorpaenidae	*Scorpaena guttata*	California Scorpionfish	1	0.6	—	—	24
Sebastidae	*Sebastes dallii*	Calico Rockfish	9	0.4	4	8	7
	Sebastes miniatus	Vermilion Rockfish	5	0.4	6	9	7
	Sebastes saxicola	Stripetail Rockfish	1	0.1	—	—	5
	Sebastes sp	Rockfish Unidentified	2	0.1	3	3	3
Hexagrammidae	*Ophiodon elongatus*	Lingcod	2	0.1	13	13	13
	Zaniolepis latipinnis	Longspine Combfish	189	4.4	8	16	14
Cottidae	*Chitonotus pugetensis*	Roughback Sculpin	156	3.4	3	11	9
	Icelinus quadriseriatus	Yellowchin Sculpin	146	1.8	4	8	7
Agonidae	*Odontopyxis trispinosa*	Pygmy Poacher	4	0.4	7	9	8
PERCIFORMES							
Sciaenidae	*Genyonemus lineatus*	White Croaker	1	0.1	—	—	10
Embiotocidae	*Cymatogaster aggregata*	Shiner Perch	15	0.5	8	10	9
PLEURONECTIFORMES							
Paralichthyidae	*Citharichthys sordidus*	Pacific Sanddab	70	1.6	4	19	7
	Citharichthys stigmaeus	Speckled Sanddab	3775	34.9	3	29	8
	Citharichthys xanthostigma	Longfin Sanddab	1352	68.3	4	23	13
	Hippoglossina stomata	Bigmouth Sole	12	2.4	18	29	22

[a] measured as total length (cm)

Appendix G.2 *continued*

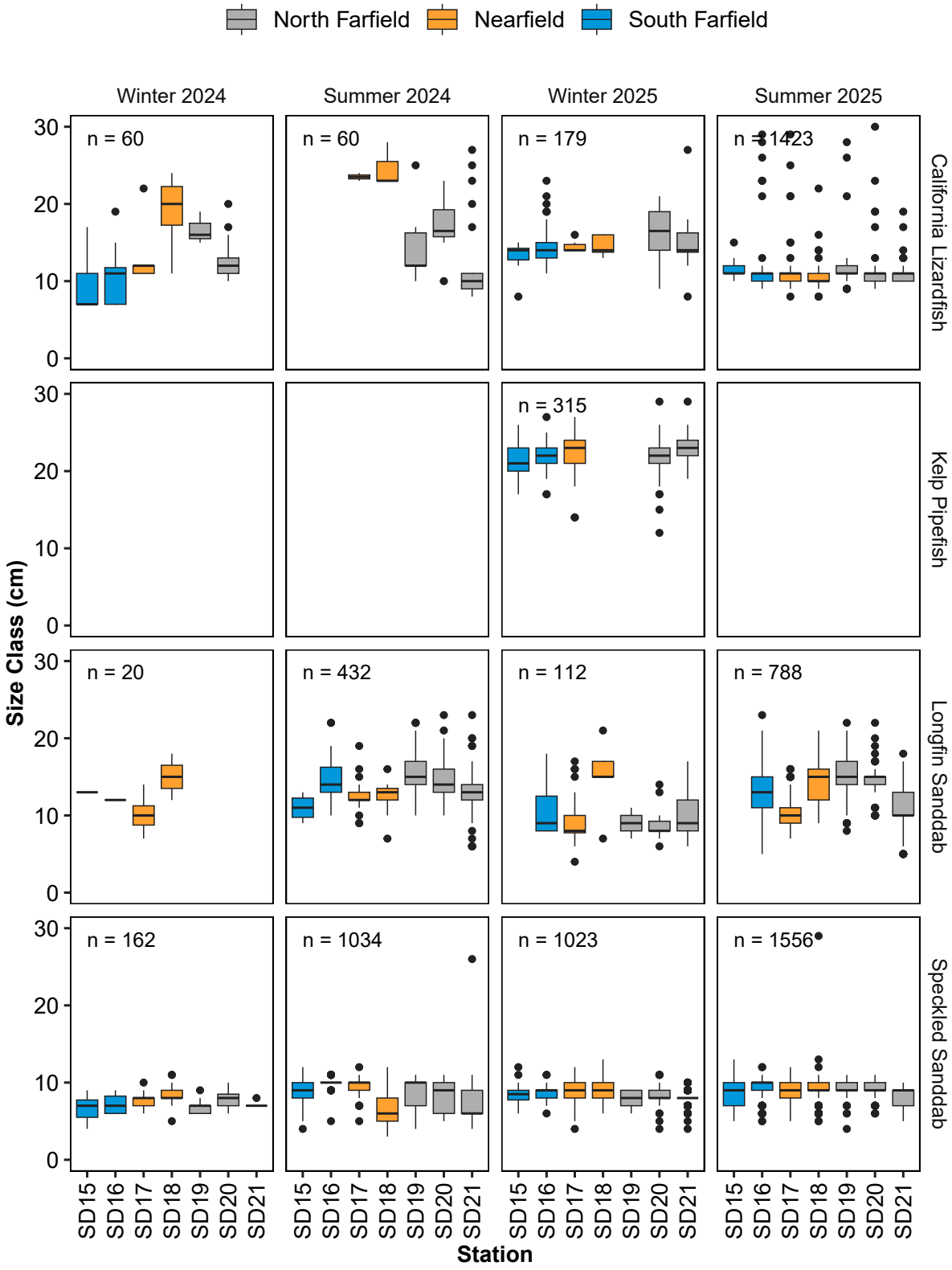
Taxonomic Classification		Common Name	n	Bm	Length (cm)		
					Min	Max	Mean
Paralichthyidae	*Paralichthys californicus*	California Halibut	57	41.6	19	57	34
	Xystreurys liolepis	Fantail Sole	25	6.6	15	31	22
Pleuronectidae	*Parophrys vetulus*	English Sole	261	35.5	9	33	20
	Pleuronichthys decurrens	Curlfin Sole	4	0.5	6	19	12
	Pleuronichthys ritteri	Spotted Turbot	41	6.3	12	22	18
	Pleuronichthys verticalis	Hornyhead Turbot	155	20.9	5	24	15
Cynoglossidae	*Symphurus atricaudus*	California Tonguefish	219	4.2	6	16	11

[a] measured as total length (cm)



Appendix G.3

Summary of fish lengths by survey and station for the four most abundant species collected in the PLOO region during 2024 and 2025. Data are median, upper and lower quartiles, 1.5 times the interquartile range (whiskers), and outliers (circles).



Appendix G.4

Summary of fish lengths by survey and station for the four most abundant species collected in the SBOO region during 2024 and 2025. Data are median, upper and lower quartiles, 1.5 times the interquartile range (whiskers), and outliers (circles).

Appendix G.5

Summary of demersal fish abnormalities and parasites at PLOO and SBOO trawl stations during 2024 and 2025.

Region	Year	Survey	Station	Species	Anomaly/Parasite	n
PLOO	2024	Winter	SD7	California Skate	Tumor	1
			SD7	Pacific Sanddab	*Phrixocephalus cininnatus*	2
			SD8	Pacific Sanddab	*Phrixocephalus cininnatus*	3
			SD10	Pacific Sanddab	*Phrixocephalus cininnatus*	2
			SD12	Dover Sole	Tumor	1
			SD12	Pacific Sanddab	*Phrixocephalus cininnatus*	6
			SD14	Pacific Sanddab	*Phrixocephalus cininnatus*	1
	2025		SD7	Pacific Sanddab	*Phrixocephalus cininnatus*	1
			SD8	Pacific Sanddab	*Phrixocephalus cininnatus*	3
			SD10	Pacific Sanddab	*Phrixocephalus cininnatus*	17
			SD12	Pacific Sanddab	*Phrixocephalus cininnatus*	10
			SD13	Pacific Sanddab	*Phrixocephalus cininnatus*	9
			SD14	Pacific Sanddab	*Phrixocephalus cininnatus*	10
		Summer	SD12	Pacific Sanddab	*Phrixocephalus cininnatus*	1
SBOO	2024	Winter	SD17	English Sole	Tumor	1
		Summer	SD18	California Halibut	*Elthusa vulgaris*	1
			SD18	Speckled Sanddab	*Elthusa vulgaris*, Fin Rot	1
			SD19	California Halibut	Tumor	1
			SD19	Speckled Sanddab	Ambicoloration	1
			SD19	Speckled Sanddab	Lesion	1
			SD19	Speckled Sanddab	Tumor	1
	2025	Winter	SD21	Hornyhead Turbot	Fin Rot	0
		Summer	SD18	English Sole	Skeletal Deformity	1
			SD19	Speckled Sanddab	*Elthusa vulgaris*	1

Appendix G.6

Description of PLOO demersal fish cluster groups defined in Figure 8.5. Data are mean abundance of the characteristic species. Highlighted/bold values indicate the most characteristic species according to SIMPER analysis.

	Cluster Group					
Species	**A**[a]	**B**[a]	**C**	**D**	**E**	**F**
Pacific Sanddab	**75**	**110**	**92**	**246**	**112**	**39**
California Lizardfish	0	0	**140**	11	<1	0
Plainfin Midshipman	**116**	**4**	1	6	**12**	<1
Halfbanded Rockfish	0	**60**	12	**29**	3	4
Dover Sole	**36**	1	**5**	**31**	**13**	**3**
Longspine Combfish	**7**	2	**7**	**24**	2	1
Squarespot Rockfish	1	**5**	4	14	5	4
Shortspine Combfish	0	**23**	0	**<1**	<1	<1
Longfin Sanddab	0	3	7	9	4	0
Greenblotched Rockfish	**4**	1	3	5	1	1
Gulf Sanddab	0	0	0	7	6	<1
Vermilion Rockfish	0	0	0	8	4	1
California Tonguefish	**3**	1	1	4	**<1**	0
Greenstriped Rockfish	2	0	1	5	1	<1
Greenspotted Rockfish	0	0	<1	<1	2	1

[a] SIMPER analysis only conducted on cluster groups that contain more than one haul. For these groups, shading indicates five most abundant species.

Appendix G.7

Description of SBOO demersal fish cluster groups defined in Figure 8.6. Data are mean abundance of the characteristic species. Highlighted/bold values indicate the most characteristic species according to SIMPER analysis.

	Cluster Group					
Species	**A**	**B**[a]	**C**	**D**[a]	**E**	**F**
Speckled Sanddab	**98**	**26**	**53**	**143**	**180**	**13**
California Lizardfish	3	**75**	**9**	**118**	**93**	1
Pacific Sanddab	<1	0	1	**153**	3	<1
Longspine Combfish	0	**79**	<1	**1**	3	0
Longfin Sanddab	1	**8**	**33**	0	**30**	1
Yellowchin Sculpin	<1	5	2	0	20	0
Hornyhead Turbot	4	3	**4**	**9**	6	**2**
White Croaker	<1	**22**	2	0	<1	0
California Tonguefish	<1	6	5	0	6	<1
English Sole	<1	6	4	1	5	<1
Roughback Sculpin	<1	5	<1	1	7	0

[a] SIMPER analysis only conducted on cluster groups that contain more than one haul. For these groups, shading indicates five most abundant species.

Appendix G.8

Taxonomic listing of megabenthic invertebrate taxa collected at all PLOO trawl stations during 2024 and 2025. Data are total number of individuals (n). Taxonomic arrangement follows SCAMIT (2023).

Taxonomic Classification				n
PORIFERA	Demospongiae	Chalinidae	*Chalinidae*	4
		Suberitidae	*Suberites latus*	4
CNIDARIA	Octocorallia	–	*Malacalcyonacea*	1
		Gorgoniidae	*Adelogorgia phyllosclera*	4
			Eugorgia rubens	1
		Plexauridae	*Plexauridae*	1
			Muricea fruticosa	2
			Thesea sp B	14
		Virgulariidae	*Acanthoptilum* sp	20
	Hexacorallia	Metridiidae	*Metridium farcimen*	3
		Parazoanthidae	*Savalia lucifica*	2
MOLLUSCA	Gastropoda	Calliostomatidae	*Calliostoma turbinum*	1
		Nassariidae	*Tritia insculpta*	1
		Cancellariidae	*Cancellaria cooperii*	1
		Pseudomelatomidae	*Antiplanes catalinae*	7
			Megasurcula carpenteriana	4
			Megasurcula stearnsiana	1
		Discodorididae	*Baptodoris mimetica*	1
			Platydoris macfarlandi	4
		Polyceridae	*Triopha catalinae*	1
		Pleurobranchaeidae	*Pleurobranchaea californica*	45
		Philinidae	*Philine auriformis*	3
	Cephalopoda	Sepiolidae	*Rossia pacifica*	8
		Octopodidae	*Octopus rubescens*	22
ANNELIDA	Polychaeta	Aphroditidae	*Aphrodita refulgida*	2
ARTHROPODA	Malacostraca	Squillidae	*Schmittius politus*	1
		Sicyoniidae	*Sicyonia ingentis*	51
			Sicyonia penicillata	22
		Crangonidae	*Crangon alaskensis*	1
		Diogenidae	*Paguristes bakeri*	4
			Paguristes turgidus	7
		Calappidae	*Platymera gaudichaudii*	2
		Epialtidae	*Loxorhynchus crispatus*	2
			Loxorhynchus grandis	1
		Inachidae	*Coryrhynchus lobifrons*	4
ECHINODERMATA	Crinoidea	Antedonidae	*Florometra serratissima*	1
	Asteroidea	Luidiidae	*Luidia armata*	3

Appendix G.8 *continued*

Taxonomic Classification				n
ECHINODERMATA	Asteroidea	Luidiidae	*Luidia asthenosoma*	46
			Luidia foliolata	88
		Astropectinidae	*Astropecten californicus*	477
			Astropecten ornatissimus	2
		–	*Granulosina*	1
		Asteriidae	*Stylasterias forreri*	2
	Ophiuroidea	Gorgonocephalidae	*Gorgonocephalus eucnemis*	3
		Ophiuridae	*Ophiura luetkenii*	144
		Ophiopholidae	*Ophiopholis bakeri*	24
		Ophiotrichidae	*Ophiothrix spiculata*	54
	Echinoidea	Diadematidae	*Centrostephanus coronatus*	1
		Toxopneustidae	*Lytechinus pictus*	49273
		Strongylocentrotidae	*Mesocentrotus franciscanus*	1
			Strongylocentrotus fragilis	13

Appendix G.9

Taxonomic listing of megabenthic invertebrate taxa collected at all SBOO trawl stations during 2024 and 2025. Data are total number of individuals (n). Taxonomic arrangement follows SCAMIT (2023).

Taxonomic Classification				n
CNIDARIA	Octocorallia	Renillidae	*Renilla koellikeri*	1
		Virgulariidae	*Stylatula elongata*	8
MOLLUSCA	Gastropoda	Turbinidae	*Megastraea turbanica*	1
		Naticidae	*Neverita lewisii*	1
		Bursidae	*Crossata ventricosa*	4
		Austrosiphonidae	*Kelletia kelletii*	8
		Nassariidae	*Caesia perpinguis*	1
		Muricidae	*Pteropurpura festiva*	1
			Pteropurpura vokesae	1
		Pseudomelatomidae	*Burchia semiinflata*	6
			Megasurcula carpenteriana	3
		Arminidae	*Armina californica*	2
		Onchidoridae	*Acanthodoris brunnea*	10
		Pleurobranchaeidae	*Pleurobranchaea californica*	10
		Philinidae	*Philine auriformis*	57
	Cephalopoda	Octopodidae	*Octopus rubescens*	7
ANNELIDA	Polychaeta	Aphroditidae	*Aphrodita* sp	1
ARTHROPODA	Malacostraca	Hemisquillidae	*Hemisquilla californiensis*	13
		Sicyoniidae	*Sicyonia ingentis*	17
			Sicyonia penicillata	86
		Thoridae	*Heptacarpus stimpsoni*	6
		Pandalidae	*Pandalus platyceros*	3
			Pandalus sp	1
		Crangonidae	*Crangon alba*	10
			Crangon nigromaculata	78
		Palinuridae	*Panulirus interruptus*	1
		Diogenidae	*Paguristes bakeri*	5
		Paguridae	*Pagurus armatus*	2
			Pagurus spilocarpus	29
		Calappidae	*Platymera gaudichaudii*	3
		Epialtidae	*Loxorhynchus crispatus*	1
			Loxorhynchus grandis	7
		Inachidae	*Ericerodes hemphillii*	1
		Inachoididae	*Pyromaia tuberculata*	22
		Parthenopidae	*Latulambrus occidentalis*	4
		Cancridae	*Metacarcinus anthonyi*	2
			Metacarcinus gracilis	5

Appendix G.9 *continued*

Taxonomic Classification				n
ARTHROPODA	Malacostraca	Portunidae	*Achelous xantusii*	9
ECHINODERMATA	Asteroidea	Luidiidae	*Luidia armata*	48
			Luidia foliolata	11
		Astropectinidae	*Astropecten californicus*	1868
	Ophiuroidea	Ophiotrichidae	*Ophiothrix spiculata*	66
	Echinoidea	Toxopneustidae	*Lytechinus pictus*	64
		Dendrasteridae	*Dendraster terminalis*	12
		Loveniidae	*Lovenia cordiformis*	22
BRACHIOPODA	Lingulata	Lingulidae	*Glottidia albida*	1
CHORDATA	Ascidiacea	Polyclinidae	*Polyclinum planum*	3

Appendix G.10

Description of PLOO megabenthic invertebrate cluster groups defined in Figure 8.10. Data are mean abundance of the characteristic species. Highlighted/bold values indicate the most characteristic species according to SIMPER analysis.

	Cluster Group					
Species	**A**	**B**	**C**	**D**	**E**	**F**
Grimothea planipes	0	**5261**	0	0	1	2
Lytechinus pictus	0	**87**	**12**	**619**	**1516**	2
Sicyonia ingentis	**89**	**59**	<1	<1	5	7
Strongylocentrotus fragilis	0	44	0	**27**	45	**24**
Acanthoptilum sp	0	0	0	3	37	**73**
Ophiura luetkenii	0	0	0	1	49	**2**
Astropecten californicus	0	<1	2	**12**	**5**	**6**
Luidia foliolata	0	<1	3	4	**4**	<1
Apostichopus californicus	0	<1	<1	1	**4**	3
Megasurcula carpenteriana	<1	0	0	**6**	<1	1
Amphichondrius granulatus	0	0	0	**5**	<1	0
Pleurobranchaea californica	0	0	0	3	2	<1
Neocrangon zacae	0	0	0	**4**	<1	<1
Octopus rubescens	0	<1	0	2	1	<1
Thesea sp B	0	0	0	2	1	<1
Octopus veligero	**3**	0	1	0	<1	0
Nymphon pixellae	0	0	0	3	<1	0
Ophiothrix spiculata	0	0	<1	1	<1	0
Doryteuthis opalescens	0	0	0	2	<1	<1
Florometra serratissima	0	<1	0	<1	1	0
Ophiopholis bakeri	0	0	0	<1	<1	0

[a] SIMPER analysis only conducted on cluster groups that contain more than one haul. For these groups, shading indicates five most abundant species.

Appendix G.11

Description of SBOO megabenthic invertebrate cluster groups defined in Figure 8.11. Data are mean abundance of the characteristic species. Highlighted/bold values indicate the most characteristic species according to SIMPER analysis.

	Cluster Group					
Species	**A**[a]	**B**[a]	**C**	**D**	**E**	**F**
Lytechinus pictus	0	0	**647**	5	<1	**2**
Ophiura luetkenii	**72**	0	0	<1	<1	0
Astropecten californicus	0	**1**	28	**39**	**2**	0
Dendraster terminalis	**3**	0	4	1	1	<1
Sicyonia penicillata	0	0	0	<1	**7**	0
Ophiothrix spiculata	**3**	0	2	1	<1	0
Pyromaia tuberculata	**1**	0	2	<1	<1	<1
Octopus rubescens	**1**	0	0	<1	**2**	<1
Kelletia kelletii	0	0	<1	<1	**1**	<1
Lovenia cordiformis	0	0	3	<1	<1	<1
Pisaster brevispinus	0	**1**	2	**<1**	0	0
Crossata ventricosa	0	**1**	0	<1	<1	**1**
Crangon nigromaculata	0	0	<1	<1	<1	**<1**
Philine auriformis	0	0	0	2	<1	<1
Latulambrus occidentalis	0	0	0	2	<1	<1
Acanthodoris brunnea	0	0	0	<1	1	0
Luidia armata	0	0	<1	<1	0	0
Platymera gaudichaudii	0	0	0	<1	<1	<1
Metacarcinus gracilis	0	0	0	<1	<1	0

[a] SIMPER analysis only conducted on cluster groups that contain more than one haul. For these groups, shading indicates five most abundant species.

Appendix H

Contaminants in Marine Fishes

2024 – 2025
Raw Data Tables & Supplemental Analyses

Appendix H.1

Lengths and weights of fishes used for each composite (Comp) tissue sample from PLOO trawl and rig fishing zones during 2025. Data are summarized as number of individuals (n), minimum, maximum, and mean values.

				Length (cm)			Weight (g)		
Zone	**Comp**	**Species**	**n**	**Min**	**Max**	**Mean**	**Min**	**Max**	**Mean**
RF1	1	Vermilion Rockfish	3	22	31	26	262	945	538
RF1	2	Vermilion Rockfish	3	22	26	24	213	370	287
RF1	3	Copper Rockfish	3	32	33	33	972	1135	1028
RF2	1	Speckled Rockfish	3	26	31	28	346	694	494
RF2	2	Mixed Rockfish[a]	3	22	33	26	211	835	433
RF2	3	Mixed Rockfish[b]	3	22	35	27	264	1009	513
TZ1	1	Pacific Sanddab	8	16	23	20	75	194	135
TZ1	2	Pacific Sanddab	8	18	21	19	89	159	108
TZ1	3	Pacific Sanddab	6	16	22	20	56	203	132
TZ2	1	Pacific Sanddab	4	20	23	22	134	208	169
TZ2	2	Pacific Sanddab	5	18	23	21	100	197	154
TZ2	3	Pacific Sanddab	4	23	24	23	174	200	191
TZ3	1	Pacific Sanddab	6	12	21	18	76	166	125
TZ3	2	Pacific Sanddab	6	17	22	19	72	198	116
TZ3	3	Pacific Sanddab	7	17	22	19	92	183	131
TZ4	1	Pacific Sanddab	8	16	21	18	59	130	85
TZ4	2	Pacific Sanddab	7	16	21	18	66	189	97
TZ4	3	Pacific Sanddab	6	15	24	20	54	204	129

[a] Includes Starry and Flag Rockfish; [b] includes Squarespot and Vermilion Rockfish

Appendix H.2

Lengths and weights of fishes used for each composite (Comp) tissue sample from SBOO trawl and rig fishing zones during 2025. Data are summarized as number of individuals (n), minimum, maximum, and mean values.

				Length (cm)			Weight (g)		
Zone	**Comp**	**Species**	**n**	**Min**	**Max**	**Mean**	**Min**	**Max**	**Mean**
RF3	1	Vermilion Rockfish	3	23	29	25	354	670	459
RF3	2	Brown Rockfish	3	24	31	27	330	805	533
RF3	3	Brown Rockfish	3	27	29	28	483	717	587
RF4	1	Honeycomb Rockfish	3	18	22	20	164	281	239
RF4	2	California Scorpionfish	3	22	26	24	342	587	465
RF4	3	Treefish	3	23	26	25	337	667	504
TZ5	1	Hornyhead Turbot	6	16	21	19	120	253	190
TZ5	2	Hornyhead Turbot	7	14	22	19	79	299	198
TZ5	3	Hornyhead Turbot	10	14	21	18	76	221	150
TZ6	1	Longfin Sanddab	11	13	19	15	48	131	64
TZ6	2	Hornyhead Turbot	6	17	21	19	112	276	194
TZ6	3	Longfin Sanddab	17	13	14	13	34	55	45
TZ7	1	Hornyhead Turbot	5	20	22	20	187	291	214
TZ7	2	Hornyhead Turbot	11	13	20	16	52	254	117
TZ7	3	Hornyhead Turbot	5	18	23	21	139	277	218
TZ8	1	Hornyhead Turbot	11	16	23	19	87	333	182
TZ8	2	Hornyhead Turbot	5	17	24	20	127	399	232
TZ8	3	Longfin Sanddab	8	13	16	14	42	83	59
TZ9	1	Hornyhead Turbot	11	16	21	19	99	209	167
TZ9	2	Spotted Turbot	15	15	23	17	74	214	119
TZ9	3	Bigmouth Sole	5	20	26	23	115	323	201

Appendix H.3

Constituents and method detection limits (MDL) used for the analysis of liver and muscle tissues of fishes collected during 2024-2025.

	MDL			MDL	
Parameter	**Liver**	**Muscle**	**Parameter**	**Liver**	**Muscle**
Metals (ppm)					
Aluminum (Al)	0.208-2.12	0.183-0.212	Lead (Pb)	0.077-0.792	0.067-0.078
Antimony (Sb)	0.282-2.9	0.246-0.284	Manganese (Mn)	0.014-0.14	0.012-0.014
Arsenic (As)	0.147-1.51	0.127-0.146	Mercury (Hg)	0.007-0.019	0.001-0.002
Barium (Ba)	0.003-0.029	0-0.003	Nickel (Ni)	0.044-0.452	0.039-0.045
Beryllium (Be)	0.004-0.042	0.004-0.004	Selenium (Se)	0.346-3.55	0.302-0.4
Cadmium (Cd)	0.013-0.13	0.011-0.013	Silver (Ag)	0.024-0.243	0.021-0.024
Chromium (Cr)	0.013-0.129	0.011-0.013	Tin (Sn)	0.078-0.804	0.068-0.079
Copper (Cu)	0.037-0.382	0.032-0.037	Zinc (Zn)	0.033-0.338	0.03-0.034
Iron (Fe)	0.489-5.01	0.425-0.491			
Chlorinated Pesticides (ppb)					
Hexachlorocyclohexane (HCH)					
HCH, Alpha isomer	1.96-6.38	0.23-0.637	HCH, Delta isomer	2.43-6.12	0.285-0.624
HCH, Beta isomer	2.15-5.96	0.252-0.607	HCH, Gamma isomer	1.76-6.28	0.206-0.64
Total Chlordane					
Alpha (cis) chlordane [A(c)C]	5.54-7.48	0.648-0.747	Heptachlor epoxide [HeptEpox]	4.62-6.44	0.552-0.643
Cis nonachlor [cNon]	5.32-7.5	0.623-0.764	Methoxychlor [Methoxy]	8.75-11.8	1.02-1.18
Gamma (trans) chlordane [G(t)C]	4.66-6.42	0.545-0.654	Oxychlordane [Oxychlor]	2.68-6.36	0.314-0.648
Heptachlor [Hept]	1.83-6.96	0.214-0.695	Trans nonachlor [tNon]	3.88-7.64	0.455-0.767
Total Dichlorodiphenyltrichloroethane (DDT)					
o,p-DDD	2.56-7.35	0.3-0.749	p,p-DDD	3.09-9.01	0.362-0.919
o,p-DDE	2.91-7.54	0.34-0.769	p,p-DDE	2.39-7.05	0.279-0.704
o,p-DDT	2.85-7.59	0.333-0.774	p,p-DDT	7.23-10.5	0.847-1.07
p,-p-DDMU	3.4-6.84	0.397-0.697			
Miscellaneous Pesticides					
Aldrin	2.24-6.58	0.262-0.671	Endrin	6.45-8.72	0.755-0.875
AlphaEndosulfan	2.71-7.17	0.317-0.72	Endrin aldehyde [EndAld]	3.42-9.62	0.401-0.981
BetaEndosulfan	2.75-7.35	0.322-0.749	Hexachlorobenzene (HCB)	4.86-6.69	0.579-0.668
Dieldrin	3.17-7.17	0.371-0.731	Mirex	3.32-6.95	0.389-0.708
EndosulfanSulfate	4.72-9.89	0.553-0.988			

Appendix H.3 *continued*

Parameter	MDL		Parameter	MDL	
	Liver	Muscle		Liver	Muscle
Polychlorinated Biphenyls Congeners (PCBs) (ppb)					
PCB 8	1.85-6.43	0.216-0.655	PCB 126	2.82-7.84	0.331-0.787
PCB 18	2.23-6.53	0.261-0.666	PCB 128	3.62-7.23	0.423-0.726
PCB 28	1.78-6.72	0.208-0.685	PCB 138	2.11-6.45	0.247-0.647
PCB 37	2.34-7.14	0.274-0.728	PCB 149	3.93-7	0.46-0.713
PCB 44	2.22-6.43	0.259-0.655	PCB 151	3.42-6.67	0.4-0.669
PCB 49	2.16-6.16	0.253-0.628	PCB 153/168	4.54-14	0.531-1.41
PCB 52	2.25-6.22	0.264-0.634	PCB 156	3.78-8.24	0.442-0.827
PCB 66	2.46-6.54	0.288-0.667	PCB 157	4.58-8.12	0.536-0.828
PCB 70	2.32-6.43	0.272-0.655	PCB 158	2.06-6.83	0.241-0.685
PCB 74	2.54-6.66	0.297-0.679	PCB 167	3.01-7.65	0.352-0.768
PCB 77	2.66-7.66	0.311-0.769	PCB 169	4.11-7.29	0.481-0.743
PCB 81	2.66-6.58	0.311-0.66	PCB 170	5.09-7.62	0.596-0.777
PCB 87	2.4-6.77	0.281-0.69	PCB 177	2-7.05	0.234-0.719
PCB 99	3.35-6.18	0.392-0.63	PCB 180	3.5-6.69	0.409-0.682
PCB 101	3.4-6.32	0.397-0.644	PCB 183	3.55-7.07	0.416-0.721
PCB 105	2.51-7.41	0.293-0.755	PCB 187	3.94-6.93	0.461-0.706
PCB 110	2.15-6.51	0.252-0.663	PCB 189	3.11-5.03	0.363-0.512
PCB 114	2.03-6.85	0.238-0.698	PCB 194	2.82-6.48	0.33-0.66
PCB 118	2.36-6.6	0.276-0.673	PCB 195	3.78-5.99	0.442-0.61
PCB 119	2.65-6.64	0.311-0.677	PCB 201	4.12-6.67	0.482-0.68
PCB 123	2.1-6.67	0.245-0.68	PCB 206	3.45-9.2	0.404-0.938
Polycyclic Aromatic Hydrocarbons (PAHs) (ppb)					
1-methylnaphthalene	67.8-165	66.7-165	Benzo[G,H,I]perylene	105-161	104-161
1-methylphenanthrene	52.4-213	51.6-213	Benzo[K]fluoranthene	78.3-172	77.1-172
2-methylnaphthalene	50-202	49.2-202	Biphenyl	75.5-255	74.4-255
2,3,5-trimethylnaphthalene	54.3-190	53.5-190	Chrysene	85.3-167	84-167
2,6-dimethylnaphthalene	56.3-194	55.4-194	Dibenzo(A,H)anthracene	94.6-156	93.1-156
3,4-benzo(B)fluoranthene	59.1-172	58.2-172	Fluoranthene	69-163	67.9-163
Acenaphthene	60-195	59.1-195	Fluorene	55.4-182	54.6-182
Acenaphthylene	52.1-216	51.3-216	Indeno(1,2,3-CD)pyrene	66.7-156	65.7-156
Anthracene	67.2-168	66.2-168	Naphthalene	49.5-210	48.8-210
Benzo[A]anthracene	64-176	63.1-176	Perylene	85.6-144	102-143
Benzo[A]pyrene	59.8-166	58.9-166	Phenanthrene	64.8-185	63.8-185
Benzo[e]pyrene	64.8-157	63.8-157	Pyrene	73.3-160	72.2-160
Polybrominated Diphenyl Ethers (PBDEs)					
BDE-17	1.24-7.7	0.148-0.768	BDE-100	1.04-8.31	0.124-0.829
BDE-28	1.29-7.32	0.154-0.731	BDE-138	1.15-6.53	0.138-0.652
BDE-47	1.1-10.4	0.982-1.04	BDE-153	1.01-7.47	0.121-0.746
BDE-49	0.828-7.86	0.099-0.784	BDE-154	1.09-7.03	0.13-0.702
BDE-66	0.602-8.22	0.072-0.82	BDE-183	1.3-8.36	0.155-0.834
BDE-85	1.21-9.71	0.145-0.969	BDE-190	1.66-9.86	0.199-0.984
BDE-99	1.05-9.66	0.836-0.964			

Appendix H.4

Concentrations of metals (ppm) detected in liver tissues of fishes collected from PLOO and SBOO trawl zones during 2025. See Appendix H.3 for MDLs and abbreviations; DNQ = detected but not quantified; ND = not detected; NR = not reportable.

	Zone	Comp	Species	Al	Sb	As	Ba	Be	Cd	Cr	Cu	Fe
PLOO	TZ1	1	Pacific Sanddab	ND	ND	3.68	0.015 DNQ	ND	5.91	0.067 DNQ	2.11	95.1
		2	Pacific Sanddab	ND	ND	4.22	0.038 DNQ	ND	3.95	0.083 DNQ	2.69	117
		3	Pacific Sanddab	0.5 DNQ	ND	3.87	0.015 DNQ	ND	4.15	0.048 DNQ	2.3	78.4
	TZ2	1	Pacific Sanddab	ND	ND	2.85	0.011 DNQ	ND	4.71	0.032 DNQ	2.6	79.7
		2	Pacific Sanddab	ND	ND	5.21	0.015 DNQ	ND	5.31	0.05 DNQ	3.13	86.7
		3	Pacific Sanddab	ND	ND	3.6	0.012 DNQ	ND	6.04	0.043 DNQ	4.1	75
	TZ3	1	Pacific Sanddab	ND	ND	3.82	0.013 DNQ	ND	4.61	0.046 DNQ	2.58	92.1
		2	Pacific Sanddab	ND	ND	4.03	0.013 DNQ	ND	5.08	0.038 DNQ	3.05	115
		3	Pacific Sanddab	ND	ND	3.48	0.021 DNQ	ND	5.89	0.037 DNQ	2.65	111
	TZ4	1	Pacific Sanddab	ND	ND	4.08	0.037 DNQ	ND	6.55	0.575	4.12	177
		2	Pacific Sanddab	ND	ND	4.1	0.02 DNQ	ND	7.08	ND	3.69	180
		3	Pacific Sanddab	ND	ND	4.36	0.015 DNQ	ND	6.62	0.089 DNQ	4.39	127
SBOO	TZ5	1	Hornyhead Turbot	0.405 DNQ	ND	4.09	0.012 DNQ	ND	3.97	0.065 DNQ	9.15	31.8
		2	Hornyhead Turbot	0.29 DNQ	ND	3.08	0.008 DNQ	ND	6.23	0.055 DNQ	9.47	33.5
		3	Hornyhead Turbot	0.455 DNQ	ND	3.88	0.021 DNQ	ND	5.09	0.075 DNQ	5.11	61.9
	TZ6	1	Longfin Sanddab	0.562 DNQ	ND	6.85	0.018 DNQ	ND	2	0.054 DNQ	5.15	92.9
		2	Hornyhead Turbot	0.58 DNQ	ND	3.32	0.006 DNQ	ND	4.82	0.064 DNQ	8.04	59.4
		3	Longfin Sanddab	ND	ND	5.66	ND	ND	1.6	0.043 DNQ	3.69	105
	TZ7	1	Hornyhead Turbot	ND	ND	3.75	0.006 DNQ	ND	3.73	0.066 DNQ	8.67	38.5
		2	Hornyhead Turbot	0.29 DNQ	ND	3.31	0.006 DNQ	ND	3.26	0.065 DNQ	8.3	43.6
		3	Hornyhead Turbot	1.116 DNQ	ND	2.92	0.007 DNQ	ND	3.47	0.067 DNQ	8.95	37.4
	TZ8	1	Hornyhead Turbot	0.732 DNQ	ND	3.22	0.009 DNQ	ND	10.6	0.08 DNQ	5.79	35.9
		2	Hornyhead Turbot	0.517 DNQ	ND	4.92	0.007 DNQ	ND	9.34	0.064 DNQ	7.01	26.8
		3	Longfin Sanddab	ND	ND	5.14	0.007 DNQ	ND	1.24	0.059 DNQ	4.17	54
	TZ9	1	Hornyhead Turbot	0.313 DNQ	ND	6.31	0.005 DNQ	ND	5.96	0.064 DNQ	7.79	87.2
		2	Spotted Turbot	0.33 DNQ	ND	10.2	0.009 DNQ	ND	0.675	0.085 DNQ	17.4	128
		3	Bigmouth Sole	ND	ND	9.24	0.042 DNQ	ND	0.862	0.099 DNQ	1.88	64.1

Appendix H.4 *continued*

	Zone	Comp	Species	Pb	Mn	Hg	Ni	Se	Ag	Sn	Zn
PLOO	TZ1	1	Pacific Sanddab	ND	0.828	0.103	ND	2.29	ND	0.384 DNQ	29.1
		2	Pacific Sanddab	ND	0.841	0.09	ND	2.206 DNQ	ND	0.42 DNQ	28
		3	Pacific Sanddab	ND	1.12	0.084	ND	2.16	ND	0.267 DNQ	28.5
	TZ2	1	Pacific Sanddab	ND	1.34	0.1	ND	1.587 DNQ	ND	ND	25.4
		2	Pacific Sanddab	ND	1.23	0.126	ND	2.39	ND	0.369 DNQ	26.6
		3	Pacific Sanddab	ND	1.24	0.126	ND	2.24	ND	0.343 DNQ	30.3
	TZ3	1	Pacific Sanddab	ND	0.87	0.092	ND	2.57	ND	0.398 DNQ	23.5
		2	Pacific Sanddab	ND	0.972	0.104	ND	2.43	ND	0.339 DNQ	28.9
		3	Pacific Sanddab	ND	0.947	0.129	ND	2.38	ND	0.361 DNQ	27.2
	TZ4	1	Pacific Sanddab	ND	0.854	0.08	ND	2.82	ND	0.372 DNQ	36.6
		2	Pacific Sanddab	ND	1.01	0.112	ND	3.04	ND	0.69	30.3
		3	Pacific Sanddab	ND	1.2	0.104	ND	2.69	0.074 DNQ	0.438 DNQ	33.3
SBOO	TZ5	1	Hornyhead Turbot	ND	0.98	0.11	ND	1.94	0.075 DNQ	0.194 DNQ	67.8
		2	Hornyhead Turbot	ND	0.979	0.239	ND	1.74	0.153	0.284 DNQ	67.6
		3	Hornyhead Turbot	ND	0.816	0.109	ND	2.06	0.064 DNQ	0.159 DNQ	57.2
	TZ6	1	Longfin Sanddab	ND	0.887	0.052	2.56	3.1	0.097 DNQ	0.492 DNQ	21.1
		2	Hornyhead Turbot	0.086 DNQ	1.04	0.125	ND	1.97	0.076 DNQ	0.205 DNQ	63.8
		3	Longfin Sanddab	0.247 DNQ	0.912	0.046	ND	3.37	0.091 DNQ	0.467 DNQ	20.3
	TZ7	1	Hornyhead Turbot	ND	1.23	0.139	ND	1.64	0.094 DNQ	0.25 DNQ	58.6
		2	Hornyhead Turbot	ND	1.17	0.117	ND	1.72	0.091 DNQ	0.183 DNQ	50.9
		3	Hornyhead Turbot	0.113 DNQ	1.5	0.143	ND	1.69	0.109 DNQ	0.164 DNQ	59.5
	TZ8	1	Hornyhead Turbot	ND	0.991	0.142	ND	1.68	0.054 DNQ	0.186 DNQ	56
		2	Hornyhead Turbot	ND	1.03	0.144	ND	2.08	0.067 DNQ	0.224 DNQ	45.2
		3	Longfin Sanddab	ND	0.622	0.034 DNQ	ND	2.14	ND	0.353 DNQ	16.6
	TZ9	1	Hornyhead Turbot	ND	0.941	0.129	ND	1.89	0.074 DNQ	0.175 DNQ	58.1
		2	Spotted Turbot	0.148 DNQ	1.42	0.088	ND	1.95	0.103 DNQ	0.238	57.5
		3	Bigmouth Sole	ND	1	0.054	ND	1.77	ND	0.199 DNQ	31.4

Appendix H.5

Concentrations of pesticides (ppb) and lipids (% weight) detected in liver tissues of fishes collected from PLOO and SBOO trawl zones during 2025. See Appendix H.3 for MDLs and abbreviations; DNQ=detected but not quantified; ND=not detected; NR=not reportable.

				Chlordane							
	Zone	Comp	Species	A(c)C	cNon	G(t)C	Hept	HeptEpox	Methoxy	Oxychlor	tNon
PLOO	TZ1	1	Pacific Sanddab	ND	ND	ND	ND	ND	ND	ND	ND
		2	Pacific Sanddab	ND	ND	ND	ND	ND	ND	ND	ND
		3	Pacific Sanddab	ND	ND	ND	ND	ND	ND	ND	ND
	TZ2	1	Pacific Sanddab	ND	ND	ND	ND	ND	ND	ND	ND
		2	Pacific Sanddab	ND	ND	ND	ND	ND	ND	ND	ND
		3	Pacific Sanddab	ND	ND	ND	ND	ND	ND	ND	ND
	TZ3	1	Pacific Sanddab	ND	ND	ND	ND	ND	ND	ND	ND
		2	Pacific Sanddab	ND	ND	ND	ND	ND	ND	ND	ND
		3	Pacific Sanddab	ND	ND	ND	ND	ND	ND	ND	ND
	TZ4	1	Pacific Sanddab	ND	ND	ND	ND	ND	ND	ND	ND
		2	Pacific Sanddab	ND	ND	ND	ND	ND	ND	ND	ND
		3	Pacific Sanddab	ND	ND	ND	ND	ND	ND	ND	ND
SBOO	TZ5	1	Hornyhead Turbot	ND	ND	ND	ND	ND	ND	ND	ND
		2	Hornyhead Turbot	ND	ND	ND	ND	ND	ND	ND	ND
		3	Hornyhead Turbot	ND	ND	ND	ND	ND	ND	ND	ND
	TZ6	1	Longfin Sanddab	ND	ND	ND	ND	ND	ND	ND	ND
		2	Hornyhead Turbot	ND	ND	ND	ND	ND	ND	ND	ND
		3	Longfin Sanddab	32.9	ND	20.4	2.27 DNQ	18.5	ND	ND	ND
	TZ7	1	Hornyhead Turbot	ND	ND	ND	ND	ND	ND	ND	ND
		2	Hornyhead Turbot	ND	ND	ND	ND	ND	ND	ND	ND
		3	Hornyhead Turbot	ND	ND	ND	ND	ND	ND	ND	ND
	TZ8	1	Hornyhead Turbot	ND	ND	ND	ND	ND	ND	ND	ND
		2	Hornyhead Turbot	ND	ND	ND	ND	ND	ND	ND	ND
		3	Longfin Sanddab	ND	ND	ND	ND	ND	ND	ND	ND
	TZ9	1	Hornyhead Turbot	ND	ND	ND	ND	ND	ND	ND	ND
		2	Spotted Turbot	ND	ND	ND	ND	ND	ND	ND	ND
		3	Bigmouth Sole	ND	ND	ND	ND	ND	25	ND	ND

Appendix H.5 *continued*

	Zone	Comp	Species	DDT							Endosulfan		
				o,p-DDD	o,p-DDE	o,p-DDT	p,-p-DDMU	p,p-DDD	p,p-DDE	p,p-DDT	Alpha	Beta	Sulfate
PLOO	TZ1	1	Pacific Sanddab	ND	ND	ND	5.22	ND	72.7	ND	ND	ND	ND
		2	Pacific Sanddab	ND	ND	ND	7.46	ND	89.4	ND	ND	ND	ND
		3	Pacific Sanddab	ND	ND	ND	7.06	ND	93.8	ND	ND	ND	ND
	TZ2	1	Pacific Sanddab	ND	ND	ND	6.92	ND	121	ND	ND	ND	ND
		2	Pacific Sanddab	ND	ND	ND	5.84	ND	65.9	ND	ND	ND	ND
		3	Pacific Sanddab	ND	ND	ND	6.8	ND	78	ND	ND	ND	ND
	TZ3	1	Pacific Sanddab	ND	ND	ND	5.21	ND	82.5	ND	ND	ND	ND
		2	Pacific Sanddab	ND	ND	ND	8.03	ND	100	ND	ND	ND	ND
		3	Pacific Sanddab	ND	ND	ND	6.59	ND	93.5	ND	ND	ND	ND
	TZ4	1	Pacific Sanddab	ND	ND	ND	12.5	ND	145	ND	ND	ND	ND
		2	Pacific Sanddab	ND	ND	ND	8.3	ND	107	ND	ND	ND	ND
		3	Pacific Sanddab	ND	ND	ND	6.1	ND	101	ND	ND	ND	ND
SBOO	TZ5	1	Hornyhead Turbot	ND	ND	ND	ND	ND	26.9	ND	ND	ND	ND
		2	Hornyhead Turbot	ND	ND	ND	ND	ND	38.2	ND	ND	ND	ND
		3	Hornyhead Turbot	ND	ND	ND	ND	ND	38.1	ND	ND	ND	ND
	TZ6	1	Longfin Sanddab	ND	ND	ND	4.5	ND	102	ND	ND	ND	ND
		2	Hornyhead Turbot	ND	ND	ND	ND	ND	33.4	ND	ND	ND	ND
		3	Longfin Sanddab	ND	ND	ND	4.17	9.03	118	ND	25.4	3.83	ND
	TZ7	1	Hornyhead Turbot	ND	ND	ND	ND	ND	12.1	ND	ND	ND	ND
		2	Hornyhead Turbot	ND	ND	ND	ND	ND	14.9	ND	ND	ND	ND
		3	Hornyhead Turbot	ND	ND	ND	ND	ND	7.03	ND	ND	ND	ND
	TZ8	1	Hornyhead Turbot	ND	ND	ND	ND	ND	14.4	ND	ND	ND	ND
		2	Hornyhead Turbot	ND	ND	ND	ND	ND	9.44	ND	ND	ND	ND
		3	Longfin Sanddab	ND	ND	ND	ND	ND	74.9	ND	ND	ND	ND
	TZ9	1	Hornyhead Turbot	ND	ND	ND	ND	ND	9.48	ND	ND	ND	ND
		2	Spotted Turbot	ND	ND	ND	ND	ND	4.37	ND	ND	ND	ND
		3	Bigmouth Sole	ND	ND	ND	ND	8.1	8.18	ND	ND	3.04	14.9

Appendix H.5 *continued*

	Zone	Comp	Species	HCH				Aldrin	Dieldrin	Endrin	EndAld	HCB	Mirex	Lipids
				Alpha	Beta	Delta	Gamma							
PLOO	TZ1	1	Pacific Sanddab	ND	ND	ND	ND	ND	ND	ND	ND	ND	ND	17.4
		2	Pacific Sanddab	ND	ND	ND	ND	ND	ND	ND	ND	ND	ND	28.1
		3	Pacific Sanddab	ND	ND	ND	ND	ND	ND	ND	ND	ND	ND	19
	TZ2	1	Pacific Sanddab	ND	ND	ND	ND	ND	ND	ND	ND	ND	ND	15
		2	Pacific Sanddab	ND	ND	ND	ND	ND	ND	ND	ND	ND	ND	15.8
		3	Pacific Sanddab	ND	ND	ND	ND	ND	ND	ND	ND	ND	ND	17.3
	TZ3	1	Pacific Sanddab	ND	ND	ND	ND	ND	ND	ND	ND	ND	ND	26.5
		2	Pacific Sanddab	ND	ND	ND	ND	ND	ND	ND	ND	ND	ND	25.9
		3	Pacific Sanddab	ND	ND	ND	ND	ND	ND	ND	ND	ND	ND	20.7
	TZ4	1	Pacific Sanddab	ND	ND	ND	ND	ND	ND	ND	ND	ND	ND	29.7
		2	Pacific Sanddab	ND	ND	ND	ND	ND	ND	ND	ND	ND	ND	24.9
		3	Pacific Sanddab	ND	ND	ND	ND	ND	ND	ND	ND	ND	ND	24.7
SBOO	TZ5	1	Hornyhead Turbot	ND	ND	ND	ND	ND	ND	ND	ND	ND	ND	5.1
		2	Hornyhead Turbot	ND	ND	ND	ND	ND	ND	ND	ND	ND	ND	7.54
		3	Hornyhead Turbot	ND	ND	ND	ND	ND	ND	ND	ND	ND	ND	4.9
	TZ6	1	Longfin Sanddab	ND	ND	ND	ND	ND	ND	ND	ND	ND	ND	24.7
		2	Hornyhead Turbot	ND	ND	ND	ND	ND	ND	ND	ND	ND	ND	3.96
		3	Longfin Sanddab	11.9	43	39.6	6.76	ND	33.5	6.79	ND	ND	ND	19.2
	TZ7	1	Hornyhead Turbot	ND	ND	ND	ND	ND	ND	ND	ND	ND	ND	4.44
		2	Hornyhead Turbot	ND	ND	ND	ND	ND	ND	ND	ND	ND	ND	4.16
		3	Hornyhead Turbot	ND	ND	ND	ND	ND	ND	ND	ND	ND	ND	5.27
	TZ8	1	Hornyhead Turbot	ND	ND	ND	ND	ND	ND	ND	ND	ND	ND	5.75
		2	Hornyhead Turbot	ND	ND	ND	ND	ND	ND	ND	ND	ND	ND	4
		3	Longfin Sanddab	ND	ND	ND	ND	ND	ND	ND	ND	ND	ND	23.5
	TZ9	1	Hornyhead Turbot	ND	ND	ND	ND	ND	ND	ND	ND	ND	ND	3.6
		2	Spotted Turbot	ND	ND	ND	ND	ND	ND	ND	ND	ND	ND	3.29
		3	Bigmouth Sole	2.59	4.69	ND	ND	ND	6.71	ND	6.93	ND	ND	2.84

Appendix H.6

Concentrations of PCBs (ppb) detected in liver tissues of fishes collected from PLOO and SBOO trawl zones during 2025. See Appendix H.3 for MDLs; DNQ=detected but not quantified; ND = not detected; NR = not reportable.

				PCB Congener									
	Zone	Comp	Species	8	18	28	37	44	49	52	66	70	74
PLOO	TZ1	1	Pacific Sanddab	ND	ND	ND	ND	ND	ND	ND	ND	ND	ND
		2	Pacific Sanddab	ND	ND	ND	ND	ND	ND	ND	ND	ND	ND
		3	Pacific Sanddab	ND	ND	ND	ND	ND	ND	ND	ND	ND	ND
	TZ2	1	Pacific Sanddab	ND	ND	ND	ND	ND	ND	ND	ND	ND	ND
		2	Pacific Sanddab	ND	ND	ND	ND	ND	ND	ND	ND	ND	ND
		3	Pacific Sanddab	ND	ND	ND	ND	ND	ND	ND	ND	ND	ND
	TZ3	1	Pacific Sanddab	ND	ND	ND	ND	ND	3.85	6.34	3.68	5	ND
		2	Pacific Sanddab	ND	ND	ND	ND	ND	3.7	3.21	3.3	3.17	ND
		3	Pacific Sanddab	ND	ND	ND	ND	ND	3.14	3.8	ND	3.38	ND
	TZ4	1	Pacific Sanddab	ND	ND	ND	ND	ND	2.67 DNQ	ND	ND	ND	ND
		2	Pacific Sanddab	ND	ND	ND	ND	ND	3.07 DNQ	4	3.19	4.58	ND
		3	Pacific Sanddab	ND	ND	ND	ND	ND	ND	ND	ND	ND	ND
SBOO	TZ5	1	Hornyhead Turbot	ND	ND	ND	ND	ND	ND	ND	ND	ND	ND
		2	Hornyhead Turbot	ND	ND	ND	ND	ND	ND	ND	ND	ND	ND
		3	Hornyhead Turbot	ND	ND	ND	ND	ND	ND	ND	ND	ND	ND
	TZ6	1	Longfin Sanddab	ND	ND	ND	ND	ND	ND	ND	ND	ND	ND
		2	Hornyhead Turbot	ND	ND	ND	ND	ND	ND	ND	ND	ND	ND
		3	Longfin Sanddab	ND	ND	ND	ND	ND	ND	ND	ND	ND	ND
	TZ7	1	Hornyhead Turbot	ND	ND	ND	ND	ND	ND	ND	ND	ND	ND
		2	Hornyhead Turbot	ND	ND	ND	ND	ND	ND	ND	ND	ND	ND
		3	Hornyhead Turbot	ND	ND	ND	ND	ND	ND	ND	ND	ND	ND
	TZ8	1	Hornyhead Turbot	ND	ND	ND	ND	ND	ND	ND	ND	ND	ND
		2	Hornyhead Turbot	ND	ND	ND	ND	ND	ND	ND	ND	ND	ND
		3	Longfin Sanddab	ND	ND	ND	ND	ND	ND	ND	ND	ND	ND
	TZ9	1	Hornyhead Turbot	ND	ND	ND	ND	ND	ND	ND	ND	ND	ND
		2	Spotted Turbot	ND	ND	ND	ND	ND	ND	ND	ND	ND	ND
		3	Bigmouth Sole	ND	ND	ND	ND	ND	ND	ND	ND	ND	ND

Appendix H.6 *continued*

	Zone	Comp	Species	PCB Congener 77	81	87	99	101	105	110	114	118	119
PLOO	TZ1	1	Pacific Sanddab	ND	ND	ND	9.35	6.07	3.59	5.18	ND	10.9	ND
		2	Pacific Sanddab	ND	ND	ND	10.8	7.51	ND	5.57	ND	10.6	ND
		3	Pacific Sanddab	ND	ND	ND	10.1	6.97	ND	5.79	ND	12	ND
	TZ2	1	Pacific Sanddab	ND	ND	ND	6.56	4.7	ND	ND	ND	7.21	ND
		2	Pacific Sanddab	ND	ND	ND	5.89	ND	ND	ND	ND	5.79	ND
		3	Pacific Sanddab	ND	ND	ND	5.43	ND	ND	2.75 DNQ	ND	5.62	ND
	TZ3	1	Pacific Sanddab	ND	ND	5.83	19.5	14.7	9.22	16.2	ND	27.9	ND
		2	Pacific Sanddab	ND	ND	2.97	17.6	12.6	5.26	8.92	ND	20.7	ND
		3	Pacific Sanddab	ND	ND	3.67	19.6	13.1	5.97	11.4	ND	27	ND
	TZ4	1	Pacific Sanddab	ND	ND	ND	13.9	10.3	ND	8.07	ND	14.9	ND
		2	Pacific Sanddab	ND	ND	4.58	17	15.9	6.34	10.3	ND	21.4	ND
		3	Pacific Sanddab	ND	ND	ND	12.8	7.63	3.4	5.94	ND	13.4	ND
SBOO	TZ5	1	Hornyhead Turbot	ND	ND	ND	ND	ND	ND	ND	ND	ND	ND
		2	Hornyhead Turbot	ND	ND	ND	ND	ND	ND	ND	ND	ND	ND
		3	Hornyhead Turbot	ND	ND	ND	ND	ND	ND	ND	ND	ND	ND
	TZ6	1	Longfin Sanddab	ND	ND	ND	6.41	ND	ND	ND	ND	6.7	ND
		2	Hornyhead Turbot	ND	ND	ND	ND	ND	ND	ND	ND	ND	ND
		3	Longfin Sanddab	ND	ND	ND	6.01	ND	ND	ND	ND	6.6	ND
	TZ7	1	Hornyhead Turbot	ND	ND	ND	ND	ND	ND	ND	ND	ND	ND
		2	Hornyhead Turbot	ND	ND	ND	ND	ND	ND	ND	ND	ND	ND
		3	Hornyhead Turbot	ND	ND	ND	ND	ND	ND	ND	ND	ND	ND
	TZ8	1	Hornyhead Turbot	ND	ND	ND	ND	ND	ND	ND	ND	ND	ND
		2	Hornyhead Turbot	ND	ND	ND	ND	ND	ND	ND	ND	ND	ND
		3	Longfin Sanddab	ND	ND	ND	4.26	ND	ND	ND	ND	5.13	ND
	TZ9	1	Hornyhead Turbot	ND	ND	ND	ND	ND	ND	ND	ND	ND	ND
		2	Spotted Turbot	ND	ND	ND	ND	ND	ND	ND	ND	ND	ND
		3	Bigmouth Sole	ND	ND	ND	ND	ND	ND	ND	ND	ND	ND

Appendix H.6 *continued*

	Zone	Comp	Species	PCB Congener 123	126	128	138	149	151	153/168	156	157	158
PLOO	TZ1	1	Pacific Sanddab	ND	ND	ND	13.2	ND	ND	25.5	ND	ND	ND
		2	Pacific Sanddab	ND	ND	ND	12.7	ND	ND	24.9	ND	ND	ND
		3	Pacific Sanddab	ND	ND	ND	13.1	5.79	ND	26.7	ND	ND	ND
	TZ2	1	Pacific Sanddab	ND	ND	ND	8.67	ND	ND	17	ND	ND	ND
		2	Pacific Sanddab	ND	ND	ND	7.91	ND	ND	15.1	ND	ND	ND
		3	Pacific Sanddab	ND	ND	ND	6.43	ND	ND	13.4	ND	ND	ND
	TZ3	1	Pacific Sanddab	2.52 DNQ	ND	6.72	27.2	5.83	3.73	44.8	ND	ND	2.76
		2	Pacific Sanddab	ND	ND	4.94	24.3	7.57	ND	44	ND	ND	ND
		3	Pacific Sanddab	ND	ND	5.74	30.4	ND	ND	44.1	ND	ND	2.56 DNQ
	TZ4	1	Pacific Sanddab	ND	ND	ND	16.9	ND	4.21	33.6	ND	ND	ND
		2	Pacific Sanddab	ND	ND	5.18	20.9	6.67	ND	36.2	ND	ND	ND
		3	Pacific Sanddab	ND	ND	ND	16.7	ND	ND	34	ND	ND	ND
SBOO	TZ5	1	Hornyhead Turbot	ND	ND	ND	ND	ND	ND	ND	ND	ND	ND
		2	Hornyhead Turbot	ND	ND	ND	2.56 DNQ	ND	ND	2.585 DNQ	ND	ND	ND
		3	Hornyhead Turbot	ND	ND	ND	ND	ND	ND	5.86 DNQ	ND	ND	ND
	TZ6	1	Longfin Sanddab	ND	ND	ND	9.2	ND	ND	17.5	ND	ND	ND
		2	Hornyhead Turbot	ND	ND	ND	ND	ND	ND	ND	ND	ND	ND
		3	Longfin Sanddab	ND	ND	ND	9.51	ND	ND	19.1	ND	ND	ND
	TZ7	1	Hornyhead Turbot	ND	ND	ND	ND	ND	ND	ND	ND	ND	ND
		2	Hornyhead Turbot	ND	ND	ND	ND	ND	ND	ND	ND	ND	ND
		3	Hornyhead Turbot	ND	ND	ND	ND	ND	ND	ND	ND	ND	ND
	TZ8	1	Hornyhead Turbot	ND	ND	ND	ND	ND	ND	ND	ND	ND	ND
		2	Hornyhead Turbot	ND	ND	ND	ND	ND	ND	ND	ND	ND	ND
		3	Longfin Sanddab	ND	ND	ND	7.57	ND	ND	14.4	ND	ND	ND
	TZ9	1	Hornyhead Turbot	ND	ND	ND	ND	ND	ND	ND	ND	ND	ND
		2	Spotted Turbot	ND	ND	ND	ND	ND	ND	ND	ND	ND	ND
		3	Bigmouth Sole	ND	ND	ND	ND	ND	ND	ND	ND	ND	ND

Appendix H.6 *continued*

	Zone	Comp	Species	PCB Congener 167	169	170	177	180	183	187	189	194	195	201	206
PLOO	TZ1	1	Pacific Sanddab	ND	ND	ND	1.24 DNQ	9.04	ND	10.5	ND	ND	ND	ND	ND
		2	Pacific Sanddab	ND	ND	ND	ND	7.43	ND	9.29	ND	ND	ND	ND	ND
		3	Pacific Sanddab	ND	ND	ND	ND	8.71	ND	9.37	ND	ND	ND	ND	ND
	TZ2	1	Pacific Sanddab	ND	ND	ND	ND	5.94	ND	6.94	ND	ND	ND	ND	ND
		2	Pacific Sanddab	ND	ND	ND	ND	6.49	ND	6.78	ND	ND	ND	ND	ND
		3	Pacific Sanddab	ND	ND	ND	ND	ND	ND	5.3	ND	ND	ND	ND	ND
	TZ3	1	Pacific Sanddab	ND	ND	ND	2.71	11	ND	12.1	ND	ND	ND	ND	ND
		2	Pacific Sanddab	ND	ND	ND	3.21	13.5	4.74	15.5	ND	3.85	ND	ND	ND
		3	Pacific Sanddab	ND	ND	ND	ND	11.4	ND	10.5	ND	ND	ND	ND	ND
	TZ4	1	Pacific Sanddab	ND	ND	ND	ND	9.24	ND	10.4	ND	ND	ND	ND	ND
		2	Pacific Sanddab	ND	ND	ND	2.58 DNQ	10.5	ND	11.1	ND	ND	ND	ND	ND
		3	Pacific Sanddab	ND	ND	ND	1.26 DNQ	11.4	ND	13	ND	ND	ND	ND	ND
SBOO	TZ5	1	Hornyhead Turbot	ND	ND	ND	ND	ND	ND	ND	ND	ND	ND	ND	ND
		2	Hornyhead Turbot	ND	ND	ND	ND	ND	ND	ND	ND	ND	ND	ND	ND
		3	Hornyhead Turbot	ND	ND	ND	ND	ND	ND	ND	ND	ND	ND	ND	ND
	TZ6	1	Longfin Sanddab	ND	ND	ND	ND	4.52	ND	7.25	ND	ND	ND	ND	ND
		2	Hornyhead Turbot	ND	ND	ND	ND	ND	ND	ND	ND	ND	ND	ND	ND
		3	Longfin Sanddab	ND	ND	ND	ND	4.1	ND	6.34	ND	ND	ND	ND	ND
	TZ7	1	Hornyhead Turbot	ND	ND	ND	ND	ND	ND	ND	ND	ND	ND	ND	ND
		2	Hornyhead Turbot	ND	ND	ND	ND	ND	ND	ND	ND	ND	ND	ND	ND
		3	Hornyhead Turbot	ND	ND	ND	ND	ND	ND	ND	ND	ND	ND	ND	ND
	TZ8	1	Hornyhead Turbot	ND	ND	ND	ND	ND	ND	ND	ND	ND	ND	ND	ND
		2	Hornyhead Turbot	ND	ND	ND	ND	ND	ND	ND	ND	ND	ND	ND	ND
		3	Longfin Sanddab	ND	ND	ND	ND	ND	ND	6.41	ND	ND	ND	ND	ND
	TZ9	1	Hornyhead Turbot	ND	ND	ND	ND	ND	ND	ND	ND	ND	ND	ND	ND
		2	Spotted Turbot	ND	ND	ND	ND	ND	ND	ND	ND	ND	ND	ND	ND
		3	Bigmouth Sole	ND	ND	ND	ND	ND	ND	ND	ND	ND	ND	ND	ND

Appendix H.7

Concentrations of PAHs (ppb) detected in liver tissues of fishes collected from PLOO and SBOO trawl zones during 2025. See Appendix H.3 for MDLs; DNQ=detected but not quantified; ND = not detected; NR = not reportable.

	Zone	Comp	Species	1-methyl naphthalene	1-methyl phenanthrene	2-methyl naphthalene	2,3,5-trimethyl naphthalene	2,6-dimethyl naphthalene	3,4-benzo(B) fluoranthene	Acenaphthene	Acenaphthylene	Anthracene	Benzo[A] anthracene	Benzo[A] pyrene
PLOO	TZ1	1	Pacific Sanddab	ND	ND	ND	ND	ND	ND	ND	ND	ND	ND	ND
		2	Pacific Sanddab	ND	ND	ND	ND	ND	ND	ND	ND	ND	ND	ND
		3	Pacific Sanddab	ND	ND	ND	ND	ND	ND	ND	ND	ND	ND	ND
	TZ2	1	Pacific Sanddab	ND	ND	ND	ND	ND	ND	ND	ND	ND	ND	ND
		2	Pacific Sanddab	ND	ND	ND	ND	ND	ND	ND	ND	ND	ND	ND
		3	Pacific Sanddab	ND	ND	ND	ND	ND	ND	ND	ND	ND	ND	ND
	TZ3	1	Pacific Sanddab	ND	ND	ND	ND	ND	ND	ND	ND	ND	ND	ND
		2	Pacific Sanddab	ND	ND	ND	ND	ND	ND	ND	ND	ND	ND	ND
		3	Pacific Sanddab	ND	ND	ND	ND	ND	ND	ND	ND	ND	ND	ND
	TZ4	1	Pacific Sanddab	ND	ND	ND	ND	ND	ND	ND	ND	ND	ND	ND
		2	Pacific Sanddab	ND	ND	ND	ND	ND	ND	ND	ND	ND	ND	ND
		3	Pacific Sanddab	ND	ND	ND	ND	ND	ND	ND	ND	ND	ND	ND
SBOO	TZ5	1	Hornyhead Turbot	ND	ND	ND	ND	ND	ND	ND	ND	ND	ND	ND
		2	Hornyhead Turbot	ND	ND	ND	ND	ND	ND	ND	ND	ND	ND	ND
		3	Hornyhead Turbot	ND	ND	ND	ND	ND	ND	ND	ND	ND	ND	ND
	TZ6	1	Longfin Sanddab	ND	ND	ND	ND	ND	ND	ND	ND	ND	ND	ND
		2	Hornyhead Turbot	ND	ND	ND	ND	ND	ND	ND	ND	ND	ND	ND
		3	Longfin Sanddab	ND	ND	ND	ND	ND	ND	ND	ND	ND	ND	ND
	TZ7	1	Hornyhead Turbot	ND	ND	ND	ND	ND	ND	ND	ND	ND	ND	ND
		2	Hornyhead Turbot	ND	ND	ND	ND	ND	ND	ND	ND	ND	ND	ND
		3	Hornyhead Turbot	ND	ND	ND	ND	ND	ND	ND	ND	ND	ND	ND
	TZ8	1	Hornyhead Turbot	ND	ND	ND	ND	ND	ND	ND	ND	ND	ND	ND
		2	Hornyhead Turbot	ND	ND	ND	ND	ND	ND	ND	ND	ND	ND	ND
		3	Longfin Sanddab	ND	ND	ND	ND	ND	ND	ND	ND	ND	ND	ND
	TZ9	1	Hornyhead Turbot	ND	ND	ND	ND	ND	ND	ND	ND	ND	ND	ND
		2	Spotted Turbot	ND	ND	ND	ND	ND	ND	ND	ND	ND	ND	ND
		3	No Sample	—	—	—	—	—	—	—	—	—	—	—

Appendix H.7 *continued*

	Zone	Comp	Species	Benzo[e] pyrene	Benzo[G,H,I] perylene	Benzo[K] fluoranthene	Biphenyl	Chrysene	Dibenzo(A,H) anthracene	Fluoranthene	Fluorene	Indeno(1,2,3-CD)pyrene	Naphthalene	Perylene	Phenanthrene	Pyrene
PLOO	TZ1	1	Pacific Sanddab	ND	ND	ND	ND	ND	ND	ND	ND	ND	ND	ND	ND	ND
		2	Pacific Sanddab	ND	ND	ND	ND	ND	ND	ND	ND	ND	ND	ND	ND	ND
		3	Pacific Sanddab	ND	ND	ND	ND	ND	ND	ND	ND	ND	ND	ND	ND	ND
	TZ2	1	Pacific Sanddab	ND	ND	ND	ND	ND	ND	ND	ND	ND	ND	ND	ND	ND
		2	Pacific Sanddab	ND	ND	ND	ND	ND	ND	ND	ND	ND	ND	ND	ND	ND
		3	Pacific Sanddab	ND	ND	ND	ND	ND	ND	ND	ND	ND	ND	ND	ND	ND
	TZ3	1	Pacific Sanddab	ND	ND	ND	ND	ND	ND	ND	ND	ND	ND	ND	ND	ND
		2	Pacific Sanddab	ND	ND	ND	ND	ND	ND	ND	ND	ND	ND	ND	ND	ND
		3	Pacific Sanddab	ND	ND	ND	ND	ND	ND	ND	ND	ND	ND	ND	ND	ND
	TZ4	1	Pacific Sanddab	ND	ND	ND	ND	ND	ND	ND	ND	ND	ND	ND	ND	ND
		2	Pacific Sanddab	ND	ND	ND	ND	ND	ND	ND	ND	ND	ND	ND	ND	ND
		3	Pacific Sanddab	ND	ND	ND	ND	ND	ND	ND	ND	ND	ND	ND	ND	ND
SBOO	TZ5	1	Hornyhead Turbot	ND	ND	ND	ND	ND	ND	ND	ND	ND	ND	ND	ND	ND
		2	Hornyhead Turbot	ND	ND	ND	ND	ND	ND	ND	ND	ND	ND	ND	ND	ND
		3	Hornyhead Turbot	ND	ND	ND	ND	ND	ND	ND	ND	ND	ND	ND	ND	ND
	TZ6	1	Longfin Sanddab	ND	ND	ND	ND	ND	ND	ND	ND	ND	ND	ND	ND	ND
		2	Hornyhead Turbot	ND	ND	ND	ND	ND	ND	ND	ND	ND	ND	ND	ND	ND
		3	Longfin Sanddab	ND	ND	ND	ND	ND	ND	ND	ND	ND	ND	ND	ND	ND
	TZ7	1	Hornyhead Turbot	ND	ND	ND	ND	ND	ND	ND	ND	ND	ND	ND	ND	ND
		2	Hornyhead Turbot	ND	ND	ND	ND	ND	ND	ND	ND	ND	ND	ND	ND	ND
		3	Hornyhead Turbot	ND	ND	ND	ND	ND	ND	ND	ND	ND	ND	ND	ND	ND
	TZ8	1	Hornyhead Turbot	ND	ND	ND	ND	ND	ND	ND	ND	ND	ND	ND	ND	ND
		2	Hornyhead Turbot	ND	ND	ND	ND	ND	ND	ND	ND	ND	ND	ND	ND	ND
		3	Longfin Sanddab	ND	ND	ND	ND	ND	ND	ND	ND	ND	ND	ND	ND	ND
	TZ9	1	Hornyhead Turbot	ND	ND	ND	ND	ND	ND	ND	ND	ND	ND	ND	ND	ND
		2	Spotted Turbot	ND	NR	ND	ND	ND	ND	ND	ND	ND	ND	ND	ND	ND
		3	No Sample	—	—	—	—	—	—	—	—	—	—	—	—	—

Appendix H.8

Concentrations of PBDEs (ppb) detected in liver tissues of fishes collected from PLOO and SBOO trawl zones during 2025. See Appendix H.3 for MDLs; DNQ=detected but not quantified; ND = not detected; NR = not reportable.

				PBDE											
	Zone	Comp	Species	17	28	47	49	66	85	99	100	138	153	154	183	190
PLOO	TZ1	1	Pacific Sanddab	ND	ND	18.3	ND	ND	ND	ND	ND	ND	ND	ND	ND	ND
		2	Pacific Sanddab	ND	ND	13.3	ND	ND	ND	ND	ND	ND	ND	ND	ND	ND
		3	Pacific Sanddab	ND	ND	17.1	ND	ND	ND	ND	ND	ND	ND	ND	ND	ND
	TZ2	1	Pacific Sanddab	ND	ND	16.1	ND	ND	ND	ND	ND	ND	ND	ND	ND	ND
		2	Pacific Sanddab	ND	ND	13.3	ND	ND	ND	ND	ND	ND	ND	ND	ND	ND
		3	Pacific Sanddab	ND	ND	18.4	ND	ND	ND	ND	ND	ND	ND	ND	ND	ND
	TZ3	1	Pacific Sanddab	ND	ND	12.5	ND	ND	ND	ND	ND	ND	ND	ND	ND	ND
		2	Pacific Sanddab	ND	ND	24	ND	ND	ND	ND	ND	ND	ND	ND	ND	ND
		3	Pacific Sanddab	ND	ND	13.2	ND	ND	ND	ND	ND	ND	ND	ND	ND	ND
	TZ4	1	Pacific Sanddab	ND	ND	17.1	ND	ND	ND	ND	ND	ND	ND	ND	ND	ND
		2	Pacific Sanddab	ND	ND	14	ND	ND	ND	ND	ND	ND	ND	ND	ND	ND
		3	Pacific Sanddab	ND	ND	9.77	ND	ND	ND	ND	ND	ND	ND	ND	ND	ND
SBOO	TZ5	1	Hornyhead Turbot	ND	ND	29.7	ND	ND	ND	21.2	10.6	ND	ND	7.02	ND	ND
		2	Hornyhead Turbot	ND	ND	23.2	ND	ND	ND	14.6	7.01	ND	ND	ND	ND	ND
		3	Hornyhead Turbot	ND	ND	33.3	ND	ND	ND	28.5	13.6	ND	ND	10.4	ND	ND
	TZ6	1	Longfin Sanddab	ND	ND	10.4	ND	ND	ND	ND	11.7	ND	ND	ND	ND	ND
		2	Hornyhead Turbot	ND	ND	24.3	ND	ND	ND	17.3	10.5	ND	ND	9.02	ND	ND
		3	Longfin Sanddab	ND	ND	17.6	ND	ND	ND	ND	14.3	ND	ND	ND	ND	ND
	TZ7	1	Hornyhead Turbot	ND	ND	ND	ND	ND	ND	ND	ND	ND	ND	ND	ND	ND
		2	Hornyhead Turbot	ND	ND	10.1	ND	ND	ND	ND	ND	ND	ND	ND	ND	ND
		3	Hornyhead Turbot	ND	ND	ND	ND	ND	ND	ND	ND	ND	ND	ND	ND	ND
	TZ8	1	Hornyhead Turbot	ND	ND	13.7	ND	ND	ND	9.96	ND	ND	ND	ND	ND	ND
		2	Hornyhead Turbot	ND	ND	ND	ND	ND	ND	ND	ND	ND	ND	ND	ND	ND
		3	Longfin Sanddab	ND	ND	11.7	ND	ND	ND	ND	10.7	ND	ND	ND	ND	ND
	TZ9	1	Hornyhead Turbot	ND	ND	ND	ND	ND	ND	ND	ND	ND	ND	ND	ND	ND
		2	Spotted Turbot	ND	ND	ND	ND	ND	ND	ND	ND	ND	ND	ND	ND	ND
		3	Bigmouth Sole	ND	ND	ND	ND	ND	ND	ND	ND	ND	ND	ND	ND	ND

Appendix H.9

Concentrations of metals (ppm) detected in muscle tissues of fishes collected from PLOO and SBOO rig fishing zones during 2025. See Appendix H.3 for MDLs and abbreviations; DNQ = detected but not quantified; ND = not detected; NR = not reportable.

	Zone	Comp	Species	Al	Sb	As	Ba	Be	Cd	Cr	Cu	Fe
PLOO	RF1	1	Vermilion Rockfish	ND	ND	2.45	0.006 DNQ	ND	ND	0.06 DNQ	0.449	1.563 DNQ
	RF1	2	Vermilion Rockfish	ND	ND	1.29	0.007 DNQ	ND	ND	0.051 DNQ	0.374	1.318 DNQ
	RF1	3	Copper Rockfish	ND	ND	2.32	0.019 DNQ	ND	ND	0.073 DNQ	0.376	1.2 DNQ
	RF2	1	Speckled Rockfish	ND	ND	0.892	0.022 DNQ	ND	ND	0.056 DNQ	0.37	2.51 DNQ
	RF2	2	Mixed Rockfish	ND	ND	1.39	0.018 DNQ	ND	ND	0.045 DNQ	0.431	2.702 DNQ
	RF2	3	Mixed Rockfish	ND	ND	1.67	0.024 DNQ	ND	ND	0.065 DNQ	0.344	2.947 DNQ
SBOO	RF3	1	Vermilion Rockfish	ND	ND	2.67	0.01 DNQ	ND	ND	0.05 DNQ	0.21 DNQ	1.35 DNQ
	RF3	2	Brown Rockfish	ND	ND	0.91	0.01 DNQ	ND	ND	0.07 DNQ	0.11 DNQ	0.9 DNQ
	RF3	3	Brown Rockfish	ND	ND	1.01	0.01 DNQ	ND	ND	0.06 DNQ	0.21 DNQ	1.23 DNQ
	RF4	1	Honeycomb Rockfish	ND	ND	1.27	0.01 DNQ	ND	ND	0.04 DNQ	0.18 DNQ	1.46 DNQ
	RF4	2	California Scorpionfish	ND	ND	1.49	0.01 DNQ	ND	ND	0.05 DNQ	0.18 DNQ	0.96 DNQ
	RF4	3	Treefish	ND	ND	1.5	0.00491 DNQ	ND	ND	0.04 DNQ	0.17 DNQ	1.08 DNQ

Appendix H.9 continued

	Zone	Comp	Species	Pb	Mn	Hg	Ni	Se	Ag	Tl	Sn	Zn
PLOO	RF1	1	Vermilion Rockfish	ND	0.083	0.081	ND	1.12	0.026 DNQ	0.106 DNQ	3.46	4.32
	RF1	2	Vermilion Rockfish	ND	0.085	0.049	ND	0.842 DNQ	0.026 DNQ	0.101 DNQ	3.39	3.64
	RF1	3	Copper Rockfish	ND	0.046	0.141	ND	1.43	0.037 DNQ	0.122 DNQ	3.93	4.31
	RF2	1	Speckled Rockfish	ND	0.052	0.088	ND	1.09	ND	0.126 DNQ	4.14	3.32
	RF2	2	Mixed Rockfish	ND	0.026	0.445	ND	1.26	0.032 DNQ	0.162 DNQ	6.88	3.14
	RF2	3	Mixed Rockfish	ND	0.072	0.194	ND	1.07	ND	0.15 DNQ	3.49	3.61
SBOO	RF3	1	Vermilion Rockfish	ND	0.08	0.037	ND	0.65 DNQ	ND	0.08 DNQ	2.98	3.75
	RF3	2	Brown Rockfish	ND	0.04	0.07	ND	0.66 DNQ	ND	0.1 DNQ	2.8	3.69
	RF3	3	Brown Rockfish	ND	0.04	0.084	ND	0.75 DNQ	ND	0.11 DNQ	3.13	4.54
	RF4	1	Honeycomb Rockfish	ND	0.06	0.188	ND	0.89 DNQ	ND	0.12 DNQ	3.31	4.68
	RF4	2	California Scorpionfish	ND	0.05	0.126	ND	0.8 DNQ	ND	0.13 DNQ	2.78	3.68
	RF4	3	Treefish	ND	0.02	0.189	ND	0.8 DNQ	ND	0.08 DNQ	3.32	4.19

Appendix H.10

Concentrations of pesticides (ppb) and lipids (% weight) detected in muscle tissues of fishes collected from PLOO and SBOO rig fishing zones during 2025. See Appendix H.3 for MDLs and abbreviations; DNQ=detected but not quantified; ND = not detected; NR = not reportable; NS=not sampled.

				Chlordane							
Zone		Comp	Species	A(c)C	cNon	G(t)C	Hept	HeptEpox	Methoxy	Oxychlor	tNon
PLOO	RF1	1	Vermilion Rockfish	ND	ND	ND	ND	ND	ND	ND	ND
	RF1	2	Vermilion Rockfish	ND	ND	ND	ND	ND	ND	ND	ND
	RF1	3	Copper Rockfish	ND	ND	ND	ND	ND	ND	ND	ND
	RF2	1	Speckled Rockfish	ND	ND	ND	ND	ND	ND	ND	ND
	RF2	2	Mixed Rockfish	ND	ND	ND	ND	ND	ND	ND	ND
	RF2	3	Mixed Rockfish	ND	ND	ND	ND	ND	ND	ND	ND
SBOO	RF3	1	Vermilion Rockfish	ND	ND	ND	ND	ND	ND	ND	ND
	RF3	2	Brown Rockfish	ND	ND	ND	ND	ND	ND	ND	ND
	RF3	3	Brown Rockfish	ND	ND	ND	ND	ND	ND	ND	ND
	RF4	1	Honeycomb Rockfish	0.975	ND	0.766	ND	ND	ND	ND	0.536
	RF4	2	California Scorpionfish	ND	ND	ND	ND	ND	ND	ND	ND
	RF4	3	Treefish	ND	ND	ND	ND	ND	ND	ND	ND

Appendix H.10 *continued*

	Zone	Comp	Species	DDT							Endosulfan		
				o,p-DDD	o,p-DDE	o,p-DDT	p,-p-DDMU	p,p-DDD	p,p-DDE	p,p-DDT	Alpha	Beta	Sulfate
PLOO	RF1	1	Vermilion Rockfish	ND	ND	ND	ND	ND	1.82	ND	ND	ND	ND
	RF1	2	Vermilion Rockfish	ND	ND	ND	ND	ND	1.31	ND	ND	ND	ND
	RF1	3	Copper Rockfish	ND	ND	ND	ND	ND	4.1	ND	ND	ND	ND
	RF2	1	Speckled Rockfish	ND	ND	ND	ND	ND	3.19	ND	ND	ND	ND
	RF2	2	Mixed Rockfish	ND	0.535	ND	0.942	0.506	19.5	ND	ND	ND	ND
	RF2	3	Mixed Rockfish	ND	ND	ND	0.617	ND	5.04	ND	ND	ND	ND
SBOO	RF3	1	Vermilion Rockfish	ND	ND	ND	ND	ND	1.05	ND	ND	ND	ND
	RF3	2	Brown Rockfish	ND	ND	ND	ND	ND	1.41	ND	ND	ND	ND
	RF3	3	Brown Rockfish	ND	ND	ND	ND	ND	3.38	ND	ND	ND	ND
	RF4	1	Honeycomb Rockfish	ND	ND	ND	ND	ND	4.9	ND	ND	ND	ND
	RF4	2	California Scorpionfish	ND	ND	ND	ND	ND	0.806	ND	ND	ND	ND
	RF4	3	Treefish	ND	ND	ND	ND	ND	2.54	ND	ND	ND	ND

Appendix H.10 *continued*

	Zone	Comp	Species	HCH				Aldrin	Dieldrin	Endrin	EndAld	HCB	Mirex	Lipids
				Alpha	Beta	Delta	Gamma							
PLOO	RF1	1	Vermilion Rockfish	ND	ND	ND	ND	ND	ND	ND	ND	ND	ND	1.02
	RF1	2	Vermilion Rockfish	ND	ND	ND	ND	ND	ND	ND	ND	ND	ND	0.875
	RF1	3	Copper Rockfish	ND	ND	ND	ND	ND	ND	ND	ND	ND	ND	1.72
	RF2	1	Speckled Rockfish	ND	ND	ND	ND	ND	ND	ND	ND	ND	ND	3.06
	RF2	2	Mixed Rockfish	ND	ND	ND	ND	ND	ND	ND	ND	ND	ND	2.67
	RF2	3	Mixed Rockfish	ND	ND	ND	ND	ND	ND	ND	ND	ND	ND	2.59
SBOO	RF3	1	Vermilion Rockfish	ND	ND	ND	ND	ND	ND	ND	ND	ND	ND	1.85
	RF3	2	Brown Rockfish	ND	ND	ND	ND	ND	ND	ND	ND	ND	ND	1.15
	RF3	3	Brown Rockfish	ND	ND	ND	ND	ND	ND	ND	ND	ND	ND	1.79
	RF4	1	Honeycomb Rockfish	ND	ND	ND	ND	ND	ND	ND	ND	ND	ND	1.06
	RF4	2	California Scorpionfish	ND	ND	ND	ND	ND	ND	ND	ND	ND	ND	0.347
	RF4	3	Treefish	ND	ND	ND	ND	ND	ND	ND	ND	ND	ND	0.579

Appendix H.11

Concentrations of PCBs (ppb) detected in muscle tissues of fishes collected from PLOO and SBOO rig fishing zones during 2025. See Appendix H.3 for MDLs; DNQ=detected but not quantified; ND = not detected; NR = not reportable.

				PCB Congener									
	Zone	Comp	Species	8	18	28	37	44	49	52	66	70	74
PLOO	RF1	1	Vermilion Rockfish	ND	ND	ND	ND	ND	ND	ND	ND	ND	ND
	RF1	2	Vermilion Rockfish	ND	ND	ND	ND	ND	ND	ND	ND	ND	ND
	RF1	3	Copper Rockfish	ND	ND	ND	ND	ND	ND	ND	ND	ND	ND
	RF2	1	Speckled Rockfish	ND	ND	ND	ND	ND	ND	ND	ND	ND	ND
	RF2	2	Mixed Rockfish	ND	ND	ND	ND	ND	0.294 DNQ	ND	ND	ND	ND
	RF2	3	Mixed Rockfish	ND	ND	ND	ND	ND	ND	ND	ND	ND	ND
SBOO	RF3	1	Vermilion Rockfish	ND	ND	ND	ND	ND	ND	ND	ND	ND	ND
	RF3	2	Brown Rockfish	ND	ND	ND	ND	ND	ND	ND	ND	ND	ND
	RF3	3	Brown Rockfish	ND	ND	ND	ND	ND	ND	ND	ND	ND	ND
	RF4	1	Honeycomb Rockfish	ND	ND	ND	ND	ND	ND	ND	ND	ND	ND
	RF4	2	California Scorpionfish	ND	ND	ND	ND	ND	ND	ND	ND	ND	ND
	RF4	3	Treefish	ND	ND	ND	ND	ND	ND	ND	ND	ND	ND

Appendix H.11 *continued*

	Zone	Comp	Species	PCB Congener 77	81	87	99	101	105	110	114	118	119
PLOO	RF1	1	Vermilion Rockfish	ND	ND	ND	ND	ND	ND	0.15 DNQ	ND	ND	ND
	RF1	2	Vermilion Rockfish	ND	ND	ND	ND	ND	ND	ND	ND	ND	ND
	RF1	3	Copper Rockfish	ND	ND	ND	ND	ND	ND	ND	ND	0.295	ND
	RF2	1	Speckled Rockfish	ND	ND	ND	ND	ND	ND	ND	ND	ND	ND
	RF2	2	Mixed Rockfish	ND	ND	ND	0.713	1.13	ND	0.552	ND	1.15	ND
	RF2	3	Mixed Rockfish	ND	ND	ND	ND	ND	ND	ND	ND	ND	ND
SBOO	RF3	1	Vermilion Rockfish	ND	ND	ND	ND	ND	ND	ND	ND	ND	ND
	RF3	2	Brown Rockfish	ND	ND	ND	ND	ND	ND	ND	ND	ND	ND
	RF3	3	Brown Rockfish	ND	ND	ND	ND	ND	ND	ND	ND	ND	ND
	RF4	1	Honeycomb Rockfish	ND	ND	ND	ND	ND	ND	ND	ND	0.309 DNQ	ND
	RF4	2	California Scorpionfish	ND	ND	ND	ND	ND	ND	ND	ND	ND	ND
	RF4	3	Treefish	ND	ND	ND	ND	ND	ND	ND	ND	ND	ND

Appendix H.11 *continued*

Zone		Comp	Species	PCB Congener									
				123	126	128	138	149	151	153/168	156	157	158
PLOO	RF1	1	Vermilion Rockfish	ND	ND	ND	0.301	ND	ND	0.725	ND	ND	ND
	RF1	2	Vermilion Rockfish	ND	ND	ND	ND	ND	ND	ND	ND	ND	ND
	RF1	3	Copper Rockfish	ND	ND	ND	0.52	ND	ND	1.15	ND	ND	ND
	RF2	1	Speckled Rockfish	ND	ND	ND	0.463	ND	ND	0.953	ND	ND	ND
	RF2	2	Mixed Rockfish	ND	ND	ND	1.8	1.17	0.472	3.95	ND	ND	ND
	RF2	3	Mixed Rockfish	ND	ND	ND	0.326	ND	ND	0.626 DNQ	ND	ND	ND
SBOO	RF3	1	Vermilion Rockfish	ND	ND	ND	ND	ND	ND	ND	ND	ND	ND
	RF3	2	Brown Rockfish	ND	ND	ND	ND	ND	ND	ND	ND	ND	ND
	RF3	3	Brown Rockfish	ND	ND	ND	ND	ND	ND	ND	ND	ND	ND
	RF4	1	Honeycomb Rockfish	ND	ND	ND	0.456	ND	ND	0.807	ND	ND	ND
	RF4	2	California Scorpionfish	ND	ND	ND	ND	ND	ND	ND	ND	ND	ND
	RF4	3	Treefish	ND	ND	ND	ND	ND	ND	ND	ND	ND	ND

Appendix H.11 *continued*

				PCB Congener											
	Zone	Comp	Species	167	169	170	177	180	183	187	189	194	195	201	206
PLOO	RF1	1	Vermilion Rockfish	ND	ND	ND	ND	ND	ND	ND	ND	ND	ND	ND	ND
	RF1	2	Vermilion Rockfish	ND	ND	ND	ND	ND	ND	ND	ND	ND	ND	ND	ND
	RF1	3	Copper Rockfish	ND	ND	ND	ND	ND	ND	ND	ND	ND	ND	ND	ND
	RF2	1	Speckled Rockfish	ND	ND	ND	ND	ND	ND	ND	ND	ND	ND	ND	ND
	RF2	2	Mixed Rockfish	ND	ND	ND	ND	0.83	ND	0.898	ND	ND	ND	ND	ND
	RF2	3	Mixed Rockfish	ND	ND	ND	ND	ND	ND	ND	ND	ND	ND	ND	ND
SBOO	RF3	1	Vermilion Rockfish	ND	ND	ND	ND	ND	ND	ND	ND	ND	ND	ND	ND
	RF3	2	Brown Rockfish	ND	ND	ND	ND	ND	ND	ND	ND	ND	ND	ND	ND
	RF3	3	Brown Rockfish	ND	ND	ND	ND	ND	ND	ND	ND	ND	ND	ND	ND
	RF4	1	Honeycomb Rockfish	ND	ND	ND	ND	ND	ND	ND	ND	ND	ND	ND	ND
	RF4	2	California Scorpionfish	ND	ND	ND	ND	ND	ND	ND	ND	ND	ND	ND	ND
	RF4	3	Treefish	ND	ND	ND	ND	ND	ND	ND	ND	ND	ND	ND	ND

Appendix H.12

Concentrations of PAHs (ppb) detected in muscle tissues of fishes collected from PLOO and SBOO rig fishing zones during 2025. See Appendix H.3 for MDLs; DNQ=detected but not quantified; ND = not detected; NR = not reportable.

	Zone	Comp	Species	1-methyl naphthalene	1-methyl phenanthrene	2-methyl naphthalene	2,3,5-trimethyl naphthalene	2,6-dimethyl naphthalene	3,4-benzo(B) fluoranthene	Acenaphthene	Acenaphthylene	Anthracene	Benzo[A] anthracene	Benzo[A] pyrene
PLOO	RF1	1	Vermilion Rockfish	ND	ND	ND	ND	ND	ND	ND	ND	ND	ND	ND
	RF1	2	Vermilion Rockfish	ND	ND	ND	ND	ND	ND	ND	ND	ND	ND	ND
	RF1	3	Copper Rockfish	ND	ND	ND	ND	ND	ND	ND	ND	ND	ND	ND
	RF2	1	Speckled Rockfish	ND	ND	ND	ND	ND	ND	ND	ND	ND	ND	ND
	RF2	2	Mixed Rockfish	ND	ND	ND	ND	ND	ND	ND	ND	ND	ND	ND
	RF2	3	Mixed Rockfish	ND	ND	ND	ND	ND	ND	ND	ND	ND	ND	ND
SBOO	RF3	1	Vermilion Rockfish	ND	ND	ND	ND	ND	ND	ND	ND	ND	ND	ND
	RF3	2	Brown Rockfish	ND	ND	ND	ND	ND	ND	ND	ND	ND	ND	ND
	RF3	3	Brown Rockfish	ND	ND	ND	ND	ND	ND	ND	ND	ND	ND	ND
	RF4	1	Honeycomb Rockfish	ND	ND	ND	ND	ND	ND	ND	ND	ND	ND	ND
	RF4	2	California Scorpionfish	ND	ND	ND	ND	ND	ND	ND	ND	ND	ND	ND
	RF4	3	Treefish	ND	ND	ND	ND	ND	ND	ND	ND	ND	ND	ND

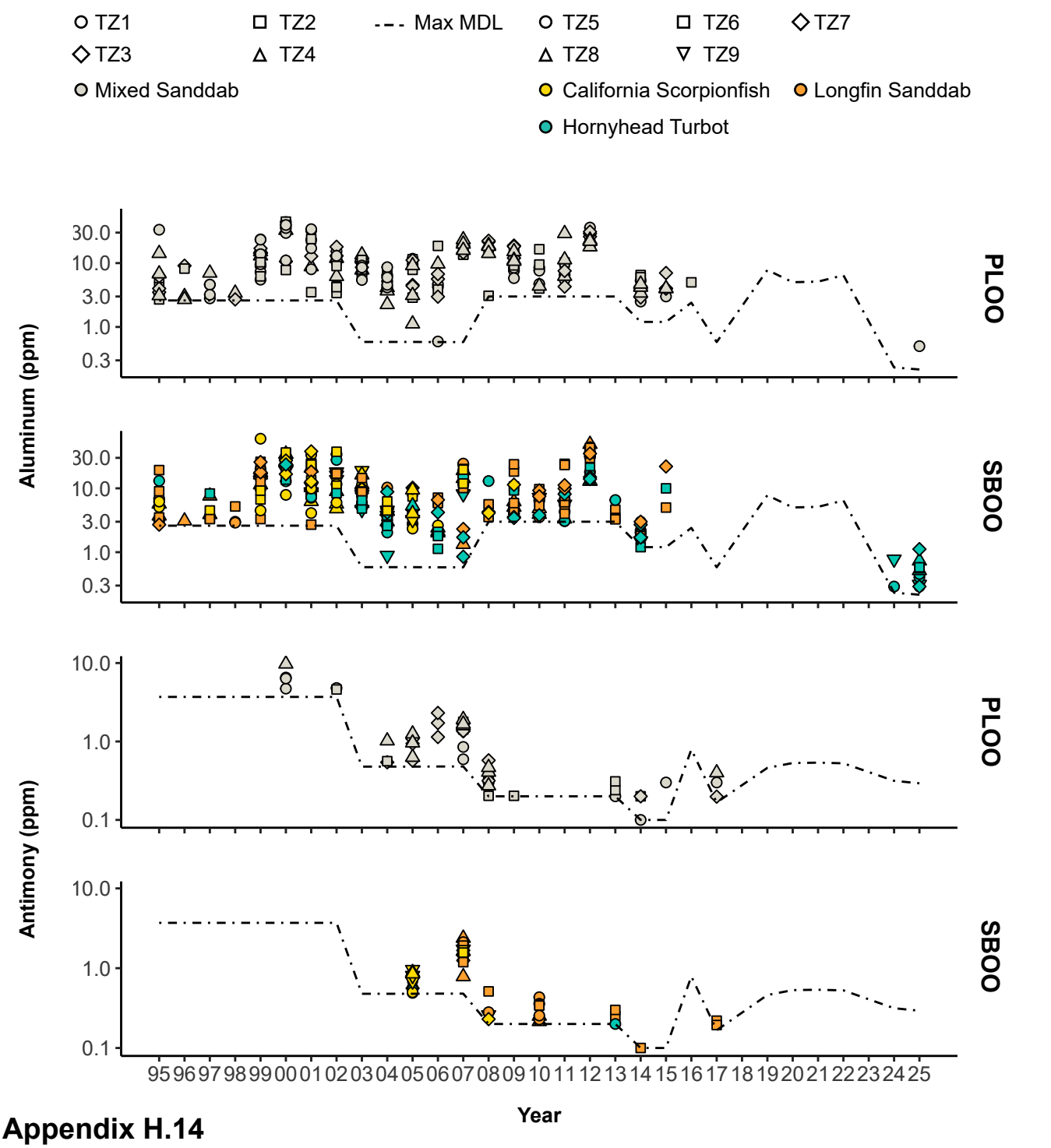
Appendix H.12 *continued*

	Zone	Comp	Species	Benzo[e] pyrene	Benzo[G,H,I] perylene	Benzo[K] fluoranthene	Biphenyl	Chrysene	Dibenzo(A,H) anthracene	Fluoranthene	Fluorene	Indeno(1,2,3-CD)pyrene	Naphthalene	Perylene	Phenanthrene	Pyrene
PLOO	RF1	1	Vermilion Rockfish	ND	ND	ND	ND	ND	ND	ND	ND	ND	ND	ND	ND	ND
	RF1	2	Vermilion Rockfish	ND	ND	ND	ND	ND	ND	ND	ND	ND	ND	ND	ND	ND
	RF1	3	Copper Rockfish	ND	ND	ND	ND	ND	ND	ND	ND	ND	ND	ND	ND	ND
	RF2	1	Speckled Rockfish	ND	ND	ND	ND	ND	ND	ND	ND	ND	ND	ND	ND	ND
	RF2	2	Mixed Rockfish	ND	ND	ND	ND	ND	ND	ND	ND	ND	ND	ND	ND	ND
	RF2	3	Mixed Rockfish	ND	ND	ND	ND	ND	ND	ND	ND	ND	ND	ND	ND	ND
SBOO	RF3	1	Vermilion Rockfish	ND	ND	ND	ND	ND	ND	ND	ND	ND	ND	ND	ND	ND
	RF3	2	Brown Rockfish	ND	ND	ND	ND	ND	ND	ND	ND	ND	ND	ND	ND	ND
	RF3	3	Brown Rockfish	ND	ND	ND	ND	ND	ND	ND	ND	ND	ND	ND	ND	ND
	RF4	1	Honeycomb Rockfish	ND	ND	ND	ND	ND	ND	ND	ND	ND	ND	ND	ND	ND
	RF4	2	California Scorpionfish	ND	ND	ND	ND	ND	ND	ND	ND	ND	ND	ND	ND	ND
	RF4	3	Treefish	ND	ND	ND	ND	ND	ND	ND	ND	ND	ND	ND	ND	ND

Appendix H.13

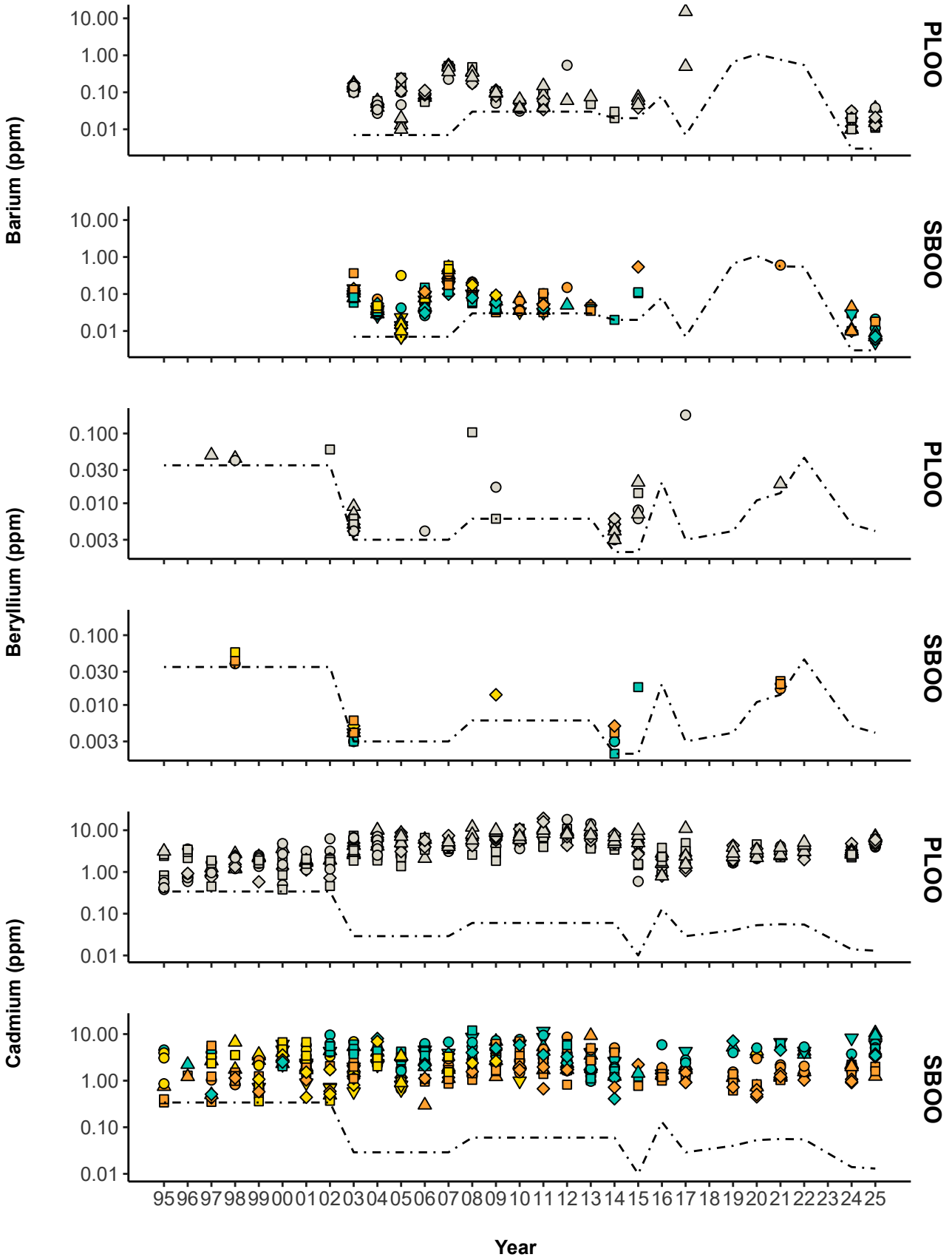
Concentrations of PBDEs (ppb) detected in muscle tissues of fishes collected from PLOO and SBOO rig fishing zones during 2025. See Appendix H.3 for MDLs; DNQ=detected but not quantified; ND = not detected; NR = not reportable.

				PBDE												
	Zone	Comp	Species	17	28	47	49	66	85	99	100	138	153	154	183	190
PLOO	RF1	1	Vermilion Rockfish	ND	ND	ND	ND	ND	ND	ND	ND	ND	ND	ND	ND	ND
	RF1	2	Vermilion Rockfish	ND	ND	ND	ND	ND	ND	ND	ND	ND	ND	ND	ND	ND
	RF1	3	Copper Rockfish	ND	ND	NR	ND	ND	ND	ND	ND	ND	ND	ND	ND	ND
	RF2	1	Speckled Rockfish	ND	ND	NR	ND	ND	ND	ND	ND	ND	ND	ND	ND	ND
	RF2	2	Mixed Rockfish	ND	ND	2.55	ND	ND	ND	ND	ND	ND	ND	ND	ND	ND
	RF2	3	Mixed Rockfish	ND	ND	ND	ND	ND	ND	ND	ND	ND	ND	ND	ND	ND
SBOO	RF3	1	Vermilion Rockfish	ND	ND	NR	ND	ND	ND	ND	ND	ND	ND	ND	ND	ND
	RF3	2	Brown Rockfish	ND	ND	ND	ND	ND	ND	ND	ND	ND	ND	ND	ND	ND
	RF3	3	Brown Rockfish	ND	ND	NR	ND	ND	ND	ND	ND	ND	ND	ND	ND	ND
	RF4	1	Honeycomb Rockfish	ND	ND	ND	ND	ND	ND	ND	ND	ND	ND	ND	ND	ND
	RF4	2	California Scorpionfish	ND	ND	ND	ND	ND	ND	ND	ND	ND	ND	ND	ND	ND
	RF4	3	Treefish	ND	ND	ND	ND	ND	ND	ND	ND	ND	ND	ND	ND	ND

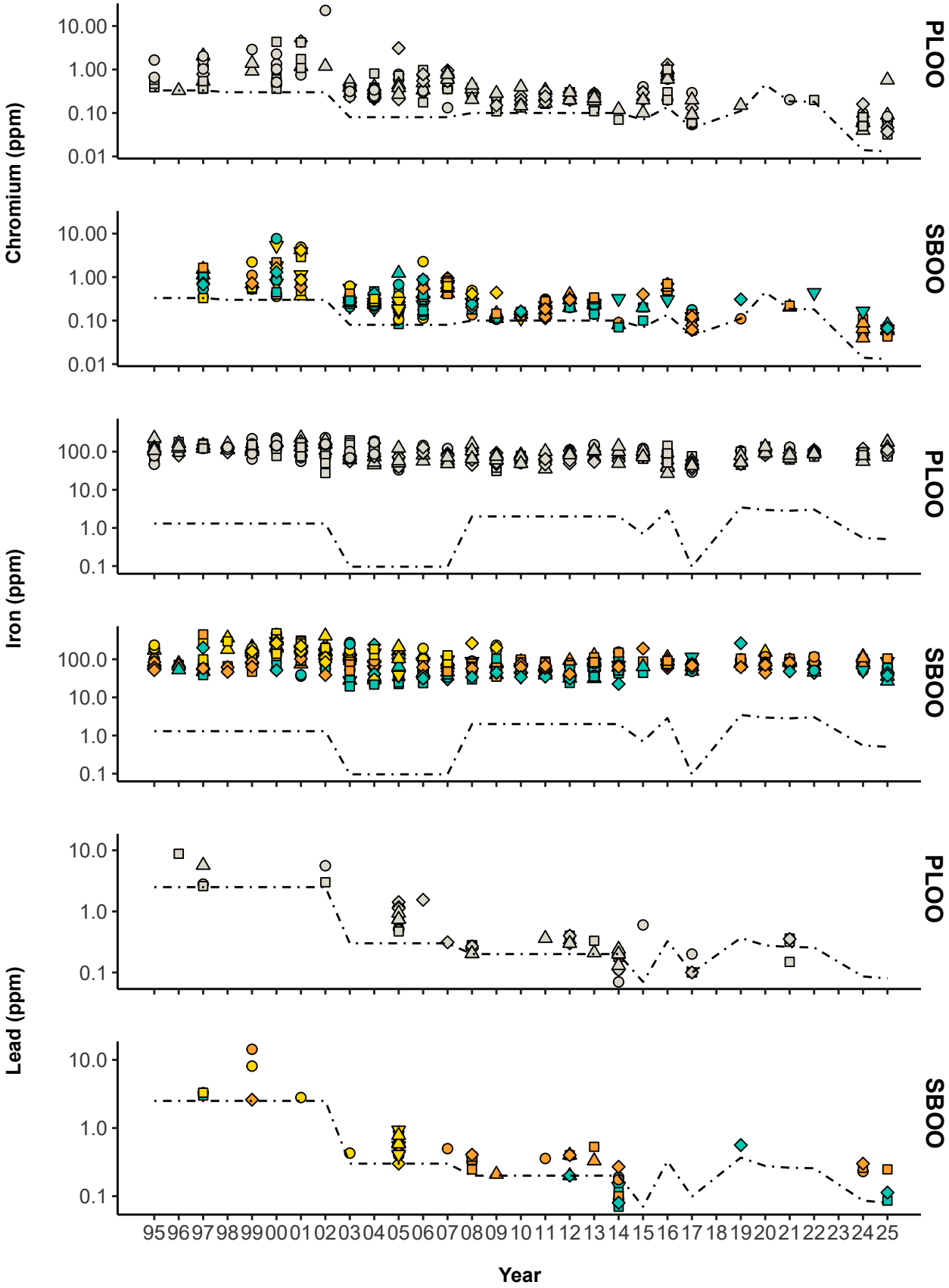


Appendix H.14

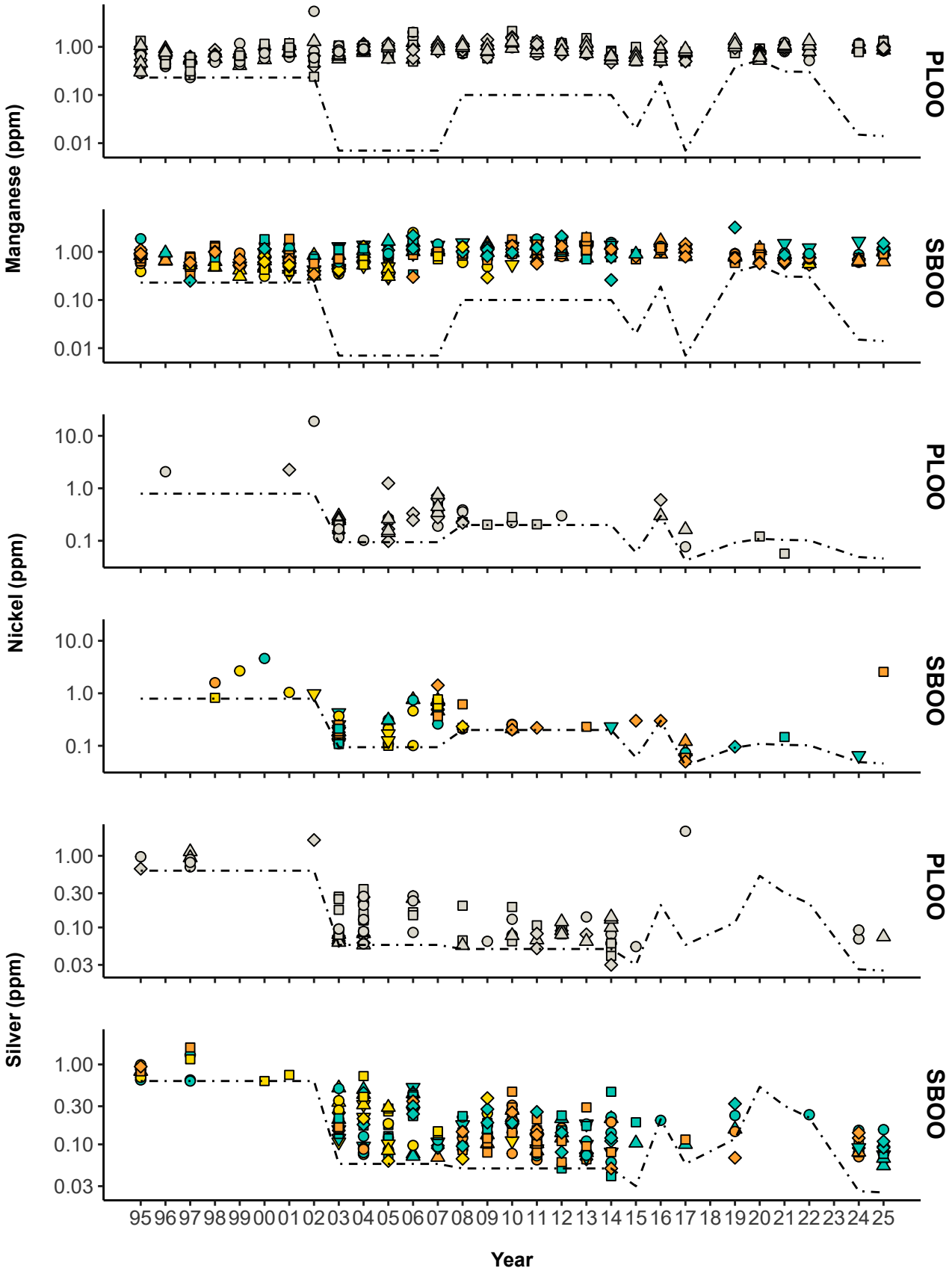
Concentrations of select metals in liver tissues of fishes collected from PLOO and SBOO trawl zones from 1995 through 2025. Zones TZ1 and TZ5 are considered nearfield. No samples were collected in 2018 and 2023 as described in text.



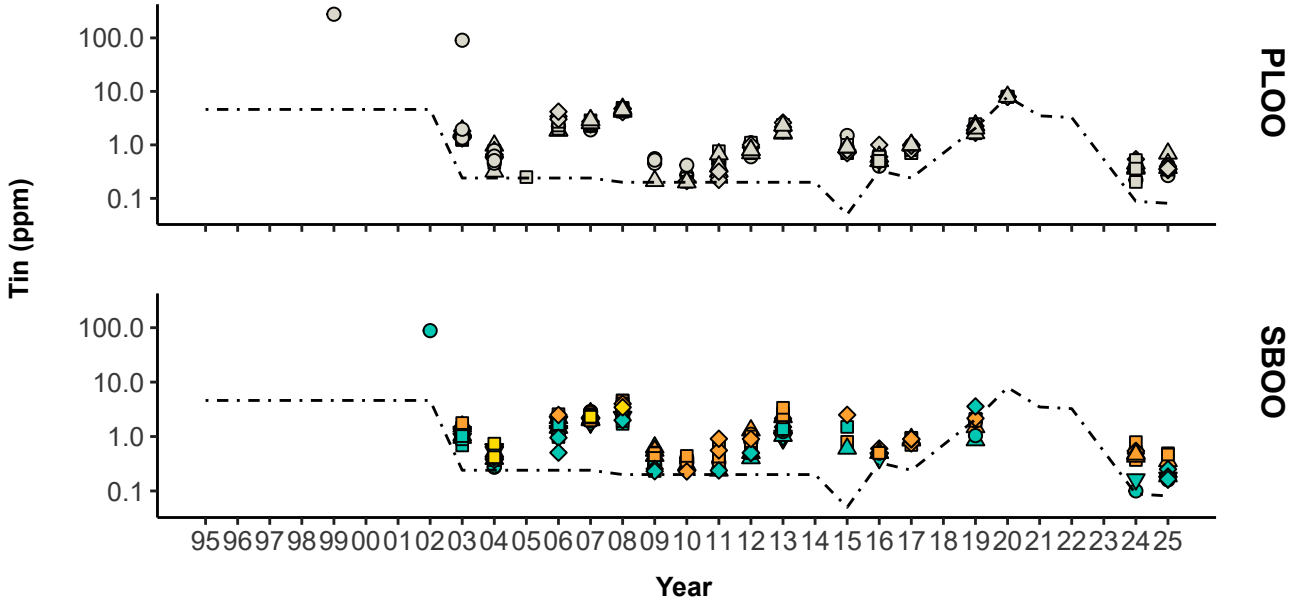
Appendix H.14 *continued*



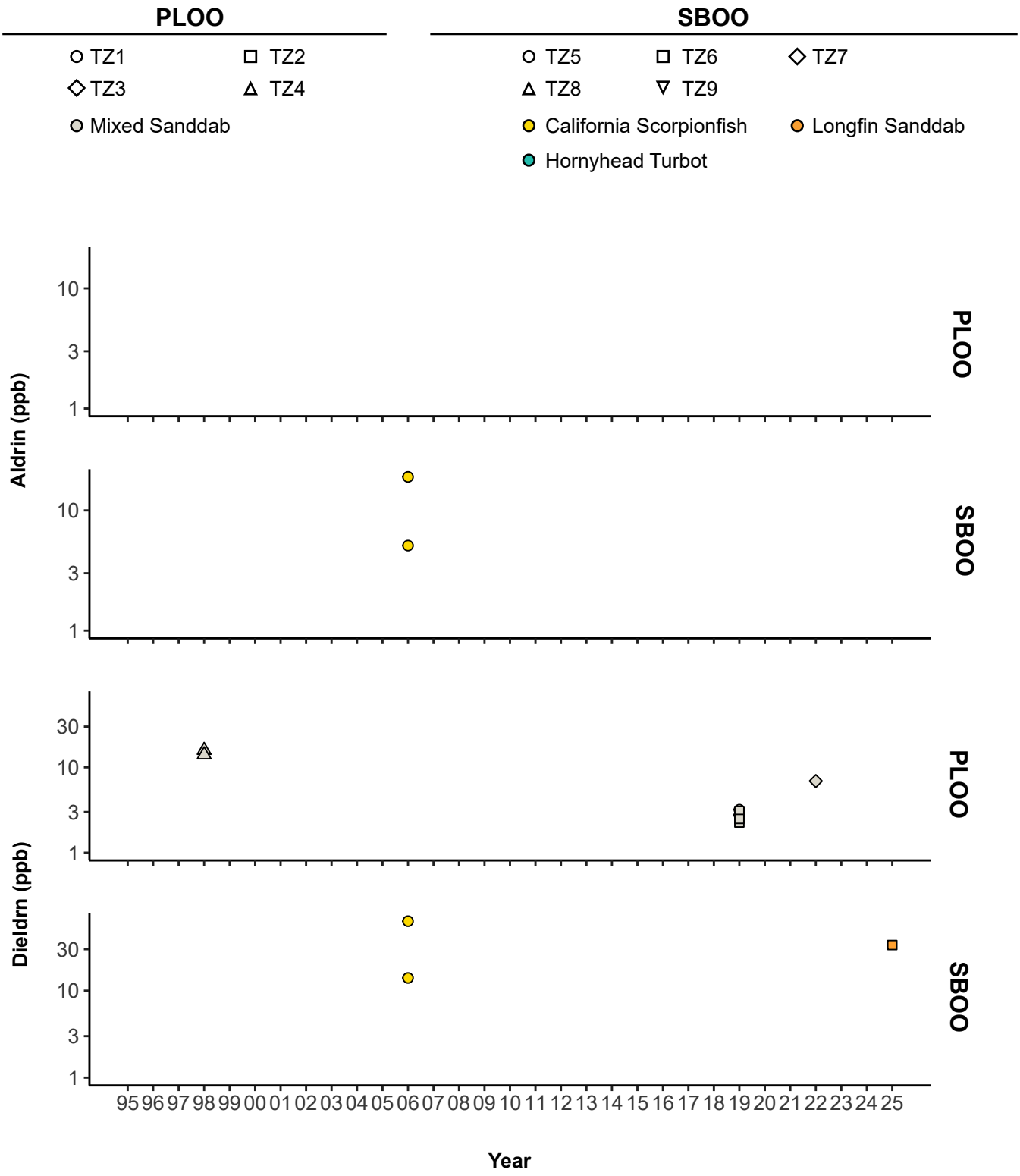
Appendix H.14 *continued*



Appendix H.14 *continued*

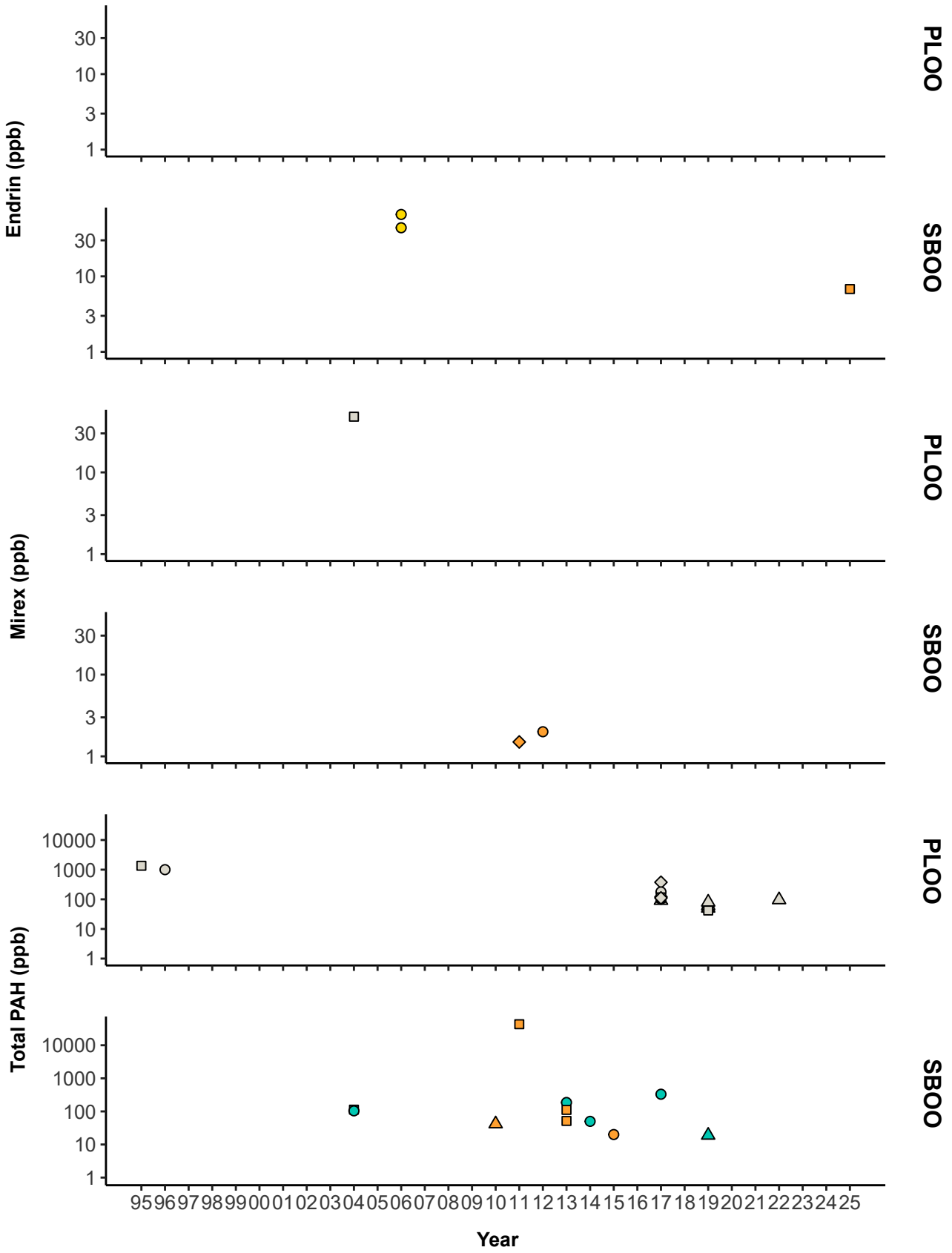


Appendix H.14 *continued*

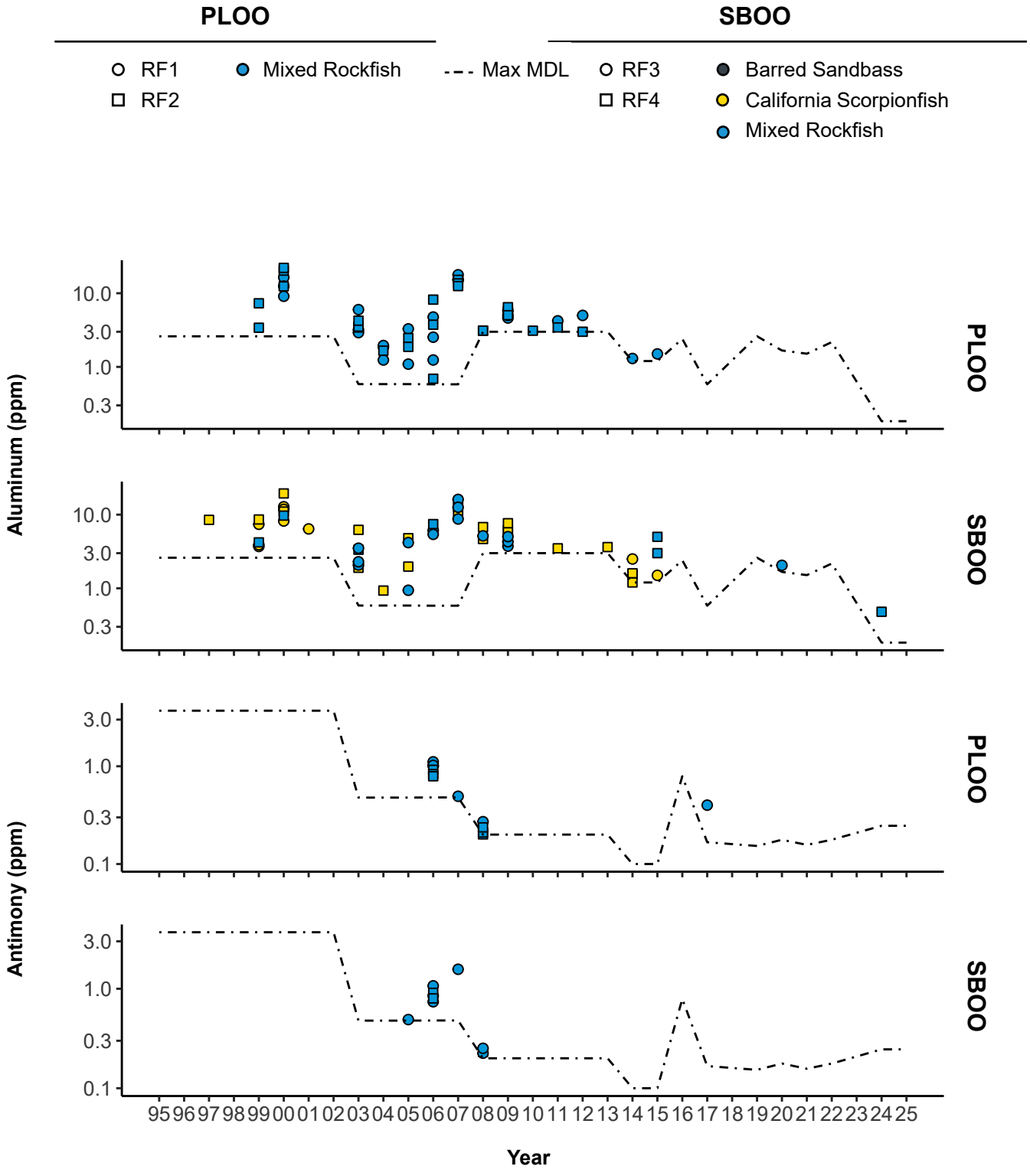


Appendix H.15

Concentrations of pesticides and total PAH in liver tissues of fishes collected from PLOO and SBOO trawl zones from 1995 through 2025. Zones TZ1 and TZ5 are considered nearfield. No samples were collected in 2018 and 2023 as described in text.

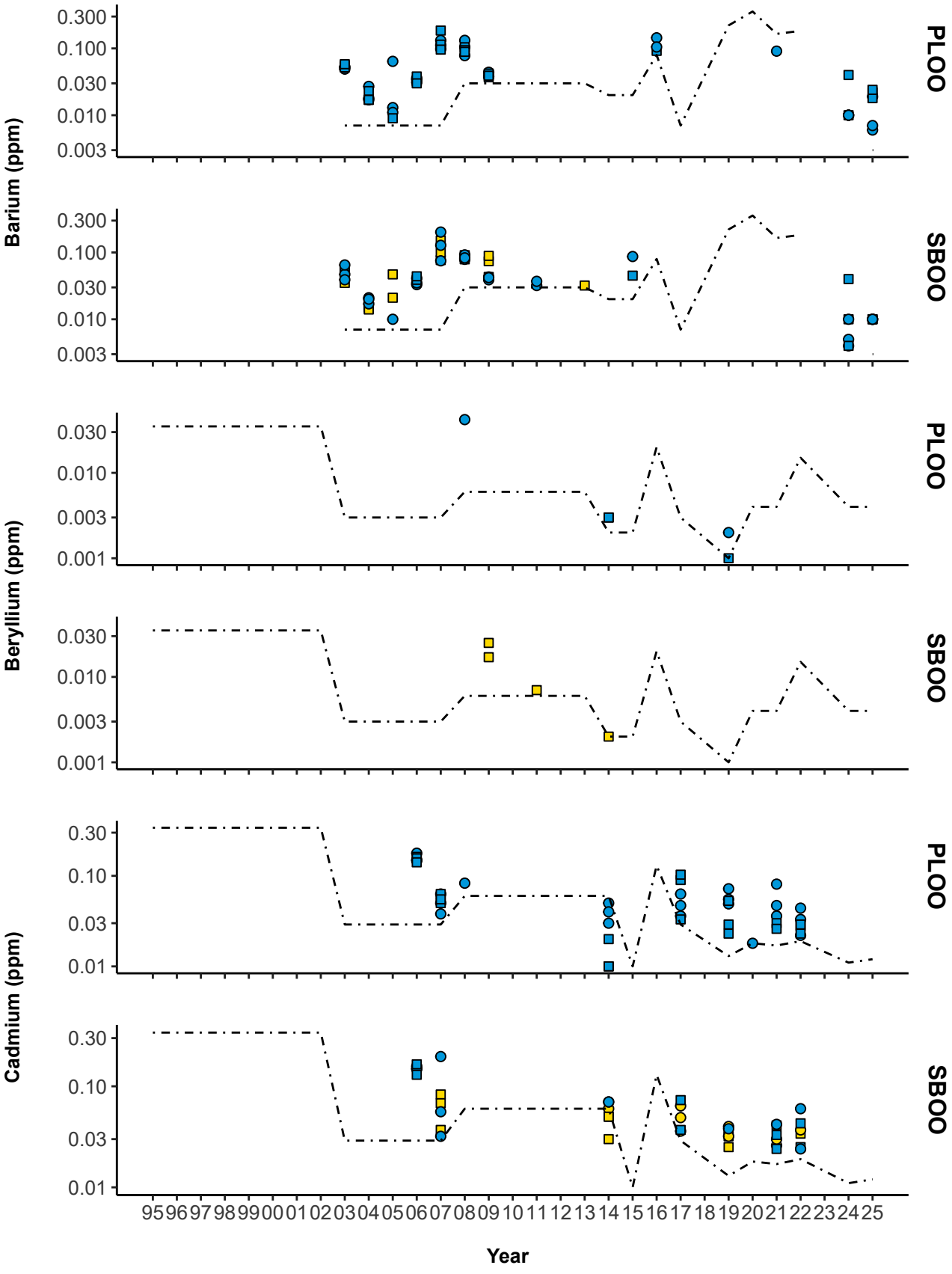


Appendix H.15 *continued*

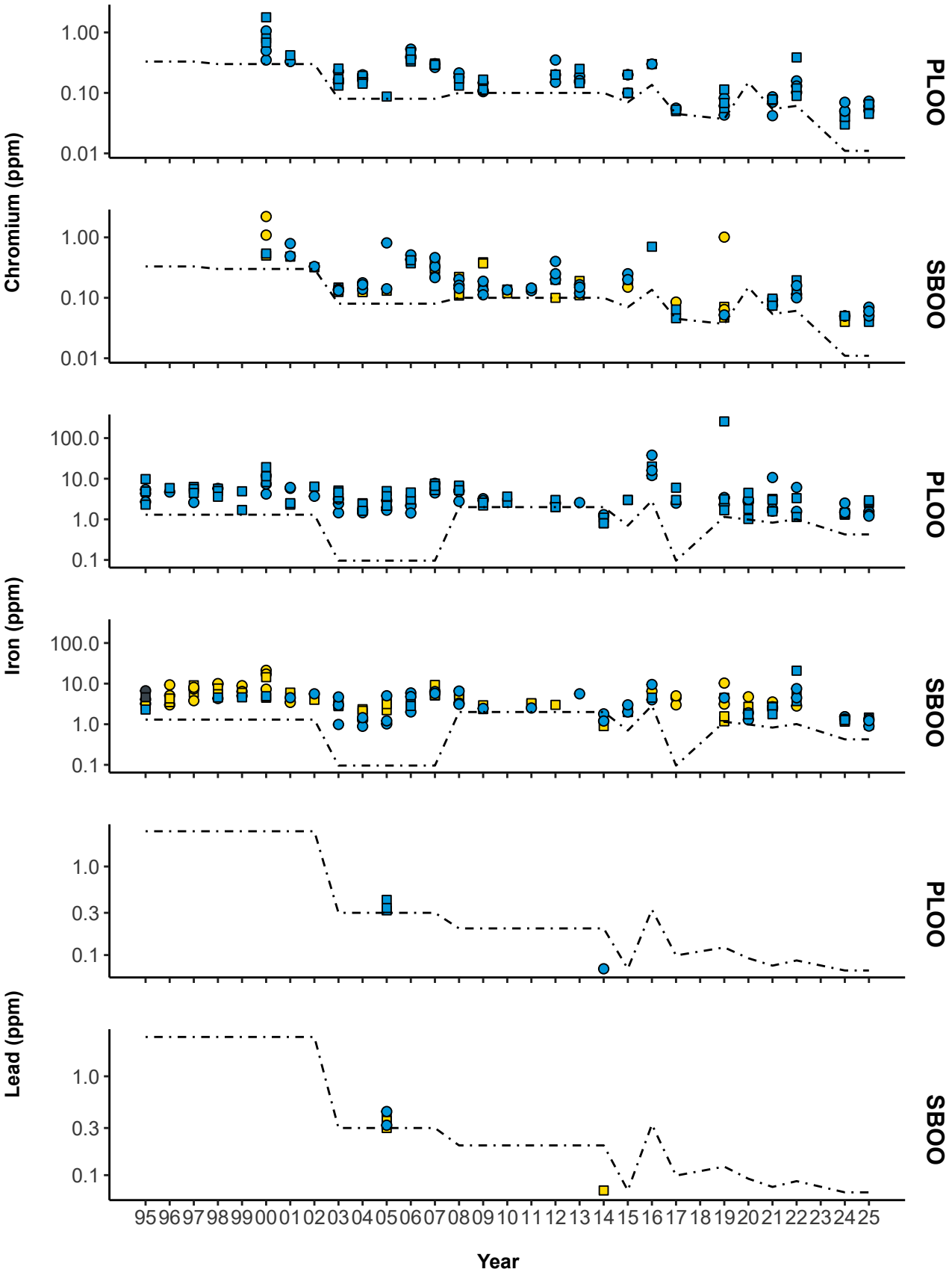


Appendix H.16

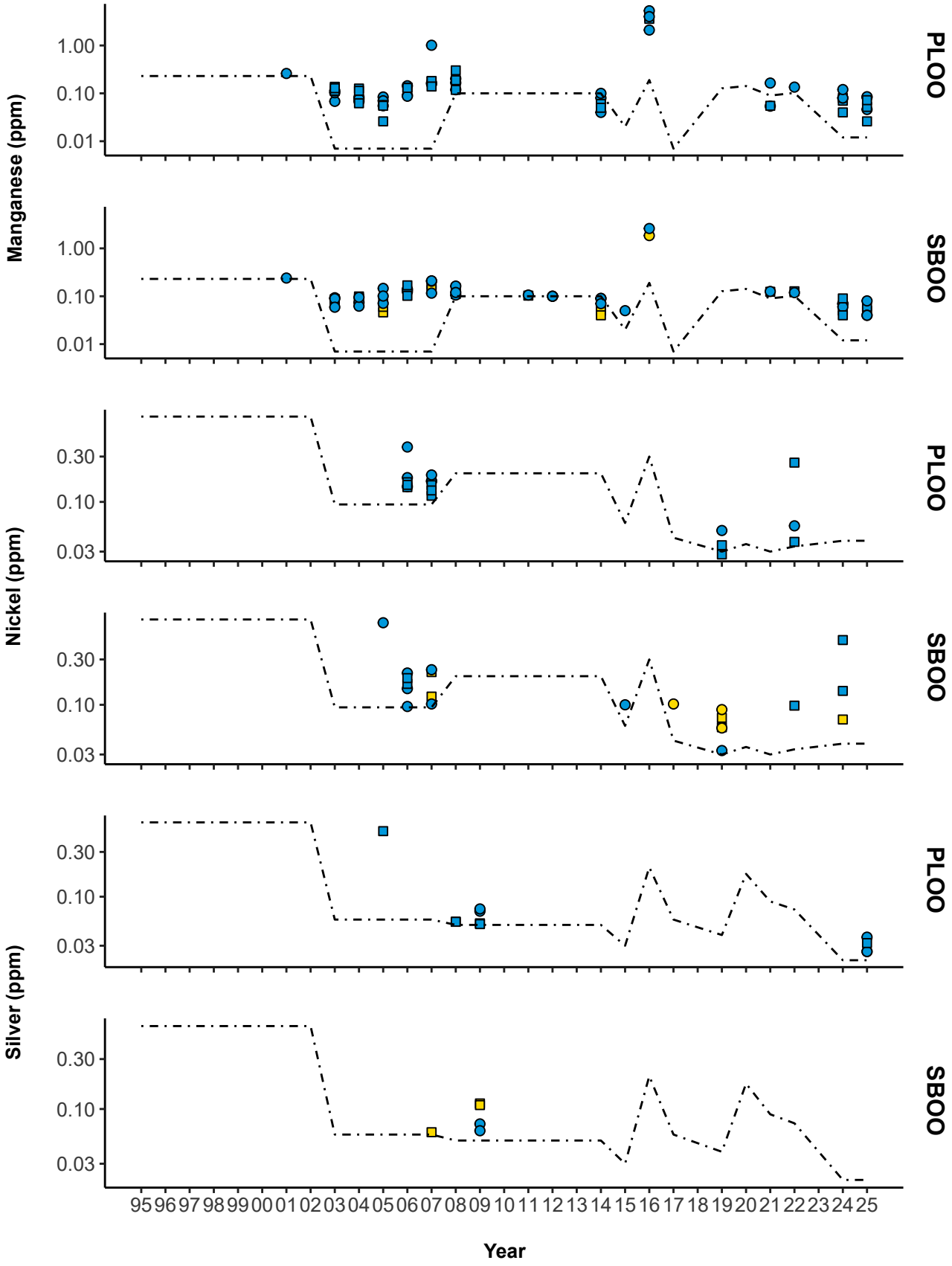
Concentrations of select metals in muscle tissues of fishes collected from PLOO and SBOO rig fishing zones from 1995 through 2025. Zones RF1 and RF3 are considered nearfield. No samples were collected in 2018 and 2023 as described in text.



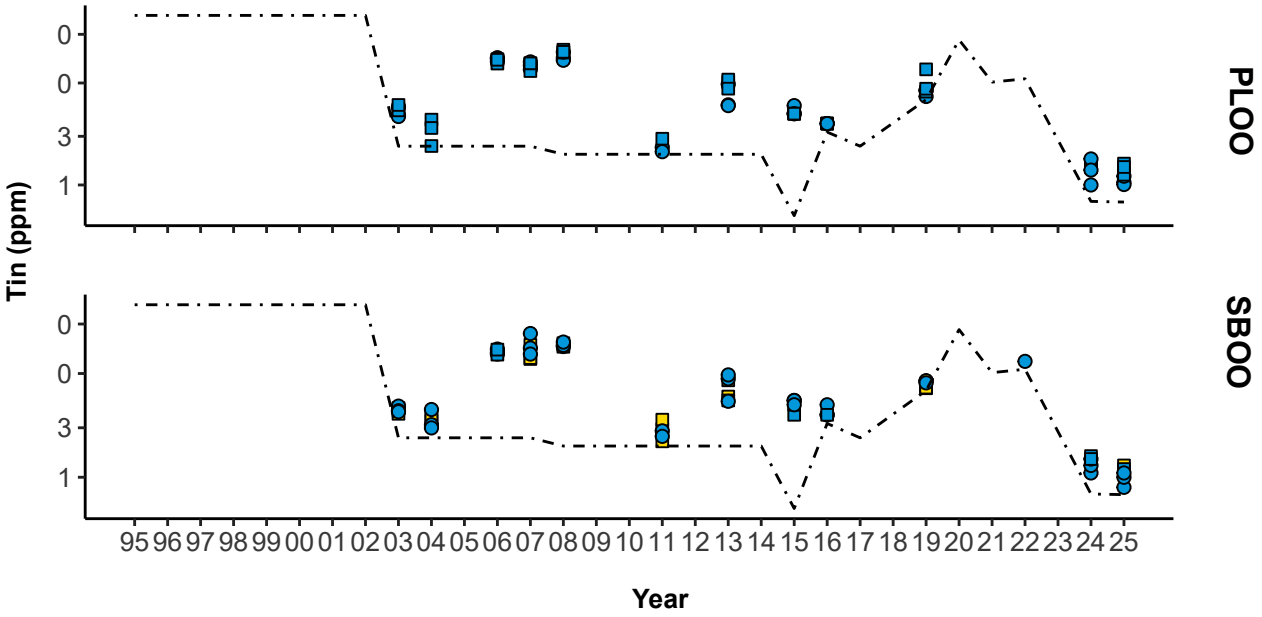
Appendix H.16 *continued*



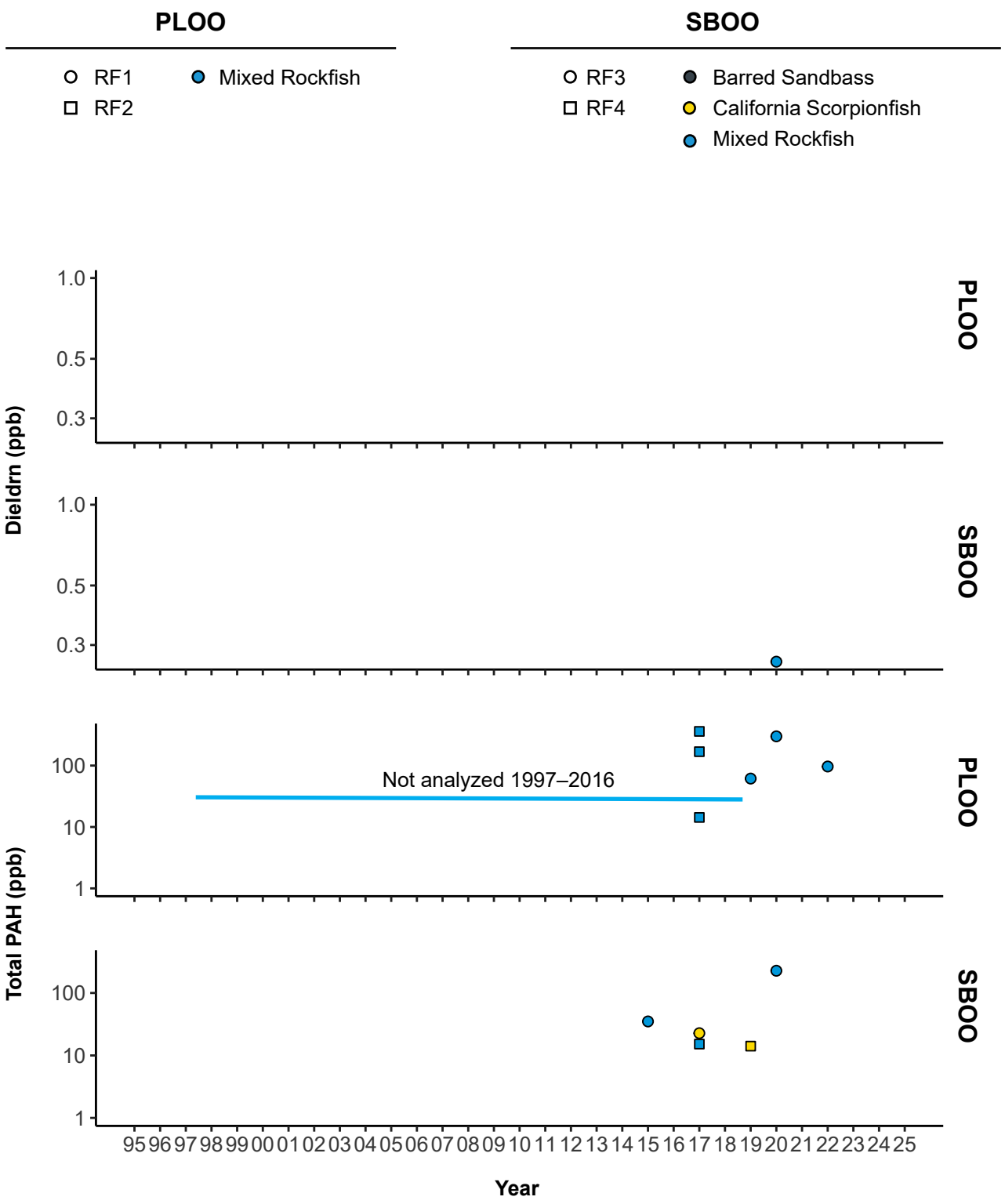
Appendix H.16 *continued*



Appendix H.16 *continued*



Appendix H.16 *continued*



Appendix H.17

Concentrations of dieldrin and total PAH in muscle tissues of fishes collected from PLOO and SBOO rig fishing zones from 1995 through 2025. Analysis of Total PAH was not a permit requirement from 1997–2016. Zones RF1 and RF3 are considered nearfield. No samples were collected in 2018 and 2023 as described in text.

Appendix I

Evaluation of Anthropogenic Impacts on the San Diego Coastal Kelp Forest Ecosystem

Biennial Project Report
Spring 2023 – Fall 2025

Lydia B. Ladah, PhD
James Leichter, PhD
Kristin Riser, BS
Brenna Bulach, MS
Rilee Sanders, MS
Paul K. Dayton, PhD

Scripps Institution of Oceanography
UC San Diego, 9500 Gilman Dr., La Jolla, CA 92093

External Report Submitted to City of San Diego
Public Utilities Department

Evaluation of Anthropogenic Impacts on the San Diego Coastal Kelp Forest Ecosystem

Biennial Project Report
Spring 2023 – Fall 2025

Lydia B. Ladah, PhD
James Leichter, PhD
Kristin Riser, BS
Brenna Bulach, MS
Rilee Sanders, MS
Paul K. Dayton, PhD

Scripps Institution of Oceanography

UC San Diego, 9500 Gilman Dr., La Jolla, CA 92093

Submitted to City of San Diego Public Utilities Department

May 15, 2026

corresponding authors: lladah@ucsd.edu, jleichter@ucsd.edu

Integrative Oceanography Division

Scripps Institution of Oceanography, UC San Diego

9500 Gilman Dr, Mail Code 0227, La Jolla, CA 92093-0227

Evaluation of Anthropogenic Impacts on the San Diego Coastal Kelp Forest Ecosystem: Biennial Project Report, Spring 2023 - Fall 2025

EXECUTIVE SUMMARY

The results presented in this biennial report (spring 2023 to fall 2025) of the City of San Diego's evaluation of anthropogenic impacts on kelp forests program show that the giant kelp forests along the San Diego coastline have experienced reduced persistence over the past decade in several historically stable beds. However, for much of the recent reporting period, the kelp forests appear to have generally benefited from extended periods of cooler than average temperatures, sufficient benthic irradiance for photosynthesis, lower wave heights, and reduced urchin densities and recruitment at most sites, indicating ample nutrient and light exposure for reproduction and growth, and reduced wave and herbivory disturbance. Although spatially variable, as a result, the kelp forests of San Diego County have shown episodic kelp recruitment, with increasing abundance and plant size. For example, during this reporting period, some of the monitoring sites showed giant kelp densities of both early and mature life stages, as well as mean plant size, within the top 10% of the time series dating back to 2007. Mean stipe density and maximum plant size were within the top 20%. These results suggest adequate conditions for giant kelp recruitment and growth at many sites.

The region has experienced strong spatial variability in temperatures, with net cool water and associated nutrient exposure being prominent features of the reporting period. Although monthly bottom temperature anomalies across the region varied by both depth and site, they did show cooler anomalies (compared to the monthly average for 2007 to 2025) across many sites in late 2024 and early 2025, and again at some sites, particularly shallow ones, in late 2025. A recent notable pattern of cooler than average temperatures occurred at 8 m depth at the Point Loma Central site, where much of the kelp recovery has been documented, with periods in 2023 and 2025 registering some of the coldest temperatures measured for the entire time series since 2007. Additionally, the monthly average Scripps pier temperatures during the reporting period compared with the monthly average temperatures for the period from 2007 to 2025, show a pattern of negative (cold) monthly anomalies for much of the reporting period, with cooler than average monthly means for some periods exceeding 2 °C cooling. Cooler temperatures in this region are related to higher nutrient concentrations, as they are inversely correlated at temperatures below 15 °C, which is the approximate temperature below which nitrate becomes available in the water column. The monthly average bottom temperatures at many monitoring sites were below this nutrient threshold temperature proxy of 15 °C for consecutive months during the reporting period. The cooler, nutrient replete waters suggested by the temperatures measured

during the reporting period should have provided ample nutrient exposure which is evidenced in giant kelp recruitment and growth.

While giant kelp recovery has been detected at some sites recently, abundance at other study sites remains historically low. The understory macroalgae that compete with giant kelp for bottom space and light have maintained growth, reproduction and stable densities for the reporting period at some of the monitoring sites, which may have limited giant kelp recruitment and growth. Additionally, invertebrate herbivore densities can influence giant kelp survivorship at all life stages. Some sites and seasons did show herbivore presence, with purple sea urchin densities exceeding 10 per 10 m^2, and with red sea urchin densities exceeding 2 per 10 m^2, falling within the upper 10% of the historical time series dating back to 2007. Along with the densities on the transects at the monitoring sites, recruitment of both sea urchin species was also documented very near some of the monitoring sites. Collectively, these factors are known to constrain giant kelp recruitment and survival, even under otherwise favorable oceanographic conditions.

Overall, giant kelp forest recovery occurred during the period from spring 2023 to fall 2025 yet was spatially variable with reduced densities and plant sizes compared to historical patterns at many sites. The measured recovery was most likely related to the cooler than average benthic temperatures indicating nutrient availability, sufficient bottom light, reduced wave action, and lower sea urchin herbivore densities at some of the monitoring sites during this reporting period.

INTRODUCTION

Kelp forests along the San Diego region provide highly valuable socioecological and socioeconomic services, with importance for coastal protection, habitat for biodiverse fauna and flora, fishing, and recreation, as well as a general cultural significance for the community. The health and resilience of kelp forests are shaped by a complex interplay of coastal oceanography, disturbance regimes, and biotic interactions in the context of a large and growing coastal urban region with myriad potential anthropogenic impacts (Dayton & Tegner 1984, Dayton et al. 1999, Parnell 2015, Parnell et al. 2026). The physical setting and environmental dynamics driving kelp communities in the nearshore environment include the availability of rocky substrata at ~5 to 30 m depth, ocean temperatures, water-column stratification, nutrient delivery, light availability, currents, upwelling intensity, internal waves, and wave-driven disturbance. This suite of factors provides a foundation upon which complex population, community, and patch-level processes unfold and vary at seasonal to annual and decadal scales. Complex interactions between the temporally and spatially variable physical environments and biological processes, especially those affecting kelp reproduction, recruitment, growth, and consumption by herbivores, result in strong spatial variability in kelp abundance, persistence, mortality, and recovery from disturbance. Kelp forests are also sensitive to a range of human impacts including direct harvesting of kelp and associated fish and invertebrate resources, surface run-off, pollution, and potential sewage discharge impacts on water quality, sedimentation, and light availability. The socioeconomic importance of kelp forests and the need to distinguish potential anthropogenic impacts from natural environmental dynamics influencing kelp abundance has motivated extensive, long-term research and monitoring including the present effort supported by the City of San Diego in partnership with researchers at Scripps Institution of Oceanography, UC San Diego.

Overall, abundance of the dominant, canopy forming giant kelp *Macrocystis pyrifera* along the San Diego coast has been extremely variable over the ~60-year duration of reliable scientific observations, with apparent sharp declines in many locations over the past decade. The San Diego region is generally characterized by weak and variable upwelling compared with regions further north, with nearshore sub-thermocline nutrient delivery highly sensitive to small changes in thermocline depth, internal wave energy, and horizontal advection. Both the physical environment and the phenology of *M. pyrifera* show predictable variability throughout years. Seasonal storms (e.g. November through March) and wave events are a dominant source of physical disturbance that can open space on benthic rocky surfaces and reduce kelp canopy cover, facilitating greater light penetration. During spring and early summer (e.g. late March through June), increased day length and periods of enhanced episodic upwelling result in generally cold water-column temperatures and exposure to nitrate-rich water

along the coast, which are associated with the highest rates of kelp reproduction, recruitment and the appearance of juvenile kelp sporophytes with rapid subsequent kelp growth. Conversely, mid to late summer and fall are typically marked by the highest annual kelp biomass and surface canopies, which reduce bottom light availability and coincide with warmer surface temperatures and increased water-column stratification, and a deepened thermocline and correlated nutracline, leading to limited nutrient supply to shallow waters with resulting decreased kelp growth. Although many of these processes affect the region in a general seasonal fashion, they are also known to vary at much smaller spatial scales.

For example, internal tides and internal bores are important along the San Diego coastal shelf resulting from the interaction of water-column density stratification with tidal forcing along the steep topography of offshore bathymetric features (Jackson & Winant 1983, Leichter et al. 2023). The spatiotemporally variable interactions of stratification and tidal forcing with bathymetry can result in short-term pulses of cold, nutrient-rich water that can temporarily enhance photosynthesis and growth, even during otherwise nutrient-poor periods such as periods of reduced upwelling. This tidally driven mechanism is thought to result in spatial variability in kelp canopy cover responses, which can vary by depth and proximity to the offshore features (Leichter et al. 2023).

Additionally, interannual and decadal climate oscillations further modulate nutrient dynamics in the California Current. For example, during El Niño events, regional warming, strong stratification with deepening thermocline depth, and suppressed upwelling of nutrient enriched waters severely limit nutrient delivery, reducing kelp growth and canopy extent (Dayton et al. 1999). In contrast, La Niña years generally bring enhanced cooling, increased nitrate, and often large kelp canopy expansions. Furthermore, widespread climatic variations such as the Pacific Decadal Oscillation (PDO) and longer term ‘regime shifts’, with generally warmer temperatures and reduced nutrient availability influence the baseline upon which other scales of oceanographic variability occur (Parnell et al. 2010). These oceanographic regimes at varying spatiotemporal scales interact strongly with biological processes such as competition, herbivory, and recruitment, and in conjunction with variable anthropogenic impacts, create temporal mosaics visible in each discrete kelp forest along depth gradients.

Light is also an important variable for kelp forests as kelps depend on photosynthesis to grow and require adequate light thresholds for gametogenesis of microscopic stages on the benthos, essential for subsequent kelp recruitment. Light dynamics contribute to fine-scale patchiness in kelp recruitment and growth and can vary across small spatiotemporal scales. Light attenuation varies significantly in space and time in coastal San Diego waters due to sediment inputs, phytoplankton blooms, storm-driven runoff, and resuspension events. Turbidity reduces benthic light availability,

very likely suppressing kelp recruitment. Light attenuation also varies with storm cycles, and summer stratification, and the quantity and quality of benthic light is greatly impacted by the canopies of understory kelps and turf algae, resulting in bottom shading. The spatial extent of where giant kelp can be found is mainly controlled by the availability of hard substrate at depths where light penetration is adequate for gametogenesis, recruitment and growth since the plants recruit and begin their life cycle at the bottom. Light is attenuated in a logarithmic fashion with depth in the ocean, and attenuation is wave length dependent across the photosynthetic spectrum.

The critical process of photosynthesis for kelp metabolism and growth is dependent on light radiation across wavelengths between ~400 and 700 nanometers. Light energy within this bandwidth is generally considered to be of primary importance for photosynthesis and is termed Photosynthetic Active Radiation (PAR). Longer wavelength red light is most rapidly attenuated with depth, while shorter wavelength blue light, most important for gametogenesis, a critical step in recruitment in Laminarian kelps including *M. pyrifera* (Lüning & Dring, 1975), penetrates further into the water column. Light availability limits the deepest depths that giant kelp can exist along the mainland shelf of southern California to ~25 m. The main limiting factor for kelp recruitment at depth, besides hard substrate, is the availability of light for gametogenesis, the lower limit of which has been estimated as a quantum dose of ~0.4 mol of photons m^{-2} d^{-1} (Deysher & Dean, 1984), and ~0.7 mol of photons m^{-2} d^{-1} for early sporophyte growth (Dean & Jacobsen, 1984). Thus, light availability is highly variable, responding to changes across seasons, atmospheric and water column conditions, and shading by kelps and other macroalgae on the seafloor. These factors influencing light availability all likely contribute strongly to variation in kelp abundance, along with disturbance, temperature and nutrient availability.

Wave exposure also exerts both constructive and destructive roles (Parnell et al. 2026). Moderate wave energy enhances nutrient exchange around kelp blades, reduces sediment accumulation, and helps maintain open substrate for recruitment. Extreme winter storm events, however, remove adult kelp plants, create canopy gaps, and trigger successional transitions. These disturbance-driven openings are the foundation of patch dynamics in kelp forests and show complex patterns also resulting in spatiotemporal variability (Dayton et al. 1984, Dayton et al. 1999, Seymour et al. 1989).

The physical drivers described above interact strongly with biological drivers of recruitment and growth, such as herbivory and competition. For example, sea urchins (notably purple urchins, *Strongylocentrotus purpuratus* and red urchins, *Mesocentrotus franciscanus*) are among the most influential herbivores in kelp forest ecosystems in San Diego County (Tegner & Dayton 1977, Parnell et al. 2026). At moderate densities, urchins contribute to the processing of detritus and the transfer of kelp-derived energy to benthic food webs, facilitating resource availability to a suite of

detritivores and invertebrates. However, urchin populations can increase rapidly, likely in response to stochastic influences on recruitment and post-settlement mortality, especially when predator control is weakened by overfishing of natural urchin consumers such as sheephead (*Bodianus pulcher*) and spiny lobsters (*Panulirus interruptus*). Urchin populations can proliferate and intensify grazing on kelp stipes and entire holdfasts in urchin feeding fronts. This can transform kelp forests into areas virtually devoid of macroalgae, termed urchin barrens, where macroalgal biomass is markedly depleted and ecosystem productivity declines (Steneck et al. 2002).

Other herbivores in the system such as abalone (*Haliotis spp*.) and snails (such as the wavy turban snail, *Megastrea undosa*) occupy both intertidal and subtidal reef habitats within kelp forests, impacting kelp forests by grazing as well as by occupying space as competitors for other grazers such as sea urchins. Abalone historically supported productive fisheries and competed for space with other herbivores. At historical abundances, abalone foraging likely influenced kelp canopy dynamics and created space for new kelp recruitment, contributing to habitat heterogeneity. However, abalone populations have declined markedly due to overharvesting and disease since the 1970s. Grazing by abalone and other gastropods can reduce epiphytic growth on kelp surfaces and may contribute to recycling of organic matter within kelp forests, although their ecological impact is generally thought to be more subtle than that of more aggressive herbivores such as sea urchins.

Sea urchins, due to their potential for overgrazing, are linchpins of possible alternate ecosystem states (e.g. kelp forest vs. urchin barrens), while snails and abalone comprise important consumers that influence algal turnover, nutrient cycling, and food web complexity. Understanding the roles of these invertebrates in the kelp forests of San Diego and their population variation, especially in response to anthropogenic impacts, is crucial for ecosystem-based management aimed at maintaining resilient kelp forest ecosystems under changing environmental conditions. Taken together, grazers interact with predators and understory algal competitors for space and light, kelp primary production, patch dynamics and oceanographic conditions to structure kelp forests in the San Diego region.

Additionally, competition for hard substrate and light is central to canopy-forming giant kelp recruitment, resilience and recovery. Understory algal species, including the benthic kelps *Pterygophora californica*, *Eisenia arborea*, and *Laminaria farlowii*, are strong spatial competitors that dominate the benthos when *Macrocystis pyrifera* canopy is reduced by warm temperatures, nutrient deficits, or storms. The stipitate *Pterygophora* kelp produces approximately 1 to 1.5 m stipes with relatively large blades impacting benthic light availability for microscopic kelp gametogenesis, an important step in kelp recruitment, and by out-shading smaller kelp recruits and juveniles (Dayton & Tegner 1984, Dayton et al. 1999). *Eisenia* is also a stipitate kelp which forms long-

lived and high-temperature tolerant individuals that can monopolize space for years and can out-shade *M. pyrifera* recruits. Stipitate understory kelps such as *Eisenia* and *Pterogophora* may serve as ecosystem engineers providing similar ecosystem services at least at small scales that are provided by canopy-forming giant kelp. *Laminaria*, a foliose kelp with blades up to several meters in length, can thrive in low-light microhabitats once canopy cover declines and prevent new recruitment by both out-shading other algae and by its whiplash effect during wave-exposure with shear impacts on a wide region of the benthos due to their flexible foliose nature. Additionally, other algae including other competitors for space and light such as invasive *Sargassum* species and foliose red macroalgae are also important components of algal assemblages.

Patch dynamics research in southern California shows that kelp forests are mosaics of different aged patches that experience asynchronous disturbance, recovery, and competitive interactions (e.g. Dayton et al. 1984, Parnell 2015, Parnell et al. 2026). Wave-driven disturbance, thermal, light and nutrient impacts on growth and recruitment, and grazing intensity all interact to produce spatially stable patches, transitional patches, and degraded patches of both canopy-forming and understory kelps and other algae, often within meters of each other. Differential patch assemblages can also alter hydrodynamic, light and sediment microhabitats in different manners. For example, understory canopies reduce near-bed flow, trap sediments, and can limit spore settlement and juvenile recruitment. In nutrient-poor years, some benthic algae may expand dramatically and inhibit canopy-forming giant kelp recovery even after oceanographic conditions improve. Thus, competition is not static and is tightly coupled to oceanographic variability and disturbance history (Parnell et al. 2026).

In response to a range of concerns about potential anthropogenic impacts on kelp abundance in the San Diego region, researchers at the Scripps Institution of Oceanography (SIO) have partnered with the City of San Diego Ocean Monitoring Program. The SIO group has conducted regular surveys of the kelp forests off San Diego County since the 1970’s and now regularly surveys the kelp forests off Point Loma, La Jolla and North County (see Figure 1). These surveys represent a continuation of ecological studies that began at SIO in the Point Loma (PLKF) and La Jolla (LJKF) kelp forests and continue at some of the sites established in the 1970's and 1980's (Dayton & Tegner 1984). Additional study sites have been established more recently in both of those kelp forests as well as in kelp forests off northern San Diego County (North County - NCKF). PLKF and LJKF are the largest contiguous kelp forests off the Western United States Coast and are historically one of the most studied kelp forest systems in the world.

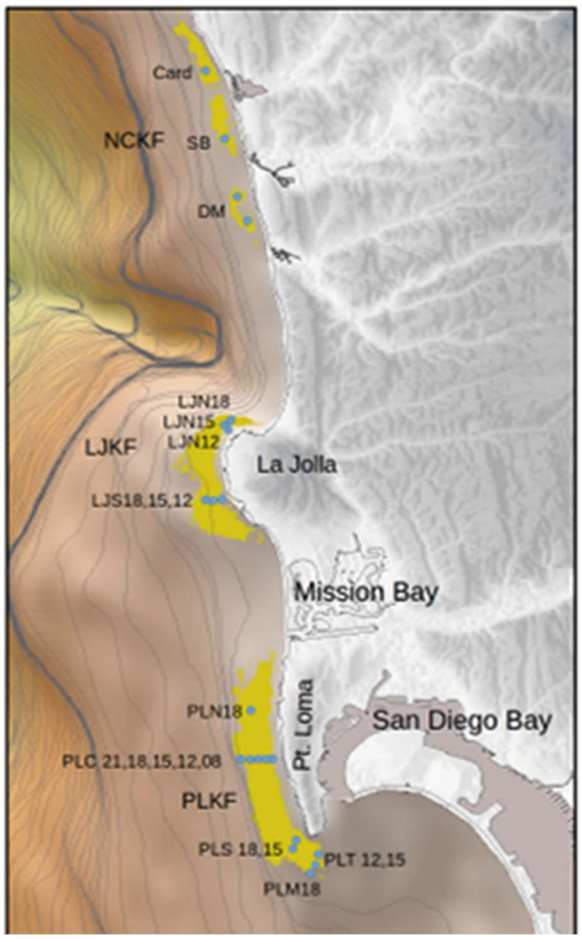


Figure 1: Map of San Diego region kelp forests (contours in meters) with yellow shading showing where surface canopy was observed from 1967-1999 in aerial photographs. NCKF, LJKF, and PLKF refer to the kelp forests off North County, La Jolla, and Point Loma, respectively. Light blue circles show the 20 permanent quarterly monitoring sites (see methods). North County, Card = Cardiff, SB = Solana Beach, DM = Del Mar; La Jolla, LJS = La Jolla South at 12, 15, and 18 m, and LJN = La Jolla North at 12, 15, and 18 m; and Point Loma, PLN = Point Loma North at 18 m, PLC = Point Loma Central (long-term monitoring sites) at 8, 12, 15, 18 and 21 m, PLS = Point Loma South at 15 and 18 m, PLT = Point Loma Tip at 12 and 15 m, and PLM = Point Loma Mouth at 18 m.

METHODS

For this biennial reporting period (spring 2023 to fall 2025), a subset of the most relevant data collected is presented. The full methods of the kelp forest monitoring program are described in a recent paper (Parnell et al. 2026) and in all previous city of San Diego kelp forest monitoring program reports. The most important methods relevant to this report are repeated here for convenience and clarity.

Macroalgae, invertebrates and bottom temperatures are monitored at 20 permanently established study sites (Figure 1). Algae and invertebrates are monitored along four replicate parallel permanent band transects oriented perpendicular to shore (25 x 4 m bands separated 3-5 m apart) except at the Del Mar study site where two sets of band transects are located ~1300 m apart due to the small size and fragmented shape of the rocky benthic habitat at that kelp forest.

The main components of the kelp forest monitoring program include measuring algal density (and for some species, benthic cover), growth, reproductive condition and recruitment; invertebrate densities; sea urchin demography (size distributions to monitor

for episodic recruitment); collection of ocean bottom temperature (a partial proxy of ocean nutrient status); and collection of benthic light data as photosynthetically active radiation.

Algae

Several stages of the giant kelp, *Macrocystis pyrifera*, are enumerated to identify recruitment events and to follow the fate of recruiting cohorts into adulthood. Giant kelp life stages include adults (≥4 stipes), pre-adults (>1 m tall but with <4 stipes), bifurcates (a late post-recruitment stage indicated by the presence of a split in the apical meristem which represents the primary dichotomous branching event), and pre-bifurcates (very early post-settlement blade stages lacking the initial dichotomous split). Stipe numbers are counted and recorded for each adult plant on each visit.

Conspicuous macroalgal species/groups are enumerated within 5 x 2 m (10 m^2) contiguous quadrats along the band transect lines at all sites.

Reproduction and growth of the giant kelp, *Macrocystis pyrifera*, and the understory kelps, *Pterygophora californica* and *Laminaria farlowii*, are measured on mapped or tagged plants along the central Point Loma study sites. Growth of *M. pyrifera* is monitored by counting the number of stipes on each mapped plant one meter above the substratum. Reproductive state (i.e. spore production by the sporophyte stage) is represented by the size of the sporophyll bundle (germ tissue) at the base of each plant. Reproductive state for each plant is ranked according to the ordinal scale: 0 representing no sporophylls present, 1 sporophylls present but no sori (sites of active reproduction) development, 2 sporophylls with sori only at the base of sporophylls, 3 sporophylls with sori over most of the sporophyll surface, 4 sporophylls with sori over all of the sporophyll surface, and 5 sporophylls with sori over all of the sporophyll surface releasing zoospores.

Growth of *Pterygophora californica* is determined by the method of DeWreede (1984). A hole (6 mm) is punched into the midrib of the terminal blade ~30 mm from the base of the blade, and another hole is punched monthly at the same location. The distance between the two holes represents the linear growth of each blade. Reproductive effort for *P. californica* is evaluated by a count of the total number of sporophyll blades on each plant and the number with active spore production. Growth of *Laminaria farlowii* is determined in a similar manner to *P. californica*. A 13 mm diameter hole is punched 100 mm from the base of each blade and is repeated each visit. The distance between the two holes represents the linear growth of each blade. The reproductive status of *L. farlowii* is evaluated as the percentage of each blade covered by sori.

Invertebrates

All conspicuous sessile and mobile invertebrates are enumerated annually in spring within the 10 m^2 quadrats.

Size frequencies of red (*Mesocentrotus franciscanus*) and purple (*Strongylocentrotus purpuratus*) sea urchins are measured semi-annually (spring and fall) for >100 individuals, when possible, for each species located near all the study sites except for the NCKF sites which do not have adequate sea urchin densities. Sea urchins are collected in 1 m^2 quadrats in suitable substrate within 50 m of each study site. Suitable substrate includes ledges and rocks which can be fully searched for sea urchins as small as 2 mm. Sea urchins are measured using calipers and then returned to their place of capture. Sea urchin recruitment is evaluated using the population size frequency data.

Temperature

Sea bottom temperatures are recorded at 10 min intervals using ONSET Tidbit recorders (accuracy and precision = 0.2˚C and 0.3˚C, respectively) at the permanent central Point Loma study sites, and at a range of additional study sites. Recently, we have updated to higher resolution and more reliable oceanographic-quality temperature recorders at all sites for redundancy and accuracy, especially with the goal of characterizing both high-frequency forcing and long-term trends.

Temperature is one of the dominant driving factors in the system and is relatively easy to measure. Temperature has a direct impact on kelp growth and reproduction, and, due to the strong inverse relationship with nutrients in the Southern California Bight region (Ladah 2003, Parnell et al. 2010), serves as a valuable proxy for nutrient availability as well. In this region, cooler temperatures tend to have enriched nitrogenous nutrients especially in the form of nitrate, which is important for kelp metabolism and inversely correlated with temperatures below ~15 °C. The physical environment of the coastal ocean is highly variable with respect to temperature across a range of scales from minutes to hours to seasons, and thus collection of high frequency temperature data is critical to evaluating the dynamics of the system.

Light

Bottom light as Photosynthetically Active Radiation (PAR) is measured at three depths off central Point Loma along a cross-shore transect near the permanent algal study sites but in areas without giant kelp canopy. These areas are dominated by low growing understory algae thus precluding shading by nearby giant kelp canopy. The measurement sites off Point Loma are located at 9, 15, and 24 m depth. Submarine light is also measured off southern La Jolla at a depth of 24 m. PME miniPAR loggers equipped with LICOR LI-192 quantum sensors are used to measure bottom

Photosynthetically Active Radiation (PAR). Sampling is conducted at 1-minute intervals, and the sensors are equipped with external wipers cleaning the sensors at 4-hour intervals to reduce biofouling and maintain sensor accuracy.

RESULTS

Temperature

SIO pier surface and bottom temperature

For much of the reporting period, the temperatures measured at the UCSD-SIO pier at both the surface and the bottom (5-7 m depth) exceeded the regional 15 °C temperature proxy for nitrate, with the primary exceptions occurring during winter and spring of 2023 and 2025 at both depths and, additionally, during winter and spring of 2024 at the bottom (Figure 2a). However, when comparing the monthly average Scripps pier temperatures for the reporting period with the monthly average temperatures for the period from 2007 to 2025, a pattern of negative (cold) monthly anomalies can be seen for most of this reporting period, with monthly averages falling below the zero-anomaly line, except for the periods from November 2023 to March 2024, and in August 2024 and 2025 (Figure 2b). For some periods, the negative monthly anomalies neared or exceeded 2 °C below the mean (cooler than average), for example in June 2023 and from November 2024 to January 2025.

Benthic temperature at the long-term Point Loma Central kelp forest monitoring sites

The time series for the Point Loma Central benthic cross-depth sites from 2007 to 2025 measured at 8, 12, 15, 18 and 21 m depth are shown in Figure 3 (a-e) with the red dotted line marking the approximate temperature below which nitrogenous nutrients, particularly sub-thermocline nitrate, become available in the region (temperature proxy for ~1 µM nitrate is near 15 °C) (Zimmerman & Robertson 1985, Ladah 2003, Parnell et al. 2010, Leichter et al. 2023).

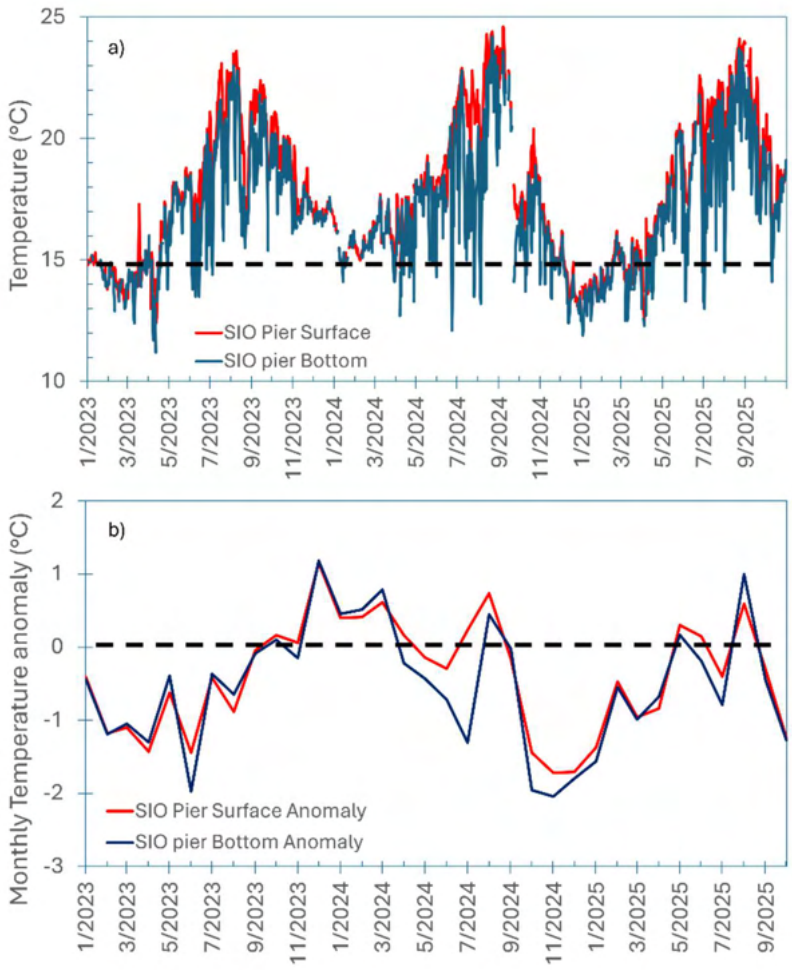


Figure 2: a) Temperature records taken at the surface (red) and bottom (blue) (5-7m depth) of the Scripps pier from January 2023 to December 2025 with the dotted black line showing 15 °C (temperature proxy for nutrients, see methods, with temperatures above this threshold generally being nutrient poor) and b) monthly mean temperature anomaly at the surface and bottom compared to the 2007-2025 monthly means, with the dotted line showing the zero (negative numbers are colder than the long-term mean for that month). See UCSD shore stations for details.

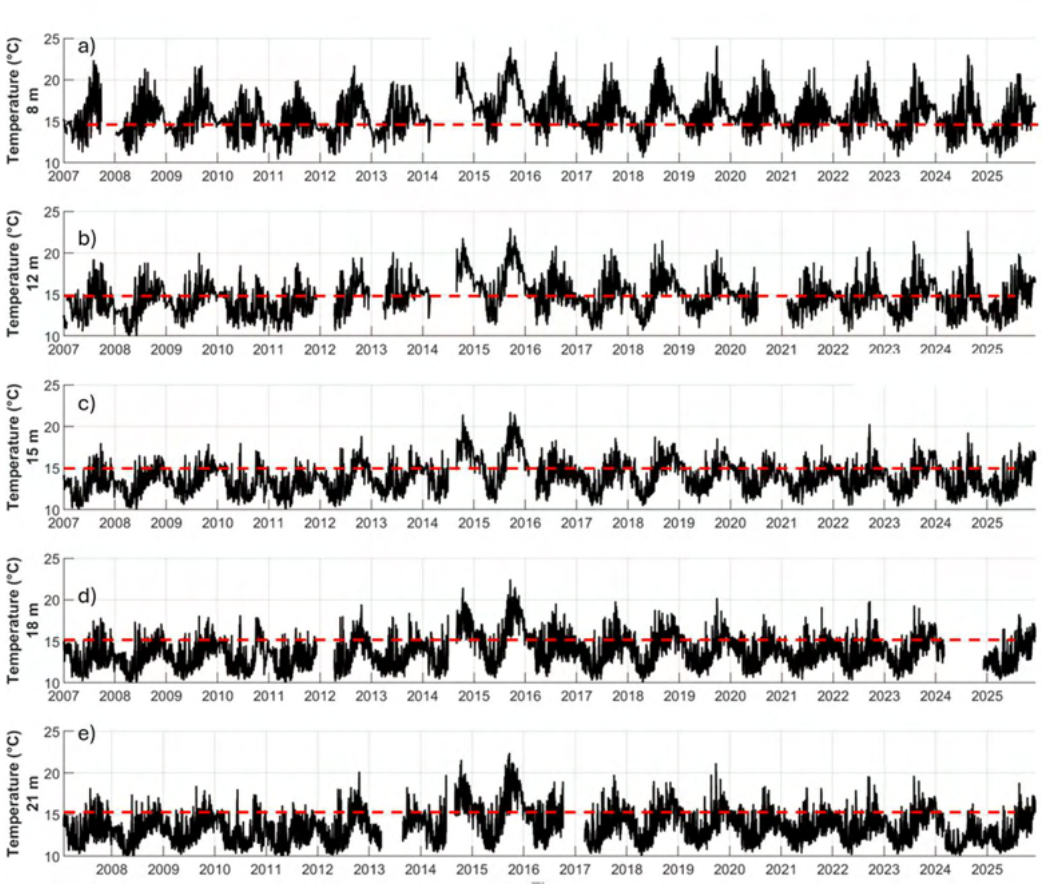


Figure 3: Benthic temperature measured at the cross-depth long-term monitoring sites from 2007 to 2025 at Point Loma Central at: a) 8 m depth, b) 12 m depth, c) 15 m depth, d) 18 m depth, and e) 21 m depth. Red dotted line shows the 15 °C temperature used as a nutrient proxy (see text).

Overall, for the time series back to 2007, the years 2008 and 2011 showed the coldest temperatures measured at all sites, while 2014 and 2015 showed the warmest. Across the sites, there is a clear pattern of increasing nitrate availability (estimated by temperature proxy) with depth, shown by the proportion of the time series below the 15 °C temperature, ranging from 41% at 8 m, 61% at 12 m, 74% at 15 m, 78% at 18 m and 80% at 21 m. In addition, cool temperatures and associated nitrate exposure appear to have been prominent features for the 2023-2025 period. A recent notable pattern of cooler than normal temperatures can be seen particularly at 8 m depth, showing periods in 2023 and 2025 registering some of the coldest temperatures measured for the entire time series since 2007.

Monthly mean benthic temperatures calculated from the data in Figure 3 for the Point Loma Central sites fell below the 15 °C nutrient-threshold proxy for multiple consecutive months at several sites during the 2023-2025 reporting period (Figure 4a). At the 8 m site, monthly mean temperatures remained below this threshold from January to June 2023, January to May 2024, and November 2024 to May 2025. At the 12 m site, monthly mean temperatures were below 15 °C from January to July 2023, January to July 2024, and October 2024 to July 2025. At the 15 m site, temperatures were below the threshold from January to August 2023, January 2024 to July 2025, and again from September to October 2025. At the 18 m site (noting a gap in the record due to a lost temperature logger from March to November 2024), temperatures were below 15 °C from January to August 2023, January to February 2024, and December 2024 to October 2025. At the 21 m site, temperatures were below the threshold from January to August 2023 and throughout the period from January 2024 to October 2025. Late February through early June represents the primary recruitment window for the giant kelp, *Macrocystis pyrifera*, and the cooler, nutrient-replete conditions indicated by these monthly averages during the reporting period would therefore be expected to provide sufficient nutrient exposure to support recruitment and early growth.

Comparing the monthly averages for the current reporting period from 2023 to 2025 (using data from Figure 4a, and using only months with 90% of the data available for that month) to the average monthly temperatures for the entire time series from 2007 to 2025 (data in Figure 3), many of the Point Loma Central benthic sites showed negative monthly anomalies (Figure 4b). For example, the monthly mean temperature at the 21 m site during October–December 2024 was more than 2 °C colder than the long-term average for those months (2007–2025). Similarly, the 8 m, 12 m, and 15 m sites also exhibited cold anomalies exceeding 2 °C below the long-term mean in December 2024. Consecutive months exceeding 1 °C below the long-term average (cold) anomaly for 8 m, 12 m and 15 m depth included the period from November 2024 to February 2025 (through March 2025 for 8 m depth), the months from May 2024 to February 2025 for the 21 m site, and again in September and October 2025 at the 8 m site. At 18 m depth, data for 2024 were limited; however, monthly mean temperatures in January and February 2025 were also more than 1 °C below the long-term average.

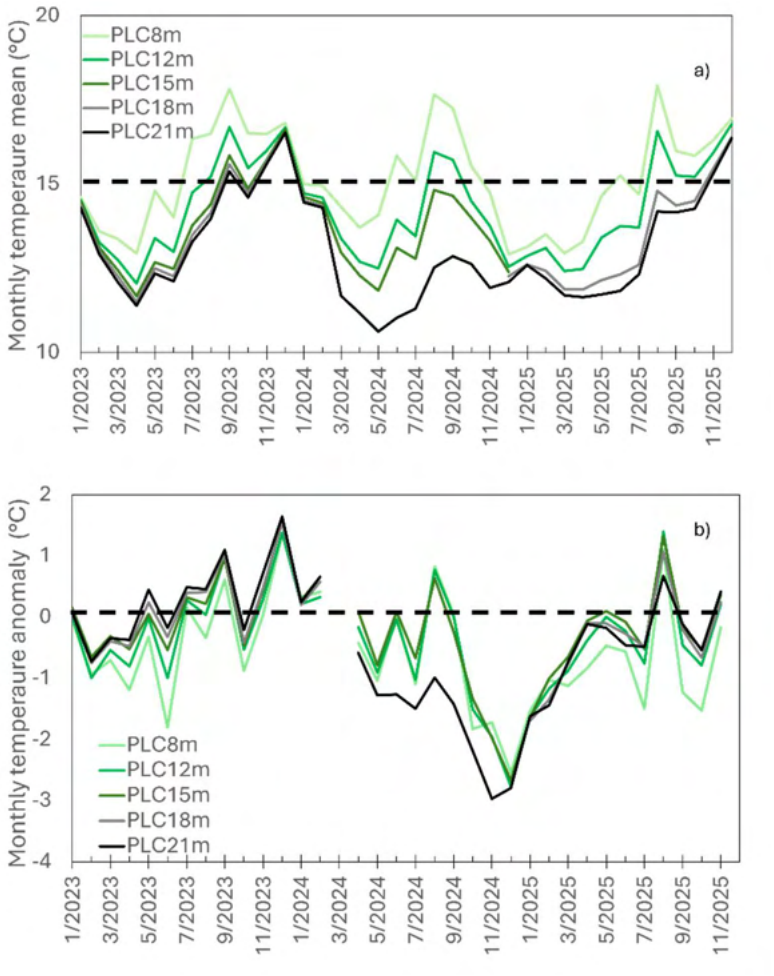


Figure 4: a) Zoom of benthic temperature measured from 2023 to 2025 at Point Loma Central 8 m, 12 m, 15 m, 18 m, and 21 m depth. Black dotted line shows the 15 °C temperature used as a nutrient proxy (see methods); b) Mean monthly temperature anomaly (deviation from the monthly means for the entire time series shown in Figure 3, from 2007 to 2025) at Point Loma Central at 8 m, 12 m, 15 m, 18 m, and 21 m depth. Black dotted line shows the zero-anomaly mark. Above (below) this line, monthly mean temperatures were warmer (colder) than the monthly mean for 2007-2025 period.

Light

Photosynthetically active radiation (PAR) significantly varies with depth in the absence of canopy cover, with the amount reaching deeper waters (24 m in Point Loma and La Jolla) being significantly less than in shallower waters (for example at 9 m depth in Point Loma) (Figure 5). Using the threshold corresponding to 0.7 moles of photons m^{-2} day^{-1} as the requirement for juvenile *Macrocystis* growth (Dean & Jacobsen, 1984), near 75% of the time series for the shallowest site (9 m depth) and near 50% for the 15 m site was above this threshold (Figure 5a,b), whereas for the deeper sites at 24 m depth at both La Jolla and Point Loma (Figure 5c,d), more than 85% of the time series was below this threshold, suggesting light limitation for juvenile growth in deeper waters for most, if not all (for example in 2020 at the 24 m sites), of the year. However, for the reporting period from 2023 to 2025, an increase in peak PAR can be seen particularly at the 15 m and 24 m sites for spring and summer 2023 compared to data available from previous years (Figure 5b-d).

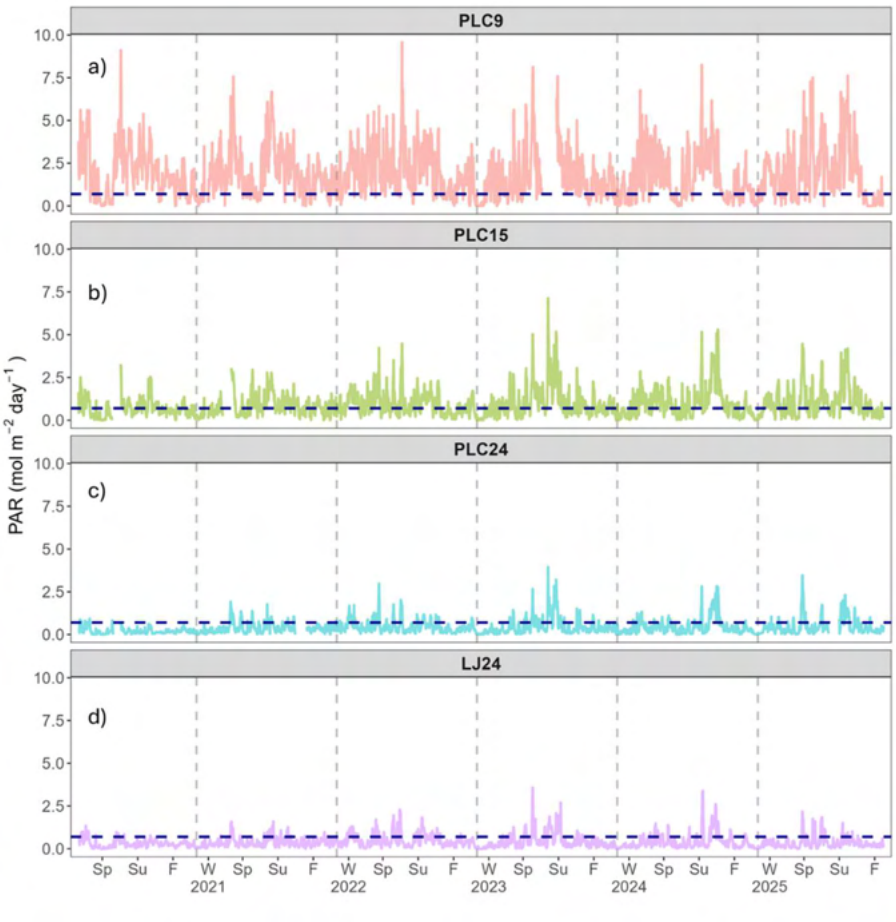


Figure 5: Benthic photosynthetically active radiation (PAR) taken near the kelp monitoring sites at, a) Point Loma Central 9 m depth, b) Point Loma Central 15 m depth, c) Point Loma Central 24 m depth, and d) La Jolla 24 m depth. The dark blue dotted line shows the 0.7 moles of photons m^{-2} day^{-1} threshold, the requirement for juvenile *M. pyrifera* growth (per Dean & Jacobsen, 1984).

Waves

Using the Point Loma South 191 CDIP buoy station (cdip.ucsd.edu), significant wave height (H_s) and wave period were used to explore wave impacts for the reporting period (Figure 6), as well as historically. Wave height and wave period are important factors influencing kelp dynamics, as larger wave heights and longer-period swells increase the depth of orbital motion and wave speed, enhancing shoaling and allowing wave energy to impact plants in deeper waters. Additionally, because wave energy scales with the square of wave height, a doubling of wave amplitude (wave height) results in a fourfold increase in wave energy (see Seymour et al. 1989).

Looking at the time series back to 2007, some of the highest historically significant wave heights (H_s) occurred on January 6, 2023, and February 22, 2023. The February 22, 2023, event ranks as the eighth highest H_s recorded since January 2017, exceeded only by several events in 2017 and 2021. For example, on January 6, 2023,

H_s exceeded 4.5 m with a long period of 18 s, while on February 22, 2023, H_s exceeded 5 m. Within the reporting period, January 2023 also exhibited the highest monthly mean H_s, at 2.1 m. In contrast, monthly mean H_s during much of 2024 and 2025 were generally at least 0.5 m lower. For example, the monthly mean H_s in January 2025 was nearly half that observed in January 2023.

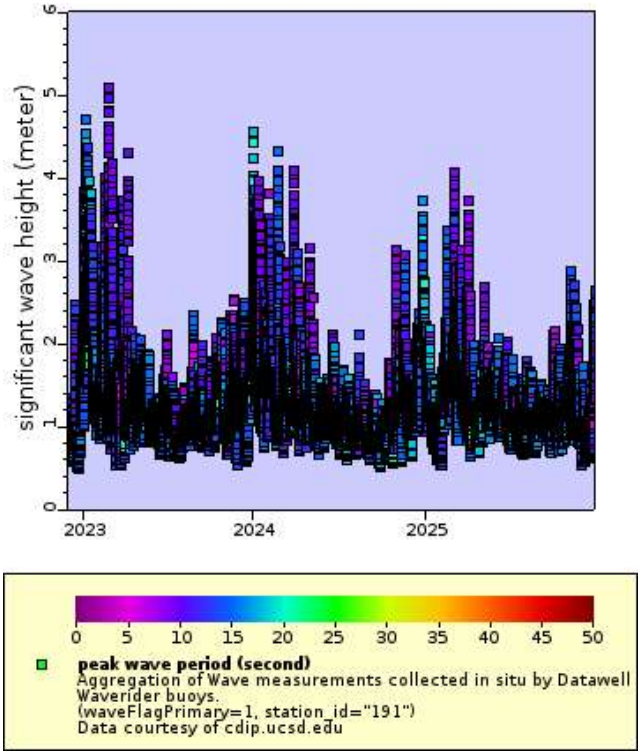


Figure 6: Aggregation of Wave measurements collected *in situ* by the Datawell Waverider buoy at station 191 Pt Loma. The CDIP Station 191 is a buoy maintained by the Coastal Data Information Program (CDIP) at Scripps Institution of Oceanography. It continuously measures swell height, wave period, direction, and marine weather conditions. The figure shows wave period in colors and significant wave height on the figure in meters. See cdip.ucsd.edu for details.

Macrocystis pyrifera (giant kelp)

Recruitment

Since 2007, the density of pre-bifurcate (or blade stage plants, Figure 7) and bifurcate plants (small juveniles, Figure 8) have shown a pattern of episodic recruitment, with recent recruitment pulses detected during the reporting period (Figure 9,10). For example, for the pre-bifurcate stage, the spring and summer seasons of the years 2007, 2010-2016, 2019 and 2024 show mean densities greater than 10 individuals per 10 m^2 with La Jolla South 18 m showing a relatively large recruitment event in spring 2024, reaching a mean of 36 individuals per 10 m^2. For the bifurcate stage or small juvenile plant recruitment, the spring and summer seasons of the years 2010-2012, and 2015-

2016 show the highest densities exceeding a mean of 10 individuals per 10 m^2, in particular at the La Jolla North 15 m and La Jolla South 18 m, Point Loma Central 18 m and 21 m, and Solana Beach sites.

For this reporting period (Figure 9,10), the spring season of 2024 at the La Jolla South 12 m, 15 m, and 18 m, and at Point Loma South 18 m sites, were among the top 10% pre-bifurcate densities for the entire series dating back to 2007, along with spring 2025 at the Point Loma Central 18 m site. For the bifurcate stage, the summer of 2023 and the spring and summer of 2024 were also among the top 10% of mean bifurcate densities at the La Jolla South 18 m site. The most recent patterns suggest an increase in recruitment after a period of recruitment failure.

Pre-adults

Since 2007, the density of pre-adults (Figure 11) reached its peak in summer 2010 and spring 2015 in the Solana Beach site near a mean of 20 individuals per 10 m^2, followed by summer 2016 at the La Jolla South 18 m site.

For this reporting period (Figure 12), the summer and fall seasons of 2023 (at the La Jolla South 18 m and Point Loma South 18 m sites), the summer and winter season of 2024 (at the La Jolla South 18 m site), the spring season of 2025 (at the La Jolla South 18 m site), and the summer and fall season of 2025 (at the Point Loma Central 18 m site) were within the top 10% mean densities of pre-adults, suggesting adequate conditions for growth of recruits to reach the pre-adult stage.

Adults

Since 2007, the highest density of adult plants (Figure 13) occurred in fall 2010 and summer 2015 in Solana Beach, and in fall 2016 and winter and spring of 2017 at the La Jolla South 18 m site, exceeding a mean of 5 adult individuals per 10 m^2.

For this reporting period (Figure 14), the mean adult density per 10 m^2 at the La Jolla South 18 m site was within the top 10% of the entire time series dating back to 2007, with mean densities of adults in spring, summer and fall of 2025, exceeding a mean of 2 adults per 10 m^2, also suggesting adequate conditions for continued adult survivorship and growth.

Stipe density

Since 2007, the highest mean stipe density (Figure 15), an indicator of the biomass carrying capacity of the system, occurred at the Cardiff (fall 2013 and winter 2014) and Point Loma 21 m (spring 2013) sites, exceeding 80 stipes per 10 m^2.

For this reporting period (Figure 16), the mean stipe density at the La Jolla South 18 m site, at 34 stipes per 10 m^2 for fall 2025 falls within the top 20% of the time series

dating back to 2007, suggesting that although stipe density is currently somewhat lower than in previous years, conditions remain adequate to maintain critical giant kelp biomass.

Adult plant size (as stipe counts)

Since 2007, the largest mean plant size (using stipe counts per individual) (Figure 17) was detected in spring and summer of 2022 at the Point Loma Central 15 m site, exceeding a mean of 74 stipes per plant. The Point Loma Central 15 m site dominated the series showing the largest mean plant size exceeding 50 stipes per plant for spring and summer 2010, and fall 2021 through fall 2022, as well as the Solana Beach site with 54 stipes per plant in fall 2025.

For this reporting period (Figure 18), the Point Loma Central 15 m site in winter 2023, the La Jolla South 15 m site from summer 2023 to spring 2024, the Point Loma Mouth 18 m site in spring and summer 2025, and the Solana Beach site in summer and fall 2025 were among the top 10% of the time series dating back to 2007 in mean plant size, all above a mean of 35 stipes per plant, again suggesting that conditions were adequate to maintain somewhat larger plants.

Since 2007, historically the largest plants (maximum stipe counts per plant) (Figure 19) were found at the La Jolla South 18 m site with a maximum of 130 stipes per plant in summer 2014 and in Cardiff in summer and fall 2010 with maxima of 117 and 128 stipes per plant, respectively. The periods and sites with the maximum plant size reaching 100 stipes or greater included Cardiff in summer and fall 2013; La Jolla North 15 m in summer and fall 2014; La Jolla North 18 m in summer 2009, 2010 and 2012; La Jolla South 12 m in fall 2013; La Jolla South 18 m in spring and summer 2014; Point Loma Central 8 m in fall 2011 and summer 2013; Point Loma Central 12 m in summer 2022, Point Loma Central 15 m in summer and fall 2011, Point Loma Central 18 m in summer 2010, spring and summer 2013; Point Loma Central 21 m in summer 2010; and Solana Beach in summer and fall 2013, and spring, summer and fall 2014.

During the reporting period (Figure 20), the largest plants, falling within the top 20% of observed sizes, occurred at the Point Loma Central 8 m site in summer 2023 and the Point Loma Mouth 18 m site in summer 2025, with maxima exceeding 70 stipes per plant. The recent documentation of larger plants at various sites does indicate that although they are not as large as in previous decades or prior to the marine heat wave of 2024-2015, larger plants do still exist in the system suggesting adequate conditions to maintain mature plant biomass.

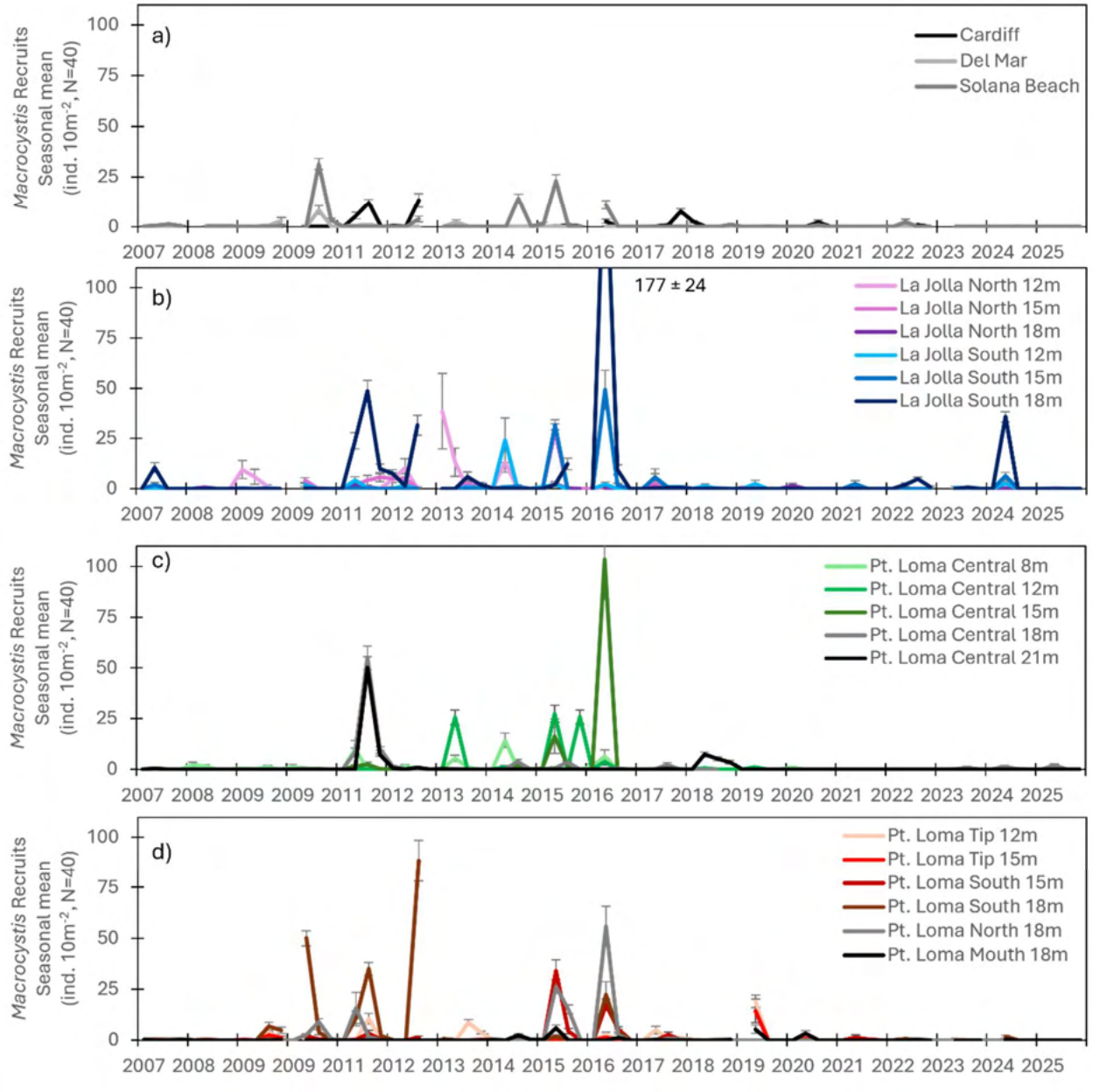


Figure 7: Density of *Macrocystis pyrifera* recruits (number of individual pre-bifurcate or blade stage individuals, shorter than 1 m); seasonal means (Winter 2007 to Fall 2025) from quarterly monitoring of 40 quadrants of 5 x 2 m^2 each, at, a) North County sites, b) La Jolla sites, c) Point Loma Central long-term sites, and d) Point Loma additional sites. Error bars show standard error of the mean.

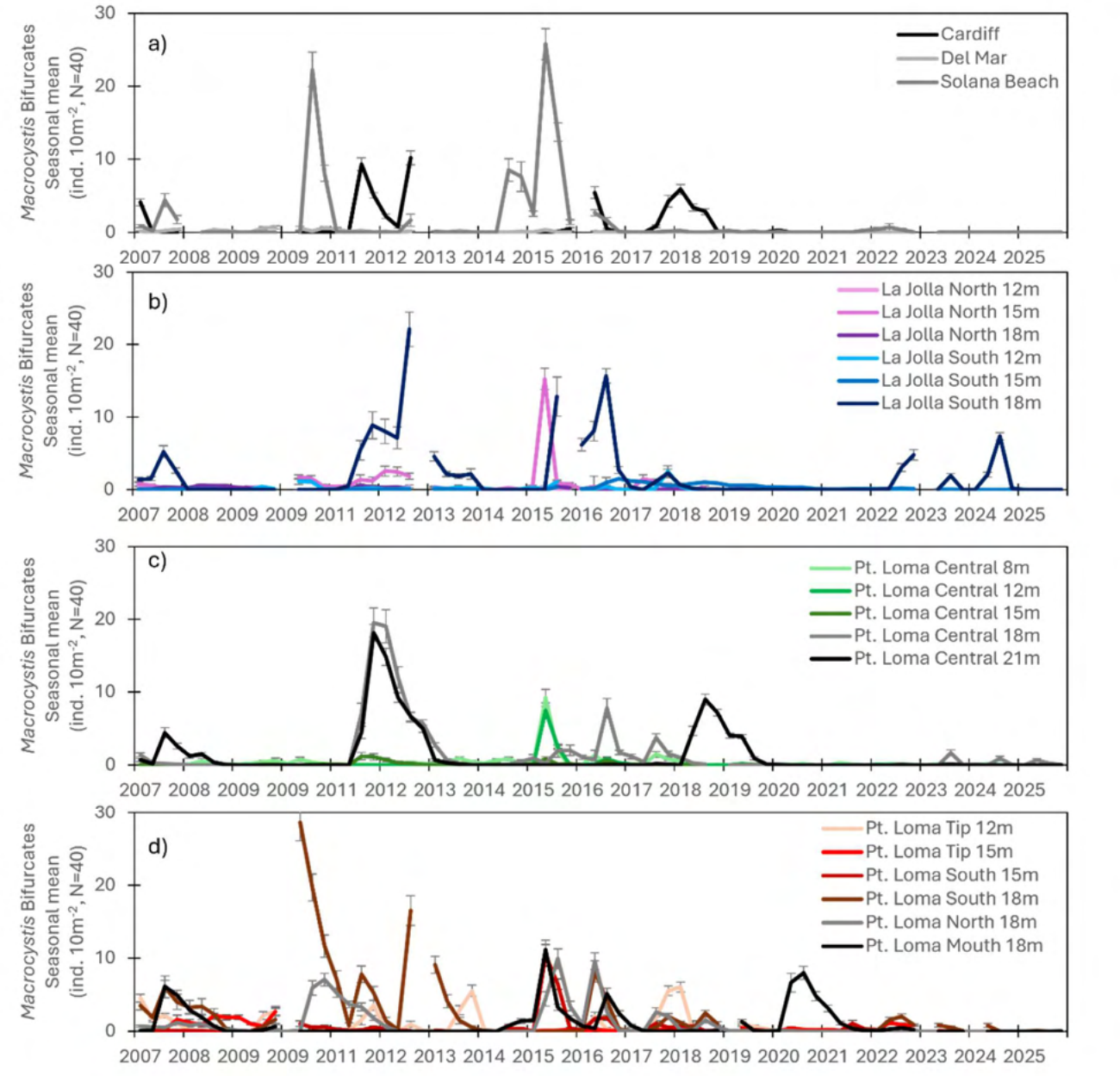


Figure 8: Density of *Macrocystis pyrifera* small juveniles (number of bifurcated individuals shorter than 1 m); seasonal means (Winter 2007 to Fall 2025) from quarterly monitoring of 40 quadrants of 5 x 2 m^2 each, at, a) North County sites, b) La Jolla sites, c) Point Loma Central long-term sites, and d) Point Loma additional sites. Error bars show standard error of the mean.

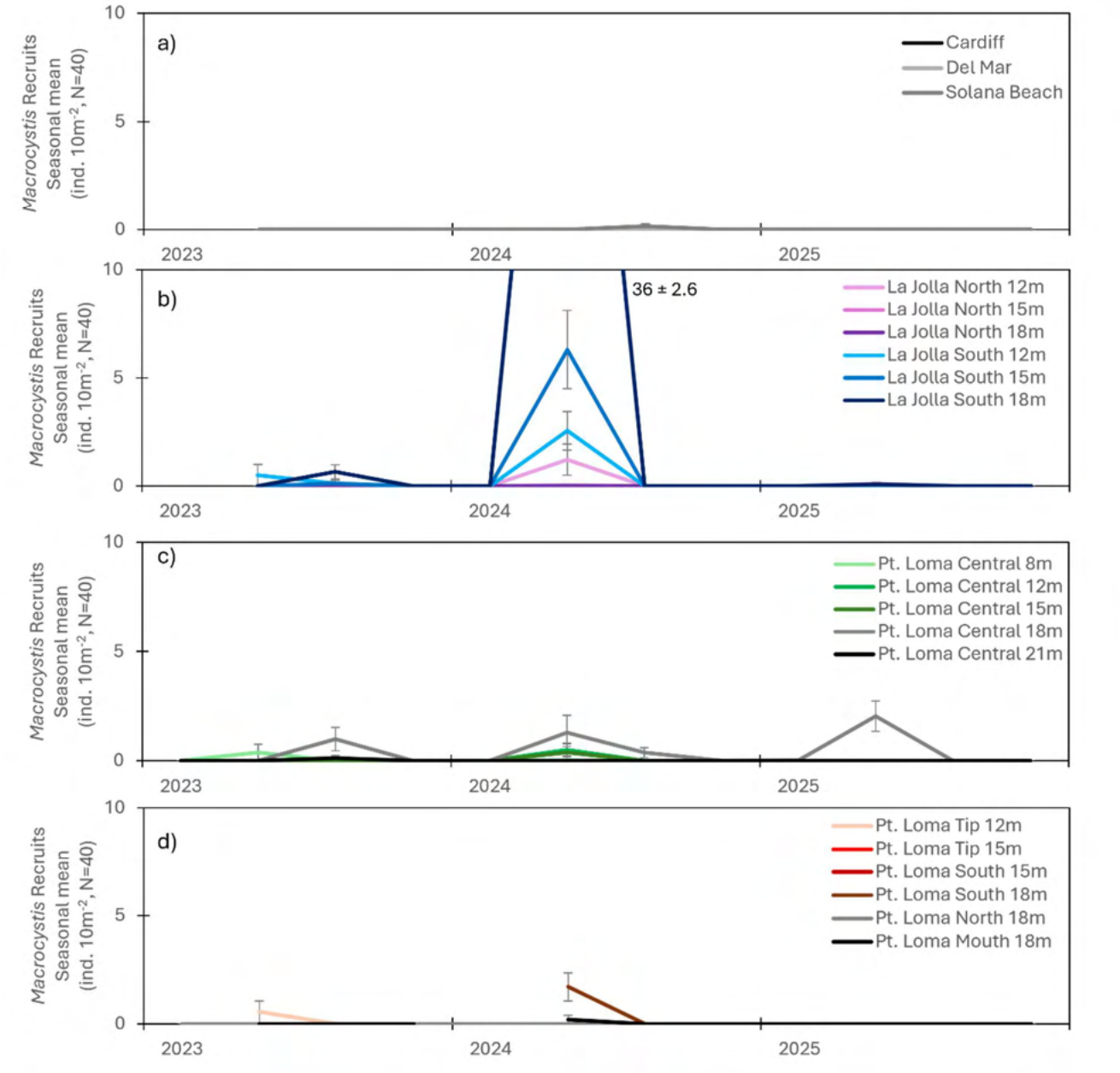


Figure 9: Zoom for reporting period (2023-2025) (note change of scale) of density of *Macrocystis pyrifera* recruits (number of individual pre-bifurcate or blade stage individuals, shorter than 1 m); seasonal means from quarterly monitoring of 40 quadrants of 5 x 2 m^2 each, at, a) North County sites, b) La Jolla sites, c) Point Loma Central long-term sites, and d) Point Loma additional sites. Error bars show standard error of the mean.

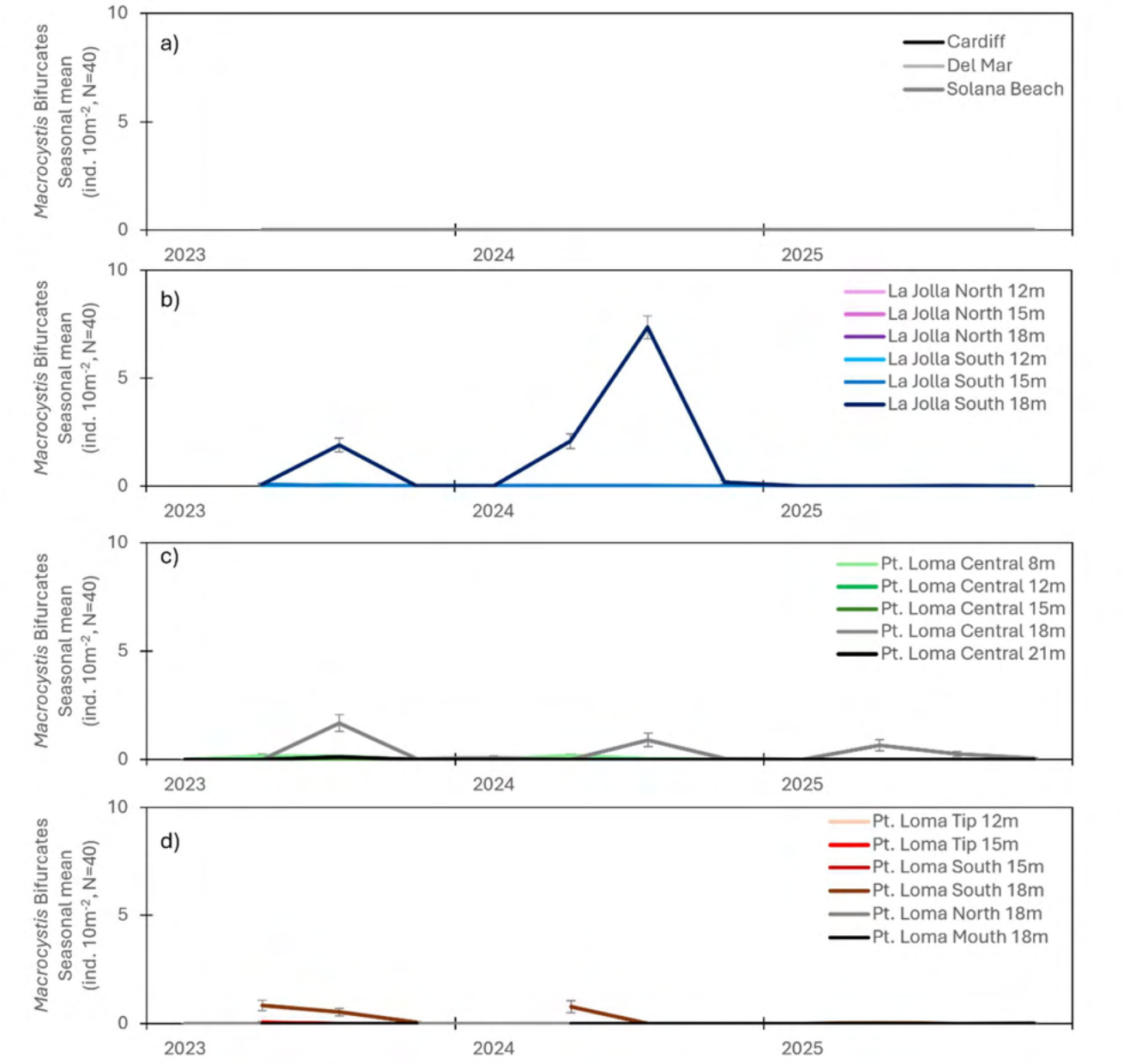


Figure 10: Zoom for reporting period (2023-2025) (note change of scale) of density of Mac*rocystis pyrifera* small juveniles (number of individual bifurcated individuals, shorter than 1 m); seasonal means from quarterly monitoring of 40 quadrants of 5 x 2 m^2 each, at, a) North County sites, b) La Jolla sites, c) Point Loma Central long-term sites, and d) Point Loma additional sites. Error bars show standard error of the mean.

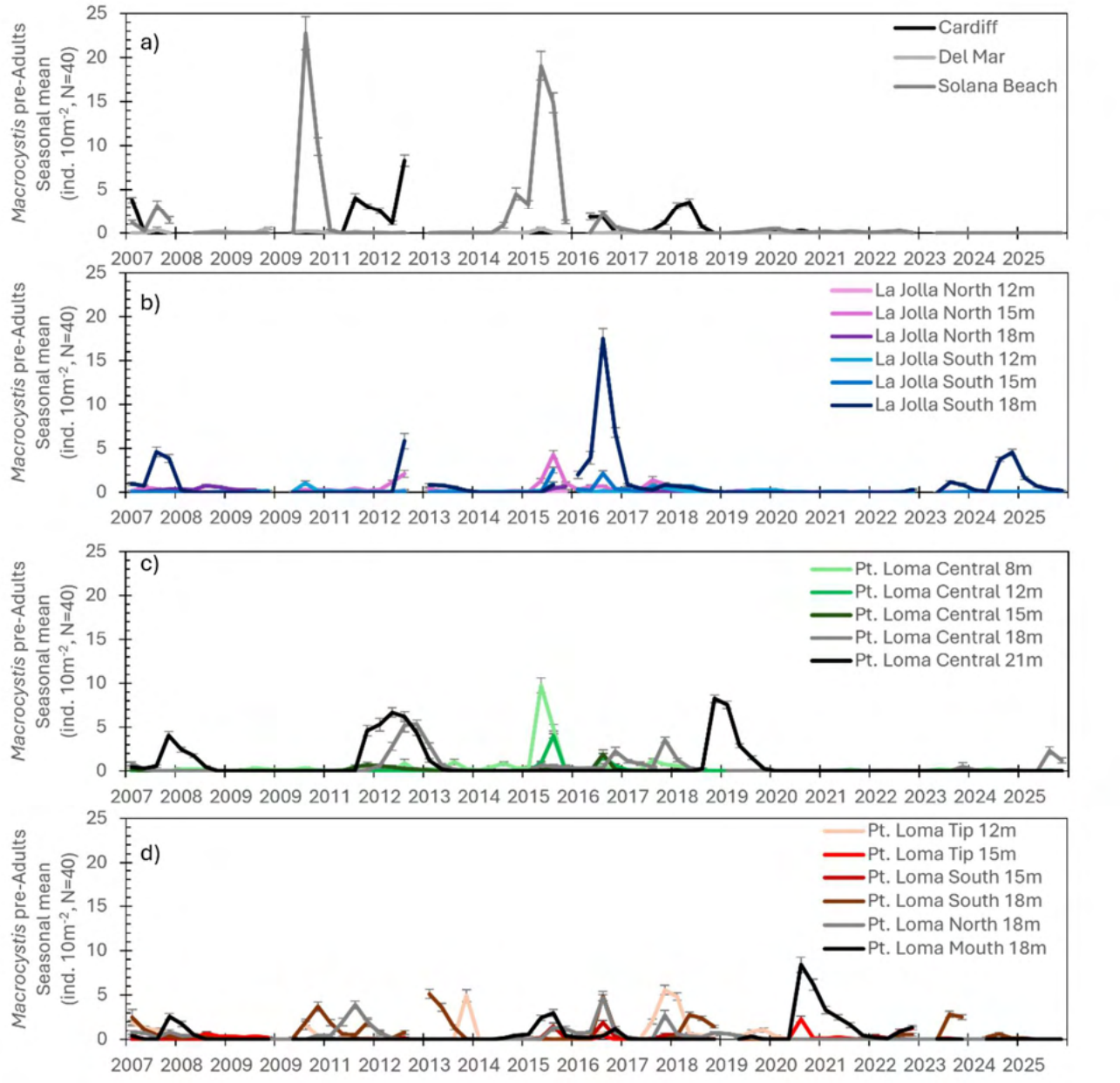


Figure 11: Density of *Macrocystis pyrifera* pre-adults (number of individuals with ≥ 2 and < 4 stipes longer than 1m); seasonal means (Winter 2007 to Fall 2025) from quarterly monitoring of 40 quadrants of 5 x 2 m^2 each, at, a) North County sites, b) La Jolla sites, c) Point Loma Central long-term sites, and d) Point Loma additional sites. Error bars show standard error of the mean.

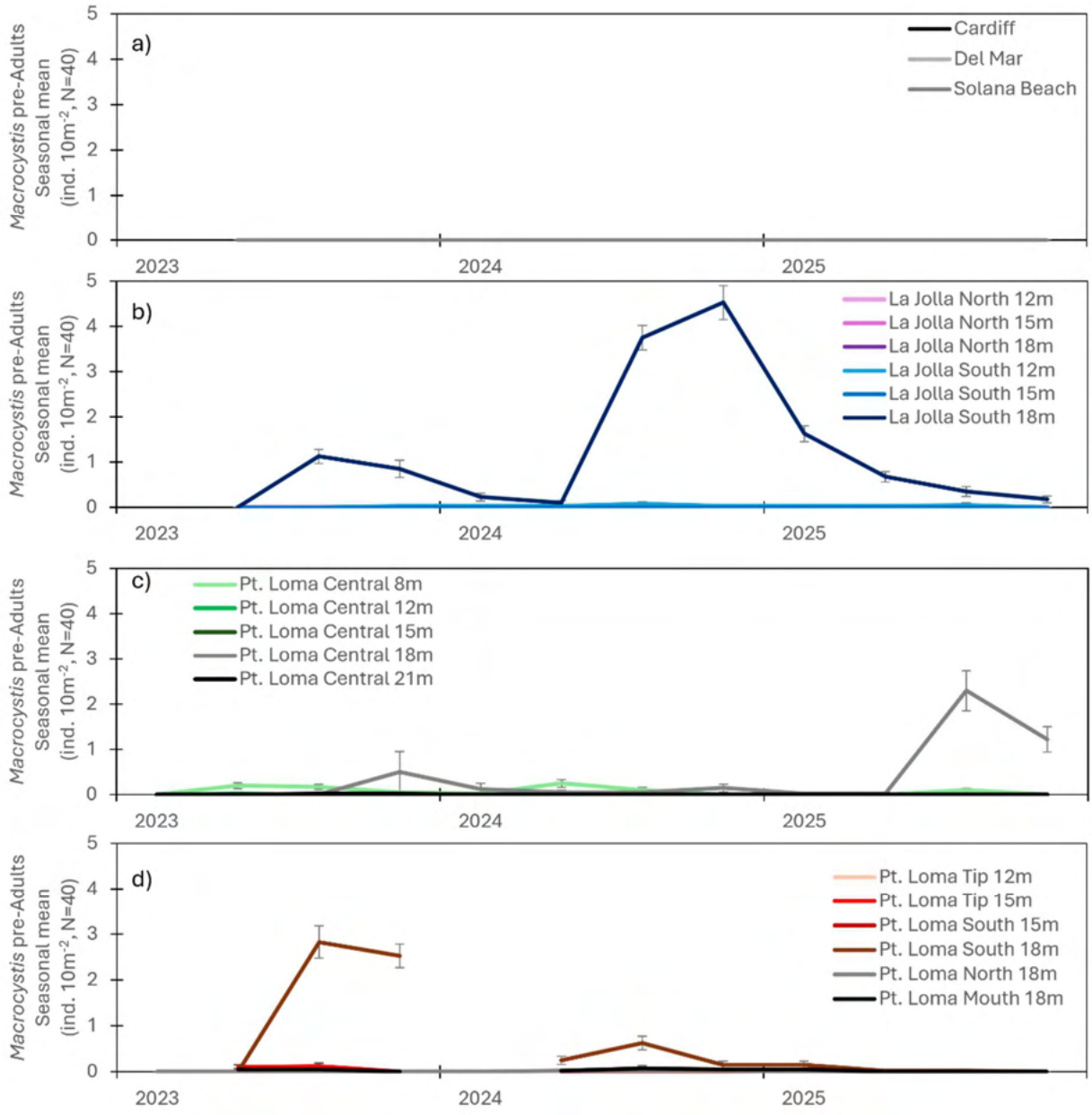


Figure 12: Zoom for reporting period (2023-2025) (note change of scale) of density of *Macrocystis pyrifera* pre-adults (number of individuals with ≥ 2 and < 4 stipes longer than 1m);); seasonal means from quarterly monitoring of 40 quadrants of 5 x 2 m^2 each, at, a) North County sites, b) La Jolla sites, c) Point Loma Central long-term sites, and d) Point Loma additional sites. Error bars show standard error of the mean.

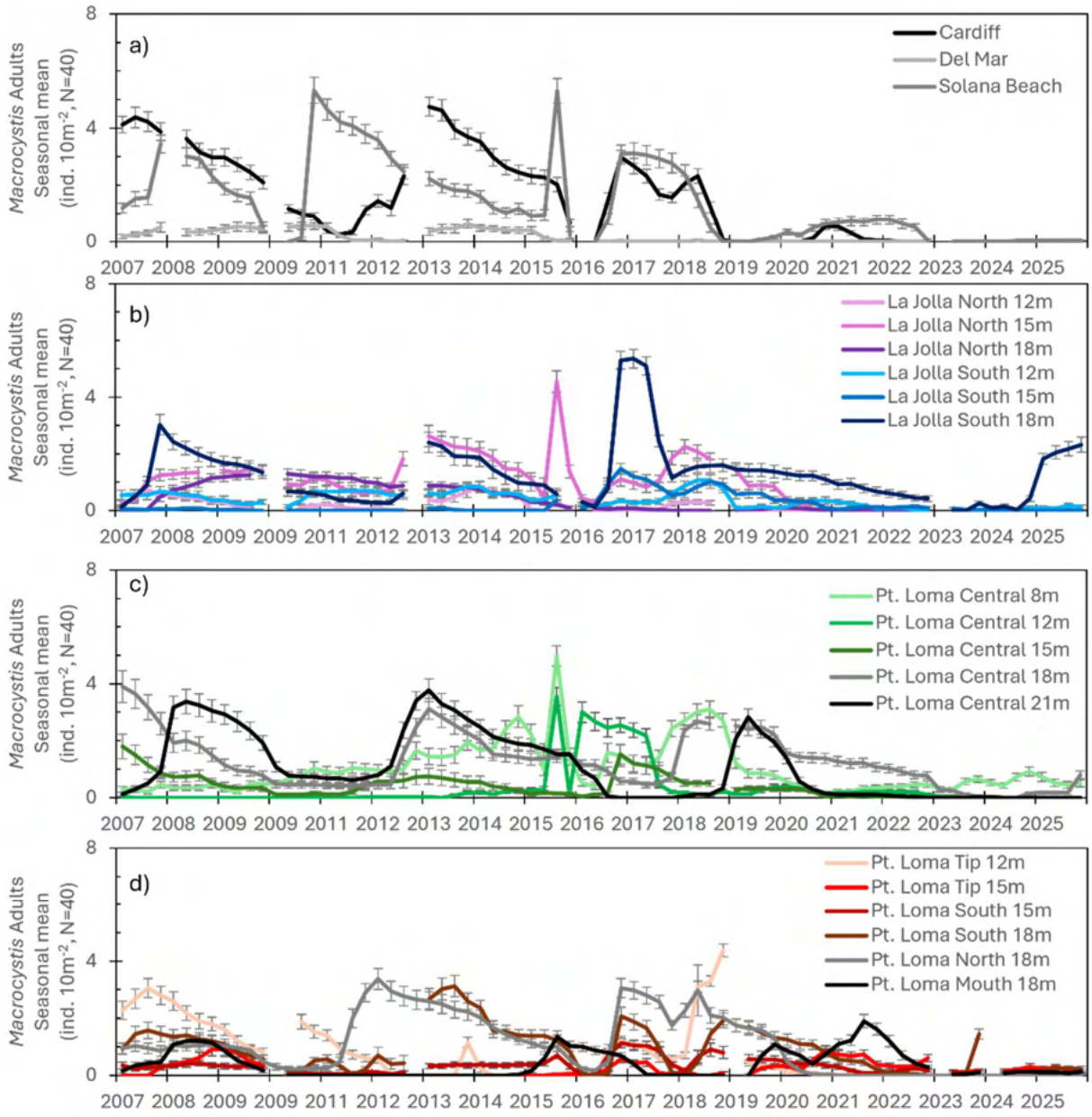


Figure 13: Density of *Macrocystis pyrifera* adults (number of individuals with ≥ 4 stipes longer than 1m); seasonal means (Winter 2007 to Fall 2025) from quarterly monitoring of 40 quadrants of 5 x 2 m^2 each, at, a) North County sites, b) La Jolla sites, c) Point Loma Central long-term sites, and d) Point Loma additional sites. Error bars show standard error of the mean.

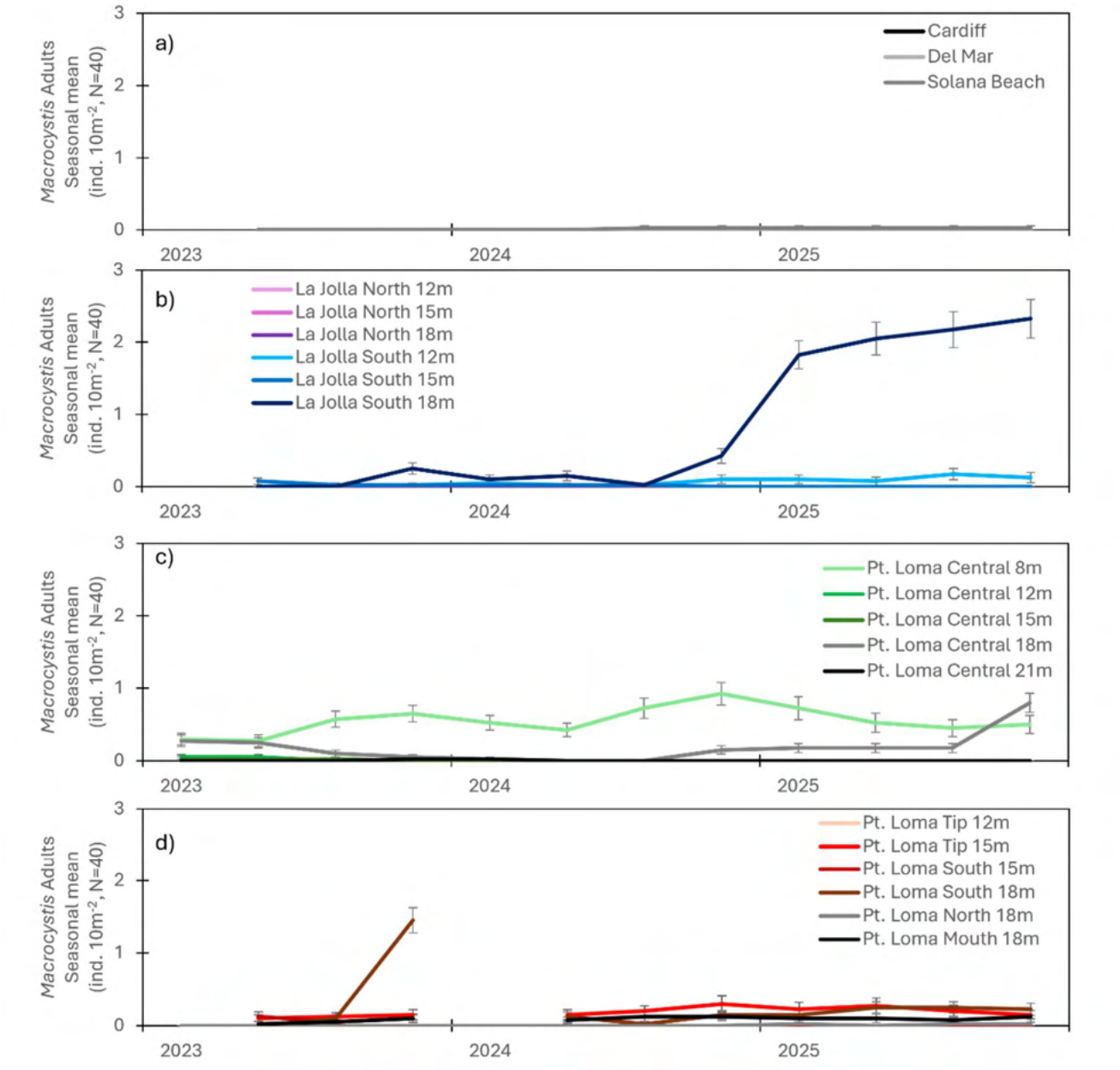


Figure 14: Zoom for reporting period (2023-2025) (note change of scale) of density of *Macrocystis pyrifera* adults (number of individuals with ≥ 4 stipes longer than 1m); seasonal means from quarterly monitoring of 40 quadrants of 5 x 2 m^2 each, at, a) North County sites, b) La Jolla sites, c) Point Loma Central long-term sites, and d) Point Loma additional sites. Error bars show standard error of the mean.

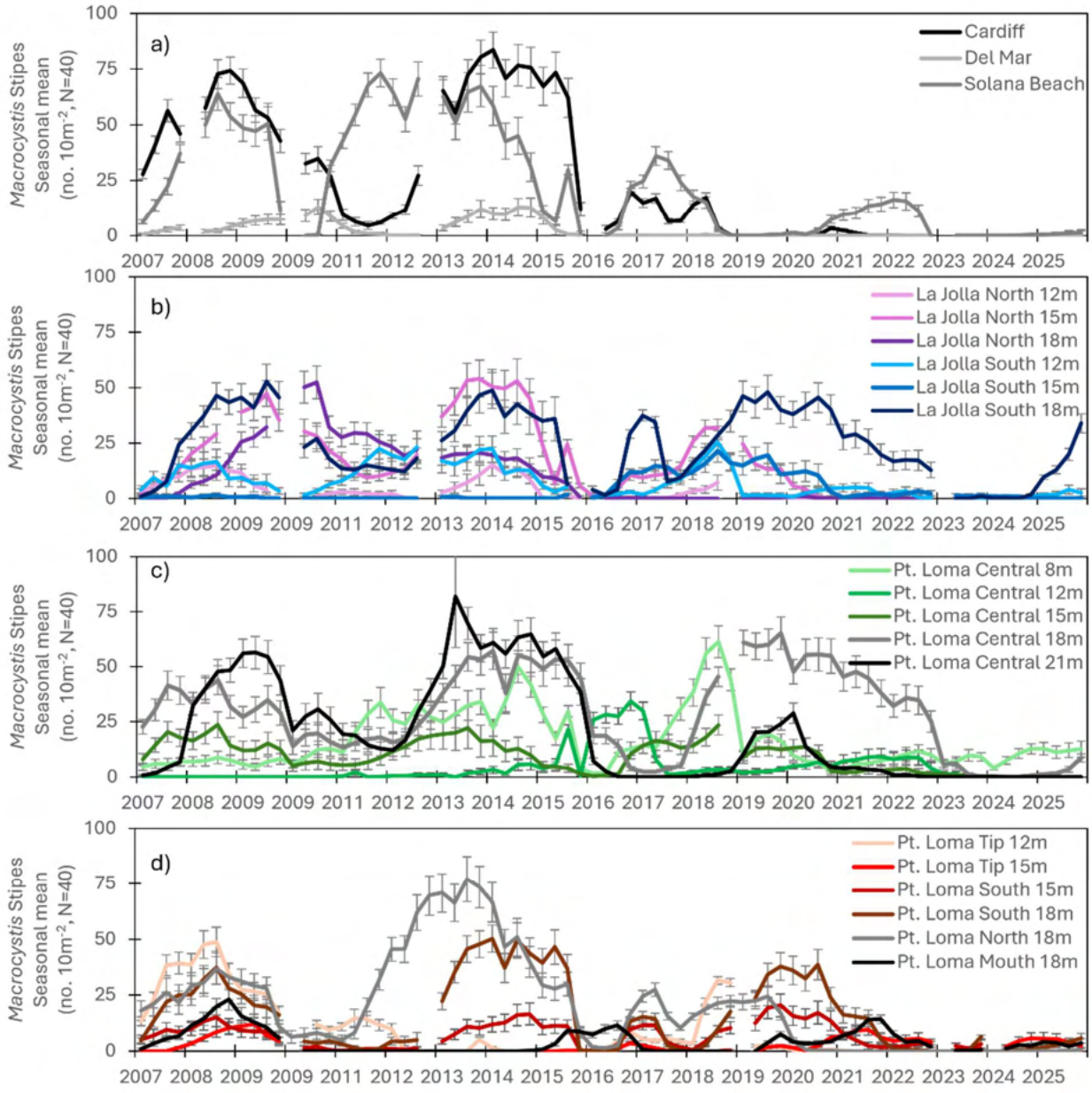


Figure 15: Density of *Macrocystis pyrifera* stipes (number of stipes longer than 1m); seasonal means (Winter 2007 to Fall 2025) from quarterly monitoring of 40 quadrants of 5 x 2 m^2 each, at, a) North County sites, b) La Jolla sites, c) Point Loma Central long-term sites, and d) Point Loma additional sites. Error bars show standard error of the mean.

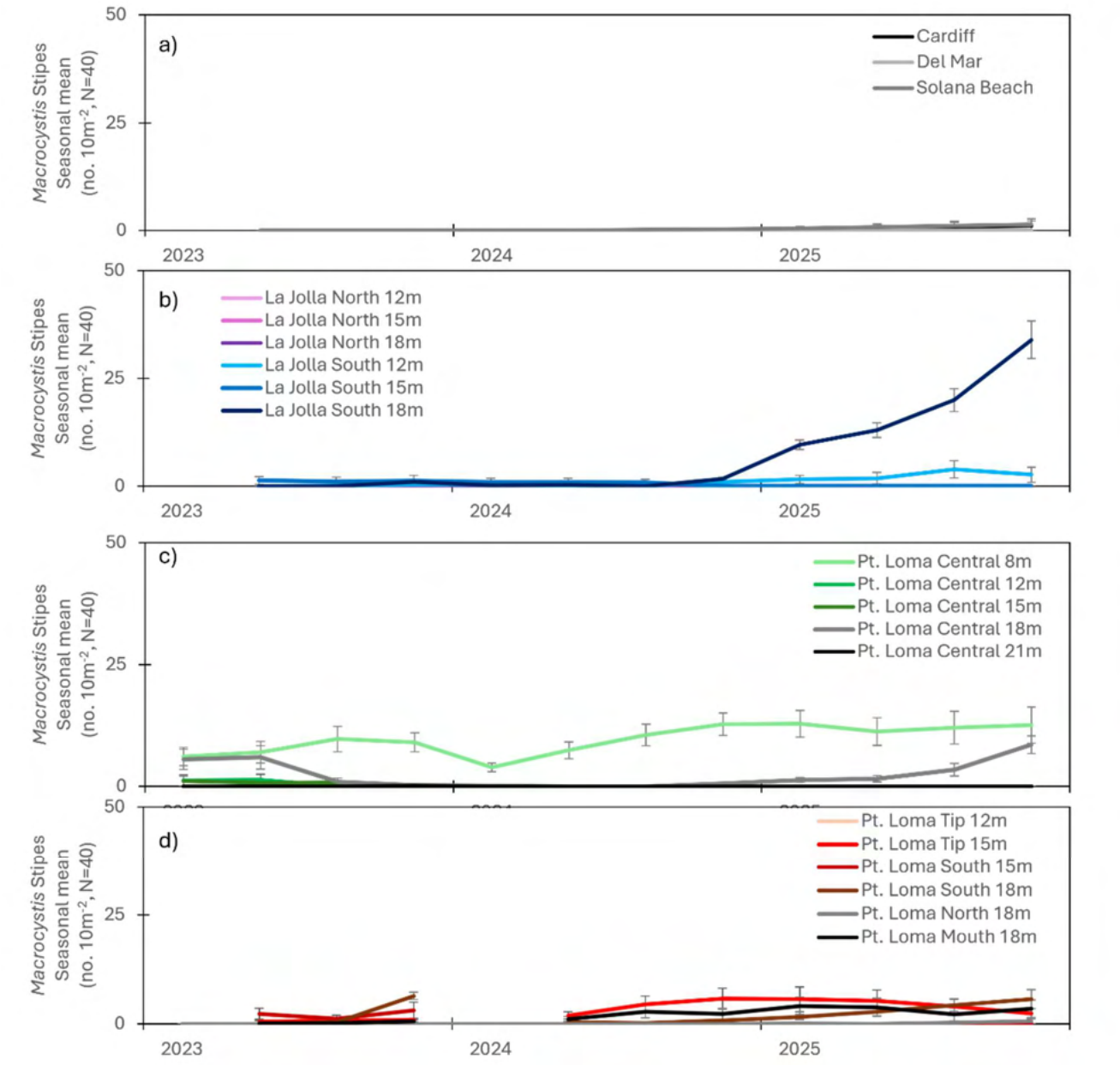


Figure 16: Zoom for reporting period (2023-2025) (note change of scale) of density of *Macrocystis pyrifera* stipes (number of stipes longer than 1m); seasonal means from quarterly monitoring of 40 quadrants of 5 x 2 m^2 each, at, a) North County sites, b) La Jolla sites, c) Point Loma Central long-term sites, and d) Point Loma additional sites. Error bars show standard error of the mean.

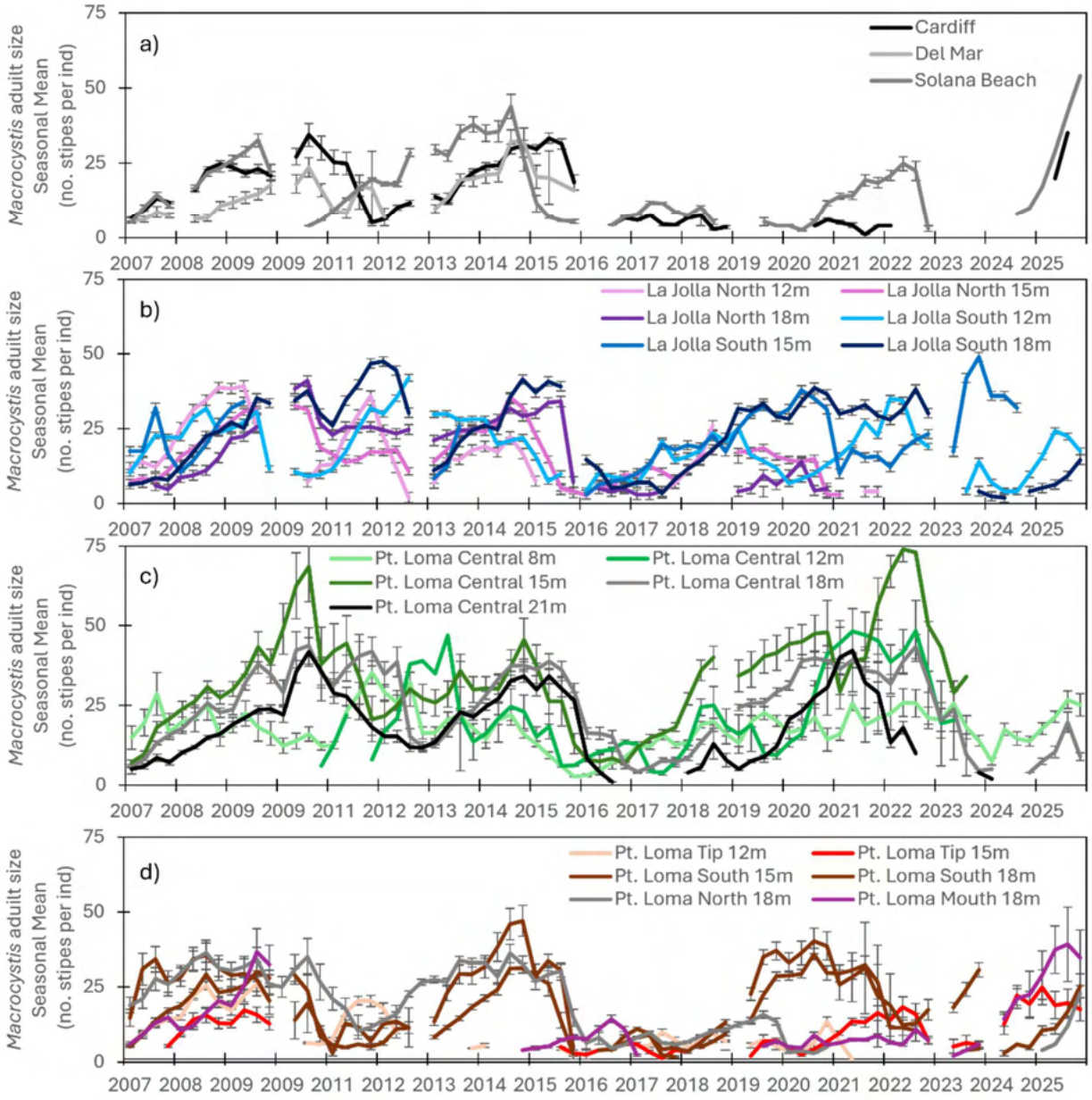


Figure 17: Size of *Macrocystis pyrifera* adults (number of stipes per adult individual longer than 1m); seasonal means from quarterly monitoring of 400 m^2 (Winter 2007 to Fall 2025); in a) North County sites, b) La Jolla sites, c) Point Loma Central long-term sites, and d) Point Loma additional sites. Error bars show standard error of the mean.

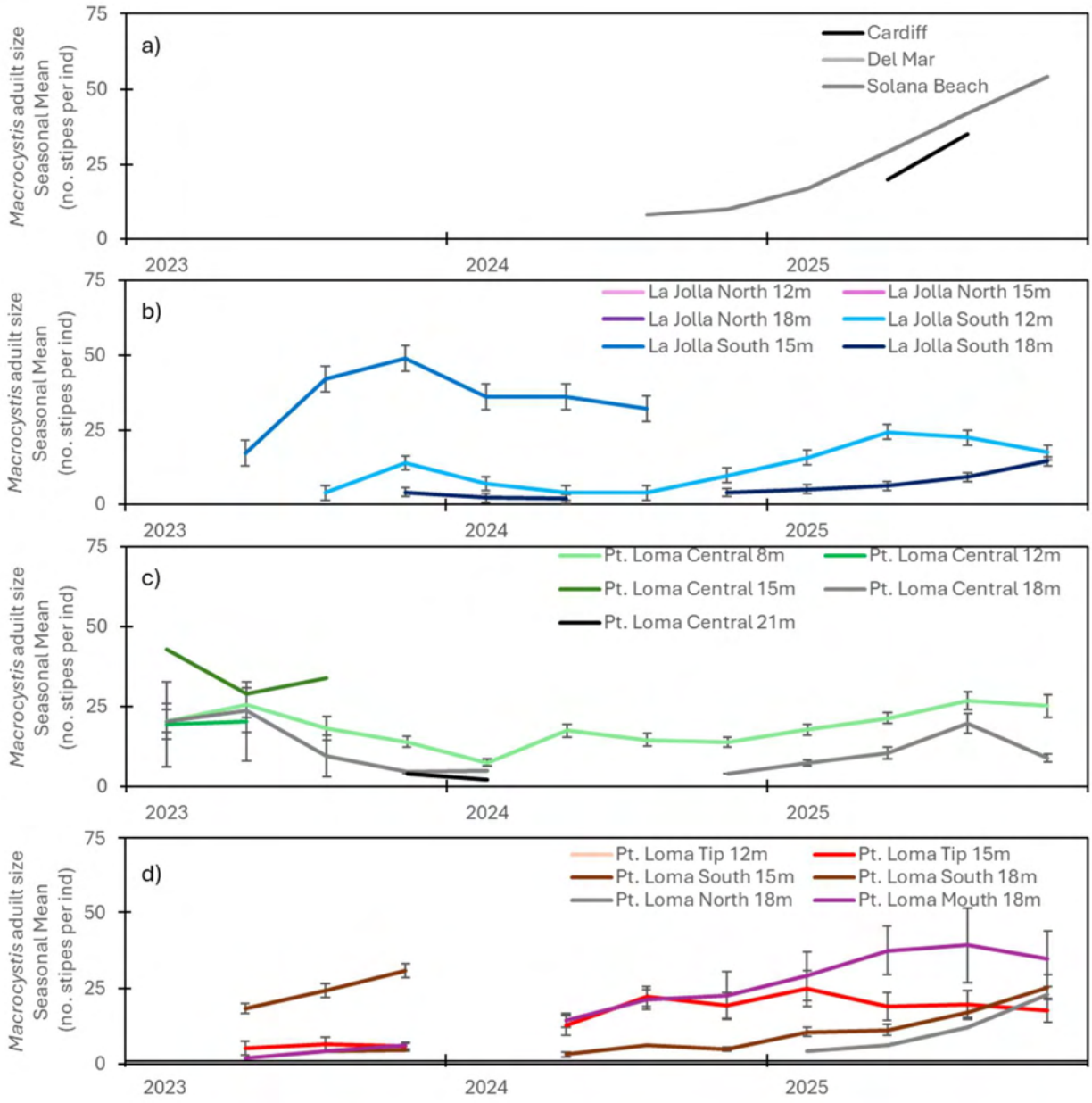


Figure 18: Zoom for reporting period (2023-2025) (no change of scale) of size of Ma*crocystis pyrifera* adults (number of stipes per adult individual longer than 1m); seasonal means from quarterly monitoring of 400 m^2 in a) North County sites, b) La Jolla sites, c) Point Loma Central long-term sites, and d) Point Loma additional sites. Error bars show standard error of the mean.

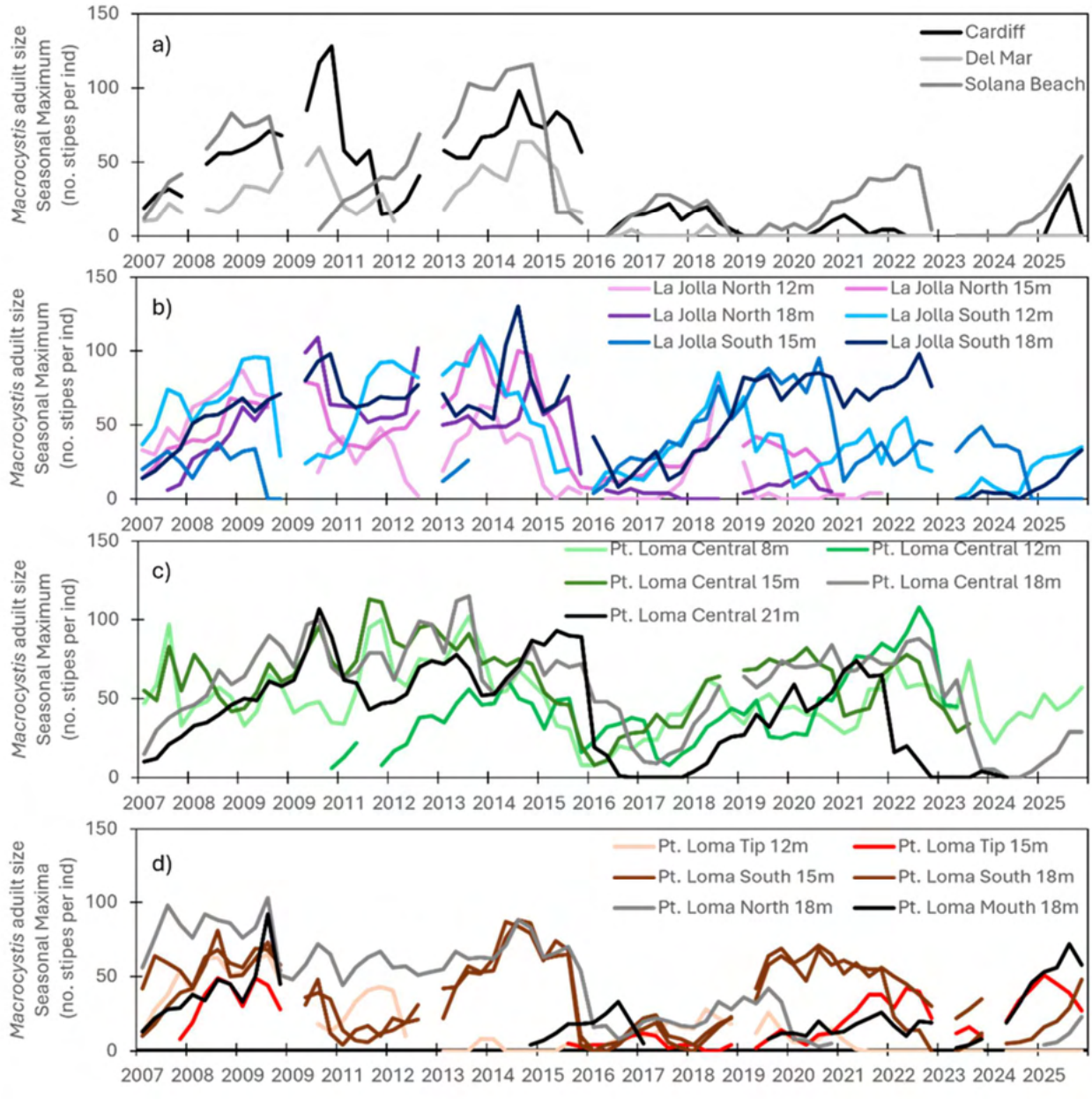


Figure 19: Size of *Macrocystis pyrifera* adults (number of stipes per adult individual longer than 1m); seasonal maxima from quarterly monitoring of 400 m^2 (Winter 2007 to Fall 2025); in a) North County sites, b) La Jolla sites, c) Point Loma Central long-term sites, and d) Point Loma additional sites.

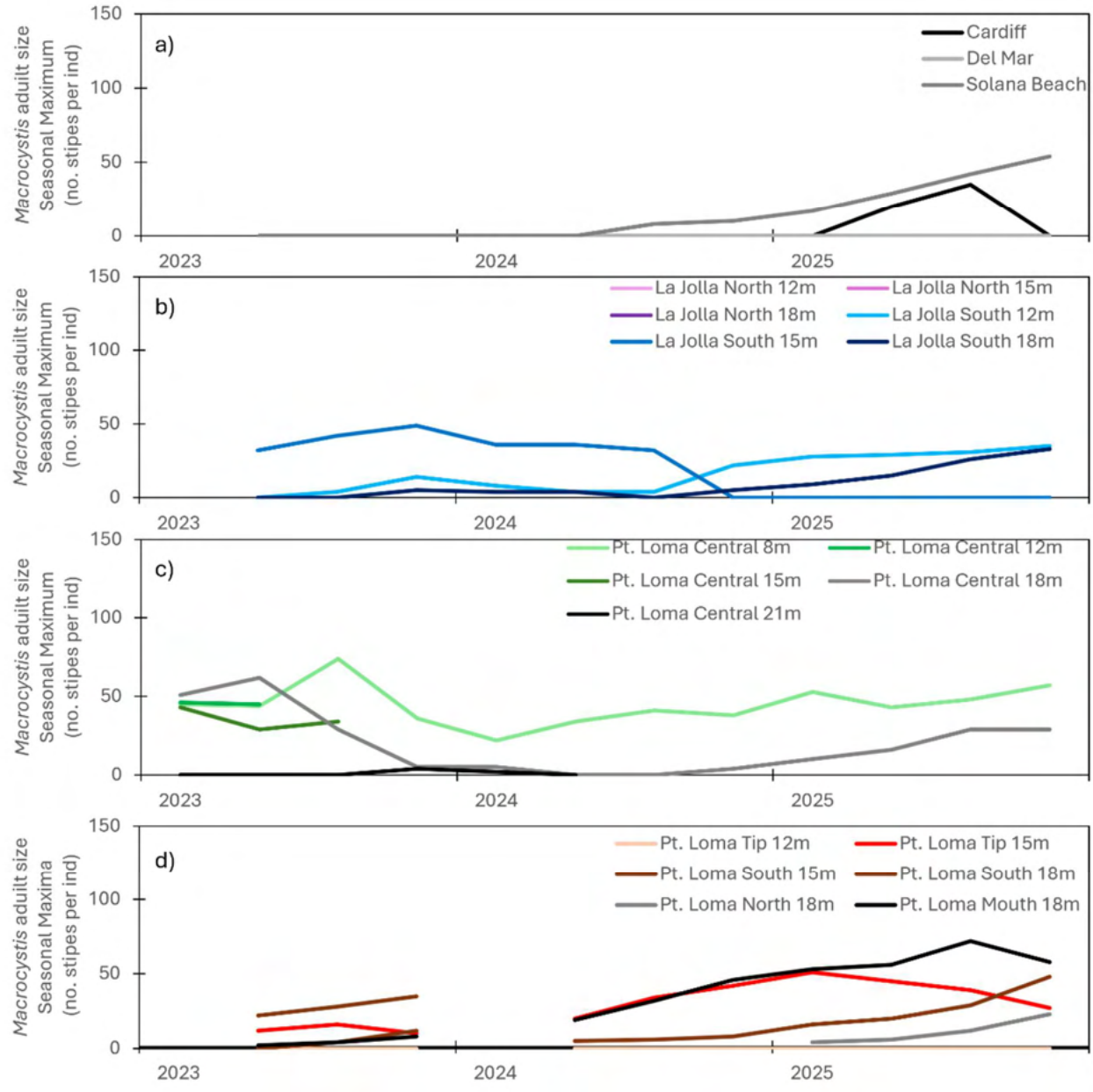


Figure 20: Zoom for reporting period (2023-2025) (no change of scale) of size of *Macrocystis pyrifera* adults (number of stipes per adult individual longer than 1m); seasonal maxima from quarterly monitoring of 400 m^2 in a) North County sites, b) La Jolla sites, c) Point Loma Central long-term sites, and d) Point Loma additional sites.

Understory kelp species

Laminaria

The understory foliose kelp*, Laminaria farlowii* (Figure 21), showed high densities at some of the monitoring sites in the San Diego region during this reporting period. The North County sites of Cardiff and Solana Beach, the La Jolla South 12 and 15 m sites, and almost all of the Point Loma Central sites showed fairly consistent mean seasonal densities reaching or exceeding 25 individuals per 10 m^2 for the reporting period, whereas Pt Loma Central 18 m only reached those densities in 2025. The Point Loma North 18 m site maintained constant mean densities exceeding 50 individuals per 10 m^2.

Pterygophora

The understory stipitate kelp, *Pterygophora californica* (Figure 22), was also abundant at many of our monitoring sites during this reporting period, with the Point Loma South 18 m and the Point Loma Tip 15 m sites exceeding seasonal mean densities of 75 individuals per 10 m^2.

Eisenia

Density of the understory stipitate kelp, *Eisenia arborea* (Figure 23) during the reporting period was high at two sites in particular: Point Loma Central 8 m, where it was relatively stable at a mean seasonal density of 6 individuals per 10 m^2; and at La Jolla South 12 m, where seasonal mean density was near 15 individuals per 10 m^2 in 2023 and dropped to near 6 individuals per 10 m^2 after 2024.

Kelp reproductive indices

Laminaria farlowii reproduction (Figure 24a) showed seasonal patterns with the percentage of tissue covered by sori being higher in summer and fall, and at the shallow sites in 2023, with all depths showing high reproductive tissue exceeding a mean of 30% of each blade covered with sori in 2024 and especially in 2025.

Pterygophora californica reproduction (Figure 24b) showed active spore production with spring and especially winter peaks, with reproduction for the reporting period being highest in winter 2024 and winter 2025.

Macrocystis pyrifera reproduction (Figure 24c) showed consistently high reproductive indices throughout the reporting period at both the Point Loma 8 m and Point Loma 18 m sites, with sporophylls showing a reproductive state above 3 (sori over

most of the sporophyll surface) and 4 (sporophylls with sori over all of the sporophyll surface), except for a brief low period in reproduction at the Point Loma 18 m site in October 2023 when sporophylls were ranked at a level 1 (sporophylls present but no sori). Other sites showed inconsistent reproduction.

Growth of understory kelps

Growth of the understory kelps *Laminaria farlowii* (Figure 25a) and *Pterygophora californica* (Figure 25b) showed seasonal growth rates for spring and summer, with higher growth in spring 2023 and summer 2025.

Invertebrate densities and recruitment

Abalone

Density

The density of all abalone species (Figure 26) has historically been the highest at the Point Loma Central 8 m site, which dominates the time series dating back to 2007, at times reaching a mean over 1 individual per 10 m^2. Additionally, the La Jolla South 18 m site has also ranked high in abalone abundance. While extremely low compared to long-term historical abundances (e.g. pre-1970), the highest abalone mean densities in recent years occurred in spring 2017 and 2018 at the Point Loma 8 m site and in spring 2009 at the La Jolla South 18 m site.

For the reporting period (Figure 27), some abalone densities are still being documented in spring 2023, 2024, and 2025 at the Point Loma Central 8 m site, with densities above 0.3 individuals per 10 m^2. These observations can be seen as encouraging as they indicate some natural abalone recruitment is occurring, even with observed densities not approaching historical levels.

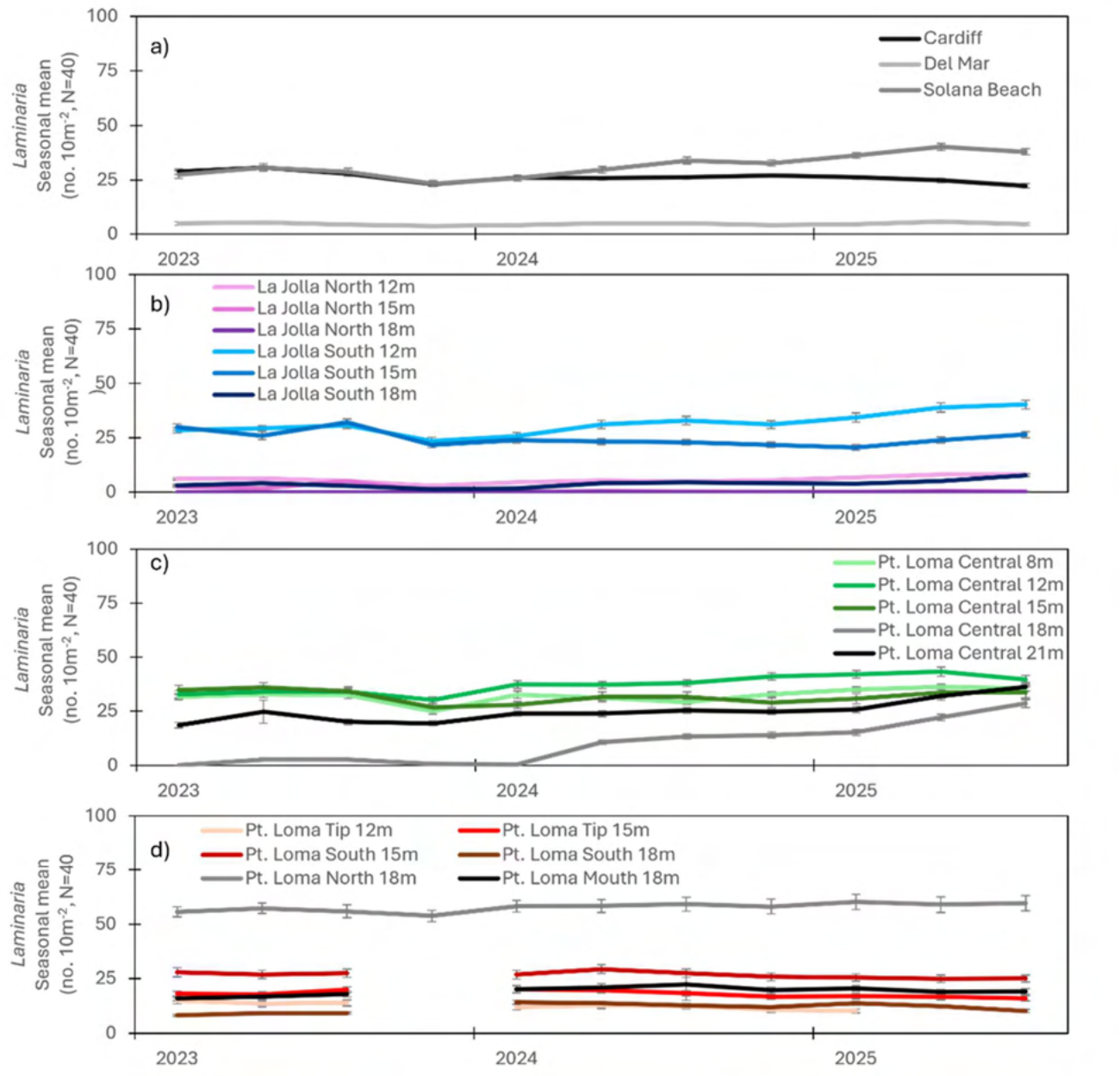


Figure 21: Zoom for reporting period (2023-2025) of density of the understory laminate kelp, *Laminaria* (number of individuals); seasonal means from quarterly monitoring of 40 quadrants of 5 x 2 m^2 each, at, a) North County sites, b) La Jolla sites, c) Point Loma Central long-term sites, and d) Point Loma additional sites. Error bars show standard error of the mean.

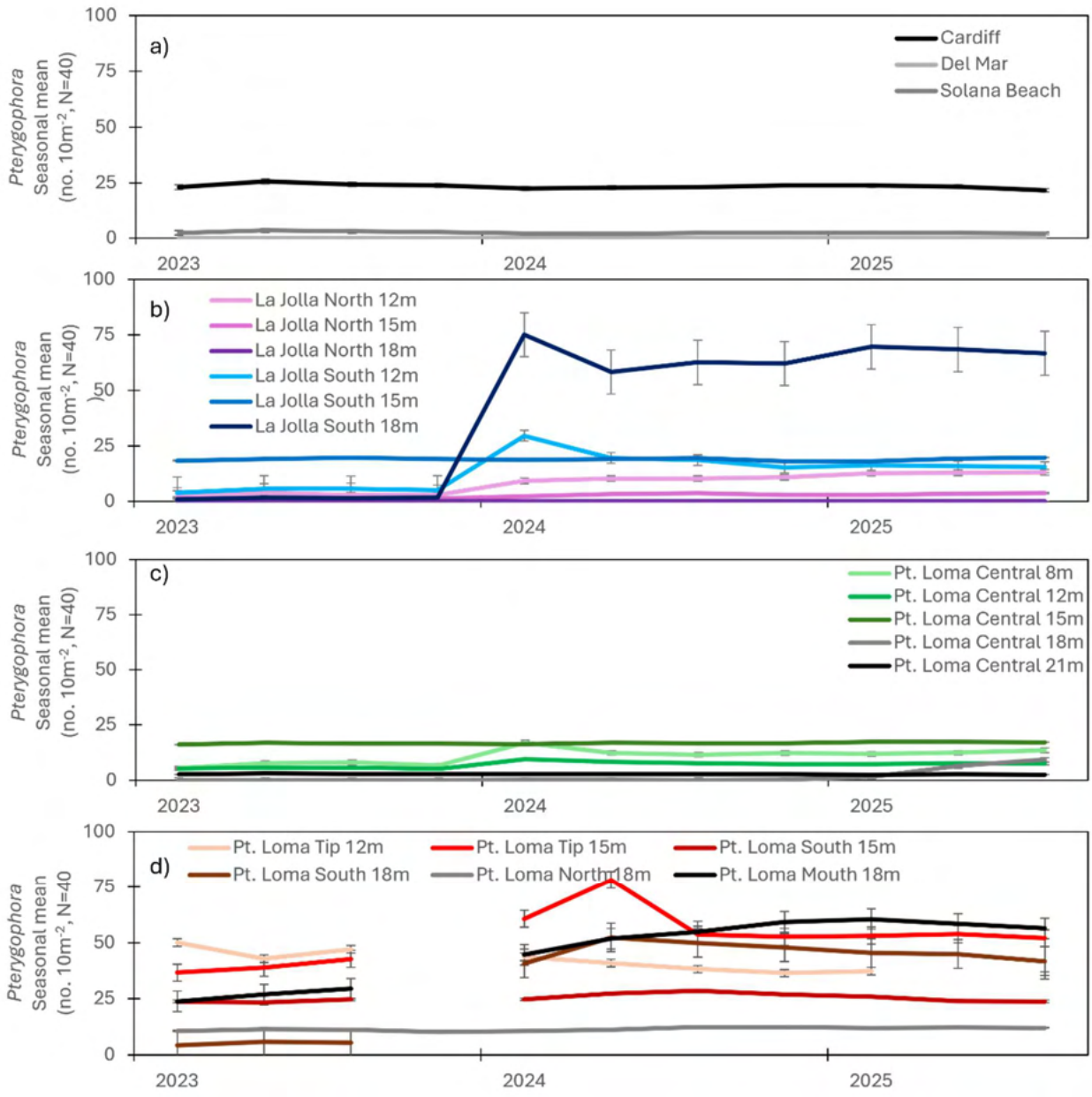


Figure 22: Zoom for reporting period (2023-2025) of density of the understory stipitate kelp, *Pterygophora* (number of individuals); seasonal means from quarterly monitoring of 40 quadrants of 5 x 2 m^2 each, at, a) North County sites, b) La Jolla sites, c) Point Loma Central long-term sites, and d) Point Loma additional sites. Error bars show standard error of the mean.

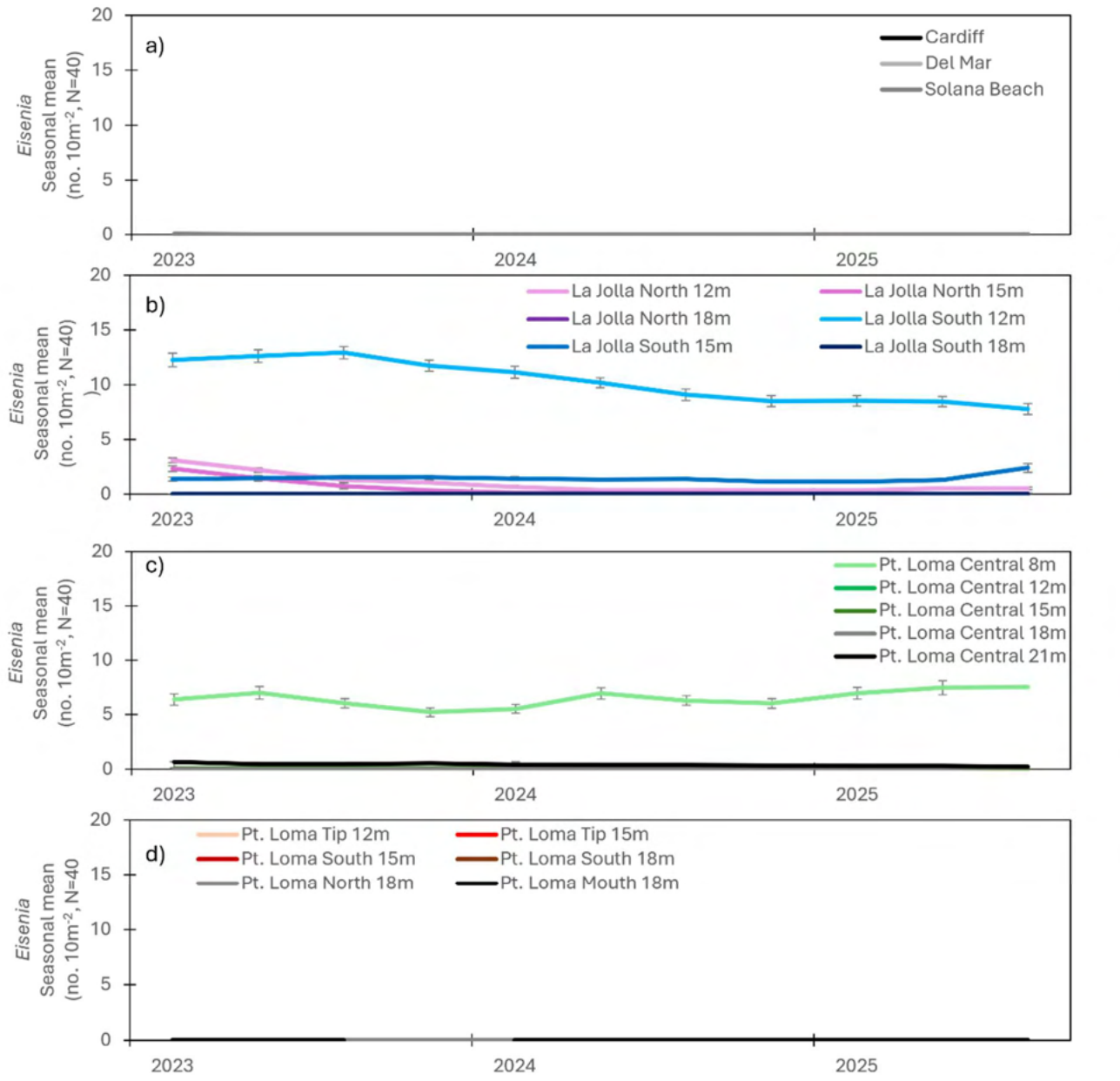


Figure 23: Zoom for reporting period (2023-2025) of density of the understory stipitate kelp, *Eisenia arborea* (number of individuals); seasonal means from quarterly monitoring of 40 quadrants of 5 x 2 m^2 each, at, a) North County sites, b) La Jolla sites, c) Point Loma Central long-term sites, and d) Point Loma additional sites. Error bars show standard error of the mean.

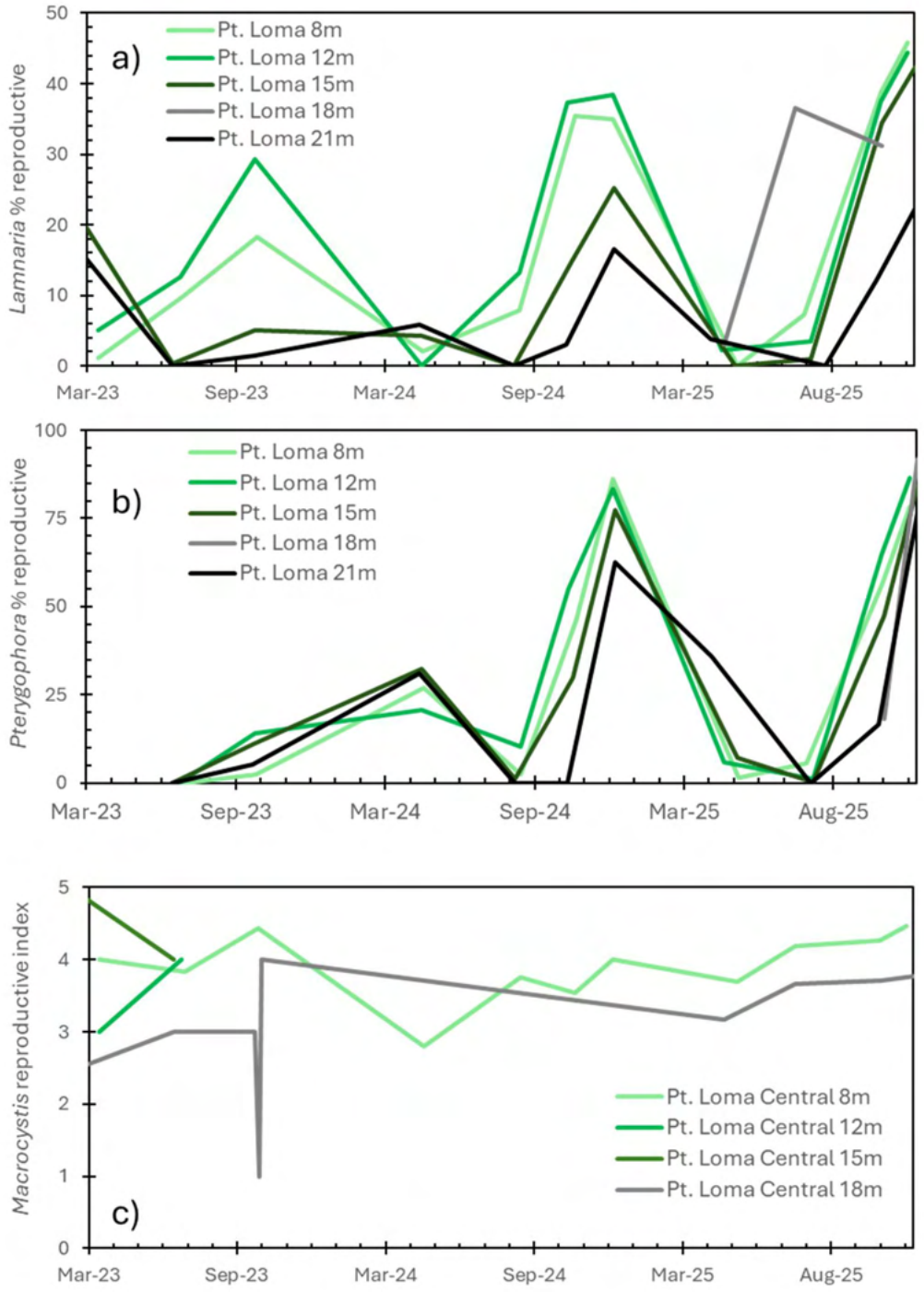


Figure 24: Zoom for reporting period (2023-2025) of the mean of reproductive indices at the Point Loma Central sites for two understory kelps, a) *Laminaria*, and b) *Pterygophora*; and c) the giant kelp, *Macrocystis pyrifera*. See methods for details.

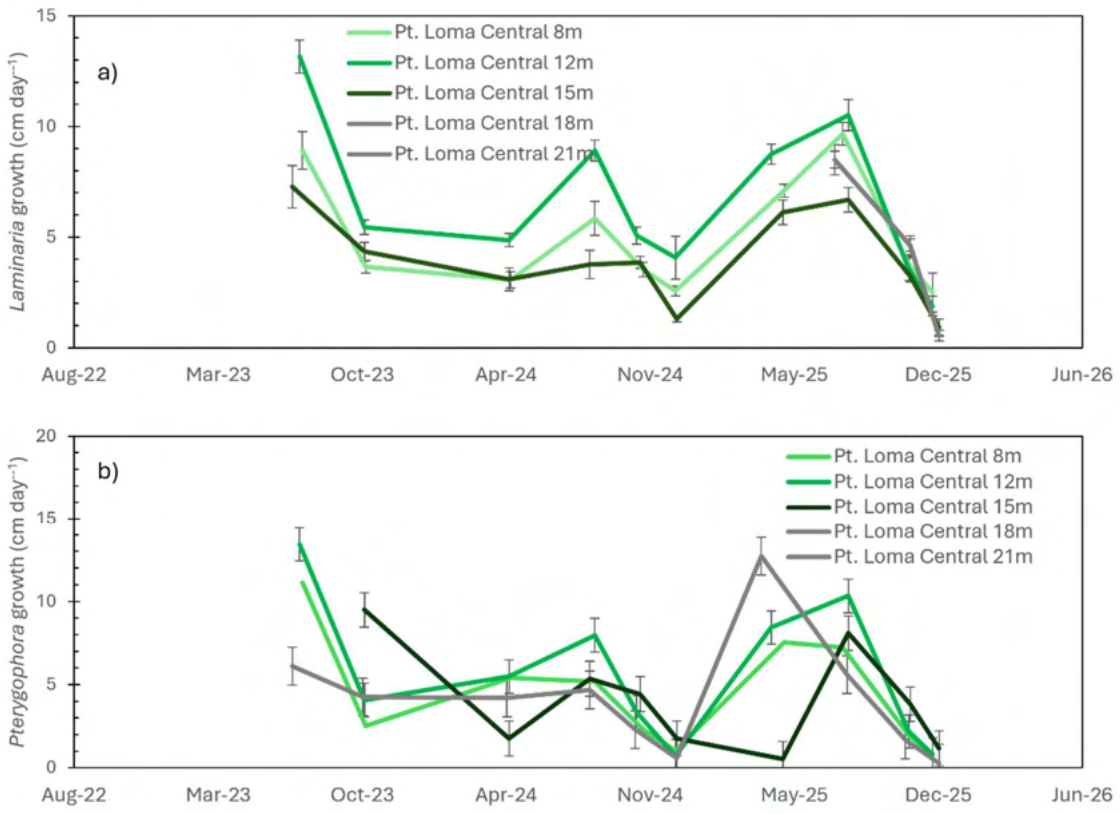


Figure 25: Zoom for reporting period (2023-2025) of mean growth rates at the Point Loma Central sites for two understory kelps, a) *Laminaria*, and b) *Pterygophora* (see details in methods).

Purple Sea Urchins

Density

Historically, the highest mean densities of purple sea urchins exceeded 100 individuals per 10 m^2 in spring 2012 and 2013 at the Point Loma Tip 15 m site, with mean densities above 50 individuals per 10 m^2 in spring 2010, 2011, 2012, and 2013, at the Point Loma Tip 12 m and 15 m sites, as well as at the Point Loma Mouth 18 m and Point Loma South 18 m sites. Most of the other sites show low or no purple urchin presence (Figure 28).

For the reporting period (Figure 29), none of the sites and periods were within the top 10% of the mean density of purple sea urchins in the time series dating back to 2007, with only the Point Loma Mouth 18 m site for spring 2023, the Point Loma Central

8 m site for spring 2023 and 2024, and the Point Loma Tip 15 m site for spring 2024 and 2025 within the top 20% of the historical time series dating back to 2007. Only the following sites and seasons for the reporting period exceeded 10 purple sea urchins per 10 m^2: Point Loma Tip 15 m in spring 2024 and 2025, Point Loma Central 18 m in spring 2023 and 2024, and Point Loma Mouth 18 m in spring 2023.

Recruitment

For this reporting period (Figure 30-32), both fall 2023 and fall 2024 showed higher numbers of purple sea urchins in the smaller size class near the La Jolla North 12 m site. Some sites, particularly in La Jolla, exceeded 50% of the purple urchins measured in the < 25 mm size class for most seasons, suggesting that more than half of the population entailed recruits, for example in fall 2023 (La Jolla North 12 and 18 m, and La Jolla South 12 m), spring 2024 (La Jolla North 12 m), fall 2024 (La Jolla North 12, 15 and 18 m), spring 2025 (La Jolla North 12 m) and fall 2025 (La Jolla North 12 and 18 m).

Notably, although the La Jolla North 18 m site showed more than 50% of the population in the smaller size classes at times, demographic evaluations there required a search effort of more than 15 quadrants to find enough purple urchins for all seasons evaluated except for in spring 2023. Additionally, for fall 2024 and spring 2025, more than 15 quadrants were required for the site west of Point Loma Central 18 m; as well as for the La Jolla South 15 m site in fall 2025.

Red Sea Urchins

Density

Historically, the highest mean densities of red sea urchins occurred in the Point Loma Mouth 18 m and Point Loma Tip 12 and 15 m sites, exceeding 10 individuals per 10 m^2 in spring 2012, 2013, 2014 and 2015 (Figure 33).

For the recent reporting period (Figure 34), only the Point Loma Central 18 m (spring 2023, 2024 and 2025), La Jolla North 15 m (spring 2023 and 2024), La Jolla North 18 m (spring 2023), and Point Loma Mouth 18 m (spring 2023) sites were within the top 10% of the historical time series of red sea urchin densities dating back to 2007, exceeding a mean of 2 red sea urchins per 10 m^2.

Recruitment

For this reporting period (Figure 35-37), higher numbers of red sea urchins in the smaller size class were detected in fall 2023 and fall 2024 near the La Jolla North 12 m site, and to a lesser degree in Fall 2024 near the Point Loma Mouth 18 m and Point Loma Central 21 m sites.

The following seasons and sites exceeded 50% of the red sea urchins found with a size lower than 35 mm (considered recruits for this analysis): spring 2023 at La Jolla North 12 m; fall 2023 at La Jolla North 12 m (reaching 100%), La Jolla South 12 and 15 m, Point Loma Central 8 and 15 m; spring 2024, La Jolla North 12 and 15 m, Point Loma Central 8 and 12 m, Point Loma South 15 m and La Jolla South 15 m; fall 2024, La Jolla North 12 m (reaching 90%), and La Jolla North 15 m, Point Loma Central 12 m, Point Loma Tip 15 m and Point Loma Mouth 18 m (reaching 88%), La Jolla South 15 m, Point Loma Central 21 m and west of Point Loma South 18 m; spring 2025, La Jolla North 12 and 15 m, La Jolla South 15 and 18 m, Point Loma Tip 15 m and Point Loma Mouth 18 m, and Point Loma South 18 m and west of Point Loma South 18 m; and fall 25, La Jolla North 12 and 15 m, La Jolla South 18 m, Point Loma Central 8 and 21 m, and Point Loma Tip 15 m.

Notably the following sites required more than 15 quadrants to find and measure sufficient red urchins: in spring 2023, La Jolla North 18 m, Point Loma Tip 12 and 18 m, La Jolla South 12 and 15 m, Point Loma North and South at 18 m; for fall 23, La Jolla North 18 m and La Jolla South 15 and 18 m, and Point Loma South 15 m (which needed 28 quadrants), and Point Loma North 18 m; for spring 2024 many of the sites repeated, for example La Jolla North and South 18 m, and Point Loma North 18 m; for fall 2024, only La Jolla North 18 m as well as Point Loma Central 18 m and west of that site required more than 15 quadrants to find sufficient urchins; for spring 2025, only La Jolla North 18 m as well as west of Point Loma Central 18 m required 15+ quadrants; and for fall 2025 again many sites did, including La Jolla North and South 15 m, Point Loma Mouth, Central and South at 18 m as well as Point Loma Central at 15 m.

Wavy Top Snails

Density

Historically, the highest mean densities of the wavy top turban snail occurred at the Point Loma Central 15 m in spring 2025 with a mean of 13.2 individuals per 10 m^2. Mean densities exceeding 8 individuals per 10 m^2 include the Point Loma Central 15 m (spring 2021, 2022, 2023 and 2025) and 18 m sites (spring 2022 and 2023), the Point Loma Tip 12 m site (spring 2023 and 2024), Point Loma Central 8m site (spring 2018), and La Jolla North 15 m site (spring 2020) (Figure 38).

For the reporting period (Figure 39), some of the highest historical mean densities dating back to 2007 have been recorded, with the Point Loma Central 8, 15, and 18 m sites, along with the Point Loma Tip 12 m site showing the highest abundances of wavy top turban snails.

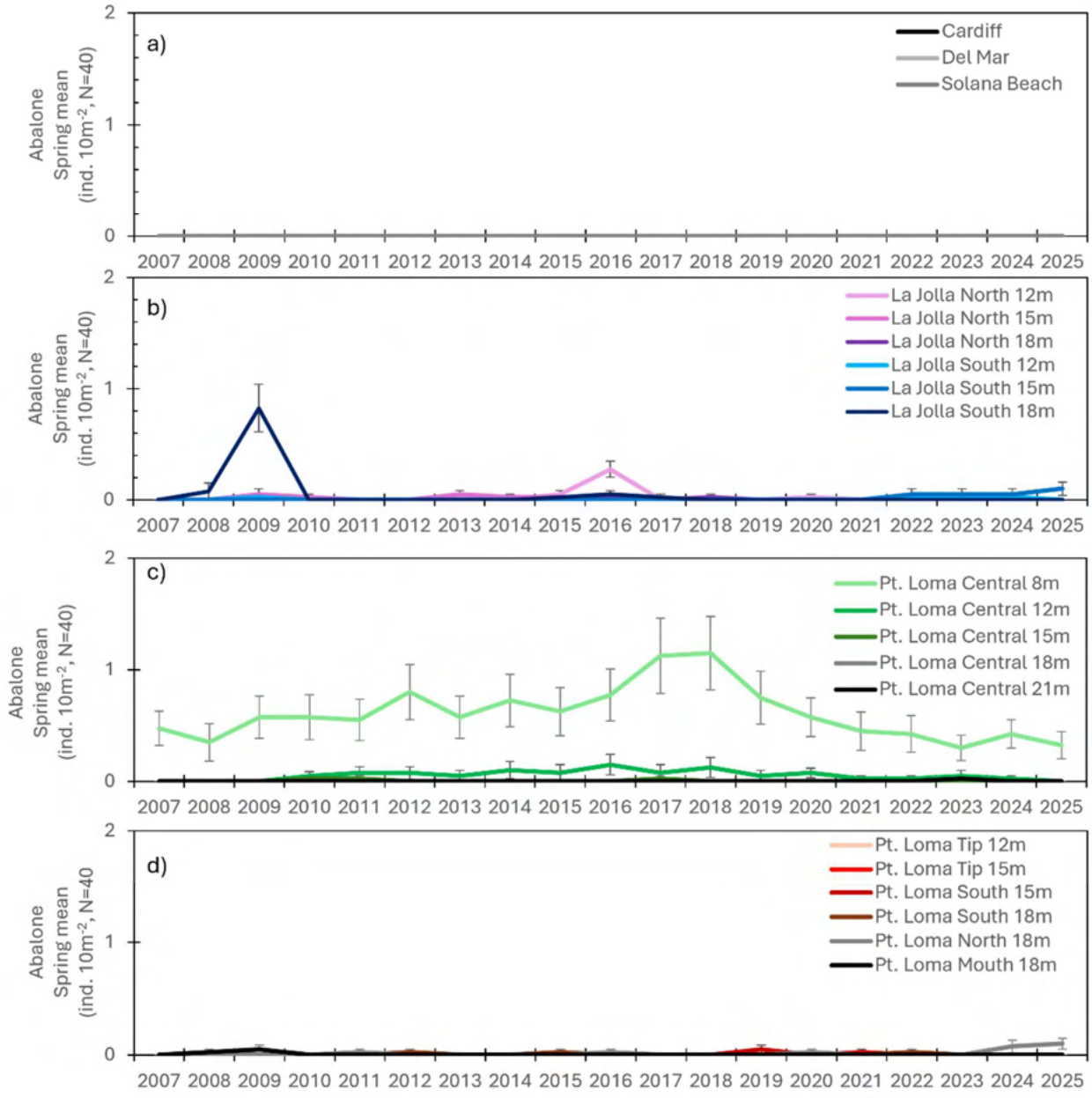


Figure 26: Density of Abalone (number of *Haliotis* spp. individuals); seasonal means (Winter 2007 to Fall 2025) from quarterly monitoring of 40 quadrants of 5 x 2 m^2 each, at, a) North County sites, b) La Jolla sites, c) Point Loma Central long-term sites, and d) Point Loma additional sites. Error bars show standard error of the mean.

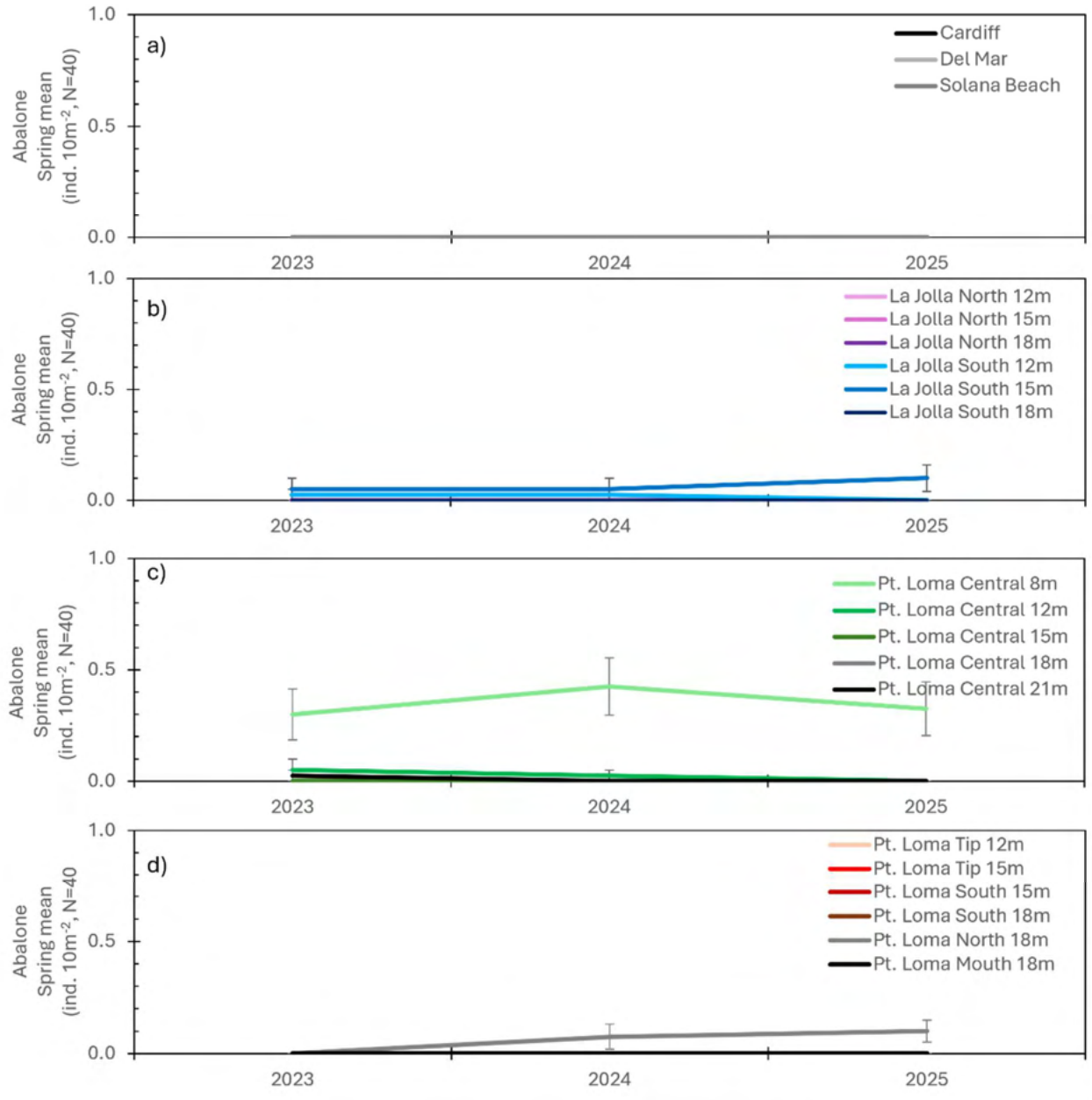


Figure 27: Zoom for reporting period (2023-2025)(note change of scale) of density of Abalone (number of *Haliotis* spp. individuals); seasonal means from quarterly monitoring of 40 quadrants of 5 x 2 m^2 each, at, a) North County sites, b) La Jolla sites, c) Point Loma Central long-term sites, and d) Point Loma additional sites. Error bars show standard error of the mean.

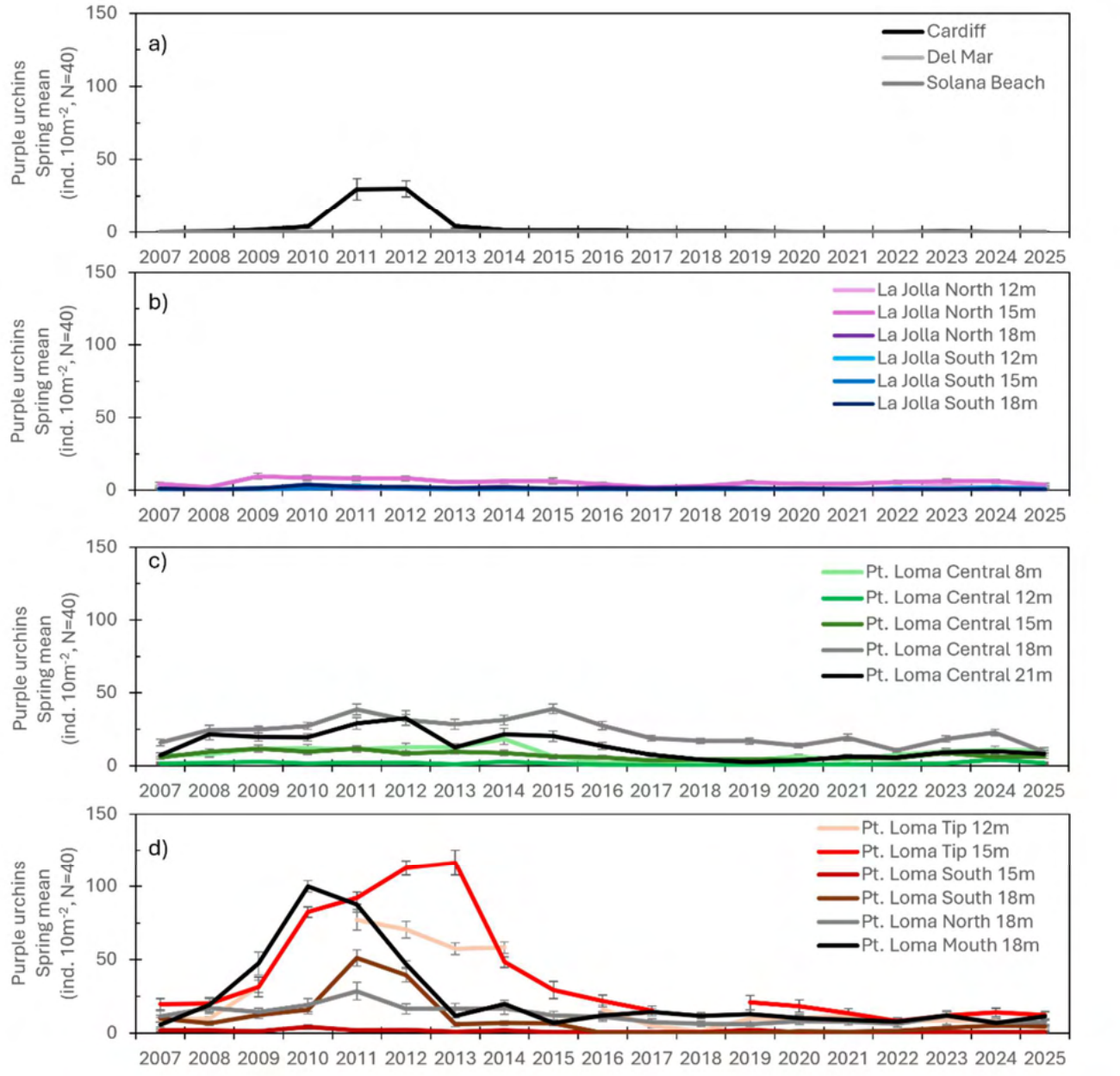


Figure 28: Density of Purple Sea Urchins (number of *Strongylocentrotus purpuratus* individuals); seasonal means (Winter 2007 to Fall 2025) from quarterly monitoring of 40 quadrants of 5 x 2 m^2 each, at, a) North County sites, b) La Jolla sites, c) Point Loma Central long-term sites, and d) Point Loma additional sites. Error bars show standard error of the mean.

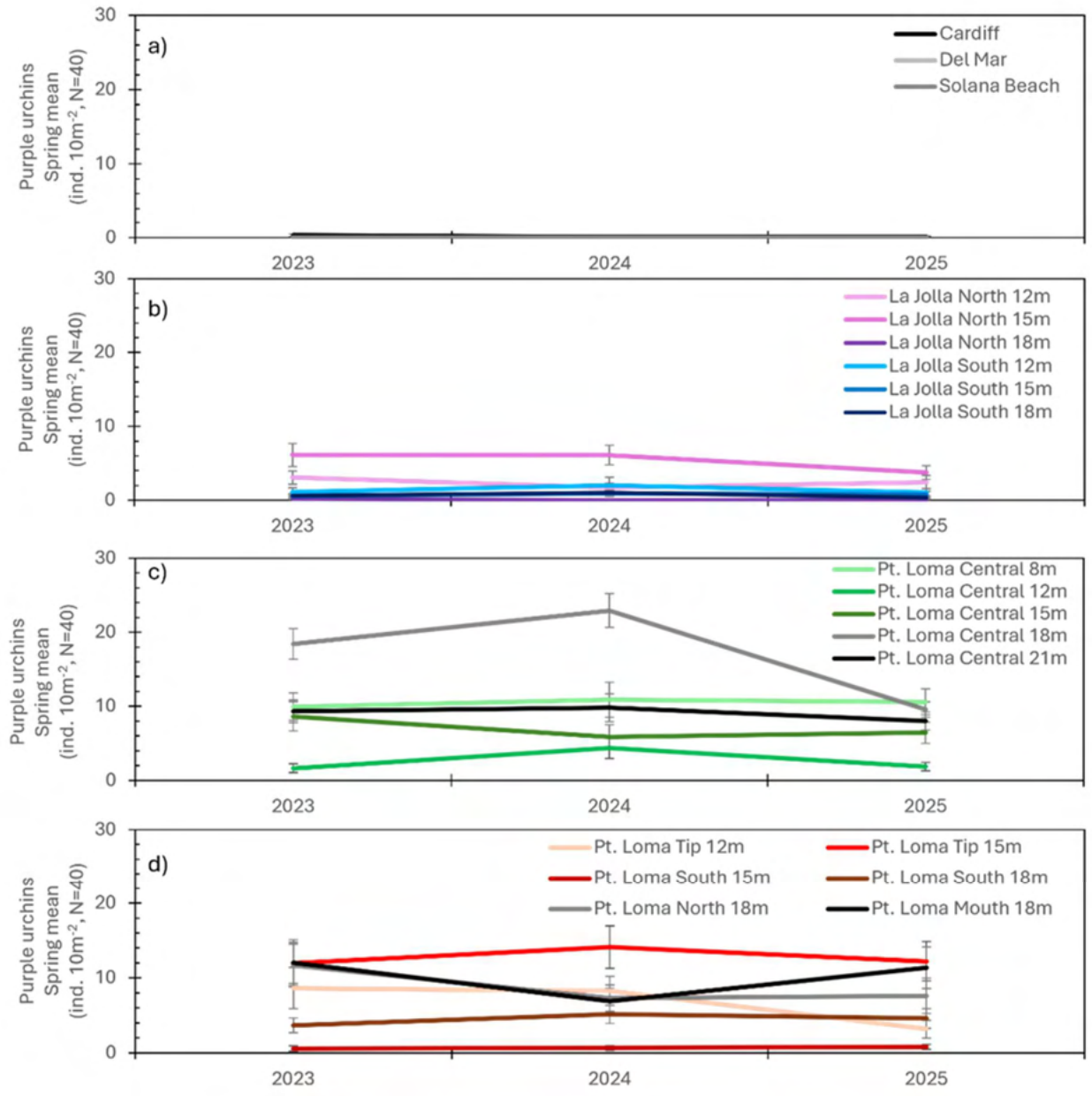


Figure 29: Zoom for reporting period (2023-2025) (note change of scale) of density of Purple Sea Urchins (number of *Strongylocentrotus purpuratus* individuals); seasonal means from quarterly monitoring of 40 quadrants of 5 x 2 m^2 each, at, a) North County sites, b) La Jolla sites, c) Point Loma Central long-term sites, and d) Point Loma additional sites. Error bars show standard error of the mean.

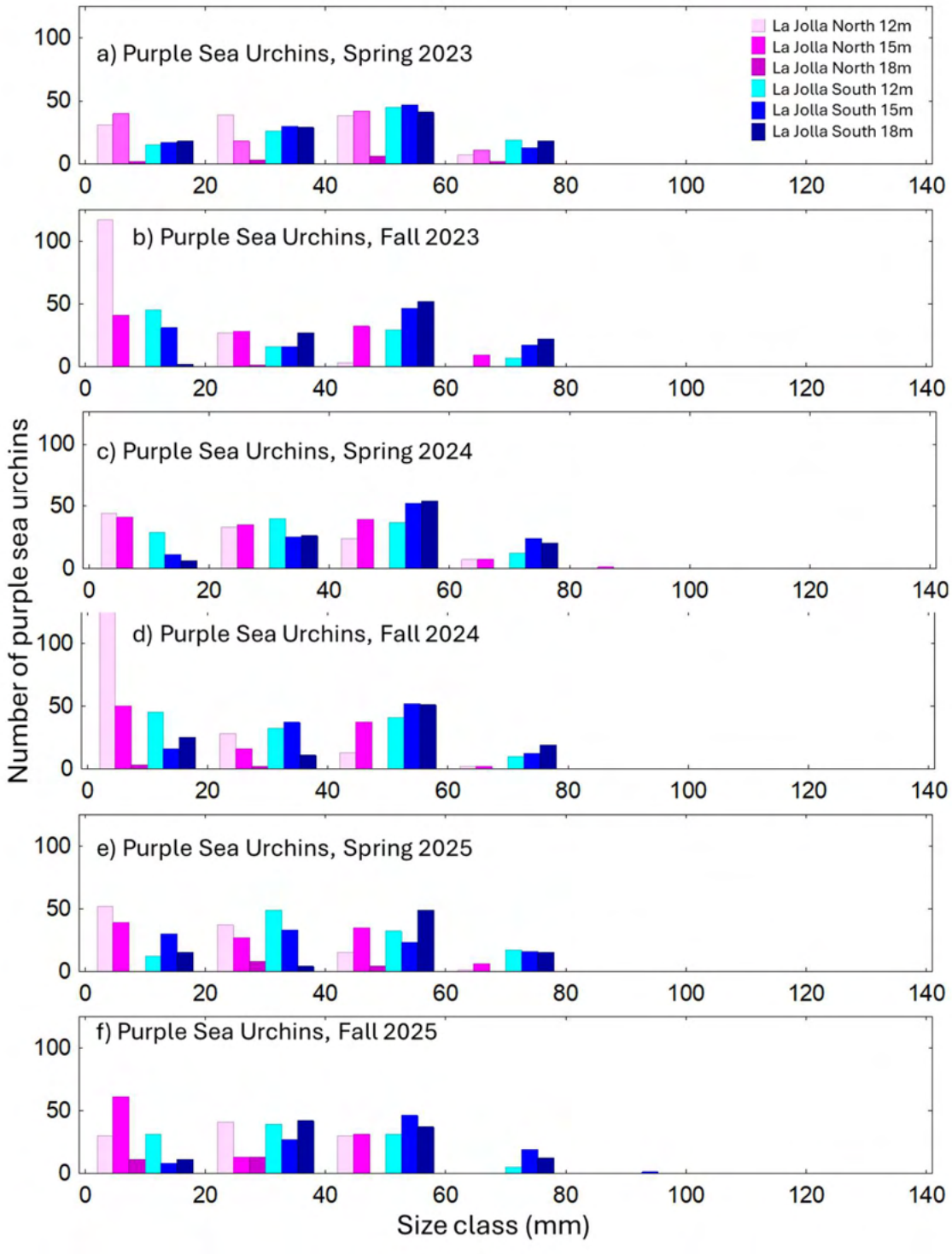


Figure 30: Size Structure (test size in mm) of Purple Sea Urchins (number of *Strongylocentrotus purpuratus* individuals in each 20 mm size class) for the La Jolla sites in spring and fall of 2023, 2024 and 2025, covering the reporting period.

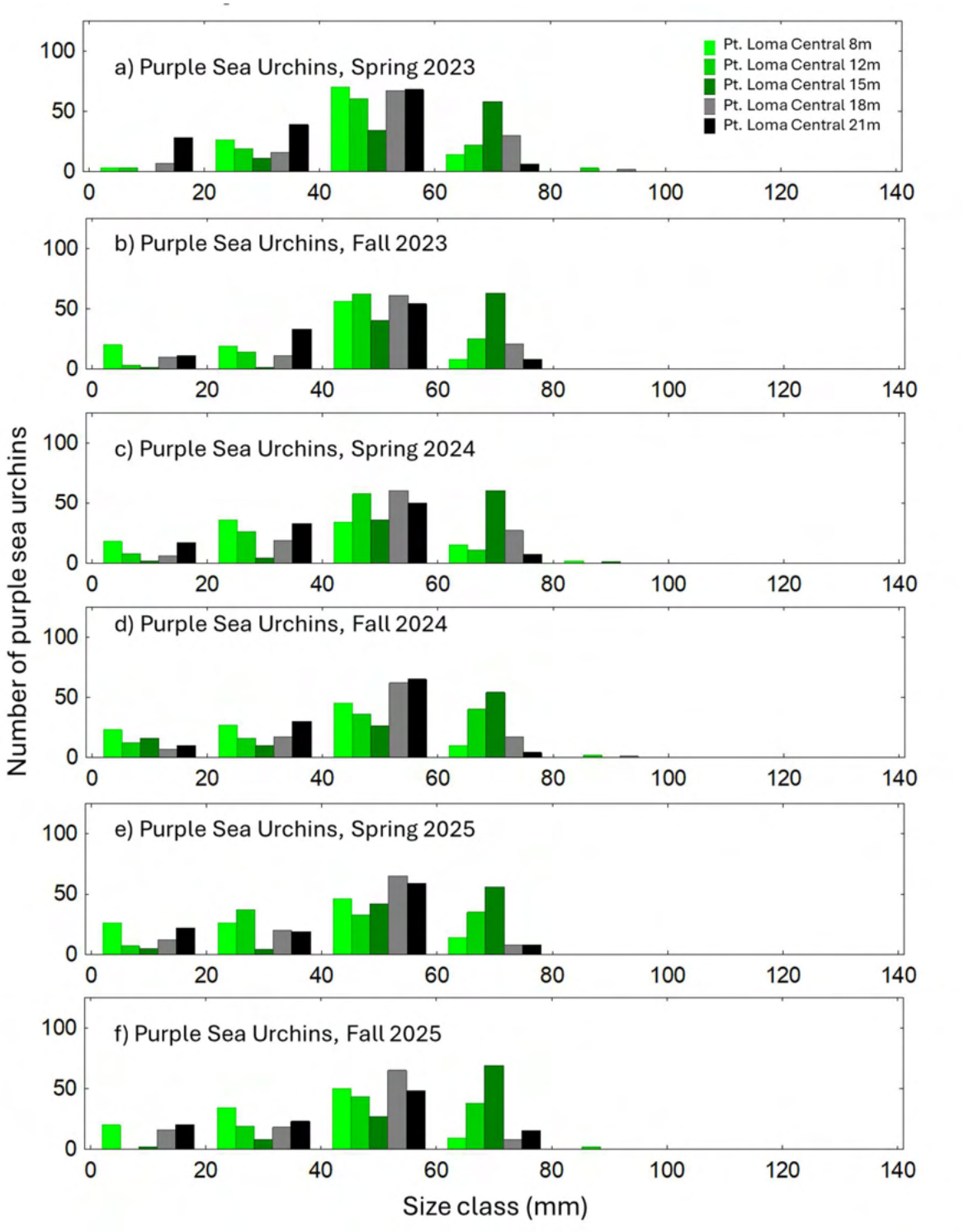


Figure 31: Size Structure (test size in mm) of Purple Sea Urchins (number of *Strongylocentrotus purpuratus* individuals in each 20 mm size class) for the Point Loma Central sites in spring and fall of 2023, 2024 and 2025, covering the reporting period.

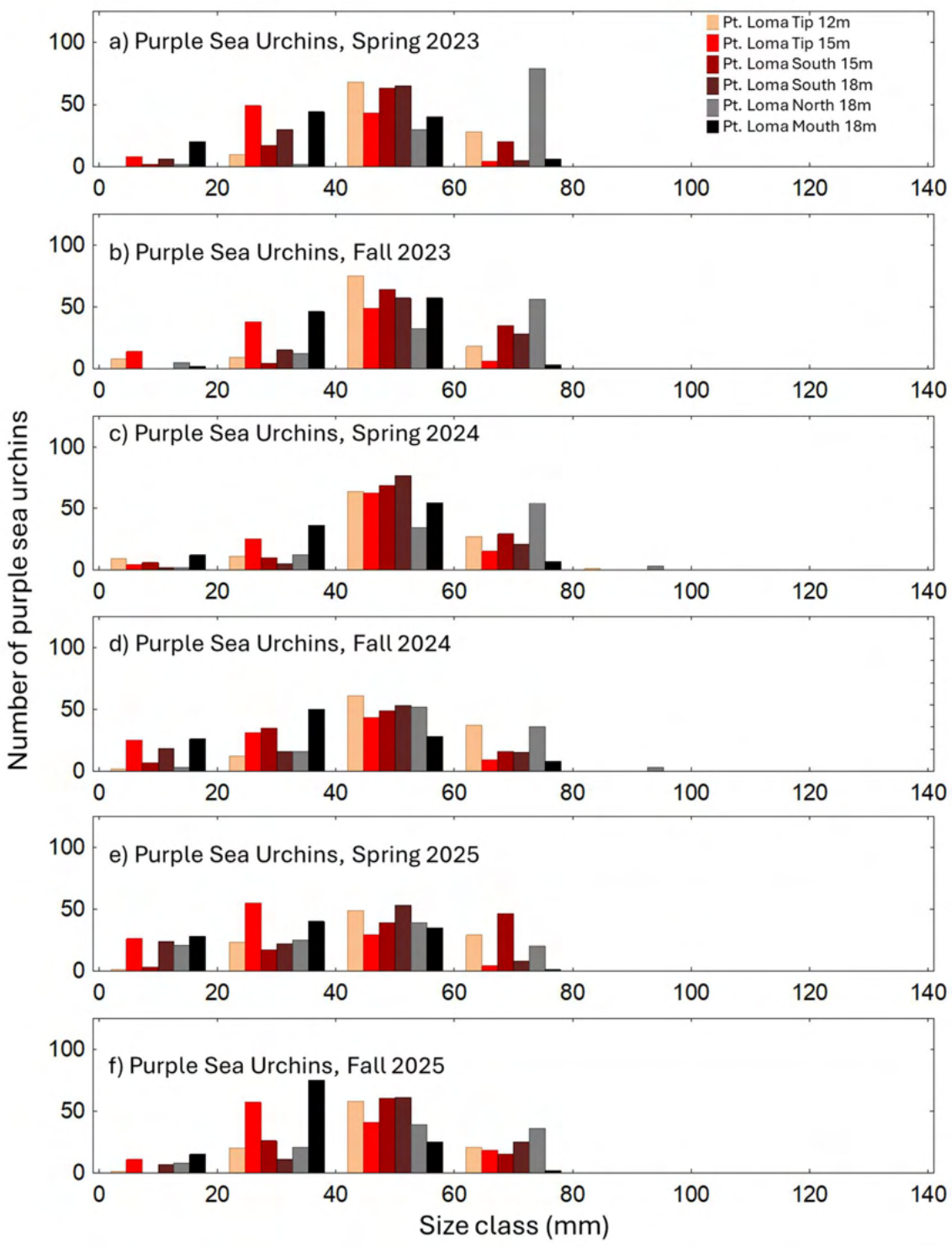


Figure 32: Size Structure (test size in mm) of Purple Sea Urchins (number of *Strongylocentrotus purpuratus* individuals in each 20 mm size class) for the Point Loma additional sites in spring and fall of 2023, 2024 and 2025, covering the reporting period.

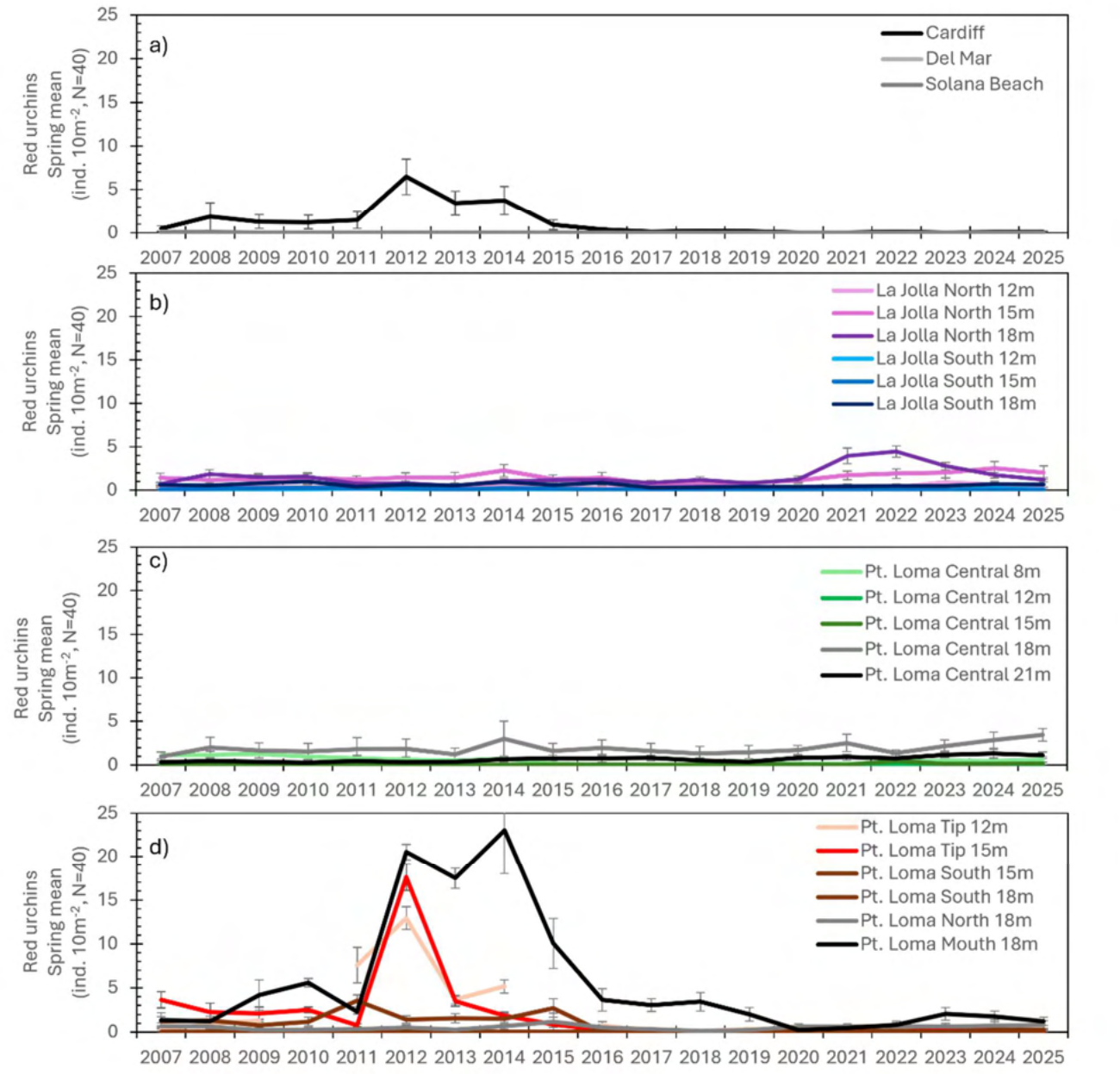


Figure 33: Density of Red Sea Urchins (number of *Mesocentratus franciscanus* individuals); seasonal means (Winter 2007 to Fall 2025) from quarterly monitoring of 40 quadrants of 5 x 2 m^2 each, at, a) North County sites, b) La Jolla sites, c) Point Loma Central long-term sites, and d) Point Loma additional sites. Error bars show standard error of the mean.

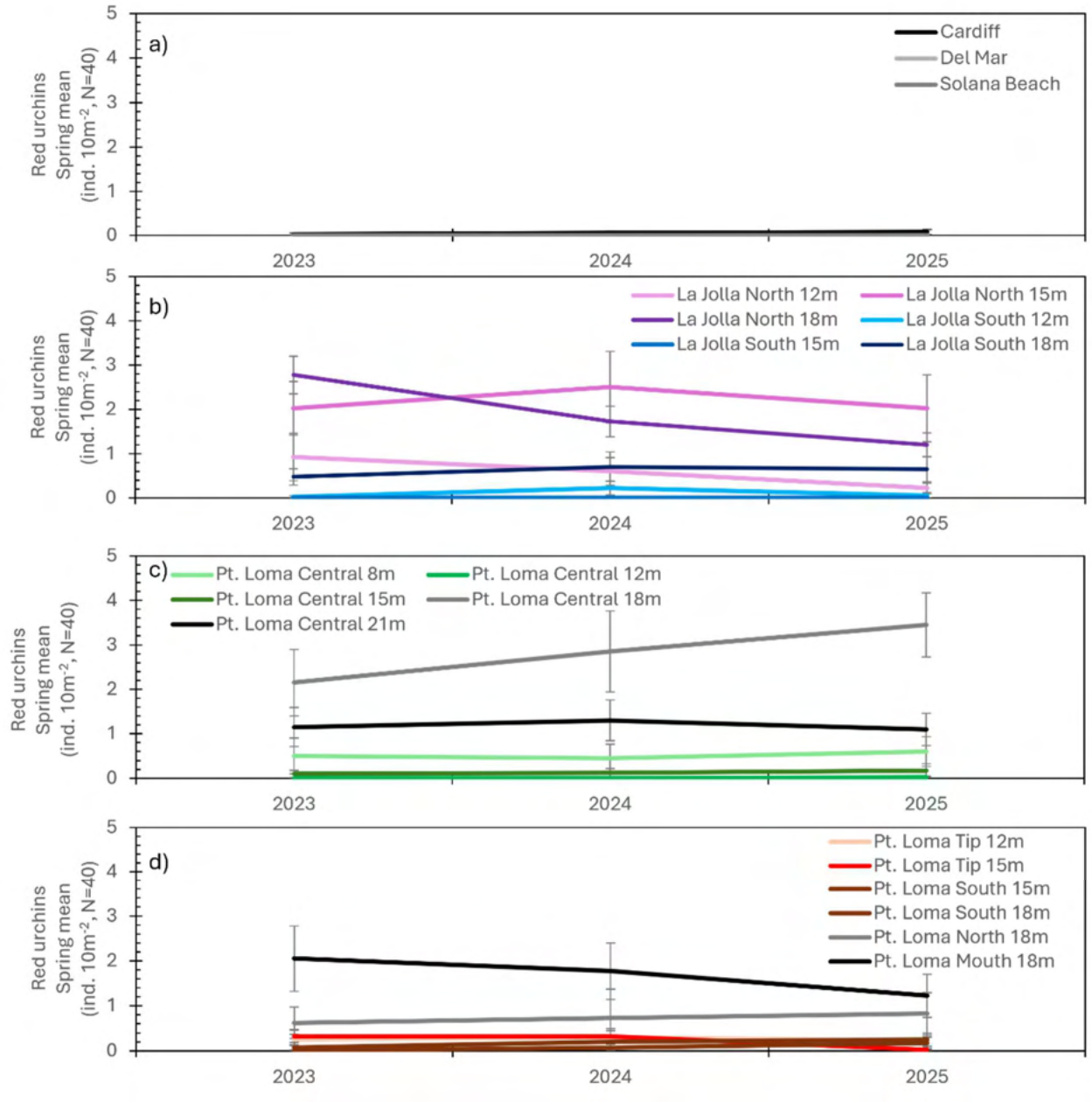


Figure 34: Zoom for reporting period (2023-2025)(note change of scale) of density of Red Sea Urchins (number of *Mesocentratus franciscanus* individuals); seasonal means from quarterly monitoring of 40 quadrants of 5 x 2 m^2 each, at, a) North County sites, b) La Jolla sites, c) Point Loma Central long-term sites, and d) Point Loma additional sites. Error bars show standard error of the mean.

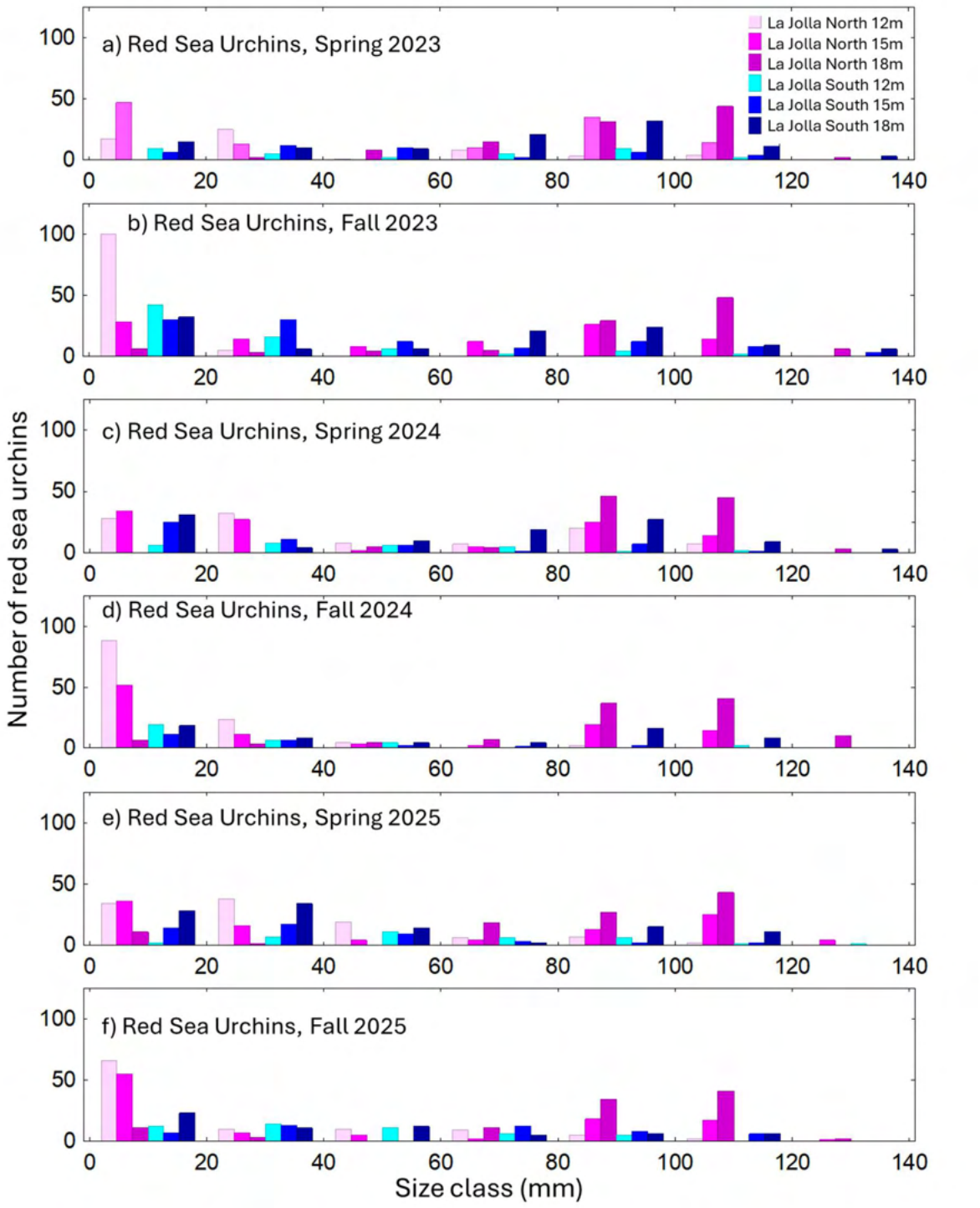


Figure 35: Size Structure (test size in mm) of Red Sea Urchins (number of *Mesocentratus franciscanus* individuals in each 20 mm size class) for the La Jolla sites in spring and fall of 2023, 2024, and 2025, covering the reporting period.

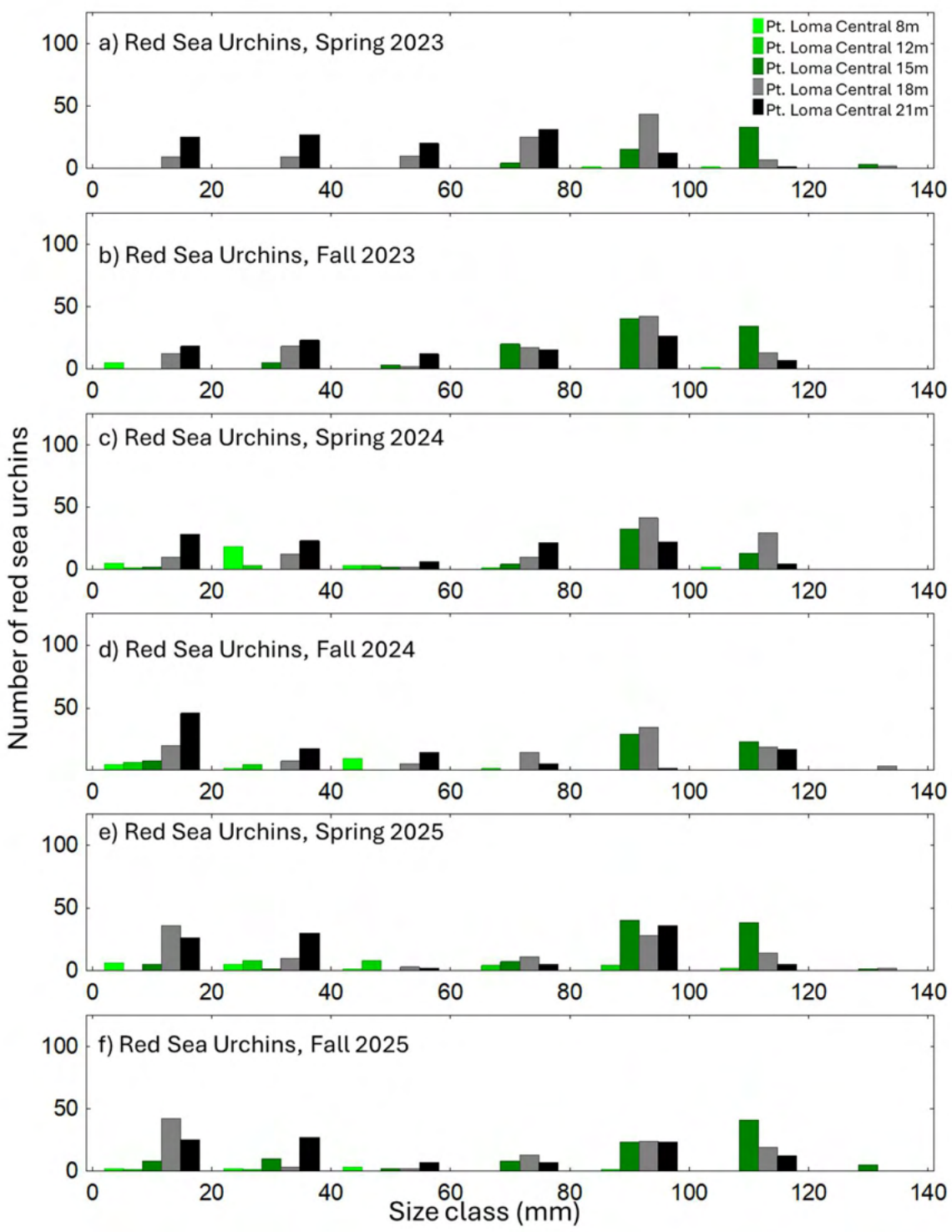


Figure 36: Size Structure (test size in mm) of Red Sea Urchins (number of *Mesocentratus franciscanus* individuals in each 20 mm size class) for the Point Loma Central sites in spring and fall of 2023, 2024 and 2025, covering the reporting period.

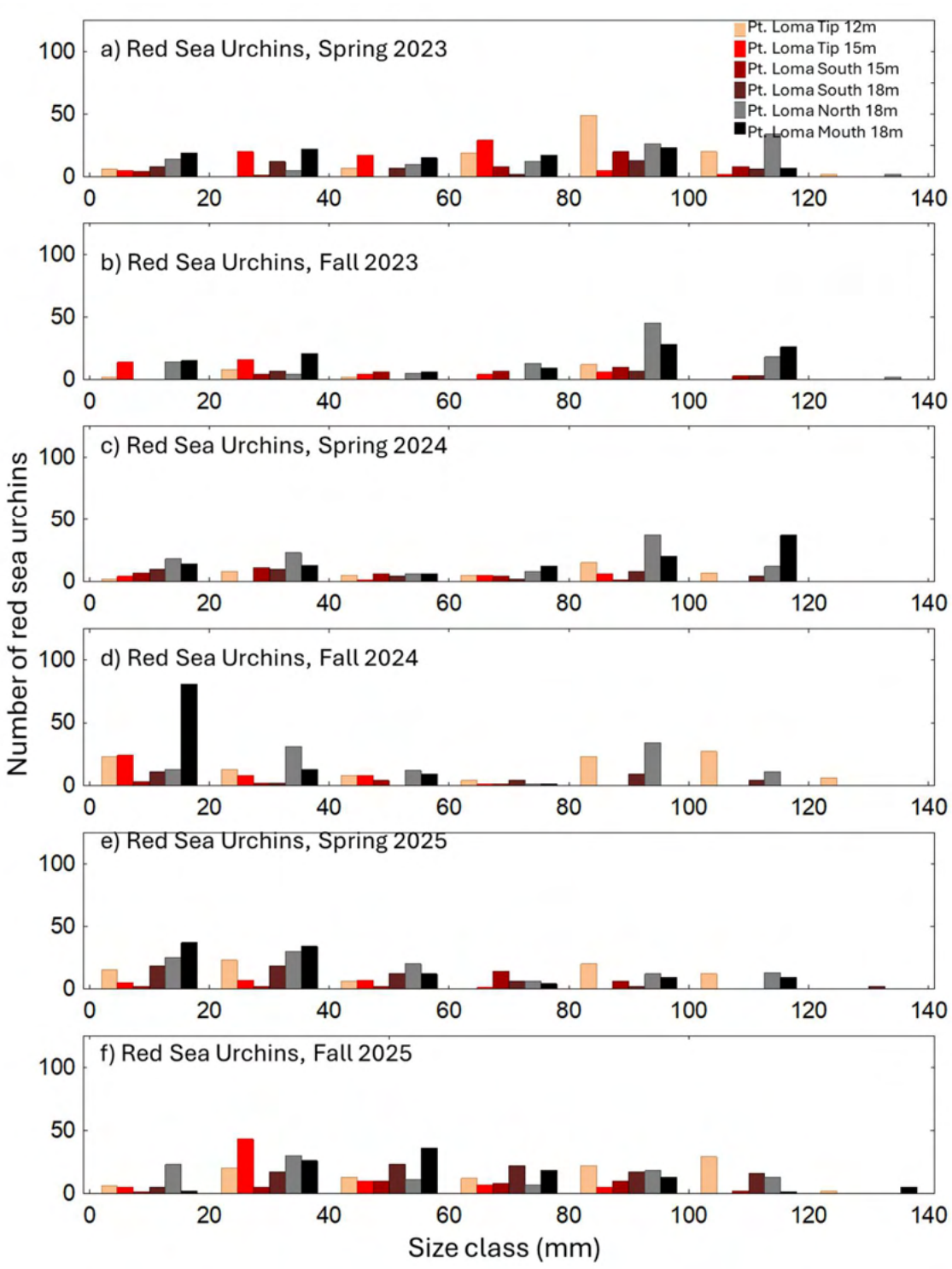


Figure 37: Size Structure (test size in mm) of Red Sea Urchins (number of *Mesocentratus franciscanus* individuals in each 20 mm size class) for the other Point Loma additional sites in spring and fall of 2023, 2024, and 2025, covering the reporting period.

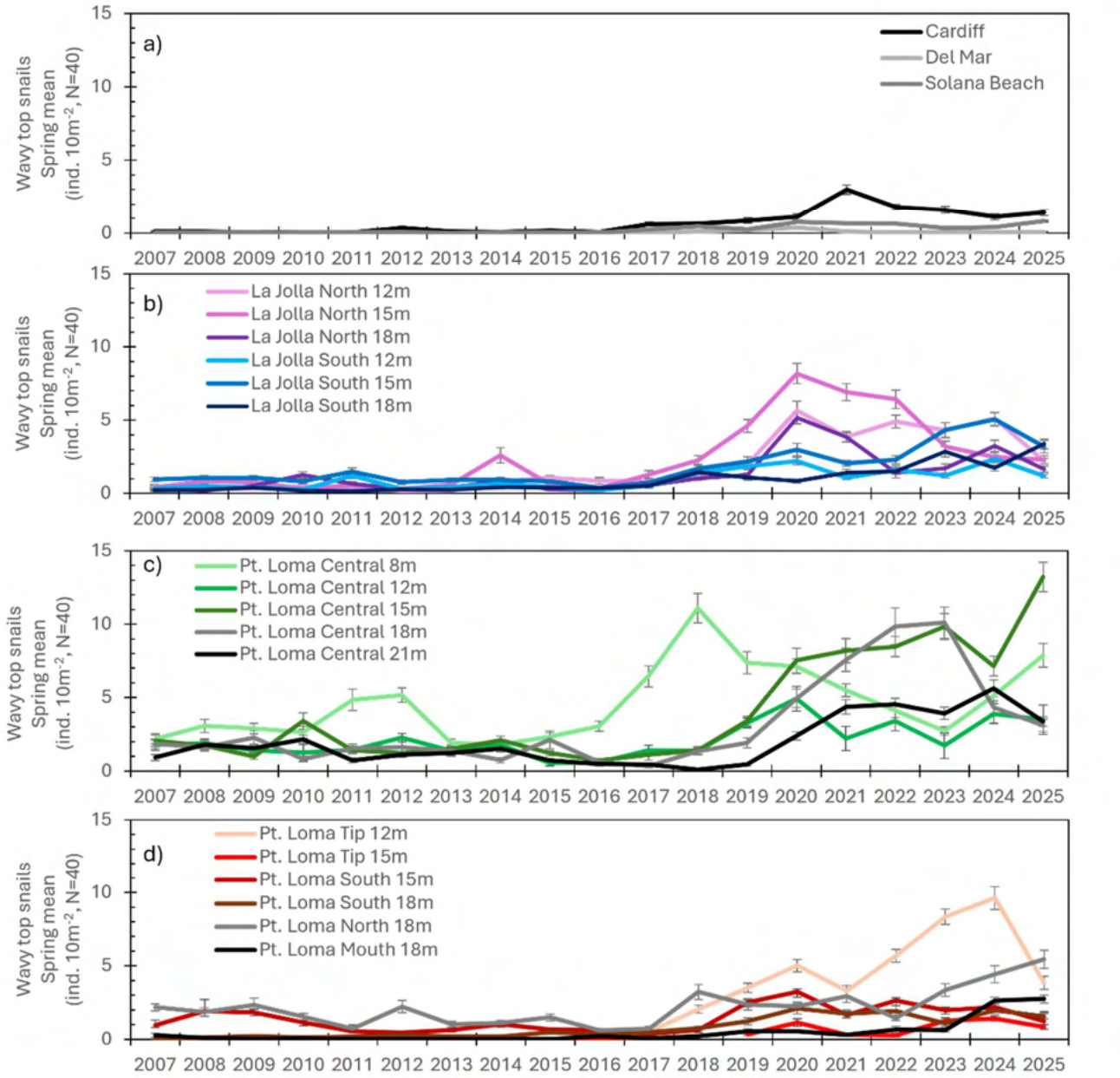


Figure 38: Density of Wavy Top Snails (number of *Megastrea* spp. individuals); seasonal means (Winter 2007 to Fall 2025) from quarterly monitoring of 40 quadrants of 5 x 2 m^2 each, at, a) North County sites, b) La Jolla sites, c) Point Loma Central long-term sites, and d) Point Loma additional sites. Error bars show standard error of the mean.

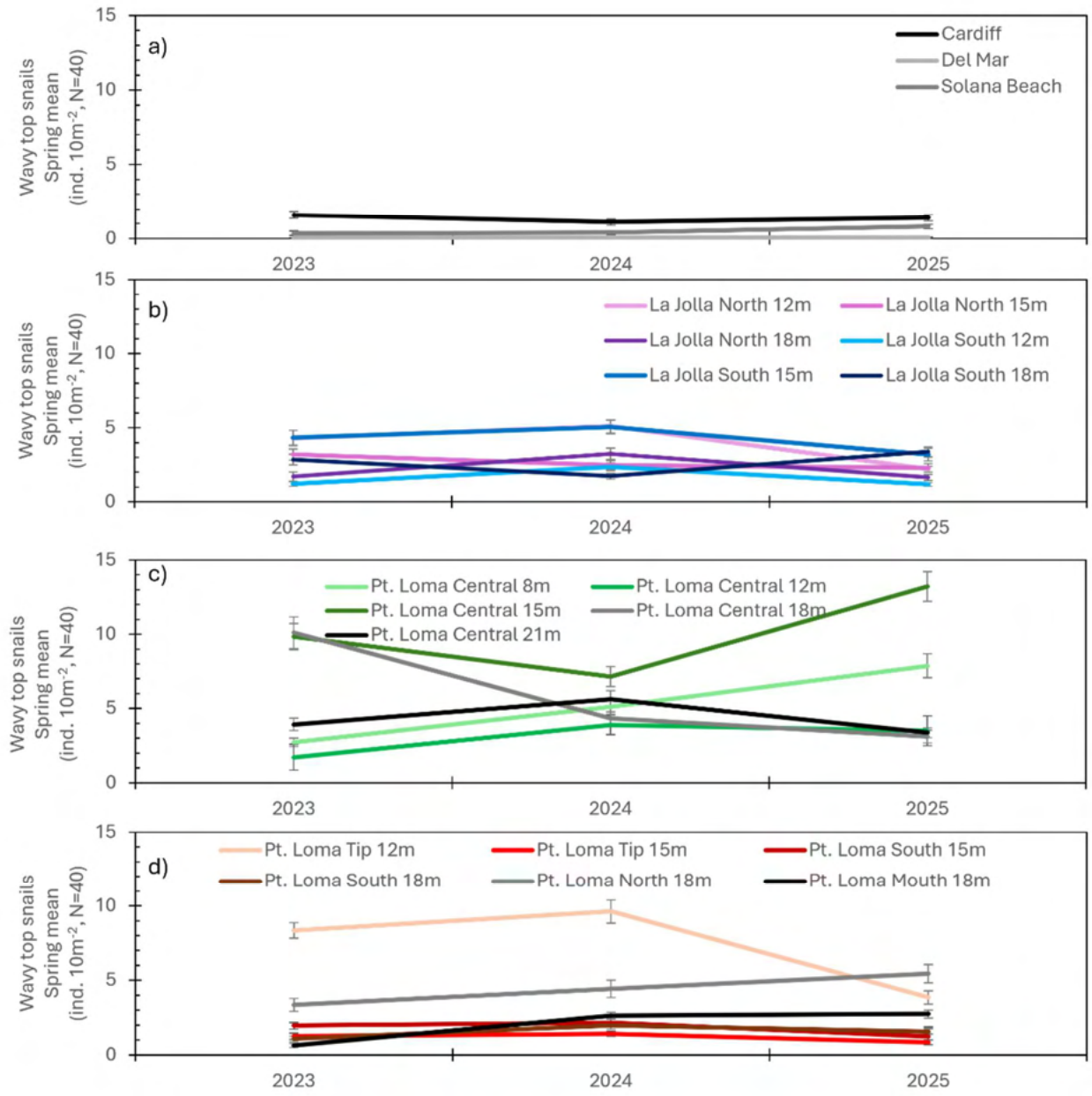


Figure 39: Zoom for reporting period (2023-2025) (note change of scale) of density of Wavy Top Snails (number of *Megastrea* spp. individuals); seasonal means from quarterly monitoring of 40 quadrants of 5 x 2 m^2 each, at, a) North County sites, b) La Jolla sites, c) Point Loma Central long-term sites, and d) Point Loma additional sites. Error bars show standard error of the mean.

CONCLUSION

The results shown in this biennial report (spring 2023 to fall 2025) of the City of San Diego's kelp forest monitoring program designed to evaluate anthropogenic impacts on the kelp forests in San Diego County, support the conclusion that the San Diego region giant kelp forests have demonstrated recent recruitment and growth at some of the monitoring sites with some recovery of density. Spatial variability was evident, recovery did not reach historical maxima, and some populations continue to show reduced persistence. In general, for much of the recent reporting period, the San Diego kelp forests appear to have benefited from cooler nutrient-rich waters and higher light exposure, supporting reproduction and growth, as well as reduced wave and herbivory disturbance reducing mortality. Overall, the results continue to show highest kelp growth and resilience at Point Loma relative to the rest of the San Diego region. As in past sampling and monitoring periods, the relative persistence of the kelp forest at Point Loma when compared with other sites along the coast, continues to suggest that point source impacts of the Point Loma outfall are not controlling kelp population fluctuations. Other factors most likely influencing kelp abundance in the San Diego area are sea water temperatures and temperature fluctuations, oceanic nutrient availability, light, especially for early life stage kelps, and benthic competition for space. This report documents spatially variable episodic kelp recruitment, with increasing abundance and plant growth at numerous sites in the monitoring program. It remains to be seen how the recently recovered populations will fare considering the potential for a significant El Niño event predicted by NOAA for late 2026-2027, which for the San Diego region could result in widespread warmer, nutrient-poor waters, with increased subtropical hurricane wave impacts.

CITED LITERATURE

Dayton, P. K., & Tegner, M. J. (1984). Catastrophic storms, El Niño, and patch stability in a southern California kelp community. Science, 224(4646), 283-285.

Dayton, P. K., Currie, V., Gerrodette, T., Keller, B. D., Rosenthal, R., & Tresca, D. V. (1984). Patch dynamics and stability of some California kelp communities. Ecological Monographs, 54(3), 253-289.

Dayton, P. K., Tegner, M. J., Parnell, P. E., & Edwards, P. B. (1992). Temporal and spatial patterns of disturbance and recovery in a kelp forest community. Ecological Monographs, 62(3), 421-445.

Dayton, P. K., Tegner, M. J., Edwards, P. B. & Riser, K. L. (1999). Temporal and spatial scales of kelp demography: the role of oceanographic climate. Ecological Monographs, (69), 219-250.

Dean, T. A., & Jacobsen, F. R. (1984). Growth of juvenile *Macrocystis pyrifera* (Laminariales) in relation to environmental factors. Marine Biology, 83(3), 301-311.

DeWreede, R. E. (1984). Growth and age class distribution of *Pterygophora californica* (Phaeophyta). Marine Ecology Progress Series 19, 93-100.

Deysher, L. E., & Dean, T. A. (1984). Critical irradiance levels and the interactive effects of quantum irradiance and dose on gametogenesis in the giant kelp *Macrocystis pyrifera*. Journal of Phycology, 20(4), 520-524.

Jackson, G., & Winant, C. (1983) Effect of a kelp forest on coastal currents. Continental Shelf Research, 2(1), 75-80.

Ladah, L. B. (2003). The shoaling of nutrient-enriched subsurface waters as a mechanism to sustain primary productivity off Central Baja California during El Niño winters. Journal of Marine Systems 42, 145-152.

Leichter, J. J., Ladah, L. B., Parnell, P. E., Stokes, M. D., Costa, M., & Dayton, P. K. (2023). Alongshore variation in nutrient exposure associated with thermal variability and internal waves in southern California Giant Kelp beds. Frontiers in Marine Research. 10,1007789.

Lüning, K., & Dring, M. J. (1975). Reproduction, growth and photosynthesis of gametophytes of *Laminaria saccharina* grown in blue and red light. Marine Biology, 29(3), 195-200.

Parnell, P., Miller, E. F., Cody, C. E. L., Dayton, P. K., Carter, M. L., & Stebbinsd, T. D. (2010). The response of giant kelp (*Macrocystis pyrifera*) in southern California to low-frequency climate forcing. Limnology and Oceanography, 55(6), 2686-2702.

Parnell, P. E. (2015). The effects of seascape pattern on algal patch structure, sea urchin barrens, and ecological processes. Journal of Experimental Marine Biology and Ecology, 465, 64-76.

Parnell, P. E., Cody, C. E. L., Ladah, L. B, Riser, K. L., Bulach B., Leichter, J. J., Latker, A. K., Schroeter S. C., & Dayton, P. K. (2026). Demography and dynamics of Giant Kelp Cohorts across four decades: Lessons for conservation and resilience planning. Ecological Applications 36(1): e70181.

Seymour, R. J., Tegner, M. J., Dayton, P. K., & Parnell, P. E. (1989). Storm wave induced mortality of giant kelp, *Macrocystis pyrifera*, in southern California. Estuarine, Coastal and Shelf Science, 28(3), 277-292.

Steneck, R. S., Graham, M. H., Bourque, B. J., Corbett, D., Erlandson, J. M., Estes, J. A., & Tegner, M. J. (2002). Kelp forest ecosystems: biodiversity, stability, resilience and future. Environmental Conservation, 29(4), 436-459.

Tegner, M. J., & Dayton, P. K. (1977). Sea urchin recruitment patterns and implications of commercial fishing. Science, 196(4287), 324-6.

Zimmerman, R. C., & Robertson, D. L. (1985) Effects of El Niño on local hydrography and growth of the giant kelp, *Macrocystis pyrifera*, at Santa Catalina Island, California, Limnology and Oceanography, 30(6), 1298-1302.

Appendix J

Ocean Imaging Annual Reports

2024 and 2025

Mark Hess

Ocean Imaging Corps
13976 West Bowles Avenue, Suite 100, Littleton CO 80127

External Report Submitted to City of San Diego
Public Utilities Department

Satellite Coastal Water Quality Monitoring in the San Diego / Tijuana Region

By Mark Hess



Annual Summary Report

1 January, 2024 - 31 December, 2024

All data and imagery contained in this report are strictly subject to Copyright by Ocean Imaging.

No data or imagery contained herein may be copied, digitally reproduced or distributed without written permission by Ocean Imaging Inc.

17 June 2025

Ocean Imaging

13976 West Bowles Avenue, Suite 100, Littleton CO 80127 Phone: 303-948-5272 www.oceani.com

Table of Contents

1. INTRODUCTION AND PROJECT HISTORY 1

2. METHODS AND TECHNOLOGY OVERVIEW 2

2.1 Imaging in the UV-Visible-Near Infrared Spectrum 2
2.2 Imaging in the Thermal Infrared Spectrum 2
2.3 Satellites and Sensors Utilized 2
2.4 Data Dissemination and Analysis 7

3. HIGHLIGHTS OF 2024 MONITORING 7

3.1 Atmospheric and Ocean Conditions 9
3.2 The South Bay Ocean Outfall Region 25
3.3 The Point Loma Outfall Region 31

3.4 KELP VARIABILITY 33

4. PRESENT AND FUTURE ENHANCEMENTS OF THE PROJECT 37

5. REFERENCES 39

APPENDIX A – HIGH RESOLUTION SATELLITE IMAGERY SHOWING SBOO-RELATED WASTEWATER PLUME 41

 © Ocean Imaging Inc. 2025

1. INTRODUCTION AND PROJECT HISTORY

In the 1990s, Ocean Imaging Corporation (OI) received multiple research grants from NASA's Commercial Remote Sensing Program for the development and commercialization of remote sensing applications in the coastal zone. As part of these projects, OI developed methods to utilize various types of remotely sensed data for the detection and monitoring of stormwater runoff and wastewater discharges from offshore outfalls. The methodology was initially demonstrated with collaboration of the Orange County Sanitation District in California (Svejkovsky and Haydock, 1998). The NASA-supported research led to a proof-of-concept demonstration project in the San Diego, California region co-funded by the EPA in 2000. Those results led, in 2002, to adding an operational remote sensing-based monitoring component to the San Diego region's established water quality monitoring program. The project continues as a joint effort between the Ocean Monitoring Program of the City of San Diego's Public Utilities Department (SDPUD) and the International Boundary and Water Commission (USIBWC).

The first phase of the project was a historical study utilizing several types of satellite data acquired between the early 1980s and 2002. The study established the prevailing near-surface current patterns in the region under various oceanic and atmospheric conditions. The current directions were deduced from patterns of turbidity, ocean temperature and surfactant slicks. In some cases, near-surface current velocity could be computed by tracking recognizable color or thermal features in time-sequential images. The historical study thus established baseline data for the region's current patterns, their persistence, their frequency, and the historical locations, size and dispersion trajectories of various land and offshore discharge sources from Publicly Owned Treatment Works (POTW) (e.g., the offshore outfalls, Tijuana River, Punta Bandera Treatment Plant discharge in Mexico, etc.).

The prime objectives of the project have expanded somewhat since its inception. Initially, emphasis was on utilizing the image data to discern and monitor surface and near-surface signatures from the South Bay Ocean Outfall (SBOO) and Point Loma Ocean Outfall (PLOO), separate them from other near-shore point and non-point runoff features, and monitor their locations, extents, and potential impact on the shoreline. Prior to this project, the spatial extents of the plumes could only be estimated from a relatively sparse spatial grid of field samples, which made it difficult to separate, for example, the SBOO near surface plume from the Tijuana River runoff plume. This ambiguity made it difficult, in turn, to objectively evaluate the potential contribution, if any, of the SBOO plume to beach contamination along the nearby shoreline. The satellite and aerial imagery helped directly establish the dispersal trajectories of the SBOO effluent during months when it reached the near-surface layer and support the claim that it likely never reaches the surf zone.

In October 2002, the operational monitoring phase of the project was initiated using the variety of satellite- and model-derived datasets discussed below. Over the past five to ten years, the project's objectives have broadened from focusing primarily on the outfalls to also provide larger-scale, regional observations of the physical and biological patterns and processes affecting the San Diego County and Tijuana River discharge regions. It is this broader-view perspective that led to the creation of supplementary image products from additional sensors and sources for the SDPUD.

This report summarizes observations made during the period 1/1/2024 – 12/31/2024.

2. METHODS AND TECHNOLOGY OVERVIEW

OI uses several remote sensing technologies to monitor San Diego's offshore outfalls and shoreline water quality. Their main principle is to reveal light reflectance and heat emission patterns that are characteristic of the different discharges, water masses, plankton blooms and suspended sediment loads. Most often this is due to specific substances contained in the effluent but absent in the surrounding water.

2.1 Imaging in the UV-Visible-Near Infrared Spectrum

This is the most common technique used with satellite and aerial images. Wavelengths (colors) within the range of the human eye are most often used but ultraviolet (UV) wavelengths are useful for detecting fluorescence from petroleum compounds (oil, diesel, etc.) and near-infrared (near-IR) wavelengths can be useful for correcting atmospheric interference from aerosols (e.g., smog and smoke). Near-IR wavelengths are also highly reflected from kelp seaweeds, so such data are particularly useful for delineating the region's kelp beds and monitoring their extents through time.

The best detection capabilities are attained when several images in different wavelengths are acquired simultaneously. These "multispectral" data can be digitally processed to enhance features not readily visible in simple color photographs. For example, two such images can be ratioed, thus emphasizing the water features' differences in reflection of the two specific wavelengths. A multi-wavelength image set can also be analyzed with multispectral classification algorithms which separate distinctive features or effluents based on the correlation relationships between the different color signals.

The depth to which the color sensors can penetrate depends on which wavelengths they see, their sensitivity and the general water clarity. In the San Diego region, green wavelengths tend to reach the deepest and, as elsewhere, UV and near-IR wavelengths penetrate the least. Generally, OI's satellite and aerial sensor data reveal reflective features in the upper one to fifteen meters of the ocean.

2.2 Imaging in the Thermal Infrared Spectrum

Some satellite and aerial sensors image heat emanating from the ground and the ocean. They thus reveal patterns and features due to their differences in temperature. Since thermal infrared (TIR) wavelengths are strongly absorbed by water, the images reveal temperature patterns only on the water's surface. Such images can help detect runoff plumes when their temperatures differ from the surrounding ocean water. Runoff from shoreline sources tends to be warmer than ocean water, although the reverse can be true during the winter. Plumes from offshore outfalls can sometimes also be detected with thermal imaging. Since the effluent contains mostly fresh water, it is less dense than the surrounding salt water and tends to rise towards the surface. How far it rises depends on outfall depth, ocean currents, and stratification conditions. If it makes it all the way to the surface, it is usually cooler than the surrounding sun-warmed surface water. A plume signature detectable in multispectral color imagery but not detectable in simultaneously collected TIR imagery indicates the rising plume has not reached the actual ocean surface and remains submerged.

2.3 Satellites and Sensors Utilized

Until 2010, the project relied heavily on acquisition of multispectral color imagery with OI's DMSC-MKII aerial sensor and TIR imagery from a Jenoptik thermal imager integrated into the system. These aerial image sets were most often collected at 2m resolution. The flights were done on a semi-regular schedule ranging from one to two times per month during the summer to once or more per week during the rainy season. The flights were also coordinated with the City of San Diego's regular offshore field sampling schedule so that the imagery was collected on the same day (usually within two to three hours)

of the field data collection. Additional flights were performed on an on-call basis immediately after major storms or other events such as sewage spills. In late 2010, OI negotiated a special data collection arrangement with Germany's RapidEye Corporation and this project began utilizing their multispectral imagery in lieu of most of the aerial Digital Multispectral Camera (DMSC) image acquisitions. The use of satellite as opposed to aerial data also enables a more frequent and regionally contiguous monitoring of events affecting the target areas. In late 2019 the RapidEye satellite constellation was decommissioned by the current operator Planet Labs. Subsequently, OI secured the regular acquisition of SPOT 6 and SPOT 7 satellite imagery covering the same geographical area beginning in 2020. Table 1 lists the properties of the remote sensing image sources routinely used during the project.

Beginning in 2017, OI also began processing and posting imagery from the Sentinel-2 satellites. Sentinel-2A and 2B are satellites operated by the European Space Agency (ESA) and are the spaceborne platforms for the Multispectral Instrument (MSI). The Sentinel-2A and 2B MSIs sample 13 spectral bands: four bands at 10 meters, six bands at 20 meters and three bands at 60-meter spatial resolution. The green band focusing in the 560 nm wavelength is ideal for detecting turbidity plumes from the outfalls both at the surface and at depths down to 15 meters depending on ocean conditions. The revisit time of the Sentinel-2A satellite is approximately ten days. The second satellite carrying the MSI sensor, Sentinel-2B, was launched into orbit by the ESA and provided the first set of data from the MSI sensor as of March 17, 2017. The revisit time of the Sentinel-2B satellite is also approximately ten days. Beginning in 2018, data from Sentinel-2B became a regular addition to the satellite imagery products posted to the OI web portal. On average the Sentinel-2A and 2B imagery processed to highlight anomalous turbidity signals emanating from the PLOO, SBOO, as well as the discharge from the Tijuana River (TJR) and San Diego River (SDR) are posted to the OI web portal within 24-36 hours of satellite data acquisition. In some cases, if the data are available to OI earlier, the image products are delivered as quickly as 12 hours post-acquisition. During 2024 the Sentinel-2A and 2B satellites provided the most temporally comprehensive set of high-resolution satellite imagery. In total, 105 high resolution, multispectral satellite images showing the offshore San Diego County region were acquired, processed, and delivered in 2024. This equates to a 27% increase in satellite data used to document the area when compared to 2023 – most probably due to fewer instances of total cloud cover over the San Diego region. Of the 105 total image sets, 65 were from Sentinel-2A or 2B data making up 62% of the high-resolution satellite data processed and posted as part of the project, roughly the same as in 2023.

In October 2018, OI began using imagery from Sentinel-3A. Shortly thereafter, in December 2018 imagery from Sentinel-3B was incorporated into the mix of observation platforms. Like Sentinel-2, Sentinel-3A and Sentinel-3B are earth observation satellites developed by the ESA for the Copernicus Program. Sentinel-3A was launched on February 16, 2016, and Sentinel-3B followed on April 25, 2018. The 3A and 3B satellites are identical and deliver products in near-real time. The satellites include four different remote sensing instruments. The Ocean and Land Colour Instrument (OLCI) covers 21 spectral bands (400–1020 nm) with a swath width of 1270 km and a spatial resolution of 300 m. Sea and Land Surface Temperature Instrument covers 9 spectral bands (550–12 000 nm), using a dual-view scan with swath widths of 1420 km (nadir) and 750 km (backwards), at a spatial resolution of 500 m for visible and near-infrared, and 1 km for thermal infrared channels. The Sentinel-3 mission's main objectives are to measure sea surface topography along with the measurement of ocean/land surface temperature and ocean/land surface color. One of the satellites' main secondary missions is to monitor sea-water quality and marine pollution. The instrument on these satellites designed for these purposes is the OLCI. Ocean Imaging creates daily products dependent on cloud cover for the entire San Diego/Tijuana region using the OLCI instrument. Between the 3A and 3B satellites this

Table 1. Satellite sensors utilized in the project and their characteristics.

Sensor	Utilization Period	Resolution (m)	Utilized Wavelength Range
AVHRR	2003 - Present	1100	Channel 4: 10.30 – 11.39 um Channel 5: 11.50 – 12.50 um
MODIS	2003 - Present	250/500/1000	Band 1 (250 m): .620 – .670 um Band 2 (250 m): .841 – .876 um Band 3 (500 m): .459 – .479 um Band 4 (500 m): .545 – .565 um
Landsat 8 OLI, TIRS	2013 - Present	30 (visible - Near-IR) 100 (Thermal-IR)	Band 2: .452 - .512 um Band 3: .533 - .590 um Band 4: .636 - .673 um Band 5: .851 - .879 um Band 10: 10.60 - 11.19 um Band 11: 11.50 - 12.51 um
Sentinel-2A/2B	2017 - Present	10 (visible - Near-IR) 60 (Vegetation Red Edge) 60 (UV, SWIR)	Band 1: .443 um Band 2: .490 um Band 3: .560 um Band 4: .665 um Band 5: .705 um Band 6: .740 um Band 7: .783 um Band 8: .842 um Band 8A: .865 um
Sentinel-3A/3B	2018 - Present	300 (all utilized bands)	Band Oa2: .412.5 um Band Oa3: .442.5 um Band Oa4: .490 um Band Oa5: .510 um Band Oa6: .560 um Band Oa7: .620 um Band Oa8: .665 um Band Oa10: .68125 um Band Oa11: .07875 um Band Oa17: .865 um
VIIRS	2019 - Present	750 (all utilized bands)	Band M1: 0.402 - 0.422 um Band M2: 0.436 - 0.454 um Band M3: 0.478 - 0.488 um Band M4: 0.545 - 0.565 um Band M5: 0.662 - 0.682 um Band M6: 0.739 - 0.754 um Band M7: 0.846 - 0.885 um Band M8: 1.23 - 1.25 um Band M9: 1.371 - 1.386 um Band M10: 1.58 - 1.64 um Band M11: 2.23 - 2.28 um Band M12: 3.61 - 3.79 um Band M13: 3.97 - 4.13 um Band M14: 8.4 - 8.7 um Band M15: 10.26 - 11.26 um Band M16: 11.54 - 12.49 um
SPOT 6	2019 - Present	6	Band 1: .450 - .745 um Band 2: .450 - .525 um Band 3: .530 - .590 um Band 4: .625 - .695 um Band 5: .760 - .890 um
Sentinel-1A SAR	2021 - Present	5 x 20	C-band operating at a center frequency of 5.405 GHz
Landsat 9 OLI-2, TIRS-2	Late 2021 - Present	30 (visible - Near-IR) 100 (Thermal-IR)	Band 2: .452 - .512 um Band 3: .533 - .590 um Band 4: .636 - .673 um Band 5: .851 - .879 um Band 10: 10.60 - 11.19 um Band 11: 11.50 - 12.51 um

results in better than daily coverage with 3A and 3B data occasionally both being available on the same day. True color, near infrared, products are posted bi-monthly along with similar resolution MODIS products. Sentinel-3-derived chlorophyll and possibly total suspended matter (TSM) products, offering a 300-meter spatial resolution, will be incorporated into the data mix in late 2025.

As stated above, the RapidEye satellites were decommissioned in late 2019 and replaced by data from the SPOT 6 and SPOT 7 satellites in January of 2020. The two SPOT satellites/sensors are identical in design and function. They both image in spectral bands similar to the RapidEye satellites at a ground sampling distance of 8.8 meters for the multispectral data (see Table 1). The dynamic range of these sensors is 12-bits per pixel. OI uses the blue, green, red, and near-infrared bands from these sensors. Empirically we have found that the SPOT data have a high signal to noise ratio and therefore produce a high-quality product for detecting wastewater surface manifestations and delineating the river run-off plumes. In March of 2023, the SPOT 7 satellite stopped functioning, however we continue to receive data from SPOT 6 and are able to acquire roughly two to three clear images per month from this sensor. Figure 1 shows a set of images from 10/19/24 and 10/21/24 from Landsat 9, SPOT and Sentinel-2 highlighting the ability to obtain high-resolution imagery from multiple satellites on the same and successive days. The three images from 10/19/24 were captured within thirteen minutes of each other. Note the heavy coastal turbidity and discharge from both the TJR as well as shoreline areas south of the border moving north toward the South Bay beaches and offshore waters. Six-kilometer-spaced 25-hour averaged High Frequency Radar-derived (HF Radar) ocean currents from these days computed for the period one to two hours of the satellite data acquisitions are overlaid on the imagery to illustrate the surface flow patterns of the turbid water. Note that the turbid water appears to be clearing up by 10/21/24, however the currents continue to push the water from the TJR and border region northward.

More discussion on river discharge moving into the South Bay region is in the following sections.

As detailed in Table 1, to date, this work utilizes 1100 m resolution Advanced Very High Resolution Radiometer (AVHRR)-derived imagery (available multiple times per day), 1000 m resolution chlorophyll and sea surface temperature (SST) Moderate Resolution Imaging Spectroradiometer (MODIS)-derived imagery (available multiple times per day), 500 m resolution MODIS true color imagery (available near-daily), 750 m resolution Visible Infrared Imaging Radiometer Suite (VIIRS) chlorophyll and SST imagery (available multiple times per day), 300 m resolution Sentinel-3A and 3B color and thermal imagery (available daily), 30 m & 60 m Landsat 8 OLI/TIRS and Landsat 9 OLI-2/TIRS-2 color and thermal imagery (each available approximately every 16 days), 10 m resolution Sentinel-2A and 2B multispectral imagery (available 2-4 times per week), and 6m resolution Satellite Pour l'Observation de la Terre (SPOT) 6 (available approximately every 5-7 days). In early 2025, Sentinel-2A started to be phased out and acquisition frequency reduced to 1-2 times per month, shortly after the Sentinel-2C system was launched and data became available.

In addition, Synthetic Aperture Radar (SAR) data from the Sentinel-1A satellite (available every 3-6 days at a spatial resolution of 5m x 20 m) were added to the suite of remote sensing products in late 2021. SAR can detect surfactant films associated with natural processes (Svejkovsky and Shandley, 2001) and plumes containing anthropogenic substances (Svejkovsky and Jones, 2001; Gierach et al., 2017) when optical sensors might be limited by cloud cover or heavy atmospheric haze. The primary purpose of these satellites for this project is to provide another look at the TJR discharge plume to assess its offshore extent and direction of flow. The river and coastal runoff often contain natural and anthropogenic surfactants that dampen the SAR signal and therefore make it detectable in the data. Phytoplankton blooms also release biological surfactants that result in low backscatter observed

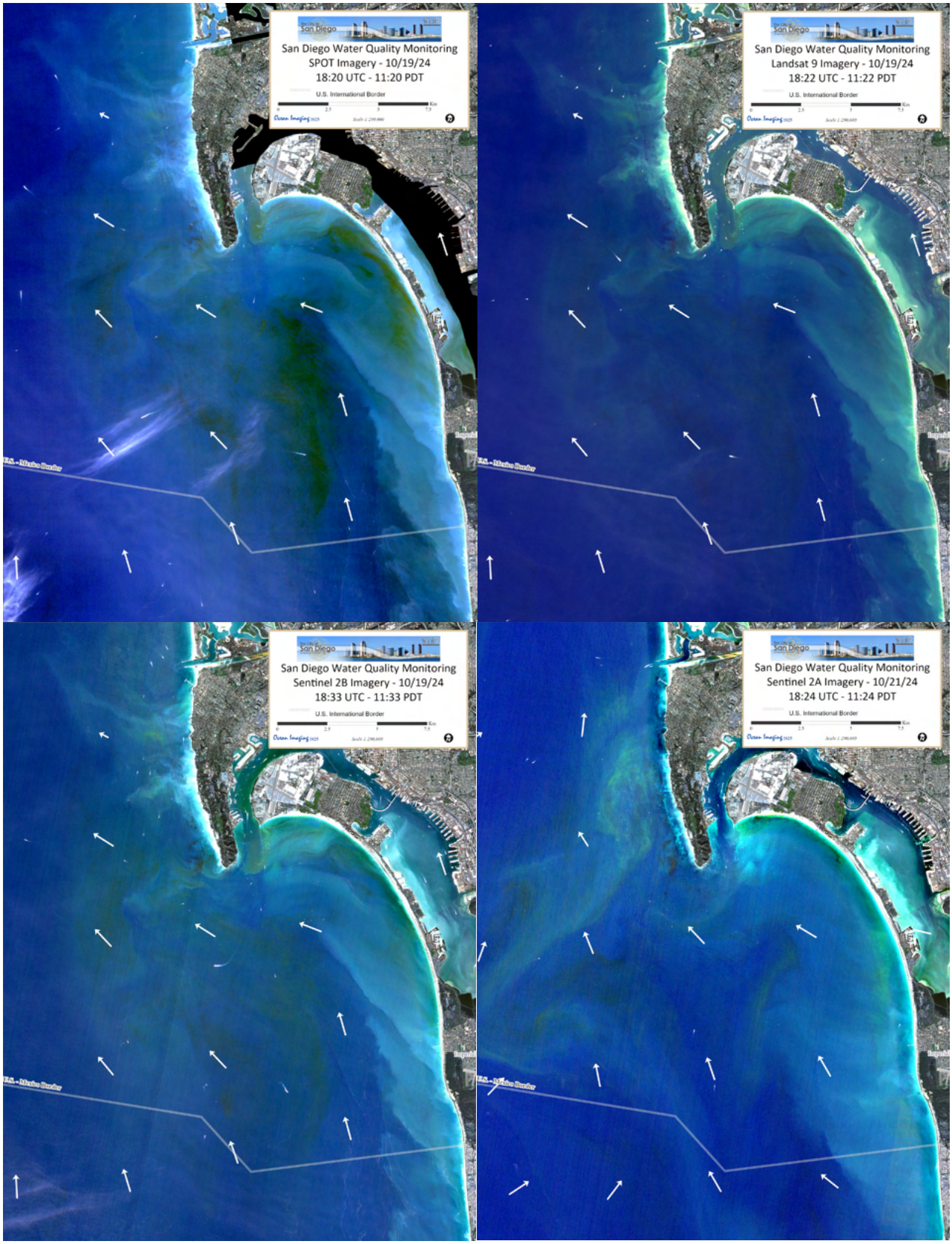


Figure 1. SPOT 6, Landsat 9 and Sentinel-2 high resolution satellite imagery from 01/19/24 and 10/21/24 with HF Radar-derived ocean currents overlaid. The three scenes from 10/19/24 were acquired thirteen minutes apart. Note that the observed movement of the coastal turbidity patterns in the South Bay area agree with the direction of the currents shown in the HF Radar-derived flow field

in the SAR data (Svejkovsky and Shandley, 2001). In 2024, 87 SAR images were acquired and processed for the San Diego region providing an additional source of information even during cloudy conditions. Figure 2 shows a sample Sentinel-1 SAR image from 11/10/24 along with SPOT 6 and Sentinel-2A scenes from the same day highlighting surfactant signatures in the SAR data created by strong phytoplankton blooms in the region. The satellite data acquisitions were approximately 5.5 hours apart. The plankton blooms clearly identifiable in both the SPOT and Sentinel-2 visible imagery (top) corroborate the supposition that the dampened SAR signal (dark areas identified by the red arrows) can help identify plankton blooms and river discharge with a high composition of surfactants. Recent attention on the severity of the TJR polluted discharge (Little, 2024) and Harmful Algal Blooms (HAB) makes monitoring and documenting the coastal and offshore waters with multiple sensor types increasingly important.

In 2012, OI added additional broad-scale products to the datasets available to the SDPUD and project partners. These include two types of ocean current data: High Frequency Radar-derived surface currents (HF Radar) and Hybrid Coordinate Ocean Model (HYCOM) model-derived surface currents (http://hycom.org). The raw data for the HF Radar currents are retrieved from National HF Radar Network via the Scripps Coastal Observing Research and Development Center (CORDC) on an hourly basis and reformatted into ESRI-compatible shapefiles. The hourly products are averages of the previous 25 hours and generated at 1 km and 6 km spatial resolutions. Additional HYCOM model-based products include daily ocean salinity, mixed layer depth, and subsurface temperature at 50, 100, 150 and 200 meters. In 2016 these products were delivered in a Web Map Service (WMS) Representational State Transfer (REST) service format compatible with the City's now retired BioMap server. They are presently being generated and archived in preparation for delivery via a next generation WMS dashboard-style data portal which will become operational in 2025. Details of this project are discussed below. The existing high resolution (6-30 m) observation region extends from approximately La Jolla southward to Rosarita Beach, Mexico and out approximately 50 miles. The coarser-scale products (250-1000 m) such as chlorophyll, SST, ocean currents and HYCOM-derived products encompass the entire Southern California Bight (SCB).

2.4 Data Dissemination and Analysis

The satellite data are made available to the SDPUD and other project constituents through a dedicated, password-protected web site. Although it is possible to process most of the data in near-real-time, earlier in the project it was decided that the emphasis of this program is not on providing real-time monitoring support and the extra costs associated with the rapid data turn-around are not warranted. Most satellite data are therefore processed and posted within 1-2 days after acquisition. As noted above, however, OI has in several cases made imagery available to the SDPUD in near-real time (within 12-24 hours) via email when observations appeared to be highly significant to ocean dynamics surrounding the outfalls or other sudden/anomalous event. The website was updated in 2022 to improve its ease of use and presentation of available imagery.

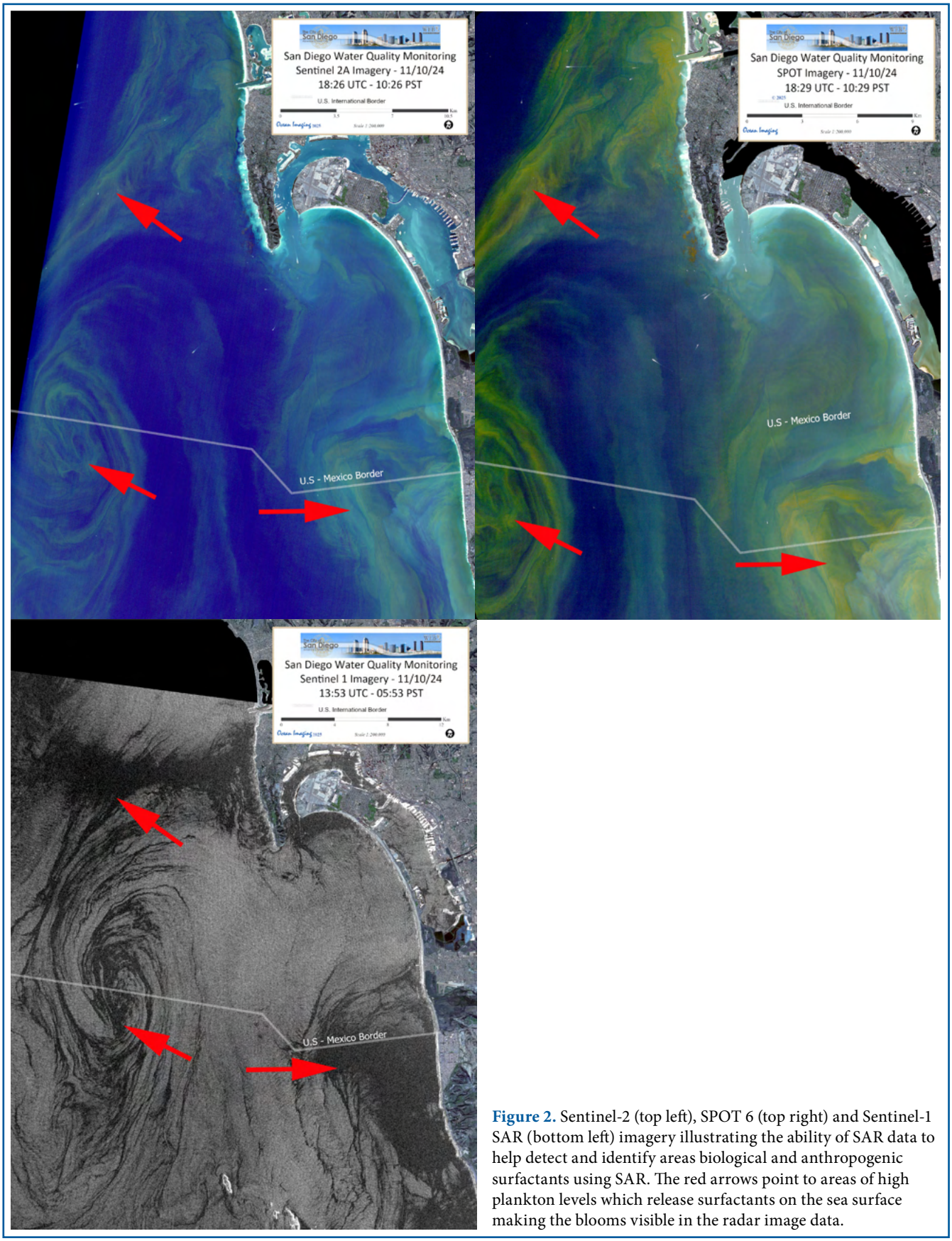


Figure 2. Sentinel-2 (top left), SPOT 6 (top right) and Sentinel-1 SAR (bottom left) imagery illustrating the ability of SAR data to help detect and identify areas biological and anthropogenic surfactants using SAR. The red arrows point to areas of high plankton levels which release surfactants on the sea surface making the blooms visible in the radar image data.

3. HIGHLIGHTS OF 2024 MONITORING

3.1 Atmospheric and Ocean Conditions

Coastal and oceanic water quality can often be correlated to rainfall events. In 2024, the San Diego International Airport station (SDIA) measured 11.37 inches of total annual rainfall and the TJR Estuary 8.67 inches, both higher than 2013-2023 averages of 8.47 and 7.85 inches respectively (see Table 2). The annual recorded precipitation recorded at the SDIA during 2024 was almost three inches above the previous 12-year average for the region. While the monthly rainfall followed normal seasonal patterns for the first four months of the year with the winter and spring months for the most part

Table 2. San Diego and Tijuana Estuary precipitation totals 2012-2024

San Diego International Airport Cumulative Monthly Precipitation in Inches

	2012	2013	2014	2015	2016	2017	2018	2019	2020	2021	2022	2023	2024
January	0.40	0.70	0.01	0.42	3.21	2.99	1.77	2.42	0.48	1.80	0.16	5.14	3.67
February	1.19	0.63	1.00	0.28	0.05	1.58	0.35	4.04	0.38	0.10	0.70	1.78	4.61
March	0.97	1.22	1.28	0.93	0.76	0.08	0.65	1.23	2.15	1.48	1.61	3.97	2.58
April	0.88	0.01	0.54	0.02	0.55	0.01	0.02	0.10	3.68	0.07	0.02	0.12	0.19
May	0.02	0.26	--	2.39	0.44	0.87	0.09	0.86	0.02	0.07	0.02	0.09	0.08
June	--	--	--	0.04	--	0.02	--	0.01	0.14	0.01	--	0.03	0.01
July	--	0.05	--	1.71	--	--	--	--	--	--	--	--	0.01
August	--	--	0.08	0.01	--	--	0.02	--	--	0.23	--	1.84	0.02
September	--	--	--	1.24	0.32	0.06	--	0.11	--	0.50	0.65	0.05	0.02
October	0.70	0.25	--	0.43	0.07	--	0.57	--	0.12	1.01	0.09	--	0.01
November	0.28	1.48	0.37	1.54	0.61	0.02	0.69	2.72	0.14	--	1.07	0.61	0.14
December	2.19	0.46	4.50	0.88	4.22	--	0.83	4.03	0.60	2.58	1.55	0.79	0.03
Annual Total	**6.63**	**5.06**	**7.78**	**9.89**	**10.23**	**5.63**	**4.99**	**15.52**	**7.71**	**7.85**	**5.87**	**14.42**	**11.37**

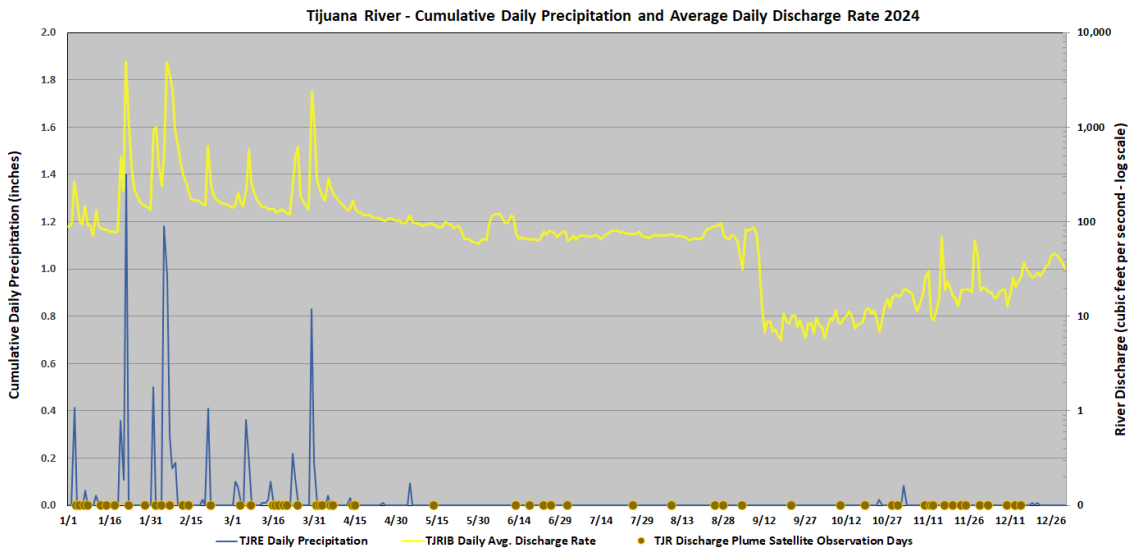
Tijuana Estuary Cumulative Monthly Precipitation in Inches

	2012	2013	2014	2015	2016	2017	2018	2019	2020	2021	2022	2023	2024
January	0.70	0.05	0.08	0.32	2.40	3.61	0.82	1.80	0.61	2.21	0.17	3.47	2.38
February	0.86	--	1.35	0.13	0.02	4.06	0.47	3.62	0.51	0.06	0.58	2.06	3.73
March	1.21	1.43	0.55	1.01	1.28	0.04	1.17	1.33	2.59	1.12	1.64	3.32	2.22
April	0.82	0.11	0.35	0.07	1.91	0.01	0.10	0.33	5.52	0.04	0.13	0.06	0.09
May	--	0.36	--	1.13	0.97	1.07	0.08	0.50	0.02	0.01	--	0.12	0.09
June	--	--	0.12	--	--	--	--	0.02	0.21	0.06	--	0.05	--
July	--	0.01	0.33	0.39	--	0.01	0.01	--	--	--	--	0.01	--
August	--	--	0.04	--	--	0.02	--	--	--	0.02	--	1.89	--
September	0.02	0.01	--	0.48	0.49	0.03	--	--	--	--	0.48	0.04	--
October	0.50	0.41	--	0.21	--	--	0.13	--	0.04	0.91	0.29	0.01	0.02
November	--	0.25	0.29	0.61	0.34	0.06	0.82	2.99	0.08	0.02	0.95	1.08	0.11
December	0.04	0.50	3.09	0.61	4.32	0.09	3.16	3.82	0.60	1.18	1.13	0.54	0.02
Annual Total	**4.15**	**3.13**	**6.20**	**4.94**	**11.73**	**8.99**	**6.76**	**14.41**	**10.18**	**5.63**	**5.38**	**12.66**	**8.67**

matching the expected rainy season and the summer months being mostly dry, the months of September through December exhibited zero to relatively low rainfall compared to the previous twelve years. The influence of an extreme early-February rain event and the occurrence of more than double the average March precipitation had an impact on coastal water quality, which is evident in the satellite imagery showing turbid waters and elevated chlorophyll levels during and subsequent to this time frame.

Figure 3 shows cumulative daily precipitation in the Tijuana Estuary along with the average daily river discharge at the Tijuana River International Boundary station (TJRIB). The table to the side of the plot gives the dates for which there was measurable precipitation at that station. As noted in previous reports, and is evident in Table 2, the monthly and annual precipitation amounts can differ at times between the SDIA and TJR reporting stations. The primary period of consistent and/or heavy precipitation occurred during the months of January, February and March with relatively little to no rainfall recorded for the remainder of the year.

We have defined a significant TJR discharge event as when the spectrally distinct "fresh core" of the river discharge plume as defined by Svejkovsky et al., (2010) is clearly visible in the imagery. There were 64 days during which the TJR discharge plume was identified as significant in the satellite imagery. Only 24 of these days were during the three rainy months at the beginning of the year and only 36 (56%) of the discharge observations can be confidently attributed to rainfall occurring one to three days prior to the observation. Figures 1 and 4 provide example imagery that show higher than normal coastal turbidity, plankton blooms and visible TJR discharge plumes even though there was no measurable rainfall prior to the imaging dates. This is likely because the TJR flow rate remained above 50 cubic feet per second (cfs) up to the month of September with an average discharge rate for 2024 of 152.8 cfs and 53.5 cfs during the months of June through October. Other possible explanations could be that the coastal turbidity was caused by significant ocean swell/wave action and ocean conditions conducive to phytoplankton blooms.



Date	CumPrcp (in)
01/03/24	0.41
01/07/24	0.06
01/11/24	0.04
01/20/24	0.36
01/21/24	0.11
01/22/24	1.40
02/01/24	0.50
02/02/24	0.01
02/05/24	1.18
02/06/24	0.97
02/07/24	0.29
02/08/24	0.16
02/09/24	0.18
02/19/24	0.02
02/21/24	0.41
03/02/24	0.10
03/03/24	0.08
03/04/24	0.01
03/06/24	0.36
03/07/24	0.17
03/12/24	0.01
03/13/24	0.01
03/14/24	0.02
03/15/24	0.10
03/23/24	0.22
03/24/24	0.11
03/30/24	0.83
03/31/24	0.18
04/05/24	0.04
04/13/24	0.03
04/25/24	0.01
05/05/24	0.09
10/24/24	0.02
11/02/24	0.08
11/23/24	0.01
11/24/24	0.01
12/19/24	0.01
12/21/24	0.01

Figure 3. Daily accumulated rainfall in the Tijuana Estuary, average daily river discharge rate measured at the Tijuana River International Boundary station and days on which significant TJR discharge was observed in the high-resolution satellite imagery including the Sentinel-1 SAR data.

When the higher coastal turbidity and river discharge levels did follow the rainfall events and water quality noticeably decreased one to two days following measurable precipitation, the coastal and offshore conditions typically improved only two to three days after the rainfall ceased. Figure 5 provides examples of heavy coastal turbidity and extensive



Figure 4. Sample high-resolution imagery from SPOT 6 highlighting turbid water, plankton blooms and TJR runoff plumes during periods when there was no measurable rainfall prior to the satellite imaging dates. Interestingly, on 10/29/24 when the TJR discharge appears to be the most prominent, the TJR flow rate for that day was only 15.8 cfs. It was 64.4, 62.7 and 72.9 cfs on 06/18/24, 07/02/24 and 08/28/24 respectively.

river runoff observed in the satellite imagery resulting from significant precipitation events.

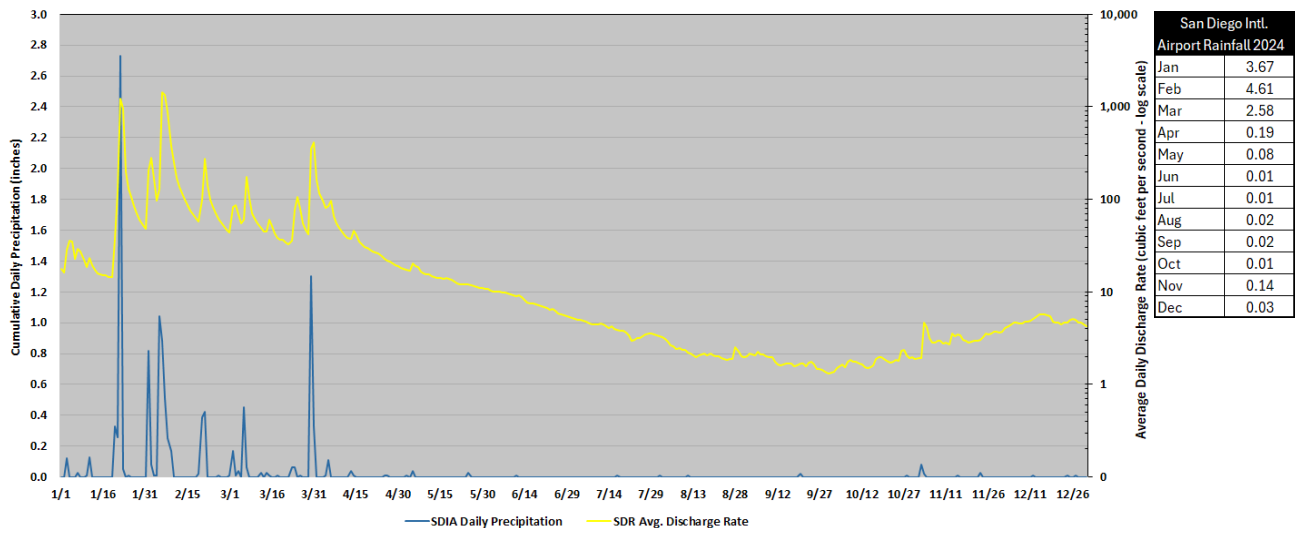
As discussed above, there was negligible measured precipitation in the San Diego region from May through October. River flow rates in cfs measured by the United States Geological Survey (USGS) Fashion Valley gauge generally correspond well with the rainfall data (Figure 6). The average flow rate in 2024 (43.0 cfs) was lower than the rate experienced during 2023 (63.6 cfs), most likely due to overall higher rainfall in 2023 (Table 2). Figures



Figure 5. Landsat, Sentinel-2 and SPOT data provide examples of days when the imagery displayed heavy TJR discharge along with coastal and offshore turbidity that can be directly correlated to rainfall events prior to the imaging dates.

5 and 7 provide examples of when the satellite data exhibited notable coastal and offshore turbid conditions as well as strong plankton blooms in the Point Loma and region and area west of Mission Bay that correlate with increased SDR flow and precipitation measurements shown in Figure 6.

In 2024 the County of San Diego issued 276 posted shoreline and/or rain advisories and 102 beach/shoreline closures. This is an 11.5% decrease in the number of advisories and a 104% increase in closures compared to 2023 (312 advisories and 50 closures respectively). The two longest contiguous 2024 closures lasted until 06/30/24 at Border Field State Park along the south end of the Tijuana Slough Shoreline and Imperial Beach. In fact, Border Field State Park had been closed for over two years prior to 2024. The majority of the closures extended from the Tijuana River mouth all the way past Avenida Del Sol to include nearly all of the Coronado City beaches. Most were associated with contamination from the TJR runoff. Generally, the closures can be attributed to a rain event prior to and/or during the closure period leading to heavy TJR discharge and coastal turbidity as shown in Figures 4 and 5. However, 25 closures were triggered by sewage spills in San Diego Bay, and several other locations. Six of the closures were attributed to an exceedance of bacterial standards with no known source. Also, 44 of the 102 closures happened between the months of May through the beginning of November when no rainfall was recorded at the Tijuana Estuary or SDIA stations within three days prior to the closure. Table 3 also shows the date(s) of the high-resolution satellite data in the project's archive acquired closest in time to the start date of the closure and/or rain advisory. Satellite data during the beach closure periods regularly show high turbidity and suspended solids and/or high plankton levels along the coastline near the closed regions as well as greater than normal TJR runoff, sometimes being carried north by the ocean currents. Figures 5 and 8 provide examples of the TJR plume extending north and ocean currents pushing the TJR discharge up past Border Field State Park towards the Coronado beaches, corresponding with shoreline closures during the same period.



San Diego Intl. Airport Rainfall 2024	
Jan	3.67
Feb	4.61
Mar	2.58
Apr	0.19
May	0.08
Jun	0.01
Jul	0.01
Aug	0.02
Sep	0.02
Oct	0.01
Nov	0.14
Dec	0.03

Figure 6. Average daily San Diego River flow rate as measured by the USGS Fashion Valley gauge plotted with daily precipitation amounts as recorded at the San Diego International Airport. Monthly precipitation totals at the SDIA station are displayed to the right of the plot.

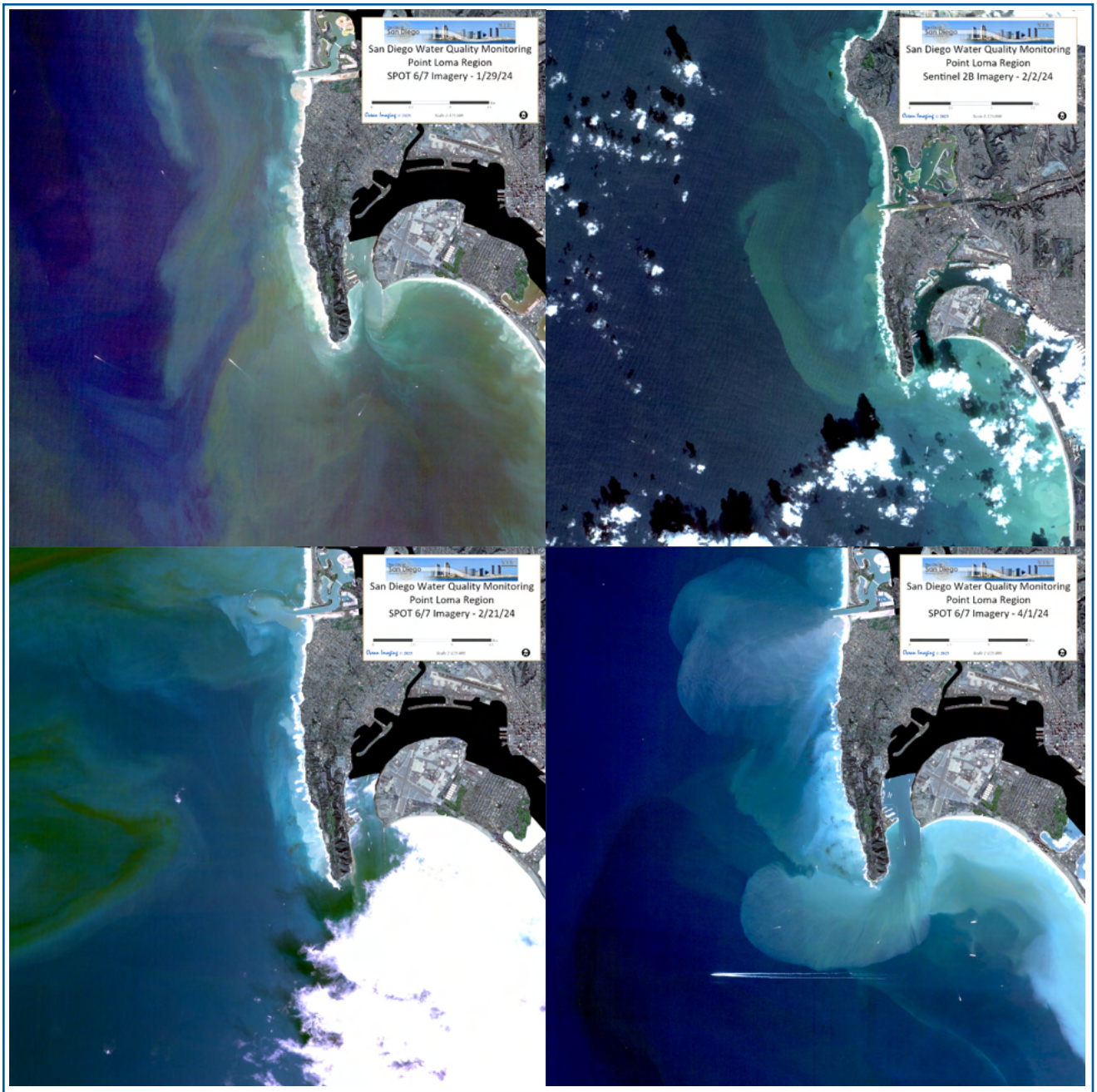


Figure 7. High-resolution SPOT data providing examples of days when the imagery displayed heavier than usual river discharge, coastal and offshore turbidity and plankton blooms that can be directly linked to a prior rainfall event. River gauge data also show higher than average flow rates on or near these dates.

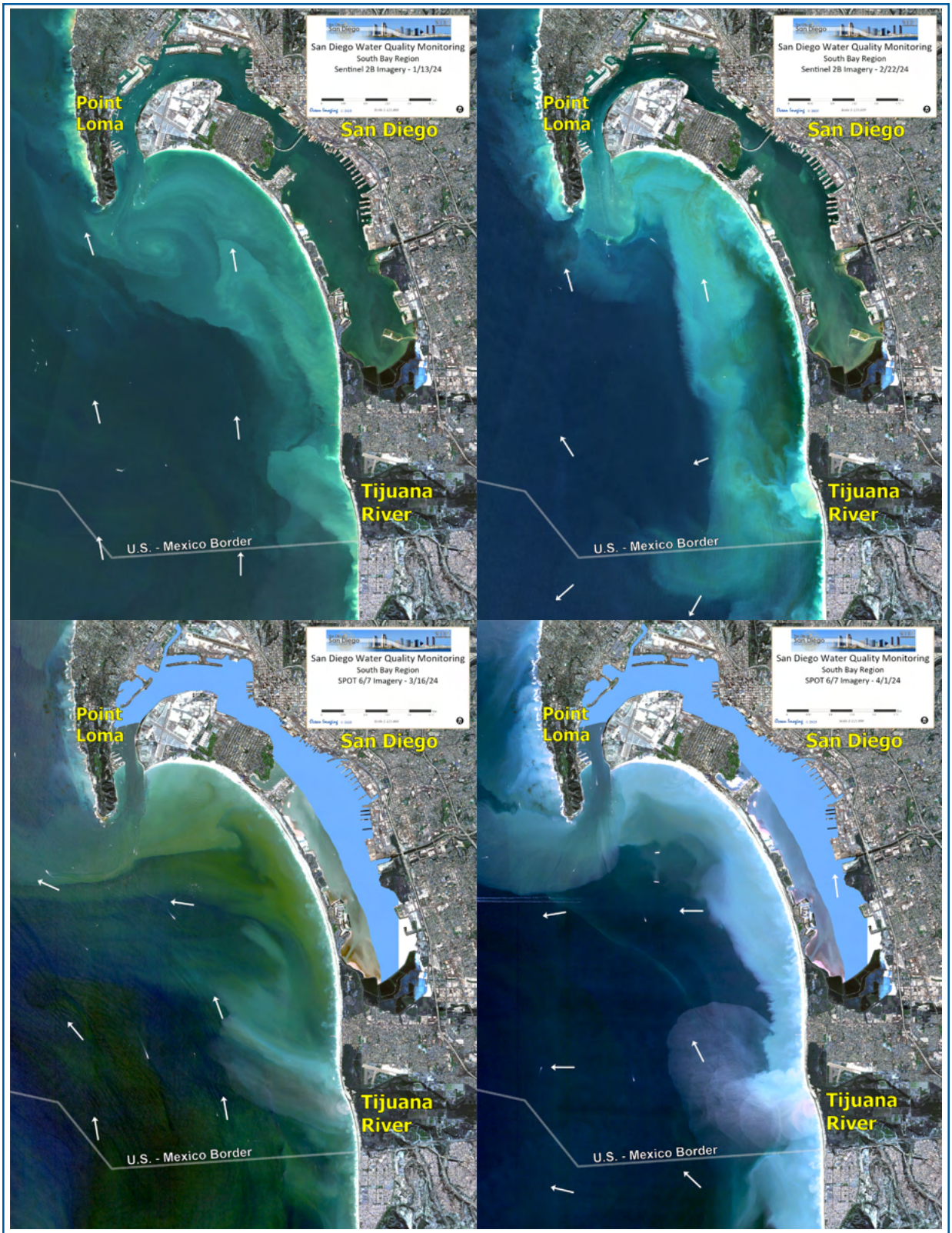


Figure 8. Sentinel-2 and SPOT 6 imagery with time-coincident 6km HF Radar currents overlaid to provide examples of when the Tijuana River plume extended to the north and/or when ocean currents pushed TJR discharge up past Border Field State Park towards the Coronado beaches, corresponding with shoreline closures during the same time period.

Table 3. 2024 County of San Diego shoreline closures, rain advisories and associated project satellite data (Source: California State Water Resources Control Board). general rain advisory beach closure associated with the Tijuana River bay or beach closure due to a sewage spill bay or beach closure due to elevated bacteria levels

Station Description	Beach Name	Station Name	Type	Cause	Source	Start Date	End Date	Duration (days)	Nearest Rain Date	Time From Rain Event	Satellite Image data
All_SanDiego County Beaches	All_SanDiego_County	All_SanDiego County Beaches	Rain			1/1/2024	1/6/2024	6	12/31/2023	0	1/2, 1/3, 1/4. 1/5, 1/7
Avenida Lunar	Coronado City beaches	IB-079	Closure	Tijuana River Associated	Sewage/ Grease	1/1/2024	1/8/2024	8	12/31/2023	0	1/2, 1/3, 1/4. 1/5, 1/7, 1/8
Loma Ave (frmrly Isabella	Coronado City beaches	EH-050	Closure	Tijuana River Associated	Sewage/ Grease	1/1/2024	1/8/2024	8	12/31/2023	0	1/2, 1/3, 1/4. 1/5, 1/7, 1/8
Navy Fence (A)	Coronado north beach	EH-060	Closure	Tijuana River Associated	Sewage/ Grease	1/1/2024	1/8/2024	8	12/31/2023	0	1/2, 1/3, 1/4. 1/5, 1/7, 1/8
Silver Strand N end (ocean)	Silver Strand State Beach	IB-070	Closure	Tijuana River Associated	Sewage/ Grease	1/1/2024	1/13/2024	13	12/31/2023	0	10 dates
End of Seacoast Dr	Imperial Beach municipal beach, other	IB-050	Closure	Tijuana River Associated	Sewage/ Grease	1/1/2024	6/30/2024	182	12/31/2023	0	86 dates
Border Fence N side	Border Field State Park	IB-010	Closure	Tijuana River Associated	Sewage/ Grease	1/1/2024	6/30/2024	182	12/31/2023	0	86 dates
Avenida Lunar	Coronado City beaches	IB-079	Closure	Tijuana River Associated	Sewage/ Grease	1/9/2024	1/13/2024	5	1/7/2024	2	1/10, 1/13, 1/14
Loma Ave (frmrly Isabella	Coronado City beaches	EH-050	Closure	Tijuana River Associated	Sewage/ Grease	1/10/2024	1/13/2024	4	1/10/2024	0	1/10, 1/13, 1/14
Navy Fence (A)	Coronado north beach	EH-060	Closure	Tijuana River Associated	Sewage/ Grease	1/11/2024	1/13/2024	3	1/10/2024	1	1/13, 1/14
Silver Strand N end (ocean)	Silver Strand State Beach	IB-070	Closure	Tijuana River Associated	Sewage/ Grease	1/17/2024	5/6/2024	111	1/11/2024	7	1/18
All_SanDiego County Beaches	All_SanDiego_County	All_SanDiego County Beaches	Rain			1/20/2024	1/26/2024	7	1/20/2024	0	1/22, 1/23, 1/26, 1/27
Bayside Park (J Street)	San Diego Bay	EH-120	Closure	Sewage Spill	Sewage/ Grease	1/22/2024	1/28/2024	7	1/22/2024	0	1/22,1/23,1/26,1/27,1/29
Sweetwater River (NR)	San Diego Bay	EH-130	Closure	Sewage Spill	Sewage/ Grease	1/22/2024	2/11/2024	21	1/22/2024	0	13 dates
Navy Fence (A)	Coronado north beach	EH-060	Closure	Tijuana River Associated	Sewage/ Grease	1/22/2024	3/19/2024	58	1/22/2024	0	33 dates
Loma Ave (frmrly Isabella	Coronado City beaches	EH-050	Closure	Tijuana River Associated	Sewage/ Grease	1/22/2024	4/10/2024	80	1/22/2024	0	53 dates
Avenida Lunar	Coronado City beaches	IB-079	Closure	Tijuana River Associated	Sewage/ Grease	1/22/2024	4/24/2024	94	1/22/2024	0	46 dates
Shelter Is shoreline park	San Diego Bay	EH-200	Closure	Sewage Spill	Sewage/ Grease	1/23/2024	1/26/2024	4	1/23/2024	0	1/23, 1/26, 1/27
Spanish Landing	Spanish Landing Park	EH-160	Closure	Sewage Spill	Sewage/ Grease	1/23/2024	1/26/2024	4	1/23/2024	0	1/23, 1/26, 1/27
Tidelands Park	San Diego Bay	EH-070	Closure	Sewage Spill	Sewage/ Grease	1/23/2024	1/28/2024	6	1/23/2024	0	1/23, 1/26, 1/27, 1/29
Glorietta Bay	San Diego Bay	EH-080	Closure	Sewage Spill	Sewage/ Grease	1/23/2024	1/28/2024	6	1/23/2024	0	1/23, 1/26, 1/27, 1/29
Centennial Park, Beach To The West	Coronado north beach	EH-063	Closure	Sewage Spill	Sewage/ Grease	1/23/2024	1/28/2024	6	1/23/2024	0	1/23, 1/26, 1/27, 1/29
Cesar Chavez Park	San Diego Bay	EH-530	Closure	Sewage Spill	Sewage/ Grease	1/23/2024	1/28/2024	6	1/23/2024	0	1/23, 1/26, 1/27, 1/29
Silver Strand (bayside)	San Diego Bay	EH-090	Closure	Sewage Spill	Sewage/ Grease	1/24/2024	1/26/2024	3	1/23/2024	1	1/26, 1/27, 1/29
All_SanDiego County Beaches	All_SanDiego_County	All_SanDiego County Beaches	Rain			2/1/2024	2/12/2024	12	2/1/2024	0	8 dates
All_SanDiego County Beaches	All_SanDiego_County	All_SanDiego County Beaches	Rain			2/1/2024	2/12/2024	12	2/1/2024	0	8 dates
Cesar Chavez Park	San Diego Bay	EH-530	Closure	Sewage Spill	Sewage/ Grease	2/6/2024	2/10/2024	5	2/6/2024	0	2/7, 2/8, 2/9, 2/12
Ruocco Park	San Diego Bay	EH-545	Closure	Sewage Spill	Sewage/ Grease	2/6/2024	2/10/2024	5	2/6/2024	0	2/7, 2/8, 2/9, 2/12
Outfall at B St Pier, Downstream (420 L)	San Diego Bay	EH-565	Closure	Sewage Spill	Sewage/ Grease	2/6/2024	2/10/2024	5	2/6/2024	0	2/7, 2/8, 2/9, 2/12
San Diego River outlet	Dog Beach, O.B.	FM-010	Closure	Sewage Spill	Sewage/ Grease	2/6/2024	2/12/2024	7	2/6/2024	0	2/7, 2/8, 2/9, 2/12, 2/14
Centennial Park, Beach To The West	Coronado north beach	EH-063	Closure	Sewage Spill	Sewage/ Grease	2/6/2024	2/12/2024	7	2/6/2024	0	2/7, 2/8, 2/9, 2/12, 2/14
Seaport Village	San Diego Bay	EH-540	Closure	Sewage Spill	Sewage/ Grease	2/6/2024	2/12/2024	7	2/6/2024	0	2/7, 2/8, 2/9, 2/12, 2/14
Tidelands Park	San Diego Bay	EH-070	Closure	Sewage Spill	Sewage/ Grease	2/6/2024	2/17/2024	12	2/6/2024	0	7 dates
Point Loma Treatment Plant	Pt. Loma shoreline	PL-050	Closure	Sewage Spill	Sewage/ Grease	2/20/2024	2/22/2024	3	2/20/2024	0	2/21, 2/22
All_SanDiego County Beaches	All_SanDiego_County	All_SanDiego County Beaches	Rain			2/20/2024	2/24/2024	5	2/20/2024	0	2/21, 2/22
All_SanDiego County Beaches	All_SanDiego_County	All_SanDiego County Beaches	Rain			3/2/2024	3/5/2024	4	3/2/2024	0	3/3, 3/4
All_SanDiego County Beaches	All_SanDiego_County	All_SanDiego County Beaches	Rain			3/7/2024	3/10/2024	4	3/4/2024	3	3/8, 3/10

Table 3 Cont'd. 2024 County of San Diego shoreline closures, rain advisories and associated project satellite data (Source: California State Water Resources Control Board). general rain advisory beach closure associated with the Tijuana River bay or beach closure due to a sewage spill bay or beach closure due to elevated bacteria levels

Station Description	Beach Name	Station Name	Type	Cause	Source	Start Date	End Date	Duration (days)	Nearest Rain Date	Time From Rain Event	Satellite Image data
Missouri St.	Pacific Beach	EH-253	Closure	Sewage Spill	Sewage/ Grease	3/8/2024	3/9/2024	2	3/7/2024	1	3/8, 3/10
Crystal Pier	Pacific Beach	FM-020	Closure	Sewage Spill	Sewage/ Grease	3/8/2024	3/9/2024	2	3/7/2024	1	3/8, 3/10
Missouri St. (150 ft North)	Pacific Beach	EH-253A	Closure	Sewage Spill	Sewage/ Grease	3/8/2024	3/9/2024	2	3/7/2024	1	3/8, 3/10
Missouri St. (150 ft South)	Pacific Beach	EH-253B	Closure	Sewage Spill	Sewage/ Grease	3/8/2024	3/9/2024	2	3/7/2024	1	3/8, 3/10
Diamond	Pacific Beach	EH-570	Closure	Sewage Spill	Sewage/ Grease	3/8/2024	3/9/2024	2	3/7/2024	1	3/8, 3/10
Law Street	Pacific Beach	EH-571	Closure	Sewage Spill	Sewage/ Grease	3/8/2024	3/9/2024	2	3/7/2024	1	3/8, 3/10
Hornblend	Pacific Beach	EH-572	Closure	Sewage Spill	Sewage/ Grease	3/8/2024	3/9/2024	2	3/7/2024	1	3/8, 3/10
Loring	Pacific Beach	EH-573	Closure	Sewage Spill	Sewage/ Grease	3/8/2024	3/9/2024	2	3/7/2024	1	3/8, 3/10
Navy Fence (A)	Coronado north beach	EH-060	Closure	Tijuana River Associated	Sewage/ Grease	3/25/2024	4/10/2024	17	3/24/2024	1	11 dates
All_SanDiego County Beaches	All_SanDiego_County	All_SanDiego County Beaches	Rain			3/30/2024	4/3/2024	5	3/20/2024	0	4/1, 4/2, 4/3, 4/4
Loma Ave (frmrly Isabella	Coronado City beaches	EH-050	Closure	Tijuana River Associated	Sewage/ Grease	4/14/2024	4/23/2024	10	4/14/2024	0	6 dates
Navy Fence (A)	Coronado north beach	EH-060	Closure	Tijuana River Associated	Sewage/ Grease	4/14/2024	4/23/2024	10	4/14/2024	0	6 dates
Oceanside pier	Oceanside municipal beach, other	OC-080	Closure	Bacterial Standards	Unknown	4/25/2024	4/27/2024	3	4/25/2024	0	4/27
Tyson Street	Oceanside municipal beach, other	OC-050	Closure	Bacterial Standards	Unknown	4/25/2024	4/27/2024	3	4/25/24	0	4/27
Surfrider Way	Oceanside municipal beach, other	OC-090	Closure	Bacterial Standards	Unknown	4/25/2024	4/27/2024	3	4/25/24	0	4/27
Avenida Lunar	Coronado City beaches	IB-079	Closure	Tijuana River Associated	Sewage/ Grease	4/25/2024	4/28/2024	4	4/25/24	0	4/27
Avenida Lunar	Coronado City beaches	IB-079	Closure	Tijuana River Associated	Sewage/ Grease	5/2/2024	5/6/2024	5	4/26/25	4	5/5, 5/7
Silver Strand N end (ocean)	Silver Strand State Beach	IB-070	Closure	Tijuana River Associated	Sewage/ Grease	5/7/2024	6/30/2024	55	5/5/24	2	19 dates
Avenida Lunar	Coronado City beaches	IB-079	Closure	Tijuana River Associated	Sewage/ Grease	5/8/2024	5/13/2024	6	5/5/24	3	5/9, 5/12, 5/13, 5/14
Loma Ave (frmrly Isabella	Coronado City beaches	EH-050	Closure	Tijuana River Associated	Sewage/ Grease	5/10/2024	5/13/2024	4	5/5/24	5	5/12, 5/13, 5/14
Navy Fence (A)	Coronado north beach	EH-060	Closure	Tijuana River Associated	Sewage/ Grease	5/10/2024	5/13/2024	4	5/5/24	5	5/12, 5/13, 5/14
Avenida Lunar	Coronado City beaches	IB-079	Closure	Tijuana River Associated	Sewage/ Grease	5/20/2024	6/16/2024	28	5/5/24	15	7 dates
Navy Fence (A)	Coronado north beach	EH-060	Closure	Tijuana River Associated	Sewage/ Grease	5/21/2024	5/26/2024	6	5/5/24	16	5/21, 5/25, 5/26
Loma Ave (frmrly Isabella	Coronado City beaches	EH-050	Closure	Tijuana River Associated	Sewage/ Grease	5/21/2024	5/30/2024	10	5/5/24	16	5/21, 5/25, 5/26, 6/2
Navy Fence (A)	Coronado north beach	EH-060	Closure	Tijuana River Associated	Sewage/ Grease	5/28/2024	5/30/2024	3	5/25/24	3	6/2
Loma Ave (frmrly Isabella	Coronado City beaches	EH-050	Closure	Tijuana River Associated	Sewage/ Grease	6/4/2024	6/14/2024	11	5/25/24	9	6/11
Navy Fence (A)	Coronado north beach	EH-060	Closure	Tijuana River Associated	Sewage/ Grease	6/4/2024	6/14/2024	11	5/25/24	9	6/11
Avenida Lunar	Coronado City beaches	IB-079	Closure	Tijuana River Associated	Sewage/ Grease	6/25/2024	6/30/2024	6	6/11/24	14	6/26, 6/30, 7/1
Navy Fence (A)	Coronado north beach	EH-060	Closure	Tijuana River Associated	Sewage/ Grease	6/26/2024	6/30/2024	5	6/11/24	15	6/26, 6/30, 7/1
Loma Ave (frmrly Isabella	Coronado City beaches	EH-050	Closure	Tijuana River Associated	Sewage/ Grease	6/26/2024	6/30/2024	5	6/11/24	15	6/26, 6/30, 7/1
Avenida Lunar	Coronado City beaches	IB-079	Closure	Tijuana River Associated	Sewage/ Grease	7/1/2024	7/1/2024	1	6/11/24	20	7/1, 7/2
Loma Ave (frmrly Isabella	Coronado City beaches	EH-050	Closure	Tijuana River Associated	Sewage/ Grease	7/1/2024	7/1/2024	1	6/11/24	20	7/1, 7/2
Navy Fence (A)	Coronado north beach	EH-060	Closure	Tijuana River Associated	Sewage/ Grease	7/1/2024	7/1/2024	1	6/11/24	20	7/1, 7/2
Silver Strand N end (ocean)	Silver Strand State Beach	IB-070	Closure	Tijuana River Associated	Sewage/ Grease	7/1/2024	8/5/2024	36	6/11/24	20	15 dates
End of Seacoast Dr	Imperial Beach municipal beach, other	IB-050	Closure	Tijuana River Associated	Sewage/ Grease	7/1/2024	9/18/2024	80	6/11/24	20	35 dates
Border Fence N side	Border Field State Park	IB-010	Closure	Tijuana River Associated	Sewage/ Grease	7/1/2024	12/31/2024	184	6/11/24	20	77 dates

Table 3 Cont'd. 2024 County of San Diego shoreline closures, rain advisories and associated project satellite data (Source: California State Water Resources Control Board). general rain advisory beach closure associated with the Tijuana River bay or beach closure due to a sewage spill bay or beach closure due to elevated bacteria levels

Station Description	Beach Name	Station Name	Type	Cause	Source	Start Date	End Date	Duration (days)	Nearest Rain Date	Time From Rain Event	Satellite Image data
Loma Ave (frmrly Isabella	Coronado City beaches	EH-050	Closure	Tijuana River Associated	Sewage/ Grease	7/8/2024	7/21/2024	14	6/11/24	28	7/8, 7/12, 7/13, 7/20
Navy Fence (A)	Coronado north beach	EH-060	Closure	Tijuana River Associated	Sewage/ Grease	7/8/2024	7/21/2024	14	6/11/24	28	7/8, 7/12, 7/13, 7/20
Avenida Lunar	Coronado City beaches	IB-079	Closure	Tijuana River Associated	Sewage/ Grease	7/8/2024	7/28/2024	21	6/11/24	28	8 dates
Loma Ave (frmrly Isabella	Coronado City beaches	EH-050	Closure	Tijuana River Associated	Sewage/ Grease	7/23/2024	7/25/2024	3	7/17/24	6	7/24, 7/25, 7/26
Navy Fence (A)	Coronado north beach	EH-060	Closure	Tijuana River Associated	Sewage/ Grease	7/23/2024	7/25/2024	3	7/17/24	6	7/24, 7/25, 7/26
Silver Strand N end (ocean)	Silver Strand State Beach	IB-070	Closure	Tijuana River Associated	Sewage/ Grease	8/8/2024	8/21/2024	14	8/1/24	7	9 dates
Avenida Lunar	Coronado City beaches	IB-079	Closure	Tijuana River Associated	Sewage/ Grease	8/17/2024	8/19/2024	3	8/11/24	6	8/17, 8/18, 8/20
Loma Ave (frmrly Isabella	Coronado City beaches	EH-050	Closure	Tijuana River Associated	Sewage/ Grease	8/17/2024	8/19/2024	3	8/11/24	6	8/17, 8/18, 8/20
Navy Fence (A)	Coronado north beach	EH-060	Closure	Tijuana River Associated	Sewage/ Grease	8/17/2024	8/19/2024	3	8/11/24	6	8/17, 8/18, 8/20
Silver Strand N end (ocean)	Silver Strand State Beach	IB-070	Closure	Tijuana River Associated	Sewage/ Grease	8/22/2024	8/26/2024	5	8/11/24	11	8/22, 8/25, 8/27
Silver Strand N end (ocean)	Silver Strand State Beach	IB-070	Closure	Tijuana River Associated	Sewage/ Grease	8/29/2024	9/11/2024	14	8/11/24	18	9/4, 9/6, 9/9, 9/11
Avenida Lunar	Coronado City beaches	IB-079	Closure	Tijuana River Associated	Sewage/ Grease	9/7/2024	9/9/2024	3	8/11/24	27	9/6, 9/9
Cortez Ave	Imperial Beach municipal beach, other	EH-010	Closure	Bacterial Standards	Unknown	9/18/2024	9/19/2024	2	8/11/2024	38	9/18, 9/19
Imperial Beach Pier	Imperial Beach pier area	EH-030	Closure	Bacterial Standards	Unknown	9/18/2024	9/19/2024	2	8/11/2024	38	9/18, 9/19
End of Seacoast Dr	Imperial Beach municipal beach, other	IB-050	Closure	Bacterial Standards	Unknown	9/18/2024	9/19/2024	2	8/11/2024	38	9/18, 9/19
End of Seacoast Dr	Imperial Beach municipal beach, other	IB-050	Closure	Tijuana River Associated	Sewage/ Grease	9/19/2024	9/21/2024	3	8/11/2024	39	9/19, 09/22
Cortez Ave	Imperial Beach municipal beach, other	EH-010	Closure	Tijuana River Associated	Sewage/ Grease	9/21/2024	9/22/2024	2	9/20/24	1	09/22, 09/23
End of Seacoast Dr	Imperial Beach municipal beach, other	IB-050	Closure	Tijuana River Associated	Sewage/ Grease	10/4/2024	10/11/2024	8	9/20/24	14	10/4, 10/5, 10/10, 10/12
Imperial Beach Pier	Imperial Beach pier area	EH-030	Closure	Tijuana River Associated	Sewage/ Grease	10/11/2024	10/12/2024	2	9/20/24	21	10/12
Cortez Ave	Imperial Beach municipal beach, other	EH-010	Closure	Tijuana River Associated	Sewage/ Grease	10/11/2024	11/6/2024	27	9/20/24	21	12 dates
End of Seacoast Dr	Imperial Beach municipal beach, other	IB-050	Closure	Tijuana River Associated	Sewage/ Grease	10/11/2024	11/6/2024	27	9/20/24	21	12 dates
Imperial Beach Pier	Imperial Beach pier area	EH-030	Closure	Tijuana River Associated	Sewage/ Grease	10/14/2024	11/7/2024	25	9/20/24	24	13 dates
Carnation Ave.	north Imperial Beach	IB-060	Closure	Tijuana River Associated	Sewage/ Grease	10/14/2024	11/7/2024	25	9/20/24	24	13 dates
Silver Strand N end (ocean)	Silver Strand State Beach	IB-070	Closure	Tijuana River Associated	Sewage/ Grease	10/17/2024	10/31/2024	15	9/20/24	27	7 dates
End of Seacoast Dr	Imperial Beach municipal beach, other	IB-050	Closure	Tijuana River Associated	Sewage/ Grease	11/12/2024	12/18/2024	37	11/3/24	9	18 dates
Carnation Ave.	north Imperial Beach	IB-060	Closure	Tijuana River Associated	Sewage/ Grease	11/12/2024	12/18/2024	37	11/3/24	9	18 dates
Cortez Ave	Imperial Beach municipal beach, other	EH-010	Closure	Tijuana River Associated	Sewage/ Grease	11/12/2024	12/18/2024	37	11/3/24	9	18 dates
Imperial Beach Pier	Imperial Beach pier area	EH-030	Closure	Tijuana River Associated	Sewage/ Grease	11/12/2024	12/28/2024	47	11/3/24	9	21 dates
End of Seacoast Dr	Imperial Beach municipal beach, other	IB-050	Closure	Tijuana River Associated	Sewage/ Grease	12/19/2024	12/31/2024	13	12/19/24	0	12/23, 12/27, 12/28
Cortez Ave	Imperial Beach municipal beach, other	EH-010	Closure	Tijuana River Associated	Sewage/ Grease	12/19/2024	12/31/2024	13	12/19/24	0	12/23, 12/27, 12/28
Carnation Ave.	north Imperial Beach	IB-060	Closure	Tijuana River Associated	Sewage/ Grease	12/20/2024	12/31/2024	12	12/19/24	1	12/23, 12/27, 12/28
Avenida Lunar	Coronado City beaches	IB-079	Closure	Tijuana River Associated	Sewage/ Grease	12/21/2024	12/22/2024	2	12/21/24	0	12/23
Silver Strand N end (ocean)	Silver Strand State Beach	IB-070	Closure	Tijuana River Associated	Sewage/ Grease	12/21/2024	12/28/2024	8	12/21/24	0	12/23, 12/27, 12/28
Avenida Lunar	Coronado City beaches	IB-079	Closure	Tijuana River Associated	Sewage/ Grease	12/25/2024	12/28/2024	4	12/24/24	1	12/27, 12/28
Loma Ave (frmrly Isabella	Coronado City beaches	EH-050	Closure	Tijuana River Associated	Sewage/ Grease	12/25/2024	12/28/2024	4	12/24/24	1	12/27, 12/28
Navy Fence (A)	Coronado north beach	EH-060	Closure	Tijuana River Associated	Sewage/ Grease	12/25/2024	12/28/2024	4	12/24/24	1	12/27, 12/28
Imperial Beach Pier	Imperial Beach pier area	EH-030	Closure	Tijuana River Associated	Sewage/ Grease	12/29/2024	12/31/2024	3	12/27/24	2	12/27, 12/28

Although discharges from the San Diego River and Mission Bay do not cause the same level of beach contamination issues as the Tijuana River, the runoff from the San Diego River did affect nearshore water clarity and quality on several days throughout the year in 2024, directly as a source of suspended sediment and indirectly as a source of high nutrient input, encouraging coastal and offshore phytoplankton blooms. While not at the scale or frequency as observed in previous years, turbidity plumes emanating from the river entrance and/or phytoplankton blooms either along the coast or offshore of the area were documented on 81 days in the medium-resolution (MODIS and Sentinel-3) and high-resolution satellite imagery throughout the year. The area surrounding the Point Loma kelp bed tended to be more often affected by direct shore runoff and discharges from the San Diego River and Mission Bay during the prevalent southward current regime. Figure 9 provides examples from a 300-meter Sentinel-3 image time series of days on which the data revealed heavy coastal turbidity and a developing phytoplankton bloom in this northern section of the project's study area. The bloom moves offshore and is entrained on a large offshore eddy and then begins to deform.

As discussed above there were significant phytoplankton and possible HABs during the spring and late summer to fall of 2024 which may have contributed to decreased offshore water quality. This is seen by dark green and brown to red reflectance in the satellite data caused by phytoplankton containing photosynthetic pigments that vary in color from brown to red and blooms often dominated by the dinoflagellate *Lingulodinium polyedra* which absorbs light in the ultraviolet part of the electromagnetic spectrum (Kahru et al.,1998, Zheng et al., 2018). Diatoms (primarily *Pseudo-nitzschia* spp) and dinoflagellates are largely responsible for the local harmful algal blooms (red tides) when they occur (Southern California Coastal Water Research Project, 2019). Figure 10 provides examples of high-resolution Landsat and SPOT data highlighting days when the imagery revealed strong coastal and offshore phytoplankton blooms that cannot be directly linked to a significant (over 0.01 inches) prior rainfall event.

The SCB experienced lower overall chlorophyll levels throughout 2024 when compared to the previous three years, especially 2021. Chlorophyll levels and thus phytoplankton abundance in the SCB were relatively low during the first three months of the year, particularly in the southern part of the region. An increase in coastal upwelling combined with rainfall events during the end of March and beginning of April likely introduced nutrients into the ocean system from river discharge and coastal runoff contributing to the increase the chlorophyll levels during April, May and June. A noticeable decrease in offshore chlorophyll levels from July through September is evident in the representative satellite imagery, as is the increase in levels from October through December. Figure 11 provides representative SCB VIIRS and MODIS-derived chlorophyll images for each month of 2024. As observed in the satellite data, the California Current relaxed during July and August and was not moving greener/nutrient-rich water into the lower part of the SCB region. The California Current appears to build strength again in September, however the chlorophyll levels in the San Diego offshore region remained relatively low. The Current appears to gain strength from October into December as does coastal upwelling. Figure 12 shows 300 and 1000-meter fused resolution monthly chlorophyll averages for the area offshore of San Diego County and south of the U.S.-Mexico border. These composites were generated from MODIS, VIIRS and OLCI data as part of a SDPUD-funded project to study plankton abundance and extent in the region from 1997 through 2024. The series provides a more coastal, regional perspective of the changes in phytoplankton throughout the year. The data correlate well with the SCB imagery in Figure 11. This is especially apparent from July through the end of the year when the offshore waters were comparatively devoid of chlorophyll during July, August and September and then coastal upwelling and hence chlorophyll levels dramatically increased during the months of

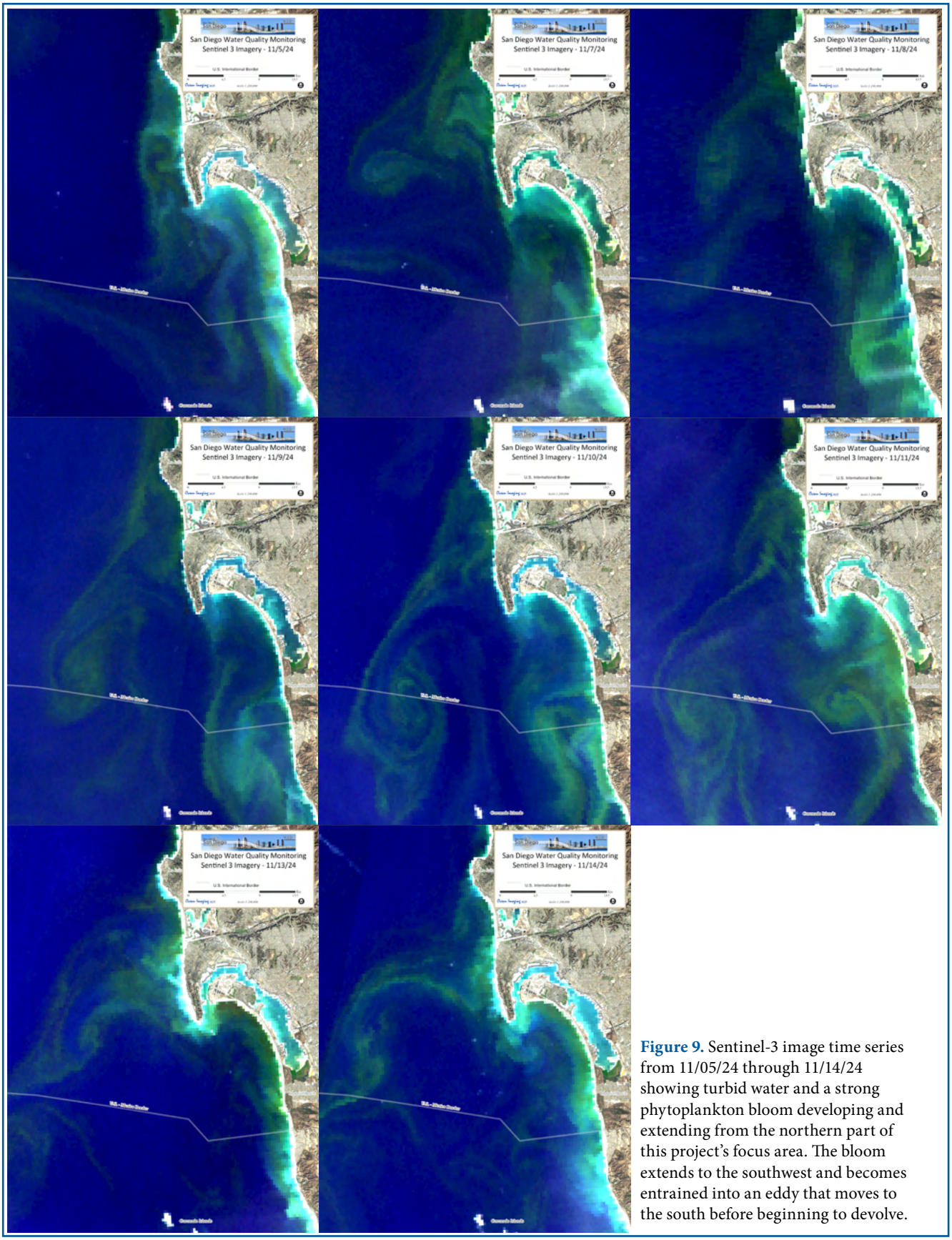


Figure 9. Sentinel-3 image time series from 11/05/24 through 11/14/24 showing turbid water and a strong phytoplankton bloom developing and extending from the northern part of this project's focus area. The bloom extends to the southwest and becomes entrained into an eddy that moves to the south before beginning to devolve.

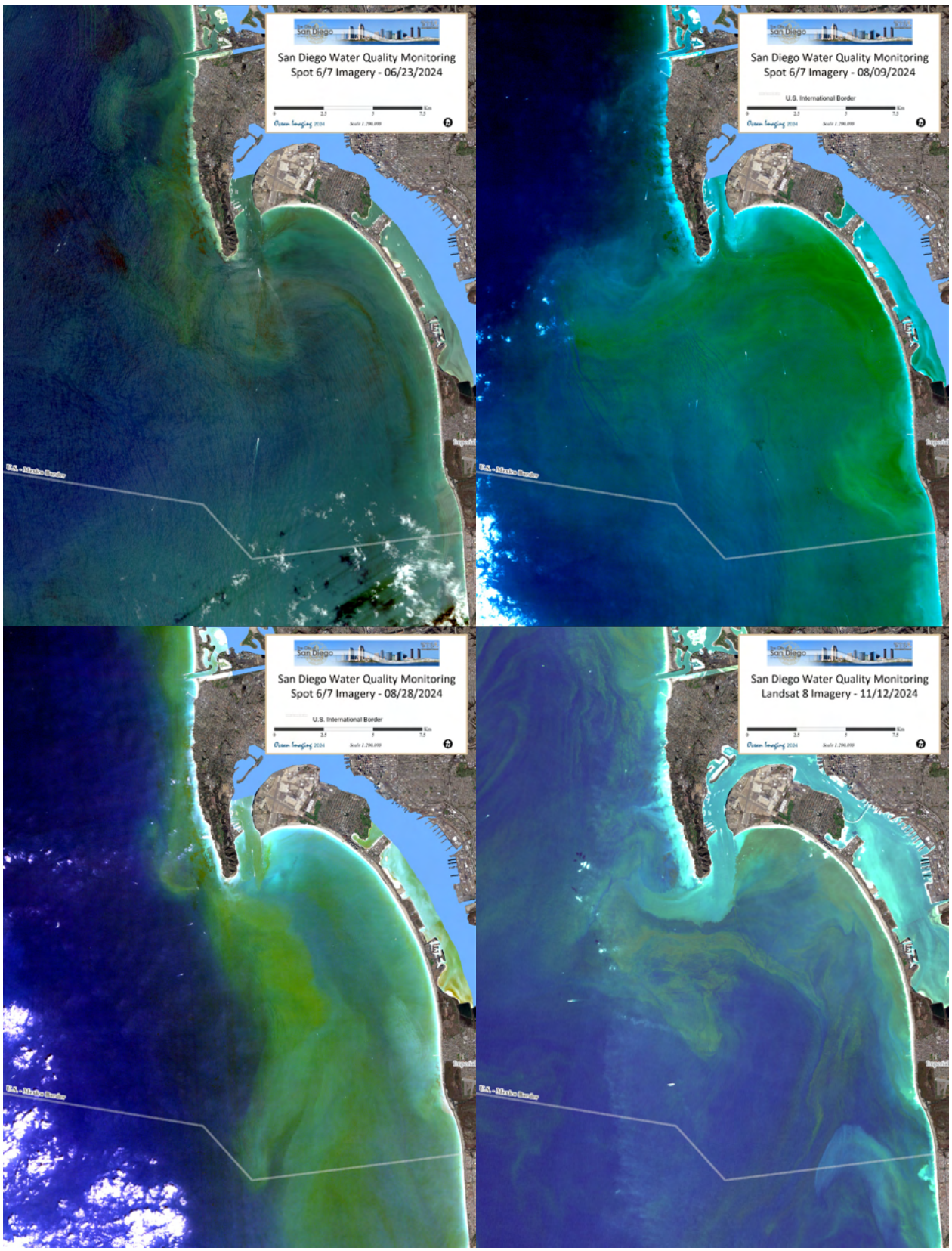


Figure 10. Sample high-resolution Landsat and SPOT data providing examples of days when the imagery revealed strong coastal and offshore phytoplankton blooms and possible HABs that cannot be directly linked to a significant (over 0.01 inches) prior rainfall event.

October through December along the entire San Diego County coastline extending well offshore and far south below the U.S.-Mexico border. Higher chlorophyll levels in the San Diego region were confined to within approximately 15 kilometers of the coast for July through September and then extended farther offshore as the year progressed.

The City of San Diego conductivity-temperature-depth (CTD) sampling results correlated well with the satellite data observations. Some of the highest chlorophyll levels recorded via CTD (as high as 63.87 mg/m^3 at station I32, 1-meter depth on 06/04/24) occurred during the month of June. More than 75% of fluorometry readings exceeding 10.0 mg/m^3 occurred from May to July, slightly later than the typical spring bloom season. The higher chlorophyll readings in the month of July were mostly confined to the shoreline stations as the phytoplankton levels in the offshore areas began to recede by the end of June. The imagery in Figures 11 and 12 corroborates these measurements, clearly documenting May and June as months exhibiting high intensities and spatial extent of phytoplankton

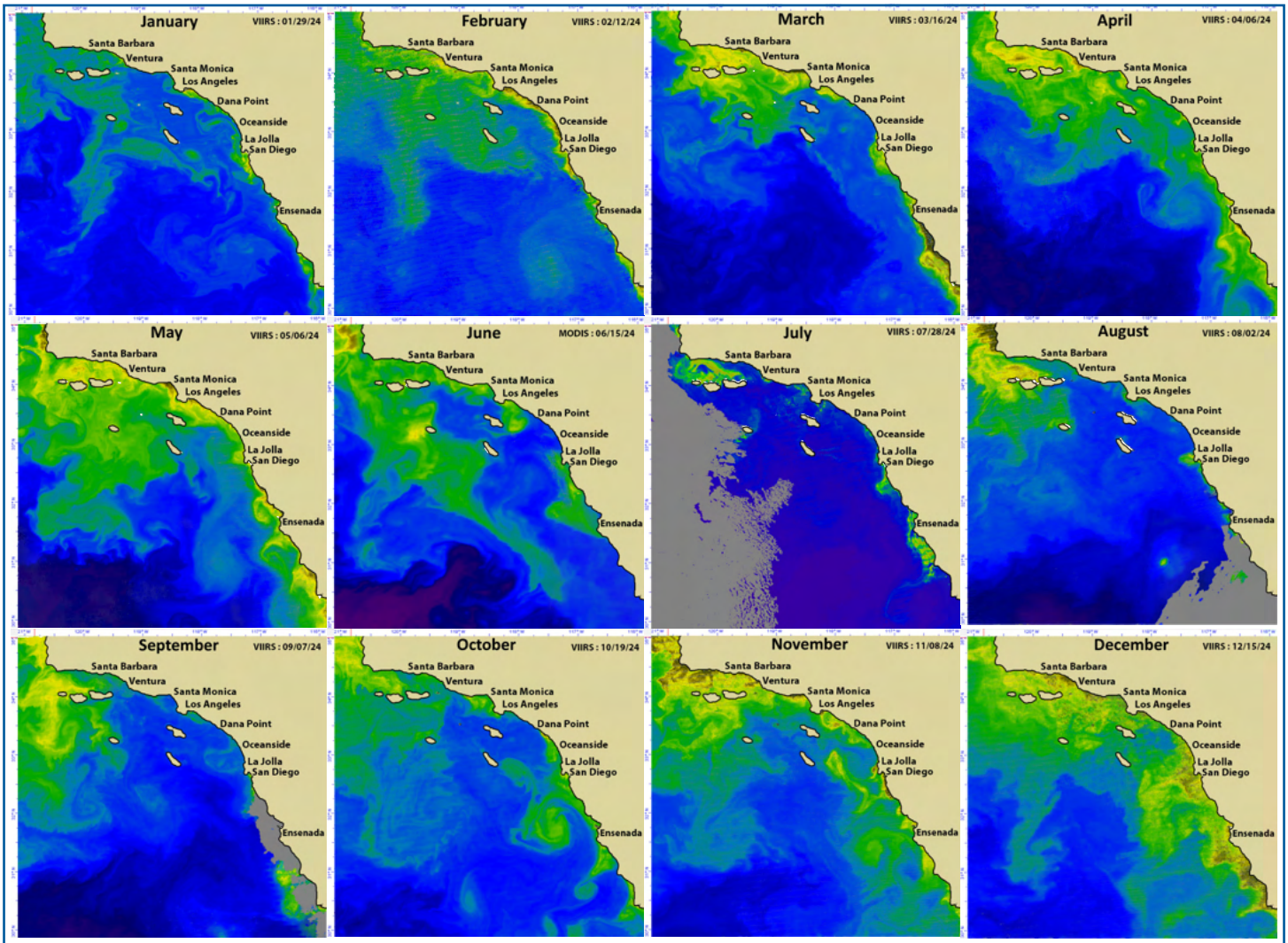


Figure 11. Representative VIIRS and MODIS-derived chlorophyll images for each month of 2024 showing relatively low levels of chlorophyll-rich water in the SCB during the months of January through March and then an increase during the months of April, May and June - likely due to the heavy rainfall and resulting eutrophication combined with coastal upwelling. SCB-wide levels decreased during the summer months and increased again in October through December, likely caused by the California Current bringing nutrient-rich water down into the region.

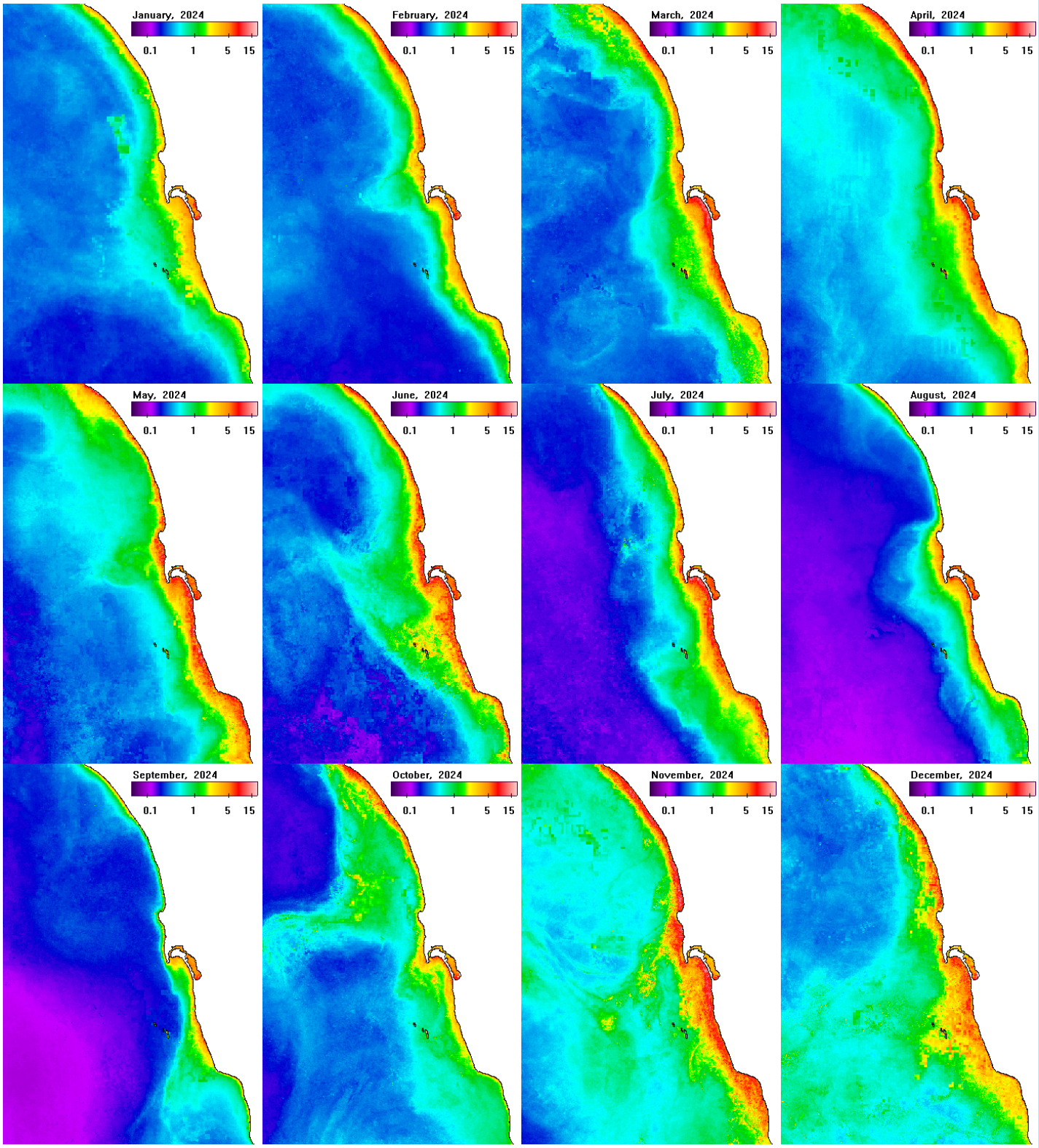


Figure 12. Monthly chlorophyll (mg/m^3) composites of the San Diego County coastal and offshore area derived from 300m and 1km MODIS, VIIRS and OCLI imagery generated by Mati Kahru of Scripps Institution of Oceanography in cooperation with OI as part of a SDPUD-funded project to study a long-term time series of satellite imagery to assess phytoplankton abundance and extent possibly related to increasing eutrophication of the ocean in this region.

blooms in the San Diego County coastal region. Figure 13 offers examples of the CTD fluorometry data in correlation with the high-resolution satellite imagery on or near the same day as the field samples.

While the high-resolution remotely sensed data do not depict quantitative chlorophyll levels, the yellow to green plankton blooms are self-evident in the imagery and correlate well with the CTD data.

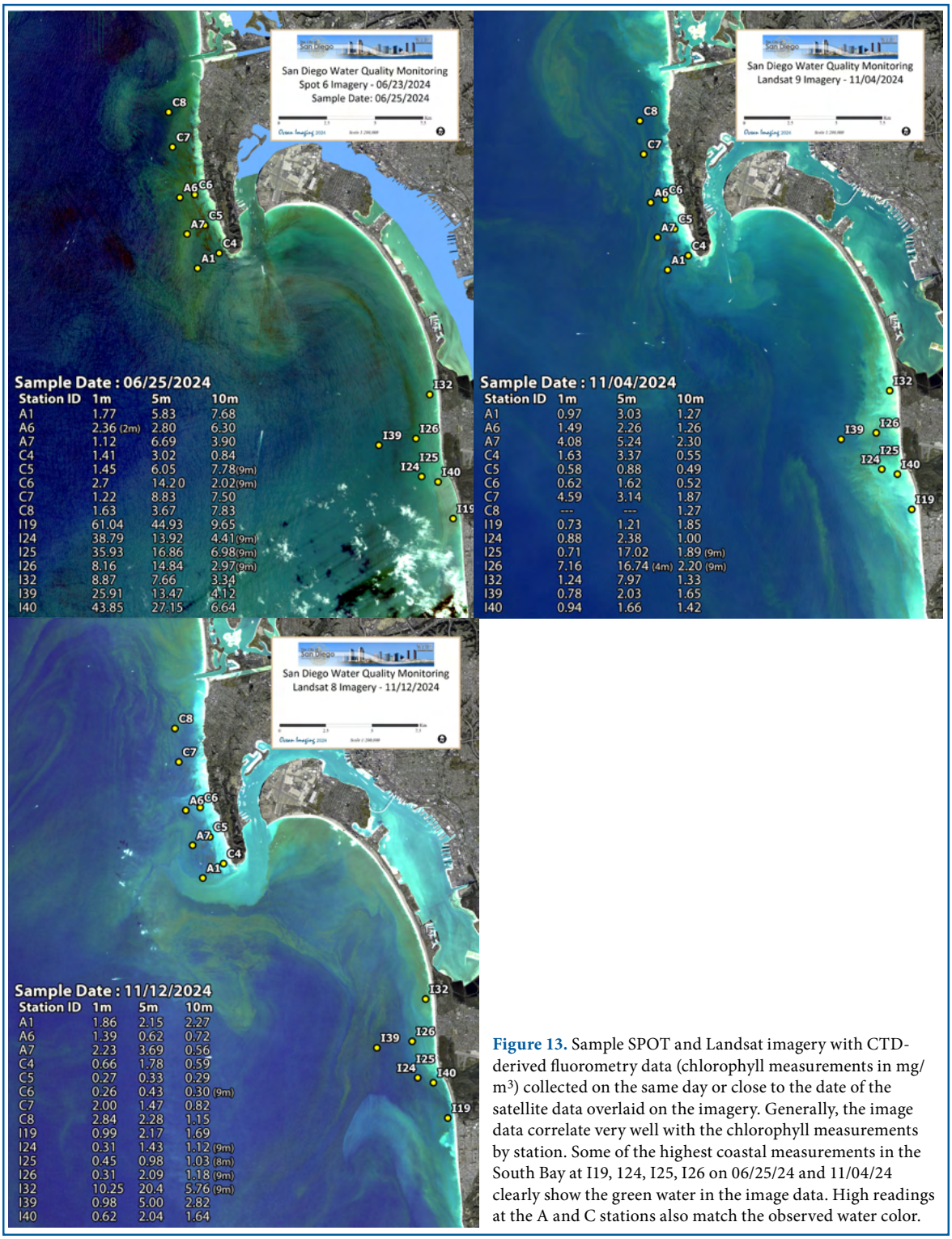


Figure 13. Sample SPOT and Landsat imagery with CTD-derived fluorometry data (chlorophyll measurements in mg/m^3) collected on the same day or close to the date of the satellite data overlaid on the imagery. Generally, the image data correlate very well with the chlorophyll measurements by station. Some of the highest coastal measurements in the South Bay at I19, 124, I25, I26 on 06/25/24 and 11/04/24 clearly show the green water in the image data. High readings at the A and C stations also match the observed water color.

3.2 The South Bay Ocean Outfall Region

The South Bay International Wastewater Treatment Plant (SBIWTP) switched from advanced primary to secondary treatment in January 2011. This change resulted in the reduction of total suspended solids (TSS) concentrations from an average of 60 mg/L for several years prior to the change to the TSS loads reading consistently below 20 mg/L until late 2020. Beginning at the end of 2020, the TSS concentrations became much more variable with daily measurements peaking over 900 mg/L in early 2024. Prior to 2011, a distinct effluent signature was regularly detected in multispectral imagery as per the seasonal fluctuation described above. Since then, the effluent signature continues to be observed with multispectral color and thermal imagery during months with weak vertical stratification, however, more intermittently. On occasion the signature is distinctly discernable in thermal images (indicating it has fully reached the ocean surface), but undetectable in the color imagery. We theorize this is due to the reduction in TSS concentrations.

The SBOO wastewater plume generally remains well below the surface between approximately mid-April and November due to vertical stratification of the water column. During that period, it usually cannot be detected with multispectral aerial and satellite imagery, which penetrate the upper 7 to 15 meters (depending on water clarity), nor can it be detected with thermal IR imaging, which does not penetrate below the surface. Seasonal breakdown of the vertical stratification results in the plume's rise closer to the surface or to reach the surface between November and April when it can often be detected with satellite imaging. This concept held true in 2024, as the last observation of a SBOO surface plume during the beginning of the year was on 04/02/24 and then was not seen again in the image data until 11/08/24. In total, there were 26 instances during which the SBOO effluent plume was observed in 2024 out of the 105 high resolution satellite scenes acquired and processed. Of the 26, there were four instances of the plume observed by different satellites on the same day. This equates to 22 days when the plume was visible in the high-resolution imagery – four more than observed in 2023. There were 89 days on which one or more of the high resolution, multispectral satellites imaged the study area and so the SBOO plume was detected on 24.7% of satellite observations days. This is more than the average for the previous 12 years (20.3% of the observations). The effluent surface plumes are most often seen moving to the south or as a stagnant body. There was only one day on which the plume was observed moving east or northeast (01/13/24) and two days (04/02/24 and 11/30/24) during which the plume was oriented directly northward. On 01/13/24 when the plume showed an eastward direction, it was effectively blocked from reaching anywhere close to the shore by the offshore movement of the TJR discharge. On 04/02/24 and 11/30/24 when the plume was observed pushing northward, the turbidity signature dissipated only a few kilometers from the SBOO wye. Therefore, from the entire set of 2024 imagery, it can be inferred that the SBOO surface plume never came anywhere near the San Diego shoreline.

Appendix A includes the 2024 SPOT, Sentinel-2 and Landsat multispectral imagery on days which the SBOO plume was detected. There were four occurrences when either Sentinel-2A or 2B data were acquired within minutes of Landsat or SPOT 6 data providing a near time-coincident validation of features observed in the imagery.

As has been the case in previous years, there was an occurrence when the SBOO effluent plume appeared in the imagery as a patch of clearer water breaking the more turbid water on the surface. As discussed in prior reports, the clear effluent signal in the imagery is most likely due to the contrast between the higher turbidity coastal surface waters and the 'normal' level of turbidity of the effluent water breaking the surface. It is also possible that the effluent plume became somewhat diluted on its way to the surface if weak vertical stratification did exist, thus slowing down its rise in the water column. This situation is exemplified in Figure 14. On 04/02/24, a mere day after the SBOO plume was visible as a turbid signature against relatively clear

water, the more turbid TJR discharge water engulfed the outfall area within the 24-hour interval between satellite data captures. The SBOO effluent is then observed as clearer than the surrounding water.

The months of January, February, November, and December exhibited the highest frequency of 2024 SBOO effluent plume observations in the satellite data. As previously discussed and documented in previous reports, it is typical to see the highest number of SBOO effluent surfacing's during these months. As is characteristically the case, the effluent surface manifestations that occurred during these periods were most probably the result of two primary factors: the lack of strong vertical stratification during the winter months and relatively weak subsurface currents over the SBOO which allowed the undispersed effluent to reach the surface.

According to the September 2024 California Regional Quality Control Board's Executive Officer Report, transboundary flows were still discharging continuously through the main channel of the Tijuana River up through September of 2024. Transboundary flows are defined as instances of groundwater, urban run-off, storm water, treated sewage wastewater, and untreated sewage wastewater from infrastructure deficiencies and other sources in Mexico coming across the U.S.-Mexico border and into the into the international treatment plant, Tijuana Estuary and U.S. coastal waters. Most of these transboundary flows occurred in the TJR main channel resulting in over 36 billion gallons coming into the U.S. system and waters from October of 2023 through June of 2024 (SDRWCB, 2024). As is discussed above, while the satellite imagery documented many of the related SBOO effluent surface manifestations and pollution discharge from the TJR, several of the TJR transboundary flow occurrences during the summer months were not detected in the satellite data. This may be because, while many were documented as caused by rain and weather events, a significant percentage during the months of June through August were considered dry weather flows from numerous sources in Mexico that exceeded the San Diego-Tijuana wastewater system capacity (SDRWCB, 2024). The relatively lower TJR discharge rate during June and July as seen in Figure 4 above also offers evidence as to why these flows are not always observed as expansive, discolored TJR plumes.

Figure 15 shows the SBIWTP effluent flow rate and TSS over the 2003 to 2024 period (top) and during 2024 plotted with the dates on which SBOO effluent was observed on the surface of the ocean in the high-resolution satellite imagery (bottom). As seen in the top plot, the variability in both the SBIWTP



Figure 14. SPOT and Sentinel imagery showing a SBOO surface signature being clearer than the surrounding, extremely turbid water (04/02/24 - right). On 04/01/24, just one day earlier, the TJR discharge had not yet reached the SBOO effluent surfacing area.

effluent flow rate and TSS increased significantly after the beginning of 2019. On the lower graph there are a few notable spikes in flow and the TSS occurred during the first quarter of 2024, however both parameters stabilized as the year progressed with the TSS levels dropping close to zero after November. Despite fluctuations in 2024, the trend line shows the average effluent flow rate of 22.70 million gallons per day (MGD) remained below the permit limit of 25 MGD. The TSS levels were highly variable over the past three years, however there is no direct correlation of the SBOO effluent surface observations to TSS measurements. Of the 22 days on which the SBOO effluent was observed breaking

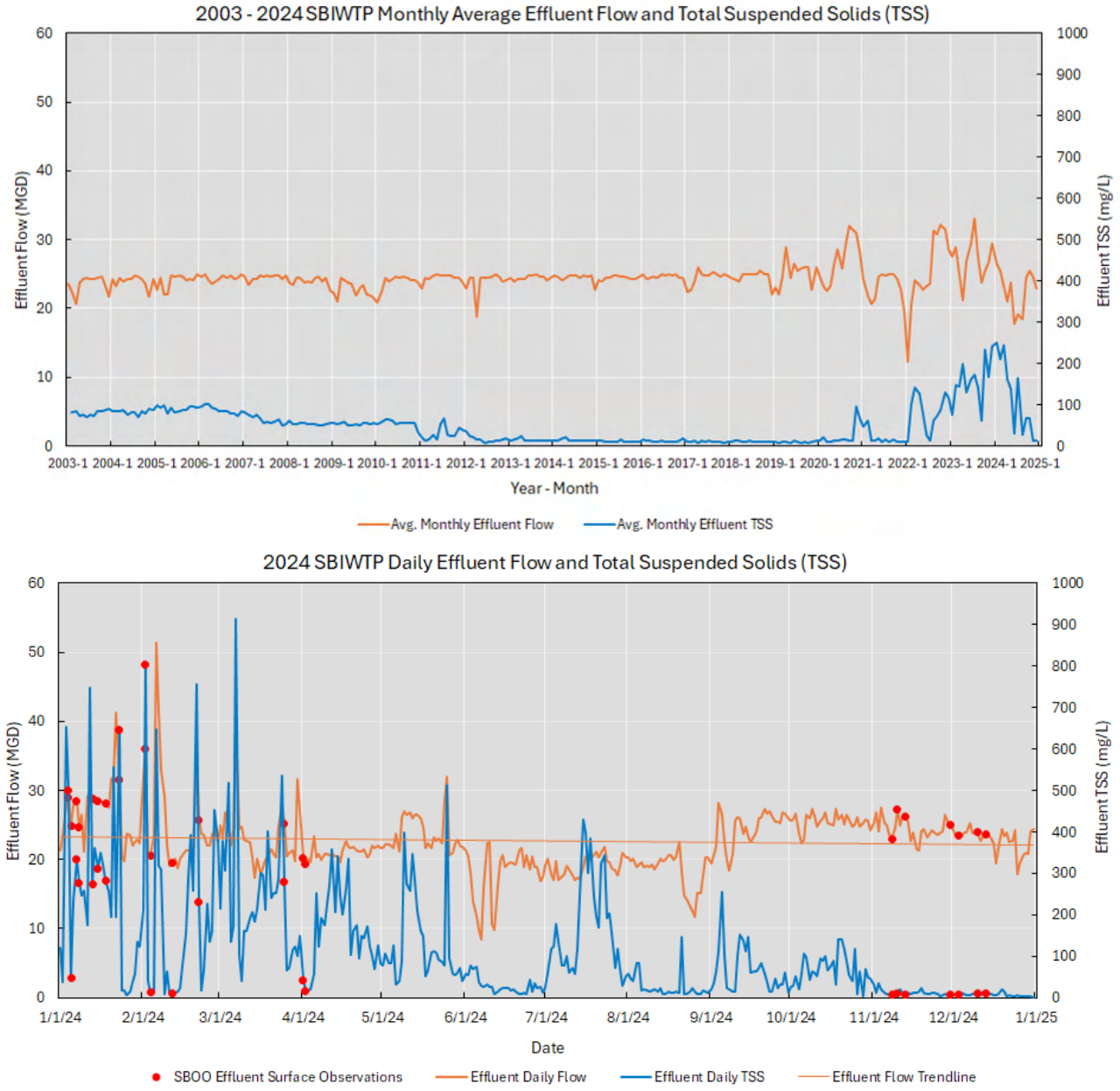


Figure 15. SBIWTP effluent flow rate and TSS from 2003 through 2024 (top) and over the 2024 period (top) plotted with the dates (red dots – bottom graph) on which SBOO effluent was observed on the surface of the ocean in the high-resolution satellite imagery. Red dots are shown on the dates corresponding with both the effluent flow and TSS data. The effluent flow trend line is shown as an orange line. Data courtesy of the USIBWC.

the surface, only ten occurred when the flow rate exceeded 25 MGD, and so it cannot be concluded that the additional flow diverted through SBIWTP resulted in the effluent reaching the ocean's surface more often. These data continue to corroborate the belief that the instances of effluent reaching the surface almost always occur because of seasonal changes in ocean conditions when the water column stratification breaks down and are rarely, if ever, related to a higher flow rate through the system or water with higher TSS levels exiting the outfall.

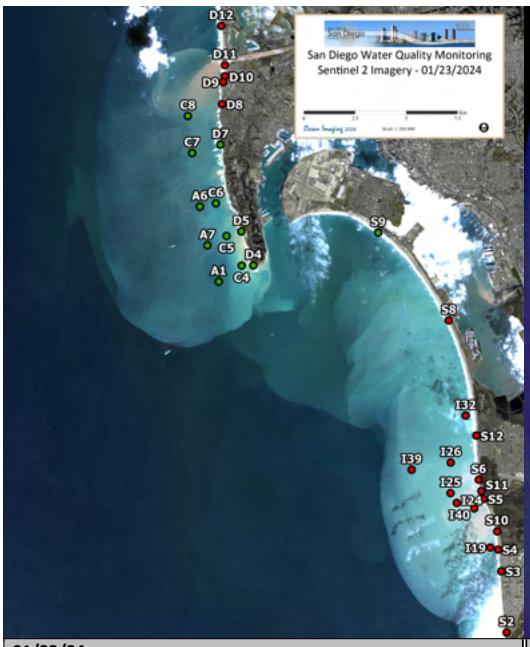
A total of 19 shoreline stations, ranging from Mission Beach to northern Baja (across the US/Mexico border) are sampled weekly by City of San Diego staff to monitor the levels of three types of fecal indicator bacteria (i.e., total coliform, fecal coliform, *Enterococcus* bacteria) in recreational waters. An additional 15 nearshore (kelp) stations are also sampled weekly to monitor Fecal Indicator Bacteria (FIB) and a range of water quality parameters (i.e., temperature, salinity, dissolved oxygen, pH, transmissivity, Chlorophyl-a, colored dissolved organic matter (CDOM). Furthermore, 69 offshore stations are sampled quarterly to monitor both water quality conditions and one or more types of FIB. PLOO stations are located along, or adjacent to, the 18, 60, 80, and 98-m depth contours, and SBOO stations are located along the 9, 19, 28, 38, and 55-m depth contours.

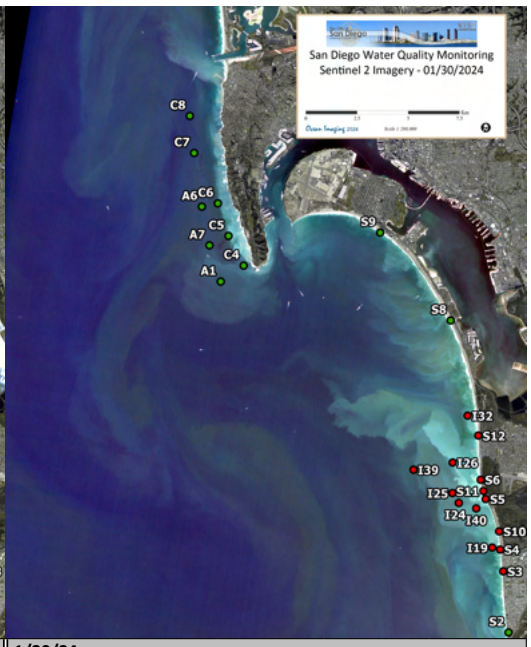
The City Marine Microbiology Laboratory (CMML) follows guidelines issued by the U.S. Environmental Protection Agency (USEPA) Water Quality Office, State Water Resources Control Board (SWRCB) including the 2019 Ocean Plan, the California Department of Public Health (CDPH), and Environmental Laboratory Accreditation Program (ELAP) with respect to sampling and analytical procedures (Bordner et. al., 1978, American Public Health Association (APHA) 2012, CDPH 2019, USEPA 2014). All bacterial analyses were initiated within eight hours of sample collection and conformed to standard membrane filtration techniques, for which the laboratory is certified (ELAP Field of Testing 126). FIB densities were determined and validated in accordance with USEPA and APHA guidelines as follows in APHA (2012).

In 2024, the sampling area of the SBOO/Tijuana River outflow region experienced 68 days, on which the field sampling showed FIB measurements exceeding the single sample maximum (SSM) for fecal coliform density for one or more sampling stations as defined by the 2019 California Ocean Plan (the SSM for fecal coliform density at a site will not exceed 400 per 100 mL) (SWRCB, 2019). The offshore SBOO region, which includes the stations over the SBOO wye, experienced only two days of elevated bacteria levels at depths of six meters or shallower and the nearshore region (referred to as the "kelp" region in previous reports) experienced 35 days on which the bacteria levels were deemed elevated. There were 55 sampling days when at least one shore station showed elevated levels. The number of sampling days for all three SBOO areas totaled 88 in 2024 and 96 in 2023. Therefore, in 2024 for the three sampling regions combined, 77.3% of the sampling days resulted in elevated bacteria levels at one station or more, which is slightly more than the 74.0% recorded in 2023 (using the same 2019 California Ocean Plan standards). As it has been in recent years, the vast majority of the samples showing elevated levels were recorded at the shore stations. Elevated levels offshore near the SBOO wye are rare. Of the three samples collected on two days when elevated bacteria levels were recorded at offshore stations, none (I3, I10 and I18) were close to the SBOO wye.

The satellite imagery showing substantial discharge from the TJR region often correlates well with times when the shoreline and kelp area sampling showed elevated bacteria levels. In past years, heavy and/or persistent rainfall was often the most plausible cause for most of the elevated bacteria samples and the turbid and/or discolored waters seen in the remote sensing data. However, given the increasing problems with untreated sewage and other pollutants flowing out of the TJR for much of the year (SDRWCB, 2024 and Little, 2024), that premise is no longer valid in many cases. Normally, the best water quality and clarity in the South Bay

region is observed during the dry season from May through August. This was generally true in terms of water clarity observed in the image data during the summer of 2024, however as noted above, there were several transboundary flow incidents due to 'dry weather flows from numerous sources in Mexico' that exceeded the San Diego-Tijuana wastewater system capacity (SDRWCB, 2024). These breeches to the system undoubtedly contributed to many of the elevated FIB measurements. Figure 16 offers a few examples of the bacteria sample data overlaid on top of imagery acquired on the same day or day prior to the water quality sampling. Note the very turbid water emanating from the TJR river and trending north in both images and that samples with FIB exceeding the SSM were taken as far north as Silver Strand beach. The satellite data examples in this figure were acquired on 01/23/24 and 01/30/24 following heavy, multi-day rain events and TJR daily average flow rates of 4,956 cfs, 1,003 cfs and 140 cfs on 01/22/24, 01/23/24 and 01/30/24 respectively. Also note the elevated FIB levels around the mouth of the San Diego River on 01/24/24. SDR average daily flow rates were 1,233 cfs, 951 cfs and 200 cfs on 01/22/24, 01/23/24 and 01/24/24 respectively. Figure 17 offers an example of a day when, with the exception of phytoplankton blooms, the turbidity levels were low, and the general water clarity was good, yet some measurements showed FIB exceeding the SSM both on the shore and offshore. In the South Bay, only the shoreline stations were sampled on the day shown in the figure. The FIB measurements exceeding the SSM were likely related to the transboundary flow problems discussed above.

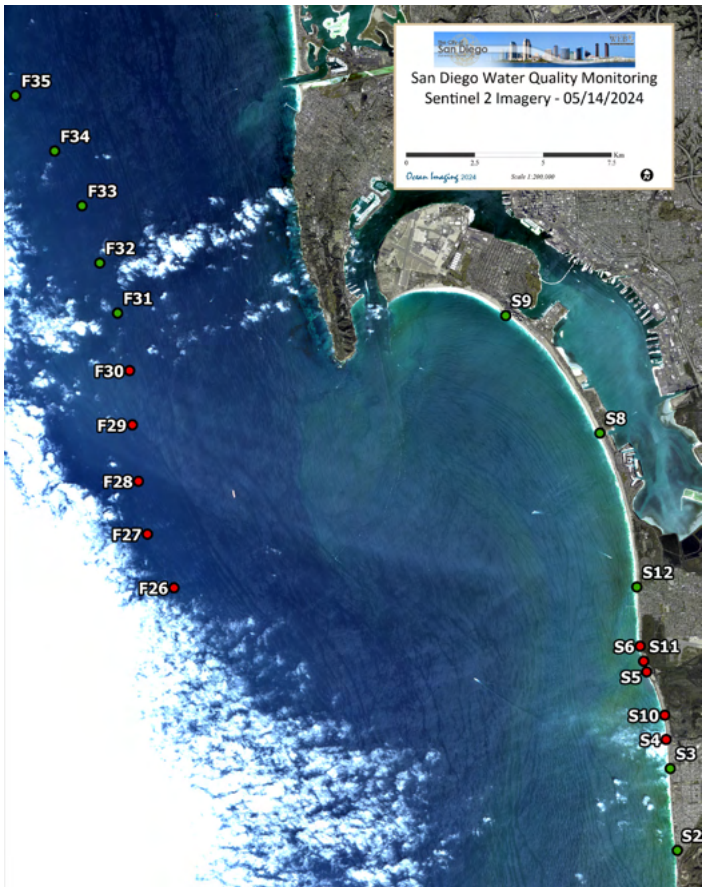




01/23/24				
Station	Depth (M)	Entero	Fecal	Total
S0	0	8000	3400	16000
S2	0	12000	4200	8800
S3	0	11000	6600	16000
S4	0	6800	8600	16000
S5	0	12000	12000	16000
S6	0	12000	12000	11000
S8	0	8200	10000	16000
S10	0	6600	6600	16000
S11	0	12000	12000	16000
S12	0	12000	9200	14000
1/24/24				
I19	2	2200	3600	16000
	6	800	1100	8000
	11	380	200	4400
I24	2	2400	5000	16000
	6	1800	1000	14000
	11	2600	2600	16000
I25	2	1600	2600	16000
	6	1400	2000	16000
	9	2600	2600	16000
I26	2	2400	3000	14000
	6	3000	2200	16000
	9	5800	2600	16000
I32	2	2800	2400	9800
	6	2000	1400	11000
	9	3800	2800	16000
I39	2	600	940	13000
	12	160	120	860
	18	300	140	1000
I40	2	5000	5600	16000
	6	5200	4200	16000
	9	3800	3000	16000
D8	0	420	140	1200
D9	0	280	400	600
D10	0	500	380	1000
D11	0	4000	1200	3400
D12	0	240	110	440

1/30/24				
Station	Depth (M)	Entero	Fecal	Total
I19	2	26	80	600
	6	120	380	4600
	11	220	880	8000
I24	2	260	3800	15000
	6	40	160	760
	11	78	220	1200
I25	2	500	5400	16000
	6	72	110	840
	9	70	120	1500
I26	2	36	2200	7200
	6	460	4000	15000
	9	820	4800	16000
I32	2	96	400	4400
	6	340	520	4000
	9	520	480	5200
I39	2	2	6	180
	12	90	620	4400
	18	100	580	4600
I40	2	600	6800	16000
	6	74	110	1000
	9	180	80	3000
S3	0	320	340	2600
S4	0	200	860	12000
S5	0	720	1600	16000
S6	0	740	1800	16000
S10	0	5800	12000	16000
S11	0	900	1800	16000
S12	0	360	300	4800

Figure 16. Sentinel-2 data with near-surface bacterial sampling data overlaid from the same day and day prior to the image acquisition date. Red dots at PLOO stations (A, C, D) indicate fecal coliform densities in exceedance of the fecal coliform SSM (2019 Ocean Plan). Red dots at SBOO (I, S) stations indicate exceedances of the total coliform, fecal coliform and/or enterococcus SSMs (2015 Ocean Plan). Green dots identify stations at which the FIB levels were in compliance. The tables below each image show the measurement values by depth for each station with elevated bacteria levels in red text. The left image and table show the satellite data acquired on 01/23/24 with sample data overlaid from 01/23/24 and 01/24/24. The right image and table show satellite and bacteria sample data from 01/30/24.



Station	Depth (M)	Entero	Fecal	Total
F26	1	2	NA	NA
	25	2	NA	NA
	60	160	NA	NA
	80	110	NA	NA
	98	16	NA	NA
F27	1	2	NA	NA
	25	2	NA	NA
	60	440	NA	NA
	80	38	NA	NA
	98	76	NA	NA
F28	1	6	NA	NA
	25	2	NA	NA
	60	620	NA	NA
	80	16	NA	NA
	98	110	NA	NA
F29	1	2	NA	NA
	25	2	NA	NA
	60	880	NA	NA
	80	100	NA	NA
	98	20	NA	NA
F30	1	6	NA	NA
	25	2	NA	NA
	60	1100	NA	NA
	80	1000	NA	NA
	98	24	NA	NA
S0	0	700	3000	16000
S4	0	800	2200	16000
S5	0	12000	12000	16000
S6	0	12000	8200	16000
S10	0	3000	10000	16000
S11	0	12000	12000	16000

Figure 17. A Sentinel-2 image from 05/14/24 with bacterial sampling data overlaid from the same day. Phytoplankton blooms are evident, however low turbidity, the lack of a significant TJR discharge plume and a lower-than-average river flow rate on 05/14 (99 cfs vs. the 2024 annual daily average of 152 cfs) point to other reasons for the high FIB readings not apparent as fouled water in the image data. Red dots at PLOO stations (F) indicate fecal coliform densities in exceedance of the fecal coliform SSM (2019 Ocean Plan). Red dots at SBOO stations (S) indicate exceedances of the total coliform, fecal coliform and/or enterococcus SSMs (2015 Ocean Plan). Green dots identify stations at which the FIB levels were in compliance. The table to the right of the image shows the measurement values by depth for each station with elevated bacteria levels in red text.

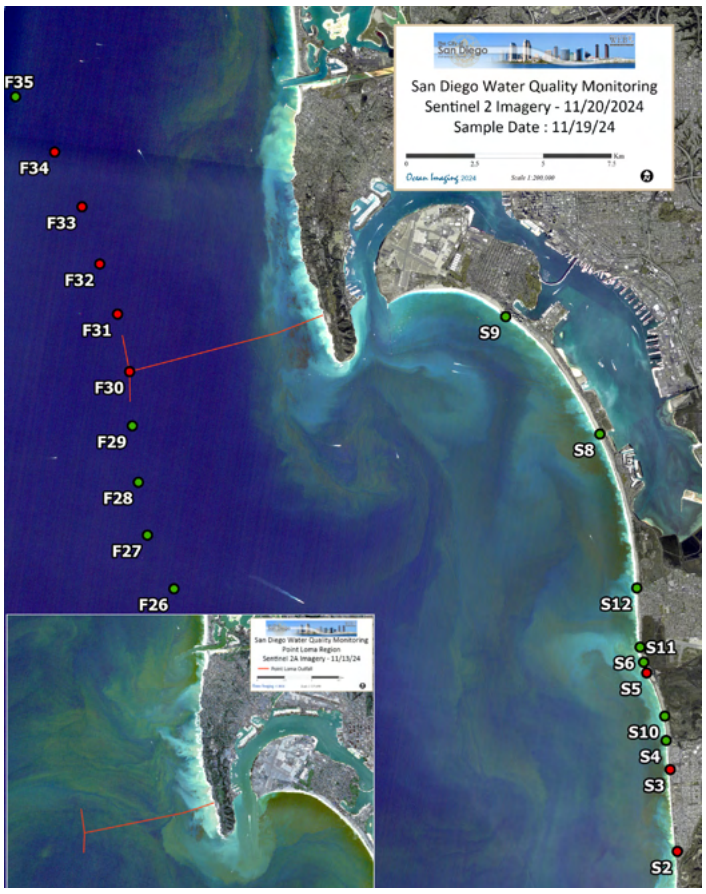
3.3 The Point Loma Outfall Region

After its seaward extension in 1993, the Point Loma Ocean Outfall (PLOO) is one of the deepest and longest wastewater outfalls in the world, discharging at a depth of 320 feet (~97.5 meters), 4.5 miles (7.25 kilometers) offshore. The outfall's plume is generally not observed directly with multispectral color or thermal imagery. It appears to not reach the surface waters, even during the winter months when the water column's vertical stratifications are weakened. We believe that on a few occasions we have observed the plume's extents indirectly through an anomalous lateral displacement of thermal or chlorophyll features around the outfall wye. This effect can be explained by the doming up of the discharged effluent and laterally displacing the near-surface waters above it.

In 2024 the Point Loma region was affected by conditions already described for general San Diego County: significant seasonal rainfall during the months of January through March and very little rainfall for the rest of the year, including November and December which experienced a total of only 0.17 inches for the two months combined. Similar to past years, compromised water clarity was likely a result of runoff from the San Diego River

and Mission Bay bringing sediment-laden water inside and outside the Point Loma kelp bed after the rain events described in section 3.1 above.

The 2024 Point Loma shoreline, kelp and offshore bacterial sampling resulted in a comparable number of elevated bacteria measurements when contrasted to previous years as defined by the 2015 California Ocean Plan (Total coliform density will not exceed 10,000 per 100 mL; or Fecal coliform density will not exceed 400 per 100 mL; or Total coliform density will not exceed 1,000 per 100 mL when the ratio of fecal/total coliform exceeds 0.1; or enterococcus density will not exceed 104 per 100 mL) (SWRCB, 2015). Out of 111 total sample days, there were 16 days on which elevated bacteria levels were measured at one or more stations in this region. In 2023 the PLOO stations were sampled on 115 days during the year. In 2024 for the three PLOO sampling areas combined, 14.4% of the sampling days resulted in elevated bacteria levels at one station or more, which is lower than recorded in 2023 (17.4%). The shoreline sampling yielded 8 days on which one or more stations experienced high bacteria counts. The offshore sampling resulted in 8 days when FIB were over the SSM. No kelp stations recorded out of compliance SSMs for FIB in 2024. Figures 17 (above) and 18 provide examples of when multiple stations in the Point Loma sampling region resulted in non-compliant SSM numbers on 05/14/24 and 11/19/24.



Station	Depth (M)	Entero	Fecal	Total
F30	1	2	NA	NA
	25	2	NA	NA
	60	100	NA	NA
	80	440	NA	NA
	98	12		NA
F31	1	2	NA	NA
	25	2	NA	NA
	60	160	NA	NA
	80	6	NA	NA
	98	1000	NA	NA
F32	1	2	NA	NA
	25	2	NA	NA
	60	12	NA	NA
	80	700	NA	NA
	98	70	NA	NA
F33	1	4	NA	NA
	25	2	NA	NA
	60	24	NA	NA
	80	280	NA	NA
	98	60	NA	NA
F34	1	2	NA	NA
	25	2	NA	NA
	60	10	NA	NA
	80	120	NA	NA
	98	74	NA	NA
S0	0	12000	12000	16000
S2	0	140	700	1600
S3	0	110	1200	4000
S5	0	100	380	1800
S10	0	3000	10000	16000
S11	0	12000	12000	16000

Figure 18. Sentinel-2 acquired on 11/20/24 with bacterial sampling data from 11/19/24 overlaid on the image. Red dots at PLOO stations (F) indicate fecal coliform densities in exceedance of the fecal coliform SSM (2015 Ocean Plan). Red dots at SBOO stations (S) indicate exceedances of the total coliform, fecal coliform and/or enterococcus SSMs (2019 Ocean Plan). Green dots identify stations at which the FIB levels were in compliance. The table to the right of the image shows the measurement values by depth for each station with elevated bacteria levels in red text. The inset image is a Sentinel-2 scene, captured one week prior to the sampling, shows SDR discharge, active coastal turbidity and offshore phytoplankton blooms, however, these prior coastal disturbances did not play a part in the increased FIB readings in the area. There is no evidence of the wastewater plume at the surface in the imagery from November 20. Instead, all bacterial exceedances were found at depths of 60 m or more, indicating that the plume was trapped by the pycnocline barrier and so any surface presence would not be visible in the satellite imagery.

The imagery both dates do not show visible evidence of any direct correlation to the offshore bacteria samples. The inset image from one week earlier 11/13/24 does display significant turbidity along the coast, visible SDR discharge and high levels of offshore chlorophyll. However, the reason for the high FIB levels at the "F" stations is in all probability linked to the PLOO effluent. The stations exhibiting elevated FIB levels are all either right over or north of the wye and at depths of 60 meters or below. This indicates that the high-bacteria effluent originating from the outfall may have been trapped by a pycnocline barrier at depth so any surface presence would not be visible in the satellite imagery.

3.4 Kelp Variability

One observation provided by the satellite image archive is the continuing variability in the size of the Point Loma kelp bed over time (Figure 19). Table 4 shows the area in km^2 of three notable kelp beds in the San Diego region over the past 17 years. The September and October dates were chosen to represent the kelp bed canopy coverage for each year since spring and fall are the time periods when the canopy size is considered to be at or near its peak - with fall being the preferred season to map kelp using remote sensing techniques. The estimated size of the Point Loma bed canopy in the fall of 2024 (0.88 km^2) was significantly smaller than the average canopy coverage for the prior 16-year period from 2008-2023 (3.95 km^2). 2024 exhibited the second smallest canopy coverage over the 17-year period only second to 2016. As reported previously, the satellite data show the bed begin to decrease in size during February of 2016, perhaps due to the storm events taking place during early to mid-January, effects from the 2014-2016 strong El Niño event and/or the Northeast Pacific marine heat wave (Di Lorenzo, 2016). Noted in the 2017 and 2018 annual reports, the kelp bed appeared to be coming back in January of 2017, but then decreased in size as the year progressed resulting in much smaller than average canopy coverage by the end of that year. Using the fall imagery as an indicator for annual health, the bed size appeared to be stabilizing since the 2016 and 2017 lows, however the 2023 and 2024 computed areal coverages show a considerable decrease in size (Figure 20). Contrary to previous years such as 2018, 2020 and 2021 when the canopy area exhibited significant intra-annual variability, during 2023 and 2024 the bed size remained consistently depleted throughout the year (Figure 21). Very little kelp canopy was visible in the high-resolution SPOT, Sentinel-2 and Landsat imagery from January through September. In fact, no exposed kelp canopy was visible in the satellite data during the entire month of September. During October through December the canopy gradually increased in size through the end of the year. Satellite data acquired throughout January of 2025 showed the kelp canopy continuing to expand, but not to the levels observed in 2017 through 2022. While there were significant differences in tidal heights at the time of each satellite image acquisition, tides cannot be flagged as the primary reason for the difference in canopy coverage observed in the satellite data. There were days when the areal coverage was high, but the tide level was also high and vice versa when the imagery revealed smaller bed size, but the tides were relatively low.

Canopy coverage for each year in Table 4 and Figure 20 was computed by first running a Normalized Difference Vegetation Index (NDVI) classification followed by an iso cluster unsupervised classification to generate a single exposed kelp class (ESRI, 2024). It is important to point out that the canopy coverage shown in Table 4 may differ slightly from those provided in the Region Nine Kelp Survey Consortium Aerial Kelp Survey Reports. This is because the canopy areas for the Point Loma bed computed for those reports are averages of four surveys performed throughout the year; while the coverage estimates shown in this report are taken from single satellite images acquired during the fall time period chosen to represent the maximum coverage experienced during that time of year. Tide levels were not a factor in the inter-year comparison as there was little variability in tide level between the years (often approximately two feet or less). However, due to the overflight times of these satellites, the canopy areas could

be underrepresented compared to the kelp survey reports because the tide levels at the time of satellite data acquisition could vary significantly from the tides during the aerial surveys. The Imperial Beach and Tijuana beds have not been visible in the satellite data since 2015. It is being documented that kelp forests along the West Coast have been experiencing noteworthy variability in canopy size for the past several years, and thus warrants keeping a close watch on the health of the kelp beds in the San Diego region (Bell et al., 2020 and Schroeder, 2019).

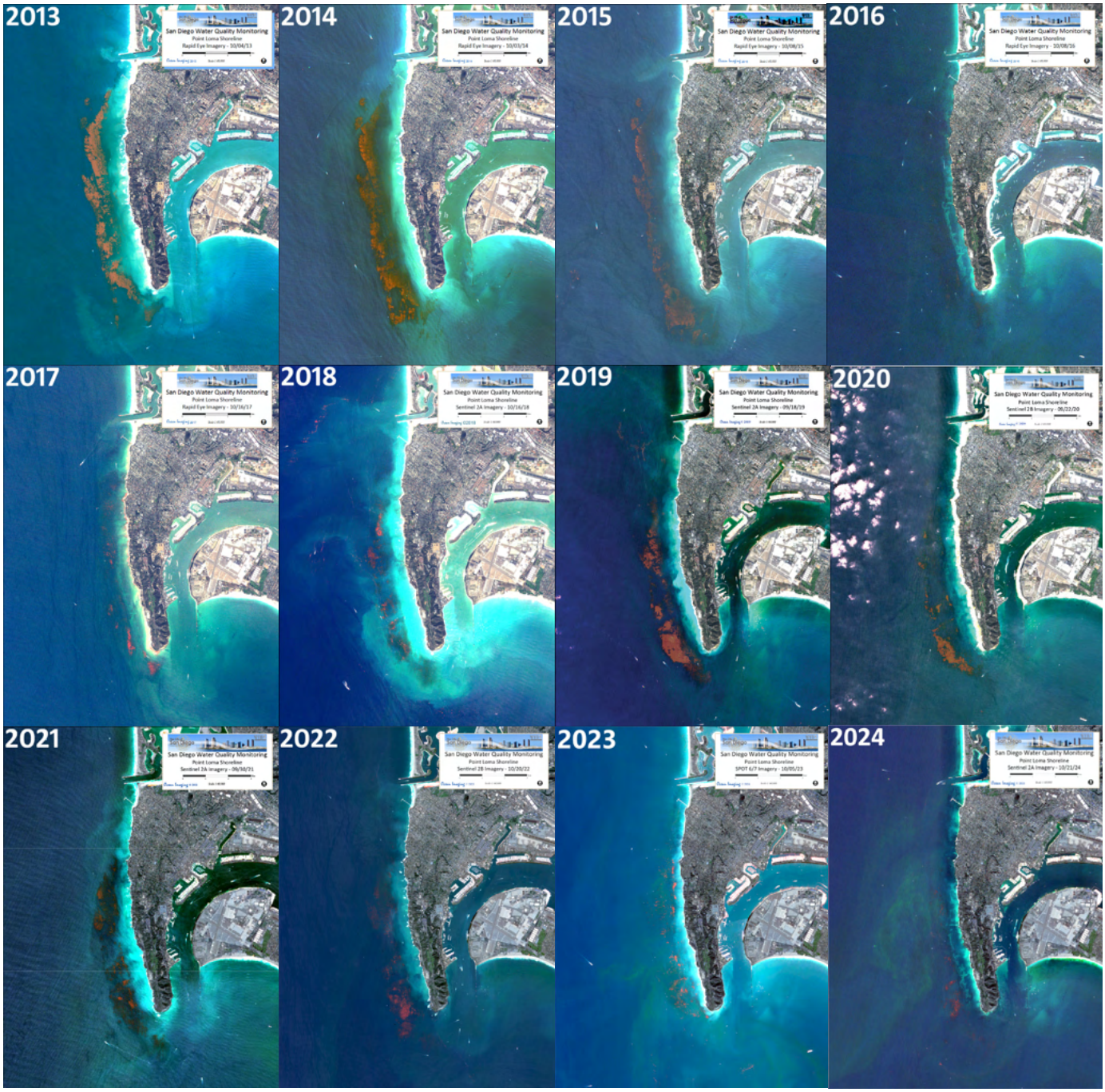


Figure 19. The Point Loma kelp bed as observed in high-resolution satellite imagery for the years 2013-2024. September and October dates were chosen to represent the kelp bed canopy coverage for each year since that period is when the canopy size is thought to be at or near its peak.

Table 4. Kelp canopy areas of three San Diego kelp beds measured from satellite imagery collected for this project.

			Kelp (km²)		
Year	**Date**	**Satellite**	**Point Loma**	**Imperial Beach**	**Tijuana**
2024	10/21/24	Sentinel-2A	0.88	0.00	0.00
2023	10/05/23	SPOT 6/7	2.14	0.00	0.00
2022	10/20/22	Sentinel-2B	4.48	0.00	0.00
2021	09/30/21	Sentinel-2B	3.82	0.00	0.00
2020	09/22/20	Sentinel-2A	2.93	0.00	0.00
2019	09/18/19	Sentinel-2A	5.17	0.00	0.00
2018	10/16/18	Sentinel-2A	2.44	0.00	0.00
2017	10/04/17	RapidEye	1.05	0.00	0.00
2016	09/08/16	RapidEye	0.22	0.00	0.00
2015	09/17/15	Landsat 7	4.11	0.39	0.29
2014	09/14/14	Landsat 8	5.42	0.59	0.30
2013	09/23/13	RapidEye	5.89	0.19	0.05
2012	09/15/12	RapidEye	2.91	0.00	0.00
2011	09/01/11	RapidEye	1.99	0.00	0.00
2010	09/27/10	Landsat 7	6.01	0.00	0.00
2009	09/16/09	Landsat 5	5.96	1.01	0.21
2008	09/05/08	Landsat 7	8.66	0.82	0.01

* Average surface canopy coverage 2008-2023 = 3.95 km²

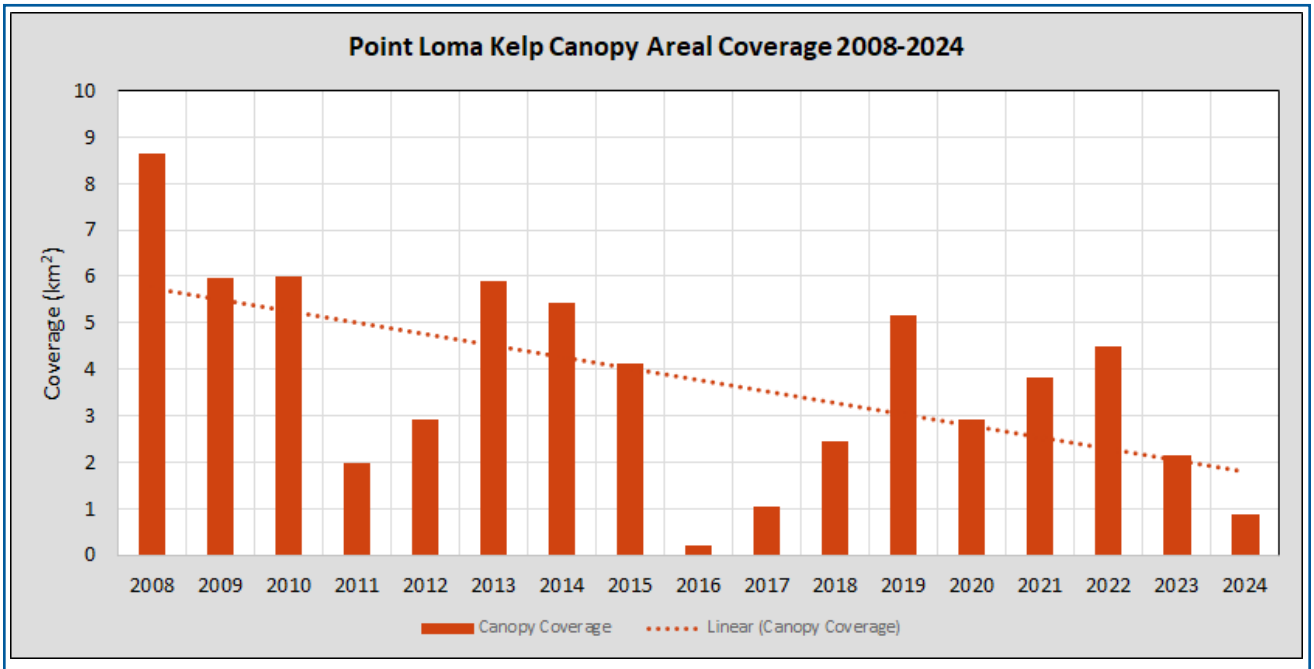


Figure 20. Point Loma kelp canopy coverage 2008-2024. Calculations were from imagery acquired on the September and October dates shown in Table 4 above. The dates were chosen to represent the kelp bed canopy coverage for each year since the September to October time period is when the canopy size is thought to be at or near its peak. The dotted line shows a linear trend line over the period.

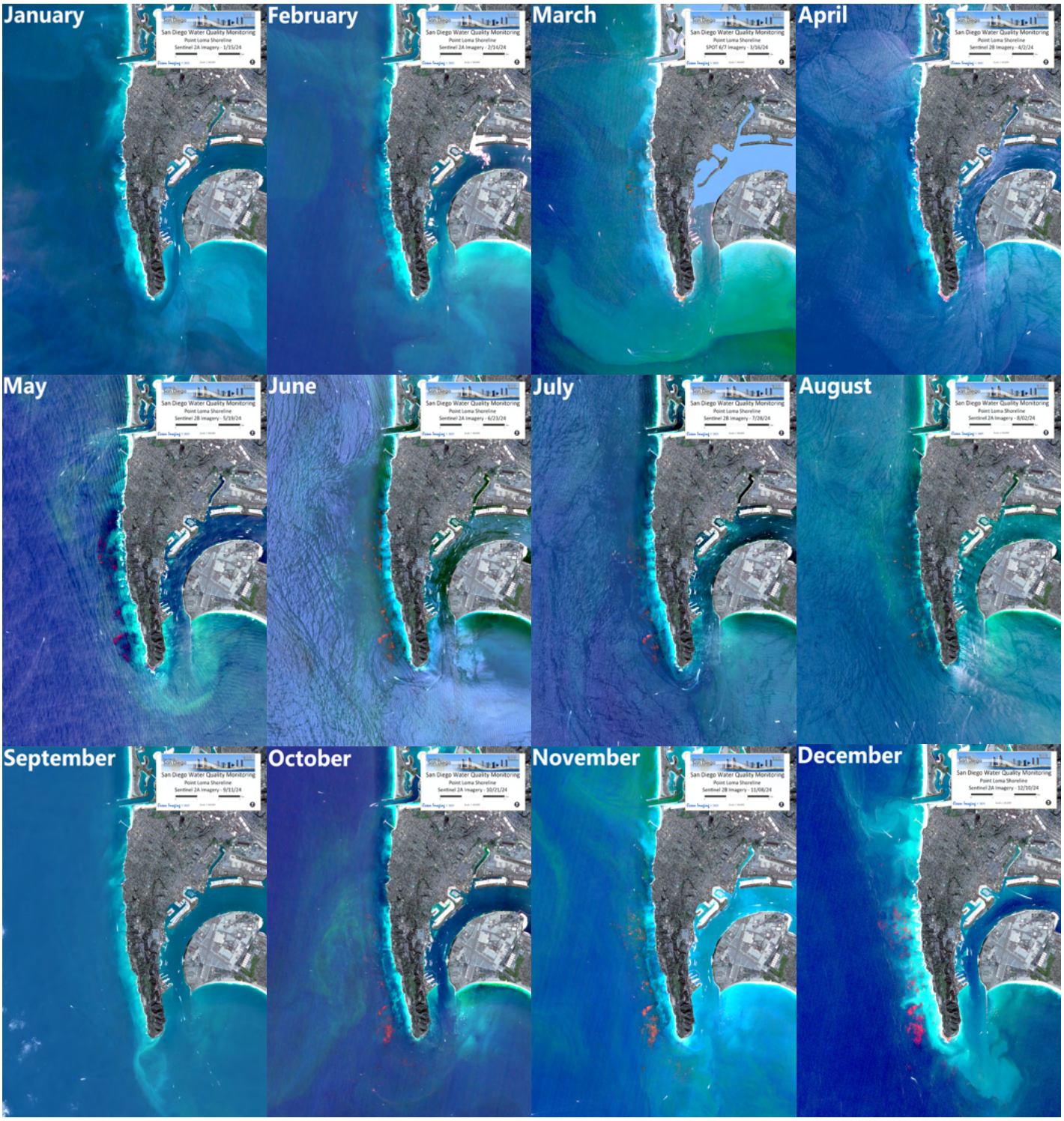


Figure 21. High-resolution satellite imagery documenting the month-to-month variability in the Point Loma kelp bed canopy coverage. The dates were chosen to best represent the maximum-observed canopy coverage for each month.

4. PRESENT AND FUTURE ENHANCEMENTS OF THE PROJECT

In 2016, OI began to generate ocean currents and other satellite- and model-derived oceanographic data products in a Web Map Service (WMS) Representational State Transfer (REST) format which would have been compatible with a WMS the City was working to implement. It was intended that all the OI-delivered data products, including all the satellite imagery would be delivered via OI's ArcGIS Server for easy ingestion into the City's WMS by fall of 2017. While this system was not implemented, OI has developed a dashboard-style web portal to fill that purpose. The site will incorporate an interactive WMS to serve as a mechanism to better facilitate the visualization viewing of existing and future satellite image data products as well as any other tabular data sets the City chooses to host on the platform. Not only will the server give the user the capability to overlay different data types on top of each other (i.e., ocean currents on top of satellite imagery) it will significantly enhance the information experience providing convenient, near real-time access to the many data products delivered as part of this project. Initially the site will be password-protected and for internal use only by SDPUD employees and their partners. The server will host present, near real-time imagery and tabular data as well as data from the previous one to two years. Discussions have also begun regarding the development of a public-facing data dashboard hosting most of the same datasets that have been vetted through the City's quality control procedures. As part of this process, the historical imagery, data, and reports will remain accessible via the existing web portal. If a public-facing dashboard style data portal is implemented by the City, OI will progressively work backwards in time to make all historical data available via this platform, including the archived imagery and additional data products. Figure 22 shows the dashboard interface which will be operational by the time of this report's release.

In mid-to-late 2025, 300m resolution chlorophyll and TSM data products derived from the Sentinel-3 satellites will be added to the project's near-daily image mix. These data should help to further identify and track turbid water resulting from offshore runoff and river discharge. The products will initially be experimental in nature to determine the ability of the ESA TSM algorithms to differentiate TSM from offshore chlorophyll blooms. Figure 23 provides an example of the upcoming TSM imagery.

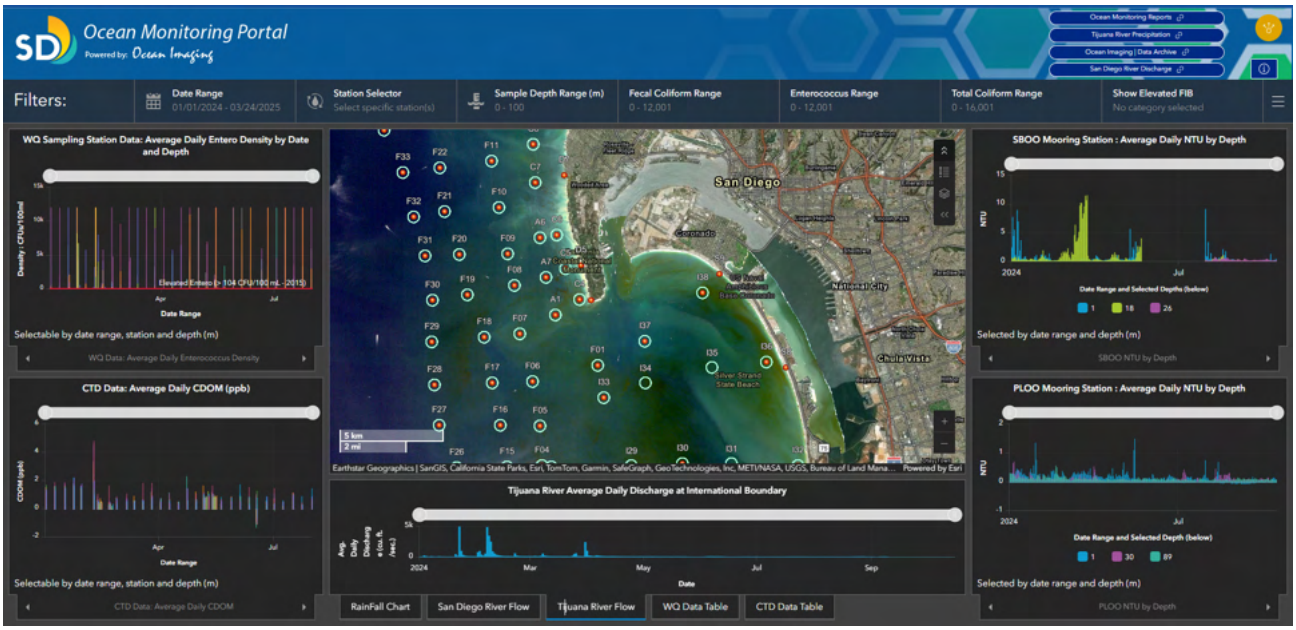


Figure 22. Dashboard-style data portal hosting access to satellite imagery along with several other oceanographic and biological datasets that can be filtered for display by date, sample depth, value range and other definable parameters.

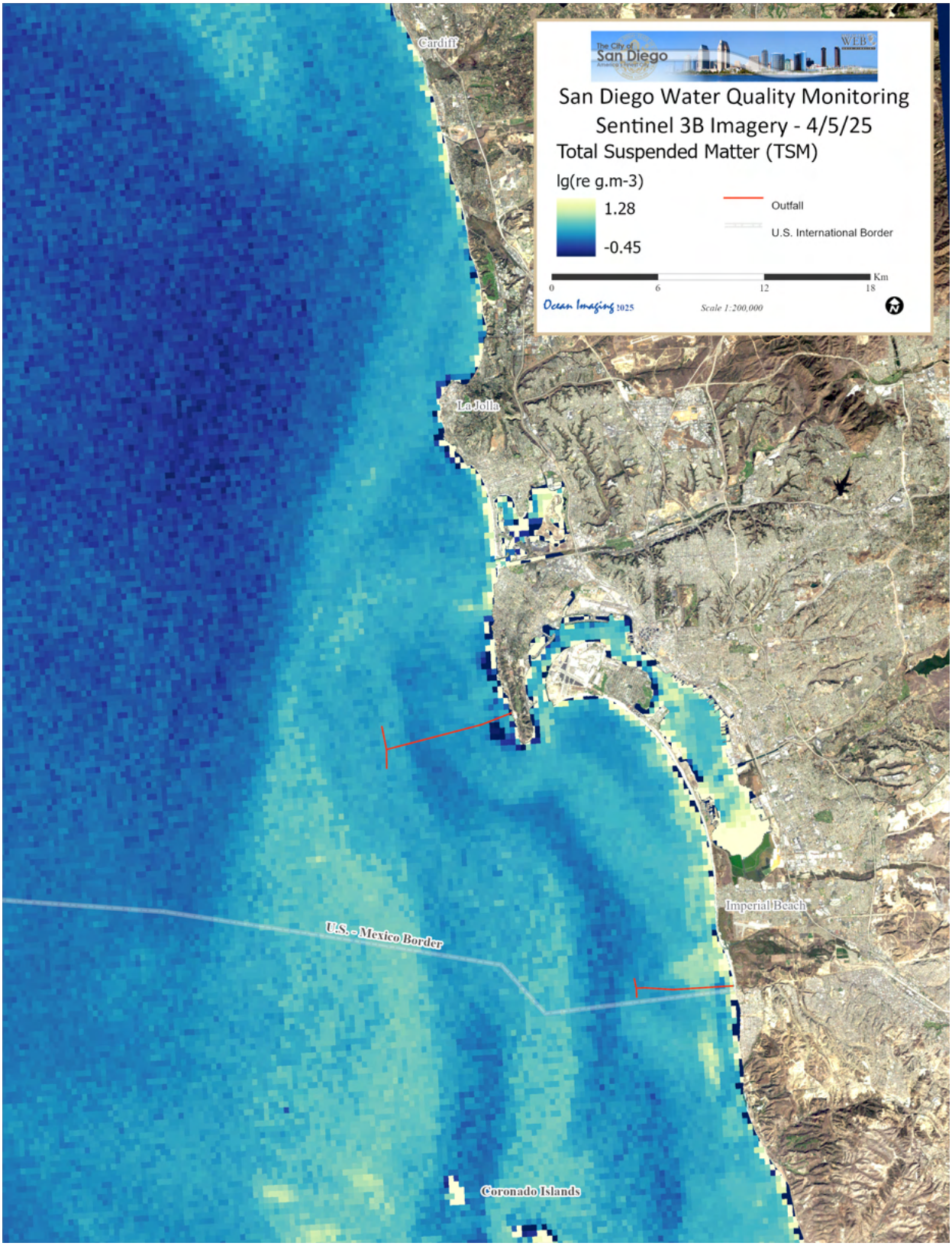


Figure 23. Sample TSM imagery from 04/05/25. This imagery will be posted near-daily beginning in mid-to-late 2025.

5. REFERENCES

[APHA] American Public Health Association. (2012). "Standard Methods for the Examination of Water and Wastewater, 22nd edition." *American Public Health Association, American Water Works Association, and Water Environment Federation*.

Bell, Tom W., et al. "Three Decades of Variability in California's Giant Kelp Forests from the Landsat Satellites." *Remote Sensing of Environment,* vol. 238, 2020, p. 110811., doi:10.1016/j.rse.2018.06.039.

Bordner, R., Winter, J., Scarpino, P., eds. 1978. "Microbiological Methods for Monitoring the Environment: Water and Wastes, EPA Research and Development," *EPA-600/8-78-017.*

[CDPH] California State Department of Public Health website. (2019). "Regulations for Public Beaches and Ocean Water-Contact Sports Areas." *Appendix A: Assembly Bill 411, Statutes of 1997, Chapter765.* https://www.cdph.ca.gov/Programs/CEH/DRSEM/Pages/EMB/RecreationalHealth/Beaches-and-Recreational-Waters.aspx

Di Lorenzo, E., Mantua, N. "Multi-year persistence of the 2014/15 North Pacific marine heatwave." *Nature Climate Change* ***6****, 1042–1047 (2016).* https://doi.org/10.1038/nclimate3082

[ESRI] "ISO Cluster Unsupervised Classification (Spatial Analyst)." *Iso Cluster Unsupervised Classification (Spatial Analyst)-ArcGIS Pro | Documentation*, pro.arcgis.com/en/pro-app/ latest/tool-reference/ spatial-analyst/iso-cluster-unsupervised-classification.htm. Accessed 15 May 2024.

Gierach, M. M., Holt, B., Trinh, R., Pan, B.J., Rains, C., 2017. "Satellite detection of wastewater diversion plumes in Southern California." *Estuarine, Coastal and Shelf Science*, 186, 171 – 182.

Kahru, Mati, and B. Greg Mitchell. "Spectral reflectance and absorption of a massive red tide off Southern California." *Journal of Geophysical Research: Oceans, vol. 103, no. C10, 15 Sept. 1998, pp. 21601–21609,* https://doi.org/10.1029/98jc01945.

Little, Joe. "Toxic Tide: The Sewage Crisis at the Border." *NBC 7 San Diego*, NBC 7 San Diego, 12 Jan. 2024, www.nbcsandiego.com/news/local/toxic-tide-the-sewage-crisis-at-the-border/3391666/.

Schroeder, Sarah B., et al. "Passive Remote Sensing Technology for Mapping Bull KELP (NEREOCYSTIS Luetkeana): A Review of Techniques and Regional Case Study." *Global Ecology and Conservation, vol. 19, 2019,* doi:10.1016/j.gecco.2019.e00683.

[SDRWCB] San Diego Regional Water Quality Control Board. "San Diego Region - Executive Officer's Reports." *Executive Officer's Report | San Diego Regional Water Quality Control Board*, www.waterboards.ca.gov/sandiego/publications_forms/publications/eoreports.html. Accessed 25 Mar. 2025.

Southern California Coastal Water Research Project, 10 May 2019, "Harmful Algal Blooms." https://www.sccwrp.org/about/research-areas/eutrophication/harmful-algal-blooms/.

[SWRCB] California State Water Resources Control Board. (2015). California Ocean Plan, Water Quality Control Plan, Ocean Waters of California. California Environmental Protection Agency, Sacramento, CA.

[SWRCB] California State Water Resources Control Board. (2019). California Ocean Plan, Water Quality Control Plan, Ocean Waters of California. California Environmental Protection Agency, Sacramento, CA.

Svejkovsky, J., Haydock, I., 1998. "Satellite remote sensing as part of an ocean outfall environmental monitoring program." *Taking a Look at California's Ocean Resources: An Agenda for the Future,* ASCE, Reston, VA (USA), 2, 1306.

Svejkovsky, J., Jones, B., 2001. "Satellite Imagery Detects Coastal Stormwater and Sewage Runoff." *EOS-Trans. American Geophys. Union*, 82(50).

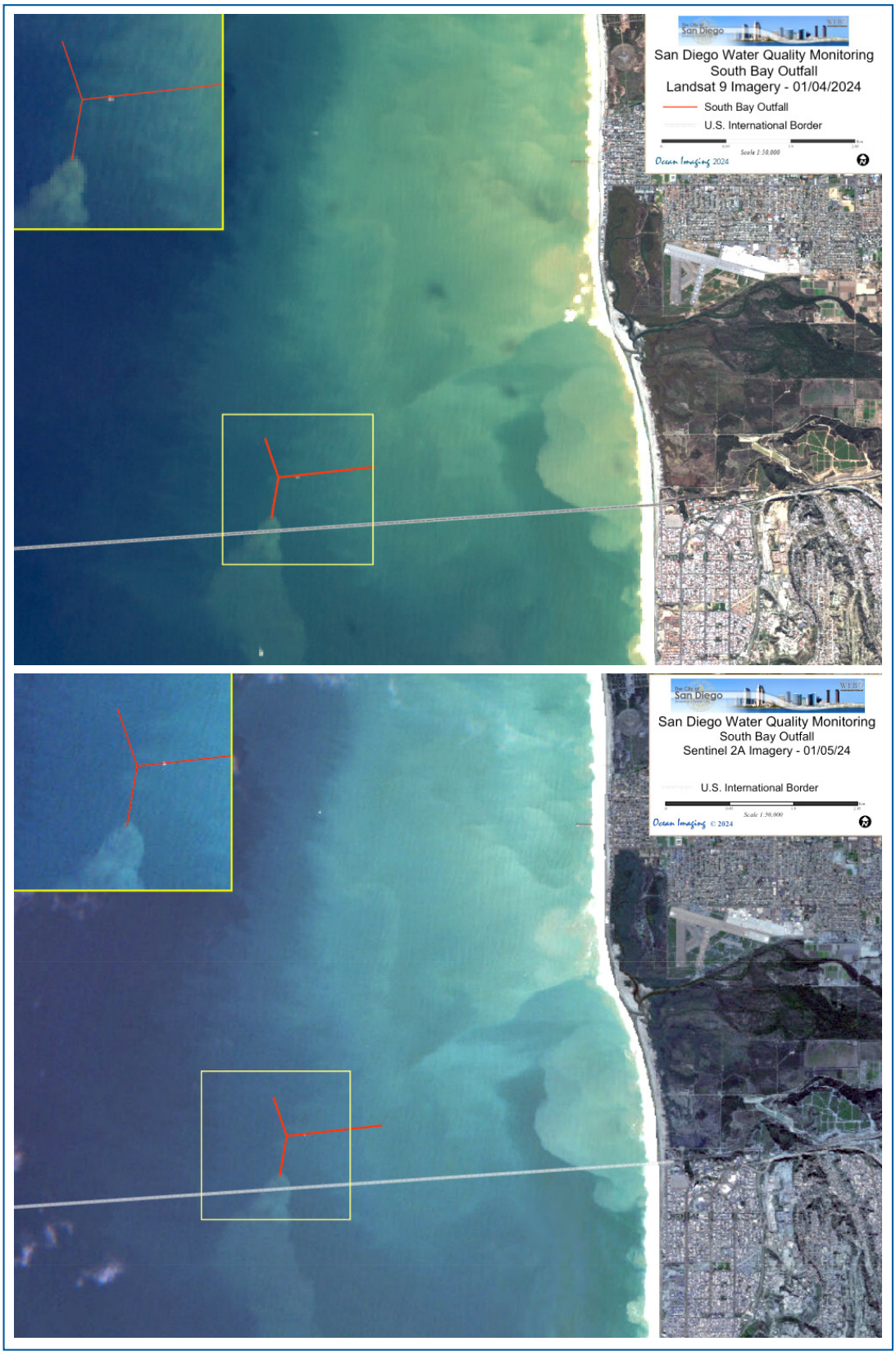
Svejkovsky, J., Shandley, J., 2001. "Detection of offshore plankton blooms with AVHRR and SAR imagery." *Int. J. of Remote Sensing*, 22 (2&3), 471-485.

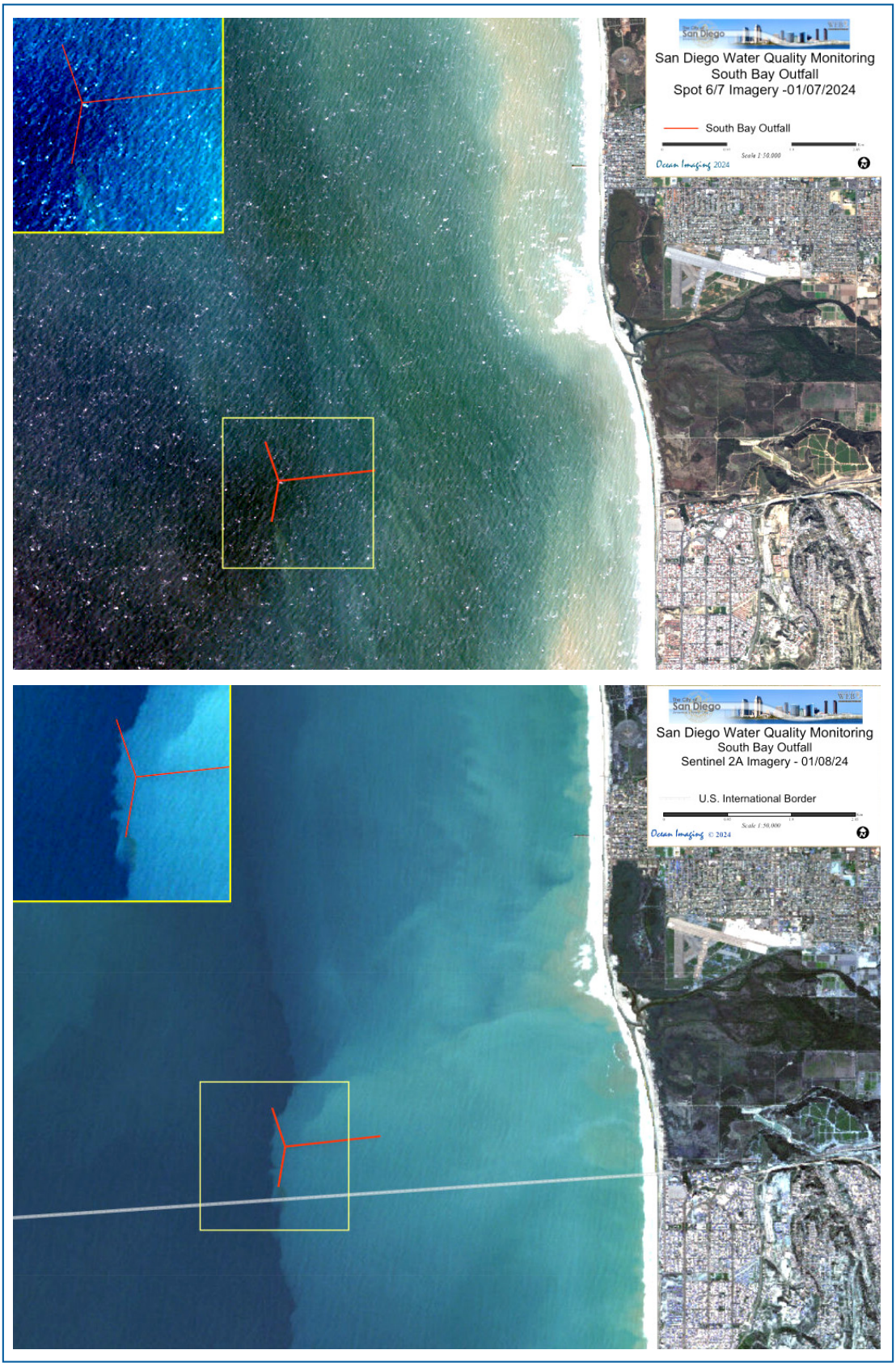
Svejkovsky, J., Nezlin, N. P., Mustain, N.M. Kum, J. B., 2010. "Tracking storm water discharge plumes and water quality of the Tijuana River with multispectral aerial imagery." *Estuarine, Coastal and Shelf Science.* 87(3), 387-398.

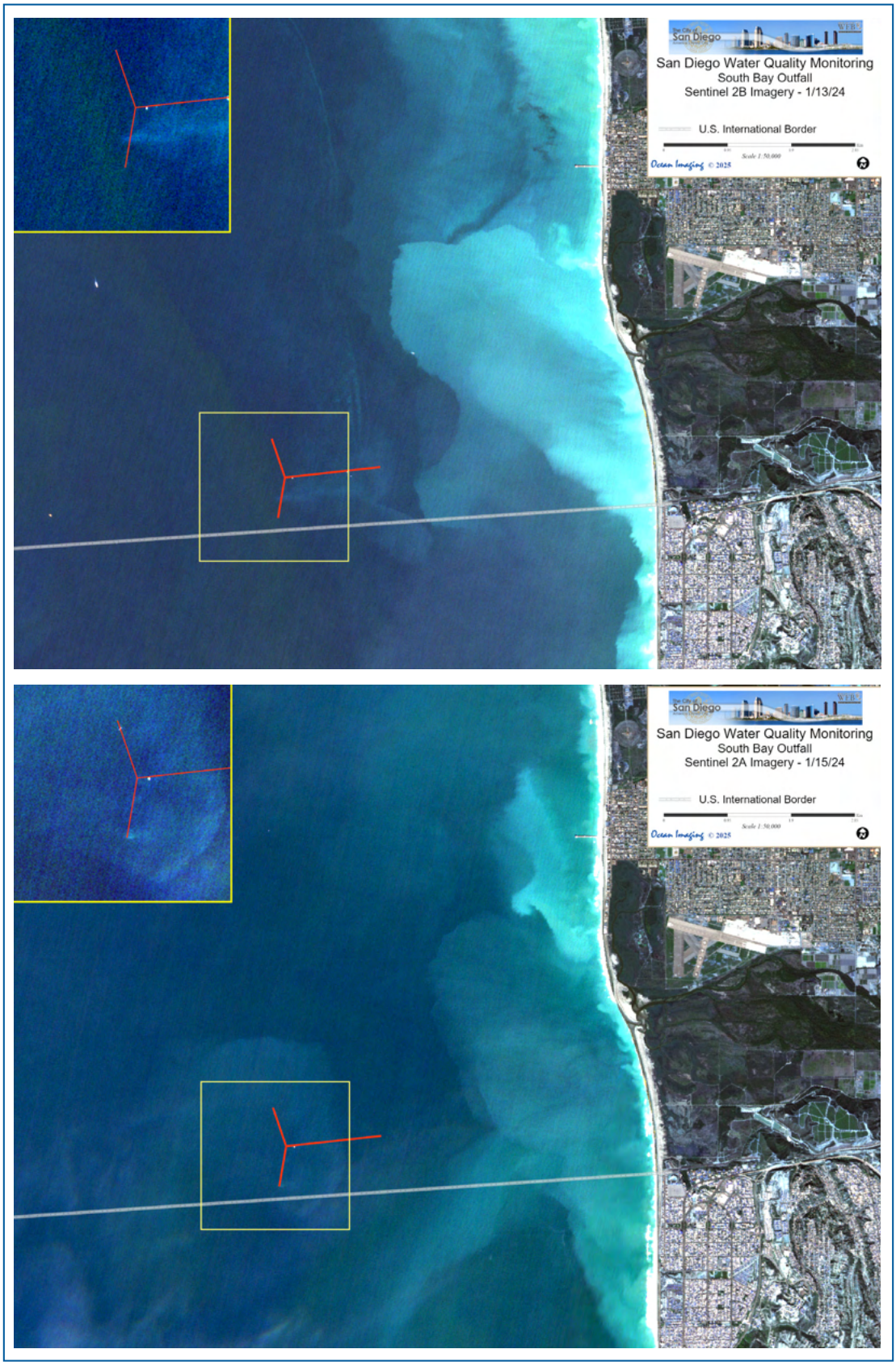
[USEPA] United States Environmental Protection Agency. (2014). Method 1600: "Enterococci in Water by Membrane Filtration Using membrane-Enterococcus Indoxyl-β-D-Glucoside Agar (mEI)." *EPA Document EPA-821-R-14-011. Office of Water* (4303T), Washington, DC.

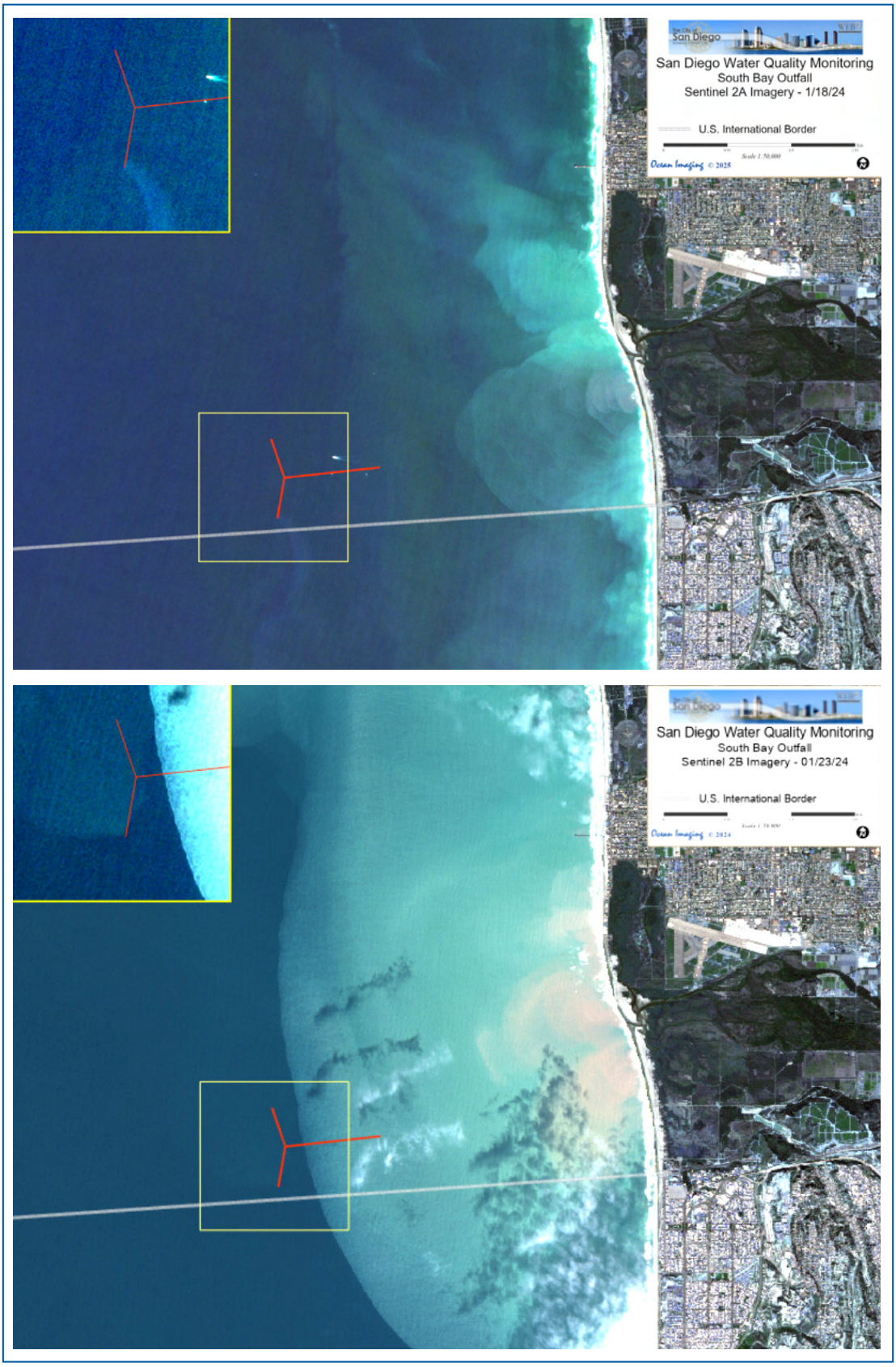
Zheng, Q., Klemas,V.V., Coastal Ocean Environment. Comprehensive Remote Sensing." *Elsevier, Amsterdam* (2018), pp. 89-120.

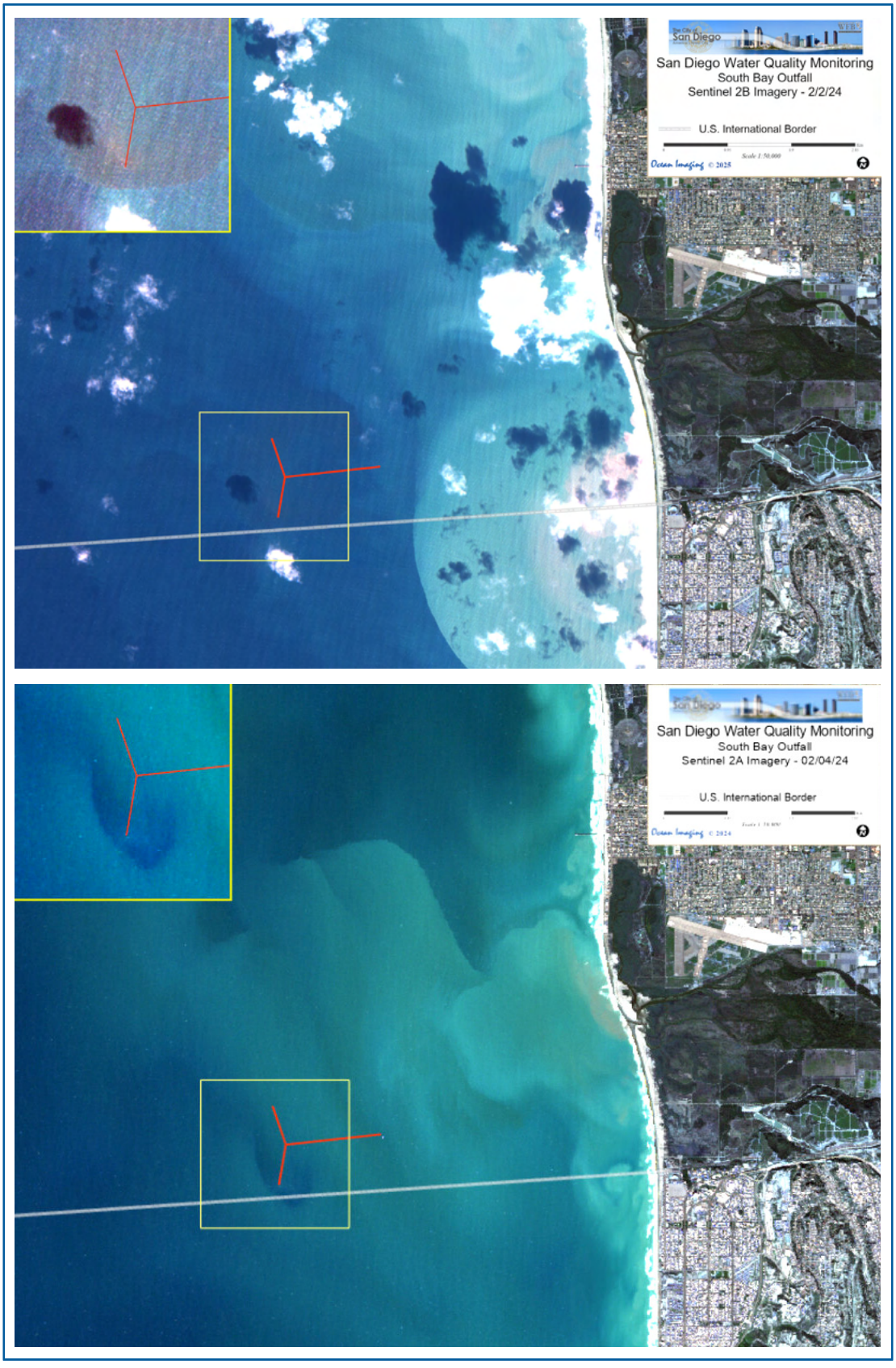
APPENDIX A – HIGH RESOLUTION SATELLITE IMAGERY SHOWING SBOO-RELATED WASTEWATER PLUME

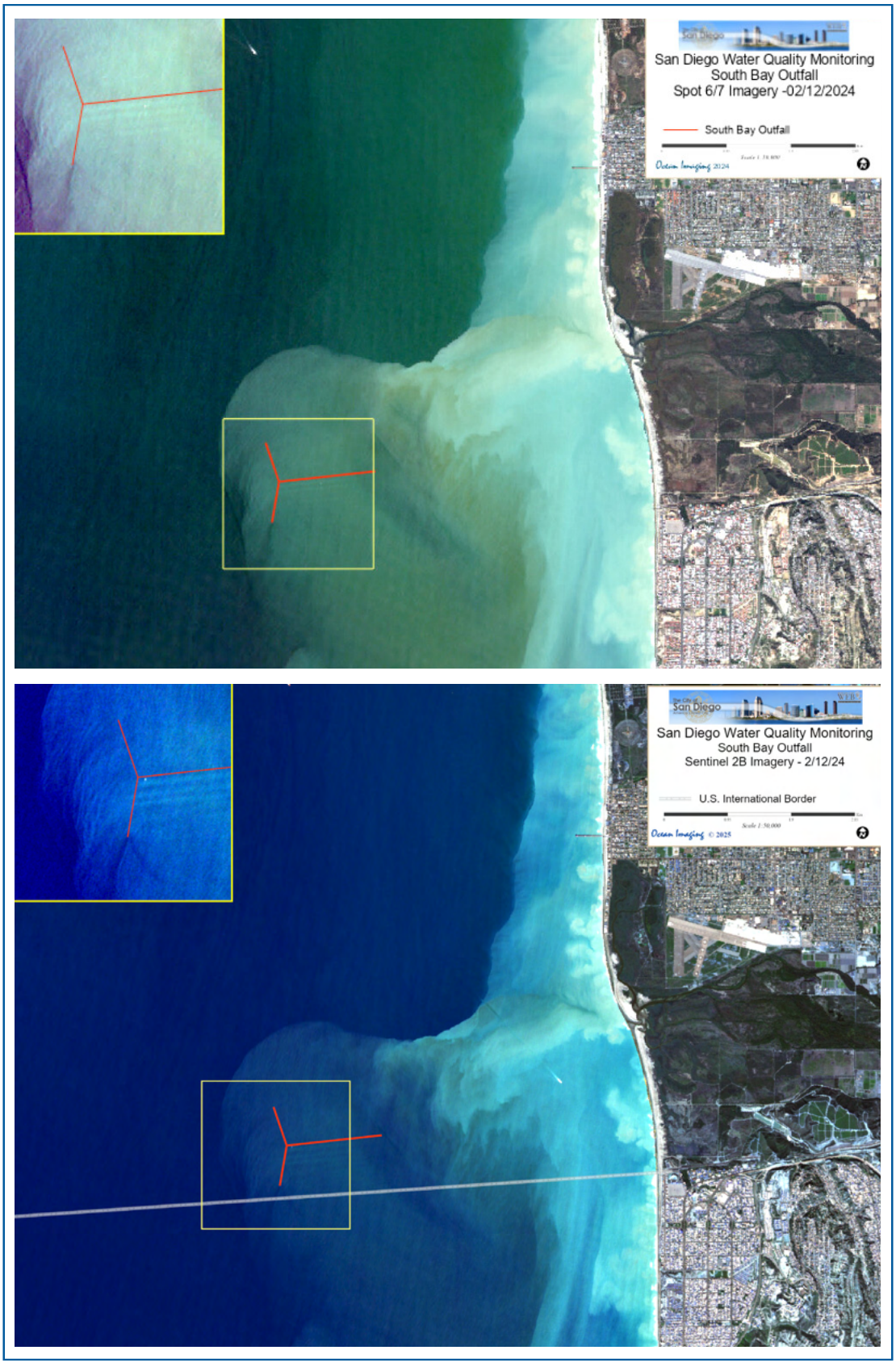


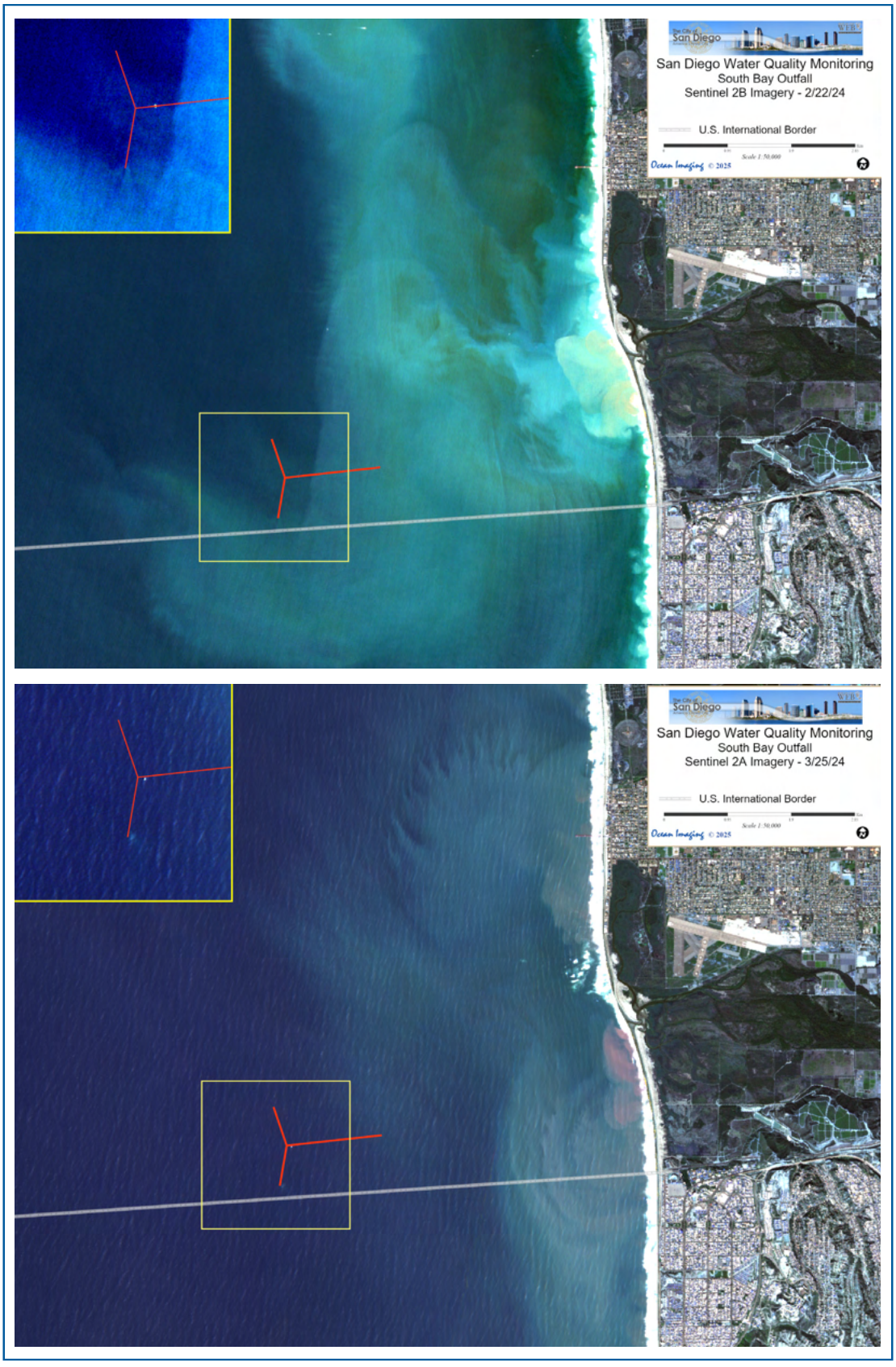

San Diego Water Quality Monitoring
South Bay Outfall
Spot 6/7 Imagery -01/07/2024
South Bay Outfall
Ocean Imaging 2024
San Diego Water Quality Monitoring
South Bay Outfall
Sentinel 2A Imagery - 01/08/24
U.S. International Border
Ocean Imaging © 2024

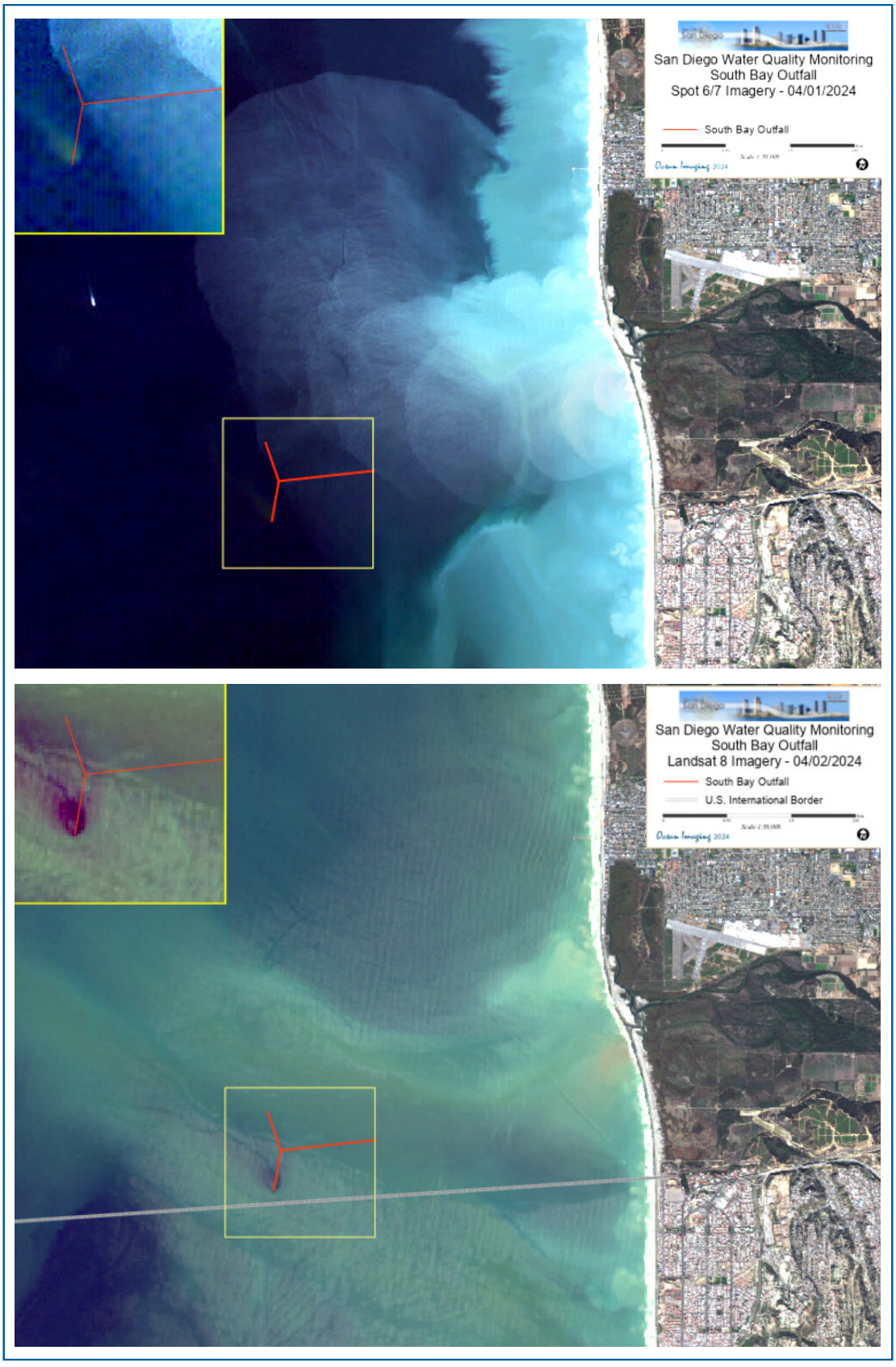

San Diego
San Diego Water Quality Monitoring
South Bay Outfall
Sentinel 2B Imagery - 1/13/24
U.S. International Border
Ocean Imaging © 2025
San Diego
San Diego Water Quality Monitoring
South Bay Outfall
Sentinel 2A Imagery - 1/15/24
U.S. International Border
Ocean Imaging © 2025

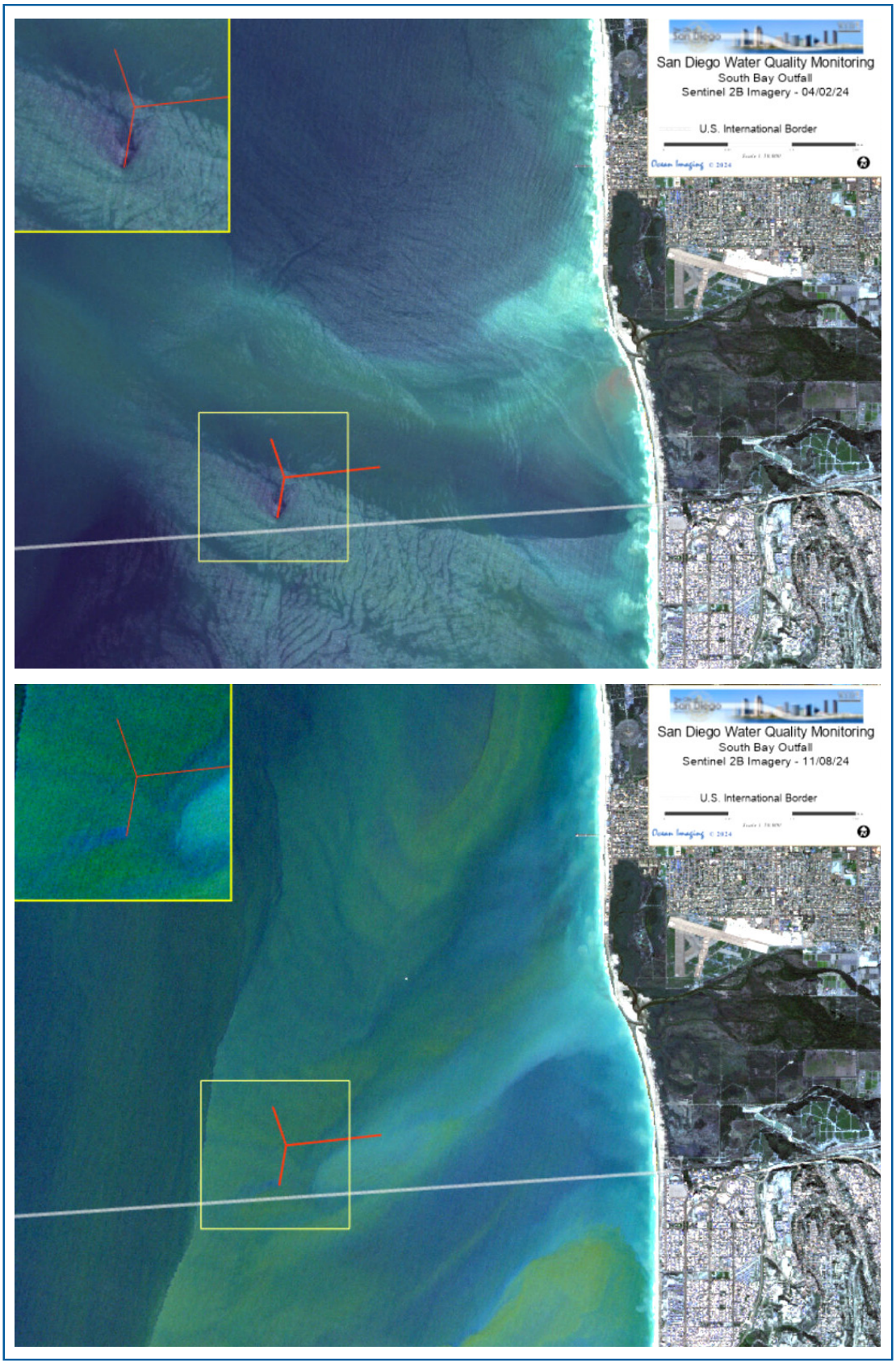

San Diego
San Diego Water Quality Monitoring
South Bay Outfall
Sentinel 2A Imagery - 1/18/24
U.S. International Border
San Diego
San Diego Water Quality Monitoring
South Bay Outfall
Sentinel 2B Imagery - 01/23/24
U.S. International Border

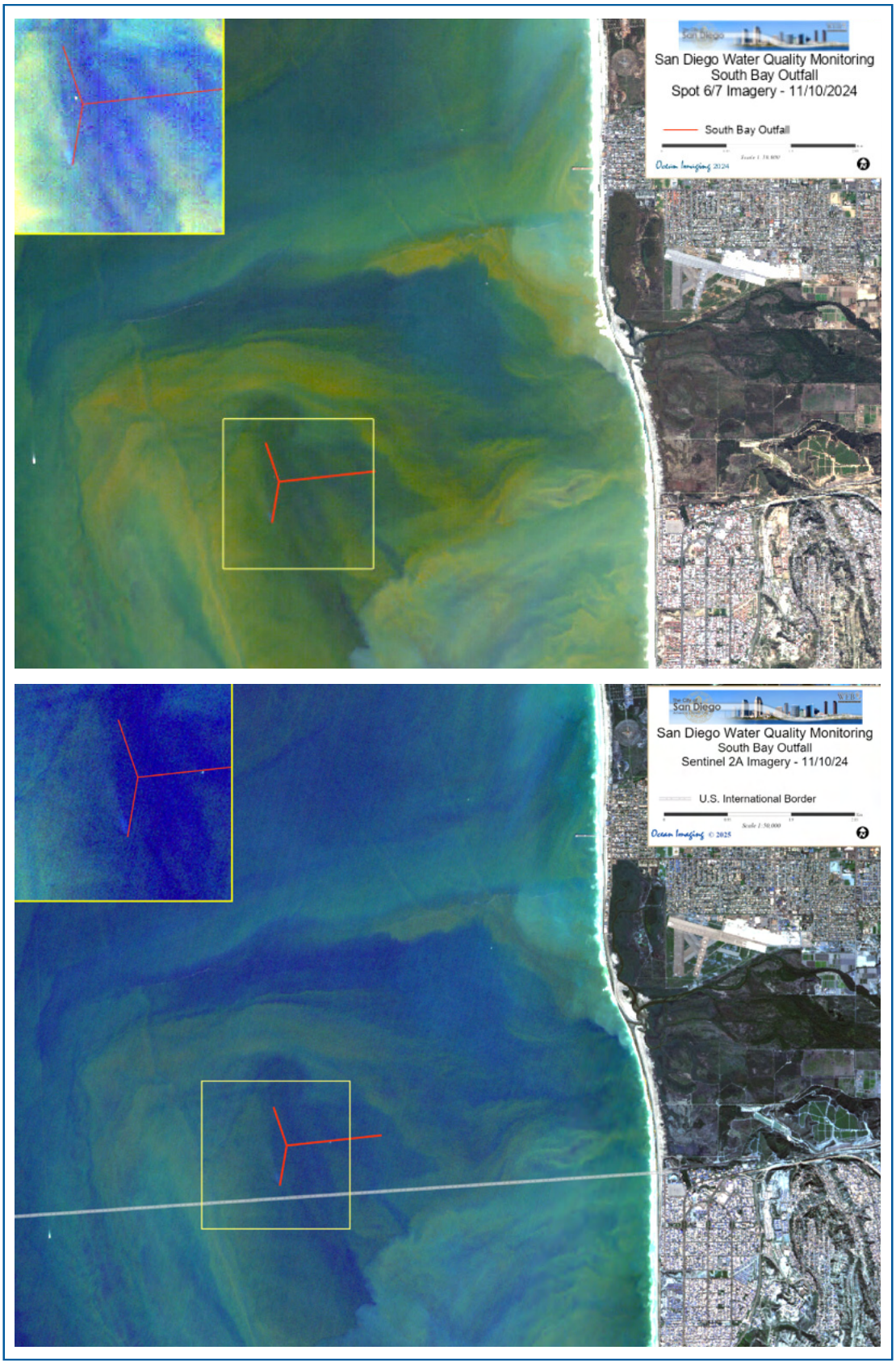

San Diego Water Quality Monitoring
South Bay Outfall
Sentinel 2B Imagery - 2/2/24
U.S. International Border
San Diego Water Quality Monitoring
South Bay Outfall
Sentinel 2A Imagery - 02/04/24
U.S. International Border

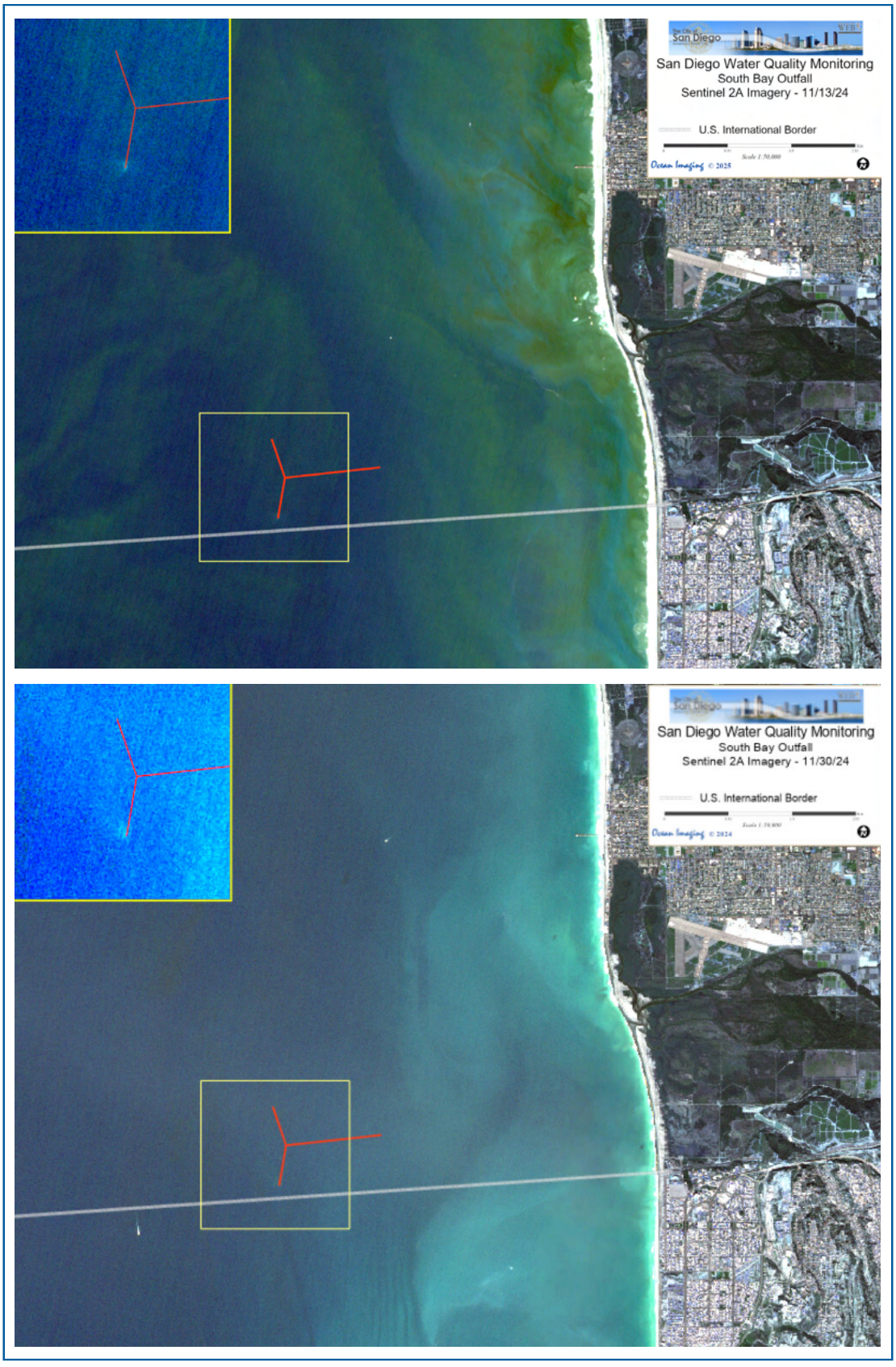

San Diego Water Quality Monitoring
South Bay Outfall
Spot 6/7 Imagery -02/12/2024
South Bay Outfall
San Diego Water Quality Monitoring
South Bay Outfall
Sentinel 2B Imagery - 2/12/24
U.S. International Border

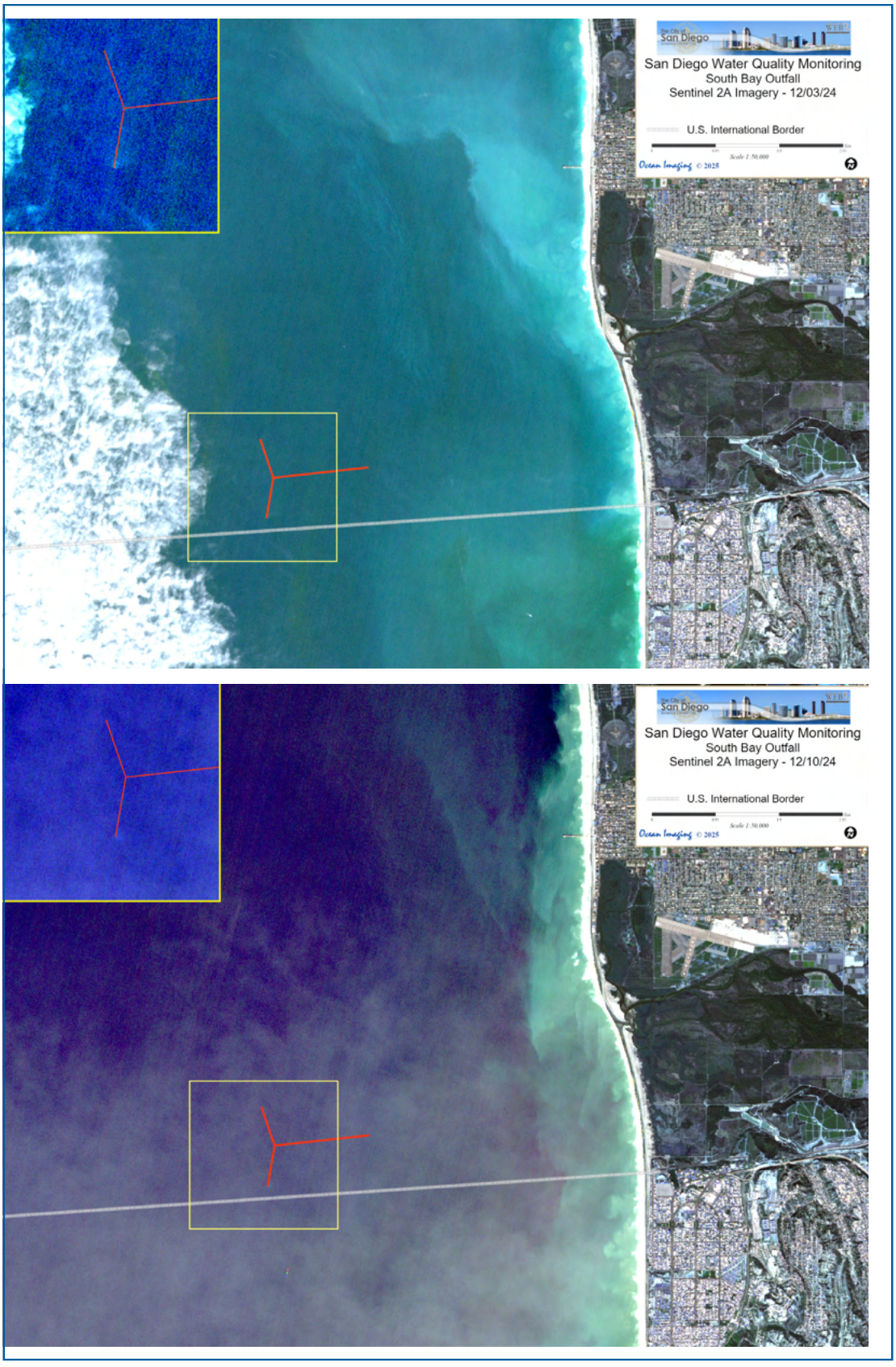

San Diego
San Diego Water Quality Monitoring
South Bay Outfall
Sentinel 2B Imagery - 2/22/24
U.S. International Border
Ocean Imaging © 2025
San Diego
San Diego Water Quality Monitoring
South Bay Outfall
Sentinel 2A Imagery - 3/25/24
U.S. International Border
Ocean Imaging © 2025

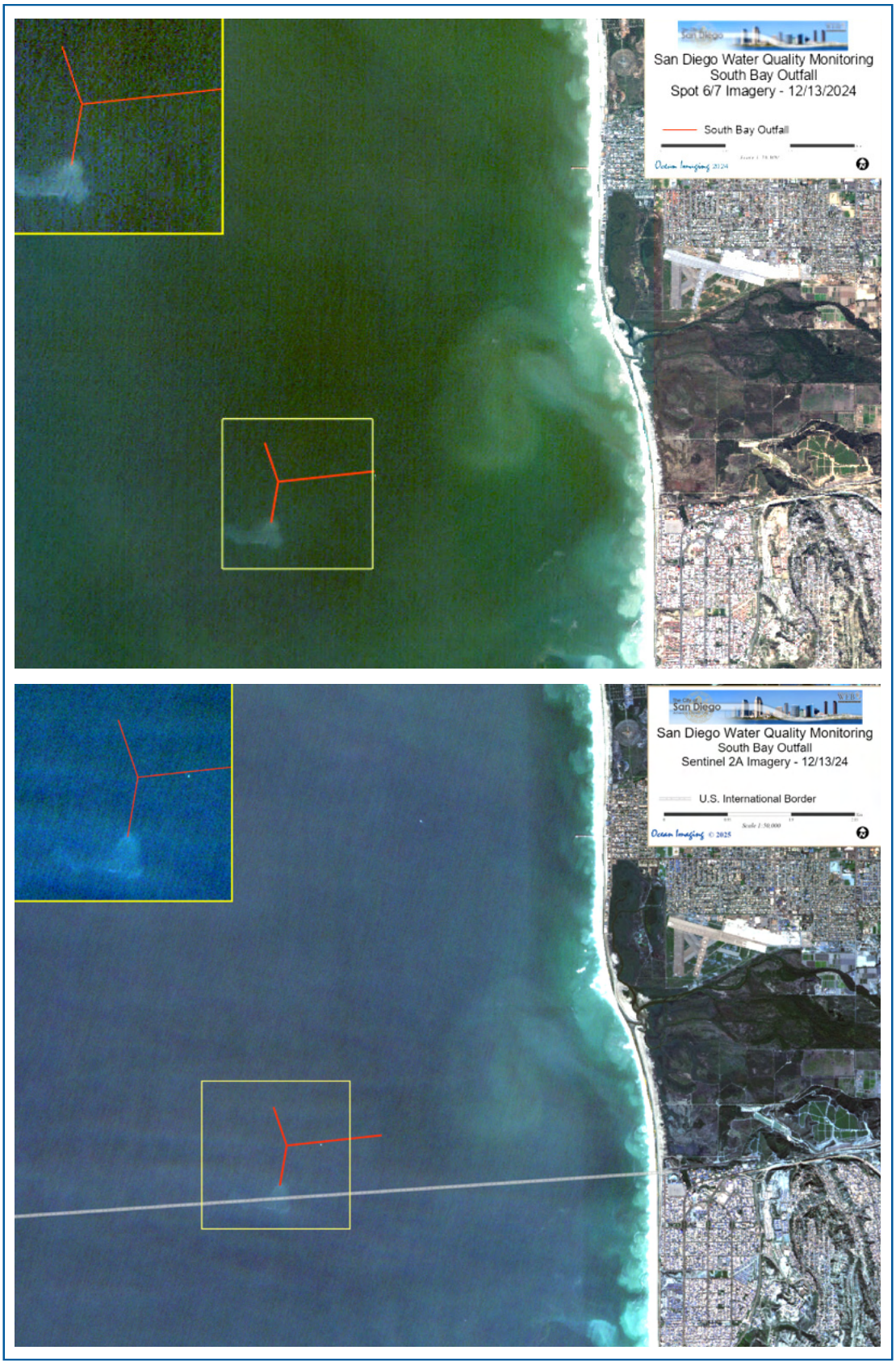

San Diego Water Quality Monitoring
South Bay Outfall
Spot 6/7 Imagery - 04/01/2024
South Bay Outfall
San Diego Water Quality Monitoring
South Bay Outfall
Landsat 8 Imagery - 04/02/2024
South Bay Outfall
U.S. International Border


San Diego Water Quality Monitoring
South Bay Outfall
Sentinel 2B Imagery - 04/02/24
U.S. International Border
San Diego Water Quality Monitoring
South Bay Outfall
Sentinel 2B Imagery - 11/08/24
U.S. International Border


San Diego Water Quality Monitoring
South Bay Outfall
Spot 6/7 Imagery - 11/10/2024
South Bay Outfall
San Diego Water Quality Monitoring
South Bay Outfall
Sentinel 2A Imagery - 11/10/24
U.S. International Border

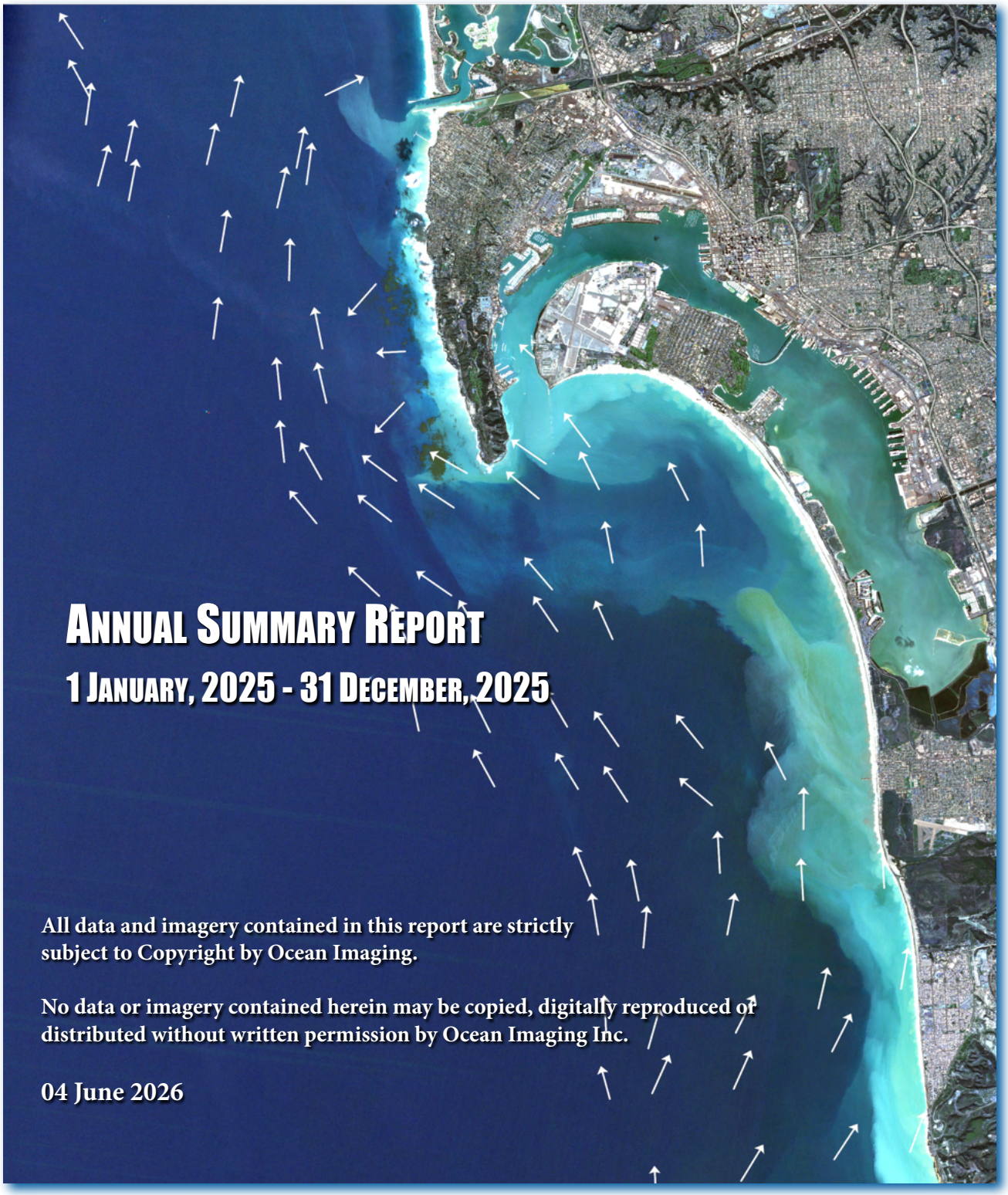

San Diego Water Quality Monitoring
South Bay Outfall
Sentinel 2A Imagery - 11/13/24
U.S. International Border
San Diego Water Quality Monitoring
South Bay Outfall
Sentinel 2A Imagery - 11/30/24
U.S. International Border


San Diego
San Diego Water Quality Monitoring
South Bay Outfall
Sentinel 2A Imagery - 12/03/24
U.S. International Border
Ocean Imaging © 2025
San Diego
San Diego Water Quality Monitoring
South Bay Outfall
Sentinel 2A Imagery - 12/10/24
U.S. International Border
Ocean Imaging © 2025


San Diego Water Quality Monitoring
South Bay Outfall
Spot 6/7 Imagery - 12/13/2024
South Bay Outfall
San Diego Water Quality Monitoring
South Bay Outfall
Sentinel 2A Imagery - 12/13/24
U.S. International Border

Satellite Coastal Water Quality Monitoring in the San Diego / Tijuana Region

By Mark Hess



Annual Summary Report

1 January, 2025 - 31 December, 2025

All data and imagery contained in this report are strictly subject to Copyright by Ocean Imaging.

No data or imagery contained herein may be copied, digitally reproduced of distributed without written permission by Ocean Imaging Inc.

04 June 2026

Ocean Imaging

13976 West Bowles Avenue, Suite 100, Littleton CO 80127 Phone: 303-948-5272 www.oceani.com

Table of Contents

1. INTRODUCTION AND PROJECT HISTORY 1

2. METHODS AND TECHNOLOGY OVERVIEW 2

2.1 Imaging in the UV-Visible-Near-Infrared Spectrum 2
2.2 Imaging in the Thermal Infrared Spectrum 2
2.3 Satellites and Sensors Utilized 2
2.4 Data Dissemination and Analysis 8

3. HIGHLIGHTS OF 2025 MONITORING 8

3.1 Atmospheric and Ocean Conditions 8
3.2 The South Bay Ocean Outfall Region 24
3.3 The Point Loma Outfall Region 30
3.4 Kelp Variability 32

4. PRESENT AND FUTURE ENHANCEMENTS OF THE PROJECT 36

5. REFERENCES 37

APPENDIX A – HIGH-RESOLUTION SATELLITE IMAGERY SHOWING SBOO-RELATED WASTEWATER PLUME 39

 © Ocean Imaging Inc. 2026

1. INTRODUCTION AND PROJECT HISTORY

In the 1990s, Ocean Imaging Corporation (OI) received multiple research grants from NASA's Commercial Remote Sensing Program for the development and commercialization of remote sensing applications in the coastal zone. As part of these projects, OI developed methods to utilize several types of remotely sensed data for the detection and monitoring of stormwater runoff and wastewater discharges from offshore outfalls. The methodology was initially demonstrated in collaboration with the Orange County Sanitation District in California (Svejkovsky and Haydock 1998). The NASA-supported research led to a proof-of-concept demonstration project in the San Diego, California region co-funded by the EPA in 2000. Those results led, in 2002, to adding an operational remote sensing-based monitoring component to the San Diego region's established water quality monitoring program. The project continues as a joint effort between the Ocean Monitoring Program of the City of San Diego's Public Utilities Department (SDPUD) and the International Boundary and Water Commission (USIBWC).

The first phase of the project was a historical study utilizing several types of satellite data acquired between the early 1980s and 2002. The study established the prevailing near-surface current patterns in the region under various oceanic and atmospheric conditions. The current directions were deduced from patterns of turbidity, ocean temperature, and surfactant slicks. In some cases, near-surface current velocity could be computed by tracking recognizable color or thermal features in time-sequential images. The historical study thus established baseline data for the region's current patterns, their persistence, their frequency, and the historical locations, sizes, and dispersion trajectories of various land and offshore discharge sources from Publicly Owned Treatment Works (POTW) (e.g., the offshore outfalls, Tijuana River, Punta Bandera Treatment Plant discharge in Mexico, etc.).

The prime objectives of the project have expanded since its inception. Initially, emphasis was on utilizing the image data to discern and monitor surface and near-surface signatures from the South Bay Ocean Outfall (SBOO) and Point Loma Ocean Outfall (PLOO), separate them from other nearshore point and non-point runoff features, and monitor their locations, extents, and potential impact on the shoreline. Prior to this project, the spatial extents of the plumes could only be estimated from a relatively sparse spatial grid of field samples, which made it difficult to separate, for example, the SBOO near-surface plume from the Tijuana River runoff plume. This ambiguity made it difficult, in turn, to objectively evaluate the potential contribution, if any, of the SBOO plume to beach contamination along the nearby shoreline. The satellite and aerial imagery helped directly establish the dispersal trajectories of the SBOO effluent during months when it reached the near-surface layer and support the conclusion that it is unlikely to reach the surf zone under observed conditions.

In October 2002, the operational monitoring phase of the project was initiated using a variety of satellite- and model-derived datasets described below. Over the past five to ten years, the project's objectives have broadened from focusing primarily on the outfalls to also providing larger-scale, regional observations of the physical and biological patterns and processes affecting the San Diego County and Tijuana River discharge regions. It is this broader-view perspective that led to the creation of supplementary image products from additional sensors and sources for the SDPUD. This report summarizes observations made during the period 1 January, 2025 through 31 December, 2025.

2. METHODS AND TECHNOLOGY OVERVIEW

OI uses several remote sensing technologies to monitor San Diego's offshore outfalls and shoreline water quality. Their primary function is to reveal light reflectance, heat emission, and radar backscatter patterns that are characteristic of the different discharges, water masses, plankton blooms, and suspended sediment loads. Most often this is due to specific substances contained in the effluent but absent in the surrounding water.

2.1 Imaging in the UV-Visible-Near-Infrared Spectrum

This is the most common technique used with satellite and aerial images. Wavelengths (colors) within the range of the human eye are most often used but ultraviolet (UV) wavelengths are useful for detecting fluorescence from petroleum compounds (oil, diesel, etc.) and near-infrared (near-IR) wavelengths can be useful for correcting atmospheric interference from aerosols (e.g., smog and smoke). Near-IR wavelengths are also highly reflected from kelp seaweeds, so such data are particularly useful for delineating the region's kelp beds and monitoring their extents through time.

The best detection capabilities are attained when several images in different wavelengths are acquired simultaneously. These "multispectral" data can be digitally processed to enhance features not readily visible in simple color photographs. For example, two such images can be ratioed, thus emphasizing the water features' differences in reflection of the two specific wavelengths. A multi-wavelength image set can also be analyzed with multispectral classification algorithms which separate distinctive features or effluents based on the correlation relationships between the different color signals.

The depth to which the color sensors can penetrate depends on which wavelengths they see, their sensitivity and the general water clarity. In the San Diego region, green wavelengths tend to reach the deepest and, as elsewhere, UV and near-IR wavelengths penetrate the least. In general, the satellite sensor data used for this program reveal reflective features in the upper one to fifteen meters of the ocean.

2.2 Imaging in the Thermal Infrared Spectrum

Some satellite and aerial sensors image heat emanating from the ground and the ocean. They thus reveal patterns and features due to their differences in temperature. Since thermal infrared (TIR) wavelengths are strongly absorbed by water, the images reveal temperature patterns only on the water's surface. Such images can help detect runoff plumes when their temperatures differ from the surrounding ocean water. Runoff from shoreline sources tends to be warmer than ocean water, although the reverse can be true during the winter. Plumes from offshore outfalls can sometimes also be detected with thermal imaging. Since the effluent contains mostly freshwater, it is less dense than the surrounding salt water and tends to rise toward the surface. How far it rises depends on outfall depth, ocean currents, and stratification conditions. If it makes it all the way to the surface, it is usually cooler than the surrounding sun-warmed surface water. A plume signature detectable in multispectral color imagery but not detectable in simultaneously collected TIR data indicates the rising plume has not reached the actual ocean surface and remains submerged.

2.3 Satellites and Sensors Utilized

Until 2010, the project relied heavily on acquisition of multispectral color imagery with OI's DMSC-MKII aerial sensor and TIR imagery from a Jenoptik thermal imager integrated into the system. These aerial image sets were most often collected at 2m resolution. The flights were done on a semi-regular schedule ranging from one to two times per month during the summer to once or more per week during the rainy season. The flights were also coordinated with the City of San

Diego's regular offshore field sampling schedule so that the aerial data were collected on the same day (usually within two to three hours) of the field data collection. Additional flights were performed on an on-call basis immediately after major storms or other events such as sewage spills. In late 2010, OI negotiated a special data collection arrangement with Germany's RapidEye Corporation, and this project began utilizing their multispectral imagery in lieu of most of the aerial Digital Multispectral Camera (DMSC) image acquisitions. The use of satellite as opposed to aerial data also enables a more frequent and regionally contiguous monitoring of events affecting the target areas. In late 2019 the RapidEye satellite constellation was decommissioned by the current operator Planet Labs. Subsequently, OI secured the regular acquisition of SPOT 6 and SPOT 7 satellite scenes covering the same geographical area beginning in 2020. Table 1 lists the properties of the remote sensing image sources routinely used during the project during 2025.

Beginning in 2017, OI began processing and posting imagery from the Sentinel-2 satellites. Sentinel-2A, 2B, and 2C are satellites operated by the European Space Agency (ESA) and are the spaceborne platforms for the Multispectral Instrument (MSI). The Sentinel-2A, 2B and 2C MSIs sample 13 spectral bands: four bands at 10 m, six bands at 20 m and three bands at 60-meter spatial resolution. The green band focusing in the 560 nm wavelength is ideal for detecting turbidity plumes from the outfalls both at the surface and at depths down to 15 m depending on ocean conditions. The revisit time of each Sentinel-2 satellite is approximately ten days. Sentinel-2C was launched into orbit by the ESA in late 2024 and provided the first set of data from the MSI sensor in early 2025. Presently with the three Sentinel satellites in orbit the revisit time over the San Diego region is approximately one to two days. This represents a significant improvement in observational frequency relative to previous years. On average the Sentinel-2A, 2B, and 2C data processed to highlight anomalous turbidity signals emanating from the PLOO, SBOO, as well as the discharge from the Tijuana River (TJR) and San Diego River (SDR) are posted to the OI web portal within 24–36 hours of satellite data acquisition. In some cases, if the data are available to OI earlier, the image products are delivered as quickly as 12 hours post-acquisition. During 2025 the Sentinel-2 suite of satellites provided the most temporally comprehensive set of high-resolution satellite data. In total, 114 high-resolution, multispectral satellite images showing the offshore San Diego County region were acquired, processed, and delivered in 2025. This equates to an 8.6% increase in satellite data used to document the area when compared to 2024 – likely due to the addition of Sentinel-2C data and fewer instances of total cloud cover over the San Diego region. Of the 114 total image sets, 87 were from Sentinel-2A/2B/2C data making up 76% of the high-resolution satellite data processed and posted as part of the project.

In October 2018, OI began using data from Sentinel-3A. Shortly thereafter, in December, 2018 imagery from Sentinel-3B was incorporated into the mix of observation platforms. Like Sentinel-2, Sentinel-3A and Sentinel-3B are Earth observation satellites developed by the ESA for the Copernicus Program. Sentinel-3A was launched on February 16, 2016, and Sentinel-3B followed on April 25, 2018. The 3A and 3B satellites are identical and deliver products in near-real-time. The satellites include four different remote sensing instruments. The Ocean and Land Colour Instrument (OLCI) covers 21 spectral bands (400–1020 nm) with a swath width of 1270 km and a spatial resolution of 300 m. The Sea and Land Surface Temperature Instrument covers 9 spectral bands (550–12 000 nm), using a dual-view scan with swath widths of 1420 km (nadir) and 750 km (backwards), at a spatial resolution of 500 m for visible and near-IR, and 1 km for thermal infrared channels. The Sentinel-3 mission's main objectives are to measure sea surface topography along with the measurement of ocean/land surface temperature and ocean/land surface color. One of the satellites' main secondary missions is to monitor sea-water quality and marine pollution. The instrument on these satellites designed for these purposes is the OLCI. Ocean Imaging creates

Table 1. Satellite sensors utilized in the project and their characteristics.

Sensor	Utilization Period	Resolution (m)	Utilized Wavelength Range
MODIS	2003 - Present	250/500/1000	Band 1 (250 m): .620 – .670 µm Band 2 (250 m): .841 – .876 µm Band 3 (500 m): .459 – .479 µm Band 4 (500 m): .545 – .565 µm
Landsat 8 OLI, TIRS	2013 - Present	30 (visible - Near-IR) 100 (Thermal-IR)	Band 2: .452 - .512 µm Band 3: .533 - .590 µm Band 4: .636 - .673 µm Band 5: .851 - .879 µm Band 10: 10.60 - 11.19 µm Band 11: 11.50 - 12.51 µm
Sentinel-2A/2B/2C	2017 - Present	10 (visible - Near-IR) 60 (Vegetation Red Edge) 60 (UV, SWIR)	Band 1: .443 µm Band 2: .490 µm Band 3: .560 µm Band 4: .665 µm Band 5: .705 µm Band 6: .740 µm Band 7: .783 µm Band 8: .842 µm Band 8A: .865 µm
Sentinel-3A/3B	2018 - Present	300 (all utilized bands)	Band Oa2: .412.5 µm Band Oa3: .442.5 µm Band Oa4: .490 µm Band Oa5: .510 µm Band Oa6: .560 µm Band Oa7: .620 µm Band Oa8: .665 µm Band Oa10: .68125 µm Band Oa11: .7875 µm Band Oa17: .865 µm
VIIRS	2019 - Present	750 (all utilized bands)	Band M1: 0.402 - 0.422 µm Band M2: 0.436 - 0.454 µm Band M3: 0.478 - 0.488 µm Band M4: 0.545 - 0.565 µm Band M5: 0.662 - 0.682 µm Band M6: 0.739 - 0.754 µm Band M7: 0.846 - 0.885 µm Band M8: 1.23 - 1.25 µm Band M9: 1.371 - 1.386 µm Band M10: 1.58 - 1.64 µm Band M11: 2.23 - 2.28 µm Band M12: 3.61 - 3.79 µm Band M13: 3.97 - 4.13 µm Band M14: 8.4 - 8.7 µm Band M15: 10.26 - 11.26 µm Band M16: 11.54 - 12.49 µm
SPOT 6	2019 - Present	6	Band 1: .450 - .745 µm Band 2: .450 - .525 µm Band 3: .530 - .590 µm Band 4: .625 - .695 µm Band 5: .760 - .890 µm
Sentinel-1A/1C SAR	2021 - Present	5 x 20	C-band operating at a center frequency of 5.405 GHz
Landsat 9 OLI-2, TIRS-2	Late 2021 - Present	30 (visible - Near-IR) 100 (Thermal-IR)	Band 2: .452 - .512 µm Band 3: .533 - .590 µm Band 4: .636 - .673 µm Band 5: .851 - .879 µm Band 10: 10.60 - 11.19 µm Band 11: 11.50 - 12.51 µm

daily products dependent on cloud cover for the entire San Diego/Tijuana region using the OLCI instrument. Between the 3A and 3B satellites this results in better than daily coverage with 3A and 3B data occasionally both being available on the same day. True color and near-IR products are posted every two months. Sentinel-3-derived chlorophyll products offering a 300-meter spatial resolution, were incorporated into the data mix in late 2025.

As stated above, the RapidEye satellites were decommissioned in late 2019 and replaced by data from the SPOT 6 and SPOT 7 satellites in January of 2020. The two SPOT satellites/sensors are identical in design and function. They both image in spectral bands similar to the RapidEye satellites at a ground sampling distance of six meters for the multispectral data (see Table 1). The dynamic range of these sensors is 12-bits per pixel. OI uses the blue, green, red, and near-IR bands from these sensors. Empirically we have found that the SPOT data have a high signal to noise ratio and therefore produce a high-quality product for detecting wastewater surface manifestations and delineating the river runoff plumes. In March of 2023, the SPOT 7 satellite stopped functioning; however, we continue to receive data from SPOT 6 and acquire two to three clear images per month from this sensor during the fall to spring period. Figure 1 shows a set of images acquired on 03/15/25 from SPOT 6 and Sentinel-2A highlighting the ability to obtain high-resolution imagery from multiple satellites on the same day. The two images from 03/15/25 were captured within twenty minutes of each other. Note the turbid effluent from the SBOO seen at the surface of the ocean in both scenes as well as heavy turbidity along the shoreline. Two-kilometer-spaced High Frequency Radar-derived (HF Radar) ocean current vectors from the same day acquired within minutes of the satellite overpasses are overlaid on the imagery to illustrate the surface flow patterns in the region. Note that the turbid water north of the U.S.-Mexico border appears to be moving north and northwest, yet the water near and south of the border (around the SBOO underwater wye) is moving south and west, pushing the SBOO effluent with it. It is also evident that the SBOO effluent plume at the ocean's surface enlarged slightly over the twenty-minute period between the two datasets. More discussion on the SBOO and visible effluent follows in subsequent sections.

The use of Advanced Very High Resolution Radiometer (AVHRR) satellite data described in prior reports was discontinued in 2025 due to phasing out of this sensor suite by NOAA in lieu of the newer Visible Infrared Imaging Radiometer Suite (VIIRS) satellites now in orbit. As detailed in Table 1, to date, this work utilizes 1000 m resolution chlorophyll and sea surface temperature (SST) Moderate Resolution Imaging Spectroradiometer (MODIS)-derived image data (available multiple times per day), 750 m VIIRS chlorophyll and SST data (available multiple times per day), 300 m resolution Sentinel-3A and 3B color and thermal image data (available daily), 30 m & 60 m Landsat 8 OLI/TIRS and Landsat 9 OLI-2/TIRS-2 color and thermal image data (each available approximately every 16 days), 10 m resolution Sentinel-2A, 2B, and 2C multispectral imagery (available 2–4 times per week), and 6 m resolution Satellite Pour l'Observation de la Terre (SPOT) 6 (available approximately every 5–7 days). Sentinel-2A was slated to be phased out of the Copernicus program in early 2025, however we continue to receive 2A data into early 2026 and so there has not been a decrease in Sentinel-2 information.

In addition, Synthetic Aperture Radar (SAR) data from the Sentinel-1A satellite (available every 3–6 days at a spatial resolution of 5m x 20 m) were added to the suite of remote sensing products in late 2021. Sentinel-1C data became available in late 2025 and was added to the suite of imagery delivered as part of this project. SAR can detect surfactant films associated with natural processes (Svejkovsky and Shandley 2001) and plumes containing anthropogenic substances (Svejkovsky and Jones 2001; Gierach et al. 2017) when optical sensors might be limited by cloud cover or heavy atmospheric haze. The primary purpose of these satellites for this project is to provide an additional

observational perspective at the TJR discharge plume to assess its offshore extent and direction of flow. The river and coastal runoff often contain natural and anthropogenic surfactants that dampen the SAR signal and therefore make it detectable in the data. Phytoplankton blooms also release biological surfactants that result in low backscatter observed in the SAR data (Svejkovsky and Shandley 2001). In 2025, 124 SAR images were acquired and processed for the San Diego region providing an additional

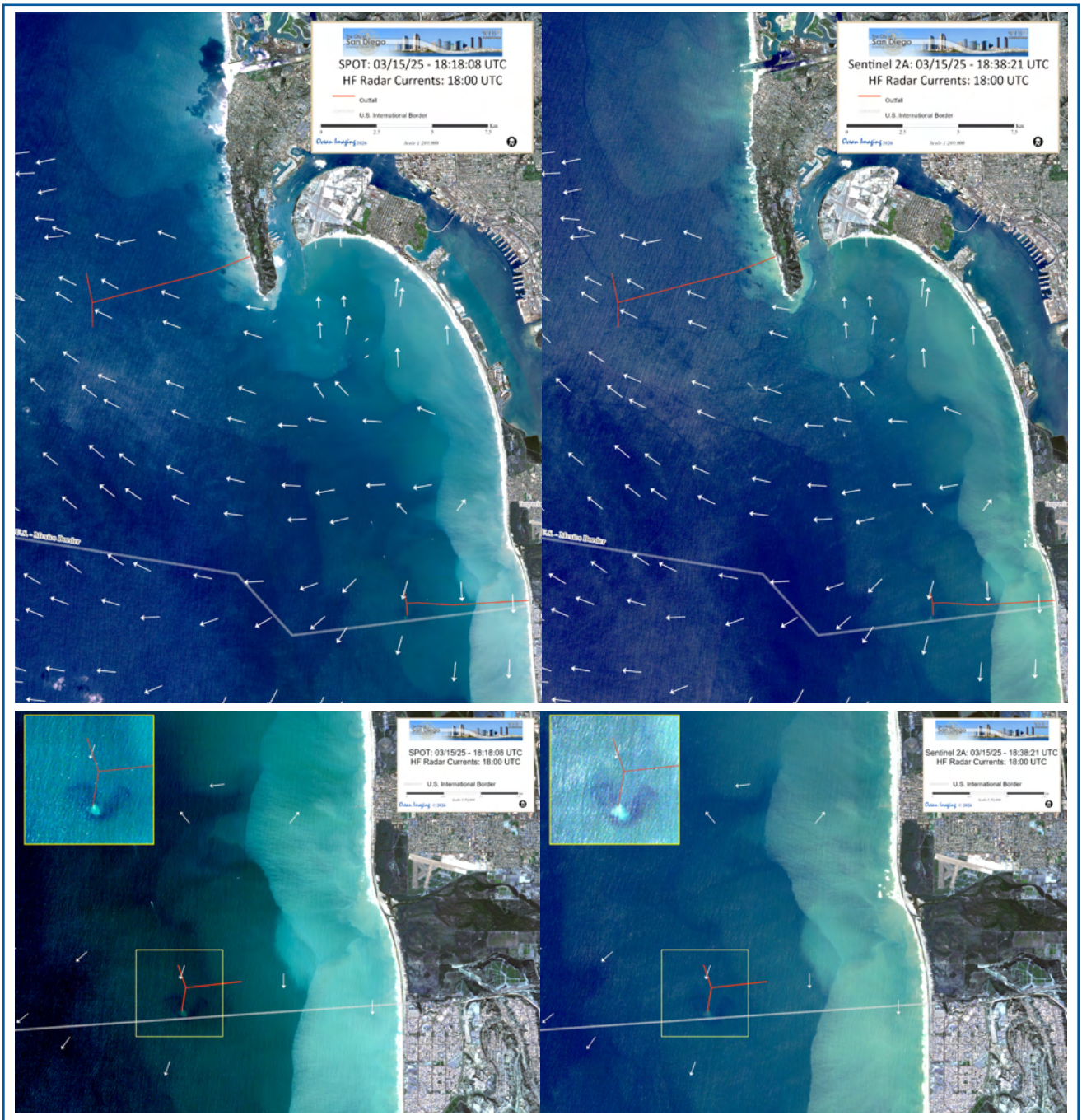


Figure 1. SPOT 6 (left) and Sentinel-2A (right) imagery acquired on 03/15/25 within twenty minutes of each other (18:18 and 18:38 UTC respectively). HF Radar-derived currents from 18:00 UTC on the same day are overlaid to show the local surface flow and illustrate the divergence of the water movement roughly at the latitude of the TJR mouth. The lower panels show the effluent surfacing from the SBOO and directed south (lighter area within the clearer patch of water).

source of information even during cloudy conditions. Figure 2 shows a Sentinel-2 image captured on 02/23/25 (left) along with a Sentinel-1A SAR image (right) captured two days later when coastal cloud cover prohibited the acquisition of optical satellite data. On 02/23/25 the ocean currents were moving the discolored, potentially impactful TJR water south along the coast. The dampened SAR signal (dark area) in the Sentinel-1A image from 02/25/25 shows that the TJR water likely containing anthropogenic surfactants (often indicative of polluted water) was constrained to the south of the river mouth and did not move north into the San Diego region. This was identifiable even during the cloudy conditions when the optical satellites could not show the core of the TJR plume and its direction. Recent attention on the severity of the TJR polluted discharge (Little 2024) and Harmful Algal Blooms (HAB) make monitoring and documenting the coastal and offshore waters with multiple sensor types increasingly important.

In 2012, OI added additional broad-scale products to the datasets available to the SDPUD and project partners. These include two types of ocean current data: High Frequency Radar-derived surface currents (HF Radar) and Hybrid Coordinate Ocean Model (HYCOM) model-derived surface currents (http://hycom.org). The raw data for the HF Radar currents are now retrieved from the NOAA National Data Buoy Center HF Radar National Server (https://hfradar.ndbc.noaa.gov/) daily and reformatted into ESRI-compatible shapefiles. The products are generated at 1 km and 6 km spatial resolutions. In 2016 these products were delivered in a Web Map Service (WMS) Representational State Transfer (REST) service format compatible with the City's

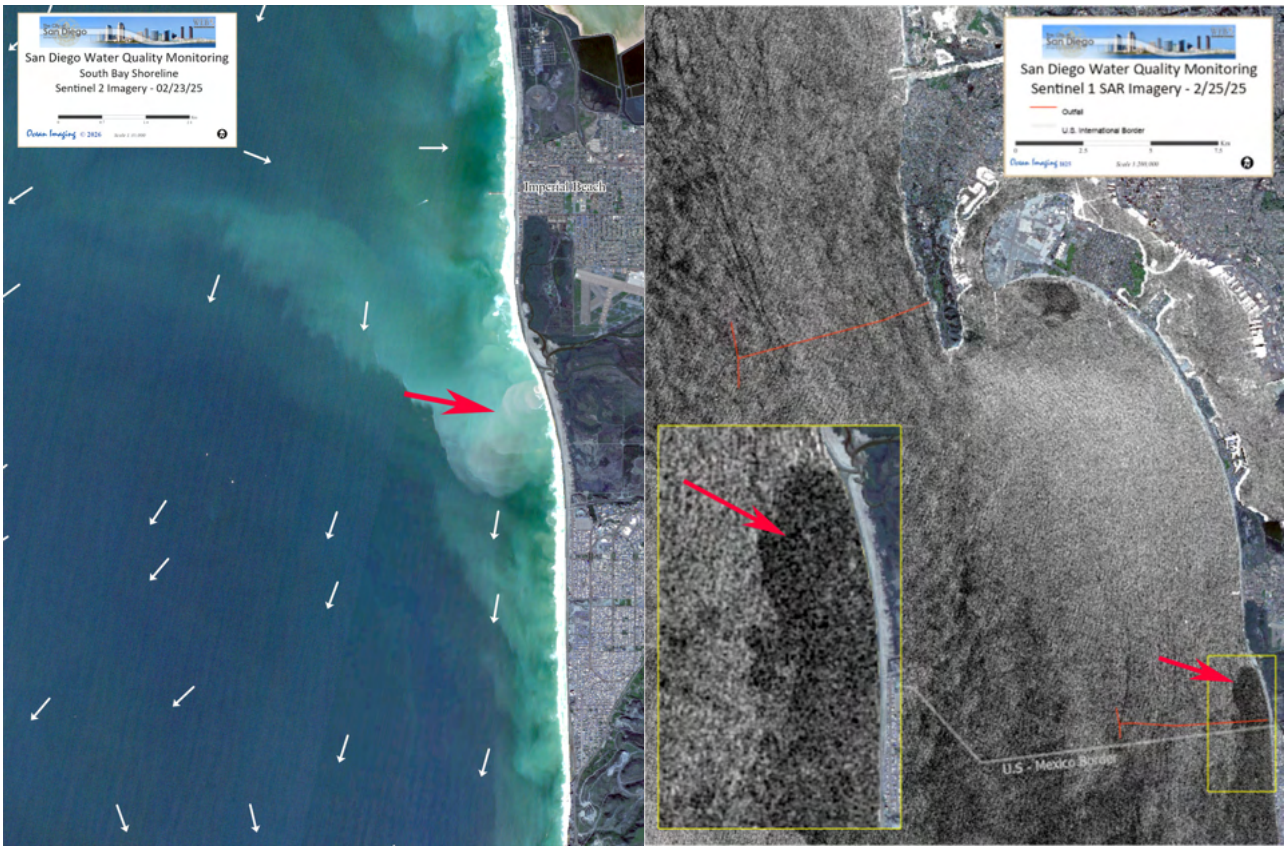


Figure 2. Sentinel-2 image (left) acquired on 02/23/25 showing highly turbid, discolored, and likely high-surfactant water being discharged from the TJR. HF Radar currents overlaid show the prevailing currents in the area at the time of the image. A Sentinel-1A SAR image acquired on 02/25/25 (right) showing a reduced SAR reflectance signal indicating high-surfactant water west and south of the TJR mouth.

now retired BioMap server. They are presently being generated and prepped for incorporation into a next-generation WMS dashboard-style data portal which became operational in 2025. The ocean currents will soon be added to the dashboard as the platform is refined and improved. The existing high-resolution (6–30 m) observation region extends from La Jolla southward to Rosarito Beach, Mexico and out approximately 50 miles. The coarser-scale products (250–1000 m) such as chlorophyll, SST and ocean currents encompass the entire Southern California Bight (SCB).

2.4 Data Dissemination and Analysis

The satellite data are made available to the SDPUD and other project constituents through a dedicated, password-protected website. Although it is possible to process most of the data in near real-time, earlier in the project it was decided that the emphasis of this program is not on providing real-time monitoring support and the extra costs associated with the rapid data turnaround are not warranted. Most satellite data are therefore processed and posted within 1–2 days after acquisition. As noted above, however, OI has in several cases made imagery available to the SDPUD in near-real-time (within 12–24 hours) via email when observations appeared to be highly significant to ocean dynamics surrounding the outfalls or other sudden/anomalous event. The website was updated in 2022 to improve its ease of use and presentation of available imagery. Future improvements are planned for the site to increase interactivity and ease of data access and visualization.

3. HIGHLIGHTS OF 2025 MONITORING

3.1 Atmospheric and Ocean Conditions

Coastal and oceanic water quality can often be correlated to rainfall events. In 2025, the San Diego International Airport station (SDIA) measured 9.84 inches of total annual rainfall and 9.03 inches at the Tijuana River International Boundary station (TJRIB), both higher than 2012–2024 averages of 8.69 and 7.91 inches respectively (see Table 2). While the monthly rainfall followed normal seasonal patterns for the first four months of the year with the winter and spring months for the most part matching the expected rainy season and the summer months being mostly dry, the months of January and February exhibited relatively low rainfall compared to the previous twelve years – especially when contrasted to 2024. March and November were the rainiest months (2.93 and 3.11 inches measured at the SDIA station respectively). The well above average precipitation in November (2.3 and 2.0 inches above the 2012–2024 averages for the SDIA and TJRIB stations) was evident in the satellite data which exhibited periods of highly turbid water along the coast and 16 observations of significant TJR discharge between mid-November and the end of the year.

Figure 3 shows cumulative daily precipitation in the Tijuana Estuary along with the average daily river discharge at the TJRIB station. The tables below the plot give the date for which there was measurable precipitation at that station. As noted in previous reports, and is evident in Table 2, the monthly and annual precipitation amounts can differ at times between the SDIA and TJR reporting stations. The primary period of consistent and/or heavy precipitation occurred during the months of February, March, November, and December with relatively little rainfall recorded between May and August.

We have defined a significant TJR discharge event as when the spectrally distinct “fresh core” of the river discharge plume as defined by Svejkovsky et al. 2010, is clearly visible in the imagery. There were 64 days

during which the TJR discharge plume was identified as significant in the satellite imagery. Thirty-four of these days were during the four rainy months identified above. Hydrologic response in the Tijuana River watershed is strongly event-driven, with the majority of runoff and sediment transport occurring during a relatively small number of larger storm events (Biggs et al. 2022). Watershed-scale modeling of the binational Tijuana River basin indicates that runoff generation increases nonlinearly with event precipitation, with analyzed storm totals ranging from 7 to 83 millimeters (mm) (0.28 to 3.27 inches), and substantially higher runoff coefficients associated with larger precipitation events (Gudino-Elizondo et al. 2019). It is also evident in Figure 3 that the TJR discharge spikes as a result of rainfall as low as 0.1 inches on a single day. We used ≥ 0.25 inches per day as a loose cutoff to identify a significant rainfall

Table 2. San Diego and Tijuana Estuary precipitation totals 2012-2025

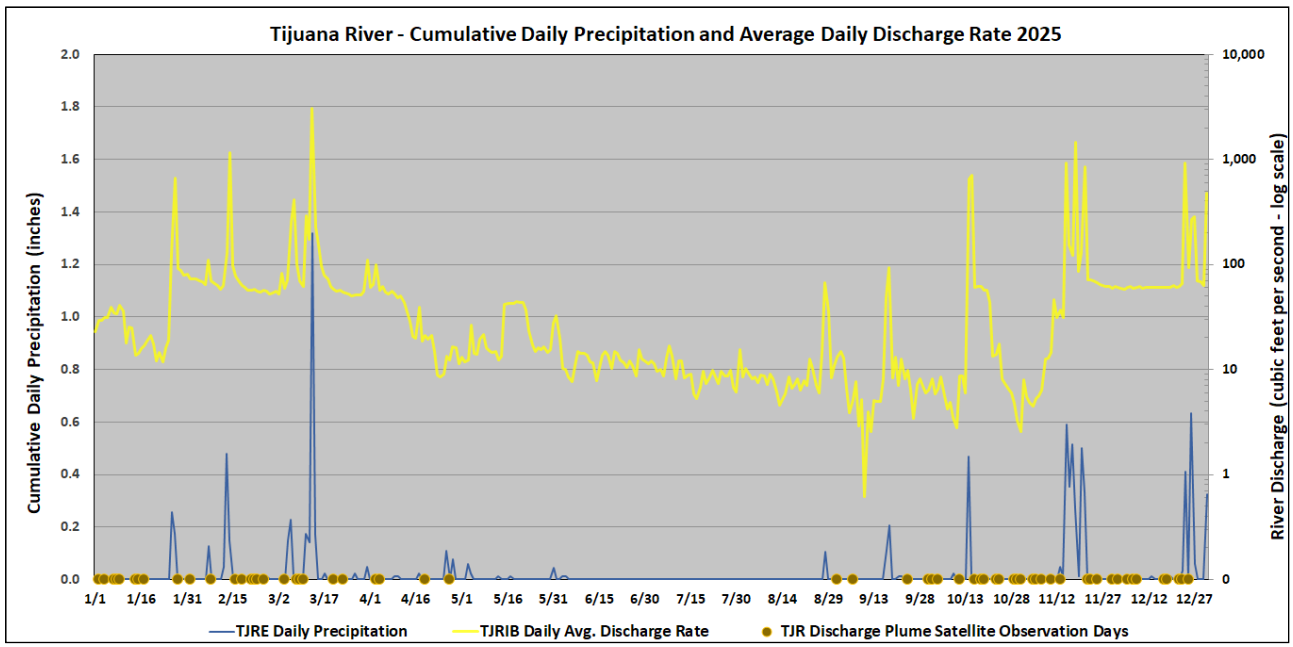
San Diego International Airport Cumulative Monthly Precipitation in Inches

	2012	2013	2014	2015	2016	2017	2018	2019	2020	2021	2022	2023	2024	2025
January	0.40	0.70	0.01	0.42	3.21	2.99	1.77	2.42	0.48	1.80	0.16	5.14	3.67	0.24
February	1.19	0.63	1.00	0.28	0.05	1.58	0.35	4.04	0.38	0.10	0.70	1.78	4.61	0.95
March	0.97	1.22	1.28	0.93	0.76	0.08	0.65	1.23	2.15	1.48	1.61	3.97	2.58	2.93
April	0.88	0.01	0.54	0.02	0.55	0.01	0.02	0.10	3.68	0.07	0.02	0.12	0.19	0.23
May	0.02	0.26	--	2.39	0.44	0.87	0.09	0.86	0.02	0.07	0.02	0.09	0.08	0.17
June	--	--	--	0.04	--	0.02	--	0.01	0.14	0.01	--	0.03	0.01	0.04
July	--	0.05	--	1.71	--	--	--	--	--	--	--	--	0.01	--
August	--	--	0.08	0.01	--	--	0.02	--	--	0.23	--	1.84	0.02	0.05
September	--	--	--	1.24	0.32	0.06	--	0.11	--	0.50	0.65	0.05	0.02	0.47
October	0.70	0.25	--	0.43	0.07	--	0.57	--	0.12	1.01	0.09	--	0.01	0.42
November	0.28	1.48	0.37	1.54	0.61	0.02	0.69	2.72	0.14	--	1.07	0.61	0.14	3.11
December	2.19	0.46	4.50	0.88	4.22	--	0.83	4.03	0.60	2.58	1.55	0.79	0.03	1.23
Annual Total	6.63	5.06	7.78	9.89	10.23	5.63	4.99	15.52	7.71	7.85	5.87	14.42	11.37	9.84

Tijuana Estuary Cumulative Monthly Precipitation in Inches

	2012	2013	2014	2015	2016	2017	2018	2019	2020	2021	2022	2023	2024	2025
January	0.70	0.05	0.08	0.32	2.40	3.61	0.82	1.80	0.61	2.21	0.17	3.47	2.38	0.44
February	0.86	--	1.35	0.13	0.02	4.06	0.47	3.62	0.51	0.06	0.58	2.06	3.73	0.82
March	1.21	1.43	0.55	1.01	1.28	0.04	1.17	1.33	2.59	1.12	1.64	3.32	2.22	2.29
April	0.82	0.11	0.35	0.07	1.91	0.01	0.10	0.33	5.52	0.04	0.13	0.06	0.09	0.24
May	--	0.36	--	1.13	0.97	1.07	0.08	0.50	0.02	0.01	--	0.12	0.09	0.15
June	--	--	0.12	--	--	--	--	0.02	0.21	0.06	--	0.05	--	0.02
July	--	0.01	0.33	0.39	--	0.01	0.01	--	--	--	--	0.01	--	--
August	--	--	0.04	--	--	0.02	--	--	--	0.02	--	1.89	--	0.11
September	0.02	0.01	--	0.48	0.49	0.03	--	--	--	--	0.48	0.04	--	0.34
October	0.50	0.41	--	0.21	--	--	0.13	--	0.04	0.91	0.29	0.01	0.02	0.50
November	--	0.25	0.29	0.61	0.34	0.06	0.82	2.99	0.08	0.02	0.95	1.08	0.11	2.64
December	0.04	0.50	3.09	0.61	4.32	0.09	3.16	3.82	0.60	1.18	1.13	0.54	0.02	1.49
Annual Total	4.15	3.13	6.20	4.94	11.73	8.99	6.76	14.41	10.18	5.63	5.38	12.66	8.67	9.03

event as recorded at the TJRIB station. As has been the case in past years, analysis of 2025 satellite observations indicates that only six observed TJR plume events occurred within 0–3 days of rainfall exceeding 0.25 inches. Precipitation events of this magnitude can be sufficient to generate runoff-driven plume formation. However, the majority (~90%) of plume observations occurred during periods of low or no measurable rainfall. Figures 2 and 4 provide imagery examples showing higher than normal coastal turbidity, plankton blooms and visible TJR discharge plumes even though there was no measurable rainfall prior to the imaging dates. The TJR average discharge rate in 2025 was 65.7 cfs which was markedly below the average rate in 2024 of 152.8 cfs (IWBC 2026). However, there were the same number of plumes deemed significant (64) observed in the image data in 2025 as were observed in 2025 indicating that the discharge rate does not necessarily correspond directly with how turbid the river plume appears via satellite.



Date	CumPrcp (in)
01/03/25	0.01
01/26/25	0.26
01/27/25	0.17
02/07/25	0.13
02/12/25	0.05
02/13/25	0.48
02/14/25	0.15
02/26/25	0.01
03/05/25	0.15
03/06/25	0.23
03/07/25	0.01
03/11/25	0.17
03/12/25	0.14
03/13/25	1.32

Date	CumPrcp (in)
03/14/25	0.17
03/17/25	0.02
03/27/25	0.02
03/31/25	0.05
04/09/25	0.01
04/10/25	0.01
04/17/25	0.02
04/26/25	0.11
04/28/25	0.08
05/03/25	0.06
05/04/25	0.02
05/13/25	0.01
05/17/25	0.01
05/31/25	0.04

Date	CumPrcp (in)
06/03/25	0.01
06/04/25	0.01
08/28/25	0.11
09/17/25	0.11
09/18/25	0.20
09/21/25	0.01
09/22/25	0.01
10/09/25	0.02
10/14/25	0.47
10/15/25	0.01
11/13/25	0.05
11/14/25	0.01
11/15/25	0.59
11/16/25	0.35

Date	CumPrcp (in)
11/17/25	0.52
11/18/25	0.27
11/19/25	0.01
11/20/25	0.50
11/21/25	0.33
12/13/25	0.01
12/19/25	0.01
12/23/25	0.04
12/24/25	0.41
12/26/25	0.63
12/27/25	0.06
12/31/25	0.32

Figure 3. Daily accumulated rainfall in the Tijuana Estuary, average daily river discharge rate measured at the Tijuana River International Boundary station and days on which significant TJR discharge was observed in the high-resolution satellite data including the Sentinel-1 SAR data.

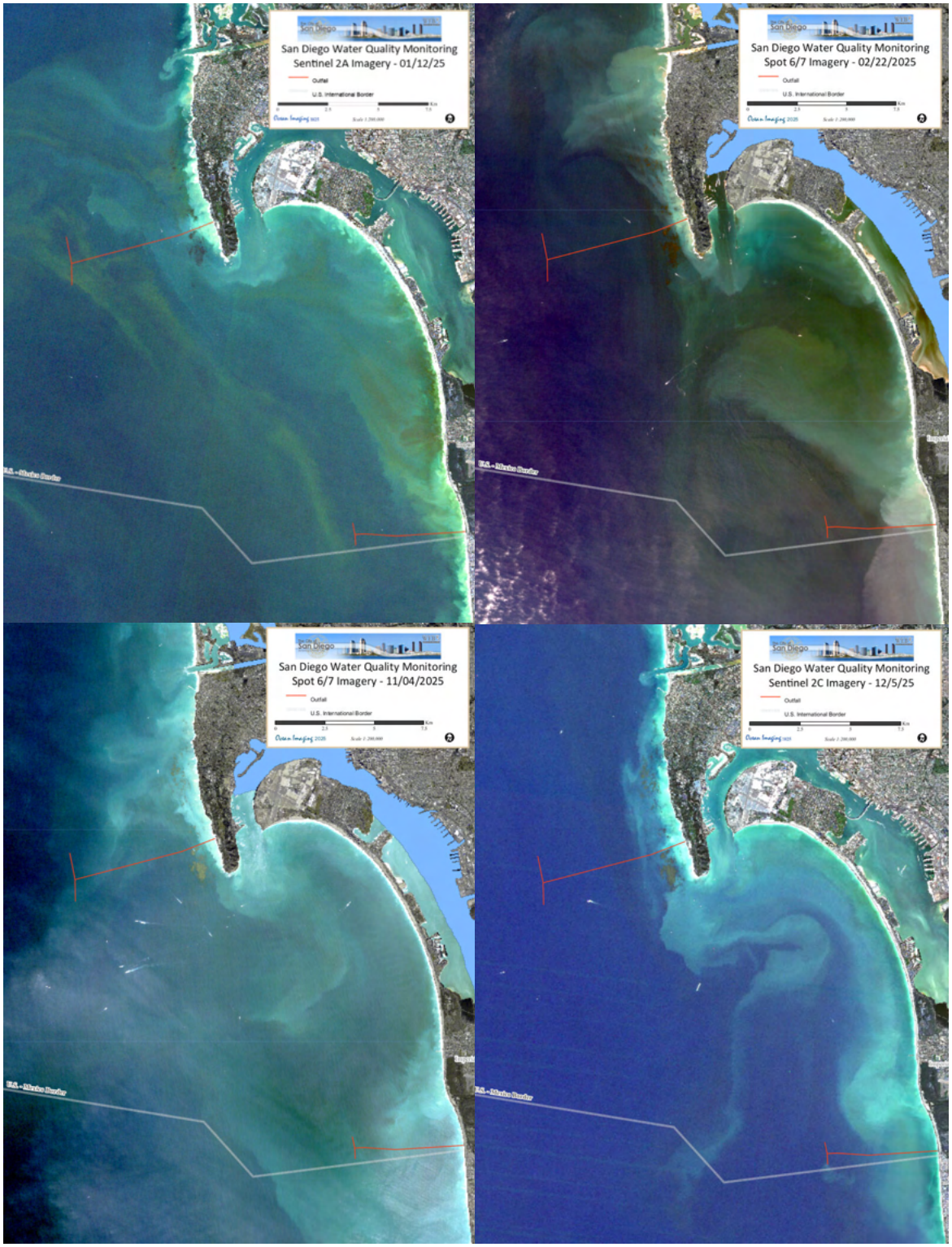


Figure 4. Sample high-resolution imagery from SPOT 6 and Sentinel-2 highlighting turbid water, plankton blooms, and TJR runoff plumes during periods when there was no measurable rainfall prior to the satellite imaging dates. Notably, on 02/22/25 when the TJR plume appears to be very prominent, the TJR discharge rate for that day was only 57.6 cfs which was below the 2025 annual average of 65.7 cfs.

Possible explanations for the observed TJR discharge plumes and reduced coastal water quality include precipitation events inland of San Diego and Tijuana creating runoff into the San Diego and Tijuana regions, coastal turbidity caused by significant ocean swell/wave action and other oceanographic conditions conducive to phytoplankton blooms. It is also possible that plume presence in the TJR coastal zone was partially driven by persistent transboundary flows and infrastructure-related discharges, with rainfall acting as an episodic amplifying factor rather than the primary control. Additional discussion of this topic is provided below.

Figure 5 provides examples of heavy coastal turbidity and extensive river runoff observed in the satellite imagery that may be linked to prior precipitation events. Contrary to previous years, in many cases when strong TJR runoff and coastal turbidity was observed in the image data following a rain event, the coastal waters did not clear up within two to three days and remained turbid for several days after the initial post-storm observation. In some situations, this was because another rain event soon followed, yet in others the exact reason is unknown. SDR river discharge in cfs measured by the United States Geological Survey (USGS) Fashion Valley gauge also tracked closely with the rainfall data recorded at the SDIA station (Figure 6). The mean discharge rate in 2025 (20.9 cfs) was lower than the rate experienced during 2024 (43.0 cfs), most likely due to overall higher rainfall in 2024 (Table 2). Figures 5 and 7 provide examples of when the satellite data exhibited notable coastal and offshore turbid conditions as well as plankton blooms in the Point Loma region and area west of Mission Bay that correlate with increased SDR flow and precipitation measurements shown in Figure 6.

In 2025 the County of San Diego issued 350 posted shoreline and/or rain advisories and 95 beach/shoreline closures. This is a 26.8% increase in the number of advisories and an 8.6% decrease in closures compared to 2024 (276 advisories and 104 closures respectively). As has been typical for the past several years, the two longest contiguous 2025 closures lasted well into October at Border Field State Park along the south end of the Tijuana Slough Shoreline and Imperial Beach which was closed from January through most of July. Most of the closures extended from the Tijuana River mouth all the way past Avenida Del Sol to include nearly all the Coronado City beaches and were attributed to contamination from the TJR runoff. Generally, the closures were associated with a rain event prior to and/or during the closure period leading to heavy TJR discharge and coastal turbidity as shown in Figure 6. However, nine closures were triggered by sewage spills, pump station failures, and/or sewer line problems. Unlike previous years, none of the closures were directly attributed to an exceedance of bacterial standards with no known source. Table 3 also shows the date(s) of the high-resolution satellite data in the project's archive acquired closest in time to the start date of the closure and/or rain advisory. Satellite data during the beach closure periods regularly show high turbidity and suspended solids and/or high plankton levels along the coastline near the closed regions as well as greater than normal TJR runoff, sometimes being carried north by the ocean currents. Figures 4, 5 and 8 provide examples of the TJR plume extending north and ocean currents pushing the TJR discharge up past Border Field State Park towards the Coronado beaches, corresponding with shoreline closures during the same period.

Although discharges from the San Diego River and Mission Bay do not cause the same level of beach contamination issues as the Tijuana River, the runoff from the San Diego River did affect nearshore water clarity and quality on several days in 2025, directly as a source of suspended sediment and indirectly as a source of high nutrient input, potentially encouraging coastal and offshore phytoplankton blooms. While not at the same scale or frequency as observed in previous years, turbidity plumes emanating from the river entrance and/or phytoplankton blooms either along the coast or offshore of the area were documented on 33 days in the medium-resolution (Sentinel-3) and high-resolution satellite data throughout the year. The area surrounding the Point Loma

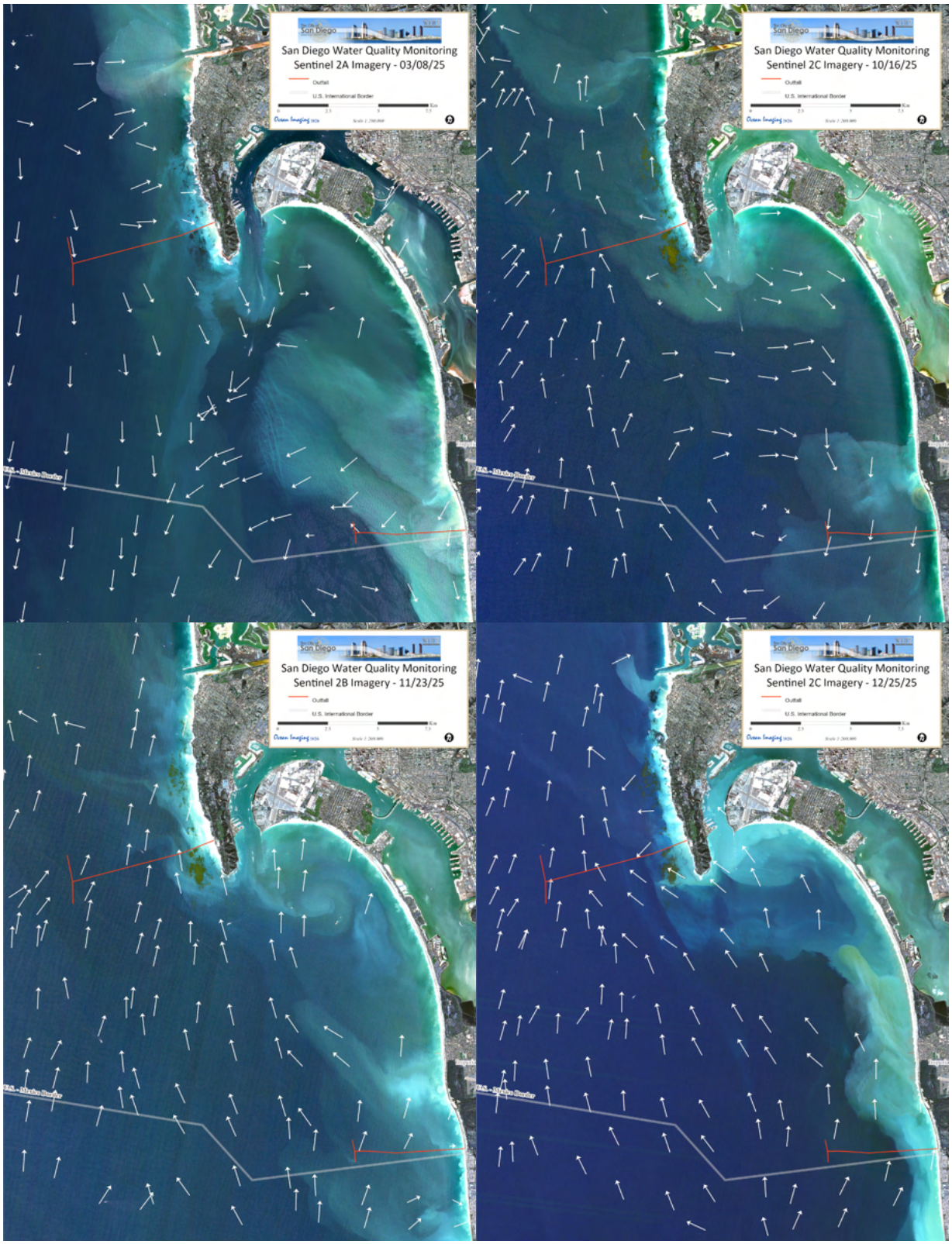
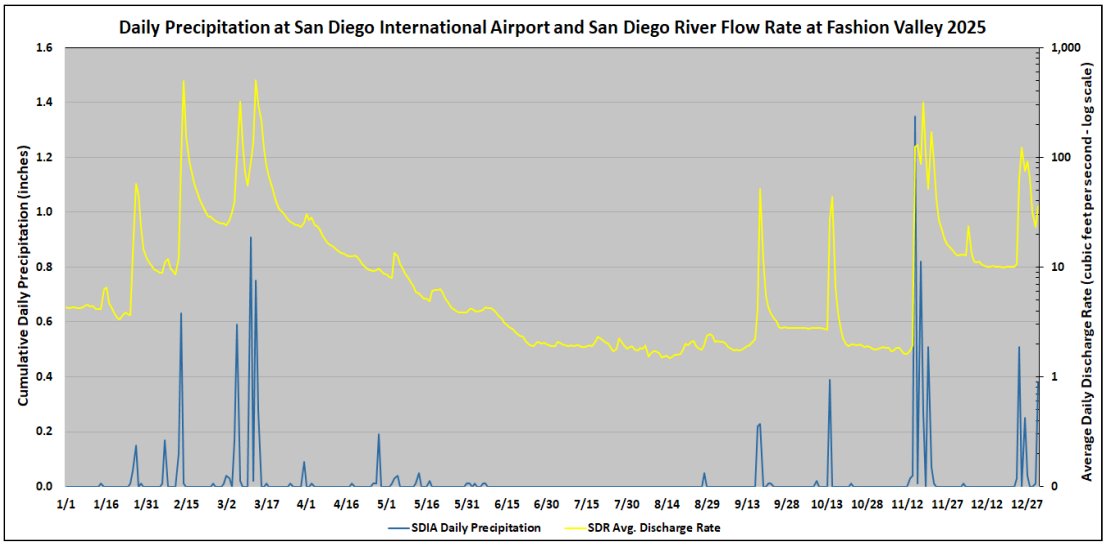


Figure 5. Examples of days when Sentinel-2 imagery displayed heavy TJR discharge along with coastal and offshore turbidity that can be correlated to rainfall events prior to the imaging dates.



San Diego Intl. Airport Rainfall 2025	
Jan	0.24
Feb	0.95
Mar	2.93
Apr	0.23
May	0.17
Jun	0.04
Jul	0.00
Aug	0.05
Sep	0.47
Oct	0.42
Nov	3.11
Dec	1.23

Figure 6. Average daily San Diego River discharge rate as measured by the USGS Fashion Valley gauge plotted with daily precipitation amounts as recorded at the San Diego International Airport. Monthly precipitation totals at the SDIA station are displayed to the right of the plot.

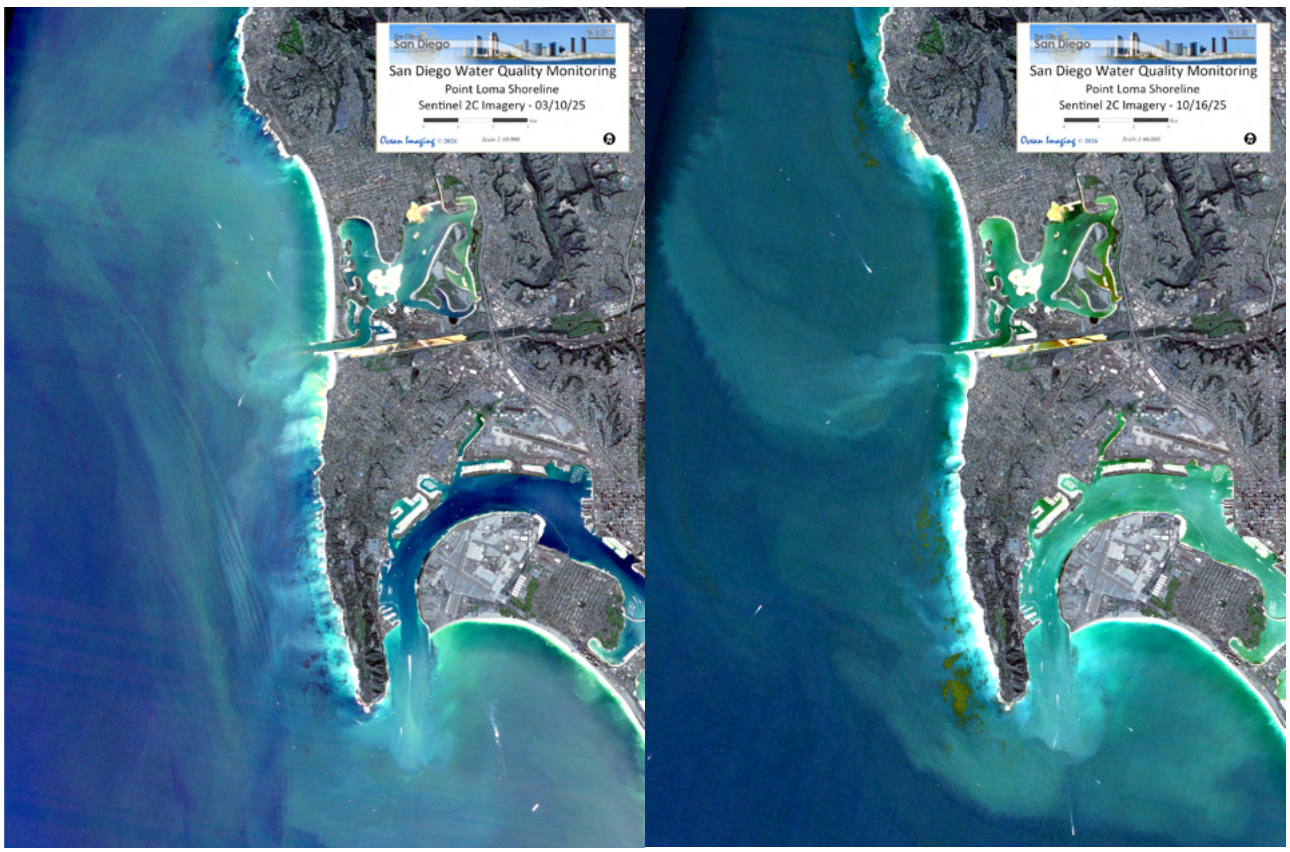


Figure 7. Examples from Sentinel-2C imagery when heavy coastal turbidity, SDR runoff and plankton blooms were observed following significant rain events in the San Diego area.

Table 3. 2025 County of San Diego shoreline closures, rain advisories, and associated project satellite data (Source: California State Water Resources Control Board). general rain advisory beach closure associated with the Tijuana River bay or beach closure due to a sewage spill bay or beach closure due to elevated bacteria level

Beach Name	Station Name	Type	Cause	Source	Start Date	End Date	Duration (days)	Nearest Rain Date	Time From Rain Event	Satellite Image Data
Border Field State Park	IB-010	Closure	Tijuana River Associated	Sewage/Grease	1/1/2025	10/12/2025	284	12/28/2024	4	74 dates
Imperial Beach municipal beach, other	IB-050	Closure	Tijuana River Associated	Sewage/Grease	1/1/2025	1/15/2025	14	12/28/2024	4	9 dates
Imperial Beach municipal beach, other	EH-010	Closure	Tijuana River Associated	Sewage/Grease	1/1/2025	1/14/2025	13	12/28/2024	4	8 dates
north Imperial Beach	IB-060	Closure	Tijuana River Associated	Sewage/Grease	1/1/2025	1/2/2025	1	12/28/2024	4	1/2
Imperial Beach pier area	EH-030	Closure	Tijuana River Associated	Sewage/Grease	1/1/2025	1/2/2025	1	12/28/2024	4	1/2
Imperial Beach pier area	EH-030	Closure	Tijuana River Associated	Sewage/Grease	1/3/2025	1/14/2025	11	1/3/2025	0	1/4, 1/7, 1/8, 1/9, 1/12
north Imperial Beach	IB-060	Closure	Tijuana River Associated	Sewage/Grease	1/3/2025	1/13/2025	10	1/3/2025	0	1/4, 1/7, 1/8, 1/9, 1/12
La Jolla Shores Beach	EH-340	Closure	Blockage	Sewer Line / Stormdrain	1/15/2025	1/16/2025	1	1/14/2025	1	1/14
La Jolla Shores Beach	SI-010	Closure	Blockage	Sewer Line / Stormdrain	1/15/2025	1/16/2025	1	1/14/2025	1	1/14
Imperial Beach municipal beach, other	IB-050	Closure	Tijuana River Associated	Sewage/Grease	1/16/2025	7/28/2025	193	1/14/2025	2	40 dates
Imperial Beach municipal beach, other	EH-010	Closure	Tijuana River Associated	Sewage/Grease	1/16/2025	7/29/2025	194	1/14/2025	2	40 dates
Imperial Beach pier area	EH-030	Closure	Tijuana River Associated	Sewage/Grease	1/16/2025	7/27/2025	192	1/14/2025	2	39 dates
north Imperial Beach	IB-060	Closure	Tijuana River Associated	Unknown	1/18/2025	7/27/2025	190	1/14/2025	4	39 dates
All San Diego County	All San Diego County beaches	Rain			1/27/2025	1/30/2025	3	1/27/2025	0	1/29
Silver Strand State Beach	IB-070	Closure	Tijuana River Associated	Sewage/Grease	1/31/2025	4/4/2025	63	1/29/2025	2	19 dates
Coronado City beaches	IB-079	Closure	Tijuana River Associated	Sewage/Grease	1/31/2025	2/5/2025	5	1/29/2025	2	2/1
Coronado City beaches	EH-050	Closure	Tijuana River Associated	Sewage/Grease	1/31/2025	2/3/2025	3	1/29/2025	2	2/1
Coronado north beach	EH-060	Closure	Tijuana River Associated	Sewage/Grease	1/31/2025	2/3/2025	3	1/29/2025	2	2/1
Coronado City beaches	IB-079	Closure	Tijuana River Associated	Sewage/Grease	2/7/2025	2/8/2025	1	2/7/2025	0	2/8
North County Beaches	Northern San Diego County beaches	Rain			2/7/2025	2/10/2025	3	2/7/2025	0	2/8
San Diego Bay	EH-211	Closure	Other	Unknown	2/12/2025	2/14/2025	2	2/12/2025	0	
All San Diego County	All San Diego County beaches	Rain			2/12/2025	2/17/2025	5	2/12/2025	0	2/16
Coronado City beaches	IB-079	Closure	Tijuana River Associated	Sewage/Grease	2/13/2025	2/23/2025	10	2/13/2025	0	2/16, 2/18, 2/21, 2/22, 2/23
Coronado City beaches	EH-050	Closure	Tijuana River Associated	Sewage/Grease	2/13/2025	2/23/2025	10	2/13/2025	0	2/16, 2/18, 2/21, 2/22, 2/23
Coronado north beach	EH-060	Closure	Tijuana River Associated	Sewage/Grease	2/13/2025	2/21/2025	8	2/13/2025	0	2/16, 2/18, 2/21
All San Diego County	All San Diego County beaches	Rain			3/6/2025	3/10/2025	4	3/6/2025	0	3/8, 3/10
All San Diego County	All San Diego County beaches	Rain			3/11/2025	3/18/2025	7	3/11/2025	0	3/15, 3/18
Coronado City beaches	EH-050	Closure	Tijuana River Associated	Sewage/Grease	3/14/2025	3/23/2025	9	3/14/2025	0	3/15, 3/18, 3/20, 3/23
Coronado north beach	EH-060	Closure	Tijuana River Associated	Sewage/Grease	3/14/2025	3/21/2025	7	3/14/2025	0	3/15, 3/18, 3/20
Coronado City beaches	IB-079	Closure	Tijuana River Associated	Sewage/Grease	3/14/2025	3/23/2025	9	3/14/2025	0	3/15, 3/18, 3/20, 3/23
Marine Street Beach	EH-290	Closure	Sewage Spill	Sewage/Grease	3/15/2025	3/17/2025	2	3/14/2025	1	3/15
Coronado north beach	EH-060	Closure	Tijuana River Associated	Sewage/Grease	3/22/2025	3/23/2025	1	3/17/2025	5	3/20, 3/23
Silver Strand State Beach	IB-070	Closure	Tijuana River Associated	Sewage/Grease	4/12/2025	5/16/2025	34	4/10/2025	2	7 dates
Coronado City beaches	IB-079	Closure	Tijuana River Associated	Sewage/Grease	4/12/2025	4/21/2025	9	4/10/2025	2	4/19
Coronado City beaches	EH-050	Closure	Tijuana River Associated	Sewage/Grease	4/13/2025	4/21/2025	8	4/10/2025	3	4/19

Table 3, Cont'd. 2025 County of San Diego shoreline closures, rain advisories, and associated project satellite data (Source: California State Water Resources Control Board). general rain advisory beach closure associated with the Tijuana River bay or beach closure due to a sewage spill bay or beach closure due to elevated bacteria level

Beach Name	Station Name	Type	Cause	Source	Start Date	End Date	Duration (days)	Nearest Rain Date	Time From Rain Event	Satellite Image Data
Coronado north beach	EH-060	Closure	Tijuana River Associated	Sewage/Grease	4/13/2025	4/21/2025	8	4/10/2025	3	4/19
Coronado City beaches	IB-079	Closure	Tijuana River Associated	Sewage/Grease	5/3/2025	5/4/2025	1	5/3/2025	0	
Coronado north beach	EH-060	Closure	Tijuana River Associated	Sewage/Grease	5/6/2025	5/7/2025	1	5/5/2025	1	5/7
Coronado City beaches	IB-079	Closure	Tijuana River Associated	Sewage/Grease	5/6/2025	5/12/2025	6	5/5/2025	1	5/7
Coronado City beaches	EH-050	Closure	Tijuana River Associated	Sewage/Grease	5/6/2025	5/7/2025	1	5/5/2025	1	5/7
Silver Strand State Beach	IB-070	Closure	Tijuana River Associated	Sewage/Grease	5/18/2025	6/24/2025	37	5/17/2025	1	5/19, 5/27, 6/20
Coronado City beaches	IB-079	Closure	Tijuana River Associated	Sewage/Grease	5/23/2025	5/28/2025	5	5/17/2025	6	5/27
Coronado City beaches	EH-050	Closure	Tijuana River Associated	Sewage/Grease	5/24/2025	5/27/2025	3	5/17/2025	7	5/27
Coronado north beach	EH-060	Closure	Tijuana River Associated	Sewage/Grease	5/24/2025	5/27/2025	3	5/17/2025	7	5/27
Coronado City beaches	IB-079	Closure	Tijuana River Associated	Sewage/Grease	6/2/2025	6/22/2025	20	6/1/2025	1	6/20
Coronado City beaches	EH-050	Closure	Tijuana River Associated	Sewage/Grease	6/4/2025	6/9/2025	5	6/4/2025	0	
Coronado north beach	EH-060	Closure	Tijuana River Associated	Sewage/Grease	6/4/2025	6/9/2025	5	6/4/2025	0	
La Jolla Shores Beach	EH-574	Closure	Sewage Spill	Sewage/Grease	6/16/2025	6/17/2025	1	6/7/2025	9	
Coronado Cays (NR)	EH-575	Closure	Pump Station Failure	Combined Sewer Discharge	7/1/2025	7/2/2025	1	6/7/2025	24	
Coronado Cays (NR)	EH-576	Closure	Pump Station Failure	Combined Sewer Discharge	7/1/2025	7/2/2025	1	6/7/2025	24	
Silver Strand State Beach	IB-070	Closure	Tijuana River Associated	Sewage/Grease	7/16/2025	7/28/2025	12	6/7/2025	39	7/16, 7/23, 7/26, 7/28
Coronado City beaches	IB-079	Closure	Tijuana River Associated	Sewage/Grease	7/16/2025	7/27/2025	11	6/7/2025	39	7/16, 7/23, 7/26
Coronado north beach	EH-060	Closure	Tijuana River Associated	Sewage/Grease	7/16/2025	7/21/2025	5	6/7/2025	39	7/16
Coronado City beaches	EH-050	Closure	Tijuana River Associated	Sewage/Grease	7/16/2025	7/25/2025	9	6/7/2025	39	7/16, 7/23
Imperial Beach municipal beach, other	EH-010	Closure	Tijuana River Associated	Sewage/Grease	8/2/2025	9/9/2025	38	6/7/2025	56	12 days
Imperial Beach pier area	EH-030	Closure	Tijuana River Associated	Sewage/Grease	8/2/2025	9/9/2025	38	6/7/2025	56	12 days
north Imperial Beach	IB-060	Closure	Tijuana River Associated	Sewage/Grease	8/2/2025	9/9/2025	38	6/7/2025	56	12 days
Imperial Beach municipal beach, other	IB-050	Closure	Tijuana River Associated	Sewage/Grease	8/2/2025	9/9/2025	38	6/7/2025	56	12 days
Coronado City beaches	IB-079	Closure	Tijuana River Associated	Sewage/Grease	8/31/2025	9/4/2025	4	8/28/2025	3	9/1, 9/3, 9/4
Silver Strand State Beach	IB-070	Closure	Tijuana River Associated	Sewage/Grease	8/31/2025	9/6/2025	6	8/28/2025	3	9/1, 9/3, 9/4, 9/6
Coronado City beaches	EH-050	Closure	Tijuana River Associated	Sewage/Grease	9/1/2025	9/4/2025	3	8/28/2025	4	9/1, 9/3, 9/4
Coronado north beach	EH-060	Closure	Tijuana River Associated	Sewage/Grease	9/1/2025	9/4/2025	3	8/28/2025	4	9/1, 9/3, 9/4
All San Diego County	All San Diego County beaches	Rain			9/18/2025	9/21/2025	3	9/18/2025	0	9/19
Imperial Beach municipal beach, other	IB-050	Closure	Tijuana River Associated	Sewage/Grease	9/21/2025	9/25/2025	4	9/21/2025	0	9/19, 9/24
Imperial Beach municipal beach, other	EH-010	Closure	Tijuana River Associated	Sewage/Grease	9/21/2025	9/25/2025	4	9/21/2025	0	9/19, 9/24
Imperial Beach pier area	EH-030	Closure	Tijuana River Associated	Sewage/Grease	9/21/2025	9/25/2025	4	9/21/2025	0	9/19, 9/24
north Imperial Beach	IB-060	Closure	Tijuana River Associated	Sewage/Grease	9/21/2025	9/25/2025	4	9/21/2025	0	9/19, 9/24
Imperial Beach municipal beach, other	IB-050	Closure	Tijuana River Associated	Sewage/Grease	9/29/2025	10/11/2025	12	9/22/2025	7	10/1, 10/2, 10/4, 10/11
Imperial Beach municipal beach, other	EH-010	Closure	Tijuana River Associated	Sewage/Grease	9/29/2025	10/9/2025	10	9/22/2025	7	10/1, 10/2, 10/4
Imperial Beach pier area	EH-030	Closure	Tijuana River Associated	Sewage/Grease	9/29/2025	10/6/2025	7	9/22/2025	7	10/1, 10/2, 10/4

Table 3, Cont'd. 2025 County of San Diego shoreline closures, rain advisories, and associated project satellite data (Source: California State Water Resources Control Board). general rain advisory beach closure associated with the Tijuana River bay or beach closure due to a sewage spill bay or beach closure due to elevated bacteria level

Beach Name	Station Name	Type	Cause	Source	Start Date	End Date	Duration (days)	Nearest Rain Date	Time From Rain Event	Satellite Image Data
north Imperial Beach	IB-060	Closure	Tijuana River Associated	Sewage/Grease	9/29/2025	10/9/2025	10	9/22/2025	7	10/1, 10/2, 10/4
Imperial Beach pier area	EH-030	Closure	Tijuana River Associated	Sewage/Grease	10/7/2025	10/9/2025	2	9/22/2025	15	
Border Field State Park	IB-010	Closure	Tijuana River Associated	Sewage/Grease	10/13/2025	12/31/2025	79	10/9/2025	4	24 dates
Imperial Beach municipal beach, other	IB-050	Closure	Tijuana River Associated	Sewage/Grease	10/13/2025	10/29/2025	16	10/9/2025	4	6 dates
Imperial Beach municipal beach, other	EH-010	Closure	Tijuana River Associated	Sewage/Grease	10/13/2025	10/29/2025	16	10/9/2025	4	6 dates
Imperial Beach pier area	EH-030	Closure	Tijuana River Associated	Sewage/Grease	10/13/2025	10/29/2025	16	10/9/2025	4	6 dates
north Imperial Beach	IB-060	Closure	Tijuana River Associated	Sewage/Grease	10/13/2025	10/30/2025	17	10/9/2025	4	7 dates
All San Diego County	All San Diego County beaches	Rain			10/14/2025	10/17/2025	3	10/14/2025	0	10/16
Coronado north beach	EH-060	Closure	Line Break	Sewer Line	10/21/2025	10/22/2025	1	10/15/2025	6	
Imperial Beach municipal beach, other	IB-050	Closure	Tijuana River Associated	Sewage/Grease	10/31/2025	11/9/2025	9	10/22/2025	9	10/31, 11/4, 11/5, 11/7
Imperial Beach municipal beach, other	EH-010	Closure	Tijuana River Associated	Sewage/Grease	10/31/2025	11/9/2025	9	10/22/2025	9	10/31, 11/4, 11/5, 11/7
Imperial Beach pier area	EH-030	Closure	Tijuana River Associated	Sewage/Grease	10/31/2025	11/9/2025	9	10/22/2025	9	10/31, 11/4, 11/5, 11/7
north Imperial Beach	IB-060	Closure	Tijuana River Associated	Sewage/Grease	10/31/2025	11/9/2025	9	10/22/2025	9	10/31, 11/4, 11/5, 11/7
Imperial Beach municipal beach, other	IB-050	Closure	Tijuana River Associated	Sewage/Grease	11/13/2025	12/31/2025	48	11/13/2025	0	12 dates
Imperial Beach municipal beach, other	EH-010	Closure	Tijuana River Associated	Sewage/Grease	11/13/2025	12/23/2025	40	11/13/2025	0	11 dates
Imperial Beach pier area	EH-030	Closure	Tijuana River Associated	Sewage/Grease	11/13/2025	12/31/2025	48	11/13/2025	0	12 dates
north Imperial Beach	IB-060	Closure	Tijuana River Associated	Sewage/Grease	11/13/2025	12/23/2025	40	11/13/2025	0	11 dates
Silver Strand State Beach	IB-070	Closure	Tijuana River Associated	Sewage/Grease	11/13/2025	11/27/2025	14	11/13/2025	0	12 dates
Coronado City beaches	IB-079	Closure	Tijuana River Associated	Sewage/Grease	11/14/2025	11/27/2025	13	11/14/2025	0	11 dates
Coronado City beaches	EH-050	Closure	Tijuana River Associated	Sewage/Grease	11/14/2025	11/27/2025	13	11/14/2025	0	11 dates
Coronado north beach	EH-060	Closure	Tijuana River Associated	Sewage/Grease	11/14/2025	11/27/2025	13	11/14/2025	0	11 dates
All San Diego County	All San Diego County beaches	Rain			11/15/2025	11/24/2025	9	11/15/2025	0	11/23
Silver Strand State Beach	IB-070	Closure	Tijuana River Associated	Sewage/Grease	12/7/2025	12/11/2025	4	12/3/2025	4	12/7, 12/8
Mission Bay	MB-031	Closure	Sewage Spill	Sewer Line	12/16/2025	12/19/2025	3	12/13/2025	3	12/17, 12/18
Tecolote Shores	MB-041	Closure	Sewage Spill	Sewer Line	12/16/2025	12/19/2025	3	12/13/2025	3	12/17, 12/18
Mission Bay	MB-043	Closure	Sewage Spill	Sewer Line	12/16/2025	12/19/2025	3	12/13/2025	3	12/17, 12/18
Mission Bay	MB-227	Closure	Sewage Spill	Sewer Line	12/22/2025	12/31/2025	9	12/19/2025	3	
Silver Strand State Beach	IB-070	Closure	Tijuana River Associated	Sewage/Grease	12/24/2025	12/31/2025	7	12/24/2025	0	12/25
Imperial Beach municipal beach, other	EH-010	Closure	Tijuana River Associated	Sewage/Grease	12/24/2025	12/31/2025	7	12/24/2025	0	12/25
north Imperial Beach	IB-060	Closure	Tijuana River Associated	Sewage/Grease	12/24/2025	12/31/2025	7	12/24/2025	0	12/25
All San Diego County	All San Diego County beaches	Rain			12/24/2025	12/29/2025	5	12/24/2025	0	12/25
Coronado City beaches	EH-050	Closure	Tijuana River Associated	Sewage/Grease	12/30/2025	12/31/2025	1	12/30/2025	0	12/25
Coronado north beach	EH-060	Closure	Tijuana River Associated	Sewage/Grease	12/30/2025	12/31/2025	1	12/30/2025	0	12/25
Coronado City beaches	IB-079	Closure	Tijuana River Associated	Sewage/Grease	12/30/2025	12/31/2025	1	12/30/2025	0	12/25
All San Diego County	All San Diego County beaches	Rain			12/31/2025	12/31/2025	1	12/31/2025	0	12/25

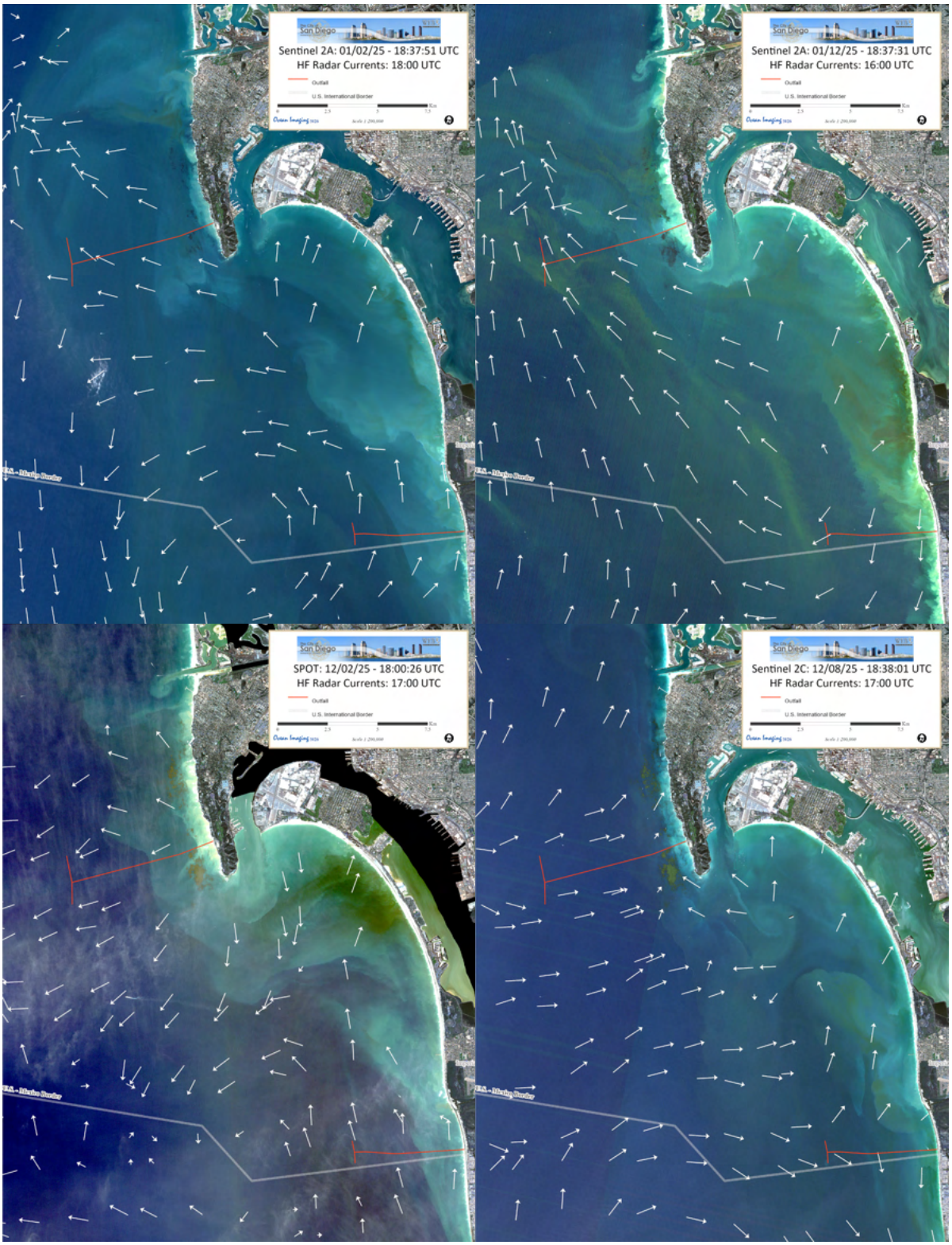


Figure 8. Sentinel-2 and SPOT 6 imagery with time-coincident 2km HF Radar currents overlaid to provide examples of when the TJR plume extended to the north and/or when ocean currents pushed TJR discharge up past Border Field State Park towards the Coronado beaches, corresponding with shoreline closures during the same period.

kelp bed was more often affected by direct shore runoff and discharges from the San Diego River and Mission Bay during the prevalent southward current regime. Figure 9 provides examples from a 300-meter Sentinel-3 image time series of days on which the data revealed heavy coastal turbidity and a developing phytoplankton bloom in this northern section of the project's study area. The bloom moves offshore and then grows larger as it extends south during the three-day period.

There were fewer phytoplankton and possible HAB observed in the satellite imagery in 2025 compared to 2024. While not measured quantitatively, HAB are recognized by dark-green and brown-to-red reflectance in the satellite data caused by phytoplankton containing photosynthetic pigments that vary in color from brown to red and blooms often dominated by the dinoflagellate Lingulodinium polyedra which absorbs light in the ultraviolet part of the electromagnetic spectrum (Kahru et al. 1998, Zheng et al. 2018). Diatoms (primarily Pseudo-nitzschia spp) and dinoflagellates are largely responsible for the local harmful algal blooms (red tides) when they occur (Southern California Coastal Water Research Project 2019). Figure 10 provides a few examples of high-resolution Landsat and SPOT data highlighting days when the imagery revealed strong coastal and offshore phytoplankton blooms.

The SCB experienced slightly higher overall chlorophyll levels throughout 2025 when compared to the previous four years, especially when compared to 2023 which showed relatively low chlorophyll levels and thus phytoplankton abundance in the SCB through much of the year (Ocean Imaging 2023). Of the years 2021–2025, 2021 exhibited the highest levels in the SCB over that time frame (Ocean Imaging 2021). Figure 11 provides representative SCB VIIRS and MODIS-derived chlorophyll images for each month of 2025. Increased coastal upwelling during February, March, and early April likely enhanced the supply of nutrient-rich subsurface water to the coastal ocean. Concurrent rainfall events likely contributed additional nutrients through river discharge and coastal runoff. Together, these processes likely contributed to the elevated chlorophyll concentrations observed during this period. Cholorphyll levels were high in the northern bight compared to previous years. The California Current appeared to maintain its strength through the summer, likely facilitating the transport of nutrient-rich waters into the Southern California Bight and contributing to the elevated chlorophyll concentrations observed during that period. The

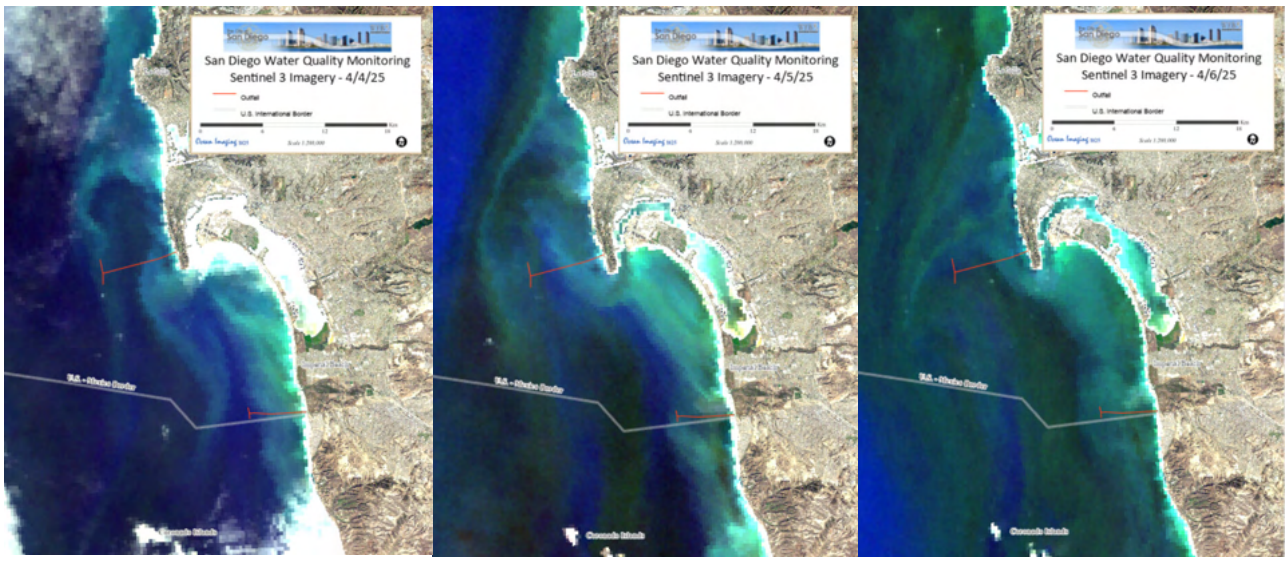


Figure 9. Sentinel-3 image time series from 04/04/25 through 04/06/25 showing turbid water and a strong phytoplankton bloom developing and extending south and west from the northern part of this project's focus area.

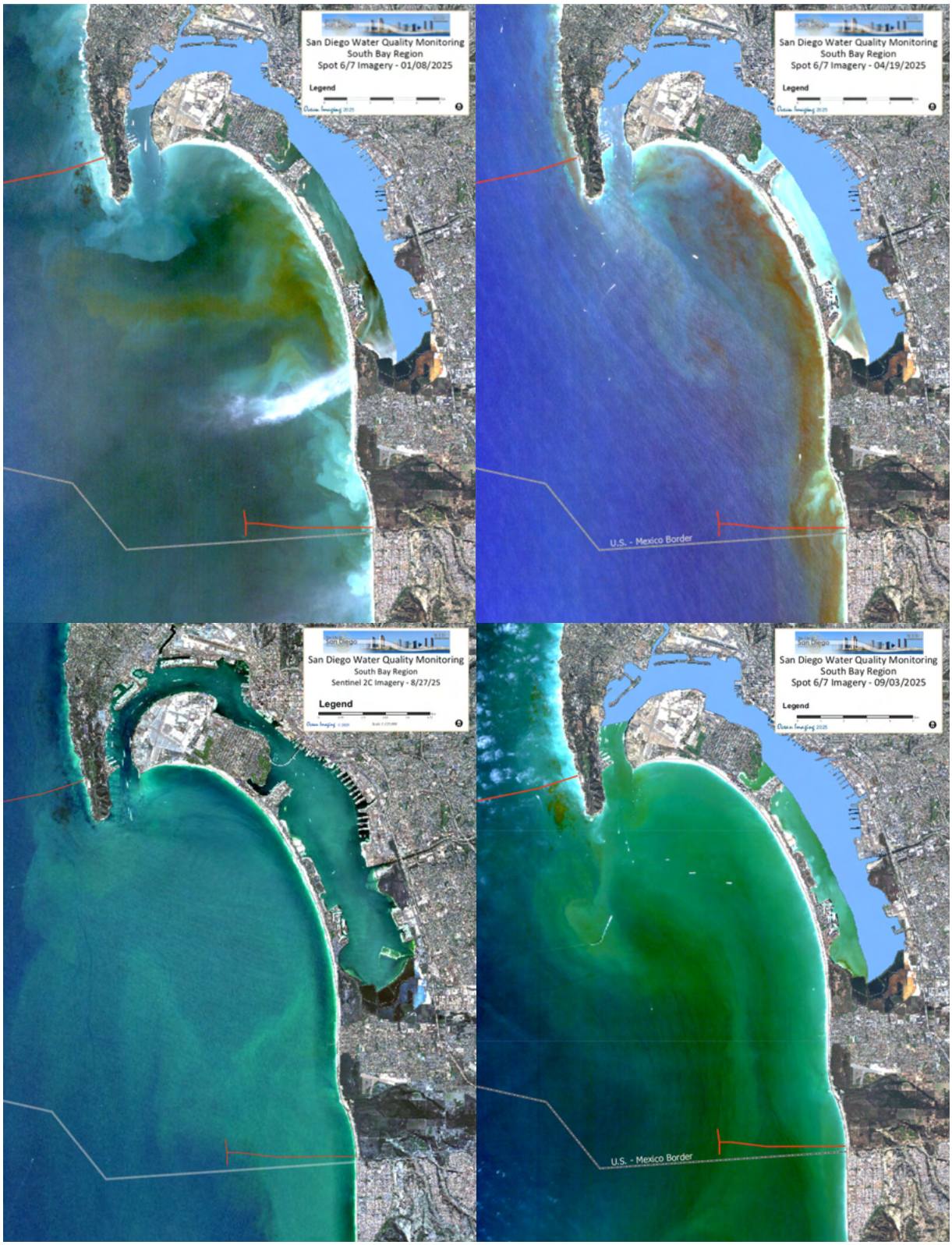


Figure 10. Sample high-resolution Sentinel-2 and SPOT data providing examples of days when the imagery revealed strong coastal and offshore phytoplankton blooms and possible HABs.

current then appeared to weaken in November and December. Figure 12 shows 300 and 1000-meter fused resolution monthly chlorophyll averages for the area offshore of San Diego County and south of the U.S.-Mexico border. These composites were generated from MODIS, VIIRS and OLCI data as part of a SDPUD-funded project to study plankton abundance and extent in the region from 1997 through 2024, however, 2025 data were obtained for this report. The series provides a more coastal, regional perspective of the changes in phytoplankton throughout the year. The data correlate well with the SCB imagery in Figure 11, however, the San Diego region exhibited higher chlorophyll abundance in April and lower levels in August and September – unlike the entire SCB.

The City of San Diego conductivity-temperature-depth (CTD) sampling results generally correlated well with the satellite data observations, the main difference being that the average chlorophyll readings from the CTD sampling stations was higher than the average measurements derived from the satellite data (Figure 13). The best explanation for this is that the satellite image data (see Figure 12) encompasses a much larger area than that of the sampling stations with the image data averages reflecting lower offshore chlorophyll

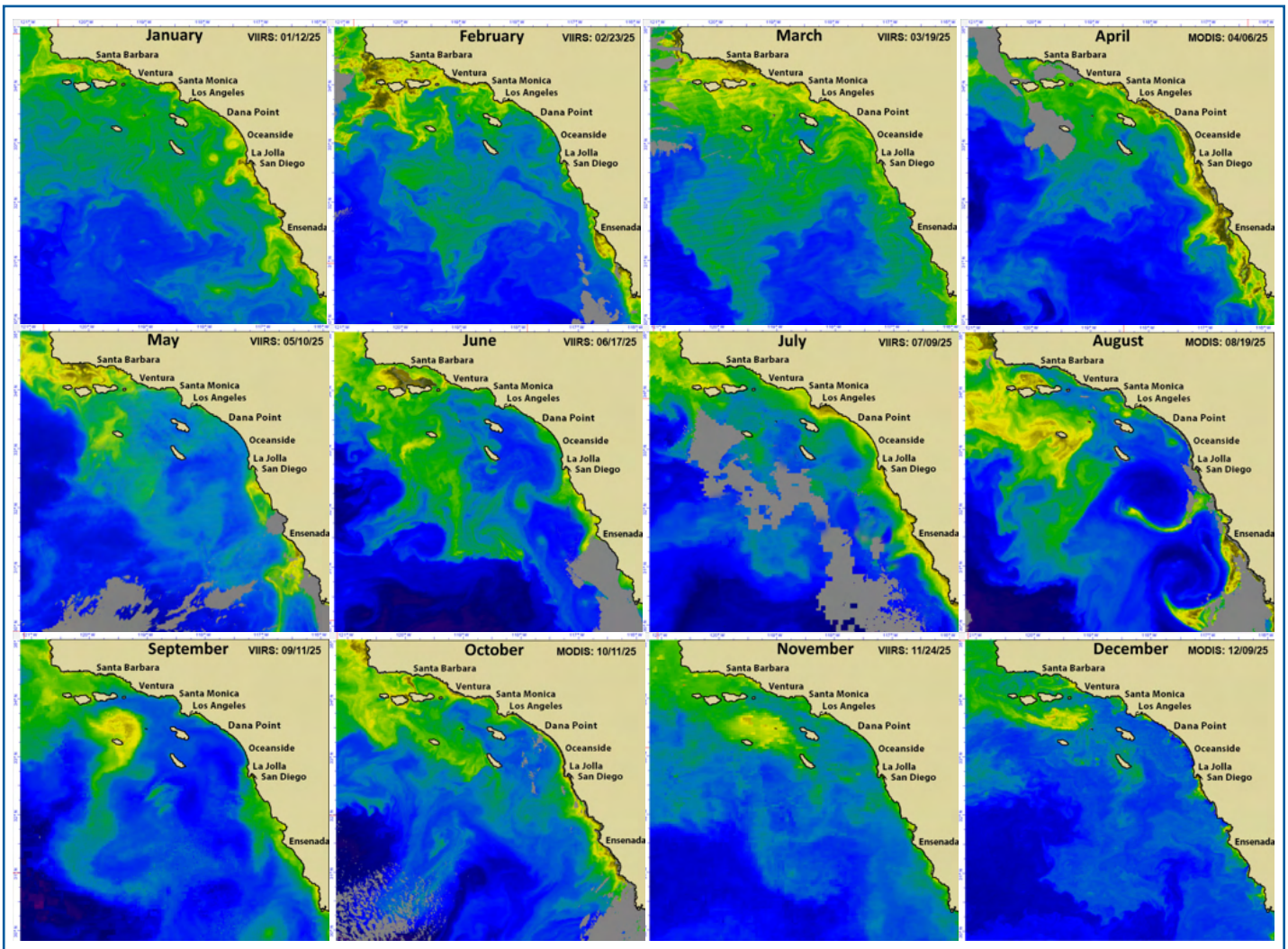


Figure 11. Representative VIIRS and MODIS-derived chlorophyll images for each month of 2025 showing relatively high levels of chlorophyll-rich water in the SCB through much of the year until December when levels decreased. Grey areas in imagery are masked cloud cover.

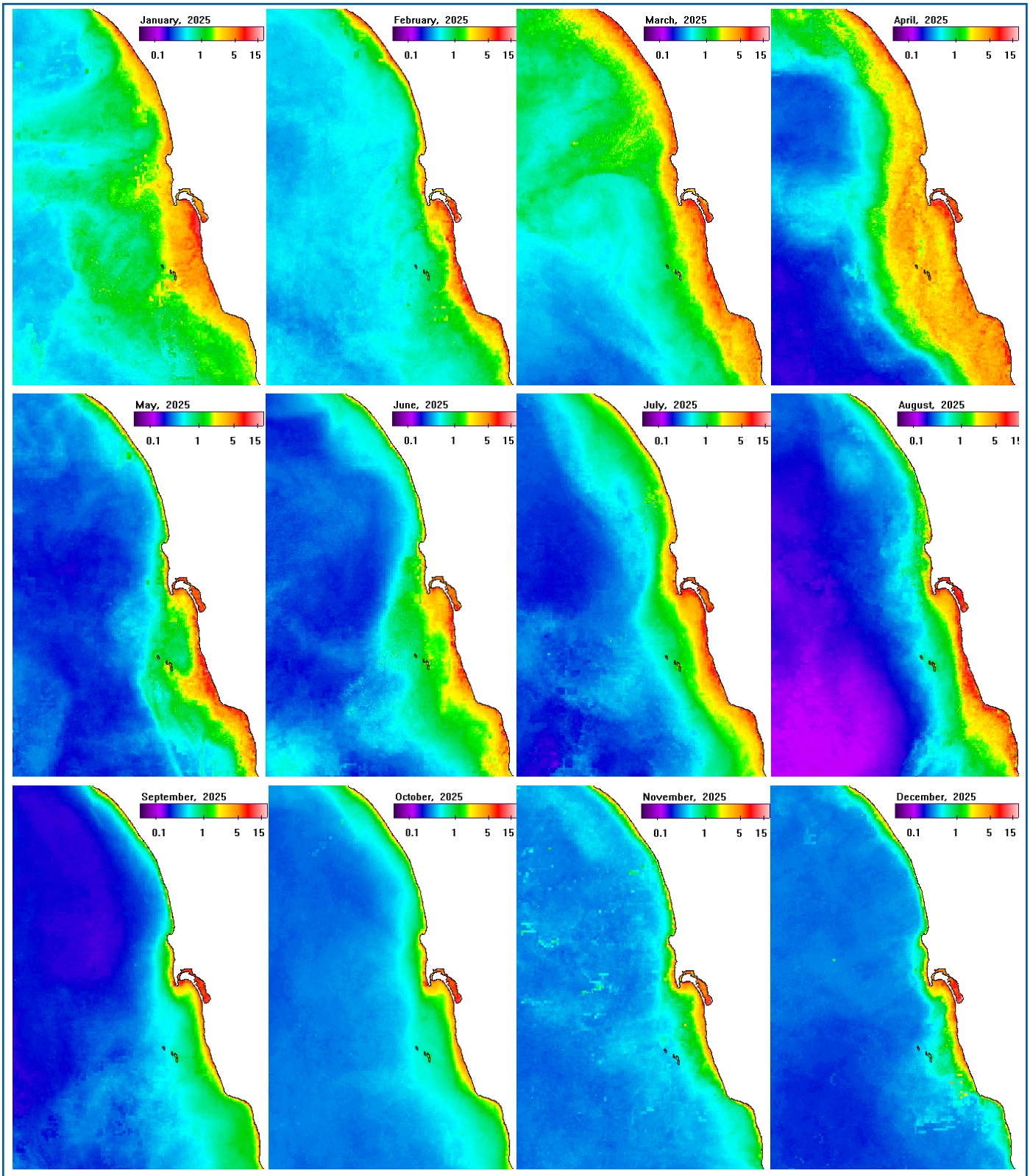


Figure 12. Monthly chlorophyll (mg/m^3) composites of the San Diego County coastal and offshore area derived from 300 m and 1 km MODIS, VIIRS and OCLI imagery generated by Mati Kahru of Scripps Institution of Oceanography in cooperation with OI as part of a SDPUD-funded project to study a long-term time series of satellite imagery to assess phytoplankton abundance and extent possibly related to increasing eutrophication of the ocean in this region.

levels and the CTD data reflecting higher levels indicative of stronger blooms closer to the coast.

Excluding a few anomalous outliers, some of the highest chlorophyll levels recorded via CTD (as high as 48.96 mg/m^3 at station I25, 7-meter depth on 05/12) occurred during the months of April and

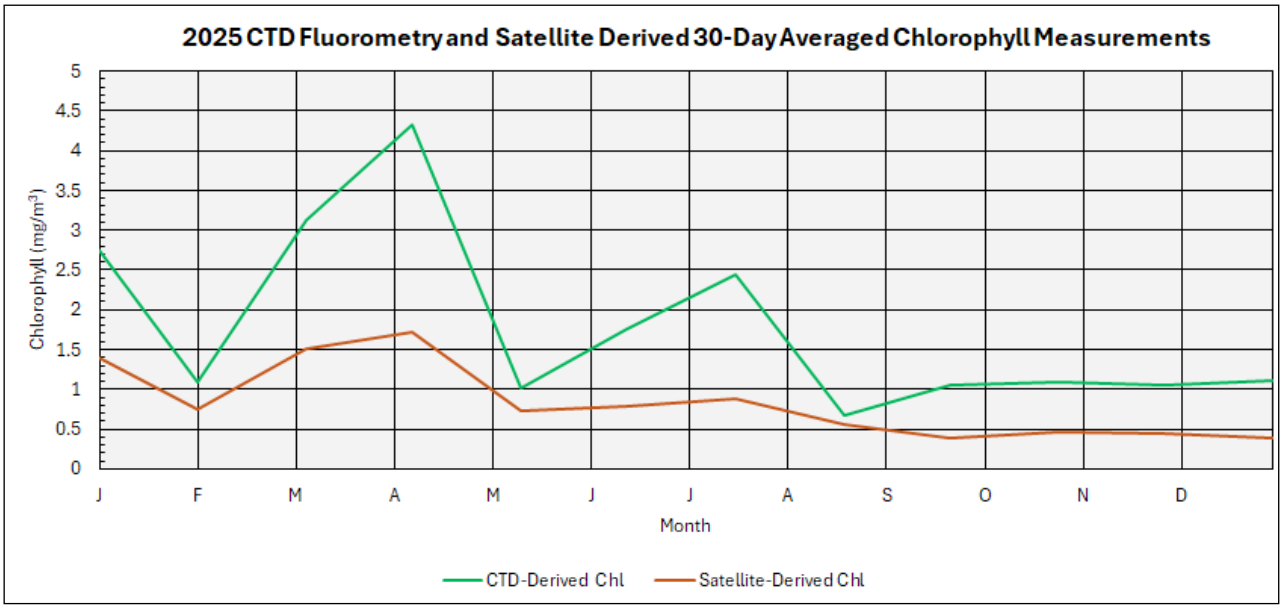


Figure 13. Monthly averaged chlorophyll measurements derived from the San Diego CTD sampling stations (all stations averaged) and the satellite image derived chlorophyll (image data and the AOI are shown in Figure 12).

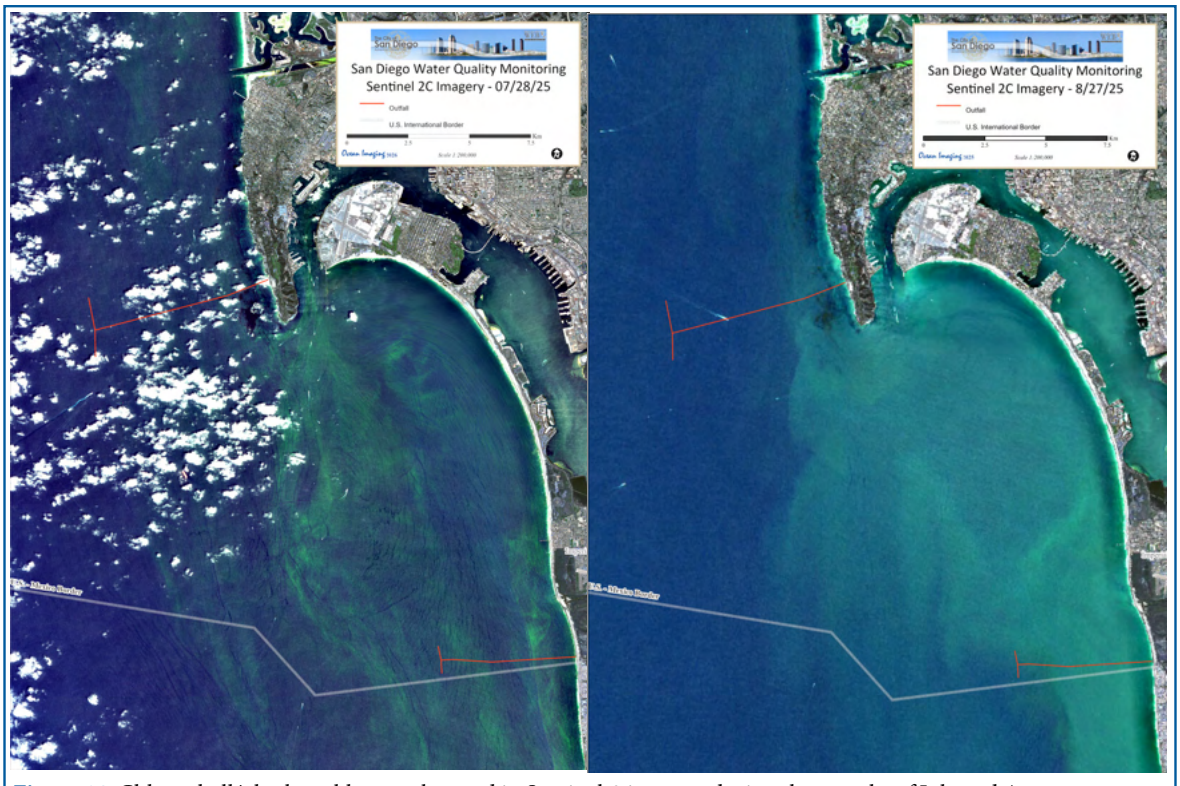


Figure 14. Chlorophyll/plankton blooms observed in Sentinel-2 imagery during the months of July and August.

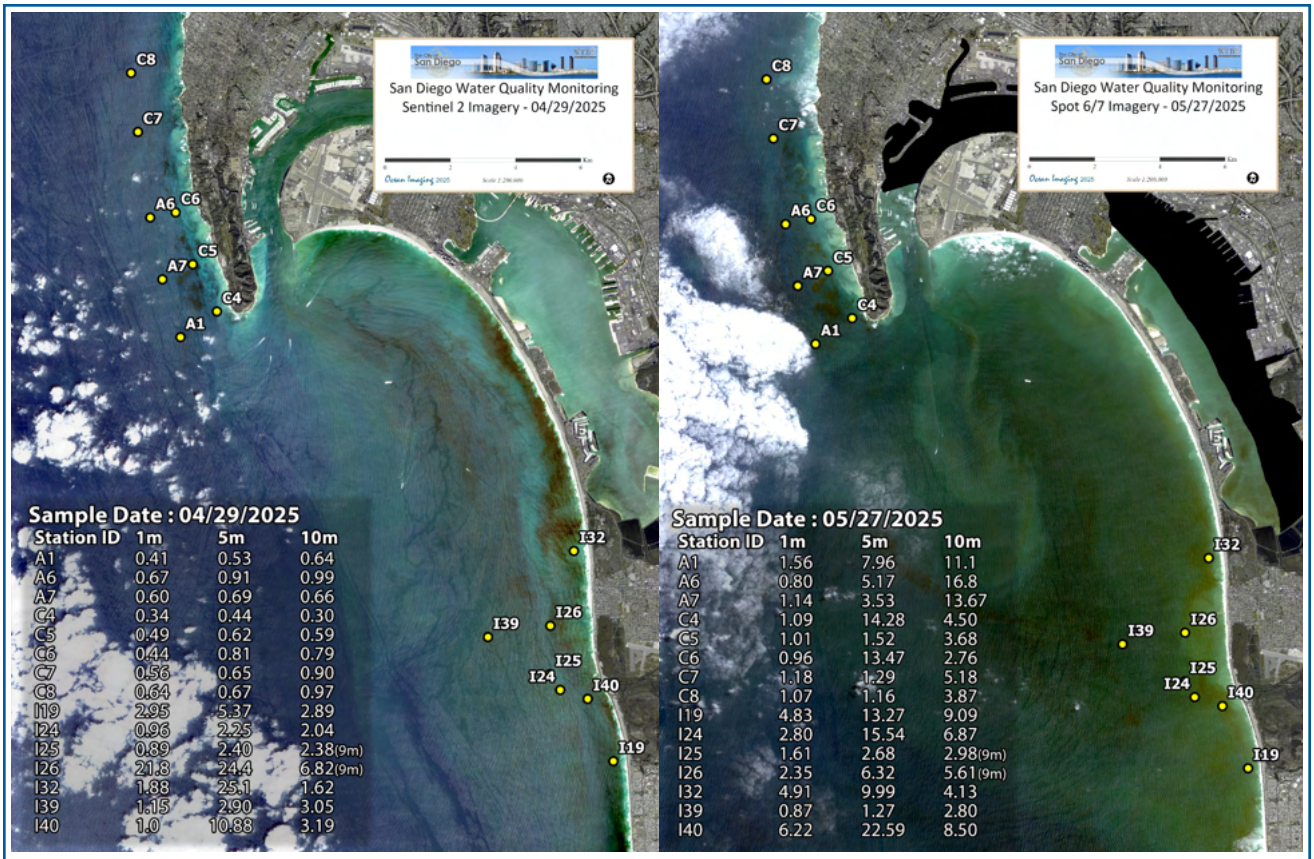


Figure 15. Sample SPOT and Sentinel-2 imagery with CTD-derived fluorometry data (chlorophyll measurements in mg/m^3) collected on the same day as the satellite acquisitions overlaid on the imagery. Generally, the image data correlates very well with the chlorophyll measurements by station. Some of the highest coastal measurements in the South Bay at I19, 124, I26 and I40 on both dates show the green or green-brown water in the image data.

May. Approximately 75% of fluorometry readings exceeding 10.0 mg/m^3 occurred during March, April, and May, which is earlier than what was observed in 2024 and more closely follows typical spring upwelling and bloom season. The higher chlorophyll readings in the months of July and August were mostly confined to the SBOO Offshore stations south of Coronado Island which is exemplified in the satellite imagery provided in Figure 14. Figure 15 offers examples of the CTD fluorometry data in correlation with the high-resolution satellite imagery on or near the same day as the field samples. While the high-resolution remotely sensed data do not depict quantitative chlorophyll levels, the green-reflecting plankton blooms are self-evident in the imagery and correlate well with the CTD data.

3.2 The South Bay Ocean Outfall Region

The South Bay International Wastewater Treatment Plant (SBIWTP) switched from advanced primary to secondary treatment in January 2011. This change resulted in the reduction of total suspended solids (TSS) concentrations from an average of 60 mg/L for several years prior to the change to the TSS loads reading consistently below 20 mg/L until late 2020. Beginning at the end of 2020, the TSS concentrations became much more variable with daily measurements peaking over 900 mg/L in early 2024. Prior to 2011, a distinct effluent signature was regularly detected in multispectral imagery as per the seasonal fluctuation described above. Since then, the effluent signature continues to be visible in the multispectral color and thermal imagery during months with weak vertical stratification,

however, more intermittently. On occasion the signature is distinctly discernable in thermal images (indicating it has fully reached the ocean surface), but undetectable in the color imagery. We theorize this is due to the reduction in TSS concentrations. Work began in 2024 to rehabilitate the SBIWTP as well as a few pump stations in Mexico. As part of a Cease-and-Desist Order in August of 2025, interim effluent limits were established for the SBIWTP and so the USIBWC increased flow through the system up to 30 MGD. In October, the flow was increased to 35 MGD but then decreased back down to 25 MGD to allow for repair of one of the pump stations (San Diego Regional Water Quality Control Board 2025).

Transboundary flows were still discharging continuously through the main channel of the Tijuana River up through early 2026. Transboundary flows are defined as instances of groundwater, urban runoff, storm water, treated sewage wastewater, and untreated sewage wastewater from infrastructure deficiencies and other sources in Mexico coming across the U.S.-Mexico border and into the into the international treatment plant, Tijuana Estuary and U.S. coastal waters via the TJR. Most of these transboundary flows occurred in the TJR main channel resulting in over 138 billion gallons coming into the U.S. system and waters from 2020 through 2025. In 2025 18,079 million gallons of this untreated water entered the U.S. (San Diego Regional Water Quality Control Board 2025). While many of these flow events were documented as increased TJR discharge visible in the 64 satellite scenes discussed above, 20 of those observations were during the dry season (May through October) and only six could be correlated to prior precipitation of 0.25 inches or more. Transboundary flows of 2,594 million gallons were recorded during the dry season (San Diego Regional Water Quality Control Board 2025). The addition of Sentinel-2C and the Sentinel-1C and 1D (data becoming available in May of 2026) will increase the amount of remote sensing data available to help in the visual documentation of this situation as the improvements to the SBIWTP and related pump stations unfold over the next few years.

From mid-April through November, the SBOO wastewater plume is predominantly confined well below the surface due to water-column stratification. During that period, it usually cannot be detected with multispectral aerial and satellite imagery, which penetrate the upper 7 m to 15 m (depending on water clarity), nor can it be detected with thermal IR imaging, which does not penetrate below the surface. Seasonal breakdown of the vertical stratification results in the plume's rise closer to the surface or to reach the surface typically between November and April when it can often be detected with satellite imaging. This concept held true in 2025, as the last observation of a SBOO surface plume during the beginning of the year was on 04/04/25 and then was not seen again in the image data until 10/29/25. In total, there were 24 instances during which the SBOO effluent plume was observed in 2025 out of the 114 high-resolution satellite scenes acquired and processed. Of the 24, there were five instances of the plume observed by different satellites on the same day. The plume was visible via three different satellites on 03/15/25. This equates to 19 days when the plume was visible in the high-resolution data – three less than observed in 2024. There were 96 days on which one or more high-resolution, multispectral satellites imaged the study area and so the SBOO plume was detected on 19.8% of satellite observations days. This is less than the average for years 2012–2024 (20.6% of the observations). The effluent surface plumes are most often seen moving to the northwest, south or as a stagnant body. There were no days when the plume was moving northeast or east toward the shoreline. Therefore, from the full set of 2025 imagery, there is no evidence in the observation data that the SBOO surface plume never came anywhere near the San Diego coast.

The months of January, November, and December exhibited the highest frequency of 2025 SBOO effluent plume observations in the satellite data. As discussed, and documented in previous reports, it is typical to see the highest number of SBOO effluent surface manifestations during these months. As is characteristically the case, the effluent surface manifestations that occurred during these periods

were most probably the result of two primary factors: the lack of strong vertical stratification during the winter months and relatively weak subsurface currents over the SBOO which allowed the undispersed effluent to reach the surface. As has been the case in previous years, there was an occurrence on 02/01/25 when the SBOO effluent plume appeared in the image data as a faint patch of clearer water breaking the more turbid water on the surface (see Appendix A). As discussed in prior reports, the clear effluent signal visible in the satellite data is most likely caused by the contrast between higher-turbidity coastal surface waters and the more typical turbidity level of effluent water as it reaches the surface. It is also possible that the effluent plume became partially diluted on its way to the surface if weak vertical stratification did exist, thus slowing down its rise in the water column. Appendix A highlights the 2025 SPOT, Sentinel-2, and Landsat multispectral imagery on days which the SBOO plume was detected. There were five occurrences when either Sentinel-2A,2B or 2C data were acquired within minutes of Landsat or SPOT 6 data providing a near time-coincident validation of features observed in then data.

Figure 16 shows the SBIWTP effluent flow rate and TSS over the 2003 through 2025 period (top) and during 2025 plotted with the dates on which SBOO effluent was observed on the surface of the ocean in the high-resolution satellite imagery (bottom). As seen in the top plot, the variability in both the SBIWTP effluent flow rate and TSS increased significantly after the beginning of 2019 and continued through 2025. On the lower graph there are a few notable spikes in flow and the TSS occurred during the year, however the TSS levels stabilized somewhat after October. Despite fluctuations in 2025, the trend line shows the average effluent flow rate of 24.6 million gallons per day (MGD) remained below the existing permit limit of 25 MGD. The TSS levels were variable between 2021–2024 with a few significant spikes in 2025, however there is no direct correlation of the SBOO effluent surface observations to TSS measurements. Of the 19 days on which the SBOO effluent was observed breaking the surface, only four occurred when the flow rate exceeded 25 MGD, and so it cannot be concluded that the additional flow diverted through SBIWTP resulted in the effluent reaching the ocean's surface more often. These data continue to support the proposed explanation that the instances of effluent reaching the surface almost always occur because of seasonal changes in ocean conditions when the water column stratification breaks down and are rarely, if ever, related to a higher flow rate through the system or water with higher TSS levels exiting the outfall.

A total of 19 shoreline stations, ranging from Mission Beach to northern Baja (across the US/Mexico border) are sampled weekly by City of San Diego staff to monitor the levels of three types of fecal indicator bacteria (i.e., total coliform, fecal coliform, Enterococcus bacteria) in recreational waters. Shore stations south of the Mesican border are sampled by the Comisión Internacional de Límites y Aguas (CILA) and analyzed by City of San Diego staff. An additional 15 nearshore (kelp) stations are also sampled weekly to monitor Fecal Indicator Bacteria (FIB) and a range of water quality parameters (i.e., temperature, salinity, dissolved oxygen, pH, transmissivity, Chlorophyl-a, colored dissolved organic matter (CDOM). Furthermore, 69 offshore stations are sampled quarterly to monitor both water quality conditions and one or more types of FIB. PLOO stations are located along, or adjacent to, the 18, 60, 80, and 98-m depth contours, and SBOO stations are located along the 9, 19, 28, 38, and 55-m depth contours.

The City Marine Microbiology Laboratory (CMML) follows guidelines issued by the U.S. Environmental Protection Agency (USEPA) Water Quality Office, State Water Resources Control Board (SWRCB) including the 2019 Ocean Plan, the California Department of Public Health (CDPH), and Environmental Laboratory Accreditation Program (ELAP) with respect to sampling and analytical procedures (Bordner et. al. 1978, American Public Health Association (APHA) 2012, CDPH 2019, USEPA 2014). All bacterial analyses were initiated within eight hours of sample collection

and conformed to standard membrane filtration techniques, for which the laboratory is certified (ELAP Field of Testing 126). FIB densities were determined and validated in accordance with USEPA and APHA guidelines as follows in APHA (2012).

In 2025, the sampling area of the SBOO/Tijuana River outflow region experienced 60 days of the 88 days sampled, on which the field sampling showed FIB measurements exceeding the single sample maximum (SSM) for fecal coliform density for one or more sampling stations as defined by the 2019 California Ocean Plan (the SSM for fecal

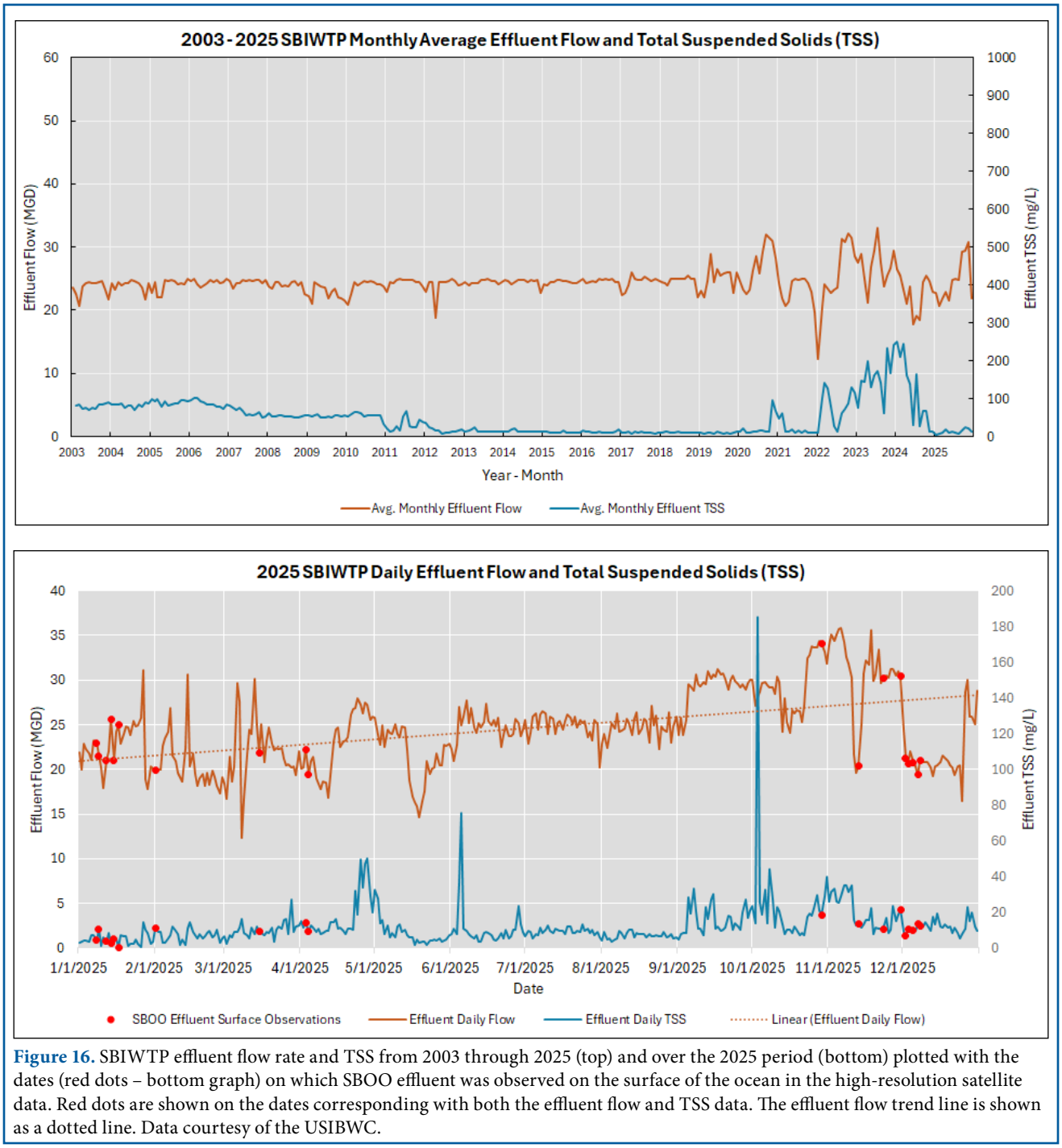
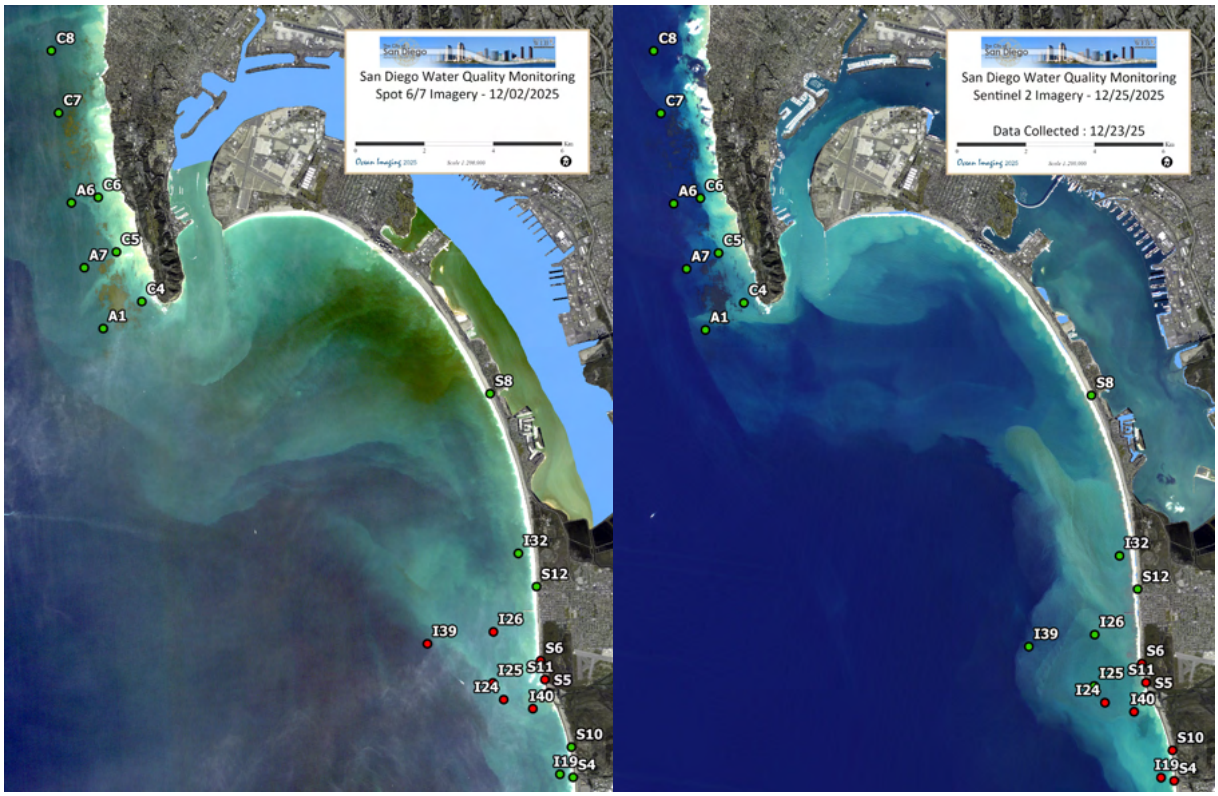


Figure 16. SBIWTP effluent flow rate and TSS from 2003 through 2025 (top) and over the 2025 period (bottom) plotted with the dates (red dots – bottom graph) on which SBOO effluent was observed on the surface of the ocean in the high-resolution satellite data. Red dots are shown on the dates corresponding with both the effluent flow and TSS data. The effluent flow trend line is shown as a dotted line. Data courtesy of the USIBWC.

coliform density at a site will not exceed 400 per 100 mL) (SWRCB 2019). The offshore SBOO region, which includes the stations over the SBOO wye, experienced only one day of elevated bacteria levels at depths of six meters or shallower and the nearshore region (referred to as the "kelp" region in previous reports) experienced 23 days on which the bacteria levels were deemed elevated. There were 48 sampling days when at least one shore station showed elevated levels. The number of sampling days for all three SBOO areas totaled 96 in 2025 and 88 in 2024. Therefore, in 2025 for the three sampling regions combined, 62.5% of the sampling days resulted in elevated bacteria levels at one station or more, which is less than the 77.3% recorded in 2024 (using the same 2019 California Ocean Plan standards). As it has been in recent years, most of the samples showing elevated levels were recorded at the shore stations. Elevated levels offshore near the SBOO wye are rare. The one sample collected when elevated bacteria levels were recorded at offshore stations (at depths of six meters or shallower), was at station I11 which is not close to the SBOO wye.

The satellite imagery showing substantial discharge from the TJR region often correlates well with times when the shoreline and kelp area sampling showed elevated bacteria levels. In past years, heavy and/or persistent rainfall was often the most plausible cause for most of the elevated bacteria samples and the turbid and/or discolored waters seen in the remote sensing data. However, given the increasing problems with untreated sewage and other pollutants flowing out of the TJR (San Diego Regional Water Quality Control Board 2025, SDRWCB 2024 and Little 2024), that premise is no longer valid in many cases. Normally, the best water quality and clarity in the South Bay region is observed during the months of May through August. This was generally true in terms of water clarity observed in the image data during the summer of 2025. However as noted above, there were transboundary flow incidents due to dry season flows from sources in Mexico prior to and after the September SBIWTP capacity ramp up (San Diego Regional Water Quality Control Board 2025). These breeches to the system undoubtedly contributed to many of the elevated FIB measurements. Figures 17 and 18 offer a few examples of the bacteria sample data overlaid on top of image data acquired on the same day (Figure 17) or a few days after the water quality sampling (Figure 18). The satellite data examples in Figure 17 were acquired on 12/02/25 and 12/23/25 neither following heavy, rain events and TJR daily mean discharge rates were 60.6 cfs, and 65.73 cfs on 12/02/25 and 12/23/25 respectively – both close to the 2025 average of 65.7 cfs. Figure 18 offers an example of a situation when the bacteria sampling (11/17/25) took place during the 11/13/25–11/18/25 rain event with the Sentinel-3 image acquired the day after on 11/19/25. The TJR discharge rate was 1,443.9 cfs on the day of image data acquisition. Note the very turbid water emanating from the TJR river and trending north in all three image examples and



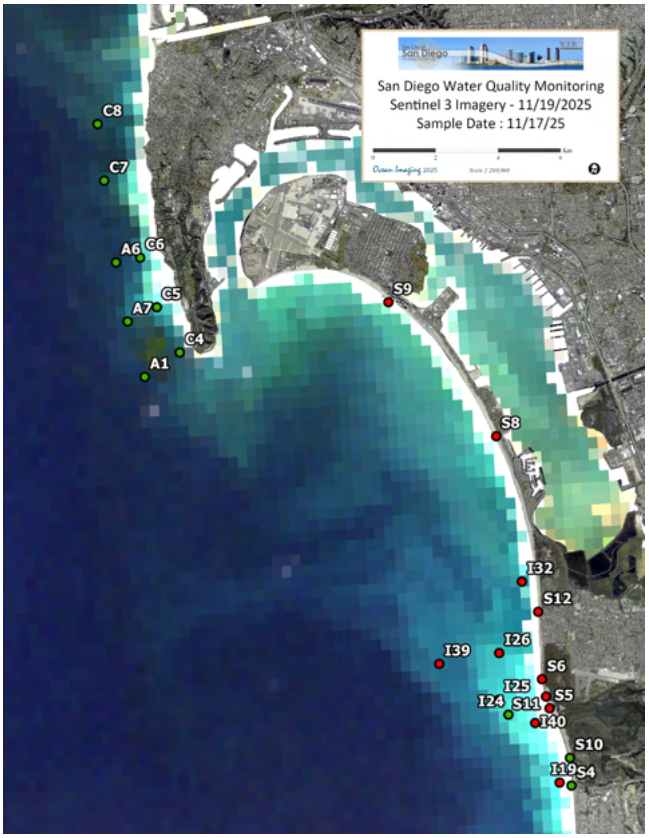
12/2/2025

STATION	DEPTH	ENTERO	FECAL	TOTAL
I19	11	110	86	280
I19	2	10	6	20
I19	6	10	6	34
I24	11	480	900	5400
I24	6	260	720	3600
I24	2	120	180	1200
I25	9	300	660	2800
I25	2	80	240	1200
I25	6	100	220	1100
I26	9	200	620	3600
I26	6	70	58	540
I26	2	90	40	800
I32	6	12	4	20
I32	2	8	2	60
I32	9	8	2	60
I39	2	340	440	3600
I39	18	98	380	940
I39	12	64	100	480
I40	2	4400	8400	16000
I40	9	3600	7400	16000
I40	6	2800	7200	16000
S0	0	6200	6000	16000
S10	0	200	40	800
S11	0	280	820	4600
S12	0	94	60	240
S2	0	100	110	340
S3	0	84	92	180
S4	0	100	78	100
S5	0	12000	12000	16000
S6	0	380	1800	4200
S8	0	2	2	20
S9	0	24	18	20

12/23/2025

STATION	DEPTH	ENTERO	FECAL	TOTAL
I19	2	1400	600	2600
I19	6	620	400	2200
I19	11	4	8	6
I24	2	1200	2000	6400
I24	6	460	600	2600
I24	11	58	80	320
I25	2	22	30	160
I25	6	26	26	80
I25	9	2	2	4
I26	2	280	380	2200
I26	6	34	38	100
I26	9	2	2	2
I32	2	2	2	2
I32	6	2	2	2
I32	9	2	2	2
I39	2	2	2	2
I39	12	2	2	2
I39	18	2	2	2
I40	6	860	3400	8600
I40	9	800	2400	7800
I40	2	1400	1200	9600
S0	0	4400	6000	16000
S10	0	3800	4000	15000
S11	0	12000	12000	16000
S12	0	2	2	2
S2	0	32	4	16
S3	0	600	52	720
S4	0	720	960	4000
S5	0	8000	4200	16000
S6	0	6800	12000	16000
S8	0	2	2	2
S9	0	2	4	18

Figure 17. SPOT and Sentinel-2 data with near-surface bacterial sampling data overlaid from the same day of the image acquisition date. Red dots at SBOO (I, S) stations indicate exceedances of the total coliform, fecal coliform, and/or enterococcus SSMs (2015 Ocean Plan). Green dots identify stations at which the FIB levels were in compliance. The tables below each image show the measurement values by depth for each SBOO station with elevated bacteria levels in red text. The left image and table show the satellite data acquired on 12/02/25 with sample data overlaid from the same day The right image and table show satellite and bacteria sample data from 12/23/25.



STATION	DEPTH	ENTERO	FECAL	TOTAL
I19	11	2000	1400	9400
I19	6	1200	1000	5200
I19	2	1400	860	10000
I24	6	460	300	3400
I24	11	180	180	1000
I24	2	120	160	1300
I25	6	400	260	1600
I25	9	320	180	2000
I25	2	100	80	1000
I26	9	700	2400	6200
I26	2	500	1100	5400
I26	6	780	1000	7400
I32	6	800	6200	16000
I32	9	900	2400	15000
I32	2	200	800	6600
I39	2	120	1000	9400
I39	12	80	820	5200
I39	18	52	380	1800
I40	6	220	440	1200
I40	9	540	400	3600
I40	2	520	320	2800
S10	0	NA	100	NA
S11	0	NA	12000	NA
S12	0	NA	7600	NA
S4	0	NA	54	NA
S5	0	NA	12000	NA
S6	0	NA	800	NA
S8	0	NA	8200	NA
S9	0	NA	5000	NA

Figure 18. Sentinel-3 data acquired on 11/19/25 with near-surface bacterial sampling data overlaid from 11/17/25. Red dots at SBOO (I, S) stations indicate exceedances of the total coliform, fecal coliform, and/or enterococcus SSMs (2015 Ocean Plan). Green dots identify stations at which the FIB levels were in compliance. The table to the right of the image shows the measurement values by depth for each SBOO station with elevated bacteria levels in red text.

that on 11/17/25 the samples with FIB exceeding the SSM were taken as far north as Coronado.

3.3 The Point Loma Outfall Region

After its seaward extension in 1993, the Point Loma Ocean Outfall (PLOO) is one of the deepest and longest wastewater outfalls in the world, discharging at a depth of 320 feet (~97.5 m), 4.5 miles (7.25 kilometers) offshore. The outfall's plume is very rarely observed directly with multispectral color or thermal imagery. It appears to not reach the surface waters, even during the winter months when the water column's vertical stratifications are weakened. We believe that on a few occasions over the past twenty years we have observed the plume's extents indirectly through an anomalous lateral displacement of thermal or chlorophyll features around the outfall wye. This effect can be explained by the doming up of the discharged effluent and laterally displacing the near-surface waters above it, however this situation is highly unusual.

In 2025 the Point Loma region was affected by conditions already described for general San Diego County: significant seasonal rainfall during the months of March and November with average or below average precipitation for all other months. Similar to past years, compromised water clarity was likely a result of runoff from the San Diego River and Mission Bay bringing sediment-laden water inside and outside the Point Loma kelp bed after the rain events described in section 3.1 above.

The 2025 Point Loma shoreline, kelp and offshore bacterial sampling resulted in a comparable number of elevated bacteria measurements when contrasted to previous years as defined by the 2015 California Ocean Plan (Total coliform density will not exceed 10,000 per 100 mL; or Fecal coliform density will not exceed 400 per 100 mL; or Total coliform density will not exceed 1,000 per 100 mL when the ratio of fecal/total coliform exceeds 0.1; or enterococcus density will not exceed 104 per 100 mL) (SWRCB 2015). Out of 111 total sample days, there were 12 days on which elevated bacteria levels were measured at one or more stations in this region. In 2025 for the three PLOO sampling areas combined, 10.8% of the sampling days resulted in elevated bacteria levels at one station or more, which is lower than recorded in 2023 and 2024 (17.4% and 14.4% respectively). The shoreline sampling yielded two days on which one or more stations experienced high bacteria counts. The offshore sampling resulted in eight days when FIB were over the SSM and the kelp stations recorded two days on which station A7 was out of compliance for

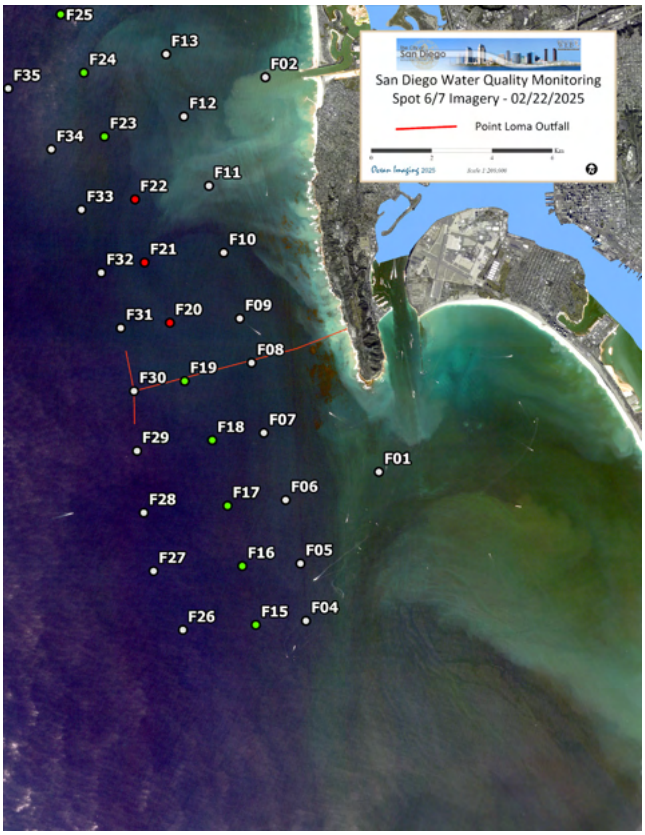


Figure 19. SPOT scenes acquired on 02/22/25 with bacterial sampling data from the same day overlaid on the image. Red dots at PLOO stations (F) indicate fecal coliform densities in exceedance of the fecal coliform SSM (2015 Ocean Plan). Green dots identify stations at which the FIB levels were in compliance and white dots show the stations that were not sampled on that day. The table to the right of the image shows the measurement values by depth for each station with elevated bacteria levels in red text. The SDR discharge was heavier than normally observed in the satellite imagery and there is no evidence of the PLOO effluent plume at the ocean's surface.

STATION	DEPTH	ENTERO	FECAL	TOTAL
F15	1	2	NA	NA
F15	25	2	NA	NA
F15	60	90	NA	NA
F15	80	2	NA	NA
F16	1	2	NA	NA
F16	25	2	NA	NA
F16	60	4	NA	NA
F16	80	8	NA	NA
F17	1	2	NA	NA
F17	25	2	NA	NA
F17	60	2	NA	NA
F17	80	14	NA	NA
F18	1	2	NA	NA
F18	25	2	NA	NA
F18	60	18	NA	NA
F18	80	52	NA	NA
F19	1	2	NA	NA
F19	25	2	NA	NA
F19	60	50	NA	NA
F19	80	62	NA	NA
F20	60	480	NA	NA
F20	1	2	NA	NA
F20	25	2	NA	NA
F20	80	68	NA	NA
F21	80	200	NA	NA
F21	1	2	NA	NA
F21	25	2	NA	NA
F21	60	22	NA	NA
F22	60	240	NA	NA
F22	80	180	NA	NA
F22	1	2	NA	NA
F22	25	2	NA	NA
F23	1	2	NA	NA
F23	25	2	NA	NA
F23	60	48	NA	NA
F23	80	68	NA	NA
F24	1	2	NA	NA
F24	25	2	NA	NA
F24	60	88	NA	NA
F24	80	100	NA	NA
F25	1	2	NA	NA
F25	25	2	NA	NA
F25	60	36	NA	NA
F25	80	86	NA	NA

the FIB SSM. Figure 19 (above) provides one example of when three of the eleven stations sampled on 02/22/25 in the Point Loma sampling region resulted in non-compliant SSM numbers. Stations F1 – F14 and F26 – F35 were not sampled on this day. The SPOT imagery reveals a possible explanation for the elevated FIB numbers as the SDR discharge is more visible than normal and is heading in the direction of the stations with elevated samples. However, the elevated levels were all found at depths between 60 and 80 meters. The stations exhibiting elevated levels were all northeast of the PLOO diffusers and so it is also inconclusive that the high SSM readings were directly related to the effluent exiting the PLOO at a depth of ~97.5 m. The HF Radar currents from that day (not depicted in the figure) show the ocean surface currents moving the water south, yet the HYCOM-derived surface currents (also not shown) contradict this with the water movement heading north. If the HYCOM currents are correct and are translated to the depth of the samples, this could indicate that high-bacteria effluent originating from the outfall may have been trapped by a pycnocline barrier below the surface and was being pushed northward to stations F20 – F22. Currents at the depths of the elevated samples were not available for analysis. Otherwise, the source of the high FIB levels could be attributed to the SDR river discharge. While the direct cause is not known, the imagery in Figure 19 is provided to show the significant discharge from the river as well as the lack of surface manifestation from the PLOO effluent which is rarely, if ever seen, due to the depth of the outfall.

3.4 Kelp Variability

One observation provided by the satellite image archive is the continuing variability in the size of the Point Loma kelp bed over time (Figure 20). Table 4 shows the area in km^2 of three notable kelp beds in the San Diego region over the past 18 years. The September and October dates were chosen to represent the kelp bed canopy coverage for each year since spring and fall are the time periods when the canopy size is considered to be at or near its peak - with fall being the preferred season to map kelp using remote sensing techniques. The estimated size of the Point Loma bed canopy in the fall of 2025 (3.22 km2) was significantly larger than measured in 2024, but still smaller than the average canopy coverage for the prior 17-year period from 2008–2024 (3.77 km2). As reported previously, the satellite data show the bed begin to decrease in size during February of 2016, perhaps due to the storm events taking place during early to mid-January, effects from the 2014–2016 strong El Niño event and/or the Northeast Pacific marine heat wave (Di Lorenzo 2016). Noted in the 2017 and 2018 annual reports, the kelp bed appeared to be coming back in January of 2017 but then decreased in size as the year progressed resulting in much smaller than average canopy coverage by the end of that year. Using the fall imagery as an indicator for annual health, the bed size appeared to be stabilizing since the 2016 and 2017 lows, with another decline in 2023 and 2024 yet we see a possible resurgence in 2025 (Figure 21). The intra-annual variability, during 2025 exhibited the same lower canopy coverage for the first half of the year, but beginning in July showed canopy growth through the end of the year. (Figure 22). An interesting observation is that the Imperial Beach kelp bed, albeit exceedingly small, was visible in the satellite data during 2025 – the first time since 2015. The first readily identifiable appearance of the canopy was in October with observations extending into December. While there were significant differences in tidal heights at the time of each satellite image acquisition, tides cannot be flagged as the primary reason for any difference in canopy coverage observed in the satellite data. There were days when the areal coverage was high, but the tide level was also high and vice versa when the imagery revealed smaller bed size, but the tides were relatively low.

Canopy coverage for each year in Table 4 and Figure 21 was computed by first running a Normalized Difference Vegetation Index (NDVI) classification followed by either a Support Vector Machine or iso cluster unsupervised classification to generate a single exposed kelp class (ESRI 2024, ESRI 2025). It is important to point out that the canopy

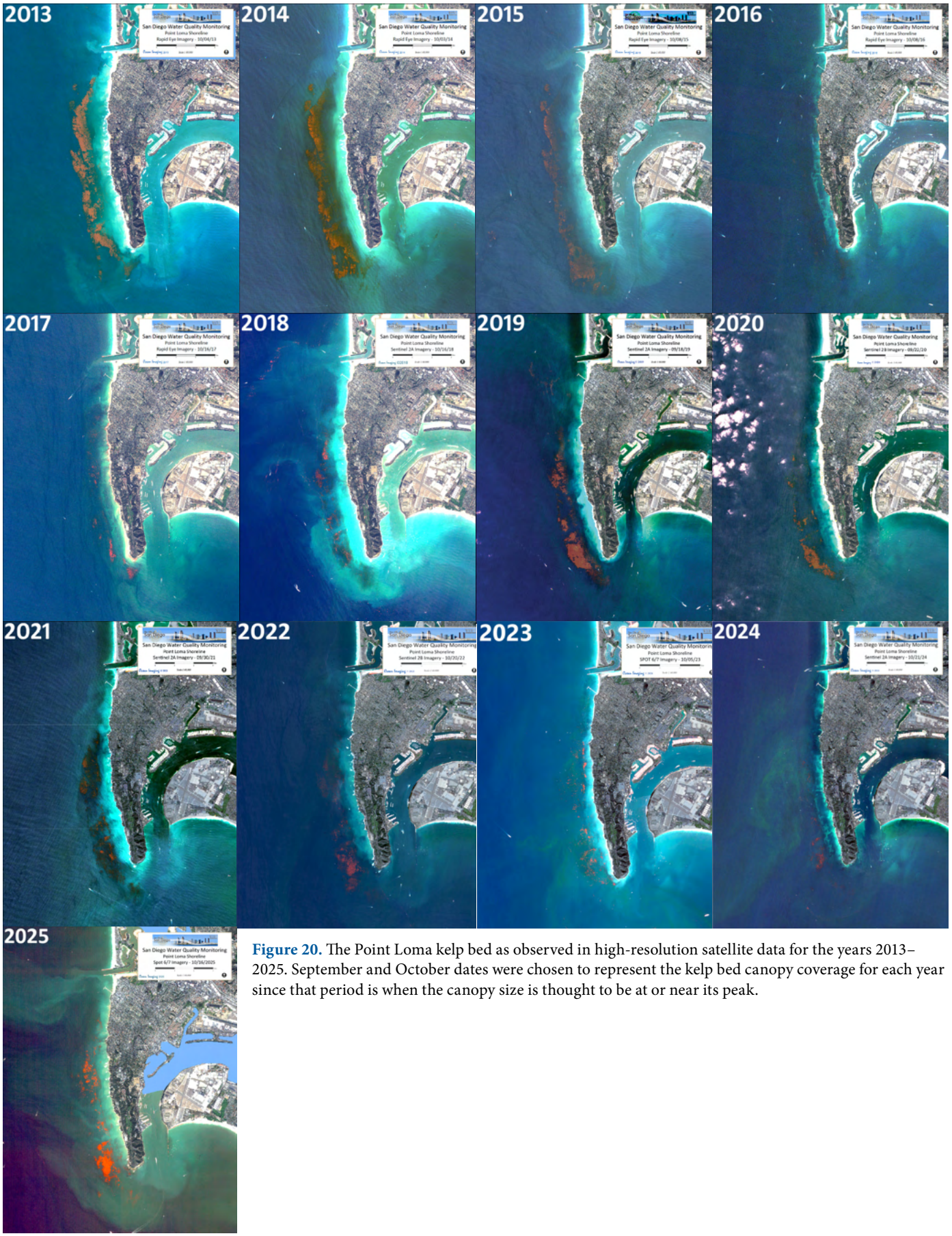


Figure 20. The Point Loma kelp bed as observed in high-resolution satellite data for the years 2013–2025. September and October dates were chosen to represent the kelp bed canopy coverage for each year since that period is when the canopy size is thought to be at or near its peak.

coverage shown in Table 4 may differ slightly from those provided in the Region Nine Kelp Survey Consortium Aerial Kelp Survey Reports. This is because in these reports for each year of surveys, photographs from quarterly surveys during which the greatest aerial coverage was observed for

Table 4. Kelp canopy areas of three San Diego kelp beds measured from satellite data collected for this project.

			Kelp (km²)		
Year	Date	Satellite	Point Loma	Imperial Beach	Tijuana
2025	10/16/25	SPOT 6/7	3.22	0.02	0.00
2024	10/21/24	Sentinel-2A	0.88	0.00	0.00
2023	10/05/23	SPOT 6/7	2.14	0.00	0.00
2022	10/20/22	Sentinel-2B	4.48	0.00	0.00
2021	09/30/21	Sentinel-2B	3.82	0.00	0.00
2020	09/22/20	Sentinel-2A	2.93	0.00	0.00
2019	09/18/19	Sentinel-2A	5.17	0.00	0.00
2018	10/16/18	Sentinel-2A	2.44	0.00	0.00
2017	10/04/17	RapidEye	1.05	0.00	0.00
2016	09/08/16	RapidEye	0.22	0.00	0.00
2015	09/17/15	Landsat 7	4.11	0.39	0.29
2014	09/14/14	Landsat 8	5.42	0.59	0.30
2013	09/23/13	RapidEye	5.89	0.19	0.05
2012	09/15/12	RapidEye	2.91	0.00	0.00
2011	09/01/11	RapidEye	1.99	0.00	0.00
2010	09/27/10	Landsat 7	6.01	0.00	0.00
2009	09/16/09	Landsat 5	5.96	1.01	0.21
2008	09/05/08	Landsat 7	8.66	0.82	0.01

* Average surface canopy coverage 2008–2024 = 3.77 km²

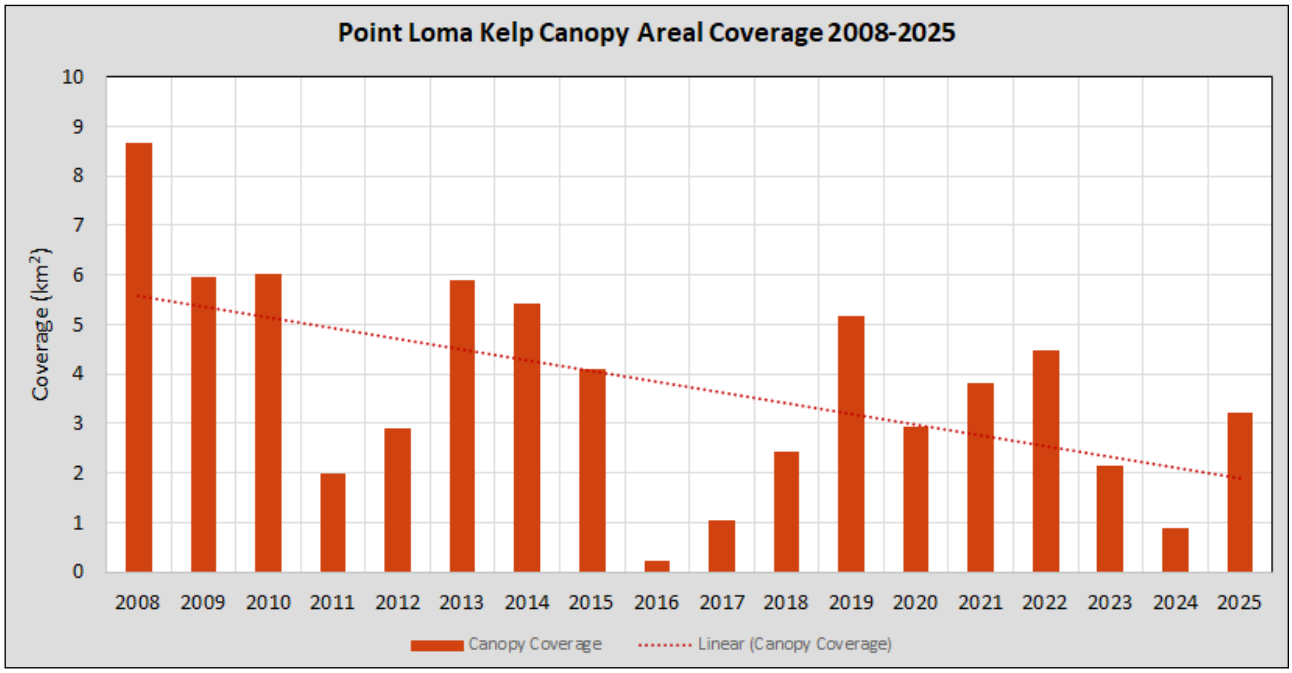


Figure 21. Point Loma kelp canopy coverage 2008–2025. Calculations were from imagery acquired on the September and October dates shown in Table 4 above. The dates were chosen to represent the kelp bed canopy coverage for each year since the September to October time period is when the canopy size is most likely at its peak. The dotted line shows a linear trend line over the period.

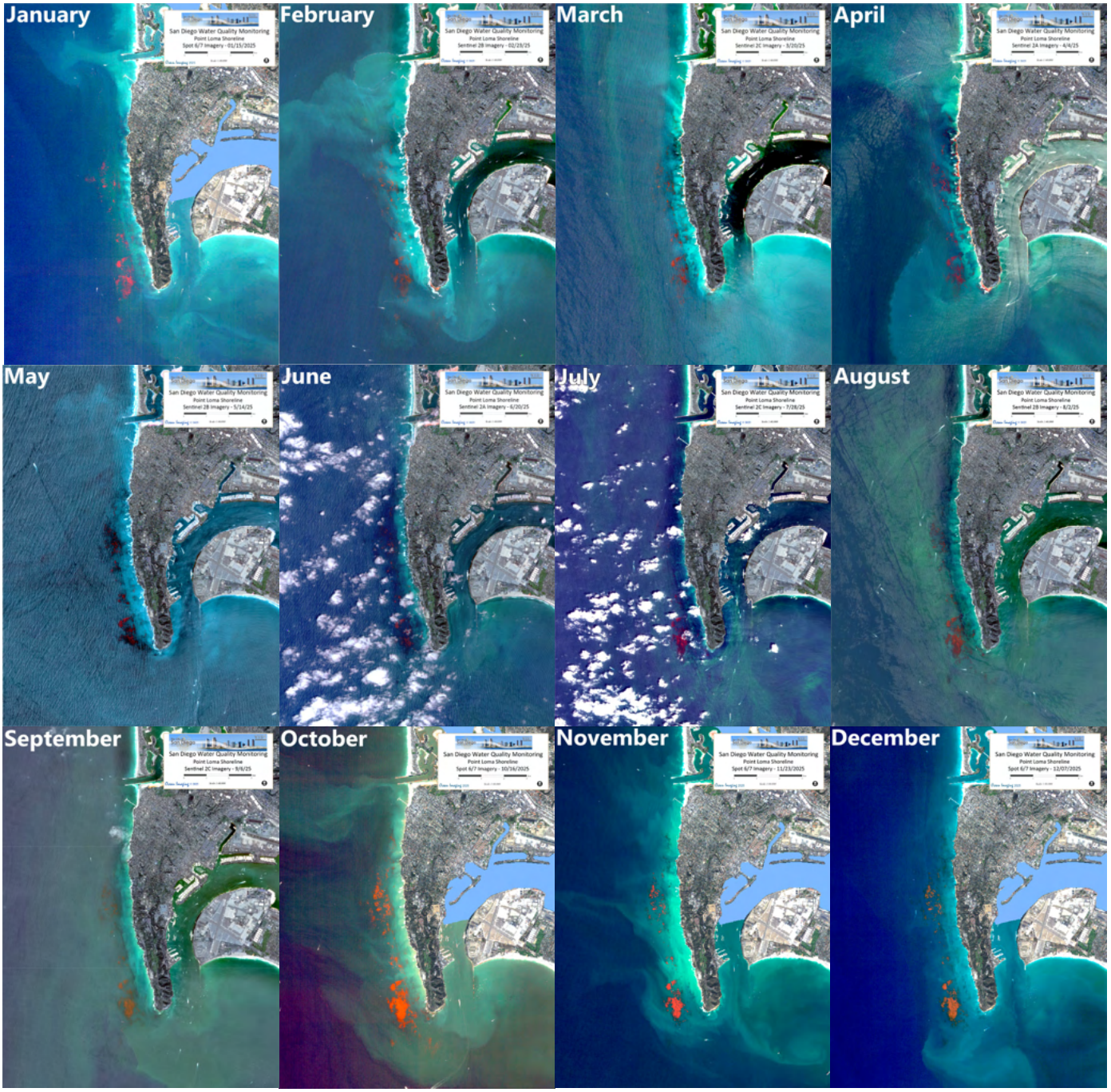


Figure 22. High-resolution satellite data documenting the month-to-month variability in the PointLoma kelp bed canopy coverage. The dates were chosen to best represent the maximum-observed canopy coverage for each month.

each kelp bed were assembled into a composite photo-mosaic representing an annual overview of the region's kelp beds canopy coverage; while the coverage estimates shown in this report are taken from single satellite images acquired during the fall time period chosen to represent the maximum coverage experienced during that time of year. Tide levels were not a factor in the inter-year comparison as there was little variability in tide level between the years (often approximately two feet or less). However, due to the overflight times of these satellites, the canopy areas could be underrepresented compared to the kelp survey reports because the tide levels at the time of satellite data acquisition could vary significantly from the tides during the aerial surveys. The Imperial Beach and Tijuana beds have not been visible in the satellite data since 2015. It is being documented that kelp forests along the West Coast have been experiencing noteworthy variability in canopy size for the past several years, and thus warrants keeping a close watch on the health of the kelp beds in the San Diego region (Bell et al. 2020 and Schroeder 2019).

4. PRESENT AND FUTURE ENHANCEMENTS OF THE PROJECT

As discussed in the 2024 report, in 2025 OI launched an interactive dashboard-style web portal to provide quicker access to select high-resolution imagery as well as many other tabular data such as water quality, CTD and river discharge data. The site incorporates an interactive WMS to serve as a mechanism to better facilitate the visualization viewing of existing and future satellite image data products as well as any other tabular data sets the City chooses to host on the platform. At present the site is password-protected and for internal use only by SDPUD employees and their partners. The server hosts present, near real-time imagery and tabular data as well as data from the previous two years. Discussions have also begun regarding the development of a public-facing data dashboard hosting most of the same datasets that have been vetted through the City's quality control procedures. As part of this process, the historical imagery, tabular data, and reports will remain accessible via the existing web portal. If a public-facing dashboard style data portal is implemented by the City, OI will progressively work backwards in time to make all historical data available via this platform, including the archived imagery and additional data products.

5. REFERENCES

[APHA] American Public Health Association. (2012). "Standard Methods for the Examination of Water and Wastewater, 22nd edition." *American Public Health Association, American Water Works Association, and Water Environment Federation.*

Bell, Tom W., et al. "Three Decades of Variability in California's Giant Kelp Forests from the Landsat Satellites." *Remote Sensing of Environment*, vol. 238, 2020, p. 110811., doi:10.1016/j.rse.2018.06.039.

Biggs, T. W., et al. (2022). Runoff and sediment loads in the Tijuana River: Dam impacts and climate variability. *Journal of Hydrology: Regional Studies,* 41, 101064. https://doi.org/10.1016/j.ejrh.2022.101064

Bordner, R., Winter, J., Scarpino, P., eds., 1978. "Microbiological Methods for Monitoring the Environment: Water and Wastes, EPA Research and Development," EPA-600/8-78-017.

[CDPH] California State Department of Public Health website. (2019). "Regulations for Public Beaches and Ocean Water-Contact Sports Areas." A*ppendix A: Assembly Bill 411, Statutes of 1997, Chapter765*. https://www.cdph.ca.gov/Programs/CEH/DRSEM/Pages/EMB/RecreationalHealth/Beaches-and-Recreational-Waters.aspx

Di Lorenzo, E., Mantua, N. "Multi-year persistence of the 2014/15 North Pacific marine heatwave." *Nature Climate Change 6*, 1042–1047 (2016). https://doi.org/10.1038/nclimate3082

[ESRI 2024] "ISO Cluster Unsupervised Classification (Spatial Analyst)." *Iso Cluster Unsupervised Classification (Spatial Analyst)-ArcGIS Pro | Documentation*, https://pro.arcgis.com/en/pro-app/3.4/tool-reference/spatial-analyst/iso-cluster-unsupervised-classification.htm. Accessed 15 May 2024.

[ESRI 2025] "Train support vector machine classifier (Spatial Analyst)." ArcGIS Pro Documentation. Retrieved March, 2025, from ArcGIS Pro tool reference

Gierach, M. M., Holt, B., Trinh, R., Pan, B.J., Rains, C., 2017. "Satellite detection of wastewater diversion plumes in Southern California." *Estuarine, Coastal and Shelf Science*, 186, 171 – 182.

Gudino-Elizondo, N., Biggs, T., Bingner, R., & Langendoen, E. (2019). Modelling runoff and sediment loads in a developing coastal watershed of the US–Mexico border. Water, 11(5), 1024. https://doi.org/10.3390/w11051024

International Boundary and Water Commission, United States and Mexico (IBWC). 2026. Tijuana River at International Boundary (Station 11-0133.00) discharge data, 2024–2025. IBWC Water Data Portal. Available at: https://waterdata.ibwc.gov/ (accessed , 2026).

Kahru, Mati, and B. Greg Mitchell. "Spectral reflectance and absorption of a massive red tide off Southern California." *Journal of Geophysical Research: Oceans, vol. 103, no. C10, 15 Sept. 1998, pp. 21601–21609*, https://doi.org/10.1029/98jc01945.

Little, Joe. "Toxic Tide: The Sewage Crisis at the Border." *NBC 7 San Diego, NBC 7 San Diego, 12 Jan. 2024*, www.nbcsandiego.com/news/local/toxic-tide-the-sewage-crisis-at-the-border/3391666/.

Ocean Imaging, Inc. 2021. Satellite Coastal Water Quality Monitoring in the San Diego/Tijuana Region: Annual Summary Report, 1 January 2021–31 December 2021. Prepared for the City of San Diego Public Utilities Department and the International Boundary and Water Commission.

Ocean Imaging, Inc. 2023. Satellite Coastal Water Quality Monitoring in the San Diego/Tijuana Region: Annual Summary Report, 1 January 2023–31 December 2023. Prepared for the City of San Diego Public Utilities Department and the International Boundary and Water Commission.

San Diego Regional Water Quality Control Board. (2025, April). San Diego Regional Water Quality Control Board April 2025 meeting [Video]. YouTube. https://www.youtube.com/live/9SpqCJsl9O4

Schroeder, Sarah B., et al. "Passive Remote Sensing Technology for Mapping Bull KELP (NEREOCYSTIS Luetkeana): A Review of Techniques and Regional Case Study." *Global Ecology and Conservation, vol. 19, 2019,* doi:10.1016/j.gecco.2019.e00683.

[SDRWCB] San Diego Regional Water Quality Control Board. "San Diego Region - Executive Officer's Reports." *Executive Officer's Report | San Diego Regional Water Quality Control Board*, www.waterboards.ca.gov/sandiego/publications_forms/publications/eoreports.html. Accessed 25 Mar. 2025.

Southern California Coastal Water Research Project, 10 May 2019, "Harmful Algal Blooms." https://www.sccwrp.org/about/research-areas/eutrophication/harmful-algal-blooms/.

[SWRCB] California State Water Resources Control Board. (2015). California Ocean Plan, Water Quality Control Plan, Ocean Waters of California. California Environmental Protection Agency, Sacramento, CA.

[SWRCB] California State Water Resources Control Board. (2019). California Ocean Plan, Water Quality Control Plan, Ocean Waters of California. California Environmental Protection Agency, Sacramento, CA.

Svejkovsky, J., Haydock, I., 1998. "Satellite remote sensing as part of an ocean outfall environmental monitoring program." *Taking a Look at California's Ocean Resources: An Agenda for the Future*, ASCE, Reston, VA (USA), 2, 1306.

Svejkovsky, J., Jones, B., 2001. "Satellite Imagery Detects Coastal Stormwater and Sewage Runoff." *EOS-Trans. American Geophys. Union*, 82(50).

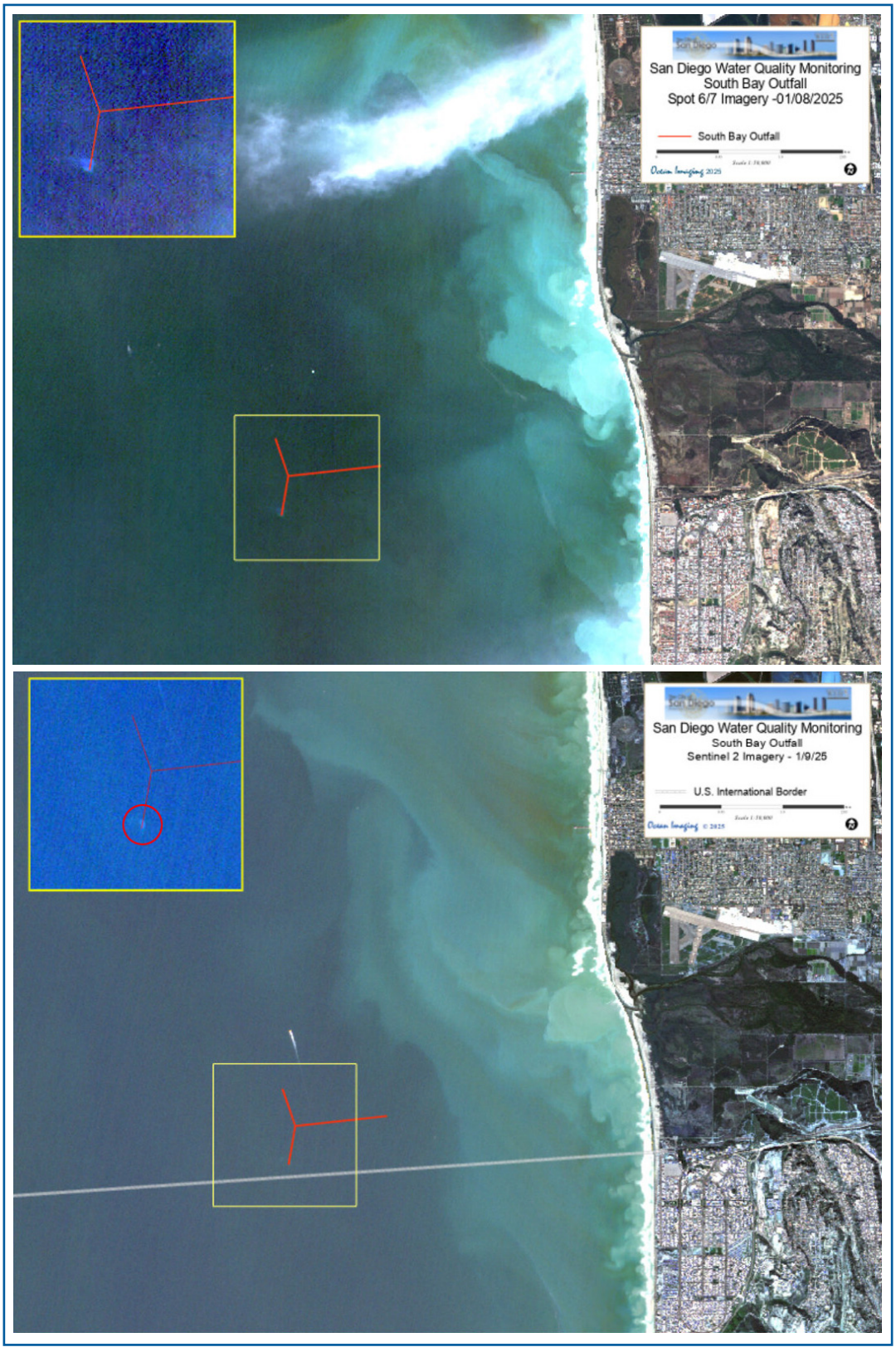
Svejkovsky, J., Shandley, J., 2001. "Detection of offshore plankton blooms with AVHRR and SAR imagery." *Int. J. of Remote Sensing*, 22 (2&3), 471-485.

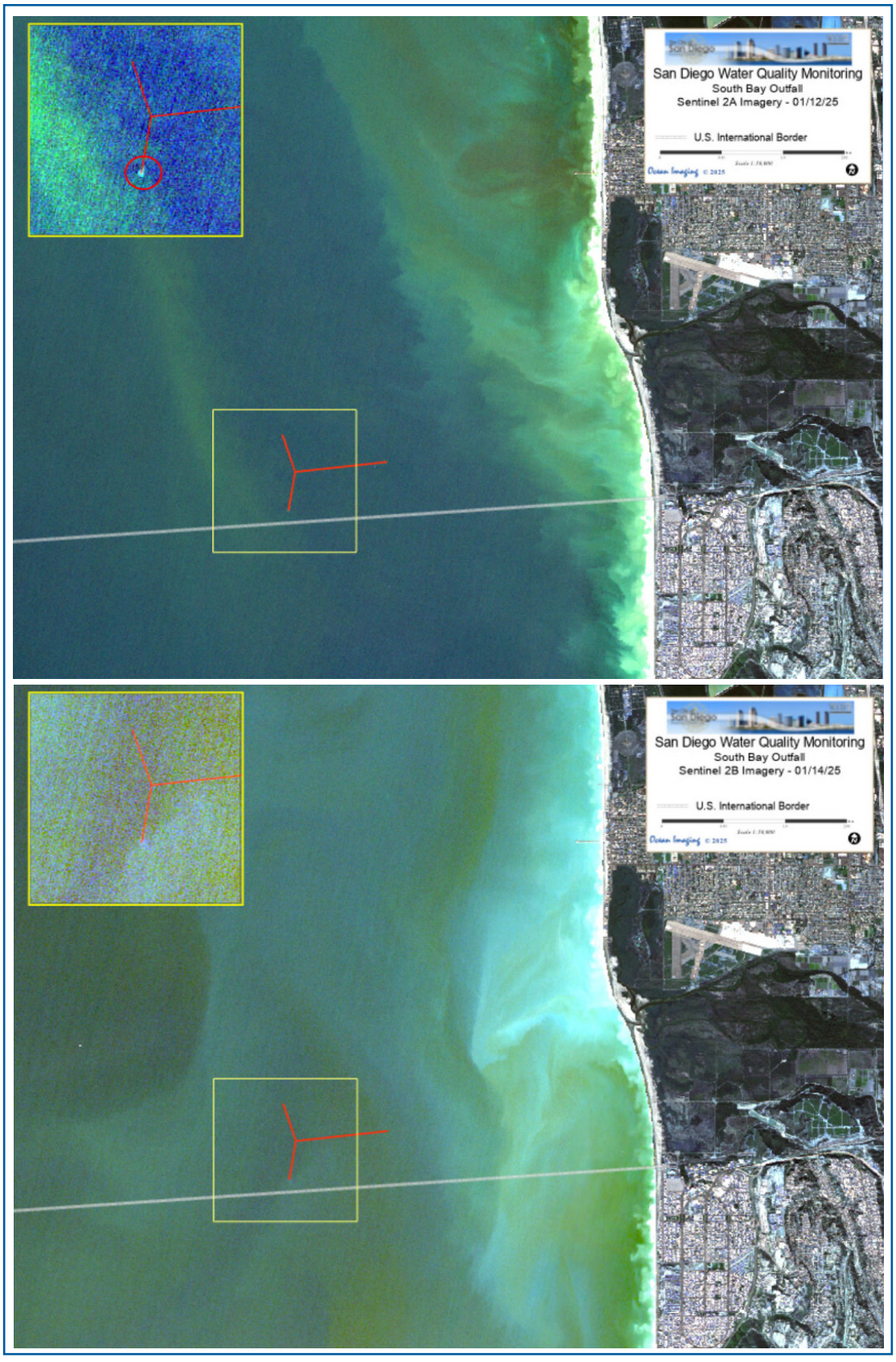
Svejkovsky, J., Nezlin, N. P., Mustain, N.M. Kum, J. B., 2010. "Tracking storm water discharge plumes and water quality of the Tijuana River with multispectral aerial imagery." *Estuarine, Coastal and Shelf Science*. 87(3), 387-398.

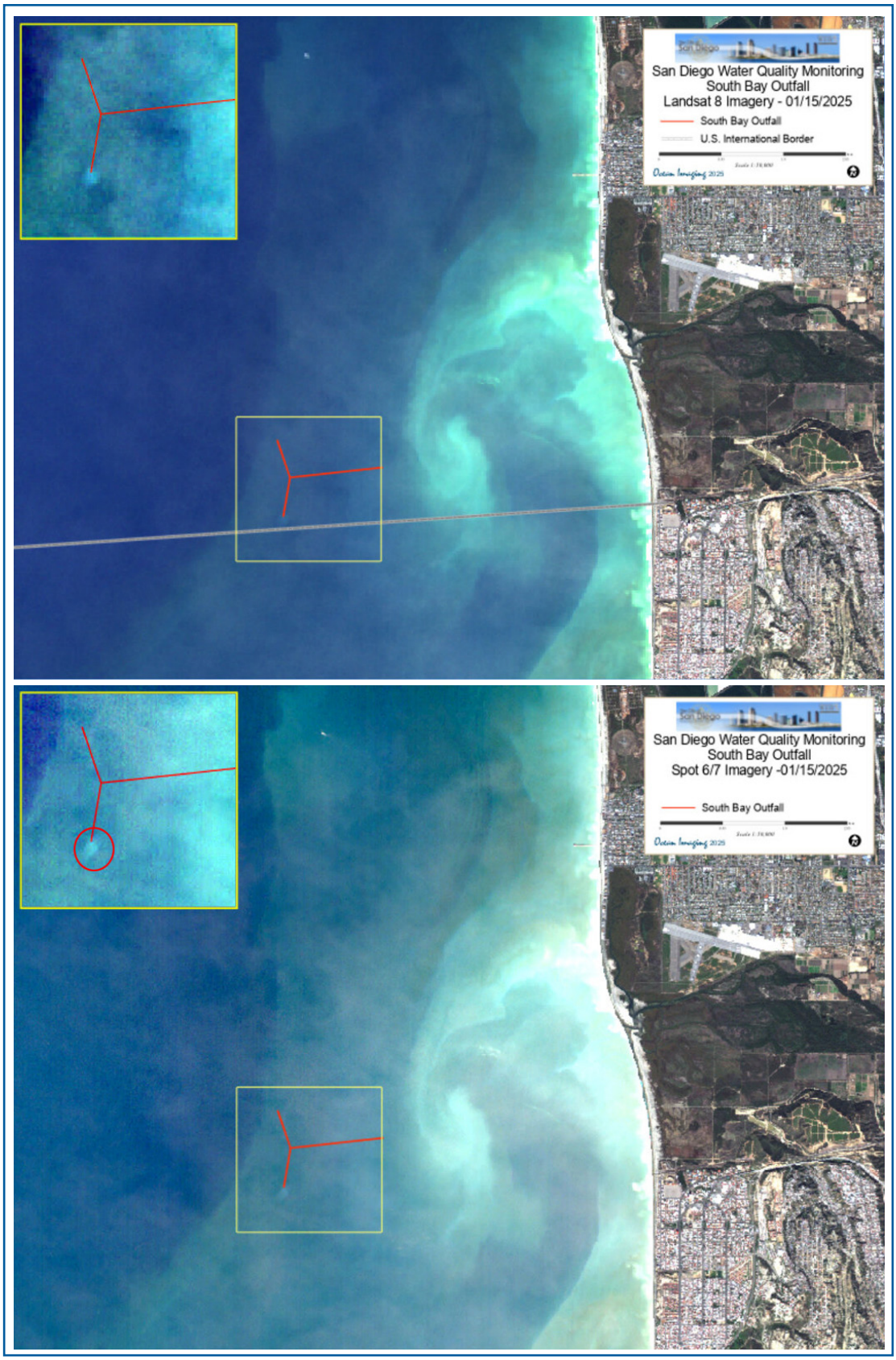
[USEPA] United States Environmental Protection Agency. (2014). Method 1600: "Enterococci in Water by Membrane Filtration Using membrane-Enterococcus Indoxyl-β-D-Glucoside Agar (mEI)." *EPA Document EPA-821-R-14-011*. Office of Water (4303T), Washington, DC.

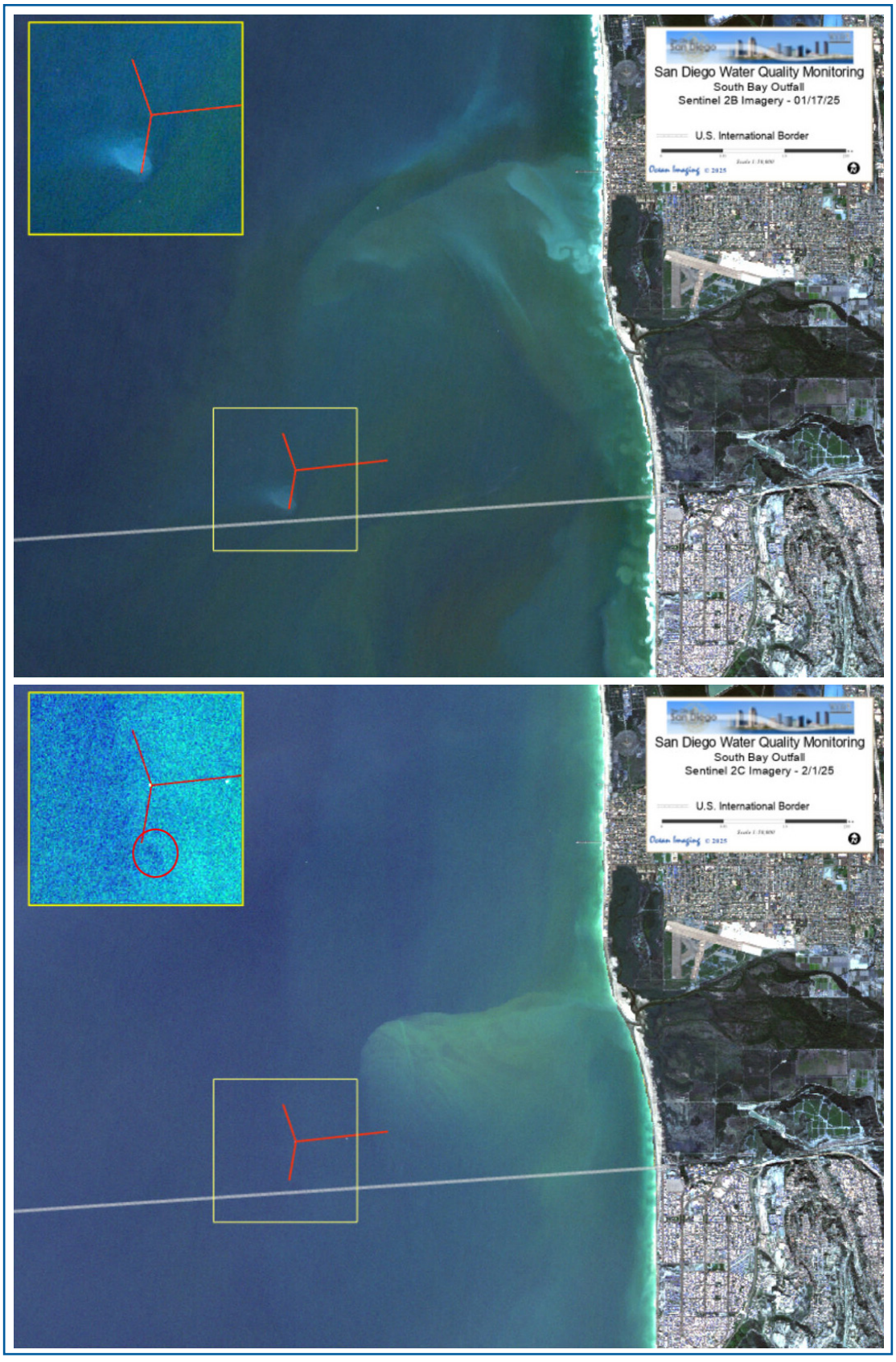
Zheng, Q., Klemas,V.V., Coastal Ocean Environment. Comprehensive Remote Sensing." *Elsevier*, Amsterdam (2018), pp. 89-120.

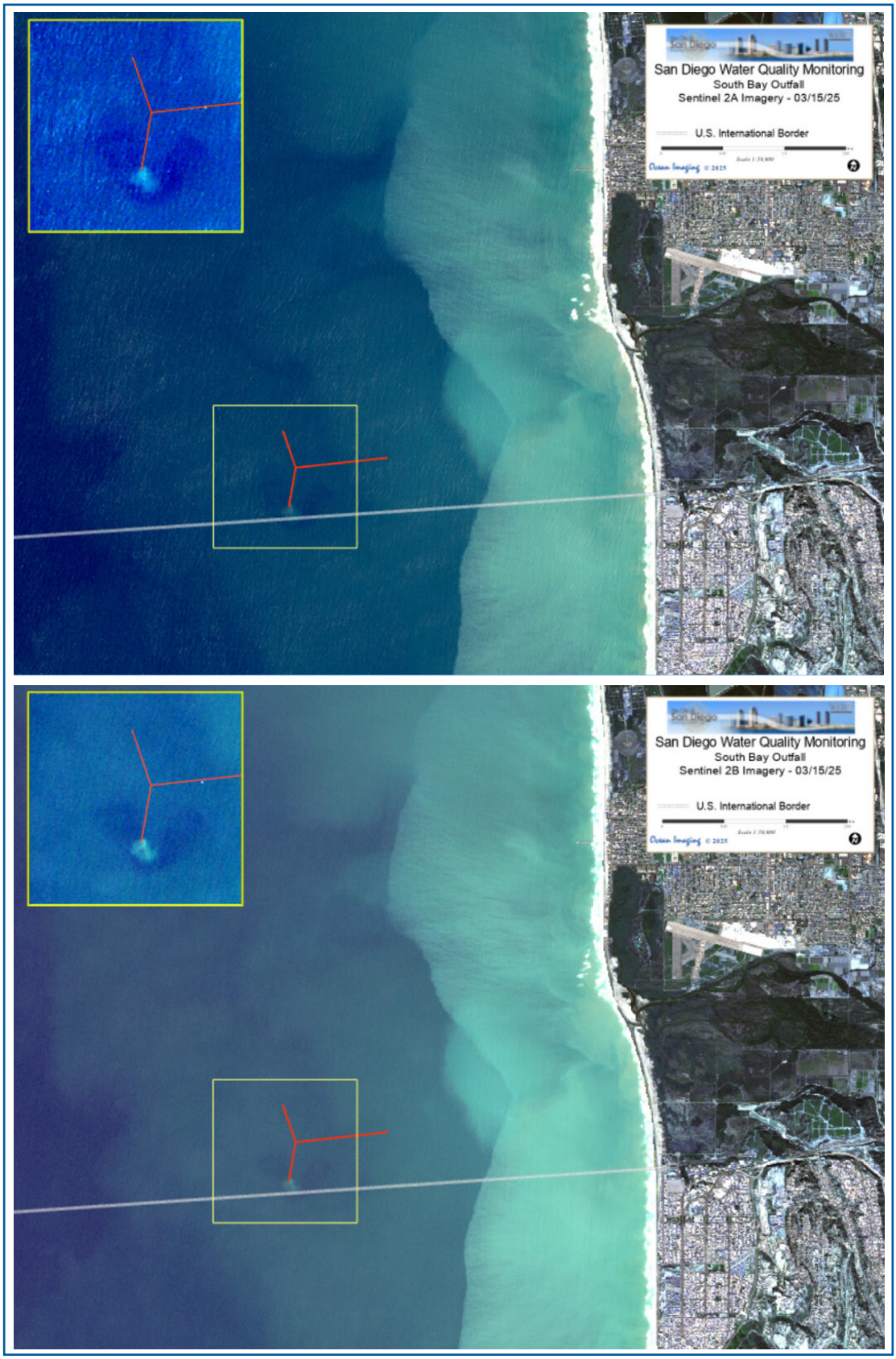
APPENDIX A – HIGH-RESOLUTION SATELLITE IMAGERY SHOWING SBOO-RELATED WASTEWATER PLUME

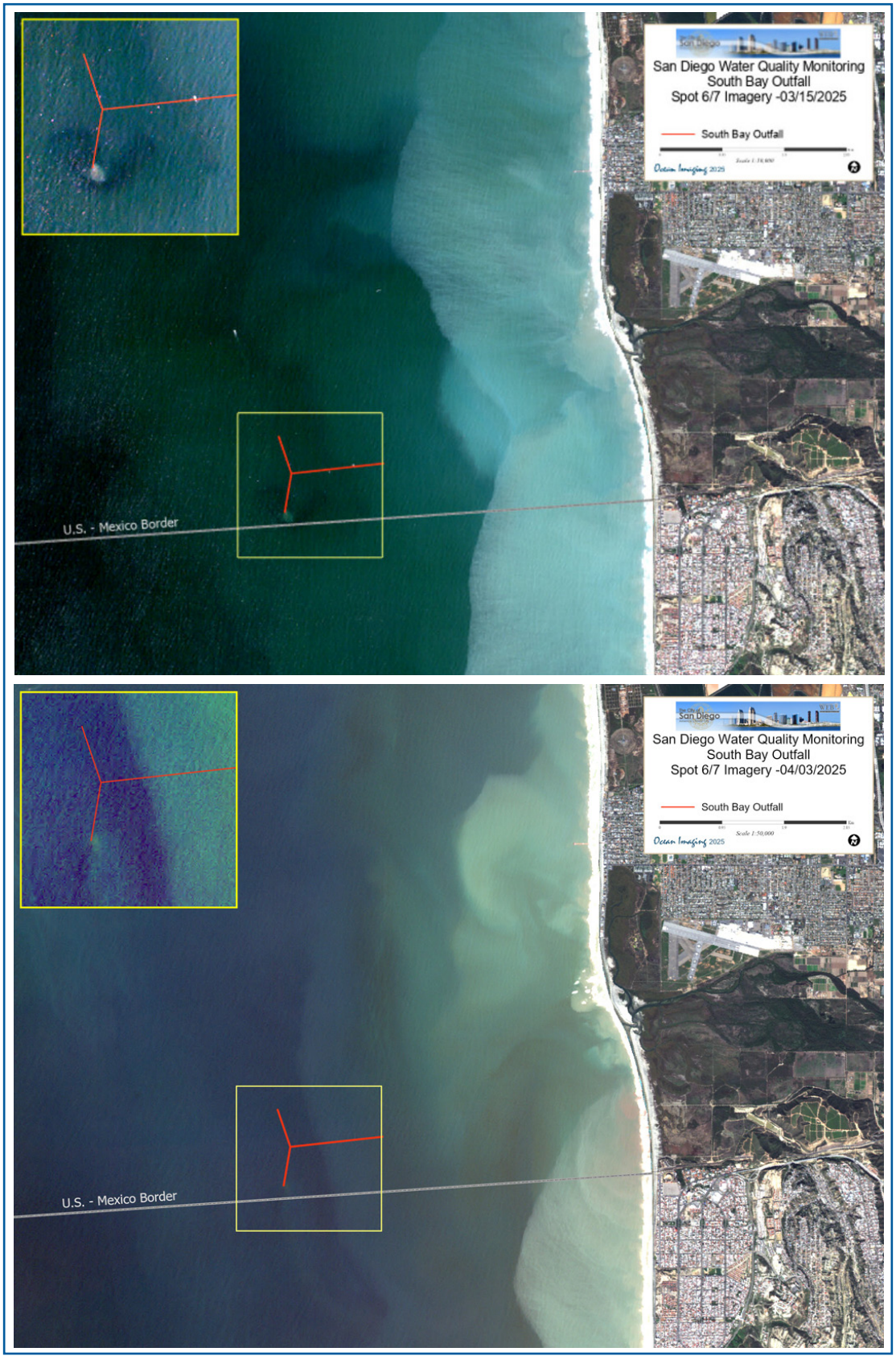


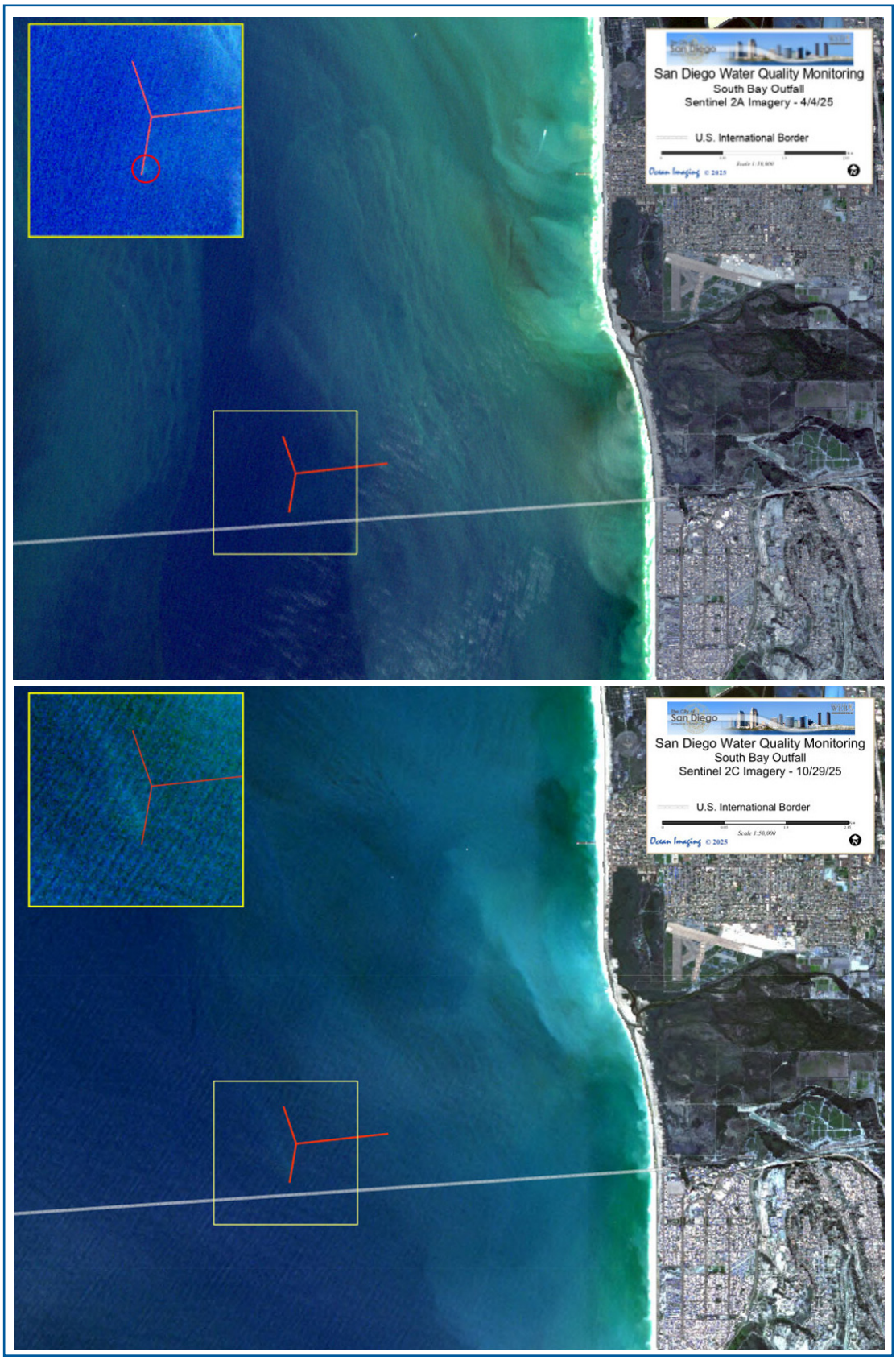

San Diego Water Quality Monitoring
South Bay Outfall
Sentinel 2A Imagery - 01/12/25
U.S. International Border
San Diego Water Quality Monitoring
South Bay Outfall
Sentinel 2B Imagery - 01/14/25
U.S. International Border

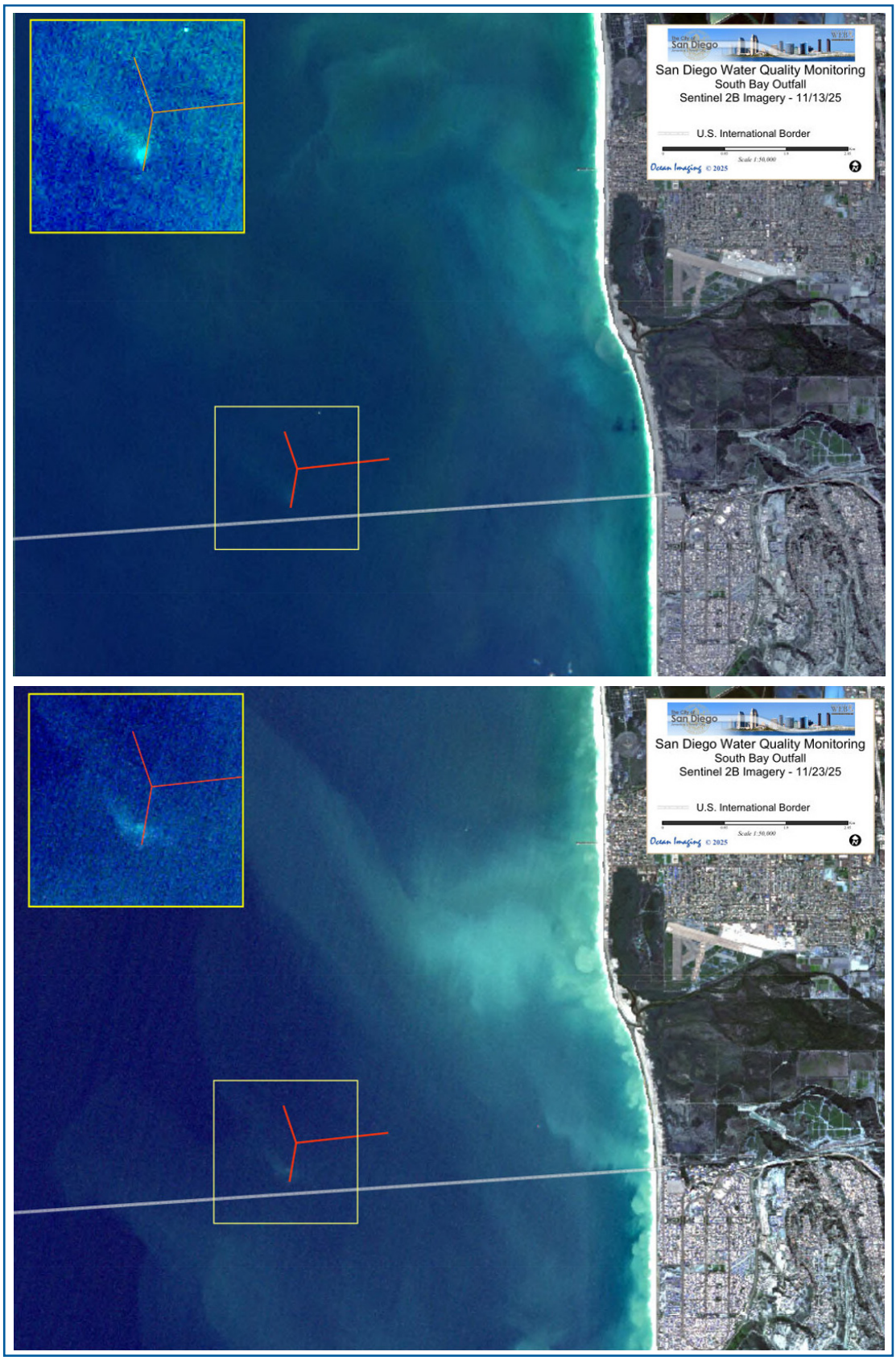

San Diego Water Quality Monitoring
South Bay Outfall
Landsat 8 Imagery - 01/15/2025
South Bay Outfall
U.S. International Border
San Diego Water Quality Monitoring
South Bay Outfall
Spot 6/7 Imagery -01/15/2025
South Bay Outfall

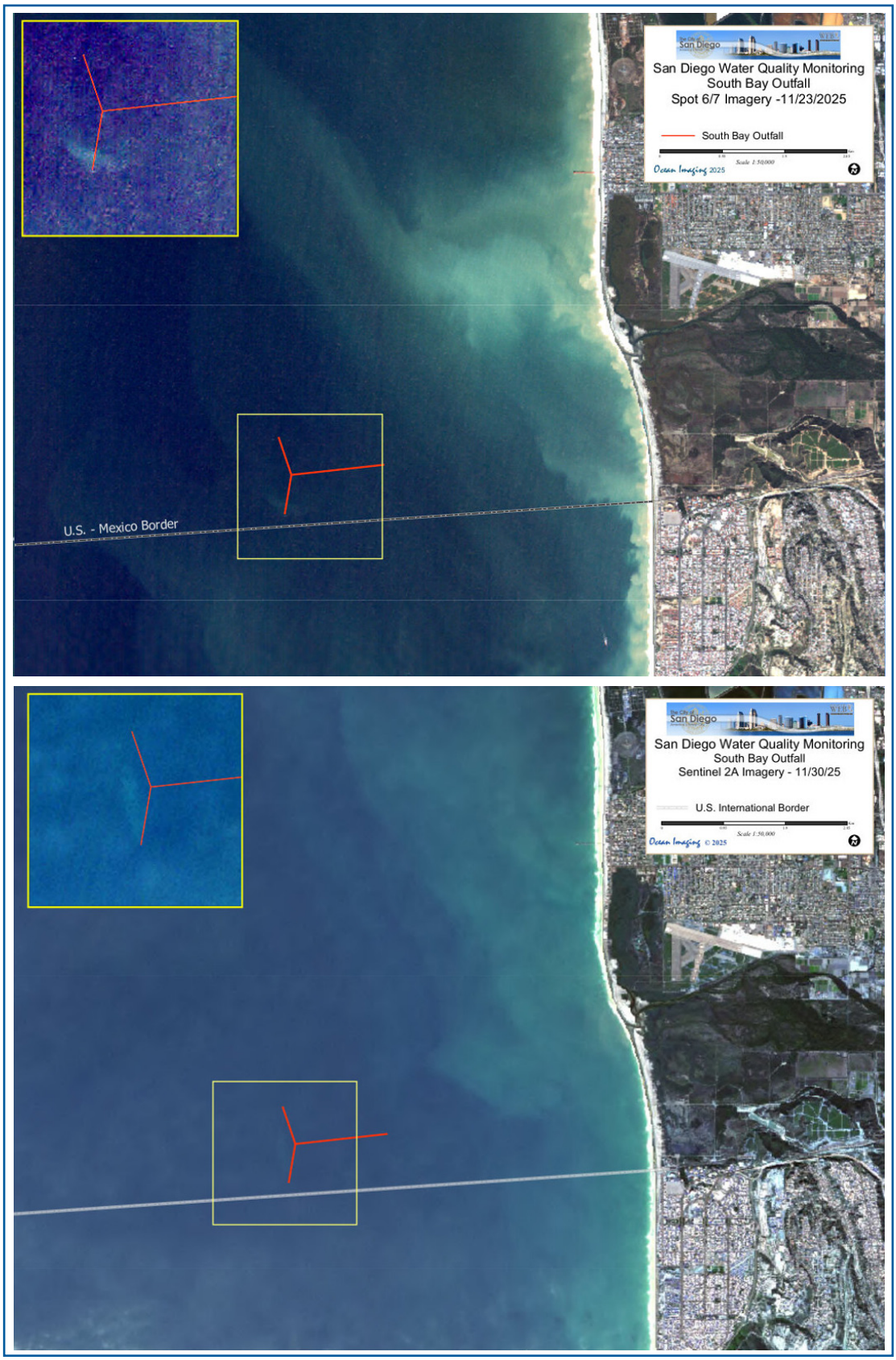

San Diego Water Quality Monitoring
South Bay Outfall
Sentinel 2B Imagery - 01/17/25
U.S. International Border
San Diego Water Quality Monitoring
South Bay Outfall
Sentinel 2C Imagery - 2/1/25
U.S. International Border

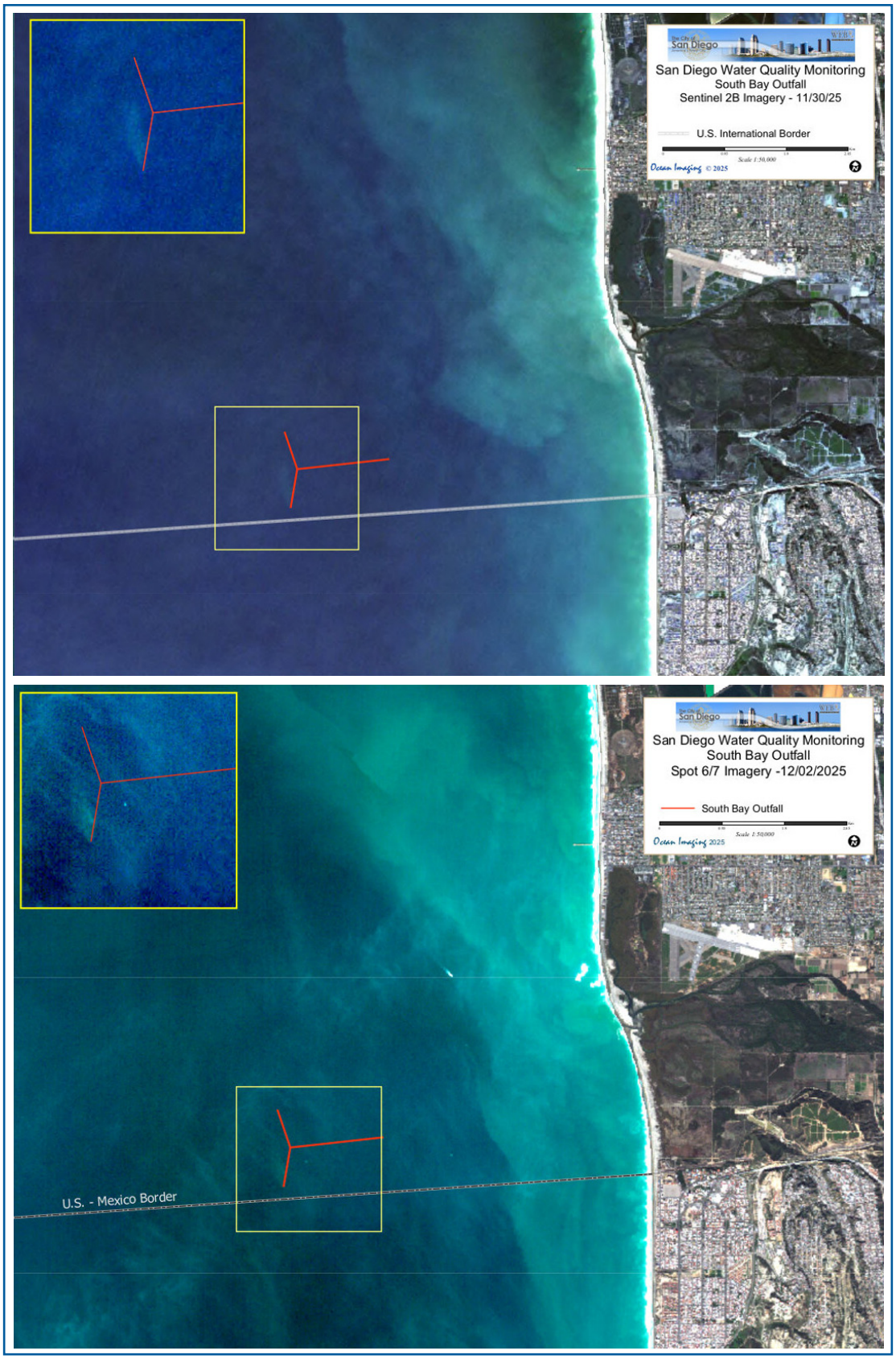

San Diego Water Quality Monitoring
South Bay Outfall
Sentinel 2A Imagery - 03/15/25
U.S. International Border
San Diego Water Quality Monitoring
South Bay Outfall
Sentinel 2B Imagery - 03/15/25
U.S. International Border

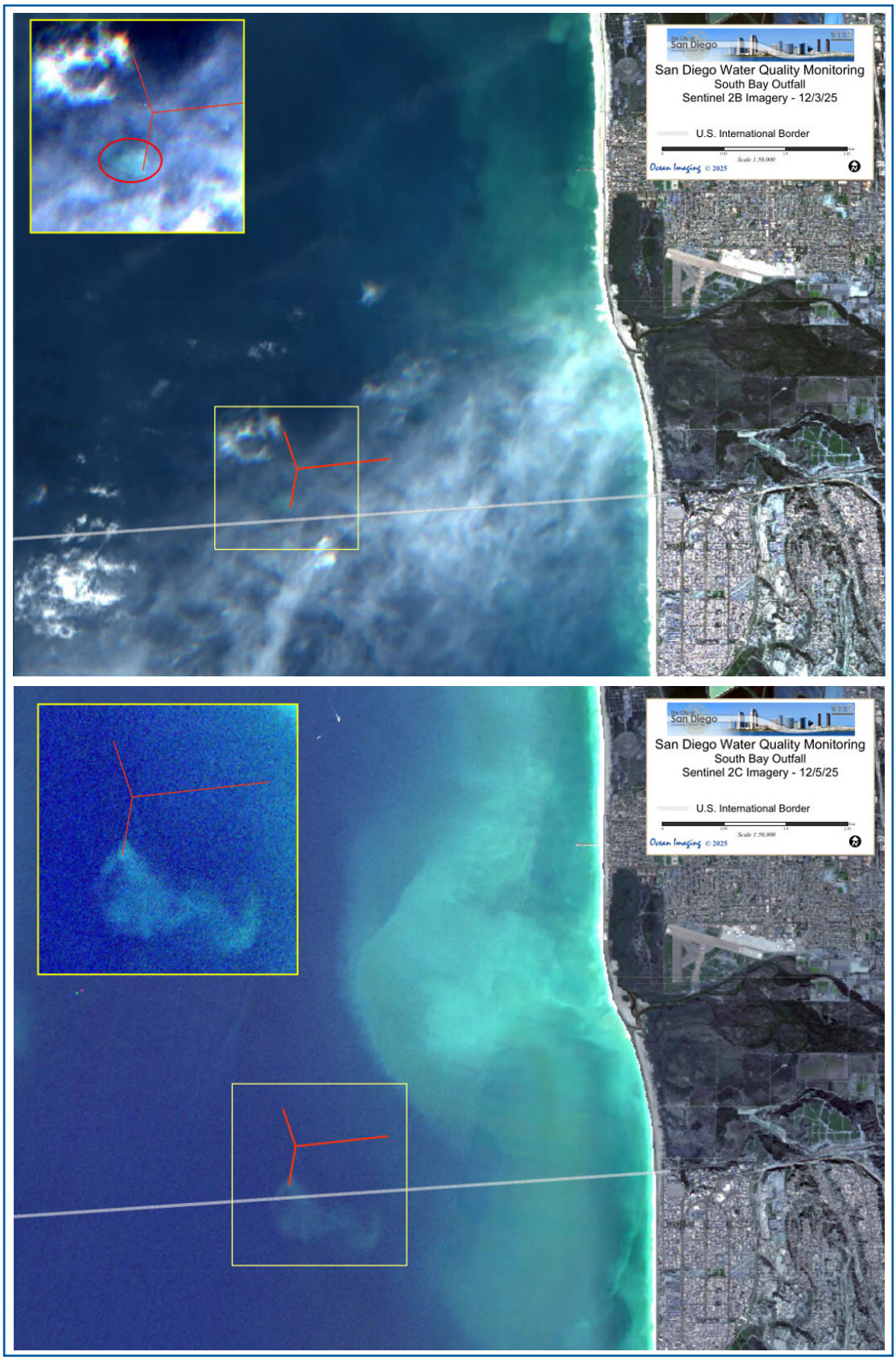

San Diego Water Quality Monitoring
South Bay Outfall
Spot 6/7 Imagery -03/15/2025
South Bay Outfall
Ocean Imaging 2025
U.S. - Mexico Border
San Diego Water Quality Monitoring
South Bay Outfall
Spot 6/7 Imagery -04/03/2025
South Bay Outfall
Scale 1:50,000
Ocean Imaging 2025
U.S. - Mexico Border

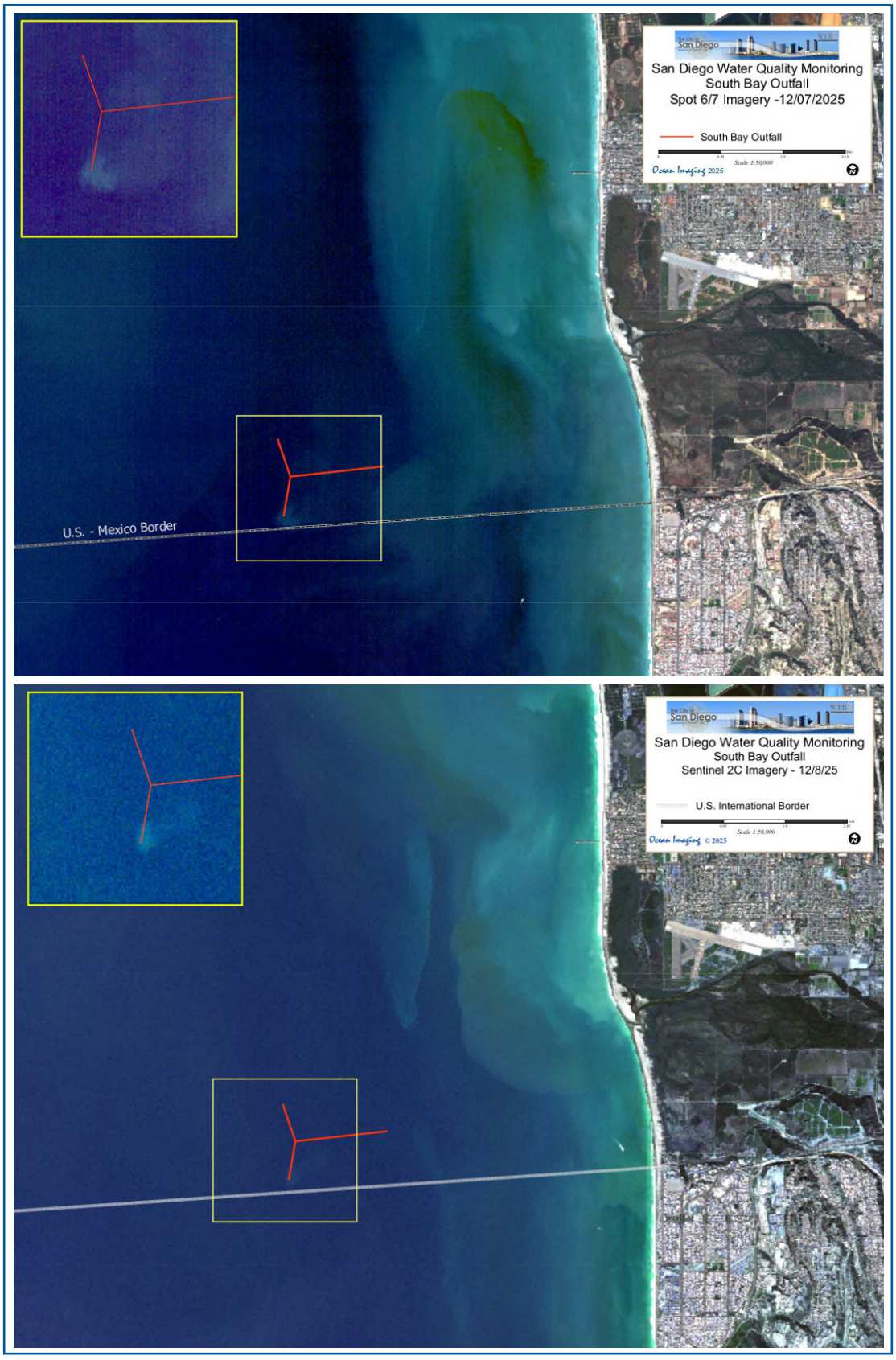

San Diego Water Quality Monitoring
South Bay Outfall
Sentinel 2A Imagery - 4/4/25
U.S. International Border
Ocean Imaging © 2025
San Diego Water Quality Monitoring
South Bay Outfall
Sentinel 2C Imagery - 10/29/25
U.S. International Border
Scale 1:50,000
Ocean Imaging © 2025


San Diego Water Quality Monitoring
South Bay Outfall
Sentinel 2B Imagery - 11/13/25
U.S. International Border
Ocean Imaging © 2025
San Diego Water Quality Monitoring
South Bay Outfall
Sentinel 2B Imagery - 11/23/25
U.S. International Border
Ocean Imaging © 2025


San Diego Water Quality Monitoring
South Bay Outfall
Spot 6/7 Imagery -11/23/2025
South Bay Outfall
Ocean Imaging 2025
U.S. - Mexico Border
San Diego Water Quality Monitoring
South Bay Outfall
Sentinel 2A Imagery - 11/30/25
U.S. International Border
Ocean Imaging © 2025


San Diego Water Quality Monitoring
South Bay Outfall
Sentinel 2B Imagery - 11/30/25
U.S. International Border
Ocean Imaging © 2025
San Diego Water Quality Monitoring
South Bay Outfall
Spot 6/7 Imagery -12/02/2025
South Bay Outfall
Ocean Imaging 2025
U.S. - Mexico Border


San Diego Water Quality Monitoring
South Bay Outfall
Sentinel 2B Imagery - 12/3/25
U.S. International Border
Ocean Imaging © 2025
San Diego Water Quality Monitoring
South Bay Outfall
Sentinel 2C Imagery - 12/5/25
U.S. International Border
Ocean Imaging © 2025


San Diego Water Quality Monitoring
South Bay Outfall
Spot 6/7 Imagery -12/07/2025
South Bay Outfall
Ocean Imaging 2025
U.S. - Mexico Border
San Diego Water Quality Monitoring
South Bay Outfall
Sentinel 2C Imagery - 12/8/25
U.S. International Border
Ocean Imaging © 2025

Appendix K

Ocean Acidification Monitoring Progress Report

2019-2024

OCEAN ACIDIFICATION MONITORING PROGRESS REPORT FOR THE POINT LOMA AND SOUTH BAY OCEAN OUTFALL REGIONS, SAN DIEGO, CALIFORNIA

Progress Report
September 2025

Report Period: 2019 - 2024

City of San Diego Point Loma Wastewater Treatment Plant
(NPDES CA0107409; Order No. R9-2017-0007 as amended by Order No. R9-2022-0078)

City of San Diego South Bay Water Reclamation Plant
(NPDES CA0109045; Order No. R9-2021-0011)

U.S. IBWC South Bay International Wastewater Treatment Plant
(NPDES CA0108928; Order No. R9-2021-0001)

Ocean Monitoring Program Manager
Ryan M. Kempster (rkempster@sandiego.gov)

Ocean Operations Supervisor
Adriano Feit (afeit@sandiego.gov)

Ocean Acidification Monitoring Lead
Coulson Lantz (clantz@sandiego.gov)

Ocean Acidification Inter-Agency Liaison
Ami Latker (alatker@sandiego.gov)

City of San Diego, Environmental Monitoring and Technical Services Laboratory,
2392 Kincaid Road, San Diego, CA 92101

Table of Contents

Ocean Acidification Monitoring Progress Report 3

1. **Background 3**
2. **Methods 3**
3. **Results 5**
4. **Conclusions and Recommendations 7**

Works Cited 9

Tables 11

Figures 16

Appendices 22

Appendix A 22

Appendix B 23

1. Background

This Ocean Acidification Monitoring Progress Report summarizes the work conducted and data collected during ocean acidification (OA) monitoring efforts by the City of San Diego (City). In 2021, new requirements were established in the NPDES permits for the South Bay Water Reclamation Plant (NPDES CA0109045; Order No. R9-2021-0011) and the South Bay International Wastewater Treatment Plant (NPDES CA0108928; Order No. R9-2021-0001) to monitor pH by spectrophotometric analysis to calibrate the pH results measured by a conductivity-temperature-depth (CTD) profiler. Further, pH and total alkalinity are required to be used to calculate aragonite saturation state for ocean acidification monitoring. To achieve these objectives, the City's Ocean Monitoring Program has been collecting discrete bottle samples for pH and total alkalinity (TA) analysis in the South Bay Ocean Outfall (SBOO) monitoring region. Although not permit mandated, the City also collected the same samples in the Point Loma Ocean Outfall (PLOO) monitoring region to enhance understanding and interpretation of these data.

The collected bottle samples were used to describe the carbonate chemistry of coastal waters as part of the City's ongoing permit required monitoring centered around the following three primary objectives:

1. Reporting bottle pH and TA data
2. Calibration of CTD pH with bottle pH data
3. Ocean acidification monitoring: aragonite saturation state

Detailed throughout this report are significant activities that have been completed between 2019 and 2024 to achieve the objectives above. Furthermore, this Progress Report details recommendations for future monitoring based on the study findings.

2. Methods

2.1 Sample Collection

A total of 69 offshore stations were sampled four times a year as part of the City's regular quarterly water quality monitoring to characterize regional ocean conditions and estimate dispersion of the PLOO and SBOO wastewater plumes. These stations were monitored during February, May, August, and November with the PLOO and SBOO stations sampled over three to five days during each survey. Stations F1–F36 are arranged in a grid surrounding the PLOO along or adjacent to the 18, 60, 80 and 98-m depth contours, while stations inclusive of I1–I40 are arranged in a grid surrounding the SBOO along the 9, 19, 28, 38 and 55-m depth contours (Figure 1).

Samples were collected using a rosette sampler fitted with Niskin bottles surrounding a central CTD fitted with an SBE18 pH electrode. Due to the critical role of pH monitoring for understanding water quality, the accuracy of pH electrode data have garnered increased attention due to the pH electrode's known propensity to drift (McLaughlin et al. 2017). To account for sensor drift, for the past 20 years the City has calibrated the SBE-18 pH electrodes to a threshold of ± 0.05 pH across a series of three standardized NBS (National Bureau of Standards) buffers (pH

of 7, 8, and 9) the morning of deployment. Should any buffer fall outside this range, a new calibration slope is calculated and updated in the Seabird software and a recalibration is performed to ensure sensor accuracy within ± 0.05 pH units. Following calibration, the electrode storage solution is switched from pH 4 (with salt [KCl]) to clean seawater for the interim period between calibration and field deployment (~ 1 hour).

To investigate SBE-18 pH electrode accuracy and monitor OA in the coastal waters of San Diego, discrete bottle samples of seawater were collected at 2 to 3 discrete depths (surface, midwater, and bottom) from a subset of the quarterly monitoring stations in the PLOO (F13, F15, F35) and SBOO regions (I1, I21, I28) during quarterly water sampling (Table 1, Figure 1; 6 stations total). Additionally, samples were collected at the location of the SBOO and PLOO real-time oceanographic mooring systems (RTOMS) when deployed (2 stations total). Seawater samples were collected and preserved in accordance with best practices for seawater carbonate chemistry measurements (Dickson et al. 2007) and shipped to a lab for spectrophotometric analysis of pH and potentiometric analysis of TA. Details on these analyses and results from estimates of precision, accuracy, and quality control (QC) can be found in Appendix A.

In addition to calibrating CTD pH measurements, laboratory-derived pH and TA were used to calculate parameters of the seawater carbonate system for the purpose of OA monitoring. Among the measurable (and calculated) parameters in the seawater carbonate system, aragonite saturation state (Ω_{arg}) has been developed as a monitoring baseline for biological impacts given its established relationship with shell formation in both pelagic and benthic organisms in the Southern California Bight (SCB) (Orr et al. 20025; Hofmann Elizondo et al. 2024). In essence, the parameter measures the availability of carbonate ions needed for a calcifying organism to form (> 1) or dissolve (< 1) their calcium carbonate shell. To calculate Ω_{arg}, at least two measurable parameters of the carbonate system are needed (i.e., pH, total alkalinity, pCO_2, and dissolved inorganic carbon (DIC)). Data received from the laboratory (pH, TA) were combined with the simultaneous in-situ data from the time of collection by the CTD (pressure, temperature, and salinity) to calculate the in-situ pH and Ω_{arg} using the R package seacarb (Gattuso et al. 2015) with K1 and K2 constants applied from Mehrbach et al. (1973) and refit by Dickson and Millero (1987).

2.2 Overview of Activities Completed and Challenges

Over the 2019 – 2024 sampling period a total of 412 seawater samples were collected for TA and pH analysis. A breakdown of collection efforts by month within each year is detailed in Table 2. Of the 412 bottle samples collected, 365 passed QC review and were used in the analysis (CTD pH correction and Ω_{arg} calculation). A breakdown of total samples analyzed, lost, or removed during QC review for each year can be found in Table 3. These data were used in combination with the corresponding CTD data from bottle files at the depth of collection (salinity, temperature, and pressure) to calculate in-situ pH on the total scale and aragonite saturation state (Ω_{arg}).

Bottle samples were initially analyzed by the Dickson Lab at the Scripps Institution of Oceanography (SIO) from 2019-2022. Challenges over this period included significantly delayed turnaround time of samples (> 2-3 years) and temporary loss of submitted samples due to staff turnover and lab throughput limitations. A temporary shutdown of this lab forced the City to move

sample analysis to the Southern California Coastal Water Research Project (SCCWRP) lab from 2023 to 2024. Additional challenges ensued due to lab establishment (setup of instruments and training of staff in carbonate chemistry analyses) and development of quality control standard operating procedures. Altogether, between 2019 and 2024, a total of 20 samples were lost (broken or misplaced) due to the various challenges highlighted above.

2.2.1. Real-time Mooring pH validation

TA/pH bottle sample collection at the location of the SBOO and PLOO real-time oceanographic mooring systems (RTOMS) was conducted to simultaneously validate CTD pH measurements and mooring pH sensor measurements (City of San Diego, 2025). These moored pH sensors collect high temporal resolution data (i.e., sample every 10 minutes) to characterize ocean conditions near the ocean outfalls. Since these moorings are deployed for up to a year at a time, these in-situ sensors are subject to a potential decrease in data quality over the deployment period due to biofouling, plumbing clogs, and instrument drift. Bottle samples were collected at discrete depths to match the location of mooring sensors on a quarterly basis and at the beginning/end of each mooring deployment (Tables 1, 2). Due to significant delays in sample turnaround time as mentioned, complete comparisons between the bottle results and mooring data have been delayed. This report is intended to focus on CTD pH validation and aragonite saturation state reporting. Mooring pH data comparisons will be included in future reports.

3. Results

3.1 Bottle pH and TA

A full table of carbonate chemistry results including metadata recorded during sample collection (sampling effort, date, and depth), analytical results (TA and pH), and contemporaneous CTD data extracted from bottle files (in-situ temperature, salinity, and pressure) can be found in Appendix B. These data were used to recalculate spectrophotometric bottle pH to in-situ conditions so the differences between bottle and CTD pH could be compared in order to apply a correction factor to CTD data.

Overall, on average, in-situ bottle pH was 7.905 ± 0.14 and in-situ bottle TA was 2240 ± 14 µmol kg^{-1}. The highest annual pH was recorded in surface waters (1-10 m) in the spring (8.125 ± 0.06) and the lowest at the bottom (51 – 150 m), also in the spring (7.761 ± 0.06). TA was highest at the surface in the fall (2315 ± 178 µmol kg^{-1}) and lowest at the bottom in the fall (2205 ± 371 µmol kg^{-1}). An overview of average pH and TA binned by season and depth can be found in Table 4. In general, depth profiles of pH agree with oceanographic expectations, where pH decreases with depth (Figure 2). TA normalized to a salinity of 35 psu ([35/Salinity]*TA; Zeebe and Wolf-Gladrow, 2001) plotted as a function of depth generally decreased with depth.

Maximum ranges across all depths and seasons for pH (Δ0.58) and TA (Δ102 µmol kg^{-1}) were within expected ranges for shallow coastal Southern California waters (McLaughlin et al. 2018) and agreed with previously established oceanographic trends for the region, where pH decreases with depth and TA was generally lower at the bottom due to density dependence (Harris et al. 2013).

3.2 CTD pH Calibration

Prior work by McLaughlin et al. (2017) examined the differences between SBE-18 pH electrodes and bottle spectrophotometric pH measurements in the SCB region to develop a correction factor for CTD pH data. This study confirmed that spectrophotometric methods were more accurate and CTD pH data could be corrected using a linear depth factor developed by plotting the difference in electrode and spectrophotometric in-situ pH as a function of depth. This depth factor was developed into a 'pH Fit Tool' and applied to the City's carbonate chemistry data.

Application of these methods to the City's 2019-2024 OA dataset shows that, similar to McLaughlin et al. (2017), the CTD pH (on NBS scale) tended to over-report in-situ seawater pH relative to spectrophotometric measurements on total pH scale (slope value > 1; Figure 3). On average, CTD pH was 0.036 ± 0.072 pH units higher than the spectrophotometric bottle measurement (ΔpH = CTD pH – Spectrophotometric pH; Table 5). This also aligns with expected differences due to the use of different pH scales (Marion et al. 2011). Plotting ΔpH as a function of depth for the entire 2019-2024 dataset (Figure 4) yielded the following equation:

$$\Delta pH = -0.0009*Depth + 0.0712$$

Application of this equation to CTD pH data increased the ΔpH by, on average, 0.071 ± 0.012 pH units (Table 5). These depth-corrected CTD pH data did not improve the offset between CTD and bottle pH and instead resulted in an over-correction of the CTD pH when applied across the dataset. This agrees with the conclusions in McLaughlin et al. (2017) where a pre-existing offset < 0.05 pH units is unlikely to be improved by a depth correction. Application of the depth correction by individual year instead of the entire 5-year span also did not improve ΔpH, and ΔpH as a function of depth was weakly correlated. These results can be found in Table 5 and Figure 5.

In summary, the depth correction outlined by McLaughlin et al. (2017) did not reduce the difference between CTD and bottle pH data or the strength of the fit (r^2) in the data (CTD pH vs. Bottle pH; Figure 6). These results align with the conclusions of prior work where an average pre-existing offset of < 0.05 ΔpH units is unlikely to be improved by the depth correction approach. Instead, these results highlight that the City's CTD pH electrode calibration procedure conducted the morning of deployment (fit to ± 0.05 pH units across a range of 7, 8, and 9 NBS buffers) is properly ensuring that the CTD pH data are not subject to drift within the accuracy range of these sensors as stated by the manufacturer (± 0.1 pH units).

3.3 OA Monitoring: Aragonite Saturation State

On average, the in-situ aragonite saturation state (Ω_{arg}) was 1.7 ± 0.5. Ω_{arg} and was highest at the surface (1 - 10 m) in the summer (3.0 ± 0.3) and lowest at the bottom (51 – 150 m) in the spring (1.0 ± 0.1). Across the PLOO and SBOO regions, Ω_{arg} ranged from a minimum of 0.9 to a maximum of 2.8 in winter, 0.8 to 3.6 in spring, 0.9 to 3.4 in summer, and 0.9 to 2.9 in fall. The average Ω_{arg} binned by season and depth can be found in Table 4. In general, the ranges of Ω_{arg} observed agree with expectations for nearshore variability in the California current system (maxima > 3 and minima < 1; Feely et al. 2008; Alin et al. 2012). Ω_{arg} decreased with depth (Figure

2) and fell below saturation (< 1) at an average depth of 78 m, which is shallower than previous estimates for undersaturation in nearshore waters of the Southern California Bight (138m; McLaughlin et al. 2018). Undersaturated values were commonly observed during spring sampling when upwelling conditions were strongest. This complements previous work which has shown that the upwelling of deep, high DIC water masses is the primary driver of Ω_{arg} variability along the southern California continental shelf (Harris et al. 2013).

4. Conclusions and Recommendations

This report describes the carbonate chemistry of San Diego's coastal waters to fulfill NPDES permit requirements and complete the three primary objectives of this study: 1) Reporting bottle pH and TA data; 2) Calibration of CTD pH with bottle pH data; and 3) Ocean Acidification monitoring: Aragonite Saturation State.

4.1. Conclusions

Based on the findings of this study, as detailed throughout this report, the City offers the following conclusions:

4.1.1. Reporting Bottle pH and TA Data

The discharge of treated wastewater to San Diego coastal waters from the PLOO and SBOO was not observed to show pH or TA to vary beyond what is expected to occur naturally and agrees with previously established oceanographic patterns for the region.

4.1.2. Calibration of CTD pH with Bottle pH Data

This study confirms that the City's approach to daily CTD pH electrode calibration is sufficient to ensure accuracy in CTD collected pH data within manufacturer specifications and is not improved by additional bottle pH calibration. However, bottle collected pH samples for calibration of real time mooring pH data may be beneficial due to the long-term deployment of these sensors.

4.3.3. Ocean Acidification Monitoring: Aragonite Saturation State

The aragonite saturation state conditions observed in San Diego coastal waters align with expectations for nearshore variability in the California current system and is primarily driven by upwelling conditions. Observations did not indicate these conditions are impacted by wastewater discharge from the PLOO or SBOO.

4.4. Recommendations

Based on the findings of this study, the City requests the following amendments to be applied upon renewal of the NPDES permits for the PLWTP, SBWRP, and the SBIWTP:

1. Discontinue quarterly pH bottle sampling for the purpose of CTD pH correction given the high quality of the City's pH calibration procedures.

2. Increase sampling depths and frequency of pH bottle sampling at PLOO and SBOO RTOMS to better support calibration and post-deployment QC of the mooring's OA-related sensors. This proposed shift would improve the function of PLOO and SBOO RTOMS as OA-monitoring platforms. Additionally, this proposed change will aid regional efforts to ground-truth SCB Ω_{arg} modeling, which currently has gaps in nearshore, shallow locations and would benefit from multi-parameter carbonate chemistry monitoring (e.g., pH + TA + pCO_2) to better constrain model predictions.

Together, this proposed shift in OA monitoring would eliminate unnecessary sampling for CTD pH correction, and the change will improve the temporal resolution of OA monitoring both locally in San Diego's coastal waters and regionally by contributing high quality validation data for region-wide OA models. However, unless directed to by the Region Nine Regional Water Quality Control Board, the City will continue the same OA monitoring conducted to date to ensure compliance with NPDES permit requirements. The City is committed to continue collection of pH and TA bottle samples as part of the Bight'23 Ocean Acidification and Hypoxia (OAH) study through February 2026. As such, sampling will continue on a quarterly basis at the same stations and in coordination with the deployment of PLOO and SBOO RTOMS. Samples will continue to be analyzed at SCCWRP using standards and protocols provided by the Dickson lab at SIO (Dickson et al. 2007).

Works Cited

Alin, S. R., Feely, R. A., Dickson, A. G., Hernández-Ayón, J. M., Juranek, L. W., Ohman, M. D., & Goericke, R. (2012). Robust empirical relationships for estimating the carbonate system in the southern California Current System and application to CalCOFI hydrographic cruise data (2005–2011). *Journal of Geophysical Research: Oceans*, *117*(C5).

City of San Diego. (2025). Annual Receiving Waters Monitoring and Toxicity Testing Quality Assurance Report, 2024. City of San Diego Ocean Monitoring Program, Public Utilities Department, Environmental Monitoring and Technical Services Division, San Diego, CA.

Clayton, T. D., & Byrne, R. H. (1993). Spectrophotometric seawater pH measurements: total hydrogen ion concentration scale calibration of m-cresol purple and at-sea results. *Deep Sea Research Part I: Oceanographic Research Papers*, *40*(10), 2115-2129.

Dickson, A. G., & Millero, F. J. (1987). A comparison of the equilibrium constants for the dissociation of carbonic acid in seawater media. *Deep Sea Research Part A. Oceanographic Research Papers*, *34*(10), 1733-1743.

Dickson, A. G., Afghan, J. D., & Anderson, G. C. (2003). Reference materials for oceanic CO2 analysis: a method for the certification of total alkalinity. *Marine Chemistry*, *80*(2-3), 185-197.

Dickson, A. G., Sabine, C. L., & Christian, J. R. (2007). *Guide to best practices for ocean CO2 measurements*. North Pacific Marine Science Organization.

Feely, R. A., Sabine, C. L., Hernandez-Ayon, J. M., Ianson, D., & Hales, B. (2008). Evidence for upwelling of corrosive" acidified" water onto the continental shelf. *Science*, *320*(5882), 1490-1492.

Gattuso, J. P., Epitalon, J. M., Lavigne, H., Orr, J., Gentili, B., Hagens, M., ... & Gattuso, M. J. P. (2015). Package 'seacarb'. *Preprint at http://cran. r-project. org/package= seacarb*.

Harris, K. E., DeGrandpre, M. D., & Hales, B. (2013). Aragonite saturation state dynamics in a coastal upwelling zone. *Geophysical Research Letters*, *40*(11), 2720-2725.

Hofmann Elizondo, U., Vogt, M., Bednaršek, N., Münnich, M., & Gruber, N. (2024). The impact of aragonite saturation variability on shelled pteropods: An attribution study in the California Current System. *Global Change Biology*, *30*(6), e17345.

Marion, G.M, F.J. Millero, M.F. Camões, P. Spitzer, R. Feistel, and C.-T.A. Chen. (2011). pH of seawater. *Marine Chemistry*. 126: 89–96.

McLaughlin, K., Nezlin, N. P., Weisberg, S. B., Dickson, A. G., Booth, J. A., Cash, C. L., ... & Terriquez, L. (2017). An evaluation of potentiometric pH sensors in coastal monitoring applications. *Limnology and Oceanography: Methods*, *15*(8), 679-689.

McLaughlin, K., Nezlin, N. P., Weisberg, S. B., Dickson, A. G., Booth, J. A. T., Cash, C. L., ... & Terriquez, L. (2018). Seasonal patterns in aragonite saturation state on the southern California continental shelf. *Continental Shelf Research*, *167*, 77-86.

Mehrbach, C., Culberson, C. H., Hawley, J. E., & Pytkowicx, R. M. (1973). Measurement of the apparent dissociation constants of carbonic acid in seawater at atmospheric pressure 1. *Limnology and oceanography*, *18*(6), 897-907.

Orr, J. C., Fabry, V. J., Aumont, O., Bopp, L., Doney, S. C., Feely, R. A., ... & Yool, A. (2005). Anthropogenic ocean acidification over the twenty-first century and its impact on calcifying organisms. *Nature*, *437*(7059), 681-686.

Zeebe, R. E., & Wolf-Gladrow, D. (2001). *CO2 in seawater: equilibrium, kinetics, isotopes* (Vol. 65). Gulf Professional Publishing.

Tables

Table 1: List of stations and depths sampled for each sampling effort. Real Time Oceanographic Mooring System (RTOMS) stations included.

Sampling Effort	Station	Depths Sampled (m)
PLOO	F13	1, 60
PLOO	F15	1, 80
PLOO	F35	1, 50, 100
PLOO	RTOMS	1, 30, 89
SBOO	I1	1, 60
SBOO	I21	1, 41
SBOO	I28	1, 55
SBOO	RTOMS	1, 26

Table 2: Overview of sample collection timing by month (abbreviated) for each sampling year. NA indicates no sample was taken when the Real Time Oceanographic Mooring System (RTOMS) was not deployed.

Year	SBOO	SBOO RTOMS	PLOO	PLOO RTOMS
2019	May, Aug, Nov	Dec	May, Aug, Nov	NA
2020	Feb, Aug, Nov	NA	Aug, Nov	Aug
2021	Feb, May, Aug, Nov	Nov	Feb, May, Aug, Nov	Nov
2022	Feb, May, Aug, Nov	Feb, May, Aug, Nov	Feb, May, Aug, Nov	May, Aug, Nov, Dec
2023	Feb, May, Aug, Nov	May, July, Aug, Nov	Feb, May, Aug, Nov	Feb, May, Aug, Nov
2024	Feb, May, Aug, Nov	Feb, May, July, Aug, Nov	Feb, May, Aug, Nov	Jan, Feb, May, Aug, Nov

Table 3: Total number of total alkalinity (TA) and pH samples collected, lost or removed in QC, and used in the final analysis (separated by sampling year). Bottom row in bold indicates the sum of all samples across the 2019 – 2024 report period.

Year	Collected	Lost in Lab	Removed in QC	Analysis Total
2019	41	0	3	38
2020	35	6	3	26
2021	61	0	4	57
2022	93	5	13	75
2023	94	9	1	84
2024	88	0	3	85
Total	**412**	**20**	**27**	**365**

Table 4: Average ± standard deviation (SD) pH (in-situ, total scale), TA (µmol kg^{-1}), and aragonite saturation state (Ω_{arg}) organized by depth (surface [1 – 10m], midwater [11 – 50m], bottom [51 – 150m]) and season (Winter, Spring, Summer, Fall) for the entire 2019-2024 study period. Bolded values represent average among all depths for the respective season.

Season & Depth	In-situ pH (total scale)	Total Alkalinity (µmol kg^{-1})	Ω_{arg}
Winter	**7.916 ± 0.13**	**2235 ± 14**	**1.7 ± 0.5**
Surface	8.048 ± 0.03	2230 ± 18	2.3 ± 0.2
Midwater	7.938 ± 0.09	2234 ± 12	1.8 ± 0.4
Bottom	7.792 ± 0.03	2241 ± 11	1.2 ± 0.2
Spring	**7.883 ± 0.18**	**2250 ± 14**	**1.7 ± 0.8**
Surface	8.094 ± 0.05	2250 ± 13	2.7 ± 0.3
Midwater	7.787 ± 0.07	2241 ± 10	1.2 ± 0.2
Bottom	7.730 ± 0.01	2255 ± 14	1.0 ± 0.1
Summer	**7.899 ± 0.13**	**2238 ± 9**	**1.8 ± 0.8**
Surface	8.053 ± 0.04	2240 ± 7	2.8 ± 0.3
Midwater	7.869 ± 0.07	2229 ± 6	1.5 ± 0.3
Bottom	7.782 ± 0.05	2241 ± 10	1.2 ± 0.1
Fall	**7.924 ± 0.12**	**2234 ± 14**	**1.8 ± 0.6**
Surface	8.069 ± 0.03	2237 ± 13	2.6 ± 0.2
Midwater	7.910 ± 0.05	2226 ± 10	1.7 ± 0.2
Bottom	7.818 ± 0.07	2237 ± 14	1.3 ± 0.2
All Seasons	**7.905 ± 0.14**	**2240 ± 14**	**1.8 ± 0.7**

Table 5: Average ± standard deviation (SD) difference between CTD pH and in-situ corrected bottle pH (ΔpH = CTD pH – Bottle pH) for each year and the entire reporting period (Total: 2019 – 2024). Using the pH Fit Tool, ΔpH (y) was plotted as a function of depth (x) and the resulting linear regression equation was re-applied to the CTD pH data. This was conducted individually for each year of data ($\Delta pH_{corrected\ (1\ year)}$) and again for all six years of data together ($\Delta pH_{corrected\ (all\ years)}$).

Year	ΔpH	$\Delta pH_{corrected\ (1\ year)}$	$\Delta pH_{corrected\ (all\ years)}$
2019	0.09 ± 0.08	0.10 ± 0.01	0.10 ± 0.01
2020	0.05 ± 0.07	0.09 ± 0.01	0.08 ± 0.01
2021	-0.04 ± 0.13	0.02 ± 0.01	0.08 ± 0.03
2022	0.03 ± 0.13	0.10 ± 0.01	0.09 ± 0.03
2023	0.04 ± 0.13	0.08 ± 0.01	0.08 ± 0.03
2024	0.08 ± 0.07	0.11 ± 0.01	0.02 ± 0.01
Total	**0.04 ± 0.07**	**0.07 ± 0.01**	**0.07 ± 0.01**

Figures

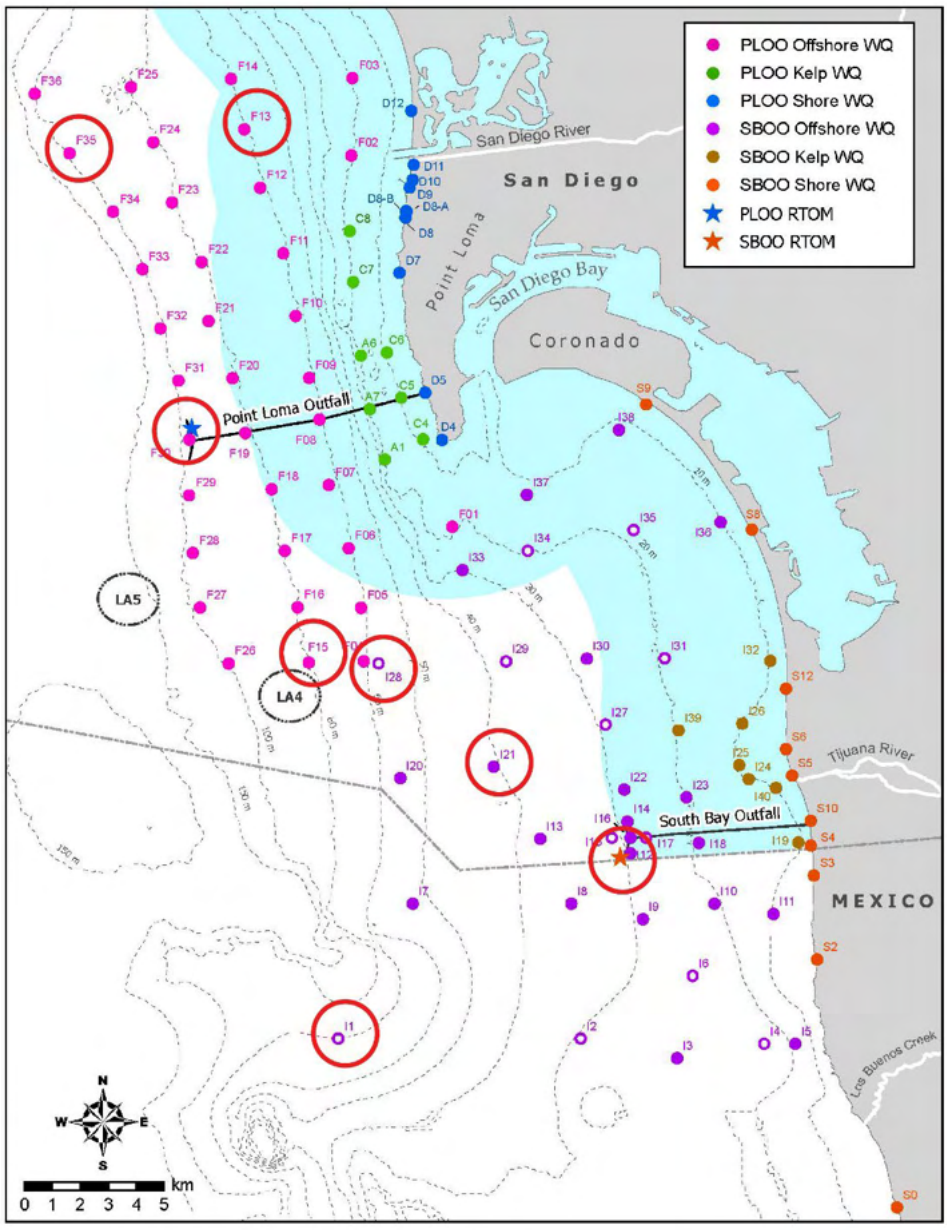


Figure 1: Map of all water quality stations sampled by the City. Red circled stations indicate those where bottle samples were collected for TA and pH analysis as part of routine quarterly water quality monitoring. Blue shading indicates the extent of California state waters.

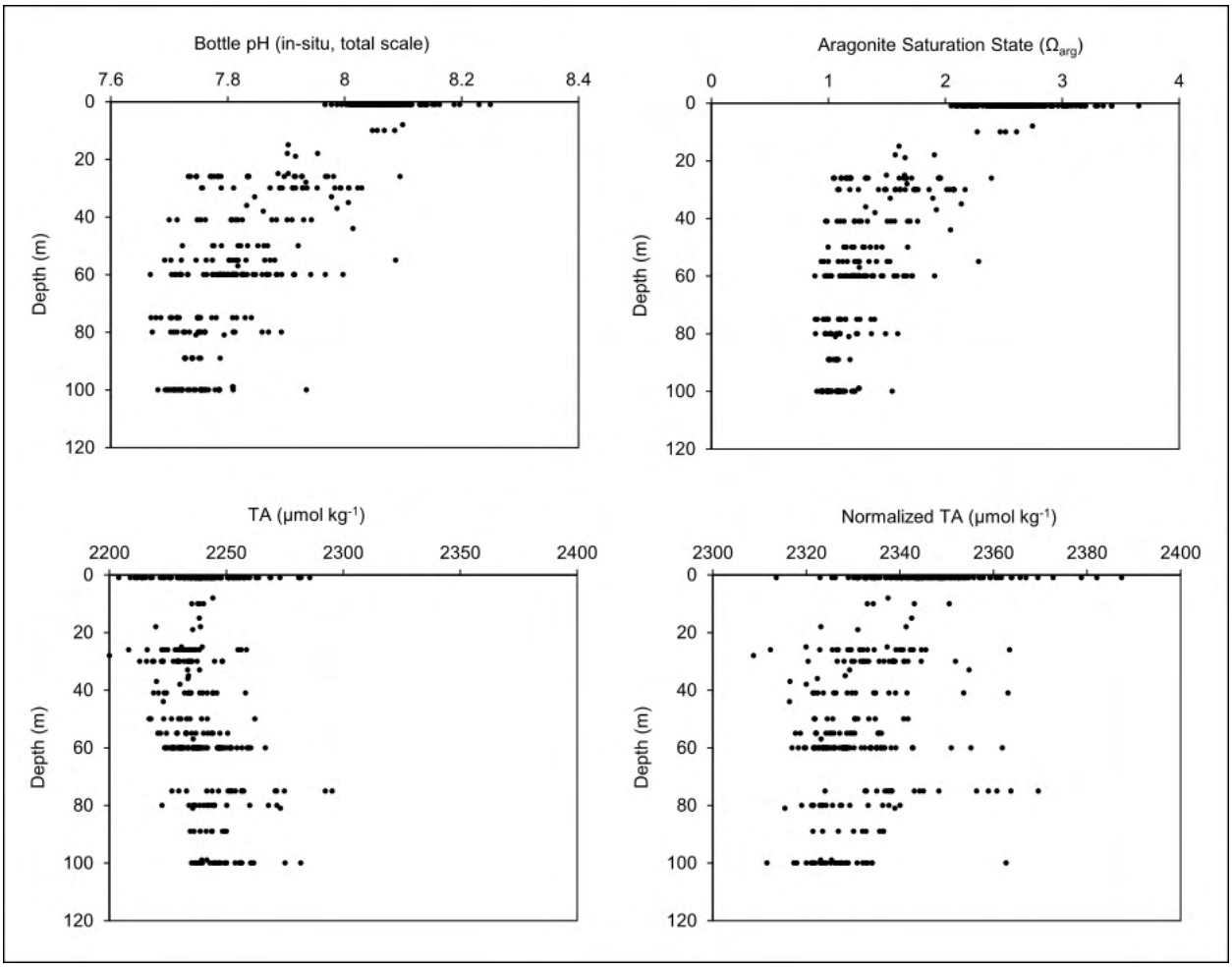


Figure 2: Profile plots of pH, total alkalinity (TA), normalized TA (to 35 psu), and aragonite saturation state (Ω_{arg}). Data presented include all stations and depths over the 2019 – 2024 report period.

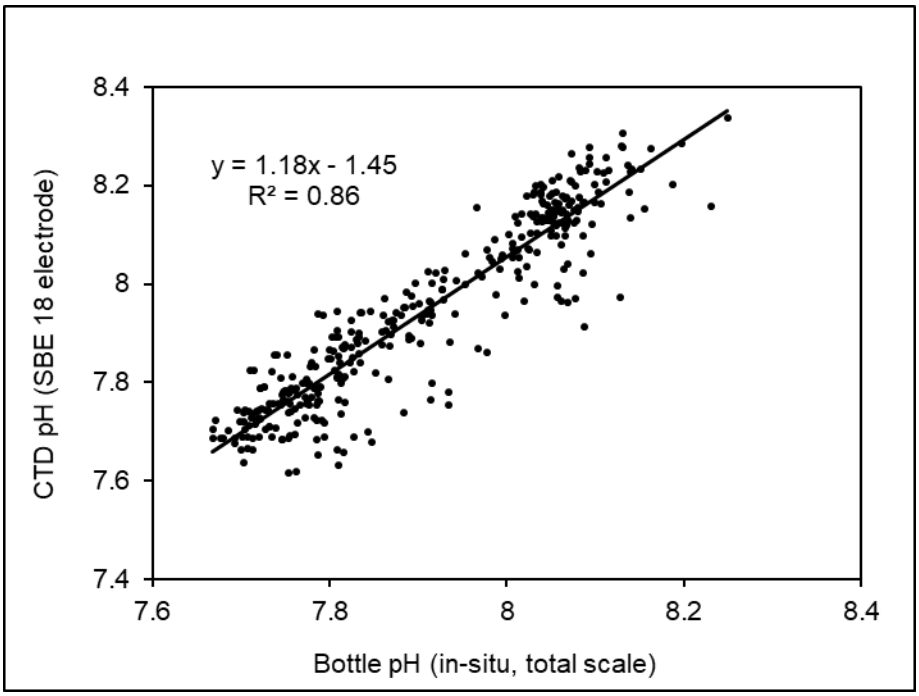


Figure 3: Linear regression of pH CTD data vs pH bottle data (corrected to in-situ conditions on the total scale) for all data collected during the 2019 –2024 study period.

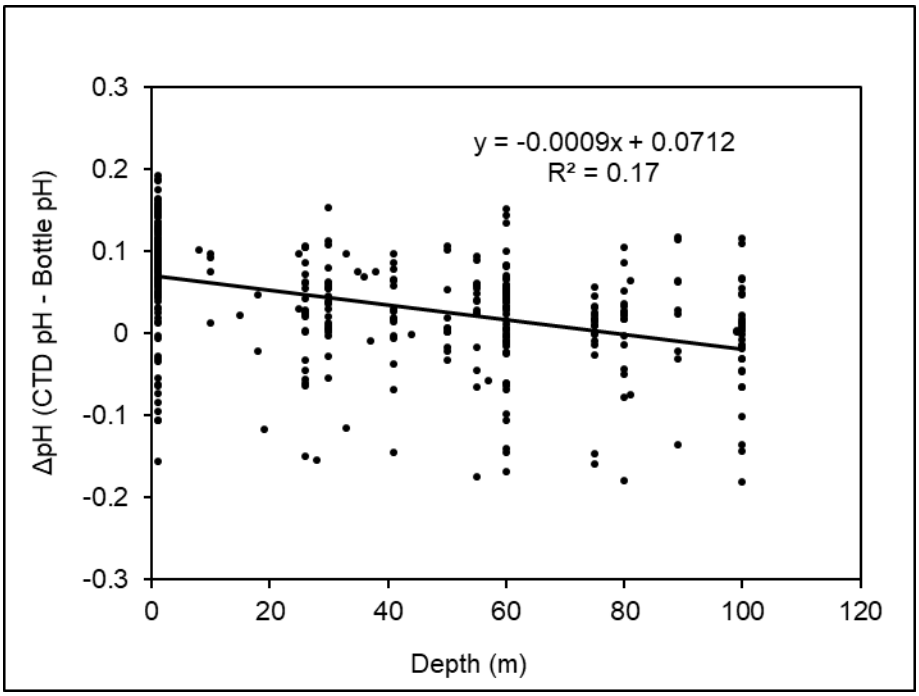


Figure 4: pH difference (ΔpH = CTD pH – Bottle pH) as a function of depth for the entire 2019 – 2024 report period.

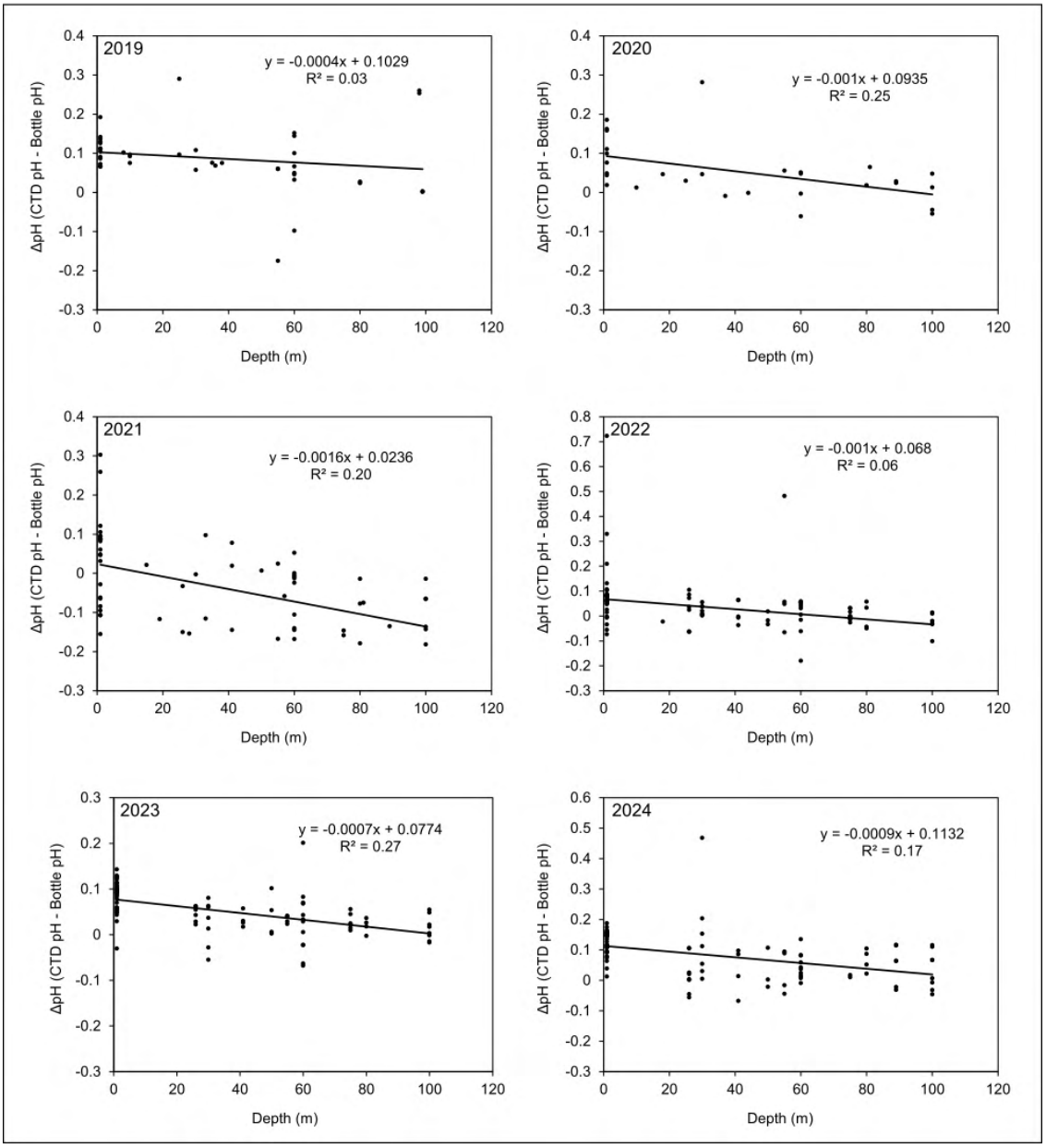


Figure 5: pH difference (ΔpH = CTD pH – Bottle pH) as a function of depth for each year of the report period (noted in top left corner of each figure).

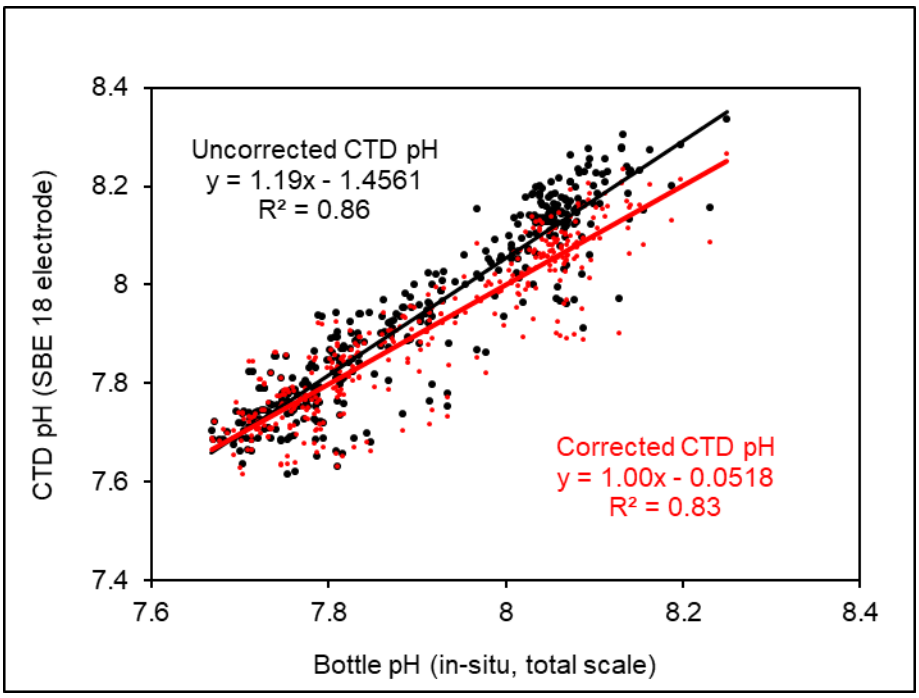


Figure 6: Linear regression of uncorrected pH CTD data (black) and corrected pH CTD data (red) vs pH bottle data corrected to in-situ conditions on the total scale for all data collected during the 2019 –2024 study period.

Appendices

Appendix A: Laboratory Methods and QC Results

Over the 2019-2024 period a total of 392 samples were analyzed for total alkalinity (TA) and pH. Seawater TA was analysed using a potentiometric open-cell titration method (Dickson et al. 2007) on an automatic titrator using ~ 40 ml of seawater per sample. Of the 392 samples analyzed, 11 were removed from the dataset for outlier analytical values (> 2400 µmol kg^{-1}) due to analytical error. Of the TA results included in this analysis, a subset of samples were measured in duplicate and precision of replicate measurements was ± 5.9 µmol kg^{-1}.

Samples for pH (~ 5 ml) were analysed with a spectrophotometer in a cuvette following the method of Clayton and Byrne (1993) using a correction factor for the m-cresol dye addition (based on the absorption at the isosbestic point detailed in Dickson et al. 2007) over the range of pH found in this study (7.6 – 8.2). Of the 392 samples analyzed, 16 were removed for outlier analytical values (ΔpH > 0.2) due to analytical error. Each pH sample was measured in triplicate, and precision was ± 0.004.

Overall analytical accuracy for TA (SD = ± 3.4 µmol kg^{-1}) and pH_T (SD = ± 0.008) measurements was estimated from frequent measurements of certified reference materials from the Scripps Institution of Oceanography (Dickson et al. 2003). Parameters for the seawater carbonate system (Aragonite saturation state (Ω_{arg}), dissolved inorganic carbon (DIC; µmol kg^{-1}), and pCO_2 (µatm)) were calculated from measured TA, pH_T, temperature, pressure, and salinity using the R package seacarb (Gattuso et al. 2015) with K1 and K2 constants applied from Mehrbach et al. (1973) and refit by Dickson and Millero (1987).

Appendix B: Carbonate Chemistry Results

Table B.1: Carbonate chemistry values for the entire 2019 – 2024 report period organized by region, station, and collection date. Values include the following: Measured by CTD: depth (m), temperature (˚C), salinity (psu), and CTD pH (SBE-18 pH electrode). Bottle samples analyzed in the lab: Bottle pH (corrected to in-situ conditions on the total scale) and total alkalinity (TA; µmol kg^{-1}). Calculated values from bottle pH and TA: aragonite saturation state (Ω_{arg}).

Region	Station	Date	Depth	Temperature	Salinity	CTD pH	Bottle pH	TA	Ω_{arg}
PLOO	F35	14 May 2019	1	18.22	33.65	8.185	8.056	2244.1	2.63
PLOO	F15	14 May 2019	60	10.94	33.73	7.848	7.802	2237.5	1.21
PLOO	F15	14 May 2019	60	10.97	33.71	7.848	7.798	2236.5	1.20
SBOO	I1	14 May 2019	10	16.38	33.57	8.143	8.068	2238.7	2.52
SBOO	I1	14 May 2019	1	17.94	33.66	8.227	8.102	2245.2	2.84
SBOO	I1	14 May 2019	36	11.62	33.66	7.901	7.833	2233.6	1.32
SBOO	I1	14 May 2019	8	17.14	33.60	8.201	8.099	2244.2	2.75
SBOO	I8	16 May 2019	1	17.99	33.66	8.23	8.088	2244.5	2.78
SBOO	I8	16 May 2019	10	16.58	33.43	8.148	8.056	2237.8	2.47
SBOO	I8	16 May 2019	55	11.06	33.70	7.877	7.818	2232.7	1.25
SBOO	I20	16 May 2019	1	16.63	33.61	8.209	8.072	2239.9	2.56
SBOO	I20	16 May 2019	10	14.64	33.53	8.144	8.048	2235.3	2.27
SBOO	I20	16 May 2019	38	11.66	33.64	7.936	7.861	2230.2	1.40
PLOO	F35	07 Aug 2019	1	21.41	33.67	8.265	8.073	2242.1	3.03
PLOO	F35	08 Aug 2019	1	19.52	33.67	8.241	8.137	2240.5	3.18
PLOO	F35	08 Aug 2019	60	11.30	33.69	7.939	7.788	2236.8	1.19
PLOO	F35	08 Aug 2019	60	11.31	33.69	7.937	7.793	2237.6	1.20
PLOO	F13	09 Aug 2019	1	20.29	33.69	8.275	8.163	2242.9	3.42
PLOO	F13	09 Aug 2019	25	12.04	33.66	7.983	7.886	2230.8	1.50
PLOO	F13	09 Aug 2019	80	10.75	33.78	7.785	7.761	2240.3	1.10
SBOO	I13	12 Aug 2019	1	18.78	33.61	8.165	8.099	2239.8	2.90
SBOO	I13	12 Aug 2019	30	12.84	33.62	8.061	7.953	2234.6	1.77

Region	Station	Date	Depth	Temperature	Salinity	CTD pH	Bottle pH	TA	Ω_{arg}
SBOO	I13	12 Aug 2019	60	11.35	33.70	7.869	7.967	2233.9	1.72
SBOO	I1	12 Aug 2019	60	11.36	33.70	7.867	7.801	2236.0	1.22
SBOO	I1	14 Aug 2019	1	17.51	33.61	8.16	8.070	2242.2	2.63
SBOO	I1	14 Aug 2019	55	11.39	33.69	7.864	7.804	2235.2	1.23
PLOO	F15	05 Nov 2019	1	18.95	33.66	8.165	8.054	2243.6	2.69
PLOO	F15	05 Nov 2019	35	15.23	33.58	8.082	8.006	2233.9	2.14
PLOO	F15	05 Nov 2019	99	11.80	33.74	7.811	7.808	2239.5	1.26
PLOO	F35	05 Nov 2019	99	11.80	33.74	7.811	7.810	2241.8	1.26
PLOO	F35	07 Nov 2019	1	17.73	33.59	8.125	8.058	2237.2	2.59
PLOO	F35	07 Nov 2019	80	12.92	33.65	7.897	7.870	2234.0	1.49
SBOO	I1	13 Nov 2019	1	17.85	33.60	8.129	8.043	2238.0	2.53
SBOO	I28	13 Nov 2019	30	15.08	33.60	8.051	7.994	2234.8	2.08
SBOO	I28	13 Nov 2019	60	13.52	33.66	7.946	7.914	2235.6	1.67
SBOO	I1	13 Nov 2019	60	13.31	33.68	7.925	7.825	2235.7	1.38
SBOO	I1	15 Nov 2019	55	12.67	33.72	7.912	8.087	2237.0	2.29
SBOO	I1	15 Nov 2019	1	16.94	33.59	8.125	8.053	2237.0	2.49
PLOO	F35	12 Feb 2020	1	15.47	33.44	8.099	8.055	2222.7	2.36
PLOO	F35	12 Feb 2020	44	13.72	33.59	8.013	8.014	2223.2	2.05
PLOO	F15	12 Feb 2020	60	12.77	33.62	7.939	7.942	2227.1	1.71
PLOO	F15	12 Feb 2020	60	12.74	33.62	7.936	7.997	2225.9	1.91
SBOO	I1	13 Feb 2020	1	15.19	33.51	8.08	8.062	2223.8	2.37
SBOO	I1	13 Feb 2020	37	13.55	33.55	7.978	7.987	2220.2	1.93
SBOO	I1	18 Aug 2020	1	22.83	33.75	8.278	8.093	2250.9	3.30
SBOO	I28	18 Aug 2020	100	10.51	33.90	7.744	7.696	2238.8	0.95
SBOO	I28	18 Aug 2020	100	10.51	33.90	7.744	7.731	2246.9	1.03
PLOO	F35	18 Aug 2020	10	16.55	33.36	8.098	8.086	2240.3	2.61
PLOO	F35	18 Aug 2020	1	23.19	33.75	8.256	8.094	2251.2	3.35
PLOO	F35	18 Aug 2020	30	13.64	33.45	8.053	8.007	2228.9	2.01

Region	Station	Date	Depth	Temperature	Salinity	CTD pH	Bottle pH	TA	Ω_{arg}
PLOO	F35	18 Aug 2020	89	10.74	33.71	7.779	7.751	2249.3	1.08
PLOO	PLOO_RTOM	18 Aug 2020	89	10.74	33.71	7.778	7.754	2250.0	1.09
PLOO	PLOO_RTOMS	20 Aug 2020	1	23.65	33.74	8.209	8.051	2252.8	3.15
PLOO	PLOO_RTOMS	20 Aug 2020	81	10.72	33.79	7.81	7.746	2235.7	1.06
SBOO	I1	25 Aug 2020	55	12.56	33.56	7.936	7.881	2233.2	1.50
SBOO	I1	25 Aug 2020	1	23.05	33.63	8.151	8.052	2246.5	3.08
SBOO	I13	03 Nov 2020	60	13.22	33.56	7.964	7.913	2239.7	1.65
SBOO	I13	03 Nov 2020	60	13.05	33.58	7.962	7.914	2240.4	1.64
SBOO	I13	03 Nov 2020	18	14.87	33.47	8	7.954	2238.9	1.91
PLOO	PLOO_RTOMS	10 Nov 2020	1	17.49	33.62	8.128	8.079	2252.4	2.69
PLOO	F15	10 Nov 2020	25	13.68	33.54	7.933	7.904	2239.7	1.65
PLOO	F15	10 Nov 2020	100	10.96	33.81	7.765	7.810	2245.1	1.23
PLOO	F35	13 Nov 2020	1	17.65	33.62	8.156	8.080	2260.1	2.72
PLOO	F35	13 Nov 2020	80	11.74	33.70	7.877	7.859	2193.6	1.37
PLOO	PLOO_RTOMS	09 Feb 2021	19	13.08	33.57	7.799	7.916	2235.7	1.66
PLOO	PLOO_RTOMS	09 Feb 2021	60	11.55	33.79	7.689	7.795	2247.0	1.22
PLOO	F13	09 Feb 2021	60	11.55	33.78	7.688	7.828	2247.1	1.31
PLOO	F13	10 Feb 2021	1	14.52	33.50	8.199	8.078	2238.9	2.40
PLOO	F15	10 Feb 2021	41	12.20	33.71	7.903	7.825	2244.5	1.34
PLOO	F15	10 Feb 2021	26	13.64	33.58	8.062	8.095	2232.2	2.40
SBOO	I1	11 Feb 2021	1	14.37	33.48	8.142	8.053	2241.4	2.28
SBOO	I1	11 Feb 2021	55	11.27	33.85	7.799	7.774	2250.6	1.16
SBOO	I28	25 Feb 2021	81	10.20	34.02	7.719	7.794	2273.2	1.18
SBOO	I28	25 Feb 2021	1	14.81	33.49	8.123	8.077	2214.0	2.39
SBOO	I1	04 May 2021	60	10.38	33.83	7.763	7.787	2250.1	1.15
SBOO	I1	04 May 2021	60	10.38	33.83	7.763	7.776	2246.4	1.12
SBOO	I21	04 May 2021	15	12.93	33.45	7.925	7.904	2238.5	1.61
SBOO	I21	04 May 2021	1	17.44	33.63	8.098	8.066	2253.2	2.62

Region	Station	Date	Depth	Temperature	Salinity	CTD pH	Bottle pH	TA	Ω_{arg}
SBOO	I12	06 May 2021	1	17.08	33.73	8.233	8.151	2257.2	3.04
SBOO	I12	06 May 2021	41	11.14	33.69	7.825	7.806	2235.0	1.23
SBOO	I1	11 May 2021	1	17.02	33.72	8.284	8.197	2253.8	3.29
SBOO	I1	11 May 2021	50	10.93	33.74	7.841	7.834	2241.9	1.29
SBOO	I1	11 May 2021	100	10.03	33.92	7.753	7.767	2256.7	1.09
SBOO	I1	11 May 2021	100	10.03	33.92	7.753	7.935	2255.7	1.55
PLOO	F15	12 May 2021	60	10.73	33.77	7.811	7.759	2252.2	1.10
PLOO	F15	12 May 2021	1	17.45	33.68	8.336	8.249	2258.2	3.65
PLOO	F35	13 May 2021	1	17.27	33.67	8.175	8.081	2251.1	2.68
PLOO	F35	13 May 2021	80	10.63	33.81	7.747	7.761	2250.3	1.10
SBOO	I28	03 Aug 2021	60	10.94	33.75	7.809	7.808	2238.4	1.22
SBOO	I28	03 Aug 2021	60	10.94	33.75	7.806	7.814	2242.0	1.24
SBOO	I1	03 Aug 2021	30	11.81	33.52	7.887	7.890	2233.8	1.49
SBOO	I1	03 Aug 2021	1	16.81	33.40	8.114	8.066	2236.8	2.54
PLOO	F35	10 Aug 2021	100	10.68	33.92	7.695	7.761	2250.0	1.10
PLOO	F35	10 Aug 2021	100	10.68	33.92	7.691	7.756	2261.1	1.09
PLOO	F13	10 Aug 2021	57	11.35	33.68	7.759	7.817	2235.9	1.26
PLOO	F13	10 Aug 2021	1	20.47	33.49	8.13	8.069	2243.5	2.91
PLOO	F15	11 Aug 2021	1	18.89	33.27	8.169	8.073	2217.5	2.73
PLOO	F15	11 Aug 2021	60	11.56	33.64	7.823	7.827	2238.6	1.30
PLOO	F35	12 Aug 2021	1	21.35	33.52	8.172	8.067	2232.7	2.97
PLOO	F35	12 Aug 2021	80	11.05	33.76	7.735	7.812	2244.9	1.24
SBOO	I1	03 Nov 2021	28	12.94	33.35	7.78	7.934	2200.1	1.67
SBOO	I1	03 Nov 2021	1	18.07	33.33	7.971	8.078	2252.9	2.73
SBOO	I21	04 Nov 2021	1	18.02	33.55	7.996	8.058	2238.9	2.61
SBOO	I21	04 Nov 2021	26	12.80	33.42	7.764	7.914	2208.3	1.61
SBOO	I1	04 Nov 2021	1	17.85	33.47	7.962	8.069	2231.8	2.64
SBOO	I1	04 Nov 2021	41	12.38	33.50	7.739	7.884	2234.6	1.51

Region	Station	Date	Depth	Temperature	Salinity	CTD pH	Bottle pH	TA	Ω_{arg}
SBOO	I1	05 Nov 2021	1	17.78	33.45	7.966	8.061	2282.0	2.66
SBOO	I1	05 Nov 2021	60	12.19	33.54	7.699	7.844	2230.1	1.37
PLOO	F35	09 Nov 2021	1	17.75	33.51	8.041	8.069	2226.5	2.63
PLOO	F35	09 Nov 2021	33	14.85	33.56	7.944	7.846	2233.5	1.53
PLOO	F13	09 Nov 2021	100	11.07	33.87	7.62	7.763	2256.5	1.13
PLOO	F13	09 Nov 2021	100	11.07	33.86	7.617	7.753	2247.6	1.10
PLOO	F15	09 Nov 2021	1	17.97	33.53	8.022	8.086	2235.1	2.75
PLOO	F15	09 Nov 2021	33	13.50	33.27	7.862	7.978	2238.6	1.89
PLOO	F35	09 Nov 2021	75	11.55	33.63	7.662	7.808	2233.0	1.25
PLOO	F35	09 Nov 2021	89	11.36	33.68	7.652	7.787	2238.9	1.19
PLOO	F35	09 Nov 2021	75	11.51	33.63	7.657	7.815	2246.7	1.27
PLOO	F35	10 Nov 2021	1	17.46	33.51	7.973	8.128	2238.3	2.92
PLOO	PLOO_RTOMS	10 Nov 2021	60	12.01	33.54	7.68	7.848	2239.0	1.38
PLOO	PLOO_RTOMS	12 Nov 2021	1	17.63	33.49	7.973	8.057	2257.5	2.60
PLOO	PLOO_RTOMS	12 Nov 2021	80	11.51	33.70	7.631	7.810	2236.8	1.25
PLOO	F15	01 Feb 2022	1	15.59	33.42	8.149	8.063	2240.8	2.42
PLOO	PLOO_RTOMS	01 Feb 2022	30	14.24	33.41	8.063	8.008	2245.0	2.07
PLOO	PLOO_RTOMS	01 Feb 2022	60	12.40	33.54	7.924	7.867	2241.3	1.46
PLOO	PLOO_RTOMS	01 Feb 2022	60	12.40	33.54	7.925	7.871	2237.5	1.47
PLOO	PLOO_RTOMS	03 Feb 2022	1	15.40	33.43	8.145	8.062	2255.9	2.42
PLOO	F35	03 Feb 2022	41	13.29	33.40	8.007	7.943	2245.9	1.76
PLOO	F35	03 Feb 2022	1	14.76	33.43	8.133	8.139	2255.1	2.74
PLOO	F35	03 Feb 2022	26	13.96	33.41	8.053	7.981	2256.4	1.96
PLOO	F35	04 Feb 2022	1	15.35	33.45	8.162	8.059	2236.9	2.38
PLOO	F13	04 Feb 2022	55	11.45	33.60	7.872	7.815	2242.1	1.26
SBOO	I28	09 Feb 2022	1	15.07	33.47	8.031	8.065	2254.3	2.41
SBOO	I28	09 Feb 2022	60	12.27	33.48	7.806	7.867	2248.9	1.45
PLOO	F13	03 May 2022	1	16.46	33.55	8.186	8.138	2268.9	2.92

Region	Station	Date	Depth	Temperature	Salinity	CTD pH	Bottle pH	TA	Ω_{arg}
PLOO	F15	03 May 2022	30	10.67	33.77	7.758	7.756	2248.5	1.09
PLOO	F15	03 May 2022	60	10.27	33.95	7.741	7.709	2260.5	0.98
PLOO	PLOO_RTOMS	03 May 2022	60	10.27	33.95	7.744	7.704	2259.0	0.97
PLOO	PLOO_RTOMS	04 May 2022	1	16.12	33.65	8.157	8.230	2281.4	3.42
PLOO	PLOO_RTOMS	04 May 2022	41	10.73	33.85	7.663	7.700	2258.2	0.98
PLOO	PLOO_RTOMS	04 May 2022	1	16.32	33.65	8.202	8.187	2257.8	3.16
SBOO	I1	04 May 2022	26	11.46	33.74	7.685	7.746	2255.0	1.11
SBOO	I1	04 May 2022	26	11.46	33.74	7.683	7.747	2258.6	1.11
SBOO	I1	05 May 2022	1	16.80	33.58	8.153	8.155	2255.4	3.03
SBOO	I1	05 May 2022	55	10.28	33.94	7.638	7.703	2247.3	0.96
SBOO	I28	18 May 2022	1	16.72	33.58	8.129	8.047	2285.8	2.50
SBOO	I28	18 May 2022	50	10.43	33.81	7.757	7.774	2262.2	1.13
SBOO	SBOO_RTOMS	18 May 2022	100	9.66	34.16	7.685	7.786	2261.8	1.13
SBOO	SBOO_RTOMS	18 May 2022	100	9.66	34.16	7.688	7.707	2275.2	0.96
SBOO	I21	18 May 2022	1	16.81	33.59	8.147	8.080	2268.8	2.65
SBOO	I21	18 May 2022	30	11.35	33.69	7.816	7.810	2248.2	1.26
SBOO	I1	18 May 2022	75	9.81	33.99	7.687	7.713	2295.2	0.99
SBOO	I1	18 May 2022	75	9.80	33.99	7.688	7.702	2292.4	0.96
PLOO	F13	19 May 2022	1	17.62	33.66	8.227	8.139	2262.8	3.03
PLOO	F13	19 May 2022	60	10.15	33.96	7.724	7.719	2266.8	1.00
PLOO	F15	20 May 2022	1	15.85	33.69	8.164	8.106	2281.0	2.71
PLOO	F15	20 May 2022	80	10.09	33.98	7.664	7.714	2268.1	0.98
PLOO	F35	20 May 2022	80	10.09	33.98	7.665	7.708	2271.7	0.98
SBOO	I21	09 Aug 2022	41	11.67	33.54	7.811	7.818	2240.0	1.28
SBOO	I21	09 Aug 2022	26	11.98	33.53	7.859	7.834	2234.8	1.34
SBOO	SBOO_RTOMS	09 Aug 2022	18	12.70	33.45	7.88	7.902	2219.9	1.57
SBOO	SBOO_RTOMS	09 Aug 2022	1	19.03	33.45	8.122	8.097	2244.2	2.91
SBOO	I28	09 Aug 2022	41	11.67	33.54	7.811	7.813	2224.4	1.26

Region	Station	Date	Depth	Temperature	Salinity	CTD pH	Bottle pH	TA	Ω_{arg}
SBOO	I28	11 Aug 2022	1	22.65	33.62	8.128	8.047	2243.9	3.01
SBOO	I1	11 Aug 2022	60	11.16	33.61	7.798	7.813	2227.7	1.24
PLOO	F35	16 Aug 2022	75	10.83	33.60	7.771	7.773	2274.9	1.15
PLOO	F35	16 Aug 2022	50	11.46	33.54	7.819	7.852	2233.1	1.36
PLOO	F35	16 Aug 2022	30	12.42	33.49	7.937	7.916	2237.6	1.61
PLOO	PLOO_RTOMS	16 Aug 2022	1	23.21	33.56	8.136	8.054	2255.8	3.12
PLOO	PLOO_RTOMS	16 Aug 2022	1	22.93	33.56	8.183	8.052	2237.0	3.05
PLOO	PLOO_RTOMS	16 Aug 2022	100	10.54	33.76	7.754	7.786	2239.9	1.15
PLOO	PLOO_RTOMS	16 Aug 2022	75	10.83	33.60	7.771	7.780	2244.0	1.15
PLOO	F13	17 Aug 2022	1	20.89	33.36	7.965	8.020	2240.6	2.68
PLOO	F13	18 Aug 2022	80	10.70	33.71	7.783	7.750	2235.7	1.07
PLOO	F15	14 Nov 2022	1	16.33	33.45	8.094	8.017	2233.6	2.27
PLOO	F15	14 Nov 2022	30	13.50	33.37	7.922	7.912	2229.7	1.66
PLOO	F15	14 Nov 2022	75	11.36	33.63	7.782	7.751	2256.7	1.11
PLOO	F35	14 Nov 2022	75	11.37	33.63	7.781	7.748	2241.8	1.09
PLOO	PLOO_RTOMS	15 Nov 2022	1	17.44	33.54	8.119	8.055	2254.2	2.57
PLOO	F35	15 Nov 2022	50	12.18	33.44	7.841	7.822	2229.7	1.31
PLOO	PLOO_RTOMS	15 Nov 2022	100	10.78	33.80	7.756	7.742	2281.9	1.08
PLOO	F35	15 Nov 2022	100	10.78	33.80	7.755	7.745	2249.3	1.07
PLOO	PLOO_RTOMS	17 Nov 2022	60	11.88	33.54	7.839	7.780	2256.8	1.20
PLOO	F35	18 Nov 2022	1	16.97	33.53	8.125	8.064	2245.2	2.55
SBOO	I1	28 Nov 2022	1	16.58	33.47	8.103	8.027	2251.0	2.36
SBOO	I1	28 Nov 2022	30	13.96	33.37	7.967	7.928	2229.0	1.74
SBOO	I1	28 Nov 2022	60	12.44	33.48	7.871	7.824	2230.9	1.33
SBOO	I21	28 Nov 2022	60	12.44	33.47	7.87	7.815	2227.0	1.30
SBOO	I21	29 Nov 2022	1	15.91	33.47	8.118	8.068	2236.7	2.47
SBOO	SBOO_RTOMS	29 Nov 2022	55	12.43	33.48	7.88	7.831	2228.9	1.35
SBOO	SBOO_RTOMS	30 Nov 2022	41	13.52	33.42	7.941	7.876	2223.5	1.54

Region	Station	Date	Depth	Temperature	Salinity	CTD pH	Bottle pH	TA	Ω_{arg}
SBOO	SBOO_RTOMS	30 Nov 2022	26	14.08	33.40	8.002	7.897	2233.2	1.64
SBOO	I28	30 Nov 2022	26	14.09	33.40	8.002	7.916	2235.2	1.71
PLOO	PLOO_RTOMS	13 Dec 2022	1	14.83	33.44	8.073	8.007	2273.0	2.15
PLOO	F13	13 Dec 2022	30	14.76	33.43	8.03	7.992	2233.4	2.04
PLOO	F13	13 Dec 2022	75	11.29	33.71	7.705	7.705	2251.8	1.00
PLOO	F15	13 Dec 2022	75	11.26	33.71	7.703	7.686	2250.8	0.96
SBOO	I28	28 Feb 2023	1	13.56	33.36	8.069	8.026	2231.9	2.09
SBOO	SBOO_RTOMS	28 Feb 2023	50	11.58	33.55	7.792	7.790	2234.5	1.20
SBOO	I21	28 Feb 2023	100	10.91	33.82	7.713	7.710	2243.0	0.99
SBOO	SBOO_RTOMS	28 Feb 2023	100	10.93	33.82	7.715	7.717	2246.8	1.01
SBOO	I28	07 Feb 2023	1	14.25	33.35	8	8.031	2230.7	2.16
SBOO	I28	07 Feb 2023	30	13.40	33.37	7.881	7.936	2229.7	1.73
SBOO	I1	07 Feb 2023	60	12.00	33.56	7.723	7.791	2237.8	1.23
SBOO	I1	07 Feb 2023	60	12.00	33.56	7.723	7.786	2232.9	1.21
SBOO	I1	08 Feb 2023	1	13.78	33.29	8.073	8.024	2232.4	2.10
SBOO	I1	08 Feb 2023	41	11.56	33.61	7.788	7.762	2233.7	1.13
SBOO	I1	09 Feb 2023	1	13.79	33.28	8.069	8.013	2229.9	2.05
SBOO	I1	09 Feb 2023	55	11.22	33.66	7.775	7.746	2240.3	1.09
SBOO	I21	02 Mar 2023	1	13.28	33.30	8.104	8.034	2239.6	2.11
SBOO	SBOO_RTOMS	02 Mar 2023	60	10.87	33.81	7.724	7.718	2254.5	1.02
SBOO	I21	03 Mar 2023	1	13.53	33.28	8.156	8.057	2233.8	2.22
SBOO	I21	03 Mar 2023	80	10.72	33.88	7.739	7.703	2245.0	0.97
PLOO	F35	16 May 2023	1	17.15	33.47	8.099	8.050	2243.2	2.50
PLOO	F35	16 May 2023	30	11.12	33.58	7.761	7.789	2235.5	1.18
PLOO	F35	16 May 2023	60	10.43	33.80	7.709	7.732	2247.8	1.03
PLOO	PLOO_RTOMS	16 May 2023	60	10.43	33.80	7.709	7.732	2246.3	1.03
PLOO	PLOO_RTOMS	18 May 2023	1	15.79	33.52	8.165	8.087	2263.9	2.58
PLOO	PLOO_RTOMS	18 May 2023	41	10.88	33.68	7.765	7.748	2238.7	1.08

Region	Station	Date	Depth	Temperature	Salinity	CTD pH	Bottle pH	TA	Ω_{arg}
PLOO	PLOO_RTOMS	18 May 2023	1	15.92	33.55	8.187	8.103	2259.6	2.67
PLOO	F13	18 May 2023	26	11.30	33.61	7.799	7.777	2236.7	1.16
PLOO	F13	18 May 2023	26	11.30	33.61	7.799	7.770	2236.3	1.15
PLOO	F15	19 May 2023	1	17.05	33.47	8.127	8.040	2245.4	2.45
PLOO	F15	19 May 2023	55	10.42	33.78	7.744	7.721	2243.6	1.00
SBOO	I28	23 May 2023	1	17.49	33.49	8.181	8.038	2238.9	2.47
SBOO	I28	23 May 2023	50	10.44	33.59	7.871	7.818	2230.6	1.22
SBOO	I21	23 May 2023	100	10.07	33.91	7.721	7.699	2253.8	0.95
SBOO	I21	23 May 2023	100	10.07	33.91	7.72	7.703	2256.1	0.95
SBOO	I12	23 May 2023	1	17.35	33.48	8.178	8.049	2238.0	2.51
SBOO	I12	23 May 2023	30	12.78	33.37	8.046	7.983	2230.0	1.86
SBOO	I12	23 May 2023	75	10.37	33.72	7.735	7.713	2252.5	0.98
PLOO	F35	23 May 2023	75	10.39	33.72	7.742	7.717	2257.5	1.00
PLOO	F35	24 May 2023	1	17.44	33.46	8.139	8.049	2238.4	2.52
PLOO	F35	24 May 2023	60	11.15	33.62	7.807	7.774	2231.4	1.14
PLOO	F35	25 May 2023	1	17.08	33.33	8.141	8.017	2229.0	2.32
PLOO	F13	25 May 2023	80	10.63	33.75	7.745	7.727	2242.6	1.02
PLOO	PLOO_RTOMS	08 Aug 2023	1	21.68	33.41	8.091	7.987	2235.3	2.59
PLOO	PLOO_RTOMS	08 Aug 2023	30	13.75	33.17	8.036	8.023	2222.3	2.07
PLOO	PLOO_RTOMS	08 Aug 2023	60	11.68	33.49	7.902	7.859	2227.6	1.39
PLOO	PLOO_RTOMS	09 Aug 2023	1	20.12	33.30	8.151	8.050	2237.7	2.76
PLOO	F35	09 Aug 2023	41	12.58	33.36	7.959	7.902	2232.2	1.57
PLOO	F35	09 Aug 2023	1	20.92	33.25	8.141	8.027	2236.8	2.71
PLOO	F35	09 Aug 2023	26	12.87	33.34	7.989	7.927	2229.1	1.67
PLOO	F35	09 Aug 2023	26	12.87	33.34	7.989	7.928	2229.7	1.67
PLOO	F13	10 Aug 2023	1	22.82	33.44	8.136	8.009	2239.3	2.81
PLOO	F13	10 Aug 2023	55	11.94	33.40	7.905	7.864	2229.1	1.41
PLOO	F13	15 Aug 2023	1	20.44	33.35	8.135	8.038	2238.5	2.73

Region	Station	Date	Depth	Temperature	Salinity	CTD pH	Bottle pH	TA	Ω_{arg}
PLOO	F15	15 Aug 2023	50	11.69	33.38	7.874	7.868	2226.6	1.41
PLOO	F15	15 Aug 2023	100	10.73	33.66	7.739	7.754	2238.4	1.08
SBOO	I1	15 Aug 2023	100	10.73	33.66	7.74	7.757	2244.6	1.09
SBOO	I1	15 Aug 2023	1	21.05	33.39	8.159	8.046	2247.5	2.84
SBOO	I1	15 Aug 2023	30	12.23	33.30	7.948	7.911	2222.9	1.57
SBOO	I1	15 Aug 2023	75	11.10	33.48	7.763	7.754	2253.9	1.10
SBOO	I21	15 Aug 2023	75	11.09	33.48	7.763	7.748	2256.6	1.09
SBOO	I21	16 Aug 2023	1	15.54	33.25	8.101	8.003	2231.8	2.14
SBOO	I28	16 Aug 2023	60	11.42	33.48	7.841	7.812	2259.6	1.26
SBOO	I28	17 Aug 2023	1	18.52	33.33	8.163	8.042	2234.8	2.57
PLOO	F35	17 Aug 2023	80	10.94	33.66	7.781	7.755	2243.8	1.09
PLOO	F35	24 Oct 2023	1	17.38	33.09	8.126	8.034	2232.0	2.42
PLOO	F35	24 Oct 2023	30	13.89	33.30	7.954	7.894	2227.4	1.62
PLOO	F35	24 Oct 2023	75	12.94	33.42	7.885	7.840	2229.7	1.40
PLOO	PLOO_RTOMS	24 Oct 2023	75	12.95	33.41	7.886	7.830	2226.8	1.37
PLOO	F15	07 Nov 2023	1	16.85	33.12	8.135	8.042	2218.4	2.40
PLOO	F15	07 Nov 2023	30	14.24	33.23	8.009	7.929	2223.1	1.75
SBOO	I1	07 Nov 2023	60	13.62	33.31	7.953	7.883	2229.7	1.56
SBOO	I1	07 Nov 2023	60	13.62	33.31	7.953	7.885	2224.0	1.57
SBOO	I1	08 Nov 2023	1	16.65	33.18	8.128	8.069	2211.6	2.50
SBOO	I1	08 Nov 2023	41	14.16	33.23	7.94	7.910	2221.1	1.68
SBOO	I21	08 Nov 2023	1	16.86	33.17	8.121	8.068	2226.1	2.53
SBOO	I21	08 Nov 2023	26	14.92	33.20	8.022	7.968	2225.0	1.94
SBOO	I12	08 Nov 2023	26	14.91	33.19	8.014	7.971	2223.6	1.95
SBOO	I12	09 Nov 2023	1	16.46	33.16	8.109	8.050	2221.8	2.41
SBOO	I12	09 Nov 2023	55	13.65	33.30	7.912	7.872	2221.9	1.53
PLOO	PLOO_RTOMS	14 Nov 2023	1	17.23	33.20	8.136	8.030	2225.7	2.39
PLOO	PLOO_RTOMS	14 Nov 2023	50	13.71	33.15	8.022	7.920	2217.1	1.68

Region	Station	Date	Depth	Temperature	Salinity	CTD pH	Bottle pH	TA	Ω_{arg}
PLOO	PLOO_RTOMS	14 Nov 2023	100	12.33	33.54	7.833	7.785	2236.5	1.22
PLOO	F13	14 Nov 2023	100	12.33	33.54	7.833	7.779	2235.2	1.20
PLOO	F13	15 Nov 2023	1	17.28	33.20	8.141	8.033	2223.2	2.40
PLOO	F15	15 Nov 2023	60	13.61	33.27	7.975	7.892	2227.0	1.59
PLOO	F15	16 Nov 2023	1	17.63	33.23	8.063	8.034	2238.7	2.45
PLOO	F35	16 Nov 2023	80	13.83	33.28	7.889	7.892	2222.5	1.59
SBOO	I28	13 Feb 2024	1	14.97	32.98	8.197	8.041	2214.0	2.23
SBOO	I28	13 Feb 2024	50	13.08	33.31	7.969	7.862	2217.8	1.46
SBOO	I1	13 Feb 2024	100	10.67	33.93	7.825	7.710	2250.1	0.99
SBOO	I1	13 Feb 2024	100	10.67	33.93	7.825	7.715	2247.0	1.00
SBOO	I1	13 Feb 2024	1	15.03	33.07	8.201	8.039	2214.1	2.23
SBOO	I1	13 Feb 2024	30	14.88	33.09	8.182	8.029	2213.0	2.17
SBOO	I21	13 Feb 2024	89	11.16	33.67	7.855	7.738	2244.0	1.06
SBOO	I21	13 Feb 2024	89	11.16	33.67	7.855	7.741	2241.4	1.07
SBOO	SBOO_RTOMS	14 Feb 2024	1	15.00	32.94	8.186	8.031	2212.1	2.19
SBOO	SBOO_RTOMS	14 Feb 2024	60	12.21	33.44	7.943	7.808	2230.9	1.27
SBOO	SBOO_RTOMS	15 Feb 2024	1	15.15	33.02	8.198	8.033	2215.5	2.21
SBOO	I28	15 Feb 2024	80	10.98	33.75	7.856	7.752	2238.6	1.09
PLOO	F35	22 Feb 2024	1	15.43	32.91	8.167	8.040	2204.0	2.25
PLOO	F35	22 Feb 2024	60	11.76	33.54	7.892	7.833	2228.9	1.32
PLOO	F35	22 Feb 2024	60	11.77	33.54	7.893	7.810	2231.9	1.26
PLOO	F35	23 Feb 2024	1	15.38	32.99	8.178	8.023	2208.9	2.18
PLOO	PLOO_RTOMS	23 Feb 2024	41	13.12	33.24	8.027	7.930	2244.2	1.70
PLOO	PLOO_RTOMS	24 Feb 2024	1	15.39	32.98	8.185	8.038	2210.9	2.25
PLOO	PLOO_RTOMS	24 Feb 2024	55	12.09	33.48	7.891	7.802	2224.4	1.25
PLOO	PLOO_RTOMS	07 May 2024	60	10.22	33.85	7.728	7.712	2251.9	0.98
PLOO	F13	07 May 2024	60	10.22	33.85	7.728	7.721	2247.1	1.00
PLOO	F13	08 May 2024	1	17.10	33.41	8.225	8.109	2247.9	2.79

Region	Station	Date	Depth	Temperature	Salinity	CTD pH	Bottle pH	TA	Ω_{arg}
PLOO	F15	08 May 2024	41	10.49	33.77	7.727	7.713	2241.9	0.99
PLOO	F15	08 May 2024	1	17.19	33.44	8.23	8.115	2247.6	2.83
PLOO	F35	08 May 2024	26	10.92	33.67	7.757	7.736	2238.5	1.05
PLOO	F35	08 May 2024	26	10.94	33.67	7.758	7.733	2234.3	1.04
PLOO	F35	10 May 2024	1	17.10	33.45	8.208	8.112	2246.9	2.81
PLOO	F35	10 May 2024	55	10.36	33.80	7.676	7.692	2244.4	0.94
SBOO	I28	14 May 2024	1	17.18	33.32	8.175	8.067	2239.3	2.58
SBOO	I1	14 May 2024	50	10.32	33.76	7.725	7.723	2239.4	1.00
SBOO	I1	14 May 2024	100	9.84	34.01	7.687	7.681	2255.8	0.90
SBOO	I1	14 May 2024	100	9.84	34.01	7.686	7.693	2260.4	0.93
SBOO	I1	14 May 2024	1	16.28	33.36	8.151	8.076	2241.6	2.55
SBOO	I21	14 May 2024	30	10.55	33.66	7.787	7.757	2231.9	1.08
SBOO	I21	14 May 2024	75	9.92	33.91	7.686	7.669	2271.0	0.89
SBOO	SBOO_RTOMS	14 May 2024	75	9.92	33.90	7.687	7.677	2271.6	0.91
SBOO	SBOO_RTOMS	15 May 2024	1	17.58	33.42	8.208	8.073	2242.9	2.65
SBOO	SBOO_RTOMS	15 May 2024	60	10.06	33.90	7.705	7.668	2251.3	0.89
SBOO	I28	16 May 2024	1	17.61	33.45	8.235	8.081	2244.4	2.69
SBOO	I28	16 May 2024	80	9.93	33.99	7.723	7.671	2260.0	0.89
PLOO	PLOO_RTOMS	31 Jul 2024	1	17.73	33.39	8.166	8.087	2250.6	2.74
PLOO	PLOO_RTOMS	31 Jul 2024	26	11.51	33.52	7.79	7.789	2228.2	1.19
PLOO	PLOO_RTOMS	31 Jul 2024	26	11.51	33.52	7.787	7.783	2231.1	1.18
PLOO	PLOO_RTOMS	06 Aug 2024	1	20.04	33.30	8.123	8.013	2236.5	2.56
PLOO	F13	06 Aug 2024	30	11.86	33.28	7.927	7.873	2218.5	1.43
PLOO	F13	06 Aug 2024	60	10.63	33.66	7.778	7.787	2248.4	1.16
PLOO	F15	06 Aug 2024	60	10.63	33.65	7.776	7.764	2233.9	1.10
PLOO	F15	07 Aug 2024	1	18.72	33.29	8.025	8.013	2235.1	2.45
SBOO	I1	07 Aug 2024	41	11.33	33.56	7.686	7.754	2234.0	1.11
SBOO	I1	07 Aug 2024	1	21.00	33.43	8.058	7.995	2239.6	2.57

Region	Station	Date	Depth	Temperature	Salinity	CTD pH	Bottle pH	TA	Ω_{arg}
SBOO	I1	07 Aug 2024	26	11.56	33.54	7.727	7.783	2237.0	1.19
SBOO	I1	07 Aug 2024	26	11.56	33.54	7.727	7.772	2234.0	1.16
SBOO	I21	08 Aug 2024	1	19.78	33.28	8.053	8.014	2238.0	2.55
SBOO	I21	08 Aug 2024	55	11.29	33.54	7.719	7.763	2232.9	1.12
PLOO	F35	13 Aug 2024	1	22.63	33.40	8.069	7.977	2241.5	2.63
PLOO	F35	13 Aug 2024	50	11.39	33.52	7.755	7.777	2223.3	1.15
PLOO	F35	13 Aug 2024	100	10.62	33.70	7.689	7.721	2237.1	1.00
PLOO	F35	13 Aug 2024	100	10.62	33.70	7.689	7.735	2238.3	1.03
PLOO	PLOO_RTOMS	13 Aug 2024	1	21.98	33.42	8.178	8.063	2234.5	3.01
PLOO	PLOO_RTOMS	13 Aug 2024	30	11.90	33.31	7.894	7.889	2219.1	1.48
PLOO	PLOO_RTOMS	13 Aug 2024	89	10.69	33.69	7.706	7.728	2234.7	1.02
PLOO	PLOO_RTOMS	13 Aug 2024	89	10.69	33.69	7.708	7.740	2236.3	1.04
PLOO	F13	14 Aug 2024	1	21.22	33.31	8.257	8.112	2235.0	3.20
PLOO	F13	14 Aug 2024	60	11.78	33.48	7.852	7.810	2230.2	1.26
PLOO	F15	15 Aug 2024	1	23.42	33.50	8.154	7.967	2241.6	2.66
PLOO	F15	15 Aug 2024	80	10.73	33.67	7.746	7.724	2236.2	1.01
SBOO	I28	06 Nov 2024	1	16.21	33.27	8.233	8.141	2229.9	2.84
SBOO	I28	06 Nov 2024	41	11.25	33.44	7.893	7.807	2219.0	1.22
SBOO	I1	06 Nov 2024	1	16.14	33.29	8.244	8.093	2229.7	2.59
SBOO	I1	06 Nov 2024	26	11.74	33.36	7.941	7.836	2216.3	1.32
SBOO	I1	06 Nov 2024	26	11.74	33.36	7.941	7.835	2222.5	1.32
SBOO	I1	07 Nov 2024	1	16.85	33.34	8.277	8.130	2235.8	2.86
SBOO	I21	07 Nov 2024	55	11.29	33.42	7.904	7.809	2220.8	1.23
PLOO	F35	19 Nov 2024	1	15.87	33.32	8.218	8.059	2226.0	2.41
PLOO	F35	19 Nov 2024	60	10.99	33.48	7.865	7.783	2224.9	1.15
PLOO	F35	19 Nov 2024	100	10.25	33.78	7.789	7.723	2245.7	0.99
PLOO	F35	19 Nov 2024	100	10.26	33.77	7.789	7.722	2245.6	0.99
PLOO	PLOO_RTOMS	19 Nov 2024	1	15.67	33.36	8.227	8.083	2233.8	2.51

Region	Station	Date	Depth	Temperature	Salinity	CTD pH	Bottle pH	TA	Ω_{arg}
PLOO	PLOO_RTOMS	19 Nov 2024	30	12.42	33.25	8.024	7.912	2216.0	1.58
PLOO	PLOO_RTOMS	19 Nov 2024	89	10.25	33.68	7.79	7.727	2248.5	1.00
PLOO	PLOO_RTOMS	19 Nov 2024	89	10.25	33.68	7.791	7.727	2243.8	1.00
PLOO	F13	20 Nov 2024	1	15.56	33.36	8.28	8.130	2233.2	2.73
PLOO	F13	20 Nov 2024	60	10.90	33.51	7.851	7.827	2223.7	1.26
PLOO	F15	21 Nov 2024	1	15.54	33.37	8.306	8.131	2235.2	2.74
PLOO	F15	21 Nov 2024	80	10.40	33.77	7.821	7.735	2241.8	1.03